F 1103 Vegyészet 04

R 1985 MÁR 0 2

ACADÉMIE DE LA RÉPUBLIQUE SOCIALISTE DE ROUMANIE

REVUE ROUMAINE DE CHIMIE

REFERÁLVA

TOME 30
N° 1
Janvier 1985

Rev. Roumaine Chim.

RRCHAX, 30, *1*, p. 1–94 (1985), Bucarest

EDITURA ACADEMIEI REPUBLICII SOCIALISTE ROMÂNIA

ACADÉMIE DE LA RÉPUBLIQUE SOCIALISTE DE ROUMANIE

COMITÉ DE RÉDACTION

Rédacteur en chef:

I. G. MURGULESCU, membre de l'Académie de la République Socialiste de Roumanie

Rédacteurs en chef adjoints:

A.T.BALABAN et V.EM. SAHINI, membres correspondants de l'Académie de la République Socialiste de Roumanie

Collège de rédaction:

EM. BRATU, ELENA CEAUŞESCU, ECATERINA CIORĂNESCU-NENITZESCU, CR. SIMIONESCU, membres de l'Académie de la République Socialiste de Roumanie; P. SPACU, membre correspondant de l'Académie de la République Socialiste de Roumanie; M. BANCIU, M. D. GHEORGHIU, I. HAIDUC, D. I. MARCHIDAN, I. MOLDOVAN, G. NIAC et D. SĂNDULESCU

La Revue Roumaine de Chimie parait 10 fois par an. Toute commande de l'étranger pour les travaux parus aux Editions de l'Académie de la République Socialiste de Roumanie sera adressée à « ROMPRESFILATELIA » — sectorul Export-Import Presă, P.O.Box 12—201 télex 10376 prsfi-r Bucureşti, Calea Griviţei nr. 64—66, Roumanie,

Les manuscrits, les livres et les revues proposés en échange, ainsi que toute correspondance seront envoyés à la rédaction :

REVUE ROUMAINE DE CHIMIE

125, Calea Victoriei, 79717 Bucarest, Roumanie, téléphone 50 76 80

EDITURA ACADEMIEI REPUBLICII SOCIALISTE ROMÂNIA
125, Calea Victoriei, 79717 Bucarest, Roumanie, téléphone 50 76 80

REVUE ROUMAINE DE CHIMIE

ORSZÁGOS MŰSZAKI INFORMÁCIÓS KÖZPONT ÉS KÖNYVTÁR 1883

Tome 30, N° 1 Janvier, 1985

C. I. LEPĂDATU, Global similarity and shape recognition in experimental chemistry 3–5

S. STERNBERG, I. LINGVAY, T. VIȘAN and LIANA MOISESCU, Electrochemical behaviour of silicon electrodes in molten chlorides . . . . . . 7–16 R

M. NICU, Synthesis and uses of α-methyl-styrene-p-sulphonate (II). Sulphonation of isopropylbenzene (IPB) with H_2SO_4 ($d = 1.831$ g/mL) 17–22

D. MUNTEANU, VIRGINIA MANOVICIU and I. MANOVICIU, Separation of oligo(1,2-propylene terephthalate)s by gradient elution high performance liquid chromatography 23–29

A. O. MOKHALLALATI, ANCA ISTUDOR, D. VÎRTOSU and C. LUCA, Potentiometric gas sensor for carbon dioxide . . . . 31–36 R

D. R. GUPTA and R. K. ARORA, Synthesis of some biologically active N′-picolinoyl-4-(substituted azo)-alkyl/aryl pyrazoles 37–40

ABOEL MAGED A. ABDEL-WAHAB, MOHAMED S. K. YOUSSEF and GUNTER HELMCHEN, Mass spectra of diastereomeric substituted secondary valer- and butyramides 41–48

ASHOK KUMAR, B. K. PURI and A. L. J. RAO, Thermodynamics of complex formation: Zinc-ε-caprolactam system 49–53

IULIA HAVLIK, T. SIMONESCU and I. HAVLIK, New pyrazolone compounds of bis-methylaminoantipyryl-propane and bis-methylaminoantipyryl-butane 55–59

SALAH M. ABD EL-KADER, MAHMOUD F. ABD EL-ALLE, MOHAMADY A. FAKHR EL-DEIN and SALAH A. TURK, Isolation and characterization of arabinogalactan from Lima Bean (*Phaseolus Limensis*) Seed 61–68

CLEOPATRA VASILIU-OPREA and M. POPA, Mechanochemically initiated copolymerizations. 6. Synthesis and characterization of acrylonitrile-vinyl acetate-α-methyl styrene copolymers obtained by vibratory milling (in Russian) 69–79

HOCINE KADI and D. P. LAZAR, Identification of aromatic hydrocarbons in different petroleum fractions. II. Component identification by HPLC (in French) 81–88

BOOK REVIEWS 89–93

Rev. Roumaine Chim. **30**, *1*, 1–94 (1985), Bucarest

Revue Roumaine de Chimie, **30**, *1*, 3–5 (1985)

GLOBAL SIMILARITY AND SHAPE RECOGNITION IN EXPERIMENTAL CHEMISTRY

C. I. LEPĂDATU

Center of Chemical Physics, Spl. Independenţei 202, Bucharest, Romania

Received July 21, 1982

The global similarity and the shape recognition of the signatures (spectrograms, gas chromatograms, etc.) are discussed. The chemometric method makes use of the properties of the convex functions defined on the set of experimental data.

The practice of various chemical branches necessitates, frequently, the comparison between mixtures of substances and a mixture considered as a standard. The usual way is to compare their signatures (IR or electronic spectra, gas chromatograms, etc.) and to see if their attributes (peaks, etc.) can be assigned to the chemical components. Another way is to make classical qualitative and quantitative analyses. There are however, many situations where, due to the complexity of the samples, the last task cannot be made or is not necessary. The problem reduces, in these circumstances, to the comparison of curves of pictures representing signatures of the samples. How to compare the curves each other and to obtain from their shapes a global similarity? This work implies the following stages :

(i) obtain the signatures (chromatograms, spectra, etc.)

(ii) compare the values of the attributes (wavenumbers, retention times, intensities, etc.) without reference to their nature.

(iii) combine the attribute-to-attribute comparisons into one single comparison.

A simple but questionable answer to the last point has been reported by Tamimoto[1,2] and applied by Dravnieks and Krotoszynski.[3] The aim of this note is to see if question (iii) may be solved using the properties of the convex functions. Let us consider an N-dimensional vector A for a mixture considered as a standard, its components $\{A_n\}_{n=1,\dots,N}$ being in one-to-one correspondence with the attributes $\{\omega_n\}_{n=1,\dots,N}$ of the standard signature. Let us consider the vector A′ of a sample, its components $\{A'_n\}_{n=1,\dots,N}$ being generally different from those of the vector A. We consider the vector A as the "true" value of the multidimensional experiment, A′ being the "result" of a measurement affected by errors. The relative error of each vector component (attribute) is:

$$e_n' = \frac{A_n - A_n'}{A_n}, \tag{1}$$

its relative similarity being given by:

$$x_n' = |1 - e_n'| = \left|\frac{A_n'}{A_n}\right|. \tag{2}$$

Note that A_n' and A_n are always considered as positive and different from zero.

Instead of x_n' values, the normalized values will be used:

$$p_n' = \frac{x_n'}{\sum_{i=1}^{N} x_i'}. \tag{3}$$

Let us choose the convex functions $f : [a, b] \to R$, $[a, b] \subset R$. The Jensen inequality[4] valid for such functions is:

$$\frac{1}{N}\sum_{n=1}^{N} f(y_n) \leqslant f\left(\frac{1}{N}\sum_{n=1}^{N} y_n\right),\ y_n \in [a, b]. \tag{4}$$

For $y_n = p_n'$ (equation 3), we have:

$$\frac{1}{N}\sum_{n=1}^{N} f(p_n') \leqslant f\left(\frac{1}{N}\right). \tag{5}$$

For $f(x) = -x^2$ (this function mapped onto the probability field is named information energy (Onicescu)[5–6]), we obtain:

$$A_0 = N\frac{\sum_{n=1}^{N} x_n'^2}{\left(\sum_{n=1}^{N} x_n'\right)^2} \geqslant 1. \tag{6}$$

For $f(x) = -x \log x$ (this function mapped onto the probability field is named information entropy (Shannon)[7]), we obtain:

$$A_S = \frac{-\sum_{n=1}^{N} p_n' \log p_n'}{\log N} \geqslant 1. \tag{7}$$

Observe that the equality for (6) and (7) takes place only if all values $x'_n = k$. For $x'_n = 1$ (i.e. $A'_n = A_n$), the two vectors A′ (sample) and A (standard) are identical ($A_{O(S)} = 1$).

Generally, for $x'_n = k$, $A_{O(S)} = 1$, formulas 6 and 7 allow therefore the "shape recognition" of the vectors A and A′, their components (attributes) being proportional. Formulas 6 and 7 can be used to estimate the global similarity between the vectors A and A′ which represent the signatures of the sample and standard. Observe that the global similarity depends on the choice of the convex function f(x).

One may also define a noneuclidian distance (Tamimoto[1-2]) between the vectors A (standard) and A′(sample), given by

$$D_T = + \log A_{O(S)}. \tag{8}$$

For $A_{O(S)} > 1$; $D_T > 0$, for $A_{O(S)} = 1$, the distance between the sample and standard being zero (A and A′ are identical or proportional).

ACKNOWLEDGEMENT. I express my thanks to Drs. S. Moldoveanu and T.Constantinescu for helpful discussions concerning the usefulness and the applicability of global similarity and of shape recognition to experimental chemistry.

REFERENCES

[1] T. T. Tamimoto, *Trans. N.Y. Acad. Sci. Ser. 2*, **23**, 567 (1961).

[2] T. T. Tamimoto, *Notices Amer. Math. Soc.* **8**, 432 (1961).

[3] A. Dravnieks and B. K. Krotoszynski, *J. Gas Chromatogr.*, **6**, 144(1968).

[4] A. J. White, "Real Analysis", Addison-Wesley Publ. Comp. London, 1968.

[5] O. Onicescu and V. Ştefănescu, "Elemente de statistică informaţională cu aplicaţii", Ed. Tehnică, Bucharest, 1979.

[6] V. Ştefănescu, "Aplicaţii ale energiei şi corelaţiei informaţionale", Ed. Academiei, Bucharest, 1979.

[7] S Guiaşu, "Aplicaţii ale teoriei informaţiei", Ed. Academiei, Bucharest, 1968.

Revue Roumaine de Chimie, **30**, *1*, 7–16 (1985)

ELECTROCHEMICAL BEHAVIOUR OF SILICON ELECTRODES IN MOLTEN CHLORIDES

S. STERNBERG, I. LINGVAY *, T. VIŞAN and LIANA MOISESCU
Chair of Physical Chemistry and Electrochemical Technology,
The Polytechnic, Bucharest, Romania
* Radio Parts and Semiconductors Factory, Bucharest, Romania

Received March 10, 1983

Electrochemical behaviour of the n-type and p-type silicon electrodes in LiCl–KCl eutectic solvent and LiCl–KCl + 1 M $PbCl_2$ melts was studied by potentiostatic technique. Anodic and cathodic polarization curves on exposed (110) faces of semiconductor have been obtained at 500 ± 5°C in the darkness. In LiCl–KCl–$PbCl_2$ systems a pronounced increase of anodic currents, especially on the p-type silicon electrodes, was observed, whereas in the cathodic region the "metallizing" potential was rapidly shifted from –2V to – 0.6 V *vs* Ag/Ag$^+$ reference electrode.

The detailed knowledge of the current/potential dependence on silicon electrode in molten salts is of interest both from a theoretical and a practical point of view. However, only a few electrochemical studies have been carried out in molten nitrates[1] and chlorides.[2,3] Thus, recently Tyagay *et al.* [2] have published the results concerning the polarization of silicon in NaCl–KCl–$AlCl_3$ melt at 140° C; the deposition of aluminium was observed at a very negative potential on *n*-type silicon with resistivity of 4.5 Ω. c.m.

Earlier[4] we described the cathodic reactions on silicon in molten potassium nitrate. We now report an investigation of potentiostatic polarization with *n*-type and *p*-type monocrystal silicon in LiCl–KCl eutectic melt with and without added $PbCl_2$, in the darkness.

EXPERIMENTAL TECHNIQUE

Steady-state potentiostatic measurements were carried out at constant temperature of 500°C on monocrystal silicon (110) surfaces. Before the preparation of electrodes, the resistivity of each silicon disk samples was measured at 27°C using "the four sondes method". The impurity concentration was calculated from these resistivity values [5] as well as the charge carriers concentration at the working temperature[6] (Table 1).

Table 1

Experimental and calculated data for polarization of silicon electrodes in molten chlorides ($t = 500°C$).

Electrode ($s = 0.75$ cm^2)			Corrosion current i_0, mA		Multiplication factor, K*
type	resistivity, $\Omega \cdot$ cm	carriers concentration, at/cm (at 500°C)	in LiCl$-$KCl eutectic	in LiCl$-$KCl$-$PbCl$_2$ solutions	$K = \left(\frac{i_{Pb}}{i}\right)_{E = +5V}$
n-Si	0.01	5×10^{18}	0.06	0.2	3
n-Si	1.4	1×10^{18}	0.025	0.1	(22)
n-Si	30	1.1×10^{17}	0.02	0.04	2.5
n-Si	70	1×10^{17}	0.003	0.005	2.2
p-Si	0.01	1.1×10^{19}	0.011	0.09	20
p-Si	0.015	7×10^{18}	0.01	0.05	23
p-Si	0.5	5×10^{17}	0.01	0.015	10
p-Si	10	1.5×10^{17}	0.012	0.01	10
p-Si	100	1.15×10^{17}	0.003	0.008	10
p-Si	200	1×10^{17}	0.003	0.004	9

* i_{Pb} represents the anodic current in LiCl$-$KCl$-$PbCl$_2$ at $+5$ V potential and i is the current in the same conditions but in LiCl$-$KCl solvent.

Both n-type and p-type silicon electrodes were made following the already described design.[4] Single crystal disks with (110) orientation were sealed in a Pyrex glass tube, the inside faces being supplementarily doped by thermal diffusion[7] and metallized by nickel deposition.[8] The reaction products formed during thermal diffusion over silicon surface were moved by a spesPal treatment.[9] In all experiments a constant surface area of 0.75 cm^2 was exposed in the melt. crior to each series of polarization measurements, surface renewal of the electrode was accomplished by the already described technique.[4]

The counter electrode was a carbon rod with a large surface area. The reference electrode consisted of an Ag wire immersed in LiCl$-$KCl $+$ 1 M AgCl melt.

Potentiostatic measurements were made by means of a P.A.R. potentiostat Model 173 provided with P.A.R. digital coulometer Model 179.

RESULTS AND DISCUSSION

Stationary potential values E_s, about of $-$ 0.6 V (*vs.* Ag/Ag$^+$ reference electrode) are obtained by introducing n-type or p-type semiconductor silicon in LiCl$-$KCl eutectic solvent. This potential is shifted at about $-$ 0.4 V by supplementary addition of Pb^{2+} ions in the melt. The E_s potential can be considered as corrosion mixed potential, corresponding to the overall reaction:

$$\mathrm{Si} + \mathrm{X}^{n+} \rightleftarrows \mathrm{Si}^{n+} + \mathrm{X} \qquad (1)$$

where X^{n+} is an oxidizing ion in the melt (Li$^+$ or Pb^{2+} ion) and X $-$ its reduced form. By extrapolating the anodic and cathodic polarization branch, corrosion currents in the range of 5$-$200 μA result. These currents increase with carriers concentration in the semiconductor. However, on the basis of corrosion potential and corrosion current values, no different behaviour between n-type and p-type silicon samples was noticed.

The obtained steady-state current/potential curves on silicon in molten chlorides are shown in Figs. 1–4. In LiCl–KCl eutectic without Pb^{2+} ions the cathodic currents have small values until very negative

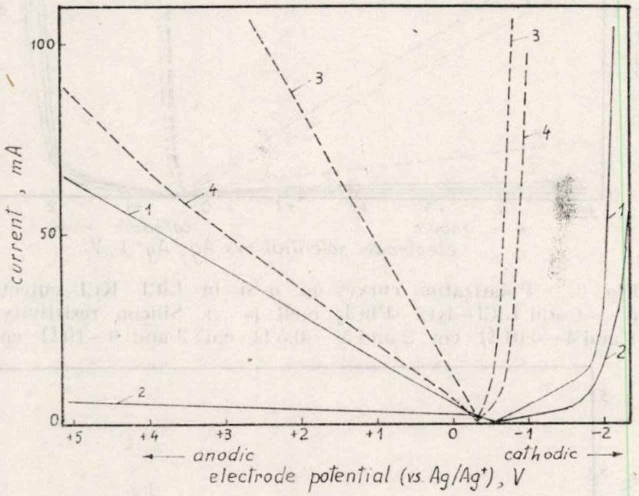

Fig. 1. – Polarization curves on n-Si in LiCl–KCl eutectic (——) and LiCl–KCl–$PbCl_2$ melt (- - -). Silicon resistivity: 1 and 3 – 0.01 Ω · cm; 2 and 4 – 1.4 Ω · cm.

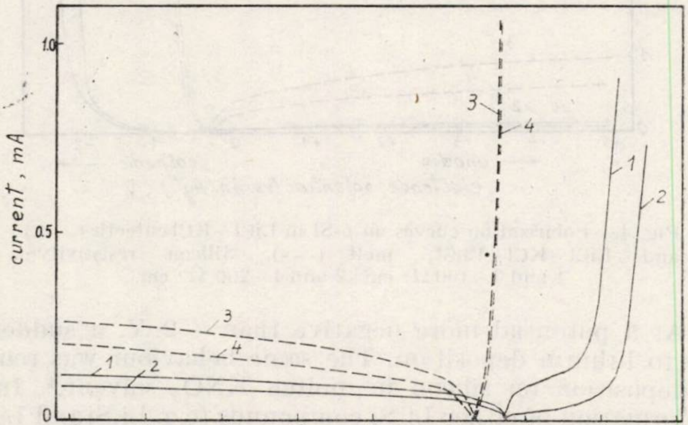

Fig. 2. – Polarization curves on n-Si in LiCl–KCl eutectic (——) and LiCl–KCl–$PbCl_2$ melt (- - -). Silicon resistivity: 1 and 3 – 30 Ω · cm; 2 and 4 – 70 Ω · cm.

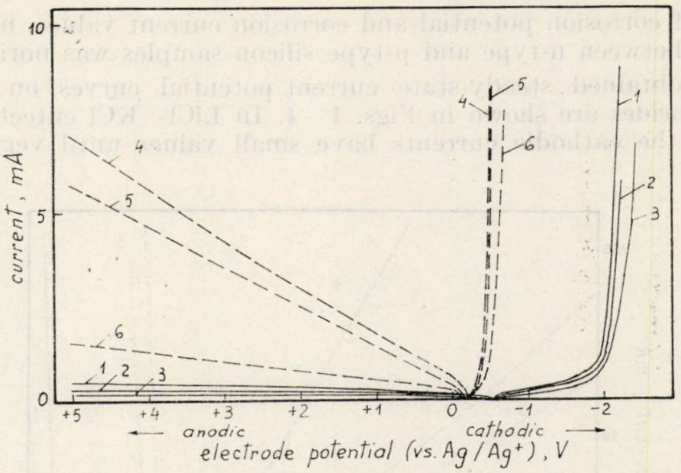

Fig. 3. — Polarization curves on *p*-Si in LiCl—KCl eutectic (——) and LiCl—KCl—PbCl$_2$ melt (- - -). Silicon resistivity: 1 and 4—0.01 Ω · cm; 2 and 5 — 0.5 Ω · cm; 3 and 6—10 Ω · cm.

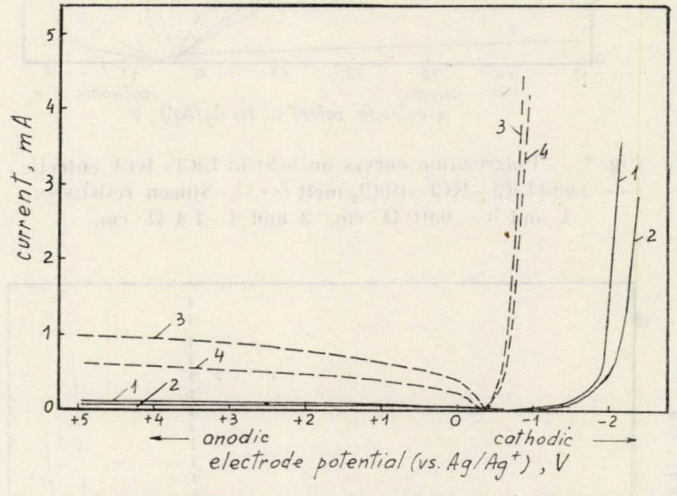

Fig. 4. — Polarization curves on *p*-Si in LiCl—KCl eutectic (——) and LiCl—KCl—PbCl$_2$ melt (- - -). Silicon resistivity: 1 and 3—100 Ω · cm; 2 and 4—200 Ω · cm.

potentials. At a potential more negative than — 2 V, a sudden increase occurs, due to lithium deposition. The same behaviour was remarked for potassium deposition on silicon in molten KNO$_3$ solvent.[4] In the first region, the formation of either Li$_n$Si compounds (e.g. Li$_4$Si and Li$_2$Si reported by Klemm[10]) or K$_n$Si compounds (for example KSi and KSi$_8$[11]) is presumed. Generally, the following reactions may be written:

$$n\,Li^+ + (n - m)e^- + Si \rightleftharpoons Li_nSi + m\,e^+ \qquad (2)$$

$$n\,K^+ + (n - m)e^- + Si \rightleftharpoons K_nSi + m\,e^+ \qquad (3)$$

where n is the number of free electrons from conduction energy band and m — the number of positive holes which participate in the electrode process. Obviously, these reactions take place at more positive potentials than lithium deposition (which appears at cca -2 V).

The effect of the added $PbCl_2$ on $i-E$ curves was then investigated. The steady-state curves in $LiCl-KCl-PbCl_2$ solutions were also presented in Figs 1—4. As shown in these figures both silicon types respond in the same way to the Pb^{2+} ion addition, *i.e.* by increasing the cathodic current at a given potential. In all cases the cathodic process is only lead deposition

$$Pb^{2+} + (2 - m)e^- \rightleftharpoons Pb + m\,e^+ \tag{4}$$

which proceeds with very high exchange current density i_0. It is known that in molten electrolytes, i_0 values of Pb^{2+}/Pb process are very high (at our Pb^{2+} ion concentration i_0 value may be several A/cm² [12]). The sudden increase of current which appears very close to the stationary potential is therefore the Pb^{2+} ion reduction with metal lead deposition. One can conclude that after the first metallic nuclei formation over the silicon surface, the "surface states" occurrence and partial metallization are possible. In these conditions, the semiconductor electrode behaves in some portions as metallic electrode, with a practically unlimited concentration of electrons.

It is also remarkable that in all the cases the Pb^{2+} ion addition provides a strong increase of anodic current. On the *p*-type Si electrodes it has a small value in the absence of Pb^{2+} ions, even at very doped electrodes. For example, on p-type Si electrode with 0.01 Ω. cm resistivity, the anodic current is 400 μA at cca $+5$ V potential; in $LiCl-KCl-PbCl_2$ systems this current rises to 8000 μA.

In Fig. 5 some semilogarithmic curves for anodic polarization are represented. The shape of E-log i curve remained the same for all silicon

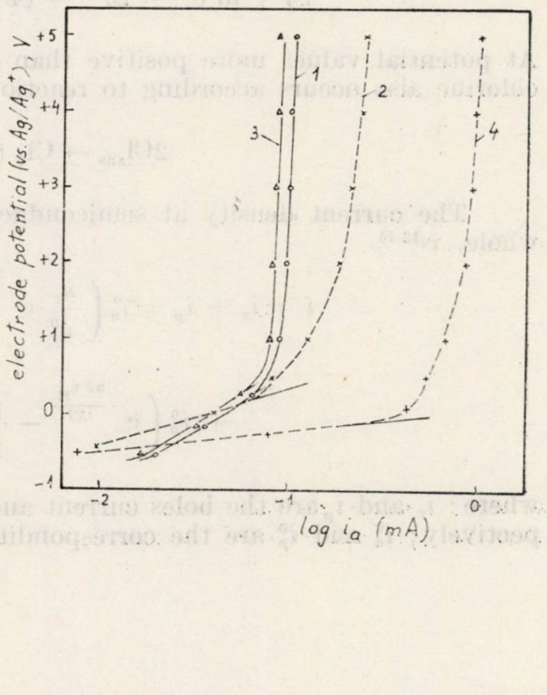

Fig. 5. — Tafel lines obtained for the silicon electrodes in $LiCl-KCl$ eutectic (——) and $LiCl-KCl-PbCl_2$ melt (- - -) 1 and 2—*n*-Si electrode, 30 Ω · cm; 3 and 4—*p*-Si electrode, 100 Ω · cm.

electrodes. Two regions are given on these curves. The first portion, from equilibrium potential to *ca* + 1 V, shows a relatively strong increase of current, the Tafel slope being within 200–400 mV range. In the present paper we make the approximation that the whole overpotential is located in the Debye layer; therefore the Tafel slope would be $\frac{RT}{F}$ (see references[13,14]) that is 173 mV at 500°C. The second portion is very differentiated, as a function both of nature and concentration of charge carriers, but in all the cases the Tafel slope has very high values (3000–15000 mV). In the most curves a current plateau (an anodic limit current) occurs, that indicates a slowness of the electrochemical process. This E-log i dependence is obtained for majority of curves excepting n-Si electrodes with very doped level (n-Si with resistivity 0.01 $\Omega \cdot$ cm) and a part of curves obtained in LiCl–KCl–$PbCl_2$ systems, too; a quasilinear dependence is observed in these last cases (see Figs. 1–4).

We further tried an interpretation of anodic processes on silicon in molten chlorides. In the Pb^{2+} ion absence, mainly silicon dissolution with $SiCl_4$ formation takes place. It is also known that at + 1 V potential value (*vs.* silver electrode) the gaseous chlorine is formed by anodic oxidation of Cl^- ions. We supposed that both anodic reactions are preceded by reaction

$$Cl^- + m\,e^+ \rightarrow Cl_{ads} + (1 - m)\,e^- \text{ (slow)} \tag{5}$$

followed by rapid dissolution of silicon:

$$Si + 4\,Cl_{ads} \rightarrow SiCl_4 \text{ (fast)} \tag{6}$$

It is also possible a direct dissolution of silicon as:

$$Si + m\,e^+ \rightarrow Si^{4+} + (4 - m)\,e^- \text{ (slow)} \tag{7}$$

At potential values more positive than + 1 V the evolution of gaseous chlorine also occurs according to reaction

$$2Cl_{ads} \rightarrow Cl_2 \text{ (fast)} \tag{8}$$

The current density at semiconductor/electrolyte interface, on the whole, is[13,14]

$$i = i_n + i_p = i_n^0 \left(\frac{n_s}{n_s^0} e^{-\frac{\alpha F \eta_H}{RT}} - e^{\frac{\beta F \eta_H}{RT}} \right) + \\ + i_p^0 \left(e^{-\frac{\alpha F \eta_H}{RT}} - \frac{p_s}{p_s^0} e^{\frac{\beta F \eta_H}{RT}} \right) \tag{9}$$

where: i_n and i_p are the holes current and the free electrons current, respectively; i_n^0 and i_p^0 are the corresponding exchange currents; n_s^0 and n^s

represent the number of electrons over the semiconductor surface at equilibrium and in polarization conditions, respectively; p_s^0 and p_s have the same meanings, but for the holes; α, β are cathodic and anodic transfer coefficients, respectively; η_H is the overpotential in the Helmholtz layer.

Experimental investigations in aqueous solutions reveal that anodic dissolution of germanium[15–18] and silicon[19–23] takes place mainly by the holes. Thus, the polarization on p-type germanium and silicon electrodes gives anodic currents higher than those on n-type electrodes. The results obtained in the present work show that in molten chlorides at high temperature, anodic behaviour of the two types of silicon is quite different; thus, in majority of cases, except very little doped electrodes, the currents on n-type silicon were several orders of magnitude higher than on p-type samples. We make therefore the approximation that the holes participation in anodic process is practically zero. Hence, on n-type and p-type silicon, the electrode process takes place with the majority carriers and the minority carriers, respectively; these carriers are the electrons in the both cases.

Assuming that the overpotential in the Helmholtz layer (η_H) is negligible and $m = 0$, respectively $i_p = 0$, equation (8) becomes:

$$i = i_n^0\left(\frac{n_s}{n_s^0} - 1\right) \tag{10}$$

In the case of Boltzmann distribution of charge carriers concentration with the potential, equation (10) may be written as:

$$i_n = i_n^0\left[\mathrm{e}^{\frac{-F(\varphi_1-\varphi_1)^0}{RT}} - 1\right] \tag{11}$$

where φ_1^0 and φ_1 are potential drops in the Debye layer at equilibrium and at polarization, respectively. In this last relation the difference $\varphi_1 - \varphi_1^0 = \eta_D$ represents the overpotential in the Debye layer.

From equation (11) at anodic polarization of n-Si electrodes and reactions with $m = 0$, results a curve with the rectification of current, respectively, a current barrier of $i_n = -i_n^0$. In LiCl—KCl eutectic melts, except very doped electrode (n—Si 0.01 $\Omega \cdot$ cm), on all the other n-Si electrodes the existence of this anodic barrier was remarked.

In both figures, 6 and 7, the anodic current at a constant overpotential of + 5 V is plotted *vs* carriers concentration. The same dependence was obtained by choosing the current at any potential from "slow portion" of anodic branch of $i-E$ curves.

In the n—Si case the anodic current (approximately equal to exchange current i_0) strongly increases with electrons concentration (c_e) From Fig. 6 the following dependence can be estimated:

$$i_a = \text{const. x } c_{e^-}^2. \tag{12}$$

According to our approximation, on p—Si the electrochemical process would be expected to take place with free electrons, therefore with the minority carriers. In all polarization curves on $p-$Si one obtained the limit currents, generally much smaller than in the $n-$Si case. These anodic currents have not significant dependence from c_{e+} (see Fig. 7), according to the following relationship :

$$i_a = \text{const. x } c_{e+}^{0,1} \tag{13}$$

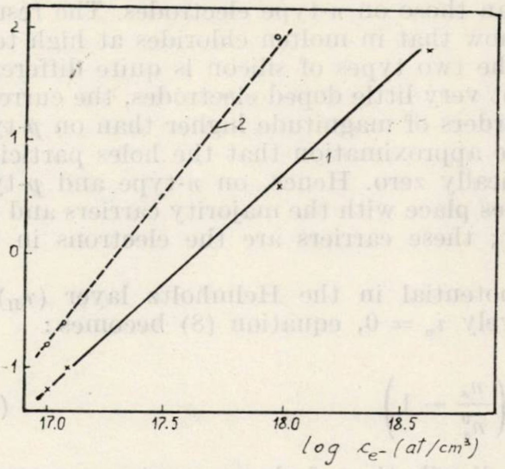

Fig. 6. — The dependence of anodic current at + 5 V potential on the doping level, for n-type silicon electrodes. 1 — in LiCl—KCl eutectic ; 2 — in LiCl—KCl—PbCl$_2$ melt.

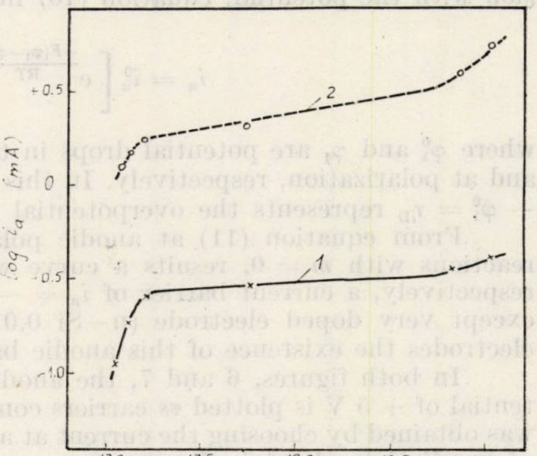

Fig. 7. — The dependence of anodic current at + 5 V potential on the doping level, for p-type silicon electrodes. 1 — in LiCl—KCl eutectic ; 2 — in LiCl—KCl—PbCl$_2$ melt.

These currents can be considered as diffusion limit currents, depending on n_s^0/n_p^0 ratio, that is depending on specific monocrystal silicon technology. In the $p-$Si case it was found that this ratio has a little variation with doping level. Hence, a kinetic barrier of current for p-type silicon is expected to appear at cathodic polarization, but it is probably masked by the "metallizing" phenomenon as mentioned above.

The addition of Pb^{2+} ions in LiCl—KCl eutectic has an electrocatalytic effect on anodic process. In some cases (n—Si 1.4 $\Omega \cdot$ cm, p—Si 0.01 $\Omega \cdot$ cm and p—Si 0.012 $\Omega \cdot$ cm) the limitative character of anodic current disappears and a linear relation $i-E$ was observed. In the other cases, the limitative shapes of $i-E$ curves are kept but, at higher limit current values.

The metallic lead deposition described by reaction (4) proceeds spontaneously even without polarization or at small values of anodic potentials. Owing to the high values of exchange current, i_0, the reaction rate of this process increases, of course, with doping. The occurrence of metallic lead over the surface of semiconductor electrode, that is "surface states", gives the same metallic character as that supposed at cathodic polarization (in much lower proportion, certainly). The rate of electrochemical process is therefore multiplied by this metallic character.

Another free electrons source can appear by lead redissolution as:

$$Pb + m\ e^{+} \rightarrow Pb^{2+} + (2 - m)\ e^{-} \tag{14}$$

where m = 0, according to the hypothesis assumed in the present paper. In Table 1 are calculated the values of "multiplication factor" $K = i_{Pb}/i$ at + 5 V potential; K is a current multiplication factor owing to Pb^{2+} ion addition. On n—Si electrodes, K has the values within 2.2—2.5 range, except n—Si 1.4 $\Omega \cdot$ cm, where the anodic curve character is completely changed. On p—Si electrodes K values are much higher; they varied within a wide range, from 9 to 23, as can be seen from Table 1, due probably to a large variation of n_s/n_p ratio.

CONCLUSIONS

Silicon/molten chlorides interface was experimentally studied by steady-state potentiostatic technique at 500° C in the darkness. Semiconductor silicon electrodes with variable doping of phosphorus (n-type) and boron (p-type) were used. The analysis of steady-state polarization curves leads to several conclusions concerning the electrochemical behaviour of (110) crystallographic face of silicon:

— At cathodic polarization, the current suddenly increases at potentials higher than — 2V in Li—KCl eutectic and — 0.6 V in LiCl—KCl + + 1 M $PbCl_2$ solutions, respectively. This fact can be explained taking into account the "metallization effect" due to discharge of Li^{+} or Pb^{2+} cations.

— At anodic polarization, after the linear region, have been remarked limit currents due to either kinetic or diffusive control, especially on p-type electrodes; the values of these currents are proportional to the doping level of silicon. Comparison of anodic currents at + 5 V potential in LiCl—KCl and LiCl—KCl—$PbCl_2$ melts indicates a multiplication coefficient of 2.2—2.5 on n—Si and of 9—23 on p—Si, in the Pb^{2+} presence.

REFERENCES

[1] V. A. Tyagay, A. V. Gorodyskiy, I. A. Stepanova, E. V. Panov and Yu. M. Shirshov, *Elektrokhimiya*, **14**, 1682 (1978).

[2] V. A. Tyagay, E. V. Panov, Yu. K. Delimarskiy, I. A. Stepanova and Yu. M. Shirshov, *Elektrokhymiya*, **14**, 1674 (1978).

[3] O. V. Snytko, "Problemy Fiziky Poverkhnosty Poluprovodnykov", Naukova Dumka, Kiev, 1981 p. 287.

[4] S. Sternberg, I. Lingvay and T. Vişan, *Rev. Roumaine Chim.*, **27**, 1085 (1982).

[5] S. M. Sze and I. C. Irvin, "Solid State Electronics", vol. II, 1968, p. 599.

[6] Ch. A. Wert and R. M. Thomson, "Physics of Solids", Mc. Graw-Hill, New York, 1964 p. 314.

[7] I. Lingvay, N. Iosif and A. Hluşcu, Romanian Patent No. 87126 (1979) ; N. Iosif, Romanian Patent No. 78127 (1980).

[8] I. Lingvay and M. Scârlete, *Rev. Chim. (Bucureşti)*, **33**, 569 (1982).

[9] I. Lingvay, Romanian Patent No. 66653 (1975).

[10] W. Klemm and M. Struck, *Z. anorg. Chem.*, **278**, 117 (1955).

[11] E. Hohmann, *Z. anorg. Chem.*, **257**, 113 (1948).

[12] S. Sternberg, A. Cotârţă and T. Vişan, to be published.

[13] V. A. Myamlin and Yu. K. Pleskov, "Electrochemistry of Semiconductors", Plenum Press, New York, 1967.

[14] H. Gerischer, *Z. phys. Chem. (Frankfurt)*, **26**, 223, 325 (1960) ; **27**, 48 (1961).

[15] F. Beck and H. Gerischer, *Z. Elektrochem.*, **63**, 500 (1959).

[16] W. H. Brattain and C. G. Garrett, *Bell System. Techn. J.*, **34**, 129 (1955).

[17] W. H. Brattain and C. G. B. Garrett, *Phys. Rev.*, **94**, 750 (1954) ; *Physica*, **20**, 885 (1954).

[18] H. Gerischer and F. Beck, *Z. phys. Chem. (Frankfurt)*, **24**, 378 (1960).

[19] I. B. Flynn, *J, Electrochem. Soc.*, **105**, 715 (1958).

[20] E. A. Efimov and I. G. Erusalimchik, *Zhuriz. Khim.*, **35**, 384 (1961) ; E. A. Efimov, I. G. Erusalimchik and G. P. Sokolova, *Zhur. fiz. Khim.*, 38, 2172 (1964).

[21] E. N. Paleolog, K. S. Korotskova and N. D. Tomashov, *Doklody Akad. Nauk S.S.S.R.*, **133**, 170 (1960).

[22] S. O. Izidinov, T. I. Borisova and V. I. Veselovskiy, *Zhur. fiz. Khim.*, **36**, 1246 (1962).

[23] A. Wolkenberg, *Electrochim. Acta*, **21**, 1165 (1976).

Revue Roumaine de Chimie, **30**, *1*, 17–22 (1985)

SYNTHESIS AND USES OF α-METHYL-STYRENE-*p*-SULPHONATE (II).

SULPHONATION OF ISOPROPYLBENZENE (IPB) WITH H_2SO_4 (d=1.831 g/mL)

M. NICU

Polytechnic Institute Jassy, Splai Bahlui no. 71, Romania

Received July 15, 1983

The sulphonation of isopropyl-benzene with sulphuric acid ($d = 1.831$) was studied and the influence of the molar ratio of the reactants, the type of the reaction system, temperature of reaction time on the *p*-isopropyl-benzene-sulphonic acid yield were established.

1. INTRODUCTION

In a previous paper[1] the possible synthesis ways of α-methyl-styrene-*p*-sulponate (MSS) as well as the sulphonating agent influence on the yield were discussed. The sulphuric acid ($d = 1.831$ g/mL) was found to be the optimal sulphonating agent for IPB.

The studies carried out on the sulphonation of the inferior homologues of IPB[2–13] revealed these reactions to be controlled by the reagent mole ratio, temperature and reaction time.

In the present paper the influence of the above mentioned factors on the IPB sulphonation was studied.

2. EXPERIMENTAL

The following reaction scheme may describe the sulphonation process:

$$\underset{(a)}{\mathrm{IPB}} + \underset{(b)}{H_2SO_4} \rightarrow \underset{(c)}{\mathrm{IPB}-SO_3H} + \underset{(d)}{H_2O} + \underset{(f)}{\mathrm{IPB}}\ \text{(unreacted)} + \underset{(e)}{H_2SO_4\ \text{(unreacted)}} + \underset{(g)}{\text{by-products}} \quad (1)$$

By-products are all compounds, excepting IPB$-SO_3H$, involving acid consumption namely sulphones, products of IPB oxidation and polysulphonation.

Two data are indicative of the process evolution: theoretical yield and real yield.

The theoretical yield represents the IPB percentage converted into IPB $-SO_3H$ if this were the only reaction product.

If a, b, c, d, e, f and g were the number of equivalents of IPB, H_2SO_4, IPB $-SO_3H$, H_2O, H_2SO_4 (unreacted), IPB (unreacted) and by-products, respectively, the relation for calculating the theoretical yield (η_t) may be derived.

At the moment $t = 0$ the number of equivalents is $n = c + e + g$ and the number of equivalents of reacted acid, $z = b - n$. The number of equivalents of consumed acid is equal to the number of equivalents of reacted IPB. The equivalent-gram of IPB is equal to 120. For A grams of IPB introduced in reaction, the theoretical yield is:

$$\eta_t = \frac{120\,z}{A} \cdot 100 \tag{2}$$

where n is determined by titration.

The real yield (η_r) is proportional to the IPB amount converted into p-IPB $-SO_3H$ (p) which may be determined gravimetrically as p-IPB $-SO_3K$. The real yield is given by the relation:

$$\eta_r = \frac{120 \cdot p}{256\ A} \cdot 100 \tag{3}$$

where 256 represents the molecular weight of IPB $-SO_3K \cdot H_2O$.

By comparing the theoretical and real yields, the significance of side reactions may be estimated as well as the efficiency of raw materials consumption.

The IPB sulphonation may be carried out either in closed or open system according to water component (for the other components the system is always closed).

The content of *ortho* and *para* isomers of the reaction product was estimated by ^{1}H-NMR spectral measurements.

The sulphonations were carried out for 5 –60 min, at 60 –185°C and H_2SO_4/IPB mole ratios of 0.5 –3.[1]

3. RESULTS AND DISCUSSIONS

3.1. Influence of the reagent mole ratio

The experimental results are illustrated in Fig. 1.

The yields are noticed to increase with increasing reagent mole ratio up to a certain value. Higher mole ratios are not justified due to rather

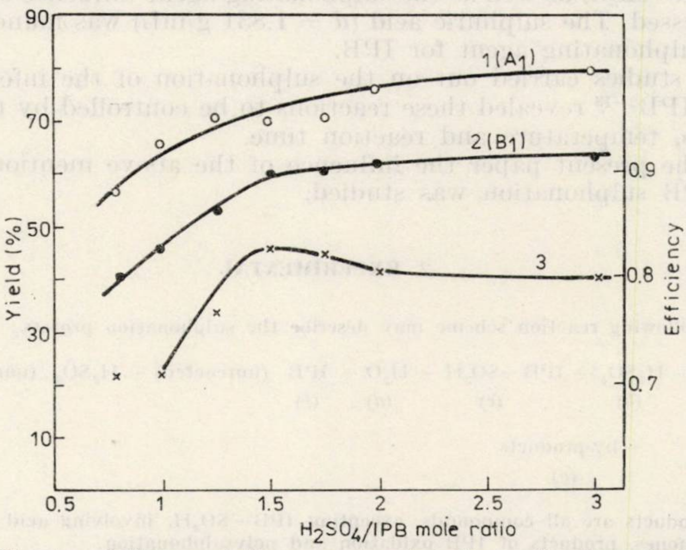

Fig. 1. — Influence of the reagent mole ratio on the theoretical yield (1), real yield (2) and on the efficiency of acid consumption (3) in a closed system, after 25 min, at 165°C.

small yield increases and to a high alkali consumption in the neutralization stage. The sulphonation efficiency shows a maximum at mole ratios lying between 1.25 and 1.75. The optimum reagent mole ratio may be thus concluded to lie between these values.

3.2. Influence of the reaction temperature

The reaction temperature strongly influences the yield (as both thermodynamic and kinetic parameter) as well as the substitution in the aromatic ring.

Depending on the temperature and the reaction system the sulphonation may be carried out either in the presence or in the absence of water.

The temperature influence on the theoretical yield was followed (Fig. 2) as well as on the real yield system in a closed reaction or in a respectively opened reaction system in relation to water.

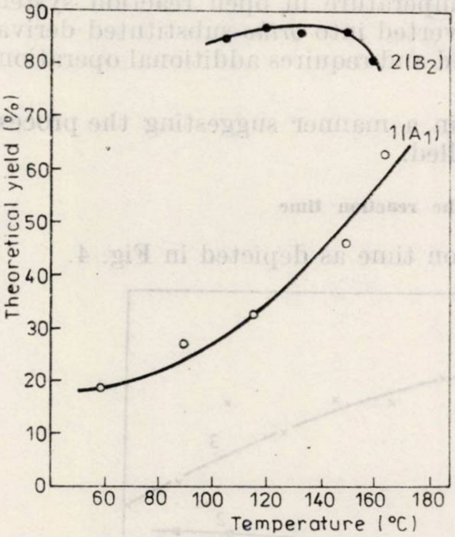

Fig. 2. — The reaction temperature influence on the sulphonation theoretical yield in closed reaction system (1) and on the sulphonation real yield in reaction system opened in relation to water (2) at a reaction time of 20 min ($H_2SO_4/IPB = 1.25$).

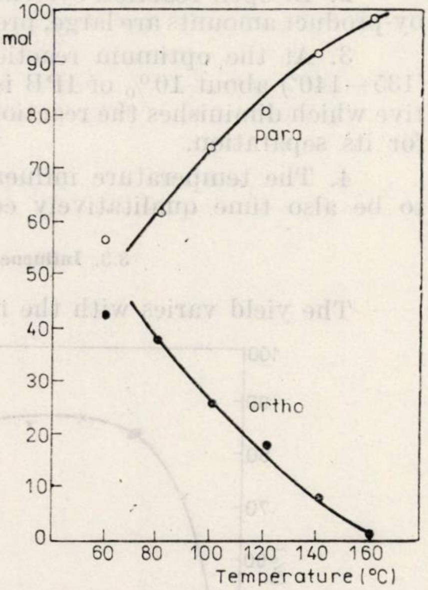

Fig. 3. — Influence of the temperature on the substitution orientation in the aromatic ring ($H_2SO_4/IPB = 1.25$; closed system).

The temperature is noticed to influence strongly the equilibrium of this reversible reaction. Under normal pressure, the optimum reaction temperature is found to be that of the boiling reaction mixture (160—164°C).

In the case of sulphonation with water removal ($T > 100°$, open system) the yields are noticed to be much higher, the temperatures lower than 140 having a rather insignificant influence. The yield decrease for the reactions carried out in open systems at temperatures above 140°C is mainly due to the formation of sulphones since the water elimination influences markedly the equilibrium shifting of this reaction.

The higher temperatures (up to 185°C) were found to promote the side reactions of oxidation, polysulphonation and formation of sulphones. At temperatures of 180—185°C, a black, viscous reaction mixture is formed from which IPB—SO_3K may be isolated rather hardly and in a low yield. It may be thus concluded that the reaction temperature must not exceed 175—180°C.

The temperature influence on the substitution orientation in the aromatic ring is illustrated in Fig. 3.

It is found that the content of *para* isomer increases with increasing temperature being formed exclusively above 160°.

The following conclusions may be drawn on the process development as a function of temperature and reaction system:

1. In a closed reaction system (in the presence of water) the yields are lower than in an open system; the by-product amounts are also lower.

2. In open reaction system the highest yields are attained, but the by-product amounts are large, prevailing at high reaction time and duration.

3. At the optimum reaction temperature in open reaction system (135—140°) about 10% of IPB is converted into *ortho*-substituted derivative which diminishes the reaction yield and requires additional operations for its separation.

4. The temperature influences in a manner suggesting the process to be also time qualitatively controlled.

3.3. Influence of the reaction time

The yield varies with the reaction time as depicted in Fig. 4.

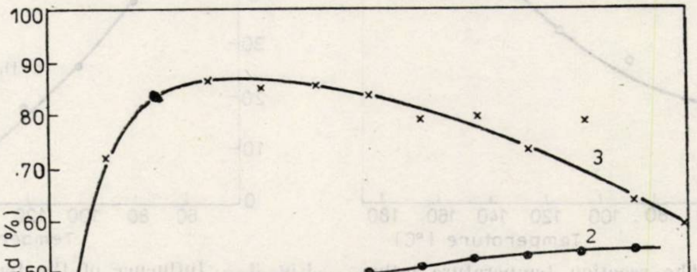

Fig. 4. — Influence of the reaction time on the real (1) and theoretical (2) yields in closed system and on the real yield in open system (3) (H_2SO_4/IPB = 1.25 : temperature).

The experimental data indicate the following:

1. The real yields (1, 3) increase up to a maximum decreasing then with increasing reaction time. This behaviour is characteristic for consecutive reaction systems. The following reactions are probable to proceed in the case of the system under investigation:

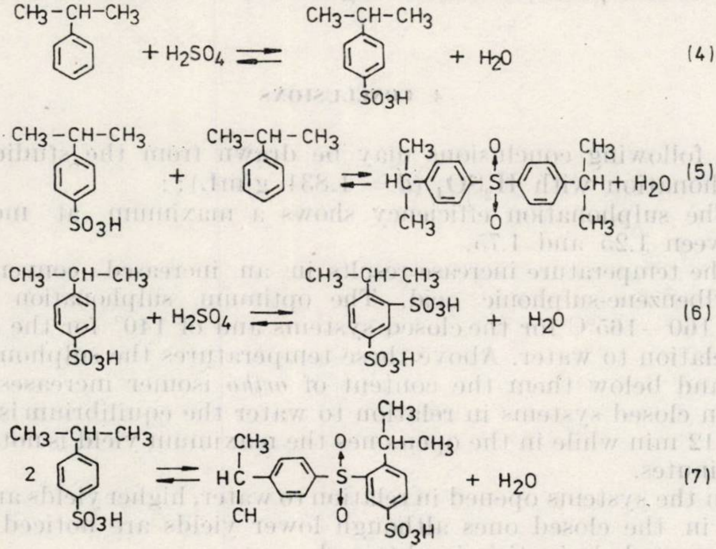

Scheme I

In the IR and ^1H-NMR spectra of the unpurified sulphonation products trisubstituted benzene rings were not identified. The relative absorptions of the sulphone group (1200 cm^{-1}) and P-disubstituted benzene ring (840 cm^{-1}) were found to increase for the products obtained at longer reaction times. These facts are indicative of the sulphone formation (2) as the only consecutive reaction.

2. The decrease in the real yields is more pronounced in the open system, a fact which may be explained by the reversibility of reaction 2. Due to the water elimination from the system the equilibrium shifts towards the sulphone formation.

3. The theoretical yields (2) are found to be inverse and about equal to the real ones (1). This fact suggests the diminution of the system acidity (theoretical yield increase) to produce rather by the diminution of $IPB-SO_3H$ concentration than by the consumption of new amounts of H_2SO_4 in sulphonation. Hence, the consecutive reactions 1 and 2 are probably to proceed since only in reaction 2 equal amounts of IPB and $IPB-SO_3H$ are consumed, which does not affect the equilibrium of reaction 1 and avoids the consumption of new amounts of acid and the equilibrium shifting. If reactions 3 and 4 proceeded they would affect significantly the equilibrium of the main reaction and the acid consumption and theoretical yields would be much higher at longer reaction times.

4. The rate of reaction 2 thus results to be negligible as compared to that of reaction 1 at temperatures below 165°. It follows that at least for shorter reaction times the evolution of the system is faithfully reflected by reaction 1.

5. The equilibrium of the main reaction is attained after 20–25 minutes at 150°C diminishing to 10–12 min. at 160–165°.

6. The side processes become significant at reaction times of 30–35 minutes.

4. CONCLUSIONS

The following conclusions may be drawn from the studies on the IPB sulphonation with H_2SO_4 ($d = 1.831$ g/mL) ; :

1. The sulphonation efficiency shows a maximum at mole ratios lying between 1.25 and 1.75.

2. The temperature increase results in an increased conversion into *p*-isopropylbenzene-sulphonic acid. The optimum sulphonation temperature is of 160–165°C for the closed systems and of 140° for the open systems in relation to water. Above these temperatures the sulphone amouts increase and below them the content of *ortho* isomer increases.

3. In closed systems in relation to water the equilibrium is attained after 10–12 min while in the open ones the maximum yield is noticed after 15–20 minutes.

4. In the systems opened in relation to water, higher yields are obtained while in the closed ones although lower yields are noticed only the *para*-sulphonated derivative is obtained.

REFERENCES

[1] M. Nicu, *Bull. Polytechnical Institute of Jassy*, **27**, 109 (1981).
[2] W. H. G. Rueggeberg, T. E. Souls, L. S. Norwood, *J. Org. Chem.*, **20**, 455 (1965).
[3] E. E. Gilbert, L. S. Giolito, Patent U.S., 2.704.285 (1955).
[4] H. Cerfontain, H. Y. Hoffmann, A. Telder, *Rec. trav. Chim.*, **83**, 493 (1964).
[5] A. Streitwiser, R. H. Zagov, R. C. Fabey, S. Suzuki, *J. Amer. Chem. Soc.*, **80**, 2326 (1958).
[6] A. E. Shilov, F. M. Voishtein, *Doklady Akad. Nauk. S.S.S.R.*, **100**, 728 (1955).
[7] H. Cerfontain, F. L. Sixma, L. Vollbrocht, *Rec. trav. Chim.*, **83**, 226 (1964).
[8] J. W. Monston, J. E. Collen, *J. Amer. Chem. Soc.*, **77**, 3151 (1955).
[9] W. A. Loro and D. W. Hein, Patent U.S., 2.681.926 (1954).
[10] G. Olah and A. Pavlath, *Acta Chim. Acad. Sci. Hung.*, **4**, 111 (1954).
[11] A. W. Koondrop and H. Cerfontain, *Rec. trav. Chim.*, **81**, 954 (1962).

Revue Roumaine de Chimie, **30**, *1*, 23–29 (1985)

SEPARATION OF OLIGO(1,2-PROPYLENE TEREPHTHALATE)S BY GRADIENT ELUTION HIGH PERFORMANCE LIQUID CHROMATOGRAPHY

D. MUNTEANU *, VIRGINIA MANOVICIU ** and I. MANOVICIU **

*ICECHIM, Center for Plastic Materials, Timişoara Laboratory, Str. Gării 25, 1900 Timişoara, Romania

**"Traian Vuia" Polytechnic Institute, Faculty of Chemical Technology, Timişoara, Romania

Received April 1, 1983

Good separation of the components of the reaction mixture from the transesterification of dimethylterephthalate with 1,2-propylene glycol was obtained by reverse phase gradient elution high performance liquid chromatography, using methanol/water as eluent system. The method allows the semiquantitative analysis of the individual oligomers and may be very useful for the study of the transesterification process, although some peaks were not identified.

INTRODUCTION

An investigation of the transesterification of dimethylterephthalate (MeTMe) with glycols assumes perfect analytical determination of all components present in the reaction mixture. Entailing the reaction of two bifunctional compounds, this process is characterized by complexity, with respect to both composition of the intermediate reaction products and the corresponding reaction mechanism. This complexity is obviously the main reason for the lack of significant kinetic and thermodynamic parameters, even for the most studied reaction with ethylene glycol (EG).

The use of branched glycols, to obtain poly(terephthalate)s with some improved properties, has been the subject of an increased interest only in recent years. Consequently, the transesterification of MeTMe with 1,2-propylene glycol (1,2-PG) is much less investigated.

It is the purpose of the present work to establish an analytical method suitable for the study of this process.

Basically, the determination methods of the individual components from the transesterification mixture are much the same, when one glycol is changed with another. However, there are differences between the solubility in alcohols of oligomers from linear and branched glycols.

Oligo(ethyleneterephthalate)s (OET) obtained by : (i) the transesterification of MeTMe with EG, (ii) the extraction from poly(ethylene terephthalate), films, (iii) the first condensation step of terephthalic acid with EG, were separated earlier by different chromatographic techniques, i.e. paper chromatography,[1] thin layer chromatography, [2,3], size exclusion chromatography, [4–7] column liquid chromatography,[8] normal phase HPLC, [3,9] and reverse phase gradient elution HPLC (RP–GE–HPLC).[10]

For the HPLC separation of OET, Van der Maeden et al.[10] employ a very unusual eluent system : 1,1,1,3,3,3-hexafluoro-isopropanol (HFI)/H_2O, because HFI is known as a good solvent for poly(ethylene terephthalate) and was used in light scattering, viscosity and SEC determination.[11] Due to the fact that oligo(1,2-propylene glycol terephthalate)s are more soluble in methanol (MeOH), the usual eluent system MeOH/H_2O could be used for their RP–GE–HPLC separation. Moreover, we used the same system for oligomers obtained from MeTMe and other branched glycols.

EXPERIMENTAL

Materials

MeTMe was a commercial product (technical grade). 1,2-PG from UCB Brussells (reagent grade). Methanol was distilled in glass through a 30 TP column. Water was freshly bidistilled from $KMnO_4$. The catalyst $Zn(CH_3COO)_2\ 2H_2O$ (purity grade) was used without further purification.

Procedures

The transesterification was carried out in the usual way, with 0.1 wt % catalyst (based on MeTMe), at 180–220°C, depending upon the molar ratio 1,2–PG : MeTMe. When the reaction was followed in time, 2 g samples were withdrawn from the reaction mixture, 0.02–0.05 g dissolved in MeOH and 10–20 µl injected in the liquid chromatograph.

Apparatus

Use was made of a high performance liquid chromatograph in the gradient mode (the gradient part consisting of two Waters Model 6000A pumps and a Model 660 solvent programmer), equipped with two UV detectors (Waters Model 440 for detection at $\lambda_1 = 254$ nm and $\lambda_2 = 280$ nm), a U6K injector and a linear potentiometric recorder with two channels, Servogor 220. The column used was a reversed phase micro-Bondapak C_{18} (30 cm × 3 · 9 mm), 10 µm particle size.

Chromatographic conditions

Linear gradient started at the injection point, from 70% (v/v) MeOH/H_2O to 100% MeOH for 20 min, flow-rate 1.5 mL/min. The column was regenerated by following the reverse gradient to the starting conditions for 5 min, and subsequent re-equilibration under these conditions for 10 min.

RESULTS AND DISCUSSION

In the transesterification of MeTMe (T : terephthaloyl group) with glycols (G : glycol group), the main oligomer series which appear as intermediates of final products, might be represented by :

I, n $Me(TG)_n H$ CH_3O and OH end groups

II, n $HG(TG)_n H$ two OH end groups

III, n – 1 $Me(TG)_{n-1} TMe$ two CH_3O end groups

Also, there could be present, among others, some by-products such as cyclic oligomers, [10] or oligomers with ether links in the glycol group,[12] but these would result more likely in the polycondensation step.[12,13]

If the process is a succession of consecutive and competitive reaction steps, the modification of the molar ratio 1,2-PG : MeTMe, and following the reaction in time, will assist identification, as it was also tried for urethane oligomers.

Figure 1 shows the chromatograms of the transesterification products at different molar rations 1,2-PG : MeTMe (2 : 1, 4 : 1, 6 : 1, 8 : 1, 20 : 1). At a molar ratio of 20 : 1, only the first member (HGTGH) of the oligomer series II, n is obtained, and could be used for identification. When the molar ratio is lowered, the number oligometric species II, n increases together with that of other compounds. Some of them are unidentified by-products and others are members of the oligomer series I, n and III, n – 1, which have been identified as it is shown below.

Figure 2 allows to follows the transesterification reaction in time. Gradient elution HPLC is known to be of limited use for quantitative analysis, because of some experimental difficulties,[14] but if the gradient procedure is strictly standardized, it may give an accurate analysis of oligomer mixtures, as Van der Maeden et al. pointed out. [10] To verify this, we made a statistical evaluation of the results of 7 consecutive injections of the final reaction mixture (molar ratio 2 : 1). The coefficients of variation were 0.2 – 0.5 % for the retention times and 1 – 5 % for the peak areas.

The fact that some peaks proportionally increase and then decrease in time (Fig. 2) was an indication of intermediary products (i.e. MeTGH). Some members of series I, n and III, n – 1 have been identified in this way.

In accordance with others, [2,3,9] the quantity could be made on the assumption of equal UV weight response, considering the same absorbance at a given wavelength per terephthaloyl equivalent. This was also proved by using two UV detectors in series and obtaining the same peak area percentage for both wavelengths ($\lambda_1 = 254$ nm and $\lambda_2 = 280$ nm).

The method is useful for the semiquantitative analysis of the individual oligomers, though some peaks remained unidentified. The time beha-

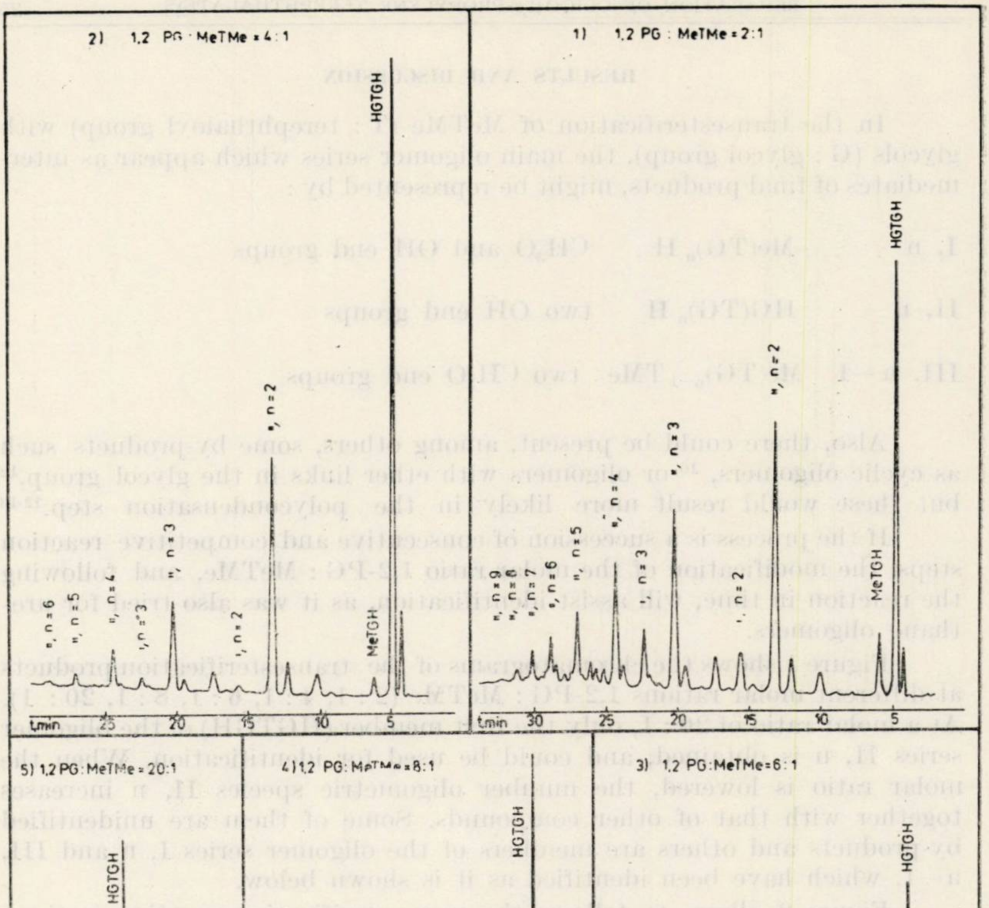

Fig. 1. — Chromatograms of the transesterification products, for different molar ratios 1,2-PG : MeTMe. 1) 2 :1, 2) 4 : 1, 3) 6 : 1, 4) 8 : 1, 5) 20 : 1 (for chromatographic conditions, see text)

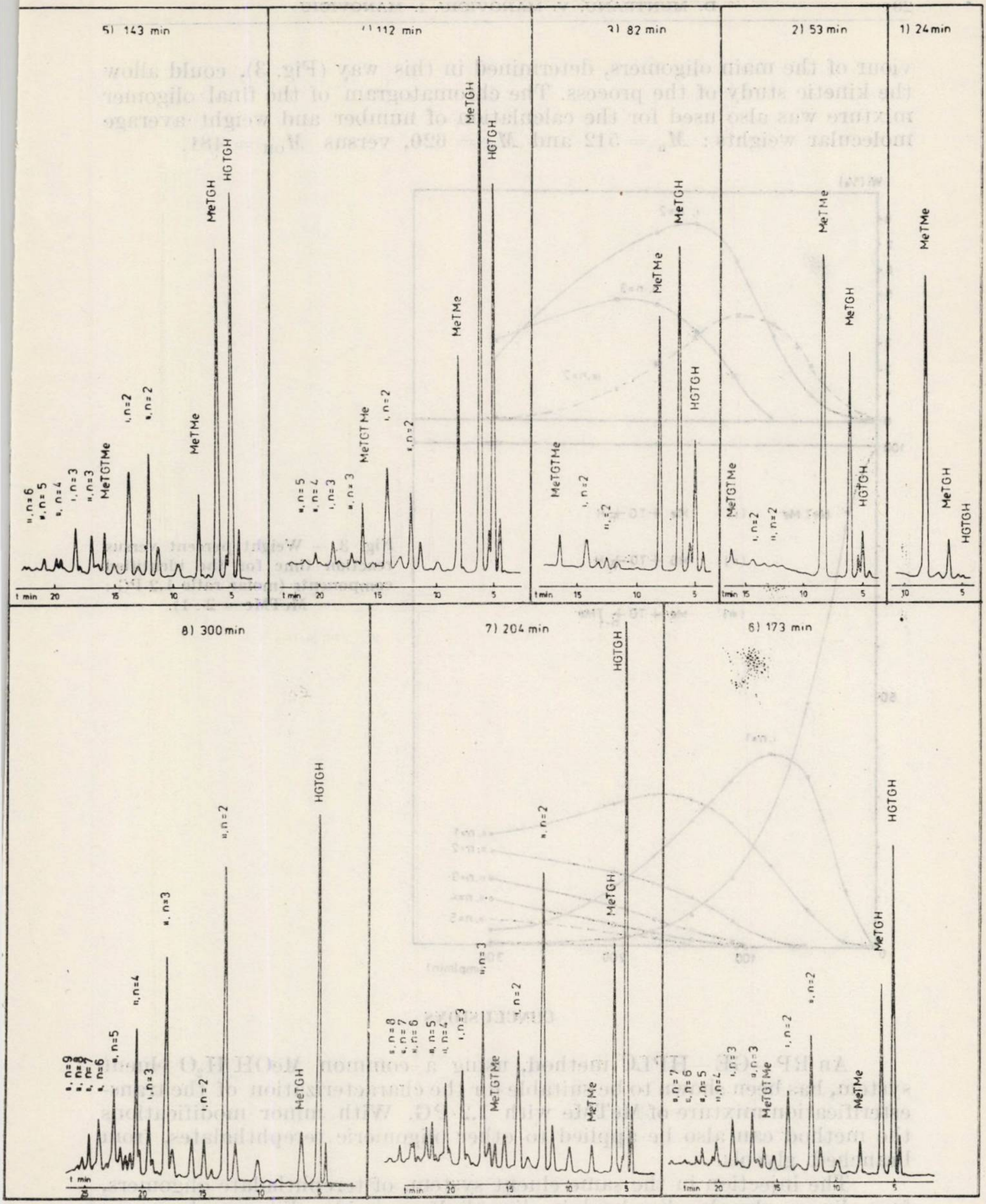

Fig. 2. — Chromatograms of samples from the MeTMe transesterification (molar ratio 1,2-PG : MeTMe = 2 : 1), at different reaction times. 1) 24 min, 2) 53 min, 3) 82 min, 4) 112 min, 5) 143 min, 6) 173 min, 7) 204 min, 8) 300 min (for chromatographic conditions, see text).

viour of the main oligomers, determined in this way (Fig. 3), could allow the kinetic study of the process. The chromatogram of the final oligomer mixture was also used for the calculation of number and weight average molecular weights : $M_n = 512$ and $M_w = 620$, versus $M_{OH} = 481$.

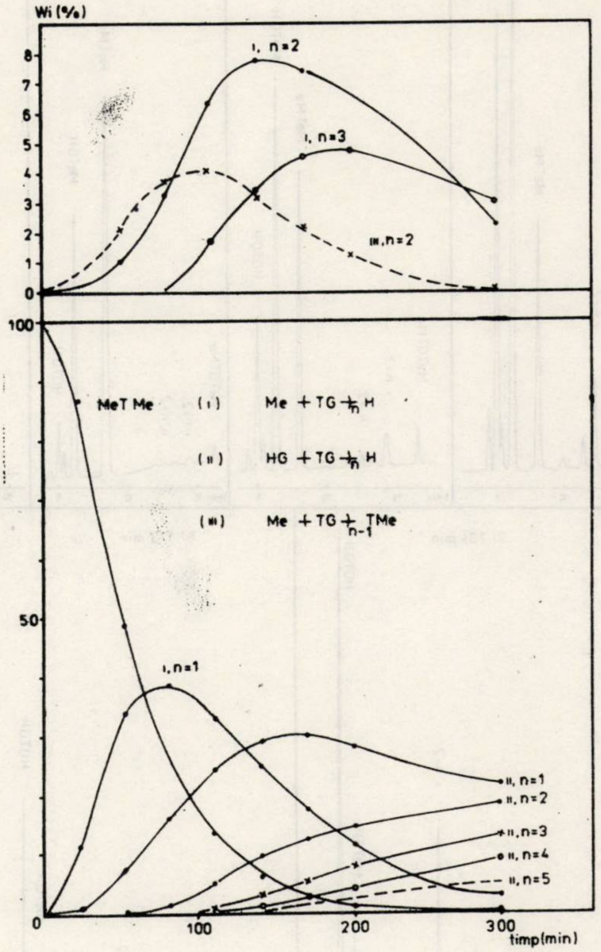

Fig. 3. — Weight percent versus reaction time for the identified components (molar ratio 1,2-PG : MeTMe = 2 : 1).

CONCLUSIONS

An RP—GE—HPLC method, using a common MeOH/H_2O eluent system, has been shown to be suitable for the characterization of the transesterification mixture of MeTMe with 1,2-PG. With minor modifications the method can also be applied to other oligomeric terephthalates, from branched glycols.

The injection in the same eluent system, of terephthalate oligomers, from linear glycols, dissolved in dimethylformamide, did not show any "sample solvent effect". The applicability and limitations to such oligomer separations are under study.

REFERENCES

[1] H. Zahn, and R. Krzikala, *Makromol. Chem.*, **23**, 31 (1957).

[2] S. Mori, S. Iwasaki, M. Furusaka and T. Takeuchi, *J. Chromatogr.*, **62**, 109 (1971).

[3] W. R. Hudgins, K. Thurer and T. Mariani, *J. Appl. Polym. Sci., Appl. Polym. Symp.*, **34**, 145 (1978).

[4] C. Gueri and J. Meybeck, *Bull. Soc. chim. France*, **1971**, 2163.

[5] D. R. Cooper, *J. Chromatogr.*, **80**, 24 (1973).

[6] M. Minarik, Z. Sir and J. Coupek, *Angew. Makromol. Chem.*, **64**, 147 (1977).

[7] S. Shiono, *J. Polym. Sci., Polym. Chem. Ed.*, **17**, 4123 (1979).

[8] L. H. Jr. Peebles, M. W. Huffmann and C.T. Ablett, *J. Polym. Sci.*, **A7**, 479 (1969).

[9] L. M. Zaborsky, *Analyt Chem.*, **49**, 1166 (1977).

[10] F. B. P. Van der Maeden, M. E. F. Biemond and P.C.G.M. Janssen, *J. Chromatogr.*, **149**, 539 (1978).

[11] E. L. Slagowski, R. C. Gebauer and G. J. Gaesser, *J. Appl. Polym. Sci.*, **21**, 2293 (1977).

[12] V. Hornof, *J. Macromol. Sci., Chem.*, A **15**, 503 (1981).

[13] D. R. Cooper and J. A. Semlyen, *Polymer*, **14**, 185 (1973).

[14] H. Knopp, R. Tenner and G. Truempler, "III Int. Polyurethane Symp.", Leipzig, 1981, p. 163

Revue Roumaine de Chimie, **30**, *1*, 31–36 (1985)

POTENTIOMETRIC GAS SENSOR FOR CARBON DIOXIDE

A. O. MOKHALLALATI, ANCA ISTUDOR, D. VÎRTOSU and C. LUCA

Polytechnic Institute, Faculty of Chemical Technology, Dept. of Analytical Chemistry,
Spl. Independenței No. 202, 79611 Bucharest, Romania

Received April 4, 1984

A Pd/PdO pH electrode, a quaternized polystyrene solid electrolyte and a polyphenyleneoxide gas permeable membrane were used to obtain a simple, flexible and reproducible carbon dioxide sensor. The probe design and construction is described in detail. It is also shown that the resulting sensor might be used for a wide range of measurements.

The first potentiometric sensor for carbon dioxide was described by Stow.[1] He utilized a rubber membrane to separate the sample from a thin film of water, the pH of which was measured with a glass electrode. Severinghaus [2] improved this sensor by replacing the rubber membrane with a Teflon one, adding sodium hydrogen carbonate to the water film and providing a water permeable "spacer" such as tissue paper to define the geometry of the electrolyte film between the gas permeable membrane and the glass electrode. Variations on this basic design are now used in all commercially available probes. More rencently it was proposed to replace the glass membrane pH electrode by other types of pH electrodes. Thus, Niedrach [3] suggested a Pd/PdO pH electrode while Mascini[4] a pH dependent electrode obtained by thermomoulding a mixture of powdered antimony and a thermoplastic polymer. Likewise, Ruzicka and Hansen[5] showed that it is possible to remove the gas permeable membrane in the so-called air-gap electrode. Besides, Van Kempen and Kreuzer [6] and later on Brand and co-workers [7] described a miniature P_{CO_2} sensor which is based on conductance measurement.

This paper reports on the use of a Pd/PdO pH-dependent electrode in a gas-sensing probe together with a quaternized polystyrene solid electrolyte and a polyphenyleneoxide gas permeable membrane.

EXPERIMENTAL

Reagents and standards

All chemicals used were of analytical grade. Carbon dioxide standards were prepared from potassium hydrogen carbonate, pH-adjustment being done by 0.1 M $NaHSO_4$ solution.

The gas permeable membrane was obtained from polyphenyleneoxide powder (ICECHIM — Bucharest).

Carbon dioxide sensor design

The carbon dioxide sensor uses a Pd/PdO pH-dependent electrode as electrochemically active region. It was elsewhere mentioned that the voltage of this electrode follows approximately the equation :

$$E = E^\circ - (2.3\,RT/F)\ \mathrm{pH} \tag{1}$$

where :

$$E^\circ = -(\Delta G^\circ \mathrm{H_2O} - \Delta G^\circ \mathrm{PdO})/2F \tag{2}$$

and the pH determining reaction is :

$$\mathrm{Pd + H_2O \rightarrow PdO + 2H^+ + 2e^-} \tag{3}$$

An Ag/AgCl electrode is the reference electrode (Fig. 1).

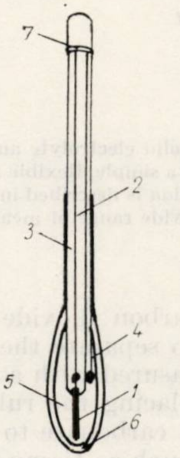

Fig. 1. — Design of a carbon dioxide sesnor. 1. Pd/PdO pH dependent electrode ; 2. Stainless steel electrical connector ; 3. polyester resin electrical insulation ; 4. Ag/AgCl reference electrode ; 5. solid polyelectrolyte ; 6. carbon dioxide permeable membrane ; 7. plastic body.

Both electrodes are successively surrounded by a solid electrolyte and a gas-permeable membrane layer. The first one consists of a quaternized polystyrene anion exchange resin, partially in chloride form and partially in hydrogen carbonate form. The second layer is a gas permeable ion-impermeable diffusion barrier made of polyphenylene oxide.

The membrane separates the interior of the electrode from the sample, so that the following equilibria will be established :

$$\mathrm{CO_2(sample) \rightleftharpoons CO_2(membrane) \rightleftharpoons CO_2(polyelectrolyte\ film)} \tag{4}$$

It was pointed out that the response of the electrode changes according to variations in the pH of the film, this pH being governed by the equilibria :

$$\mathrm{CO_2(g) + H_2O \rightleftharpoons H_2CO_3} \tag{5}$$

$$K = a_{\mathrm{H_2CO_3}}/P_{\mathrm{CO_2}} \tag{6}$$

$$\mathrm{H_2CO_3 \rightleftharpoons H^+ + HCO_3^-} \tag{7}$$

$$K_{a_1} = a_{\mathrm{H^+}} \cdot a_{\mathrm{HCO_3^-}}/a_{\mathrm{H_2CO_3}} \tag{8}$$

$$\mathrm{HCO_3^- \rightleftharpoons H^+ + CO_3^{2-}} \tag{9}$$

$$\mathrm{K_{a_2}} = a_{\mathrm{H^+}} \cdot a_{\mathrm{CO_3^{2-}}}/a_{\mathrm{HCO_3^-}} \tag{10}$$

As for the carbon dioxide level in the sample and polyelectrolyte film, it can be written :

$$\mathrm{CO_2(sample)} = K_D \cdot P_{\mathrm{CO_2}}\ \mathrm{(polyelectrolyte\ film)} \tag{11}$$

where K_D is a constant at a given temperature.

The relationship between the e.m.f. of the electrode and the carbon dioxide concentration in the film can be established by considering the next cell:

$$\mathrm{Ag/AgCl},\ m\mathrm{M\ NaHCO_3},\ c\mathrm{M\ NaCl},\ v\mathrm{M\ CO_2},\ \mathrm{Pd/PdO} \tag{12}$$

where mM is the concentration of sodium hydrogen carbonate, cM the concentration of sodium chloride and vM the concentration of carbon dioxide in the polyelectrolyte film.

The potential generated by this cell is:

$$E = E^0_{\mathrm{Pd/PdO}} + 2.303\ RT/F \lg a_{\mathrm{H^+}} - E^0_{\mathrm{Ag/AgCl}} + 2.303 RT/F \lg a_{\mathrm{Cl}} \tag{13}$$

The chloride concentration is constant and, as the system is at constant ionic strength, the chloride activity is also constant, so from equation (13) we obtain:

$$E = E' + 2.303\ RT/F \lg a_{\mathrm{H^+}} \tag{14}$$

Substituting successively for $a_{\mathrm{H^+}}$, $a_{\mathrm{H_2CO_3}}$ and $P_{\mathrm{CO_2}}$ the potential can be described by:

$$E = E' + 2.303\ RT/F \lg K_{a_1} \cdot K \cdot K_{\mathrm{D}} - 2.303\ RT/F \lg a_{\mathrm{HCO_3^-}} + K \lg |\mathrm{CO_2}|\ \text{sample} \tag{15}$$

The Ka_1 constant is so small that the changes in the hydrogen carbonate ion concentration in the film, which are due to the changes in the carbon dioxide equilibrum across the membrane are neglected, provided that the initial sodium hydrogen carbonate concentration is moderately high and at constant ionic strength the hydrogen carbonate ion activity can be regarded as a constant. So we can rewrite equation (15) as:

$$E = E'' + RT/F \lg |\mathrm{CO_2}|\ \text{sample} \tag{16}$$

Construction of Pd/PdO pH electrode

The Pd/PdO pH electrode was obtained[9] by coating one end of a palladium wire with 50% aqueous sodium hydroxide, exposing it to high temperature, e.g 800°C in air or oxygen. Before this oxidizing step, the wire has been cleaned by dipping it into aqua regia for about 20 seconds. This procedure led to a black palladium oxide coating on the portion of wire that has been covered with NaOH.

The wire was grit-blasted to a point about 0.5 cm above its lower end to remove excess oxide and to define a sharp boundary for the active end of the electrode. The bare portion of the wire was then electrically insulated by dipping all the bare wire area just meeting or slightly overlapping the oxide, in a polyester resin, dried at 100°C for 10 min. and cured at 140°C for 1 h.

Synthesis of quaternized polystyrene

The solid electrolyte must fulfil the following requirements:

- to provide at a constant concentration the Cl^- ions for the reference electrode.
- to contain HCO_3^- ions at a moderately high level so that, small changes in the hydrogen carbonate ion concentration. that are due to changes in the carbon dioxide equilibrium across the membrane be neglected:
- to provide good electrical conductivity;
- to swell slightly and to present a very low solubility.

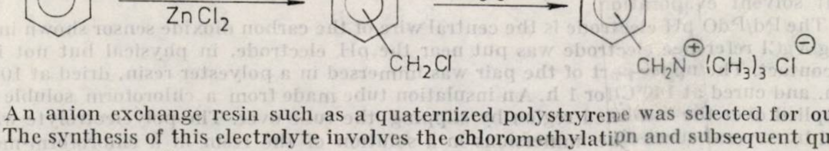

(17)

An anion exchange resin such as a quaternized polystryrene was selected for our purposes. The synthesis of this electrolyte involves the chloromethylation and subsequent quaternization of polystyrene [3].

During this process a secondary reaction of alkylation is encountered and it would result in connecting different polymer chains with methylene bridges. Thus a cross-linked structure is produced which would be expected to swell, but not to dissolve in the solvent.

There appears to be a competition between the chloromethyl ether and substituted benzyl chloride for the unsubstituted benzene rings.

The cross-linking reaction is therefore minimized by dilution with chloromethyl ether. The literature shows that if the polystyrene concentration decreases it is necessary to increase the catalyst/polystyrene ratio. The chloromethylation of polystyrene was carried out to obtain a chloromethylated resin with an optimal chlorine content of 3.8–4.2%. The adopted procedure required a polystyrene/chloromethyl ether ratio of 1/15 and a catalyst/polystyrene ratio of 1/3. Aluminium chloride was used as catalyst, because of its better solubility in chloromethyl ether. Polystyrene and catalyst were separately dissolved in portions of chloromethyl ether, then the solutions were mixed together, under moderate stirring.

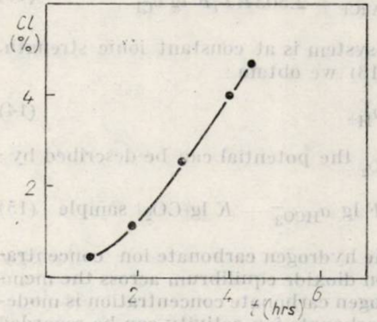

Fig. 2. — Increase in chlorine content during chloromethylation reaction.

As figure 2 points out, a polymer chlorine content of about 4% was obtained within four hours at 25°C.

At the end of this period, the chloromethylation was stopped by adding a 9:1 (v/v) water-dioxane mixture. The chloromethylated polystyrene was precipitated with methanol as a white fibrous precipitate.

To ensure complete removal of aluminium chloride the polymer was redissolved in dioxane and reprecipitated by pouring it into water.

The quaternization of chloromethylated polystyrene was accomplished by reacting it with triethylamine.

Complete conversion to a quaternary resin was achieved by treating the chloromethyl polystyrene dioxane solution with a 20–30% excess of a 20% triethylamine dioxane solution. The product had precipitated before the quaternization was completed. Water was then added to redissolve the polymer and the solution was left over night at room temperature to complete the amination. The final product was then recovered by adding the reaction mixture to petroleum ether under stirring.

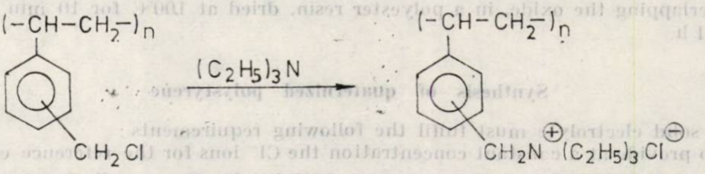

(18)

The resin was washed in petroleum ether to remove completely ethylamine. The material was broken up mechanically and vacuum dried at 50°C. An exhange capacity of 0.9 meq per gram was evaluated for the final product.

Construction of carbon dioxide sensor

The carbon dioxide sensor was formed by successive immersions steps of the pH electrode — reference electrode pair in organic solutions of materials already mentioned and subsequent solvent evaporation.

The Pd/PdO pH electrode is the central wire of the carbon dioxide sensor shown in Fig. 1. The Ag/AgCl reference electrode was put near the pH electrode, in physical but not in electrical contact. The upper part of the pair was immersed in a polyester resin, dried at 100°C for 10 min. and cured at 140°C for 1 h. An insulation tube made from a chloroform soluble plastic was applied over the insulated region by slipping the tube over. The polyelectrolyte was then applied by several successive immersions in a solution of the resin in a chloroform-methanol mixture. This structure was then heated in nitrogen at 50°C to eliminate solvents. The polyelectrolyte was converted to a partially bicarbonate form and partially chloride form, by immersing in an aqueous 0.1 M $KCl-0.1$ M $KHCO_3$ solution, rinsing in water and drying in flowing nitrogen (about 1 min.) at 50°C.

Finally, the carbon dioxide permeable ion — impermeable diffusion barrier was applied by successive dipping of the electrode in a polyphenylene oxide chloroform solution.

RESULTS AND DISCUSSION

All potential measurements were carried out in a 20 mL. seald and thermostated cell. To determine the electrode calibration and response time curves, a 10.0 mL solution of 0.1 M $NaHSO_4$ (pH 1.5) was placed in the thermostated cell and degassed with water saturated N_2 for 15 min. Thus the carbon dioxide was removed from the bisulfate solution.

The cell was sealed when the electrode with a rubber "O"-ring was placed in the cell. The electrode was allowed 15 min. to reach thermal echilibrium. The progressive additions of hydrogen carbonate stock solutions, maintained at the same temperature as the cell, were then added by injection through a rubber septum.

The electrode response times were determined by measuring the strip chart recorder trace from the point where the injection was made to the point where the electrode potential corresponds to 90 % of the actual CO_2 concentration.

It can be seen in Fig. 3 that the sensor described here has a useful response range over the P_{CO_2} values which are important in blood gases analysis, in carbon dioxide determination in power stations waters or in CO_2, HCO_3^- and CO_3^{2-} analysis in natural waters.

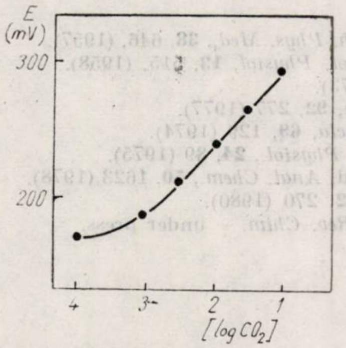

Fig. 3. — Potential response of carbon dioxide sensor.

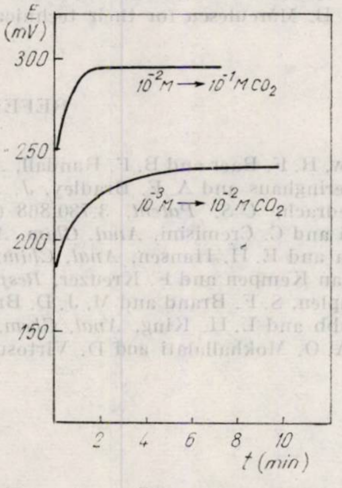

Fig. 4. — Dynamic response curves of carbon dioxide sensor.

The calibration curve has a slope of 53 mv per decade concentration change of carbon dioxide which is comparable to that obtained for the commercial probes.

The dynamic response at two different concentration levels is shown in Fig. 4. The response time is short (2—4 min.) particularly at high carbon levels. In Fig. 5 the response time of the sensor to step changes in carbon dioxide concentrations was evaluated by adding 1.0 mL hydrogen bicarbonate stook solution to 10 mL 0.1 M $NaHSO_4$ solution as to obtain a 0.001 M carbon dioxide concentration in the thermostated cell. After 2 min., 1 mL of 1M NaOH solution was added to neutralize the acid and convert carbon doxide to carbonate. Thus the carbon dioxide concentration was reduced to near zero. The experimental data are in accordance with theoretical models for this type of sensor.

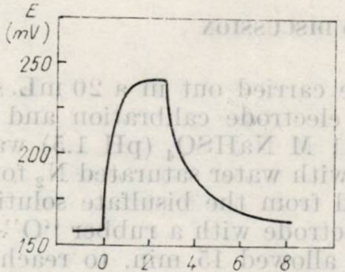

Fig. 5. — Response of carbon dioxide sensor to step changes in carbon dioxide concentration. To 10 mL of 0.1 M $NaHSO_4$ was added, at $t = 0$ min., 1.0 mL bicarbonate stock solution to give a $[CO_2] = 10^{-2}$M and at $t=2$ min., 1 mL of 1.0 M NaOH solution.

The characteristics of this probe have not been fully examined but the performances already presented and the simplicity in design made it attractive for the *in vivo* measurements, as well as for manufacturing micro biosensors.

ACKNOWLEDGEMENT. We thank Doina Caravaniez, C. Tărăbășanu and B. Mărculescu for their technical assistance.

REFERENCES

[1] R. W. Stow, R. F. Baer and B. F. Randall, *Arch. Phys. Med.*, **38**, 646, (1957).
[2] J. W. Severinghaus and A. F. Bradley, *J, Appl. Physiol*, **13**, 515, (1958).
[3] L. W. Niedrach, *U.S. Patent*, 3.730.868 (1973).
[4] M. Mascini and C. Cremisini, *Anal. Chim. Acta*, **92**, 277 (1977).
[5] J. Ruzicka and E. H. Hansen, *Anal. Chim. Acta*, **69**, 129 (1974).
[6] L. H. J. Van Kempen and F. Kreuzer, *Respir. Physiol.*, **24**, 89 (1975).
[7] H. A. Himplen, S. F. Brand and M. J. D. Brand, *Anal. Chem.*, **50**, 1623 (1978).
[8] W. T. Grubb and L. H. King, *Anal. Chem.*, **52**, 270 (1980).
[9] C. Luca, A. O. Mokhallalati and D. Vîrtosu, *Rev. Chim.* — under press.

Revue Roumaine de Chimie, **30**, *1*, 37–40 (1985)

SYNTHESIS OF SOME BIOLOGICALLY ACTIVE N′-PICOLINOYL-4-(SUBSTITUTED AZO)-ALKYL/ARYL PYRAZOLES

D. R. GUPTA and R. K. ARORA

Department of Chemistry, University of Roorkee
Roorkee – 247667, India

Received December 7, 1983

Syntheses of two new series of N′-picolinoyl-3,5-diphenyl-4-(substituted phenyl azo)-pyrazoles and N′-picolinoyl-3-methyl-5-phenyl-4-(substituted phenyl-azo)-pyrazoles are reported. The compounds have been synthesized through the reaction of picolinic acid hydrazide with the corresponding 2-substituted azo derivatives of 1,3-diphenylpropane-1,3-dione and 1-phenylbutane-1,3-dione respectively and their subsequent cyclisation. The characterization and structural assignments are made on the basis of elemental analysis and spectroscopic criteria (IR, NMR and MS).

INTRODUCTION

Five membered heterocyclic compounds especially pyrazoles have recently engaged the attention of medicinal chemists as they are widely employed as potential drugs.[1–6] Organic molecules containing azo, sulphanilamido and picolinoyl groupings exhibit anticancerous,[7–9] antibacterial,[10] anticonvulsant[11] and antitubercular[12] activities. The above moieties when attached to a pyrazole nucleus may produce chemotherapic agents with enhanced activity. With this aim in view, the synthesis of a few alkyl and aryl derivatives of pyrazoles having these substituents, was performed.

The present communication describes the synthesis of N′-picolinoyl-3,5-diphenyl-4-(substituted azo)-pyrazoles(I) and N′-picolinoyl-3-methyl-5-phenyl-4-(substituted azo)-pyrazoles (II) shown in scheme 1.

EXPERIMENTAL

All the reagents used were of A.R. grade. Picolinic acid hydrazide was prepared from picolinic acid (K. L.). All the melting points are uncorrected. The purity and homogeneity of these compounds were checked by TLC. Infrared spectra were recorded on a Beckman IR-20 spectrophotometer. ^{1}H–NMR spectra were recorded on a Joel FX-100 spectrophotometer.

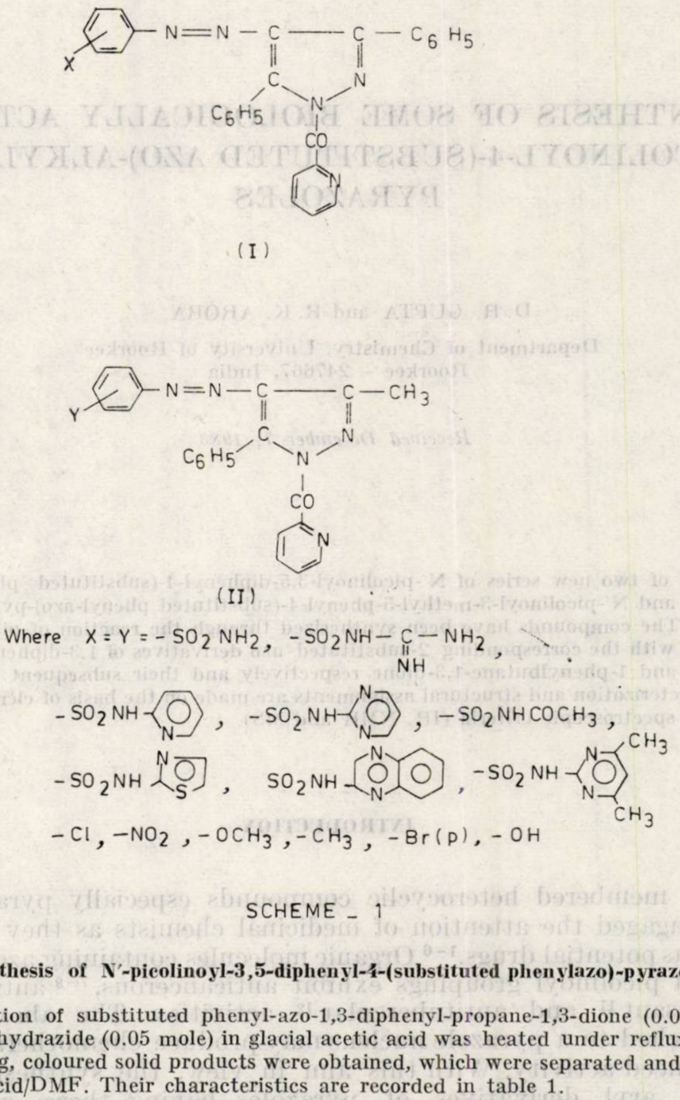
X
N=N
C
C
C6 H5
C
N
C6H5
N
CO
N
(I)
Y
N=N
C
C
CH3
C
N
C6 H5
N
CO
N
(II)
Where X = Y = - SO2 NH2 , - SO2 NH - C - NH2 ,
NH
- SO2 NH
- SO2 NH
N
N
- SO2 NH COCH3 ,
- SO2 NH
N
S
SO2 NH
N
N
- SO2 NH
N
N
CH3
CH3
- Cl , - NO2 , - OCH3 , - CH3 , - Br (p) , - OH

SCHEME _ 1

Synthesis of N′-picolinoyl-3,5-diphenyl-4-(substituted phenylazo)-pyrazoles

A solution of substituted phenyl-azo-1,3-diphenyl-propane-1,3-dione (0.05 mole) and picolinic acid hydrazide (0.05 mole) in glacial acetic acid was heated under reflux for about 4 hrs. On cooling, coloured solid products were obtained, which were separated and recrystallised from acetic acid/DMF. Their characteristics are recorded in table 1.

IR(KBr) : 1580 (N=N), 1600(C=N), 1740(C=O) amide and 780 (aromatic ring) cm^{-1}.

^{1}H−NMR(CDCl$_3$) : δ 7.15−8.25 (m, 18H, Ar-*H*) ppm.

MS : M$^+$ 508 (compound No. 1, Table 1).

Synthesis of N′-picolinoyl-3-methyl-5-phenyl-4-(substituted phenylazo)-pyrazoles

A solution of substituted phenyl-azo-1-phenylbutane-1,3-dione (0.05 mole) and picolinic acid hydrazide (0.05 mole) in glacial acetic acid was heated under reflux for about 4 hrs. The coloured solid products obtained on cooling, were recrystallised from acetic acid/DMF. Their characteristics are recorded in table 2.

IR(KBr) : 1580 (N=N), 1630 (C=O) amide, 1480 (C=N) cm^{-1} .

^{1}H−NMR spectrum of N′-picolinoyl-3-methyl-5-phenyl-4-(2-methylphenyl-azo)-pyrazole

$CDCl_3$: δ 2.4 (s, 3H, CH_3-Ar) ; 2.65 (s, 3H, CH_3-C_3) ; 7.0—7.50 (m, 11H, Ar H) ; 7.80—7.95 (m, 2H, *ortho* to N of pyridine ring) ppm.
MS : M^+ 446 (Compound No. 1, Table 1).

Table 1

Physical data of N′-picolinoyl-3,5-diphenyl-4-(substituted phenylazo)-pyrazoles

X =	M.P. °C	Colour *	Yield %	Analytical data Nitrogen % Found	Analytical data Nitrogen % Calcd
2-Sulphanilamido benzene	232	Y	72	16.58	16.53
N′-2-guanyl sulphanilamido-benzene	221	PeY	78	20.38	20.36
N′-2-pyridyl sulphanilamido-benzene	244	LY	74	16.71	16.75
N′-2-pyrimidyl sulphanilamido-benzene	178	Bn	75	19.16	19.11
N′-2-acetyl sulphanilamido-benzene	197	Y	80	15.24	15.27
N′-2-thiazolyl sulphanilamido-benzene	237	DY	67	16.60	16.58
N′-2-quinoxalyl sulphanilamido-benzene	188	PeY	72	17.58	17.61
N′-2-(4,6-dimethyl) pyrimidyl sulphanilamido-benzene	228	Y	78	18.24	18.24
Phenyl	186	Y	74	16.36	16.31
2-Chlorophenyl	165	DY	65	15.14	15.11
3-Chlorophenyl	169	DY	65	15.10	15.11
4-Chlorophenyl	189	PeY	65	15.16	15.11
2-Nitrophenyl	184	DY	74	16.65	17.72
3-Nitrophenyl	213	DY	72	17.64	17.72
4-Nitrophenyl	227	DY	72	17.68	17.72
2-Methoxyphenyl	179	PeY	65	15.28	15.25
3-Methoxyphenyl	201	Y	68	15.26	15.25
4-Methoxyphenyl	188	DY	70	15.29	15.25
2-Methyl phenyl	177	Bn	70	15.82	15.80
3-Methyl phenyl	180	DY	72	15.78	15.80
4-Methyl phenyl	209	OY	66	15.82	15.80
4-Bromo phenyl	162	PeY	64	13.79	13.77
2-Hydroxy phenyl	197	PeY	80	15.80	15.73
3-Hydroxy phenyl	204	Y	72	15.78	15.73
4-Hydroxy phenyl	168	Y	68	15.80	15.73

*Bn = Brown, D = Deep, L = Lemon, O = Orange. Pe = Pale, Y = yellow

Table 2

Physical data of N′-picolinoyl-3-methyl-5-phenyl-4- (substituted phenylazo)-pyrazoles

Y	M. P. °C	Colour*	Yield %	Analytical data Nitrogen % Found	Analytical data Nitrogen % Calcd
2-Sulphanilamido benzene	205	DY	70	18.87	18.83
N′-2-guanyl sulphanilamido-benzene	256	PeY	74	22.90	22.95
N′-2-pyridyl sulphanilamido-benzene	221	Y	76	18.67	18.73

Table 2 (continued)

Y	M. P. C°	Colour*	Yield %	Analytical data Nitrogen % Found	Calcd
N -2-pyrimidyl sulphanilamidobenzene	270	DY	80	21.32	21.37
N′-2-acetyl sulphanilamidobenzene	250	PeY	74	17.24	17.21
N′-2-thiazolyl sulphanilamidobenzene	238	Bn	75	18.51	18.52
N′-2-quinoxalyl sulphanilamidobenzene	182	Y	68	19.44	19.51
N′-2-(4,6-dimethyl)pyrimidyl sulphanil-amido benzene	236	Y	70	20.26	20.28
Phenyl	160	Bn	72	19.10	19.07
2-Chlorophenyl	239	LY	64	17.40	17.45
3-Chlorophenyl	184	Y	80	17.41	17.45
4-Chlorophenyl	167	PeY	78	17.42	17.45
2-Nitrophenyl	220	DY	65	22.34	20.38
3-Nitrophenyl	188	DY	70	20.40	20.38
4-Nitrophenyl	242	Y	72	20.34	20.38
2-Methoxyphenyl	176	PeY	71	17.61	17.63
3-Methoxyphenyl	169	Y	71	17.62	17.63
4-Methoxyphenyl	198	Bn	70	17.68	17.63
2-Methylphenyl	274	Y	75	18.34	18.37
3-Methylphenyl	237	PeY	80	18.32	18.37
4-Methylphenyl	255	DY	68	18.40	18.37
4-Bromophenyl	264	Bn	64	15.71	15.69
2-Hydroxyphenyl	195	Y	70	18.25	18.27
3-Hydroxyphenyl	177	PeY	70	18.24	18.27
4-Hydroxyphenyl	183	DY	72	18.27	18.27

*Bn = Brown, D = Deep, L = Lemon, O = Orange, Pe = Pale, Y = yellow

ACKNOWLEDGEMENTS. The authors wish to express their cordial thanks to Dr. B. B. Agarwal and Dr. A. K. Sharma for recording ^1H-NMR and MS. One of us (R.K.A) is grateful to U.G.C., New Delhi, India for award of a Junior Research Fellowship.

REFERENCES

[1] E. C. Herrmann and J. Grablicks, *Cancer Chemotherapy Reports*, **14**, 85 (1961).

[2] E. L. Anderson, J. E. Casey, L. C. Green, J. J. Lafferty and H. E. Reife, *J. Med. Chem.*, **1**, 259 (1964).

[3] J. B. Wright, W. E. Dulin and J. H. Markillie, *J. Med. Chem.*, **7**, 102 (1964).

[4] W. Wilson and N. Bottiglieri, *Cancer Chemotherapy*, **72**, 137 (1962).

[5] C. W. Noell and C. C. Cheng, *J. Med. Chem.*, **12**, 545 (1969).

[6] H. G. Garg and R. A. Sharma, *J. Pharm. Sci.*, **59**, 350 (1970).

[7] E.J. Modest, H.N. Schlein and G. E. Foley, *J. Pharm. Pharmacol.*, **9**, 68 (1957).

[8] R. E. Harmen, F. E. Dutton and H. D. Waren, *J. Med. Chem.*, **11**, 627 (1968).

[9] H. G. Garg and C. Prakash, *J. Med. Chem.*, **14**, 175 (1971).

[10] R. D. Desai, G. S. Saharia and H. S. Sodi, *J. Indian Chem. Soc.*, **46**, 115 (1969).

[11] E. H. Jenney and C. C. Pfeiffer, *J. Pharmacol. Exptl. Therap.*, **122**, 110–23 (1958).

[12] H. H. Fox and J. T. Gibbs, *J. Org. Chem.*, **17**, 1653–60 (1952).

Revue Roumaine de Chimie, **30**, *1*, 41–48 (1985)

MASS SPECTRA OF DIASTEREOMERIC SUBSTITUTED SECONDARY VALER- AND BUTYRAMIDES

ABOEL-MAGED A. ABDEL-WAHAB, MOHAMED S. K. YOUSSEF and GUNTER HELMCHEN*

Chemistry Department, Faculty of Science, Assiut University Assiut, Egypt
* Institute of Organic Chemistry, Stuttgart University, W. Germany

Received October 25, 1983

Mass spectra of six substituted secondary valer- and butyramides (1, 3, 5, 7, 9, 11) and their corresponding diastereomers (2, 4, 6, 8, 10, 12) were obtained and interpreted. Simple N-alkyl cleavage or double α and C–N cleavages with hydrogen rearrangements are the two main routes of fragmentation. However, the presence of methyl group on the secondary carbon prefers the N-alkyl cleavage. A clear-cut distinction between the diastereomers can be made by comparing the abundance of certain peaks in the spectra.

Mass spectra of a wide variety of aliphatic amides were studied by many authors.[1–4] However, the differentiation between diastereomeric secondary amides by fragmentation under the effect of electron beam has not been approached. Owing to the growing use of diastereoisomeric amides in resolution, determination of optical purity and determination of absolute configuration of amines and acids, [5] the interpretation of mass spectra of diastereomeric N-substituted amides is thus very necessary. In the present work the mass spectra of six γ or δ hydroxy N-substituted valer-and butyramides and their corresponding diastereomers were interpreted. These include

N-(α′-phenyl)ethyl-α-benzyl-δ-hyroxyvaleramides (1,2),
N-(α′-phenyl)propyl-β-phenyl-γ-hydroxybutyramides (3,4),
N-(α′-methyl)heptyl-β-phenyl-γ-hydroxybutyramides (5,6),
N-(α′-phenyl)ethyl-β-phenylbutyramides (7,8), N-(α′-phenyl-β′-hydroxy) ethyl-β-phenylbutyramides (9, 10) and N-(α-phenyl-β-hydroxy) ethyl-α-phenylbutyramides (11, 12).[6]

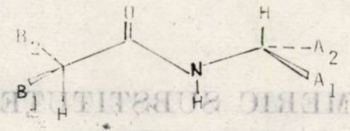

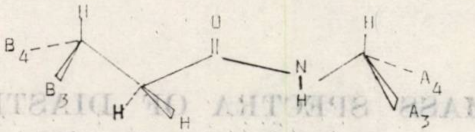

	A_1	A_2	B_1	B_2
1(D°)	CH_3	Ph	CH_2PHh	$-(CH_2)_3OH$
2(D_u)	CH_3	Ph	$-(CH_2)_3OH$	CH_2Ph
11(D°)	CH_2OH	Ph	Ph	CH_2CH_3
12(D_u)	CH_2OH	Ph	CH_2C_3	Ph
	A_3	A_4	B_3	B_4
3(D°)	CH_2CH_3	Ph	Ph	CH_2OH
4(D_u)	Ph	CH_2CH_3	Ph	CH_2OH
5(D°)	CH_3	C_6H_{13}	Ph	CH_2OH
6(D_u)	C_6H_{13}	CH_3	Ph	CH_2OH
7(D°)	CH_3	Ph	Ph	CH_3
8(D_u)	CH_3	Ph	CH_3	Ph
9(D°)	Ph	CH_2OH	CH_3	Ph
10(D_u)	Ph	CH_2OH	Ph	CH_3

The most important ions in the mass spectra are given in Table 1. The most abundant ion in the spectra of 1 and 2, at m/z 105, indicates that simple cleavage or N-alkyl bond (Scheme 1—A) is easier than cleavage of other bonds due to the stability of the formed radical. The low abundance of the ion m/z 206 may be ascribed to its further fragmentation to ions of m/z 189, m/z 188, m/z 163 and m/z 91. Also, the ion m/z 91 could be originated directly through Scheme 1—G. A simple α-cleavage to the carbonyl (Scheme 1—B) was confirmed by the presence of peaks at m/z 163, m/z 146, m/z 145, m/z 148 and m/z 120. While the double α and C—N cleavages with hydrogen rearrangement[1] (Scheme 1—C) is responsible for ions at m/z 106, m/z 190 and ions therefrom at m/z 172, m/z 162 and M/z 161, a simple C—N cleavage with hydrogen rearrangement (Scheme 1—D) originates ions at m/z 121 and m/z 190. Interestingly, McLafferty rearrangement was accomplished in three different pathways (Scheme 1—H, 1—I and 1—J) resulting in the formation of ions at m/z 207 and m/z 104; at m/z 219 and m/z 92 and at m/z 253 and m/z 58, respectively. Furthermore, their behaviours as alcohols,[7-9] although less predominant, was demonstrated by the appearance of ions at m/z 266 and m/z 252 *via* a simple β-and γ-cleavages (Scheme 1—E and 1—F, respectively) and ion m/z 293 by loss of water.

The most stable ion in the fragmentation of 3 and 4, at m/z 106, was originated from a double α and C—N cleavages with hydrogen rearrangement (Scheme 2—G). This was confirmed by the appearance of ions at m/z 268 and m/z 162. The ion at m/z 119 derived from simple N-alkyl cleavage of 3 (or 4) has low abundance (16.6%, Scheme 2—A) compared with that obtained from the simple cleavage of 1 (or 2) at m/z 105 (100%, Scheme 1—A). This is because the loss of ethyl group (M_3-29, m/z 268) is easier than the loss of methyl group[10] (M_1-15, m/z 252). The ion at m/z 105 in the fragmentation pattern of 3 and 3 may be originated from the loss of ethyl radical followed by fragmentation (Scheme

Table 1

Partial mass spectra of 1—12

m/z	% Abundance													
	1	2	3	4		5		6	7	8	9	10	11	12
41	4.3	32.9	4.6	4.4	10.0	—*	9.5	—*	7.8	11.8	3.1	4.0	7.0	10.2
42	5.4	20.5	—	1.1	2.5	—	2.6	—	8.7	9.2	—	1.7	—	—
43	1.9	36.0	1.3	2.5	12.9	—	12.6	—	2.2	4.9	1.1	1.7	2.8	1.1
44	7.6	5.7	2.8	8.5	100.0	33.1	100.0	75.9	9.5	7.6	3.9	11.7	5.9	—
56	1.1	36.0	1.0	1.3	1.7	—	1.9	—	—	1.9	—	—	—	—
57	—	29.7	—	—	2.9	2.7	13.5	7.1	—	—	—	—	—	—
58	—	1.4	1.5	1.4	7.3	3.7	8.7	9.0	—	—	—	—	—	—
77	16.6	11.8	11.8	13.5	5.1	—	5.2	—	29.4	31.0	13.6	—	—	13.8
79	17.9	18.5	12.5	14.6	2.9	—	2.6	—	10.2	29.6	16.3	15.5	7.9	10.7
91	55.9	54.5	48.0	41.7	10.3	—	11.7	2.3	31.9	30.1	12.4	18.0	77.0	85.6
92	6.0	6.3	4.6	4.0	1.2	—	1.4	—	3.3	3.2	1.4	1.7	6.1	7.2
103	13.3	13.2	13.0	10.7	8.9	—	9.3	—	19.6	20.4	10.9	11.8	14.0	15.6
104	18.5	20.3	21.3	21.1	11.8	3.1	13.8	8.6	23.6	24.0	9.2	9.0	9.0	—
105	100.0	100.0	7.0	7.7	7.7	—	7.5	2.9	100.0	100.0	39.1	35.8	3.4	4.4
106	43.5	45.4	100.0	100.0	2.1	—	2.2	—	55.5	52.7	100.0	100 0	100.0	100.0
113	—	—	—	—	—	2.1	1.8	2.6	—	—	—	—	—	—
117	18.4	18.8	11.4	10.9	7.0	—	8.1	3.3	—	4.4	2.3	3.1	4.7	5.8
118	4.0	5.0	17.5	15.1	4.3	20.9	20.3	31.5	7.2	7.4	5.9	6.9	6.3	7.9
119	2.5	2.7	15.6	12.1	2.3	2.0	3.3	4.6	50.9	49.4	5.8	7.2	28.1	31.7
120	48.1	50.8	4.0	4.7	1.5	—	1.4	1.7	57.9	55.2	6.2	10.0	13.9	17.6
121	9.0	17.3	2.9	2.3	2.4	—	2.8	—	7.5	8.0	1.8	2.4	12.6	14.1
145	14.4	13.3	2.6	2.8	4.2	2.8	7.1	5.6	1.6	1.8	—	—	—	—
146	4.9	5.2	—	1.1	—	—	1.7	—	2.4	1.7	—	—	3.4	3.2
147	1.6	2.5	—	—	—	—	—	—	4.6	—	1.2	1.2	—	—
148	56.0	58.7	1.9	3.8	—	—	—	—	5.6	5.1	8.3	7.8	—	—
161	4.5	5.5	2.0	2.5	1.1	2.2	1.4	4.5	—	—	—	—	—	—
162	11.7	10.9	2.7	5.0	3.5	8.6	6.5	10.3	70.5	71.0	—	—	—	—
163	3.6	3.4	—	1.1	1.2	—	1.4	2.1	21.5	22.6	—	—	—	—
177	—	—	3.4	3.7	4.1	9.6	8.0	14.3	—	—	—	—	—	—
188	3.1	2.9	—	—	3.0	8.7	5.5	9.9	—	—	—	—	—	—
189	2.3	2.9	—	—	1.7	5.8	3.6	8.2	—	—	—	—	—	—
190	3.0	2.6	—	—	1.5	5.6	3.7	7.4	—	—	—	—	—	—
202	4.6	4.4	—	—	—	1.9	1.1	2.7	—	—	—	—	—	—
206	2.9	2.2	—	—	1.7	4.4	2.4	4.7	—	—	—	—	—	—
207	1.9	2.2	1.3	1.6	1.1	4.4	2.3	5.5	—	—	—	—	—	—
220	11.5	12.3	—	—	—	—	—	—	—	—	—	—	—	—
252	67.1	65.3	—	—	—	—	—	—	3.9	3.7	27.5	23.4	51.3	52.1
253	17.2	17.3	—	—	—	—	—	—	—	—	17.6	12.9	24.3	25.6
255	—	—	—	—	—	—	—	—	—	—	—	—	1.1	1.0
261	—	—	—	—	19.9	100.0	36.9	100.0	—	—	—	—	—	—
265	—	—	—	—	—	—	—	—	—	—	4.6	3.3	2.1	2.4
266	10.5	9.5	—	—	—	—	—	—	—	—	1.2	1.2	0.6	—
267	2.0	1.8	11.1	11.5	—	—	—	—	84.8	92.3	—	—	—	—
268	—	—	12.8	10.6	—	—	—	—	—	—	—	—	—	—
273	—	—	—	—	7.3	44.9	16.0	46.7	—	—	—	—	—	—
283	—	—	—	—	—	—	—	—	—	—	4.2	2.9	0.1	0.2
291	—	—	—	—	1.3	6.4	1.8	4.9	—	—	—	—	—	—
293	3.4	2.5	—	—	—	—	—	—	—	—	—	—	—	—
297	—	—	10.3	6.4	—	—	—	—	—	—	—	—	—	—
311	57.3	58.3	—	—	—	—	—	—	—	—	—	—	—	—

* These spectra were obtained at 20 eV and 0.1 mA.

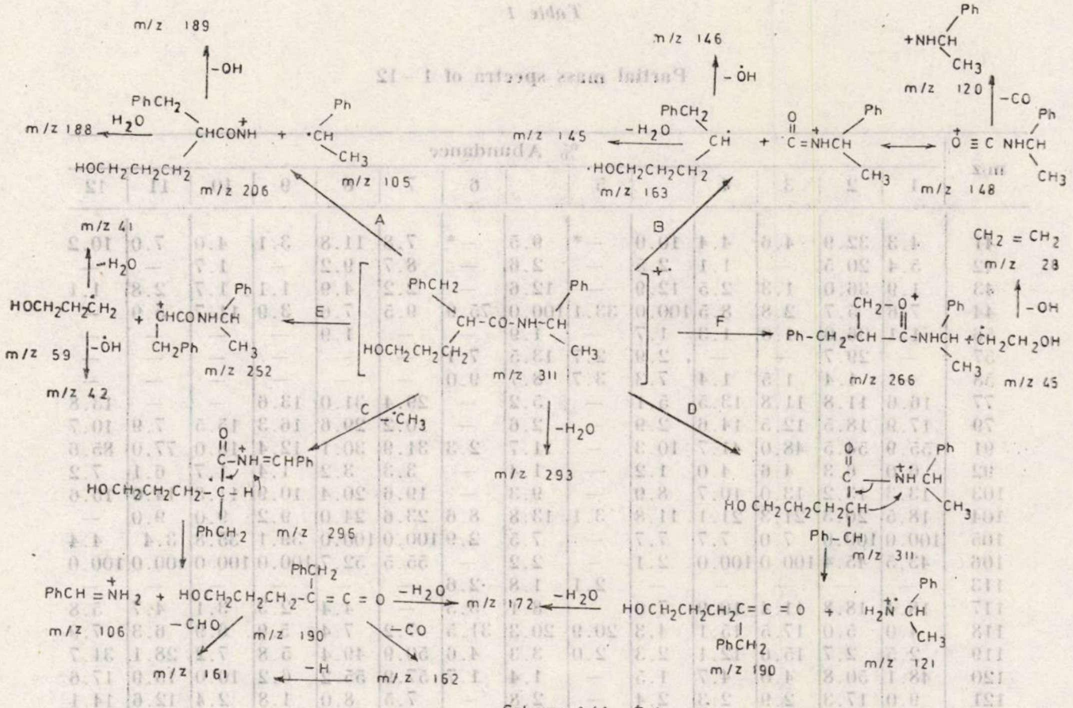
m/z 189
-OH
m/z 188
H2O
PhCH2
CHCONH
HOCH2CH2CH2
m/z 206
Ph
CH
CH3
m/z 105
A
m/z 146
-ȮH
m/z 145
-H2O
PhCH2
CH
HOCH2CH2CH2
m/z 163
B
C=NHCH
Ph
CH3
O≡C NHCH
m/z 148
+NHCH
Ph
CH3
m/z 120
-CO
m/z 41
-H2O
HOCH2CH2CH2
CHCONHCH
CH2Ph
CH3
m/z 252
m/z 59
-ȮH
m/z 42
E
PhCH2
CH-CO-NH-CH
HOCH2CH2CH2
Ph
CH3
m/z 311
F
CH2-O
Ph-CH2-CH — C-NHCH + ĊH2CH2OH
m/z 266
m/z 45
CH2 = CH2
m/z 28
-OH
C
-ĊH3
C-NH=CHPh
HOCH2CH2CH2-C-H
PhCH2
m/z 296
-H2O
m/z 293
D
HOCH2CH2CH2CH
NH CH
Ph-CH
m/z 311
PhCH=NH2
m/z 106
HOCH2CH2CH2-C=C=O
PhCH2
m/z 190
-H2O
m/z 172
-H2O
HOCH2CH2CH2C=C=O
PhCH2
m/z 190
H2N CH
Ph
CH3
m/z 121
-CHO
m/z 161
-CO
m/z 162
-H

Scheme 1 (A– F)

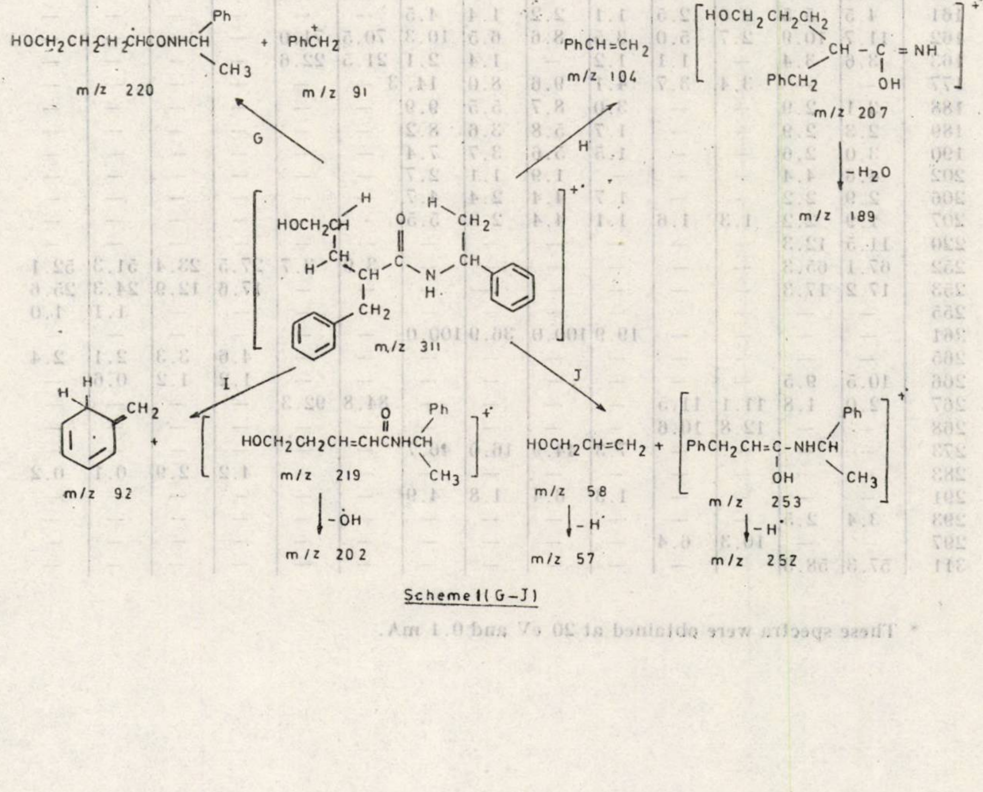
HOCH2CH2CH2CHCONHCH
Ph
CH3
m/z 220
PhCH2
m/z 91
G
PhCH=CH2
m/z 104
H
HOCH2CH2CH2
CH - C = NH
PhCH2
OH
m/z 207
-H2O
m/z 189
HOCH2CH
H
CH
CH
C
N
H
CH2
CH
CH2
m/z 311
I
J
m/z 92
HOCH2CH2CH=CHCNHCH
Ph
CH3
m/z 219
-ȮH
m/z 202
HOCH2CH=CH2
m/z 58
-H˙
m/z 57
PhCH2CH=C-NHCH
OH
Ph
CH3
m/z 253
-H˙
m/z 252

Scheme 1 (G–J)

2—G). Also, McLafferty type rearrangement has been accomplished in four different pathways (Scheme 2—C, 2—D, 2—E and 2—F).

The most stable ion, m/z 44, in the mass spectra of 5 and 6 at 70 eV was also originated from double α and C—N cleavages with hydrogen rearrangement (Scheme 3—C). It was noticed that the loss of hexyl group is very much easier than the loss of methyl group,[10,11] otherwise a peak at m/z 101 should be obtained via double α and C—N cleavages with hydrogen rearrangement. This is also clear from the low abundance of ion m/z 113 (Scheme 3—A). The presence of n-hexyl group is also responsible for the formation of ions m/z 58 and m/z 162 through double β and C—N cleavages with hydrogen rearrangement [2] (Scheme 3—D). Noteworthy, fragmentation at 20 eV resulted in the formation of a base ion at m/z 261 via McLafferty rearrangement (Scheme 3—E).

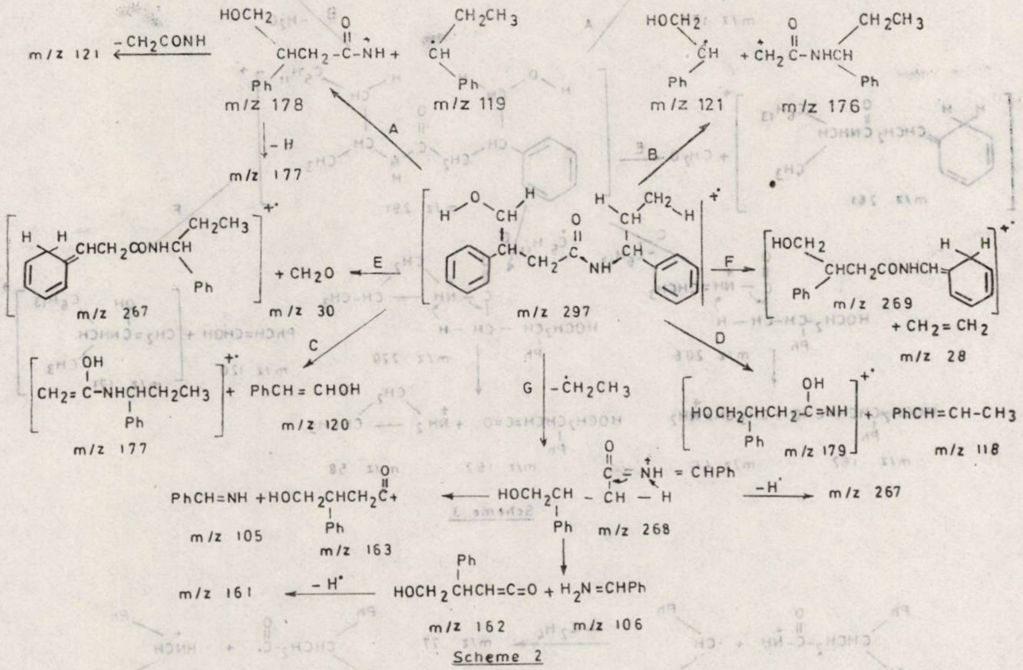
m/z 121
- CH2CONH
m/z 178
m/z 119
m/z 121
m/z 176
A
B
- H
m/z 177
m/z 267
+ CH2O
m/z 30
E
m/z 297
F
m/z 269
+ CH2= CH2
m/z 28
C
D
m/z 177
PhCH = CHOH
m/z 120
G
- ĊH2CH3
HOCH2CHCH2C=NH
m/z 179
PhCH=CH-CH3
m/z 118
PhCH=NH
m/z 105
HOCH2CHCH2C+
m/z 163
m/z 268
- H˙
m/z 267
m/z 161
- H˙
HOCH2CHCH=C=O + H2N=CHPh
m/z 162
m/z 106

Scheme 2

Compounds 7 and 8 revealed a base ion, as with 1 and 2, at m/z 105 (Scheme 4—A) and a less abundant ion at m/z 120 and m/z (Scheme 4—B). The two possible pathways of McLafferty rearrangement (Scheme 4—E and 4—F) led to the formation of ions m/z 104 and m/z 163. The m/z 106 ion is also observed in high abundance as a result of double α and C—N cleavages with hydrogen rearrangement.

As expected, the most abundant ion in the spectra of 9, 10, 11 and 12 (m/z 106) was originated from the double α and C—N cleavages with hydrogen rearrangement. The low abundance of the ion m/z 121 is not unexpected due to the loss of CH_2OH radical (Scheme 5—C and 6—C). In addition, McLafferty rearrangement took place through routes D, E and F in Schemes 5 and 6.

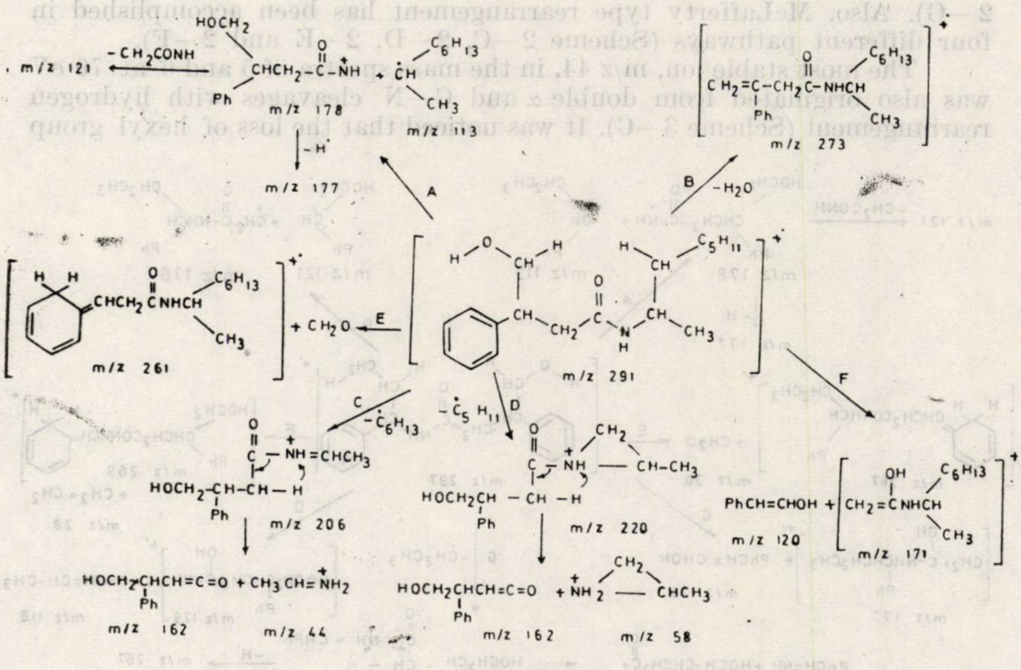
m/z 121
- CH2CONH
HOCH2
m/z 178
m/z 113
-H
m/z 177
m/z 273
A
B
-H2O
E
+ CH2O
m/z 261
m/z 291
C
-C6H13
D
-C5H11
F
m/z 206
m/z 220
PhCH=CHOH
m/z 120
m/z 171
m/z 162
m/z 44
m/z 162
m/z 58

Scheme 3

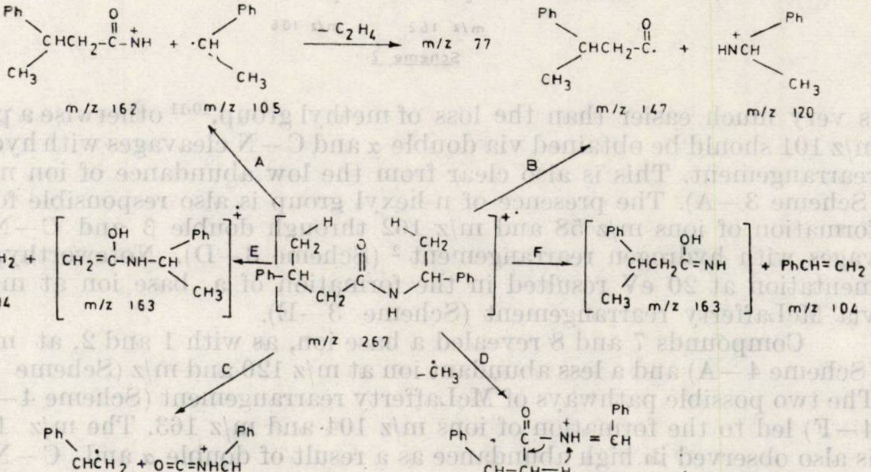
m/z 162
m/z 105
-C2H4
m/z 77
m/z 147
m/z 120
A
B
PhCH=CH2
m/z 104
m/z 163
E
m/z 267
F
m/z 163
m/z 104
D
CH3
m/z 119
m/z 148
m/z 252
m/z 106
m/z 146
-CO
m/z 118

Scheme 4

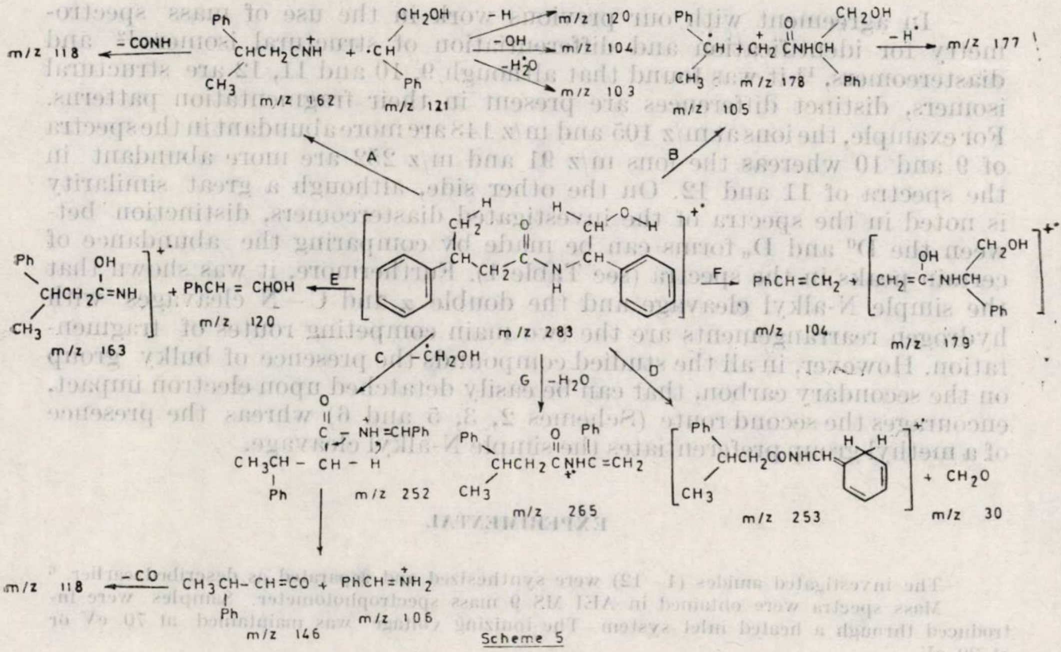
m/z 283
A
B
C
D
E
F
G
m/z 118
m/z 162
m/z 121
m/z 120
m/z 104
m/z 103
m/z 105
m/z 178
m/z 177
m/z 163
m/z 120
m/z 179
m/z 252
m/z 265
m/z 253
m/z 30
m/z 146
m/z 106

Scheme 5

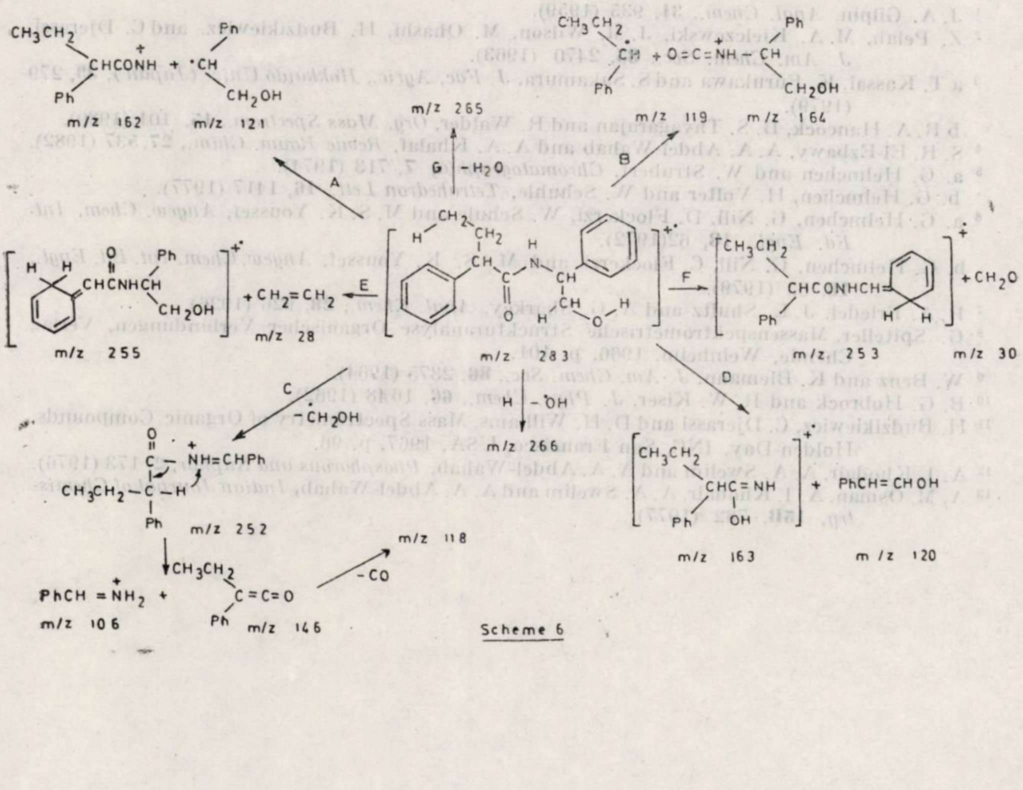
m/z 283
A
B
C
D
E
F
G
m/z 162
m/z 121
m/z 265
m/z 119
m/z 164
m/z 255
m/z 28
m/z 253
m/z 30
m/z 266
m/z 252
m/z 163
m/z 120
m/z 118
m/z 106
m/z 146

Scheme 6

In agreement with our previous work in the use of mass spectrometry for identification and differentiation of structural isomers [12] and diastereomers, [13] it was found that although 9, 10 and 11, 12 are structural isomers, distinct differences are present in their fragmentation patterns. For example, the ions at m/z 105 and m/z 148 are more abundant in the spectra of 9 and 10 whereas the ions m/z 91 and m/z 252 are more abundant in the spectra of 11 and 12. On the other side, although a great similarity is noted in the spectra of the investigated diastereomers, distinction between the D^0 and D_u forms can be made by comparing the abundance of certain peaks in the spectra (see Table 1). Furthermore, it was shown that the simple N-alkyl cleavage and the double α and C—N cleavages with hydrogen rearrangements are the two main competing routes of fragmentation. However, in all the studied compounds the presence of bulky group on the secondary carbon, that can be easily detatched upon electron impact, encourages the second route (Schemes 2, 3, 5 and 6) whreas the presence of a methyl group preferentiates the simple N-alkyl cleavage.

EXPERIMENTAL

The investigated amides (1—12) were synthesized and separated as described earlier. [6] Mass spectra were obtained in AEI MS 9 mass spectrophotometer. Samples were introduced through a heated inlet system. The ionizing voltage was maintained at 70 eV or at 20 eV.

REFERENCES

[1] J. A. Gilpin, *Anal. Chem.*, **31**, 935 (1959).

[2] Z. Pelah, M. A. Kielczewski, J. M. Wilson, M. Ohashi, H. Budzikiewicz, and C. Djerassi, *J. Am. Chem. Soc.*, **85**, 2470 (1963).

[3] a T. Kassai, K. Furukawa and S. Sakamura, *J. Fac. Agric., Hokkaido Univ. (Japan)*, **39**, 279 (1979).
b R. A. Hancock, B. S. Thyagarajan and R. Walder, *Org. Mass Spectrom.*, **15**, 101 (1980).

[4] S. R. El-Ezbawy, A. A. Abdel-Wahab and A. A. Khalaf, *Revue Roum. Chim.*, **27**, 537 (1982).

[5] a. G. Helmchen and W. Strubert, *Chromatographia*, **7**, 713 (1974).
b. G. Helmchen, H. Volter and W. Schuhle, *Tetrahedron Lett.*, **16**, 1417 (1977).

[6] a. G. Helmchen, G. Nill, D. Flockerzi, W. Schule and M. S. K. Youssef, *Angew. Chem, Int. Ed. Engl.*, **18**, 62(1972).
b. G. Helmchen, G. Nill, C. Flockerzi and M. S. K. Youssef, *Angew. Chem. Int. Ed. Engl.*, **18**, 63 (1979).

[7] R. A. Friedel, J. L. Shultz and A. G. Sharkey, *Anal. Chem.*, **28**, 926 (1926).

[8] G. Spiteller, Massenspektrometrische Strucktauranalyse Organischer Verbindungen, Verlag Chemie, Weinheim, 1966, p. 101.

[9] W. Benz and K. Biemann, *J. Am. Chem. Soc.*, **86**, 2375 (1964).

[10] B. G. Hobrock and R. W. Kiser, *J. Phys. Chem.*, **66**, 1648 (1962).

[11] H. Budzikiewicz, C. Djerassi and D. H. Williams, Mass Spectrometry of Organic Compounds, Holden-Day, INC, San Francisco, USA, 1967, p. 96.

[12] A. I. Khodair, A. A. Swelim and A. A. Abdel-Wahab, *Phosphorous and Suphur*, **2**, 173 (1976).

[13] A. M. Osman, A. I. Khodair, A. A. Swelim and A. A. Abdel-Wahab, *Indian Journal of Chemistry*, **15B**, 782 (1977).

Revue Roumaine de Chimie, **30**, *1*, 49—53 (1985)

THERMODYNAMICS OF COMPLEX FORMATION : ZINC-ε-CAPROLACTAM SYSTEM

ASHOK KUMAR *, B.K.PURI * and A.L.J. RAO**

* Department of Chemistry, Indian Institute of Technology, Delhi, New Delhi — 110 016, India
** Department of Chemistry, Punjabi University, Patiala

Received December 7, 1983

Polarographic techniques have been used to investigate the complexing reactions in aqueous solution between ε-caprolactam and zinc ion. The co-ordination number and stability constants of the complexes have been determined polarographically. The method of Ringbom and Erikson using cadmium as indicator ion was used on the basis of reversible and irreversible character of electrode reactions at dropping mercury electrode. The values of the kinetic parameters, αn and $k^0_{\mathrm{f,h}}$ have been calculated. The effect of temperature has been discussed in terms of the variations in the values of the kinetic parameters. The values of thermodynamic parameters ΔG, ΔH and ΔS have also been calculated.

INTRODUCTION

In continuation of our earlier polarographic studies[1] on the complexation reaction of Cd(II) with ε-caprolactam, we report in this paper the results of studies on the behaviour of zinc-ε-caprolactam at the d.m.e. (Table 1). The stability constants, rates of electrode reactions and thermodynamic functions of the complexation reactions have been evaluated. Zinc showed irreversible behaviour and therefore, Ringbom and Eriksson[2-3]

Table 1

$E_{1/2}$ Data for the cadmium-ε-caprolactam system in the absence and presence of 0.05 M Zn(II)

[Cp1] M	$-E_{3/4}$ vs SCE Zn(II) absent	$\Delta E_{1/2}$	$-E_{1/2}$ vs. SCE Zn(II) present	$\Delta E_{1/2}$
0.0	0.615	0.000	0.615	0.000
0.1	0.617	0.002	0.617	0.002
0.2	0.621	0.006	0.620	0.005
0.3	0.625	0.010	0.622	0.007
0.4	0.632	0.017	0.627	0.012
0.5	0.636	0.021	0.630	0.015
0.6	0.642	0.027	0.635	0.020
0.7	0.657	0.042	0.640	0.025
0.8	0.671	0.056	0.647	0.032

ion indicator method was applied to calculate the stability constants using cadmium as indicator ion. Saraiya and Sundaram[4] have reported the stability constants of thiosulphate complexes by the method of Rosotti and Rosotti.[5] Owing to the weakly basic nature of ε-caprolactam, strong complexation is not expected but the polarographic behaviour of Zn(II) in the absence and presence of ε-caprolactam was sufficiently distinct to indicate complex formation and to allow quantitative assessment of stability constants.

EXPERIMENTAL

Solutions

All the chemicals used were of analytical grade and their stock solutions were prepared in conductivity water. Ionic strength was maintained constant with potassium nitrate. The pH's of all the experimental solutions were maintained at 6.2 ± 0.05. Triton X-100 (Sigma) was used as maximum suppressor.

Apparatus and Procedure

Polarograms in all instances were recorded at various temperatures with a manual Adopt polarograph (Toshniwal CLO 2) in conjunction with polyflex galvanometer (Toshniwal PL 50) and pH's of the solutions were measured with an Elico pH meter. A saturated calomel electrode was used as the reference electrode and was connected to the polarographic cell through a potassium chloride-agar bridge. Oxygen was expelled by passing a stream of purified nitrogen into the test solution. The d.m.e. had the typical characteristics $m = 2.90$ mg/s and $t = 2.9$ s in open circuit. The number of electrons (n) involved in the reduction process was determined by millicoulmetric method of De Vries and Kroon[6].

Methods of calculation

The stability constants were investigated by the indicator ion method of Ringbom and Eriksson, cadmium being the indicator ion in all cases. This technique was involved in the determination of the half-wave potentials of the indicator ion over a wide range of ligand concentration both in the absence and the presence of the metal ion whose stability constants were required. Half-wave potential shifts of the indicator ion were smaller in the presence of added metal ion than in its absence and served for the direct determination of the free ligand concentration. The ligand number, $\bar{n}$ of the metal-ligand system was given, at each of the free ligand concentration by

$$\bar{n} = \frac{C_x - [X]}{C_m}$$

where C_x = Total ligand concentration

$[X]$ = Free ligand concentration

C_m = Concentration of the metal. Then stability constants followed from the plot of the formation curve ($\bar{n}$ vs. log [X]), which was integrated graphically to give the Fronaeou[7] relation.

$$\mathrm{Fo}[X] = \exp \int_0^x \bar{n}\ \mathrm{dlog}\ [X] \qquad (2)$$

RESULTS AND DISCUSSION

A single well-defined diffusion-controlled wave appeared in each solution containing 0.5 mM of Ni(II) with varying amounts of ligand. The values of slope from conventional log plots showed the reduction to be irreversible. Hence, the method of Ringbom and Erikson was applied to determine the stepwise stability constants.

The shifts in half-wave potential of 5×10^{-4} M Cd^{+2} in the presence of 0.1 M KNO_3 as a function of ε-caprolactam concentration were reported previously.[1] The procedure was repeated in the presence of 0.05 mM Ni^{+2}. The $E_{1/2}$ data obtained are plotted in Fig. 1 as a function of the total ε-caprolactam concentration. The information obtained from these curves made possible the determination of the formation curve (Fig. 2), indicating the maximum co-ordination number 3 for Zn(II) (Table 2). The graphical integration of this curve was carried out by weighing areas under the

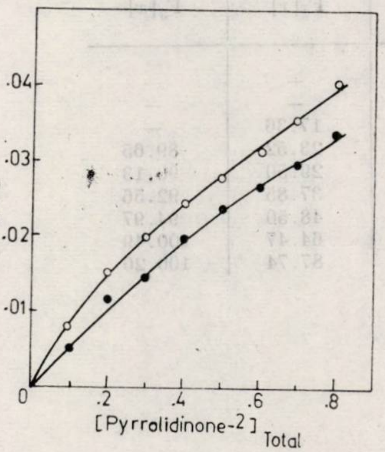

Fig. 1. — Plots of $E_{1/2}$ for the zinc-ε-caprolactam system in the absence (○) and presence (●) of 0.05 M Zn (II).

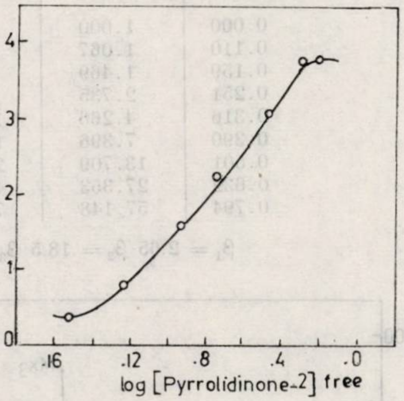

Fig. 2. — Formation curve of the zinc (II) -ε-caprolactam system.

Table 2

Formation curve data of Zn(II)-ε-caprolactam complex

[Cpl] M	$[Cpl]_{free}$ M	$-\log[Cpl]_{free}$ M	$\bar{n}$
0.05	0.05	1.300	0.0
0.1	0.09	1.046	0.2
0.2	0.15	0.824	1.0
0.3	0.225	0.648	1.5
0.4	0.300	0.523	2.0
0.5	0.380	0.420	2.4
0.6	0.460	0.319	2.8
0.7	0.545	0.233	3.1
0.8	0.645	0.181	3.1

curve bounded by values of log [cpl] corresponding to a range of $[\mathrm{cpl}]_{\mathrm{free}}$ values. Values of $F_o[\mathrm{cpl}]$ were calculated from equation (2). Using the fact that the residual integral is given by

$$\lim_{[x] \to 0} F_0[\mathrm{cpl}] = \frac{1}{1 - \bar{n}} \tag{3}$$

the calculation of stability constants then followed in the normal way, by graphical extrapolation. The data are being summarized in table 3. The distributions of the various species were presented in Fig. 3 as a function of ligand concentration.

Table 3

Derived functions for zinc-ε-caprolactam system

$[\mathrm{Cpl}]_{\mathrm{free}}$	$\mathrm{Fo}(x)]$	$F_1[x]$	$F_2[x]$	$F_3[x]$
0.000	1.000	—	—	—
0.110	1.067	—	—	—
0.159	1.469	2.959	17.36	—
0.251	2.735	6.908	23.52	89.65
0.316	4.266	10.328	29.50	90.13
0.390	7.396	16.067	37.85	92.56
0.501	13.709	25.357	48.50	94.97
0.632	27.353	41.720	64.47	100.49
0.794	57.148	70.690	87.74	100.20

$\beta_1 = 2.65$ $\beta_2 = 18.5$ $\beta_3 = 90.0$

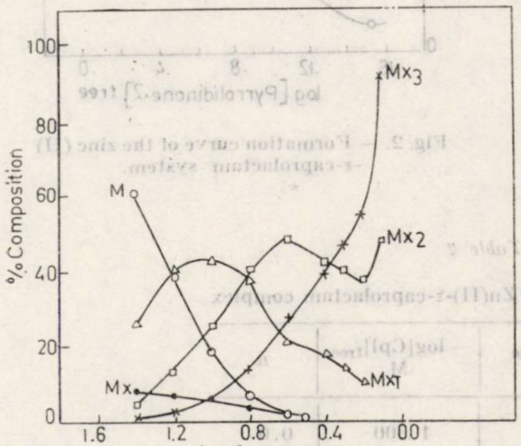

Fig. 3. — Distribution diagram for zinc (II) -ε-caprolactam system.

The kinetic parameters were calculated by Koutechy's theoretical treatment as extended by Meites and Israel.[8] The value of αn was obtained by equating the slope of $E_{\mathrm{d.e}}$ vs. $\log \frac{i}{i_d - i}$ plot to $\frac{-0.0542}{\alpha n}$, and the intercept of the same plot giving $E_{1/2}$ was used to calculate $k^0_{f,h}$. The values of $k^0_{f,h}$ increase with temperature (Table 4). The shift in half-wave potential towards more positive values shows the easier reduction of the complex at higher temperatures (Table 4) and is in accordance with the irreversible nature of the processes.

Table 4

Data for rate constants and thermodynamic functions

Temp. °C	i_d (μa)	$-E_{1/3}$ vs SCE	Slope (mV)	k° (cm/sec)	ΔH kcal/mole	ΔG kcal/mole	ΔS cal/mole
30	10.15	1.050	83	1.18×10^{-12}	1.70	20.85	−63.02
40	14.99	0.922	75	9.10×10^{-12}		20.28	−59.36
50	16.42	0.838	70	3.25×10^{-11}		20.13	−57.06

The enthalpy of activation (ΔH) for the electrode reaction has been calculated by equating the slope of $\log k^0_{f,h}$ vs. $\frac{1}{T}$ plot to $\left(\frac{-\Delta H}{2.3031\ R}\right)$.

The free energy of activation (ΔG) could be determined from the following equation

$$k^0_{f,h} = \frac{kT}{h} \exp\left(\frac{-\Delta G}{RT}\right)$$

where k = Boltzman constant, h = Plank's constant, $\varnothing = 2.0 \times 10^{-8}$ cm and other terms have their usual meaning. The activation entropy (ΔS) was calculated from the relation.

$$\Delta S = \frac{\Delta H - \Delta G}{T}$$

Entropy change is negative as must be the case with common ligands.

REFERENCES

[1] B. K. Puri and Ashok Kumar, *Microchem. J.* (In press).

[2] A. Ringbom, and L. Eriksson, *Acta Chem. Scand.* **7**, 1105 (1953).

[3] L. Eriksson, *Acta Chem. Scand.*, **7**, 1146 (1953).

[4] S. C. Saraiya and A. K. Sundaram, *Proc. Indian Academy of Science*, **70**, 120 (1969).

[5] F. J. C. Rosotti and N. S. Rosotti, *Acta Chem. Scand*, **9**, 1166 (1955).

[6] T. de Vries, J. L. Kroon, *J. Am. Chem. Soc.*, **75**, 2484 (1953).

[7] S. Fronaeous, *Acta Chem. Scand.* **4**, 72 (1950).

[8] L. Meites, "Polarographic Technique" Interscience, New York 1965.

Revue Roumaine de Chimie, **30**, *1*, 55–59 (1985)

NEW PYRAZOLONE COMPOUNDS OF BIS-METHYLAMINOANTIPYRYL-PROPANE AND BIS-METHYLAMINO-ANTIPYRYL-BUTANE

IULIA HAVLIK [a], T. SIMONESCU [b] and I. HAVLIK [a]
a Chemical Research Center, Timişoara, Blvd Mihai Viteazul No. 24, Romania
b University of Timişoara, Blvd Vasile Pârvan No. 4, Timişoara, Romania

Received September 21, 1983

A number of six new complex compounds of bis-methylaminoantipyrylpropane and five of bis-metylaminoantipyryl-butane have been synthesized and characterized by elemental analysis, electronic and vibrational spectra, as well as by magnetic measurements.

The present paper continues the sequence of the works which deal with the complex compounds of the ligands N,N′-bisantipyryl-piperazine,[1,2] bis-methylaminoantipyryl-ethane [3] and N,N′-bis-antipyrylmethyl-piperazine.[2,4,5]

The two ligands used in this paper are bis-methylaminoantipyryl-propane (L(1)) and bis-methylaminoantipyryl-butane (L(2)), with formula :

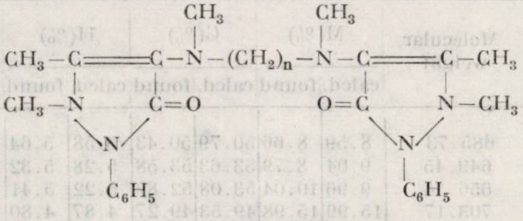

n = 3 for L(1)

n = 4 for L(2)

These ligands are not described in the literature, their synthesis was described in a patent.[6]

The aim of their preparation was to verify their capacity of complexation with different 3d transitional metals like cobalt, nickel, zinc and with cadmium.

EXPERIMENTAL

For the synthesis of the complexes metal salts like : $CoAc_2 \cdot 4H_2O$, $CoCl_2 \cdot 2H_2O$, $NiAc_2 \cdot 4H_2O$, $NiSO_4 \cdot 7H_2O$, $CdCl_2 \cdot 2H_2O$ and water solution of $ZnCl_2$ were used, all of analytical purity.

The syntheses were carried out mainly according to the same general procedure, with small differences, which will be given.

Further an example of preparation is described.

Preparation of $CoL(1)(SCN)_2 \cdot 2H_2O$: $5 \cdot 10^{-4}$M(0.1142 g) $CoCl_2 \cdot 2H_2O$ dissolved in 5 mL ethanol, 10^{-3}M(0.0761 g) NH_4SCN, dissolved in 5 mL ethanol were added dropwise. The solution became turbid, the mixture was stirred continously at 25°C during 30 min, then was concentrated on water bath to 25 mL and cooled stepwise to 25°C, when fine crystals of blue-greenish colour began to appear. The solution was kept at +5°C for 24 hours, after which it was filtered, washed with water and ethanol and dried at 70°C.

The $NiL(1)(SCN)_2$, $CoL(2)(SCN)_2$, $NiL(2)(SCN)_2$ and $ZnL(2)(SCN)_2$ compounds were prepared by the same procedure. As the $ZnL(1)(SCN)_2$, $CdL(1)(SCN)_2$ and $CdL(2)(SCN)_2$ compounds are formed immediately, concentration on water bath is no more needed.

The $CdL(1)Cl_2 \cdot CdCl_2$ and $CdL(2)Cl_2$ compounds respectively are formed also instantaneously in ethanolic, medium, the reactives being in these cases $CdCl_2 \cdot 2H_2O$ and L(1) and L(2) respectively.

The $CdL(1)J_2 \cdot 0.5CdJ_2$ compound forms instantaneously, but in order to avoid the hardly soluble CdJ_2 formation, one has to proceed in another way, namely, at the ligand solution KJ will be added, and then $CdCl_2 \cdot 2H_2O$, all reactives being previously dissolved in ethanol p.a

The compounds were separated from solution with yields between 28.5% (for $CdL(2)(SCN)_2$) and 87% (for $CoL(1)(SCN)_2 \cdot 2H_2O$), depending on their solubility.

The solubilities of the compounds are different, some are insoluble in water and sparingly soluble in organic solvents like ethanol, acetone, chloroform, ethoxy ethane, namely $CoL(1)(SCN)_2 \cdot 2H_2O$, $NiL(1)(SCN)_2$ and $ZnL(1)(SCN)_2$, others are soluble in water and insoluble in organic solvents : $CdL(1)(SCN)_2$, $CdL(1)Cl_2 \cdot CdCl_2$ and $CdL(1)J_2 : 0.5CdJ_2$, and those of the ligands L(2) are insoluble in water, ethanol and ethoxy ethane and very sparingly soluble in chloroform and acetone.

The compounds were analysed determining the metal, halogen, C and the H content. The results of the elemental analysis and of melting point determinations for the compounds are given in tables 1 and 2.

Table 1

Analytical data of complex compounds

Compound	Molecular weight	M(%)		C(%)		H(%)		SCN, Cl, J(%)		Melting point (°C)
		calcd.	found	calcd.	found	calcd.	found	calcd.	found	
$CoL(1)(SCN)_2 \cdot 2H_2O$	685.73	8.59	8.66	50.79	50.43	5.58	5.64	16.94	17.35	173–176
$NiL(1)(SCN)_2$	649.45	9.04	8.79	53.63	53.58	5.28	5.32	17.89	18.03	263–266
$ZnL(1)(SCN)_2$	656.14	9.96	10.04	53.08	52.89	5.22	5.41	17.70	17.52	330*
$CdL(1)(SCN)_2$	703.17	15.99	15.98	49.53	49.27	4.87	4.80	16.52	16.07	215–216
$CdL(1)Cl_2 \cdot CdCl_2$	841.24	26.72	26.76	38.55	38.27	4.07	4.21	16.86	16.81	265–266
$CdL(1)J_2 \cdot O \cdot 5CdJ_2$	1023.93	16.47	16.52	31.66	31.42	3.35	3.20	18.59	18.23	199–201

* with decomposition

The electronic spectra of the compounds were recorded on a Unicam SP 800 spectrophotometer, in quartz cells, using solutions of the samples in absolute ethanol.

The vibrational spectrum was registered on a Specord IR 75 spectrophotometer, in the range of 400–4000 cm^{-1}, using the KBr mulls technique.

The magnetic measurements were made on a Gouy balance, at 21°C, using $Hg[Co(SCN)_4]$ for calibration.

Table 2

Analytical data of complex compounds

Compound	Molecular weight	M(%)		C(%)		H(%)		SCN, Cl(%)		Melting point (°C)
		calcd.	found	calcd.	found	calcd.	found	calcd.	found	
$CoL(2)(SCN)_2$	663.72	8.88	9.01	54.28	54.36	5.47	5.32	17.50	17.41	143 –145
$NiL(2)(SCN)_2$	663.47	8.85	8.71	54.30	54.05	5.47	5.29	17.51	17.32	263 –265*
$ZnL(2)(SCN)_2$	670.16	9.76	9.63	53.76	53.62	5.41	5.27	17.33	17.20	<360*
$CdL(2)Cl_2$	671.94	16.73	16.69	50.05	49.94	5.40	5.30	10.55	10.42	330*
$CdL(2)(SCN)_2 \cdot Cd(SCN)_2$	945.77	23.77	23.52	40.64	40.41	3.84	3.67	24.65	24.42	238.5 –240.5

* with decomposition

RESULTS AND DISCUSSIONS

The data of elemental analyses show that the compounds are pure, free of uncomplexed ligands.

λ and ε values are given in table 3.

Table 3

Electronic spectral data

Compound	λ(nm)	ε
L(1)	280	9,403.44
$CoL(1)(SCN)_2 \cdot 2H_2O$	275	10,311.10
$NiL(1)(SCN)_2$	272.5	17,430.50
$ZnL(1)(SCN)_2$	277.5	10,550.99
$CdL(1)(SCN)_2$	263	18,931.50
$CdL(1)Cl_2 \cdot CdCl_2$	265	13,397.54
$CdL(1)J_2 \cdot O \cdot 5CdJ_2$	266	15,033.43
L(2)	273	18,323.21
$CoL(2)(SCN)_2$	273.5	19,438.82
$NiL(2)(SCN)_2$	272.5	21,712.50
$ZnL(2)(SCN)_2$	269	20,968.43
$CdL(2)Cl_2$	271	20,325.12
$CdL(2)(SCN)_2 \cdot Cd(SCN)_2$	270.5	18,973.40

The spectra of the ligands contain a very intense maximum at 280 nm, respectively 273 nm, which remains unmodified after complexation, but grows in intensity. The high values for the molar extinction coefficient suggest a charge transfer mechanism.

Table 4 shows the characteristic vibrational bands of the free ligands and those of the complexes.

Table 4

IR spectra assignments of the bands involved in complex formation (cm^{-1})

Compound	$\nu_{C=O}$	ν_{C-O}	$\nu_{C=C}/\nu_{C=N}$ combined with the phenyl ring	ν_{C-N}	ν_{NCS}
L(1)	1640	—	1587	1540*	1137	—
$CoL(1)(SCN)_2 \cdot 2H_2O$	1667	1027	1580	1540*	1153	2047
$NiL(1)(SCN)_2$	1613	1040	1580	1553*	1157	2083
$ZnL(1)(SCN)_2$	1607	1013	1580	1553*	1163	2073
$CdL(1)(SCN)_2$	1620	1027	1593	1567*	1163	2070
$CdL(1)Cl_2 \cdot CdCl_2$	1613	1023	1590	1550*	1167	—
$CdL(1)J_2 \cdot O \cdot 5CdJ_2$	1607	1030	1580	1540*	1167	—
L(2)	1653	—	1593	1556*	1140	—
$CoL(2)(SCN)_2$	1627	1043	1590	1543*	1147	2067
$NiL(2)(SCN)_2$	1613	1070	1587	1540*	1160	2080
$ZnL(2)(SCN)_2$	1607	1073	1587	1543*	1160	2067
$CdL(2)Cl_2$	1657	1073	1587	1553*	1140	—
$CdL(2)(SCN)_2 \cdot Cd(SCN)_2$	1617	1077	1590	1547*	1163	—

* shondler

In the IR spectra of the compounds, both the characteristic vibrations of group $C_5 = O$, as well as those of C_5-O appear. Thus only one of the two pairs of donor atoms participates at the coordination, the complexes are tetracoordinated, having two coordinative bonds $C_4-N \rightarrow$ and $C_5-O \rightarrow$ and two covalent ones $M-X$.

The magnetic measurements performed for the Co and Ni complexes (Table 5) prove the presence of three, respectively two unpaired electrons, a fact which corresponds to high spin (O_h or T_d) or low spin (T_d) Co complexes and to high spin (O_h or T_d) or low spin (O_h or T_d) Ni complexes.

Table 5

Magnetic data of complexes

Compound	$\chi_m \cdot 10^6$ c.g.s.u.	μ_{eff}(B.M.)	No. of unpaired electrons
$CoL(1)(SCN)_2 \cdot 2H_2O$	7,875.70	4.32	3
$NiL(1)(SCN)_2$	5,136.22	3.48	2
$CoL(2)(SCN)_2$	9,804.28	4.82	3
$NiL(2)(SCN)_2$	3,672.53	2.95	2

The results of vibrational spectrum and magnetic measurements suggest for the complexes the probable structures $CoL(1)(SCN)_2 \cdot 2H_2O$, $NiL(1)(SCN)_2$, $CoL(2)(SCN)_2$ and $NiL(2)(SCN)_2$ T_d.

CONCLUSIONS

1. Six new complexes of bis-methylaminoantipyryl-propane and five of bis-methylaminoantipyryl-butane with $3d^7$, $3d^8$, $3d^{10}$ and $4d^{10}$ transitional metals have been prepared.

2. The electronic spectra recorded for the complexes, compared with the spectra of ligands, suggest a charge transfer origin of the bands.

3. From the IR spectrum results, in agreement with the magnetic measurements, that only one of the two pairs of donor atoms C_4-N and C_5-O participates at coordination, forming tetracoordinated compounds.

REFERENCES

[1] I. Havlik, T. Simonescu, I. Havlik, A. Maurer and S. Policec, *Bul. Inst. Polit. Timişoara,* **28**(42), 93(1983).

[2] S. Policec, A. Maurer, I. Havlik, O. Costişor, M. Mracec and C. Csunderlik, *Bul. Inst. Polit. Timişoara,* **25**(39), 57(1980).

[3] I. Havlik, T. Simonescu and I. Havlik, *Rev. Roumaine Chim.*, **28**, 357(1983).

[4] O. Costişor, A. Maurer and S. Policec, *Bul. Inst. Polit. Timişoara,* under press.

[5] O. Costişor, A. Maurer, A. Tomescu and S. Policec, *Bul. Inst. Polit.* Timişoara, under press.

[6] I. Havlik, T. Simonescu, A. Maurer and I. Havlik, Rom. Pat. Appl., nr. 80370, 29 oct. 1980.

Revue Roumaine de Chimie, 30, *1*, 61–68 (1985)

ISOLATION AND CHARACTERIZATION OF ARABINOGALACTAN FROM LIMA BEAN (*PHASEOLUS LIMENSIS*) SEED

SALAH M. ABD EL-KADER[a], MAHMOUD F. ABD EL-ALLE[b]
MOHAMADY A. FAKHR EL-DEIN[a] and SALAH A. TURK[a]
Department of Agricultural Chemistry, El-Minia University, Egypt
[a] Agricultural Chemistry Department, Faculty of Agriculture, El-Minia University, Egypt
[b] Chemistry Department, Faculty of Science, Tanta University, Egypt

Received March 10, 1984

An arabinogalactan type of polysaccharide ($[\alpha]_D = -30°$) was isolated in 1.9–3.7% yield from the ground dehulled seeds of Lima bean. It is composed of L-arabinose, D-galactose, L-rhamnose and D-galacturonic acid (molar ratio about 1.5 : 5.5 : 1.5 : 1.0). Periodate oxidation revealed that some units were attacked. Polarimetry and hydrolysis of the methylated polysaccharide showed the predominance of the β-(1 $\rightarrow$ 3) linked galactopyranoside units, which are attached to L-arabinose, L-rhamnose and D-galacturonic acid at the C_2, C_3 and C_6 positions. The optical rotation in cuprammonium complex is discussed.

Dixie Butter Pea White variety of Lima bean *(Phaseolus limensis)* is a leguminous plant which is widely grown in United States, Southern Canada and Latin America. It has high nutritional value,[1,2] and is used as an essential ingredient in native food in different forms. It was introduced in Egypt from U.S.A. in 1978. [3] A series of studies on Black grame (*phaseolus mungo*) polysaccharide, indicated a composition of L-arabinose, D-galactose, D-galacturonic acid and L-rhamnose as 30 : 20 : 3 : 5,[4] somewhat similar to that reported by Kadkal *et al.* as 18 : 13 : 2 : 3.[5] Thus arabinose and galactose are the major constituents in the ratio 3 : 2. Usually the tentative model of polysaccharide in phaseolus species is one of these types : xylogalactan, arabinogalactane and rhamnogalacturonan.[6] Arabinogalactane types of polysaccharide occur as part of pectic substance from several sources,[7–10] and may have a branched chain structure.[11–13]

MATERIALS AND METHODS

Materials

Lima bean seeds were obtained from the Farm of Faculty of Agriculture, El-Minia University, Egypt. The dehulled seeds were ground in coffee grinder and used for extracting the polysaccharide.

Methods

All specific rotations are equilibrium values and were measured at room temperature. Evaporations were carried out under reduced pressure at temperature not exceeding 40°C, unless otherwise stated. Protein was removed either by treatments with aqueous cold sodium chloride (10% W/V) or with aqueous trichloroacetic acid (10% W/V).

Paper chromatography was carried out by the descending technique on Whatman No. 1 filter paper, with the following solvent systems (V/V). (a) 1-butanol-acetic acid-water (4 : 1 : 5), (b) ethylacetate-acetic acid-water (7 : 1 : 1), for unsubstituted sugars and (c) benzene-ethanol-water (190 : 50 : 5) for methylated sugars. Sugars on a paper chromatogram were detected with benzidine-trichloroacetic acid,[14] and aniline phosphate.[15]

Gas-liquid chromatography (glc) of methylated sugars was usually performed after conversion into their corresponding alditol acetates, with a Shimadzu gas chromatograph Model-GC—GAM, fitted with a flame-ionization detector using a glass column (0.4×200 cm) packed with 5% OV—101, at 180°C. Methylated uronic acids were also analyzed as their methyl glycoside methyl esters on a column of 15% butanediol succinate polyester on Neosorb Wat; 175°C.

The hydrolysate of acidic polysaccharide gave arabinose, galactose and rhamnose, and a small proportion of galacturonic acid.

Determination of carbohydrate was generally made by phenolsulfuric acid.[16] Colorimetric determination of uronic acid was done by the carbazol method.[17]

Isolat on of polysaccharide

For removal of protein and lipids, the dehulled ground seeds were stirred successively with 10% (W/V) cold sodium chloride solution (4×500 ml, for 1 hr. each time), then with 10% (W/V) trichloroacetic acid (3×200 ml for 4 hrs each time). After centrifugation, the defatted ground seeds (68 g) were used for extracting the polysaccharide : — (A) By suspension in water (3×500 ml) and autoclavisation at 120°C for 20 min. After each extraction the residual seed material was separated by centrifugation. The combined extracts were treated with diastase for 24 hrs, then poured into ethanol (1 L) after concentrating it to 500 ml. The solid precipitate was washed several times with alcohol and dissolved in warm water (500 ml). The solution was washed with chloroform (2×100 ml), and it (Fraction I) was poured into ethanol (1L) yielding a pale-yellow powder (4.6 g). In order to purify the acidic polysaccharide, the water-extract was dissolved in 0.02N sodium sulfate (500 ml) to which cetylpyridinium chloride (CPC, 6 g) was added, until no more precipitate was formed. The precipitate was collected and dissolved in 10% sodium chloride (400 ml). The solution was filtered, dialyzed, concentrated to 200 ml, and (Frac. Ia) was poured into ethanol (400 ml) yielding a white powder (1.9 g) of an acidic polysaccharide. The supernatant solution of the precipitate was dialyzed, concentrated and (Frac. Ib) then poured into ethanol, yielding a neutral polysaccharide (2.1 g).

(B). The insoluble residue, after hot water extraction, was extracted with 0.1N sodium hydroxide with continuous stirring at 65°C (3×500 ml, for 2 hrs each time). The combined extracts were neutralized, dialyzed, concentrated to 500 ml, and (Frac II) poured into alcohol (1L) yielding a white powder (3.7 g). Since fraction II also contained an acidic polysaccharide it was purified as CPC complex as in the case of the hot water extract. However in the supernatant solution of the insoluble complex no appreciable amount of polysaccharide was precipitated by the addition of ethanol, indicating the absence of neutral polysaccharide.

(C) To fraction Ia or fraction II (500 ml), Fehling's solution (100 ml) was added and the mixture was allowed to stand for ten days. The resulting copper complex (2.0—3.2 g) was separated by centrifugation, washed with alcohol several times, and dried in a desiccator.

Anal. Calcd. for $[C_7H_{10.8}O_{5.7}-0.4\ Cu(NH_3)_2]_n$; Cu = 11.3%. Found : Cu = 14.9%

The polysaccharide was recovered from the copper complex by treatment with 1N hydrochloric acid (100 ml) with stirring and pouring into ethanol (200 ml). The white precipitate was filtered off, washed successively with ethanol and ether, then dried under reduced pressure. It had $[\alpha]_D$ — 30° for both acidic polysaccharides (C, 0.1% in H_2O).

Acid hydrolysis of acidic arabinogalactan

Acidic polysaccharide (300 mg) was hydrolysed with M sulphuric acid (15 ml) for 8 hrs at a boiling water bath. After neutralization with $BaCO_3$, filtration, deionization on Rexyn-101 (H^+) resin and concentration, the mixture of acidic and neutral sugars was fractionated on a column of IR-48 resin. The column was eluted first with 250 ml water to remove the neutral sugars, and gradient elution by ethanolic ammonia (100 ml) followed in order to obtain the uronic acids.

(a) Neutral sugars. The column eluates were concentrated, and on examination on paper chromatograms they were found to contain three components. These gave the same colour reactions, moved to the same extent and were undistinguished from authentic samples of D-galactose (R_f—0.1), L-arabinose (R_f 0.19) and L-rhamnose (R_f 0.4), respectively (solvent a). The ratio of sugars was determined after eluting the corresponding zones from the paper chromatograms run in solvent a), by phenolsulphuric acid method.

(b) Uronic acid fractions were pooled, concentrated and subjected to paper electrophoresis,[18] along with authentic standards in 0.2 M borate buffer, pH 8.92 at 320 V for 7 hrs, and were undistinguished from authentic sample of D-galacturonic acid (R_f 0.01). The ratio of galacturonic acid was estimated after eluting the corresponding zone, by colorimetric determination with carbazole reagent (uronic acid 11.5 %).

Methylation of the polysaccharide: The dried polysaccharide (1.5 g) was dispersed in liquid ammonia by stirring at -55 to $-60°C$, and methylated by addition of metalic sodium (1.6 g) and methyl iodide (40 ml) in portions during 5 hrs with vigorous stirring.[19] After one more treatment with the same reagents, the ammonia was evaporated at room temperature.

A portion (1.0 g) of the partially methylated polysaccharide was then refluxed in methanol (10 ml) with methyl iodide (12 ml) and silver oxide (2.4 g; added in portion) for 20 hrs. The reaction mixture was then evaporated to dryness and the solid material was extracted with chloroform. The chloroform extract was concentrated to a syrup which was treated with methyl iodide (4 ml) and silver oxide (1.2 g) as before, yielding a yellowish solid product (0.6 g). The IR absorption spectrum of this product revealed the absence of hydroxyl group.

Anal. Calcd. For 79.7 % methylation; $[C_7H_{8.8}O_{3.1}(OCH_3)_{2.6}]_n = OCH_3$, 36.14 %.
found: OCH_3, 36.5 %.

Identification of the products

The methylated polysaccharide (C 500 mg) was allowed to stand in 40 % sulfuric acid (5 ml), at room temperature for 2 hrs, then diluted again with water (10 ml) and heated at 60°C for 2 more hrs. After further dilution with water (20 ml), the reaction mixture was heated on water bath for 14 hrs, and neutralized with barium carbonate. The barium salt was filtered off and the filtrate concentrated to a syrup (350 mg) which on examination by paper chromatography using solvent C, was found to contain at least nine components with R_f values of 0.016, 0.021, 0.067, 0.37, 0.38, 0.58, 0.63, 0.76 and 0.95. The methylated sugars were reduced with sodium borohydride, converted into their corresponding alditol acetates and were analyzed by gas-liquid chromatography.

2,3,4-tri-*O*-Methyl-*D*-galacturonic acid, which could not be resolved under this condition, was confirmed by GLC as their methyl galactoside methyl ester (column; 15 % butanediol succinate polyester at 175°C, retention time relative to β-methyl-*D*-galactoside, 2.3 and 3.1).

Periodate Oxidation: Phaseolus acidic arabinogalactan (100 mg) was oxidized with 0.3 M sodium metaperiodate (150 ml) at room temperature in the dark.[20] Aliquots (5 ml) were removed after 24 hrs and the consumption of periodate and production of formic acid were determined.[21,22] The results based on 155.5 g of polysaccharide (calculated on the arabinose-galactose-rhamnose-galacturonic acid ratios of 1.5 : 5.5 : 1.5 : 1.0) were as follows: periodate consumed: 0.6 g mole, ormic acid produced: 0.32 mole.

The remaining solution from periodate oxidation was treated with ethylene glycol[23] (few drops) and dialysed for 24 hrs against running tap-water. The nondialyzable material was recovered by concentration and was then hydrolysed with 0.5 M sulphuric acid for 5 hrs at 100°C. The neutralised ($BaCO_3$) hydrolysate was examined by paper chromatography. Large amounts of only *L*-arabinose (R_f 0.187) and *D*-galactose (R_f 0.123) were detected in an approximate molar ratio of 1.0 : 2.5.

RESULTS AND DISCUSSION

The polysaccharides were extracted successively with hot water at 120°C (Fraction I), and 0.1N sodium hydroxide at 65°C under a nitrogen atmosphere (Fraction II). The procedure for fractionation is shown in Scheme I. The polysaccharides in the water extract were further fractionated by treatment with CPC to give an acidic polysaccharide (Fraction IA) and a neutral polysaccharide (Fraction IB; discarded). The acidic polysaccharide in each fraction (IA and II) was purified by repeated fractional precipitations with ethanol, and then *via* its copper-complex. Examination of the carbohydrate components by paper chromatography, after hydrolysis with acid, indicated the presence of L-arabinose, D-galactose, L-rhamnose and D-galacturonic acid. The quantitative estimation of the molecular proportions of the four sugars indicated that they were present in an approximate ratio (1.5 : 5.5 : 1.5 : 1.0). This ratio remained essentially the same when three different methods for isolating the polysaccharide were applied, indicating the homogeneity of the acidic polysaccharide (Arabino-Galacturono-Rhamno-Galactan).

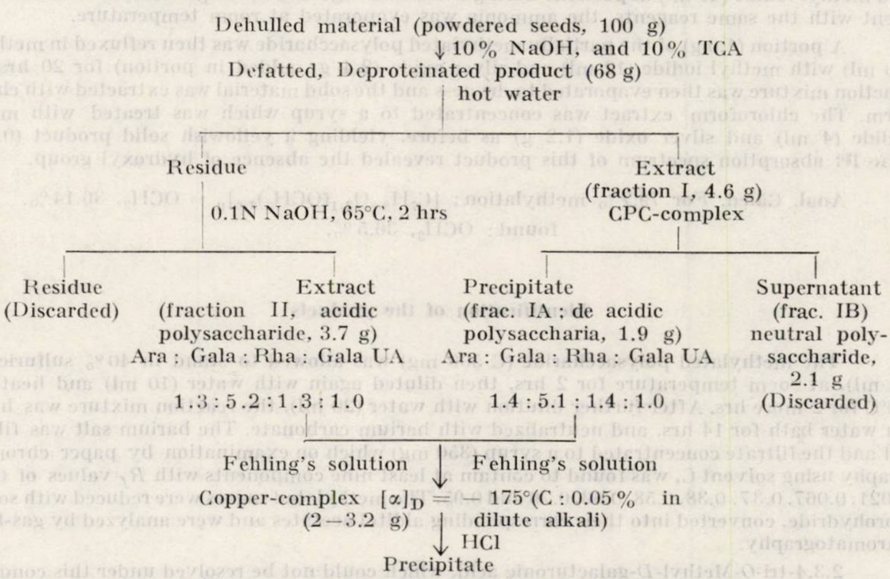
Dehulled material (powdered seeds, 100 g)
10% NaOH, and 10% TCA
Defatted, Deproteinated product (68 g)
hot water
Residue
Extract
(fraction I, 4.6 g)
0.1N NaOH, 65°C, 2 hrs
CPC-complex
Residue
(Discarded)
Extract
(fraction II, acidic
polysaccharide, 3.7 g)
Ara : Gala : Rha : Gala UA
1.3 : 5.2 : 1.3 : 1.0
Precipitate
(frac. IA ; de acidic
polysaccharia, 1.9 g)
Ara : Gala : Rha : Gala UA
1.4 : 5.1 : 1.4 : 1.0
Supernatant
(frac. IB)
neutral poly-
saccharide,
2.1 g
(Discarded)
Fehling's solution
Fehling's solution
Copper-complex
(2–3.2 g)
[α]D = – 175°(C : 0.05% in
dilute alkali)
HCl
Precipitate
(the same acidic polysaccharide, [α]D = – 30°
(C, 0.1% in dilute alkali)
Ara : Gala : Rham : Gala UA
1.5 : 5.5 : 1.5 : 1.0

Scheme I. Fractionation of Polysaccharide from Lima Bean Seed (*Phaseolus limensis*)

The polysaccharide was then exhaustively methylated with methyl iodide and sodium metal in liquid ammonia. The acidic polysaccharide exhibited considerable resistance towards complete methylation and five successive methylation processes were required to yield a methylated product containing 0.797 OCH_3 per hydroxyl group, as judged from the infrared spectrum (the absence of OH-band at 3400–3600 cm^{-1}). The high negative value for the specific rotation of the polysaccharide $[\alpha]_D = -30°$), and the presence of absorption band at 890 cm^{-1} in the infrared spectrum are characteristic for β-configuration (Fig. 1).

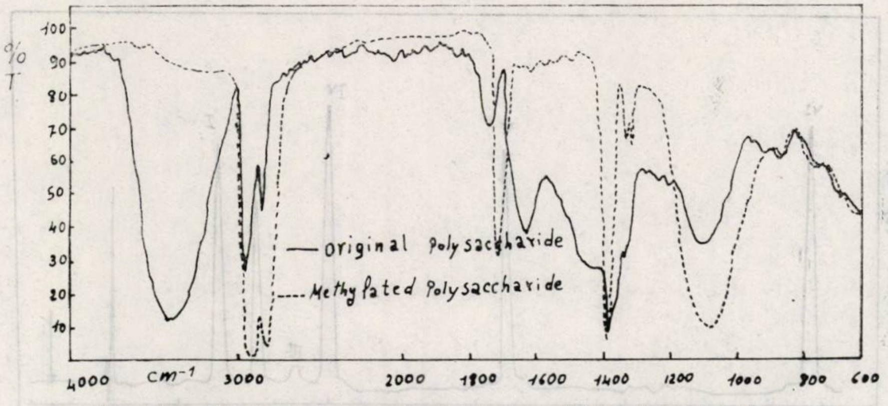

Fig. 1. — IR-absorption spectrum of the acidic polysaccharide.

Examination of the fission products of the methylated polysaccharide on paper chromatograms showed the presence of nine components. As shown in Figure 2, gas-liquid chromatography of the methylated product revealed the presence of 2,4-di-O-methyl-L-arabinose (Peak I, Tg 1.27), 2,3,4-tri-O-methyl-L-rhamnose (Peak III, Tg 1.53), 2,4,6-tri-O-methyl-D-galactose (Peak IV, Tg 2.03), and 4,6-di-O- and 2,4-di-O-methyl-D-galactose (Peak V and VI, Tg 3.2 and 5.26), together with a trace of 2,4-di-O-methyl-L-rhamnose (Peak III, Tg 1.8). The presence of 2,3,4-tri-O-methyl-D-galacturonic acid was confirmed by glc as its methyl glycoside methyl ester. No tetra-O-methyl-D-galactose or tri-O-methyl-L-arabinose was detected. The procedure used for detection of methylated sugars is capable of detecting less than one part of tetra-O-methyl-D-galactose (indicative of end groups) in a hundred parts of tri-O-methyl-D-galactose [24] and therefore the methylated material has a chain length greater than one hundred units. Thus, the molar ratios of the methyl sugar fragments are listed in Table 1. Comparison of the molecular ratio of methylated arabi-

Table 1

Molar ratios of products in the hydrolysis of methylated acidic polysaccharide

O-Methyl sugar	Linkage indicated	Tg*	Molar ratio
2,4-Di-O-methyl-L-arabinose	→3(Arb)1→	1.27	1.7
2,3,4-Tri-O-methyl-L-rhamnose	(Rhm)1→	1.53	1.2
2,4-Di-O-methyl-L-rhamnose	→3(Rhm)1→	1.80	trace
2,4,6-Tri-O-methyl-D-galactose	→3(Gala)1→	2.03	1.7
4,6-Di-O-methyl-D-galactose	→2(Gala)1→	3.20	1.6
2,4-Di-O-methyl-D-galactose	→3 →6(Gala)1→	5.26	1.8
2,3,4-Tri-O-methyl-D-galactouronic acid	(Gala UA)1→	—	1.0

* Retention time relative to that of 2,3,4,6 -tetra-O-methyl-D-glucose.

nose to methylated galactose (1 : 3) with that of arabinose to galactose (1 : 3.7) in the original polysaccharide and the similar comparison between arabinose and rhamnose in methylated and original polysaccharide were present in (1.0 : 0.7) to (1.0 : 1.0) respectively the results showed that some galactose and rhamnose units were lost during methylation and hydrolysis.

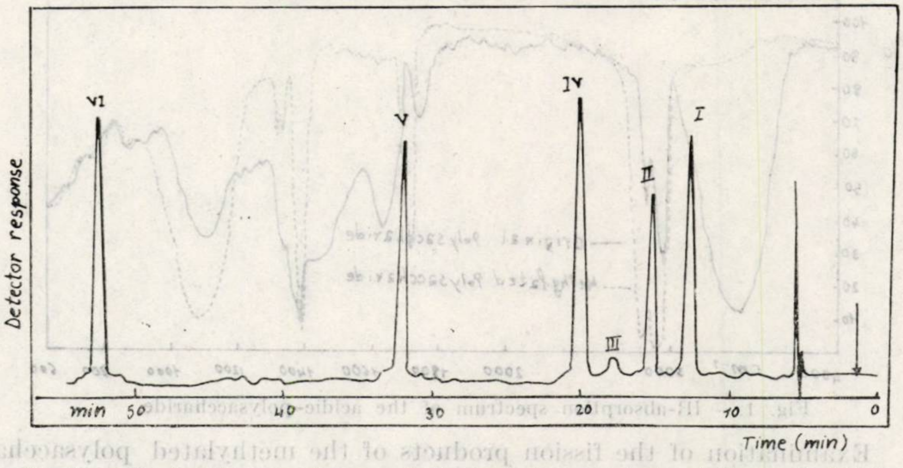

Fig. 2. — Gas-liquid chromatogram of the hydrolysis products of the methylated acidic polysaccharide (fractions Ia and II) as their alditol acetates

The methylation data strongly suggest that the polysaccharide has relatively high branched structure. The fact that (1 → 3) linked-D-galactose residues appear only as non-terminal units, some of which are branched by (1 → 3) and also (1 → 6) linkages, strongly suggests that the polysaccharide has (1 → 3) linked galactane backbone chain, though there is a possibility that a small proportion of (1 → 3) linked galactose units are also present as tri-O-methyl-D-galactose.

Condition : 5 % OV—101,0.7 nitrogen, at 180° C(I) 2,3-di-O-methyl-L-arabinose, (II) 2,3,4-tri-O-methyl-L-rhamnose, (III) 2,4-di-O-methyl-L -rhamnose, (IV) 2,4,6-tri-O-methyl-D-galactose, (V) 4,6-di-O-methyl-D-galactose, (VI) 2,4-di-O-methyl-D-galactose.

The L-arabinose and D-galacturonic acid are both attaching to the galactane backbone at C_2 or C_6, but the galacturonic acid is located only in the terminal position.

The rhamnose units are also attaching either on arabinose units or on galactose units in (1 → 3) links. Figure 3 illustrates one of the possible structures of the arabino-galacturono-rhamnogalactan.

However, in view of the failure to detect any 2,3,4,6-tetra-O-methyl-D-galactose in the hydrolyzate of the methylated polysaccharide it has been suggested that incomplete methylation of the polysaccharide and demethylation during hydrolysis might be the reason for the presence of most of the di-O-methyl derivatives. The isolation of 2,4-di-O-methyl-L-rhamnose as a trace quantity of L-rhamnose derivative is suggestive of branching at positions 1 and 3 of the rhamnose units. However, similarly, the presence of di-O-methyl-L-rhamnose may be due to incomplete methylation or to demethylation. Others[25,26] have reported similar observations.

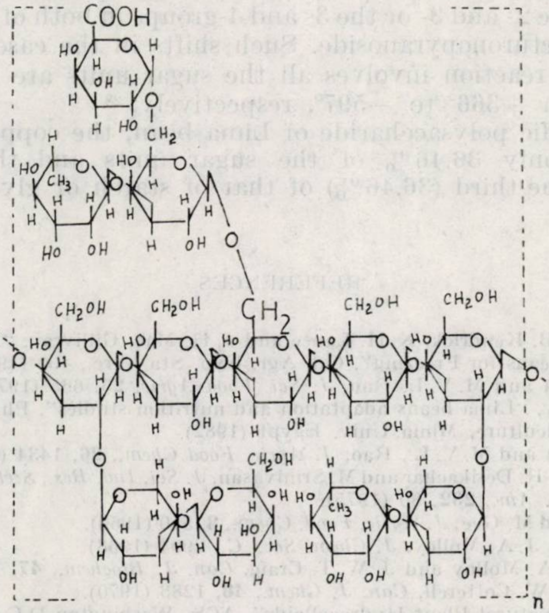

Fig. 3. — A possible structure of the acidic polysaccharide.

On periodate oxidation, the acidic polysaccharide consumed about 0.7 mole of oxidant per mole of sugar residue (Table 2). This and the presence of L-arabinose and D-galactose in the hydrolyzate of the periodate oxidized polysaccharide indicated that the L-arabinose and D-galactose units were branched on forming (1 → 3) linkages. Comparison of the molar ratio of arabinose to galactose in the hydrolyzate of the periodate oxidized and in the original polysaccharide (1.0 : 2.5) and (1.8 : 3.7) respectively, may indicate that some galactose units were lost during the overoxidation.

Table 2

Periodate oxidation of polysaccharide

Time(h)	0.5	1	2	8	14	24	38	50	64	88
Uptake	0.12	0.17	0.37	0.55	0.61	0.69	0.72	0.77	0.81	0.81
HCOOH	0.02	0.05	0.12	0.23	0.29	0.32	0.36	0.37	0.39	0.39
CH_2O	—	—	—	—	—	—	—	—	—	—

On reacting polysaccharide with Fehling's solution a copper complex which contained one-third atomic equivalent of copper per mole of sugar unit was formed. Comparison of the specific rotation of the arabino-galacturono-rhamno-galactan in dilute alkali (−30°) with that in cuprammonium solution (−175°), showed that a levorotatory complex was formed in cuprammonium solution. This solution has been shown[27] to occur in reactions involving the 2- and 3-hydroxyl groups of L-rhamnopyranoside as well as the 2- and 3- or the 3- and 4-groups in both of D-galactopyronoside and galacturonopyranoside. Such shifts in the case of starch and glycogen where reaction involves all the sugar units are from + 375° to −115° and from +366° to −597°, respectively.[28]

In the acidic polysaccharide of Lima bean, the copper complex isolated involves only 36.46% of the sugar units and the levorotatory shift is about one-third (36.46%) of that of starch or glycogen.

REFERENCES

[1] A. H. Holland, J. B. Kendrick, N. H. Lance and J. H. Mac. Gillivray, "Production of green Lima beans for Freezing", Cal. Agr. Exp. Sta. Circ., 430 (1953).

[2] N. S. Susheelamma and M. V. L. Rao, *J. Sci. Food Agric.* **25**, 665 (1974).

[3] M. Y. A. El-Maziny, "Lima beans adaptation and nutrition studies", Ph. D. Thesis, Faculty of Agriculture, Minia Univ. Egypt (1982).

[4] N. S. Susheelamma and M. V. L., Rao, *J. Agric. Food Chem.*, **26**, 1434 (1978).

[5] S. B. Kadkol, H. S. R. Desikachar and M. Srinivasan, *J. Sci. Ind. Res., Sect. C*, **20**, 252 (1961).

[6] P. Albersheim, *Sci. Am.*, **232**, 80 (1975).

[7] R. M. Mccready and M. Gee, *J. Agric. Food. Chem.*, **8**, 510 (1960).

[8] G. O. Aspinall and J. A. Molloy, *J. Chem. Soc., C.*, 2994 (1968).

[9] G. O. Aspinall, J. A. Molloy and J. W. T. Craig, *Can. J. Biochem.*, **47**, 1063 (1969).

[10] G. O. Aspinall, I. W. Cotterell, *Can. J. Chem.*, **48**, 1283 (1970).

[11] R. L. Whistler, "Natural Plant Hydrocolloids", ACS. Washington D.C.P. 45(1954).

[12] R. L. Whistler, *Cereal Foods World*, **20**, 96(1975).

[13] M. Glicksman "Gum Technology in the Food Industry", Academic Press, New York, N.Y. (1969).

[14] J. S. D. Bacon and J. Edelman, *Biochem. J.*, **48**, 114(1951).

[15] J. L. Bryson and T. J. Mitchel; *Nature London*, **164**, 864 (1951).

[16] M. Dubois, K. A. Gilles, J. K. Hamilton, P. A. Rebers and F. Smith, *Anal. Chem.*, **28**, 350 (1956).

[17] Z. Disch, *J. Biol. Chem.* **196**, 189 (1947).

[18] B. J. Block, E. L. Durrum and G. Zweig, "A Manual of Paper Chromatography and Paper Electrophoresis", 1st ed. Academic Press, New York, N. Y. p. 131 (1955).

[19] I. E. Muskat, *J. Amer. Chem. Soc.*, **56**, 693, 2449 (1934).

[20] G. Neumuller and E. Vasseur, *Arkiv Kemi*, **5**, 235 (1953).

[21] T. G. Halsall, E. L. Hirst and J. K.N. Jones, *J. Chem. Soc.*, 1427 (1947).

[22] G. F. O'Dea and R. A. Gibbons, *Biochem. J.*, **55**, 580 (1953).

[23] G. A. Adams, *Can. J. Chem.*, **38**, 280 (1960).

[24] L. Hough, J. K. N. Jones and W. H. Wadman, *J. Chem. Soc.*, 3393 (1952).

[25] G. O. Aspinall, E. L. Hirst and R. S. Mohamed, *J. Chem. Soc.*, 1734 (1954).

[26] C. P. J. Glaudemans and T. E. Timell, *J. Amer. Chem. Soc.*, **80**, 1209 (1958).

[27] E. A. Davidson, "Carbohydrate Chemistry", Holt and Winston, Inc. New York, Chap. 5, 108−112 (1967).

[28] R. E. Reeves, *Advan. Carbohydrate Chem.*, **6**, 108 (1951).

Revue Roumaine de Chimie, **30**, *1*, 69–79 (1985)

МЕХАНОХИМИЧЕСКИ ИНИЦИИРОВАННЫЕ СОПОЛИМЕРИЗАЦИИ

6. МЕХАНОХИМИЧЕСКИЙ СИНТЕЗ ПРИ ВИБРАЦИОННОМ РАЗМОЛЕ ТРОЙНОГО СОПОЛИМЕРА НА ОСНОВЕ АКРИЛОНИТРИЛА-ВИНИЛАЦЕТАТА-α-МЕТИЛСТИРОЛА

КЛЕОПАТРА ВАСИЛИУ-ОПРЕА, МАРЧЕЛ ПОПА
Ясский Политехнический Институт, Кафедра по органической и макромолекулярной химии, Румыния

Получена 7-го декабря 1983 г.

В работе описывается возможность осуществления, при помощи вибрационного размола, механохимического синтеза сополимера на основе акрилонитрила-винилацетата и α-метилстирола. Рассматривается влияние некоторых факторов механохимического режима, а также влияние реакционной среды на эффективность синтеза, выраженную достигнутой степенью превращения (выходом сополимера). Полученные сополимеры охарактеризованы их структурными особенностями и их физико-химическими свойствами.

The paper reports on the synthesis, by vibratory milling, of acrylonitrile — vinyl acetate — α-methyl styrene copolymers. The influence of some reaction parameters on synthesis efficiency is presented. The obtained copolymers were characterized by means of their structural and physico-chemical properties.

ВВЕДЕНИЕ

Возможность инициирования реакций механохимической сополимеризации винильных мономеров указана в литературе ещё в 1963 г.[1] но с тех пор этому типу синтеза было посвящено мало работ[2–4]. Недавно, было доказано возможность механохимической сополимеризации вибрационным размолом довольно большого числа бинарных систем на основе акрилонитрила, стирола и др.[5–9] при отсутствии добавок, играющих роль «Механоинициаторов». Этим путём были получены также и тройные сополимеры на основе акрилонитрила, винилацетата и α-метилстирола.[9]

В настоящей работе исследуется влияние параметров механохимического синтеза на эффективность реакции и выявляется ряд свойств, отличающих эти продукты от аналогичных, полученных классическими методами.

ЭКСПЕРИМЕНТАЛЬНАЯ ЧАСТЬ

Подвергаемые сополимеризации мономеры очищали перегонкой, сишили на молекулярных ситах и снова перегоняли (акрилонитрил и винилацетат перегоняли под азотом и α-метилстирол перегонял в вакууме). Для полимеризации использовали АН с $n_d^{20} = 1{,}392$, ВА с $n_d^{20} = 1{,}395$ и α-МС с $n_d^{20} = 1{,}538$. Синтезы осуществлялись в вибромельницах типа Labowi LS 60, с частотой 25 гц и амплитудой 2—4 мм; реакционные сосуды были построены из нержавеющей стали марки $\overline{V}_2A$, вместимостью 4 л. Они термостатируются путем цирккуляции воды в кожухном пространстве аппарата и позваляют создать желаемую атмосферу реакции. Все проведенные синтезы осуществлялись в инертной (азотной) атмосфере, с использованием мелющих тел сферической формы (Ø 9 мм) в количестве 6 кг.

Для исследования влияния полярности реакционной среды на синтез тройного сополимера были использованы жидкости с различными значениями диэлектрической постоянной (ε), при объёмном отношении 1: 1 к смеси сомономеров. Использованные радикальные акцепторы вводились при концентрации 1% к смеси сомономеров. Полученные продукты реакции отделялись путем вытяжки в течение 48 часов в аппарате Soxhlet для удаления не вступившего в реакцию мономера и фракций с небольшой молекулярной массой, после чего подвергались сушке в вакууме при температуре 40°C.

Растворимость в ДМФ (диметилформамиде) определялась путем растворения 2,5 г полимера в 100 мл растворителя, с перемешиванием и периодическим прогревом в течение 24 часов. Растворимая фракция осаждалась в метаноле, после чего подвергалась фильтрованию, сушке взвешиванию.

ИК-спектры были сняты на спектрофотометре SPECORD-IR 71 (ГДР) использовая метод таблетирования с КБр.

Спектроскопия Мёсбауэра осуществлялась на спектрометре ELRON при комнатной температуре, используя в качестве эталона нитропрусиат натрия.

Состав продуктов реакции устанавливали путем элементарного анализа; содержание азота определялось методом Къелдаля.

Термостабильность продуктов реакции определялась при помощи дифференциального термического анализа, с использованием дериватографа ,,Erdely-Paulik'' (Венгерская Н. Р.), при градиенте температуры 12°С/мин и образца в порошковом состоянии (50 мг).

РЕЗУЛЬТАТЫ И ИХ ОБСУЖДЕНИЯ

Для получения информации, касающейся механизма тройной сополимеризации и реакционной способности использованных сомономеров в синтезах этого типа, было исследовано влияние некоторых параметров механического режима и природы реакционной среды.

Влияние некоторых факторов на процесс механохимической сополимеризации. Систематическое исследование было проведено для четырёх факторов, оказавшихся важными и в процессах механохимической гомополимеризации [10].

Влияние продолжительности. Для того, чтобы установить влияние этого фактора на процесс сополимеризации, были проведены синтезы в диапазоне продолжительностей от 24 до 240 часов. Для этого осуществляли вибрационный размол двух бинарных смесей (акрилонитрил (АН)-винилацетат (ВА) 9: 1 и АН — α-метилстирол (МС) 9: 1) и одной тройной смеси (АН: ВА: МС — 18:1: 1), с получением косвенной информации о реакционной способности сомономеров субстрата.

Кинетические кривые синтеза вышеуказанных трёх сополимеров показаны на рис. 1; вид этих кривых типичен для процессов механохимического синтеза: восходящая ветвь до достижения максимального выхода сополимера, затем падение этой величины, что указывает на протекание интенсивных процессов механодеструкции. Наивысшее значение выхода сополимера получается в случае сополимера АН: ВА; для системы АН: МС имеет место снижение этой величины примерно на 10%; в обоих случаях максимум достигается после 192 часов (кривые 1,2). В случае тройного сополимера, максимальное значение выхода, соответствующее продолжительности 144 ч., меньше (см. кривую 3), что очевидно указывает на гораздо более низкую реакционноспособность ВА и МС сравнительно с АН.

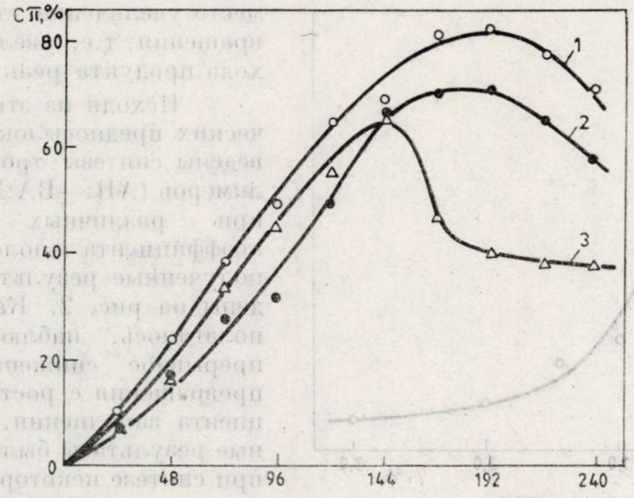

Рис. 1. — Влияние продолжительности на выход при синтезе некоторых сополимеров. 1 — АН: ВА 9:1; 2 — АН: МС 9:1; 3 — АН: ВА: МС 18:1:1 (η = 0,5%, Ø 9мм, инертная среда, Т = 18 ± 2°С).

Эти результаты хорошо сходятся с результатами, полученными раньше, при гомополимеризации вибрационным размолом акрилонитрила.[11] В последнем случае, на всем исследуемом временном диапазоне получаются более высокие значения выходов продукта гомополимеризации по сравнению с сополимерами; максимум достигается после 96 часов от начала реакции.

Влияние коэффициента заполнения. Эффективность процессов механохимического синтеза, выраженная степенью превращения возрастает с ростом количества энергии, отнесённой единице массы мономера. Энергия развиваемая во время виброразмола, являющаяся следствием ударов между мелющими телами или между ними и стенками реакционного сосуда, пропорциональна количеству мелющих тел. Если при постоянном количестве мелющих шариков (6 кг) изменять количество смеси сомономеров (т.е. коэффициент заполнения[11]), можно ожидать увеличение эффективности реакции, так как одна и та же энергия, развиваемая во время синтеза, будет отнесена к различным количествам мономера. Отсюда следует, что при сижении коэффициента заполнения должно иметь место увеличение степень превращения, т.е. увеличение выхода продукта реакции.

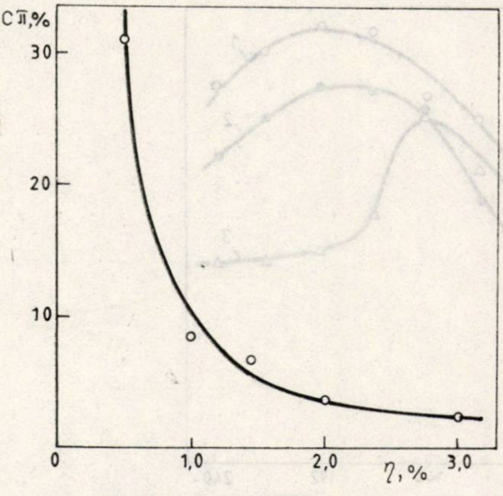

Рис. 2. — Влияние коэффициента заполнения на степени превращения при синтезе тройного сополимера АН: ВА: МС 18: 1:1 (6 кг шариков, инертная среда, Т = 18 ± ± 2°С, 72 часа).

Исходя из этих теоретических предпосылок, были проведены синтезы тройных сополимеров (АН: —ВА:МС —18:1:1) при различных значениях коэффициента заполнения (η%); полученные результаты приведены на рис. 2. Как и предполагалось, наблюдается непрерывное снижение степени превращения с ростом коэффициента заполнения. Аналогичные результаты были получены при синтезе некоторых гомополимеров или бинарных сополимеров[5,11].

Влияние химической природы среды. Кинетическая энергия, выделяемая в условиях вибрационного размола, создаёт состояние плазмы в реакционной среде, в которой имеются атомы, свободные радикалы, электроны, металлические катионы, радикалы-анионы; каждая из вышеупомянутых частиц способна инициировать процессы полимеризации. В цели получения информаций о механизме реакции сополимеризации, было исследовано влияние химической природы среды.

Влияние радикальных акцепторов. В качестве радикальных акцепторов использовались фенол и гидрохинон; синтезы проводились во временном диапазоне 0 —192 ч. Полученные кинетические кривые представлены на рис. 3. В присутствии радикальных акцепторов наблюдаются, во всех случаях, более низкие значения степеней превращения; из исследованных радикальных акцепторов более сильный ингибирующий эффект дает гидрохинон (кривая 3). Полученные результаты указывают на то, что активные центры радикальной природы оказывают существенное влияние на протекание механохимической сополимеризации в исследованной системе сомономеров.

Влияние полярности среды. Результаты ранее проведенных исследований[10] показали, что полярность реакционной среды сильно влияет на степень превращения в случае гомополимеризации акрилонитрила. Для того, чтобы проверить этот эффект, были проведены сополимеризации в присутствии полярных жидкостей с различными значениями диэлектрической постоянной: гексан, метанол, вода. Полученные кинетические кривые для временного диапазона 24 — 168 ч, представлены на рис. 4. Эти кривые имеют один и тот же вид для всех исследованных случаев; в присутствии полярных жидкостей наблюдается сдвиг максимума степени превращения в сторону значения 96 часов. С ростом величины диэлектрической постоянной (ε), степень превращения падает.

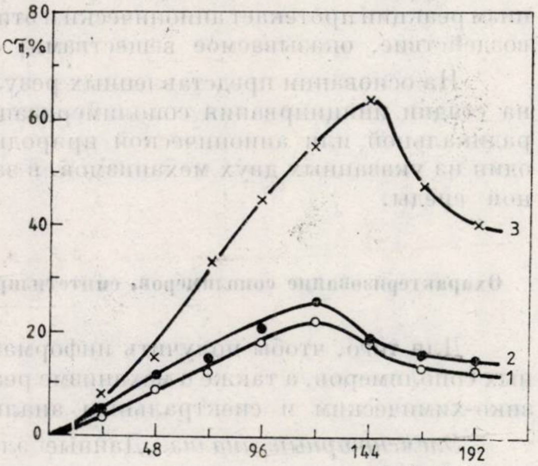

Рис. 3. — Изменение степени превращения при синтезе тройного сополимера АН: ВА:МС 18: :1: 1 в присутствии радикальных акцепторов. 1 — гидрохинон, 2 — Фенол; 3 — инертная среда;

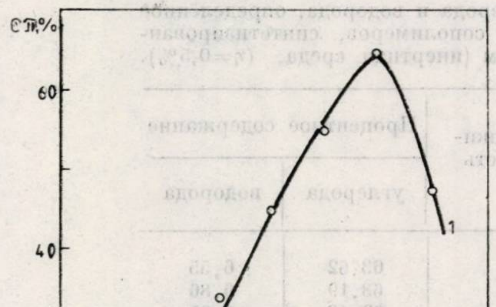

Рис. 4. — Изменение степени превращения с продолжительностью при синтезе тройного сополимера АН : ВА : МС 18: 1: 1 в средах с различной полярностью. 1 — инертная среда; 2 — гексан; 3 — метанол; 4 — вода. ($\eta = 0{,}5\%$, T=18±2°C).

Так как в серии использованных полярных жидкостей способность переноса протона растёт от гексана к воде, то уменьшение степени превращения следует обьяснить прекращением полимеризации вследствие этого эффекта. Отсюда следует, что в присутствии полярных сред, механизм реакции протекает анионически и этим можно объяснить возмущающее воздействие, оказываемое веществами, отдающими протон.

На основании представленных результатов можно сделать вывод, что на стадии инициирвания сополимеризации появляются активные центры радикальной или анионической природы и рост цепи происходит через один из указанных двух механизмов, в зависимости от природы реакционной среды.

Охарактеризование сополимеров, синтетизированных механохимическим путем

Для того, чтобы получить информации о структуре синтетизированных сополимеров, а также о механизме реакции, сополимеры подвегали физико-химическим и спектральным анализам.

Элементарный анализ. Данные элементарного анализа указывают на то, что исследуемые сополимеры имеют состав, отличающийся от состава сополимеров, получаемых обычными методами. Содержание углерода и водорода для трёх серий синтетизированных сополимеров дается в таблице 1, а изменение содержания азота с продолжительностью синтеза — на рис. 5 (для фракции, расстворимых в ДМФ).

Таблица 1

Процентное содержание углерода и водорода, определённое элементарным анализом, для сополимеров, синтетизированных механохимическим путём (инертная среда, ($\eta = 0{,}5\%$).

Сополимеры	Продолжительность (ч)	Процентное содержание	
		углерода	водорода
АН :МС—9 :1	72	63,62	6,55
	96	63,19	6,86
	120	62,48	6,85
	144	60,58	6,43
АН :ВА—9 :1	96	67,20	5,40
	120	67,36	5,49
	144	67,59	5,21
	168	63,80	5,20
АН : МС : ВА —18 :1 :1	72	54,57	5,03
	96	53,75	5,61
	120	53,97	5,27
	144	53,32	5,62
	168	51,62	5,35

Следует отметить изменение содержания углерода с ростом времени синтеза для всех синтетизированных сополимеров; этот эффект объясняется ростом количества химически связанного металла который сбивается во времени размола из стенках сосуда, переходит в колоидальном состоянии [12] механохимически активируется и реагирует с полимерными цепями.

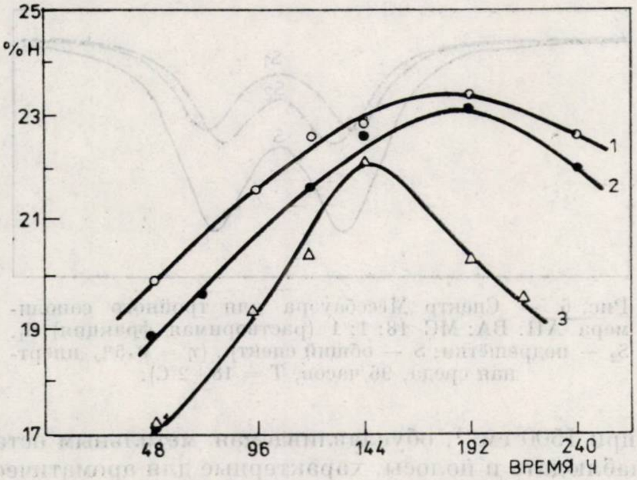

Рис. 5. — Изменение содержания азота с продолжительностью синтеза для следующих механохимически синтетизированных сополимеров. 1 — сополимер АН: МС 9: 1; 2 — сополимер АН: ВА 9: 1; 3 — сополимер АН: ВА: МС 18: 1: 1 ($\eta = 0{,}5\%$, инертная среда, $T = 18 \pm 2°C$).

У всех синтетизированных сополимеров, содержание азота увеличивается до деличины, соответствующей продолжительности, дающей максимум степени превращения (рис. 5 сравнительно с рис. 4), после чего падает. Этот эффект следует объяснить усилением процесса механодеструкции при продолжительностях, превышающих величину, соответствующую максимальной степени превращения, следствием чего является, в первую очередь, уменьшение количества акрилонитрила в структуре образованных сополимеров и обогащение их винилацетатом или α-метилстиролом. Возможны также и реакции выделения HCN, что отмечено при механохимической деструкции поли (акрилонитрила) и другими авторами [13]. В то же время, количество азота может уменьшаться и вследствие химического связывания большого количества металла из стенок реакционного сосуда при увеличении продолжительности синтеза. Следует отметить тот факт, что наиболее существенные изменения состава происходят в случае тройного сополимера, у которого как содержание углерода (таблица 1), так и содержание азота (рис. 6, кривая 3) меньше соответствующих содержаний в бинарных сополимерах.

ИК-спектроскопия. Спектральный анализ в ИК-области некоторых бинарных и тройных сополимеров подтверждает наличие в цепи высокомолекулярного соединения мономеров из исходной смеси. Так, в спектрах всех сополимеров наблюдается полоса поглощения, соответствующая группе — CN(2235 см$^{-1}$). Сополимеры с винилацетатом дают полосы поглощения, соответствующее эфирной группе (1240 см$^{-1}$). Наконец, у сополимеров, содержащих α-метилстирол, появляется полоса

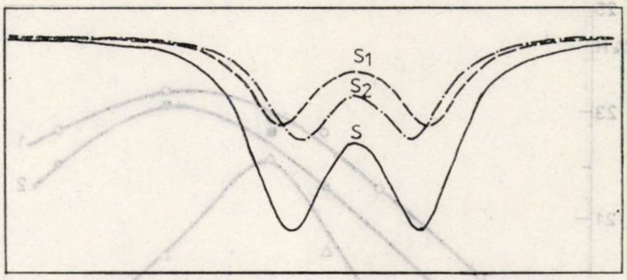

Рис. 6. — Спектр Мёссбауэра для тройного сополимера АН: ВА: МС 18: 1: 1 (растворимая фракция) S_1, S_2 — подрешётки; S — общий спектр. (η = 0,5% инертная среда, 96 часов, T = 18±2°C).

поглощения при 1500 см$^{-1}$, обуславливаемая метильным остатком; кроме того можно наблюдать и полосы, характерные для ароматического кольца (700—760 см$^{-1}$). Следует отметить также присутствие во всех спектрах широкой полосы поглощения при 1600—1700 см$^{-1}$. В других исследованиях [10] было установлено, что эта полоса обусловлена сопряжённой структурой, получающейся при отщеплении группы — CN, способной принимать участие в полимеризации в условиях вибрационного размола [14].

Спектроскопия Мёссбауэра. Убедительные данные, которые говорят о присутствие химически связанных в структуре сополимеров металла представляют собой спектры Мёссбауэра. Присутствие в спектре под-решёток S_1 и S_2 обусловлена ионами Fe^{2+} и Fe^{3+}, пропорция которых в структуре сополимеров может быть определена количественно. На рис. 6 представлен спектр Мёссбауэра для расстворимой фракции тройного сополимера а в таблице 2 представлены величины, определенные путем вычисления из спектра Мёссбауэра. Как видно, общее содержание химически ,связанного железа в структуре исследуемого тройного сополимера равно 1,15%; этот результат сравним с предыдущими результатами (0,87%)[10], полученными при механохимическом синтезе поли (акрилонитрила).

Таблица 2

Параметры, вычисленные из спектра Мёссбауэра

Изомерический сдвиг (мм/с)	Четырёхполярное расклинивание (мм/с)	Эффект Мёссбауэра (%)	Fe %
— 0,1009	0,5327	0,550	1,150
— 0,1004	0,4059	0,600	

Растворимость. Механохимически синтетизированные соединения имеют более низкую расстворимость чем их аналоги, полученные классическими методами, что было замечено раньше и у гомополимеров на основе акрилонитрила[10]. Снижение растворимости определяется присутствием химически связанного полимером металла. Исследуя изменение этого свойства с продолжительностью синтеза для трёх типов сополимеров на основе акрилонитрила, установили, что при продолжительности размола до 120 ч, значения растворимости не превышают 40% (рис. 7). При более высоких значениях продолжительности реакции наблюдается непрерывный рост растворимости, что объясняется процессами механодеструкции, следствием которых является снижение молекулярной массы, а также отрывом привитого сополимера с металлической поверхности коллоидных частиц, образованных вследствие сильных ударов мелющих тел, сталкивающихся между собой и со стенками сосуда.

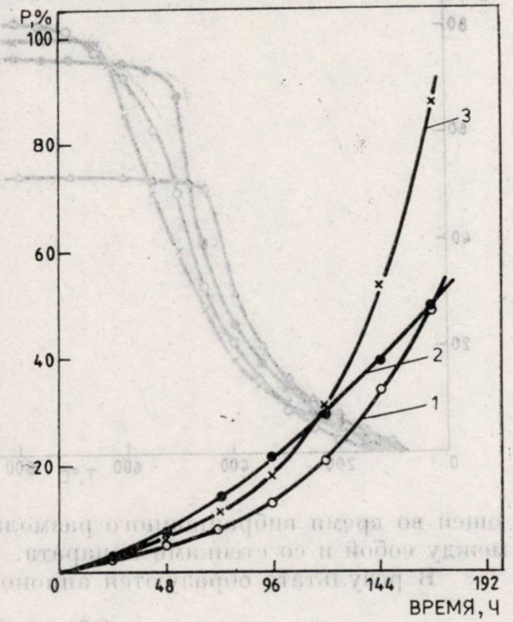

Рис. 7. — Изменение весовых потерь с температурой для некоторых сополимеров, синтетизированных в различных условиях. 1 — АН: ВА: МС — 18: 1: 1, инертная среда, 96; часов; 2 — АН: ВА: МС 18: 1: 1, метанол; 3 — АН: МС 9: 1, инертная среда, 96 часов; 4 — АН : ВА 9 : 1, инертная среда, 96 часов.

Термостойкость. Особые химические структуры, характеризующиеся присутствием в них химически связанного железа, позволяют сщитать синтетизированные соединения металлополимеры, характеризующихся высокой термостойкостью [12].

Дифференциальный термический анализ некоторых сополимеров, полученных в различных условиях синтеза, подтверждают эту гипотезу. Результаты, представленные на рис. 8 показают, что до температуры 100°С полимеры практически не теряютв весе при температуре Т = 200°С процентные потери в весе не превосходят 10%.

Как видно, наибольшей термостойкостью обладает сополимер АН: ВА. Сравнительный анализ двух синтетизированных тройных сополимеров показывает, что большей термостойкостью при температурах выше 600°С обладает сополимер, полученный в присутствии метанола. Это можно объяснить большим количеством металла, химически связанного в структуре полимера что является следствием коррозионного действия, оказываемого метаналом на металлическую аппаратуру.

Все представленные результаты подтверждают, следовательно, возможность синтеза механохимическим путём некоторых сополимеров. Механизм протекания этого синтеза является комплексным, с одной стороны из-за разнообразия активных центров, с другой стороны из-за протекания, одновременно с синтезом, реакций механодеструкции. Инициирование полимеризации является результатом механоэмисии, неизбежно протекающей во время вибрационного размола из-за столкновения мелющих тел между собой и со стенками аппарата.

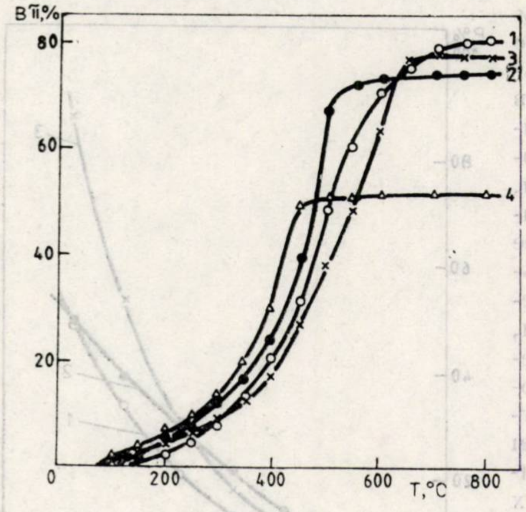

Рис. 8. — Изменение растворимости с продолжительностью синтеза для сополимеров, полученных механохимическим путём. 1 — АН: ВА 9: 1; 2 — — АН: МС 9: 1; 3 — АН: ВА: МС: 18: 1 : 1 ($\eta = 0{,}5\%$, инертная среда, $T = 18 \pm 2°$ С).

В результате образуются анионо-радикальные частицы.

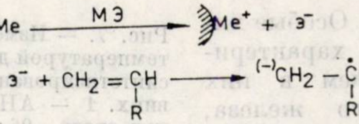

$$\mathrm{Me} \xrightarrow{\text{МЭ}} \mathrm{Me}^{+} + \text{э}^{-}$$

$$\text{э}^{-} + CH_2 = \underset{R}{\underset{|}{CH}} \longrightarrow {}^{(-)}CH_2 - \underset{R}{\underset{|}{\dot{C}H}}$$

В зависимости от природы реакционной среды, механизм роста цепи будет радикальным или анионическим. Металлические ионы, образованные вследствие протекания ,,механоэмисии'', входят в структуру синтетизированных сополимеров либо путем участия в стадии прекращения — привязываясь к анионическом концу (особенно в случае растворимой фракции), либо путем комплексации с атомами азота и кислорода с электронами, неучаствующими в химических связях (нерастворимая фракция).

Следовательно, продукты этого типа синтеза являются макромолекулярными комплексами, со следующими характеристическими для данных соединений свойствами: нерастворимость в обычных растворителях, хорошая термостойкость, парамагнетизм.

ВЫВОДЫ

Вибрационный размол некоторых двойных и тройных смесей мономеров позволяет осуществлять синтез соответствующих сополимеров. На процесс механохимического синтеза тройного сополимера АН: ВА: МС влияют такие факторы, как продолжительность, коэффициент заполнения, присутствие радикальных акцепторов или жидкостей с различными значениями полярности. Продукты механохимического синтеза имеют низкую растворимость в обычных растворителях, а их элементарный состав отличается от элементарного состава обычно синтетизированных аналогов. Нерастворимая фракция механохимически синтетизированного тройного сополимера является типичным примером высокомолекулярного комплекса и входит в разряд металло-сополимеров.

ЛИТЕРАТУРА

[1] N. Plate and V. A. Kargin, *J. Polym. Sci.*, **4**, 1027(1963).
[2] Н. А. Плате и Л. Б. Строганов, *Высокомол. соедин.*, **2**, 240 (1972).
[3] Н. К. Барамбойм и Л. Н. Антонова, *Высокомол. соедин.*, **3**, 675(1976).
[4] Л. А. Антонова, Н. А. Хрусталеев, Н. К. Барамбойм и Н. А. Кротова, *Коллоидн. ж.*, **3**, 535 (1976).
[5] C. I. Simionescu, C. Vasiliu Oprea and C. Negulianu, *Eur. Polymer J.*, **15**, 1037 (1979).
[6] C. Vasiliu Oprea and M. Popa, *Polymer Bulletin*, **3**, 269(1984).
[7] C. Vasiliu Oprea and F. Weiner, *Angew. Makromol. Chem.*, **106**, 207(1982).
[8] C. Vasiliu Oprea and M. Popa, *Acta Polymerica*, **10**, 612(1983).
[9] C. Vasiliu Oprea and M. Popa, *Acta Polymerica*, **35**, 261(1984).
[10] C. Vasiliu Oprea and M. Popa, *Angew. Makromol. Chem.*, **92**, 73(1980).
[11] C. Vasiliu Oprea and M. Popa, *Angew. makromol. Chem.*, **90**, 13(1980).
[12] Е. М. Натансон и З. А. Ульберг, «Коллоидные металлы и металлополимеры», Наукова Думка, Киев, 1971.
[13] H. Grohn und K. Bischoff, *Plaste und Kautschuk*, **4**, 180(1962).
[14] C. Vasiliu Oprea and M. Popa, *Polymer J.*, **16**, 4, 191(1984).

Revue Roumaine de Chimie, 30, 1, 81–88 (1985)

IDENTIFICATION D'HYDROCARBURES AROMATIQUES DE QUELQUES FRACTIONS PÉTROLIÈRES. II[1]

IDENTIFICATION DE COMPOSANTS PAR HPLC

HOCINE KADI et D. P. LAZAR *

Département de Génie chimique, Ecole Polytechnique, Université d'Alger, Algérie,

* Département de Chimie physique, Faculté de Technologie chimique, Splai Bahlui, 71, 6600 Jassy, Roumanie

Reçu le 2 septembre, 1983

The interest for both separation and identification of aromatic hydrocarbons in different petroleum fractions is mainly justified by their economical value and by a particular scientific importance. The separation and identification of aromatic hydrocarbons are analyticaly interesting because these operations can be simoultaneously accomplished through three different physical methods : HPLC chromatography, the composite method of n.d. PA and the IR spectral analysis.

L'intérêt porté à la séparation et à l'identification des hydrocarbures aromatiques s'explique par la valeur économico-industrielle et par l'intérêt scientifique qu'ils représentent. Du point de vue analytique, la séparation et l'identification des hydrocarbures aromatiques peuvent se faire par trois méthodes physiques differéntes : méthode chromatographique HPLC, méthode composée n.d. PA et méthode d'analyse spectrale IR.

1. PARTIE EXPÉRIMENTALE

Durant les essais préliminaires pour l'établissement des conditions de travail standard dans la technique HPLC [1], on a constaté que pour maintenir le débit de l'éluent constant (2 mL min^{-1}), on doit utiliser une pression de plus en plus grande (de 102 à 238 atm).

Cette condition est imposée pour deux raisons :

1° le tassement, avec le temps, du remplissage de la colonne,

2° le colmatage des filtres terminaux à la sortie de la colonne.

Les fractions 1—23 sont réparties en deux groupes, en fonction de la température d'ébullition et du poids moléculaire des constituants individuels.

Le groupe « A » se compose des fractions 1—15, distillées entre $t_i^0 = 90°$ et $t_f^0 = 182°$, donc jusqu'au voisinage de la température d'ébullition du n-butylbenzène (égale à 183,3°) ; ce groupe contient les homologues supérieurs du benzène ayant des températures d'ébullition comprises entre 90° et $2 \times 90°$ et de poids moléculaires compris entre 78 et 134. Pour l'analyse chromatographique des fractions de ce groupe on a utilisé un éluent riche en eau (eau : acetonitrile = 60 : 40).

Le groupe « B » se compose des fractions 16—23, distillées entre 182° et 209°, donc jusqu'à une température d'ébullition tout près de 4-méthylindène. Ce groupe comprend des homologues supérieurs du benzène ayant des poids moléculaires supérieurs à 134 et une structure moléculaire complexe. Pour l'analyse chromatographique des fractions de ce groupe on a utilisé un éluent riche en composant organique (eau : acétonitrile = 40 : 60).

Tableau 1

Résultats généraux obtenus par l'identification chromatographique HPLC, groupe « A »
Eluent : eau : acétonitrile = 60 : 40 ; débit : 2 ml min^{-1}

Fraction	$t°_i$ (°C)	$t°_f$ (°C)	$\Delta t°$ (°C) a)	PE_m (°C) b)	Aire du pic (%) c)	$t_{R,i}$ sec	$t_{R,i}$ min	Résolution R d)	Facteur de résolution, R_C e)	Composants séparés	Composants identifiés f)
1	2	3	4	5	6	7	8	9	10	11	12
Pression de l'éluent = 187 atm											
1	90,0	99,0	9,0	94,50	69,3 30,7	450 726	7,5 12,1	6,13	1,00	2	1 ; 2
2	99,0	103,5	4,5	101,25	9,4 90,6	450 726	7,5 12,1	6,13	1,00	2	1 ; 2
3	103,5	115,0	11,5	109,25	100,0	726	12,1			1	2
Pression de l'éluent = 129 atm											
4	115,0	123,5	8,5	119,25	97,0 3,0	684 1122	11,4 18,7	6,00	1,00	2	2; 3
5	123,5	131,0	7,5	127,25	58,8 1,7 39,5	684 1008 1122	11,4 16,8 18,7	5,30 1,32	1,00 1,00	3	2; 3; 4
6	131,0	137,0	6,0	134,00	7,0 9,0 84,0	684 1008 1122	11,4 16,8 18,7	4,10 1,12	1,00 1,00	3	2; 3; 4
7	137,0	145,5	8,5	141,25	2,5 28,3 29,2	675 1008 1128	11,25 16,8 18,7	3,96 1,03	1,00 0,78	3	3; 4; 5
8	145,5	151,0	5,5	148,25	32,0 68,0	1008 1128	16,8 18,7	1,18	0,80	2	4; 5
9	151,0	157,5	6,5	154,25	14,4 31,6 1,7 10,0 31,1 11,2	1008 1128 1422 1476 1554 1614	16,8 18,7 23,7 24,6 25,9 26,9	1,14 * * * *	0,72 1,00 0,60 0,34 0,21	6	4; 5; 6; n.i. ; 7; 8

Pression de l'éluent = 119 atm

Tableau 1 (suite)

1	2	3	4	5	6	7	8	9	10	11	12
10	157,5	164,5	7,0	160,75	7,2 12,1 2,4 4,9 32,4 31,5 9,5	996 1098 1506 1596 1686 1830 1896	16,6 18,3 25,1 26,6 28,1 30,5 31,6	2,26 * * * * *	0,84 1,00 0,69 0,66 0,49 0,37	7	5 ; 6 ; 9 ; 7 8 ; 11 ; n.i.
11	164,5	169,0	4,5	166,75	3,2 6,6 7,4 2,4 45,0 35,4	996 1098 1506 1596 1686 1830	16,6 18,3 25,1 26,6 28,1 30,5	* * * * *	0,62 0,29 0,70 0,88 0,16	6	5 ; 6 ; 9 ; 7 8 ; 11
12	169,0	172,0	3,0	170,50	2,8 2,5 18,1 53,1 23,5	996 1098 1506 1686 1830	16,8 18,3 25,1 28,1 30,5	1,06 3,40 1,18 *	1,00 1,00 0,80 0,49	5	5 ; 6 ; 12 ; 8 ; 11 5

Pression de l'éluent = 129 atm

13	172,0	175,0	3,0	173,5	17,7 46,2 15,4 12,4 8,3	1524 1716 1842 2880 3210	25,4 28,6 30,7 48,0 53,5	1,19 * * *	0,79 0,53 1,00 0,78	5	12 ; 8 ; 11 ; 10 ; n.i.
14	175,0	178,0	3,0	176,50	22,0 40,5 11,0 20,3 6,2	1650 1752 1902 2970 3390	26,0 29,2 31,7 49,5 56,5	1,19 * * *	0,80 0,50 1,00 0,78	5	12 ; 8 ; 11 ; 10 ; n.i.
15	178,0	182,0	4,0	180,00	15,1 23,5 6,0 34,6 20,8	1620 1818 1962 3520 3540	27,0 30,3 32,7 58,66 59,00	1,14 * * *	0,80 0,56 1,00 0,65	5	12 ; 8 ; 11 : 10 ; n .i.

a) $t^0 = t_f^0 = t_i^0$; b) $PE_m = (t_f^0 + t_i^0)/2$; c) Rapportée à la somme des surfaces de tous les pics du chromatogramme de la fraction respective. d) Conformément à la relation (2)[1].

e) Conformément à la relation (1)[1]. f) Correspondance des chiffres : 1 = benzène ; 2 = toluène ; 3 = éthylbenzène ; 4 = xylène (*m*, *p*) ; 5 = *o*-xylène ; 6 = *n*-propylbenzène ; 7 = isopropylbenzène ; 8 = 1,2,4-triméthylbenzène ; 9 = 1,3,5-triméthylbenzène ; 10 = 1,2,3-triméthylbenzène ; 11 = t-butylbenzène ; 12 = iso-butylbenzène ; 13 = *n*-butylbenzène.

* = résolution difficile

n.i. = non identifié

Tableau 2

Résultats généraux obtenus par séparation et identification partielle (approximative) des constituants du groupe « B »

Eluent : eau : acétonitrile — 40 : 60 ; débit = 2 mlmin^{-1}; pression unique = 238 atm

Fraction	t_i^0 (°C)	t_f^0 (°C)	$\Delta t°$ (°C) a)	PE_m (°C) b)	Aire du pic (%) c)	$t_{R,i}$ sec	$t_{R,i}$ min	Résolution d)	Facteur de résolution, R_C e)	Composants séparés	Composants Identification approximative f)
1	2	3	4	5	6	7	8	9	10	11	12
16	182,0	184,5	2,5	183,25	6,5	396	6,6	*	0,39	7	1 ; 2 ; 3
					10,4	420	7,0	*	0,40		
					3,7	468	7,8	*	0,10		
					4,4	486	8,1	*	0,02		
					3,7	498	8,3	*	0,65		
					31,7	546	9,1	*	0,21		
					39,6	582	9,7				
17	184,5	188,0	3,5	186,25	0,6	318	5,3	2,40	1,00	11	1 ; 2 ; 3
					4,6	390	6,5	*	0,57		
					9,4	414	6,9	*	0,59		
					2,5	456	7,6	*	0,27		
					8,0	498	8,3	*	0,77		
					33,4	546	9,1	*	0,45		
					28,6	582	9,7	*	0,61		
					3,0	678	11,3	*	0,20		
					3,9	720	12,0	*	0,13		
					2,2	750	12,5	*	0,06		
					3,8	780	13,0				
18	188,0	191,0	3,0	189,5	1,6	318	5,3	2,67	1,00	11	1 ; 2 ; 3
					3,5	390	6,5	*	0,61		
					6,0	414	6,9	*	0,70		
					3,3	462	7,7	*	0,43		
					7,6	504	8,4	*	0,78		
					36,7	546	9,1	*	0,56		
					21,4	588	9,8	*	0,61		
					4,1	684	11,4	*	0,24		
					5,4	726	12,1	*	0,11		
					4,0	750	12,5	*	0,08		
					6,5	792	13,2				
19	191,0	197,5	6,5	194,25	4,7	318	5,3	2,89	0,95	11	1 ; 2 ; 3
					2,0	396	6,6	*	0,50		
					2,6	420	7,0	*	0,70		
					2,5	468	7,8	*	0,55		
					7,4	510	8,5		0,76		
					35,2	552	9,2		0,54		
					21,7	600	10,0		0,45		
					4,5	690	11,5		0,17		
					5,5	732	12,2		0,05		
					4,8	762	12,7		0,05		
					9,1	804	13,4				

Tableau 2 (suite)

1	2	3	4	5	6	7	8	9	10	11	12
20	197,5	200,5	3,0	198,75	18,0	324	5,4	2,89	0,96	11	1 ; 2 ; 3
					1,2	402	6,7		0,61		
					1,1	426	7,1		0,89		
					2,1	474	7,9		0,68		
					9,0	510	8,5		0,77		
					21,4	558	9,3		0,61		
					20,4	606	10,1		0,48		
					6,0	696	11,6		0,16		
					5,7	744	12,4		0,06		
					7,0	780	13,0		0,10		
					8,1	816	13,6				
21	200,5	202,0	1,5	201,25	24,0	336	5,6	2,46	0,88	11	1 ; 2
					0,7	414	6,9		0,50		
					0,5	438	7,3		0,86		
					3,7	486	8,1		0,70		
					12,0	528	8,8		0,66		
					28,8	564	9,4		0,85		
					5,8	708	11,8		0,08		
					4,2	750	12,5		0,15		
					11,7	792	13,2		0,15		
					5,3	828	13,8		0,11		
					5,5	858	14,3				
22	202,0	205,0	3,0	203,50	32,4	330	5,5	2,73	0,97	9	2
					1,5	486	8,1		0,62		
					6,1	528	8,8		0,42		
					19,0	564	9,4		0,37		
					8,6	684	11,4		0,21		
					9,0	732	12,2		0,12		
					8,7	798	13,3		0,07		
					4,3	822	13,7		0,02		
					10,4	864	14,4				
23	205,0	209,0	4,0	207,00	38,0	330	5,5	3,57	0,98	8	2
					2,4	480	8,0		0,77		
					7,7	528	8,8		0,49		
					10,4	564	9,4		0,54		
					7,1	660	11,0		0,40		
					9,6	738	12,3		0,30		
					13,1	804	13,4		0,23		
					11,7	870	14,5				

a), b), c), d), e), f) = même signification que dans le Tableau 1 ;

Correspondance des chiffres (v. col. 12) : 1 = 1-méthyl, 3-isopropylbenzène ; 2 = *n*-butylbenzène ; 3=1,3-diméthyl, 5-éthylbenzéne.

* = résolution difficile

Les fractions ont été par la suite réparties en sous-groupes de 3 fractions, ce qui a permis une corrélation plus commode des temps de retention, $t_{R,i}$, surtout que dans le groupe « A », certaines analyses chromaotgraphiques on tété effectuées sous quatre pressions différentes : 102, 119, 123 et 187 atm.

Le groupe « B » a été analysé sous une même pression, 238 atm (voir Tabl. 1 et 2).

L'identification des constituants individuels sur les chromatogrammes des fractions 1—15 a été effectuée à l'aide d'une collection d'étalons où sont inclus les homologues suivants du benzène : toluène. éthylbenzène, *orto*-, *meta*- et *para*-xylène, *n*-propylbenzène, isopropylbenzène 1,2,3,-1,2,4- et 1,3,5-trimethylbenzène, isobuthylbenzène, 1-méthyl, 3-isopropylbenzène, n-buthylbenzène et benzène (total 14 étalons).

L'évaluation quantitative, en pourcentage de chaque composant, a été faite d'après les procédés standard utilisés en CG comme en HPLC[2-5]. Même si la vitesse du papier d'enregistrement n'influence pas beaucoup la qualité de séparation chromatographique, on a choisi une vitesse de 1 cm min^{-1}, considérée comme la plus convenable.

L'identification des constituants individuels du groupe « A » a été réalisée à l'aide des étalons disponibles mais le critère chromatographique a été complété par le critère de la température d'ébullition et de la courbe de distribution des composants, qui se prolonge sur un certain nombre de fractions successives (Tabl. 1 et 2, col. 10).

Dans le groupe « B », à cause du manque d'étalons, l'identification des composants (Tabl. 2, col. 11) est basée seulement sur le critère de la température d'ébullition et sur les courbes de distribution (voir Tabl. 3) et, par conséquent, elle est approximative.

Tableau 3

Répartition des constituants (numérotés 1—15) séparés par fractions

Constituant aromatique	$t_{R,i}$ (min)	FRACTIONS								Identification approximative de constituant
		16	17	18	19	20	21	22	23	
1	5,6 —5,3=0,3		×	×	×	×	×	×	×	
2	6,9 —6,5=0,4	×	×	×	×	×	×			
3	7,3 —6,9=0,4	×	×	×	×	×	×			1-methyl, 3, isopropylbenzène
4	7,9 —7,6=0,3	×	×	×	×	×				
5	8,5 —8,0=0,5	×	×	×	×	×	×	×	×	
6	$t_{R,6}=8,3$	×								
7	$t_{R,7}=8,8$						×	×	×	
8	9,4 —9,1=0,3	×	×	×	×	×	×	×	×	*n*-buthylbenzène
9	10,1 —9,7=0,4	×	×	×	×	×				1-3-diméthyl, 5-éthylbenzène
10	11,8 —11,0=0,8		×	×	×	×	×	×	×	
11	12,5 —12,0=0,5		×	×	×	×	×	×	×	
12	12,7 —12,5=0,2		×	×	×					
13	13,4 —13,0=0,4		×	×	×	×	×	×	×	
14	13,8 —13,6=0,2						×	×		
15	14,5 —14,3=0,2						×		×	

2. DISCUSSIONS

2.1. Dans le groupe « A » , on a mis en évidence 16 composants individuels dont 10 ont été identifiés et 6 se sont manifestés sous forme de substances non identifiées et présentes dans une seule fraction. Les fractions 1—8 sont caractérisées par $\Delta t°$ élevé (4°—11°) et par un petit nombre de constituants (2—3). Les fractions 9—11 contiennent chacune 7 constituants mais les fractions 12—15, avec un $\Delta t° = 3°$, ne contiennent que 5 constituants. Dans les fractions 1—8 un des constituants est quantitativement dominant parceque ceci représente 58 à 97 % de la composition de la fraction respective.

La fraction 3 contient un seul hydrocarbure aromatique, le toluène.

Avec l'augmentation de la température d'ébullition on observe que la composition, en pourcentage, des fractions tend à devenir uniforme (par exemple, la fraction 15).

2.2 Les fractions du groupe «B» ont été analysées par chromatographie HPLC à une même pression, 236 atm; mais, avec un autre éluent, plus riche en composant organique. Ceci a permis une corrélation commode des temps de retention, $t_{R,i}$, pour les constituants distribués sur plusieurs fractions (voir Tabl. 3).

Chaque fraction contient un nombre relativement élevé des composants (de 7 à 11, mais predominant 11). Le nombre total de constituants identifiés est 15. A la différence de la première moitié du groupe « A », dans le groupe « B] » la contribution (en pourcentage massique) des constituants majeurs est beaucoup réduite (30% à 40%).

Les constituants moyens contribuent avec 10—20 %, alors que ceux mineurs se trouvent à un pourcentage inférieur à 10 %. Certains constituants se présentent sous forme de traces (inférieures à 1 %).

Dans chaque fraction, seuls deux à trois constituants présentent des contributions supérieures à 20 %, le reste de constituants participent avec un pourcentage inférieur à 10 %. Dans le groupe « B », les valeurs $\Delta t°$ sont, en général, plus petites que celles du groupe « A », alors que le nombre de constituants y est à peu près double.

L'identification des constituants ayant les formules brutes $C_{19}H_{12}$, $C_{10}H_{14}$, $C_{11}H_{16}$ est difficile à cause des valeurs très voisines des temps de retention, des températures d'ébullition rapprochées et des nombreux cas d'isomérie. De même, l'utilisation d'une pression d'éluent très élevée (238 atm) diminue l'efficacité de la colonne chromatographique.

3. CONCLUSIONS

a. La méthode cromatographique HPLC est très efficiente en ce qui concerne les constituants des fractions 1—15; ainsi, on a pu mettre en évidence les constituants se trouvant à une très faible concentration de 1—2 % et même inférieure à 1 % (voir Tabl. 1 et 2, col. 5). L'efficacité de la séparation peut être constatée surtout dans le cas des fractions de composition complexe (par exemple, les fractions 17—21), les constituants étant des hydrocarbures aromatiques avec des masses moléculaires et des températures d'ébullition très voisines.

b. En ce qui concerne l'identification des constituants, la méthode chromatographique HPLC dépend des performances de la colonne et de l'existence d'une collection complète d'étalons; mais, dans ces circonstances s'impose l'utilisation d'une méthode auxiliaire d'identification ou d'une corrélation des données chromatographiques avec d'autres méthodes physiques.

c. L'efficacité de la méthode HPLC, concernant la séparation et l'identification des constituants individuels dépend de la composition des fractions obtenues après la distillation VPE (vrai point d'ébullition), de la sélection correcte de la colonne chromatographique, de l'éluent et d'autres paramètres expérimentaux spécifiques pour la méthode HPLC.

BIBLIOGRAPHIE

[1] H. Kadi et D. P. Lazăr, *Rev. Roumaine Chim.*, **29**, 6, 497–505(1984).

[2] N. Brenner et R. J. Olson, dans « The Practice of Gas Chromatography » (L. S. Ettre et A. Zlatkis, Editeurs), Interscience Publishers, New York, 1967, p. 15.

[3] L. S. Ettre, dans « The practice of Gas Chromatography » (L. S. Ettre et A. Zlatkis, Editeurs), Interscience Publishers, New York, 1967, p. 390–92.

[4] J. M. Gill et F. T. Tao, Technical Bulletin 135–67, édité par VARIAN AEROGRAPH, California, 1967, p. 12–14.

[5] E. L. Johnston et R. Stevenson, « Basic Liquid Chromatography », VARIAN Ass., Inc., Palo Alto, California, 1978, p. 207–214.

Revue Roumaine de Chimie, **30**, *1*, 89–93 (1985)

COMPTES RENDUS

W. L. HAWKINS, *"Polymer Degradation and Stabilization"*, in *"Polymers. Properties and Applications"*, vol. 8, Springer-Verlag, Berlin, 1984, 120 pages, 88 DM (hard-cover).

Degradation is a major factor which limits the application of polymers. Loss of mechanical strength, dielectric quality, and aesthetic aspect often leads to failure of polymeric materials, before reaching the required service life. Therefore stabilization is necessary. There are two main possibilities to improve stability of polymers : modification of polymer structure and compounding with selective additives (stabilizers). The first method is rather limited because certain chemical structures and physical properties are required for a certain application of the polymeric material. Thus stabilization with additives is the most usual method to obtain polymers with desired qualities. Polymer stabilisation became an important part of polymeric science after achieving an understanding of degradation chemistry.

W. L. Hawkins who has a long experience in the field of polymer science describes in his monograph two aspects of stabilization :

i) the most important mechanisms of oxidative and non-oxidative degradation, photooxidation, and thermal degradation :

ii) stabilization with additives for the three kinds of degradation mentioned above.

The book has the following chapters :

A. Introduction
B. Polymer Degradation
  I. Thermal Degradation in the Absence of Oxygen
  II. Oxidative Degradation – An Historical Introduction
  III. Recent Developments in Oxidative Degradation
  IV. Degradation by Hydrolysis
C. Stabilization Against Non-oxidative Thermal Degradation
D. Stabilization Against Thermal Degradation
E. Stabilization Against Degradation by Radiation
F. Stabilizatilon Against Degradation by Ozone
G. Test Procedures
H. Future Trends

It is emphasized that the introduction of light stabilizers (hindered amines) has been a major advance in the protection of polymers against photodegradation. But only a few aspects are known about the mechanism of photodegradation. Combined efforts of polymer researchers, photochemists, physical chemists, and organic chemists can contribute to the generation of new stabilizers making polymers able to compete with more conventional materials.

The book provides the background for selection of the most effective stabilizers or stabilizer combinations to protect a specific polymer against degradation. The subject is clearly and understandably presented. Ungraduated and graduated students, industrial chemists and polymer researchers will be interested in this review.

Like all the books edited by Springer Verlag, the printing is excellent and error-free. Figures and tables are drawn clearly.

Ursula Bologa

"Anionic Polymerization" (Advances in Polymer Science vol. 56), Springer-Verlag, Berlin, 1984, 165 pages, 98 DM (hard-cover).

The first article in this volume, "Anionic Polymerizations of Non-Polar Monomers Involving Lithium" is written by R. N. Young, R. P. Quirk, and L. J. Fetters. The paper deals with carbanionic polymerizations involving lithium and non-polar monomers that have achieved a special interest as a result of the possibility for obtaining systems lacking spontaneous termination reactions. This method is used for preparations of polymers of narrow molecular weight distributions and predictable molecular weight. The non-terminating nature of these systems facilitates kinetic studies, the synthesis of block copolymers of uniform composition and allows controlled termination reactions where star-shaped or comb-type polymers can be formed as well as chains having functional groups at one or both ends. The topics discussed include structure and bonding of organolithium compounds, the initiation and propagation reactions in hydrocarbon solvents, the influence of polar co-solvents on chain propagation, the stereochemistry of polydienes and chain end functionalization.

The second review, "Anionic Copolymerization of Cyclic Ethers with Cyclic Anhydrides", is written by J. Lustoň, and F. Vašš. The anionic copolymerization of cyclic ethers with cyclic anhydrides is a reaction of great interest and practical importance, especially as curing reaction of epoxy resins. Attention is focussed on the kinetics and mechanisms of copolymerization, the effect of epoxide and anhydride structure on copolymerization, the effect of type and structure of initiator on the rate and the course of copolymerization. The reaction in the presence of proton-donor compounds is also considered, as well as the effect of the proton-donors. The author emphasizes that it should be necessary to study copolymerization involving anionic mechanism on model compounds.

The book represents an excellent up-to-date collection of information on the progress that has been made in recent years on anionic polymerization. It provides a deep insight on the kinetics and thermodynamics of the phenomena.

Ursula Bologa

A. MIZUIKE, "Enrichment Techniques for Inorganic Trace Analysis. Chemical Laboratory Practice", Springer-Verlag, Berlin, 1983, 144 pages, 72 DM (hard-cover).

The author of this book has also written the chapter "Separations and Preconcentrations" in "Trace Analysis: Physical Methods" edited by G. H. Morrison, Wiley- Interscience, New York, 1965. Since then the progress in the field of trace analysis has been remarkable. The author gives in the present book updated information (785 references for literature through 1982).

This monograph contains the newest techniques of analysis and enrichments based on volatilization, liquid-liquid extraction, selective dissolution, precipitation, electrochemical deposition and dissolution, sorption, ion exchange, liquid chromatography, flotation, freezing and zone melting.

The book contains 13 chapters:

1. Introduction
2. General Aspects of Enrichment Techniques
3. Control of Contamination and Loss
4. Volatilization
5. Liquid-liquid Extraction
6. Selective Dissolution
7. Precipitation
8. Electrochemical Deposition and Dissolution
9. Sorption, Ion Exchange and Liquid Chromatography
10. Flotation
11. Freezing and Zone Melting
12. Enrichment Techniques in Water Analysis
13. Enrichment Techniques in Gas Analysis

The Appendix contains useful data for analytical chemists:

1. Physical properties of solvents
2. Masking agents for cations
3. Ion exchange data for all cations in Mendeleev's periodic table.

Each chapter contains the theoretical fundamentals of each technique. The most important apparatus used in laboratory are drawn with care in 41 figures.

The book is recommended to analytical chemists as well as to the chemists working in industry. It is readable and well systematized. The printing is excellent. The figures and tables are clear and highly readable.

Ursula Bologa

"*Transition Metal Complexes — Structures and Spectra*" (Structure and Bonding, vol. 55), Springer-Verlag, Berlin, 1983, 209 pages, 98 DM (hard-cover).

Structures and spectra of transition metal complexes are the subject of volume 55 in the series "Structure and Bonding" edited by Springer-Verlag. The book contains four contributions by M. H. Gubelmann, A. F. Williams, M. Bacci, F. Valach, B. Koreň, P. Sivý, M. Melník, F. Mathey, J. Fischer, and J. H. Nelson.

"The Structure and Reactivity of Dioxygen Complexes of the Transition Metals" written by M. H. Gubelmann and A. F. Williams is the first review. Three aspects of these complexes are discussed in detail : the structural classification, the electronic structure, and the reactivity. The electronic structure is considered first in qualitative terms which allows the rationalisation of the different classes of compounds. Calculations and spectroscopic data are analysed critically. The reactivity of the complexes is discussed for each structural class in terms of the electronic structure. The article gives a clear summary of current knowledge of these compounds (529 references) for workers interested in their application.

The second paper is "The Role of Vibronic Coupling in the Interpretation of Spectroscopic and Structural Properties of Biomolecules" written by M. Bacci. The term vibronic coupling is widely spread in literature, although it is sometimes misleading. The adjective vibronic derives from the contraction of two adjectives, vibrational and electronic, and, in its common meaning, indicates a dynamic interaction between vibrational and electronic motions.

The aim of the article is to review the spectroscopic and structural properties of several biomolecules. The importance of the vibronic coupling in the interpretation of physical properties of molecules and crystals is widely recognized, but a desultory attention has been paid to the role played by such a coupling in biological systems. After a brief outline of the Jahn-Teller effect, the whole problem is critically re-examined. Some suggestions are given for the inclusion of vibronic coupling in future analysis on biomolecules.

"Crystal Structure Non-Rigidity of Central Atoms for Mn(II), Fe(II), Fe(III), Co(II), Co(III), Ni(II), Cu(II) and Zn(II) Complexes" is the title of the next article written by F. Valach, B. Koreň, P. Sivý, and M. Melnik. This paper deals with the conception of crystal structure non-rigidity for central atoms of selected complexes by using statistical distributions of interatomic central-nearest ligand atom. The compounds are classified with respect to the geometry of their inner coordination sphere and to their crystal structure aspect. The square-planar geometry is found to be the most stable for Cu(II) and Ni(II)$_{LS}$ complexes, tetragonal-pyramidal for Zn(II) complexes, while for Fe(II)$_{HS}$, Mn(II)$_{HS}$, Fe(III)$_{HS}$, Co(II)$_{HS}$, Ni(II)$_{HS}$, and Co(III)$_{LS}$ complexes it is the regular octahedral geometry (HS and LS denote high-spin and respective low-spin states).

"Complexing Modes of the Phosphole Moiety" is the last review written by F. Mathey, J. Fischer and J. H. Nelson. The review shows that the growing interest aroused by phospholes in coordination chemistry can be attributed to three main reasons : i) the influence of the partial delocalization of the phosphorus lone pair on the complexing ability of phospholes ; ii) the discovery of phosphametallocenes ; iii) the variety of complexing modes found for the phosphole nucleus. For a given phosphole, no less than ten different types of complexes can be obtained.

Volume 55 in the series "Structure and Bonding" edited by Springer-Verlag is concerned with new aspects related to experimental and theoretical chemistry of transition metal complexes. It has to be noted that all the articles are valuable sources of up-to-date information and keys to the voluminous primary literature.

Ursula Bologa

J. ŠTĚPEK and H. DAOUST, "*Additives for Plastics, Polymers. Properties and Applications*" vol. 5, Springer Verlag, Berlin, 1983, 243 pages, 168 DM (hard-cover).

Plastics have become competitive materials in industry and technology. Because of their practical importance attention is focused on the improvement of their physical properties (mechanical strength, dielectric quality and aesthetic aspect) without changing their molecular structure. Stabilization of polymers with additives is an important part of polymer science which developed from art to science after an understanding of basic phenomena has been achieved. The author defines additives as "substances that are dispersed within polymeric materials in order to modify their behavior in the course of processing and to improve the desired properties, of final products".

The book deals with the most important additives utilized for plastic materials. They are classified into two main groups :

i) additives that modify the physical properties (part A of the book, 134 pages) ;
ii) antiaging agents and antidegradants (part B of the book, 94 pages).

The 14 chapters of the monograph are :

Part A :

1. Plasticizers

2. Lubricants and Mold-Release Agents
3. Macromolecular Modifiers
4. Reinforcing Fillers, Reinforcing Agents, and Coupling Agents
5. Colorants and Brightening Agents
6. Chemical and Physical Blowing Agents
7. Antistatic Agents

Part B :

8. Difficulty Stabilizable and Nonstabilizable Factors Provoking Plastic Degradation
9. Heat Stabilizers
10. Antioxidants and Metal Ion Deactivating Agents
11. Ultraviolet Protecting Agents
12. Flame Retardants
13. Biocides Against Biological Degradation of Plastics
14. Brief Survey of Methods Used to Incorporate Additives into Polymer Matrices.

Each chapter takes the reader from the fundamental theory through practical commercial applications for a wide range of additive types.

Special attention is paid to homogenization processes that should be in conformity with thermodynamic principles, to permeation of polymer by the additive, and to the efficiency of combined additives. The preparation of polymer-additive mixtures is a complicated process involving theoretical considerations. Sometimes such mixtures have antagonistic effects; the optimal cases are those of synergetic effects of combined additives.

Despite the 650 references, this book is only an introduction to the many aspects of additives for plastics. It is complementary to volume 8 in this series, namely "Polymer Degradation and Stabilization" written by W. L. Hawkins, Springer Verlag, Berlin, 1984. It is addressed to students, technologists, and researchers of plastic technology. It is readable, systematic and well documented. Printing is excellent.

Ursula Bologa

G. W. GOKEL and S. H. KORZENIOWSKI, "*Macrocyclic Polyether Syntheses*" (Reactivity and Structure Concepts in Organic Chemistry, vol. 13) Springer-Verlag, Berlin, 1982, 410 pages, 238 DM (hard-cover).

About fifteen years have passed since Pedersen published his paper on crown ether chemistry. Several articles predate his paper, but Pedersen was the first one who recognized the complexing ability of polyethers synthetized by him. Numerous excellent reviews have been published since 1967 dealing with particular aspects of macrocyclic ether chemistry. There was a need for a single source of information in this field considering the rapid development of synthetic methods and various applications of crown ethers.

This book edited by Springer-Verlag is the most comprehensive and well-documented survey of methods used in polyether syntheses published till now.

The reader is introduced at the beginning of the book into the nomenclature and the organization of the topic. A systematic scheme of table usage is given as a useful guide. Each chapter contains a brief theoretical background and the description of the most important methods used for the corresponding group of compounds, followed by tables of the known substances Detailed preparations are omitted because their inclusion would have made the book quite lengthy.

The eight chapters are :

1. Introduction and General Principles
2. The Template Effect
3. Syntheses of Oxygen Macromolecules
4. Syntheses of Azacrowns
5. Crown Ethers and Macrocyclic Polyethers Lactones
6. Miscellaneous Macrocycles
7. Open-chain Equivalents of Crown Ethers
8. Cryptands and Related Polycyclic Systems

The following systematization of the listed substances is used. The compounds are arranged according to increasing carbon number. Within groups with the same number of carbons, the compounds are arranged by increasing size of the ring. Among compounds having the same number of carbons and the same ring size, the compounds are arranged by increasing number of heteroatoms ; and lastly by increasing order of Cahn- Ingold-Prelog priority of the pendant group or other substituents.

References are given for each chapter. The book contains an author index and a subject index.

The book is recommended to organic chemists interested in macrocyclic polyether syntheses, inorganic and analytical chemists concerned with coordination chemistry of alkali metals and transition metals, as well as to those chemists who want to begin their research in this field.

Ursula Bologa

NOTE POUR LES AUTEURS

La Revue Roumaine de Chimie publie des articles en anglais, français, russe, allemand ou espagnol. Les auteurs sont priés d'envoyer des articles et des comptes rendus inédits.

Les manuscrits seront dactylographiés à double interligne. La bibliographie, les tableux et la légende des figures seront placés après le texte.

Si l'article fait partie d'une série numérotée, la partie précédente sera donnée comme première référence.

Chaque article sera précédé d'un résumé comprenant quinze lignes au maximum.

Les références bibliographiques dans le texte seront faites par des exposants sans parenthèses et paraîtront à la fin de l'ouvrage.

Les publications périodiques mentionnées dans la bibliographie seront présentées suivant les prescriptions internationales: le nom de l'auteur précédé de l'initiale du prénom, le titre du périodique abrégé conformément à « Chemical Abstracts » et souligné par une ligne, le numéro du tome indiqué par des chiffres arabes et souligné par deux lignes, suivi de la première page de l'article; à la fin, l'année de la parution sera placé entre parenthèses. Le numéro de la revue ne sera pas indiqué si les pages du volume sont numérotées consécutivement.

Les textes des livres ou traités inclueront : le nom des auteurs, l'initiale du prénom, le titre du livre entre guillemets et sans être souligné, le numéro du tome précédé par l'abréviation « vol. » (ou «Bd. »), le numéro de l'édition, les éditions (the publisher), la localité de la parution du livre, l'année de la parution et la page de la référence précédée(s) par l'abréviation « p. » (ou « S. »).

Les brevets seront indiqués comme suit : l'auteur ou la firme, le pays et le numéro du brevet, la date et la revue *(Chem. Abstr.)*. Par ex. : M. Jones (to Union Carbide Co), Brit. Pat. 601 238, 2 Sept. 1959; cf. *Chem. Abstr.*, **54**, 12808 (1960).

Si la référence n'a pas été lue en original, on indiquera aussi la revue de référence consultée.

Les diagrammes seront tracés à l'encre de Chine sur papier calque. Les tableaux et les figures (en nombre strictement nécessaire) ainsi que les courbes dans les figures seront numérotés par des chiffres arabes. Leur explication sera donnée dans la légende des figures. Prière de ne pas inscrire les mêmes données dans les tableaux et les figures. Chaque tableau aura un titre. On indiquera dans le texte la place approximative des tableaux et des figures. Les formules chimiques seront incluses dans le texte; en outre, elles seront transcrites sur papier calque, à l'encre de Chine.

Les auteurs sont priés d'indiquer les caractères italiques (en soulignant les lettres au crayon), ainsi que tout autre caractère spécial; les préfixes *ortho, meta, para, cis, trans*, etc. seront soulignés pour indiquer leurs caractères italiques et ne seront jamais écrits avec des majuscules.

Aucune correction à la main ne sera admise sur le manuscrit. Les corrections seront tapées à la machine. Les lettres grecques ou d'autres symboles spéciaux seront insérés à la main à l'encre clairement.

Le manuscrit sera signé par l'auteur.

Le titre-courant aura 50 lettres au maximum.

L'entière responsabilité du contenu des articles appartient aux auteurs.

Sur demande on peut obtenir une note plus complète.

PRINTED IN ROMANIA

TRAVAUX PARUS AUX ÉDITIONS DE L'ACADÉMIE DE LA RÉPUBLIQUE SOCIALISTE DE ROUMANIE

GH. MARCU, **Chimia compuşilor coordinativi**, 1984, 415 p.

E. CORDOŞ, C. MANOLIU, **Spectrometria de absorbţie şi fluorescenţă atomică**, 1984, 178 p.

C. BODEA editeur, **Tratat de biochimie vegetală**, p. I vol. 5, 1984, 438 p.

ELENA CEAUŞESCU, **Cercetări în chimia şi tehnologia polimerilor**, 1983, 519 p.

N. ASANDEI, A. GRIGORIU, **Chimia şi structura fibrelor**, 1983, 395 p.

N. IONESCU, M. CĂLDĂRARU, **Oxidarea catalitică a olefinelor inferioare**, 1983.

C. CAŞCAVAL, **Studiul polimerilor prin piroliză şi cromatografie de gaze**, 1983, 220 p.

C. I. SIMIONESCU, F. DANEŞ, **Originea vieţii**, 1983, 110 p.

C. BODEA (editeur), **Tratat de biochimie vegetală**, p. II, vol. IV, 1982, 408 p.

I. G. MURGULESCU, RODICA VÎLCU, **Introducere în chimia fizică. Vol. III, Termodinamica chimică**, 1982, 624 p.

I. G. MURGULESCU, J. PĂUN, **Introducere în chimia fizică, Vol. I.3 Nucleul atomic, reacţii nucleare, particule elementare**, 1982 606 p.

ELENA JERCAN, **Analiza cromatografică**, 1982, 286 p.

ELENA CEAUŞESCU, **Noi cercetări în domeniul compuşilor macromoleculari**, 1981, 536 p.

I. G. MURGULESCU, TATIANA ONCESCU, E. SEGAL, **Introducere în chimia fizică, Vol. II.2. Cinematică chimică şi cataliză**, 1981, 1024 p.

V. DRĂGUŢAN, A. T. BALABAN, M. DIMONIE, **Metateza olefinelor şi polimerizarea prin deschidere de inel a cicloolefinelor**, 1981, 254 p.

LYDIA-MARIA VAICUM, **Epurarea apelor uzate cu nămol activ. Bazele biochimice**, 1981, 218 p.

I. GĂLĂŢEANU, **Procese şi metode radiochimice în energetica nucleară**, 1981, 234 p.

O. IORDACHE, **Procese polistocastice aplicate la fenomenele de transfer**, 1981, 186 p.

CR. SIMIONESCU, VALERIA GORDUZA, **Polimeri biocompatibili şi biologic activi**, 1980, 479 p.

ELENA CEAUŞESCU, **Polimerizarea stereospecifică a izoprenului**, 1979, 307 p.

CONST. GH. MACAROVICI, **Analiza chimică cantitativă anorganică**, 1979, 457 p.

M. FLORESCU, **Metode ştiinţifice în dezvoltarea industriei chimice moderne**, 1979, 256 p.

A. T. BALABAN, I. GĂLĂŢEANU, G. GEORGESCU, LIGIA SIMIONESCU, **Compuşi marcaţi şi radiofarmaceutici cu aplicaţii în medicina nucleară**, 1979, 495 p.

I. G. MURGULESCU, E. SEGAL, **Introducere în chimia fizică. Vol. II. 1. Teoria molecular-cinetică a materiei**, 1979, 1036 p.

S. STERNBERG, FL. DANEŞ, **Termodinamica chimică aplicată**, 1978, 400 p.

I. G. MURGULESCU, V. EM. SAHINI, **Introducere în chimia fizică. Vol. I.2. Structura şi proprietăţile moleculelor**, 1978, 604 p.

I. ZUGRĂVESCU, MAGDA PETROVANU, **N-ylid chemistry**, coèdition avec McGraw-Hill International Book Company, U.S.A., 1977, 396 p.

I. G. MURGULESCU, **Introducere în chimia fizică. Vol. I.1. Atomi, molecule, legătură chimică**, 1976, 560 p.

ELENA CEAUŞESCU, **Research Work on synthesis and characterization of macromolecular compounds. Contributions**, 1974, 251 p.

CR. SIMIONESCU, VIORICA RUSAN, V. POPA, **Chimia algelor marine**, 1974, 212 p., 1 pl.

ISSN 0035—4090

I.P. INFORMAŢIA c. 2608

43 426

LEI 40

$ 75 (pour un abonnement annuel)

F1103

04

R 1985 MAR 0 8

ACADÉMIE DE LA RÉPUBLIQUE SOCIALISTE DE ROUMANIE

Veggészet

REVUE ROUMAINE DE CHIMIE

TOME 30

N° 2

Février 1985

Rev. Roumaine Chim. RRCHAX, 30, 2, p. 95–186 (1985) Bucarest

EDITURA ACADEMIEI REPUBLICII SOCIALISTE ROMÂNIA

ACADÉMIE DE LA RÉPUBLIQUE SOCIALISTE DE ROUMANIE

COMITÉ DE RÉDACTION

Rédacteur en chef :

I. G. MURGULESCU, membre de l'Académie de la République Socialiste de Roumanie

Rédacteurs en chef adjoints :

A. T. BALABAN et V. EM. SAHINI, membres correspondants de l'Académie de la République Socialiste de Roumanie

Collège de rédaction :

EM. BRATU, ELENA CEAUȘESCU, ECATERINA CIORĂNESCU-NENITZESCU, CR., SIMIONESCU, membres de l'Académie de la République Socialiste de Roumanie; GH. SPACU, membre correspondant de l'Académie de la République Socialiste de Roumanie; M. BANCIU, M. D. GHEORGHIU, I. HAIDUC, D. I. MARCHIDAN, I. MOLDOVAN, G. NIAC et D. SĂNDULESCU

La Revue Roumanie de Chimie paraît 10 fois par an. Toute commande de l'étranger sera adressée à « ROMPRESFILATELIA » — sectorul Export-Import-Presă, P.O. Box 12—201, télex 10376 prsfi r 78104, Calea Griviței nr. 64—66, București, Roumanie

Les manuscrits, les livres et les revues proposés en échange, ainsi que toute correspondance seront envoyés à la rédaction :

REVUE ROUMAINE DE CHIMIE
125, Calea Victoriei, 79717 Bucarest, Roumanie, téléphone 50 76 80

EDITURA ACADEMIEI REPUBLICII SOCIALISTE ROMÂNIA
125, Calea Victoriei, 79717 Bucarest, Roumanie, téléphone 50 76 80

REVUE ROUMAINE DE CHIMIE

INFORMÁCIÓS

Tome 30, N° 2 **Février, 1985**

MARIANA CIUREANU, MIHAELA HILLEBRAND, VICTOR EM. SAHINI and ELENA VOLANSCHI, U.H.F. spin density calculations on substituted nitroaromatic anion radicals 97–103

S. STERNBERG, MIHAELA UNGUREANU, V. BRÂNZOI and LILIANA APĂTEANU, Polarization behaviour of the *n*-type and *p*-type silicon in sulphuric acid — hydroquinone solutions 105–110

C. I. LEPĂDATU, The concept of electroenegativity in *Slater's* theory of the atom 111–116

C. CRISTESCU, *as*-triazine derivatives with potential therapeutic action. XIX. Synthesis of 5-(substituted-benzyl)thio-6-azauridines 117–123

HANS-HORST GLATT, MAMADOU FOULA BARRY, CAROL CSUNDERLIK, RADU BACALOGLU, MIHAI MEDELEANU and MARIA LANTOS, Imines of aminoazoles. I. Synthesis and characterization of some imines of 2-aminobenzoimidazole (in German) 125–131

MARIUS H. TERDIC and VICTORIA A. SMARANDACHE, Disubstituted phenothiazones. III. Syntheses of dimethyl-3H-phenothiazin-3-ones 133–139

RAMESH KUMARI, A. D. TANEJA and V. P. KUDESIA, Studies of enolization of some substituted acetoacetarylamides at different temperatures and concentrations 141–150

RADU VLĂDEA, Catalytic influences in the electrooxidation of olefins in non-aqueous solutions. I. Experimental aspects 151–155

RADU VLĂDEA and FRANCISC KEREK, Catalytic influences in electrooxidation of olefins in non-aqueous solutions II. Diisobutylene and styrene oxidation products 157–170

HOCINE KADI and D. P. LAZĂR, Identification of aromatic hydrocarbons from petroleum fractions. II. Identification by means of HPLC (in French) 171–178

H. A. EL-NAGGAR, A. RAMADAN and A. A. ABDEL-RASSOUL, Synergistic and antagonistic extraction of protactinum (V) by bis(2-ethyl hexyl) phosphoric acid and tributyl phosphate mixture 179–185

Rev. Roumaine Chim. 30, *2*, 95–186 (1985), Bucarest

Revue Roumaine de Chimie, **30**, 2, 97—103 (1985)

U.H.F. SPIN DENSITY CALCULATIONS ON SUBSTITUTED NITROAROMATIC ANION RADICALS

MARIANA CIUREANU, MIHAELA HILLEBRAND, VICTOR EM. SAHINI
and ELENA VOLANSCHI
Department of Physical Chemistry, Polytechnic Institute, Blvd. Republicii 13, Bucharest,
Romania

Received September 6, 1983

Unrestricted Hartree-Fock spin density calculations were performed on some substituted nitroaromatic anion radicals. The calculated proton hyperfine splittings reflect well the experimental differences brought about by the character of the substituents. New values for the nitrogen spin polarization parameters were obtained by the method of multiple regression using the UHF spin densities.

The ESR spectra of the nitroaromatic anion-radicals have been extensively investigated, the experimental results being mainly correlated with McLachlan spin densities. [1–3] All these studies revealed the dominating influence of the nitro group, even in the presence of other substituents.

The present paper aims to discuss the features of the spin density distribution calculated by a more refined procedure, the Unrestricted Hartree-Fock (UHF) method, in terms of Amos and Snyder's equations, [4] for a series of differently substituted nitroaromatic anion radicals. Therefore, various nitroderivatives (Fig. 1) containing substituents with different character, like methyl as electron repelling, — CHO as electron withdrawing and vinyl as a conjugative group, were considered. Since experimental results concerning some thioacyl nitrocompounds were available from a previous work, [5] these derivatives were enclosed too.

Moreover, since the existing spin polarization parameters for the nitro group are fitted for McLachlan spin densities, we consider interesting to use the UHF data for a new parametrization, using the method of multiple regression.

METHOD OF CALCULATION

The spin density calculations were performed by the UHF method with the annihilation of the superior spin component, using a program written in Fortran IV. [6] The semiempirical parameters used throughout the paper are listed in Table 1. The ionization potential of the thioamide nitrogen atom was taken to be smaller than the generally accepted value (—28.5 eV), in order to account for the inductive effect of the saturated ring. The methyl and methylene groups in compounds IIa, b and VI a, b were treated by a hyperconjugative model.

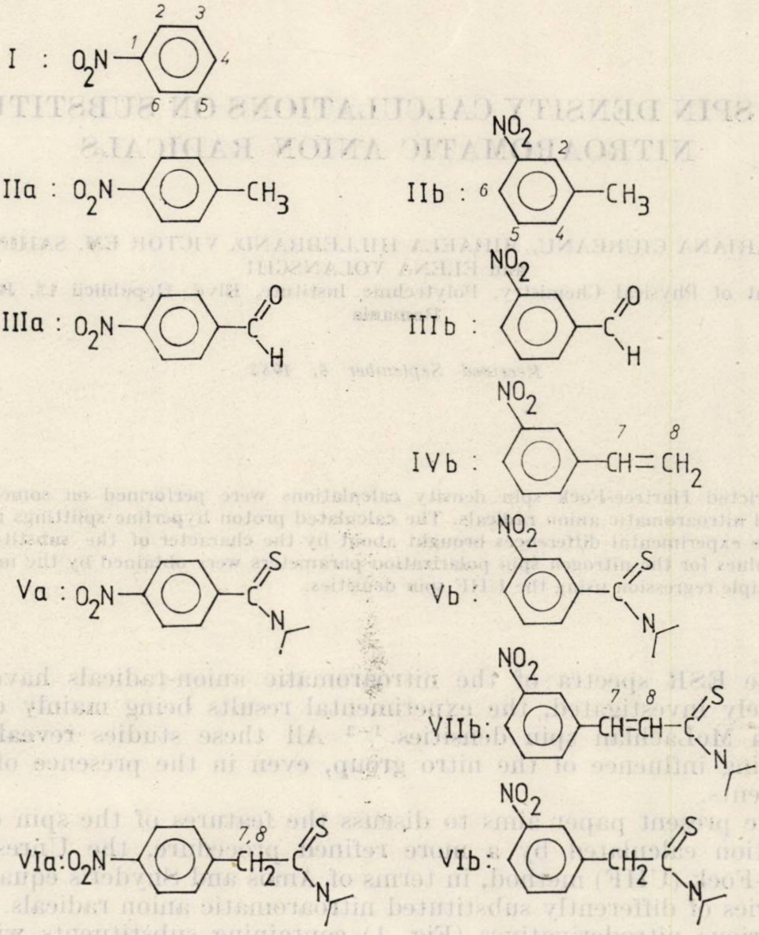
I
IIa
IIb
IIIa
IIIb
IVb
Va
Vb
VIIb
VIa
VIb
O_2N
NO_2
CH_3
O
H
S
N
CH=CH$_2$
CH=CH
CH$_2$
1
2
3
4
5
6
7
8
7,8

Fig. 1. — The substituted nitroaromatic compounds under investigation.

Table 1

Mono- and bicentric semiempirical MO parameters (eV)

Monocentric					Bicentric	
X	W_x	γ_{xx}	X−Y	β_{xy}	X−Y	β_{XY}
C	−11.16	11.13	C⋯C (aromatic)	−2.39	C(H_2)−H_2	−3.00
Ȯ	−17.28	15.23	C=O	−2.70	C(H_3)−H_3	−3.00
N̈ (NO_2)	−28.53	16.76	C=C (vinyl)	−2.79	CH_3-phenyl	−1.40
N̈ (amide)	−26.53	16.76	C=S	−1.83	C(phenyl)-C(vinyl)	−2.00
Ṡ	−11.86	9.92	C−N (VO_2)	−2.60	C(CH_2)−C(S)	−1.40
H_2(CH_2)	− 9.50	9.33	C(S)-N(amide)	−2.32	C(phenyl)-C(S)	−1.63
H_2(CH_3)	− 9.50	9.33	C(phenyl)-C(H_2)	−1.40	N−O (NO_2)	−2.60

The bielectronic bicentric repulsion integrals (γ_{ij}) were first evaluated by the Nishimoto-Mataga approximation, but even after the annihilation of the superior spin component, the $\langle S^2 \rangle$ values obtained were larger than 0.75. This effect, noted also in our previous work on some aminyloxide radicals, [7] as well as in other literature data [8] was shown to be independent of the parameter choice. In order to avoid this "spin contamination", it was foud convenient to follow the procedure indicated by Tino and Klimo[9] and use larger values for the repulsion integrals. Actually, the Pariser-Parr integrals were found to produce a decrease of the $\langle S^2_{aa} \rangle$ values to about 0.75, and the reported spin densities were evaluated using these values for the repulsion matrix.

RESULTS AND DISCUSSION

1. Proton hyperfine splittings

The theoretical proton hyperfine splittings (hfs) are collected in table 2, together with the experimental data taken from the references quoted in the last column.

Considering nitrobenzene as a typical nitroderivative, the data in table 2 reflect the features of the experimental hyperfine pattern (large splittings for the *ortho* and *para* protons). Although the theoretical values are somewhat overestimated, the theoretical a_p/a_o ratio (1.16) is nearly equal to the experimental one (1.09).

Table 2

Calculated and experimental proton hf splittings

Radical		a_2	a_3	a_4	a_5	a_6	a_7	a_8	Reference
I	exp.	0.330	0.103	0.382	0.103	0.330	—	—	10
	calc.	0.354	0.085	0.387	0.085	0.354	—	—	
II a	exp.	0.339	0.114	—	0.114	0.339	0.398	0.398	11
	calc.	0.353	0.082	—	0.082	0.353	0.413	0.413	11
IIIa	exp.	0.310	0.044	—	0.044	0.238	0.123	—	11
	calc.	0.320	0.004	—	0.007	0.256	0.069	—	
V a	exp.	0.324	0.100	—	0.085	0.324	—	—	5
	calc.	0.365	0.039	—	0.035	0.295	—	—	
VI a	exp.	0.300	0.112	—	0.112	0.300	0.355	0.355	5
	calc.	0.417	0.084	—	0.066	0.334	0.367	0.367	
II b	exp.	0.339	—	0.384	0.109	0.339	0.108	—	12
	calc.	0.332	—	0.350	0.084	0.333	0.056	—	
IV b	exp.	0.338	—	0.390	0.108	0.338	0.042	0.042	12
	calc.	0.336	—	0.445	0.092	0.408	0.019	0.025	
V b	exp.	0.353	—	0.428	0.112	0.353	—	—	5
	calc.	0.287	—	0.507	0.091	0.448	—	—	
VI b	exp.	0.348	—	0.410	0.108	0.348	0.108	0.108	5
	calc.	0.410	—	0.372	0.097	0.352	0.040	0.040	
VII b	exp.	0.307	—	0.420	0.102	0.360	0.053	0.045	5
	calc.	0.302	—	0.505	0.115	0.484	0.026	0.023	

The presence of the methyl in *para* vs. the nitro group (IIa) has only a minor effect on the experimental splittigs of nitrobenzene, a fact which is well accounted for by the UHF calculations : the calculated methyl and *ortho* proton splittings are almost equal to the corresponding protons in the anion radical I.

In comparison with the freely rotating methyl group, which does not affect the symmetry of the molecule, the —CHO substituent (anion radical IIIa) determines the nonequivalence of the two *ortho* (2,6) positions as a result of the restricted rotation around the phenyl-(C=O) bond. This nonequivalence is well reflected by the UHF hfs, as evidenced by the ratios : $(a_2/a_6)_{\mathrm{calc}} = 1.25$ vs. $(a_2/a_6)_{\mathrm{exp}} = 1.30$.

Although some ressemblance between the anion radicals of *p*-nitrothiobenzoylamide (Va) and *p*-nitrobenzaldehyde (IIIa) might be expected, the *ortho* protons (2,6) are equivalent for Va, pointing out a less restricted rotation around the phenyl-(C=S) bond. The UHF distribution does not account for this equivalence, but the calculated π-bond order $p_{\Phi-(\mathrm{C=O})}$ (0.4279) is higher than $p_{\Phi-(\mathrm{C=S})}$ (0.3108), in agreement with the above discussed experimental trends.

The calculated spin distributions for the anion radicals Va and VIa are less uniform than the experimental ones: the *ortho* proton hfs. are larger (the largest values are those of VIa), and the *meta* hfs. are smaller (i.e. about half of the experimental values) than the measured splittings. It should be noted that, in order the improve the calculated hfs. for these anion radicals, other parameters for the thioamide group were tried, but they were found to affect the overall agreement for the other compounds ; therefore, the values presented in table 1 were retained throughout the calculations.

If either the experimental or the theoretical hfs. of the anion radical VIa are compared to those of IIa, no noticeable differences are observed ; the splittings of the methyl protons in VIa are somewhat smaller, a fact which may be explained by the extended conjugation via the thioamide moiety.

In all the *meta* substituted nitroderivatives (b-series) excepting VIIb, the protons in *ortho vs.* the nitro group (2,6) are equivalent. In the calculated spin distribution these splittings are not equal, the difference being negligeable for *m*-nitrotoluene and maximum for VIIb, in agreement with the experimental data.

A comparison of the hfs. for the thioamide-containing radicals qIΛ and VIIb with those of the simpler related radicals IIb, respectively IVb, reveals the following experimental effects produced by the thioamide moiety :

— An increase of a_4 and a decrease of a_2 when the connection with the nitrosubstituted ring is assured by the conjugative group CH=CH, i.e. $(a_{\mathrm{VIIb}}/a_{\mathrm{IVb}})_2 < 1$, $(a_{\mathrm{VIIb}}/a_{\mathrm{IVb}})_4 > 1$.

— An increase of all the large splittings (a_2, a_4, a_6) when the —C=S group is connected to the benzenic ring via a methylene group, $(a_{\mathrm{VIb}}/a_{\mathrm{IIb}})_{2,4,6} > 1$.

Although the theoretical hfs. values are generally larger than the experimental ones, the ratios of the theoretical splittings (Table 3) reflect in a reasonably good manner the experimental statements.

However, for VIb the effect on site 2 in the calculated spin distribution is overemphasized, leading to a value exceeding that of a_4 (*para* to the nitro group), which is generally the greatest in all the nitroanion radicals.

Table 3

Experimental and theoretical ratios of the hfs. in the thioamide-containing vs. the corresponding simpler anion radicals

Site i	$(a_{\mathrm{VIIb}}/a_{\mathrm{IVb}})_i$		$(a_{\mathrm{VIb}}/a_{\mathrm{IIb}})_i$	
	Exp.	Calc.	Exp.	Calc.
2	0.908	0.900	1.026	1.239
4	1.076	1.133	1.068	1.069
6	1.065	1.188	1.026	1.058

2. Nitrogen splittings

The nitrogen hyperfine splittings were evaluated from the calculated spin densities using four sets of spin polarization parameters, recommended by different authors.

However, no one of the values employed (Table 4) gave a reasonable agreement with the experimental data. This is obviously due to the fact that all the four sets of spin polarization parameters were fitted for other kinds of spin density calculations (McLachlan, HF with nonorthogonal atomic orbitals, etc.). Consequently, we used the method of multiple regression to obtain new nitrogen spin polarization parameters in connection with the UHF spin densities.

Table 4

UHF spin densities for the nitro group and nitrogen hfs. evaluated by different methods (mT)

Rad.	ρ_N	ρ_O	ρ_C	a_N^{calc}				a_N^{exp}
				1	2	3	4	
I	0.311	0.134	0.050	1.606	2.119	0.631	0.609	1.062
IIa	0.307	0.133	0.049	1.584	2.087	0.623	0.601	1.079
III a	0.187	0.107	0.101	0.879	1.085	0.302	0.366	0.583
V a	0.217	0.107	0.089	1.076	1.381	0.391	0.425	0.825
VI a	0.241	0.120	0.078	1.191	1.524	0.450	0.472	1.065
II b	0.341	0.140	0.038	1.785	2.373	0.710	0.668	1.070
III b	0.266	0.124	0.059	1.343	1.745	0.523	0.520	0.892
IV b	0.295	0.121	0.055	1.544	2.054	0.593	0.578	0.983
V b	0.257	0.116	0.069	1.311	1.713	0.495	0.503	0.977
VI b	0.323	0.133	0.038	1.692	2.247	0.670	0.632	1.020
VII b	0.275	0.115	0.052	1.433	1.899	0.552	0.538	0.950

1. $a_N = 3.295\,(2\rho_N - \rho_0)$ [13]
2. $a_N = 9.90\,\rho_N - 3.58 \sum_i \rho_{0_i}$ [1]
3. $a_N = 2.273\,\rho_N - 0.929\,\rho_C - 0.108 \times 2\rho_0$[14]
4. $a_N = 1.958\,\rho_N$[14]

We have selected for this purpose only the anion radicals which do not contain the thioamide group. The omission of the thioamide-containing radicals is justified by the increased number of semiempirical MO parameters introduced by this structural entity. Further reason for this choice, which makes the UHF nitro group spin densities more reliable for a calibration, is the better agreement between the experimental and theoretical proton hyperfine splittings.

Considering the nitrogen and oxygen spin densities for the anion radicals, I, IIa, IIb, IIIa, IIIb, and IVb, the following relationship was found to hold :

$$a_{\mathrm{N}}(\mathrm{mT}) = 3.576\,\rho_{\mathrm{N}}^{\pi} - 0.285 \sum_{i} \rho_{\mathrm{O}_i}^{\pi} \qquad (1)$$

Table 5

Nitrogen splittings calculated with eq. (1) (mT)

Rad.	$a_{\mathrm{N}}^{\mathrm{calc}}$	$a_{\mathrm{N}}^{\mathrm{exp}}$	Rad.	$a_{\mathrm{N}}^{\mathrm{calc}}$	$a_{\mathrm{N}}^{\mathrm{exp}}$
I	1.036	1.062	II b	1.139	1.070
II a	1.022	1.079	III b	0.880	0.892
III a	0.608	0.583	IV b	0.986	0.983
V a	0.715	0.825	V b	0.987	0.977
VI a	0.793	1.065	VI b	1.078	1.020
			VII b	0.918	0.950

This equation was used to evaluate the nitrogen hyperfine coupling constants for all the anion radicals (Table 5). The results are in a considerably better agreement with the experimental data than those calculated by other procedures, even for the radicals not taken into account in the estimation of $Q_{\mathrm{N}}^{\mathrm{N}}$ and $Q_{\mathrm{O}}^{\mathrm{N}}$.

Inspection of the data in table 5 reveals the following features, well accounted for by the UHF calculations :

— The introduction of an electron accepting substituent (CHO, 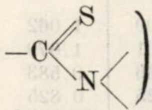 in nitrobenzene (I) results in a decrease of the nitrogen hfs ; this effect is more important for the *para*-substituted anion radicals (IIIa, Va) as compared to the *meta*-nitrothiobenzoyl anion radical (Vb). The lowest value is noted for the anion radical IIIa, owing to the larger electron withdrawing power of the —CHO substituent.

— The trend experimentally observed for the nitrogen hyperfine splittings, consistent with the decrease of conjugation in the series

$$a_{\mathrm{N}}(\mathrm{VIII}) < a_{\mathrm{N}}(\mathrm{V}) < a_{\mathrm{N}}(\mathrm{VI})$$

is well accounted for by the UHF calculated hfs. for the *meta* series ; as the *para*-substituted series is concerned, although the agreement of the calculated to the experimental hfs is poor, the same trend is observed ($a_{\mathrm{N}}(\mathrm{Va}) < a_{\mathrm{N}}(\mathrm{VIa})$).

In conclusion, it may be inferred that, in spite of the diversity substituents and parameters, the agreement of the UHF calculated spin densities with the experimental data is reasonably good for all the proton splitting constants.

The present values determined for the nitrogen spin polarization parameters were found to be suitable for the evaluation of the nitrogen splittings in terms of UHF spin densities.

REFERENCES

[1] P. H. Rieger and G. K. Fraenkel, *J. Chem. Phys.*, **39**, 609 (1963).

[2] A. H. Maki and A. J. Stone, *J. Chem. Phys.*, **38**, 1999 (1963).

[3] D. H. Geske, J. L. Ragle, M. A. Bambenek and A. L. Balch, *J. Amer. Chem. Soc.*, **86**, 987 (1964).

[4] A. T. Amos and J. Snyder, *J. Chem. Phys.*, **41**, 1773 (1964); **42**, 3670 (1964).

[5] C. Cercasov, F. Cornea, M. Ciureanu, M. Hillebrand, V. E. Sahini and E. Volanschi, *Org. Magn. Resonance*, **20**, 217 (1982).

[6] M. Huillebrand and V. E. Sahini, *Bul. I.P.B., Seria Chimie-Metalurgie*, **40**, 23 (1978).

[7] M. Hillebrand and A. T. Balaban, *Rev. Roumaine Chim.*, **25**, 995 (1980).

[8] J. Ladik, G. Biczo, I. Kande and L. Sumegi, *Acta Chimica Acad. Scient. Hung.*, **61**, 381 (1969).

[9] J. Tino and V. Klimo, *Collection Czechoslovak Chem. Commun.*, **41**, 960 (1976).

[10] T. Fujinaga, Y. Deguki and K. Umemoto, *Bull. Chem. Soc. Japan*, **37**, 822 (1964).

[11] A. H. Maki and D. H. Geske, *J. Amer. Chem. Soc.*, **83**, 1853 (1961).

[12] M. Barzaghi, A. Gamba. G. Morossi and M. Simonetta, *J. Phys. Chem.*, **78**, 49 (1974).

[13] M. Barzaghi, P. L. Beltrame, A. Gamba and M. Simonetta, *J. Amer. Chem. Soc.*, **100**, 251 (1978).

[14] D. N. Nanda and P. T. Narashimhan, *Theor. chim. Acta*, **32**, 231 (1973).

Rev. Roumaine de Chimie, 30, 2, 105—110 (1985)

POLARIZATION BEHAVIOUR OF THE *n*-TYPE AND *p*-TYPE SILICON IN SULPHURIC ACID – HYDROQUINONE SOLUTIONS

S. STERNBERG*, MIHAELA UNGUREANU*, V. BRÂNZOI* and LILIANA APĂTEANU**

* Polytechnic Institute of Bucharest, Romania

** Institute of Chemical and Biochemical Energetics, Bucharest, Romania

Received December 21, 1983

The polarization behaviour of the *n*- and *p*-type silicon electrodes with different dopping levels in sulphuric acid solutions with and without hydroquinone addition was studied by means of the potentiostatic method.

INTRODUCTION

The present paper represents a contribution to the semiconductor silicon electrodes study that means the polarization behaviour of the silicon electrodes in different electrolytical media. The poor data in the literature in this field could be explained by the fact that the monocrystalline silicon of high purity is obtained very difficultly and at the contact with an aqueous electrolyte an oxide layer of complex and variable composition is formed at the silicon [1,2].

The paper contains the study of the behaviour of semiconductor silicon, at anodic and cathodic polarization, in an aqueous solution of H_2SO_4, in the presence and absence of hydroquinone, in steady state conditions.

EXPERIMENTAL

Measurements were carried out by potentiostatic technique, using a Model 173 Princeton Apllied Research potentiostat. The scheme of the potentiostatic device is presented in figure 1.

The working cell was in Pyrom glass and is presented in figure 2. The working electrodes, as described previously, [3] were disks of monocrystalline semiconductor silicon of 1—2 mm thickness, sealed in a Pyrom glass tube, as shown in figure 3.

The electric contact at the polarization of the silicon disk was realized by a copper wire in mercury.

In order to prevent a Hg—Si rectifier contact the inside of the n-type silicon disks was doped by diffusion with phosphorus from $POCl_3$ at 1255 °C. In the same way the inside of the p-type silicon disks was saturated with boron by painting with B_2O_3 and heating up to 1255 °C. The reaction products formed during the thermal diffusion were moved by a special electrochemical treatment. [4] The silicon slices, nn^+ and pp^+ doped, were metallized by chemical deposition of Ni and by gold electrodeposition in aqueous solutions. The electrode was assembled as shown in figure 3. Before each determination a renewal of the silicon disk surface was realized by the following treatment : etching in HNO_3 (70 %) and HF (50 %) 1 :1 mixture, etching in HF (50 %) solution rinsed (3—4 times) in distilled water. Prior to each experiment the silicon electrode was maintained for 15 minutes at a potential which assures the complete cleaning of the surface by an intense evolution of H_2. After that the silicon electrode was polarized by steps of 50 mV. For each step the value of the steady state current was registered. (In order to compare the results, a polarization curve on a Pt sheet of 1 cm² area was also registered in steady conditions). As a reference electrode a saturated calomel electrode was used, joined by a Luggin capillary. The reagents were of p.a. purity. Experiments were carried out at a constant temperature of 20 °C in dark.

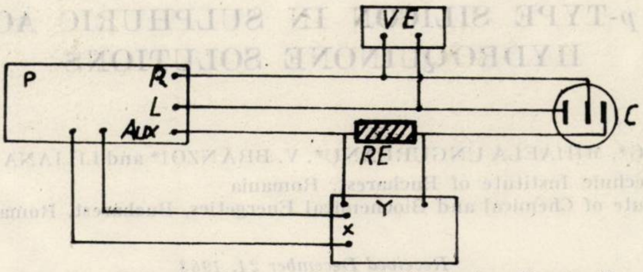

Fig. 1. — Scheme of the potentiostatic device. P-potentiostat ; X—Y — recorder ; V.E. — electronic voltmeter, C — electrolytical cell ; R.E. — standard load.

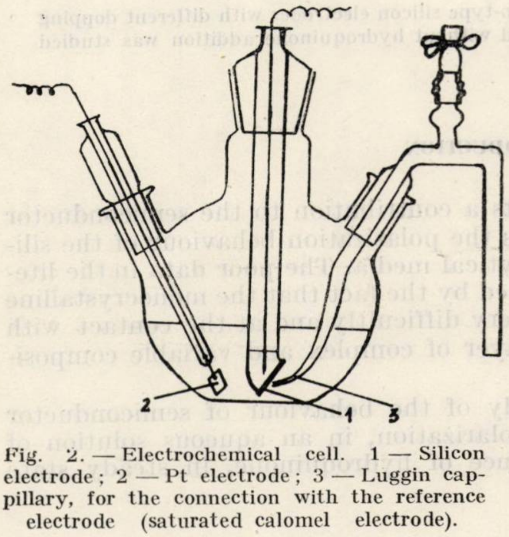

Fig. 2. — Electrochemical cell. 1 — Silicon electrode ; 2 — Pt electrode ; 3 — Luggin cappillary, for the connection with the reference electrode (saturated calomel electrode).

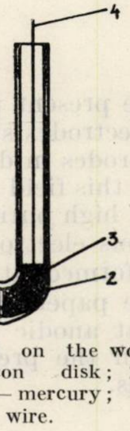

Fig. 3. — Detail on the working electrode. 1 — Silicon disk ; 2 — Pyrom glass tube ; 3 — mercury ; 4 — copper wire.

RESULTS AND DISCUSSIONS

The anodic and cathodic polarization behaviour of the silicon electrodes, in sulphuric acid solutions of 1.24 g/cm³ density, in steady state conditions, was studied. In parallel, the behaviour of these electrodes in sulphuric acid solutions containing an organic substance, 10^{-2} M hydroquinone, capable to support an electrode process, was also studied. Figure 1 shows a representative curve, obtained at the polarization of an *n*-type silicon electrode in sulphuric acid solution, in the absence and presence of hydroquinone.

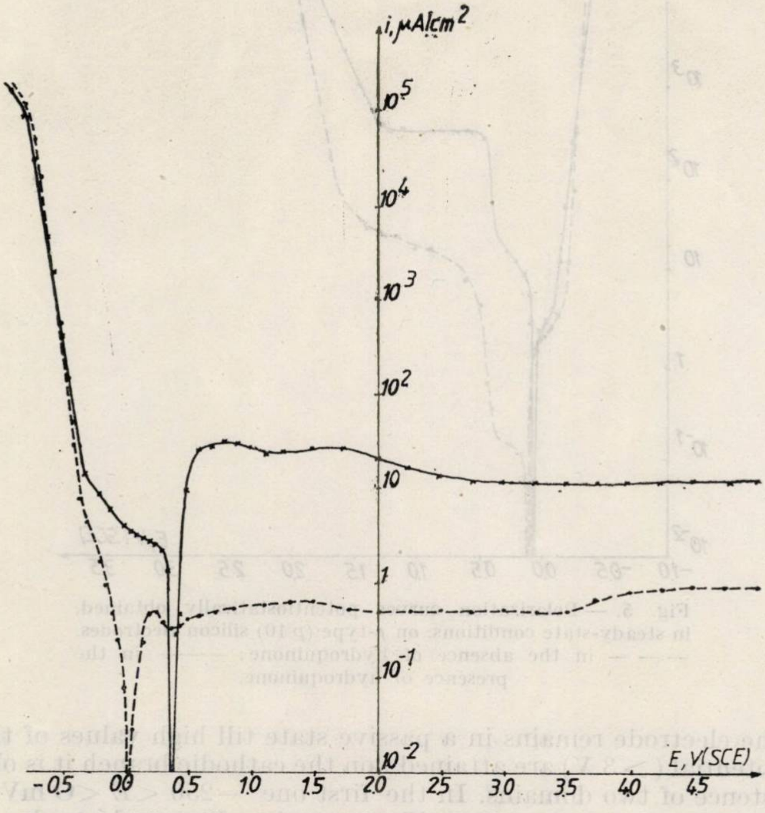

Fig. 4. — Polarization curves potentiostatically obtained, in steady state conditions on *n*-type (*n* 1,6) silicon electrodes. — — — in the absence of hydroquinone; ——— in the presence of hydroquinone.

In figure 5 are given the polarization curves on the platinum electrode, in the same solutions. Figure 5 shows a representative curve obtained at the polarization of a *p*-type silicon electrode in sulphuric acid solution in the absence and presence of hydroquinone. Table 1 contains the electrochemical parameters for the five types of the studied electrodes.

The polarization curves of the electrodes have the following shape: — on the anodic branch it is initially observed an increase of the current till the dissolution rate of the silicon becomes equal with the rate of formation of the silicon oxides; after that the surface covers gradually with an oxide layer which passivates the electrode and the current density decreases to a very small value, of about 1μA/cm².

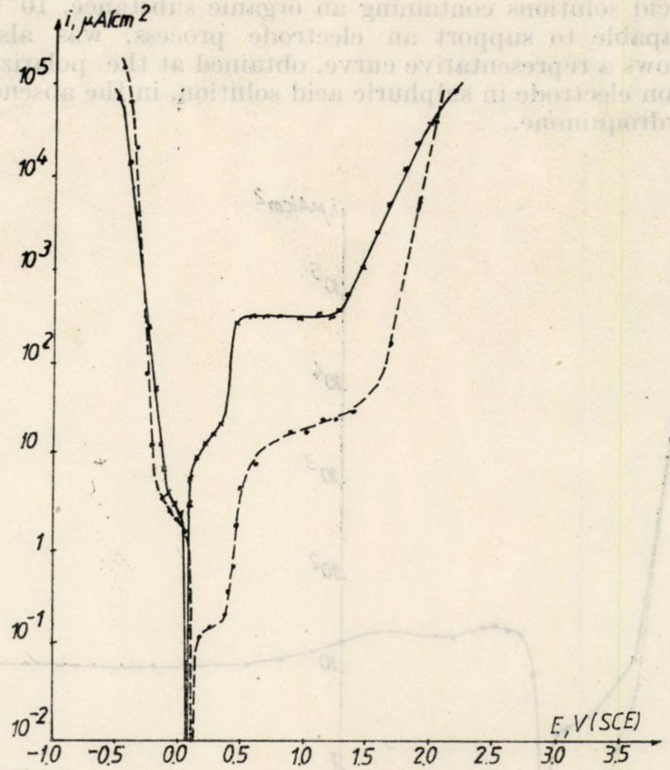

Fig. 5. — Polarization curves potentiostatically obtained, in steady-state conditions, on *p*-type (*p* 10) silicon electrodes. — — — in the absence of hydroquinone ; ——— in the presence of hydroquinone.

The electrode remains in a passive state till high values of the electrode potential (> 3 V) are attained : on the cathodic branch it is observed the existence of two domains. In the first one $-250 < E < 0$ mV (SCE)/ a cathodic process which is specific to semiconductor electrodes occurs, with small current and a braking determined by a relatively small concentration of the charge carriers. In the second one/$E < -250$ mV (SCE)/ the cathodic current is much higher and can be compared with that one obtained on platinum. On the cathodic branch the process of evolution of hydrogen occurs with a high limiting current density, of about $10^5 \mu A/cm^2$.

The steady state potential is within the /0−160 mV (SCE)/ range. In the presence of hydroquinone a change is observed of the shape of the polarization curve, which results in the appearance of a cathodic limiting current, the movement of the steady state potential $\Delta E = E_0^* - E_0$ ($E_0^* =$ = the equilibrium potential in the presence of hydroquinone) with about 300 mV, in the positive direction, the increase of the anodic current of about 40 times.

A dependency in noticed between the steady state potential and the charge carriers concentration of the silicon electrode (an increase with the

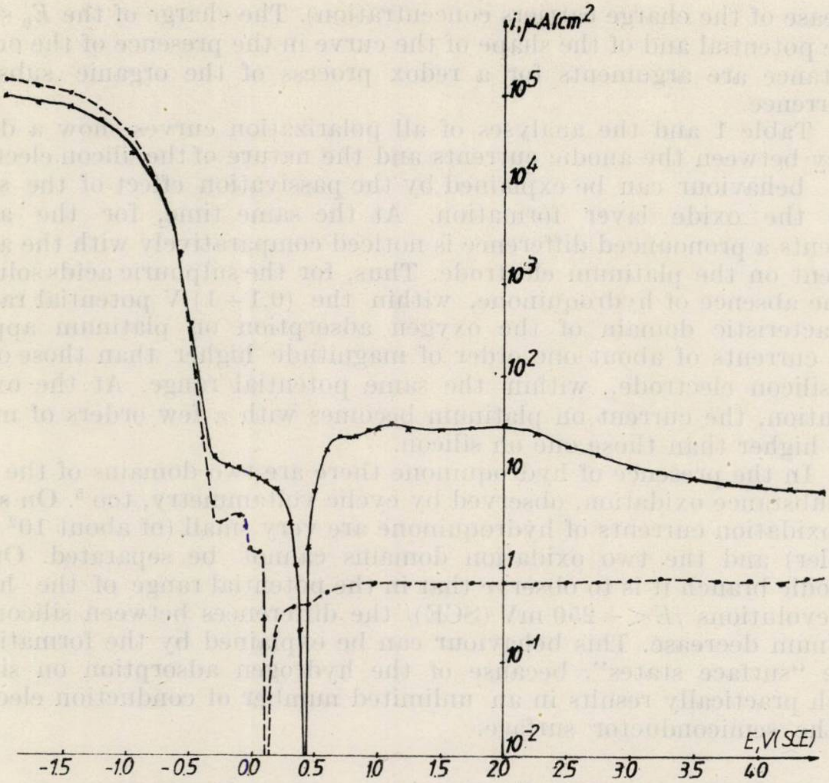

Fig. 6. — Polarization curves, potentiostatically obtained, in steady-state conditions, on p-type (p 10) silicon electrodes. — — — in the absence of hydroquinone ; ——— in the presence of hydroquinone.

Table 1

Electrochemical parameters at the polarization of n- and p-type silicon in sulphuric acid solutions, in the absence and in the presence of hydroquinone.

Type of silicon electrode (resistivity)		n (0.01 Ωcm)	n (1.6 Ωcm)	n (70 Ωcm)	p (10 Ωcm)	p (100 Ωcm)
Equilibrium potential, E_0 (SCE), V		−0.020	0.020	0.115	0.125	0.160
E_0 change in the presence of hydroquinone $\Delta E = E_0^* - E_0$ (V)		0.395	0.360	0.150	0.310	0.215
Tafel slope for hydrogen, mV		85	101	115	115	140
Tafel slope for hydrogen in the hydroquinone presence, mV		89	102.5	120	115	145
Passivation current, μA/cm²		1.4	0.5	0.6	0.7	0.6
The limiting current in the presence of hydroquinone μA/cm²	Cathodic	5	3.5	10	10	15
	Anodic	45	32	45	30	28

increase of the charge carriers concentration). The charge of the E_0 steady state potential and of the shape of the curve in the presence of the organic substance are arguments for a redox process of the organic substance occurrence.

Table 1 and the analyses of all polarization curves show a dependency between the anodic currents and the nature of the silicon electrode. This behaviour can be explained by the passivation effect of the silicon with the oxide layer formation. At the same time, for the anodic currents a pronounced difference is noticed comparatively with the anodic current on the platinum electrode. Thus, for the sulphuric acids solutions in the absence of hydroquinone, within the $(0.1 \div 1)$ V potential range a characteristic domain of the oxygen adsorption on platinum appears, with currents of about one order of magnitude higher than those one on the silicon electrode, within the same potential range. At the oxygen evolution, the current on platinum becomes with a few orders of magnitude higher than those one on silicon.

In the presence of hydroquinone there are two domains of the organic substance oxidation, observed by cyclic voltammetry, too [5]. On silicon the oxidation currents of hydroquinone are very small (of about 10^2 times smaller) and the two oxidation domains cannot be separated. On the cathodic branch it is to observe that in the potential range of the hydrogen evolutions $/E < -250$ mV (SCE)/ the differences between silicon and platinum decrease. This behaviour can be explained by the formation of some "surface states", because of the hydrogen adsorption on silicon, which practically results in an unlimited number of conduction electrons on the semiconductor surface.

REFERENCES

[1] V. A. Myamlin, and Yu, V. Pleskov, "Electrochemistry of semiconductors", Plenum Press, New York, 1967.

[2] S. Sternberg, V. Brânzoi, L. Apăteanu and M. Ungureanu, *Revista de Metalurgie* (under press).

[3] S. Sternberg, I. Lingvay and T. Vișan, *Rev. Roumaine Chim.*, **27**,, 1985 (1982).

[4] I. Lingvay, F. Daneș and M. Scarlat, *Rev. Roumaine Chim.* (under press)

[5] S. Sternberg, M. Ungureanu, *Rev. Roumaine Chim.*, (under press).

Revue Roumaine de Chimie, **30**, 2, 111–116 (1985)

THE CONCEPT OF ELECTRONEGATIVITY IN *SLATER'S* THEORY OF THE ATOM

C.I. LEPĂDATU

Center of Chemical Physics, Spl. Independenței 202, Bucharest, Romania

Received July 21, 1982

It is shown that the double of Mulliken's electronegativity means the energy required to bring a couple of electron charges to a distance equal to that between nucleus and the valence shell of a chemical element. The connection with the Fermi energy of the atom is also discussed.

I. INTRODUCTION

Quite recently, the concept of electronegativity has received a great deal of attention. Parr et al. [1] based on the density functional theory of Hohenberg and Kohn,[2] have shown that the electronegativity may be identified with the negative of the chemical potential. This fundamental idea has been discussed in a series of papers. [3–8]

The aim of the present note is to give another interpretation of the atomic electronegativity, in the frame of Slater's theory of the atom.[9] We shall define the electronegativity as the sum of ionization potential and electron affinity of the element

$$X_Z = I\,(Z, Q = +1) + I\,(Z, Q = -1), \tag{1}$$

where the first term is the ionization potential, the second term the electron afinity, Z the atomic number and Q the ionic charge (for a neutral element, $Q = 0$).

X_z represents the double of Mulliken's electronegativity, [10] usually estimated from experimental ionization potentials and electron affinities.[11–14] We shall attempt, in the following, to derive analytical expressions for $I(Z, Q = \pm 1)$, in order to obtain the electronegativity as a function of Z and Q. The expression thus found, leads to a very simple meaning of electronegativity.

II. FORMULAS FOR ATOMIC ENERGY, IONIZATION POTENTIAL AND ELECTRON AFFINITY

For this purpose, we use Wilson's formula [15] for the exact nonrelativistic ground state energy of an atom

$$E = -\int_{z'=0}^{Z}\left[\int_{0}^{\infty}\frac{\rho(r, z')}{r}\,\mathrm{d}r\right]\mathrm{d}z', \tag{2}$$

where $\rho\ (r, z')$ is the electron density function.
An expression for the ground state energy of an atom may be derived, using an approximate density function built from Slater type orbitals :

$$\rho\ (r, z') \approx \sum_{n} N_n \,|\, r\, R_n(r, z')\,|^2, \tag{3}$$

where n is the principal quantum number, N_n the electron population of a shell and $R(r, z')$ the radial part of the Slater type orbitals. Note that the integration in equation 2 must be done over z', from zero to Z_{ef} (effective nuclear charge). In this case, equation 2 becomes :

$$E = -\sum_{n} N_n \frac{Z_{ef}^2}{2n^2}. \tag{4}$$

Formula 4 may be used to obtain the ground state energy as a function of Z and Q. For this purpose, the following relationship is used for the efective nuclear charge of the valence shell :

$$Z_{ef} = aZ + (1 - a)\,Q - C_n, \tag{5}$$

where Z is the atomic number, Q the ionic charge, negative or positive, $a = 0.65$ and C_n is a constant equal to $+\,a$ (for $2s$, $2p$) and $3a +$ $+\,3$(for $3s$, $3p$). This expression has been obtained with Slater's rules.[9]

The ground state energy of the atoms having the electronic configurations $(1s)^2\,(2s, 2p)^{Z-Q-2}$ and $(1s)^2\,(2s, 2p)_8\,(3s, 3p)^{Z-Q-10}$ may be found from (4)—(5) and Slater's rules for the inner shells.[9] It is of the form :

$$E(Z, Q) = I_0\,(Z) + I(Z, Q), \tag{6}$$

where (in atomic units) :

$$I_0(Z) = -\frac{1}{2n^2}\,\frac{1}{400}\,[169Z^3 + 2524Z^2 - 1075Z - 50] \tag{7}$$

$$I(Z, Q) = \frac{1}{2n^2}\,\frac{1}{400}\,[49Q^3 + (133Z - 84)\,Q^2 + (-13Z^2 + 208Z - 195)Q],$$

for $(2s, 2p)$ — row $(Z = 3-10)$, and

$$I_0(Z) = -\frac{1}{2n^2}\frac{1}{400}[169Z^3 + 10136Z^2 - 28539Z + 26640] \tag{8}$$

$$I(Z, Q) = \frac{1}{2n^2}\frac{1}{400}[49Q^3 + (133Z - 896)Q^2 + (-13Z^2 + 632Z - 4059)Q],$$

for $(3s, 3p)$ — row $(Z = 11-18)$.

$I_0(Z)$ represents the ground state energy for the neutral elements. $I(Z, Q)$ is the ionization energy $(Q > 0)$ or affinity $(Q < 0)$.

$I_0(Z)$ reproduces fairly well the Hartree-Fock ground state energies and may be favourably compared with those experimentally determied.[17] $I(Z, Q)$ gives satisfactorily the first ionization energies $(Q = +1)$, but the electron affinities $(Q = -1)$ are rather poor if they are compared with the experimental ones.[18] Higher ionization energies are not generally reproduced.

Note that $E(Z, Q)$ function has its minimum for $Q < 0$. Indeed, the minimum

$$\frac{dE(Z,Q)}{dQ} = \frac{dI(Z,Q)}{dQ} = 0,$$

for the $(2s, 2p)$—row lies for the Q values within -0.57 (Li) and -0.238(Ne) and for the $(3s, 3p)$—row between -1.428(Na) and -1.09(Ar). The energy versus Q curve is very smooth near its minimum, the difference between $E(Z, Q)_{Q=0}$ and $E(Z, Q)_{\min}$ being of only some eV's.

III. THE CONCEPT OF ELECTRONEGATIVITY

If the quantities $I(Z, Q = \pm 1)$, eqs. 7—8, are introduced into (1), using equation 5, one obtains (in eV):

$$X_Z \simeq 13.9\frac{Z_{ef}e^2}{n^2} + 0.8. \tag{9}$$

We have thus found a unique formula for the electronegativity of the neutral elements $Z = 3-18$. Because the Rydberg constant is equal to 13.6 eV and $r_n^{-1} = Z_{ef}/n^2$, (9) becomes:

$$X_Z \simeq R\frac{e^2}{r_n} + 0.8, \tag{10}$$

where the first term would represent the energy required to remove the electron from an imaginary hydrogen atom, namely from the distance of the valence shell of the element to infinity. The meaning of the second term may be guessed, if we put $r_n = a_0$, the Bohr radius. According to (1) and (9), the constant 0.8 eV must be the affinity of the hydrogen atom (experimental value[18] 0.747 eV).

An expression similar to (10) can be also obtained with the vector model of the atom :[19]

$$X_Z \simeq = \pi\,(ll) \approx R\frac{e^2}{r_n}, \tag{11}$$

where $\pi\,(ll)$, $l = s, p, d, f$ represents the interaction energy for pairs of identical electrons .[20] As has been shown, [19] π (and therefore X) is roughly equal to the energy necessary to bring a hydrogenlike couple of electron charges to a distance equal to that between nucleus and the valence shell of the element.

Table 1 gives the electronegativity of the (2*s*, *sp*)-row of elements, obtained with (11) (or (10) without the free term), where $r_n^{-1} = Z_{ef}/n^2$ is calculated using expression (5).

Table 1

Atomic electronegativitaties for the (2s, 2p)-row of elements

Element	Li	Ba	B	C	N	O	F
X_Z (eV)	4.42	6.63	8.84	11.05	13.26	15.47	17.68
in X_{Li} units	1.0	1.5	2.0	2.5	3.0	3.5	4.0
Pauling's system[a)]	1.0	1.5	2.0	2.5	3.0	3.5	4.0

a) L. Pauling, "The Nature of the Chemical Bond" (Cornell Univ. Press., Ithaca, 1960).

As may be seen in Table 1, there is a striking parallelism between the relative electronegativites and those given by Pauling [21] (both are expressed in units of Lithium electronegativity). This parallelism is less obvious for the other rows of elements.

IV. ELECTRONEGATIVITY AND FERMI ENERGY

The present interpretation of the electronegativity may be connected with the Fermi energy of the atoms, i.e. with the energy of the highest occupied levels. For this purpose, we shall assume that the electrons behave in the valence shells of the atoms as a gas of free electrons. According to the free electron gas theory (tridimensional case), the Fermi energy is given by the formula [22] :

$$\varepsilon_F = \frac{\hbar^2}{2m}\,(3\pi^2\rho)^{2/3}, \tag{12}$$

where ρ is the electron concentration. For a single electron in the valence shell, the electron concentration coincides with the atomic one .[22] Table 2 gives the eletronegativities obtained with (11), where $r_n^{-1} = Z_{ef}/n^2$ is calculated using expression (5) and Slater's rules [9] for the effective principal quantum number. They are compared with the Fermi energy values calculated using the atomic concentrations given by Kittel [22].

Table 2

Electronegativities and Fermi energies (in eV)

$(ns)^1$	X_{Slater}	ε_F	$(ns)^2$	C_{Slater}	ε_F
Li	4.42	4.75	Be	6.63	8.91
Na	3.32	3.24	Mg	4.26	4.47
K	2.19	2.12	Ca	2.83	2.95
Rb	1.87	1.85	Sr	2.42	2.48
Cs	1.70	1.58	Ba	2.20	2.31
$(ns)^2(np)^1$			$(ns^2)(np)^2$		
B	8.84	9.35	C	11.05	11.44
Al	5.29	5.60	Si	6.27	4.95
Ga	4.97	5.01	Ge	5.61	4.56
In	4.25	4.14	Sn	4.80	3.99
Tl	3.85	3.90	Pb	4.36	3.75

As may be seen in Table 2, the agreement between X_Z and ε_F is satisfactory for those elements having for their valence shell, $n = 3-6$. The agreement is less satisfactory for some other elements (Be, B, Si, Ge, Sn, Pb). A reason could be the inequivalency [23] between the (ns) — and (np) — shells, neglected in Slater's model of the atom.

Table 3 gives the Fermi energy and the electronegativity values calculated on the one hand with Slater's rules [24] and on the other hand with Burns' rules[24] which make the difference between the (ns) — and (np) — shells.

Table 3

Electronegativities* and Fermi energies (in eV)

$(ns)^2(np)^2$	X_S	X_{ns}	X_{np}	ε_F	$(ns)^2(np)^3$	X_S	X_{ns}	X_{np}	ε_F
Si	6.27	6.95	4.91	4.95	P	7.25	7.93	5.89	—
Ge	5.61	8.16	5.31	4.56	As	6.26	8.71	5.87	4.71
Sn	4.80	5.22	3.40	3.99	Sb	5.36	5.58	3.75	3.76
Pb	4.36	3.62	2.36	3.75	Bi	4.86	3.87	2.61	3.38
$(ns)p^2(np)^4$					$(ns)^2(np)^5$				
S	8.23	8.92	6.88	—	Cl	9.21	9.90	7.86	—
Se	6.90	9.27	6.42	4.02	Br	7.55	9.82	6.97	—
Te	5.91	5.93	4.11	3.47	I	6.46	6.28	4.46	3.0
Po	5.36	4.12	2.85	3.26	At	5.86	11.55	8.20	—
$(n—1)d^{10}(ns)^1$					$(n—1)d^{10}(ns)^2$				
Cu	3.68	6.55	—	7.01	Zn	4.32	7.06	—	5.92
Ag	3.15	4.19	—	5.49	Cd	3.70	4.52	—	4.70
Au	2.85	2.91	—	5.52	Hg	3.35	3.14	—	4.44

* X_{ns}, X_{np} are electronegativities obtained with Burns atomic orbitals.[16]

We have used Burns' wavefunctions ,[24] because they claim to reproduce fairly well the moments $r^q (q = -3 \text{ to } +4)$, which have to do with r_n^{-1} involved in (11). As may be seen in Table 3, the values obtained with (11) and (12) agree satisfactorily if X_{np} values are compared with the Fermi energies.

REFERENCES

[1] R. G. Parr, R. A. Donnelly, M. Lavy and W. E. Palke, *J. Chem. Phys.*, **68**, 380 (1978).
[2] P. Hohenberg and W. Kohn, *Phys. Rev. B*, **136**, 864 (1964).
[3] N. K. Ray, L. Samuels and R. G. Parr, *J. Chem. Phys.*, **70**, 3680 (1970).
[4] P. Politzer and H. Weinstein, *J. Chem. Phys.*, **71**, 4218 (1979).
[5] N. H. March. *J. Chem. Phys.*, **71**, 1004 (1979).
[6] W. E. Palke, *J. Chem. Phys.*, **72**, 2511 (1980).
[7] J. A. Alonso and L. A. Girifalco, *J. Chem. Phys.*, **73**, 1313 (1980).
[8] N. K. Ray and R. G. Parr, *J. Chem. Phys.*, **73**, 1334 (1980).
[9] J. C. Slater, *Phys. Rev.*, **36**, 57 (1930).
[10] R. S. Mulliken, *J. Chem. Phys.*, **2**, 782 (1934) ; **3**, 573 (1935) ; **46**, 497 (1949).
[11] J. Hinze and H. H. Jaffé, *J. Amer. Chem. Soc.*, **84**, 540 (1962).
[12] J. Hinze, M. A. Whitehead and H. H. Jaffé, *J. Amer. Chem. Soc.*, **85**, 148 (1963)
[13] J. Hinze and H. H. Jaffé, *Canad. J. Chem.*, **41**. 1315 (1963).
[14] G. Pilcher and H. A. Skinner, *J. Inorg. Nuclear Chem.*, **24**, 137 (1962).
[15] E. B. Wilson, Jr., *J. Chem. Phys.*, **36**, 2232 (1962).
[16] E. Clementi, "Tables of Atomic Functions", I. B. M., San José, Calif. 1965.
[17] A. Veillard and E. Clementi, *J. Chem. Phys.*, **49**, 2415 (1968).
[18] V. I. Vedeneyev, L. V. Gurvich, V. N. Kondratyev, V. A. Medvedev and E. L. Frankevich, "Bond Energies, Ionization Potentials and Electron Affinities", Arnold, London, 1965.
[19] C. I. Lepadatu, *Rev. Roumaine Chim.* **27**, 897(1982).
[20] R. Stevenson, "Multiplet Structure of Atoms and Molecules", Saunders Comp., Philadelphia, 1965.
[21] L. Pauling, "The Nature of the Chemical Bond", Cornell Univ. Press, Ithaca, 1963.
[22] C. Kittel, "Introduction to Solid State Physics", J. Wiley, New York, 1963.
[23] E. Clementi and D. L. Raimondi, *J. Chem. Phys.*, **38**, 2686 (1963).
[24] G. Burns, *J. Chem. Phys.*, **41**, 1521 (1964).

Revue Roumaine de Chimie, **30**, 2, 117—123 (1985)

as-TRIAZINE DERIVATIVES WITH POTENTIAL THERAPEUTIC ACTION XIX*.

SYNTHESIS OF 5-(SUBSTITUTED-BENZYL) THIO-6-AZAURIDINES

C. CRISTESCU
Chemical and Pharmaceutical Research Institute,
Şos. Vitan 112, 74351 Bucharest, Romania

Received February 11, 1984

5-Mercapto-6-azauracil (I) reacts in aqueous medium with substituted-benzyl chloride derivatives giving 5-(substituted-benzyl) thio-6-azauracils (II). Treatment of II with hexamethyldisilazane led to 2,4-bis (trimethylsilyloxy)-derivatives (III). They were further condensed with 1-0-acetyl-2,3,5-tri-O-benzoyl-D-ribofuranose in the presence of anhydrous stannic chloride to afford the corresponding blocked-nucleosides (IV). Under the action of sodium methoxide, the IV derivatives were debenzoylated with the formation of the title compounds.

In connection with our studies on the preparation and biological activity of 6-aza-analogues of the naturally occurring pyrimidine nucleosides, we were interested in the synthesis of 6-aza-analogues substituted at position 5 by benzyl-thio- group with potential cancerostatic activity. In a preliminary communication, [1] we reported on the synthesis of 5-benzylthio-6-azauridine. These compounds have interesting physico-chemical and biological properties. We now wish to report further studies related to the stereoselectivity of the coupling reaction, by applying the Friedel-Crafts catalyzed silyl Hilbert-Johnson reaction, [2,3] used in the synthesis of such nucleosides, and to describe the preparation and some physico-chemical properties of several new compounds in this series. The study was initiated by the assumption that electronegative substituents on the benzyl ring especially halogens or nitro-group, may produce the most active derivatives.

5-Mercapto-6-azauracil [4] (I) reacts in aqueous medium with substituted benzyl chloride derivatives leading to 5-(substituted-benzyl) thio-6-azauracils (IIa—o). The azauracil derivatives prepared by the procedure described above are listed in table 1.

The silyl ethers used in this work were prepared by reaction of the appropiate 5-(substituted-benzyl) thio-6-azauracil with hexamethyldisilazane in the presence of traces of trimethylsilyl chloride, under reflux.

---

* Part XVIII, C. Cristescu, *Rev. Roumaine Chim.*, **28**, 989 (1983).

Table 1

5 (substituted-benzyl) thio-6-azauracils (IIa—0) and 2,4-bis (trimethylsilyloxy)-5 (substituted-benzyl) thio-6-azauracils (IIIa—o)

No.	R	m.p. °C	Yield %	T.L.C[a]	U.V. Specra (EtOH) λmax(logε)	IR Spectra(KBr)cm^{-1}		Formula[b].	No.	b.p. °C (m/mHg)	Yield %
						$\tilde{\nu}$—(CO)	$\tilde{\nu}$(C=C)				
II—a	2—F—C_6H_4—	228—230	90	0.58	310 (3.83)	1730, 1676	1596, 1500	$C_{10}H_8N_3O_2SF$	III—a	195—197 (0.4)	90
II—b	3—F—C_6H_4—	230—231	91	0.57	310 (3.84)	1760, 1726	1600, 1500	$C_{10}H_8N_3O_2SF$	III—b	192—193 (0.4)	95
II—c	4—F—C_6H_4—	230—231	92	0.57	310 (3.83)	1730, 1686	1610, 1510	$C_{10}H_8N_3O_2SF$	III—c	220—222 (0.8)	97
II—d	2—Cl—C_6H_4—	259—261	91	0.58	310 (3.81)	1716, 1663	1626, 1520	$C_{10}H_8N_3O_2SCl$	III—d	198—200 (0.4)	93
II—e	3—Cl—C_6H_4—	229—230	85	0.60	310 (3.84)	1763, 1726	1610, 1483	$C_{10}H_8N_3O_2SCl$	III—e	220—222 (0.4)	92
II—f	4—Cl—C_6H_4—	247—248	83	0.58	310 (4.10)	1706, 1666	1580, 1480	$C_{10}H_8N_3O_2SCl$	III—f	225—228 (0.4)	93
II—g	2—Br—C_6H_4—	260—261	91	0.58	310 (3.83)	1716, 1683	1580, 1473	$C_{10}H_8N_3O_2SBr$	III—g	203—205 (0.4)	95
II—h	3—Br—C_6H_4—	237—239	92	0.60	310 (3.90)	1740, 1713	1593, 1480	$C_{10}H_8N_3O_2SBr$	III—h	230—232 (0.4)	95
II—i	4—Br—C_6H_4—	257—258	92	0.58	310 (4.08)	1710, 1673	1583, 1480	$C_{10}H_8N_3O_2SBr$	III—i	235—237 (0.4)	93
II—j	2,4—Cl_2—C_6H_3—	260—261	92	0.58	310 (3.79)	1716, 1663	1590, 1500	$C_{10}H_7N_3O_2SCl_2$	III—j	240—242 (0.4)	94
II—k	3,4—Cl_2—C_6H_3—	257—258	93	0.58	310 (3.84)	1716, 1683	1580, 1493	$C_{10}H_7N_3O_2SCl_2$	III—k	240—242 (0.4)	94
II—l	2,6—Cl_2—C_6H_3—	228—230	83	0.58	310 (3.81)	1716, 1663	1626, 1520	$C_{10}H_7N_3O_2SCl_2$	III—l	245—247 (0.4)	95
II—m	2—NO_2—C_6H_4—	231—233	73	0.57	307 (3.89)	1726, 1686	1600, 1510	$C_{10}H_8N_4O_4S$	III—m	248—250 (0.4)	95
II—n	4—NO_2—C_6H_4—	247—248	73	0.57	278 (4.08)	1706, 1666	1590, 1500	$C_{10}H_8N_4O_4S$	III—n	248—250 (0.4)	96
II—o	4—CH_3O—C_6H_4—	237—239	64	0.60	311 (4.12)	1750, 1720	1616, 1516	$C_{11}H_{11}N_3O_3S$	III—o	238—240 (0.4)	95

a. Spots detected as UV absorbing (254 nm); solvent system : chloroform-methanol (8 :2)
b. Analytical results were within ±0.4% of the theoretical value for C, H, N, S

Several of these silyl ethers were obtained as crystalline solids after prolonged standing at low temperatures; however, in most cases, the freshly distilled viscous 2,4-bis(trimethylsilyloxy)- derivatives (III a—o) (Table 1) were used directly in the condensation reaction. In the infrared spectrum of III, the absorption bands at 700 cm^{1}, 1020 cm^{-1} $\bar{\nu}$(SiO); 850 cm^{-1}, 1275 cm^{-1} $\bar{\nu}$(SiMe$_3$), and 1080 cm^{-1} $\bar{\nu}$(OSiMe$_3$) were observed.

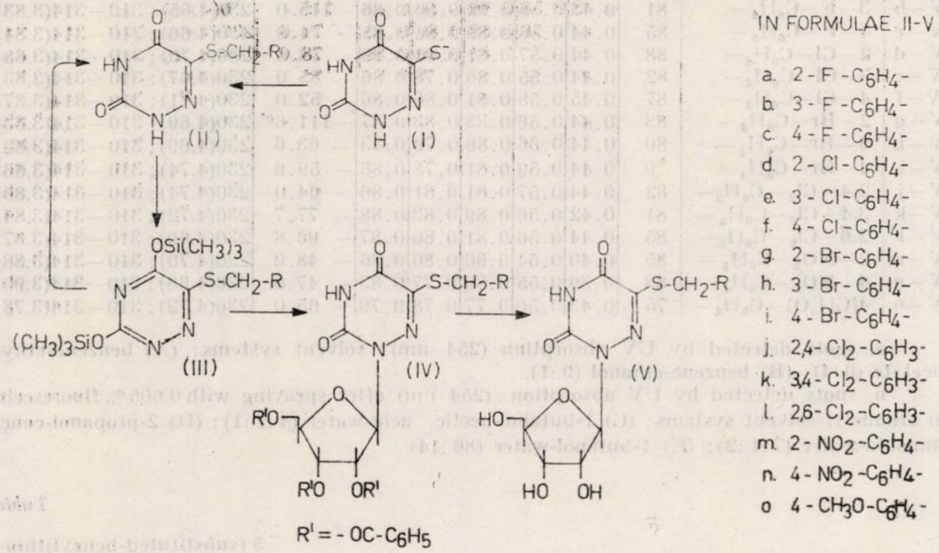
O
HN
S-CH$_2$-R
N
H (II)
S$^-$
H (I)
OSi(CH$_3$)$_3$
(CH$_3$)$_3$SiO
(III)
S-CH$_2$-R
(IV)
R'O
R'O OR'
(V)
HO
HO OH
R' = - OC-C$_6$H$_5$
IN FORMULAE II-V
a. 2 - F - C$_6$H$_4$-
b. 3 - F - C$_6$H$_4$-
c. 4 - F - C$_6$H$_4$-
d. 2 - Cl - C$_6$H$_4$-
e. 3 - Cl - C$_6$H$_4$-
f. 4 - Cl - C$_6$H$_4$-
g. 2 - Br - C$_6$H$_4$-
h. 3 - Br - C$_6$H$_4$-
i. 4 - Br - C$_6$H$_4$-
j. 2,4 - Cl$_2$ - C$_6$H$_3$-
k. 3,4 - Cl$_2$ - C$_6$H$_3$-
l. 2,6 - Cl$_2$ - C$_6$H$_3$-
m. 2 - NO$_2$ - C$_6$H$_4$-
n. 4 - NO$_2$ - C$_6$H$_4$-
o 4 - CH$_3$O - C$_6$H$_4$-

Condensation of III a—o with 1-0-acetyl-2,3,5-tri-O-benzoyl-D-ribofuranose in dry 1,2-dichloroethane, 12 hours at 22°C, in the presence of anhydrous stannic chloride affords IV a—o in 74—88% yields (Table 2). A slight excess (8—10%) of the silylated derivatives is often advantageous to effect a complete conversion of the sugar component and to simplify the reaction work-up, because the hydrolyzed 5-(substituted-benzyl) thio-6-azauracil can usually be much more easily removed than the unreacted sugar.

The resulting blocked nucleosides (IV a—o) were deacylated by the methoxide catalysed transesterification method to the 5-(substituted-benzyl)thio-6-azauridines (V a—o) (Table 3).

The assignment of carbohydrate moiety to the N-1 position of the 5-(substituted-benzyl)thio-6-azauracil ring is based on the fact that the nucleosides V exhibit a hypsochromic shift of the absorption maximum in the ultraviolet spectrum by passing from acidic to basic media. This is typical of an N$_1$ substituted 6-azauracil.[5,6]

In the infrared spectrum of tri-0-benzoyl-derivatives (IV) the strong absorption of the acyl groups overlaps a considerable number of bands of the heterocyclic and sugar moieties of the molecule. As a consequence of these overlaps the spectra show fewer bands. The carbonyl groups absorb in the 1710±10 cm^{-1} region. The absorption bands of the

Table

1(2,′, 3′, 5′-tri-O-benzoyl-β-D-ribofuranosyl)-5-

No.	R	Yield %	T.L.C.[a]		Paper chrom[b]			c. $[\alpha]_D^{25}$	UV Spectra λ max(logε) (EtOH)
			A	B	C	D	E		
IV−a	$2-F-C_6H_4-$	84	0.44	0.56	0.91	0.79	0.87	−111.0	230(4.66); 310−314(3.84)
IV−b	$3-F-C_6H_4-$	81	0.43	0.56	0.90	0.80	0.86	−115.0	230(4.65); 310−314(3.83)
IV−c	$4-F-C_6H_4-$	85	0.44	0.56	0.89	0.80	0.85	− 71.0	230(4.66); 310−314(3.84)
IV−d	$2-Cl-C_6H_4-$	88	0.44	0.57	0.81	0.80	0.89	− 78.0	230(4.70); 310−314(3.88)
IV−e	$3-Cl-C_6H_4-$	82	0.44	0.55	0.86	0.78	0.86	− 85.0	230(4.67); 310−314(3.83)
IV−f	$4-Cl-C_6H_4-$	87	0.45	0.58	0.81	0.80	0.86	− 52.0	230(4.71); 310−314(3.87)
IV−g	$2-Br-C_6H_4-$	83	0.44	0.56	0.83	0.83	0.87	−111.6[c′]	230(4.69); 310−314(3.83)
IV−h	$3-Br-C_6H_4-$	80	0.44	0.56	0.86	0.79	0.83	− 63.6	230(4.69); 310−314(3.82)
IV−i	$4-Br-C_6H_4-$	79	0.44	0.59	0.81	0.78	0.86	− 59.6	230(4.74); 310−314(3.86)
IV−j	$2,4-Cl_2-C_6H_3-$	82	0.44	0.57	0.81	0.81	0.86	− 64.0	230(4.74); 310−314(3.86)
IV−k	$3,4-Cl_2-C_6H_3-$	81	0.42	0.56	0.89	0.83	0.88	− 77.7	230(4.72); 310−314(3.84)
IV−l	$2,6-Cl_2-C_6H_3-$	85	0.44	0.56	0.81	0.80	0.87	− 96.8	230(4.69); 310−314(3.87)
IV−m	$2-NO_2-C_6H_4-$	85	0.40	0.54	0.86	0.80	0.86	− 48.0	230(4.70); 310−314(3.88)
IV−n	$4-NO_2-C_6H_4-$	83	0.39	0.55	0.80	0.77	0.83	− 47.0	230(4.68); 310−314(3.90)
IV−o	$4(CH_3O)-C_6H_4-$	75	0.43	0.56	0.77	0.78	0.79	− 65.0	230(4.72); 310−314(3.78)

a. spots detected by UV absorption (254 nm); solvent systems: (A) benzene-ethyl aacetate (6 :4); (B) benzene-ethanol (9 :1).

b. spots detected by UV absorption (254 nm) after spraying with 0.005 % fluorescein (in ethanol); solvent systems: (C) 1-butanol-acetic acid-water (4 :1 :1); (D) 2-propanol-conc. ammonia-water (7 :1 :2); (E) 1-butanol-water (86 :14).

Table

5 (substituted-benzyl)thio-

No.	R	m.p. °C	Re-cryst.[a] solv.	Yield %	T.L.C.[b]	Paper chrom.[c]			$[\alpha]_D^{25}$ (C₁EtOH)
					A	B	C	D	
V−a	$2-F-C_6H_4-$	119−120	F	91	0.27	0.65	0.62	0.57	−40.0
V−b	$3-F-C_6H_4-$	164−166	F	90	0.26	0.66	0.63	0.57	−51.0
V−c	$4-F-C_6H_4-$	172−173	F	91	0.25	0.64	0.63	0.55	−60.0
V−d	$2-Cl-C_6H_4-$	123−124	G	92	0.30	0.66	0.63	0.57	−61.0
V−e	$3-Cl-C_6H_4-$	155−156	H	87	0.27	0.66	0.65	0.59	−60.3
V−f	$4-Cl-C_6H_4-$	194−196	C	92	0.29	0.66	0.65	0.58	−78.0
V−g	$2-Br-C_6H_4-$	143−145	E	86	0.31	0.64	0.60	0.58	−30.5
V−h	$3-Br-C_6H_4-$	172−173	E	85	0.29	0.66	0.63	0.55	−52.5
V−i	$4-Br-C_6H_4-$	191−192	C	94	0.30	0.68	0.62	0.60	−65.0
V−j	$2,4-Cl_2-C_6H_3-$	154−155	D	94	0.31	0.70	0.65	0.60	−76.0
V−k	$3,4-Cl_2-C_6H_3-$	157−158	G	90	0.30	0.71	0.68	0.63	−35.5
V−l	$2,6-Cl_2-C_6H_3-$	173−175	B	93	0.32	0.69	0.67	0.63	−59.0
V−m	$2-NO_2-C_6H_4-$	139−141	F	90	0.28	0.58	0.55	0.47	−55.0
V−n	$4-NO_2-C_6H_4-$	210−212	A	93	0.26	0.58	0.54	0.44	−58.5
V−o	$4-CH_3O-C_6H_4-$	187−189	C	85	0.28	0.60	0.58	0.57	−61.0

a. (A) methanol; (B) methanol-chloroform (1 :3); (C) ethanol; (D) ethanol-chloroform (1 :5); (E) ethanol-water (1 :1); (F) 2-propanol; (G) ethyl acetate; (H) ethyl acetate-hexane (2 :1)

b. spots detected by UV absorption (254 nm); solvent systems: (A) chloroform-methanol (8 :2).

c. spots detected by UV absorption (254 nm) after spraying with 0.005 % fluoresceine (in ethanol); solvent systems: (B) 1-butanol-acetic acid-water (4 :1 :1); (C) 2-propanol-conc. ammonia-water (7 :1 :2); (D) 1-butanol-water (86 :14).

2

(substituted-benzyl) thio-azauracils (IVa—o)

IR Spectra ($CHCl_3$) cm^{-1}				^1H—NMR Spectra ($CDCl_3$/TMS) H_1 ($J_{1'2'}$)d.	Formula^{e}
$\tilde{\nu}$ (CO)	$\tilde{\nu}$ (CO.O)	$\tilde{\nu}$ (C.CO)	$\tilde{\nu}$ (C=C)		
1713	1183,1100	1320,1280	1610,1500	6.47 (d, 3.00)	$C_{36}H_{28}N_3O_9SF$
1720	1183,1100	1320,1273	1606,1500	6.48 (d, 2.50)	$C_{36}H_{28}N_3O_9SF$
1700	1193,1096	1320,1286	1603,1510	6.50 (d, 3:00)	$C_{36}H_{28}N_3O_9SF$
1716	1173,1120	1313,1260	1600,1490	6.54 (d, 3.25)	$C_{36}H_{28}N_3O_9SCl$
1713	1180,1100	1316,1273	1603,1500	6.48 (d, 2.50)	$C_{36}H_{28}N_3O_9SCl$
1716	1178,1116	1312,1260	1600,1513	6.52 (d, 2.75)	$C_{36}H_{28}N_3O_9SCl$
1713	1176,1120	1313,1266	1600,1493	6.52 (d, 2.50)	$C_{36}H_{28}N_3O_9SBr$
1713	1186,1116	1310,1266	1600,1493	6.49 (d, 2.75)	$C_{36}H_{28}N_3O_9SBr$
1716	1173,1120	1310,1260	1600,1500	6.47 (d, 3.00)	$C_{36}H_{28}N_3O_9SBr$
1713	1170,1113	1313,1253	1600,1513	6.53 (d, 3.50)	$C_{36}H_{27}N_3O_9SCl_2$
1713	1173,1113	1306,1263	1600,1490	6.56 (d, 3.50)	$C_{36}H_{27}N_3O_9SCl_2$
1716	1170,1116	1313,1260	1600,1513	6.63 (d, 3.50)	$C_{36}H_{27}N_3O_9SCl_2$
1713	1170,1100	1303,1260	1593,1516	6.52 (d, 2.50)	$C_{36}H_{28}N_4O_{11}S$
1716	1170,1113	1306,1260	1593,1510	6.54 (d, 2.25)	$C_{36}H_{28}N_4O_{11}S$
1720	1175,1110	1310,1260	1605,1500	6.57 (d, 2.70)	$C_{37}H_{31}N_3O_{10}S$

c. c = 1 % in chloroform

c′. c = 2 % in chloroform

d. chemical shifts in δ ppm and J values in Hz.

e. analytical results were within ± 0.4 % of the theoretical values for C, H, N, S.

3

6-azauridines (Va—0)

UV Spectra λmax(logε)			IR Spectral (KBr)cm^{-1}		^1H-NMR Spectra (DMSO—d/TMS) $H_{1'}(J_{1'2'})^d$	Formula^{e}.
EtOH	0.1N HCl	0.1N NaOH	$\tilde{\nu}$(CO)	$\tilde{\nu}$(C=C)		
312(3.79)	310(3.75)	300(3.67)	1686, 1726	1586, 1493	5.88 (d, 3.25)	$C_{15}H_{16}N_3O_6SF$
312(3.82)	310(3.77)	300(3.69)	1693, 1713	1605, 1500	5.90 (d, 3.50)	$C_{15}H_{16}N_3O_6SF$
312(3.85)	310(3.80)	300(3.71)	1686, 1710	1596, 1500	5.86 (d, 3.25)	$C_{15}H_{16}N_3O_6SF$
312(3.84)	310(3.78)	300(3.70)	1700, 1713	1600, 1466	5.96 (d, 3.25)	$C_{15}H_{16}N_3O_6SCl$
312(3.84)	310(3.77)	300(3.71)	1696, 1710	1595, 1473	5.86 (d, 3.50)	$C_{15}H_{16}N_3O_6SCl$
312(3.88)	310(3.82)	300(3.78)	1686, 1713	1595. 1490	5.91 (d, 3.50)	$C_{15}H_{16}N_3O_6SCl$
312(3.84)	310(3.78)	300(3.71)	1686, 1720	1593, 1495	5.93 (d, 3.00)	$C_{15}H_{16}N_3O_6SBr$
312(3.87)	310(3.80)	300(3.71)	1700, 1733	1600, 1493	5.90 (d, 3.00)	$C_{15}H_{16}N_3O_6SBr$
312(3.85)	310(3.80)	300(3.71)	1673, 1733	1600, 1496	5.90 (d, 3.00)	$C_{15}H_{16}N_3O_6SBr$
312(3.85)	310(3.82)	300(3.73)	1690, 1713	1596, 1480	5.92 (d, 3.00)	$C_{15}H_{15}N_3O_6SCl_2$
312(3.86)	310(3.79)	300(3.71)	1700, 1720	1593, 1466	5.90 (d, 3.50)	$C_{15}H_{15}N_3O_6SCl_2$
312(3.86)	310(3.84)	300(3.73)	1693, 1726	1596, 1490	5.99 (d, 2.75)	$C_{15}H_{15}N_3O_6SCl_2$
312(3.92)	310(3.92)	302(3.85)	1700, 1726	1613, 1520	5.93 (d, 3.50)	$C_{15}H_{16}N_4O_8S$
271(4.16)	279(4.19)	270(4.19)	1700, 1713	1610, 1500	5.90 (d, 3.50)	$C_{15}H_{16}N_4O_8S$
312(3.82)	310(3.80)	300(3.75)	1700, 1710	1600, 1496	5.91 (d, 3.00)	$C_{16}H_{19}N_3O_7S$

d. chemical shifts in ppm and J values in Hz.

e. analytical results were within ± 0.4 % of the theoretical values for C, H, N, S.

acyl group, linked to the ribose residue, are 1270±10 cm^{-1}, 1310±10 cm^{-1} $\tilde{\nu}$(C.CO) and 1100±10 cm^{-1}, 1180±10 cm^{-1} $\tilde{\nu}$(CO.O) respectively. In the spectra of all tri-O-benzoyl-derivatives, three bands regularly occurred (1090, 1128 and 1237 cm^{-1}). These bands are probably due to the strong absorption of the ribose component. [7,8]

The infrared absorption of the V-derivatives in the carbonyl stretching region confirms the N_1 substitution of the 6-azauracil-5-substituted component since the spectra of these nucleosides are similar to those of 1-methyl-6-azauracil and different from 3-methyl-6-azauracil. Horak and Gut [9] described the use of the infrared spectra to distinguish between the N_1 and N_3 substituted 6-azauracils and nucleosides.

The anomeric protons of nucleosides IV and V, appear in ^1H-NMR spectra as a doublet at δ 6.57 ppm and 5.90 ppm respectively, with a coupling constant 2—3.5 Hz. The position of the signal indicates that the nucleosides may be the β-anomer by comparison with the ^1H-NMR spectra of other nucleosides of the same type.[10–14]

EXPERIMENTAL

The melting points were determined with a heating microscope plate and are not corrected. Thin layer chromatography was performed on precoated silicagel plates 60 F_{254} (Merck). Paper chromatography was performed by ascending tehnique on Schleicher & Schüll 2043 b mgL paper. The preparative column chromatography was performed on silicagel 60 (70—230 mesh ASTM) (Merck), a flow-rate of 100 mL per hour being maintained. The fractions were collected at 6 minutes' intervals. The ultraviolet absorbing substances were determined in eluates by running registration of UV absorption (UVICORD LKB 254 nm). The optical rotation was measured on a Hilger & Watts automatic polarimeter. The ultraviolet spectra were recorded on a Pye Unicam SP 1800 ultraviolet spectrophotometer. The infrared spectra were recorded on a Zeiss-Jena UR — 20 spectrophotometer. The ^1H-NMR spectra were recorded at 60 MHz on a Varian EM 360 spectrophotometer.

General procedure for the preparation of 5-(substituted-benzyl) thio-6-azauracils (II a—o)

5-Mercapto-6-azauracil sodium salt (15 mM) was dissolved at 60° C in water (40 mL) and ethanol (40 mL) was added. A solution of substituted-benzyl chloride (15 mM) in ethanol (20 mL) was added. The mixture was stirred at 70 °C for 90 minutes, cooled overnight at 4°C and filtered. Compounds II a—o were recrystallized from ethanol (Table 1).

General procedure for the preparation of 1-(2′, 3′, 5′-tri-O-benzoyl- β -D-ribofuranosyl-5-(substituted-benzyl)thio-6-azauracil (IV a—o)

A mixture of II a—o (5.5 mM), hexamethyldisilazane (10 mL) and trimethylsilyl chloride (0.5 mL) was refluxed for 2 hours, until a clear solution was obtained. The excess of hexamethyldisilazan was removed under vaccum 15 mm Hg and the residue was distilled under reduced pressure to give 2,4-bis(trimethylsilyloxy)-5-(substituted-benzyl)thio-6-azauracil (III a—o) as shown in table 1.

The freshly distilled viscous 2,4-bis(trimethylsilyloxy)-derivatives (5 mM) were dissolved in dry 1,2-dichloroethane and added to 1-O-acetyl-2,3,5-tri-O-benzoyl-D-ribofuranose (4.5 mM), previously dissolved in dry 1,2-dichloroethane (150 mL). The mixture was stirred 12 hours at 22°C in the presence of anhydrous stannic chloride (3.5 mM). The solution was treated with a saturated aqueous sodium hydrogen carbonate solution (2 × 50 mL) and the organic phase was filtered over Celite 535, dried on sodium sulphate and evaporated. The residue was chromatographed on a silicagel column (60 g) with chloroform and chloroform-methanol (99 :1 v/v). The collected fractions were combined and evaporated in vacuum to give the pure corresponding blocked nucleosides (IV a—o) shown in table 2.

General procedure for the preparation of 5-(substituted-benzyl)thio-6-azauridines (V a—o)

A mixture of the blocked nucleoside IV (2 mM), 1 N sodium methoxide solution (2 mL) and dry methanol (60 mL), was stirred under reflux for 2 hours. The solvent was evaporated in vacuum and the resulting oil was dissolved in water (50 mL) and extracted with ethyl acetate — ether (2 :1 v/v ; 2 × 25 mL). The aqueous layer was treated with DOWEX 50 W × × 8 (H) at pH 2, filtered and evaporated in vacuum. The residue crystallized from the solvent is indicated in table 3.

ACKNOWLEDGEMENT. The author thanks Mrs. Veronica Vişan and Mrs. Ileana Costea of the Analytical Department of our Institute for recording the IR and UV spectra, Mrs. Cornelia Ioan for the elemental analyses and Mr. D. Ionescu for the NMR spectra. The author expresses his gratitude to Mrs. Anca Sava for her invaluable help.

REFERENCES

[1] C. Cristescu, *Rev. Roumaine Chim.*, **20**, 1287 (1975).
[2] U. Niedbala and H. Vorbrüggen, *Angew. Chem. Internat. Edit.*, **9**, 461 (1970).
[3] U. Niedbala and H. Vorbrüggen, *J. Org. Chem.*, **39**, 3654 (1974).
[4] C. Cristescu and J. Marcus, *Pharmazie*, **16**, 135 (1961).
[5] J. Johnas and J. Gut, *Coll. Czech. Chem. Comm.*, **26**, 2155 (1961).
[6] K. V. Zee-Cheng and C. C. Cheng, *J. Org. Chem.*, **27**, 976 (1962).
[7] C. L. Angell, *J. Chem. Soc.*, **1961**, 504.
[8] J. Pitha and J. Zemlika, *Coll. Czech. Chem. Comm.*, **29**, 410 (1964).
[9] M. Horak and J. Gut., *Coll. Czech. Chem. Comm.*, **26**, 1680 (1961).
[10] J. Beranek, *Coll. Czech. Chem. Comm.*, **34**, 618 (1969).
[11] M. P. Sweizer, E. B. Banta, J. T. Witkowsky and R. K. Robins, *J. Amer. Chem. Soc.*, **95**, 3770 (1973).
[12] D. J. Wood, F. E. Hruska, R. Mynott and R. H. Sarma, *Canad. J. Chem.*, **51**, 2571 (1973).
[13] J. D. Stewens and H. G. Fletcher, *J. Org. Chem.*, **33**, 1799 (1968).
[14] F. E. Hruska, A. A. Grey and I. C. Smith, *J. Amer. Chem. Soc.*, **92**, 4088 (1970).

Revue Roumaine de Chimie, **30**, *2*, 125—131 (1985)

IMINE DER AMINOAZOLE. 1.

SYNTHESE UND CHARAKTERISIERUNG EINIGER IMINE DER 2-AMINOBENZIMIDAZOLE

HANS-HORST GLATT, MAMADOU FOULA BARRY, CAROL CSUNDERLIK,
RADU BACALOGLU, MIHAI MEDELEANU und MARIA LANTOS
Technische Hochschule „Traian Vuia", Laboratorium für Organische Chemie,
str. Bocşa Nr. 6, 1900 Timişoara, S.R. Rumänien

Eingegangen den 21 März, 1984

Es wird die Synthese von acht in der Literatur nicht angeführten Benzyliden-2-aminobenzimidazolen anhand der Kondensierung 5(6)-substituierter 2-Aminobenzimidazole mit Benzaldehyden beschrieben. Die dargestellten Imine wurde durch ihren Schmelzpunkt, die Elementaranalyse, sowie IR—, UV— und ^1H—NMR-spektroskopisch charakterisiert. Es wird bewiesen, dass die Moleküle in allen Fällen eine ebene Konfiguration und eine erweiterte Konjugierung aufweisen.

Eight new benzylidene 2-aminobenzimidazoles were obtained from the corresponding 5(6)-substituted 2-aminobenzimidazoles and benzaldehydes. The products were characterized by their melting point, elemental analysis, IR-, UV- and ^1H-NMR-spectra. It has been proved that all compounds have a plane configuration and an extended conjugation.

Obzwar die Synthese der Azomethine anhand der direkten Kondensierung der Amine mit Benzaldehyden schon oftmals beschrieben wurde, [1] sind Synthesen heterocyclischer Imine nur selten in der Literatur angegeben. [2,3] Aus der Reihe der Imine des 2-Aminobenzimidazols wurden bloss die aus 2-Amino-1-alkylbenzimidazolen und Nitrobenzaldehyden zugänglichen beschrieben.[4-7]

Die vorliegende Arbeit befasst sich mit der Synthese und Charakterisierung von Iminen der 5(6)-substituierten 2-Aminobenzimidazole und Benzaldehyden.

Die Synthese der Imine **3** aus der Klasse der Benzyliden-2-aminobenzimidazole wurde anhand folgender Reaktion ausgeführt:

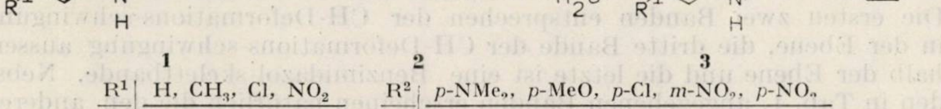

1 **2** **3**

R^1	H, CH_3, Cl, NO_2
1	**A**, **B**, **C**, **D**,

R^2	*p*-NMe_2, *p*-MeO, *p*-Cl, *m*-NO_2, *p*-NO_2
2	**a**, **b**, **c**, **d**, **e**,

Das aus äquimolaren Mengen an 5(6)-substituierten 2-Aminobenzimidazol **1** und Benzaldehyd **2** bestehende Gemisch wurde in Dioxan-Toluen (1 :1/Vol :Vol) im Beisein katalytischer Mengen von *p*-Toluensulphonsäure unter Rückfluss gekocht. Anhand dieser Methode wurden acht in der Literatur nicht angegebene Imine hergestellt.

In den IR-Spektren der Azomethine der Benzylidenanilinreihe erscheint eine mittelstarke Bande um 1610—1630 cm^{-1} die in der Regel der C=N—Valenzschwingung zugeordnet wird.[8,9] Das Benzimidazolsystem anderseits weist charakteristische Skelett-banden unter anderen auch bei 1620, 1600, 1500 cm^{-1} auf.[4,10] Hinzu kommen noch die 3—4 Skelettbanden des aromatischen Benzenrings im 1450—1610 cm^{-1}—Bereich.[11] Es ist nun zum Erwarten, dass im 1450—1620 cm^{-1}—Bereich der IR-Spektren der Imine aus der Reihe des 2-Aminobenzimidazols zahlreiche Banden erscheinen, deren Zuordnung anhand der Methode der empirischen Infrarotspektroskopie unsicher ist. Aus Tabelle 1 folgt, dass im angegebenen Bereich im allgemeinen 5—7 gut ausgeprägte Banden verschiedener Intensität erscheinen. Starke Banden sind die um 1575—1590 und bzw. um 1520 cm^{-1}.

Tabelle 1

Charakteristische IR-Banden der Benzyliden-2-aminobenzimidazole **3**.

Benzimidazol-system[a]	ν_{NH}	1620	1600	1500	1460	1420	1000	960	880	760
Benzimidazol	3400	1611	1596 1580	1494	1472 1453	1402	998	950	880	758
3 Aa	3420	1609[b]	1580	1527	1472	1435 1411	1000	978	900	743
3 Ab	3443	1604[b]	1575	1529	1478	1430 1400	1000	968	873	769
3 Ac	3400	1624[b] 1605	1593 1564	1512	1486	1426 1403	989	969	878	790
3 Ad	3380	1613[b]	1567	1527	1469	1424	991	930	898	748
3 Ae	3400	1612[b]	1585	1502	1475	1422	992	957	883	764
3 Ba	3380	1612[b]	1580	1527	1467	1432	1000	943	880	748
3 Ca	3400	1611[b]	1578	1527	1464	1430	1002	951	892	764
3 Da	3395	1608[b]	1572	1518	1461	1405	998	941	878	761

[a] nach [10]

[b] wahrscheinlich zusammen mit der C=N—Valenzschwingungsbande

Die Benzimidazolbanden von unter 1000 cm^{-1} können jedoch zugeordnet werden. Diese vier Banden erscheinen in den 989—1002, 943—970, 873—900 und 743—790 cm^{-1}—Bereichen, und sind mittelstark oder schwach. Die ersten zwei Banden entsprechen der CH-Deformations-schwingung in der Ebene, die dritte Bande der CH-Deformations-schwingung ausserhalb der Ebene und die letzte ist eine Benzimidazol-skelettbande. Nebst den in Tab. 1. angegebenen Banden erscheinen natürlich die den anderen Strukturelementen entsprechenden Banden.

Die UV-Spektren der Benzyliden-2-aminobenzimidazole weisen ein Absorptionsmaximum im 352—441 nm-Bereich von molarem Extinktionskoeffizienten von 16000—46000 l/Mcm auf (Tabelle 2). Durch den Vergleich der Absorptionsmaxima der heterocyclischen Imine mit jenen der entsprechend substituierten 2-Aminobenzimidazole und bzw. Benzaldehyde ist eine starke bathochrome Verschiebung offensichtlich. Dies bedeutet — so wie es auch für andere Benzylidenimine gezeigt wurde[15,16] dass die Moleküle eine ebene Konfiguration und eine auf das ganze Molekül erweiterte Konjugierung aufweisen. Aus der Abhängigkeit der Lage des Absorptionsmaximums von der Art der Substituenten folgt der elektronenspendende Charakter des Benzenrings in bezug auf das Benzimidazolsystem. So erklärt sich der grössere bathochrome Effekt bei dem mit einer 4-Dimethylaminogruppe substituierten Benzenkern (3Aa) im Vergleich mit dem des 4-Chlorbenzylidenderivats (3Ac Tabelle 2). Im Falle der 4-Nitrobenzylidenverbindung ist jedoch ein kleiner bathochromer Effekt im Vergleich mit dem entsprechenden 4-Chlorderivat zu verzeichnen. Das kann bedeuten, dass in diesem Fall der Benzolkern gegenüber dem Imidazol einen elektronenanziehenden Effekt aufweist. Natürlich ist die grösste bathochrome Verschiebung bei dem mit einer Nitrogruppe

Tabelle 2

UV-Spektren der Benzyliden-2-aminobenzimidazole

Verbindung	a) λ_{Max} (nm)	$\varepsilon_{Max} 10^{-4}$ (L/Mcm)	f	c) λ_{Max} (nm)	d) λ_{Max} (nm)	e) λ_{Max} (nm)
3 Aa	392	4,3161	0,835	454	283 242	340 242
3 Ab	352	2,4624	0,688	372	283 242	273
3 Ac	355	1,9760	0,599	355	283 242	254
3 Ad	359	1,7070	0,478	359	283 242	233
3 Ae	386	1,6312	0.457	386	283 242	265
3 Ba	393	2,5202	0,549	451	288 245	340 242
3 Ca	396	4,1847	0,877	454	292 250	340 242
3 Da	441	4,5428	0,942	498	258 232	340 242

a) in dioxanischer Lösung

b) berechnet anhand der Gleichung: $f = 4{,}315\ 10^{-9}\ \varepsilon_{Max} \Delta \nu_{1/2}$.[12]

c) Absorptionsmaximum in 0,4 M/1 CF_3COOH-Dioxan

d) Absorptionsmaxima der entsprechend substituierten 2-Amino-benzimidazole.[13]

e) Absorptionsmaxima der entsprechende substituierten Benzaldehyde.[14]

am Imidazolring und mit einer 4-Dimethylaminogruppe am Benzolring substituierten Imin zu bemerken.

Die Verschiebung der Absorptionsmaxima der Imine durch Protonierung legt dieselben Schlüsse nahe. So hat die Protonierung des Benzimidazolrings im Falle der Imine mit stark elektronenspendenden Gruppen am Benzenkern (*p*-NMe_2 : 3Aa, 3Ba, 3Ca, 3Da) eine wesentliche bathochrome Verschiebung des Absorptionsmaximus zur Folge. Diese Verschiebung wird um so kleiner je unbedeutender der elektronenabstossende Effekt der Substituenten am Benzenkern wird (3Ab, *p*-OMe). Wie es zum Erwarten war, ist der elektronenanziehende Effekt des Benzimidazolringes durch die Protonierung wesentlich gestiegen.

Es ist interessant, dass die Stärke des harmonischen Oszillators mit der Bedeutung des elektronenabstossenden Charakters der Substituenten am Benzimidazolkern ansteigt. Dies kann als weiterer Beweis der erweiterten Konjugation des Iminsystems ausgelegt werden.

Die ^1H-NMR-Spektren der Benzyliden-2-aminobenzimidazole (Tabelle 3) beweisen die Struktur dieser Verbindungen. So erscheint das stark entschirmte Aldiminproton als Singulett im 9,14–9,51 ppm-Bereich. Stark elektronenanziehende Substituenten am Benzenkern des Imins verursachen erwartungsgemäss eine Tieffeldverschiebung dieses Signals,

Tabelle 3

^1H-NMR-Spektren der Benzyliden-2-aminobenzimidazole 3

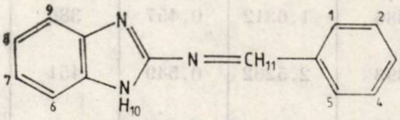

Verbindung$^{c)}$	Signale der Protonen δ (ppm)										
	1	2	3	4	5	6	7	8	9	10	11
3 Aa	7.80^{a}	6.76^{a}	3.00 NMe_2	6,76^{a}	7,80^{a}	7,08–7,39^{b}				6,75	**9,16**
3 Ab	7,95	7,05^{a}	3,80 MeO	7,05^{a}	7,95^{a}	7,0–7,39^{b}				7,13	9,30
3 Ac	8,08^{a}	7,58^{a}	Cl	7,58^{a}	8,08^{a}	7,16–7,48				7,50	**9,41**
3 Ad	8,80	NO_2	8,38	8,38	7,83	7,13–7,50				8,38	**9,51**
3 Ae	8,15	8,15	NO_2	8,15	8,15	7,18–7,50				7,18	**9,51**
3 Ba	7,49^{a}	6,75^{a}	2,99^{a} N Me_2	6,75^{a}	7,49^{a}	7,21	6,95	2.45 Me	7,56	6,75	**9,15**
3 Ca	7,78^{a}	6,74^{a}	2,98^{a} NMe_2	6,74^{a}	7,78^{a}	7,09	6,99	Cl	7,39	7,30	**9,10**
3 Da	7,81^{a}	6,76^{a}	2,99 NMe_2	6,76^{a}	7,81	7,53^{a}	7,41	NO_2	8,20	7,88	**9,14**

a) Dublett, J = 9Hz
b) Multiplett AA′BB′.
c) Standard : HMDS

während der Einfluss der elektronischen Effekte der Substituenten am Benzimidazolkern auf die Lage dieses Signals nur unbedeutend ist. Im ersteren Falle lassen sich die chemischen Verschiebungen mit den Substituentenparametern (aus L.c. [17]) gut korrelieren:

$$\delta_{CH} = 0{,}22\ \sigma + 9{,}35 \qquad (r = 0.998)$$

Das dem Benzimidazol-NH entsprechende Signall lässt sich im allgemeinen nur schwer lokalisieren, da es breit ist und von den aromatischen Protonen abgedeckt wird. Es erscheint um 7,1—8,4 ppm und wird von der Konzentration und von der Temperatur beeinflusst.

Die den Protonen der zwei aromatischen Systeme entsprechenden Signale erscheinen als komplexe Multiplette im 7,0—8,2 ppm-Bereich. Die NMR-Spektren der am Benzimidazolring unsubstituierten Imine (3Aa — 3Ae) weisen ein AA′BB′-Multiplett um 7,1—7,5 ppm auf. Das Erscheinen eines solchen Multipletts anstelle des erwarteten ABCD-Systems lässt sich anhand der Tautomerie-bedingten Äquivalenz der zwei N-Atome des Benzimidazolkerns erklären.

Im Falle der Imine mit substituiertem Benzimidazolkern (3Ba, 3Ca, 3Da) erscheinen dessen Protonen als ABC-Multiplett um 7,4—8,0 (H_9), 7,1—7,5 (H_6) und bzw. 7,0—7,4 ppm (H_7). Die Protonen des *p*-substituierten Benzenkerns erscheinen als AB-System mit chemischen Verschiebungen von 7,5—8,1 und bzw. 6,7—7,6 ppm (Kopplungskonstanten um 9 Hz). Im Falle der Verbindung 3Ae scheint sich der elektronenanziehende Effekt des Benzimidazolrestes mit jenem der Nitrogruppe am Benzenkern zu kompensieren, und anstelle des erwarteten AB-Systems erscheint ein „pseudo A_2"-System bei 8,15 ppm. Dieser Fall ähnelt dem in der Literatur angegebenen Falle des 5-Chlor-2-(4′-phenyl)-benzimidazols [18] und beweist dass die Benzimidazolgruppe einen der Nitrogruppe in bezug auf einen Benzenring gleichkommenden elektronenanziehenden Charakter aufweist. Es ist zu unterstreichen dass sich die NMR-spektroskopischen Befunde vollkommen mit jenen der UV-spektroskopischen Untersuchungen decken. Nebst den oben angegebenen Signale erscheinen in den NMR-Spektren der Imine auch die den Substituenten entsprechenden Signale. Die Protonen der Dimethylaminogruppe erscheinen als 6-Protonen-Singulett bei 2,99 ppm, und die Methoxygruppe weist ein 3-Protonen-Singulett mit einer chemischen Verschiebung von 3,8 ppm auf.

BESCHREIBUNG DER VERSUCHE

Die IR-Spektren der KBr-Presslinge wurden mit einem IR-75-SPECORD (Carl Zeiss Jena) aufgezeichnet. Die UV-Spektren wurden mit einem Cary 17 (Varian) aufgenommen. Die ^{1}H-NMR-Untersuchungen wurden mit einem TESLA BS 487-C (80MHz) vorgenommen. Die Proben wurden in DMSO-d_6 gelöst (Konzentration zirka 1—5 %, bedingt von der Löslichkeit des Imins) und als inneres Standard wurde Hexamethyldisiloxan benützt. Die Multiplette wurden als Systeme erster Ordnung behandelt wobei anähernde Werte der chemischen Verschiebungen und der Kopplungskonstanten erhalten wurden. Die Elementaranalysen wurden mit einem PERKIN ELMER (Elemental Analyzer Modell 240 B) durchgeführt. Die Schmelzpunkte wurden mit einem Boethius-Heiztisch bestimmt. Darstellung der 5(6)-substituierten Benzyliden-2-aminobenzimidazole *3* (allgemeine Arbeitsweise):

In 100 cm^3 Dioxan-Toluen (1 : 1/Vol : Vol) werden 10 mM 2-Aminobenzimidazol **1** und bzw. 10 mM Benzaldehyd **2** gelöst, mit zirka 0,004 mM *p*-Toluensulphonsäure versetzt und 1,5—15 Stunden am Wasserabscheider unter Rückfluss gekocht. Das Reaktionsgemisch wird sodann i. Vak. auf ein Drittel seines Anfangsvolumens eingeengt. Beim langsamen Erkalten fällt das Imin in den meissten Fällen mit analytischer Reinheit aus. Das imin wird abgesogen, mit etwas Petrolether gewaschen und gegebenenfalls aus Toluen oder *o*-Xylen umkristallisiert. Die Ausbeute beträgt 68—85%. Aus der Mutterlauge kann durch Fällen mit Petrolether weiteres Imin gewonnen werden. Anhand dieser Methode wurden folgende Imine dargestellt:

p-Dimethylaminobenzyliden-2-aminobenzimidazol **3Aa**, aus 2-Aminobenzimidazol **1A** und *p*-Dimethylaminobenzaldehyd **2a**, Rückfluss 4 Stn (ohne Katalysator 30% Ausbeute, mit Katalysator 80,4%), gelbe Nadeln mit grünlichem Schimmer, Schp. 239—41°C; $C_{16}H_{16}N_4$ ($M = 264{,}33$) ber. %C 72,70 %H 6,10 %N 21,20; gef. %C 72,38 %H 6,15 %N 21,28.

p-Methoxybenzyliden-2-aminobenzimidazol **3Ab**, aus- 2-Aminobenzimidazol **1A** und Anisaldehyd **2b**, Rückfluss 14,5 Stn, Ausbeute 78,4%, gelbe Kristalle, Schp. 225—7°C $C_{15}H_{13}N_3O$ ($M = 251{,}29$) ber. %C 71,70 %H 5,21 %N 16,72; gef. %C 70,59 %H 5,42 %N 17,47.

p-Chlorobenzyliden-2-aminobenzimidazol **3Ac**, aus 2-Amidobenzimidazol **1A** und *p*-Chlorobenzaldehyl **2c**, Rückfluss 5,5 Stn. Ausbeute 82,1%, gelbe Nadeln Schp. 217—9°C, $C_{14}H_{10}N_3Cl$ ($M = 255{,}71$) ber. %C 65,76 %H 3,94 %N 16,43; gef. %C 64,42 %H 4,04 %N 16,86.

m-Nitrobenzyliden-2-aminobenzimidazol **3Ad**, aus- 2-Aminobenzimidazol **1A** und *m*-Nitrobenzaldehyd **2d**, Rückfluss 1,5 Stn, Ausbeute 80,6%, rost-braune Nadeln, Schp. 192—5°C; $C_{14}H_{10}N_4O_2$ ($M = 266{,}26$) ber. %C 63,15 %H 3,79 %N 21,04; gef. %C 63,05 %H 3,94 %N 20,94.

p-Nitrobenzyliden-2-aminobenzimidazol **3Ae**, aus 2-Amidobenzimdazol **1A** und *p*-Nitrobenzaldehyd **2e**, Rückfluss 4 Stn. Ausbeute 84,5 %, goldgelbe nadelförmige Gebilde Schp. über 230°C, $C_{14}H_{10}N_4O_2$ ($M= 266{,}26$) ber. %C 63,15 %H 3,79 %N 21,04; gef. %C 62,53 %H 3,83 %N 21,49.

p-Dimethylaminobenzyliden-2-amino-5(6)-methylbenzimidazol **3Ba**, aus 2-Amino-5(6)-methylbenzimidazol **1B** und *p*-Dimethylaminobenzaldehyd **2a**, Rückfluss 7,0 Stn, Ausbeute 73,4%, braune Kristalle Schp. 132—5°C, $C_{17}H_{18}N_4$ ($M = 278{,}36$);ber. %C 73,35 %H 6,52 %N 20,13; gef. %C 72,93 %H 6,52 %N 19,47.

p-Dimethylaminobenzyliden-2-amino-5(6)-chlorbenzimidazol **3Ca**, aus 2-Amino-5(6)-chlorbenzimidazol **1C** und *p*-Dimethylaminobenzaldehyd **2a** Rückfluss 7,5 Stn, Ausbeute 68,5%, goldgelbe Nadeln, Schp. 227—9°C; $C_{16}H_{15}N_4Cl$ ($M = 298{,}78$) ber. %C 64,32 %H 5,06 %N 18,75 %C 63,16 %H 4,74 %N 18,14.

p-Dimethylaminobenzyliden-2-amino-5(6)-nitrobenzimidazol **3Da** aus 2-Amino-5(6)-nitrobenzimidazol **1D** und *p*-Dimethylaminobenzaldehyd **2a** Rückfluss 15,5 Stn, Ausbeute 78,9%, braune Kristalle Schp. 180—4°C.

LITERATURÜBERSICHT

[1] Methoden der organischen Chemie (Houben-Weyl), Sauerstoffverbindungen II, Georg Thieme Verlag, Stuttgart 1954, S. 455.

[2] H. O. Hankovszky und K. Hideg, *Acta Chim. Acad. Sci. Hung.*, **53**, 405 (1967).

[3] J. Bödeker und K. Courault. *J. prakt. Chem.*, **322**, 336 (1980).

[4] P. N. Preston, „Benzimidazoles", Wiley, New York, 1981, S. 167.

[5] A. M. Simonov und N. D. Vitkevich, *Zh. Obshch. Khim.*, **30**, 590 (1960).

[6] A. M. Simonov und A. F. Pozharskii, *Zh. Obshch. Khim.*, **31**, 3970 (1961).

[7] N. D. Vitkevich und A. M. Simonov, *Zh. Obshch. Khim.*, **29**, 2614 (1959).

[8] G. Vergoten und G. Fleury. *Mol. Cryst. Liq. Cryst.*, **30**, 213 (1975).

[9] L. E. Clougherty, J. A. Sousa und G. M. Wyman, *J. Org. Chem.*, **22**, 462 (1957).

[10] A. R. Katritzky, "Physical Methods in Heterocyclic Chemistry", Academic Press, New York, 1963, S. 239.

[11] K. Nakanishi und P. H. Solomon, "Infrared Absorption Spectroscopy Holden-Day", San Francisco 1977, S. 19.

[12] A. T. Balaban, M. Banciu und I. Pogany, ,,Aplicaţii ale metodelor fizice în chimia organică" Ed. Ştiinţifică şi Enciclopedică, Bucureşti, 1983, S. 33.

[13] H. H. Glatt, Dissertationsschrift, Timişoara 1981.

[14] CRC-Atlas of Spectral Data and Physical Constants for Organic Compounds (Editors J. G. Grasselli und W. M. Richey), 2-nd. Ed. Bd. II, CRC-Press Inc., Ohio.

[15] R. Gawinecki und F. Muzalewski, *Pol. J. Chem.*, **54**, 1177 (1980).

[16] F. Muzalewski und R. Gawinecki, *Pol. J. Chem.*, **55**, 565 (1981).

[17] J. E. Leffler und E. Grunwald, "Rates and Equilibria of Organic Reactions", Wiley, New York 1963, S. 173.

[18] I. Silberg, "Spectrometria RMN a compuşilor organici", Ed. Dacia, Cluj-Napoca 1978, S. 210.

Revue Roumaine de Chimie, 30, 2, 133—139 (1985)

DISUBSTITUTED PHENOTHIAZONES. III[1]

SYNTHESES OF DIMETHYL-3H-PHENOTHIAZIN-3-ONES

MARIUS H. TERDIC and VICTORIA A. SMARANDACHE

Institute of Chemistry, 3400-Cluj-Napoca,
str. Fîntînele 30, Romania

Received November 7, 1983

For the preparation of twenty dimethyl-3H-phenothiazin-3-ones (dimethyl-phenothiazones) two general synthetic methods were used. The first one consists in the condensation of the properly substituted zinc 2-aminophenyl sulfides with *p*-benzoqinones. From different reaction mixtures, beside the expected dimethyl-phenothiazones, eleven halogeno-dimethyl-phenothiazones were also isolated and characterized (Scheme 1 and Table 1). The second method comprises the thionation of the dimethyl-4′-hydroxy-diphenyl-amines followed by oxidation (Scheme 2 and Table 2). Only 4,6-dimethylphenothiazone could not be obtained by any method used in this work probably due to a steric hindrance.

3H-Phenothiazin-3-one (phenothiazone) has 7 hydrogen atoms which may be substituted with various radicals, so that for a single substituent 7 position isomers exist. With two identical substituents the number of the possible isomers is 21 and with 2 different substituents we could have 42 isomers, etc.

In this work we report the preparation of twenty dimenthyl- and eleven halogeno-dimethyl-phenothiazones. They are new compounds except the 1,2-dimethyl-phenothiazone which was very recently described in the literature.[2] Only the 4,6-dimethyl-phenothiazone could not be obtained by any method used in our previous works, [1,4] probably due to a steric hindrance. This phenomenon is difficultly explainable having in view the fact that both 4-methyl- and 6-methyl-phenothiazones are known compounds. [3]

For the preparation of the dimethyl-phenothiazone isomers two general synthetic methods were used, namely the condensation of the properly substituted zinc mercaptides of 2-amino-thiophenols with *p*-benzoquinones (method A) and the thionation of dimethyl-4′-hydroxy-diphenylamines followed by oxidation (method B). The first method was used to obtain the dimethyl-phenothiazones with the two methyl-groups located on the quinoide part of the nucleus, or one CH_3-group on the quinoide and the other one on the benzenoide part of the phenothiazone ring. The second method was used for the preparation of the dimethyl-phenothiazones having both CH_3-groups on the benzenoide part of the molecule.

Method A. This reaction proceeds very easily by simple stirring of the reactants at room temperature in ethanol (suspension) and only to completion the reaction mixture was boiled for 5 minutes. The reaction product was in most cases a complex mixture, which contains the expected dimethyl-phenothiazone and in addition one or two halogeno-dimethyl-phenothiazones with the halogene atom located on the quinoide part of the molecule. The formation of several phenothiazone derivatives in this reaction was explained by the superposition of several reaction mechanisms by which the starting compounds may react.[3,4]

Scheme 1

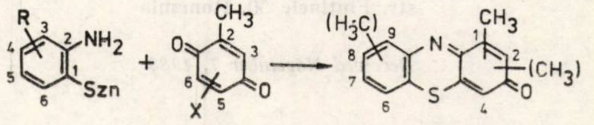

1a, R = H
b, R = 3CH$_3$
c, R = 4CH$_3$
d, R = 5CH$_3$
e, R = 6CH$_3$
zn = 1/2 Zn

2a, X = H
b, X = 3CH$_3$
c, X = 5CH$_3$
d, X = 6CH$_3$
e, X = 3Cl
f, X = 5Cl
g, X = 6Br

3a, 1,2-Dimethyl-
b, 1,4-Dimethyl-
c, 1,6-Dimethyl-
d, 1,7-Dimethyl-
e, 1,8-Dimethyl-
f, 1,9-Dimethyl-
g, 2,4-Dimethyl-
h, 2,6-Dimethyl-
i, 2,7-Dimethyl-
j, 2,8-Dimethyl-
k, 2,9-Dimethyl-
l, 4,7-Dimethyl-
m, 4,8-Dimethyl-
n, 4,9-Dimethyl-
phenothiazone

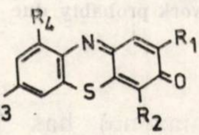

4a, R$_1$ = Br, R$_2$ = R$_3$ = CH$_3$, R$_4$ = H
b, R$_1$ = Br, R$_2$ = R$_4$ = CH$_3$, R$_3$ = H
c, R$_1$ = R$_3$ = CH$_3$, R$_2$ = Br, R$_4$ = H
d, R$_1$ = R$_4$ = CH$_3$, R$_2$ = Br, R$_3$ = H

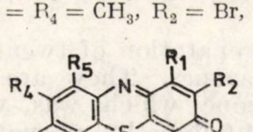

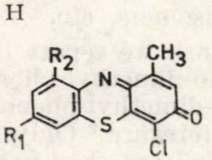

5a, R$_1$ = Cl, R$_2$ = R$_3$ = CH$_3$, R$_4$ = R$_5$ = H
b, R$_1$ = Cl, R$_2$ = R$_4$ = CH$_3$, R$_3$ = R$_5$ = H
c, R$_1$ = Cl, R$_2$ = R$_5$ = CH$_3$, R$_3$ = R$_4$ = H
d, R$_2$ = Cl, R$_1$ = R$_3$ = CH$_3$, R$_4$ = R$_5$ = H
e, R$_2$ = Cl, R$_1$ = R$_4$ = CH$_3$, R$_3$ = R$_5$ = H

6a, R$_1$ = CH$_3$, R$_2$ = H
b, R$_1$ = H, R$_2$ = CH$_3$

By the reaction of zinc mercaptides **1a – e** with the *p*-benzoquinones **2a – g** we have obtained the dimethyl-phenothiazones **3a – n** and the halogeno-dimethyl-phenothiazones **4a – d**, **5a – e** and **6a – b**. The halogeno-dimethyl-phenothiazones are classified in 3 groups depending on the type of the substitution of the *p*-benzoquinone submitted to the reaction. Thus, the compounds **4** resulted when the *p*-benzoquinone was substituted in the positions 2 and 6; the derivatives **5** are formed by the reaction of 2,3-disubstituted-*p*-benzoquinones and the phenothiazone derivatives of type **6** are synthetized with the *p*-benzoquinone substituted in the positions 2 and 5. The different dimethyl- and halogeno-dimethyl-phenothiazone mixtures obtained by this method were separated in their components by column chromatography on alumina and silicagel. The purity of the compounds was verified by TLC. The dimethyl- and halogeno-dimethyl-phenothiazones obtained by this method are shown in table 1.

From the starting compounds only the zinc mercaptide of 2-amino-amino-6-methyl-thiophenol (**1e**) was not a pure substance, but a mixture the 4-methyl-isomer **1c**. This mixture of **1c** + **1e** was submitted to the reaction with toluquinone (**2a**) when four different dimethyl-phenothiazones were formed (Table 1, reaction 3). Only in this way it was possible to prepare dimethyl-phenothiazones **3c** and **3h** carrying a CH_3—group in the position 6. The zinc mercaptide of 2-amino-4-methyl-thiophenol (**1c**) could be obtained without the isomer **1e** and it was used for the preparation of 4,8-dimethyl-phenothiazone (**3m**, Table 1, reaction 10).

In order to check the structures of the halogeno-dimethyl-phenothiazones, for the compounds with the halogen atom located in the position 4, that is for **4c**, **4d**, **6a** and **6b** the chemical method was used, i.e. the corresponding dimethyl-phenothiazones were submitted to the selective halogenation following the known method.[1,5] The structures of the other halogeno-dimethyl-phenothiazones were established with the aid of the ^1H—NMR spectra and the chromatographic study which will be published elsewhere.

Scheme 2

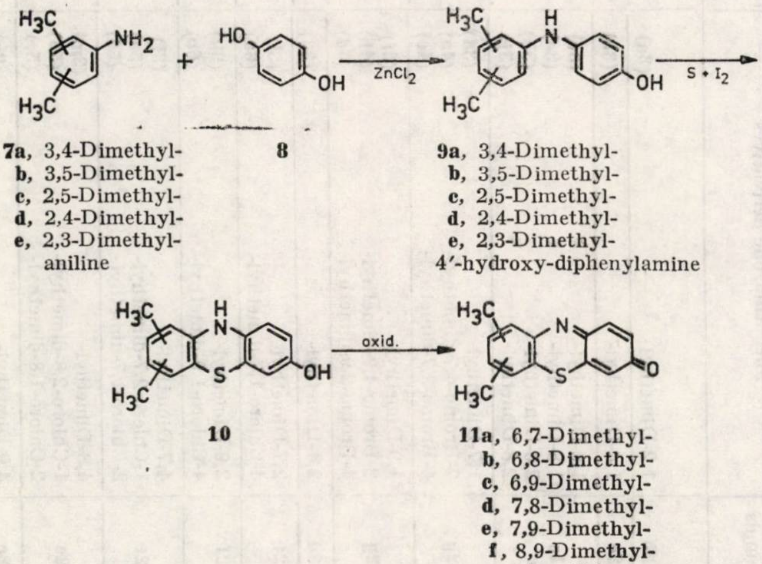

7a, 3,4-Dimethyl-
b, 3,5-Dimethyl-
c, 2,5-Dimethyl-
d, 2,4-Dimethyl-
e, 2,3-Dimethyl-
aniline

8

9a, 3,4-Dimethyl-
b, 3,5-Dimethyl-
c, 2,5-Dimethyl-
d, 2,4-Dimethyl-
e, 2,3-Dimethyl-
4'-hydroxy-diphenylamine

10

11a, 6,7-Dimethyl-
b, 6,8-Dimethyl-
c, 6,9-Dimethyl-
d, 7,8-Dimethyl-
e, 7,9-Dimethyl-
f, 8,9-Dimethyl-
phenothiazone

Method B. By reaction of dimethyl-anilines (xylidines, **7a** — **e**) with hydroquinone (**8**) in the presence of zinc chloride we obtained dimethyl-4'-hydroxy-diphenylamines (**9a** — **e**). The method was used in our previous

Table 1

Dimethyl- and halogeno-dimethyl-phenothiazones obtained by method A

No.	Starting compounds	Phenothiazone derivatives		Yield %	m.p. °C	Analysis (calcd.)				IR[CO] cm^{-1}
						*C*69.70 ;	*H*4.56 ;	*Cl*12.86 ;	*Br*24.96	
						found				
1	**1a** + **2b**	1,2-Dimethyl-	(**3a**)	51.9	180–183	69.64	4.63	—	—	1615
2	**1a** + **2c**	1,4-Dimethyl-	(**3b**)	15.1	144–145	70.04	5.02	—	—	1640
3	**1c** + **1e** + **2a**	1,6-Dimethyl-	(**3c**)	1.3	185–186	70.64	4.77	—	—	1629
		1,8-Dimethyl-	(**3e**)	12.8	207–208		*	—	—	1627
		2,6-Dimethyl-	(**3h**)	3.8	197–198		*	—	—	1633
		2,8-Dimethyl-	(**3j**)	18.5	189–191	69.36	4.21	—	—	1630
4	**1d** + **2g**	1,7-Dimethyl-	(**3d**)	35.1	175–177	69.53	4.80	—	—	1631
		2-Bromo-4,7-dimethyl-	(**4a**)	0.7	173–174		*	—	—	1612
		4-Bromo-2,7-dimethyl-	(**4c**)	4.4	186–188	—	—	—	25.30	1615
5	**1b** + **2g**	1,9-Dimethyl-	(**3f**)	23.9	194–196	68.87	4.76	—	—	1627
		2-Bromo-4,9-dimethyl-	(**4b**)	1.4	180–181	—	—	—	24.77	1623
		4-Bromo-2,9-dimethyl-	(**4d**)	6.5	171–172	—	—	—	25.45	1613
6	**1a** + **2d**	2,4-Dimethyl-	(**3g**)	16.6	175–176	69.71	4.41	—	—	1642
7	**1d** + **2f**	2,7-Dimethyl-	(**3i**)	31.9	178–180	69.64	4.80	—	—	1632
		4-Chloro-1,7-dimethyl-	(**6a**)	4.7	209	—	—	12.91	—	1638
8	**1b** + **2f**	2,9-Dimethyl-	(**3k**)	47.9	199–200	69.78	4.56	—	—	1633
		4-Chloro-1,9-dimethyl-	(**6b**)	0.9	236–237	—	—	12.92	—	1638
9	**1d** + **2e**	4,7-Dimethyl-	(**3l**)	2.1	192–193	69.79	4.75	—	—	1615
		1-Chloro-2,7-dimethyl-	(**5a**)	4.7	188–189	—	—	12.86	—	1615
		2-Chloro-1,7-dimethyl-	(**5d**)	2.4	181–182	—	—	12.92	—	1623
10	**1c** + **2e**	4,8-Dimethyl-	(**3m**)	2.2	177–178	70.10	4.77	—	—	1618
		1-Chloro-2,8-dimethyl-	(**5b**)	8.9	198–199	—	—	12.99	—	1620
		2-Chloro-1,8-dimethyl-	(**5e**)	5.3	209–210	—	—	12.53	—	1616
11	**1b** + **2e**	4,9-Dimethyl-	(**3n**)	2.1	172–173	70.61	4.77	—	—	1628
		1-Chloro-2,9-dimethyl-	(**5c**)	5.6	185–187	—	—	12.93	—	1625

* This compound burns very difficultly.

works for the preparation of other 4′-hydroxy-diphenylamine derivatives.[1,3] The compounds **9** did not require a special purification for thionation. By treating with the calculated amount of sulphur and a small quantity of iodine, the crude dimethyl-4′-hydroxy-diphenylamines (**9a** — **e**) were converted into dimethyl-3-hydroxy-phenothiazines (**10**), which were not isolated but further oxidized with potassium dichromate in boiling glacial acetic acid. The obtained dimethyl-phenothiazones **11a** — **f** were purified by chromatography on alumina using toluene as eluant. The dimethyl-phenothiazones prepared by this method are presented in table 2.

Table 2

Dimethyl-phenothiazones obtained by method B

Compound	Yield %	m.p. °C	Analysis (calcd.)		IR[CO] cm^{-1}
			C 69.70	H 4.56	
			found		
6,7-Dimethyl-phenothiazone (**11a**)	1	205–207	*		1620
6,8-Dimethyl-phenothiazone (**11b**)	3.8	209–210	69.66	4.58	1624
6,9-Dimethyl-phenothiazone (**11c**)	0.4	183–184	69.78	4.66	1630
7,8-Dimethyl-phenothiazone (**11d**)	3.5	207–209	69.66	4.51	1624
7,9-Dimethyl-phenothiazone (**11e**)	0.7	177–179	69.66	4.54	1617
8,9 Dimethyl-phenothiazone (**11f**)	27.0	237–238	69.65	4.85	1615

* This compound burns very difficultly.

The compounds **11a** and **11d** were obtained together and their separation was difficult. The derivative **11d** has a little higher R_f value than **11a**. The isomers **11c** and **11e** were accompanied by some impurities which were completely eliminated only by repeated chromatography. Therefore the yields with which these compounds were obtained were very low.

The substances described in this work will serve for a study concerning the substituent-nucleus interaction.

EXPERIMENTAL

The melting points are corrected. The IR spectra were recorded with a Carl Zeiss Jena UR—10 spectrophotometer; the substances were prepared as KBr pellets.

Starting materials

Zinc mercaptides

Zinc 2-amino-thiophenolate[6] (**1a**), zinc mercaptide of 3-methyl-[7] (1b), 5-methyl-[8] (**1d**) and 6-methyl-2-amino-thiophenol[7,9] (**1e**) were obtained according to the methods described in literature. The preparation of zinc mercaptide of 2-amino-4-methyl-thiphenol (**1c**) will be reported in detail elsewhere.

p-Benzoquinones

Methyl-*p*-benzoquinone[10] (toluquinone, **2a**), 2,3-dimethyl-[11] (**2b**), 2-chloro-3-methyl-[12] (**2e**), 2-chloro-5-methyl-[13] (**2f**) and 2-bromo-6-methyl-*p*-benzoquinone[3] (2g) were prepared by the methods found in literature. 2,5-Dimethyl- (**2c**) and 2,6-dimethyl-*p*-benzoquinone (**2d**) were prepared by analogy following a method given for the preparation of 2,3-dimethyl-*p*-benzoquinone (**2b**).[14]

Dimethyl-4′-hydroxy-diphenylamines

General method. 13 g Dimethyl-aniline (**7a**—**e**) was heated at 180—190°C, 1.5 hour with 20 g hydroquinone (**8**) and 2 g zinc chloride. The reaction product was worked up as previously described for the preparation of 2-methyl-4′-hydroxy-diphenylamine.[3]

3,4-Dimethyl-4′-hydroxy-diphenylamine (**9a**). The crude product was a green-yellowish solid obtained with 95% yield.

3,5-Dimethyl-4′-hydroxy-diphenylamine (**9b**). This compound was obtained as a black solid with 85% yield.

2,5-Dimethyl-4′-hydroxy-diphenylamine (**9c**). The substance was a brown-black glue obtained with 26% yield.

2,4-Dimethyl-4′-hydroxy-diphenylamine (**9d**). This substance was prepared with 57% yield. The product was a brown-reddish oil.

2,3-Dimethyl-4′-hydroxy-diphenylamine (**9e**). The compound was obtained with 45% yield as a viscous oil which became solid on standing.

SYNTHESES OF DIMETHYLPHENOTHIAZONES

Method A. The mixture of 6.4 mmoles zinc thiophenolate **1a** — **e** with 12.8 mmoles chloromethyl- or dimethyl-*p*-benzoquinones **2a** — **g** and 40 ml 95% ethanol was stirred for 1 hour and then boiled for 5 minutes. The reaction product, a red suspension, was cooled, poured into water (400 mL), extracted with toluene (3 × 200 mL) and dried over $CaCl_2$ during the night. The next day the red solution was filtered, concentrated to 250—300 mL, cooled and then purified by column chromatography on 1 kg alumina (activity II). In the cases when this first chromatography was not satisfactory, the operation was repeated with 250 g silicagel columns deactivated with 13% water. Pure toluene was used as eluant. The results of our experiments are presented in table 1. The order in which the different phenothiazone derivatives were eluted from the chromatographic column is shown in table 3.

Table 3

Elution order from the chromatographic column of the different phenothiazone derivatives obtained by method A

Reaction number (see table 1)	$R_{f_1} > R_{f_2} > R_{f_3} < R_{f_4}$			
3	**3h**	**3j**	**3c**	**3e**
4	**4c**	**4a**	**3d**	
5	**4d**	**4b**	**3f**	
7	**6a**	**3i**		
8	**6b**	**3k**		
9	**5a**	**5d**	**3l**	
10	**5b**	**5e**	**3m**	
11	**5c**	**3n**		

In some cases from the reaction mixtures orange-coloured compounds were isolated and characterized, but this study will be published in another work.

We remark that in all cases the dimethyl-phenothiazones were the last compounds which left the chromatographic column. The substances have the lowest R_f value as compared with the halogeno-dimethyl-phenothiazones.

Method B. 6 g Dimethyl-4′-hydroxy-diphenylamine **9a** — **e** was mixed with 1.92 g sulphur, a small amount of iodine and 10 mL 1,2-dichlorobenzene and boiled for 1 hour. The reaction mixture was submitted to water steam distillation in order to remove the organic solvent and then the water was decanted. The residue was oxidized by boiling with 6 g potassium dichromate and 200 mL glacial acetic acid for 3 minutes. The red solution was poured into water (800 mL), extracted with toluene and the solution was worked up as above under method A. The dimethyl--phenothiazones obtained by this method are shown in table 2.

ACKNOWLEDGEMENTS. The authors are indebted to Miss Rodica Grecu for recording the IR spectra and to Mrs. Maria Duma and Ileana Roșu for the microanalytical determinations.

REFERENCES

[1] Part II, M. H. Terdic, *Rev. Roumaine Chim*, **29**, 489 (1984).
[2] U. Yoshio, T. Yukata, K. Jinya and Y. Takatoshi, *J. Heterocycl. Chem.*, **18**, 645 (1981).
[3] M. H. Terdic, *Liebigs Ann. Chem.*, **746**, 200 (1971).
[4] M. H. Terdic and C. Bodea, *Rev. Roumaine Chim.*, **13**, 833 (1968).
[5] M. H. Terdic and C. Bodea, *Rev. Roumaine Chim.*, **13**, 1244 (1968).
[6] A. W. Hoffman, *Ber. dtsch. chem. Ges.*, **13**, 20 (1880).
[7] C. E. Dalgliesh and F. G. Mann, *J. Chem. Soc.*, **1945**, 893.
[8] R L. Mital and S. K. Jain, *J. Chem. Soc.* (C), **1969**, 2148.
[9] F.Kurzer, C. S. Hamilton and D. B. Capps, *Org. Synth.* Coll. Vol. IV, 1980 (1963).
[10]. D·F.Chattaway and G. D. Parkes, *J. Chem. Soc.*, **127**, 1309 (1925).
[11] O. H.Emeson and L. I. Smith, *J. Am. Chem. Soc.*, **62**, 141 (1940).
[12] J. Cason, C. F. Allen and S. Goodwin, *J. Org. Chem.*, **13**, 403 (1948).
[13] K . Schniter, *Ber. dtsch. chem.Ges.* , **20**, 2282 (1887).
[14] L.F. Fiser and M. I. Ardao, *J. Amer. Chem. Soc.*, **78**, 774 (1956).

Revue Roumaine de Chimie, **30**, 2, 141—150 (1985)

STUDIES OF ENOLIZATION OF SOME SUBSTITUTED ACETOACETARYLAMIDES AT DIFFERENT TEMPERATURES AND CONCENTRATIONS

RAMESH KUMARI[a], A. D. TANEJA[b] and V. P. KUDESIA[c]
[a] Chemistry and Biochemistry, Dept. HAU, Hissar
[b] Biochemistry Dept., HAU, Hissar
[c] D. N. College, Meerut (U.P.), India

Received December 19, 1983

Enol contents of the acetoacetarylamides and substituted acetoacetarylamides have been determined by different methods in ethanolic medium at different temperatures and at different concentrations. From this data the equilibrium constants, free energies of tautomerisation, the changes in enthalpy, and changes in entropy of tautomerisation have been calculated. It is observed that the percentage enol increases with increase in temperature. The maximum change in the enthalpy of tautomerisation was observed for AAAH, OAATH, AAXH, OAAAH, PAAAH, PCAAAH, α-Br AAAH, α-Br OAATH, α-Br AAXH, α-Br OAAAH, α-Br PAAAH, α-Br PCAAAH, ω-Br AAAH, ω-Br OAATH, ω-Br AAXH, ω-Br OAAAH, ω-Br PAAAH and ω-Br PCAAAH. An electronic interpretation has been provided to account for the substituent effect.

INTRODUCTION

Determination of enol contents of acetoacetarylamides is of great importance in many physico-chemical investigations. Several methods have been used for studying keto-enol equilibrium which includes volumetric and spectroscopic methods. Mankad and Patel have studied the enol contents in acetoacetarylamides by Meyer's technique.[9] From the survey of literature it appears that practically no work has been done to determine the effect of temperature and concentration on the extent of enolisation of acetoacetarylamides. The present studies were undertaken in order to study the effect of temperature and concentration on the enol contents of acetoacetarylamides and substituted acetoacetarylamides and thereby to calculate the thermodynamic parameters.

EXPERIMENTAL

The compounds viz. acetoacetanilide (AAAH), *ortho*-acetoacetotoluidide (OAATH). 2,4-acetoacetoxylidide (AAXH), *ortho*-acetoacetanisidide (OAAAH), *para*-acetoacetanisidide (PAAAH), *para*-chloroacetonisidide (PCAAAH) (Aldrich Chemicals Co. Inc. Wisconsin), α-bromoacetoacetanilide (α-Br AAAH); α-bromo-*ortho*-acetoacetotoluidide (α-Br OAATH); α-bromo-2,4-acetoacetoxylidide (α-Br AAXH); α-bromo-*ortho*-acetoacetanisidide (α-Br OAAAH);

α-bromo-*para*-acetoacetanisidide (α-Br PAAAH); α-bromo-*para*-chloro-acetoacetanilide (α-Br PCAAAH); ω-bromo-acetoacetanilide (ω-Br AAAH); ω-bromo-*ortho*-acetoacetotoluidide (ω-Br OAATH); ω-bromo-2,4-acetoacetoxylidide (ω-Br AAXH); ω-bromo-*ortho*-acetoacetanisidide (ω-Br OAAH); ω-bromo-*para*-acetoacetanisidide (ω-Br PAAAH) and ω-bromo-*para*-chloro-acetoacetanilide (ω-Br PCAAAH) were synthesized and were used for the present studies. All the chemicals used were either of BDH Analar or E. Merck G.R. of extrapure quality. All the measurements were carried out at 30 ± 0.1°C. The samples were equilibrated at experimental temperature for four hours before the analysis. A blank consisting of the solvent alone was also run. The enol percentage of all these compounds in ethanol was determined by alkali as well as bromometric titration method at different intervals and not much increase in enol contents with passage of time was observed. The results indicated that all these compounds undergo a rapid tautomerism.

Alkali titration method

Standard solutions of the above given aromatic acetoacetamides and its derivatives were prepared in alcohol. An indirect alkali titration technique was adopted for determination of enol contents in these compounds. Twenty mL of these solutions of substituted aromatic acetoacetamides were transferred and the latter were placed in a thermostat maintained at 30° ± 0.1°C for 5 hours. Aldehyde free absolute ethanol was added to the contents of the flask to freeze the equilibrium and then a slight excess of standard NaOH solution was added. This solution was then back titrated with standard oxalic acid to determine unreacted base from which the amount of enol in these compounds was calculated. The titrations were repeated under the same conditions for obtaining concordant values. A similar study was undertaken for all these compounds at different concentrations viz. 0.0025, 0.0033, 0.005, 0.01, 0.02, 0.033 and 0.05 M.

Direct bromine titration method

An established direct bromometric procedure was used for the measurements. A set of solutions of these substituted acetoacetarylamides having the concentrations viz. 0.0025, 0.0033, 0.005, 0.01, 0.02, 0.033 and 0.05 M were prepared in ethanol and allowed to stand for 4 hours to attain equilibrium. Twenty mL of these solutions were transferred to separate conical flask and placed in a thermostate maintained at 30° + 0.1°C for 4 to 5 hours. 50 mL of aldehyde-free absolute ethanol cooled at −10°C were added to the contents of the flask to freeze the equilibrium and the contents were titrated immediately with standard 0.05 M ethanolic bromine solution to a faint yellow solution, which persisted for ten seconds.

Hibber's method

To check the correctness of the results obtained by the above methods we used another method given by Hibber,[10] the principle of which is the estimation of copper in the chloroform soluble chelate copper salt which is the enol form of addition product of copper acetate. From this solution on acidifying with H_2SO_4, $CuSO_4$ separates which is estimated iodometrically. One half atom of copper corresponds to one molecule of enol.

Effect of temperature

The effect of temperature on enolization percentage of substituted acetoacetarylamides was studied by determining the enol contents of these compounds in ethanol by using alkali titration method at different temperatures viz. 10°, 20°, 30°, 40° and 50°C. A blank consisting of the solvent alone was run for each sample. The results are reported in table 3.

From these data, the equilibrium constants enol/ketone were determined at various temperatures, from the relationship between equilibrium constant and absolute temperature. The change in enthalpy for tautomerisation may be obtained from the slope of the plot of log k_{eq} *versus* $1/T$. Free energies of tautomerisation have been calculated by using the equation : $\Delta G = -RT \ln k_e$. Finally the change in entropy for tautomerisation was calculated by using the standard equation. Values of these thermodynamic quantities are listed in table 3 for the systems studied.

RESULTS AND DISCUSSION

The percent enol contents of AAAH, OAATH, AAXH, OAAAH, PAAAH, PCAAAH, α-Br AAAH, α-Br OAATH, α-Br AAXH, α-Br OAAAH, α-Br PAAAH, α-Br PCAAAH, ω-Br AAAH, ω-Br OAATH, ω-Br AAXH, ω-Br OAAAH, ω-Br PAAAH and ω-Br PCAAAH in ethanol estimated by alkali-titration, direct bromine titration and by Hibber's method are given in table 1. Enol contents were estimated in AAAH, OAATH, AAXH, OAAAH, PAAAH, PCAAAH, α-Br AAAH, α-Br OAATH, α-Br PAAAH, α-Br PCAAAH, ω-Br AAAH, ω-Br OAATH and ω-Br PAAAH at different concentrations by bromine-titration method only and the results are given in table 2. No effect of concentration was observed on enol contents, when these were estimated by alkali-titration and Hibber's method. Bromine-titration method could not be applied in the case of α-Br AAHX, α-Br OAAAH, ω-Br AAXH, ω-Br OAAAH and ω-Br PCAAAH whereas alkali-titration method could not be used for determining enol contents in the case of α-Br OAAAH and ω-Br OAAAH because the end point could not be judged accurately as these

Table 1

Percent enol contents of different substituted acetoacetarlymides (by different methods).

$M = 5.00 \times 10^{-3}$ Temperature $t = 30 \pm 0.1$°C

No.	Compound	% enol by		
		Hibber's method	Alkali titration method	Direct bromine titration method
1	AAAH	11.97	11.37	12.85
2	OAATH	10.05	9.69	11.20
3	AAXH	9.05	8.68	9.70
4	OAAAH	9.25	8.86	9.40
5	PAAAH	10.19	10.09	10.80
6	PCAAAH	11.08	10.78	11.40
7	α-Br AAAH	28.32	27.92	30.24
8	α-Br AATH	26.83	26.23	27.50
9	α-Br AAXH	25.45	25.05	—
10	α-Br OAAAH	26.10	—	—
11	α-Br PAAAH	27.15	26.84	27.75
12	α Br PCAAAH	27.82	27.52	28.75
13	ω-Br AAAH	26.28	26.18	27.65
14	ω-Br OAATH	24.02	23.81	24.75
15	ω-Br AAXH	22.71	22.31	—
16	ω-Br OAAAH	23.11	—	—
17	ω-Br PAAAH	24.20	23.90	25.05
18	ω-Br PCAAAH	25.05	24.80	—

Table 2

Effect of concentration on the enol percentage (%) of some substituted acetoacetarylamides in ethanol by direct bromine titration method

Temperature 30 ± 0.1°C

No.	Compound	Molarity	% Enol
1	AAAH	2.50×10^{-3}	19.60
		3.33×10^{-3}	17.50
		5.00×10^{-3}	12.85
		10.00×10^{-3}	5.40
		20.00×10^{-3}	3.90
		33.00×10^{-3}	3.40
		50.00×10^{-3}	2.90
2	OAATH	2.50×10^{-3}	17.60
		3.33×10^{-3}	15.70
		5.00×10^{-3}	11.20
		10.00×10^{-3}	4.10
		20.00×10^{-3}	2.50
		33.00×10^{-3}	1.80
		50.00×10^{-3}	1.40
3	AAXH	2.50×10^{-3}	16.20
		3.33×10^{-3}	14.05
		5.00×10^{-3}	9.70
		10.00×10^{-3}	3.50
		20.00×10^{-3}	2.10
		33.00×10^{-3}	1.60
		50.00×10^{-3}	1.35
4	OAAAH	2.50×10^{-3}	16.30
		3.33×10^{-3}	13.60
		5.00×10^{-3}	9.40
		10.00×10^{-3}	3.90
		20.00×10^{-3}	2.20
		33.00×10^{-3}	1.90
		50.00×10^{-3}	1.50
5	PAAAH	2.50×10^{-3}	17.80
		3.33×10^{-3}	15.50
		5.00×10^{-3}	10.80
		10.00×10^{-3}	4.05
		20.00×10^{-3}	2.80
		33.00×10^{-3}	2.30
		50.00×10^{-3}	1.95

Table 2 (continued)

No.	Compound	Molarity	% Enol
6	PCAAAH	2.50×10^{-3}	19.10
		3.33×10^{-3}	15.80
		5.00×10^{-3}	11.40
		10.00×10^{-3}	5.30
		20.00×10^{-3}	3.90
		33.00×10^{-3}	3.40
		50.00×10^{-3}	2.95
7	α-Br-AAAH	2.50×10^{-3}	37.20
		3.33×10^{-3}	34.05
		5.00×10^{-3}	30.24
		10.00×10^{-3}	21.60
		20.00×10^{-3}	19.90
		33.00×10^{-3}	19.50
		50.00×10^{-3}	19.20
8	α-Br-OAATH	2.50×10^{-3}	33.85
		3.33×10^{-3}	31.90
		5.00×10^{-3}	27.50
		10.00×10^{-3}	20.40
		20.00×10^{-3}	18.60
		33.00×10^{-3}	18.05
		50.00×10^{-3}	17.40
9	α-Br PAAAH	2.50×10^{-3}	34.75
		3.33×10^{-3}	32.40
		5.00×10^{-3}	27.75
		10.00×10^{-3}	21.00
		20.00×10^{-3}	19.40
		33.00×10^{-3}	18.80
		50.00×10^{-3}	18.30
10	α-Br PCAAAH	2.50×10^{-3}	35.60
		3.33×10^{-3}	32.25
		5.00×10^{-3}	28.75
		10.00×10^{-3}	22.25
		20.00×10^{-3}	20.45
		$33,00\times10^{-3}$	19.80
		50.00×10^{-3}	19.10
11	ω-Br-AAAH	2.50×10^{-3}	34.40
		3.33×10^{-3}	31.55
		5.00×10^{-3}	27.65
		10.00×10^{-3}	18.95
		20.00×10^{-3}	17.05
		33.00×10^{-3}	16.45
		50.00×10^{-3}	15.90

Table 2 (continued)

No.	Compound	Molarity	% Enol
12	ω-Br OAATH	2.50×10^{-3}	31.40
		3.33×10^{-3}	29.35
		5.00×10^{-3}	24.75
		10.00×10^{-3}	17.65
		20.00×10^{-3}	16.10
		33.00×10^{-3}	15.50
		50.00×10^{-3}	14.85
13	ω-Br PAAAH	2.50×10^{-3}	31.65
		3.33×10^{-3}	29.30
		5.00×10^{-3}	25.05
		10.00×10^{-3}	18.10
		20.00×10^{-3}	16.45
		33.00×10^{-3}	16.05
		50.00×10^{-3}	15.70

compounds are coloured. Enol contents in these compounds except α-Br OAAAH and ω-Br OAAAH were determined at different temperatures viz. 10°, 20°, 30°, 40° and 50°C by alkali-titration method and the results are given in table 3.

Table 3

Efect of temperature on percent enol and thermodynamic functions of substituted acetoacetarylamides (in ethanol by alkali titration method).

Concentration $= 5.00\times10^{-3}$

No.	Compound	Temperature	% Enol	K_{eq}	ΔG kcal/mole	$-\Delta H$kcal/mole	$-\Delta S$ cal/mole/deg.
1	AAAH	283.16	7.90	0.0850	1.3821	3.7482 (average)	18.12
		293.16	9.67	0.1070	1.3018		17.23
		303.16	11.37	0.1282	1.2371		16.44
		313.16	13.85	0.1607	1.1325		15.59
		323.16	16.45	0.1968	1.0566		14.87
2	OAATH	283.16	6.30	0.0672	1.5191	4.1600 (average)	20.06
		293.16	7.90	0.0857	1.4309		19.07
		303.16	9.69	0.1072	1.3448		18.16
		313.16	11.95	0.1357	1.2414		17.25
		323.16	14.45	0.1689	1.1563		16.45
3	AAXH	283.16	5.20	0.0548	1.6336	4.4762 (average)	21.58
		293.16	6.90	0.0741	1.5160		20.44
		303.16	8.68	0.0950	1.4179		19.44
		313.16	10.88	0.1220	1.3089		18.47
		323.16	13.22	0.1523	1.2238		17.64

Table 3 (continued)

No.	Compound	Temperature	% Enol	K_{eq}	ΔG kcal/mole	$-\Delta H$kcal/mole	$-\Delta S$ cal/mole/deg.
4	OAAAH	283.16	5.45	0.0576	1.6056	4.4554 (average)	21.41
		293.16	7.15	0.0770	1.4936		20.29
		303.16	8.86	0.0972	1.4043		19.33
		313.16	11.06	0.1243	1.2967		18.37
		323.16	13.46	0.1555	1.2093		17.53
5	PAAAH	283.16	6.70	0.0718	1.4820	3.5942 (average)	17.93
		293.16	8.25	0.0899	1.4033		17.05
		303.16	10.09	0.1122	1.3179		16.21
		313.16	12.29	0.1401	1.2229		15.38
		323.16	14.60	0.1709	1.1484		14.68
6	PCAAAH	283.16	7.30	0.0787	1.4302	3.7523 (average)	18.31
		293.16	9.01	0.0990	1.3472		17.40
		303.16	10.78	0.1208	1.2735		16.58
		313.16	12.98	0.1491	1.1842		15.76
		323.16	15.35	0.1813	1.1102		15.05
7	α-Br AAAH	283.16	24.25	0.3201	0.6410	1.8928 (average)	8.95
		293.16	26.05	0.3522	0.6078		8.53
		303.16	27.95	0.3879	0.5704		8.13
		313.16	30.30	0.4347	0.5184		7.70
		323.16	32.75	0.4869	0.4678		7.31
8	α-Br OAATH	283.16	22.50	0.2903	0.6959	1.9469 (average)	9.33
		293.16	24.33	0.3215	0.6610		8.90
		303.16	26.23	0.3555	0.6230		8.48
		313.16	28.53	0.3991	0.5714		8.04
		323.16	30.88	0.4467	0.5238		7.65
9	α-Br AAXH	283.16	21.20	0.2690	0.7388	2.0426 (average)	9.85
		293.16	23.15	0.3012	0.6990		9.35
		303.16	25.05	0.3342	0.6603		8.92
		313.16	27.35	0.3764	0.6078		8.46
		323.16	29.75	0.4234	0.5585		8.05
10	α-Br PAAAH	283.16	23.14	0.2934	0.6757	1.9926 (average)	9.45
		293.16	24.94	0.3322	0.6416		8.99
		303.16	26.84	0.3668	0.6042		8.57
		313.16	29.24	0.4132	0.5498		8.12
		323.16	31.65	0.4630	0.5004		7.71
11	α-Br PCAAAH	283.16	23.95	0.3149	0.6505	1.8304 (average)	8.76
		293.16	25.75	0.3468	0.6169		8.35
		303.16	27.52	0.3796	0.5834		7.96
		313.16	29.88	0.4261	0.5310		7.54
		323.16	32.05	0.4716	0.4886		7.18

Table 3 (continued)

No.	Compound	Temperature	% Enol	K_{eq}	ΔG kcal/mole	$-\Delta H$ kcal/mole	$-\Delta S$ cal/mole/deg.
12	ω-Br AAAH	283.16	22.45	0.2971	0.6828	1.8720 (average)	9.05
		293.16	24.28	0.3206	0.6627		8.65
		303.16	26.18	0.3546	0.6246		8.24
		313.16	28.58	0.4001	0.5700		7.80
		323.16	30.88	0.4467	0.5238		7.41
13	ω-Br OAATH	283.16	19.95	0.2492	0.7808	2.1549 (average)	10.37
		293.16	21.90	0.2804	0.7385		9.87
		303.16	23.81	0.3125	0.7007		9.42
		313.16	26.21	0.3561	0.6441		8.94
		323.16	28.71	0.4027	0.5897		8.49
14	ω-Br AAXH	283.16	18.41	0.2256	0.8379	2.2797 (average)	11.01
		293.16	20.40	0.2562	0.7932		10.48
		303.16	22.31	0.2871	0.7517		10.00
		313.16	24.71	0.3281	0.6932		9.49
		323.16	27.21	0.3738	0.6395		9.03

From the results it is observed that the percentage of enol obtained by bromine-titration method is higher in all the cases as compared to those obtained by alkali-titration and Hibber's method. It is assumed that this reaction i.e. keto-enol tautomerisation is instantaneous as no time effect was observed on enol contents. During the process of enolisation it is thought that the $-\underset{\underset{\textstyle O}{\|}}{C}-$ group gives rise to the $-\underset{\underset{\textstyle OH}{|}}{C}=$ group due to the proton shift from carbon adjacent to the carbonyl grpup and keto-enol tautomerisation in β-dicarbonyls may be considered as an equilibrium between keto and enol forms through the anions as pictured below :

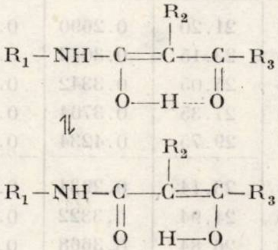

Acetoacetarylamides, AAAH, have maximum enol content while AAXH minimum enol content. In α-bromosubstituted acetoacetarylamides the enol contents are in the order : α-Br AAAH >, α-Br PCAAAH > α-Br PAAAH > α-Br OAATH > α-Br OAAAH > α-Br AAXH > and in ω-bromo acetoacetarylamides the order of enol contents is found as : ω-Br AAAH > ω-Br PCAAAH > ω-Br PAAAH > ω-Br OAATH > ω-Br OAAH > ω-Br AAXH. If we compare the enol contents of substituted-

-acetoacetarylamides in general the following order is observed : α-bromo substituted acetoacetarylamides > ω-bromo substituted acetoacetarylamides > acetoacetarylamides.

For the sake of easy comparison the percentage enol content obtained by direct bromine-titration method at different concentrations of each compound is plotted against molar concentrations. The curves seem to be almost perpendicular to the enol concentration axis. This is in accord with the observation made by Meyer and Kappelmeir.[11] The tendency towards a large increase in enolisation is clearly marked out from the bands of the curves shown by dotted lines which run parallely to the axis of the percentage enol. The data presented in these figures show that the enol content increases with the dilution of the solution, the increase in enol content is minimum as the concentration decreases. This observation is in agreement with the results reported for ethylacetoacetate[11] and in acetoacetarylamides by Patel and Mankad.[9] The replacement of $-COOC_2H_5$ by $-CONHR$ (viz. acetoacetarylamides) decreases the enol content. This can be explained on the basis of Zuffanti's results.[12] In ethylacetoacetate $-OC_2H_5$ is an electron releasing group and therefore the percent enol at 0.05M is 17.48 but in acetoacetarylamides viz. AAAH, at the same concentration, the percentage of enolization is lower, namely 12.85, and this is due to the higher electron releasing character of phenyl radical. The effect of aryl group on α-H is increased by intervening $-NH-$ group with a lone pair of electrons. The introduction of a methyl or methoxy group at *ortho* position, a chloro or methoxy group at *para* position or two methyl groups at 2,4-position in the benzene ring should appreciably increase the electron releasing ability of C_6H_5-NH group thereby further lowering the enol contents in OAATH, AAXH, OAAAH, PAAAH and PCAAAH in comparison with AAAH. Steric hindrance also plays its own role in decreasing the percent enol in these compounds. So the difference in enol content appears to be due to the presence of the different substituents in the phenyl group. From Table 1 it can be seen that α--bromo-substituted acetoacetarylamides have more percent enol (25.45 to 28.32) than ω-bromo substituted acetoacetarylamides (22.71 to 26.28) or acetacetarylamides (9.05 to 11.97). This may be due to the fact that the presence of bromine, a strong electron withdrawing group, at α-position favours the creation of region of low electron density at carbon thereby helping the transfer of proton from methylenic carbon to carbonyl oxygen and hence the increase of the percent enol in bromo-substituted acetoacetarylamides. Among all these compounds in α-Br AAAH a maximum percent enol (28.32) whereas in α-Br AAXH a minimum percent enol (25.45) were observed. The presence of $-CH_2$-Br group instead of $-CH_3$ group at ω-position in acetoacetarylamides, increases the percent enol of acetoacetarylamides. This effect is less marked in comparison with α-bromo substituted-acetoacetarylamides because of the lengthening of the chain of carbon atom which keeps bromine away from 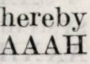 $-\underset{\overset{|}{O}}{C}-$ link ; the $-CH_2$-Br group lowers the electron density at 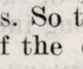 $-\underset{\overset{|}{O}}{C}-$ thereby enhancing the transfer of proton from $-CH_2-$ (methylenic) group to carbonyl oxygen and hence increases the enol contents of these compounds. Among all ω-bromo substituted acetoacetarylamides, ω-Br AAAH has the maximum percent enol (26.28) and ω-Br AAXH has the minimum percent enol (22.71).

The generality of the high percentage of enol in α-bromo and ω-bromo-substituted acetoacetarylamides as compared to those of acetoacetarylamide may be due to the fact that the bromine substituent at α- or ω-position causes steric hindrance, forcing the carbonyls closer together and thus the greater tendency to enolise in order to reduce the electrical repulsion between the carbonyls.

Equilibrium constant (K_{eq}) and thereby thermodynamic parameters such as free energy change (ΔG), enthalpy change (ΔH) and entropy change (ΔS) have been determined at various temperatures and are recorded in table 3. While studying the effect of temperatures on enolisation it is observed that an increase in temperature results in increasing the enol contents of these substituted acetoacetarylamides. Our results are different from the results of Taneja *et. al.* [13-16] in the case of acetoacetarylamides. Higher positive values of free energy (cf. Table 3) indicate an increased keto tautomer and vice versa. Positive value of ΔG signifies a reaction in which at equilibrium a considerable preponderance of reactant molecules i.e. ketone was observed. The greatest change in the enthalpy of tautomerisation occurs for AAXH. On the other hand there is comparatively little effect of temperature upon the position of equilibrium in α-Br-PCAAAH. The entropies of tautomerisation indicate more ordered systems for the enol tautomers as compared to the keto tautomers. AAXH, OAAAH, α-Br AAAH and ω-Br AAXH have large negative entropies of tautomerisation. It is suggested that these compounds have very strong intermolecular hydrogen bonding.

ACKNOWLEDGEMENTS. Thanks are due to the authorities of D.N. College, Meerut for providing the necessary facilities. The help rendered by Dr S. K. Arora, Senior Biochemist, Sorghum, in using certain instruments is gratefully acknowledged.

REFERENCES

[1] K. Meyer, *Liebigs Annal. Chem.*, **212**, 380 (1911).

[2] K. Meyer, *Chem. Ber.* 47, 845 (1941).

[3] A. Gero, *J. Amer. Chem. Soc.* **75**, 5119 (1953).

[4] G. Schwarzenback, *Helv. Chim. Acta*, **30**, 657 (1947).

[5] H. E. Acly and H. S. French, *J. Amer. Chem. Soc.* **47**, 847 (1927).

[6] J. L. Burdett and M. T. Rogers, *J. Amer. Chem. Soc.* **86**, 2105 (1966).

[7] G. Allen and R. A. Dwek, *J Chem. Soc. (B)*, **1966**, 161.

[8] G. K. Schweitzer and E. W. Benson, *J. Chem. Eng. Data*, **13**, 452 (1968).

[9] B. N. Mankad and M. R. Patel, *Indian J. Chem.*, **3**, 137 (1965).

[10] M. M. Bokadia and S. S. Desphande, *J. Indian Chem. Soc.* **26**, 3455 (1949).

[11] K. H. Mayer and Kappelmeier, *Ber. dtsch. Chem. Ges.* **44**, 2718 (1911).

[12] S. Zuffanti, *J. Chem. Educ.*, **22**, 230 (1945).

[13] A. D. Taneja and K. P. Srivastava, *Chimia*, **25**, 92 (1971).

[14] A. D. Taneja and K. P. Srivastava, *J. Indian Chem. Soc.*, **49**, 889 (1972).

[15] A. D. Taneja and K. P. Srivastava, *J. Chin. Chem. Soc.*, **19**, 115 (1972).

[16] A. D. Taneja and K. P. Srivastava, *Bulletin of the Institute of Chemistry, Academia Sinica* (1973).

Revue Roumaine de Chimie, **30**, 2, 151–155 (1985)

CATALYTIC INFLUENCES IN THE ELECTROOXIDATION OF OLEFINS IN NON-AQUEOUS SOLUTIONS. I

EXPERIMENTAL ASPECTS

RADU VLĂDEA
"Traian Vuia" Polytechnic Institute
Blvd. 30 Decembrie No. 2 Timişoara, Romania

Received October 13, 1982

The paper is dealing with the experimental techniques used in the investigation of anodic reactions of weakly- or nonactivated olefins. The oxidation process of these olefins is completely irreversible as was also certified by cyclic voltammetry. The preliminary polarization curves gave some information on the behaviour of different types of electrodes.

In recent years, much interest has been given to the electrochemical synthesis of organic compounds. However, much attention has been concentrated on the anodic oxidation of aromatic compounds[1] and very little study has been accomplished on the electrochemical reactions of aliphatic olefins.[2]

The "functionalization" of aliphatic hydrocarbons remains a great challenge to synthetic organic chemists. Electrode reactions allow the introduction of large quantities of energy into molecules in a controlled manner and at room temperature and are known to be successful in the activation of inert substrates. Hence it would seem appropriate to examine the conditions under which aliphatic hydrocarbons undergo a partial anodic oxidation and also to consider the use of such electrode reactions for the preparations of useful organic compounds in a single step starting from these very cheap feedstocks. At the present time it is possible to suggest at least five types of systems by which the electrochemical functionalization of aliphatic olefins may be carried out. These are :

1. One electron direct transfer, followed by a reaction of the radical cation with a nucleophile Nu^-. The intermediate may be the subject of a radical-radical dimerization or of a new one-electron oxidation and a new reaction with Nu^- :

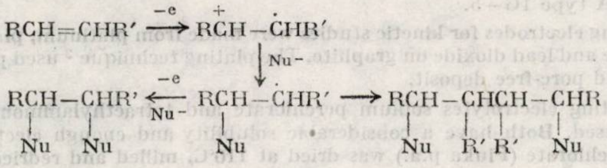

$$RCH{=}CHR' \xrightarrow{-e} \overset{+}{R}CH-\dot{C}HR'$$

$$\underset{Nu}{RCH}-\underset{Nu}{CHR'} \xleftarrow[Nu^-]{-e} \underset{Nu}{RCH}-\dot{C}HR' \longrightarrow \underset{Nu}{RCH}-\underset{R'}{CH}\underset{R'}{CH}-\underset{Nu}{CHR}$$

where Nu⁻ could be : OH, OCH_3, aciloxy, CN, N_3, OCN, halide, SCN, and other organic anions.

2. Direct electron transfer (two successive steps of one electron transfer) resulting an allylic cation which reacts with Nu⁻ :

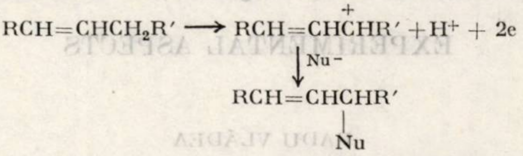

$$\begin{array}{c} RCH{=}CHCH_2R' \longrightarrow RCH{=}CH\overset{+}{C}HR' + H^+ + 2e \\ \big\downarrow {\scriptstyle Nu^-} \\ RCH{=}CH\underset{\displaystyle Nu}{\underset{|}{C}}HR' \end{array}$$

3. The electrooxidation of the system solvent-supporting electrolyte may produce radicals which react in two pathways with an alkene, either by addition or by substraction of an allylic hydrogen followed by a reaction with a Nu⁻.

4. Discharge of a halide ion followed by a chemical reaction of the olefin, halide and a Nu⁻ ("halofunctionalization").

5. Functional groups may also be introduced into alkenes by their reaction with inorganic intermediates produced at the anode.

It is the aim of this paper to present the experimental techniques used in the investigation of anodic reactions of weakly- and non-activated olefins.

EXPERIMENTAL TECHNIQUE

The measured current/voltage curves and Tafel plots were obtained at rotating electrodes. The rod electrodes were rotated with a high enough speed to eliminate any interference of mass transfer hindrance of alkenes to the anodes. A thermostated "beaker" cell with a fitted cork was used. The working electrode was in the form of a wire fitted in a glass tube full of mercury. Electrical contact was made from a platinum contact placed in mercury. The electrodes were fitted directly to the drive shaft of a variable speed motor. The counter electrode was a cylindrical platinum lamina. The reference electrode against which all potentials were quoted was an Ag/Ag⁺ system connected via a salt-bridge arrangement on a sliding Luggin probe. The reference electrode consisted of a high-purity silver wire soaked into a $AgClO_4$ solution. The electrode Ag/Ag⁺ 10^{-2} M in acetonitrile having + 0.300 V vs. SCE (saturated calomel electrode)[4] is recommended for non-aqueous solutions.[5,6] Gas for deaeration could be introduced by a tube, fitted through the cork and leading near the working electrode, a gas bubbler being placed in the gas vent.

The electrolytic cell formed part of the negative feedback circuit (Fig. 1). The electrical equipment was Tacussel—SOLEA : a potentiostat type PRT—20—2x, a potentiometer type Servovit 10 and a potentiometric recorder type EPL-2B with interchangeable plug-ins.

Preparative electrolyses at controlled potential were made in a thermostated "beaker" cell provided with magnetic stirrer, condenser, tube for gas deaeration and a gas bubbler. The working electrode was a pyrolytic graphite in cylindrical shape, the counter-electrode was a platinum cylindrical gauze, and the reference electrode Ag/Ag⁺ was connected with a Luggin capillary.

The cell formed part of an electrical circuit (Fig. 2). The electronic integrator was Tacussel—SOLEA type IG—5.

The working electrodes for kinetic studies were made from platinum, platinized titanium, pyrolytic graphite and lead dioxide on graphite. The plating technique [3] used produced a bright, smooth, hard, and pore-free deposit.

As supporting electrolytes sodium perchlorate and tetraethylammonium tosylate respectively, were used. Both have a considerable solubility and enough electrochemical inertness. Sodium perchlorate (Fluka p.a.) was dried at 110°C, milled and redried just before use.

Tetraethylammonium tosylate was synthesized in the laboratory by using a known method.[7] The crude material was recrystallized from acetone and dried in vacuum. Acetonitrile and methanol were used as solvents. Kinetic studies were conducted in acetonitrile, reproducible polarisation curves for all electrodes materials being achieved.

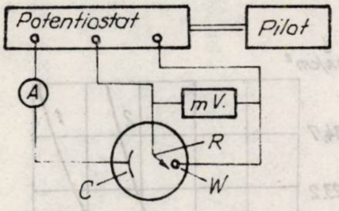

Fig. 1. — The electrical connection in a potentiostatic assembly: W — working electrode, R — reference electrode and C — counter electrode.

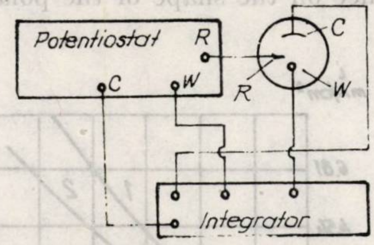

Fig. 2. — The electrical connection in an assembly for controlled potential electrolysis: W — working electrode, R — reference electrode and C — counter electrode.

Acetonitrile was purified through a derived method from the known ones [8-11]: consecutive cycles of refluxing and rapid distillation on NaH, P_2O_5, $KHSO_4$, and CaH_2, and a final distillation on a 2 meter column filled with glasses.

Methanol was purified by 10 hours refluxing with Mg and I_2 followed by a distillation at 64.7°C (760 mm Hg).

Residual water determination was made both by amperometrical titration with Karl-Fischer reactants and by gas-chromatography using the "Chromatron GCHF 18.3" type equipped with catharometer and a 2 meter long column filled with Porapak Q.

The product analyses were run on a gas chromatograph Perkin Elmer, model 990, coupled with a double-focusing mass spectrometer MAT 311 with reversed Nier-Johnson geometry, provided with a 50 m capillary column with squalan. In the case of styrene a 50 m capillary column filled with OV—7 and a temperature programme between 150—280°C with 10°C/min were used. All of the spectra were measured at an ionization potential of 70 eV and a trap current of 60 μA. The two-stage jet separator was maintained at 275°C and the temperature of the source was ca. 250°C.

Diisobutylene (BDH analytical grade) was used. Styrene was freshly distilled before use.

RESULTS

The oxidation of weakly- or non-activated olefins is a completely irreversible process [12,13] as was also certified by cyclic voltammetry.[14]

The preliminary polarization curves gave some information on the behaviour of different types of electrodes. They were obtained with a potential sweep rate of 1100 mV/min. All experiments were conducted at 25°C.

The polarization curve for a DIB solution in methanol and $NaClO_4$ (10^{-1} M/L) as supporting electrolyte is presented in figure 3. The working electrode was a platinum wire with a surface of 0.088 cm^2.

The addition of small olefin amounts leads to a potential shift to more positive values (curve 2), perhaps in connection with a surface blocking of the electrode due either to polymer formation or to a strong chemosorption of the olefins.

Using other materials as electrode, e.g. platinized titanium, graphite and lead dioxide on graphite, normal polarization curves were achieved (Figs 4 and 5).

It is obvious from these plots that the anode material has a strong influence on the shape of the polarization curves as well as on the half-wave potential of olefins which are shifted to more negative values in the series platinized titanium, lead dioxide on graphite and graphite. It is worthwhile to mention the big difference which exists between platinum and platinized titanium electrodes.

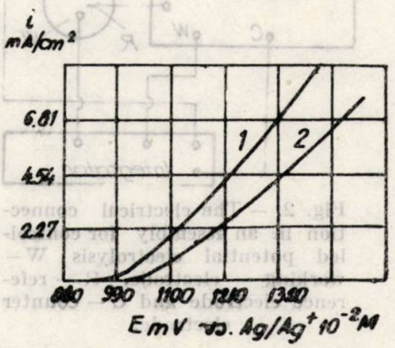

Fig. 3. — Current-potential curves on paltinum electrode : 1 : Methanol + sodium perchlorate (10^{-1} M/L) 2 : *Ibid.* 1 + Diisobutylene (DIB) (5.5×10^{-2} M/L).

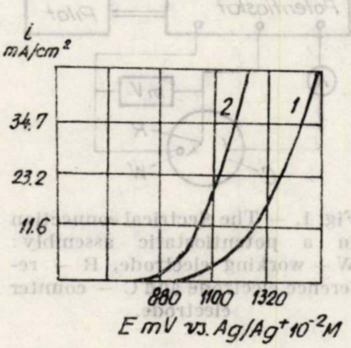

Fig. 4. — Current-potential curves on graphite electrode : 1 : Methanol + sodium perchlorate (10^{-1} M/L)) 2 : *Ibid.* 1 + Diisobutylene (DIB) 5.5×10^{-2} M/L).

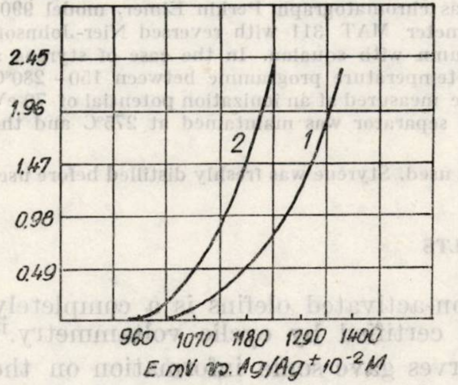

Fig. 5. — Current-potential curves on PbO_2/C electrode : 1 : Methanol + + sodium perchlorate (10^{-1} M/L) 2 : *Ibid.* 1 + Diisobutylene (DIB) ($5.5 \times \times 10^{-2}$ M/L).

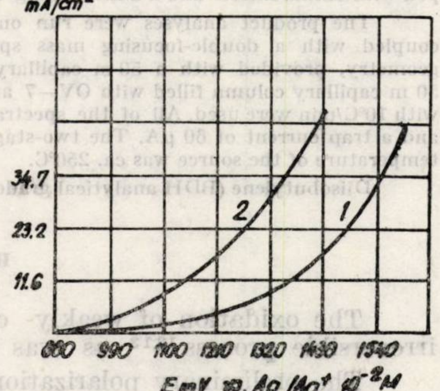

Fig. 6. — Current-potential curves on graphite electrode : 1 : Methanol + + tetraethylammonium tosylate (10^{-1} M/L) 2 : *Ibid.* 1 + Diisobutylene (DIB) (5.5×10^{-2} M/L).

On the other hand, the use of tetraethylammonium tosylate instead of $NaClO_4$ had a pronounced influence on the shape and position of the polarization curves (Fig. 6). By comparing the curves in figures 4 and 6, it can be shown that at the same potential, the values for current densities are smaller in the case of tosylate.

All these influences may be attributed to a concurrent electrosorption of different species (solvents, supporting electrolytes, reactants) on the electrode.

A similar behaviour was noticed in the case of styrene electrooxidation.

It is obvious that the rate of an electrochemical reaction is strongly affected both by the nature and morphology of the electrodes and by the presence in the system of species not directly involved in the reaction (ions of electrolyte, solvents, etc.).

REFERENCES

[1] N. L. Weinberg and H. R. Weinberg, *Chem. Rev.*, **68**, 449 (1968).

[2] G. Foita, M. Fleischmann and D. Pletcher, *J. Chem. Soc. C.* 1968, 2055.

[3] Gh. Facsko and F. Golumbioschi, "Proceedings of the Analytical Chemical Conference", Akademiai Kiadó, Budapest, 1966, p. 382.

[4] R. C. Larson, R. T. Iwamoto and R. N. Adams, *Analyt. Chim. Acta*, **25**, 371 (1961).

[5] H. Lund, *Acta Chem. Scand.*, **11**, 1323 (1957).

[6] V. A. Pleskov, *Zhur. fiz. Khim.*, **22**, 351 (1948).

[7] R. H. McKee, *Infd. Eng. Chem.*, **38**, 382 (1946).

[8] J. F. Coetzee, G P. Cunningham D., K. McGuise and G. R. Padmanabhan, *Analyt.Chem.*, **34**, 1138 (1962).

[9] A. Weissberger, E. Proskauer, J. Riddik and E. Toops, "Technique of Organic Chemistry" vol. 7, Interscience, New York, 1955, p. 435.

[10] J. F. O'Donnell, J. T. Ayeres and Ch. K. Mann, *Analyt. Chem.*, **37**,, 1161 (1965).

[11] N. Rabjolm ed., "Organic Synthesis", Wiley, New York, vol. 4, 1963, p. 473.

[12] V. D. Parker and L., Eberson, *Chem. Comm.*, **1969**, 340.

[13] M. Katz, P. Riemenschneider and H. Wendt, *Electrochim. Acta*, **17**, 1595 (1972).

[14] R. Vlădea, Dissertation, "Traian Vuia", Polytechnic Institute, Timișoara, 1976, p. 101.

Revue Roumaine de Chimie, **30**, *2*, 157–170 (1985)

CATALYTIC INFLUENCES IN ELECTROOXIDATION OF OLEFINS IN NON-AQUEOUS SOLUTIONS. II*.

DIISOBUTYLENE AND STYRENE OXIDATION PRODUCTS

RADU VLĂDEA[a] and FRANCISC KEREK[b]

[a] "Traian Vuia" Polytechnic Institute Timișoara
Blv. 30 Decembrie Nr. 2
[b] Icechim-Centrul de Chimie —Timișoara
Blv. M. Viteazu Nr. 24

Received October 13, 1982

The anodic oxidation products of diisobutylene and styrene in methanol were identified using a GC—MS system. Most of diisobutylene derivatives were constitutional isomers of some unsaturated ethers with molecular formula $C_9H_{18}O$. The styrene oxidation led to the predominant production of methoxylated monomers and dimers.

There are now clear indications that the anodic oxidation of aliphatic and aromatic hydrocarbons in aprotic solvents may be used to synthesize a range of partially oxidized products. At the same time it was demonstrated[1] that the direct anodic oxidation of asymmetric olefins at carbon anodes in methanolic solutions leads in some cases to the predominant production of anodic dimers. However only in very few cases the anodic dimerization of asymmetric olefins is a very selective reaction.

It is the aim of this paper to describe the electrochemical behaviour of an olefin susceptible to anodic allylic substitution (diisobutylene-DIB) and of styrene which tends to dimerize.

The anodic electrooxidations were run on a preparative scale, in which the reactions were not necessarily carried out under the optimum conditions.

The choice of DIB was made in an attempt to prove either a radicalic mechanism which leads to structurally different products or a carbocationic one supposing a common intermediate and identical products in an ECEC type mechanism. At the same time the knowledge of types and structures of styrene oxidation products is also very important for a better understanding of the electrode mechanism.

The electrolyses were run in a diaphragmless thermostated "beaker" cell provided with magnetic stirrer, condenser, gas bubbler and tub for gas deaeration. The working electrodes were pyrolytic graphite or lead dioxide on graphite in cylindrical shape, the counter-electrode was a platinum electrode, and the reference electrode Ag/Ag$^+$ was connected with a Luggin capillary. The equipment for controlled potential electrolysis was previously shown.[2] The process variables are given in table 1.

---

* Previous part is ref. [2]

Table 1

The process variables for DIB and Styrene anodic oxidation

Anode material	Olefin conc. Mol/L	Supp. electrolyte conc. Mol/L	Work potential mV	Total passed current C	Current yield %
	DIB				
Carbon	2	0.2 $NaClO_4$	1200	22890	60
Carbon	2	0.3 $NaClO_4$	1200	30100	62.5
Carbon	4	0.3 $NaClO_4$	1200	30058	48
Carbon	2	0.5 $NaClO_4$	1200	32163	66
Carbon	2	0.2 $TsNEt_4$	1500	54100	67
Carbon	2	0.4 $TsNEt_4$	1500	36150	69
PbO_2/C	2	0.2 $NaClO_4$	1100	42000	74
PbO_2/C	2	0.2 $TsNEt_4$	1200	36840	80
	Styrene				
Carbon	2	0.3 $NaClO_4$	1300	—	—
Carbon	2	0.3 $TsNEt_4$	1300	—	—
PbO_2/C	2	0.3 $NaClO_4$	1200	—	—
PbO_2/C	2	0.3 $TsNEt_4$	1200	—	—

Methanol was the common solvent used. After the electrolysis was completed, most of the methanol was evaporated under reduced pressure. The residue was washed with water for removing the supporting electrolyte and extracted with ether. After drying on anhydrous magnesium sulfate, the ether was removed by distillation. Each product was identified by mass spectrometry and the yields were determined by gas chromatography using correction factors. The chromatographic separations were made using a capillary column (50 m) filled with squalan, at 110°C, with helium as carrier gas (flow rate 30 mL /min) for DIB oxidation products and a capillary column (50 m) with OV—7 and a temperature programme between 150—280°C with 10°C /min. for styrene oxidation products.

DIISOBUTYLENE OXIDATION PRODUCTS

A mixture of DIB isomers (BDH p.a.) of 97% I and 3% II and another with 74.4% II and 25.6% I were used

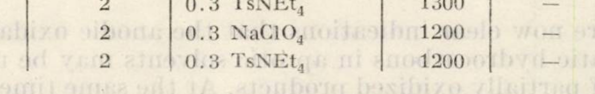

$$(CH_3)_3C - CH = C(CH_3)_2 \quad \text{and} \quad (CH_3)_3C-CH_2-C\begin{array}{l}\nearrow CH_2\\ \searrow CH_3\end{array}$$

I II

There is evidence for the presence of about 22 components in the organic phase noted from A to T in figure 1.

The mass spectra were concludent in the case of A–E, H, I, K–N peaks. The relatively small amounts of other compounds and the background noise due to squalan leakage have hindered the obtention of good spectra for other peaks.

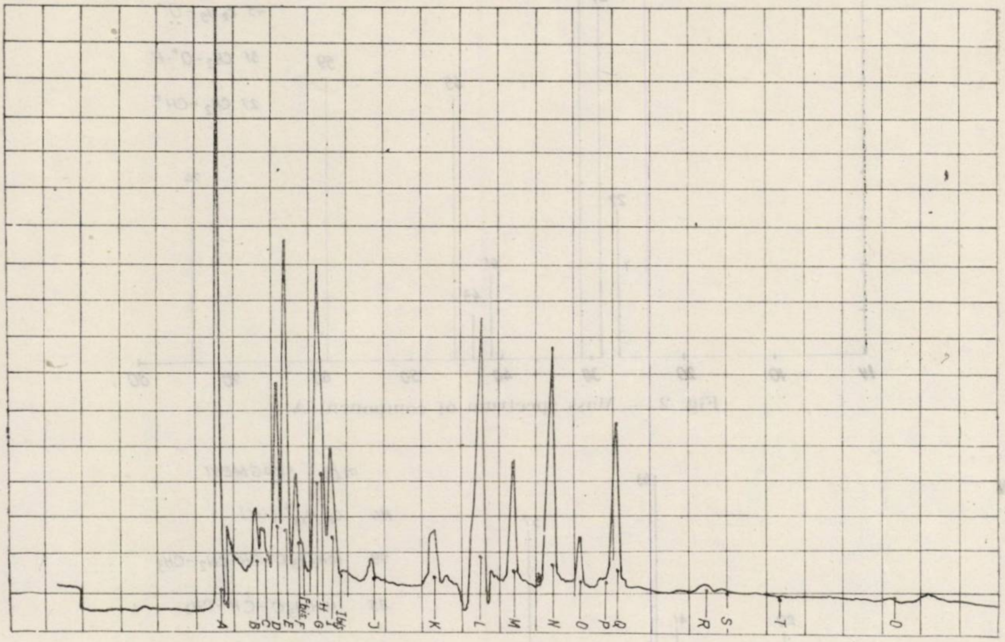

Fig. 1. — Gas-chromatogram of diisobutylene oxidation products.

The more important mass spectra and the supposed structure for the corresponding compounds are presented in the following.

The component A (Fig. 2) gave a mass spectrum which contains a molecular ion peak at *m/e* 74, and $M^+ - CH_3$ peak at *m/e* 59, another for $M^+ - C_2H_5$ peak at *m/e* 45, and usual peaks at *m/e* 31 and *m/e* 27.

The mass spectrum is identical with the known one for diethylether, used for organic phase extraction.

The mass spectrum of the peak B is shown in figure 3 and agrees with the DIB structure.

The mass spectrum of the peak C is characterized by a very low intensity of the molecular ion peak at *m/e* 160 (Fig. 4). The fragments with *m/e* 99, *m/e* 85 and especially with *m/e* 31 indicate an alcohol-ether with a tertiary carbon (*m/e* 57), [3] the structure of which is :

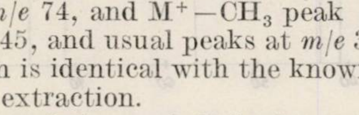

$$(CH_3)_3C-CH_2-\underset{CH_3}{\overset{OH}{C}}-CH_2-OCH_3$$

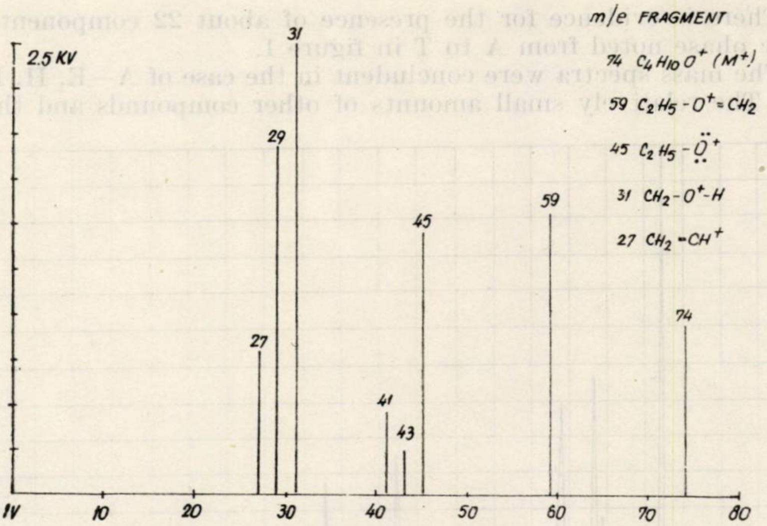

Fig. 2. — Mass spectrum of component A.

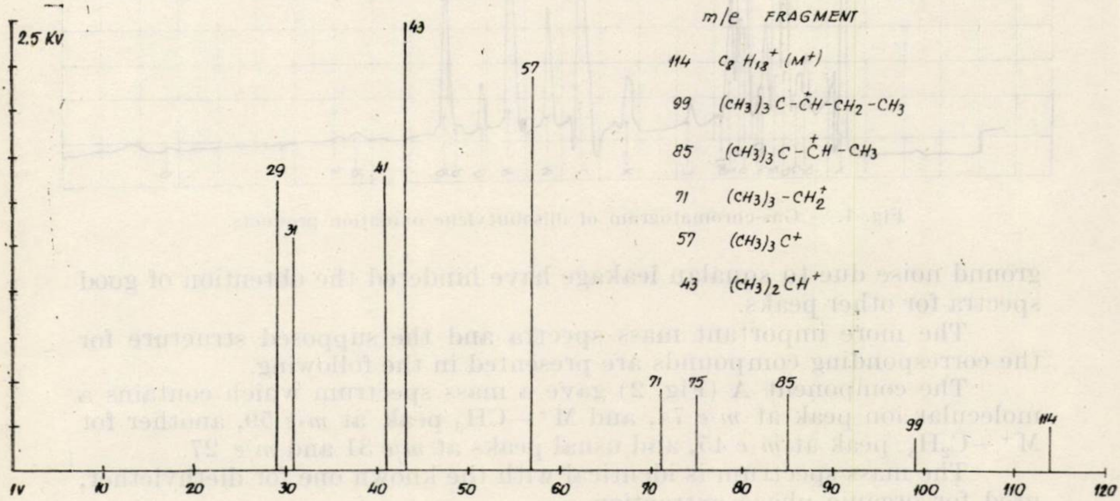

Fig. 3. — Mass spectrum of component B.

Compound D was supposed to have the structure

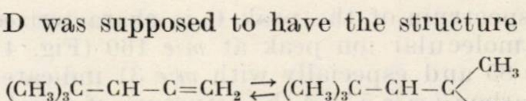

$$(CH_3)_3C-\underset{OH}{\underset{|}{CH}}-\underset{CH_3}{\underset{|}{C}}=CH_2 \rightleftarrows (CH_3)_3C-\underbrace{CH-C}_{O}\begin{matrix}CH_3\\CH_3\end{matrix}$$

The mass spectrum of this peak (Fig. 5) contains typical elements for a secondary alcohol, e.g. it shows a very weak molecular ion peak at *m/e* 128, and intense peaks at *m/e* 71, 57, 43 and 31.

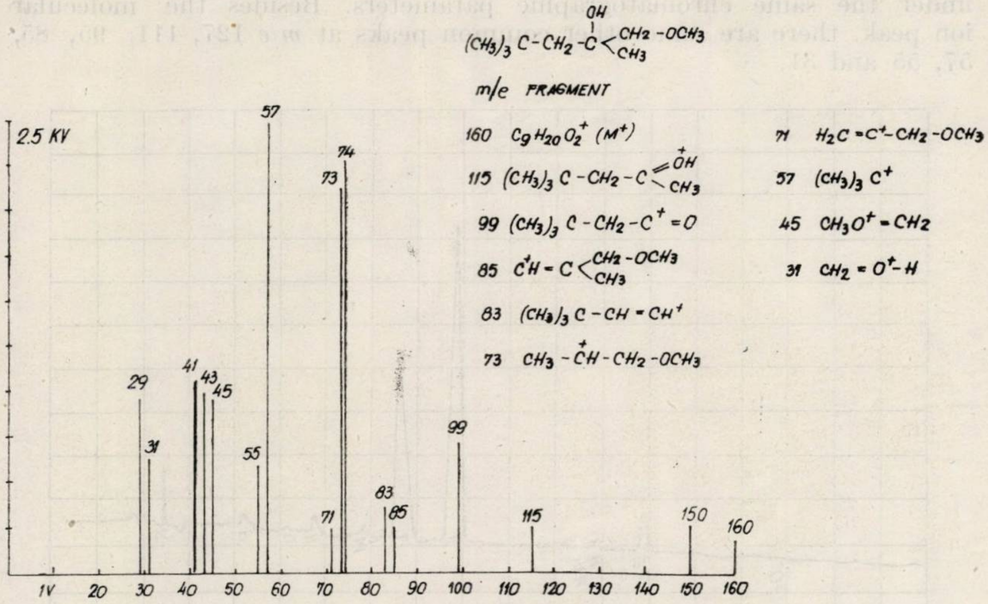

Fig. 4. — Mass spectrum of component C.

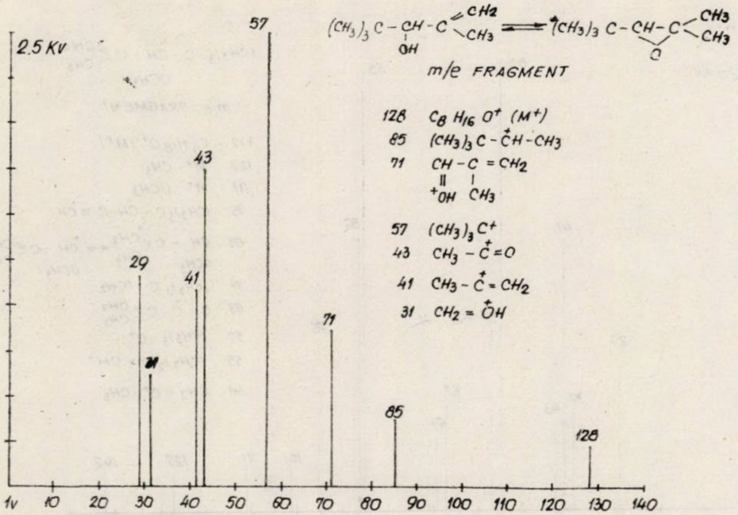

Fig. 5. — Mass spectrum of component D.

The presence of the fragment ion at *m/e* 71 is attributed to a stable structure due to double bonds conjugation.

Nine of the following components (E, H, I, K—P) have the same, value for molecular ion peaks at *m/e* 142. The common value for these molecular ion peaks was verified by a fragmentogram (Fig. 6) at *m/e* 142, under the same chromatographic parameters. Besides the molecular ion peak, there are some other common peaks at *m/e* 127, 111, 95, 85, 57, 55 and 31.

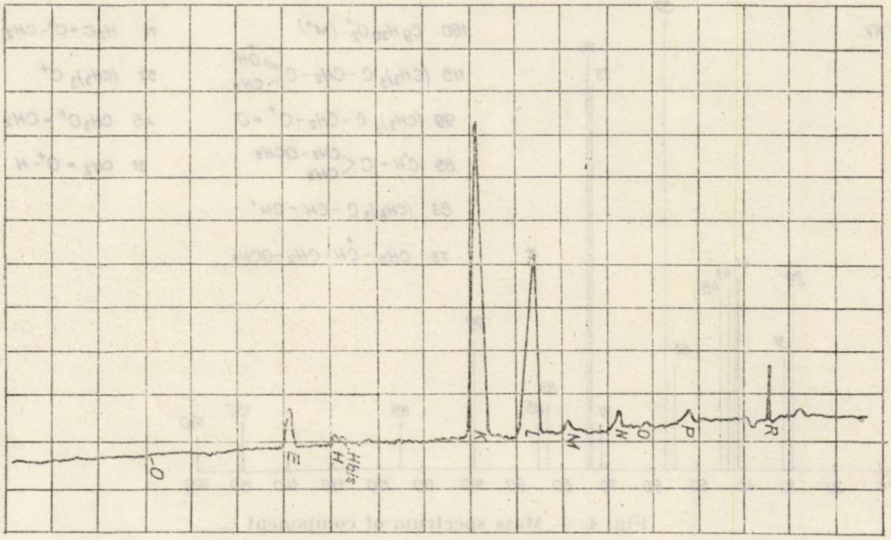

Fig. 6. — Fragmentation at m/c 142.

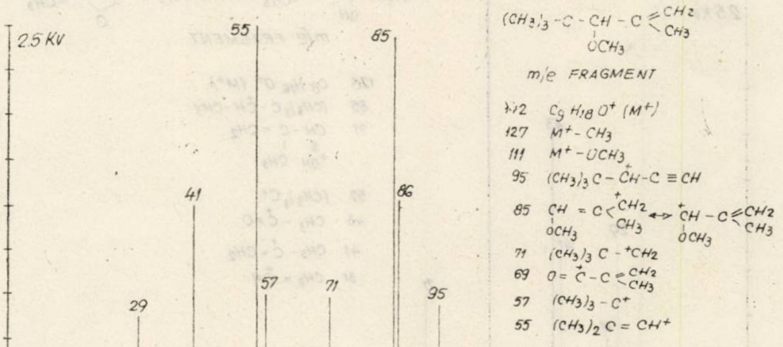

Fig. 7. — Mass spectra of component E.

In fact, all of the compounds mentioned above are constitutional isomers with molecular formula $C_9H_{18}O$. The exhibited fragment ions provide useful information about the structure of these isomers and plead for unsaturated ethers.

The mass spectrum of the compound E is shown in figure 7. After identification of fragment ions at *m/e* 127, 111, and, especially at *m/e* 85 it was possible to put forward the structure of an unsaturated ether.

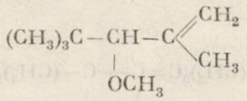

$$(CH_3)_3C-\underset{\displaystyle OCH_3}{\underset{|}{CH}}-C\begin{smallmatrix}\nearrow CH_2 \\ \searrow CH_3\end{smallmatrix}$$

A t-butylic structure was supposed due to the presence of a fragment ion at *m/e* 57. The stability of both the t-butylic cation and the cation with *m/e* 85 may explain the weak intensity of molecular ion peak.

A very interesting behaviour have the compounds H and N, whose mass spectra are quite similar (Figs 8 and 9). It was supposed that they

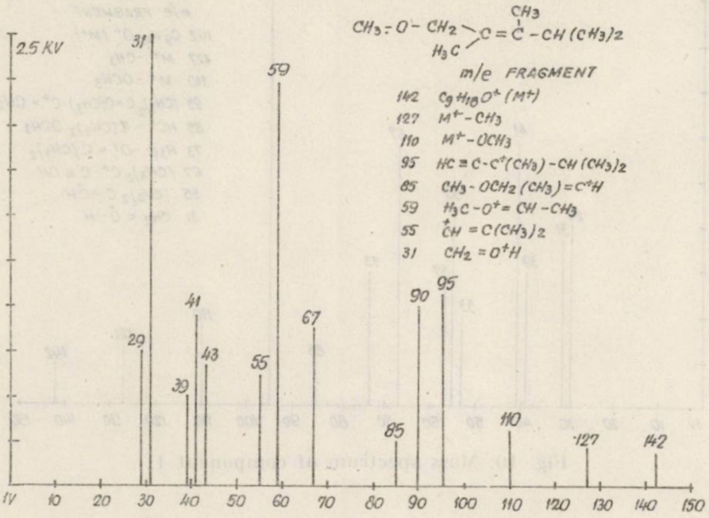

Fig. 8. — Mass spectra of component H.

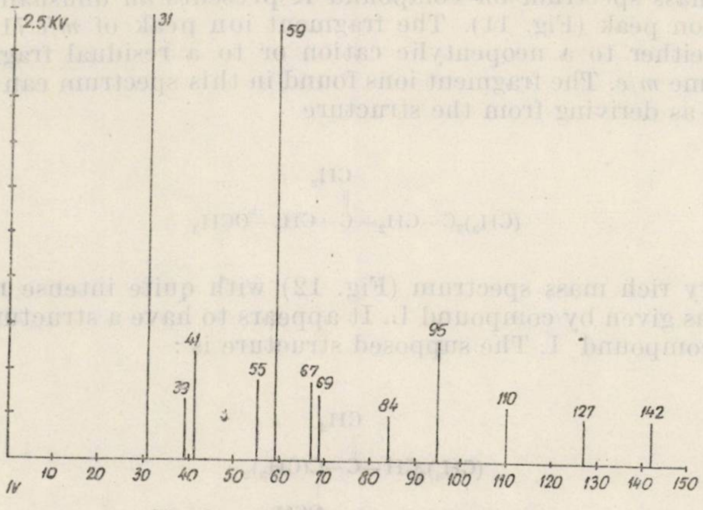

Fig. 9. — Mass spectra of component N.

are *cis-trans* isomers, a possibility also suggested by the unidentity of the radicals attached to the double bond.

In figure 10 is shown the mass spectrum for component I, the structure of which is :

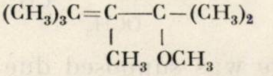

$$(CH_3)_3C{=}\underset{\displaystyle CH_3}{\underset{|}{C}}{-\!\!-}\underset{\displaystyle OCH_3}{\underset{|}{C}}{-}(CH_3)_2$$

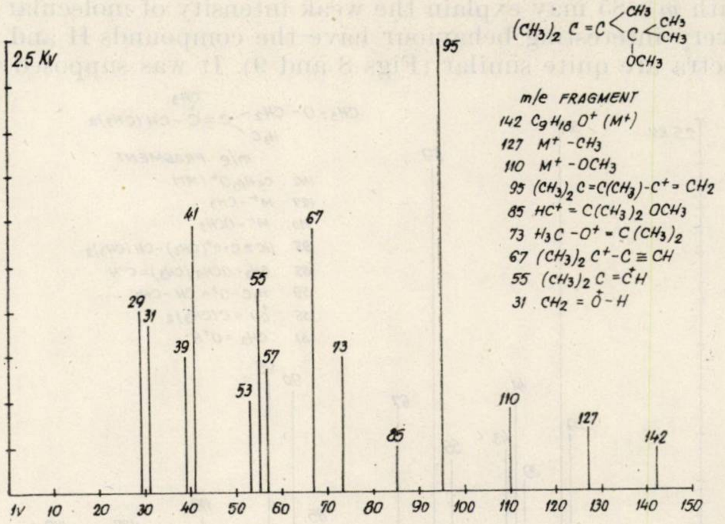

Fig. 10. Mass spectrum of component I.

The mass spectrum for compound K presents an unusually intense molecular ion peak (Fig. 11). The fragment ion peak of *m/e* 71 may be attributed either to a neopentylic cation or to a residual fragment ion with the same *m/e*. The fragment ions found in this spectrum can be easily interpreted as deriving from the structure

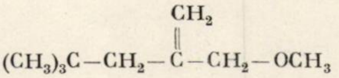

$$(CH_3)_3C-CH_2-\overset{\displaystyle CH_2}{\overset{\|}{C}}-CH_2-OCH_3$$

A very rich mass spectrum (Fig. 12) with quite intense molecular ion peak was given by compound L. It appears to have a structure similar to that of compound I. The supposed structure is :

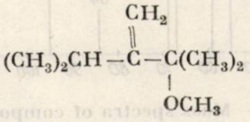

$$(CH_3)_2CH-\overset{\displaystyle CH_2}{\overset{\|}{C}}-\underset{\displaystyle OCH_3}{\underset{|}{C}}(CH_3)_2$$

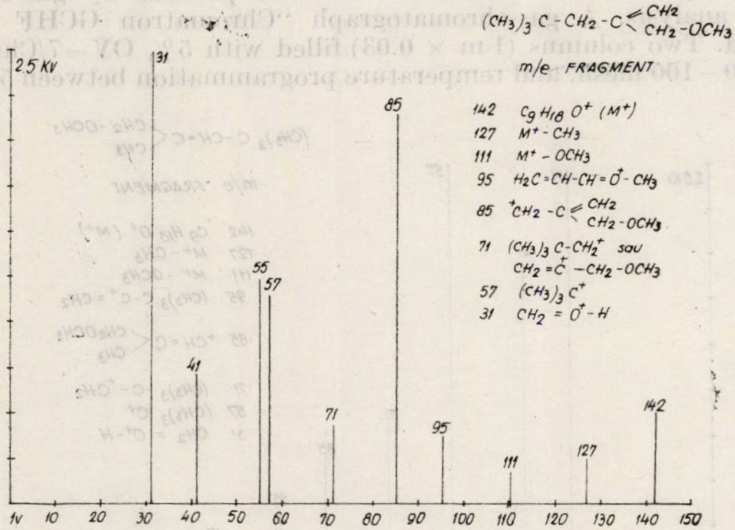

Fig. 11. — Mass spectrum of component K.

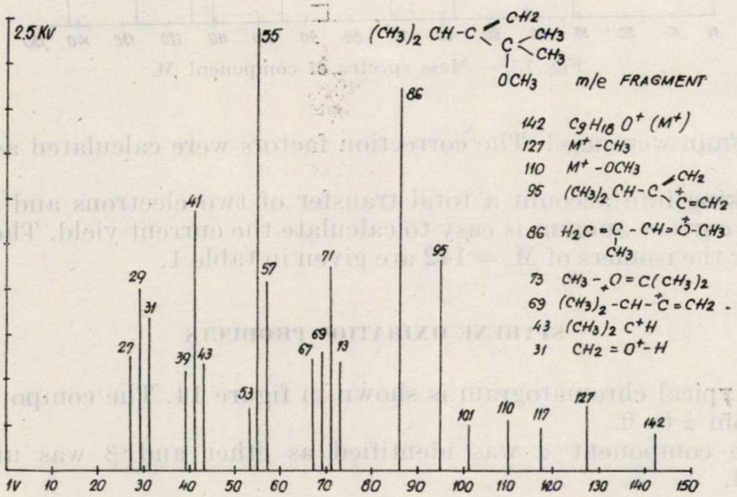

Fig. 12. — Mass spectrum of component L.

Another isomer of compound M has a mass spectrum shown in figure 13 for which was suggested the structure :

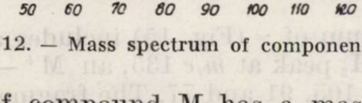

$$(CH_3)_3C-CH=\underset{\displaystyle CH_3}{\underset{|}{C}}-CH_2-OCH_3$$

It can be seen that the majority of DIB electrooxidation products are the results of an allylic substitution.

The quantitative evaluation was also possible by gas-chromatographic analysis. A gas-chromatograph "Chromatron GCHF 18.3–4" was used. Two columns (1 m × 0.03) filled with 5% OV–7/Chromosorb W sil., 80–100 mesh, and temperature programmation between 50–150°C with 8°C/min were used. The correction factors were calculated as usually for FID.

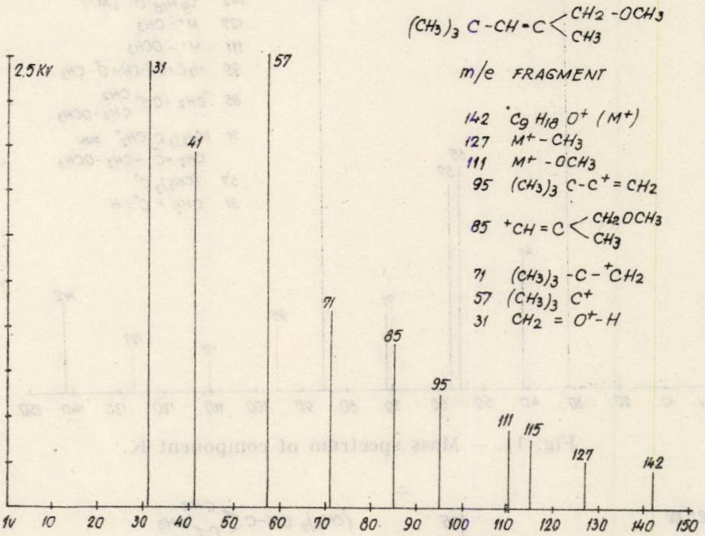

Fig. 13. — Mass spectra of component M.

Taking into account a total transfer of two electrons and knowing the total current amount is easy to calculate the current yield. The current yields for the isomers of M = 142 are given in table 1.

STYRENE OXIDATION PRODUCTS

A typical chromatogram is shown in figure 14. The components are noted from α to θ.

The component α was identified as ether and β was unreacted methanol.

The mass spectrum of γ (Fig. 15) includes a molecular ion peak at *m/e* 166, an M^+-OCH_3 peak at *m/e* 135, an $M^+-CH_2-OCH_3$ at *m/e* 121, and also peaks at *m/e* 105, 91 and 77. The fragment ions at *m/e* 121, 105, and *m/e* 91 were also measured at high resolution. The measured and calculated values, respectively are given in table 2.

The masses are esentially the same, which is a strong argument for the supposed structure

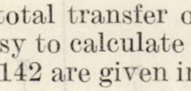

$$\begin{array}{l} C_6H_5-\underset{|}{\overset{}{CH}}-\underset{|}{CH_2} \\ \qquad\;\; OCH_3\ OCH_3 \end{array}$$

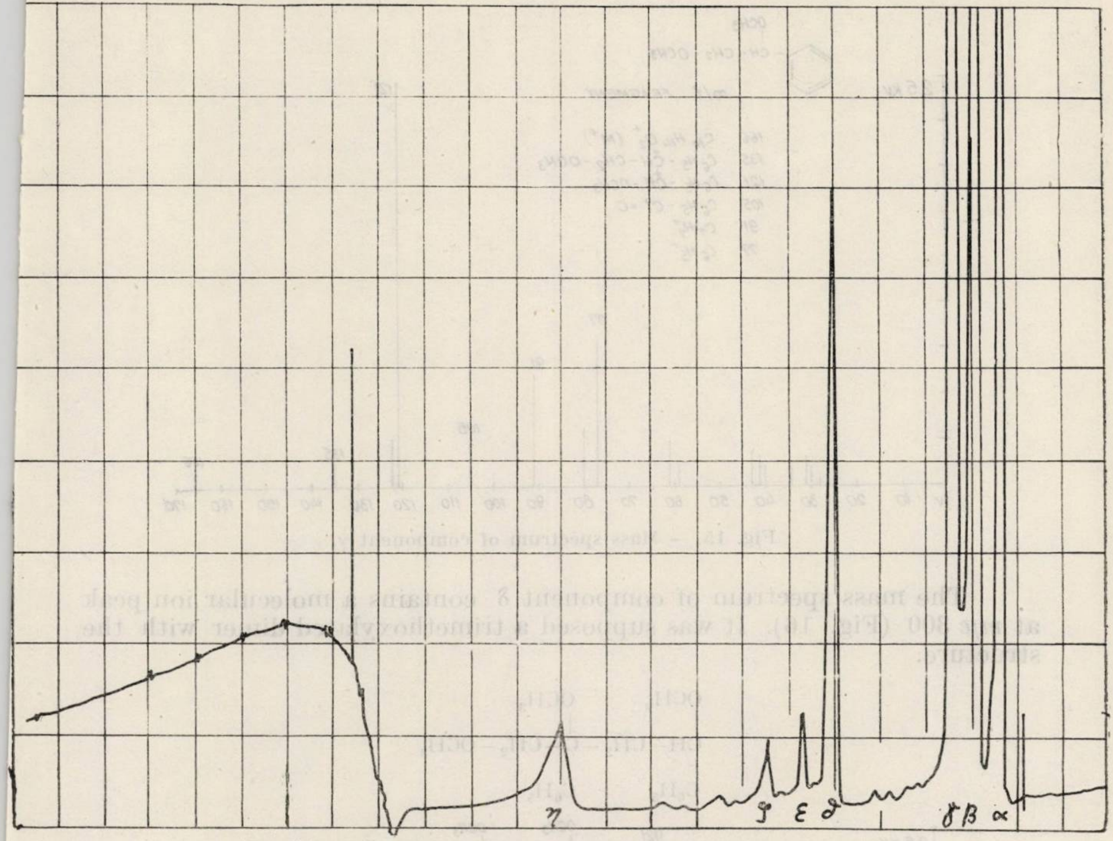

Fig. 14. — Gas-chromatogram of styrene oxidation products.

Table 2

The formula determination by comparison of high precision measured and theoretically calculated masses

Peak at *m/e*	High precision measured mass	Theoretically calculated mass	Formula
121	121.065336	121.064851	C_8H_9O
105	105.033288	105.034037	C_7H_5O
91	91.0548	91.054773	C_7H_7

The weak intensity of the molecular ion peak is due to a detachment of CH_2-OCH_3 radical with the formation of a stable cation $C_6H_5-\overset{+}{C}H-OCH_3$.

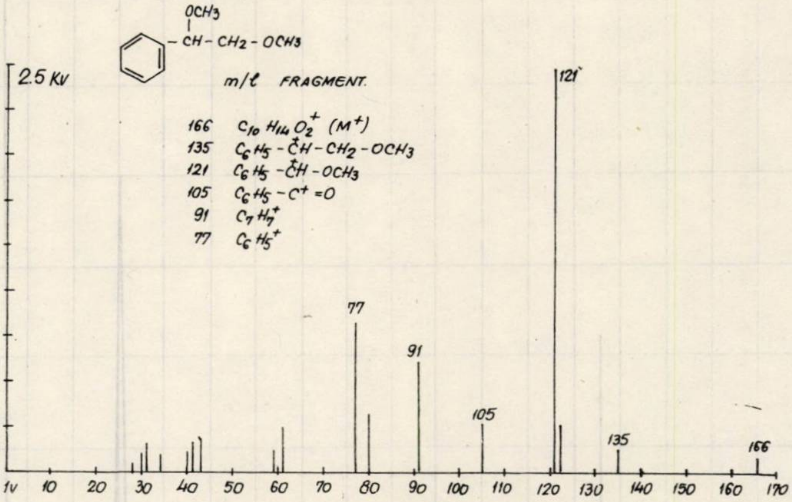

Fig. 15. — Mass spectrum of component γ.

The mass spectrum of component δ contains a molecular ion peak at *m/e* 300 (Fig. 16). It was supposed a trimethoxylated dimer with the structure.

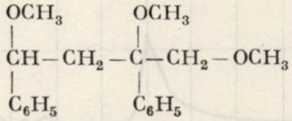

$$\underset{\displaystyle C_6H_5}{\overset{\displaystyle OCH_3}{CH}}-CH_2-\underset{\displaystyle C_6H_5}{\overset{\displaystyle OCH_3}{C}}-CH_2-OCH_3$$

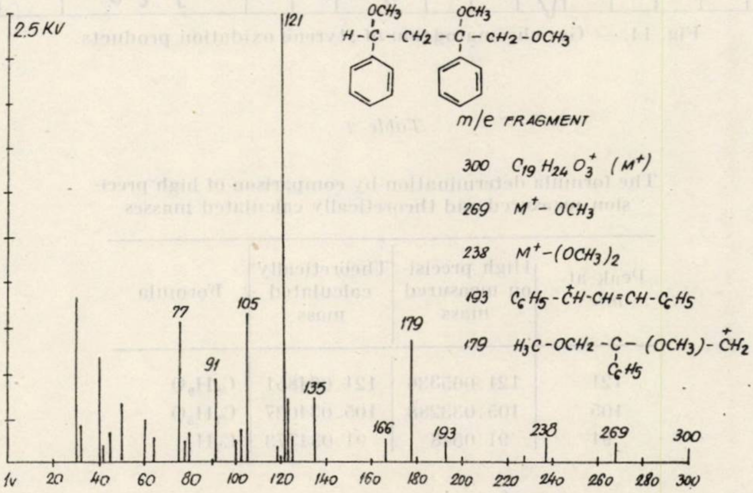

Fig. 16. — Mass spectrum of component δ.

The fragment ion peaks at *m/e* 166, 135, 121, 105, 91, and 77 have the same assignment as in the mass spectrum of the former peak. The presence of identical fragment ion peaks as for compound γ, is consistent with the above mentioned structure. The difference of 45 m.u. between peaks at *m/e* 238 and 193 is attributed to a fragmentation of CH_3OCH_2. The most intense peak is at *m/e* 121 as for the former component and is an argument for the great stability of the ion $C_6H_5-\overset{+}{C}H-OCH_3 \leftrightarrow C_6H_5-$ $-CH=\overset{+}{O}CH_3$.

The component ε has the structure of a tetramethoxylated styrene dimer

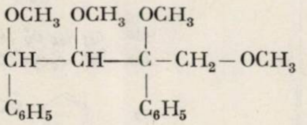

$$\begin{array}{ccccc} OCH_3 & OCH_3 & OCH_3 & & \\ | & | & | & & \\ CH- & CH- & C- & CH_2- & OCH_3 \\ | & & | & & \\ C_6H_5 & & C_6H_5 & & \end{array}$$

The mass spectrum for this compound has a molecular ion peak at *m/e* 330, and characteristic peaks at *m/e* 238, 135, and 121 (very intense) and also at *m/e* 91, 89, 77, and 73.

The component ζ is a polymethoyxlated dimer as results from mass spectrum (Fig. 17). The structure would be

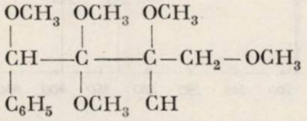

$$\begin{array}{ccccc} OCH_3 & OCH_3 & OCH_3 & & \\ | & | & | & & \\ CH- & C- & C- & CH_2- & OCH_3 \\ | & | & | & & \\ C_6H_5 & OCH_3 & CH & & \end{array}$$

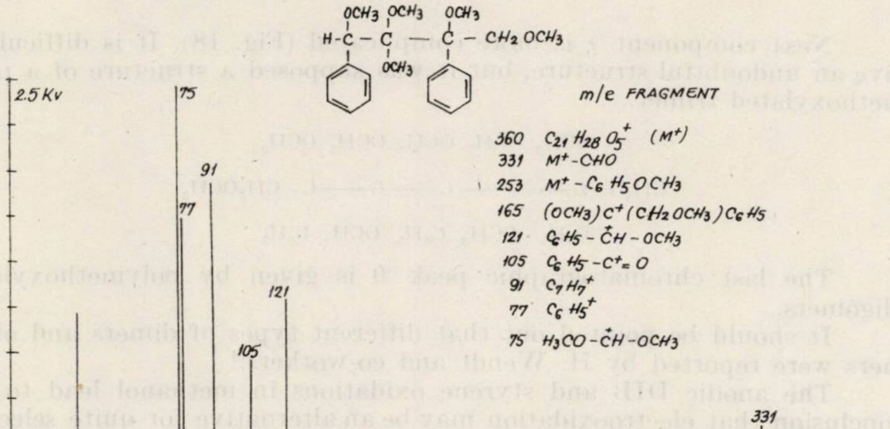

Fig. 17. — Mass spectrum of component ζ.

The most intensive peak is at *m/e* 75 corresponding to a fragment ion with a great stability $CH_3O-\overset{+}{C}H-OCH_3$ due to a + M effect of methoxy groups. This ion agrees with a structure with methoxy groups in germinal position.

The fragment ion peaks at *m/e* 165, 121, 105, 91, and 77 are identical with those of the component γ suggesting the above structure.

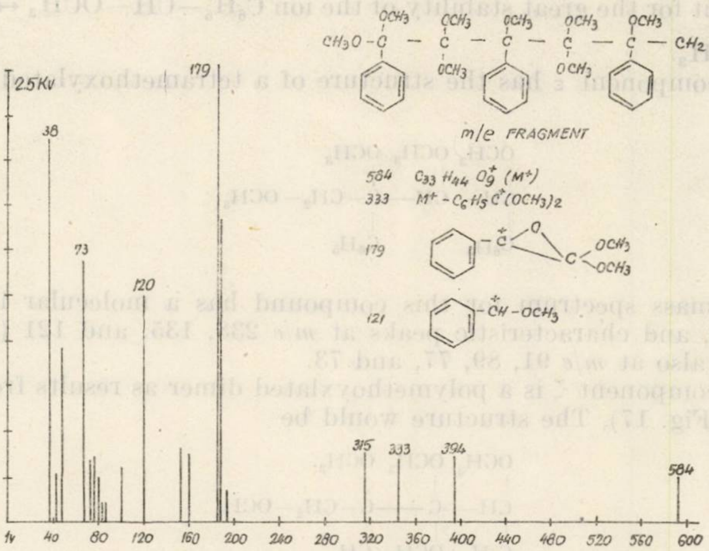

Fig. 18. Mass spectra of component η.

Next component η is more complicated (Fig. 18). It is difficult to give an undoubtful structure, but it was supposed a structure of a polymethoxylated trimer.

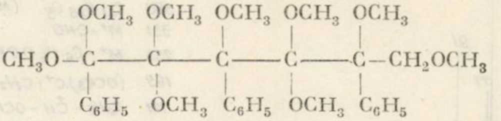

$$\begin{array}{c}
\qquad\ \ OCH_3\ \ OCH_3\ \ OCH_3\ \ OCH_3\ \ OCH_3 \\
CH_3O-\underset{C_6H_5}{\overset{|}{C}}-\underset{OCH_3}{\overset{|}{C}}-\underset{C_6H_5}{\overset{|}{C}}-\underset{OCH_3}{\overset{|}{C}}-\underset{C_6H_5}{\overset{|}{C}}-CH_2OCH_3
\end{array}$$

The last chromatographic peak θ is given by polymethoxylated oligomers.

It should be pointed out that different types of dimers and oligomers were reported by H. Wendt and co-workers.[4]

The anodic DIB and styrene oxidations in methanol lead to the conclusion that electrooxidation may be an alternative for quite selective olefins methoxylation. However, it has been proved that the results as obtained in methanol are valid, too, in higher alcohols.

REFERENCES

[1] H. Schäfer and E. Steckan, *Angew. Chem.*, **81**, 532 (1969).

[2] R. Vlădea, *Rev. Roumaine de Chim.*, **30**, 151 (1985).

[3] M. C. Hamming and N. G. Foster, "Interpretation of Mass Spectra of Organic Compounds" Academic Press, New York, 1972, p. 243.

[4] V. Plzak, H. Schneider and H. Wendt, *Ber. Bunsen Ges. Phys. Chem.*, **78**, 1373 (1974).

Revue Roumaine de Chimie **30**, *2*, 171—178 (1985)

IDENTIFICATION D'HYDROCARBURES AROMATIQUES DE QUELQUES FRACTIONS PÉTROLIÈRES. II[1]

IDENTIFICATION DES COMPOSANTS PAR HPLC

HOCINE KADI[a] and D. P. LAZĂR[b]
[a] Département de Génie chimique, Ecole Polytechnique, Université d'Alger, ALGERIE,
[b] Département de Chimie physique, Faculté de Technologie chimique, Splai Bahlui, 71, 6600 Jassy, ROUMANIE

Reçu le 2 septembre 1983

The concern for both separation and identification of aromatic hydrocarbons from different petroleum fractions is first justified by their economic value and then by a particular scientific importance. The separation and identification of aromatic hydrocarbons are analytically interesting because these operations can be simultaneously accomplished through three different physical methods : HPLC chromatography, the composite method of n.d. PA and IR spectral analysis.

L'intérêt porté à la séparation et l'identification des hydrocarbures aromatiques s'explique par leur valeur économico-industrielle et par l'intérêt scientifique qu'ils représentent. Du point de vue analytique, la séparation et l'identification des hydrocarbures aromatiques peuvent se faire par trois méthodes physiques différentes : méthode chromatographique HPLC, méthode composée n.d.PA et méthode d'analyse spectrale IR.

1. PARTIE EXPÉRIMENTALE

Durant les essais préliminaires pour l'établissement des conditions de travail standard dans la technique HPLC,[1] on a constaté que pour maintenir constant le débit de l'éluent (2 ml min^{-1}), on doit utiliser une pression de plus en plus grande (entre 102 et 238 atm).

Cette condition est nécessaire pour deux raisons :

1° le tassement, avec le temps, du remplissage de la colonne ;

2° le colmatage des filtres terminaux à la sortie de la colonne.

Les fractions 1—23 sont réparties en deux groupes, en fonction de la température d'ébullition moyenne et du poids moléculaire des constituants individuels.

Le groupe « A » comprend les fractions 1—15, distillées entre $t_i^{\circ} = 90°$ et $t_f^{\circ} = 182°$, donc jusqu'au voisinage de la température d'ébullition du *n*-butylbenzène (égale à 183,3°) ; ce groupe contient les homologues supérieurs du benzène ayant des températures d'ébullition comprises entre 90° et 2 × 90° et des poids moléculaires compris entre 78 et 134. Pour l'analyse chromatographique des fractions de ce groupe on a utilisé un éluent riche en eau (eau : acétonitrile = = 60 :40).

Le groupe « B » comprend les fractions 16—23, distillées entre 182° et 209°, donc jusqu'à une température d'ébullition tout près de 4-méthyl indène. Ce groupe comprend des homologues supérieurs du benzène ayant des poids moléculaires supérieurs à 134 et une structure moléculaire complexe. Pour l'analyse chromatographique des fractions de ce groupe on a utilisé un éluent riche en composant organique (eau : acétonitrile = 40 :60).

Les fractions ont été par la suite réparties en sous-groupes de 3 fractions, ce qui a permis une corrélation plus commode des temps de rétention $t_{R,i}$, surtout que dans le groupe « A », certaines analyses chromatographiques ont été effectuées sous quatre pressions différentes : 102, 119, 123 et 187 atm.

Le groupe « B » a été analysé sous une même pression, 238 atm (voir Tabl. 1 et 2).

Tableau 1

Résultats généraux donnés par l'identification chromatographique HPLC, groupe « A » ; Eluent : eau : acétonitrile = 60 :40 ; débit : 2 ml min^{-1}

Fraction	t_i^0 (°C)	t_f^0 (°C)	$\Delta t°$ (°C) a)	PE_m (°C) b)	Aire du pic (%) c)	$t_{R,i}$		Résolution R d)	Facteur de résolution R_C e)	Composants	
						sec	min			séparés	identifiés f)
1	2	3	4	5	6	7	8	9	10	11	12
Pression de l'éluent = 187 atm											
1	90,0	99,0	9,0	94,50	69,3 30,7	450 726	7,5 12,1	6,13	1,00	2	1 ; 2
2	99,0	103,5	4,5	101,25	9,4 90,6	450 726	7,5 12,1	6,13	1,00	2	1 ; 2
3	103,5	115,0	11,5	109,25	100,0	726	12,1			1	2
Pression de l'éluent = 129 atm											
4	115,0	123,5	8,5	119,25	97,0 3,0	684 1122	11,4 18,7	6,00	1,00	2	2 ; 3
5	123,5	131,0	7,5	127,25	58,8 1,7 39,5	684 1008 1122	11,4 16,8 18,7	5,30 1,32	1,00 1,00		2 ; 3 ; 4
6	131,0	137,0	6,0	134,00	7,0 9,0 84,0	684 1008 1122	11,4 16,8 18,7	4,10 1,12	1,00 1,00	3 3	2 ; 3 ; 4
7	137,0	145,5	8,5	141,25	2,5 28,3 29,2	675 1008 1128	11,25 16,8 18,7	3,96 1,03	1,00 0,78	3	3 ; 4 ; 5
8	145,5	151,0	5,5	148,25	32,0 68,0	1008 1128	16,8 18,7	1,18	0,80	2	4 ; 5
9	151,0	157,5	6,5	154,25	14,4 31,6 1,7 10,0 31,1 11,2	1008 1128 1422 1476 1554 1614	16,8 18,7 23,7 24,6 25,9 26,9	1,14 * * * *	0,72 1,00 0,60 0,34 0,21	6	4 ; 5 ; 6 ; n.i. ; 7 ; 8

Pression de l'éluent = 119 atm

10	157,5	164,5	7,0	160,75	7,2	996	16,6	2,26	0,84	7	5 ; 6 ; 9 ; 7 8 ; 11 ; n.i.
					12,1	1098	18,3	*	1,00		
					2,4	1506	25,1	*	0,69		
					4,9	1596	26,6	*	0,66		
					32,4	1686	28,1	*	0,49		
					31,5	1830	30,5	*	0,37		
					9,5	1896	31,6				
11	164,5	169,0	4,5	166,75	3,2	996	16,6	*	0,62	6	5 ; 6 ; 9 ; 7 8 ; 11
					6,6	1098	18,3	*	0,29		
					7,4	1506	25,1	*	0,70		
					2,4	1596	26,6	*	0,88		
					45,0	1686	28,1	*	0,16		
					35,4	1830	30,5				
12	169,0	172,0	3,0	170,50	2,8	996	16,8	1,06	1,00	5	5 ; 6 ; 12 ; 8 ; 11
					2,5	1098	18,3	3,40	1,00		
					18,1	1506	25,1	1,18	0,80		
					53,1	1686	28,1	*	0,49		
					23,5	1830	30,5				

Pression de l'éluent = 129 atm

13	172,0	175,0	3,0	173,5	17,7	1524	25,4	1,19	0,79	5	12 ; 8 ; 11 ; 10 ; n.i.
					46,2	1716	28,6	*	0,53		
					15,4	1842	30,7	*	1,00		
					12,4	2880	48,0	*	0,78		
					8,3	3210	53,5				
14	175,0	178,0	3,0	176,50	22,0	1650	26,0	1,19	0,80	5	12 ; 8 ; 11 ; 10 ; n.i.
					40,5	1752	29,2	*	0,50		
					11,0	1902	31,7	*	1,00		
					20,3	2970	49,5	*	0,78		
					6,2	3390	56,5				
15	178,0	182,0	4,0	180,00	15,1	1620	27,0	1,14	0,80	5	12 ; 8 ; 11 ; 10 ; n,i.
					23,5	1818	30,3	*	0,56		
					6,0	1962	32,7	*	1,00		
					34,6	3520	58,66	*	0,65		
					20,8	3540	59,00				

a) $t° = t_f^0 - t_i^0$; b) $PE_m = (t_i^0 + t_f^0/2$; c) Rapportée à la somme des aires des pics du cromatogramme de fraction. d) Conformément à la relation $(2)^1$. e) Conformément à la relation $(1)^1$. f) Correspondance des chiffres : 1 = benzène ; 2 = toluène ; 3 = éthylbenzène ; 4 = xylène (*m.p.*) ; 5 = *o*-xylène ; 6 — *n*-propyl benzène ; 7 = isopropylbenzène ; 8 = 1,2,4-triméthylbènzène ; 9 = 1,3,5-triméthylbenzène ; 10 = 1,2,3-triméthylbenzène ; 11 = *t*-butylbenzène ; 12 = isobutylbenzène ; 13 = *n*-butylbenzène.

* résolution difficile.

n.i. = non identifié.

Tableau 2

Résultats généraux par séparation et identification partielle (approximative) des constituants du groupe « B ».
Eluent : eau : acétonitrile = 40 :60 ; débit = 2 ml min^{-1} ; pression unique = 238 atm

Fraction	t_i° (°C)	t_f° (°C)	Δt° (°C) a)	PE_m (°C) b)	Aire du pic (%) c)	$t_{R,i}$ sec	$t_{R,i}$ min	Résolution R d)	Facteur de résolution R_c e)	Composants Séparés	Composants Identification approximative f)
1	2	3	4	5	6	7	8	9	10	11	12
16	182,0	184,5	2,5	183,25	6,5	396	6,6	*	0,39	7	1 ; 2 ; 3
					10,4	420	7,0	*	0,40		
					3,7	468	7,8	*	0,10		
					4,4	486	8,1	*	0,02		
					3,7	498	8,3	*	0,65		
					31,7	546	9,1	*	0,21		
					39,6	582	9,7				
17	184,5	188,0	3,5	186,25	0,6	318	5,3	2,40	1,00		1 ; 2 ; 3
					4,6	390	6,5	*	0,57		
					9,4	414	6,9	*	0,59		
					2,5	456	7,6		0,27		
					8,0	498	8,3		0,77		
					33,4	546	9,1		0,45		
					28,6	582	9,7		0,61		
					3,0	678	11,3		0,20		
					3,9	720	12,0	*	0,13		
					2,2	750	12,5	*	0,06		
					3,8	780	13,0				
18	188,0	191,0	3,0	189,5	1,6	318	5,3	2,67	1,00	11	1 ; 2 ; 3
					3,5	390	6,5	*	0,61		
					6,0	414	6,9	*	0,70		
					3,3	462	7,7	*	0,43		
					7,6	504	8,4	*	0,78		
					36,7	546	9,1	*	0,56		
					21,4	588	9,8	*	0,61		
					4,1	684	11,4	*	0,24		
					5,4	726	12,1	*	0,11		
					4,0	750	12,5	*	0,08		
					6,5	792	13,2				
19	191,0	197,5	6,5	194,25	4,7	318	5,3	2,89	0,95	11	1 ; 2 ; 3
					2,0	396	6,6	*	0,50		
					2,6	420	7,0	*	0,70		
					2,5	468	7,9	*	0,55		
					7,4	510	8,5		0,76		
					35,2	552	9,2		0,54		
					21,7	600	10,0		0,45		
					4,5	690	11,5		0,17		

					5,5	732	12,2		0,05		
					4,8	762	12,7		0,05		
					9,1	804	13,4				
20	197,5	200,5	3,0	198,75	18,0	324	5,4	2,89	0,96	11	1 ; 2 ; 3
					1,2	402	6,7		0,61		
					1,1	426	7,1		0,89		
					2,1	474	7,9		0,68		
					9,0	510	8,5		0,77		
					21,4	558	9,3		0,61		
					20,4	606	10,1		0,48		
					6,0	696	11,6		0,16		
					5,7	744	12,4		0,06		
					7,0	780	13,0		0,10		
					8,1	816	13,6				
21	200,5	202,0	1,5	201,25	24,0	336	5,6	2,46	0,88	11	1 ; 2
					0,7	414	6,9		0,50		
					0,5	438	7,3		0,86		
					3,7	486	8,1		0,70		
					12,0	528	8,8		0,66		
					28,8	564	9,4		0,85		
					5,8	708	11,8		0,08		
					4,2	750	12,5		0,15		
					11,7	792	13,2		0,15		
					5,3	828	13,8		0,11		
					5,5	858	14,3				
22	202,0	205,0	3,0	203,50	32,4	330	5,5	2,73	0,97	9	2
					1,5	486	8,1		0,62		
					6,1	528	8,8		0,42		
					19,0	564	9,4		0,37		
					8,6	684	11,4		0,21		
					9,0	732	12,2		0,12		
					8,7	798	13,3		0,07		
					4,3	822	13,7		0,02		
					10,4	864	14,4				
23	205,0	209,0	4,0	207,00	38,0	330	5,5	3,57	0,98	8	2
					2,4	480	8,0		0,77		
					7,7	528	8,8		0,49		
					10,4	564	9,4		0,54		
					7,1	660	11,0		0,40		
					9,6	738	12,3		0,30		
					13,1	804	13,4		0,23		
					11,7	870	14,5				

a), b), c), d), e), f) = même signification que dans le Tableau 1.
Correspondance des chiffres (v. col. 12) : 1 = l-méthyl,3-isoprophylbenzène ; 2 = n-butylbenzène ; 3 = 1,3-diméthyl,1-5-éthylbenzène.
* = résolution difficile.

L'identification des constituants individuels sur les chromatogrammes des fractions 1—15 a été effectuée à l'aide d'une collection d'étalons où sont inclus les homologues suivants du benzène : toluène, éthylbenzène, *ortho-*, *méta-* et *para*-xylène, *n*-propylbenzène, isopropylbenzène, 1,2,3-, 1,2,4- et 1,3,5-triméthylbenzène, isobutylbenzène, 1-méthyl, 3-isopropylbenzène, *n*-butylbenzène et benzène (au total 14 étalons).

L'évaluation quantitative, en pourcentage de chaque composant, a été faite d'après les procédés standard utilisés en CG comme en HPLC.[2-5] Bien que la vitesse du papier d'enregistrement n'influence pas beaucoup la qualité de la séparation chromatographique, on a choisi une vitesse de 1 cm·min^{-1}, considérée comme la plus convenable.

L'identification des constituants individuels du groupe « A » a été réalisée à l'aide des étalons disponibles mais le critère chromatographique a été complété par le critère de la température d'ébullition et de la courbe de distribution des composants, qui se prolonge sur un certain nombre de fractions successives (Tabl. 1 et 2, col. 10).

Dans le groupe « B », à cause du manque d'étalons, l'identification des composants (Tabl. 2, col. 11) est basée seulement sur le critère de la température d'ébullition et sur les courbes de distribution (voir Tabl. 3) et par conséquent elle est approximative.

Tableau 3

Répartition des constituants (numérotés 1—15) séparés par fractions

Constituant aromatiue	$t_{R,i}$ (min)	FRACTIONS								Identification approximative du constituant
		16	17	18	19	20	21	22	23	
1	5,6— 5,3=0,3		*	*	*	*	* *	*	*	
2	6,9— 6,5=0,4	*	*	*	*	*	*			
3	7,3— 6,9=0,4	*	*	*	*	*	*			1-méthyl, 3-isopropylbenzène
4	7,9— 7,6=0,3	*	*	*	*	*				
5	8,5— 8,0=0,5	*	*	*	*	*	*	*	*	
6	$t_{R,6}$ = 8,3	*								
7	$t_{R,6}$ = 8,8						*	*	*	
8	9,4— 9,1=0,3	*	*	*	*	*	*	*	*	*n*-butylbenzène
9	10,1— 9,7=0,4	*	*	*	*	*				1,3-diméthyl, 5-éthylbenzène
10	11,8—11,0=0,8		*	*	*	*	*	*	*	
11	12,5—12,0=0,5		*	*	*	*	*	*	*	
12	12,7—12,5=0,2		*	*	*					
13	13,4—13,0=0,4		*	*	*	*	*	*	*	
14	13,8—13,6=0,2					*	*	*		
15	14,5—14,3=0,2						*	*	*	

2. DISCUSSIONS

2.1. Dans le groupe « A », on a mis en évidence 16 composants individuels dont 10 ont été identifiés et 6 se sont manifestés sous forme de substances non identifiées et présentes dans une seule fraction. Les fractions 1—8 sont caractérisées par un $\Delta t°$ élevé (4°—11°) et par un petit nombre de constituants (2—3). Les fractions 9—11 contiennent chacune 7 constituants mais les fractions 12—15, avec un $\Delta t° = 3°$, ne contiennent que 5 constituants. Dans les fractions 1—8 un des constituants est quantitativement dominant parce qu'il représente 58 à 97 % de la composition de la fraction respective.

La fraction 3 contient un seul hydrocarbure aromatique, le toluène.

Avec l'augmentation de la température d'ébullition on observe que la composition, en pourcentage, des fractions tend à devenir uniforme (par exemple, la fraction 15).

2.2. Les fractions du groupe « B » ont été analysées par chromatographie HPLC à une même pression, 236 atm, mais avec un autre éluent, plus riche en composant organique. Ceci a permis une corrélation commode des temps de rétention, $t_{R,i}$, pour les constituants distribués sur plusieurs fractions (voir Tabl. 3).

Chaque fraction contient un nombre relativement élevé de composants (de 7 à 11, mais surtout 11). Le nombre total de constituants identifiés est 15. A la différence de la première moitié du groupe « A », dans le groupe « B » la contribution (en pourcentage massique) des constituants majeurs est très réduite (30 % à 40 %).

Les constituants moyens contribuent avec 10—20 %, tandis que les constituants mineurs se trouvent à un pourcentage inférieur à 10 %. Certains constituants se présentent sous forme de traces (inférieures à 1 %).

Dans chaque fraction, seuls deux à trois constituants présentent des contributions supérieures à 20 %; le reste des constituants participent avec un pourcentage inférieur à 10 %. Dans le groupe « B », les valeurs Δt° sont, en général, plus petites que celles du groupe « A », tandis que le nombre de constituants est à peu près double.

L'identification des constituants ayant les formules brutes $C_{19}H_{12}$, $C_{10}H_{14}$, $C_{11}H_{16}$ est difficile à cause des valeurs très voisines des temps de rétention, des températures d'ébullition proches et des nombreux cas d'isomérie. De même, l'utilisation d'une pression d'éluent très élevée (238 atm) diminue l'efficacité de la colonne chromatographique.

3. CONCLUSIONS

a. La méthode chromatographique HPLC est très efficiente en ce qui concerne les constituants des fractions 1—15 ; ainsi, on a pu mettre en évidence les constituants se trouvant à une très faible concentration, de 1—2 % et même inférieure à 1 % (voir Tabl. 1 et 2, col. 5). L'efficacité de la séparation peut être constatée surtout dans le cas des fractions de composition complexe (par exemple, les fractions 17—21), les constituants étant des hydrocarbures aromatiques avec des masses moléculaires et des températures d'ébullition très voisines.

b. En ce qui concerne l'identification des constituants, la méthode chromatographique HPLC dépend des performances de la colonne et de l'existence d'une collection complète d'étalons ; mais, dans ces circonstances, l'utilisation d'une méthode auxiliaire d'identification ou d'une corrélation des données chromatographiques avec d'autres méthodes physiques s'impose.

c. L'efficacité de la méthode HPLC, concernant la séparation et l'identification des constituants individuels dépend de la composition des fractions obtenues après la distillation VPE (vrai point d'ébullition), de la sélection correcte de la colonne cromatographique, de l'éluent et d'autres paramètres expérimentaux spécifiques pour la méthode HPLC.

BIBLIOGRAPHIE

[1] H. Kadi et D. P. Lazăr, *Rev. Roumaine Chim.*, **29**, 497 (1984).

[2] N. Brenner et R. J. Olson, dans ,,The Practice of Gas Chromatography" (L.S. Ettre et A. Zlatkis, Editeurs), Interscience, New York, 1967, p. 15.

[3] L. S. Ettre, dans ,,The Practice of Gas Chromatography" (L. S. Ettre et A. Zlatkis, Editeurs) Interscience New York, 1967, p. 390–92.

[4] J. M. Gill et F. T. Tao, Technical Bulletin 135–67, édité par VARIAN AEROGRAPH, California, 1967, p. 12–14.

[5] E. L. Johnston et R. Stevenson, « Basic Liquid Chromatography », VARIAN Ass,. Inc., Palo Alto, California, 1978, p. 207–214.

Revue Roumaine de Chimie, **30**, 2, 179–185 (1985)

SYNERGISTIC AND ANTAGONISTIC EXTRACTION OF PROTACTINUM (V) BY BIS-(2-ETHYL HEXYL) PHOSPHORIC ACID AND TRIBUTYL PHOSPHATE MIXTURE

H. A. EL-NAGGAR, A. RAMADAN and A. A. ABDEL-RASSOUL *
Nuclear Chemistry Department, Nuclear Research Centre,
Atomic Energy Establishment, Cairo, Egypt

Received June 15, 1983

$PaO(OH)^{2+}$ was extracted by bis (2-ethyl hexyl) phosphoric acid (HDEHP) mixed with TBP. The stability constants of different species extracted by HDEHP alone and by mixture of extractants have been investigated. Thermodynamic parameters of the synergistic and antagonistic reactions have been calculated and reaction mechanisms were suggested and confirmed. A parasite organic-organic reaction responsible for antagonism was anticipated.

INTRODUCTION

Pa(V) has been extracted as chelates mixed with alcohols[1,2] or neutral organophosphorus compounds,[3] and the physical parameters of the formed species were calculated.[1-3] Extraction by thenayltrifluoroacetone, (HTTA), formed $Pa(OH)_3(TTA)_2$. nADD, where the solvation number (n) equals 1 or 2, depending upon the type and polarity of the adduct used.[3] In our previous investigation,[4] the formed species through the synergic extraction of Pa(V) by HDEHP mixed with a number of organic adducts, proved to be $PaO(OH)[H(DEHP)_2]_2 n$ ADD, where $n = 1$ in the case of TOPO; $n = 2$ in the case of TBP, and $n = 1$ or 2 in the case of TPPO, depending upon the concentration of the adduct used. It has been also found that very low concentrations of TBP (0.8M) in such systems decrease the distribution coefficient (D) of Pa(V). This phenomenon aroused our interest to investigate such a behaviour, almost quantitatively, in the present work.

EXPERIMENTAL

1. Chemicals and Reagents

^{233}Pa (V) was prepared and separated according to a standard method mentioned before.[5] HDEHP, Eastman Kodak product, and all other chemicals are of Analar grade and were used without further purification ; while TBP, a (B.D.H.) product, has been purified according to the classical technique.[6]

---

* Director of Hot Laboratory Centre (A.E.E., Cairo, Egypt).

2. Procedure and Measuring Techniques

The solvent extraction procedure adapted has been previously described.[7]

Equilibration was carried out at a constant temperature, ± 0.1°C, using a Gallencamp water thermostat. ^{233}Pa activity, in both organic and aqueous phases, has been assayed by Orted γ-scalar provided with NaI(T1) crystal. The acidity of the aqueous solutions was measured using a digital Beckman pH-meter model 3500, with a deviation in pH measurement no more than ± 0.01

RESULTS AND DISCUSSION

1. Pa-HDEHP system

Figure 1 shows the effect of HDEHP concentration on the distribution ratio of Pa(V) between $NaClO_4-HClO_4$ aqueous phase (pH = zero) and benzene solutions of HDEHP. The data fit a series of parallel straight lines with slope about 2. The pH dependency in such a system proved to

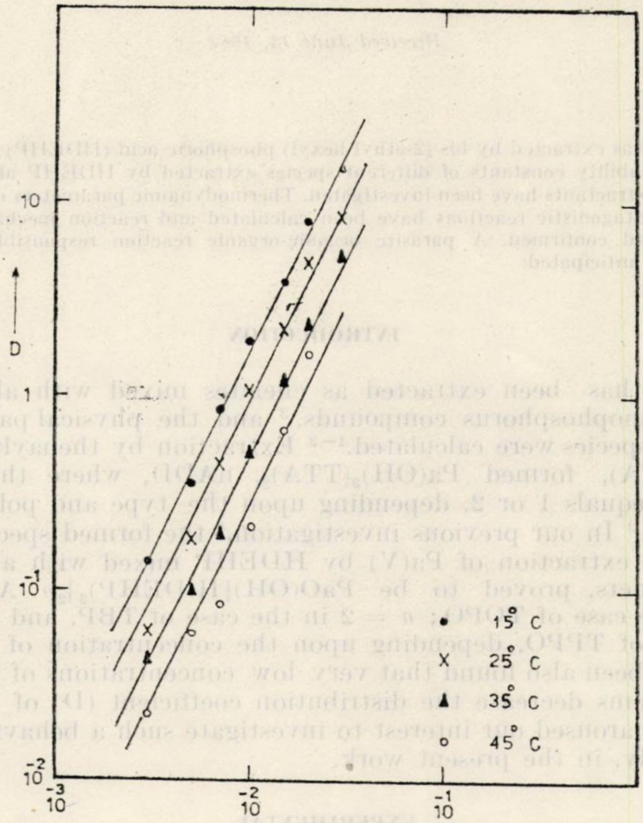

Fig. 1. — Extraction of Pa(V) from 1M (Na^+, $HClO_4$) at pH = zero by HDEHP in benzene.

follow a similar behaviour. Accordingly, the reaction representing such equilibrium could be written in the form:

$$\mathrm{PaO(CH)^{2+}_{(aq)} + 2(HDEHP)_{2_{(or)}} \overset{K_1}{\rightleftharpoons} PaO(OH)\,[H(DEHP)_2]_{2_{(or)}} + 2H^{*}_{(aq)}} \quad (1)$$

where: HDEHP exists in benzene solution as a dimer $(\mathrm{HDEHP})_2$ and the hydrolysed species of Pa(V) is considered as $\mathrm{PaO(OH)^{2+}}$[(9)]. The equilibrium constant (K_1) of the above reaction could be expressed as:

$$K_1 = \frac{\mathrm{PaO(OH)\,[H(DEHP)_2]_{2_{or}}\,[H^+]^2_a}}{\mathrm{[PaO(OH)^{2+}]_a\,[HDEHP]_{or}}} = \frac{D\mathrm{(H^+]^2_{(a)}}}{\mathrm{(HDEHP)_{2_{(or)}}}}$$

where: D is the distribution coefficient of Pa(V). In table 1, K_1 has been calculated at different temperatures and the thermodynamic functions obtained reveal that the reaction is exothermic and is thermodynamically stable ($\Delta G = -$ 22.7 KJ/mole), in spite of the negative ΔS value, which seems to oppose the reaction.

2. Pa (HDEHP-TBP) system

The factors affecting the stability of the extracted species include:

a. *TBP-concentration dependency*

The effect of TBP concentration on the extraction of Pa(V) has been studied from solutions containing different TBP concentrations 5×10^{-3} — 2.5 M while the HDEHP concentration was kept constant at 0.007 M. The data obtained are represented in figure 2. From solutions containing

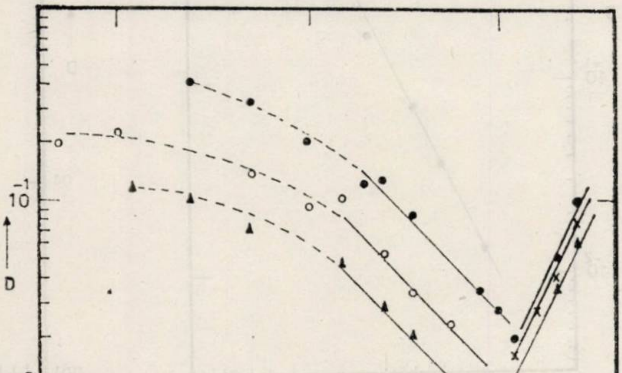

Fig. 2.— Extraction of Pa(V) from 1M ($\mathrm{Na^+}$, $\mathrm{HClO_4}$), at PH= zero by 0.007M HDEHP in benzene as a function of [TBP].

low TBP concentrations, the *D* values decrease gradually, then take a straight line behaviour, with a slope −1 by increasing the TBP concentration in used mixture, till it reaches a minimum at 1 M TBP and shows a reversible behaviour, giving straight lines with positive slope (+2) at higher concentrations.

The descending part may be attributed to an organic-organic interaction between HDEHP and TBP, as will be discussed later (equations 2−4).

b. *HDEHP concentration dependency*

The HDEHP concentration in the used organic mixture varied from 0.003 to 0.02 M, while the TBP concentration was kept constant at 0.2 M. The data obtained showed a straight line relationship with a positive second order dependency for D on (HDEHP) (Fig. 3).

c. *Hydrogen ion-concentration dependency*

The effect of $[H^{+-}]$ on the extraction behaviour of Pa(V), was investigated by the studied system Pa (HDEHP−TBP), using organic mixture containing constant [HDEHP] = 0.007 M and constant [TBP] = 0.2 M.

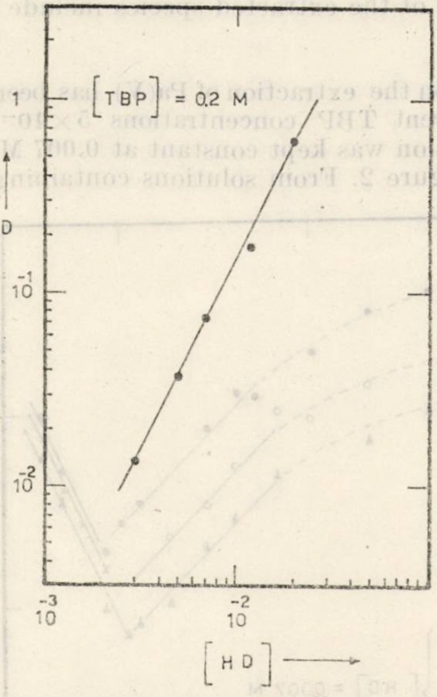

Fig. 3. — Extraction of Pa (V) from 1M (Na^+, $HClO_4$) at pH = zero as a function of [HDEHP] at constant [TBP] = 0.2 M.

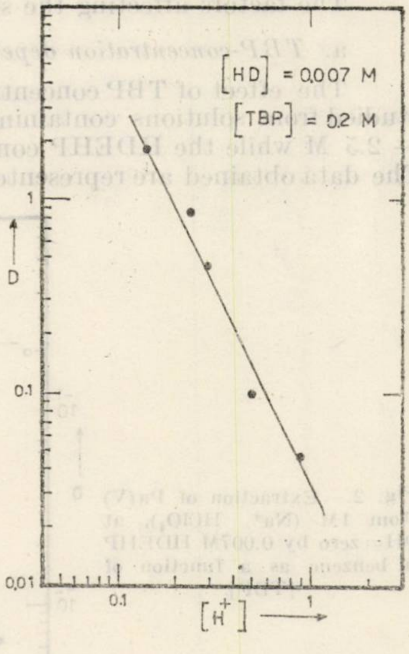

Fig. 4. — Effect of hydrogen ion concentration on the extraction of Pa(V) from 1M (Na^+, $HClO_4$) at constant [HDEHP]=0.007 M and [TBP]=0.2 M.

The data revealed an inverse second proton concentration dependency, Fig. 4, which is numerically equal to the charge on the cation $PaO(OH)^{2+}$.

In the light of the experimental data obtained, one would expect that the Pa(V) complexed species extracted by HDEHP is mostly $PaO(OH)\ [H\ (DEHP)_2]_2$.

Using HDEHP – TBP mixture, the extraction behaviour of Pa(V) is obviously affected by changes in the TBP concentration (Fig. 2). At low TBP concentration (TBP) <0.8 M), two possibilities are suggested to explain the decrease in D by the gradual increase in TBP concentration in the mixed organic solvent used ; in the first, the exchange reaction complex $PaD\ (OH)\ [H\ (DEHP)_2]_2$ first formed tends to react with TBP giving back Pa(V) in the aqueous phase ; this approach could be represented by :

$$PaO(OH)\ [H(DEHP)_2]_{2_{(or)}} + TBP_{(or)} + 2H^+_{(aq)} \overset{K_2}{\rightleftharpoons} PaO(OH)^{2+}_{(aq)} + \\ + TBP.\ 2(HDEHP)_{2_{(or)}} \qquad (2)$$

The second possibility is that an organic-organic interaction may take place prior to the ion exchange reaction ; this can be expressed as :

$$PaO(OH)^{2+}_{(aq)} + TBP - 2\ (HDEHP)_{2_{(or)}} \overset{K_3}{\rightleftharpoons}$$

$$PaO(OH)\ [H(DEHP)_2]_{2(or)} + 2H^+_{(aq)} + TBP_{(or)} \qquad (3)$$

The equilibrium constants for both reactions 2 & 3 were calculated at different temperatures and the respective thermodynamic parameters determined. By comparing the data of reactions 2 & 3 (Table 2) it seems that reaction 3 is more favourable due to the negative sign of ΔG value ; also, the negative ΔH means that the reaction is exothermic which is proved experimentally (Fig. 2). It is quite evident that the dependency with respect to TBP being -1 ; -2 with respect to $[H^+]$ and finally $+2$ with respect to [HDEHP], favours the mechanism suggested in reaction (3).

Table 1

Thermodynamic functions of the reaction of Pa(V) with HDEHP in benzene

Species	Log k	ΔH kJ/mole	ΔG kJ/mole	ΔS J/log/mole
$PaO(OH)[H(DEHP)_2]_2$	3.956	−50.08	−22.697	−91.889

Subtracting equation (3) from (1) one gets :

$$TBP_{(or)} + 2(HDEHP)_{2(or)} \overset{K_4}{\rightleftharpoons} TBP.\ 2(HDEHP)_{2(or)} \qquad (4)$$

$$K_4 = \frac{[TBP.\ 2(HDEHP_2)_{(or)}}{[TBP]_{(or)}\ [(HDEHP)_2]^2_{(or)}} = \frac{K_1}{K_3}$$

or $\log K_4 = \log K_1 - \log K_3 = 1.525$.

From the thermodynamic functions for reaction (4) given in table 2 the positive ΔH is attributed to the rupture of physical bonds of the solvent molecules around the organic species (reaction 4), which is reflected by the disordering of the system ($\Delta S = 34.98$).

At a higher TBP concentration ($[\mathrm{TBP}] > 1\mathrm{M}$) the slope analysis of the synergic reaction that occurs, after passing the minima in figure 2, illustrates that two molecules of TBP participate in the extracted species, following the expression :

$$\mathrm{PaO(OH)}^{2+}_{(aq)} + 2\,(\mathrm{HDEHP})_{2(or)} + 2\mathrm{TBP}_{(or)} \overset{K_5}{\rightleftarrows}$$

$$\mathrm{PaO(OH)}\,[\mathrm{H(DEHP)_2}]_2.\ 2\mathrm{TBP}_{(or)} + 2\mathrm{H}^+_{(aq)} \qquad (5)$$

Subtracting equation (1) from (5), the following organic phase reaction or the synergic reaction will be.

$$\mathrm{PaO(OH)}\,[\mathrm{H(DEHP)_2}]_{2(or)} + 2\mathrm{TBP}_{(or)} \overset{K_6}{\rightleftarrows}$$

$$\mathrm{PaO(OH)}\,[\mathrm{H(DEHP)_2}]_2.\ 2\mathrm{TBP}_{(or)} \qquad (6)$$

giving :

$$K_5 = \frac{D[\mathrm{H}^{2+}]^2}{[(\mathrm{HDEHP})_2]^{-2}[\mathrm{TBP}]^2}$$

The values obtained for K_5 at 3 temperatures 15°, 20° and 35°C were plotted as log K vers. $1/T$, which gave a straight line with a positive slope, and a negative ΔH value ($\Delta H = -\ 18.336$ KJ/mole). The thermodynamic functions obtained for both reactions (5) and (6) (Table 2), show that

Table 2

Thermodynamic functions for the reactions of Pa(V)/HDEHP/TBP system

Reaction number	log K	ΔH kJ/mole	ΔG kJ/mole	ΔS J/deg./mole
2	−2.4311	52.198	13.948	128.356
3	2.4311	−51.756	−13.948	−126.872
4	1.525	1.676	− 8.749	34.983
5	2.32	−18.336	−13.311	−16.862
6	−1.636	31.744	9.386	75.03

reaction (5) is exothermic, spontaneous, favoured by enthalpy changes and is opposed by entropy. Concerning reaction (6): the reaction proved to be disordering, being endoergic, and is favoured by entropy and opposed by enthalpy changes. Equation 6 shows apparently that the reaction is accompanied by ordering behaviour but actually the reaction could take place by displacement of different water molecules from the sphere complex which is proved by high positive values for both ΔS and ΔH. One could conclude that the organic-organic interaction[4] is a competing reaction prior to the synergistic extraction reaction, [6] which seems to cause depression in the distribution coefficient of Pa(V), and to be responsible for the antagonistic extraction by the ion exchanger HDEHP mixed with TBP, in the low concentration range of the latter.

REFERENCES

[1] R. T. Kolarich, V. A. Ryan and R. P. Schuman, *J. Inorg. Nucl. Chem.*, **29**, 783 (1967).

[2] S. Suzuki and Y. Inoue, *Bull. Chem. Soc. Japan*, **42**, 2523 (1969).

[3] A. T. Kandil, A. S. Abdel-Gawad and A. Ramadan, *Radiochimica Acta*, **27**, 39 (1980).

[4] H. A. El-Naggar, H. B. Maghrawy, and A. Ramadan, "Separation Science and Technology" accepted for Pub. (1982).

[5] A. G. Goble and A. G. Maddock, *J. Inorg. Nucl. Chem. Z*, **94** (1958).

[6] J. R. Flanary, Proceeding of the Int. Conf. on the Peaceful Uses of Atomic Energy, **9**, 528 (1958).

[7] H. A. El-Naggar, H. B. Maghrawy and A. Ramadan, *J. Radioanal. Chem.*, **77**, 29 (1983).

[8] Y. Marcus and A. S. Kertes, "Ion Exchange and Solvent Extraction of Metal Complexes", Wiely-Interscience, London (1969).

[9] R. Gaullaumont, *Rev. de Chimie Minérale*, **3**, 339 (1966).

NOTE POUR LES AUTEURS

La Revue Roumaine de Chimie publie des articles en anglais, français, russe, allemand ou espagnol. Les auteurs sont priés d'envoyer des articles et des comptes rendus inédits.

Les manuscrits seront dactylographiés à deux intervalles. La bibliographie, les tableaux et la légénde des figures seront placés après le texte.

Si l'article fait partie d'une série numérotée, la partie précédente sera donnée comme première référence.

Chaque article sera précédé d'un résumé comprenant quinze lignes au maximum.

Les références bibliographiques dans le texte seront faites par des exposants sans parenthèses et paraîtront à la fin de l'ouvrage.

Les publications périodiques mentionnées dans la bibliographie seront présentées suivant les prescriptions internationales : le nom de l'auteur précédé de l'initiale du prénom, le titre du périodique abrégé conformément à « Chemical Abstracts » et souligné par une ligne, le numéro du tome indiqué par des chiffres arabes et souligné par deux lignes, suivi de la première page de l'article : à la fin, l'année de la parution sera placée entre parenthèses. Le numéro de la revue ne sera pas indiqué si les pages du volume sont numérotées consécutivement.

Les textes des livres ou traités incluceront : le nom des auteurs, l'initiale du prenom, le titre du livre entre guillemets et sans être souligné, le numéro du tome précédé par l'abréviation, « vol. » (ou « Bd »), le numéro de l'édition, les éditions (the publisher), la localité de la parution du livre, l'année de la parution et la page de la référence précédée(s) par l'abréviation « p. » (ou « S. »).

Les brevets seront indiqués comme suit: l'auteur ou la firme, le pays et le numéro du brevet, la date et la revue (*Chem. Abstr.*). Par ex. : M. Jones (to Union Carbide Co.), Brit. Pat. 601 238, 2 sept. 1959, ef. *Chem. Abstr.*, **54**, 12808 (1960).

Les diagrammes seront tracés à l'encre de Chine sur papier calque. Les tableaux et les figures (en nombre strictement nécessaire), ainsi que les courbes dans les figures seront numérotes par des chiffres arabes. Leur explication sera donnée dans la légende des figures. Prière de ne pas inscrire les mêmes données dans les tableaux et les figures. Chaque tableau aura un titre. On indiquera dans le texte la place approximative des tableaux et des figures. Les formules chimiques seront incluses dans le texte: en outre, elles seront transcrites sur papier calque, à l'encre de Chimie.

Les auteurs sont priés d'indiquer les caractères italiques (en soulignant les lettres au crayon), ainsi que tout autre caractère spécial: les préfixes *ortho, meta, para, cis, trans,* etc. seront soulignes pour indiquer leurs caractéres italiques, et ne seront jamais écrits avec des majuscules.

Aucune correction à la main ne sera admise sur le manuscrit. Les corrections seront frappés à la machine. Les lettres greques ou d'autres symboles spéciaux seront insérés à la main à l'encre clairement.

Le manuscrit sera signé par l'auteur.

Titre-courant aura 50 lettres au maximum.

L'entière responsabilité du contenu des articles appartient aux auteurs.

Sur demande on peut obtenir une note plus complète.

PRINTED IN ROMANIA

TRAVUX PARUS AUX ÉDITIONS DE L'ACADÉMIE DE LA RÉPUBLIQUE SOCIALISTE DE ROUMANIE

GH. MARCU, **Chimia compuşilor coordinativi**, 1984, 415 p.

E. CORDOŞ, C. MANOLIU, **Spectrometria de absorbţie şi fluorescenţă atomică**, 1984, 178 p.

C. BODEA, **Tratat de biochimie vegetală**, p. II, vol. 5, 1984, 438 p.

ELENA CEAUŞESCU, **Cercetări în chimia şi tehnologia polimerilor**, 1983, 519 p.

N. ASANDEI, A. GRIGORIU, **Chimia şi structura fibrelor**, 1983, 395 p.

N. IONESCU, M. CĂLDĂRARU, **Oxidarea catalitică a olefinelor inferioare**, 1983.

C. CAŞCAVAL, **Studiul polimerilor prin piroliză şi cromatografie de gaze**, 1983, 220 p.

C. I. SIMIONESCU, F. DANEŞ, **Originea vieţii**, 1983, 110 p.

C. BODEA, (sub redacţia), **Tratat de biochimie vegetală**, II, Vol. IV, 1982, 408 p.

I. G. MURGULESCU, RODICA VÎLCU, **Introducere în chimia fizică, Vol. III. Termodinamica chimică**, 1982, 624 p.

I. G. MURGULESCU, J. PĂUN, **Introducere în chimia fizică, Vol. I.3. Nucleul atomic, reacţii nucleare, particule elementare**, 1982, 606 p.

ELENA JERCAN, **Analiza cromatografică**, 1982, 286 p.

ELENA CEAUŞESCU, **Noi cercetări în domeniul compuşilor macromoleculari**, 1981, 536 p.

I. G. MURGULESCU, TATIANA ONCESCU, E. SEGAL, **Introducere în chimia fizică. Vol. II, 2. Cinematică chimică şi cataliză**, 1981, 1024 p.

V. DRĂGUŢAN, A. T. BALABAN, M. DIMONIE, **Metateza olefinelor şi polimerizarea prin deschidere de inel a cicloolefinelor**, 1981, 254 p.

LYDIA-MARIA VAICUM, **Epurarea apelor uzate cu nămol activ. Bazele biochimice**, 1981, 218 p.

I. GĂLĂŢEANU, **Procese şi metode radiochimice în energetica nucleară**, 1981, 234 p.

O. IORDACHE, **Procese polistocastice la fenomenele de transfer**, 1981, 186 p.

CR. SIMIONESCU, VALERIA GORDUZA, **Polimeri biocompatibili şi biologic activi**, 1980, 479 p.

ELENA CEAUŞESCU, **Polimerizarea stereospecifică a izoprenului**, 1979, 307 p.

CONST. GH. MACAROVICI, **Analiza chimică cantitativă anorganică**, 1979, 457 p.

M. FLORESCU, **Metode ştiinţifice în dezvoltarea industriei chimice moderne**, 1979, 256 p.

A. T. BALABAN, I. GĂLĂŢEANU, G. GEORGESCU, LIGIA SIMIONESCU, **Compuşi marcaţi şi radiofarmaceutici cu aplicaţii în medicina nucleară**, 1979, 495 p.

I. G. MURGULESCU, E. SEGAL, **Introducere în chimia fizică. Vol. II.1. Teoria molecular cinetică a materiei**, 1979, 1036 p.

S. STERNBERG, FL. DANEŞ, **Termodinamica chimică aplicată**, 1978, 400 p.

I. G. MURGULESCU, V. EM. SAHINI, **Introducere în chimia fizică. Vol. 1.2. Structura şi proprietăţile moleculelor**, 1978, 604 p.

I. ZUGRĂVESCU, MAGDA PETROVANU, **N-ylid chemistry**, coédition avec McGrow-Hill, International Book Company, U.S.A., 1977, 396 p.

G. MURGULESCU, **Introducere în chimia fizică. Vol. I.1. Atomi, molecule, legătură chimică**, 1976, 560 p.

ELENA CEAUŞESCU, **Research work on synthesis and characterization of macromolecular compounds. Contributions**, 1974, 251 p.

CR. SIMIONESCU, VIORICA RUSAN, V. POPA, **Chimia algelor marine**, 1974, 212 p. 1 pl.

ISSN 0035—4090

I. P. Informaţia c. 2649

43426

Lei 40

$80 (pour un abonnement annuel)

= 1103
66
1985 APR 2 –
04
Vegyészet

ACADÉMIE DE LA RÉPUBLIQUE SOCIALISTE DE ROUMANIE

REVUE ROUMAINE DE CHIMIE

TOME 30

N° 3

Mars 1985

EDITURA ACADEMIEI REPUBLICII SOCIALISTE ROMÂNIA

Rev. Roumaine Chim.

RRCHAX, **30**, *3*, p. 187–286 (1985), **Bucarest**

ACADÉMIE DE LA RÉPUBLIQUE SOCIALISTE DE ROUMANIE

COMITÉ DE RÉDACTION

Rédacteur en chef :

I. G. MURGULESCU, membre de l'Académie de la République Socialiste de Roumanie

Rédacteurs en chef adjoints :

A. T. BALABAN et V. EM. SAHINI, membres correspondants de l'Académie de la République Socialiste de Roumanie

Collège de rédaction :

EM. BRATU, ELENA CEAUŞESCU, ECATERINA CIORĂNESCU-NENITZESCU, CR. SIMIONESCU, membres de l'Académie de la République Socialiste de Roumanie : P. SPACU, membre correspondant de l'Académie de la République Socialiste de Roumanie : M. BANCIU, M. D. GHEORGHIU, I. HAIDUC, D. I. MARCHIDAN, I. MOLDOVAN, G. NIAC et D. SĂNDULESCU

La Revue Roumaine de Chimie paraît 10 fois par an. Toute commande de l'étranger sera adressée à ROMPRESFILATELIA – sectorul Export-Import Presă, P.O. Box 12–201, télex 10376 prsfi r Bucarest, Calea Griviţei nr. 64–66, Roumanie

Les manuscrits, les livres et les revues proposés en échange, ainsi que toute correspondance seront envoyés à la rédaction.

REVUE ROUMAINE DE CHIMIE
125, Calea Victoriei, 79717 Bucarest, Roumanie, téléphone 50 76 80

EDITURA ACADEMIEI REPUBLICII SOCIALISTE ROMÂNIA
125, Calea Victoriei, 79717 Bucarest, Roumanie, téléphone 50 76 80

ORSZÁGOS MŰSZAKI INFORMÁCIÓS KÖZPONT ÉS KÖNYVTÁR 1983

REVUE ROUMAINE DE CHIMIE

Tome 30, N° 3 **Mars, 1985**

F. BADEA, F. IORDACHE, AURELIA MEGHEA, A. T. BALABAN, ROXANA MARINESCU and ANA-MARIA GHIVIRIGĂ, Carbanions and free radicals derived from 1,2-diphenylpyrazolidine-3,5-diones. I. Trapping of the free radical formed in phenylbutazone oxidation . . . . 189—198
V. BRÂNZOI, S. STERNBERG and LILIANA APĂTEANU, Electrode processes in $Pb/H_2SO_4 + Na_2SO_4$ system . . . . 199—207
S. STERNBERG and MIHAELA DRĂGĂNOIU, The mean thermodynamic activity of $CuSO_4$ in the ternary systems : $CuSO_4+MgSO_4+H_2O$ and $CuSO_4+MnSO_4+H_2O$ . . . . 209—215
C. I. LEPĂDATU and MARIUS ANDRUH, Factorisation of orbital energies in transition — metal complexes. I. Factorisation of the overlap integrals . . . . 217—221
DUMITRU MĂNOIU, MARIA MĂNOIU, ILIE G. DINULESCU and MARGARET AVRAM, Friedel — Crafts acylation of alkynes. V. Reaction of alkynes with aroyl chlorides in the presence of silver perchlorate 223—227
MARIA BREZEANU, M. ANDRUH, LUMINIȚA PATRON and V. T. POPA, Coordination compounds formation within the MCl_2-$SnCl_2$-α,α'-bipyridine (M=Co, Ni) system . . . . 229—231
C. CRISTESCU and SILVIA SITARU, *as*-Triazine derivatives with potential therapeutic action. XX. Cyanoethylation of 5-substituted-6-azauracil and 4-thioxo-5-substituted-6-azauracil . . . . 233—238
MARIA BRUMĂ and ION SAVA, Ordered polyesterimides . . . . 239—244
M. A. HASSAN, M. EL-KADY, M. EL-BORAI and A. A. ABD EL-MOATY, Base catalyzed additions of dehydroacetic acid and its 3-cinnamoyl derivatives . . . . 245—248
RADU VLĂDEA, Catalytic influences in electrooxidation of olefins in non-aqueous solutions. III. Kinetic study of diisobutylene and styrene oxidation . . 249—256
A. A. EL-BARBARY, Some chemical aspects of 5-aryl-1,3,4-oxadiazoles . . . 257—265
I. A. ATTIA and E. A. SOLIMAN, Synthesis and some reactions of acetylcyclohexenone derivatives . . . . 267—271
CLEOPATRA VASILIU OPREA and FELICIA WEINER, Mechanochemically initiated polymerizations. 6. Influence of mechanical parameters on the polymerization of styrene by vibratory grinding . . . . 273—280

BOOK REVIEWS . . . . 281—286

Rev. Roumaine Chim. **30**, *3*, 187—286 (1985), Bucarest

Revue Roumaine de Chimie, **30**, *3*, 189—198 (1985)

CARBANIONS AND FREE RADICALS DERIVED FROM 1,2-DIPHENYLPYRAZOLIDINE-3,5-DIONES. I

TRAPPING OF THE FREE RADICAL FORMED IN PHENYLBUTAZONE OXIDATION

F. BADEA, F. IORDACHE, AURELIA MEGHEA, A. T. BALABAN, ROXANA MARINESCU and ANA-MARIA GHIVIRIGĂ

Polytechnic Institute, Department of Organic Chemistry, Splaiul Independenței 313, 76206 Bucharest, Romania

Received October 18, 1984

4-n-Butyl-1,2-diphenylpyrazolidine-3,5-dione (phenylbutazone) was treated with nitrosobenzene and 3,5-di-t-butylnitrosobenzene in order to obtain the corresponding hydroxylamines. Air oxidation of these compounds afforded the corresponding persistent nitroxide radicals, identified by their ESR spectra. Air oxidation of phenylbutazone, followed by treatment with nitrosobenzene yielded the same nitroxide (ESR identification) as that obtained from the corresponding hydroxylamine by oxidation, but on using 3,5-di-t-butylnitrosobenzene instead of nitrosobenzene, no ESR signal for a nitroxide radical has been observed. The results were interpreted as indicating that the free radical derived from phenylbutazone is stable enough to be trapped by an unhindered reagent, but otherwise it is more rapidly destroyed than it is trapped. The measurement of the deuteration rates of 4-substituted 1,2-diphenylpyrazolidine-3,5-diones (4-H, 4-Et, 4-n-Bu and 4-CH_2-Ph) showed that the 4-substituent in the pyrazolidinedione system affects markedly the reaction rates of the corresponding carbanion.

Derivatives of 1,2-diphenylpyrazolidine-3,5-dione, **1**, present a well-known antirheumatic and antiphlogistic action.[1] The most convenient method for the synthesis of these compounds was proposed by Ruhkopf in 1941[2] and consists in the condensation of the substituted malonic ester with hydrazobenzene in the presence of the alkoxide corresponding to the alkyl in the dialkyl malonate :

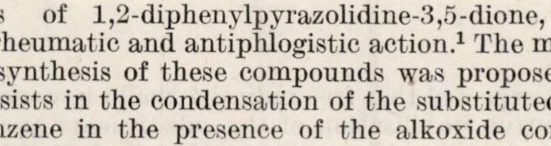

(1)

Alternative routes are to condense the unsubstituted 1,2-diphenylpyrazolidine-3,5-dione (**1a**), either with an alkyl halide or with a carbonyl compound followed by hydrogenation.[3,4]

The best known and most widely used drug in this class is phenylbutazone **1b** (Butazolidine, Butazone). However, phenylbutazone is easily degradable, especially in solution.[5,6] It was observed that even during the preparation of **1b** an oxidized side-product was formed, identified to be 1,2-diphenyl-4-butyl-4-hydroxypyrazolidine-3,5-dione **2**,[7] identical with one of the degradation products of phenylbutazone. It was supposed that **2** is formed during the condensation (1) by air oxidation of the resulted phenylbutazone. In agreement with that supposition it has been shown that the air oxidation of **1b** leading to **2** is accelerated by the presence of hydrazobenzene.[8] Bases such as triethylamine, in their turn, promote the transformation of **1b** in **2**.[5,6] The oxidation of phenylbutazone in alcoholic solutions depends upon the pH of the solution.[9] More easily, **2** can be obtained from **1b** by treatment with hydrogen peroxide.[10]

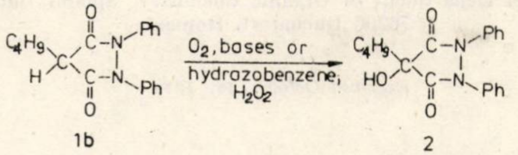

(2)

We considered from these data that a possible intermediate in the oxidation of phenylbutazone is the free radical **4**, formed by an electron transfer from the corresponding carbanion **3** :

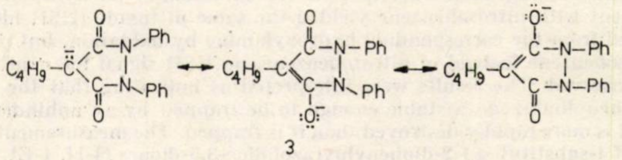

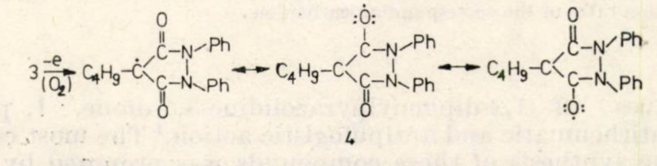

It could be expected that free radical **4** would have some persistence, due to a captodative stabilisation of the substituents at the radical centre.[11] This paper describes the trapping of radical **4** with nitrosoarenes, confirming the stability of the radical, comparable with the stability of carbanion **3**.

RESULTS

The 1,2-diphenyl-4-alkylpyrazolidine-3,5-diones **1a** — **1d** were prepared by the method described by Ruhkopf[2] from the corresponding alkylmalonates and hydrazobenzene. The melting points and the ^{1}H-NMR spectra of the obtained pyrazolidinediones agree well with the known values quoted in the literature.

Measurement of the hydrogen—deuterium exchange rates. In the measurement of the hydrogen—deuterium exchange rate, the variation in time of the NMR signal of the 4-H bonded to the pyrazolidinedione ring was used (Fig. 1). The deuterium exchange rate constants k_D were determined in

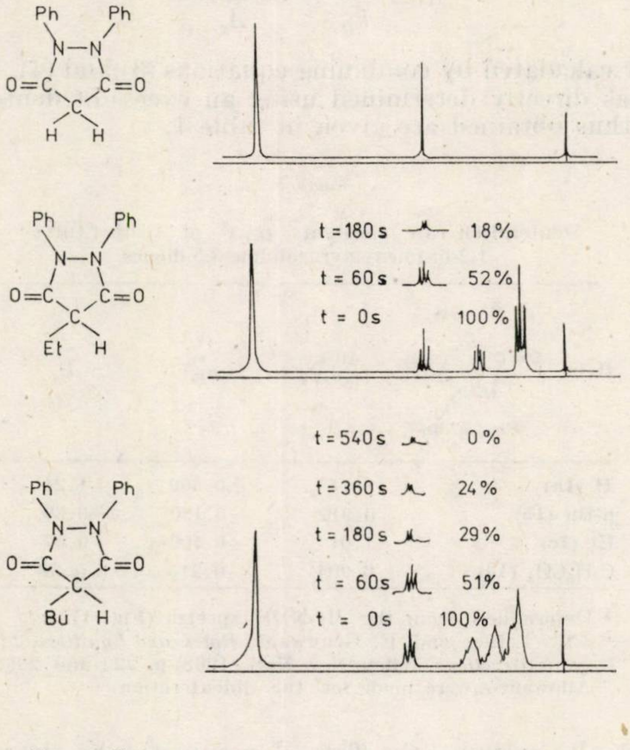

Fig. 1. — ^{1}H-NMR spectra of phenylbutazone derivatives in acetone-d$_6$: from top to bottom ; **1a** with D$_2$O for the specified times ; **1b** in similar conditions, **1c** in similar conditions, and **1d** in similar conditions.

two different ways. For fast reactions, the alkylpyrazolidinedione was treated with diluted deuterated water in order to assure the reversibility of the exchange reaction. The following equation was used :

$$k_D + k_H = \frac{2.303}{t} \lg \frac{A_0 - A_e}{A_t - A_e} \tag{3}$$

where A_0, A_e and A_t are the intensities of the 4-H signals at time zero, at equilibrium and at time t, respectively. Considering that the equilibrium constant K is :

$$K = \frac{k_D}{k_H} = \frac{A_0 - A_e}{A_e} \tag{4}$$

k_D was easily calculated by combining equations (3) and (4). For slow processes, k_D was directly determined using an excess of deuterated water. The values thus obtained are given in table 1.

Table 1

Deuteration rate constants $(k_D)^a$ of 4-substituted 1,2-di-phenylpyrazolidine-3,5-diones

R in 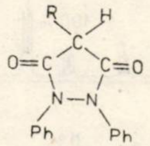	10^2k (s^{-1})	σ_R^{*b}	E_s^b
H (**1a**)	$5-8^c$	+0.490	+1.24
n-Bu (**1b**)	0.912	−0.130	−0.39
Et (**1c**)	1.01	−0.100	−0.07
$C_6H_5CH_2$ (**1d**)	0.904	−0.215	−0.38

[a] Determined from the ^{1}H-NMR spectra (Fig. 1).
[b] J.E. Leffler and E. Grunwald, *Rates and Equilibria of Organic Reactions*, Wiley, New York, 1963, p. 222 and 228.
[c] Allowances were made for the dideuteration.

Table 1 also includes the Taft σ_R^* parameters of the substituent R in position 4 of the ring as well as the steric parameter E_s of the alkyl R. It can be easily observed that the electronic effect of the 4-substituent is shadowed by the steric effect.

Trapping of the radical derived from phenylbutazone. The pure phenylbutazone was condensed either with nitrosobenzene or with 3,5-di-t-butylnitrosobenzene, in the presence of triethylamine. The resulting hydroxylamines **5** are initially white crystals which soon after filtration become yellow and in a few hours acquire a brownish colour.

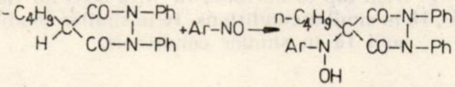

(5)

1b

5 a, Ar = Ph
b, Ar = 3,5-$(t\text{-}C_4H_9)_2C_6H_3$

The condensation requires about two hours with nitrosobenzene, and about 4 hours with 3,5-di-t-butylnitrosobenzene. Compound **5b** separates easily on cooling from the reaction mixture as white crystals, whereas

5a needs the solution to be concentrated in order to precipitate as a yellow solid.

The benzene solutions of the hydroxylamines **5** were vigorously shaken with air and the ESR spectra were recorded shortly afterwards. Both spectra have the same pattern, three equidistant broad lines of the same intensity, in agreement with the interaction of an unpaired electron with a neighbouring nitrogen nucleus ($I = 1$, number of lines $= 2I + 1$). After deaeration of the benzene solutions, the ESR spectrum of compound **5a** presents 18 lines, each initial signal being split into six lines (Fig. 2).

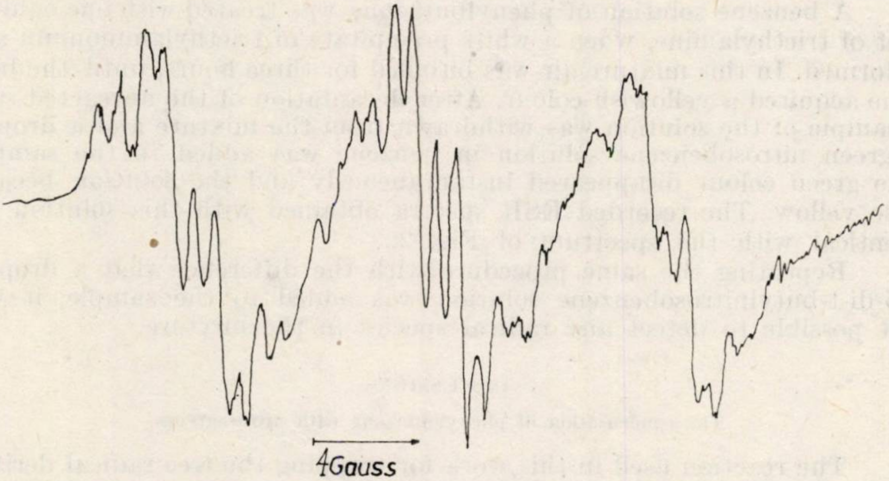

Fig. 2. — First-derivative ESR spectrum of the free radical **7a** in deaerated benzene.

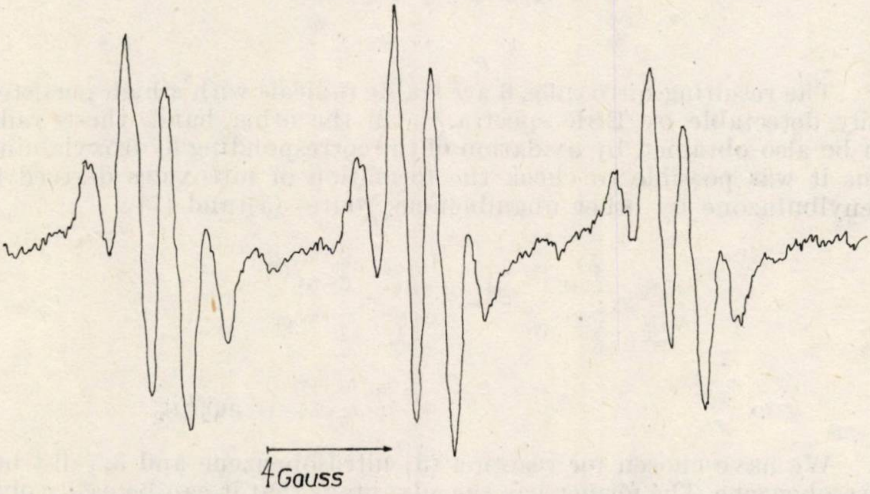

Fig. 3. — First-derivative ESR spectrum of the free radical **7b** in deaerated benzene.

This indicates the coupling of the unpaired electron with the five hydrogen atoms from the benzene ring.

The benzene solution of compound **5b** after deaeration gives an ESR spectrum composed from 12 lines, each initial line being split into four lines with the relative intensity 1 : 3 : 3 : 1 (Fig. 3). The ESR spectra are discussed in a subsequent section.

A benzene solution of phenylbutazone was treated with one equivalent of triethylamine, when a white precipitate of triethylammonium salt is formed. In this mixture air was bubbled for three hours, until the benzene acquired a yellowish colour. After decantation of the unreacted salt, a sample of the solution was withdrawn from the mixture and a drop of a green nitrosobenzene solution in benzene was added to the sample. The green colour disappeared instantaneously and the solution became pale yellow. The recorded ESR spectra obtained with this solution are identical with the spectrum of Fig. 2.

Repeating the same procedure with the difference that a drop of 3,5-di-t-butylnitrosobenzene solution was added to the sample, it was not possible to detect any radical species in the mixture.

DISCUSSIONS

The condensation of phenylbutazone with nitrosoarenes

The reaction used in this work for trapping the free radical derived from phenylbutazone was reaction (6), which presents some advantages, as compared to other trapping reactions :[12]

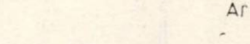

$$\text{Alk}\cdot + \text{Ar{-}N{=}O} \longrightarrow \text{Alk}{-}\underset{\text{Ar}}{\underset{|}{\text{N}}}{-}\ddot{\underset{\cdot\cdot}{\text{O}}}\cdot \qquad (6)$$

The resulting nitroxides **6** are stable radicals with a high persistency, easily detectable by ESR spectra.[13] On the other hand, these radicals can be also obtained by oxidation of the corresponding hydroxylamines.[12] Thus it was possible to check the formation of nitroxides derived from phenylbutazone by other unambiguous routes (5) and (7) :

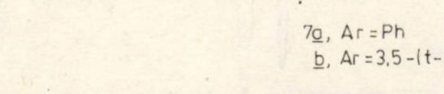

(7)

7a, Ar = Ph

b, Ar = 3,5-(t-C_4H_9)$_2$$C_6H_{10}$

We have chosen for reaction (5) nitrosobenzene and 3,5-di-t-butylnitrosobenzene. The former has the advantage that it can be easily obtained in the laboratory and can be used as standard in comparing the reactivity of other substituted nitrosoarenes. The latter, on the other hand, is advantageous in studying the ESR spectra of the radicals **7**, which are more easily interpreted than those of the radicals formed from nitrosobenzene. We have also considered that the bulky t-butyl groups will not affect markedly the reactions at the nitroso group. However, in the condensation of phenylbutazone with nitrosoarenes, nitrosobenzene reacts twice as fast as 3,5-di-t-butylnitrosobenzene. The difference in reactivity can be the result of an inductive effect of the two alkyl groups. Indeed, considering the σ^*_{m-t-Bu} Hammett values, an approximate value of the ρ^* parameter can be evaluated ($\rho^* \cong +1.5$). The positive sign of ρ^* is in good agreement with the development of a negative charge in the transition state at the reaction site. Nevertheless, the large value of the ρ^* parameter does not rule out a steric effect between the remote t-butyl groups and the n-butyl group situated at the reaction centre in carbanion **3**.

In order to determine the steric requirements of the 4-substituted 1,2-diphenylpyrazolidine-3,5-diones in a base-catalyzed reaction, we studied the deuteration rates of four pyrazolidinediones, including phenylbutazone (Table 1). Excepting the value for the unsubstituted pyrazolidinedione (**1a**), the deuteration rates are little affected by the 4-substituent of the heterocyclic ring. However, had the observed differences been determined only by the inductive effects of the R substituent, the benzyl derivative **1d** would have reacted faster than phenylbutazone **1b** ($\sigma^*_{C_6H_5CH_2} = +0.215$; $\sigma^*_{n-C_4H_9} = -0.130$). Actually, the two derivatives react with about the same rate, in good agreement with their similar E_s value. Thus, even in a reaction with small steric requirements (deuteration), the steric effects play a more dominant role than the inductive effects. We feel from these results that the reactivity difference between the two nitrosoarenes studied by us is a consequence of the repulsion of the remote t-butyl groups in the nitrosoarene and the n-butyl group situated at the reaction centre in carbanion **3**. Figure 4 shows a model of the approach of the two reagents in the transition state of the condensation.

The attack of carbanion **3** must be *exo*, due to the bulky phenyl groups in 1,2-diphenylpyrazolidine-3,5-diones. The steric interaction between the phenyl groups and the alkyl group determines the approximate configuration of the n-butyl group indicated in figure 4. As Dreiding models show, this conformation allows the collision between the t-butyl groups in the nitrosoarene and the n-butyl group in carbanion **3**.

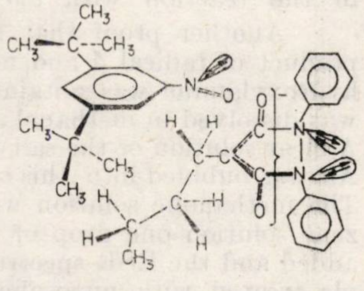

Fig. 4. – Model of the attack by the phenylbutazone anion on 3,5-di-t-butylnitrosobenzene.

We feel that the deuteration experiments recorded in table 1 are a proof that the steric requirements in the condensation of **3** play an overwhelming role in the reaction. Other more quantitative experiments are in progress at this moment in our laboratory.

The nitroxides 7 and their ESR spectra

The hydroxylamines **5** were simply oxidized to the nitroxides **7** with atmospheric oxygen. This shows, in its turn, the high stability of the radicals relative to the hydroxylaminic precursors. The ESR spectra of the radicals (**Fig.** 2) demonstrate their structure.

The ESR spectrum of deaerated benzene solutions of **7b** (Fig. 3) is easily interpreted in terms of just two hyperfine coupling constants : $a_N = 12.27$ and $a_H = 1.54$ Gauss for the three *ortho* and *para* hydrogen atoms bonded to the 3,5-di-t-butylphenyl group.

The nitrogen hyperfine coupling constant of the radical **7a** (Fig. 2) is $a_N = 11.36$, Gauss a value which is close to that of the preceding radical and of various other alkyl-aryl-nitroxides **6**.[13] The coupling constants were determined by means of a potassium peroxylaminedisulfonate standard (Frémy salt). The same standard was used for the determination of the g values, which were found to be 2.0059 in both cases (**7a** and **7b**).

The trapping of the radical 4

In the generation of radical **4** we have initially prepared the salt of phenylbutazone with triethylamine, which was aerated until a yellowish colour was observed. A small amount of the nitrosoarene was then added to the solution and the ESR spectrum of the resulting mixture was recorded.

In order to avoid any reaction between the unreacted carbanion **3** and the nitrosoarene to yield the hydroxylamine **5**, able to generate by oxidation the nitroxide **7**, we performed the reaction in benzene with an excess of triethylamine, in which the salt of carbanion **3** is insoluble. Only the coloured layer, after decantation of the unreacted salt, was withdrawn from the reaction mixture. The corresponding ESR signals of the nitroxide were observed only in the reaction with nitrosobenzene and not in the reaction with 3,5-di-t-butylnitrosobenzene.

Another proof that the observed nitroxide radical is a trapping product of radical **4** and not an oxidation product of the corresponding hydroxylamine was obtained in the following manner : phenylbutazone was dissolved in methanol and an equivalent of triethylamine was added. A clear solution of the salt of phenylbutazone and triethylamine resulted. Air was bubbled into this solution until a yellowish colour was developed. The methanolic solution was extracted with benzene, to the dried benzene solution one drop of the benzene solution of the nitrosoarene was added and the ESR spectrum was recorded shortly afterwards. The sample treated with nitrosobenzene gave similar ESR spectra with those already mentioned, indicating the presence of the nitroxide radical. The sample treated with 3,5-di-t-butylnitrosobenzene gave no signal for a nitroxide radical. We conclude from those experiments that the identification of a nitroxide radical is a proof for the existence and the persistence of the radical **4**. Radical **4** seems to be stable enough, if generated in methanolic solution, to persist until it is extracted with benzene, in order to react with an unhindered nitrosoarene. However, with a hindered nitrosoarene, 3,5-di-t-butylnitrosobenzene, the reaction is too slow to enable the observation of the nitroxide radical. The steric requirements of radical **4** are also demonstrated by the deuteration experiments of compounds **1a**–**1d**. It is very likely that radical **4** and carbanion **3** are subjected in their reactions to the same steric interactions. Moţoc and Balaban [14] have amply demonstrated that in the reactions of the free radicals the steric effects in radicals and in the reagent play a more drastic effect that the inductive effects of the substituents of the two reaction partners. The fact that the hindered nitrosoarene does not trap radical **4**, whereas nitrosobenzene yields the same nitroxide radical, either by oxidation of the hydroxylamine derivative **5a** or by oxidation of the carbanion **3** seems to be a very convincing proof for the intermediate formation of radical **4**, *via* carbanion **3**, in the oxidation of phenylbutazone.

EXPERIMENTAL

Syntheses of the pyrazolidinediones. In the synthesis of derivatives **1a**—**1d**, the procedure of Ruhkopf[2] was adopted. The substituted malonic ester was condensed with hydrazobenzene in the presence of the alkoxide corresponding to the alkyl in the dialkyl malonate. The best results were obtained in n-butanol with sodium n-butoxide. The following melting points were determined : **1a** : 173—174 ; **1b** : 105—106° ; **1c** : 104—105° ; **1d** : 135—136°. The ^{1}H-NMR spectra of the these derivatives are given in figure 1.

Deuteration experiments. The hydrogen-deuterium exchange rates were determined by treating the 1,2-diphenyl-4-R-pyrazolidine-3,5-dione with deuterated water and measuring the variation in intensity of the 4-H signal of the pyrazolidinedione ring in the ^{1}H-NMR spectra (see text and Fig. 1). The calculated rate constants k_D are listed in table 1.

Condensation of phenylbutazone (**1b**) *with nitrosobenzene.* Phenylbutazone (3 g, 0.61 mol) was disolved in 20 ml methanol containing 1 ml triethylamine (6.01 mol). To the clear solution, 1.1 g nitrosobenzene (0.01 mol) was added, resulting in a clear greenish solution. After two-hour refluxing, the greeen colour of the nitrosobenzene disappeared completely. No solid separated on cooling. By concentrating the methanolic solution, a yellow solid separated, which on standing in air became very soon dark-brown. In order to avoid the decomposition of compound **7a**, the methanolic solution of the compound was diluted with 50 ml benzene, then repeatedly washed with water, with a concentrated solution of $CaCl_2$, again with water and finally dried over $CaCl_2$. The filtered benzene solution was vigorously shaken with air and the ESR spectrum was recorded (Fig. 2).

Condensation of phenylbutazone with 3,5-di-t-butylnitrosobenzene. The same procedure described above was applied using 1.2 g (0.005 mol) of 3,5-di-t-butylnitrosobenzene. [15] The disappearance of the green colour of the nitrosoarene required about four hours. On cooling, a white solid separated (m.p. 145°), which was dissolved in dry benzene, the benzene solution was agitated with air and the ESR spectrum was recorded shortly afterwards. The spectrum is given in Fig. 3.

Trapping of radical **4**. Phenylbutazone (3 g, 0.01 mol) was dissolved in 25 ml benzene and 0.01 triethylamine (1 ml) was added. A white solid was formed. In the agitated suspension of the triethylammonium salt of phenylbutazone in benzene, air was bubbled for 3 hours. After decantation of the ammonium salt, 5 ml of the yellow benzene solution were withdrawn from the reaction mixture and to this solution 1—2 drops of a benzene solution of the nitrosoarene (0.01 mol in 25 ml benzene) were added. The ESR spectra were immediately recorded afterwards.

The ESR determination of the radicals. The ESR spectra were recorded on an ART-5 spectrometer, in the X-band frequency (9060 MHz), using peroxylamine disulphonate as internal standard ($a_N = 13$ Gauss ; $g = 2.0055$).

Samples, either directly withdrawn from the reaction mixture or prepared by dissolving compound **7b** in benzene, presented only three equidistant broad lines of the same intensity, corresponding to the interaction of the unpaired electron with the neighbouring nitrogen atom. The hyperfine structures shown in figures 2, 3 were obtained by drying the benzene solutions on $CaCl_2$ and by careful deaeration of the resulted dry solutions.

In the case of radical **7a**, some anisotropy was observed and the hyperfine structure due to the coupling with the aromatic protons was not completely resolved.

ACKNOWLEDGEMENT. The authors are indebted to Dr. M. T. Căproiu for a generous supply of 3,5-di-t-butylnitrosobenzene and helpful discussions during the progress of this work.

REFERENCES

[1] H. Stenzl, A. Staub, C. Simon and W. Baumann, *Helv. Chim. Acta*, **33**, 1183 (1950); J. R, Geigy AG, Swiss Pat. 267222 (1950); H. K. von Rechenberg, "Phenylbutazone". Edward Arnold Ltd., London, 1962.

[2] H. Ruhkopf, *Ber. dtsch. chem. Ges.*, **73**, 820 (1940).

[3] J. R. Geigy, AG, Brit. Pat., 646597; *Chem. Abstr.*, **45**, 7602 (1951); W. Michaelis and H. Röhmer, *Ber. dtsch chem. Ges.*, **31**, 3003 (1898).

[4] R. Denis, *Experientia*, **15**, 95 (1959); J. R. Geigy AG, Swiss Pat. 269236; *Chem. Abstr.*, **46**, 539 (1952).

[5] V. N. Sokolova and O. Yu. Magidson, *Zhurn. Obshch. Khim.*, **26**, 604 (1956).

[6] S. Veibel, S. Linholter and P. Sorensen, *Acta Chim. Scand.*, **12**, 1359 (1959); E. Pawelczyk and R. Wachowiak, *Dissert. Pharm. Pharmacol.*, **20**, 653 (1968); **22**, 475 (1970); *Acta Polon. Pharm.*, **26**, 433 (1969).

[7] G. Adembri and M. Ghelardoni, *Gazz. chim. ital.*, **89**, 700 (1959); see also references 5 and 6.

[8] S. Veibel, S. Linholter and P. Sorensen, *Acta Chem. Scand.*, **12**, 1364 (1959).

[9] E. Pawetczyk, R. Wachowiak and A. Romanovski, *Dissert. Pharm. Pharmacol.* **19**, 567 (1967).

[10] W. Awe and H. J. Kienert, *Pharm. Acta Helv.*, **38**, 805 (1963); M. Woodruff and J. B. Polya, *Aust. J. Chem.*, **28**, 421 (1975); cf. *Chem. Abstr.*, **82**, 111992 (1975).

[11] H. G. Viehe, R. Merenyi, L. Stella and Z. Janousek, *Angew. Chem.*, **91**, 1028 (1979); A. T. Balaban, *Bul. Inst. Politehnic Bucureşti, ser. chim.—metal.*, **43**(4), 65 (1980).

[12] A. R. Forrester, J. M. Hay and R. H. Thomson, *"Organic Chemistry of Stable Free Radicals"*, Academic Press, London—New York, 1968, p. 180.

[13] A. T. Balaban, N. Negoiţă and L. Pescaru, *Rev. Roum. Chim.*, **16**, 721 (1971); A. T. Balaban, N. Negoiţă and R. Baican, *J. Magn. Res.*, **9**, 1 (1973); M. T. Căproiu, Ph.D Thesis, Bucharest, 1984; see also ref. 12.

[14] A. T. Balaban, A. Chiriac, I. Moţoc and Z. Simon, Steric Fit in QSAR, Lecture Notes in Chem., No 15, Springer, Berlin, 1980; I. Moţoc, Ph.D. Thesis, Bucharest, 1980

[15] H. G. Aurich, *Chem. Ber.*, **101**, 1761 (1968).

Revue Roumaine de Chimie, **30**, *3*, 199–207 (1985)

ELECTRODE PROCESSES IN $Pb/H_2SO_4 + Na_2SO_4$ SYSTEM

V. BRÂNZOI*, S. STERNBERG*, and LILIANA APĂTEANU**

* Dept. of Physical Chemistry, The Polytechnic Institute of Bucharest, Polizu Street, No. 1, Romania

** ICECHIM-IECB-Institute of Chemical and Biochemical Energetics, Bucharest, Splaiul Independenței Street, No. 206, Romania

Received March 5, 1984

The polarization behaviour of lead in mixtures of $H_2SO_4+Na_2SO_4$ was studied. The increase of concentration of Na_2SO_4 leads to the height increase of the anodic and cathodic peaks. Up to 0.7 M Na_2SO_4 the shape of the curve is the same with those obtained in 1 M Na_2SO_4. The concentrations greater than 0.8 M Na_2SO_4 lead to the appearance of new anodic peaks and to the decrease of cathodic peaks. We got to the conclusion that the addition of Na_2SO_4 in H_2SO_4 solutions up to 0.7 M Na_2SO_4 favours the charge and discharge of the lead acid battery.

INTRODUCTION

The present paper is a contribution to the elucidation of the mechanism of the electrode processes occurring in the intricate Pb-H_2SO_4 system; this system lies at the basis of the lead acid batteries. For this purpose the polarization curves of the lead in $H_2SO_4+Na_2SO_4$ solutions were studied by potentiodynamic method. The Na_2SO_4 addition permits the variation of the pH of the solution. More meaningful information concerning the basic lead sulphate formation is obtained. The study of different additions to the lead acid battery electrolyte fits in the general preoccupation of improving the performances and that of turning the lead acid battery into a good account. [1–24]

EXPERIMENTAL PART

The experimental determinations were carried out by means of potentiodynamic technique. The scheme of the device, the cell for electrochemical polarizations, the preparation of the electrode surface are described in an earlier paper. [24]
Specification is made only that before each determination the electrode was cathodically polarized for 45 minutes, at —2700 mV in order to assure the complete removal of any oxide. Polarization curves were registered only after that, by scanning the potential in the $(-2700 \div +2400)$ mV range and back; thus a cycle was obtained. A number of eight cycles was done for each determination. The scan rate of the potential was of 300 mV/min. The studied solutions were 1M sulphuric acid, 1M natrium sulphate and (XM H_2SO_4 + YM Na_2SO_4) mixtures (where $X+Y=1$) with the maintenance of the sulphate ion concentration at a constant value. All the determinations were carried out at a temperature of 25°C.

RESULTS AND DISCUSSIONS

Figure 1 shows the polarization curves of pure lead in a 1M H_2SO_4 solution (solution I), at a potential scan rate of 300 mV/min.

Analysis of these curves shows the following: on the increasing anodic curve a peak appears (A), which represents the lead to lead sulphate oxidation with the formation on the metal surface of a dense and compact layer which results in a current drop to a practically constant value on the whole passive range of about 1550 mV.

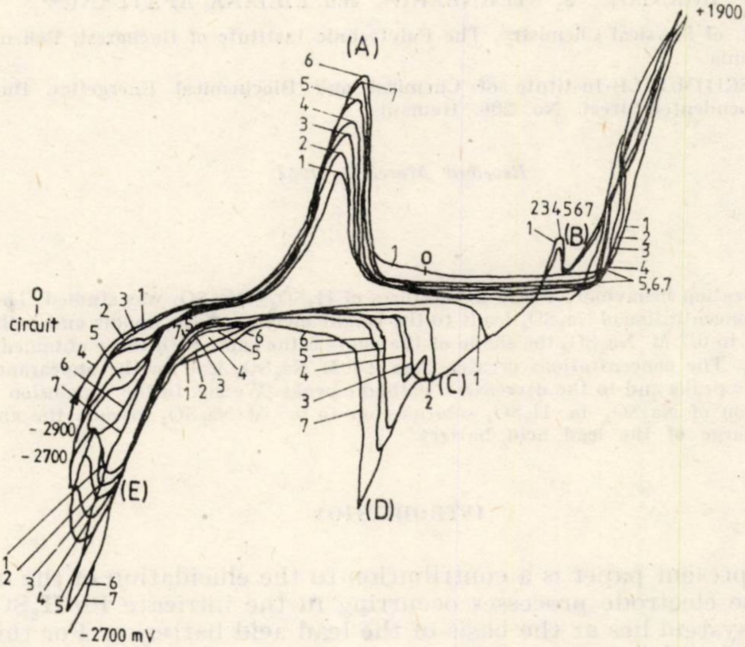

Fig. 1. — Polarization curves of pure lead in 1M H_2SO_4 solution (solution I), at a potential scan rate of 300 mV/min.

However, the passivation current has a value which is different from zero (~0.1 mA) which means that some anodic reactions are taking place in this range, too. In fact "the passivation current" is the limited current of these reactions. The dense lead sulphate film hinders the SO_4^{2-} — and HSO_4^- ions penetrability at the metal surface. Thus, between the metal surface and the lead sulphate layer, the alkalinity of the medium will be stressed. This will cause the formation of the basic lead compounds ($PbO \cdot PbSO_4$; $3PbO \cdot PbSO_4 \cdot H_2O$; $4PbO \cdot PbSO_4$; $Pb(OH)_2$; PbO; $5PbO \cdot PbSO_4 \cdot 2H_2O$) simultaneously with the potential move towards more and more positive values.[2-8] At potential values higher than +1100 mV, hence near $PbO_2/PbSO_4$ equilibrium electrode potential, the hydrated divalent lead oxides and basic sulphates oxidations are starting at α-PbO_2. This is the characteristic form for solutions with higher pH and potentials of about +1200 mV. The penetrability of the passive film increases simultaneously with the α-PbO_2 formation and the acidity of the adjacent medium to the metal surface increases again. This fact combined with a further potential move to more positive values leads to the β-PbO_2 formation (the tetragonal form of PbO_2) simultaneously with the oxygen evolution. Hence, at the end of the increasing anodic scan a corrosion layer appears on the electrode surface, consisting of an inner layer rich in α-PbO_2 and an outer layer rich in β-PbO_2. At the reverse potential sweep a (B) oxidation peak can be seen in the potential range of (+1000 mV) ÷ (+850 mV) which is followed by a small reduction peak (C) and two great reduction peaks (D) and (E). The (B) oxidation peak which appears at the decreasing anodic sweep represents a new oxidation of the metallic lead (under the lead bioxide layer) to lead basic oxides and even to α-PO_2. The first reduction peak (C) represents in fact the formed β-PbO_2 reduction, the Pb^{4+} to Pb^{2+} ion reduction respectively. The (D) peak represents the basic lead compounds reduction, while the (E) peak represents the lead sulphate, the Pb^{2+} ion, respectively to metallic lead reduction. The characteristic of solution I is the progressive increase of the cathodic and of the anodic peaks during the cyclings. The explanation of this behaviour is the following : in solutions with high acidity, the oxidation of Pb to Pb^{2+} occurs. A microporous layer of the thickness of about 1μ is formed. It hinders the anodic process on a large potential range. At the end of the reverse potential scan, after passing through different stages of oxidation ($Pb^{2+} \rightarrow Pb^{4+}$) and of reduction ($Pb^{4+} \rightarrow Pb^{2+}$) as it has been described above, the initial $PbSO_4$ layer is formed again. It is an active, porous lead layer, which can be called microelectrode. It is similar to the negative plate from the lead acid battery. During the second cycle the active spongeous lead turns into a sulphate. At the same time a supplementary amount of lead sulphate is formed from basic lead and at the end of the cycle an increased amount of spongeous lead is obtained. During the next cycles the phenomenon repeats itself leading to the gradual increase of the electrode capacity. (It has been shown, in a recent paper, that after about 100 cycles a constant value of the microelectrode capacity is attained).

The discussion will continue with the analysis of the results obtained in 1M Na_2SO_4 solution (solution II). Figure 2 shows a change in the voltammograms' shape, as well as a change of intensity of the anodic and cathodic processes. Thus, in solution I there is only a relatively small passivation current, with an average of about 0.1 mA, on the whole anodic potential scan range between −350 mV and +1150 mV; in solution II there are very high anodic currents of about 12 mV.

At the same time, a characteristic is the appearance of a peak (A_2) at positive potentials of about +750 mV, which does not exist in solution. I. This peak can be attributed to the PbO and basic lead sulphates formation, which are stable at pH $\geqslant$ 7 according to the Pourbaix lead diagram. Figure 2 shows that the anodic peaks height decreases when repeating the recyclings ; this behaviour is reverse compared to that in solution I. At the same time one can notice that during the first cycling a very high anodic current is obtained. It extends over a potential range of −700 mV and +1750 mV. The passive range practically does not exist.

This potential range includes the $PbSO_4$ formation zone as well as that of the basic lead sulphates formation. The microelectrode capacity which corresponds to this potential range is the following : Q_{II} (first cycle) = = 2.45C hence, of about 7 times higher than the microelectrode capacity obtained in solution I, Q_I (first cycle) = 0.35C. In such conditions (the

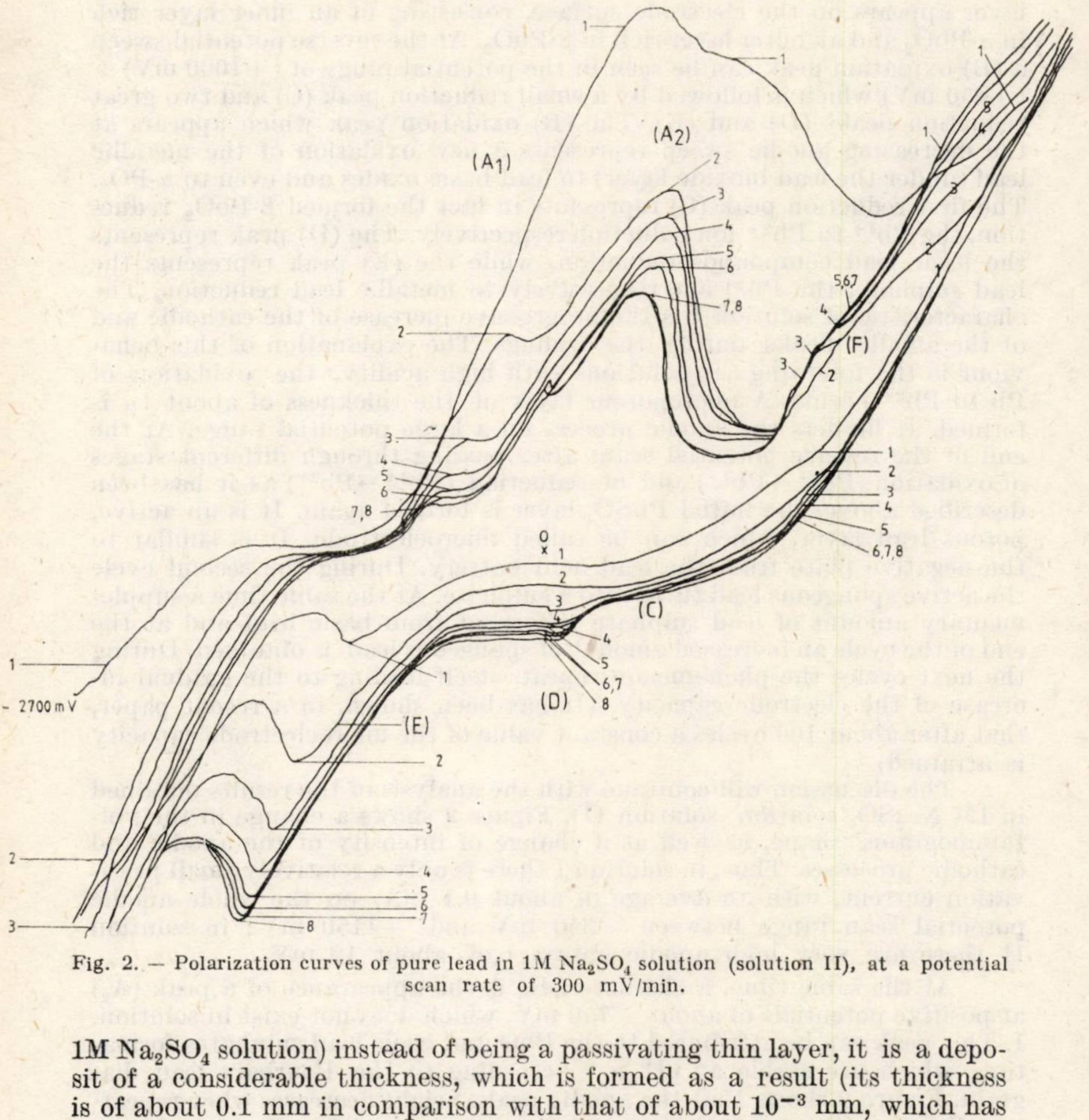

Fig. 2. — Polarization curves of pure lead in 1M Na_2SO_4 solution (solution II), at a potential scan rate of 300 mV/min.

1M Na_2SO_4 solution) instead of being a passivating thin layer, it is a deposit of a considerable thickness, which is formed as a result (its thickness is of about 0.1 mm in comparison with that of about 10^{-3} mm, which has been attained in solution 1.) This deposit (at the end of the first anodic scan) hinders the penetrability of SO_4^{2-} and H^+ ions in the triphasic contact zone (anodic deposit-basic lead-solution acting as a diffusion layer). At about +1750 mV a new increase of current takes place, caused by the oxidation of Pb_b^{2+} at α and β forms of PbO_2 as well as the gaseous oxygen evolution. At the reverse potential scan (first cycle) the cathodic current average is much smaller than that of the anodic one. Hence, the cathodic process is hindered by the diffusion layer and it is obvious that only part of the anodic deposit is reduced.

The (C) and (D) reduction peaks do not appear at the first cycle, but the Pb^{4+} to Pb^{2+} reduction still takes place by means of a cathodic limiting current. A peak of low intensity (E) appears at a potential of -1150 mV, in the Pb^{2+} to metallic lead reduction range. The first cycle has a different behaviour from that of the next cycles and it could be called a cycle "of intensified anodic capacity". During the next cycles (from the second cycle up to the eighth) one can see that at the anodic scan a net peak (A_1) of $PbSO_4$ formation, as well as another peak (A_2) of PbO and basic lead sulphate formation appear. Anodic currents and capacity are more reduced than during the first cycle. The formation of $Pb \rightarrow Pb^{2+}$ oxidation compounds takes place on the surface of the metallic basic lead and it is not hindered. At the next anodic potential scan (the second cycle) the amount of activated spongeous lead obtained during the first cycle is very small and the anodic oxidation of Pb^{2+} takes place at the expense of metallic basic lead, but the anodic deposit of the oxidation products which has remained from the first cycle is acting as a diffusion layer, which hinders the occurrence of the electrode process; thus, the increase of (A_1) and (A_2) peaks which is taking place during the second cycle may be explained. With recycling the thickness of the diffusion anodic layer is increased and the anodic peaks height decreases. But the repeated recyclings result in the activation of the cathodic processes. Hence the cathodic limiting currents from the $Pb^{4+} \rightarrow Pb^{2+}$ processes zone and the (E) cathodic peak are increasing with the increase of the number of cycles.

The cathodic activation can be explained by means of the appearance of PbO_2, which is semiconductor; its reduction to Pb^{2+} takes place at the biphasic contact interface PbO_2-solution and the weight of hindering by diffusion is smaller and smaller at the repeated recyclings. One can see that in the recycling process the (A_1) and (A_2) peaks decrease and the (E) peak increases; the whole system reaches an equilibrium, that is the whole amount of the oxidation solid product which is obtained at the anodic potential scan is reduced at the cathodic potential scan. Hence in solution II the "microelectrode" is formed only after several recyclings and the 7th and 8th cycles are practically superposed. In the 0.1M $H_2SO_4 + 0.9M\ Na_2SO_4$ (solution III) with pH $= 1.757$ and 0.2M $H_2SO_4 + 0.8M\ Na_2SO_4$ (solution IV) with pH $= 1.487$ solutions (see Figs 3 and 4), the characteristic of the first cycle, of "intensified anodic capacity" is maintained, but with a smaller height of the (A) peak. At the same time, the same succession of anodic and cathodic peaks is maintained, depending on the number of cycles as in solution I. One may notice the disappearance of the (A_2) peak starting with the second cycle. This behaviour may be explained by means of the decrease of the pH, which disfavours the basic lead sulphates formation. These ones are certainly formed in the potential range of 0 mV up to 800 mV, at the appearance of limiting currents but in a smaller amount. At the same time the appearance o some limiting currents (F) can be noted in the $Pb^{2+} \rightarrow Pb^{4+}$ oxidation zone. A (D) peak of final reduction (at the cathodic potential scan) corresponding to the oxidation anodic products to Pb^{2+} and an (E) peak of the Pb^{2+} to Pb reduction appear.

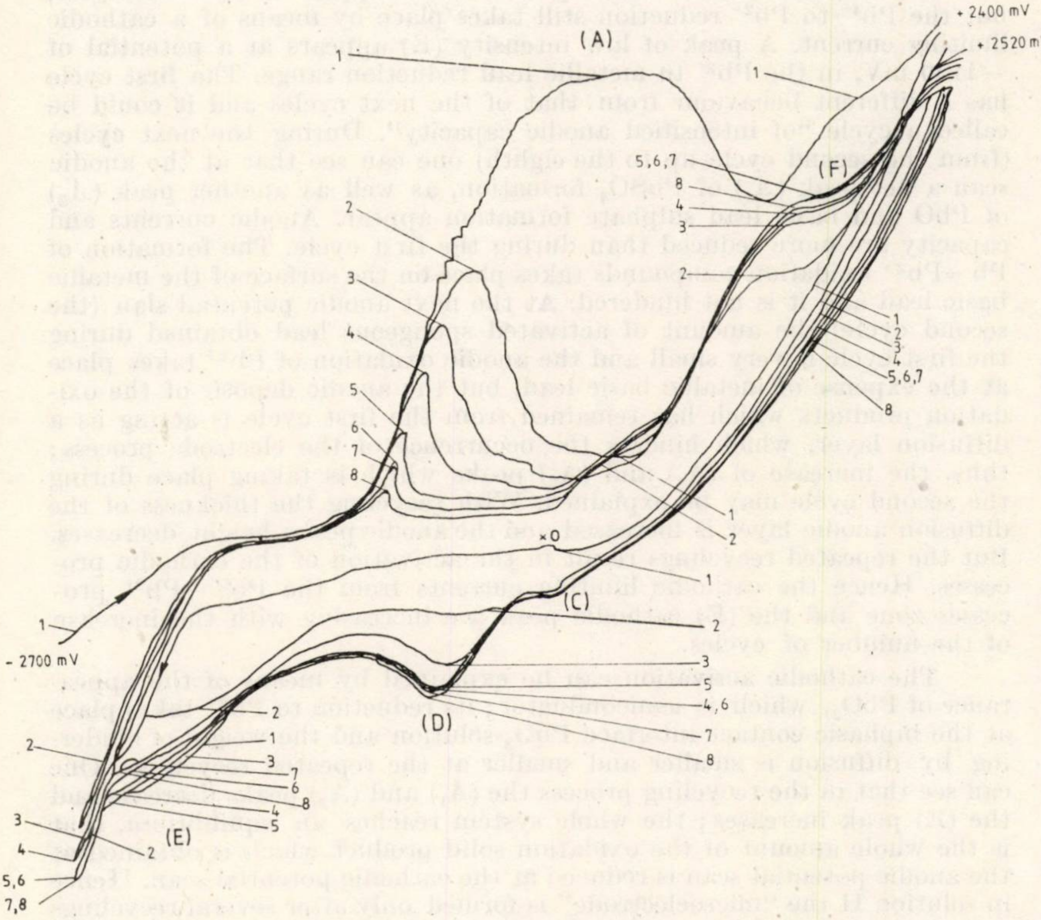

Fig. 3. — Polarization curves of pure lead in 0.1M H_2SO_4+0.9M Na_2SO_4 mixture (solution III), at a potential scan rate of 300 mV/min.

First, in the 0.4 M H_2SO_4 + 0.6M Na_2SO_4 solution (V) with a pH = = 1.293 one can notice the disappearance of the cycle with "intensified anodic intensities" (see Fig. 5).

In solution (V) the first cycle shows an (A) peak in the $PbSO_4$ formation domain, but the limiting current in the zone of basic lead sulphates formation is higher than at the next cycles. In solution (V) the shape of the polarization curves, the succession of the anodic and cathodic peaks, as well as the shape of (D) peaks are similar to those obtained in solution

I. Perhaps here the (A) peak is corresponding to a passivating thin layer and not to a diffusion layer like the one described above, which is correlated to the appearance of a first cycle with high current densities.

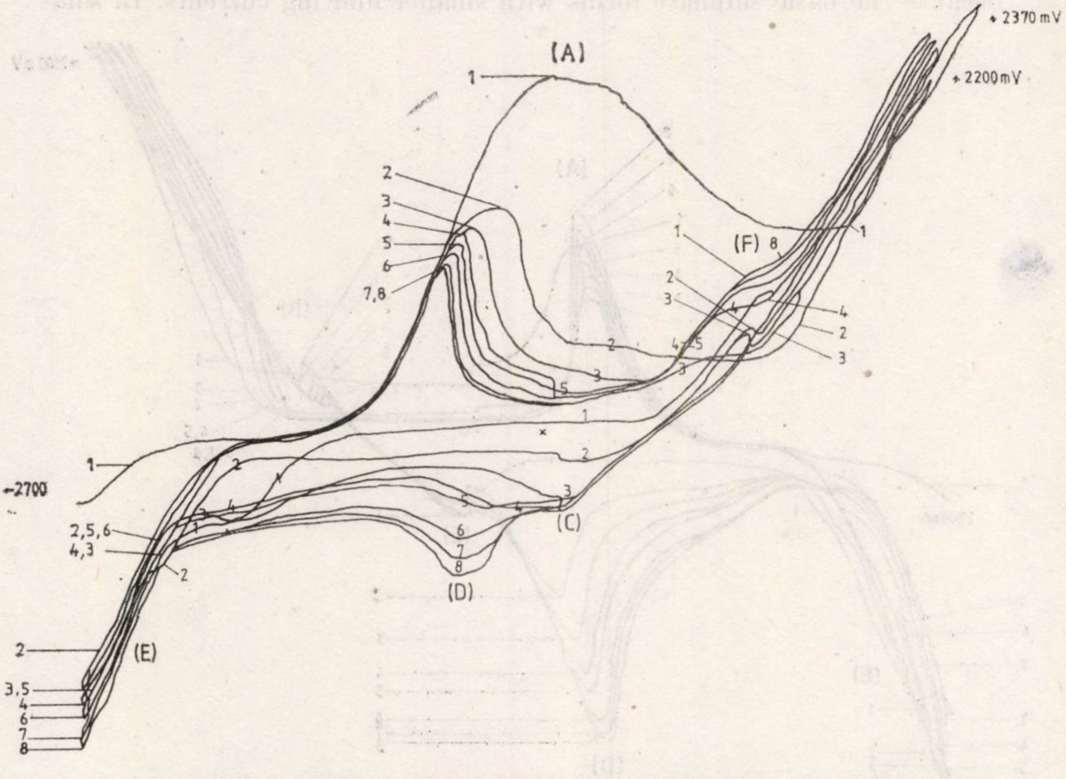

Fig. 4—Polarization curves of pure lead in 0.2M H_2SO_4 + 0.8M Na_2SO_4 (solution IV), at a potential scan rate of 300 mV/min.

CONCLUSIONS

The cyclovoltammograms which have been obtained are very different in H_2SO_4 and Na_2SO_4. In 1M H_2SO_4 an (A) peak is obtained which is corresponding to the process of $PbSO_4$ formation from metallic lead, followed by a very extended quasi-passive range situated between -350 mV and +1150 mV. The height of the (A) peak is increasing progressively from the first cycle up to the 8th. The same happens to the active lead microelectrode capacity, which is obtained at the end of each cycle. A characteristic of solutions II, III, and IV is the existence of a cycle of intensified anodic currents (the first cycle) which results in the formation of an anodic deposit. This anodic deposit is much thicker than in solution I, which acts as a diffusion layer and hinders the electrode processes intensity. In all the voltammograms in which that first characteristic cycle appears the intensity of the (A) anodic peak decreases from the first cycle to the 8th. In the 1M Na_2SO_4 solution (solution II) with pH = 7, two anodic peaks (A_1) and (A_2) appear corresponding to the lead sulphate formation as well as to the basic lead oxides and sulphates formation. In solutions III and IV with a much smaller pH, the (A_2) peak disappears because the basic sulphate forms with smaller limiting currents. In solution V the first cycle has a normal shape and it does not have the characteristic of a zone of intensified anodic currents anymore. Under these conditions the (A) peaks become increasing again in the process of recycling and the shape of the obtained voltammograms becomes very similar to the shape of those from 1M Na_2SO_4 solution (solution I).

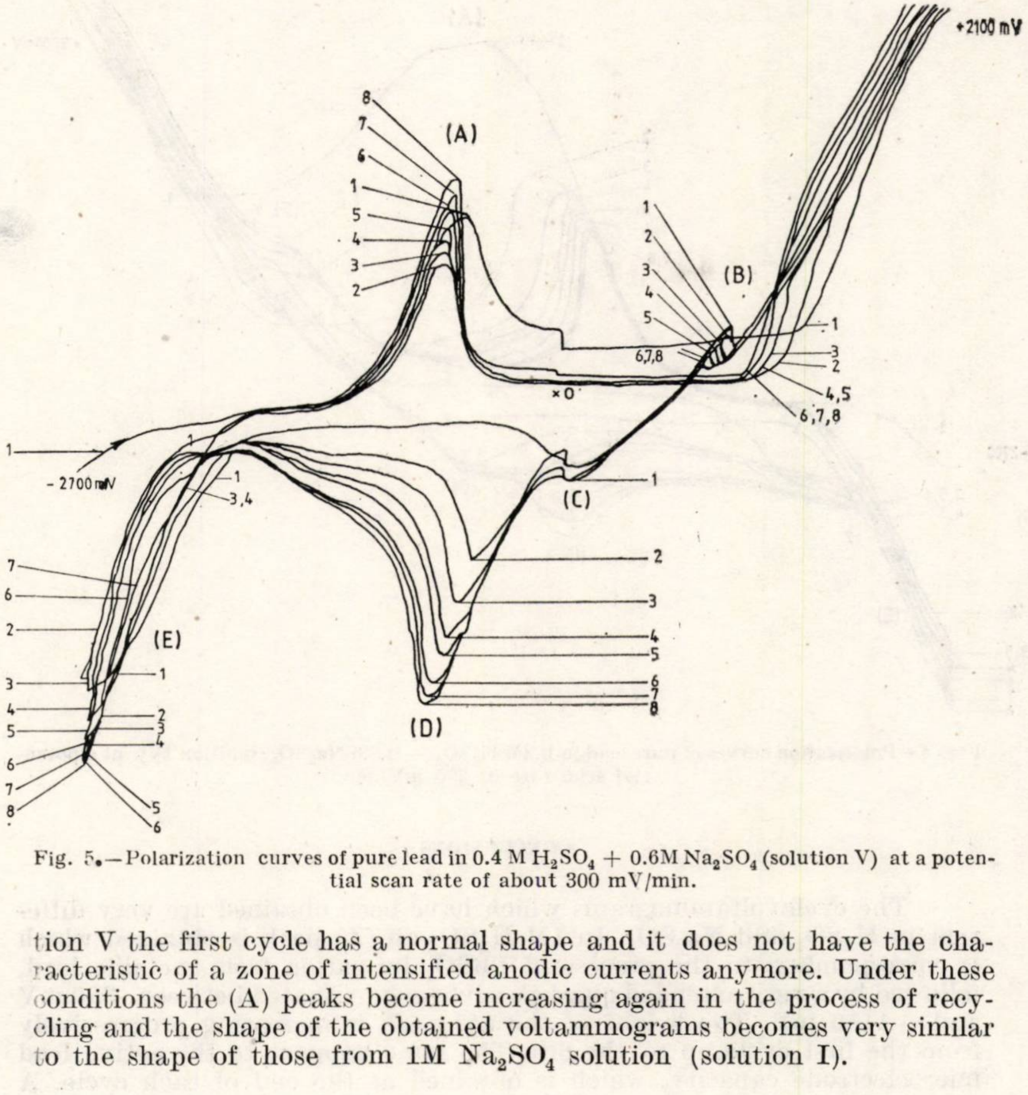

Fig. 5.—Polarization curves of pure lead in 0.4 M H_2SO_4 + 0.6M Na_2SO_4 (solution V) at a potential scan rate of about 300 mV/min.

REFERENCES

[1] J. Perkins and T. M. Coyle, *J. Electrochem. Soc.*, **124**, no4, 524 (1977).
[2] J. L. Sudworth and J. Dugdale, "Power Sources", Ed. Colins, 1968, p. 552.
[3] A. C. Simon and E. Jones, *J. Electrochem. Soc.*, **109**, 760 (1962).
[4] M. J. Gillibrand and J. Wilde, *Electrochim Acta*, **9**, 401 (1964).

[5] P. Delahay and W. C. Tobias, "Advances in Electrochemistry and Electrochemical Engineering" Vol. **8**, New York, 1971.
[6] T. F. Sharpe, *J. Electrochem. Soc.*, **124**, 168 (1977).
[7] P. Ness, *Electrochim Acta*, **12**, 161–178 (1967).
[8] S. A. Awod and Z. A. Elhady, *J. Electroanal. Chem.*, **20**, 79 (1969).
[9] S. Tudor, A. Weisstuch and S. H. Davang, *Electrochem. Technol.*, **3**, 90 (1965).
[10] S. Tudor, A. Weisstuch and S. H. Davang, *Electrochem Technol.*, **4**, 406 (1966).
[11] S. Tudor, A. Weistuch and S. H. Davang, *Electrochem. Technol.*, **5**, 21 (1967).
[12] J. Visscher, *Power Sources*, **1**, 257 (1977).
[13] K. R. Bullock, *J. Electrochem. Soc.*, **11**, 360 (1979).
[14] D. Pavlov and G. Papazov, *J. Electrochem. Soc.*, **127**, 10 (1980).
[15] A. Pierson, *Electrochem. Technol.*, **5**, 323 (1967).
[16] D. Pavlov, G. Papazov and V. Iliev, *J. Electrochem. Soc.*, **119**, 1 (1972).
[17] P. Ruetschi and R. Angstadt, *J. Electrochem. Soc.*, **111**, 1323 (1964).
[18] C. F. Yarnell and M. C. Weeks, *J. Electrochem. Soc.*, **126**, 1 (1979).
[19] C. F. Yarnell, *J. Electrochem. Soc.*, **119**, 1 (1972).
[20] R. H. Greensburg and B. Finan, *J. Electrochem. Soc.*, **98**, 474 (1951).
[21] J. Gerche, N. Anastasjevic and K. Wiesener, *Electrochim. Acta*, **26**, 10 (1981).
[22] K. R. Bullock and D. H. McClelland, *J. Electrochem. Soc.*, **124**, 1478 (1981).
[23] T. F. Sharpe, *J. Electrochem. Soc.*, **122**, 845 (1975).
[24] S. Sternberg, V. Brânzoi, L. Apăteanu and A. Mateescu, *Rev. Roumaine Chim.* **28**, 6 (1983).

Revue Roumaine de Chimie, **30**, *3*, 209—215 (1985)

THE MEAN THERMODYNAMIC ACTIVITY OF $CuSO_4$ IN THE TERNARY SYSTEMS: $CuSO_4 + MgSO_4 + H_2O$ and $CuSO_4 + MnSO_4 + H_2O$

S. STERNBERG and MIHAELA DRĂGĂNOIU
Dept. of Physical Chemistry and Electrochemical Technology, Polytechnical Institute Bucharest, str. Polizu 1, Romania

Received March, 21, 1984

The mean thermodynamic activity coefficient of $CuSO_4$ has been determined in the ternary systems $CuSO_4 + MgSO_4 + H_2O$ and $CuSO_4 + MnSO_4 + H_2O$, respectively, using measurements of electromotive forces. The difference $\Delta \ln \gamma_{1\pm}$ between the values in the ternary systems and in the binary system $CuSO_4 + H_2O$ is calculated and discussed as a function of the conventional ratio y_2. A comparison with the systems discussed in a previous work [1] is made.

The study of the equilibrium properties of the electrolyte solutions is essential for understanding the interactions appearing in such systems. As a result of the ionic interactions, of the ion-solvent interactions, the solutions of a single electrolyte are not ideal, thus the existence of multicomponent electrolyte solutions implies the study of even greater deviations from the ideality – the result of specific interactions among the components of such a solution.

In setting us the task to bring new contributions to the thermodynamic study of these systems of an outstanding practical interest, in the present work we have determined the variation of the mean activity coefficient of a 2 : 2 electrolyte ($CuSO_4$) in the presence of another symmetrical electrolyte with common anion ($MgSO_4$ respectively $MnSO_4$).

The determinations were made in aqueous solutions, at 25°C, using measurements of electromotive forces (the method presents the advantage of varying the concentrations of the two electrolytes, with the condition of maintaining constant the total ionic strength). [2,3]

The determinations were made at six given total ionic strengths for the system $CuSO_4 + MgSO_4 + H_2O$, and respectively four total ionic strengths for the system $CuSO_4 + MnSO_4 + H_2O$ and varying proportions of the two electrolytes.

EXPERIMENTAL PART

The cells used for the determinations were of the type:

$$\text{Pt-Hg}, Hg_2SO_4/CuSO_4\ (m_1),\ MeSO_4\ (m_2)/Cu$$

where: Me = Mg, Mn

The electrodes we used are as follows :

— the mercury-mercurous sulphate electrode, chosen as reversible electrode to sulphate ion, because of the excellent reproducibility of the results (comparable to that of the hydrogen electrode). [4]

Table 1

Determinations for the stability of the electrodes

Molality of $CuSO_4$ mol/1000 g H_2O	$\Delta E \cdot 10^{-3}$ (V)	Period of time (days)
0.375	1.4	4
	0.6	5
0.45	2.4	3
	0.6	10
0.525	0.86	8
	0.2	10
	1.1	5
0.6	0	14
	0.3	11
	2	11
0.675	2.1	6
	0.3	5
0.75	2.1	7
	2.2	7
	2.3	5
	0.9	7

— the copper electrode- a plate made of copper, scaled, washed and dried before each determination.

Repeated tests were made in the binary system $CuSO_4+H_2O$ at different periods of time (days) for the stability of the electrodes (Table 1). The differences in the emf values, less than 2.5 mV, have been considered as a satisfactory proof of the stability of the cell, taking into account that in calculation the difference $(E^t—E^b)$ is used.

The equilibrium criterion for each determination was the maintenence of the emf value in an interval of 0.1 mV for half an hour.

As far as the method of calculation is concerned, we consider having obtained an increase in accuracy compared to the classic method (that of calculating $a_{\pm}$, respectively $\gamma_{\pm}$, from Nernst's relation, using E°) by determining directly the difference $\Delta \ln \gamma_{1\pm}$, which is :

$$\Delta \ln \gamma_{1\pm} = \ln \gamma^t_{1\pm} - \ln \gamma^b_{1\pm} \tag{1}$$

where :

— $\gamma^t_{1\pm}$ is the mean activity coefficient of $CuSO_4$ in the studied ternary systems ;

— $\gamma^b_{1\pm}$ — similar, in the binary system $CuSO_4 + H_2O$.

The calculation is made by means of the relations :

$$E^b = E^{\circ} - \frac{\nu RT}{nF} \ln a_{1\pm} = E^{\circ} - \frac{RT}{F} \ln m^b_{1\pm} - \frac{RT}{F} \ln \gamma^b_{1\pm} \tag{2}$$

where, for the systems studied by us :

$$n = 2$$

$$\nu = 2$$

$m^b_{1\pm}$ — the mean molality of $CuSO_4$ in the binary system ; $m^t_{1\pm}$ — similar, in the ternary system.

The superior index b indicates the binary system and t the ternary one.

Likewise, for the ternary system we can write :

$$E^t = E^{\circ} - \frac{\nu RT}{nF} \ln a_{1\pm} = E^{\circ} - \frac{RT}{F} \ln m^t_{1\pm} - \frac{RT}{F} \ln \gamma^t_{1\pm} \tag{3}$$

Substracting relation (2) from (3), we obtain directly $\Delta \ln \gamma_{1\pm}$.

$$\Delta \ln \gamma_{1\pm} = \frac{E^b - E^t}{\dfrac{RT}{F}} - \ln \frac{m^t_{1\pm}}{m_{1\pm}} \tag{4}$$

In this way we avoid the use in the calculation of E° (or $\bar{E}^\circ$) obtained from personal experimental determinations combined with the use of the data in the literature.

The main advantage is the direct obtention of $\Delta \ln \gamma_{1\pm}$ an extent proved to be the most significant for the study of the ternary system as compared to the binary one.

RESULTS AND DISCUSSION

The results are presented in tables 2 and 3. In figure 1 we present the dependences $\ln \gamma^t_{1\pm} = f(m_{1\pm})$ for the two studied systems in comparison with that corresponding to the binary system $CuSO_4 + H_2O$.

Table 2

The determination of $\gamma_{1\pm}$ values in the ternary system $CuSO_4 + MgSO_4 + H_2O$

Ionic strength	Concentrations mol/1000 g H_2O	$\Delta E \cdot 10^2$ (V)	$a_{1\pm} \cdot 10^2$	$\gamma_{1\pm} \cdot 10^2$
$I = 3$	$m_1 = 0.75$ $m_2 = 0$	0	3.67	4.90
	$m_1 = 0.65$ $m_2 = 0.1$	0.11	3.39	4.86
	$m_1 = 0.55$ $m_2 = 0.2$	0.44	3.08	4.81
	$m_1 = 0.45$ $m_2 = 0.3$	0.63	2.86	4.94
	$m_1 = 0.35$ $m_2 = 0.4$	0.90	2.58	5.04
	$m_1 = 0.25$ $m_2 = 0.5$	1.31	2.19	5.08
	$m_1 = 0.15$ $m_2 = 0.6$	1.93	1.72	5.15
	$m_1 = 0.05$ $m_2 = 0.7$	3.23	1.03	5.37
$I = 2.7$	$m_1 = 0.675$ $m_2 = 0$	0	3.53	5.23
	$m_1 = 0.575$ $m_2 = 0.1$	0.38	3.04	4.88
	$m_1 = 0.475$ $m_2 = 0.2$	0.61	2.78	4.91
	$m_1 = 0.375$ $m_2 = 0.3$	0.86	2.52	5.01
	$m_1 = 0.275$ $m_2 = 0.4$	1.07	2.32	5.39
	$m_1 = 0.175$ $m_2 = 0.5$	1.66	1.84	5.37
	$m_1 = 0.075$ $m_2 = 0.6$	2.63	1.26	5.61
$I = 2.4$	$m_1 = 0.6$ $m_2 = 0$	0	3.32	5.54
	$m_1 = 0.5$ $m_2 = 0.1$	0.19	3.00	5.48
	$m_1 = 0.4$ $m_2 = 0.2$	0.34	2.77	5.66
	$m_1 = 0.3$ $m_1 = 0.3$	0.84	2.39	5.64
	$m_1 = 0.2$ $m_2 = 0.4$	1.16	2.01	5.81
	$m_1 = 0.1$ $m_2 = 0.5$	2.11	1.45	5.95
$I=2.1$	$m_1 = 0.525$ $m_2 = 0$	0	3.13	5.98
	$m_1 = 0.425$ $m_2 = 0.1$	0.30	2.79	5.91
	$m_1 = 0.325$ $m_2 = 0.2$	0.69	2.39	5.80
	$m_1 = 0.225$ $m_2 = 0.3$	1.06	2.07	6.03
	$m_1 = 0.125$ $m_2 = 0.4$	1.74	1.60	6.21
	$m_1 = 0.025$ $m_2 = 0.5$	3.72	0.74	6.48

Table (continued)

Ionic strength	Concentrations mol/1000 g H_2O	$\Delta E\cdot 10^2$ (V)	$a_{1\pm}\cdot 10^2$	$\gamma_{1\pm}\cdot 10^2$
$I=1.8$	$m_1 = 0.45$ $m_2 = 0$	0	2.95	6.56
	$m_1 = 0.35$ $m_2 = 0.1$	0.44	2.50	6.30
	$m_1 = 0.25$ $m_2 = 0.2$	0.79	2.18	6.50
	$m_1 = 0.15$ $m_2 = 0.3$	1.37	1.72	6.65
	$m_1 = 0.05$ $m_2 = 0.4$	2.69	1.03	6.88
$I=1.5$	$m_1 = 0.375$ $m_2 = 0$	0	2.73	7.30
	$m_1 = 0.275$ $m_2 = 0.1$	0.46	2.28	7.12
	$m_1 = 0.175$ $m_2 = 0.2$	1.05	1.81	7.09
	$m_1 = 0.075$ $m_2 = 0.3$	2.13	1.19	7.10

Table 3

The determination of $\gamma_{1\pm}$ values in the ternary system $CuSO_4 + MnSO_4 + H_2O$

Ionic strength	Concentrations mol/1000 g H_2O	$\Delta E\cdot 10^2$ (V)	$a_{1\pm}\cdot 10^2$	$\gamma_{1\pm}\cdot 10^2$
$I=3$	$m_1 = 0.75$ $m_2 = 0$	0	3.67	4.90
	$m_1 = 0.65$ $m_2 = 0.1$	0.11	3.35	4.81
	$m_1 = 0.55$ $m_2 = 0.2$	0.38	3.16	4.93
	$m_1 = 0.45$ $m_2 = 0.3$	0.47	2.91	5.02
	$m_1 = 0.35$ $m_2 = 0.4$	0.96	2.61	5.10
	$m_1 = 0.25$ $m_2 = 0.5$	1.24	2.26	5.22
	$m_1 = 0.15$ $m_2 = 0.6$	2.08	1.76	5.25
	$m_1 = 0.05$ $m_2 = 0.7$	3.57	1.04	5.41
$I=2.4$	$m_1 = 0.6$ $m_2 = 0$	0	3.32	5.54
	$m_1 = 0.5$ $m_2 = 0.1$	0.37	2.87	5.25
	$m_1 = 0.4$ $m_2 = 0.2$	0.58	2.64	5.40
	$m_1 = 0.3$ $m_2 = 0.3$	0.86	2.37	5.59
	$m_1 = 0.2$ $m_2 = 0.4$	1.30	1.99	5.77
	$m_1 = 0.1$ $m_2 = 0.5$	2.19	1.41	5.76
$I=1.8$	$m_1 = 0.45$ $m_2 = 0$	0	2.95	6.56
	$m_1 = 0.35$ $m_2 = 0.1$	0.39	2.54	6.42
	$m_1 = 0.25$ $m_2 = 0.2$	0.76	2.20	6.57
	$m_1 = 0.15$ $m_2 = 0.3$	1.38	1.71	6.66
	$m_1 = 0.05$ $m_2 = 0.4$	2.72	1.03	6.84
$I=1.5$	$m_1 = 0.375$ $m_2 = 0$	0	2.73	7.30
	$m_1 = 0.275$ $m_2 = 0.1$	0.40	2.32	7.23
	$m_1 = 0.175$ $m_2 = 0.2$	0.99	1.85	7.25
	$m_1 = 0.075$ $m_2 = 0.3$	2.03	1.23	7.38

We can remark that for all the ionic strengths studied, the values remain almost constant by the ln $\gamma_{1\pm}^{b}$ value (in the binary system at the same ionic strength), which implies practically an exclusive dependence

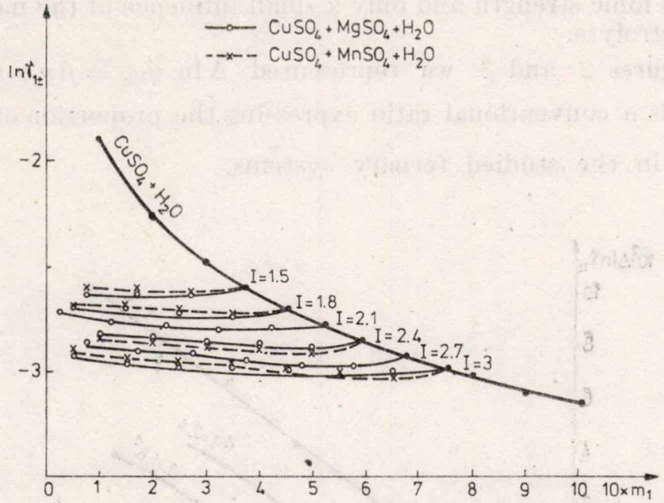

Fig. 1. — The dependence $\ln \gamma_{1\pm} = f(m_1)$ in the ternary systems :

——— ● ——— ● ——— $CuSO_4 + MgSO_4 + H_2O$

.... × .... × .... $CuSO_4 + MnSO_4 + H_2O$

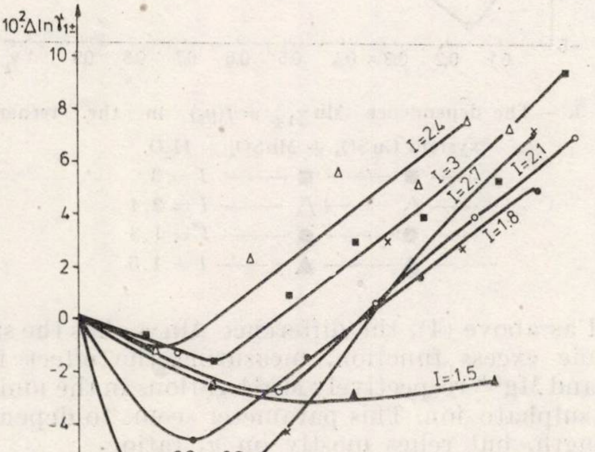

Fig. 2. — The dependence $\Delta\ln \gamma_{1\pm} = f(y_2)$ in the ternary system $CuSO_4 + MgSO_4 + H_2O$.

——— ■ ——— ■ ——— $I = 3$

——— × ——— × ——— $I = 2.7$

——— △ ——— △ ——— $I = 2.4$

——— ○ ——— ○ ——— $I = 2.1$

——— ● ——— ● ——— $I = 1.8$

——— ▲ ——— ▲ ——— $I = 1.5$

on the total ionic strength and only a small influence of the nature of the second electrolyte.

In figures 2 and 3 we represented $\Delta \ln \gamma_{1\pm} = f(y_2)$ where $y_2 = \frac{m_2}{m_1 + m_2}$ is a conventional ratio expressing the proportion of the second electrolyte in the studied ternary systems.

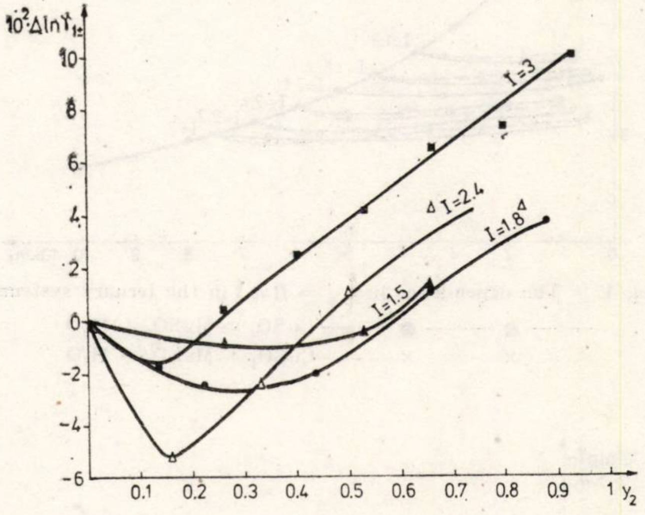

Fig. 3. — The dependence $\Delta \ln \gamma_{1\pm} = f(y_2)$ in the ternary system $CuSO_4 + MnSO_4 + H_2O$.

——■——■—— $I = 3$
——△——△—— $I = 2.4$
——●——●—— $I = 1.8$
——▲——▲—— $I = 1.5$

Expressed as above (4), the difference $\Delta \ln \gamma_{1\pm}$ has the significance of a thermodynamic excess function, measuring the effect following the mixing of Cu^{2+} and Mg^{2+} respectively Mn^{2+} cations in the ionic atmosphere of the common sulphate ion. This parameter seems to depend less on the total ionic strength, but relies mostly on y_2 ratio.

For this symmetrical type of systems $Cu^{2+} - Mg^{2+}$ and $Cu^{2+} - Mn^{2+}$ the interactions in the ionic atmosphere of SO_4^{2-} seem to be barely modified, the difference $\Delta \ln \gamma_{1\pm}$ being small.

Figure 4 presents a comparison to systems discussed previously,[1] $ZnSO_4 + MgSO_4 + H_2O$ and $ZnSO_4 + MnSO_4 + H_2O$ respectively. Although the systems are also symmetrical, and with the same valence types, for a similar aspect of the dependences $\Delta \ln \gamma_{1\pm} = f(y_2)$ we can notice that in the second case the deviation is much greater (the difference increases with the increase of y_2, reaching a difference of one order of magnitude at large values of the concentration of the second electrolyte).

The difference in behaviour is due — in our opinion — to the greater tendency of complexing zinc as compared to copper.

For the systems with zinc the difference ($\ln \gamma^t_{1\pm} - \ln \gamma^b_{1\pm}$) being small could be a proof that the second cation does not disturb significantly the zinc-sulphate interactions.

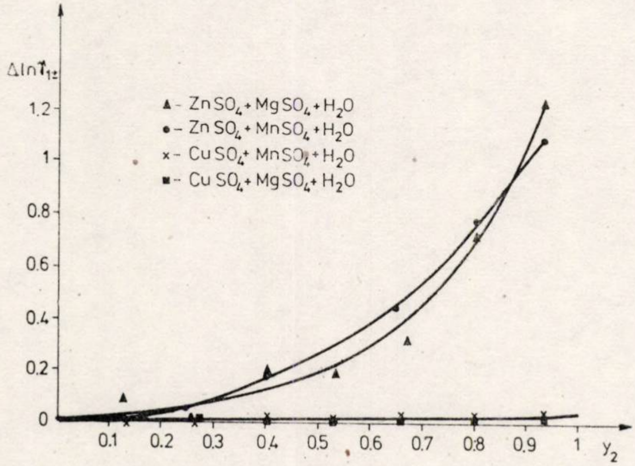

Fig. 4. — The dependence $\Delta \ln \gamma_{1\pm} = f(y_2)$ in the ternary systems :

—— ▲ —— ▲ —— $ZnSO_4 + MgSO_4 + H_2O$
—— ● —— ● —— $ZnSO_4 + MnSO_4 + H_2O$
—— ■ —— ■ —— $CuSO_4 + MgSO_4 + H_2O$
—— × —— × —— $CuSO_4 + MnSO_4 + H_2O$
$I = 3$

Both in the systems studied in the present work ($CuSO_4 + MgSO_4 + H_2O$ respectively $CuSO_4 + MnSO_4 + H_2O$) and in those containing zinc sulphate with the same added electrolytes, we cannot notice a significant difference between Mg^{2+} and Mn^{2+} ions.

REFERENCES

[1] S. Sternberg and M. Drăgănoiu, *Rev. Roumaine Chim.* **29**, 105 (1984).

[2] H. Harned and B. Owen, "The Physical Chemistry of Electrolytic Solutions", third ed., Reinhold Publishing, New York, 1958, p. 592.

[3] H. Harned and R. Robinson, "Multicomponent Electrolyte Solutions", Pergamon Press, London, 1969, p. 13.

[4] D. J. D. Ives and G. J. Janz, "Reference Electrodes", Academic Press, New York, 1961, p. 403.

Revue Roumaine de Chimie, **30**, *3*, 217–221 (1985)

FACTORISATION OF ORBITAL ENERGIES IN TRANSITION – METAL COMPLEXES. I

FACTORISATION OF THE OVERLAP INTEGRALS

C.I. LEPĂDATU and MARIUS ANDRUH
Center of Chemical Physics- ICECHIM, Spl. Independenţei 202, Bucharest, Romania

Received September 2, 1983

The factorisation of the orbital energies (radial part) into metal and ligand contributions is proved. The demonstration is mainly based on the factorisation of the overlap integral :

$$S_{ML} = \langle \Psi_M | \Psi_L \rangle = s_M \cdot s_L$$

where s_M and s_L are the metal and ligand contributions respectively.

1. INTRODUCTION

The factorisation of the orbital energies involved in the d–d transitions occurring in the electronic spectra of the transition-metal complexes has been empirically established.[1] It may be expressed as a product of two quantities :

$$\Delta \simeq f_M \cdot g_L \qquad (1)$$

where Δ is the splitting parameter and f_M, g_L the metal and ligand contributions. This experimental observation has firstly been considered as an obvious success of the crystal field approach.

The subsequent development of the theory has shown that the background of the crystal field model is quite insatisfactory for the majority of transition-metal complexes. The mentioned approach has survived under its parametrical form, usually named ligand field theory (LFT). Furthermore, it has been demonstrated that LFT derives actually from the general LCAO MO theory as applied to coordination compounds, the LFT-parameters being expressed in terms of MO quantities. This fact is not surprising if one takes into account that MO-theory is the only one deriving from basic quantum principles, being able to explain satisfactorily the chemical bond. Despite the apparent difficulty to express the MO energies as a product of metal and ligand contributions (see eq. 1), the present paper tries to show that the factorisation (1) can be in principle considered as deriving from a simple MO perturbation approach of second order.

As may be seen, equation (1) shows that the splitting parameter

$$\Delta = E_{\sigma^*} - E_{\pi^*}, \tag{2}$$

where $E_{\sigma^*(\pi^*)}$ are the $\sigma(\pi)$ antibonding energies, could be factorized if:

$$\begin{aligned} E_{\sigma^*} &= f_M \cdot \sigma_L \\ E_{\pi^*} &= f_M \cdot \pi_L \end{aligned} \tag{3}$$

and hence expression (1), where $g_L = \sigma_L - \pi_L$ represents the ligand contribution. If relationships (3) are true, the following rules are valid[2]:

$$\text{The ratios:} \quad \frac{\Delta(ML_6)}{\Delta(ML'_6)} \quad \text{(i)} \quad \text{and} \quad \frac{\Delta(ML_6)}{\Delta(M'L_6)} \quad \text{(ii)}$$

do not depend on the nature of metal and ligand respectively. These rules have been successfully used to construct the so-called tridimensional spectrochemical series, the third dimension being the metal ion contribution.

To demonstrate expressions (3), the antibonding orbital energies are expressed as MO-perturbation contributions of second order:

$$E_a = \alpha_M^0 + \sum_i \Delta^*_{ML_i} \tag{4}$$

$$\Delta^*_{ML_i} = \Xi^2_{ML_i} S^2_{ML_i} \frac{\alpha^2_{L_i}}{\alpha_M - \alpha_{L_i}} = \Xi^2_{ML_i} \delta^*_{ML_i} \tag{5}$$

where δ^* is the radial parameter, S_{ML_i} being the diatomic overlap integral Ξ the adapted symmetry angular coefficient, $\alpha_{M(L_i)}$ the energies of metal and ligand respectively.

2. FACTORIZATION OF THE OVERLAP INTEGRAL

Preliminary observations[3] have shown that the overlap integra could be factorized as follows:

$$\langle \Psi_M | \Psi_L \rangle \doteq s_M \cdot s_L. \tag{6}$$

where s_M and s_L are the metal and ligand contributions respectively. To prove this expression, Mulliken's master formulas[4] expressed in terms of incomplete gamma integrals A and B, have been used.

The proof contains three stages:

a) factorization of Q_{ML} factor;

b) factorization of $A_n(p)$ integrals;

c) factorization of $B_n(pt)$ integrals.

a) The factorization of Q_{ML} factor is almost direct :

$$Q_{ML} = \frac{1}{2}\,[p(1+t)]^{n_M+\frac{1}{2}}\,[p(1-t)]^{n_L+\frac{1}{2}}\,[(2n_M)!\,(2n_L)!]^{-1/2} =$$

$$= \frac{1}{2}\,[(2n_M)!\,]^{-1/2}\,(\zeta_M R)^{n_M+\frac{1}{2}}\,[(2n_L)!\,]^{-1/2}(\zeta_L R)^{n_L+1/2} \tag{7}$$

b) To factorize the $A_n(p)$ integral, the average theorem well known in mathematical analysis was used. The mentioned theorem asserts that if f and p are two bounded and integrable functions onto a $[a, b]$ interval and if 1) $p(x) \geqslant 0,\ x \in [a, b]$;

2) $f(x)$ is continuous on $[a, b]$, there is a point $\xi \in (a, b)$ such that

$$\int_a^b f(x)\cdot p(x) = f(\xi)\int_a^b p(x)\,dx.$$

If one takes into account that $A_n(1, p)$ integrals are rapidly convergent, one may consider that they are defined on a bounded interval [5]:

$$A_n(1, p) = \int_1^\infty \alpha^n e^{-\alpha p}\,d\alpha = \frac{n!\,e^{-p}}{p^{n+1}}\sum_{k=0}^{n}\frac{p^k}{k!}$$

$$p = \frac{\zeta_M R}{2} + \frac{\zeta_L R}{2}$$

$$A_n(1, p) = \int_1^\infty \alpha^n e^{-\alpha\frac{\zeta_L R}{2}}\,e^{-\alpha\frac{\zeta_M R}{2}}\,d\alpha =$$

$$\simeq e^{-\frac{\zeta_M R}{2}\xi}\int_1^\infty \alpha^n e^{-\frac{\zeta_L R}{2}\alpha}\,d\alpha \tag{8}$$

where the function $\alpha^n e^{-\frac{\zeta_L R}{2}\alpha}$ is positively defined onto the whole integrating domain, in accord with the average theorem.

c) Factorization of $B_n(pt)$ integrals can be done as follows :

$$B_n(pt) = \int_{-1}^{1}\beta^n e^{-\beta pt}\,d\beta \int_{-1}^{1}\beta^n e^{+\beta\frac{\zeta_L R}{2}}\,e^{-\beta\frac{\zeta_M R}{2}}\,d\beta$$

$$pt = \frac{\zeta_M R}{2} - \frac{\zeta_L R}{2}$$

According to the average theorem (∃) $\xi'(n) \in (-1, 1)$ such that

$$B_n(pt) = \xi'^n(n)\, e^{+\xi'(n)\frac{\zeta_L R}{2}} \int_{-1}^{1} e^{-\beta\frac{\zeta_M R}{2}}\, d\beta =$$

$$= \frac{4}{\zeta_M R}\, \xi'^n(n)\, e^{+\xi'(n)\frac{\zeta_L R}{2}} \cdot \mathrm{sh}\,\frac{\zeta_M R}{2} \tag{9}$$

Expressions (7−9) allow to factorize in principle the overlap integral into metal and ligand contributions. As may be seen below, Mulliken's master formulas for the overlap integral can be expressed as sums of products of A and B integrals, as follows:

$$S_{ML} = Q_{ML} \sum_{i,j} I_{p,t}(i, j) \tag{10}$$

where Q_{ML} is given by (7) and $I_{p,t}(i, j)$ by

$$I_{p,t}(i, j) = \int_{1}^{\infty}\int_{-1}^{1} (\alpha + \beta)^i (\alpha - \beta)^j \exp[-p(\alpha + \beta t)]\, d\alpha\, d\beta =$$

$$= \sum_{l=0}^{i+j} \sum_{k=0}^{l} (-1)^{l-k} \binom{i}{k} \binom{j}{l-k} \int_{1}^{\infty} \alpha^{i+j-l} \exp(-p\alpha)\, d\alpha \int_{-1}^{1} \beta^l \exp(-pt\beta)\, d\beta =$$

$$= \exp\left(-\frac{\zeta_M R}{2}\xi\right) \frac{4}{\zeta_M R}\, \mathrm{sh}\,\frac{\zeta_M R}{2} \sum_{l=0}^{i+j} \sum_{k=0}^{l} (-1)^{l-k} \binom{i}{k} \binom{j}{l-k} \times$$

$$\times \left[\xi'^l(e) \exp\left(+\xi'(l)\frac{\zeta_L R}{2}\right) \int_{1}^{\infty} \alpha^{i+j-l} \exp\left(-\frac{\zeta_L R}{2}\alpha\right) d\alpha\right] \tag{11}$$

Observe that the points ξ' depend on the rank of $B_l(pt)$ integrals.

The factorization of $I_{p,t}(i, j)$ integrals and of Q_{ML} factor allows therefore, to factorize any type of overlap integral. One may easily observe that s_M in (6) in given, according to (7, 9−11), by

$$s_M = \frac{1}{\sqrt{2}} [(2n_M)!]^{-1/2} (\zeta_M R)^{n_M + \frac{1}{2}} \exp\left(-\frac{\zeta_M R}{2}\xi\right) \frac{4}{\zeta_M R}\, \mathrm{sh}\,\frac{\zeta_M R}{2} \tag{12}$$

3. FACTORIZATION OF THE ORBITAL ENERGIES

The radial parameter δ^* in (5) becomes :

$$\delta^* = \frac{s_M^2}{\alpha_M - \alpha_L} \cdot s_L^2 \alpha_L^2 \tag{13}$$

where $\alpha_{M(L)}$ are the diagonal matrix elements of metal and ligand respectively.

For metal complexes of the same coordination geometry (the same angular coefficients Ξ) the orbital energies ratios become :

(iii)
$$\frac{\Delta^*(ML)}{\Delta^*(ML')} = \frac{\delta^*_{ML}}{\delta^*_{ML'}} = \frac{s_L^2 \alpha_L^2 \left(1 - \frac{\alpha_{L'}}{\alpha_M}\right)}{s_{L'}^2 \alpha_{L'}^2 \left(1 - \frac{\alpha_L}{\alpha_M}\right)}$$

where $\frac{\alpha_L}{\alpha_M}$ and $\frac{\alpha_{L'}}{\alpha_M}$ are the relative energies of the ligands L, L′

(iv)
$$\frac{\Delta^*(ML)}{\Delta^*(M'L)} = \frac{\delta^*_{ML}}{\delta^*_{M'L}} = \frac{s_M^2 \left(\frac{\alpha_M}{\alpha_L} - 1\right)}{s_{M'}^2 \left(\frac{\alpha_{M'}}{\alpha_L} - 1\right)}$$

where α_M/α_L and $\alpha_{M'}/\alpha_L$ are the relative energies of the metals M, M′.

The ratios (iii) and (iv) may justify the spectrochemical series. As may be seen the ratio (iii) allows to construct a ligand spectrochemical series for a given metal ion. If $\alpha_L \ll \alpha_M$, valid for rare earth complexes, expression (13) becomes

$$\delta^*_{ML} \approx \frac{s_M^2}{\alpha_M} s_L^2 \alpha_L^2 = \chi_M \cdot \sigma_L$$

which is similar to that earlier proposed elsewhere. [2]

REFERENCES

[1] C. K. Jørgensen, "Absorption Spectra and Chemical Bonding in Complexes", Pergamon Press, London, 1962, p. 113.

[2] C. I. Lepădatu, *Z. phys. Chem. (Frankfurt)*, **57**, 27 (1968).

[3] C. I. Lepădatu and M. Andruh, unpublished data.

[4] R. S. Mulliken, C. A. Rieke, D. Orloff, and H. Orloff, *J. Chem. Phys.*, **17**, 1248 (1949).

[5] Y. A. Kruglyak and D. P. Whitman, "Tablitsy integralov kvantovoi khimii", vol. I, Akad. S.S.S.R., Moskow, 1965, p. XII.

Revue Roumaine de Chimie, **30**, *3*, 223—227 (1984)

FRIEDEL—CRAFTS ACYLATION OF ALKYNES. V[1]

REACTION OF ALKYNES WITH AROYL CHLORIDES IN THE PRESENCE OF SILVER PERCHLORATE

DUMITRU MĂNOIU [a], MARIA MĂNOIU [a], ILIE G. DINULESCU [b] and MARGARET AVRAM [b]

[a] Institute for Research of Technological Engineering and Design for Rafineries (ICITPR), Bd. Republicii 291, 2000 Ploieşti, Romania

[b] Laboratory of Organic Chemistry, Polytechnic Institute — TCH, Spl. Independenţei 313, 72206 Bucharest 16, Romania

Received March 17, 1984

The behaviour towards aroyl chlorides and $AgClO_4$ of some alkynes with different stabilisation possibilities of the intermediate vinylic cation was investigated.

Our studies concerning the reaction of alkynes with acyl chlorides in the presence of $AgClO_4$ [1,2] were extended on the investigation of the behaviour of aroylvinyl cations generated from alkynes and aroyl chlorides in the presence of $AgClO_4$.

In this paper we present the reactions of benzoyl chloride and *p*-methoxy-benzoyl chloride with propyne, 1-butyne, *t*-butyl-acetylene and methyl-*t*-butyl-acetylene.

The reactions of alkynes with aroyl chlorides and $AgClO_4$ were performed according to the standard procedure used in the previously reported paper.[2]

The reaction of propyne with benzoyl chloride and $AgClO_4$, in dichloromethane, at −20°, yielded as exclusive reaction product *E*-β-chloro-α, β-unsaturated ketone **1**.

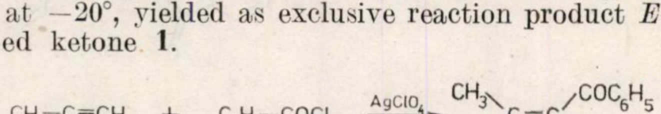

1

1-Butyne, in the same experimental conditions, led to a mixture of *E*-β-chloro-α,β-unsaturated ketone **2** and the allenic compound **3**.

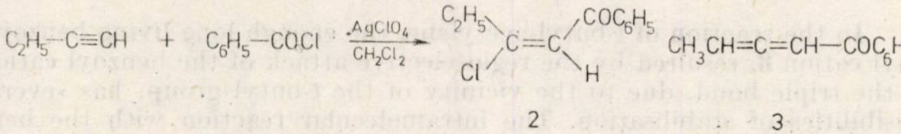

2 3

It is notable that the reaction of benzoyl chloride with the investigated alkynes, unlike reactions with acetyl chloride, does not lead to higher dienic compounds.

The formation of β-chloro-α, β-unsaturated ketones (**1** and **2**) as well as the formation of the allenic ketones, observed when alkynes with higher alkyl groups are used as starting materials, occurs according to the previously established reaction mechanism,[1,2] involving the benzoylvinyl cation **4**. This reactive intermediate gives rise – by chloride abstraction from the solvent – to **1** and **2**, respectively, whereas by proton elimination, it leads to the allenic ketone **3**.

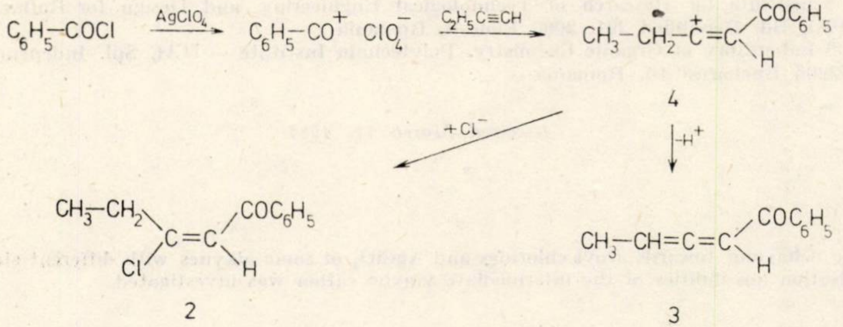
C_6H_5–COCl
$AgClO_4$
C_6H_5–CO^+ ClO_4^-
$C_2H_5C{\equiv}CH$
CH_3–CH_2–$\overset{+}{C}$=C(COC$_6H_5$)(H)
4
+Cl⁻
–H⁺
CH_3–CH_2(Cl)C=C(COC$_6H_5$)(H)
2
CH_3–CH=C=C(COC$_6H_5$)(H)
3

The reaction of *t*-butyl-acetylene with benzoyl chloride and $AgClO_4$ in dichloromethane – dichloroethane, at −50°, afforded a more complex reaction mixture. By means of preparative GLC coupled with THLC, the major component (63%) was isolated and it was identified as being the 3-*t*-butyl-indenone (**5**). Some of the minor components could also be isolated and identified: 3,4,4-trimethyl-1-keto-1,4-dihydro-naphthalene (**6**, 3.7%) and the β-chloro-α, β-unsaturated ketone **7** (<1%).

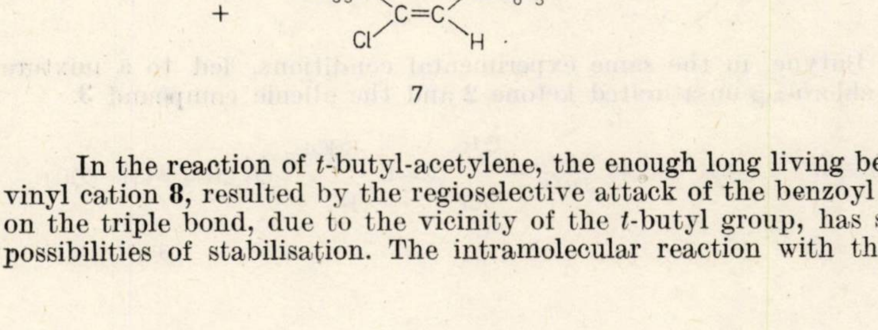
$(CH_3)_3C$–C≡CH + C_6H_5–COCl
$AgClO_4$
+
H_3C
CH_3
CH_3
O
O
5
6
+
$(CH_3)_3C$(Cl)C=C(COC$_6H_5$)(H)
7

In the reaction of *t*-butyl-acetylene, the enough long living benzoylvinyl cation **8**, resulted by the regioselective attack of the benzoyl cation on the triple bond, due to the vicinity of the *t*-butyl group, has several possibilities of stabilisation. The intramolecular reaction with the benzenic ring gives the indenone **5**. The neopentylic rearrangement leads to the cation **9** which by intramolecular cyclisation yields the dihydronaphthalenic compound **6**. Chloride abstraction from the halogenated solvents affords the chloroketone **7**.

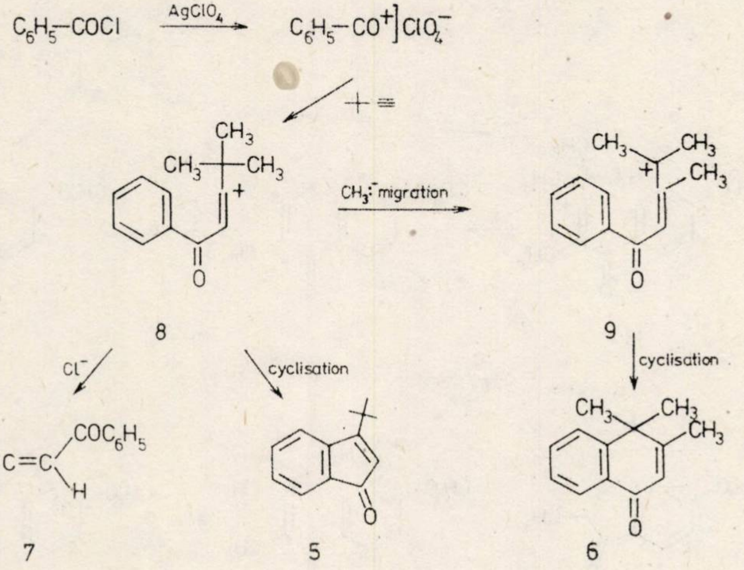
C_6H_5–COCl
AgClO$_4$
C_6H_5–CO$^+$] ClO$_4^-$
CH$_3^-$ migration
8
9
Cl$^-$
cyclisation
cyclisation
(CH$_3$)$_3$C
COC$_6$H$_5$
Cl
H
7
5
6

The results show that the intramolecular reactions are favoured over the intermolecular stabilisation by chloride abstraction.

In order to bring supplementary information about the regioselectivity of the attack of aroyl ion on the triple bond, the investigation of the behaviour of methyl-*t*-butyl-acetylene was further taken into account.

In the reaction of methyl-*t*-butyl-acetylene with *p*-methoxybenzoyl chloride and $AgClO_4$, in dichloromethane, the methoxy-indenone **10** (84.3%) and the 1,4-dihydro-naphthalenic ketone **11** (15.2%) together with traces of β-chloro-α, β-unsaturated ketone **12** were obtained.

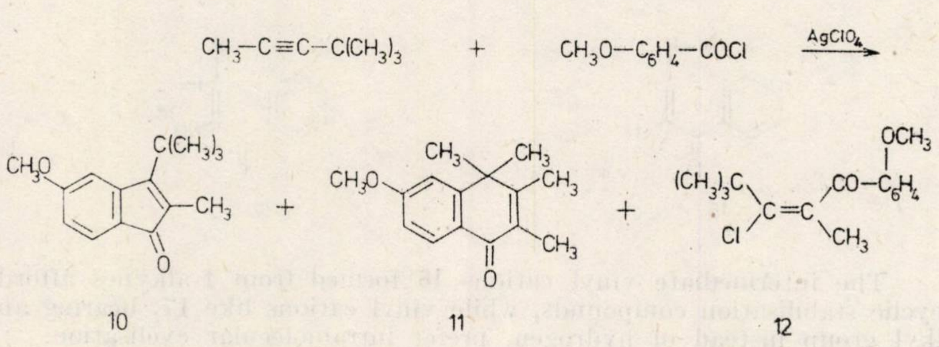
CH$_3$–C≡C–C(CH$_3$)$_3$ + CH$_3$O–C$_6$H$_4$–COCl
AgClO$_4$
C(CH$_3$)$_3$
CH$_3$O
–CH$_3$
10
CH$_3$O
11
OCH$_3$
(CH$_3$)$_3$C
CO–C$_6$H$_4$
Cl
CH$_3$
12

In this reaction two possibilities of attack of the *p*-methoxy-benzoyl ion to the triple bond of methyl-*t*-butyl-acetylene are available leading to the intermediate *p*-methoxy-benzoylvinyl cations **13** or **14**.

$$CH_3O{-}C_6H_4{-}COCl \; + \; AgClO_4 \longrightarrow CH_3O{-}C_6H_4{-}CO^+\,]\,ClO_4^-$$

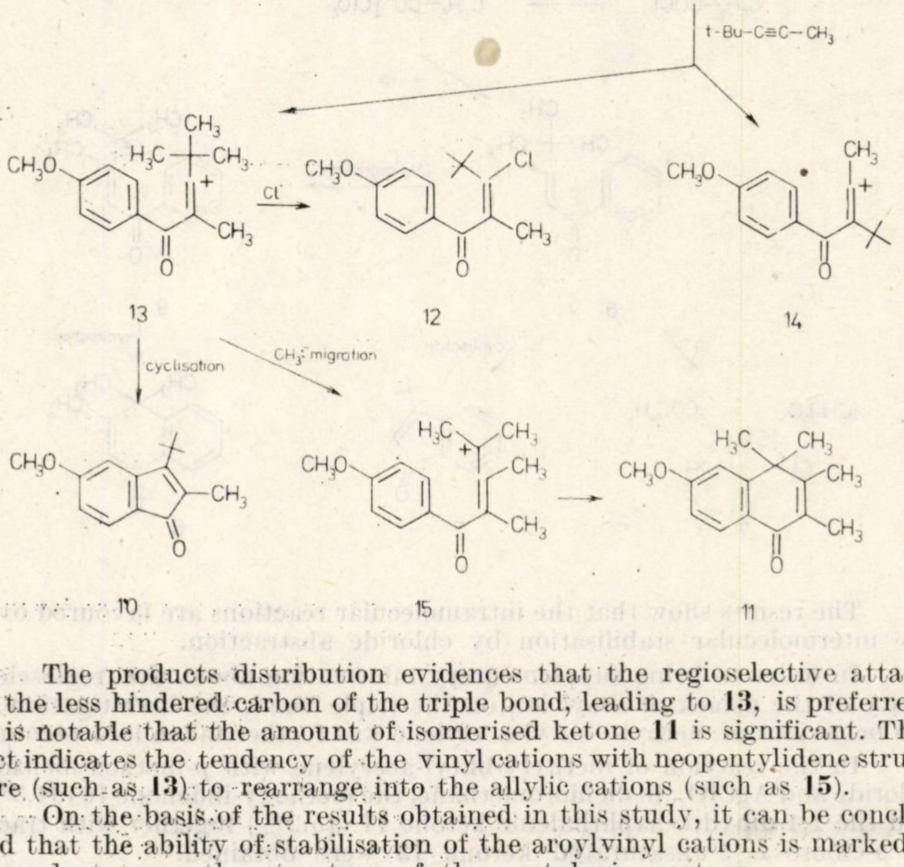
t-Bu—C≡C—CH₃
CH₃O
H₃C
CH₃
CH₃
+
CH₃
O
Cl⁻
CH₃O
Cl
CH₃
O
CH₃O
CH₃
+
O
13
12
14
cyclisation
CH₃⁻ migration
CH₃O
CH₃
O
CH₃O
H₃C
CH₃
+
CH₃
CH₃
O
CH₃O
H₃C
CH₃
CH₃
CH₃
O
10
15
11

The products distribution evidences that the regioselective attack to the less hindered carbon of the triple bond, leading to **13**, is preferred. It is notable that the amount of isomerised ketone **11** is significant. This fact indicates the tendency of the vinyl cations with neopentylidene structure (such as **13**) to rearrange into the allylic cations (such as **15**).

On the basis of the results obtained in this study, it can be concluded that the ability of stabilisation of the aroylvinyl cations is markedly dependent upon the structure of the acetylenic partner.

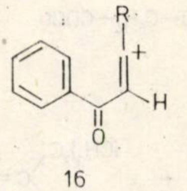

16

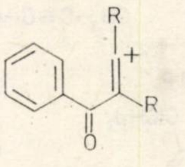

17

The intermediate vinyl cations **16** formed from 1-alkynes afford acyclic stabilisation compounds, while vinyl cations like **17**, bearing an alkyl group instead of hydrogen, prefer intramolecular cyclisation.

EXPERIMENTAL

IR spectra were recorded with a double beam UR-20 spectrophotometer. ^{1}H-NMR were determined with a Tesla 60 and Varian A60-A spectrometer. GLC analysis and GLC preparative separations were carried out as described earlier.[3,4]

Standard procedure. The reactions were carried out according to the previously described standard procedure;[2] a mixture of 1 : 1 dichloromethane —dichloroethane was used as solvent.

Reaction of propyne with benzoyl chloride and $AgClO_4$. The reaction, performed according to the standard procedure, at —20°, yielded *E*-1-benzoyl-2-chloro-prop-1-ene (**1**) as exclusive reaction product; the spectral data are identical with those previously described.[5] — IR (CCl_4, cm^{-1}) : $\nu_{C=C}$ 1603, $\nu_{C=O}$ 1678. — UV (λ^{EtOH}_{max}, nm, ε) : 265 (16700). — ^{1}H-NMR ($CDCl_3$, δ, ppm) : 7.14 (H—C=), 2.60 (CH_3).

Reaction of 1-butyne with benzoyl chloride and $AgClO_4$. Working as above, a mixture was formed in 52 % yield, containing the compounds **2** and **3**, in ratio 2 : 1.

E-1-Benzoyl-2-chloro-but-1-ene (**2**) shows spectral data identical with those previously described.[5] — IR (CCl_4, cm^{-1}) : $\nu_{C=C}$ = 1605, $\nu_{C=O}$ 1672. — UV(λ^{EtOH}_{max}, nm, ε) : 261 (16800).— ^{1}H-NMR ($CDCl_3$, δ, ppm) : 2.99 (C_2H_5), 7.04 (H—C=).

1-Benzoyl-buta-1,2-diene (**3**). — IR (CCl_4, cm^{-1}) : $\nu_{C=C=C}$1960. — ^{1}H-NMR (CCl_4, δ, ppm) : 5.06 (H—C=).

Reaction of t-butyl-acetylene with benzoyl chloride and $AgClO_4$. Working as above, from the crude reaction product the compounds **5**, **6** and **7** were isolated.

3-*t*-Butyl-indenone (**5**), 63.0 % — IR (CCl_4, cm^{-1}) : $\nu_{C=C}$ 1618, $\nu_{C=O}$ 1706. — ^{1}H-NMR ($CDCl_3$, δ, ppm) : 1.41 (*t*-Bu), 6.31 (H—C=).

3,4,4-Trimethyl-1-keto-1,4-dihydro-naphthalene (**6**), identical with earlier described product,[6] 3.7 % — IR (CCl_4, cm^{-1}) : $\nu_{C=C}$ 1630, $\nu_{C=O}$ 1660. — ^{1}H-NMR ($CDCl_3$, δ, ppm) : 6.17 (H—C=), 2.06 (CH_3-3), 1.52 (CH_3-4), 7.15 — 8.15 (aromatic).

E-1-Benzoyl-2-chloro-3,3-dimethyl-but-1-ene (**7**), <1 %. — ^{1}H-NMR ($CDCl_3$, δ, ppm) : 1.18 (*t*-Bu), 6.57 (H—C=).

Reaction of methyl-t-butyl-acetylene with p-methoxy-benzoyl chloride and $AgClO_4$. The reaction was carried out according to the standard procedure. After working-up, the crude reaction product was determined to contain 84.3 % **10** and 15.2 % **11**, together with traces of **12**.

2-Methyl-3-*t*-butyl-5-methoxy-indenone (**10**) — IR (CCl_4, cm^{-1}) : $\nu_{C=C}$1618, $\nu_{C=O}$ 1710. — ^{1}H-NMR ($CDCl_3$, δ, ppm) : 1.96 (CH_3-2), 1.42 (*t*-Bu), 3.86 (CH_3O), 6.50 (H-4, H-6), 6.80 (H-7).

6-Methoxy-2,3,4,4-tetramethyl-1-keto-1,4-dihydro-naphthalene (**11**). — IR (CCl_4, cm^{-1}) : $\nu_{C=C}$ 1630, $\nu_{C=O}$ 1645.— ^{1}H-NMR ($CDCl_3$, δ, ppm) : 2.03 (CH_3-2, CH_3-3), 1.52 (CH_3-4), 3.89 (CH_3O), 6 68 (H-5, H-7), 7.41 (H-8). (The spectra are quite similar to those of the parent compound, without methoxy group[6]).

E-2-*p*-Methoxy-benzoyl-3-chloro-4,4-dimethyl-pent-2-ene (**12**). — ^{1}H-NMR ($CDCl_3$, δ, ppm) : 1.91 (CH_3), 1.19 (*t*-Bu).

REFERENCES

[1] Part IV : D. Mănoiu, M. Mănoiu, I. G. Dinulescu and M. Avram, *Rev. Roumaine Chim.* **29**, 857 (1984).

[2] D. Mănoiu, M. Mănoiu, I. G. Dinulescu and M. Avram, *Rev. Roumaine Chim.*, **29**, 671 (1984).

[3] D. Mănoiu, M. Mănoiu, I. G. Dinulescu and M. Avram, *Rev. Roumaine Chim.*, **29**, 201 (1984).

[4] D. Mănoiu, M. Mănoiu, I. G. Dinulescu and M. Avram, *Rev. Roumaine Chim.*, **29**, 193 1984).

[5] H. Martens, G. Hoornaert and S. Toppet, *Tetrahedron*, **29**, 4241 (1973).

[6] H. Hart and R. K. Murray, jr., *J. Org. Chem.*, **35**, 1535 (1970); J. F. Huffman and T. W. Bethea, *J. Org. Chem.*, **30**, 2956 (1965).

Revue Roumaine de Chimie, **30**, *3*, 229–231 (1985)

COORDINATION COMPOUNDS FORMATION WITHIN THE MCl_2-$SnCl_2$-α,α′-BIPYRIDINE (M=Co, Ni) SYSTEM

MARIA BREZEANU*, MARIUS ANDRUH**, LUMINIȚA PATRON** and
V. T. POPA**

* Chair of Inorganic Chemistry, Polytechnical Institute of Bucharest, Spl. Independenței 202, Bucharest, Romania

** Center of Chemical Physics, Spl. Independenței 202, Bucharest, Romania

Received September 2, 1983

This work presents the synthesis of some complexes of the type $[M(bipy)_3](SnCl_3)_2$, M=Co(II), Ni(II). The thermal analysis (DSC-TGA) of this compounds indicates that the organic ligands migrate at ~ 200°C from the Co(II) or Ni(II) ions to the Sn(II) ion, resulting in mixtures of the $[M(bipy)Cl_2] \cdot 2[SnCl_2\ bipy]$-type. These compounds were characterized by IR, UV-VIS spectroscopy and magnetic measurements.

1. INTRODUCTION

In coordination chemistry, the complexes containing ligands such as α, α′-bipyridine and *o*-phenanthroline were extensively studied. The most of these are the $[ML_3]X_2$ -type complexes. The $[ML_2X_2]$ – type complexes are in general more difficult to prepare. An effective method to synthesize such compounds seems to be the stepwise controlled decomposition[1,2] of the α, α′-bipyridine complexes of Co(II) and Ni(II) chlorides. Similar studies of thermal decomposition were carried on the $H_2SnCl_4 \cdot$ (α, α′-bipy), H_2SnCl_4(4,4′-bipy)-type complexes. [3]

The present work is concerned with the complexes formation in systems such as MCl_2-SnCl_2-α, α′-bipyridine.

2. EXPERIMENTAL

We prepared two complexes containing the anion $SnCl_3^-$. The $[M(bipy)_3]\ (SnCl_3)_2$ precipitates from alcoholic solutions of $[M(bipy)_3]\ Cl_2$,[4] while adding a $SnCl_2$ hydrochloric solution (HCl favoured the formation of the $SnCl_3^-$ ion). The compounds $[Co(bipy)_3]\ (SnCl_3)_2$ – yellow (I) and $[Ni(bipy)_3]\ (SnCl_3)_2$ – pink (II) were filtered, washed with ether and dried in vacuum. They were characterized by chemical analysis, electrical conductivity measurements, IR and electronic spectra. Upon heating to 200°C, the $[M(bipy)_3](SnCl_3)_2$ – type complexes change their colour without any loss of weight. Indeed, the DSC curves clearely showed slightly exothermic processes at 120–130°C while the TGA curves indicated to weight loss, within this temperature range. The resulted compounds were also studied by IR and electronic spectroscopy and magnetic measurements.

3. RESULTS AND DISCUSSIONS

The electronic spectra for $[M(bipy)_3](SnCl_3)_2$ support the assigned formulas, with (MN_6) chromophores, in high-spin octahedral environment. [5]

The thermal analysis provided the following information :

— the complexes (I) and (II) are more stable than those containing the Cl^- anion ,their decomposition proceeding over 200°C for (I) (140°C for $[Co(bipy)_3]Cl_2$ [1]) and over 250°C for (II) (210°C for $[Ni(bipy)_3]Cl_2$ [1]).

— until the decomposition temperature both compounds undergo phase transformation accompanied by colour changes :

Cobalt : yellow → green

nickel : pink → yellow

These transformations took place both in air and inert atmosphere, leading to the same products.

Table 1

Electronic and spectral data

	$[Co(bipy)Cl_2]$		$[Ni(bipy)Cl_2]$	
$\nu_1(cm^{-1})$	—		12,270	$^3T_{1g} \rightarrow {}^3A_{2g}$
$\nu_2(cm^{-1})$	10,690	$^4T_1(P) \leftarrow {}^4A_2$	19,230	$^3T_{2g} \rightarrow {}^3A_{2g}$
$\nu_3(cm^{-1})$	15,870 14,810 14,290	$^4T_1(P) \leftarrow {}^4A_2$	—	
$10Dq(cm^{-1})$	4,710		12,270	
$B(cm^{-1})$	758		840	
β	0.78		0.8	
$\mu_{eff}(MB)$	4.64		3.19	
$\lambda(cm^{-1})$	−220		−390	

The electronic spectrum and magnetic moments of the green modification (Table 1) suggest a tetrahedral environment of the Co(II) ion. We can emphasize the strong resemblance with the electronic spectrum of β-$[Co(bipy)\,Cl_2]$ whose assigned structure was also tetrahedral. [1]

The following equations were applied to calculate 10Dq, B and λ :

$$\begin{matrix} d^7 \\ (T_d) \end{matrix} \begin{cases} 10Dq = \dfrac{1}{34}\left[9(\nu_2 + \nu_3) \pm \{81(\nu_2^2 + \nu_3^2) - 178\,\nu_2\nu_3\}^{1/2}\right] \\ B = (\nu_2 + \nu_3 - 30Dq)/15 \end{cases}$$

$$\begin{matrix} d^8 \\ (O_h) \end{matrix} \begin{cases} 10Dq = \nu_1 \\ B = (2\nu_1^2 + \nu_2^2 - 3\,\nu_1\nu_2)/(15\,\nu_2 - 27\,\nu_1) \end{cases}$$

$$\mu_{exp} = \mu_{s.o.}\left(1 - \frac{4\lambda}{10Dq}\right)$$

Consequently we may assume the following sequence of thermal transformations :

$$Co(bipy)_3^{2+} \rightarrow Co(bipy)_2^{2+} \rightarrow Co(bipy)^{2+}$$

and, as no weight loss was observed, we may conclude that the expelled bipyridine molecules coordinate to the tin ions :

$$[Co(bipy)_3](SnCl_3)_2 \rightarrow [Co(bipy)Cl_2] \cdot 2[SnCl_2bipy]$$

The behaviour of the $[Ni(bipy)_3]$ $(SnCl_3)_2$ complex was studied in the same way. The analysis of the electronic spectrum (Table 1) suggests an octahedral environment of the Ni(II) ion. Accepting the transformation :

$$[Ni(bipy)_3]\ (SnCl_3)_2 \xrightarrow{t°C} [Ni(bipy)Cl_2]2[SnCl_2\ bipy]$$

the octahedral environment of the nickel ion cannot be supported by a structure other than polynuclear, with the (NiN_2Cl_4) chromophore.

The IR spectra within the range 400—4000 cm^{-1} provided an additional proof of the bipyridine coordination to both Co(II) (or Ni(II)) and Sn(II) ions. Upon comparing the IR spectra for $[M(bipy)_3](SnCl_3)_2$ and $[M(bipy)Cl_2]2 \cdot [SnCl_2(bipy)]$, a splitting of the $\sim 1630\ cm^{-1}$ band was observed for the latter, assigned to the $-\underset{|}{C}=N-$ heterocyclic bond vibration.[7]

This splitting may be accounted for by the different interaction of cobalt or nickel ions with the nitrogen atoms of the bypyridine molecule (the different interaction of metal ions with the nitrogen atoms leads to different modifications of the $-\underset{|}{C}=N-$ bond).

Therefore, the experimental data are in agreement with the supposition that the organic ligand migrates from M(II) to Sn(II).

REFERENCES

[1] R. H. Lee, E. Griswood and J. Kleinberg, *Inorg Chem.*, **3**, 1278 (1964).

[2] W. M. Reiff, B. Dockum, M. A. Weber and R. B. Frankel, *Inorg. Chem.*, **14**, 800 (1975).

[3] D. M. Czakis-Solikowska and J. Radwanska-Doezekalska, *Rev. Roumaine Chim.*, **27**, 1105 (1982).

[4] G. T. Morgan and F. H. Burstall, *J. Chem. Soc.*, **1931**, 2213.

[5] G. L. Roberts and F. H. Field, *J. Amer. Chem. Soc.*, **72**, 4232, (1950).

[6] E. Konig, *Structure and Bonding*, **9**, 175 (1971).

[7] J. G. Gibson and E. D. McKenzie, *J. Chem. Soc. (A)*, **1969**, 2637.

Consequently we must assume the following reciprocal [illegible] transformations:

$$[Co(bipy)_3]^{2+} \to [Co(bipy)_2]^{2+} + Co(bipy)^{2+}$$

and, as no [illegible] was observed, we may conclude that the expelled bipyridine molecule coordinates to the tin ion:

$$[Co(bipy)_3](SnCl_3)_2 \to [Co(bipy)Cl_2] \cdot 2[Sn(bipy)Cl_2]$$

The behaviour of the $[Ni(bipy)_3](SnCl_3)_2$ complex was studied in the same way. The analysis of the electronic spectrum (Table 1) suggests an octahedral environment of the Ni(II) ion. Accepting the transformation:

$$[Ni(bipy)_3](SnCl_3)_2 \xrightarrow{t^\circ} [Ni(bipy)_2Cl_2][Sn(bipy)Cl_2]_2 \cdot bipy$$

the octahedral environment of the nickel ion cannot be supported by a structure other than polymeric, with the NiN_4Cl_2 chromophore.

The IR spectra within the range 400–4000 cm⁻¹ provided an additional proof of the bipyridine coordination to both Sn(II) (or Sn(IV)) and M(II) ions. Upon comparing the IR spectra for $[M(bipy)_3](SnCl_3)_2$ and $M(bipy)Cl_2 \cdot [Sn(bipy)Cl_2]$, a splitting of the ~1630 cm⁻¹ band was observed for the latter, assigned to the C=N heterocyclic bond vibration.[7]

This splitting may be accounted for by the different interaction of cobalt or nickel ions with the nitrogen atoms of the bipyridine molecule (the different interaction of metal ions with the nitrogen atoms leads to different modifications of the C=N bonds).

Therefore, the experimental data are in agreement with the supposition that the entire ligand migrates from M(II) to Sn(II).

REFERENCES

[illegible]

Revue Roumaine de Chimie, **30**, *3*, 233—238 (1985)

as-TRIAZINE DERIVATIVES WITH POTENTIAL THERAPEUTIC ACTION. XX*.

CYANOETHYLATION OF 5-SUBSTITUTED-6-AZAURACIL AND 4-THIOXO-5-SUBSTITUTED-6-AZAURACIL

C. CRISTESCU and SILVIA SITARU
Chemical and Pharmaceutical Research Institute, Şos. Vitan 112, 74351 Bucharest, Romania

Received February 11, 1984

Cyanoethylation of 5-substituted-6-azauracil (I) with acrylonitrile in aqueous media afforded the corresponding 1-(2-cyanoethyl)-derivatives II. Similarly, the treatment of 4-thioxo-5-substituted-6-azauracil (III) with acrylonitrile led to the formation of 1-(2-cyanoethyl)-derivatives (IV). The structure of the resulting IV was established by an unequivocal synthesis from II by thionation with P_2S_5 in pyridine. Treatment of IV with methyl iodide afforded the S-methyl derivatives V, which were converted by hydrolysis into the corresponding II.

6-Azauracil derivatives, including N_1-substituted compounds, ribo- and 2-deoxy-ribonucleosides exhibit cytostatic, virustatic and coccidiostatic properties. [1–4]

In connection with the preparation of new 5-substituted-6-azauracil derivatives with potential cytostatic, virustatic or coccidiostatic activity it seems interesting to convert 5-substituted-6-azauracil and 4-thioxo-5-substituted-6-azauracil in 1-(2-cyanoethyl)-derivatives. Such derivatives show a high solubility in water which is of importance in view of their administration.

The preparation of 1-(2-cyanoethyl)-5-alkyl(aryl)thio-6-azauracil was based on the same methodology, previously employed by Novacek et al.[5–6] to synthesize 1-(2-cyanoethyl)-6-azauracil.

The treatment of 5-alkyl(aryl) thio-6-azauracil [7] (I) with acrylonitrile, in aqueous media, in the presence of triethylamine and traces of sodium hydroxide at 50—60°C afforded 1-(2-cyanoethyl)-5-alkyl(aryl) thio-6-azauracil (II). The 1,3-bis-cyanoethyl-derivatives are not formed when a molar ratio 5-substituted-6-azauracil/acrylonitrile of 1 : 3—4 was employed.

The course of the cyanoethylation is determined by the different nucleophilicity of the nitrogen atom at positions 1 and 3 which indirectly results from the corresponding values of the dissociation constant. Thus

---

*Part XIX, C. Cristescu, *Rev. Roumaine Chim.*, **30**, 117 (1985).

5-alkyl (aryl)thio-6-azauracil which shows a considerable difference in the nucleophilicity of both NH groups (one of them is considerably acid) affords the mono-cyanoethyl derivative.

The structure of the products II could unequivocally be deduced from their spectral properties. The UV spectrum exhibits a hypsochromic shift of the absorption maximum by passing from acidic to basic media. This is a typical behaviour for N_1-substituted-6-azauracils[8,9] In the infrared spectra, the ring carbonyl group bands were found at 1655 ± 15 cm^{-1} and 1696 ± 14 cm^{-1} and the absorption of the cyano-group occurs at ~ 2236 cm^{-1}.

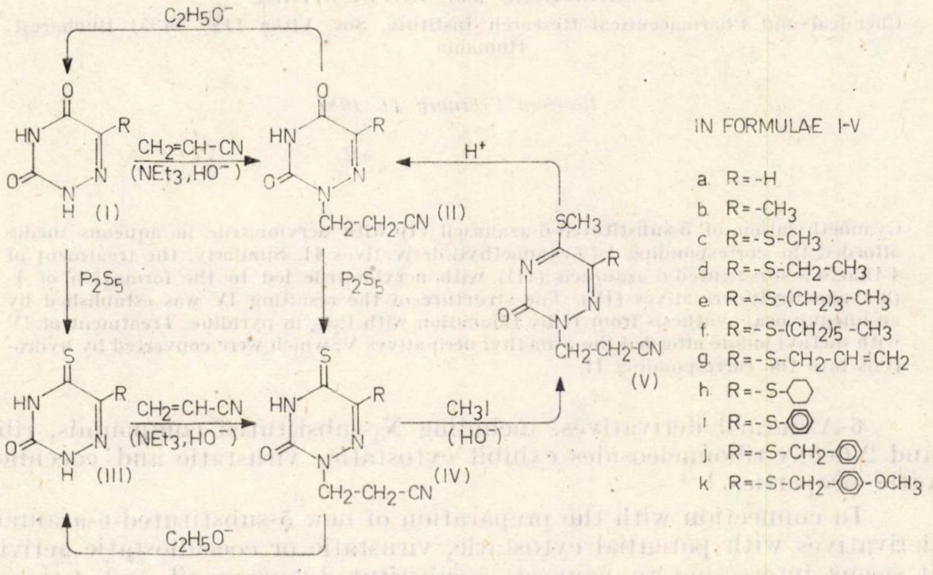

On refluxing with excess of sodium ethoxide in ethanol, the 1-(2-cyanoethyl)-derivatives II were converted into the starting 5-substituted-6-azauracil derivatives (I).

Cyanoethylation of 5-substituted-6-azauracil was studied concomitantly with the reaction of acrylonitrile with 4-thioxo-5-substituted-6-azauracil[10,11] (III). Under identical conditions, acrylonitrile reacts with III to give 1-(2-cyanoethyl)-4-thioxo-5-substituted-6-azauracil (IV).

The structure assigned to the resulting IV compounds was verified by an unequivocal synthesis. By treatment with phosphorus pentasulphide in pyridine (containing 0.1—0.3 % water), II was selectively thionated in position 4 to give the 4-thioxo-derivatives (IV) identical in all respects with the products obtained by the cyanoethylation of II. Treatment of IV with methyl iodide afforded the S-methyl-derivatives V. The lability of the methyl-mercapto group from the 4-position of the derivatives V facilitates the replacement of mercapto-group by the oxo-group. Thus V treated with diluted hydrochloric acid gives the 4-oxo-derivatives II identical in all respects with the products obtained by cyanoethylation of I.

On refluxing the mono-cyanoethyl derivatives IV with excess of sodium ethoxide in ethanol, a total decyanoethylation takes place with the formation of the starting 4-thioxo-5-substituted-6-azauracil derivatives (III).

The replacement of an oxygen atom by a sulphur atom produces a bathochromic effect in the ultraviolet spectrum of 6-azauracil.[12] The monocyanoethyl derivatives IV exhibit two intense bands at 247—254 nm and 336—340 nm. The ionization of compounds IV produces a bathochromical shift of the 340 nm band. This is in concordance with N_1-substituted-4-thioxo-6-azauracil. In the infrared spectra of compounds IV an intense absorption $\bar{\nu}$ (CO) band at $1690 \pm 10\ cm^{-1}$ occurs indicating the 2-oxo-structure of these derivatives, the $\bar{\nu}(C{=}S)$ vibration is found near $1100\ cm^{-1}$ and the cyano group absorption at $\sim 2246\ cm^{-1}$.

EXPERIMENTAL

The melting points were determined with a heating microscope plate and are not corrected. Thin layer chromatography (TLC) was performed on precoated silicagel plates 60 F_{254} (Merck). Ultraviolet spectra of products were recorded on a Unicam SP 1800 ultraviolet spectrophotometer. The infrared spectra were recorded with a Zeiss-Jena UR 20 infrared spectrophotometer.

General procedure for the preparation of 1-(2-cyanoethyl)-5-substituted-6-azauracil (II)

5-Alkyl(aryl)thio-6-azauracil (10 mM) was dissolved in a 1% aqueous solution of sodium hydroxide (40 mL) and treated at 50°C with triethylamine (14 mM) and acrylonitrile (30 mM). The mixture was stirred at 45—50°C for one hour and then at room temperature for 18 hours. The solution was filtered with charcoal and the filtrate adjusted at pH 2 with 10% hydrochloric acid. The precipitate was collected and recrystallized from the solvents indicated in table 1.

Decyanoethylation of 1-(2-cyanoethyl)-5-substituted-6-azauracil

1-(2-Cyanoethyl)-5-alkyl(aryl)thio-6-azauracil (20 mM) was added to a 1N sodium ethoxide solution in ethanol (20 mL) and refluxed for two hours. The solution was acidified

TABLE 1 1(2-cyanoethyl)-5-substituted-6-azauracils (II)

No.	RECRYSTN SOLVENT[a]	m.p. °C	YIELD %	T.L.C[b]			UV SPECTRA λmax (log ε)			IR SPECTRA (KBr) cm⁻¹		FORMULA[c]
				A	B	C	EtOH	0,1N HCl	0,1N NaOH	$\bar{\nu}$ (CO)	$\bar{\nu}$(CN)	
II-c	A	173-175	73	0.31	0.42	0.37	316 (4.16)	314-316(4.14)	304-306(4.06)	1656, 1695	2226	$C_7H_8N_4O_2S$
II-d	A	122-125	68	0.35	0.47	0.37	316 (3.81)	316(3.78)	306(3.71)	1640, 1683	2226	$C_8H_{10}N_4O_2S$
II-e	B	119-120	76	0.39	0.47	0.37	316 (3.82)	316(3.79)	306(3.72)	1660, 1696	2233	$C_{10}H_{14}N_4O_2S$
II-f	B	103-105	70	0.39	0.48	0.34	320(3.82)	320(3.78)	306(3.69)	1686, 1710	2246	$C_{12}H_{18}N_4O_2S$
II-g	A	146-148	79	0.33	0.42	0.38	318(4.10)	316 (4.13)	306(4.05)	1670, 1700	2246	$C_9H_{10}N_4O_2S$
II-h	A	253-255	42	0.06	0.17	0.26	279(3.94)	279 (3.91)	269(3.97)	1653, 1713	2233	$C_{12}H_{16}N_4O_2S$
II-i	B	184-186	65	0.29	0.58	0.43	316(3.78)	320(3.77)	306(3.58)	1666, 1686	2240	$C_{12}H_{10}N_4O_2S$
II-j	B	149-151	80	0.32	0.59	0.43	316(3.85)	317(3.79)	304(3.57)	1653, 1696	2226	$C_{13}H_{12}N_4O_2S$
II-k	C	163-165	80	0.31	0.60	0.43	318(3.89)	318(3.81)	304(3.73)	1660, 1693	2226	$C_{14}H_{14}N_4O_3S$

a. (A) water; (B) water-ethanol (1:1); (C) ethanol; (D) 2-propanol

b. Spots detected as UV absorbing (254 nm); solvent systems (A) iso-octane-ethylacetate-methanol (10:5:4); (B) chloroform-methanol (9:1); (C) benzene-methanol (8:2)

c. Analytical results were within ± 0.4% of the teoretical values for C,H,N,S with 10% hydrochloric acid to pH 4 and evaporated to dryness under reduced pressure. The residue was recrystallized from the adequate solvent[7] to afford 5-alkyl(aryl-)thio-6-azauracil (I) identical in all respects with an authentic sample.

General procedure for the preparation of 1-(2-cyanoethyl)-4-thioxo-5-substitued-6-azauracil (IV

Method I

4-Thioxo-5-substituted-6-azauracil (5 mM) was dissolved in a 1% aqueous solution of sodium hydroxide (20 mL) and treated at 50°C with triethylamine (7 mM) and acrylonitrile (15 mM). The mixture was stirred at 45–50°C, under nitrogen, for one hour and then for two days at room temperature. The solution was filtered with charcoal and the filtrate was concentrated under reduced pressure. The residue was dissolved in water and the solution was adjusted to pH 3.5 with 10% hydrochloric acid and cooled at 4°C over night. The precipitate was filtered and recrystallized from the solvent indicated in table 2.

Method II

1-(2-Cyanoethyl)-5-substituted-6-azauracil (3 mM) was dissolved in pyridine (25 mL) containing 0.1–0.3% water and phosphorus pentasulphide (1.5 mM) was added at 50°C. The mixture was heated under reflux for 4–6 hours with stirring. The clear orange-red solution was decanted after cooling at room temperature (over night) and concentrated at 40°C under reduced pressure. The dry residue was dissolved in 1 N sodium hydroxide (8–10 mL) treated with active charcoal, filtered and adjusted to pH 2.5 with 10% hydrochloric acid. After cooling at 4°C (over night), the product was filtered and recrystallized from the solvent indicated in table 2, yielding IV identical in all respects with a sample prepared by the first method.

Decyanoethylation of 1-(2-cyanoethyl)-4-thioxo-5-substituted-6-azauracil

1-(2-Cyanoethyl)-4-thioxo-5-substituted-6-azauracil (10 mM) was added to a 1 N solution of sodium ethoxide in ethanol (10 mL) and refluxed, under nitrogen, for two hours. The solution was acidified with 10% hydrochloric acid to pH 2.5 and evaporated in vacuum. The residue was recrystallized from the adequate solevent[10,11] to afford 4-thioxo-5-substituted 6-azauracil identical in all respect with an authentic sample.

General procedure for the preparation of 1-(2-cyanoethyl)-4-methylthio-5-substituted-6-azauracil (V)

1-(2-Cyanoethyl)-4-thioxo-5-substituted-6-azauracil (1 mM) was dissolved in ethanol (5 mL) and treated with a 1 N sodium hydroxide solution to pH 10. Methyl iodide (3 mM) in ethanol (1 mL) was added and the reaction mixture was stirred for one hour at room temperature. The solvent was removed in vaccum and the residue was dissolved in water (3 mL), adjusted to pH 8–9 with 1 N sodium hydroxide solution and extracted with 1,2-dichloroethane (3 × 5 mL). The combined 1,2-dichloroethane layers were dried (sodium sulphate) and evaporated in vaccum. The residue was recrystallized from the solvent indicated in table 2.

Hydrolysis of 1-(2-cyanoethyl)-4-methylthio-5-substituted-6-azauracil

1-(2-Cyanoethyl)-4-methylthio-5-substituted-6-azauracil (0.3 mM) was dissolved in ethanol (4 mL) and the solution was acidified with 10% hydrochloric acid to pH 1. The reaction mixture was stirred at room temperature for 72 hours and evaporated to dryness under reduced pressure. The residue was recrystallized from the solvent indicated in table 1 yielding 1-(2-Cyanoethyl)-5-substituted-6-azauracil identical in all respects with an authentic sample.

ACKNOWLEDGEMENT. The authors thank Mrs. Veronica Vişan and Mrs. Ileana Costea of the Analytical Department of our Institute for recording the IR and UV spectra, and Mrs. Cornelia Ioan for the elemental analyses. The authors wish to express their gratitude to Mrs. Anca Sava for her invaluable help.

REFERENCES

[1] H. Neunhoeffer, in "The Chemistry of Heterocyclic Compounds" Vol. 33, p. 1025, Wiley Interscience, New York, 1978.

[2] B. L. Mylari, M. W. Miller, H. L. Howes, Jr., S. K. Figdor, J. E. Lynch and R. C. Koch, *J. Med. Chem.*, **20**, 475 (1977).

TABLE 2

1 (cyano-ethyl) - 4 thio - 5-substituted-6-azauracils (IV) and 1(2-cyanoethyl)-4-methylthio-5-substituted-6 azauracils(V)

No.	RECRYSTN SOLVENT[a]	m.p. °C	YIELD %	T.L.C[b]			UV SPECTRA λmax(logε)			IR SPECTRA (KBr pellets) cm⁻¹			FORMULA[c]
				A	B	C	EtOH	0.1 N HCl	0.1 N NaOH	$\tilde{\nu}$(CO)	$\tilde{\nu}$(CN)	$\tilde{\nu}$(CS)	
IV-a	D	120 - 123	43	0.43	0.62	0.45	247 (4.06), 333 (4.35)	247 (4.04), 334 (4.38)	249 (4.14), 336 (4.31)	1686	2246	1140	$C_6H_6N_4OS$
IV-b	D	167 - 169	44	0.45	0.65	0.46	241 (3.69), 333 (4.08)	242 (3.73), 332 (4.13)	242 (3.82), 336 (4.06)	1700	2263	1146	$C_7H_8N_4OS$
IV-c	C	211 - 213	49	0.40	0.62	0.45	250 (4.07), 330 (4.22)	250 (4.09), 330 (4.23)	336 (4.29)	1666	2246	1173	$C_7H_8N_4OS_2$
IV-d	D	151 - 152	55	0.43	0.65	0.47	254 (4.11), 330 (4.24)	254 (4.12), 330 (4.23)	336 (4.31)	1666	2246	1173	$C_6H_{10}N_4OS_2$
IV-e	B	102 - 104	78	0.47	0.62	0.54	250 (3.75), 330 (3.40)	250 (3.73), 330 (3.84)	340 (3.42)	1680	2253	1166	$C_{10}H_{14}N_4OS_2$
IV-f	B	118 - 121	78	0.40	0.61	0.51	253 (4.14), 330 (4.25)	253 (4.12), 330 (4.10)	336 (4.33)	1683	2250	1166	$C_{12}H_{18}N_4OS_2$
IV-i	B	139 - 141	70	0.34	0.58	0.48	255 (4.21), 330 (4.23)	256 (4.24), 330 (4.24)	338 (4.27)	1673	2250	1166	$C_{12}H_{10}N_4OS_2$
IV-j	C	131 - 133	52	0.41	0.57	0.51	253 (3.91), 330 (3.96)	253 (3.93), 330 (3.97)	338 (3.99)	1670	2246	1173	$C_{12}H_{12}N_4OS_2$
IV-k	C	156 - 158	55	0.36	0.59	0.50	276 (3.60), 330 (3.96)	276 (3.61), 330 (3.92)	340 (3.93)	1680	2260	1176	$C_{14}H_{14}N_4OS_2$
V-a	C	110 - 114	60	0.28	0.61	0.45	304 (4.01)	–	–	1670	2253	–	$C_7H_8N_4OS$
V-c	C	137 - 139	72	0.33	0.67	0.52	292 (3.81)	–	–	1653	2240	–	$C_8H_{10}N_4OS_2$
V-d	D	102 - 104	70	0.46	0.69	0.61	296 (3.81)	–	–	1680	2246	–	$C_9H_{12}N_4OS_2$

a. (B) water-ethanol (1:1); (C) ethanol; (D) 2-propanol

b. Spots detected as UV absorbing (254 nm); solvent systems (A) iso-octane-ethyl acetate-methanol (10:5:4) (B) chloroform-methanol (9:1); (C) Benzene-methanol (8:2)

c. Analytical results were within ± 0.4% of the theoretical values for C,H,N,S

[3] M. W. Miller, B. L. Mylari, H. L. Howes Jr., J. E. Lynch, M. L. Lynch and R. C. Koch, *J. Med. Chem.*, **22**, 1483 (1979).

[4] M. W. Miller, B. L. Mylari, H. L. Howes Jr., S. K. Figdor, M. J. Lynch, J. E. Lynch and R. C. Koch, *J. Med. Chem.*, **23**, 1083 (1980).

[5] A. Nováček, *Coll. Czech. Chem. Comm.*, **30**, 2480 (1965).

[6] A. Nováček and M. Lissnerová, *Coll. Czech. Chem. Comm.*, **33**, 1003 (1968).

[7] C. Cristescu and T. Panaitescu, *Pharmazie*, **17**, 209, (1962).

[8] J. Johnas and J. Gut, *Coll. Czech. Chem. Comm.*, **26**, 2155 (1961).

[9] K. V. Zee-Cheng and C. C. Cheng, *J. Org. Chem.*, **27**, 976 (1962).

[10] C. Cristescu and V. Badea, *Rev. Roumaine Chim.*, **14**, 135 (1969).

[11] C. Cristescu and S. Sitaru, *Rev. Roumaine Chim.*, **16**, 135 (1971).

[12] J. Johnas and J. Gut, *Coll. Czech. Chem. Comm.*, **27**, 1886 (1962).

Revue Roumaine de Chimie, **30**, *3*, 239–244 (1985)

ORDERED POLYESTERIMIDES

MARIA BRUMĂ and ION SAVA
Institute of Macromolecular Chemistry "P. Poni", Aleea Gr. Ghica Vodă No. 41 A, — Iași, Romania

Received February 20, 1984

Ordered polyesterimides have been synthesized by solution polycondensation of certain dihydroxy compounds with diacid chlorides of dicarboxylic acids, both monomers containing preformed imide rings. The thermal stability of these polyesterimides is discussed.

INTRODUCTION

In the field of heterocyclic thermostable polymers, aromatic polyimides have been largely studied due to their superior thermal stability in oxidative atmosphere, chemical resistance and good mechanical and electrical properties. [1] However, because of their rigid structure polyimides are insoluble and infusible which causes great processing difficulties. Many attempts have been made to synthesize polyimide type polymers which contain flexible groups such as ester in order to improve their solubility. [2] But ester groups in polyesterimides lead to a decrease of their resistance at high temperatures; one method to avoid, to a certain degree, this inconvenience would be the synthesis of ordered polyesterimides.

In the present paper we describe the synthesis of ordered polyesterimides by polycondensation reaction of dihydroxy-compounds with diacid chlorides, both monomers containing preformed imide rings.

RESULTS AND DISCUSSION

The dihydroxy compounds used in the synthesis of ordered polyesterimides are: N,N′-bis(hydroxyethyl)pyromellitic diimide, N,N′-bis (hydroxyphenyl)pyromellitic diimides, N,N′-bis(hydroxyethyl)benzophenontetracarboxylic diimide and N,N′-bis(hydroxyphenyl)benzophenontetracarboxylic diimides, I. They have been prepared by the reaction of 2-aminoethanol or m- or p-aminophenol with the corresponding dianhydride [3,4], as shown in scheme 1 :

Scheme 1

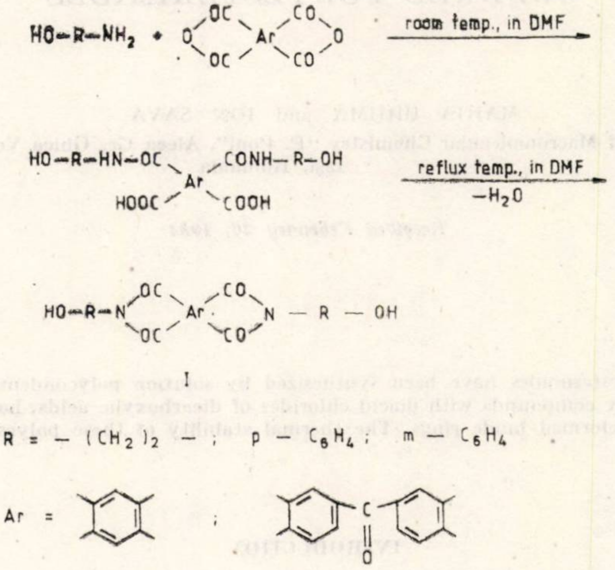
HO—R—NH₂
room temp., in DMF
reflux temp., in DMF
−H₂O
I
R = —(CH₂)₂— ; p — C₆H₄ ; m — C₆H₄
Ar =

Diacid chorides used in the polycondensation reaction with the above-mentioned dihydroxy-compounds are : oxy-bis-N(4-phenylene)-4′-(chloroformyl) phthalimide and methylene-bis-N-(4-phenylene)-4′-(chloroformyl)phthalimide II. They have been prepared by treating with thionyl chloride the corresponding dicarboxylic acids which had been synthesized from trimellitic anhydride and 4,4′-diaminodiphenylmethane or 4,4′-diaminodiphenylether, [5] as shown in scheme 2 :

Scheme 2

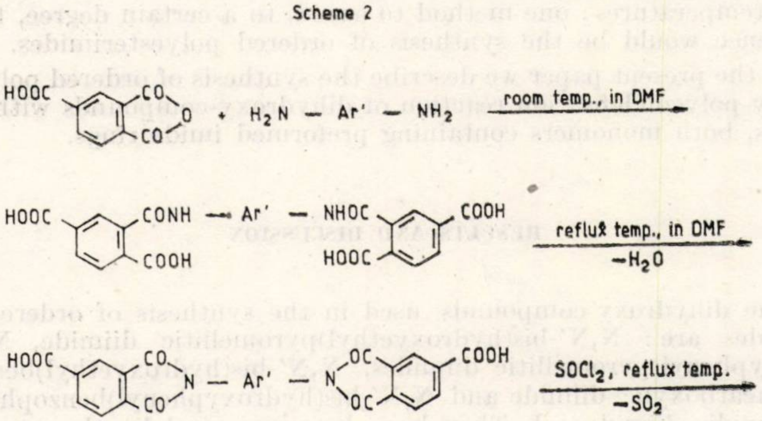
room temp., in DMF
H₂N — Ar′ — NH₂
reflux temp., in DMF
−H₂O
SOCl₂, reflux temp.
−SO₂
−HCl

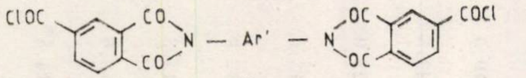

II

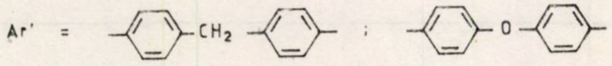

Solution polycondensation of the equimolecular amounts of the two monomers in N-methylpyrolidone containing 6% lithium chloride gave ordered polyesterimides, III, according to scheme 3:

Scheme 3

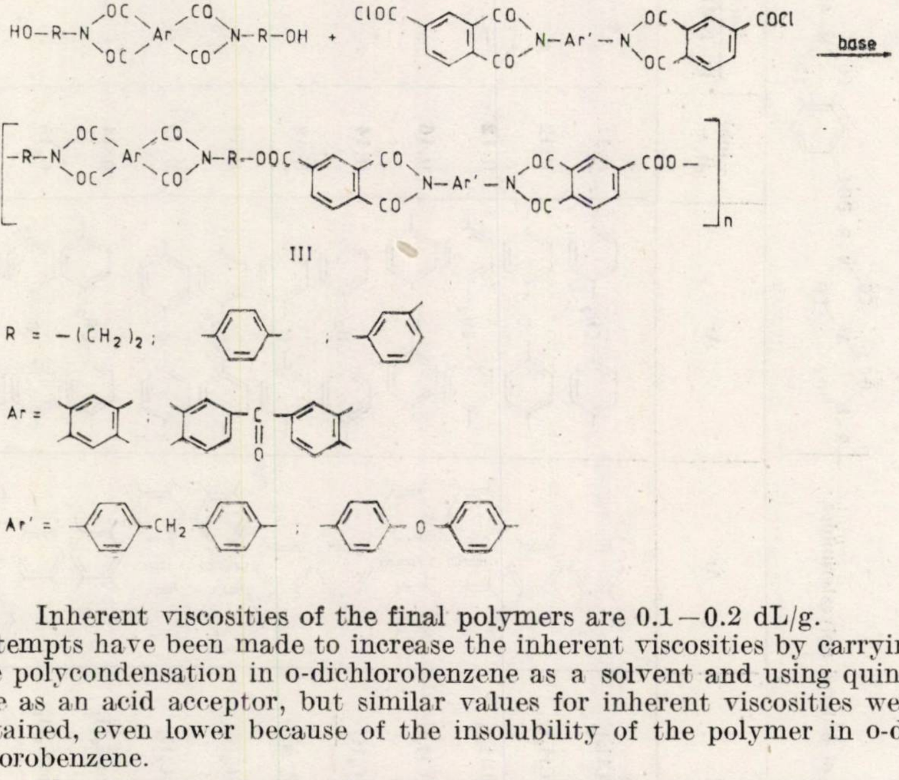

III

Inherent viscosities of the final polymers are 0.1–0.2 dL/g. Attempts have been made to increase the inherent viscosities by carrying the polycondensation in o-dichlorobenzene as a solvent and using quinoline as an acid acceptor, but similar values for inherent viscosities were obtained, even lower because of the insolubility of the polymer in o-dichlorobenzene.

The structure of the polyesterimides were identified by IR spectra and elemental analyses. Strong bands appeared at 1770–1780 cm^{-1}, 1710–1720 cm^{-1} and 715–720 cm^{-1} assigned to the imide cycle.

All these polyesterimides are soluble in polar aprotic solvents containing 6% lithium chloride. Polymers derived from N,N′-bis(hydroxyethyl)diimides are more soluble, even without adding lithium chloride.

The thermal stability of these polyesterimides was evaluated by thermogravimetric analysis (TGA) in air at a heating rate of 9.8°/minute.

Table 1

Properties of ordered polyesterimides :

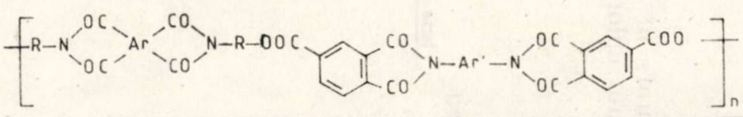

Polymer	R	Ar	Ar′	η inh[1] dL/g.	Solubility		TGA, weight loss %[2]	
					in NMP	in NMP + 6 % LiCl	at 400°	at 500°
IIIa	$(CH_2)_2$	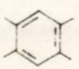	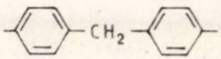	0.11	+	+	11.5	21
IIIb	$(CH_2)_2$	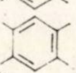	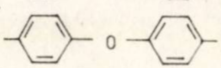	0.12	+	+	10	19.5
IIIc	$(CH_2)_2$	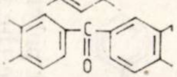	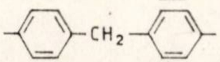	0.12	+	+	13.4	22.5
IIId	$(CH_2)_2$	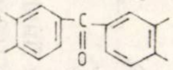	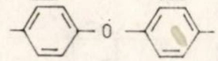	0.16	+	+	12.2	23.0
IIIe	p-C_6H_4	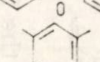	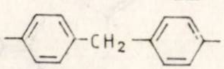	0.14	–	+	2.5	13.5
IIIf	p-C_6H_4	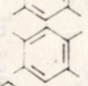	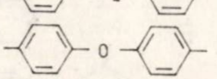	0.18	–	+	1.8	12.0
IIIg	p-C_6H_4	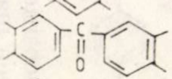	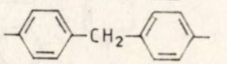	0.14	–	+	3.0	14.8
IIIh	p-C_6H_4	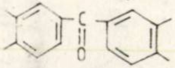	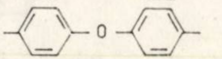	0.19	–	+	3.5	13.6
IIIi	m-C_6H_4	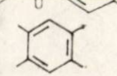	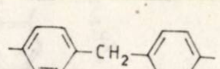	0.14	–	+	3.8	14.8
IIIj	m-C_6H_4	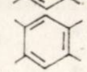	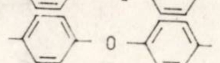	0.15	–	+	3.5	12.5
IIIk	m-C_6H_4	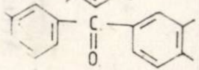	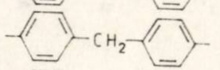	0.12	–	+	4.0	16.5
IIIl	m-C_6H_4	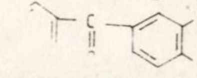	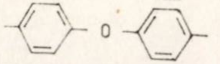	0.2	–	+	3.0	15.0

---

[1] Measured at a concentration of 0.5 g/100 mL NMP + 6% LiCl at

N,N′-bis-(hydroxyphenyl)diimides gave more thermally stable polymers than N,N′-bis(hydroxyethyl)diimide. Polymers obtained from N,N′-bis (hydroxyphenyl) diimides do not decompose up to 420°C while polymers obtained from N,N′-bis(hydroxyethyl)diimide begin to decompose within the range of 360—380°.

The thermal resistance of ordered polyesterimides containing ethylene units is comparable to that of related polyesterimides reported before but not having an ordered structure.[6]

Thus, polyesterimides synthesized in the present paper are soluble in polar aprotic solvents and have a good thermal stability due to their ordered structure.

EXPERIMENTAL

Preparation of monomers

N,N′-bis(hydroxyethyl)pyromellitic diimide, N,N′-bis (hydroxyphenyl)pyromellitic diimides, N,N′-bis(hydroxyethyl) benzophenontetracarboxylic diimide and N,N′-bis(hydroxyphenyl) benzophenontetracarboxylic diimides were prepared by the reaction of 2 mol of 2-aminoethanol or m- or p-aminophenol with 1 mol of the corresponding dianhydride, using dimethylformamide as a solvent. The general reaction procedure is as follows. In a three-necked flask equipped with mechanical stirrer, reflux condenser and N_2-inlet and -outlet, 0.4 mol. aminoethanol (or amino-phenol) and 180 mL dimethylformamide were placed. 0.2 mol pyromellitic dianhydride were added gradually to the stirred solution while the temperature of the reaction mixture increased rapidly up to 60°. Stirring was continued for other 30 minutes at room temperature and 15 minutes at reflux temperature. Imidization water was distilled off. After cooling to room temperature the precipitated product was filtered, washed with methanol and dried in vacuum oven. It was purified by recrystallization from DMF. All the products were characterized by elemental analysis, IR spectra and melting points.

To prepare diacid chlorides, first the corresponding dicarboxylic acids have been synthesized from 2 mol of trimellitic anhydride and 1 mol of 4,4′-diaminodiphenylmethane or 4,4′-diaminodiphenylether. The following example illustrates the general procedure : In a three-necked flask equipped with mechanical stirrer, reflux condenser, N_2-inlet and outlet, were introduced 0.1 mol diamine, 0.2 mol trimellitic anhydride and 140 mL dimethylformamide. The reaction mixture was stirred for 40 minutes at room temperature, and then for other 30 minutes at reflux temperature. Imidization water was distilled off. The dicarboxylic acid precipitated and it was filtered and washed with acetone. It was recrystallized from dimethylformamide.

30 grames of dicarboxylic acid and 100 mL thionyl chloride were heated under reflux for 30 minutes. 1 mL dimethylformamide was added to the reaction mixture and heating was continued for other 2 h. The light-yellow product was filtered, washed with n-hexane and dried in vacuum.

Preparation of polymers

Polycondensation was run with equimolecular amounts of the two monomers, using as a solvent N-methylpyrolidone containing 6% lithium chloride. Pyridine was used as an acid acceptor. A three-necked flask fitted with stirrer and reflux condenser was flushed with nitrogen and charged with dihydroxycompound and solvent to obtain a 10—20% final solution of polymer. Diacid chloride as a finely divided powder was added all at once to the stirred solution. The flask content was kept at room temperature 30 minutes and then pyridine was added. The reaction mixture was heated at 80–90° for 6–8 h. The polymer was precipitated by pouring into water. Inherent viscosities are 0.1–0.2 dL/g. Elemental analysis data were in good agreement with the calculated theoretical values.

REFERENCES

[1] C. E. Sroog, *J. Polymer Sci., Macromol. Reviews*, **11**, 161 (1976).

[2] M. M. Koton, *Visokomol. Soedin. A*, **15**, 310 (1973).

[3] W. A. Mosher and S. J. Chlystek, *J. Heterocycl. Chem.*, **9**, 319 (1972).

[4] K. Y. Choi and S. K. Choi, *J. Polymer. Sci., Polymer Chem. Ed.*, **20**, 1107 (1982).

[5] M. Brumă and G. Neamţu, *Rev. Roumaine Chim.*, **26**, 87 (1981).

[6] M. Brumă and I. Sava, "Aromatic polyesterimides", paper presented at the Second National Congress of Chemistry, Bucharest, 5–9 Sept. 1981.

Revue Roumaine de Chimie, **30**, 3, 245–248 (1985)

BASE CATALYZED ADDITIONS OF DEHYDROACETIC ACID AND ITS 3-CINNAMOYL DERIVATIVES

M. A. HASSAN, M. EL-KADY, M. EL-BORAI and A. A. ABD EL-MOATY
Chemistry Department, Faculty of Science, Ain Shams University, Cairo, Egypt

Received June 10, 1981

Base catalyzed addition of dehydroacetic acid (**1**) to some chalcones was investigated. Condensations of 3-cinnamoyl-4-hydroxy-6-methyl-2-pyrone (**3**) with hydrazines, acetyl acetone, diethyl malonate, ethyl acetoacetate and ethyl phenylacetate were studied. The structures of the products have been established by elemental analysis and spectroscopic evidences.

As an extension of our previous works [1-3] we describe the base catalyzed addition of dehydroacetic acid (**1**) to some chalcones affording the Michael adducts, namely 3,5-diarylpentan-1-(4′-hydroxy-6′-methyl-2′-oxopyran-3′-yl)-1, 5-diones (**2 a–d**). The IR spectra of compounds **2** showed bands at 1000, 1640, 1710, and 3220 cm^{-1} attributable to stretching frequencies of C–O–C, C=O (α-pyrones), C=O (1,5-diketones), and OH groups respectively. The ^{1}H-NMR spectrum of **2b** in $CDCl_3$ showed signals at δ 1.73 (m, 1H, Ar′–CH–), 2.3 (s, 3H, C_6-CH_3), 3.6 (d, 4H, $COCH_2$), 4.12 (s, 3H, Ar′–OCH_3), 5.7 (s, 1H, C_5-H) and 6.8–7.6 ppm (m, 9H, Ar–H).

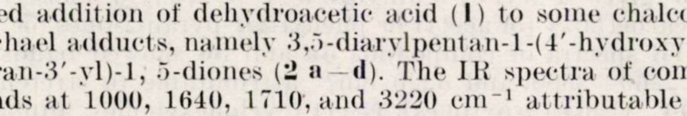

a) Ar = Ar′ = C_6H_5
b) Ar = C_6H_5 ; Ar′ = $C_6H_4-OCH_3-p$
c) Ar = $C_6H_4-OCH_3-p$; Ar′ = C_6H_5
d) Ar = Ar′ = $C_6H_4-OCH_3-p$

Claisen-Schmidt condensation[4] of dehydroacetic acid (**1**) with aromatic aldehydes in boiling chloroform in the presence of piperidine gives 3-cinnamoyl-4-hydroxy-6-methyl-2H-pyran-2-ones (**3 a–d**), which condense with phenylhydrazine in boiling acetic acid to give 5-aryl-1-phenyl-3-(4′hydroxy-6′-methyl-2′-oxopyran-3′-yl)-2-pyrazolines (**4 a–d**). The IR spectra of compounds **3** showed bands at 1000, 1600, 1650, 1705 and 3230 cm^{-1} attributable to stretching frequencies of C–O–C, C=C, C=O (α-pyrones), C=O (α, β-unsaturated ketones) and OH respectively, while the IR spectra of **4** showed the absence of νC=O (of α, β-unsaturated ketones). The ^{1}H-NMR spectrum of **3b** in $CDCl_3$ showed signals at δ 2.24 (*s*, 3H, C'_6-CH_3), 4.2 (*s*, 3H, $Ar-OCH_3$), 5.87 (*s*, 1H, C_5-H), 7.3 (*dd*, 4H, $Ar-H$), and 8.1 ppm (*dd*, 2H, $CH=CH$), while the ^{1}H-NMR spectrum of **4a** in d_6-DMSO showed signals at δ 2.18 (*s*, 3H, C_6-CH_3), 3.3–4.0 (*m*, 3H, C_4-H_2 and C_5-H), 6.1 (*s*, 1H, C_5-H), and 6.9–7.3 ppm (*m*, 10H, Ar–H).

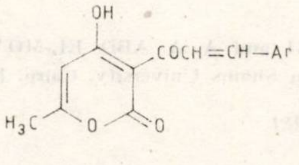

(3)

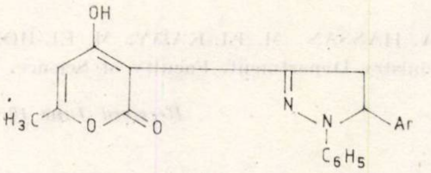

(4)

a) $Ar = C_6H_5$; b) $Ar = C_6H_4-OCH_3-p$

c) $Ar = C_6H_3-O_2CH_2-3{,}4-$; d) $Ar = C_6H_4-NO_2-p$

Base catalyzed cycloaddition of acetyl acetone on **3b** or **3c** in the presence of sodium methoxide at 170° gives 6-acetyl-5-aryl-3(4′-hydroxy-6′-methyl-2′-oxopyran-3′-yl)-cyclohex-3-en-1-ones (**5a** and **5b**). Also base catalyzed cycloaddition of diethyl malonate, ethyl acetoacetate, and ethyl phenylacetate to **3** gives 4-aryl-5, 6-dihydro-6-(4′-hydroxy-6′-methyl-2′-oxopyran-3′-yl)-3-carbethoxy (or acetyl/or phenyl-2*H*-pyran-2-ones (**5c–f**) respectively. The IR spectra of compounds **5a** and **5b** showed bands at 1000, 1650, 1685, 2260–2980, and 3220 cm^{-1} attributable to stretching frequencies of C-O-C, C=O (α-pyrones), C=O (cyclohexenone), aliphatic CH, and OH respectively, while IR spectra of **5c** and **5d** showed an additional band at 1755 cm^{-1} due to νC=O of ester. The ^{1}H-NMR spectrum of **5a** in d_6–DMSO showed signals at δ 2.12 (*s*, 3H, C_6-COCH_3), 2.2 (*s*, 3H, C'_6-CH_3), 2.37 (*dd*, C_2-2H, C_5-H and C_6-H), 3.9 (*s*, 3H, $Ar-OCH_3$), 5.8 (*s*, 1H, C'_5-H), 6.2 (*d*, 1H, C_4-H), and 7.5 (*dd*, 4H, $Ar-H$). The ^{1}H-NMR spectrum of compound **5c** in d_6–DMSO showed signals at δ 1.7 (*t*, 3H, $C_3-COOC-CH_3$), 2.2 (*s*, 3H, C_4-COCH_3), 2.3 (*s*, 3H, C'_6-CH_3), 2.4–2.6 (*dd*, 2H, C_3-H and C_4-H), 3.9 (*s*, 3H, $Ar-OCH_3$), 4.3 (*q*, 2H, $C_3-COOCH_2-$), 5.7 (*s*, 1H, C'_5-H), 6.2 (*s*, 1H, C_5-H), and 7.5 (*dd*, 4H, $Ar-H$).

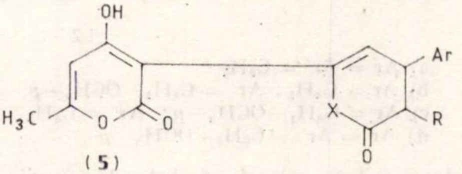

(5)

	X	R	Ar		X	R	Ar
a)	CH_2	$COCH_3$	$C_6H_4-OCH_3-p$	b)	CH_2	$COCH_3$	$C^2H_3-O_2CH_2-3{,}4-$
c)	O	$CO_2C_2H_5$	$C_6H_4-OCH_3-p$	d)	O	$CO_2C_2H_5$	$C_8H_4-NO_2-p$
e)	O	$COCH_3$	$C_6H_3-O_2CH_2-3{,}4-$	f)	O	C_6H_5	$H_6C_4-OCH_3-p$

EXPERIMENTAL

All melting points are uncorrected. The IR spectra were determined on a Unicam SP 200 G spectrometer using KBr wafer technique and the ^{1}H-NMR spectra were recorded on a Bruker WP-80 Cw spectrophotometer.

3,4-Diaryl-pentan-1-(4′-hydroxy-6′-methyl-oxopyran-3′-yl)-1,5-diones (2a – d)

To a solution of dehydroacetic acid (**1**) (0.012 mol) in alcoholic potassium hydroxide (2.0 g KOH in 50 mL ethanol), chalcones (0.01 mol) in ethanol (20 mL) were added and then the reaction mixture was allowed to stand 7 days at room temperature. The reaction mixture was poured into dilute hydrochloric acid, and the solid product which separated was filtered and crystallized from benzene-light petroleum mixture to give **2a – d** as colourless crystals (yields 50 – 53%)(cf. Table 1).

Table 1

Physical data of compounds **2 – 5**

Compound	m.p. °C	Mol. formula	Analysis % Calcd./Found		
			C	H	H
2a	95	$C_{23}H_{20}O_5$	73.40 73.53	5.32 5.23	— —
2b	91	$C_{24}H_{22}O_6$	70.94 71.03	5.42 5.37	— —
2c	100	$C_{24}H_{22}O_6$	70.94 70.88	5.42 5.36	— —
2d	88	$C_{25}H_{24}O_7$	68.81 69.02	5.50 5.43	— —
3a	128	$C_{15}H_{12}O_4$	70.31 70.25	4.67 4.71	— —
3b	203	$C_{16}H_{14}O_5$	67.13 67.04	4.89 4.92	— —
3c	185	$C_{16}H_{13}O_6$	63.79 63.82	4.32 4.27	— —
3d	243	$C_{15}H_{11}NO_6$	59.80 59.94	3.65 3.58	4.65 4.72
4a	178	$C_{21}H_{18}N_2O_3$	76.36 76.43	5.45 5.37	7.76 7.59
4b	148	$C_{22}H_{19}N_2O_4$	70.40 70.52	5.07 5.13	7.47 7.31
4c	186	$C_{22}H_{18}N_2O_5$	67.69 67.73	4.62 4.60	7.18 7.06
4d	208	$C_{21}H_{17}N_3O_5$	67.20 67.34	4.53 4.58	10.74 10.67
5a	201	$C_{21}H_{20}O_6$	68.48 68.32	5.43 5.51	— —
5b	231	$C_{21}H_{18}O_7$	65.97 66.11	4.71 4.68	— —
5c	206	$C_{21}H_{20}O_8$	63.00 63.12	5.00 4.78	— —
5d	249	$C_{20}H_{17}NO_9$	57.83 57.96	4.10 4.14	3.37 3.22
5e	236	$C_{20}H_{16}O_8$	62.50 62.63	4.17 4.13	— —
5f	208	$C_{24}H_{20}O_6$	71.29 71.34	4.95 4.82	— —

3-Cinnamoyl-4-hydroxy-6-methyl-2-pyrones (3a – d)

A solution of dehydroacetic acid (0.01 mol), aromatic aldehyde, namely benzaldehyde, anisaldehyde, piperonal, or *p*-nitrobenzaldehyde, piperidine (5 drops) in chloroform (30 mL) was refluxed for 4 hrs. The yellowish red product which separated after distillation the water-chloroform azeotrope was filtered off and recrystallized from benzene to give **3 a – d** respectively as yellow crystals (yields 56 – 62%) (cf. Table 1).

5-Aryl-1-phenyl-3-(4′-hydroxy-6′-methyl-2′-oxopyran-3′-yl)-2-pyrazolines (4a – d)

A solution of **3** (0.01 mol) and phenylhydrazine in acetic acid (30 mL) was refluxed for 6 hrs. The product which separated after concentration and cooling was filtered off and crystallized from acetic acid-ethanol mixture to give **4 a – d** as yellow to orange crystals (yields 42 – 56%) (cf. Table 1).

6-Acetyl-5-aryl-3(4′-hydroxy-6′-methyl-2′-oxopyran-3′-yl)-cyclohex-3-en-1-ones (5a and 5b), and 4-aryl-5,6-dihydro-6-(4′-hydroxy-6′-phenyl-2′-oxoypran-3′-yl)-3-carbethoxy(or acetyl/or phenyl)-2H-pyran-2-ones (5 c – f) :

A mixture of **4** (0.01 mol), acetyl acetone, diethyl malonate, ethyl acetoacetate, or ethyl phenyl acetate (0.012 mol), and sodium methoxide (0.022 mol) was heated in a sealed tube for 4 hrs at 170°. The mixture was poured into dilute hydrochloric acid. The solid product which separated was filtered and recrystallized from acetic acid-ethanol mixture to give **5 a – f** as pale yellow crystals (yields 38 – 47%) (cf. Table 1).

REFERENCES

[1] M. A. Hassan, A. A. Afifi and S. H. Eltamany, *Pakistan J. Sci., Ind. Res.*, **20**, 79 (1977).
[2] A. Sammour, A. Raouf, M. Elkasaby and M. A. Hassan, *J. Prakt.* Chem., **315**, 1175 (1973).
[3] A. Sammour, A. Raouf, M. Elkasaby and M. A. Hassan, *Acta Chim. Acad. Sci. Hung.*, **83**, 209 (1974).
[4] V. K. Mahesh and R. S. Gupta, *Indian J. Chem.*, **12**, 956 (1974).

Revue Roumaine de Chimie, **30**, *3*, 249–256 (1985)

CATALYTIC INFLUENCES IN ELECTROOXIDATION OF OLEFINS IN NON-AQUEOUS SOLUTIONS. III*

KINETIC STUDY OF DIISOBUTYLENE AND STYRENE OXIDATION

RADU VLĂDEA
The Polytehnic Institute "Traian Vuia" Timişoara, Blvd. 30 Decembrie No. 2, Romania

Received October 13, 1982

The kinetic study of diisobutylene and styrene anodic oxidation in acetonitrile or methanol gave evidence of the influence of concurrent electrosorption of solvent, olefin and supporting-electrolyte on the electrode process. The nature and the morphology of the electrodes also play an important role in the anodic oxidations of olefins.

The preparative scale electrolyses were only a first step in the electrode processes investigation for olefin oxidation using methanol as solvent. It was possible to point out very interesting conclusions about the influence of electrode material on the selectivity of olefin oxidation. Since the detailed knowledge of the electrode kinetics and the mechanism of olefins oxidation is not only of theoretical interest but will enable the electrochemist to optimize the process towards high selectivities and yields, an attempt to establish this mechanism for olefins oxidation in methanol was done.

The main products of diisobutylene oxidation have all the same molecular mass (142), and their structure suggests the idea of a common intermediate. In the same context are the results for styrene oxidation. Provided the rate determining step of the overall reaction is the formation of these intermediates, which is truthlikely from the electrochemical point of view, the influences of operating parameters on the current-voltage curves could give useful information on the kinetics and the mechanism of olefins oxidation.

A kinetic study of this process was very attractive too, as much controversial mechanisms are given.$^{1-6}$

According to their anodic half-wave potentials, one can distinguish between (anodically) strongly activated, weakly activated and unactivated olefins.

Activated and weakly activated olefins possess electron donating substituents like ether-, aromatic- and aliphatic groups which either by inductive or mesomeric effects decrease the HOMO-energy of the olefin and enhance thus the anodic attack on the olefinic double bond.

---

* Previous part in *Rev. Roumaine Chim.* **30**, 151 (1985).

Whereas unactivated olefins like propylene or butylene posssess half-wave potentials of approximately 3 to 2.7 V (all half-wave potentials measured in acetonitrile at Pt-anodes vs. SCE), weakly activated olefins are oxidized with $E_{1/2} = 1.2$ to 2 V, and strongly activated olefins have an $E_{1/2}$ below 1 V.[13] Strongly activated olefins i.e. p,p'-dimethoxystilbene or 1,4-diphenyl-butadiene-like highly conjugated aromates — are oxidized in two separate one-electron-waves, the first bearing a reversible character whereas the second is irreversible.[7,8]

Kinetic determinations were carried out in a previously reported equipment.[9] The applied voltage sweep rate was 1100 mV/min since at lower sweep rates irreproducible current/voltage waves were obtained. The solvents (acetonitrile and methanol), olefins and supporting electrolytes were of analytical grade (p.a.) or were purified in the laboratory. Acetonitrile has a wide anodic potential range, its upper limit being imposed by the supporting electrolyte only.[10] When $NaClO_4$ is used, this limit is +2.5 V vs. SCE.

In figures 1 and 2 are shown the current/voltage curves obtained on a platinum electrode in the system acetonitrile +sodium perchlorate, for different olefin amounts.

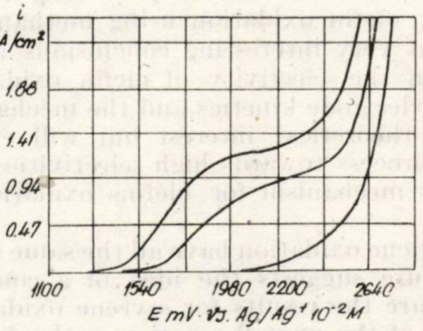

Fig. 1. — Current-potential curves for styrene oxidation in ACN + $NaClO_4$ (10^{-1}M/l) on platinized titanium: 1. ACN+$NaClO_4$; 2. ACN+$NaClO_4$ ($1.35.10^{-3}$M/l); 3. ACN+ $NaClO_4$ (1.10^{-2}M/l).

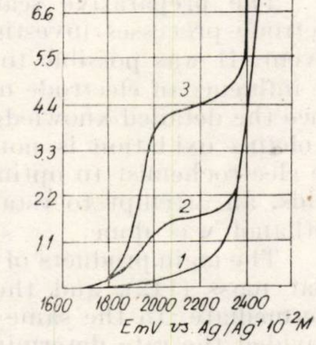

Fig. 2.—Current-potential curves for DIB oxidation in ACN + +$NaClO_4$ (10^{-1} M/l) on platinum electrode: 1. ACN + $NaClO_4$; 2. Ibid. 1 + $0.88.10^{-3}$ M/l DIB; 3. Ibid. 1+$1.35.10^{-3}$ M/l DIB.

Similar current/voltage curves were obtained on other electrodes such as the carbon one but with shifted half-wave potentials (Fig. 3).

For apparent half-wave potentials determination the Reilley and Murray method[11] was used. The method is recommended[8,12] especially for irreversible reactions. The relationship is

$$\ln \frac{i_d - i}{i} = -\frac{(1-\alpha)}{nRT}(E - E_{1/2}) \qquad (1)$$

where i_a — limiting current density, n — the number of electrons involved in the rate determinating step, α-charge-transfer coefficient, other symbols having usual signification.

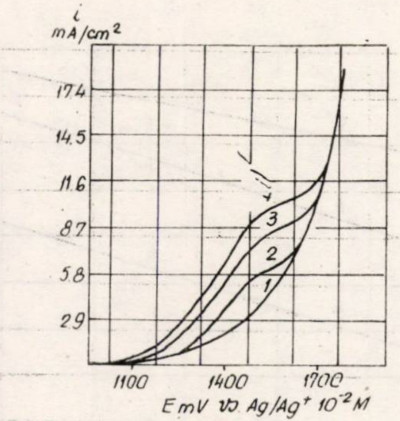

Fig. 3. — Current-potential curves for DIB oxidation in ACN + $NaClO_4$ (10^{-1}M/l) on carbon electrode: 1. ACN+ $NaClO_4$; 2. Ibid. 1 + $0.88.10^{-3}$ M/1; 3. Ibid. 1 + $1.35.10^{-3}$/M/1; 4. Ibid. 1 + $5.5.10^{-3}$ M/l.

The plotting $\ln (i_a - i)/i$ vs. E has led to the "apparent" half-wave potentials and the "apparent" charge-transfer coefficient (Fig. 4).

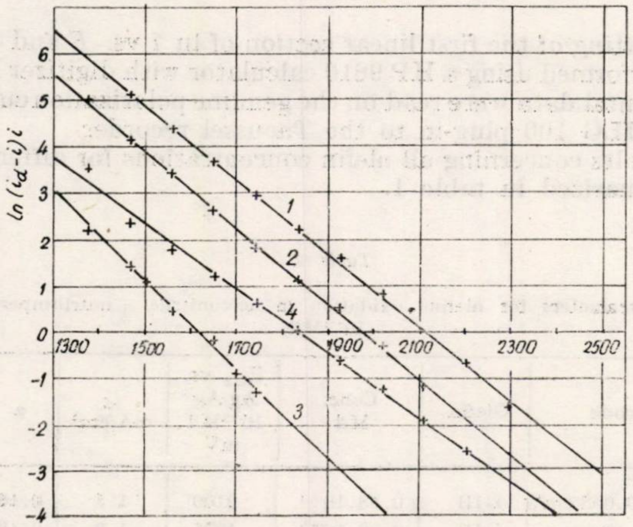

Fig. 4. — The plotting of $\ln(i_a - i)/i$ vs. E for DIB oxidation ($0.88.10^{-3}$ M/l) in ACN + $NaClO_4$:1. Platinum electrode : 2. Platinized titanium ; 3. Carbon electrode ; 4. PbO_2/C electrode.

It is evident from figure 4 that the anode material has a strong influence on the half-wave potentials.

In the range of pure charge-transfer the Tafel current-potential curves have been analyzed in order to obtain the kinetic parameters required to elucidate the reaction mechanism (Fig. 5).

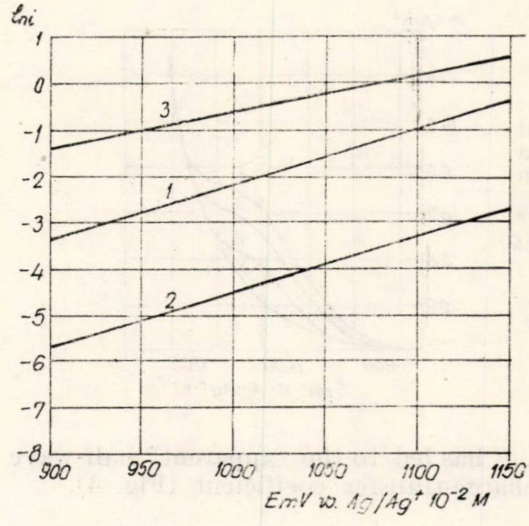

Fig. 5. — The plotting of ln *i* vs. *E* for styrene oxidation (1.10^{-2} M/l) in ACN + $NaClO_4(10^{-1}M/l)$: 1. Platinized titanium ; 2. PbO_2/C ; 3. Carbon.

The plotting of the first linear section of ln *i* vs. *E* and the calculations were performed using a HP 9810 calculator with digitizer and plotter. The experimental data were read on the genuine polarization curves obtained using a TILG 100 plug-in to the Tacussel recorder.

The results concerning all olefin concentrations for different electrodes are summarized in table 1.

Table 1

Kinetic parameters for olefine oxidation in acetonitrile + natriumperchlorate (10^{-1}M/l)

Electrode	Olefin	Conc. M/l	$E_{1/2}$ vs. Ag/Ag⁺ 10^{-2}M/l mV	i_d mA/cm²	α	ν
Platinum 0.088 cm²	DIB	$0.88.10^{-3}$	2100	1.8	0.18	0.64
Platinized titanium 0.17 cm²	DIB	$0.88.10^{-3}$	1975	1.9	0.19	0.71
Carbon 0.173 cm²	DIB	$0.88.10^{-3}$	1610	2.2	0.21	0.82
PbO_2/C 0.41 cm²	DIB	$0.88.10^{-3}$	1840	4.2	0.18	0.88
Platinized titanium 0.17 cm²	Styrene	1.10^{-2}	1590	8.5	0.31	0.71
Carbon 0.17 cm²	Styrene	1.10^{-2}	1540	11.0	0.30	0.92
PbO_2/C 0.41cm²	Styrene	1.10^{-2}	1470	26.0	0.20	0.87

The determination of the formal electrochemical reaction order for the olefin oxidation was possible by using the relationship :

$$\nu = \left(\frac{\partial \ln i}{\partial \ln c_{\mathrm{olef}}} \right) E, c_{\mathrm{solvent}} \qquad (2)$$

It is noteworthy to ascertain that in the acetonitrile-natrium perchlorate system the half-wave potentials vary both with the electrode materials and with the olefin nature. For instance, on platinized titanium $E_{1/2} = 1590$ mV for styrene and 1975 mV for DIB ; on carbon electrode $E_{1/2} = 1470$ mV for styrene and 1610 mV for DIB. At the same time, the half-wave potential is $E_{1/2} = 2100$ mV for DIB oxidation on platinum electrode and only 1610 mV on carbon. This obviously shows the great influence of the electrode material on the olefin oxidation and the direct involvement of the olefin in the electrode process.

The value of reaction order, very small on platinum electrode, suggests a stronger adsorption of the olefin on this electrode so that the oxidation process tends to become independent of the bulk olefin concentration.

The replacement of acetonitrile with methanol as solvent gives rise to essential modification in the electrode process. The polarisation curves on platinum electrode were shifted to more positive potentials with the increasing amounts of olefin (Fig. 6).

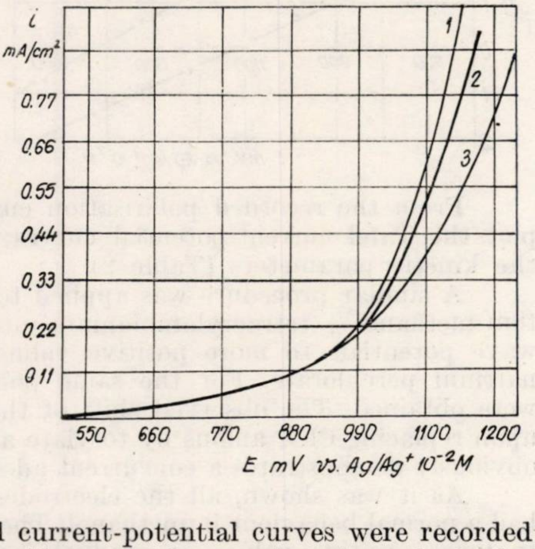

Fig. 6. — Current-potential curves for DIB oxidation in $CH_3OH + NaClO_4$ on platinum electrode : 1. $CH_3OH + NaClO_4$; 2,3 — increasing amounts of olefin.

On the other hand, normal current-potential curves were recorded on platinized titanium, lead dioxide on carbon and carbon electrodes but with different shapes (Fig. 7).

The plotting of $\ln(i_d - i)/i$ vs. E pointed out that, unlike acetonitrile, practically the same value for half-wave potentials irrespective of the olefin nature were obtained (Figs 8 and 9).

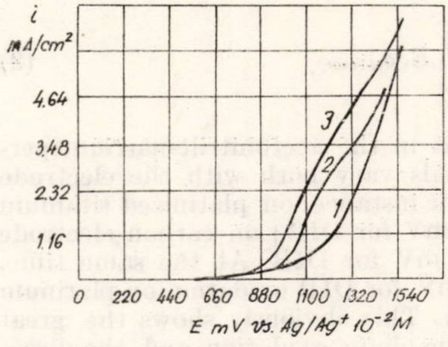

Fig. 7. — Current-potential curves for DIB oxidation in $CH_3OH + NaClO_4$ (10^{-1}M/l) on carbon electrode: 1. $CH_3OH + NaClO_4$; 2. Ibid. 1 + DIB $0.88 \cdot 10^{-3}$ M/l; 3. Ibid. 1 + DIB $1.35 \cdot 10^{-3}$ M/l.

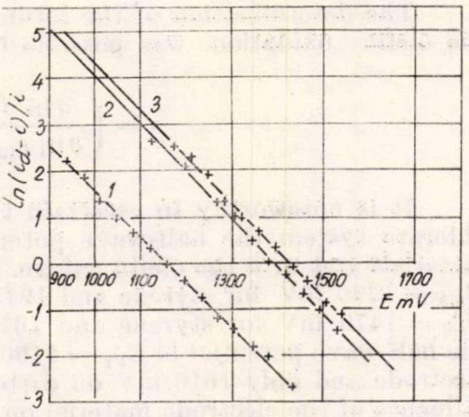

Fig. 8. — The plotting of $\ln(i_d - i)/i$ vs. E for DIB oxidation (2.10^{-3} M/l) on different electrodes, in methanol + sodium perchlorate (10^{-1}M/l): 1. Carbon; 2. PbO_2/C and 3. Platinized titanium.

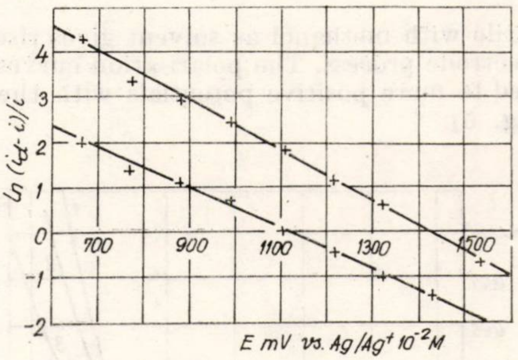

Fig. 9. — The plotting of $\ln(i_d - i)/i$ vs. E for styrene oxidation (1.10^{-1}M/l) in methanol + $NaClO_4$ (10^{-1} M/l) on: 1 Carbon electrode; 2. PbO_2/carbon.

From the recorded polarisation curve (Fig. 10) it was possible to plot the Tafel current-potential curves (Fig. 11), in order to calculate the kinetic parameters (Table 2).

A similar procedure was applied to the olefin oxidation in the system methanol + tetraetylammonium p-toluene-sulfonate. A shift of half-wave potentials to more positive values was observed compared with natrium perchlorate. For the same potentials, lower current densities were obtained. The observed shift of the apparent half-wave potentials upon replacing ClO_4^- anions by tosylate anions having aromatic character obviously demonstrates a concurrent adsorption on the electrode surface.

As it was shown, all the electrodes, excepting platinum electrode, had a normal behaviour in methanol. The shift of current-potential curves to more positive values at gradual increasing of olefin concentration suggests a hindering of the initial methanol oxidation either by polymeric insulating layers formation on the electrode surface[8.13] or by a strong chemosorption of olefins on the platinum electrode. The first assumption is rather difficult to accept in the case of a very stable and sterically hindered olefin like diisobutylene. On the other hand, an attempt for carrying out the anodic polymerization of styrene has failed. [14] There are a lot of arguments for olefin adsorption on platinum. [15] It was pointed out that an irreversible chemosorption takes place on the platinum surface, [16] the removal of olefins being impossible by washing or electrolysis, and requiring the use of strong oxidants.

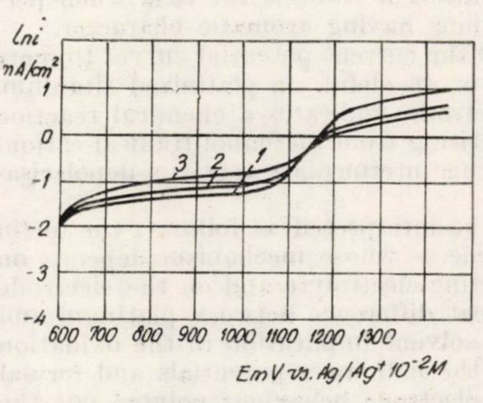

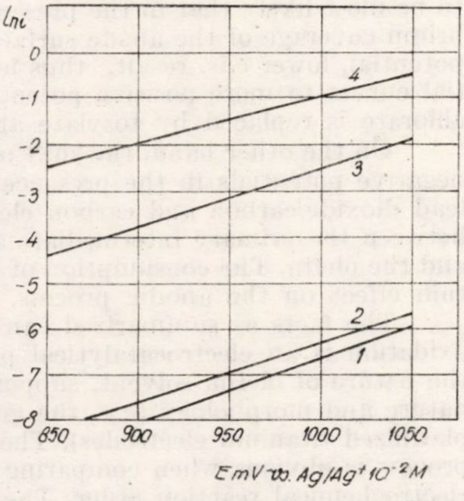

Fig. 10. — The recorded Tafel curves for DIB oxidation in CH_3OH + $NaClO_4$ (10^{-1} M/l) on carbon electrode: 1. +DIB 3.10^{-4} M/l; 2. + $5.2 \cdot 10^{-4}$ M/l; 3. + $8.4 \cdot 10^{-4}$ M/l.

Fig. 11. — The plotting of ln i vs. E for DIB oxidation in CH_3OH + $NaClO_4$ (10^{-1} M/l) on carbon electrode: 1. + $1.35 \cdot 10^{-3}$ M/l; 2. $4.85 \cdot 10^{-3}$ M/l; 3. 1.10^{-2} M/l; 4.1 10^{-1}M/l.

Table 2

Kinetic parameters for olefin oxidations in CH_3OH

Electrode	Olefin	Supporting electrolyte	α	ν
Platinum	DIB	$NaClO_4$	—	—
Platinized titanium	DIB	$NaClO_4$	0.20	0.85
Carbon	DIB	$NaClO_4$	0.12	0.91
PbO_2/C	DIB	$NaClO_4$	0.19	0.95
Carbon	DIB	$TsNEt_4$	0.31	0.88
PbO_2/C	DIB	$TsNEt_4$	0.40	0.91
Platinized titanium	Styrene	$NaClO_4$	0.22	0.83
Carbon	Styrene	$NaClO_4$	0.15	0.90
PbO_2/C	Styrene	$NaClO_4$	0.20	0.95
Platinized titanium	Styrene	$TsNEt_4$	0.20	0.81
Carbon	Styrene	$TsNEt_4$	0.34	0.88
PbO_2/C	Styrene	$TsNEt_4$	0.38	0.91

There are two generally accepted types of chemosorption[17] each of them becoming efficient under certain conditions : the *associative* model which assumes the double bond fission which is well accepted especially for maximum coverage, and the *disociative* chemosorption when the double bond is maintained and new Pt-H and Pt-H bonds are formed.

The electrosorption is a competing process among the present chemical species and is dependent upon the electrode potential. It seems to be most likely that in the presence of the olefins, the methanol equilibrium coverage of the anode surface, is decreased, and at constant overpotential, lower cds. result, thus leading to a shift of the current-potential curves to more positive potentials. The same is the case when perchlorate is replaced by tosylate anions having aromatic character.

On the other hand, the shift of the current-potential curves to more negative potentials in the presence of an olefin, on platinized titanium, lead dioxide/carbon and carbon electrodes indicates a chemical reaction between the primary intermediate arising from methanol (radical-cation) and the olefin. The consumption of this intermediate acts as a depolarisation effect on the anodic process.

The facts as summarized can be interpreted as follows: the olefin oxidation is an electrocatalytical process whose mechanism depends on the nature of olefin, solvent, supporting-electrolyte and on the electrode nature and morphology (e.g. the great difference between platinum and platinized titanium electrodes). The solvent implication in the oxidation process is obvious when comparing the half wave potentials and formal electrochemical reaction order. The electrode behaviour pointed out the influence of anode material on the chemosorption process.

REFERENCES

[1] T. Shono and A. Ikeda, *J. Amer. Chem. Soc.*, **94**, 7892 (1972).
[2] K. Sasaki, H. Urata and K. Uneyama, *Electrochim. Acta*, **12**, 137 (1967).
[3] H. Katz, Oe. Saygin and H. Wendt, *Electrochim. Acta*, **19**, 193 (1974).
[4] E. J. Rudd, M. Finkelstein and S. D. Ross, *J. Org. Chem.*, **37**, 1763 (1972).
[5] T. Shono and Y. Matsumura, *J. Amer. Chem. Soc.*, **91**, 2803 (1969).
[6] V. D. Parker and B. E. Burger, *Tetrahedron Lett.*, **1968**, 2415.
[7] V. D. Parker and L. Eberson *Chem. Comm.*, **1969**, 340.
[8] M. Katz, P. Riemenschneider and H. Wendt, *Electrochim. Acta*, **17**, 1595 (1972).
[9] R. Vlădea, Rev. Roumaine de Chim., **30**, 153(1985).
[10] L. Eberson and N. L. Weinberg, *Chem. Eng. News*, **49**, 40 (1971).
[11] C. N. Reilley and R. W. Murray, "Introduction to Electrochemical Techniques", in : "Treatise on Analytical Chemistry", Ed. Kolthoff, J.M. and Elving P. J., J. Wiley, New York, 1963, vol. IV, Part V, p. 2177.
[12] D. Koch, H. Schäfer and E. Steckan, *Chem. Ber.*, **107**, 3640 (1974).
[13] V. Plzak, H. Schneider and H. Wendt, *Ber. Bunsenges. physik. Chem.*, **78**, 1373 (1974).
[14] S. Goldschmidt and E. Stöckl, *Chem. Ber.*, **85**, 630 (1952).
[15] R. F. Lane and A. T. Hubbard, *J. Phys. Chem.*, **77**, 1401 (1973).
[16] E. Gileadi, "Electrosorption", Plenum Press, New York, 1967, p. 135.
[17] L. L. Holbrook and H. Wise, *J. Catalysis*, **38**, 294 (1973).

Revue Roumaine de Chimie, **30**, *3*, 257–265 (1985)

SOME CHEMICAL ASPECTS OF 5-ARYL-1,3,4-OXADIAZOLES

A.A. EL-BARBARY
Department of Chemistry, Faculty of Science, University of Tanta, Tanta, Egypt

Received February 15, 1983

Some 5-Aryl-1,3,4-oxadiazole-2-thiols, I, reacted with maleic anhydride, maleic acid and *p*-benzoquinone affording compounds II, III and IV, respectively. With amines compound V gave VI. With aromatic aldehydes VIe gave the corresponding chalcones, VII, which on bromination afforded the dibromo derivative VIII. Compound VII with hydroxylamine yielded IX a, b. With hydrazine hydrate in acetic acid VIIa, c, d gave Xa-c. Xa with benzaldehyde afforded XI. VIIa with acetylacetone and ethylacetoacetate gave XIIa and XIIb, respectively.

INTRODUCTION

For some time we have been occupied with the chemistry of 1,3,4-oxadiazoles[1–4] owing to their prominent use as pharmacological agents and also as intermediates in pharmaceutical industry.[5–10] In the present investigation the behaviour of certain 5-aryl-1,3,4-oxadiazoles towards a number of reagents, has been studied. The biological activity screenings will be published elsewhere.

RESULTS AND DISCUSSION

5-Aryl-1,3,4-oxadiazole-2-thiols (I)[1–3] reacted with maleic anhydride in anhydrous boiling xylene to give 5-aryl-1,3,4-oxadiazol-2-ylthio-succinic anhydrides, (IIa–c).

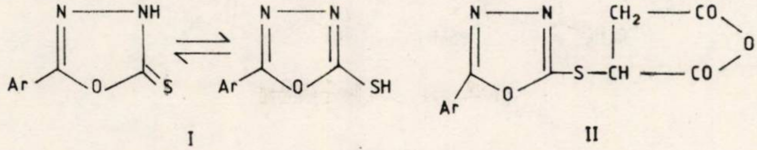
I
II

I, II; a, Ar=C_6H_5
b, Ar=$C_6H_4CH_3$–(p–)
c, Ar=C_6H_4Cl–(p–)

Compounds II were also obtained by the fusion of compounds I with maleic anhydride at 120°. Compounds II a and IIb could be hydrolysed to the corresponding dicarboxylic acids IIIa and IIIb, respectively. Also IIIa and IIIb were obtained by the reaction of compounds Ia and Ib with maleic acid in anhydrous boiling xylene.

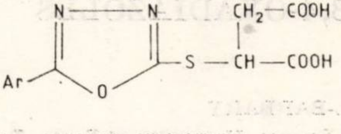

III

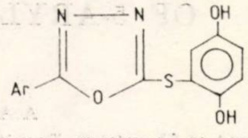

IV

a, $Ar=C_6H_5$

b, $Ar=C_6H_4CH_3-(p-)$

The structural proofs for II and III use spectroscopic data and elemental analyses. The IR spectrum of IIa showed a characteristic absorption at 1800 cm^{-1}(C=O). Compound IIIa showed the carboxylic absorption bands at 1710 cm^{-1} and 3000 cm^{-1}.The ^{1}H-NMR spectrum of IIIa showed the CH_2 protons (2H) as a doublet centered at δ3.20 ppm, the CH proton (1H) as a triplet centered at 4.85 ppm. The aromatic protons appeared as a multiplet at 7.50–8.15 ppm and the two OH protons as a singlet at 10.90 ppm. The mass spectrum of IIIa showed the molecular ion peak at *m*/*e* = 294 ($M^{+\cdot}$). The fragmentation of $M^{+\cdot}$ proceeds through elimination of H_2O to give the ion peak at 276 ($M^{+\cdot} - H_2O$).

Compounds Ia and Ib reacted with *p*-benzoquinone in anhydrous xylene at 140° to give 2-(2,5-dihydroxyphenylthio)-5-aryl-1,3,4-oxadiazoles, IVa and IVb, respectively.

The structure of compounds IV was supported by IR, ^{1}H-NMR, mass spectra and elemental analyses. In the IR spectrum of IVa, the OH band appeared at 3300 cm^{-1}. Its ^{1}H-NMR spectrum showed the two OH protons as a singlet at 10.70 ppm. The mass spectra of IVa and IVb showed the peaks at *m*/*e* 286 and 300 ($M^{+\cdot}$), respectively. The peaks $M^{+\cdot}$–OH and $M^{+\cdot}$–20H were also observed in the MS of IVa and IVb.

2-Methylthio-5-phenyl-1,3,4-oxadiazole (V) (prepared according to known methods[11,12]) reacted with different amines giving compounds VI.[13]

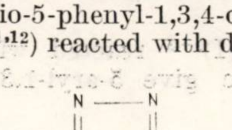

V

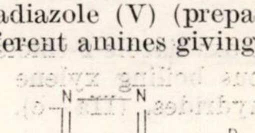

VI

a, $R=H$; $R_1=C_2H_5$

b, $R=H$; $R_1=C_6H_5$

c, $R=C_2H_5$; $R_1=C_2H_5$

d, $R=H$; $R_1=NH\ C_6H_5$

e, $R=H$; $R_1=C_6H_4\ COCH_3(p-)$

The structure of compounds VI was confirmed by the spectral data and elemental analyses. The IR spectrum of VIa showed absorption bands at 3300 cm^{-1}(NH) and at 1640 cm^{-1} (C=N). In the IR spectrum of VIe the C=O group absorption appeared at 1675 cm^{-1} and the NH group one at 3310 cm^{-1}. The mass spectra of VIa and VIe showed the molecular ion peaks at *m/e* 189 and *m/e* 279, respectively. In MS of VIa, peaks at *m/e* 160 ($M^+_\circ - C_2H_5$), *m/e* 112 ($M^+_\circ - C_6H_5$) could be assigned. In MS of VIe, peaks at *m/e* 264 ($M^+_\circ - CH_3$), 236 ($M^+_\circ - CH_3.CO$), and 159 ($M^+_\circ -$ $-C_6H_5COCH_3$) were observed.

Compound VIe condensed with some aromatic aldehydes in ethanolic potassium hydroxide to give 2-(*p*-cinnamoylanilino)-5-phenyl-1,3,4-oxadiazoles (VII). Reaction of compounds VIIa and VIIb with bromine in chloroform at room temperature afforded the corresponding dibromo derivatives VIIIa and VIIIb, respectively. [13]

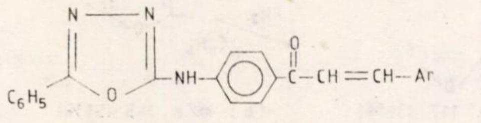

VII

a, $Ar=C_6H_5$
b, $Ar=C_6H_4OH(p-)$
c, $Ar=C_6H_4Cl(p-)$
d, $Ar=C_6H_4NO_2(p-)$
e, $Ar=C_6H_5B_r(p\_)$

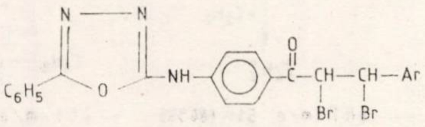

VIII

a, $Ar=C_6H_5$
b, $Ar=C_6H_4Cl(p-)$

The IR spectra of VIIa and VIIIa showed absorption bands at 1650 cm^{-1} and 1660 cm^{-1} (C=O) and 3200 cm^{-1} and 3300 cm^{-1}(NH), respectively. The MS spectrum of VIIa showed *m/e* at 367 ($M^+_\circ$).

The mass spectrum of VIIIa ($C_{23}H_{17}Br_2\ N_3O_2$) brought an additional evidence for the assigned structure. It reveals the presence of the peaks at *m/e* 527, *m/e* 529, and *m/e* 531, of relative abundance : 1 : 2 : 1 characteristic for the presence of two bromine atoms. The fragmentation of $M^+_\circ$ 527 (100%) involves fission in the molecule and depict ion (a) at *m/e* 173 (27%). This ion suffers loss of carbon monoxide to produce ion (b) at *m/e* 145 (51%), which loses N_2 to give the ion (c) at *m/e* 117 (39%). Also the fragmentation of the parent $M^+_\circ$. at *m/e* 527 involves debromination to furnish species (d) at *m/e* 447 (29%) and species (e) at *m/e* 367 (45%). In addition the ion (f) at *m/e* 105 (73%) could be seen which suffers loss of carbon monoxide to give the ion (g) at *m/e* 77 (38%). This new ion loses acetylene to give the ion (h) at *m/e* 51 (64%). Another ion (i) ($M^+_\circ -$ Ph) at *m/e* 450 (29%) was also observed.

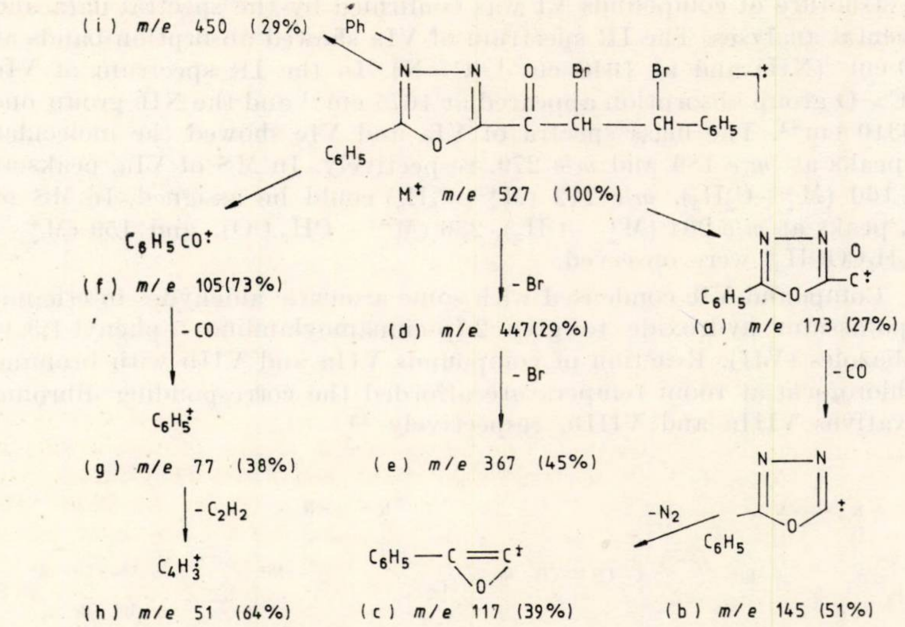
(i) m/e 450 (29%)
Ph
N—N
O
Br
Br
C—CH—CH—C6H5
O
C6H5
M+ m/e 527 (100%)
C6H5CO+
(f) m/e 105 (73%)
-CO
-Br
(d) m/e 447 (29%)
-Br
N—N
O
C+
C6H5
O
(a) m/e 173 (27%)
-CO
C6H5+
(g) m/e 77 (38%)
(e) m/e 367 (45%)
N—N
-C2H2
-N2
O
C6H5
C4H3+
C6H5—C=C+
O
(h) m/e 51 (64%)
(c) m/e 117 (39%)
(b) m/e 145 (51%)

Compounds VIIa and VIIc reacted with hydroxylamine to give 2-[4-(2-aryl-1,2-Δ^2-oxazolin-3-yl) anilino]-5-phenyl-1,3,4-oxadiazoles (IXa and IXb), respectively.

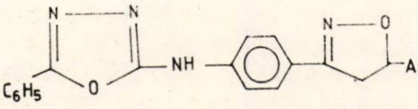
N—N
N—O
NH
Ar
C6H5
O

IX

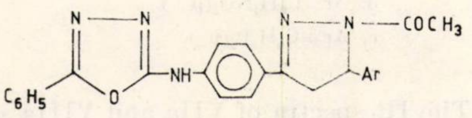
N—N
N—N—COCH3
NH
Ar
C6H5
O

X

a, Ar = C_6H_5
b, Ar = $C_6H_4Cl(p-)$

a, Ar = C_6H_5
b, Ar = $C_6H_4Cl(p-)$
c, Ar = $C_6H_4NO_2(p-)$

The ^{1}H-NMR spectrum of compound IXa showed the CH proton (1H) of the oxazole ring as a triplet centered at 4.80 ppm, the CH_2 protons (2H) as a doublet at 3.85 ppm, the NH proton (1H) as a broad singlet at 4.40 ppm and the aromatic protons (13H) as a multiplet at 6.70–8.15 ppm region. The mass spectrum of IXa showed the presence of the molecular ion peak at m/e 382 ($M^{+\cdot}$). The fragmentation of $M^{+\cdot}$ gives the ions at m/e 306 ($M^{+\cdot}-C_6H_5$) and m/e 277 ($M^{+\cdot}-C_6H_5CO$).

Compounds VIIa, c, d reacted with hydrazine hydrate in acetic acid to give 2-[4-(2-aryl-1,2-Δ^2-pyrazoline-3-yl) anilino]-5-phenyl-1,3,4-oxadiazoles (Xa-c). Condensation of Xa with benzaldehyde in boiling ethanolic potassium hydroxide afforded compound XI.[13]

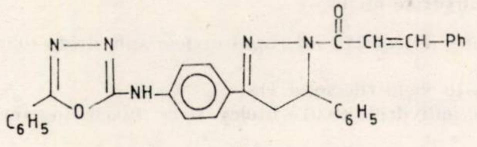

XI

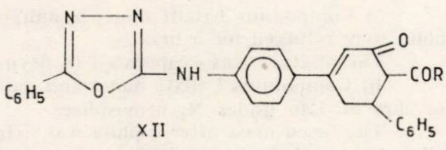

XII

a, $R=CH_3$
b, $R=OC_2H_5$
c, $R=OH$

The structure of compounds X and XI was confirmed by spectral data and elemental analyses. The IR spectrum of Xa showed absorption bands at 1630 cm^{-1} (CON), and 3200 cm^{-1} (NH). The ^{1}H-NMR spectrum of Xa showed the $NCH-C_6H_5$ proton (1H) as a triplet at δ2.90 ppm, the CH_2 protons (2H) as a doublet at 3.45 ppm and the aromatic protons (14H) as a multiplet at 7.10–8.20 ppm. The mass spectra of Xa and Xb showed the peaks at *m/e* 423 and 457 (M^{+}), respectively. The peaks $M^{+}-CH_3$ and $M^{+}-COCH_3$ were observed in the MS of Xa and Xb.

The IR spectrum of XI showed the CO absorption band at 1680 cm^{-1} and the NH one at 3210 cm^{-1}. Its MS spectrum showed the molecularion peak at 512 (M^{+}).

Furthermore, the action of acetylacetone and ethyl acetoacetate in sodium methoxide, on VIIa was investigated. The reactions afforded compounds XIIa and XIIb,[13] respectively.

The structure of compounds XII is inferred, beside IR, mass spectra and elemental analyses from the hydrolysis of compound XIIb with sodium hydroxide yielding the corresponding acid XIIc. The IR spectra of XIIa and XIIb showed absorption bands at 1655 and 1650 cm^{-1} (CO), at 1675 cm^{-1}($COCH_3$), 1770cm^{-1} ($COOC_2H_5$), and the NH band at 3290 cm^{-1} and 3280 cm^{-1}, respectively. The mass spectrum of XIIb showed the molecular ion peak at *m/e* 466 (M^{+}). The ions at *m/e* 421 ($M^{+}-OC_2H_5$), *m/e* 393 ($M^{+}-COOC_2H_5$) and at *m/e* 361 ($M^{+}-C_6H_5CO$) were observed. The IR spectrum of compound XIIc showed the absorption bands at 1655 cm^{-1} (C=O) and the carboxylic absorption bands at 1710 cm^{-1} and 3000 cm^{-1}.

EXPERIMENTAL

IR spectra were recorded using a UNICAM S.P. 1200 spectrophotometer. The KBr pellets technique was used. ^{1}H-NMR spectra were recorded at 60 MHz on a Varian EM-360 spectrometer; $CDCl_3$ was used as a solvent and TMS as internal reference standard. Chemical shifts are expressed as δ values. Mass spectra were recorded on a Micromass 7070F mass spectrometer operating at 70 eV using direct inlet. Elemental analyses were carried out by the Microanalytical Laboratory of the National Research Centre, Cairo, A.R.E. All melting points are uncorrected.

Starting materials

The starting compounds were prepared by known methods : Ia – Ic[1-3,14,15], V[11,12].

Action of maleic anhydride on Ia – c

a) Compounds I (0.01 mole) in anhydrous xylene (10 mL) and maleic anhydride (0.01 mole) were refluxed for 5 hrs.

The mixture was evaporated to dryness to yield the solid IIa-c.

b) Compounds I (0.01 mole) and maleic anhydride (0.015 mole) were fused together for 2hrs at 120° under N_2 atmosphere.

The fused mass after cooling was extracted with benzene. The solvent was evaporated till dryness and the residual solid was recrystallised from the proper solvent (Table 1). All had the same melting points and mixed m.p.'s as those prepared by method a.

Preparation of 5-Aryl-1,3,4-oxadiazol-2-yl-thiosuccinic acids (III a, b)

Method a : Compounds I (0.01 mole) in anhydrous xylene (10 mL) and maleic acd (0.01 mole) were refluxed for 5 hrs. The mixture was evaporated to dryness to yield the solid IIIa,b (Table 1).

Method b : *Hydrolysis of IIa and IIb*

A suspension of IIa,b (0.01 mole) in 20 mL of water was refluxed for 3 hrs. The precipitate was filtered off and crystallised to give compounds IIIa,b. Both had the same melting points and mixed m.p.'s as those prepared by method a.

Attempts to obtain the acid by alkaline (NaOH) hydrolysis of the anhydride IIa led to the formation of 5-phenyl-1,3,4-oxadiazole-2-one (m.p. and mixed m.p.).[16]

Action of *p*-benzoquinone on Ia and Ib

Compounds I (0.01 mole) in anhydrous xylene (10 mL) and *p*-benzoquinone (0.01 mole) were refluxed for 8 hrs. The solvent was decanted and distilled under reduced pressure. The residual solid was crystallised to give IV (Table 1).

Table 1

Experimental and analytical data of the products II – IV

Product	M.P. (°C)	Sol-vent*	Yield (%)	Analyses Calcd/Found (%)			
				C	H	N	S
IIa	161	E	72	52.17 52.00	2.90 3.11	10.14 10.21	11.59 11.78
IIb	154	E	69	53.79 53.68	3.45 3.41	9.66 9.50	11.03 10.89
IIc	141	M	75	46.45 46.40	2.26 2.21	9.03 8.91	10.32 10.21
IIIa	130	P	72	48.98 49.30	3.40 3.31	9.52 8.99	10.88 10.75
IIIb	124	P	67	50.65 50.50	3.89 3.81	9.09 8.89	10.39 10.82
IVa	143	E	66	58.74 58.83	3.50 3.41	9.79 9.64	11.19 11.03
IVb	157	M	70	60.00 60.21	4.00 3.91	9.33 9.25	10.66 10.49

*E = ethanol ; M = methanol ; P = petroleum ether

Action of amines on V

A mixture of compound V (0.01 mole) and the appropriate amine (0.01 mole) in ethanol (20 mL) was refluxed for 3 hrs.

The ethanol was distilled off and the residual solid was filtered off and crystallised from the proper solvent (Table 2).

Compound VIe was prepared by heating a mixture of V (0.01 mole) with *p*-aminoacetophenone (0.01 mole) at 150°C for 1 hr. The reaction product was collected and crystallised (Table 2).

Table 2

Experimental and analytical data of products VI

Product	M.P. (°C)	Solvent*	Yield (%)	Analyses Calcd/Found(%)		
				C	H	N
VIa	71	D	78	63.49 63.37	5.82 5.81	22.22 22.10
VIb	153	D	81	70.88 71.00	4.64 4.61	17.72 17.63
VIc	92	E	74	66.35 66.28	6.91 6.84	19.35 19.24
VId	173	M	83	66.66 66.54	4.76 4.70	22.22 22.04
VIe	195	D	71	68.81 69.00	4.66 4.49	15.05 15.00

*D = dioxane ; E = ethanol ; M = methanol

Action of aldehydes on VIe

The aromatic aldehyde (0.012 mole) was added dropwise to a solution of VIe (0.01 mole) in 20 mL ethanolic potassium hydroxide (5%). The mixture was refluxed for 3 hrs and then evaporated to a small volume and cooled. The solid that separated was filtered off and recrystallised from the proper solvent (Table 3).

Table 3

Experimental and analytical data of the products VII and VIII

Product	M.P. (°C)	Solvent*	Yield (%)	Analyses Calcd/Found(%)			
				C	H	N	Halogen
VIIa	201	D	60	75.20 75.13	4.63 4.70	11.44 11.35	— —
VIIb	209	M	63	72.06 72.19	4.43 4.32	10.97 10.85	— —
VIIc	198	E	69	68.82 68.65	3.99 4.00	10.47 10.39	8.72 8.68
VIId	220	E	80	66.99 67.14	3.88 3.80	13.59 13.65	— —
VIIe	233	P	78	61.88 61.80	3.59 3.49	9.41 9.34	17.93 17.78
VIIIa	179	E	64	52.37 52.44	3.23 3.20	7.97 7.84	30.36 30.51
VIIIb	192	B	59	49.19 49.15	2.85 2.81	7.49 7.39	28.52 28.70

D* = dioxane ; M = methanol ; E = ethanol ; P = petroleum ether ; B = benzene

Bromination of VIIa and VIIb

Bromine (0.01 mole) was added dropwise to a solution of compounds VII (0.01 mole) in chloroform (20 mL) with stirring at room temperature for 1 hr, left overnight and evaporated under vaccum. The residual solid was crystallised from the proper solvent (Table 3).

Action of hydroxylamine on VIIa and VIIb

A mixture of compounds VIIa, b (0.01 mole), hydroxylamine hydrochloride (0.01 mole) and sodium hydroxide (0.1 g) in ethanol (20 mL) was refluxed for 3 hrs. The reaction mixture was poured into cold water and the solid formed was collected and crystallised (Table 4).

Action of hydrazine hydrate on VIIa – c

Compounds VII (0.01 mole) in acetic acid (10 mL) and hydrazine hydrate (0.5g, 98 %; 0.01 mole) were refluxed for 5 hrs, cooled and then poured into water. The solid formed was filtered off and crystallised (Table 4).

Action of benzaldehyde on Xa

Benzaldehyde (0.012 mole) was added dropwise to a solution of Xa (0.01 mole) in 10 mL ethanolic potassium hydroxide (5%). The mixture was refluxed for 5 hrs, then concentrated and cooled. The residual solid was filtered off and crystallised (Table 4).

Action of acetylacetone and ethyl acetoacetate on VIIa and VIIb

Compounds V (0.01 mole) in sodium methoxide (prepared from 0.5 g sodium metal in 10 mL methanol) and acetylacetone or ethyl acetoacetate (0.01 mole) were refluxed for 6 hrs. The reaction mixture was cooled to room temperature, then poured into water. The residual solid was collected and crystallised (Table 4).

Table 4

Experimental and analytical data of products IX – XII

Product	M.P. (°C)	Solvent*	Yield (%)	Analyses Calcd/Found (%)			
				C	H	N	Halogen
IXa	178	E	57	72.25 72.11	4.71 4.63	14.66 14.58	
IXb	188	E	61	66.35 66.10	4.09 4.00	13.46 13.29	Cl 8.52 Cl 8.39
Xa	210	M	64	70.92 71.14	4.96 4.90	16.55 16.39	
Xb	217	E	63	65.65 65.50	4.38 4.31	15.32 15.41	Cl 7.66 Cl 7.31
Xc	250	M	59	64.10 64.21	4.27 4.18	17.95 18.12	
XI	293	P	73	72.66 72.71	4.30 4.21	13.67 13.52	
XIIa	225	P	75	74.83 74.70	5.12 5.00	9.35 9.21	
XIIb	183	M	80	72.65 72.50	5.22 5.09	8.77 8.68	
XIIc	204	M	91	71.84 71.92	4.66 4.71	9.31 9.44	

E = Ethanol, M = Methanol, P = Petroleum ether.

Hydrolysis of compound XIIb

Compound XIIb (0.01 mole) was refluxed in methanolic sodium hydroxide (20 mL, 7%) for 3 hrs. On acidification a solid was precipitated that crystallised (Table 4).

REFERENCES

[1] A. A. El-Barbary, M. Anwar, A. A. Ghattas and A. F. Hashem, *Rev. Roumaine Chim.*, **26**, 449 (1981).
[2] M. Anwar, A. A. El-Barbary, A. A. Ghattas and A. F. Hashem, *Polish J. Chem.*, **55**, 599 (1981).
[3] A. A. El-Barbary and M. El-Borai, *Polish J. Chem.* (In Press).
[4] A. A. El-Barbary and H. Hammouda, *Arch. Pharm.* (In Press).
[5] A. E. Wilder-Smith, E. Frommel, S. Radouco — Thomas, *Arznemittel Forsch.*, **13**, 338 (1963).
[6] A. E.-Wilder-Smith, *Hungarian Patent* 159, 568 (1963), *C.A.* **61**, 3118 (1964).
[7] J. J. Goodman, M. Matrishim. R. W. Young, and J. R. McCormick, *J. Bacteriol.*, **78**, 492 (1959).
[8] M. A. Salama, F. A. Moti, A. A. Ghattas, *Bull. NRC, Egypt*, **3**, 87 (1978).
[9] T. R. Vakula and V. R. Srinivasan, *Ind. J. Chem.*, **7**, 583 (1969).
[10] F. M. E. Abdel-Meegeid, M. A.-F. Elkaschef and A. A. Ghattas, *Egypt. J. Chem.*, **20**, 235 (1977), *ibid.*, **20**, 279 (1977).
[11] J. H. Boyer, in "Heterocyclic Compounds" (R. C. Elderfield, ed.), Vol. 7, Wiley, New York, p. 525 (1961); L. G. Behr, in "Five and Six-membered Compounds with Nitrogen and Oxygen" Vol. 17 of "The Chemistry of Heterocyclic Compounds" (R.H. Wiley, ed.), (Interscience), p. 268, 1962.
[12] M. Hashimoto and M. Ohta, *Bull. Chem. Soc., Japan*, **33**, 1394 (1960).
[13] N. M. Yousif, *Doctoral Thesis, University of Cairo* (1981).
[14] E. Hoggarth, *J. Chem. Soc.*, (1952) 4811.
[15] R. W. Young and K. H. Wood, *J. Amer. Chem. Soc.*, **77**, 4400 (1955).
[16] T. Sato and M. Ohta, *J. Pharm. Soc. Japan*, **75**, 1535 (1955).

Revue Roumaine de Chimie, **30**, *3*, 267–271 (1985)

SYNTHESIS AND SOME REACTIONS OF ACETYL-CYCLOHEXENONE DERIVATIVES

I. A. ATTIA and E. A. SOLIMAN
Chemistry Department, Faculty of Science, Ain Shams University, Abbassia, Cairo, Egypt

Received March 21, 1984

β-Tetroylacrylic acid (I) reacts with acetyl-acetone under Michael condition to give the corresponding cyclohexenone derivative II. Reactions of II with hydrazine hydrate in boiling alcohol, acetic, formic, propionic or butyric acid, as well as reaction with phenylhydrazine, hydroxylamine hydrochloride, urea and thiourea have been investigated. Reduction of indazole derivatives IV, benzoylation, sulphonation and nitrosation of indazole III have been also described.

As a sequel to our recent studies [1–3] we present some new reactions of acetyl-cyclohexenone derivatives. β-Tetroylacrylic acid (I) under Michael conditions gives 6-acetyl-5-oxo-3-tetroyl-3-cyclohexene-1-carboxylic acid (II) which easily condenses with hydrazine hydrate in boiling ethanol to give 4,5-dihydro-3-methyl-6-tetralyl-1H-indazol-4-carboxylic acid (III).

Refluxing compound III in different acids, like formic, acetic, propionic or *n*-butyric acid [4] caused replacement of the active hydrogen of imino group in indazol ring by acyl group giving 1-formyl, 1-acetyl, 1-propionyl and 1-*n*-butyryl-4,5-dihydro-3-methyl-6-tetralyl-1H-indazol-4-carboxylic acids (IVa-d) respectively.

Structures of IVa-d were confirmed by reacting cyclohexenone (II) directly with hydrazine hydrate in boiling formic, acetic, propionic or *n*-butyric acid. Reduction [5] of compounds IVa,b, by lithium aluminium hydride in ether gave 1-methyl and 1-ethyl-4,5-dihydro-3-methyl-6-tetralyl-1H-indazol-4-carboxylic acids V and VI respectively.

Heating III with benzoyl chloride gave 1-benzoyl derivative VII, whereas treatment of III with sodium nitrite and hydrochloric acid gave rise to the corresponding 1-nitroso derivative VIII. Compound III reacts with benzene-sulphonyl chloride to give the corresponding sulphone derivative IX. Similarly, condensation of II with phenyl hydrazine in boiling ethanol or acetic acid afforded the same product 1-phenyl-4,5-dihydro-3-methyl-6-tetralyl-1H-indazol-4-carboxylic acid (X). 4,5-Dihydro-3-methyl-6-tetralyl-1,2-benzisoxazole-4-carboxylic acid XI was obtained by the reaction of II with hydroxylamine hydrochloride in pyridine. Quinazoline derivatives XII and XIII were prepared by reaction of II with thiourea and urea in boiling ethanol and a few drops of glacial acetic acid.

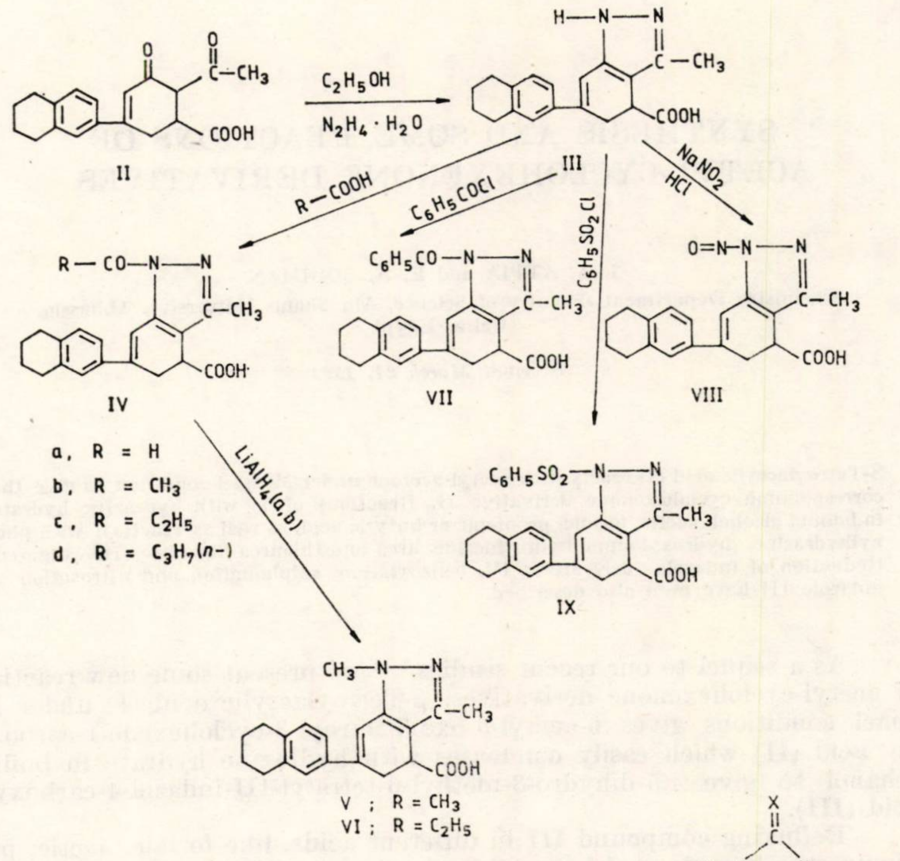
II
C_2H_5OH
$N_2H_4 \cdot H_2O$
III
R—COOH
C_6H_5COCl
$C_6H_5SO_2Cl$
$NaNO_2$
HCl
IV
a, R = H
b, R = CH_3
c, R = C_2H_5
d, R = $C_3H_7(n-)$
VII
VIII
$LiAlH_4(a,b)$
IX
V ; R = CH_3
VI ; R = C_2H_5
X
XI
XII X = S
XIII X = O

EXPERIMENTAL

The IR spectra were determined with a Unicam SP. 1200 Spectrophotometer using KBr wafer technique. All melting points are uncorrected.

Cycloaddition of acetylacetone to β-tetroyl-acrylic acid. Formation of (II)

A mixture of β-tetroyl acrylic acid (0.01 mole), acetylacetone (0.01 mole) and sodium methoxide (0.015 mole) was fused in an oil bath at 150°C for 6 hrs. The reaction mixture was poured into water to get rid of unreacted organic materials. The aqueous layer was acidified with diluted hydrochloric acid. The precipitate was crystallized from a mixture of toluene and ethanol to give II as yellow crystals (cf. Table 1).

Table 1

The physical and IR data of new compounds II–XIII

Compd	M.p. °C	Solvent* (yield) %	Formula	Analyses %		IR-Group frequencies (KBr; cm^{-1})		
				Found	Required			
II	185	T/E (60)	$C_{19}H_{20}O_4$	C, 72.92 H, 6.22	73.07 6.44	νC=O, 1670 1690 1725	νOH, 3430	νCH_2 2690
III	263–4	E/B (80)	$C_{19}H_{20}O_2N_2$	C, 73.94 H, 6.42 N, 8.92	74.03 6.49 9.69	νC=O, 1720	νOH, NH 3420	νC=N 1690
IVa	275–6	E/T (60)	$C_{20}H_{20}O_3N_2$	C, 71.23 H, 5.64 N, 8.11	71.42 5.95 8.23	νC=O 1670 1710	νC=N, 1650	νOH 3420
IVb	291–2	E/T (80) (80)	$C_{21}H_{22}O_3N_3$	C, 71.92 H, 5.94 N, 7.92	72.00 6.28 8.00	νC=O, 1660	νC=N, 1630,	νOH 3280
IVc	300	E/T (70)	$C_{22}H_{24}O_3N_2$	C, 72.22 H, 6.34 N, 7.44	72.51 6.59 7.69	νC=O, 1660, 1725	νC=N, 1640	νOH 3360
IVd	222–3	E/T (60)	$C_{23}H_{26}O_3N_2$	C, 73.00 H, 6.44 N, 7.20	73.11 6.87 7.42	νC=O, 1680, 1795	νC=N, 1640,	νOH 3410
V	234–5	E/B (50)	$C_{20}H_{22}O_2N_2$	C, 74.22 H, 6.64 N, 8.54	74.53 6.83 8.64	νC=O, 1725	νC=N, 1650	νOH 3440
VI	250–1	B (40)	$C_{21}H_{24}O_2N_2$	C, 74.83 H, 6.93 N, 8.32	75.00 7.14 8.36	νC=O, 1715	νC=N 1660	νOH 3890
VII	257–8	B (45)	$C_{26}H_{24}O_3N_2$	C, 75.54 H, 5.63 N, 6.53	75.72 5.88 6.79	νC=O, 1670 1700	νC=N, 1650	νO H 3340
VIII	286	E (60)	$C_{19}H_{19}O_3N_3$	C, 67.42 H, 5.42 N, 12.22	67.65 5.65 12.46	νC=O 1720	νC=N 1640	νOH 3280
IX	280–1	E (75)	$C_{25}H_{24}O_4N_2S$	C, 66.74 H, 5.12 N, 5.98	66.96 5.35 6.25	νC=O, 1725	νC=N, 1630	νOH 3422
X	220	T/E (45)	$C_{25}H_{24}O_2N_2$	C, 77.89 H, 6.11 N, 7.15	78.12 6.25 7.29	νC=O, 1710,	νC=N, 1640	νOH 3620
XI	192–3	B (65)	$C_{19}H_{17}O_3N$	C, 74.26 H, 5.53 N, 4.56	74.08 5.33 4.85	νC=O 1720	νC=N 1660	νOH 4330
XII	167–8	E (55)	$C_{20}H_{20}O_2N_2S$	C, 67.94 H, 5.54 N, 7.66 S, 9,09	68.18 5.68 7.95 8.76	νC=O, 1715 C=N 1630	νC=S, 1530	νOH, NH 3380
XIII	175–6	B (50)	$C_{20}H_{20}O_3N_2$	C, 71.22 H, 5.82 N, 7.99	71.40 5.95 8.83	νC=O, 1680 1720	νOH, NH 3470	νC=N 1640

* B = Benzene E = Ethanol T = Toluene

Reaction of II with hydrazine hydrate. Formation of III and IVa-d

To a solution of II (0.01 mole) in ethanol, formic, acetic, propionic or *n*-butyric acid (0.01 mole), hydrazine hydrate (0.01 mole) was added and the reaction mixture was refluxed for 5 hrs. After cooling the solid separated was crystallized from a proper solvent to give the indazole derivatives III and IVa-d (cf. Table 1).

Alternate synthesis of IVa-d

To a solution of III (0.01 mole) in 20 mL of formic, acetic, propionic, or *n*-butyric acid, 0.01 mole of hydrazine hydrate was added and the mixture was refluxed for 5 hrs. The solid that separated after concentration and cooling was crystallized from a proper solvent to give compounds, which were found to be identical by melting point and mixed melting point determination with IVa-d. (cf. Table 1).

Reduction of compounds IVa, b with lithium aluminium hydride. Formation of V and VI

A solution of IVa, b(0.01 mole) and lithium aluminium hydride (0.1 mole) in dry ether (20 mL) was refluxed on water bath for 5 hrs and filtered while hot. The solid product obtained after evaporation of the solvent was crystallized from proper solvent to give the corresponding 1-alkyl derivatives V and VI respectively (cf. Table 1).

Action of benzoyl chloride and benzene sulphonyl chloride on III. Formation of VII and IX

A solution of III (0.01 mole) in pyridine (10 mL) was treated with (0.01 mole) of benzoyl- or benzene sulphonyl chloride. The reaction mixture was heated on water bath for 2 hrs, then cooled and poured into dil. HCl. The precipitate thus obtained was crystallized from a proper solvent to give the corresponding benzoyl and sulphonyl derivatives VII and IX respectively (cf. Table 1).

Nitrosation of III. Formation of VIII

A solution of III (0.01 mole) in hydrochloric acid (8 mL) was mixed with a concentrated solution of sodium nitrite. The whole mixture was refluxed for 1/2hr on water bath. The solid that separated on cooling was filtered and crystallized from ethanol to give the nitroso derivative VIII as yellow crystals (cf. Table 1).

Condensation of II with phenylhydrazine. Formation of X

A solution of II (0.01 mole) with phenylhydrazine (0.01 mole) in ethanol or acetic acid was refluxed for 4 hrs. After concentration and cooling, the solid obtained was crystallized from a proper solvent to give the corresponding phenylindazole derivative X as yellow crystals (cf. Table 1).

Condensation of II with hydroxylamine hydrochloride. Formation of XI

A mixture of II (0.01 mole) hydroxylamine hydrochloride (0.02 mole) and pyridine (20 mL) was refluxed for 4 hrs. The reaction mixture was poured into cold water and the solid obtained was crystallized from benzene to give the corresponding benzisoxazole derivative XI as colourless crystals. (cf. Table 1).

Reaction of II with urea and thiourea. Formation of XI and XII

A mixture of II (0.01 mole), absolute ethanol (20 mL), glacial acetic acid (2 mL) and urea or thiourea (0.01 mole) was refluxed for 4 hrs. The products separated after concentration and cooling were crystallized from a proper solvent to give the corresponding quinazoline thione and quinazoline derivatives XI and XII respectively (cf. Table 1).

REFERENCES

[1] E. A. Soliman, *Rev. Roumaine Chim.*, **23**, 1597 (1978);

[2] E. A. Soliman and G. H. Sayed, *Ind. J. Chem.*, **16** (B), 884 (1978); *C.A.*, **90**, 203645 (v), (1979).

[3] E. A. Soliman and M. A. Salem, *Ind. J. Chem.*, **19** (B), 406 (1980); *C.A.*, **94**, 46897 (s) (1981).

[4] G. H. Sayed, *Ind. J. Chem.*, **19** (B), 364 (1980).

[5] D. N. Kost, M. A. Lepitskaya, G. A. Golubova, S. M. Seruivoka, *Zh. Org. Khim.*, **4**, 732 (1969).

Revue Roumaine de Chimie, **30**, *3*, 273–280 (1985)

MECHANOCHEMICALLY INITIATED POLYMERIZATIONS[6*].

INFLUENCE OF MECHANICAL PARAMETERS ON THE POLYMERIZATION OF STYRENE BY VIBRATORY GRINDING

CLEOPATRA VASILIU OPREA and FELICIA WEINER
Polytechnic Institute of Jassy, Department of Organic and Macromolecular Chemistry, Jassy, Romania

Received February 11, 1984

New results concerning the polymerization of styrene by vibratory grinding are presented. The influence of mechanical parameters such as: duration, size of grinding bodies, filling ratio upon the conversion degree is discussed.
The resulting products were characterized by spectral chemical methods.

1. INTRODUCTION

It has been proved that the mechanical dispersion of various crystalline substances of organic nature (monomers)[1,2] or of inorganic nature (salts, oxides, metals) is likely to bring about paramagnetic centres capable of initiating homo-, and copolymerization reactions.

The first results in this line of research were obtained by Deuel and Gentili[3] and Benson and co-workers.[4] Grinding quartz sand in the presence of organic substances they proved the formation of chemical bonds on the surfaces, newly uncovered in the process of destruction with the organic substances introduced.

These studies have been continued by Grohn and Paudert.[5]

The vibratory grinding of NaCl, $BaSO_4$, $CaCO_3$, SiO_2 TiO_2, graphite in the presence of unsaturated monomers initiates their mechanochemical polymerization.[6–9]

It has been proved recently that the polymerization reaction can be activated even in the absence of any activating additives. The reaction proceeds on the surfaces of the reaction vessels and the grinding bodies during the process of vibratory grinding or under the action of streams electronic fluxes unavoidably generated under the given conditions.

Thus, polymers have been made of vinylic, acrylic, dienic, cyclic monomers and the influence of some factors on these reactions has been rigorously investigated.[10–15]

---

* Previous part: Cr. Simionescu, C. Vasiliu Oprea and J. Nicoleanu, *Europ. Polym. J.* **19**, 525 (1983).

This paper reports on the effect of the mechanic regime (duration, size of grinding bodies, filling ratio) on the mechano-chemical polymerization of styrene.

2. EXPERIMENTAL

Materials and apparatus

The apparatus and the working methods have already been described in a series of earlier papers. [10–17]

3. RESULTS AND DISCUSSION

3.1. Influence of filling ratio

The filling ratio η is defined as :

$$\eta = \frac{p}{P} \times 100$$

where : p = the amount of monomer (g)
P = the amount of grinding balls (g) (balls in a V_2A).

The syntheses were carried out under inert atmosphere, for periods of 24–144 hours and at filling ratios of: 0.5 ; 0.75 ; 1 and 2%.

The filling ratio was varied by varying the amount of grinding balls at constant monomer amount (30 g).

The obtained results are set out in figure 1, which also displays the influence of duration.

The conversion (variation versus) time curves for different values of the filling ratio have the same shape, i.e. they reach a maximum which testifies to the fact that two simultaneous processes occur during vibratory grinding: polymerization and mechanodegradation.

The latter starts at the very moment when the macromolecular chain reaches the critical length. These results are in keeping with earlier ones concerning the polymerization of a great many other monomers. [10–17]

The maximum conversion degrees approximately 73 % (Fig. 1, curve 1) are obtained at minimum values of the filling ratio ($\eta = 0.5\%$), and decrease correspondingly at higher values, so that for $\eta = 1\%$ and 2% respectively, they become less than 5%.

The position of the maximum of conversion also depends on the filling ratio. At a minimum value of the latter ($\eta = 0.5\%$) the conversion increases and reaches 73% by prolonging the process up to 144 hours.

With high ratios, the process is a great deal slower, maximum conversion is reached earlier (120 hours), but it stops at values under 20%.

The filling ratio conditions: 1) The free volume in the reaction vessels which, in its turn, determines the amplitude of the mechanic vibrations, the frequency of collisions between grinding bodies, on the one hand and the walls of the vessel, on the other hand as well as among themselves, and 2) the setting up of more or less intense friction forces.

The filling ratio variation influences the joint action of mechanical energy components without the system : shock forces being set up on the one hand and friction on the other hand.

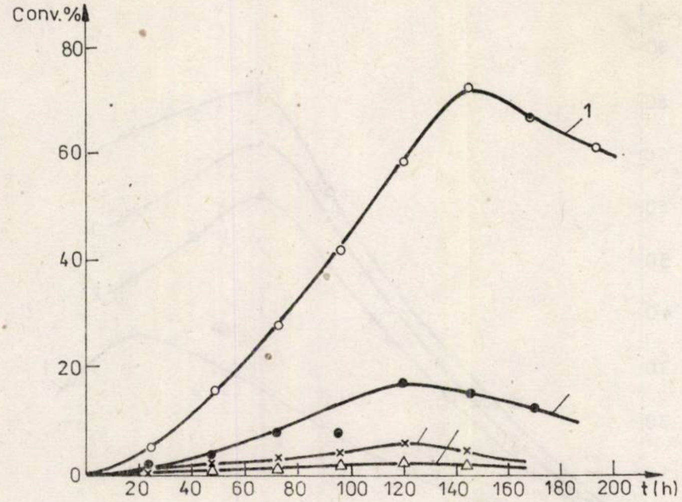

Fig. 1. — Influence of the filling ratio on the conversion degree :
1. $\eta = 0.5\%$; 2. $\eta = 0.75\%$; 3. $\eta = 1\%$; 4. $\eta = 2\%$

In any actual mechanical regime they are equilibrated. The increase of the filling ratio results in a reduction of the amount of grinding bodies, which, in its turn, influences the frequency of collissions and the amplitude of the ball trajectories. The latter determines the intensity of shock forces, and hence, the efficiency of promoting the activation of polymerization by mechanoemission.

The fact that conversion degrees achieved by increasing the filling ratio are smaller, indicates the importance of the collision frequency of grinding bodies which, under these conditions reduces the rate of metal being converted into a colloidal state, as well as the effect of mechanoexcitation of the network and the mechanoemission of electrons.

Conversely, when the filling ratio is small, the amount of balls increases. Consequently, friction forces intensify leading to a substantial rise in temperature, capable of stimulating polymerization.[18]

3.2. Dimension of grinding bodies

With a view to pointing out this particular influence syntheses have been carried out at a filling ratio of 0.5%.

The dimensions of grinding bodies were : 3, 6, 9 and 12 mm.

The conversion/time curves pass through a maximum corresponding to the duration of 144 hours (curves 2,3,4, Fig. 2).

With balls having the smallest diameter ⌀ = 3 mm, the formation of the polymer is much slower (curve 1) and the maximum is only reached after 192 hours. It is easily seen that the efficiency of polymerization increases with increasing dimensions of the grinding bodies, reaching a maximum value for the largest dimension (Ø = 12 mm). Under the assumption that mechanopolymerization is initiated by active centres brought

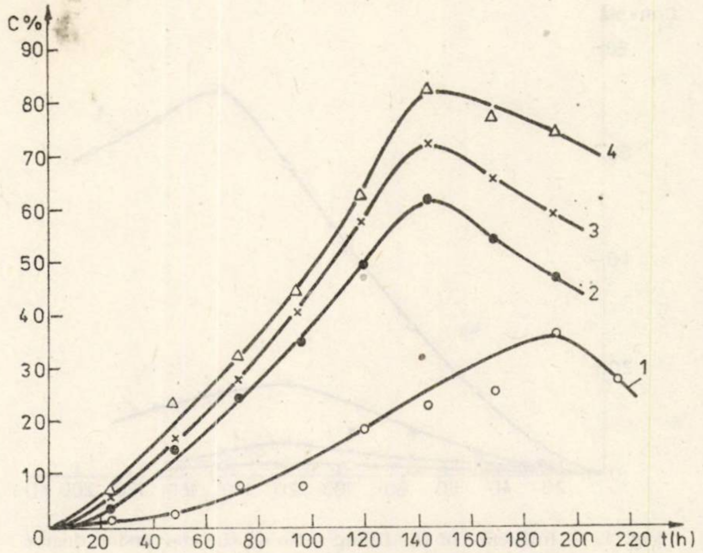

Fig. 2. — Influence of the dimension of grinding bodies on the conversion degree. 1. Ø = 3 mm ; 2. Ø = 6 mm ; Ø = 9 mm ; 4. Ø = = 12 mm

about by collisions among balls or between balls on the one hand and the walls of the apparatus on the other hand it follows that the efficiency of the process increases with increasing intensity of shock forces. The impact force is related to the kinetic energy of the balls. Thus, it is ultimately related to their mass. Obviously, the conversion degree increases with increasing ball dimensions.

4. CHARACTERIZATION OF POLYSTYRENE SYNTHESIZED BY VIBRATORY GRINDING UNDER THE INFLUENCE OF MECHANICAL PARAMETERS VARIATION

The resulting products have been subjected to chemical analyses, having as object the gathering of information on the mechanism of polymerization reactions activated through vibratory grinding.

4.1. Solubility

The activation of the polymerizations reaction on metallic surfaces newly uncovered during vibratory grinding, causes the obtained polymer to be impurified by exceedingly fine metallic particles (having colloidal dimensions) generated during the grinding process. At the same time, small quantities of chemically bound metal (by coordination) cause the final product to have a lower solubility. In order to provide a quantitative characterization of the behaviour of these polymers in the presence of solvents, a systematic study has been carried out, by use of four solvents : p-xylene, benzene, toluene and dimethyl-formamide. The first three are the common solvents of polystyrene.

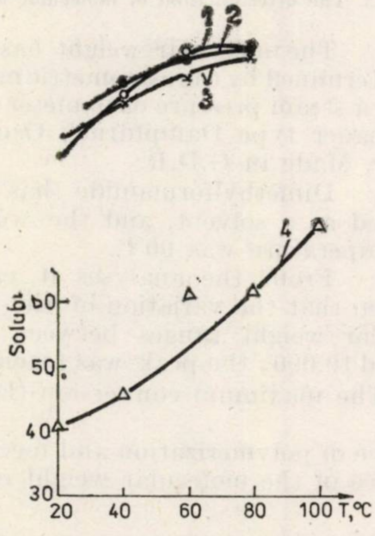

Fig. 3. — Variation of the solubility of polystyrene with temperature at a constant duration (Condition of synthesis : 144 hr ; $\eta = 0.5\,\%$) ; 1. p-xylene ; 2. DMF ; 3. benzene ; 4. toluene.

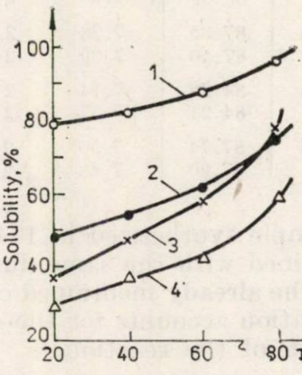

Fig. 4. — Variation of the solubility of polystyrene (72 hr ; $\eta = 0.5\,\%$) with temperature : 1. benzene ; 2. toluene ; 3. DMF ; 4. p-xylene.

The influence of the temperature variation on solubility has been investigated, maintaining a constant duration of 24 hours (Figs 3 and 4). The results showed dimethylformamide to be the most efficient solvent, strongly polarized being followed by toluene, *p*-xylene and benzene. The solubility/temperature curves display a continuous increase in solubility. The temperature ensures an increase in contents in the soluble fraction.

4.2. Elemental analysis

The percentage of C and H was determined by elemental analysis. Filtered and reprecipitated soluble fractions separated by dissolving the raw product in dimethylformamide have been subjected to this analysis.

With polystyrene synthesized under inert medium (nitrogen) using an optimum filling ratio of 0.5 % and grinding bodies with $\varnothing = 9$ mm, for various grinding durations the results for carbon range between 89.46 % and 84.28 % and then for hydrogen between 7.74 and 7.14 %, as compared to the theoretical values i.e. 92.3 % C and 7.7 % H.

Then deviations from the theoretical values are due to the presence of iron in the structure of the poylmer.

Table 1

The C, H contents and the residue in calcination contents of polystyrene synthesized by vibratory milling ($\eta = 0.5\,\%$; Ø = 9 mm)

Duration	C%	H%	Residue
48 hours	89.46	7.74	2.65
	89.50	7.79	2.70
120 hours	89.35	7.40	2.12
	89.39	7.60	2.30
144 hours	87.35	7.28	2.13
	87.40	7.30	2.25
168 hours	84.28	7.14	2.39
	84.21	7.37	2.42
192 hours	87.74	7.50	2.69
	87.90	7.68	2.70

It may be noticed that the values for the C% and H% contents vary over a rather narrow range and are a little smaller than the calculated results.

4.3. The determination of molecular weight

The molecular weight has been determined by the osmometric method on a steam pressure osmometer of the Knauer type Dampfdruck Osmometer, Made in G.D.R.

Dimethylformamide has been used as a solvent, and the working temperature was 90°C.

From the analyses it can be seen that the variation of the molecular weight ranges between 5.000 and 10.000; the peak was reached by the sample synthesized in 144 hours. The maximum conversion (Fig. 5) is obtained with the same duration.

The already mentioned concurrence of polymerization and mechanodegradation accounts for the dependence of the molecular weight on the duration of the reaction.

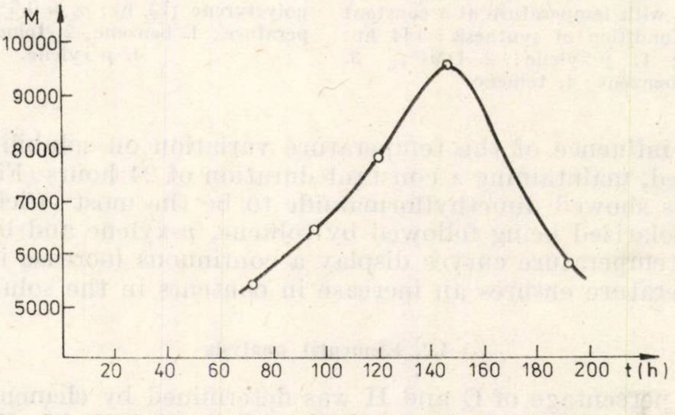

Fig. 5. — Variation of the molecular weight of polystyrene as a function of the milling duration.

4.4. The determination of the temperature for vitrous transition

In the present paper the temperature for vitrous transition has been determined by using gas chromatography.

The polystyrene was dissolved in chloroform. CROMOSORB W 60—80 mesh was added to the solution, as a support so that the concentration of the polymer on the support was 5%. After the evaporation of the solvent the polymer covered the surface of the support in the shape of a film. The filling (support + polymer) was introduced in a 1 m long column to be thermostated at 100°C for two hours. After that, heptane was injected and the netto retention time was determined during which the mobile component (heptane) contacts solely the polymer. The temperature then rose up to 130°C when the heptane started to elute the column. The transition temperature determined in this way is 90.63°C, rather close to that of isotactic polystyrene viz. $T_{tr} = 100°C$.[19–21] (Fig. 6). The obtained value is characteristic of polystyrene whose molecular weight is 9600.

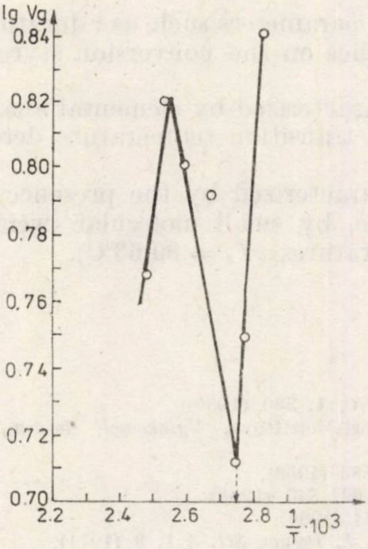

Fig. 6. — Determination of the transition temperature for polystyrene synthesized with milling durations of 144 hours.

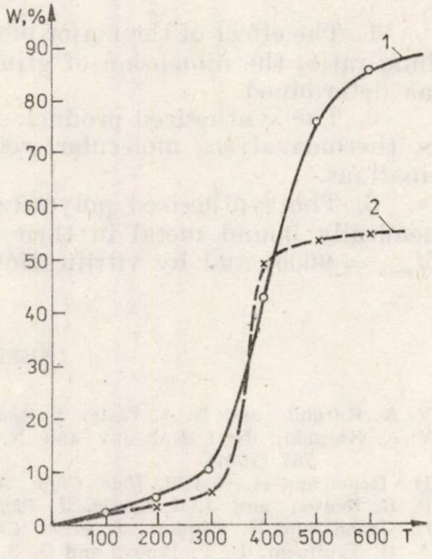

Fig. 7. — Variation of weight losses as a function of temperature : 1. polystyrene synthesized after 72 hours of milling; 2. polystyrene synthesized after 144 hours of milling.

4.5. Thermostability

In order to achieve a thorough characterization of the products synthesized by vibratory milling, the differential thermal analysis has been carried out.

The determinations were carried out on the polystyrene synthesized within the period 72–144 hours with a filling ratio of 0.5%, a temperature range of 20–1000°C and a heating speed of 9°C/min.

Starting from those determinations the variation of weight losses as a function of temperature has been calculated (Fig. 7).

The thermostability of the polymer obtained in 72 hours of milling is lower than that of the polymer resulting after 144 hours. It may be noticed that the weight losses at 300°C stand at 10% in the first case whereas in the polymer obtained in 144 hours they make up 5 %. They add up to 88 % at 600°C in the polystyrene synthesized in 72 hours and reach 55 % in the polymer obtained in 144 hours.

CONCLUSIONS

1. The effect of the major mechanical parameters such as : duration, filling ratio, the dimension of grinding bodies on the conversion styrene was determined.

2. The synthesized products were characterized by elemental analysis, thermoanalysis, molecular weight and transition temperature determinations.

3. The synthesized polymers are characterized by the presence of chemically bound metal in their structure, by small molecular weight ($M_{\max} = 9600$) and by vitrification temperatures ($T_v = 90.63$°C).

REFERENCES

[1] V. A. Karghin and N. A. Plate, *Vysokomol. Soedin.*, **1**, 330 (1959).
[2] V. A. Karghin, N. I. Kabanov and N. I. Rapaport-Moleltsova, *Vysokomol. Soedin.*, **3**, 787 (1961)
[3] H. Deuel and R. Gentili, *Helv. Chim. Acta*, **39**, 1586 (1956).
[4] R. E. Benson and J. E. Castle, *J. Phys. Chem.*, **62**, 840 (1958).
[5] H. Grohn and R. Paudert, *J. Prakt. Chem.*, **11**, 64 (1960).
[6] A. B. Taubman, L. P. Ianova and G. S. Blyskosh, *J. Polym. Sci. A* 1, **9** (1971).
[7] N. K. Baramboim and L. A. Antonova, *K. Zh* ., **38**, 5 (1976).
[8] L. P. Ianova, V. Kuznetsov and S. N. Tolstaya, *Plast. u. Kautschuk*, **26**, 3 (1979).
[9] L. P. Ianova, V. A. Kuznetsov and A. B. Taubman, *Koloidînîi jurnal*, **37**, 3 (1975).
[10] C. Vasiliu Oprea, I. Avram and R. Avram, *Angew. Makromol. Chem.*, **68**, 18 (1972).
[11] Cr. Simionescu, Cl. Vasiliu Oprea and Cl. Negulianu, *Eur. Polym. J.*, **15**, 1037 (1980).
[12] Cl. Vasiliu Oprea and M. Popa, *Angew. Makromol. Chem.*, **90**, 13 (1980).
[13] Cl. Vasiliu Oprea and M. Popa, *Angew. Makromol. Chem.*, **92**, 73 (1980).
[14] Cl. Vasiliu Oprea, Cl. Negulianu, M. Popa and F. Weiner, *Bul. I.P. Iaşi fasc.* ***1—2**, Seria chimie*, **87** (1980).
[15] Cl. Vasiliu Oprea and F. Weiner, *Angew .Makromol. Chem.*, **106**, 207 (1982).
[16] Cr. Simionescu, Cl. Vasiliu Oprea and J. Nicoleanu, *Europ. Polymer. J.*, **19**, 6, 525 (1983).
[17] Cl. Vasiliu Oprea and M. Popa, *Angew. Makromol. Chem.*, **116**, 125—138 (1983).
[18] M. T. Bryk, "Polimerizatsia na tverdoi povernosti nergamiceshih vescestv", Kiev, 1981.
[19] T. Volintiru and G. Ivan, "Introducere în fizico-chimia polimerilor", Ed. tehnică, Bucharest, 1980.
[20] M. J. Brown and E. J. Guelled, *J. Polym. Sci.*, **1**, 1073 (1976).
[21] M. J. Brown and E. J. Guelled, *Adv. Polym. Sci.*, **21**, 108 (1977).

Revue Roumaine de Chimie, **30**, *3*, 281–286 (1985)

COMPTES RENDUS

"Solar Energy, Phase Transfer Catalysis, Transport Processes" (Advances in Polymer Science, vol. 55), Springer-Verlag, Berlin, 1984, 163 pages, 98 DM (hard-cover).

Volume 55 in the series "Advances in Polymer Science" contains three contributions concerned with three new and interesting applications of polymers.

An old dream of chemists is to manage chemical reactions in conditions similar to those of biological systems (at normal temperatures and pressures, and at $pH \approx 7$). This dream seems to come true at the beginning of this decade. An argument for this statement is the first article in this volume entitled "Solar Energy Conversion by Functional Polymers" written by M. Kaneko and A. Yamada. The authors begin with a suggestive description of chemical conversion of solar energy in photosynthesis. Photosynthesis is the reduction of carbon dioxide by electrons from water with the help of visible radiation producing carbohydrates and oxygen. The chlorophyll molecules, which are magnesium complexes of porphyrin containing a long alkyl chain, play the role for the excitation, energy concentration, and charge separation. It is pointed out that for the chemical photoconversion of energy, a heterogeneous reaction system is needed to prevent energy-consuming back reactions. In plants molecular assemblies such as micelles, liposomes, and bilayer membranes provide microheterogeneous reaction environment which facilitates one-direction electron flow. This one-direction electron flow is the key point of the photosynthesis process. Once the mechanism of natural chemical conversion of solar energy is known, one can design a conventional photochemical reaction system in which the role of chlorophyll is taken by other polymeric complexes, and that of bilayer membrane by synthetic polymers.

The simplest photochemical conversion of solar energy is the photolysis of water which is described in detail. Conversion of solar energy into a fuel in order to avoid intermittence and irregularity of irradiation is another important aspect. For a fuel an electron source is needed. Water is the electron source for the most economical reduction.

It is known that nitrogen reduction to ammonia and carbon dioxide reduction to hydrocarbons take place at elevated temperatures and pressures, and in the pressence of catalysts. It is an important future task to construct solar energy conversion systems in which these reactions can be carried out under "natural" conditions.

"Polymer-Supported Phase Transfer Catalysts : Reaction Mechanisms" is the second paper written by W. T. Ford. Polymer-supported phase transfer catalysts are insoluble polymers having covalently bound functional groups active as catalysts for reactions between anions and natural organic substrates. The active functional groups may be quaternary ammonium salts, cryptands, grafted poly (ethylene glycols), or analogues of dipolar aprotic solvents. The reactions are carried out in triphase mixtures of organic liquid, solid or aqueous inorganic salt, and solid catalyst. The chemical reactions take place within the polymer matrix or on the polymer surface. The aim of the article is an analysis of the experimental parameters which affect catalytic activity and their mechanisms of action.

The last review is "Rapid Polymer Transport in Concentrated Solutions" written by W. D. Comper and B. N. Preston. The aim of the article is to introduce new observations of diffusive-convective phenomena in polymer chemistry. The processes discussed are of significance to all those interested in transport phenomena. The article reviews polymer and solvent diffusion in binary systems, polymer transport in ternary systems, macromolecular transport in transient polymeric networks, detailed discussion of measurement and of factors involved in rapid polymer transport in multicomponent systems, identification of structured flows associated with polymer transport, and biopolymers.

The present volume continues to maintain the excellent quality of the previous numbers in this series. All the articles are valuable source of up-to-date information and key to the preimary literature. Diagrams and formulas are presented clearly. The printing is excellent.

Ursula Bologa

G. A. PARKER, "Analytical Chemistry of Molybdenum", Springer-Verlag, Berlin, 1983, 173 pages, 98 DM (hard-cover).

Like the other transition metals in group V1 B of the Periodic Table of elements, molybdenum occurs in nature in minor concentrations in complex mixtures and sometimes poor ores. It is an important material in industry. It is an alloying element in high temperature and high strength steels. It appears in other types of steels and in various iron-based alloys either alone or in combination with other elements. Molybdenum is also an essential element in biological systems; its role is only now starting to be understood. Because of its multiple applications, more sensitive and selective methods for determination in any sample type have been developed. Literature data on this subject are increasing. The author felt the need of a single source of information.

The aim of the book is to present completely and systematically the available methods for molybdenum analyses. The 20 chapters are divided into two parts. The first 12 chapters are concerned with different techniques used in molybdenum determination. Detection and separation methods, gravimetric, titrimetric, volumetric, spectroscopic methods, voltammetry, catalytic and radiochemical and activation methods are reviewed and discussed. The next 8 chapters deal with sample treatment in order to obtain working solutions. These solutions can be processed by the experimental techniques mentioned earlier. Alloys, biological systems (both animals and plants) are considered.

The book is an important source of up-to-date information in the field of molybdenum chemistry. It contains 45 extensive tables, and selected detailed laboratory procedures enabling one to carry out experiments. It is a useful guide to analytical chemists. The book is error-free. Printing is excellent. Figures and tables are drawn with care.

Ursula Bologa

,,Ion Cyclotron Resonance Spectrometry, II" (Lecture Notes in Chemistry, vol. 31), Springer-Verlag, Berlin, 1982, 538 pages, 82 DM (soft cover).

H. Hartmann and K.-P. Wanczek are the editors of "Ion Cyclotron Resonance Spectrometry, I" published in the series "Lecture Notes in Chemistry", vol. 7 by Springer-Verlag, Berlin, 1978. Several recent developments have stimulated renewed interest in the use of the ion cyclotron resonance principle in different fields of physics and chemistry. Long storage time of ions and electrons can be achieved under ultrahigh vacuum conditions and in strong electromagnetic fields. This long storage time offers the possibility of studying slow-rate reactions and of precision measurements of photon-ion interactions.

The editors felt the need to publish a new volume with the newest developments in Ion Cyclotron Resonance (ICR). Volume 31 in "Lecture Notes in Chemistry" contains 28 papers which cover all the fields studied with ICR today. There are review papers as well as original contributions and short notes. The articles are arranged in four groups:

— studies of basic properties of molecules and ions (photochemistry, photodissociation, on energetics, electron affinity);

— ion chemistry (structure and reactivity of positive and negative ions, and metal ions);

— instrumentation (Fourier transform ICR spectrometry, tandem instruments, frequency scanning detectors, high magnetic field);

— theory (ion-molecule reactions, ion motion and detection).

Most of the contributions were presented at the 2nd International Symposium on Ion Cyclotron Resonance Spectrometry, held at the Akademie der Wissenschaften und der Literatur, Mainz, March, 1981.

Most of the papers describe experimental results obtained in the laboratories by their authors. The book is addressed to specialists in ICR spectrometry and mass spectrometry as well as to inorganic and organic theoretical chemists. It is readable, systematic and well documented. Printing is excellent.

Ursula Bologa

"Polymerization Reactions" (Advances in Polymer Science vol. 58), Springer-Verlag, Berlin, 1984, 131 pages, 82 DM (hard-cover).

"Macromonomers : Synthesis, Characterization and Applications" written by P. F. Rempp and E. Fanta is the first article in this volume. Macromolecular monomers, generally referred to as macromonomers or as macromers, are linear macromolecules carrying at their chain end some polymerizable functions. In most cases, this function is a double bond, an oxirane ring or another heterocycle which can undergo polymerization. The interest in macromonomers arises from the fact that they give an easy access to graft copolymers.

The first part of the review examines various methods of preparation. In the second part, homopolymerization of macromonomers yielding highly branched structures, as well as copolymerization with a classical monomer are presented.

The second paper "Linear Amino Polymers : Synthesis, Protonation and Complex Formation" written by P. Ferruti and R. Barbucci deals with recent developments of polymeric amines. Linear amino polymers containing basic nitrogen atoms are considered with regard to their synthesis, protonation and complex formation with metal ions. Cross-linked resins having essentially the same structure as linear polymers are also mentioned. As far as protonation is concerned, special care is given to thermodynamic aspects, and to the most probable protonation mechanism. Practical implications of the properties are considered.

The last paper, "Polymerization of Quinodimethane Compounds", written by S. Iwatsuki discusses the following aspects :

— flash pyrolysis of *p*-xylene ;
— preparations of poly-*p*-xylylenes other than by pyrolysis ;
— pyrolysis of paracyclophane : the vapor-coating process ;
— polymerization of halo-*p*-xylylenes ;
— polymerization behavior of quinodimethanes as acceptor monomer.

Volume 58 in the series "Advances in Polymer Science" edited by Springer-Verlag, Berlin, is concerned with interesting aspects of polymerization reactions. All the articles are important reviews on the subjects which are discussed. This volume contains an author and a subject index. The printing is excellent. The figures and tables are clear and highly readable.

Ursula Bologa

"New Developments" (Structure and Bonding, vol. 56), Springer-Verlag, Berlin, 1984, 155 pages, 82 DM (hard-cover).

Volume 56 in the series "Structure and Bonding" contains three contributions concerned with new aspects in inorganic chemistry.

The first article "Design of Inorganic Oscillators" is written by I. R. Epstein and K. Kustin. Temporal and spatial periodicities occur frequently in nature. Biorythmus and biological clocks are detectable, and periodical variations in chemical components of biological systems are also known. Despite the fact that "inorganic oscillators" are no more laboratory curiosities, this field was not intensively and systematically studied till 1980. "Inorganic oscillators" are homogeneous reactions maintained far from equilibrium, in which the reaction mechanism involves coupled feedback steps so that periodical returns to some initial state are possible. The few known chemical oscillators were discovered accidentally. The aim of the article is to present mechanistic details for the chloride-iodide-arsenite oscillator, to give a classification scheme of the known oscillators and to indicate how to design an oscillator.

"Synergetic Extraction of Actinides" written by V. V. Ramakrishna is the second review. Enhanced solvent extraction of metal ions by certain combinations of extractants is a general phenomenon which is of both practical and theoretical interest. The author presents the literature data appeared till the end of 1982. Fundamentals of synergetic extraction are discussed briefly. Physico-chemical methods for structural characterization of the extracted species are presented, and combinations of extractants are indicated. Useful tables and figures with physico-chemical constants for a large number of solvents are given. Because the compositions of the complexes are sometimes uncertain and the equilibria involved are often complex, it is a rich field here for structural chemists, who can separate and purify the complexes, determine their structure and other physico-chemical properties and then through spectroscopic techniques compare the isolated compounds with those in solution.

B. Dobiáš is the author of the last article entitled "Adsorption of Surfactants on the Mineral-Water Interface in the Flotation System". Theoretical aspects of mineral flotation, in particular the adsorption of flotation reagents at the mineral-water interface are reviewed in this paper. The principle of the flotation method consists of the different adhesion of hydrophobized and hydrophilic mineral particles to an air bubble. The hydrophobized mineral particles adhere to the air bubble and form a foam. With this method it is possible to obtain highly pure mineral components from complex and especially poor ores.

This book provides a deep insight on the subjects discussed. It is addressed to inorganic chemists and to theoretical chemists as well as to chemists working in industry. All the articles are readable, and well systematized. The printing is excellent.

Ursula Bologa

E. BERECZ and M. BALLA-ACHS, *"Gas Hydrates"*. Akadémiai Kiadó, Budapest, 1983, 340 p.

In a review published in 1927, Schroeder stated that one of the important tasks of modern chemistry was the investigation of the specific affinities occurring in the interaction of different chemical materials with water. At that time, a vast amount of practical work had already proved that not only water-soluble solid materials, but also many extremely poorly soluble gases and liquids, interact with water as a solvent, and that under appropiate circumstances solid-state hydrates, known as gas hydrates and liquid hydrates, separate out. Schroeder concluded that these gas hydrates are the product of the "secondary valence" effects, and display characteristic features ; in comparison with their real importance they have given very little attention in the systems that have been investigated. The book consists of seven chapters.

The first and second chapters are dedicated to a historical survey of the literature on gas hydrates studies and fundamentals of the structures of gas hydrates, structures, compositions and systematization of crystalline gas hydrates, simple gas hydrates, liquid hydrates, double hydrates and mixed hydrates.

The third chapter represents stability relations of gas hydrates, concerning conditions of formation and decomposition of gas hydrates, effect of third component on stability of gas hydrates, effect of gases on stability effect of electrolytes on stability, effect of alcohols on stability, effect of a condensed apolar phase and of other compounds on stability, hydrates of liquid hydrocarbons and stability of mixed hydrates.

Chapter 4 describes thermodynamics of gas hydrates, chemical thermodynamic and statistical thermodynamic investigations of gas hydrates.

Chapter 5 is devoted to properties and characteristic data of individual gas hydrate systems, single gas component (nitrogen, oxygen, noble gases, halogens, carbon dioxide, sulphur dioxide, hydrogen sulphide), hydrates of pure hydrocarbons (methane, ethane, ethylene, propane, propylene, butane and freon), hydrate systems containing more than one gas component (methane + carbon dioxide, hydrogen, sulphide, propane, ethylene), (propane + hydrogen sulphide, nitrogen), methan + propylene, propane + propylene, (hydrogen sulphide + chloroform, carbon tetrachloride, difluoroethane) and hydrates of natural gases.

Chapter 6 presents some technological aspects of the role and application of gas hydrates, application of gas hydrates for gas storage purposes, methods for the separation of components in the gaseous and liquid states by means of gas hydrates, desalination of water via gas hydrate formation.

Chapter 7 describes the fundamental methods for the experimental determination of the conditions of formation and decomposition of gas hydrates.

The special literature has been surveyed up to the end of 1980, (587 citations) thereby providing an overall picture of the present situation of investigations into gas hydrates, and the results obtained in this field. The aim of this book has been to survey the literature currently available on the topic of gas hydrates. Attention has been given both to the practical and to the theoretical importance of this class of compounds. Further, authors' investigations are drawn upon to discuss the conditions of hydrate formation, the properties of these hydrates, and the conclusions suggested by the results in the case of gaseous hydrocarbon systems containing carbon dioxide, which have so far been comparatively little studied elsewhere. This is an important field, because many gas wells contain appreciable amounts (10—80 %) of carbon dioxide, which exerts a powerful influence on the hydrate-forming properties, and hence on the transportability and applicability of these hydrocarbon systems.

The book denotes a high level editorial effort and so far, has needed contributions of high standard from its authors. The volume due to its structure, may well be used as a textbook — at the same time introductory and advanced.

The book is meant to meet requirements of the scientists and tehnologists who are confronted by gas-hydrate problems in the course of their work.

D. I. Marchidan

"Polymers in Medicine" (Advances in Polymer Science, vol. 57 Springer-Verlag, Berlin, 1984, 190 pages, 108 MD (hard-cover).

Volume 57 in the series "Advances in Polymer Science" edited by Springer-Verlag, contains four contributions by J. Drobnik, R. Duncan, A. S. Hoffman, Y. Ikada, J. Kopeček, and F. Rypaček. The papers deal with a novel application of polymers, namely with their utilization in medicine and biology. Recent progress in macromolecular chemistry had led to the hope that synthetic polymers could simulate better the desired functions in biological systems than natural polymers. Much work has to be done for understanding the action mechanisms of these synthetic polymers in the human body.

"Soluble Synthetic Polymers in Biological Systems" written by J. Drobnik and F. Rypáček is the first review. It summarizes facts and theories on the fate of a soluble polymer in the body. Analytical methods which are the main source of knowledge are discussed. A compartmental model is suggested. The importance of the individual compartmental barriers and the peculiarity of the polymer pharmacokinetics are documented. Synthetic polymers may elicit antibody production, induce immunological tolerance, serve as non-specific immunostimulator. The authors emphasize that specialists in biology, cell biology, physiology, immunology, pathology, pharmacology, together with specialists in organic chemistry and macromolecular chemistry should cooperate in the rational design of a polymer for a given purpose. These polymers should provide effective and versatile tools in biological and fundamental medical research as models of biopolymers and probes barriers, membranes and transport mechanisms, for specific manipulations of cellular processes, as hormone models and antigens. Consequently new disciplines such as polymer biochemistry and polymer pharmacology are likely to appear in the future.

A comprehensive review on polymers utilized in medicine and biology written by Cr. Simionescu and V. Gorduza, entitled "Biocompatible and Bioactive Polymers", Ed. Academiei, Bucharest, 1980 (480 pages), with 2900 references is not included in the 297 literature quotations of the article.

"Soluble Synthetic Polymers as Potential Drug Carriers" is the title of the second paper written by R. Duncan. The article discusses the consequence of the attachment of pharmaceuticals to macromolecular carriers with special reference to endocytosis and lysosomotropic drug delivery. The types of polymers are reviewed with particular regard to the methodology currently available in polymer chemistry for the synthesis of polymers bearing cell-specific targeting residues and incorporating effective polymer drug linkages. The idea of using drug carriers to improve the therapeutic efficacy of pharmacological agents is receiving increasing attention.

"Blood-Compatible Polymers" is the third review written by Y. Ikada. This article describes polymers which are blood-compatible not by the addition of anticoagulants or by the formation of anticoagulants or due to the formation of neointima, but because they consist of antithrombogenic biomaterial that does not include blood-soluble additives either. Since research in this area is in its infancy, the author has placed the emphasizis on his own experimental results.

"Ionizing Radiation and Gas Plasma (or Glow) Discharge Treatments for Preparation of Novel Polymeric Biomaterials" written by A. S. Hoffman is the last paper of the volume. In biomaterials ionizing rediation and plasma discharges have a unique ability to initiate free radical and ionic reactions without the need to add catalysts or to heat. The author analyses three basic processes which are utilized for preparing new or modified polymeric biomaterials : i) surface modification via radiation graft copolymerization or plasma gas discharge; ii) radiation of pure monomers in solution, in the solid state, or in an emulsion ; iii) radiation crosslinking in solution, in swollen state, or in the solid state.

Volume 57 in the series "Advances in Polymer Science" edited by Springer-Verlag is concerned with new aspects of applications of polymers in biology and medicine. All the articles are valuable sources of up-to-date information in this field. They are highly readable, and well systematized.

Ursula Bologa

A. MAEHLY and L. STRÖMBERG, "Chemical Criminalistics", Springer-Verlag, Berlin—Heidelberg—New York, 1981, 322 pages, (hard-cover).

R. L. Kirk was one of the first important chemists who was interested in the field of criminalistics. He established a school of criminalistics at the University of California in Berkley where, for the first time, degrees in forensic science could be obtained. He is also the author of the most important book, "Crime Investigations", published in 1953. The first triannual meeting of the International Association of Forensic Science took place in Belgium in 1957. The International Reference Organization in Forensic Medicine published in 1974 a bibliography in the history of criminalistics.

These seem to be the most important events in the area of criminalistics. Under these circumstances Springer-Verlag published in 1981 "Chemical Criminalistics" written by A. Maehly and L. Strömberg. The authors tried to cover fundamental concepts and to address also to active workers in the field of forensic chemistry.

A general introduction is concerned with a historical overview of criminalistics and with the concept of forensic science today. It is pointed out that the expression "Forensic Science" is not yet clearly defined. The authors define it as a "conglomerat of bits of human knowledge endeavour". It is emphasized that a single scientist is not able to master all aspects of forensic science. Useful figures and tables suggest the interconnection between branches of human endeavour and forensic science, as well as the development of forensic science laboratories in the world in the last decade.

The second part is concerned with :
I. Narcotics and Dangerous Drugs
II Explosives
III. Polymers
IV. Fibers
V. Paints, Varnishes and Lacquers
VI. Glass
VII. Soil
VIII. Firearm Discharge Residues
IX. Fire Investigation
X. Questioned Documents
XI. Toxic Substances in Food
XII. Restoration of Erased Markings
XIII. Miscellaneous

General and specific references are given at the end of each chapter. As can be seen, all analytical methods are used in forensic chemistry. Such techniques are : thin-layer chromatography, gas chromatography, high pressure liquid chromatography, ultraviolet and infrared spectrophotometry, mass spectrometry and fluorescence. Combined chemical methods are used with success in various fields of criminalistics.

The last part, "Auxiliary Activities", contains the following chapters :
I. The Forensic Significance of Physical Evidence and its Collection
II. Reference Collection
III. The Forensic Expert
IV. Sources of Information on Forensic Science
V. The Organization of a Forensic Science Laboratory

During the last two decades the development has been so rapid that it is now hardly possible for either a legal pathologist or a criminalist to keep abreast of this whole field. The most explosive development has taken place in three topics : toxicology, serology and chemical analysis. Thus compromises must be accepted. These compromises depend on the task to be performed by the laboratory and on the size of the organization. Some aspects of this problem are discussed in the last part.

A highly interesting feature of the book is that each chapter is illustrated with actual examples of forensic puzzles from the authors' experience in Stockholm. Many of these examples are documented with photographs so that the reader can grasp the wide variety and the important implications of the expertise. All examples cited in the book contain the factual data followed by the conclusion with its exact wording (this is of capital importance in legal procedures).

The book is recommended as well-informed, readable and systematic. The 70 figures, 65 tables, and all the formulas are drawn clearily. The quality of the printing is excellent.

Ursula Bologa

ORSZÁGOS MŰSZAK. INFORMÁCIÓS KÖZPONT ÉS KÖNYVTÁR 1883

NOTE POUR LES AUTEURS

La Revue Roumaine de Chimie publie des articles en anglais, français, russe, allemand ou espagnol. Les auteurs sont priés d'envoyer des articles et des comptes rendus inédits.

Les manuscrits seront dactylographiés à deux intervalles. La bibliographie, les tableaux et la légende des figures seront placés après le texte.

Si l'article fait partie d'une série numérotée, la partie précédente sera donnée comme première référence.

Chaque article sera précédé d'un résumé comprenant quinze lignes au maximum.

Les références bibliographiques dans la texte seront faites par des exposants sans parenthèses et paraîtront à la fin de l'ouvrage.

Les publications périodiques mentionnées dans la bibliographie seront présentés suivant les prescriptions internationales : le nom de l'auteur précédé de l'initiale de prénom, le titre du périodique abrégé conformément à « Chemical Abstracts » et souligné par une ligne, le numéro du tome indiqué par des chiffres arabes et souligné par deux lignes, suivi de la première page de l'article : à la fin, l'année de la parution sera placée entre parenthèses. Le numéro de la revue ne sera pas indiqué si les pages du volume sont numérotées consécutivement.

Les textes des livres ou traités inclueront : les nom des auteurs, l'initiale du prénom, le titre du livre entre guillemets et sans être souligné, le numéro du tome précédé par l'abréviation « vol. » (ou « Bd. »), le numéro de l'édition, les éditions (the publisher), la localité de la parution du livre, l'année de la parution et la page de la référence précédée(s) par l'abréviation « p » (ou « S »).

Les brevets seront indiqués comme suit : l'auteur ou la firme, le pays et le numéro du brevet, la date et la revue (*Chem. Abstr.*). Par ex. : M. Jones (to Union Carbide Co.), Brit. Pat. 601 238, 2 Sept. 1959, cf. *Chem. Abstr.*, **54**, 12808 (1960).

Les diagrammes seront tracés à l'encre de Chine sur papier calque. Les tableaux et les figures (en nombre strictement nécessaire), ainsi que les courbes dans les figures seront numérotés par des chiffres arabes. Leur explication sera donnée dans la légende des figures. Prière de ne pas inscrire les mêmes données dans les tableaux et les figures. Chaque tableau aura un titre. On indiquera dans le texte la place approximative des tableaux et des figures. Les formules chimiques seront incluses dans le texte : en outre, elles seront transcrites sur papier calque, à l'encre de Chine.

Les auteurs sont priés d'indiquer les caractères italiques (en soulignant les lettres au crayon), ainsi que tout autre caractère spécial : les préfixes *ortho, meta, para, cis, trans,* etc. seront soulignés pour indiquer leurs caractères italiques, et ne seront jamais écrits avec des majuscules.

Aucune correction à la main ne sera admise sur le manuscrit. Les corrections seront frappées à la machine. Les lettres grecques ou autres symboles spéciaux seront insérés à la main à l'encre clairement.

Le manuscrit sera signé par l'auteur.

Le titre-courant aura 50 lettres au maximum.

L'entière responsabilité du contenu des articles appartient aux auteurs.

Sur demande on peut obtenir une note plus complète.

PRINTED IN ROMANIA

TRAVAUX PARUS AUX ÉDITIONS DE L'ACADÉMIE DE LA RÉPUBLIQUE SOCIALISTE DE ROUMANIE

1985 APR 18

GH. MARCU, **Chimia compuşilor coordinativi**, 1984, 415 p.

E. CORDOŞ, C. MANOLIU, **Spectrometria de absorbţie şi fluorescenţă atomică**, 1984, 178 p.

C. BODEA, **Tratat de biochimie vegetală**, p. II, vol. 5, 1984, 438 p.

ELENA CEAUŞESCU, **Cercetări în chimia şi tehnologia polimerilor**, 1983, 519 p.

N. ASANDEI, A. GRIGORIU, **Chimia şi structura fibrelor**, 1983, 395 p.

N. IONESCU, M. CĂLDĂRARU, **Oxidarea catalitică a olefinelor inferioare**, 1983.

C. CAŞCAVAL, **Studiul polimerilor prin piroliză şi cromatografie de gaze**, 1983, 220 p.

C. I. SIMIONESCU, F. DANEŞ, **Originea vieţii**, 1983, 110 p.

C. BODEA, (sub redacţia), **Tratat de biochimie vegetală**, partea II, volumul IV, 1982, 408 p.

I. G. MURGULESCU, RODICA VÎLCU, **Introducere în chimia fizică. Vol. III.Termodinamica chimică**, 1982, 624 p.

I. G. MURGULESCU, J. PĂUN, **Introducere în chimia fizică. Vol. I. 3. Nucleul atomic, reacţii nucleare, particule elementare**, 1982, 606 p.

ELENA CEAUŞESCU, **Noi cercetări în domeniul compuşilor macromoleculari**, 1981, 536 p.

I. G. MURGULESCU, TATIANA ONCESCU, E. SEGAL, **Introducere în chimia fizică, Vol. II. 2, Cinematică chimică şi cataliză**, 1981, 1024 p.

V. DRĂGUŢAN, A. T. BALABAN, M. DIMONIE, **Metateza olefinelor şi polimerizarea prin deschidere de inel a cicloolefinelor**, 1981, 254 p.

LYDIA-MARIA VAICUM, **Epurarea apelor uzate cu nămol activ. Bazele biochimice**, 1981, 218 p.

I. GĂLĂŢEANU, **Procese şi metode radiochimice în energetica nucleară**, 1981, 234 p.

O. IORDACHE, **Procese polistocastice aplicate la fenomenele de transfer**, 1981, 186 p.

CR. SIMIONESCU, VALERIA GORDUZA, **Polimeri biocompatibili şi biologic activi**, 1980, 479 p.

ELENA CEAUŞESCU, **Polimerizarea stereospecifică a izoprenului**, 1979, 307 p.

CONST. GH. MACAROVICI, **Analiza chimică cantitativă anorganică**, 1979, 457 p.

M. FLORESCU, **Metode ştiinţifice în dezvoltarea industriei chimice moderne**, 1979, 256 p.

A. T. BALABAN, I. GĂLĂŢEANU, G. GEORGESCU, LIGIA SIMIONESCU, **Compuşi marcaţi şi radiofarmaceutici cu aplicaţii în medicina nucleară**, 1979, 495 p.

I. G. MURGULESCU, E. SEGAL, **Introducere în chimia fizică. Vol. II. 1. Teoria molecular cinetică a materiei**, 1979, 1036 p.

S. STERNBERG, FL. DANEŞ, **Termodinamica chimică aplicată**, 1978, 400 p.

I. G. MURGULESCU, V. EM. SAHINI, **Introducere în chimia fizică. Vol. I.2. Structura şi proprietăţile moleculelor**, 1978, 604 p.

I. ZUGRĂVESCU, MAGDA PETROVANU, **N-ylid chemistry**, coédition avec McGraw-Hill, International Book Company, U.S.A., 1977, 396 p.

I.G. MURGULESCU, **Introducere în chimia fizică. Vol. I. 1. Atomi, molecule, legătură chimică** 1976, 560 p.

ELENA CEAUŞESCU, **Research work on synthesis and characterization of macromolecular compounds. Contributions**, 1974, 251 p.

CR. SIMIONESCU, VIORICA RUSAN, V. POPA, **Chimia algelor marine**, 1974, 212 p., 1 pl.

ISSN 0035—4090

I.P. INFORMAŢIA c. 2716

43 426

Lei 40

$80 (pour un abonnement annuel)

F 1103 04

ACADÉMIE DE LA RÈPUBLIQUE SOCIALISTE DE ROUMANIE

REVUE ROUMAINE DE CHIMIE

R 1985 MAJ 1 4

MG

TOME 30

N° 4

Avril 1985

EDITURA ACADEMIEI REPUBLICII SOCIALISTE ROMÂNIA

Rev. Roumaine Chim. RRCHAX **30**, *4*, p. 287–372 (1985), Bucarest

REVUE ROUMAINE DE CHIMIE

Tome 30, N° 4 Avril, 1985

R. VÎLCU, E. LUCINESCU and M. DRĂGUŢ, Excess values in binary systems of carboxylic acids with n-heptane and benzene . . . . 289—295

AURELIA MEGHEA, FLORICA ZĂLARU and D. IONESCU, Some new copper (II) complex compounds with nitroimidazole derivatives . . . . 297—307

I. GĂNESCU, N. CALU, GH. BRÎNZAN und C. VÁRHELYI, New substitution products of $K_3[Cr(NCS)\ ]$ with chinaldine (in German) . . . . 309—316

ILEANA BARACU, EUTANŢA TĂRNĂUCEANU, V. DOBRE and I. NICULESCU-DUVĂZ, Potential anticancer agents. XXV. Aliphatic and cycloaliphatic N-nitrosoureas and N-nitrosourethanes . . . . 317—327

C. GHIRVU, M. CONSTANTINESCU, GH. IONESCU and I. M. POPA, Considerations on the electronic spectra and barrier to internal rotation of α- and β-naphthalenesulphonic acids . . . . 329—332

M. C. MARTINEZ, M. R. BERMEJO and M. GAYOSO, Dipolar study of titanium octahedral compounds with TMDTO and TEDTO (in Spanish) . . . . . . 333—337

GRIGORE TEODORESCU, CRISTINA MANDRAVEL, MELANIA GUŢUL and GABRIELA TEODORESCU, Synthesis and characterisation of a Pd(II) complex with 2,5-methoxy-4-chloro-benzenamine . . . . 339—342

MOHAMED A. ABD-ALLA, MOHAMED T. ISMAIL and AHMED M. EL-KHAWAGA, Studies on substituted diarylidenecycloheptanones . . . . 343—347

F. GARCIA, O. COLLERA, J. L. SÁNCHEZ, R. CRUZ, R. SAUCEDO and M. C. PÉREZAMADOR, Carbon-13 NMR spectra of some 16,17-glycol diterpenes 349—352

C. I. CHIRIAC, A convenient one-step conversion of aromatic aldehydes into nitriles . . . . 353—355

ADRIAN O. FULEA, About the calculation of the I. R. and Raman active fundamentals of polymers . . . . 357—364

HOCINE KADI, and D. P. LAZĂR, Identification d'hydrocarbures aromatiques de quelques fractions pétrolières. III (in French) . . . . 365—369

ADRIAN O. FULEA, Corrigenda ,,On a correction technique for fractionation data and its application to the fractionation of polyethylene terephthalate'' . . 371—372

Rev. Roumaine Chim. **30**, *4*, 287—372 (1985), Bucarest

Revue Roumaine de Chimie, **30**, *4*, 289–295 (1985)

INFORMÁCIÓS ÉS KÖNYVTÁR 1883

EXCESS VALUES IN BINARY SYSTEMS OF CARBOXYLIC ACIDS WITH N-HEPTANE AND BENZENE

R. VÎLCU, E. LUCINESCU and M. DRĂGUȚ
Department of Physical Chemistry, Polytechnic Institute, Blvd Republicii 13, Bucharest, Romania

Received May 8, 1984

The variation of ultrasonic velocity (C) and density (ρ) with the acid concentration (x_1) has been measured in binary mixtures of acetic and propionic acids, with n-heptane and benzene.
Excess volumes (VE), adiabatic compressibility (β) and excess adiabatic compressibility (βE) were calculated.
These data show a variation with x_1, significantly different from that expected for ideal liquid mixtures.
This behaviour is interpreted in terms of the molecular association of carboxylic acids.

Deviations of ultrasonic propagation velocity with solution concentration from additivity can contribute to the elucidation of nature of intermolecular forces. Several studies characterize ultrasonic velocity in mixtures of organic compounds ; in the most of examined cases the deviations from linearity were attributed to hydrogen bond formation or dipole association. But frequently, the results obtained by several author sare different and do not permit the deduction of a unitary conclusion. The systematic studies on a certain class of substances in common solvents can clear up the nature of the ultrasound velocity deviations from additivity in the same class of substances and in different solvents.

This paper continues the study of low carboxylic acids behaviour in non-aqueous solvents, as n-heptane and benzene. The results for aqueous systems were presented.[1]

Pinkerton[2] have been suggested a phenomenological classification of the liquids according to ultrasound wave absorption ; class A_1 of non-associated liquids and class A_2 of associated liquids. In the mixtures of two liquids of class A_1, both density and velocity of the sound depend almost linearly on concentration.

In this case, ultrasound absorption is due to the so-called "molecular absorption", similar to that in the gases.

In the case of A_2 class liquids, most of the ultrasound absorption is due to the intermolecular state i.e. molecular association. Consequently, the ultrasonic absorption measurements allow the study of equilibrium between associated units.

In the mixtures of two A_2 liquids or one A_2 with an A_1 type the density and ultrasonic velocity present anomalous behaviour with positive or negative deviations from additive rule. The class A_2 includes also the carboxylic acids.

The complexity of intermolecular structure of such acids, both in pure state and in different solvents, was studied by means of several physical and chemical methods. Among these acids, the acetic acid was the object of a large volume of investigations. The most representative contributions are quoted in the previous papers.[3,4] Despite this large volume of data, there still exist interesting aspects to be revealed.

EXPERIMENTAL DATA

Both experimental part and derived values were given in a previous paper[1]. We have determined experimentally, the density (ρ) of binary systems and ultrasonic propagation velocity (C) through such systems at a temperature of 25°C. From these data we obtained:

Adiabatic compressibility: $\beta = 1/\rho\, C^2$ (1)

Excess adiabatic compressibility:

$$\beta^E = \beta - \left(\frac{x_1 V_1}{x_1 V_1 + x_2 V_2}\, \beta_1 - \frac{x_2 V_2}{x_1 V_1 + x_2 V_2}\, \beta_2 \right) \tag{2}$$

index "1" refers to the acid and "2" to the solvent), where: x, is the molar fraction: V, the molar volume.

The excess volume is:

$$V^E = \overline{M}/\rho - (x_1 V_1 + x_2 V_2) \tag{3}$$

where $\overline{M}$ is the average molecular weight of the mixture. The consistency of experimental values was tested by means of a Redlich-Kister composition function with four constants: A_0, A_1, A_2 and A_3.

$$V^E = x_1 x_2 \sum_{n=0}^{n=3} A_n (x_1 - x_2)^n \tag{4}$$

The four coefficients calculated by the least squares method are given in table 1.

Table 1

Coefficients in the smoothing equation (4)

System	A_0	A_1	A_2	A_3
Acetic acid—*n* heptane	+5.367	+2.220	+1.044	−8.815
Propionic acid-*n* heptane	+1.890	−0.633	+0.355	−0.483
Acetic acid-benzene	+3.078	+0.395	+0.279	−0.074
Propionic acid-benzene	+1.125	−0.686	+0.132	−0.064

The substances used were of analytical grade, checked by determination of densities and refractive index which comply with the literature values. In order to determine the ultrasonic propagation velocity we used a double quartz crystal interferometer as previously described,[5] which works at a unique resonance frequency of 1 MHz. The density of solutions at 25°C have been determined by a pyconometer with an error of 0.01 %. The validity of such measurements has been checked by comparison with the literature values[6], found for the whole composition range for the acetic acid-benzene system. For the other systems, we did not have comparative data except for pure components ; however, the perfect concordance in the case of previously mentioned systems assures us of the experimental data validity also for the other systems similarly obtained.

DISCUSSION

Both measured and calculated values are given in tables 2—5. Excess values are represented as a function of the acid concentration, (x_1) over the whole composition range, in figs 1—4.

Table 2

Acetic acid-n heptane

x_1	ρ(25°C) g/cm³	C m/s	$\beta \cdot 10^{12}$ cm²/dyn	$\beta^E \cdot 10^{12}$ cm²/dyn	V^E_{exp} cm³/mol	V^E_{calc} cm³/mol
0	0.6790	1154	110.59	0	0	0
0.0992	0.6912	1114	116.51	7.35	0.57	0.60
0.2298	0.7099	1097	117.05	10.07	1.25	1.23
0.3510	0.7328	1090	114.69	10.53	1.40	1.43
0.5003	0.7718	1077	111.62	10.86	1.28	1.29
0.5996	0.8037	1075	107.60	9.78	1.13	1.15
0.8507	0.9248	1082	92.20	5.49	0.46	0.47
0.9060	0.9623	1090	87.46	4.23	0.34	0.33
1.0000	1.0440	1123	75.95	—	0	0

Table 3

Propionic acid-n-heptane

x_1	ρ(25°C) g/cm³	C m/s	$\beta \cdot 10^{12}$ cm²/dyn	$\beta^E \cdot 10^{12}$ cm²/dyn	V^E_{exp} cm³/mol	V^E_{calc} cm³/mol
0.000	0.6790	1154	110.59	0	0	0
0.100	0.6944	1125	113.68	4.92	0.21	0.21
0.2955	0.7306	1116	109.90	5.33	0.45	0.45
0.5074	0.7818	1119	102.16	3.35	0.46	0.46
0.7004	0.8437	1122	94.00	2.04	0.33	0.34
0.8996	0.9313	1136	83.18	0.72	0.07	0.08
1.000	0.9878	1152	76.28	0	0	0

Table 4

Acetic acid-benzene

x_1	ρ(25°C) g/cm³	C m/s	$\beta \cdot 10^{12}$ cm²/dyn	$\beta^E \cdot 10^{12}$ cm²/dyn	V^E_{exp} cm³/mol	V^E_{calc} cm³/mol
0.000	0.8738	1322	65.48	0	0	0
0.0992	0.8823	1281	69.06	2.89	0.26	0.26
0.2992	0.9034	1233	72.71	4.97	0.62	0.62
0.4961	0.9301	1189	75.93	6.39	0.76	0.76
0.7017	0.9663	1150	78.21	6.42	0.68	0.68
0.9064	1.0154	1126	77.59	3.09	0.29	0.30
1.000	1.0440	1123	75.95	0	0	0

Table 5

Propionic acid-benzene

x_1	ρ(25°C) g/cm^3	C m/s	$\beta \cdot 10^{12}$ cm^2/dyn	$\beta^E \cdot 10^{12}$ cm^2/dyn	V^E_{exp} cm^3/mol	V^E_{calc} cm^3/mol
0.000	0.8738	1322	65.48	0	0	0
0.1006	0.8819	1285	68.07	2.26	0.16	0.16
0.3018	0.9009	1249	71.10	2.74	0.30	0.29
0.5178	0.9247	1216	73.09	2.49	0.27	0.27
0.7173	0.9493	1188	74.63	1.80	0.17	0.17
0.9128	0.9755	1164	75.66	0.48	0.05	0.05
1.000	0.9878	1152	76.28	0	0	0

In all investigated cases we obtained the ultrasonic propagation velocity values with negative deviation from aditivity.

For the acetic acid-benzene system, the same curve is also presented in paper,[7] while Rao *et al.* [8] give a variation with a maximum at 90% molar value and a minimum at 67% molar value.

But in a system where no significant associations take place, one component (benzene) being non-polar and non-associated, such a complicated behaviour is hardly probable. The propagation velocity values for pure compounds[8] are also different from the values obtained by us. In a series of other papers one can find comparable data with our values ; 1322 m/s for velocity of ultrasound in benzene at 25°C, complies with 1323 m/s[9,10] or 1326 m/s[11] . For the acetic acid velocity of 1123 corresponds to 1126 m/s[10] or 1125 m/s [12].

Searching for literature data one can find that the ultrasonic propagation velocities for the same substance presents rather different values because of experimental conditions non-mentioned in detail.

From all representations of the obtained values, sensitive deviations from the ideal behaviour are noticed, in these systems where one of the components is a hightly associated, class A_2, while the other is a non-associated component of class A_1. In the case of n-heptane and benzene as solvents, the deviations have the same sense, but opposite to that in aqueous systems[1] where the solvent is also highly associated. It has been ascertained that the changes of adiabatic compressibility and ultrasonic propagation velocity through such mixtures are mainly connected to the changes of mixing volumes.

The increased volume resulting by mixing ($V^E > 0$), for the four systems, occurs as a result of cohesive forces lower than in the pure components. This fact brings about a decrease of propagation velocity and an increase of compressibility ($\beta^E > 0$) as compared with the ideal mixing behaviour. These correlations between the excess volume and excess compressibility comply with the theory of ultrasonic propagation in liquids. Another rule to be noticed is that the acetic acid in the two solvents gives for a certain value the same deviation sense, comparative to the corresponding amount of propionic acid : i.e. higher excess volumes and compressibilities and lower propagation velocities.

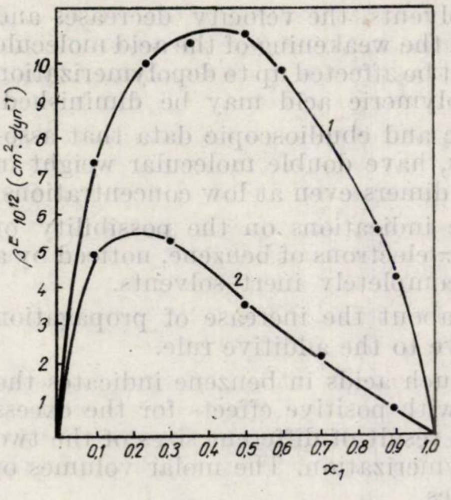

Fig. 1. — Excess compressibility-composition curves 1. system acetic acid-n-heptane ; 2. system propionic acid-n-heptane ; points, experimental values.

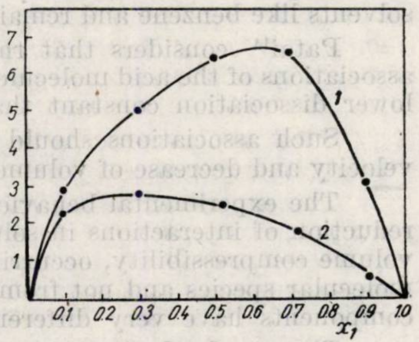

Fig. 2. — Excess compressibility-composition curves 1. system acetic acid-benzene ; 2. system propionic acid-benzene ; points, experimental values.

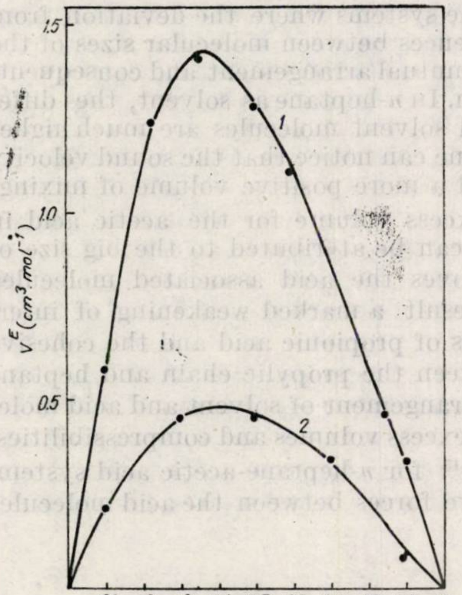

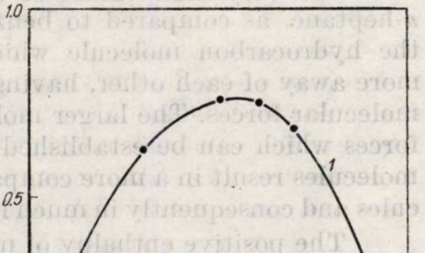

Fig. 3. — Excess volume-composition curves. 1. system acetic acid-n-heptane ; 2. system propionic acid-n-heptane ; points, experimental values ; curves (V^E), calculated from equation (4).

Fig. 4. — Excess volume-composition curves 1. system acetic acid-benzene ; 2. system propionic acid-benzene ; points, experimental values ; curves (V^E), calculated from equation (4).

These solvents of non polar type do not have a depolymerization effect on the associated acids, followed by a combined association which determined the increase of propagation velocity and decrease of compresibility as occurs in the acid systems with polar solvents.

For n-heptane and benzene as solvents, the velocity decreases and compressibility increases can arise from the weakening of the acid molecule interactions. The hydrogen bonds cannot be affected up to depolymerization but the dispertion forces between polymeric acid may be diminished.

It is well known from cryoscopic and ebullioscopic data that associated liquids such as carboxylic acids, have double molecular weight in solvents like benzene and remained as dimers even at low concentrations.

Patai[14] considers that there are indications on the possibility of associations of the acid molecules with π electrons of benzene, noticed by a lower dissociation constant than in completely inert solvents.

Such associations should bring about the increase of propagation velocity and decrease of volume relative to the additive rule.

The experimental behaviour of such acids in benzene indicates the reduction of interactions in solution, with positive effects for the excess volume compressibility, occurring as a result of different sizes of the two molecular species and not from depolymerization. The molar volumes of components have very different values.

The sound velocity is lower in the systems where the deviation from the ideal values is given by the differences between molecular sizes of the components, introducing a disorder in mutual arrangement and consequently a difficulty in the sound propagation. In n-heptane as solvent, the differences between the sizes of acid and solvent molecules are much higher than in the benzene-acid system and one can notice that the sound velocity presents more negative deviation and a more positive volume of mixing.

The very high values of the excess volume for the acetic acid in n-heptane, as compared to benzene, can be attributed to the big size of the hydrocarbon molecule which moves the acid associated molecules more away of each other, having as result a marked weakening of intermolecular forces. The larger molecules of propionic acid and the cohesive forces which can be established between the propylic chain and heptane molecules result in a more compact arrangement of solvent and acid molecules and consequently in much lower excess volumes and compressibilities.

The positive enthalpy of mixing[15] for n-heptane-acetic acid system, also indicates a weakening of cohesive forces between the acid molecules during mixing.

REFERENCES

[1] R. Vîlcu, E. Lucinescu and M. Drăguț, *Bull. Inst. Polit. Buc.*, seria Chimie-Metalurgie, **XLIII** *4*, p. 39 (1981).

[2] J. M. M. Pinkerton, *Proc. Phys. Soc. B.*, **62**, 129 (1949).

[3] R. Vîlcu and E. Lucinescu, *Rev. Roumaine Chim.*, **19**, 791 (1974).

[4] M. A. Goldman and M. T. Emerson, *J. Phys. Chem.*, **77**, 2295 (1973).

[5] R. Vîlcu and A. Simion, *Rev. Roumaine Chim.*, **20**, 1359 (1975).

[6] V. I. Anisimov, *Zh. Fiz. Khim.*, **27**, 1797 (1953).

[7] R. Vîlcu and A. Simion, *Rev. Roumaine Chim.*, **19**, 977 (1974).

[8] M. G. Seshagir Rao and B. Ramachandra Rao, *Indian J. Pure Appl. Phys.*, **3**, 207 (1965).
[9] W. Schaaffs, *Z. Phys. Chem.*, **194**, 28 (1944).
[10] S. Parthasarathy, M. Pancholy and A.F.-Chhapgar, *Il Nuovo Cimento*, **10**, 111 (1958).
[11] B. Jacobson, *J. Chem. Phys.*, **20**, 927 (1952).
[12] K. Wenkateswarlu and P. Bhamambal, *Bull. Soc. Royale Sciences Liége*, **35**, 327 (1966).
[13] Y. Wada and S. Shimbo, *J. Acoust. Soc. Amer.*, **24**, 199 (1952).
[14] Saul Patai, "The Chemistry of Carboxylic Acids and Esters", Interscience Publishers, John-Wiley-Sons, 1969.
[15] M. Woycicka, *Pure and Appl. Chem.*, **2**, 147 (1961).

Revue Roumaine de Chimie, **30**, 4, 297–307 (1985)

SOME NEW COPPER(II) COMPLEX COMPOUNDS WITH NITROIMIDAZOLE DERIVATIVES

AURELIA MEGHEA, FLORICA ZĂLARU and D. IONESCU
The Polythechnic Institute, Department of Chemical
Technology, Bucharest, Romania

Received April 24, 1984

The synthesis and properties of some new Cu(II) complex compounds with 5-nitro-1H-imidazole 4-carboxamide (A) and the corresponding ethylic ester (B) are reported. On the basis of the results of the elemental chemical and thermodifferential analyses, as well as electronic, IR and ESR spectra, these complexes were formulated as follows: $CuACl \cdot 2H_2O$, $CuACl$, $CuBCl \cdot C_2H_5OH$. The ESR spectra determined on the samples obtained in the Cu : Zn system taken in varied proportions, emphasized the importance of the dipolar coupling, implying dimer structures.

INTRODUCTION

As already known, imidazole is of particular importance as ligand owing to its presence in many biological systems, as it is that part of the molecule within which the coordination of the metal ions is considered to take place. That is why it is very useful to know the coordination properties of imidazole and its derivatives for a better understanding of the role of metal ions in such systems.

In order to follow up the coordination possibilities of the ligands and the influence of the R substituent on the type of the complex, some new Cu(II) complex compounds containing nitroimidazole derivatives ligands of type

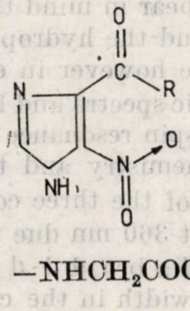

where R = $-OCH_3$; $-NH_2$; $-NHCH_2COOC_2H_5$ are obtained and characterized.

RESULTS AND DISCUSSION

Syntheses were carried out in an ethanol : water (10 : 1) medium, working at a $CuCl_2$: Ligand molar ratio 1 : 1. Under these conditions we obtained compounds I and III formulated on the basis of the elemental chemical analysis (Table 1). Compound II (green) was obtained following the transformation in time of compound I (blue). The green compound becomes blue in the presence of water, thus proving a hydration equilibrium I $\rightleftarrows$ II :

$$\underset{\text{I (blue)}}{\mathrm{CuClA\cdot 2H_2O}} \xrightleftharpoons[+2\mathrm{H_2O}]{-2\mathrm{H_2O}} \underset{\text{II (green)}}{\mathrm{CuClA}}$$

Under these working conditions no definite compound containing the ligand with R = $-OCH_3$ was obtained.

Table 1

Results of the elemental chemical analysis

No.	Compound	%Cu		%Cl		%N		%C		%H	
		calcd	found	calcd	found	calcd	found	calcd	found	calcd	found
I	$CuClA\cdot 2H_2O$ (blue)	21.83	21.04	12.18	12.92	19.24	19.49	16.47	17.30	2.71	2.05
II	CuClA (green)	24.91	24.38	13.90	13.35	21.96	21.87	18.82	19.04	1.56	1.90
III	$CuClB\cdot C_2H_5OH$ (green)	16.41	17.62	9.17	9.66	14.47	15.55	31.00	30.32	4.13	3.94

The presence of the two water molecules retained by compound I was also confirmed by thermodifferential analysis. TG curve shows a loss of weight in two steps, each corresponding to a water molecule, one at 160°C and the other at 240°C (Fig. 1).

The differences noticed between compounds I and III as regards the solvent retained in the coordination sphere (water and ethanol respectively) can be explained if we bear in mind the hydrophilic character of the unsubstituted amide group and the hydrophobic character of the corresponding ethylic ester, soluble however in ethanol.

The reflectance electronic spectra and IR spectra were recorded and a detailed study by electronic spin resonance spectra (ESR) was carried out for determining the stereochemistry and the mode of coordination.

The electronic spectra of the three compounds (Fig. 2) are similar, presenting two bands : one at 360 nm due to the $\pi-\pi^*$ transition proper to the imidazole nucleus[1] and a broad d-d band, centered at 780 nm of higher intensity and greater width in the case of the hydrated blue compound. The position of the absorption maximum and the width of this band are usually connected with pentacoordination of Cu(II) in a square pyramid geometry.[2–6]

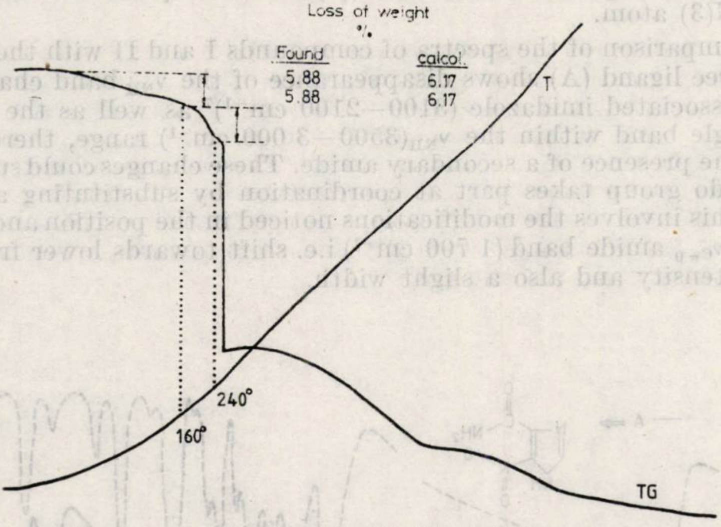

Fig. 1. — TG curve of the CuClA · 2 H_2O compound.

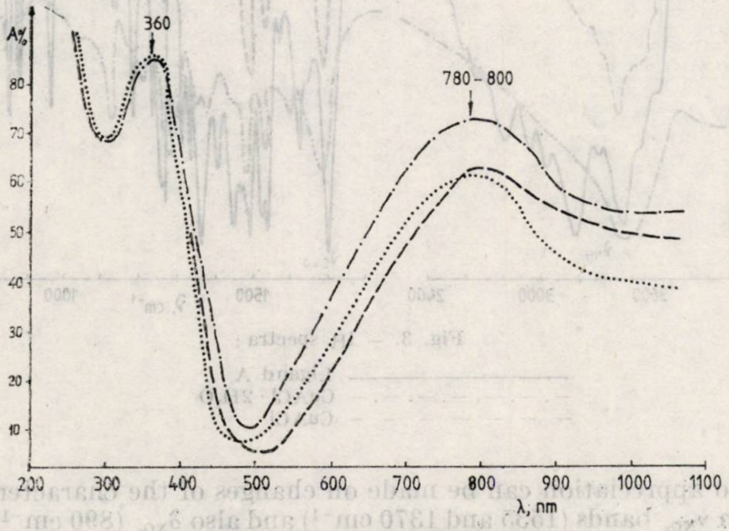

Fig. 2. — Electronic reflectance spectra :

.—.—.—.—.—.—.— CuClA · $2H_2O$ (blue)

— — — — — — — — CuClA (green)

. . . . CuClB · C_2H_5OH (green)

The IR spectra were determined by disk technique in KBr for complexes and ligands (Fig. 3).

The ligands show three functional groups which could potentially coordinate the metallic ion : a) unsubstituted and ester substituted amide groups by nitrogen and oxygen atoms ; b) nitrogroup ; c) imidazole nitrogen atoms by deprotonation of the N(1) atoms or by the electronic doublet of the N(3) atom.

Comparison of the spectra of compounds I and II with the spectrum of the free ligand (A) shows disappearance of the ν_{NH} band characteristic of the associated imidazole ($3100-2100$ cm^{-1})[7] as well as the existence of a single band within the ν_{NH}($3500-3\,000$ cm^{-1}) range, therefore indicating the presence of a secondary amide. These changes could suggest that the amido group takes part at coordination by substituting a hydrogen atom. This involves the modifications noticed in the position and intensity for the $\nu_{C=0}$ amide band ($1\,700$ cm^{-1}) i.e. shift towards lower frequencies, weak intensity and also a slight width.

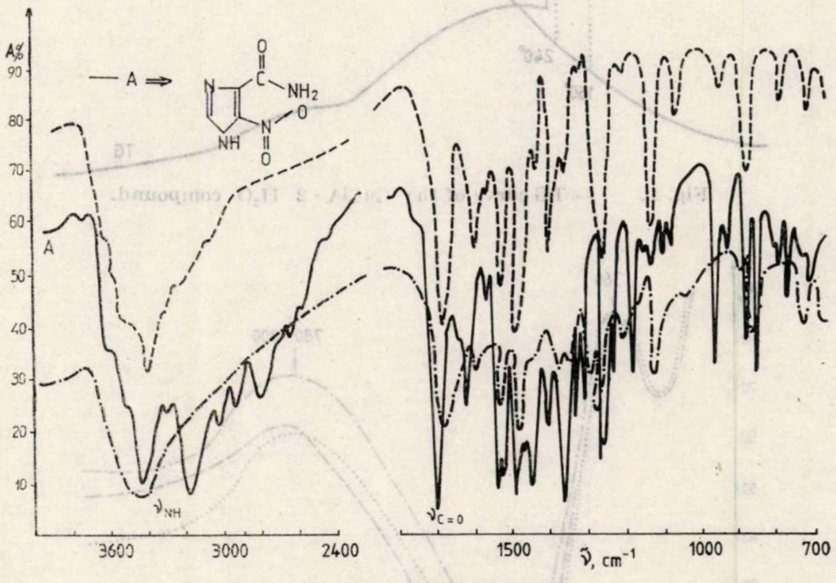

Fig. 3. — IR spectra :

———————— Ligand A
—.—.—.—.—.—.— $CuACl \cdot 2H_2O$
— — — — — — — — CuACl

No appreciation can be made on changes of the characteristic asym and sym ν_{NO_2} bands (1535 and 1370 cm^{-1}) and also δ_{NO_2} (890 cm^{-1}) as within these ranges the imidazole ring presents bands due to its stretching and deformation.

The important changes noticed within the range of the stretching ($1500-1000$ cm^{-1}) and deformation ($1000-700$ cm^{-1}) vibrations of the imidazole ring[8] would suggest that the second donor atom is the neighbouring imidazole nitrogen atom (N_3).

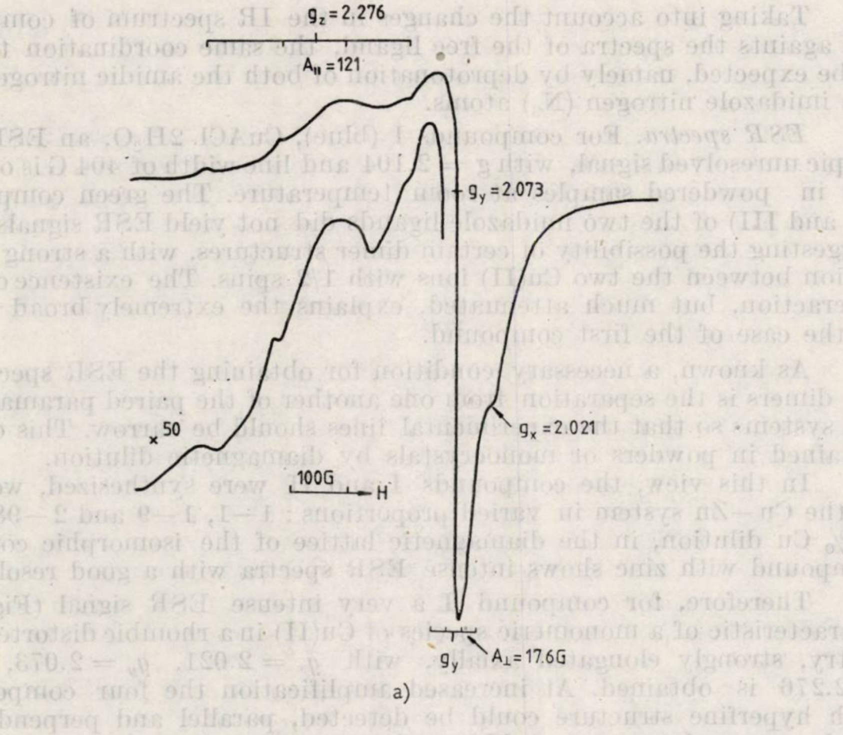

Fig. 4. — ESR spectra : a) $CuClA \cdot 2H_2O$ magnetically diluted ($Cu - Zn = 1 : 9$) ; $CuClB \cdot C_2H_5OH$ magnetically diluted ($Cu - Zn = 1 : 9$).

Taking into account the changes in the IR spectrum of compound III againts the spectra of the free ligand, the same coordination type is to be expected, namely by deprotonation of both the amidic nitrogen and the imidazole nitrogen (N_3) atoms.

ESR spectra. For compounds I (blue), CuACl. $2H_2O$, an ESR isotropic unresolved signal, with $g = 2.104$ and line width of 404 G is obtained in powdered samples at room temperature. The green compounds (II and III) of the two imidazole ligands did not yield ESR signals, thus suggesting the possibility of certain dimer structures, with a strong interaction between the two Cu(II) ions with 1/2 spins. The existence of this interaction, but much attenuated, explains the extremely broad signal in the case of the first compound.

As known, a necessary condition for obtaining the ESR spectra of the dimers is the separation from one another of the paired paramagnetic ion systems so that the experimental lines should be narrow. This can be obtained in powders or monocrystals by diamagnetic dilution.

In this view, the compounds I and II were synthesized, working in the Cu—Zn system in varied proportions : 1—1, 1—9 and 2—98. The 10% Cu dilution, in the diamagnetic lattice of the isomorphic complex compound with zinc shows intense ESR spectra with a good resolution.

Therefore, for compound I a very intense ESR signal (Fig. 4a) characteristic of a monomeric species of Cu(II) in a rhombic distorted geometry, strongly elongated axially, with $g_x = 2.021$, $g_y = 2.073$, $g_z = 2.276$ is obtained. At increased amplification the four components with hyperfine structure could be detected, parallel and perpendicular to the external magnetic field, coupling constants being :

$$A_z = 121 \text{ G}, \; A_y = 18 \text{ G}$$

Correlation of the spectral data with elemental analysis and the molecular models led, for compound I, CuACl · $2H_2O$-monomer : to a formulation in which the central ion is pentacoordinated, in a geometry of square pyramid with a stronger asymmetrical interaction in the equatorial plane and another weaker one in the axial direction, as shown by anisotropy of the ESR spectrum (Fig. 5).

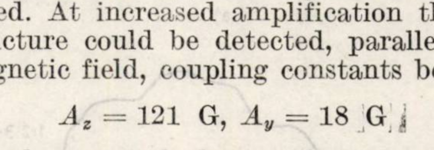

Fig. 5. — Molecular structure proposed for CuClA · $2H_2O$.

For compound III with nitroimidazole with the substituted amide an ESR spectrum is obtained in a magnetically diluted powder at room temperature (Fig. 4b). This spectrum with its sharply different shape was assigned to a dimeric species, with $\Delta M = \pm 1$ transition in a field of 3100–3200 G and double quantum transition ($\Delta M = 2$) at 1400 G. On both bands, but especially at $\Delta M = \pm 1$, one can easily detect the hyperfine splitting into 7 equidistant components with the ratio of the intensities 1 : 2 : 3 : 4 : 3 : 2 : 1 due to the two equivalent copper nuclei ($2 \cdot 2 \cdot \frac{3}{2} + 1 = 7$).

In the interpretation of this spectrum the main types of magnetic interactions between the ion pairs at 1/2 spins have to be considered.

a) The best known is the *isotropic exchange* which results from the combined effect of electrostatic repulsion of electrons (e^2/r_{12}) and Pauli's exclusion principle. It has the effect of coupling the states for giving a singlet and a triplet separated by quantity—the exchange integral, J.

The isotropic exchange can be represented by the scalar product of the two vectors corresponding to the spin magnetic moments

$$\mathscr{H}_{\text{sch}} = -JS_1 \cdot S_2$$

b) The most important magnetic interaction for the interpretation of the dimer ESR spectra is the *dipole-dipole* interaction indicated by operator :

$$\mathscr{H}_{\text{dip}} = \frac{\mu_1 \cdot \mu_2}{r^3} - \frac{3(\mu_1 \cdot r)\ (\mu_2 \cdot r)}{r^5}$$

where μ_1 and μ_2 are the magnetic dipole moments of the two ions and r is the internuclear distance.

In terms of the electronic spin operators, this expression can be written as a second order tensor

$$\mathscr{H}_T = S_1 \cdot \mathbf{J} \cdot S_2$$

where the coupling tensor **J** has generally 9 components and is not necessarily symmetrical.

c) The combined effect of the spin-orbit coupling and isotropic exchange on the ensemble of the energy levels of the fundamental and excited states brings a supplementary contribution to the interaction energy called *anisotropic or pseudo-dipolar coupling.*

When $|J| \leqslant 30\ \text{cm}^{-1}$, the pseudo-dipolar coupling is neglected and the Hamiltonian interaction is :

$$\mathscr{H}_{\text{int}} = \mathscr{H}_{\text{sch}} + \mathscr{H}_T = -JS_1 \cdot S_2 + S_1 \cdot \mathbf{J} \cdot S_2$$

The theoretical treatment for calculating the energies and transition probabilities and simulation on the computer of the ESR spectra were elaborated by Smith and Pilbrow for a great number of dimers of varied geometries.[9]

As a function of the relative values of the exchange integral (J), energy of the microwave quantum ($h\nu$) and splitting parameter in the zero field (D), several situations can be distinguished, of which two limit cases permit rigorous interpretation of the ESR spectra for dimers.

1) The most important are the cases in which *exchange coupling is slight* ($J \lesssim 30\ cm^{-1}$) and the dominant interaction which determines the characteristic form of the ESR spectrum for dimers is of *dipole-dipole* origin. The minimum Cu—Cu distance is about 2.6 Å, corresponding to a splitting parameter in the zero field, $D \cong 0.2\ \text{cm}^{-1}$, a much smaller value than the exchange coupling that can be determined from magnetic susceptibility measurements at low temperatures (between 77K—4K).

In this case the treatment foresees application of the theory of time-independent nondegenerated perturbations, in the Zeeman representation.

In this way Smith and Pilbrow simulated on computer different shapes of the lines, following variation of different parameters : geometry of the elementary cell, orientation with respect to the external magnetic field, value of the exchange integral J, line width, Cu—Cu distance.

Of the numerous simulated spectra, the ones closest to the experimental spectrum recorded by us, were selected, at the same time showing the influence of the Cu—Cu distance (Fig. 6).

2) The other case considers the existence of an intense exchange coupling, when the pseudo dipolar coupling is appreciable and the perturbation theory can no longer be applied. For $-\mathbf{J} > 100\ cm^{-1}$, the ESR spectra can be described only in terms of the triplet state.

In some cases the Wasserman procedure was used for the triplet spectra' at free radicals, [10] but the metallic dimers have broader lines, marked anisotropy of the g factor and a high anisotropic hyperfine interaction.

Figure 7 shows a set of calculated spectra [9] in which the parameter of the axial distortion D varies from 0.05 to 0.40 cm^{-1} and in which a certain similarity with our spectra for $D = 0.05$ can be found.

For selecting the present case, the ESR spectrum has to be recorded at low temperatures (77 K). Below 100 K the triplet state is strongly depopulated and the intensity of the ESR spectrum appreciably decreases.

The determinations with liquid nitrogen showed the increase in the intensity of the signal for the complex compound (III), therefore the exchange coupling is negligible, the existence of the triplet state is excluded. We now come back to the first alternative, according to which the main interaction in dimer is of *dipole-dipole* origin.

Of the calculated spectra shown in Fig. 6 (a, b, c), distance $r_{\text{Cu-Cu}} \simeq$ $\simeq 5.5$ Å can be evaluated. On the basis of these data and of molecular models, two dimer structures can be formulated, in which the coordination between the two planes of the molecules of the complex compound is mediated by the imidazole ring (Fig. 8a), or by the amide carbonyl group (Fig. 8b).

On the basis of the $r > 5$ Å distance, appreciated by interpretation of the ESR spectrum, the first structure can be selected.

Fig. 6.—ESR spectra calculated for axial copper dimers with $J = -24\ \mathrm{cm}^{-1}$, $\Delta M_s = \pm 1$ [9]; a) $r = 3\cdot5$ Å, b) $r = 5.0$ Å; c) experimental spectrum for $CuClB \cdot C_2H_5OH$ compound, $r = 5.5$ Å.

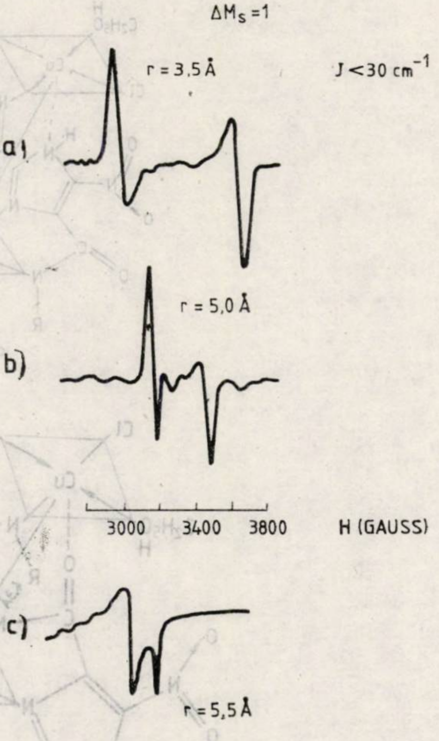

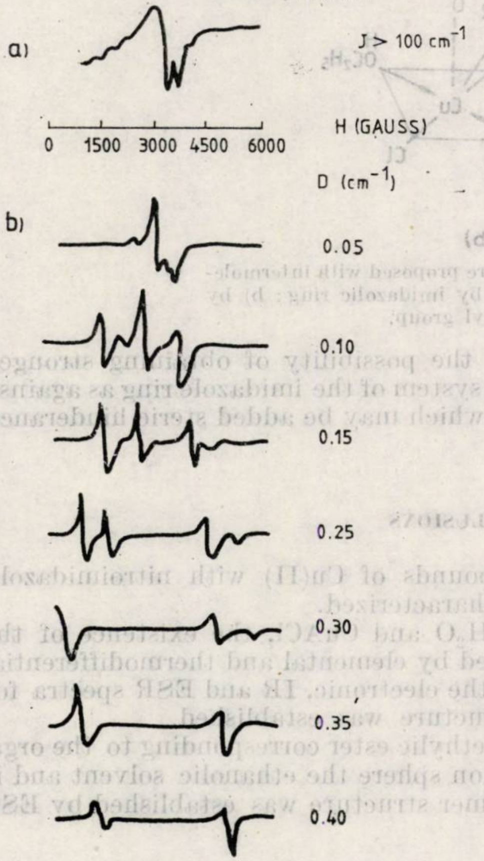

Fig. 7. — a) Experimental ESR spectra for $CuClB \cdot C_2H_5OH$ compound; b) spectra calculated for $g_{\parallel} = 2.36$ and $g_{\perp} = 2.09$, $\nu = 9160$ MHz [9].

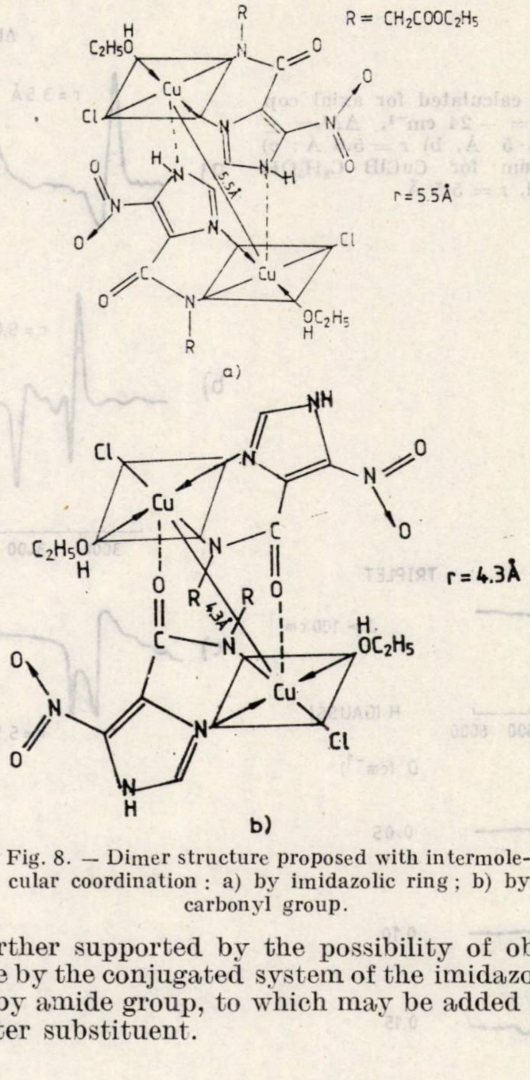

Fig. 8. — Dimer structure proposed with intermolecular coordination : a) by imidazolic ring ; b) by carbonyl group.

This is further supported by the possibility of obtaining stronger dipolar exchange by the conjugated system of the imidazole ring as against the interaction by amide group, to which may be added steric hinderance of the ethyl ester substituent.

CONCLUSIONS

— Three new complex compounds of Cu(II) with nitroimidazole derivatives were synthesized and characterized.

— For compounds $CuACl \cdot 2H_2O$ and CuACl, the existence of the hydration equilibrium was confirmed by elemental and thermodifferential chemical analyses. On the basis of the electronic, IR and ESR spectra for these compounds, a monomer structure was established.

— The compound containing ethylic ester corresponding to the organic ligand retains in the coordination sphere the ethanolic solvent and in magnetically diluted powders, a dimer structure was established by ESR spectra.

EXPERIMENTAL

$CuCl_2 \cdot 2H_2O$ p.a. was used and ligands prepared according to the indications in the literature.[11] Molar ratio $CuCl_2 \cdot 2H_2O : L = 1 : 1$, in ethanol-water medium = 10 : 1. The compounds obtained were separated by filtration under vacuum, washed with small quantities of ethanol-water and dried at room temperature.

$CuClA \cdot 2H_2O$ separates as a gelatinous blue precipitate, which by drying at room temperature changes into a compact blue mass (I). This compound (I) kept at room temperature is transformed into a green powder (compound II) that turns blue in the presence of water.

$CuClB \cdot C_2H_5OH$. By adding the ethanolic solution to the ligand solution, a blue green powder precipitate is obtained.

Copper was determined gravimmetrically after breakdown of the complex with H_2O_2 and concentrated H_2SO_4. Chlorine was determined gravimmetrically.

Electronic reflectance spectra were obtained with a VSU_2 Zeiss-Jena spectrophotometer within the 230—110 nm range in dilution with MgO at a compound/MgO ratio of 1 : 3.

Thermodifferential analysis was carried out with a Paulik-Paulik Erdey derivatograph in a mixture with Al_2O_3 ($m = 0.340$, $S = 500$, DTA, DTG = 1/40, $TC = 1200°C$, $\beta = 10°/min$).

IR spectrum was determined with a Specord 71 spectrophotometer, within the 700—4000 cm^{-1} range using the disk technique in KBr.

ESR spectra were recorded at room temperature and at 77 K on polycrystalline powders, magnetically diluted in the Cu : Zn system, with an ART-5-IFA spectrograph. The klystron frequency was 9060 MHz and the modulation of the magnetic field was 100 kc/sec. ESR spectrum parameters were calculated versus an Mn(II) standard.

REFERENCES

[1] C. N. R. Rao, "Ultraviolet and Visible Spectroscopy", Batterworths, London, 1967.

[2] B. J. Hathaway and D. E. Billing, *Coord. Chem. Rev.*, **5**, *2*, 143 (1970).

[3] B. J. Hathaway, *J. Chem. Soc., A*, 1196 (1972).

[4] M. C. Lim, Ekk Sinn and B. Martin, *Inorg. Chem.*, **15**, 4, 807 (1976).

[5] D. Mastropaolo, Dana A. Powers, J. A. Potenza and H. J. Schugar, *Inorg. Chem.*, **15**, *6*, 1444 (1976).

[6] R. W. Brooks and R. L. Martin, *Inorg. Chem.*, **14**, 3, 528 (1975).

[7] H. Zimmermann, *E. Electrochem.*, **63**, 601 (1959).

[8] R. H. Carslon and T. L. Brown, *Inorg. Chem.*, **5**, *2* 268 (1966).

[9] T. D. Smith and J. R. Pilbrow, *Coord. Chem. Rev.*, **13**, 173 (1974).

[10] E. Wasserman, L. C. Snyder and W. A. Yager, *J. Chem. Phys.*, **41**, 1763 (1964).

[11] D. Ionescu, "Compuşi organici de sinteză cu acţiune biologică", Doctoral Thesis, I.P.B. (1981).

Revue Roumaine de Chimie, **30**, *4*, 309–316 (1985)

NEUE SUBSTITUTIONSPRODUKTE VON $K_3[Cr(NCS)_6]$ MIT CHINALDIN

I. GĂNESCU *, N. CALU **, GH. BRÎNZAN * und C. VÁRHELYI ***

* Lehrstuhl für Anorganische Chemie der Universität Craiova, str. Al. I. Cuza, 13
** Lehrstuhl für Anorganische Chemie der Universität Jassy, str. 23 August, 22
*** Lehrstuhl für Anorganische Chemie der Babeş-Bolyai Universität Cluj-Napoca, str. Arany Janoş, 11

Eingegangen am 2 September, 1983

Es wurde ein rhodanylatähnliches Komplexanion $[Cr(NCS)_4(Chinaldin)_2]^-$ durch eine Substitutionsreaktion aus entwässertem $K_3[Cr(NCS)_6]$ und Chinaldin, ohne Werwendung von Lösungsmitteln, erhalten. Die Herstellung von 31 Salzen mit Chlorhydraten einiger aliphatischer und heterocyclischer Ammine, Alkaloiden und Kobalt (III)-amin komplexen bestätigt die Zusammensetzung des obenerwähnten Komplexanions. Die thermische Stabilität und der Mechanismus des Pyrolysenvorganges wurde auf thermogravimetrischen Wege untersucht. Für die Klärung einiger Strukturfragen wurden auch spektrophotometrische Untersuchungen im UV-und IR-Bereiche des Spektrums durchgeführt.

By substitution, a thiocyanate containing complex anion $[Cr(NCS)_4(Chinaldine)_2]^-$ was prepared from anhydrous $K_3[Cr(NCS)_6]$ and chinaldine in the absence of solvents. The formation of 31 salts using hydrochlorides of aliphatic and heterocyclic amines, alkaloids, and Co(III) ammine, confirms the structure of the above anion. Thermal stabilities and the mechanism of pyrolysis were investigated thermogravimmetrically. For the clarification of structural problems, UV and IR spectra were recorded.

Die von Roessler[1] entdeckte dreibasische komplexe Säure $H_3[Cr(NCS)_6]$ ergibt mit Metallionen—besonders mit Hexammin, Monoacidopentammin und Diacido-tetrammin-kobalt (III)-komplexion — neine Reihe von kristallinen, in Wasser relativ schwer löslichen Niederschläge. [2,3]

Die sehr schwer löslichen Verbindungen $Ag_3[Cr(NCS)_6]$ und $Bi[Cr(NCS)_6]$ wurden auch für analytische Zwecke verwendet. [4,5] Es wurden auch ammoniumsalzähnliche Verbindungen mit heterocyclischen Basen erhalten, wie $(Pyridin)_3.\ H_3[Cr(NCS)_6]$ und $(Chinolin)_3.\ H_3[Cr(NCS)_6]$.[6,7] Die nichtionogen gebundenen NCS-Gruppen im $K_3[Cr(NCS)_6]$ kann man leicht mit neutralen ein- und zweizähnigen Komplexbildnern stufenweise verdrangen und damit eine Reihe von Komplexanionen oder Komplexkationen auch als Nichtelektrolyte erhalten. [7–14]

Ausgehend von $K_3[Cr(NCS)_6]$ und aliphatischen und heterocyclischen Mono- und Diamminen haben Pfeiffer und Mitarbeiter[8–12] 1,6-$[Cr\ en_2(NCS)_2]NCS$, 1,6-$[Cr\ pn_2(NCS)_2]NCS$, $K[Cr(NCS)_4(o\text{-}Phen)]$ und auch das $K[Cr(NCS)_4Py_2]$ dargestellt und charakterisiert. („en" -Äthylendiammin, „p_m" — Propylendiammin, „*o*-phen"-ortho-Phenantrolin).

Wir haben systematische Untersuchungen über Substitutionsreaktionen mit entwässertem $K_3[Cr(NCS)_6]$ und primaren aromatischen Mono-

und Diamminen (mit pK-werten von 8—12 bzw. sek. und tert. Amminen, mit und ohne Lösungsmittel, durchgeführt.[15,16]

Die viel schwäheren basischen Nitroaniline, Dinitroaniline, Nitrotoluidine, Anthranilsäuren (pK-Werte 13—16) gaben keine Verbindungen vom Typus : Ammin $[Cr(NCS)_4(Amin)_2]$.[17]

Substitutionsreaktionen des $K_3[Cr(NCS)_6]$ mit Chinaldin wurden noch nicht beschrieben; wir haben beobachtet das Chinaldin sehr leicht an Chrom (III) koordiniert werden kann :

$$[Cr(NCS)_6]^{3-} + 2\text{Chinaldin} \rightarrow [Cr(NCS)_4(\text{Chinaldin})_2]^- + 2NCS^-$$

Die Zusammensetzung des $[Cr(NCS)_4(\text{Chinaldin})_2]^-$ Anions wurde auf präparativen Wege untersucht. Es wurden 31 Ammoniumsalze aus der verd. dimethylformamid Lösung von Chinaldin $H(Cr(NCS)_4(\text{Chinaldin})_2]$ durch Umsetzung mit den Chlorhydraten einiger aliphatischen und heterocyclischer Ammine bzw. Alkaloide dargestellt. Ferner wurden Salze mit Metallionen und Kobalt (III)-Komplexen vom Hexammin, Monoacidopentammin und Diacido-tetrammin-Typ in Kristallinem Zustand erhalten und charakterisiert.

Mit Hilfe von thermogravimetrischen Untersuchungen konnten die thermischen Stabilitätsbereiche der neuen Komplexsalzen bestimmt und Daten hinsichtlich des Mechanismus des Pyrolysenvorganges erhalten werden. Krausz und Kovacs[19] sowie Boda und Mitarb. [18] haben festgestellt, das bei der Thermolyse des Reineckesalzes und der Reineckate der N-Basen $Cr(NCS)_3$ und die Säure $H[Cr(NCS)_4(NH_3)_2]$ als pyrolytische Abbauzwischenprodukte auftreten. Várhelyi und Gănescu[20] haben gefunden das bei der Thermolyse von Ammin $H[Cr(NCS)_4(\text{Chinaldin})_2]$ auch $[Cr(NCS)_3 \cdot \text{Chinaldin}]$ als labiles zwischenprodukt entsteht.

Es ist wahrscheinlich das auch im Falle der Chinaldinderivate in der ersten Phase der Thermolyse in einem endothermen Prozes die Basen der äuseren Koordinationssphere frei werden :

$$\text{Ammin}\,H[Cr(NCS)_4(\text{Chinaldin})_2] \rightarrow \text{Ammin} + H[Cr(NCS)_4(\text{Chinaldin})_2]$$

Die so entstandene freie Säure $H[Cr(NCS)_4(\text{Chinaldin})_2]$ zerfällt dann schnell nach der Gleichung :

$$H[Cr(NCS)_4(\text{Chinaldin})_2] \rightarrow Cr(NCS)_3 + HNCS + 2\,\text{Chinaldin}$$

In fester Phase kann auch das Additionsprodukt $[Cr(NCS)_3 \cdot \text{Chinaldin}]$ als Abbauzwischenprodukt auftreten (Abb.1). Wie des derivatographischen Kurven des Chinaldin. $H[Cr(NCS)_4(\text{Chinaldin})_2]$ konnte die Bildung der freien $H[Cr(NCS)_4(\text{Chinaldin})_2]$ auch mit Hilfe von thermogravimetrischen Messungen nicht bestätigt werden. Die stoichiometrische ber. Säurenmengen- mit „/" bezeichnet- und der erste Knickpunkt der Thermogramme stehen nicht im Einklang. Der zweite Inflexionspunkt der thermogravimetrischen Kurven (um 320—400°C) entspricht bei fluchtigeren äseren Amminkomponenten dem Additionsprodukt $[Cr(NCS)_3 \cdot \text{Chinaldin}]$, dessen thermischer Zerfall über $Cr(NCS)_3$ zu Cr_2O_3 führt. Der thermische Zerfall und die Oxidation der Abbauzwischenprodukte über 450°C sind stark exotherme Vorgange. Die Zersetzungstemperaturen liegen zwischen 150 und 200°C. Das Endprodukt der Ammin $H[Cr(NCS)_4(Chinaldin)_2]$ bzw. Chinaldin $H[Cr(NCS)_4(Chinaldin)_2]$ ist in allen Fallen Cr_2O_3. Der Rückstand der thermischen Zersetzung der Co(III)-Ammin-Komplexen ist ein Gemisch von $Co_3O_4 + Cr_2O_3$, welches bei 910° im stochiometrischen Verhaltnissen entsteht (abb. 2).

Die Verbindungen : Ammin $H[Cr(NCS)_4(Chinaldin)_2]$ mit farblosen N-Basen sind rotviolette, kristalline Substanzen. Ihre Löslichkeit im Wasser bei Zimmertemperatur ist hauptsächlich von der in der äuseren Koordinationssphäre gebundenen Amminkomponente bestimmt. Sie beträgt 10^{-3} bis 10^{-4} mol/L.

Die Salze des $[Cr(NCS)_4(Chinaldin)_2]^-$ Ionen mit Silber, Quecksilber und Kobalt (III)-Amminen sind sehr schwer löslich in Wasser und unlöslich in apolaren organischen Lösungsmittel für diese Substanzen sind Ketone wie Aceton, Acetylaceton, Methyläthylketon, ferner Essigester, Dimethylformamid und Pyridin. In Wasser-Dimethylformamid Lösungen erleidet das $[Cr(NCS)_4(Chinaldin)_2]^-$ — Ionen weitgehende Hydrolyse nach den Gleichungen : [21,12]

$$[Cr(NCS)_4(Chinaldin)_2]^- + H_2O \rightarrow [Cr(NCS)_3(H_2O)(Chinaldin)_2]^\circ + NCS^-$$

$$[Cr(NCS)_3H_2O(Chinaldin)_2]^\circ + H_2O \rightarrow [Cr(NCS)_2(H_2O)_2(Chinaldin)_2]^+ + \\ + NCS^-$$

Die anfangs negative Farbreaktion mit Fe(III) auf freie NCS^- Ionen verstärkt sich mit der Zeit und die stark positive Fallungsreaktion von $[Cr(NCS)_4(Chinaldin)_2]^-$ — Ionen mit den chlorhydraten der Alkaloiden bleibt langsam aus.

Für die Klärung einiger Strukturfragen wurden auch spektrophotometrische Untersuchungen im UV und IR-Bereich des Spektrums durchgeführt.

EXPERIMENTELLER TEIL

Chinaldin $H[Cr(NCS)_4(Chinaldin)_2]$

In einem mit Korkstopfen versehenen Erlemmeyer-Kolben werden 0,1 Mol entwässerttes $K_3[Cr(NCS)_6]$ (53 g) und 0,3 Mol Chinaldin (42 g) inning vermischt und etwa 5—6 Stdn. auf dem Wasserbade unter mehrmaligen Umschutteln erhitzt, wodurch die anfangs blauviolette Farbe der Masse im Dunkelrot übergeht. Nach Abkuhlen wird das Produkt mit 10% Essigsäure behandelt um die entstehenden Reineckesalzanalogen Verbindungen von dem KSCN und nicht umgesetztem $K_3[Cr(NCS)_6]$ zu befreien.

Die ruckständige mikrokristalline Masse wird abfiltriert, mit verd. Äthanol und Wasser gewaschen und an der Luft getrocknet : Ausbeute : 70—80% d.Th.

Analyse : Gef : Cr 7,19 S 17,75
Aus Chinaldin $H[Cr(NCS)_4(Chinaldin)_2]$ (714,88)
Ber : Cr 7,27 S 17,91

Ammin H $[Cr(NCS)_4(Chinaldin)_2]$

Je 20 mMol Ammin werden mit 10 mL konz. HCl behandelt und das Chlorhydrat im 80—100 mL Wasser gelöst. Diese säure Flussigkeit wird mit 10 mMol chinaldin $H[Cr(NCS)_4(Chinaldin)_2]$ in 25 mL Dimethylformamid behandelt. Nach 15 Minuten stehenlassen werden, die ausgeshiedenen Kristallinen Massen auf einer Nutsche abgesaugt mit 30% Äthanol ausgewaschen, dann bei Raumtemperatur an der Luft getrocknet.

Tabelle 1

Neue Reineckesalz-Analoga vom type Ammin $H[Cr(NCS)_4(Chinaldin)_2]$

Verbindung	Mol. Gew.	Ausb. % d.Th.	Charakteristik	Analyse		
					ber.	gef.
Diäthilamin H. Rein	644,84	54	Agregate aus hellrosa Prismen	Cr S	8,06 19,85	7,97 19,21
Diprophylamin H. Rein	672,89	57	hellrosa dunne Nadeln	Cr S	7,73 19.02	7,63 18.88
Dibuthylamin H. Rein	700,94	55	rotviolette Mi- krokrist. Masse	Cr S	7,42 18,26	7,34 18,06
Triäthylamin H. Rein	672,89	59	rotviolette Mi- krokrist. Masse	Cr S	7,73 19,02	7,70 18,94
Triprophylamin H. Rein	714,97	60	rotviolette Mi- krokrist. Masse	Cr S	7,27 17,90	7,15 17,97
Tributhylamin H. Rein	757,04	57	rotviolette Mi- krokrist. Masse	Cr S	6,87 16,91	6,81 16,35
Pyridin H. Rein	650,80	60	rotviollete Mi- krokrist. Masse	Cr S	7,99 19,67	7,92 19,52
γ-Picolin H. Rein	644,77	58	rotviolette Mi- krokrist. Masse	Cr S	7,82 19,25	7,79 19,04
2.6-Lutidin H. Rein	678,85	64	grosse Tafeln Prismen	Cr S	7,66 18,85	7,59 18,49
Sim. Collidin H. Rein	683,88	69	hellrosa Nedeln	Cr S	7,60 18,72	7,58 18,57
Piperidin H. Rein	656,85	84	romb. Platten	Cr S	7,92 19,49	7,88 19,04
Piramidon H. Rein	803,61	94	rotviolette Mi. krokrist.	Cr S	6,47 15,93	6,40 15,72
Papaverin H. Rein	911,09	94	rotviolette Mi- krokrist.	Cr S	5,71 14,06	5,66 13,94
Procain H. Rein	807,93	96	rotviolette Mi- krokrist.	Cr S	6,44 15,84	6,38 15,70
Codein H. Rein	871,06	98	rotviolette Mikro- krist.	Cr S	5,97 14,69	5,91 14,50
Chinin H_2Rein	1467,83	91	rotviolette Mikro- krist.	Cr S	7,09 17,44	6,98 17,02
Levomepromazin H_2Rein	1475,42	97	rotviolette Mikro- krist.	Cr S	7,05 17,35	7,00 17,04
Chinidin H_2Rein	1467,83	93	rotviolette Mikro- krist.	Cr S	7,09 17,44	7,01 17,20
Morphyn H. Rein	857,04	95	rotviolette Mikro- krist.	Cr S	6,07 14,94	5,98 14,66
Spartein H. Rein	806,07	90	rotviolette Mikro- krist.	Cr S	6,45 15,88	6,24 15,70

H. Rein = $H[Cr(NCS)_4(Chinaldin)_2]$

$[Co(DH)_2(Ammin_2)]$ $[Cr(NCS)_4$ (Chinalhin$)_2]$

Diese Verbindungen wurden aus den alkoholischen Lösungen der $[Co(DH)_2(Ammin)_2]$-Acetat-Komplexen und aus Chinaldin $H[Cr(NCS)_4$ (Chinaldin$)_2]$ in Dimethylformamid durch doppelte Umsetzung erhalten. 2mMol Chinaldin $H[Cr(NCS)_4$ (Chinaldin$)_2]$ werden in 25 mL Dimethylformamid gelöst und mit 100 mL $[Co(DH)_2(Ammin)_2]$-Acetat-Lösung versetzt. Nach 5–10 Minuten stehenlassen werden die ausgeschiedenen mikrokristallinen Niederschlage filtriert, mit verd. Alkohol und Wasser gewaschen und dann bei Raumtemperatur an der Luft getrocknet.

Tabelle 2

Neue Komplexsalze der $H[Cr(NCS)_4(Ammin)_2]$ – saure mit Metallen und Metall-aminen

Verbindung	Mol. Gew.	Ausb. %d.Th.	Charakteristik	Analyse	
				ber.	gef.
Ag Rein.	678,59	98	Rotviolette Mikrokrist. Masse	Ag 15,89 Cr 7,66 S 18,86	15,68 7,60 18,66
Tl Rein.	775,08	96	Rotviolette Mikrokrist. Masse	Tl 26,36 Cr 6,71 S 16,51	26,02 6,68 16,12
Hg $Rein_2$.	1342,03	97	Rotviolette Mikrokrist. Masse	Hg 14,94 Cr 7,75 S 19,07	14,86 7,66 18,88
$[Co(NH_3)_6]$ $Rein_3$.	1873,26	97	Braunviolette Mikrokrist.	Co + 3Cr 11,47 S 20,49	11,28 20,15
$[Co\ en_3]$ $Rein_3$	1951,31	67	Braunviolette Mikrokrist.	Co + 3Cr 15,30 S 27,33	14,40 27,00
$[Co(NH_3)_5Cl]$ $Rein_2$	1320,97	64	Rotviolette kleine kristallaggregatte	Co + 2Cr 12,33 S 19,38	12,20 19,00
$[Co\ en_2Cl$-benzilamin$]$ $Rein_2$	1373,05	62	Rotviolette Tafeln.	Co + 2Cr 11,86 S 18,64	11,70 18,20
$[Co\ en_2Cl_2]$ Rein	820,72	65	Dunne helviolette kleine Nadeln	Co + Cr 13,51 S 15,59	13,40 15,20
$[Co(DH_2)Py_2]$ Rein	1019,91	78	Rotviolette kristallaggreg.	Co + Cr 10,87 S 12,55	10,80 12,10
$[Co(DH)_2(anilin)_2]$ Rein	1047,93	80	Rotviolette prismen.	Co + Cr 10,58 S 12,21	10,50 12,20
$[Co(DH)_2(Chinald)_2]$ Rein	1148,20	82	Rotviolette Nadeln.	Co + Cr 9,66 S 11,14	9,50 11,00

Rein = $[Cr(NCS)_4(Chinaldin)_2]^-$

Der Thiocyangehalt der Proben wurde gravimetrisch als $BaSO_4$ und der Metallgehalt als Cr_2O_3 bzw. als $Cr_2O_3 + Co_3O_4$ bestimmt.

Darstellung der $[Co(DH)_2$ $(Ammin)]_2$ – Acetat-Komplexen

6 mMol Dimethylglyoxim und 9 mMol Ammin (aromatische und heterocyclische Ammine) werden in 70 mL Äthanol unter Ruhren auf dem Wasserbad, 3 mMol $Co(CH_3-COO)_2 \cdot 4H_2O$ in 10 mL Wasser gelöst und die Mischung beider Lösungen mit einem starken Luftstrom 2–3 Stunden oxidiert. Die braune Flussigkeiten werden dann filtriert, mit 70% Alkohol auf 100 mL

Volumen aufgefüllt und zur Umsetzungsreaktionen verwendet. Diese Lösungen enthalten annähernd 3 mMol $[Co(DH)_2(Amin)_2]$-Acetat [23].

Die thermogravimetrische Messungen wurden mit einer ülichen Thermowage und mit einer Heizungsgeschwindigkeit 10°/Min durchgeführt. Es wurde annähernd 100 mg Substanzen zur Pyrolise verwendet (Abb. 1).

Die derivatographischen Messungen wurden mit einer Derivatograph M.O.M. mit einer Aufheizgeschwindigkeit von 8°/Min durchgeführt (Abb. 2).

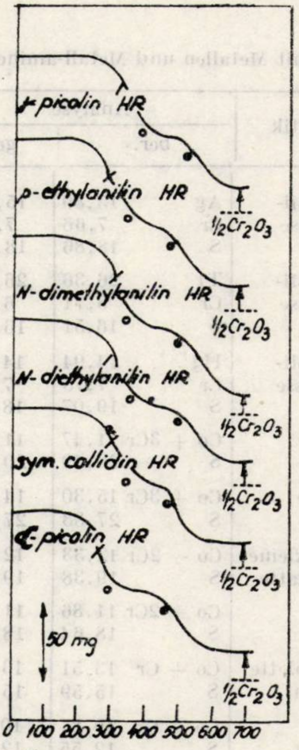

Abb. 1. — Thermogravimetrische Kurven von einigen Ammin $H[Cr(NCS)_4 (Chinaldin)_2]$ — Verbindungen : / die berechnete Menge von $H[Cr(NCS)_4 (Chinaldin)_2]$; ○ die berechnete Menge von $[Cr(NCS)_3 . Chinaldin]$; ● die berechnete Menge von $Cr(NCS)_3$; ↑ die gefundene Menge von Cr_2O_3.

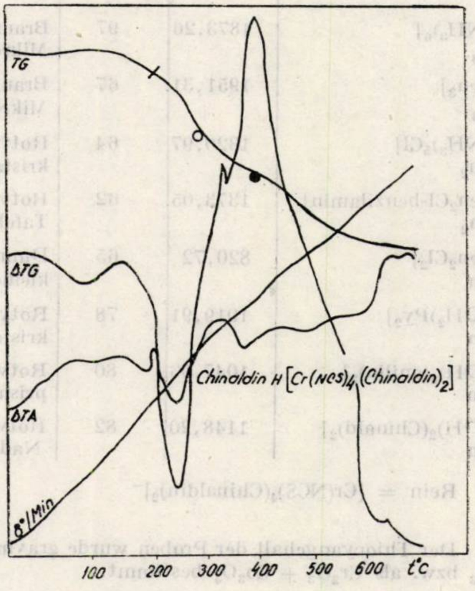

Abb. 2. — Derivatographische Kurven des Chinaldin. $H[Cr(NCS)_4 (Chinaldin)_2]$ Probemenge : 100,0 mg ; Heizungsgeschwindigkeit : 8°/Min.

Spektrophotometrische Untersuchungen : Die Lichtabsorption von Chinaldin $H[Cr(NCS)_4 (Chinaldin)_2]$ wurde im Vergleich mit der von $NH_4[Cr(NCS)_4(NH_3)_2]$ bzw. $K_3[Cr(NCS_6)]$ in Dimethylformamid gemessen. Die Absorptionsspectren zeigen 4 Maxima in Sichtbaren Bereiche (Tabelle 3 und Abb. 3).

Die Ultrarotspektren der Chinaldin $H[Cr(NCS)_4(Chinaldin)_2]$ wurden als KBr-Presslinge mit einem U.R.10 Spektrophotometer (Karl Zeiss Jena) gemessen.

Tabelle 3

Spektraldata von $K_3[Cr(NCS)_6]$ und von Ammin $H[Cr(NCS)_4 (Amimn)_2]$ Verbindung

Formel	$\lambda_1$nm	lgε_1	$\lambda_2$nm	lgε_2	$\lambda_3$nm	lgε_3	$\lambda_4$nm	lgε_4
$K_3[Cr(NCS)_6]$	550	2,01	450	1,98	380	1,90	310	4 4,2
$NH_4[Cr(NCS)_4(NH_3)_2]$	525	2,05	395	1,95	308	4,27	235	4,37
Chinaldin $H[Cr(NCS)_4$ Chinaldin$)_2]$	535	2,25	450	2,12	316	4,32	—	—

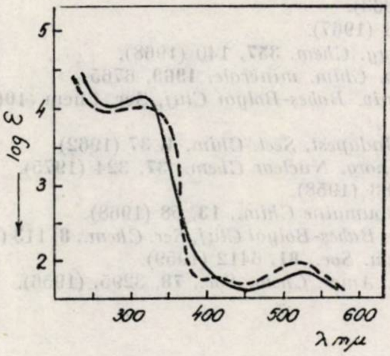

Abb. 3. — Absorptionsspektrum von : . . . $NH_4[Cr(NCS)_4(NH_3)_2]$; — Chinaldin $H[Cr(NCS)_4(Chinaldin)_2]$.

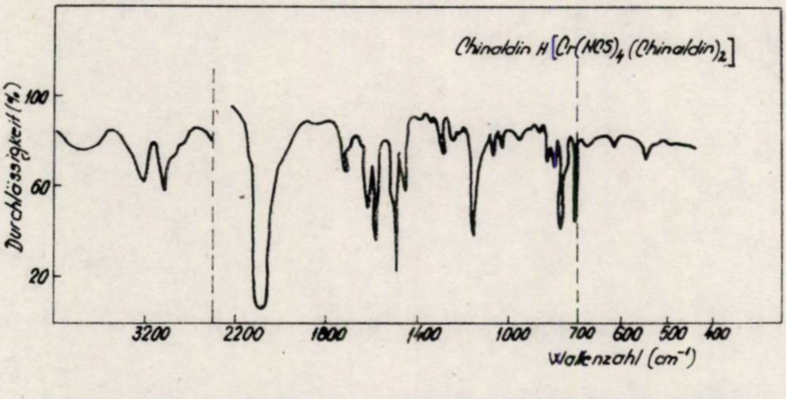

Abb. 4. — Ultrarotspektrum von Chinaldin. $H[Cr(NCS)_4(Chinaldin)_2]$.

Von Chamberlain und Bailar [24] sowie Fujita und Mitarbeiter [25] wurde festgestellt dass die $\nu_{C=N}$und $\nu_{C=S}$ Valenzschwingungen der NCS-Gruppe bei den Rhodanato-Kobalt (III)-Komplexen um 2110—2140 cm^{-1} bzw. 760 cm^{-1} auftreten. Bei einiger Klassischen Rhodanat-Chrom (III)-Komplexen wie z.b. $[Cr\ en_2(NCS)_2]NO_3$ sind diese Frequenzen bei nidrigeren Werten um 2060—2080 cm^{-1} bzw. um 730—750 cm^{-1} erkenbar. Diese Verschiebung nach niedrigeren Werten zeigt die Steigerung des Kovalenten Charakters der M—NCS-Bindung von Co(III) nach Cr(III) an. Bei Chinaldin $H[Cr(NCS)_4(Chinaldin)_2]$ erscheinen die $\nu_{C=N}$Valenzschwingungsfrequenzen um 2095 cm^{-1} und die $\nu_{C=S}$ Frequenzen bei 708—710 cm^{-1}. Dies ist ein direkter Beweis für den Kovalenten Charakter der Cr—NCS Bindung.

LITERATUR

[1] J. Roessler, *Liebigs Ann. Chem.*, **141**, 189 (1867).
[2] R. Ripan, I. Gănescu und Cs. Várhelyi, *Rev. Roumaine Chim.*, **11**, 473 (1966).
[3] R. Ripan, Cs. Várhelyi und I. Gănescu, *Rev. Roumaine Chim.*, **11**, 717 (1966).
[4] C. Mahr, *Z. analyt. Chem*, **120**, 6 (1940).
[5] C. Mahr, *Z. analyt. Chem.*, **208**, 313 (1932).
[6] A. Scagliarini und B. Tartarini, *Gazz. chim. Ital.*, **53**, 5617 (1923).
[7] J. Brönsted und H. Pedersen, *J. Amer. Chem. Soc.*, **44**, 817 (1922).
[8] P. Pfeiffer, *Ber. dtsch. chem. Ges.*, **34**, 4303 (1901).
[9] P. Pfeiffer, *Z. anorg. Chem.*, **29**, 107 (1902).
[10] P. Pfeiffer und M. Haimann, *Ber. dtsch. chem. Ges.*, **36**, 1063 (1903).
[11] P. Pfeiffer, *Ber. dtsch. chem. Ges.*, **37**, 4255 (1904).
[12] P. Pfeiffer und B. Werdelmann, *Z. anorg. Chem.*, **263**, 31 (1950).
[13] K. Issleib und A. Tzschach, *Z. anorg. Chem.*, **297**, 121 (1958).
[14] A. Reinecke, *Liebigs Ann. Chem.*, **126**, 114 (1863).
[15] Cs. Várhelyi und I. Gănescu, *Monatsh*, **98**, 478 (1967).
[16] R. Ripan, I. Gănescu und Cs. Várhelyi, *Z. anorg. Chem*, **357**, 140 (1968).
[17] I. Gănescu, Cs. Várhelyi und D. Oprescu, *Rev. Chim. minèrale*, **1969**, 6765.
[18] G. Boda, Cs. Várhelyi und A. Mostis, *Stud. Univ. Babeş-Bolyai Cluj*, Ser. Chem. **10(2)**, 63 (1965)
[19] P. J. Krausz und J. Kovacs, *Ann. Univ. Sci. Budapest, Sect. Chim*, **4**, 37 (1962).
[20] I. Gănescu, Cs. Várhelyi und D. Oprescu, *J. Inorg. Nuclear Chem.*, **37**, 324 (1975).
[21] A. W. Adamson, *J. Amer. Chem. Soc.*, **80**, 3183 (1958).
[22] J. Zsakó, Cs. Várhelyi und I. Gănescu, *Rev. Roumaine Chim.*, **13**, 58 (1968).
[23] R. Ripan, Cs. Várhelyi und B. Böhm, *Stud. Univ. Babeş-Bolyai Cluj, Ser. Chem.*, **8**, 113 (1963).
[24] M. Chamberlain und J. C. Bailar, *J. Amer. Chem. Soc.*, **81**, 6412 (1959).
[25] Y. Fujita, K. Nakamoto und M. Kobayashi, *J. Amer. Chem. Soc.*, **78**, 3295, (1956).

Revue Roumaine de Chimie, **30**, *4*, 317–327 (1985)

POTENTIAL ANTICANCER AGENTS. XXV[*] ALIPHATIC AND CYCLOALIPHATIC N-NITROSOUREAS AND N-NITROSOURETHANES

ILEANA BARACU, EUTANŢA TĂRNĂUCEANU, V. DOBRE
and I. NICULESCU-DUVĂZ
Oncological Institute, Bucharest, Romania

Received December 12, 1983

Seven aliphatic and cycloaliphatic 2-chloroethyl-nitrosoureas 1(n=7), 2(n=7,8), 5, 11–15-16(derived from 1,7-heptamethylene-, 1,8-octamethylene diamines, 5,6-benzohexahydroc indane, etc.) and two 2-hydroxyethyl-nitrosoureas (derived from 1,6-hexamethylene diamine and cyclohexyl amine) were synthesized and studied. Their isomeric structure was assigned on the basis of ^{1}H–NMR spectra and the unequivocal synthesis of th- 1-(2-chloroethyl)-1-nitrosoureas which were achieved using 2-chloroethyl-nitroso-carboa, moyl azide. Four N-nitrosourethanes (derivied from cyclohexanol, methyl-cyclohexanol cholic and desoxycholic acids) were obtained by the nitrosation of the corresponding urethanes.The most effective compounds against L1210 were 1,7-heptamethylene-bis-/1-(2-chloroethyl)-3-nitrosourea/, 1(n = 7), and especially 1,8-octamethylene-bis-1-(2-chloroethyl)-1-nitrosourea/, 2(n = 8).

Chloroethyl nitrosoureas represent a very attractive group of anticancer agents, which proved to be useful in the treatment of a large spectrum of human cancer.[1] A number of highly active lipophilic (BCNU, CCNU, Me-CCNU, etc.)[**] as well as hydrophilic nitrosoureas (Chlorozotocin, GANU, ACNU, etc.)[**] are actually under clinical evaluation.[2–7]

Although the mechanism of action of nitrosoureas has not been fully understood, a number of data indicate that they underwent nonenzymatical decompositions in aqueous media at relatively high rates, generating a number of reactive species with carbamoylating or alkylating capacities.[8,9] In human and rodents the enzymatic hydroxylation (by liver microsomal enzyme systems) of some cycloaliphatic nitrosoureas (i.e. CCN , Me-CCNU) was also demonstrated. In this case the rate of the metabolic hydroxylation exeeds the rate of the chemical breakdown.[10]

---

[*] Potential Anticancer Agents XXIV, Physicochemical and Biological Investigation of Some New Aliphatic and Cycloaliphatic Nitrosoureas, Ileana Baracu, G. Botez, R. Deneş V. Dobre, B. Ureche, T. Crăescu, N. Voiculeţ and I. Niculescu-Duvăz, *Rev. Roumaine Biochem.*, **18**, 175 (1981).

[**] Abbreviation list : BCNU, 1,3-bis-(2-chloroethyl)-1-nitrosourea ; CCNU, 1-(2-chloroethyl)-3-cyclohexyl-1-nitrosourea ; Me-CCNU, 1-(2-chloroethyl)-3-(*trans*-4-methylcyclohexyl)-1-nitrosourea ; Chlorozotocin, 2-/3-(2-chloroethyl)-3-nitrosoureido/-D-glucopyranose ; GANU, 1-(2-chloroethyl)-3-(β-D-glucopyranosyl)-1-nitrosourea ; ACNU, 1-(4-amino-2-methyl-5-pyrimidinyl)-3-(2-chloroethyl)-3-nitrosourea.

It is likely that the reaction of the resulted reactive species with the target biological macromolecules may account for the pharmacological properties of the nitrosoureas. In this respect their carbamoylating ability was related to their toxicity and the two-step DNA alkylation, by the *in vivo* generated carbocations (i.e. 2-chloroethyl carbocation, etc.) is probably responsible for their antitumor activity.[6-11]

In a previous paper we described the synthesis of the 3-nitroso isomers of aliphatic bis-N, N′-nitrosoureas $^1(n = 2-6,8)$.[12] According to the literature data, these isomers could be considered as "wrong", being biologically less effective than the corresponding 1-nitroso isomers.* However, some of these "wrong" nitrosourea isomers exhibited interesting inhibitory properties against experimental leukemia L1210. For example, compound $^1(n = 6)$ is definitely effective against leukemia L1210 (ILS% = = 63% by respect to 113% for CCNU, at equimolecular doses) and moderately toxic (LD_{50} = 1.18 mmol/kg · bw by respect to 0.32 mmol/kg · bw for CCNU).[12]

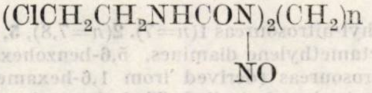

$(\mathrm{ClCH_2CH_2NHCO}\underset{\mathrm{NO}}{\mathrm{N}})_2(\mathrm{CH_2})\mathrm{n}$

1 $(n = 2-6.8)$

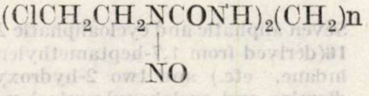

$(\mathrm{ClCH_2CH_2}\underset{\mathrm{NO}}{\mathrm{N}}\mathrm{CONH})_2(\mathrm{CH_2})\mathrm{n}$

2 $(n = 2-6)$

It is of interest to mention that the most effective nitrosourea (against L5222) from the corresponding series of "good" isomers $\mathbf{2}(n = 2-6)$ synthesized by Eisenbrand, is also the compound with $n = 6$.[13]

However, because of the different screening systems used, no direct comparison could be made, in respect to their antitumor properties between the both series of compounds (**1** and **2**). In order to compare more "good" and "wrong" nitrosoureas from both series, we decided to synthesize additional derivatives, namelly **1**, $n = 7$ and **2**, $n = 7,8$.

Independently, we were interested in increasing the number of structurally related nitrosourea, available for QSAR analysis. Accordingly we synthesized nine new compounds and studied their biological properties. These additional derivatives are aliphatic, cycloaliphatic and aromatic 1-(2-chloroethyl)-1-nitrosoureas, 1-(2-chloroethyl)-nitrosourethanes and 1-(2-hydroxyethyl)-1(3)-nitrosoureas.

SYNTHESES

1 Synthesis of 1-(2-chloroethyl)-1-nitrosoureas

A. The unequivocal synthesis of 1-(2-chlorethyl)-1-nitrosoureas **2**, $n = 7, 8$ was carried out according to Eisenbrand's procedure, by coupling the desired diamines **3**, $n=7,8$ to 2-chloroethyl-N-nitroso-carbamoyl azide **4**.[13-15] Compound **5** was obtained in the same way. The analytical data of the new compounds are given in table 1.

---

* The numbering was derived from that of CCNU, the nitrogen atom linked to the 2-chloroethyl moiety being noted as N_1.

Table 1

Analytical data of new urea derivatives

Compound	Formula	mp°C	% Yield	Analytical data %							
				Calculated				Found			
				C	H	N	Cl	C	H	N	Cl
8	$C_{16}H_{21}ClN_2O$	142 dec.	59	65.62	7.14	9.57	12.11	65.54	7.08	9.49	12.53
9	$C_9H_{18}N_2O_2$	98–101	65	58.02	9.76	15.04	—	58.06	9.68	15.05	—
10	$C_{15}H_{13}Cl_3N_4O$	125	63	48.47	3.50	15.08	28.61	48.92	3.91	15.15	29.16
14	$C_{13}H_{26}Cl_2N_4O_2$	120	75	45.74	7.69	16.42	20.77	46.08	7.45	16.21	20.38
15	$C_{12}H_{28}N_4O_4$	180	95	49.28	9.67	19.16	—	49.66	9.36	19.21	—

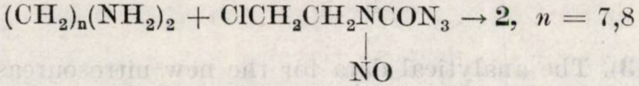

$$(CH_2)_n(NH_2)_2 + ClCH_2CH_2\underset{NO}{\underset{|}{N}}CON_3 \rightarrow \mathbf{2},\ n = 7,8$$

3, $n = 7,8$ **4**

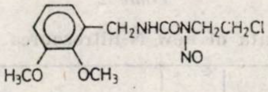

5

2-Chloroethyl-N-nitroso-carbamoyl azide (**4**) was prepared by nitrosation of 2-chloroethyl carbamoyl azide (**7**) with N_2O_4, according to the literature data.[13,14] Our attempts to obtain azide **7** by Eisenbrand's procedure partially failed, giving nonreproductible yields of an impure material. This method was however definitely improved by our finding that the addition of azothydric acid to 2-chloroethylisocyanate (**6**) proceeds in high yields in the presence of catalytically amounts of DMSO; the completion of this reaction was spectrophotometrically followed (by following the disappearance, respectivelly, the appearance of the $\nu_{NCO} = 2270\ cm^{-1}$ and $\nu_{N_3} = 2150\ cm^{-1}$).

$$ClCH_2CH_2NCO + NH_3 \xrightarrow[CHC]{DMSO} ClCH_2CH_2NHCON_3$$

6 **7**

B. Compounds **11**, **12**, **13** were obtained by normal nitrosation of the precursor ureas **8**, **9** and **10** in 98–100% HCOOH with solid sodium nitrite. This reaction afforded, after isomer purification (from 98–100% HCOOH),[2] the expected 1-nitroso isomers, practically pure (the isomeric purity was checked by ^1H–NMR in each case). This selectivity of the nitrosation is probably due to the steric control of the cyclohexyl ring (for compounds **11** and **12**) or electronic effects exerted by the arly moiety

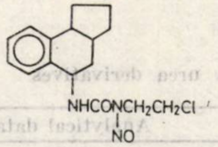

11

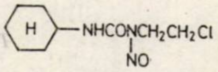

12

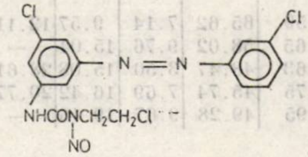

13

(compound **13**). The analytical data for the new nitrosoureas **11**—**13**, as well as for their corresponding precursor ureas 8—10, are summarized in tables 1 and 2.

Table 2

Analytical data of new N-nitrosourea derivatives

Compound	Formula	mp°C	% Yield	Analytical data %							
				Calculated				Found			
				C	H	N	Cl	C	H	N	Cl
1(n = 7)	$C_{13}H_{24}Cl_2N_6O_4$	75.5—77	84	39.10	6.07	21.05	17.75	39.57	6.39	21.23	18.23
2(n = 7)	$C_{13}H_{24}Cl_2N_6O_4$	86—89	60	39.10	6.07	21.05	17.75	38.80	6.36	20.96	17.37
3(n = 8)	$C_{14}H_{26}Cl_2N_6O_4$	71—71.5	60	40.68	6.35	20.34	17.15	40.97	6.66	20.11	16.82
5	$C_{12}H_{16}ClN_3O_4$	36—38	75	47.76	5.36	13.93	11.75	48.20	5.65	14.00	12.14
11	$C_{16}H_{20}ClN_3O_2$	116—118	92	59.71	6.28	13.06	11.01	60.00	6.69	13.30	11.51
12	$C_{15}H_{12}Cl_3N_5O_2$	86	85	—	—	17.48	—	—	—	17.00	—
13	$C_9H_{17}N_3O_3$	57—58	60	50.21	7.97	19.52	—	50.03	7.99	19.03	
16	$C_{12}H_{24}N_6O_6$	74—76	80	41.36	6.96	24.13	—	41.20	7.04	23.85	—

2. Synthesis of 3-nitrosoureas, 1 (n = 7) and 16

As we have previously found, the nitrosation of polymethylene-N,N′-bis-(2-chloroethyl)-ureas with solid sodium nitrite in 98—100% HCOOH led to the 3-nitroso isomers, **1**(n = 2—6,8).[12]

Unexpectedly, the nitrosation of heptamethylene-1,7-bis-(2-chloroethyl)-urea, **14**, in the standard conditions, failed. This reaction was achieved, with satisfactory yields, by addition of the solid sodium nitrite to a mixture of 98—100% HCOOH : 6N HCl/1 : 1, the desired 3-nitrosourea **1**(n = 7) of isomeric purity (^{1}H—NMR controlled) being obtained (for analytical data see table 1). The precursor urea **14** was prepared according to the usual procedure[12] (the analytical data are presented in table 2).

Hexamethylene-1,6-bis-/12-(2-hydroxyethyl)-3-nitrosourea/, **16**, was obtained by the nitrosation of the precursor urea **15** in 6N HCl with solid sodium nitrite, followed by methanolysis[17] and isomeric purification (recrystallization from 98—100% HCOOH). For their analytical data see tables 1 and 2.

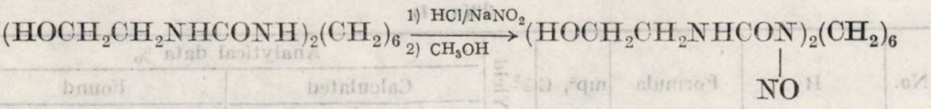

$$(HOCH_2CH_2NHCONH)_2(CH_2)_6 \xrightarrow[2)\ CH_3OH]{1)\ HCl/NaNO_2} (HOCH_2CH_2NHCO\underset{NO}{\underset{|}{N}})_2(CH_2)_6$$

15 **16**

3. 2-Chloroethyl isocyanate

2-Chloroethyl isocyanate (**6**) is, undoubtely, the key intermediate in the synthesis of 2-chloroethyl ureas. Since the known procedures for its preparation[18-23] give, generally, poor yields of unsatisfactory pure 2-chloroethyl isocyanate, we tried, previously, to improve Wenker's method of synthesis[12,20]. In this report a new synthetic route to 2-chloroethyl isocyanate was described, which affords this product with unexpectedly high yields (≃70%) and satisfactory purity. Starting from 3-chloropropionic acid chloride (**18**) its conversion to 2-chloroethyl isocyanate was achieved in one step procedure, by treatment of **18** with activated sodium azide,[24] at 30—40°, followed by thermal decomposition (at 60—80°) of the organic azide **19** thus formed.

$$\underset{\mathbf{17}}{ClCH_2CH_2COOH} \xrightarrow[DMF]{SOCl_2} \underset{\mathbf{18}}{ClCH_2CH_2COCl} \xrightarrow{NaN_3} \underset{\mathbf{19}}{ClCH_2CH_2CON_3} \rightarrow$$

$$\rightarrow \underset{\mathbf{6}}{ClCH_2CH_2NCO}$$

The reaction is practically complete when the gase evolution has ceased The best results (purity and yield) were obtained when the reaction was carried out in high boiling point aprotic solvents (such as tetraline or decaline).

34. Synthesis of new N-nitrosourethanes

N-(2-chloroethyl)-urethanes derived from cyclohexanols, **23**(**a**, **b**), steroidic hormones or biliary acids **23** (**c**—**f**) were obtained by the reaction between a) 2-chloroethyl amine (**20**) and the desired chloroformates **21**, or b) 2-chloroethyl isocyanate (**6**) and the corresponding alcohols **22** (see Scheme I). The estradiol derivative, **23d**, was prepared by both procedures. For analytical data see table 3.

Nitrosourethanes, **24** (**a**, **b**, **e**, **f**), were obtained by nitrosation of the precursors **23** in 98—100% HCCOH with solid sodium nitrite. Not all of the desired derivatives could be isolated, because they underwent, probably, decompositions during manipulations. Analytical data are presented in table 4.

Table 3

Analytical data of new N-2-chloroethyl urethanes

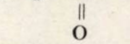

$ClCH_2CH_2NH\underset{\underset{O}{\|}}{C}OR$

23(a–f)

No.	R	Formula	mp°, C	% Yield	Analytical data %							
					Calculated				Found			
					C	H	N	Cl	C	H	N	Cl
23a	cyclohexyl	$C_9H_{16}ClNO_2$	36–40	99	52.54	7.86	6.81	17.23	52.96	8.17	6.54	17.54
23b	4-methyl-cyclohexyl	$C_{10}H_{18}ClNO_2$	61–64	91	54.66	8.27	6.38	16.13	54.68	8.61	6.04	16.11
23c	3-β-cholesteryl	$C_{30}H_{50}ClNO_2$	126–9	86	73.19	10.25	2.85	7.20	73.28	10.49	2.86	7.68
23d	3-(17β-estradiyol)	$C_{21}H_{27}ClNO_3$	93–95	14	66.90	7.23	3.69	9.40	66.40	7.27	3.91	10.01
23e	methyl, 3α-cholyl carboxylate	$C_{28}H_{46}ClNO_6$	132–4	60	63.67	8.84	2.65	6.71	63.21	8.45	2.83	7.20
23f	methyl, 3α-desoxycholyl-carboxylate	$C_{28}H_{48}ClNO_5$	75–77	55	66.65	9.07	2.73	6.92	65.49	9.36	2.75	7.36

Table 4

Analytical data of new N-2-chloroethyl-nitrosourethanes

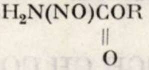

$ClCH_2CH_2N(NO)\underset{\underset{O}{\|}}{C}OR$

24 (a, b, e, f)

No	R	Formula	mp°, C	% Yield	Analytical data %							
					Calculated				Found			
					C	H	N	Cl	C	H	N	Cl
24a	cyclohexyl	$C_9H_{15}ClN_2O_3$	oil	62	46.05	6.45	11.94	15.10	46.54	6.84	11.86	15.46
24b	4-methyl-cyclohexyl	$C_{10}H_{17}ClN_2O_3$	49–50	77	48.28	6.90	11.26	14.25	48.62	6.80	11.08	13.92
24e	methyl, 3α-cholyl-carboxylate	$C_{28}H_{45}ClN_2O_7$	180–2	54	60.35	8.15	5.03	6.38	59.93	8.39	4.86	6.65
24f	methyl, 3α-desoxycholyl-carboxylate	$C_{28}H_{45}ClN_2O_6$	145–9	51	62.14	8.40	6.55	5.18	61.80	8.32	4.85	6.72

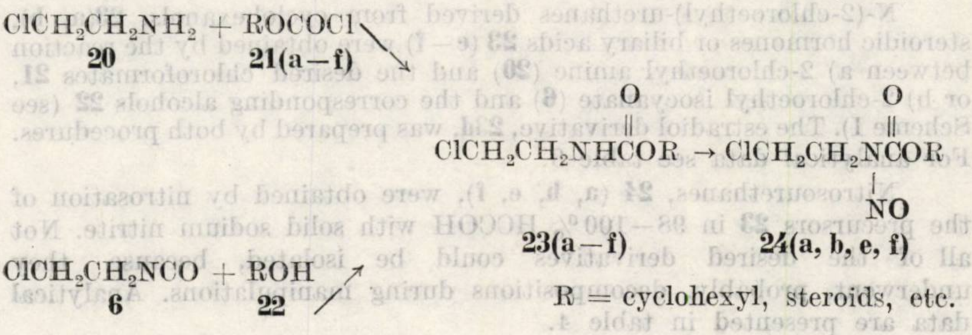

SPECTRAL DATA

A. *IR spectra* of the urea derivatives were in good agreement with the literature data. [2,5,6,8,13]By nitrosation, the carbonyl absorption is shifted with a $\Delta\nu = 75-90$ cm^{-1}, being located at 1705–1720 cm^{-1}. This band was very useful in following the nitrosation reactions.

B. ^{1}H–NMR spectra are very useful in establishing the isomeric structure and purity of the nitrosourea derivatives.

The protons belonging to the 2-chloroethyl moiety of the urea derivatives presented an A_2B_2X spectrum, which appeared as a psedosinglet located at $\delta = 3.54 \pm 0.05$ ppm. [2] There are some cases where the signal appeared as two triplets, as in the case of 1-(2-chloroethyl)-3-thymidinyl urea derivatives ($\delta = 3.57$ ppm, 2H, CH_2NH ; $\delta = 3.26$ ppm, 2H, CH_2Cl).[25]

The ^{1}H–NMR spectral pattern of the 1-(2-chloroethyl)-1-nitroso (A_2B_2, two triplets, $\Delta\nu/J = 10$ Hz) and 1-(2-chloroethyl)-3-nitroso isomers (A_2B_2X, pseudo singlet) are sufficiently different to allow a quite sure structural assignment. From the data presented before[12] and those summarized in table 5 resulted that :

Table 5

Chemical shifts δ(ppm) of the methylenic protons belonging to 2-chloroethyl moiety in the N-nitrosourea derivatives.

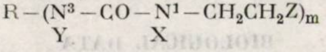

$$\underset{Y}{R-(N^3}-CO-\underset{X}{N^1}-CH_2CH_2Z)_m$$

No.	R	m	X	Y	Z	Chemical shift, δ(ppm)[1] CH_2Z	Chemical shift, δ(ppm)[1] N_1CH_2	$J_{1,2}$(Hz)
1	1,7-heptamethylene	2	H	NO	Cl	3.74 – 3.78 [2]		
2	1,7-heptamethylene or 1,8-octamethylene	2	NO	H	Cl	3.42	4.12	–
5	2,3-dimethoxy-benzyl	1	NO	H	Cl	3.50–3.56	4.20–4.26	6.0
11	5,6-benzo-hexahydro-indanyl	1	NO	H	Cl	3.53	4.20	6.0
12	cyclohexyl	1	NO	H	HO	3.60	4.09	6.0
13	2-(3,3′-dichloro)-azo-benzene	1	NO	H	Cl	3.50	4.42	10.0

[1] the signals appeared as triplets, when no otherwise noted ; [2] multiplet

1. 1-nitroso isomers present always two triplets which are characteristic of an A_2B_2 spectrum pattern. This is unequivocally demonstrated in the case of N-(2-chloroethyl)-N-nitrosocarbamoyl azide (**4**) as well as in the case of the nitrosoureas **2**(n = 7, 8) resulted from its coupling with the corresponding diamines.

The literature data regarding the assignment of the two triplets exhibited by the methylenic protons of the 2-chloroethyl-nitroso moiety are conflicting. Imbach[7] attributed the lowfield triplet to the CH_2Cl protons, while Johnston[8] assigned it to the (NO)NCH_2 ones. It is logical to assume that the upfield triplet ($\delta = 3.43-3.56$ ppm) belongs to the protons of the CH_2Cl group, since it is not shifted by nitrosation. However, because inversions could arise, we collected the following additional data, which support the Johnston's assignment :

— in compound **25** the NHCH_2 protons are located at $\delta = 3.53$ ppm, being easily recognizable as a multiplet. By nitrosation at the adjacent nitrogen atom (as in compound **25**) a downfield shift occurs, the absorption of N(NO)CH_2 protons arising as a quartet located at $\delta = 3.89$ ppm. [27]

$CH_3N(NO)CONHCH_2CH_3$ **25** $CH_3NHCON(NO)CH_2CH_3$ **26**

— for compound **9** the $-N(NO)CH_2CH_2OH$ protons, located at $\delta = 3.60$ ppm could be easily recognised as a quartet, which by deuteration colapsed to a triplet (and the OH triplet disappeared).

2. The nitrosourea **1**($n = 2-8$) exhibited in ^1H-NMR spectra a pseudosinglet centered at $\delta = 3.74-3.78$ ppm. The assignments were pone in relation to BCNU spectrum.

PHYSICO-CHEMICAL DATA

Lipophilicity, log P, alkylation rate of 4-nitro-benzyl-pyridine and chemical reactivity, $T_{0.5}$, were measured for all the new compounds and were used in computing the QSAR. These data will be published elsewhere.

BIOLOGICAL DATA

The toxicity (LD_{50} mmole/kg b.w) and the antitumor effectiveness against W_{25} carcinosarcoma (TGI%) and L1210 leukemia (ILS%) were summarized in table 6.

From the available biological data the following conclusions could be emphasized :

a) compounds **2**($n = 7,8$), 1-nitroso isomers are highly active against L1210, and more effective than the corresponding 3-nitroso isomers **1**($n = 7,8$) ;

b) however, compound **1**($n = 7$), a 3-nitroso isomer, exhibited a therapeutic index very close to that of CCNU ;

c) halogen substitution, in 2-chloroethyl moiety, by a hydroxyl group, as in compounds **9** and **16**, resulted in the loss of antileukemic activity, although they retain some activity against W_{256} carcinosarcoma ;

d) replacement of the ureidic structure by an urethanic one provides highly toxic compound s, devoid of antitumor activity.

EXPERIMENTAL SECTION

Melting points were determined with a Franz Küstner-Dresden apparatus and were uncorrected.

IR spectra were determined in KBr discs (ureas, nitrosoureas) or $CHCl_3$ and CCl_4 solutions nitrosoureas, urethanes, nitrosourethanes) on a Specord IR—75 spectrophotometer (Carl Zeiss, Jena).

Table 6

Toxicity and antitumor activity of the previous N-nitroso derivatives

No.[1]	Toxicity[2] LD_{50}mmoles/kg	Antitumor activity	
		TGI%[3]	ILS%[4]
1 ($n = 7$)	0.16	44	166
2 ($n = 7$)	2.05	nd[5]	93
2 ($n = 8$)	0.21	nd	200
5	4.91	60	nd
10	2.33	nd	nd
12	2.40	43	0
13	0.09	0	29
16	0.87	33	0
24a	0.89	33	0
24b	0.20	0	19
CCNU	0.32	nd	113

[1] the numbering is the same as in text and tables 1–4; [2] single dose on Wistar rats (according to J. Cornfield and N. Mantel, *J. Amer. Statist. Ass.*, **43**, 181 (1950); [3] Walker 256 carcinosarcoma, the treatment began 7 days after tumor transplantation; TGI% = tumor growth inhibition (T – C)/T × 100 (*T* = tumor weights in treated animals; C = idem for control); [4] Leukemia L1210 on DB2 mice; the treatment began 24 hrs after inoculation of 10^6 leukemic cells: ILS% = increase in life span (T/C–1)100: [5]nd = not determined

^1H–NMR spectra were run in $CDCl_3$, CCl_4 or $(CD_3)_2CO$ on a Varian EM–360 L spectrometer, with tetramethylsilane as internal standard.

TLC was performed on precoated Merck silicagel F_{254} plates using as eluent a mixture of benzene : ethanol/9 : 1. Nitroso derivatives could be detected in UV light or by iodine vapors. All analytical samples were essentially tlc homogenous.

1. 1,7-Heptamethylene-bis-/1-(2-chloroethyl)-3-nitrosourea,/1 (n = 7).

Solid $NaNO_2$ (0.42 g, 6.50 mmoles) was added in small portions to a cold (0–5°) stirred solution of 1,7-heptamethylene-bis-/1-(2-chloroethyl)-urea/, **14** (0.47 g, 1.40 mmoles) dissolved in 10 mL 6N HCl. The resulted yellow mixture was stirred at 0–5° for 1 hr, and then slowly (dropwise) diluted with cold H_2O (10 mL). The oily product separated was extracted with C_6H_6 (3 × × 10 mL). The combined benzenic extracts were washed with H_2O (3 × 10 mL), dried (Na_2SO_4) and evaporated to dryness in vacuo. The resulted yellow precipitate, purified by reprecipitation with water from 98–100% HCOOH,[2,12] yielded pure **1**($n = 7$)/0.52 g, 84.4%/. For analytical data see table 2.

2. 2-Chloroethyl carbamoyl azide (7)

To a cold (0–5°) stirred solution of HN_3 (5% in $CHCl_3$, 860 mL) containing DMSO (25 mL), 2-chloroethyl isocyanate (8.5 g, 80.5 mmoles) was added dropwise under cooling. Then the mixture was kept overnight at room temperature. Evaporation of the reaction mixture under reduced presure and temperature, afforded an oily residue, which was crystallized from petroleum ether (b.p. 30–60°). The solid dried in vacuo (P_2O_5) gave **7** (6.00 g, 90%), m.p. 49°.

3. 1,7-Heptamethylene-bis-1-(2-chloroethyl)-1-nitrosourea/,2 (n = 7)

To a cold solution (0–5°) of 2-chloroethyl-nitroso carbamoyl azide 4 (0.98 g, 5.50 mmoles) in CH_2Cl_2 (15 mL) 1,7-heptamethylene-diamine **3** ($n = 7$) (1.30 g, 10 mmoles) dissolved in DMFA (50 mL) was added dropwise under stirring. The mixture was stirred for 1 hr at 0–5° and for 2 hrs at room temperature. The solution thus obtained was filtered, the filtrate successively washed with water (3×25 mL), 1 %HCl (3×35 mL), water (3×25 mL), dried ($MgSO_4$) and concentrated to dryness in vacuo. The resulted oil was purified on Fluorisil using benzene as eluent. Benzenic solution was concentrated in vacuo to a final volume of 30 mL. By addition of 200 mL petroleum ether (b.p. 30–60°) to this solution, a yellow precipitate resulted, which after purification from benzene-petroleum ether gave **2** (n = 7)/2.58 g, 60 %/.

Similarly, 1,8-octamethylene-bis-/1-2(chloroethyl)-1-nitrosourea/, **2** (n = 8) was obtained. For analytical data see table 2.

4. 1-(2-Chloroethyl)-3-/8-(5′,6′-benzo)-hexahydroindanyl/-urea, 8.

2-Chloroethyl isocyanate **6** (0.80 g, 7.60 mmoles) was added dropwise at 15° to a stirred solution containing 8-(5′, 6′-benzo)-hexahydroindanil amine* (1.40 g, 7.50 mmoles), Et_3N (1 mL) and $CHCl_3$. The solution was stirred for 5 hrs at room temperature and then washed with water 2×25 mL), 1 % HCl (15 mL) and again with water (2×15 mL). The organic layer was separated, dried (Na_2SO_4) and evaporated in vacuo to a final volume of 10 mL. By addition of 100 mL petroleum ether (30–60°) to this solution the urea **8** precipitated as a white solid (1.10 g, 60 %). For, analytical data see table 1.

5. 1-(2-Chloroethyl)-3-/8-(5′,6′-benzo)-hexahydroindanyl/-1-nitrosourea (11)

Solid $NaNO_2$ (2.50 g, 36.20 mmoles) was added in small portions to a cold (0–5°) and stirred solution of urea **8** (1.00 g, 3.41 mmoles) dissolved in a mixture of 98–100 % HCOOH (5 mL and 36 % HCl (5 mL). The mixture was stirred for 1 hr at 0–5°, diluted with cold water (0–5°, 20 mL added dropwise) and stirred for 0.5 hrs (0–5°). The solid thus obtained, filtered, washed with cold water and dried (P_2O_5, vacuo), yielded **11** (1.01 g, 92 %). Analytical data are given in table 2.

6. 1-(2-Chloroethyl)-3-/2-(3,3′-dichloro)-azobenzene/-urea (10)

To a stirred solution of 1-amino-2-(3,3′-dichloro)-azobenzene (13.30 g, 50.0 mmoles) in benzene (50 mL), 2-chloroethyl isocyanate **6** (5.50 g, 52.10 mmoles) was added dropwise at 10–15°. The mixture was stirred for 1 hr more at room temperature and then cooled and filtered. The precipitate thus obtained washed with petroleum ether, dried (P_2O_5) and recrystallized from methanol gave **10** (11.65 g, 63 %). For analytical data see table 1.

7. 1-(2-Chloroethyl)-3-/2-(3,3′-dichloro)-azobenzene/-1-nitrosourea (13)

Solid $NaNO_2$ (1.80 g, 26.10 mmoles) was added in small portions to a cold (0–5°) stirred solution of **12** (3.40 g, 9.10 mmoles) in 98–100 % HCOOH (75 mL). The mixture was stirred for 1 hr at 0–5°, diluted with cold water (0–5°, 50 mL) and after 1.5 hrs was filtered. The solid thus obtained washed with cold water afforded **13** (3.11, g, 85 %). Analytical data are given in table 2.

8. 2-Chloroethyl isocyanate (6)

Activated NaN_3 (50 g, 769 mmoles) was added slowly at 30–40° to a stirred solution of 3-chloropropionic acid chloride (50 g, 394 mmoles) in tetraline (150 mL). Then the reaction mixture was heated slowly, up to 80–85°, and maintained at this temperature until the gas (N_2) evolution ceased. The end of the reaction could be spectrometrically determined following the decrease of the acid chloride and azide characteristic absorption bands at 1800 and 2150 cm^{-1} respectively. The crude 2-chloroethyl isocyanate (**6**) was purified by distillation. The fraction boiling at 28–30°/10 mmHg (lit. 41°/12 mmHg)[19] was collected (32 g, 77 %).

---

* This amine was kindly supplied by dr. A. Glatz

9. 1,6-Hexamethylene-bis-/1-(2-hydroxyethyl)-3-nitrosourea (16)

1,6-Hexamethylene-bis-/1-(2-hydroxyethyl)-urea, **15**, (2.90 g, 8.90 mmoles) was dissolved in cold (0—5°) concentrated HCl (20 mL). To this solution 30 mL of water were added and the solution was maintained at 0—5° under stirring. Solid $NaNO_2$ (2.97 g, 43.00 mmoles) was added slowly. After 1 hr stirring at this temperature, the reaction mixture was diluted with cold water (30 mL). The yellow precipitate thus formed was dried (vacuo, P_2O_5), dissolved in MeOH (35 mL) and heated at 35—40° for 0.5 hrs. The solvent was evaporated in vacuo and the resulted solid was purified by precipitation from cold 98—100% HCOOH (0—5°, 40 mL) with water (40 mL). The resulted solid filtered and dried (P_2O_5) gave **16** (2.78 g, 80%). For analytical data see table 1.

10. Synthesis of N-nitrosourethanes. General procedure

To a cold (0—5°) stirred solution of urethane (400 mmoles) in 98—100% HCOOH (80 mL) solid $NaNO_2$ (800 mmoles) was added in small portions, and the stirring was continued for 1 hr, Cold water (0—5°, 100 mL) was added dropwise to this mixture and the stirring was continued at 0—5° for 1 hr. The nitrosourethanes were isolated by filtration (when a solid was obtained) or by extraction with ethylic ether (when an oily layer resulted). In the case of nitrosourethane carrying HO-groups, the crude product was submitted to methanolysis at 35—40° for 0.5 hrs, the pure product being obtained by solvent evaporation in vacuo.

REFERENCES

[1] J. A. Montgomery, T. P. Johnston and Y. F. Shealy, Burger's Medicinal Chemistry, 595 (1979).

[2] J. A. Montgomery, R. James, G. S. McCaleb and T. P. Johnston, *J. Med. Chemistry*, **10**, 668 (1967).

[3] S. K. Carter and J. W. Neman, *Cancer Chemother. Rept.*, **1**, 115 (1968).

[4] S. C. Barranco and R. M. Humphrey, *Cancer Res.*, **31**, 191 (1971).

[5] T. P. Johnston, G. S. McCaleb, P. S. Oplinger, W. R. Laster and J. A. Montgomery, *J. Med. Chemistry*, **14**, 600 (1971).

[6] T. P. Johnston, G. S. McCaleb and J. A. Montgomery, *J. Med. Chemistry*, **18**, 104 (1975).

[7] J. L. Montero, A. Moruzzi, J. Oiry and J. L. Imbach, *Eur. J. Med. Chem.*, **12**, 397 (1977).

[8] J.A. Montgomery, R. James, G. S. McCaleb, M. C. Kirk and T. P. Johnston, *J. Med. Chemistry*, **18**, 568 (1975).

[9] M. Colvin, J. W. Cowen, R. B. Brundrett, B. S. Kramer and D. B. Ludlum, *Biochem, Biophys. Res. Commun.*, **60**, 515 (1974).

[10] H. E. May, R. Boose and D. J. Reed, *Biochem. Biophys. Res. Commun.*, **57**, 426 (1974).

[11] K. W. Kohn, *Cancer Res.*, **37**, 1450 (9177).

[12] I. Baracu, E. Tărnăuceanu and I. Niculescu-Duvăz, *Rev. Roumaine Chim.*, **22**, 885 (1977).

[13] G. Eisenbrand, H. H. Fiebig and W. J. Zeller, *Z. Krebsforsch.*, **86**, 279(1976).

[14] I. Baracu, I. Niculescu-Duvăz and V. Dobre, Rom. Pat. 100 296/1980.

[15] G. Eisenbrand, *Ger. Offen*, **2**, 659, 862; *Chem. Abstr.*, **88**, 120 126.

[16] I. Baracu, I. Niculescu-Duvăz, R. Deneș, and V. Dobre, Rom. Pat. 73 679/1981.

[17] T. P. Johnston, G. S. McCaleb, P. S. Oplinger, W. R. Laster and J. A. Montgomery, *J. Med. Chemistry*, **9**, 892 (1966).

[18] W. Siefken, *Liebigs Ann. Chem.*, **562**, 74 (1949).

[19] F. Lengfild and J. Stiglitz, *J. Amer. Chem. Soc.*, **16**, 71 (1894).

[20] H. Wenker, *J. Amer. Chem. Soc.*, **58**, 2608 (1936).

[21] C. K. Johnston, *J. Org. Chem.*, **32**, 1509 (1967).

[22] H. Najer, P. Chanrier and R. Guidicelli, *Bull. Soc. Chim. France*, **1960**, 956.

[23] A. Krantz, *Tetrahedron Lett.*, **1975**, 695.

[24] P. A. S. Smith, Organic Reactions, Coll. Vol. III, 373 Wiley, New York.

[25] T. Lin, P. H. Fischer, G. T. Shiau and W. A. Prusoff, *J. Med. Chemistry*, **21**, 130 (1978).

[26] T. P. Johnston, G. S. McCaleb, T. Anderson and D. S. Murison, *J. Med. Chemistry*, **22**, 597 (1979).

Revue Roumaine de Chimie, **30**, *4*, 329–332 (1985)

CONSIDERATIONS ON THE ELECTRONIC SPECTRA AND BARRIER TO INTERNAL ROTATION OF α- AND β-NAPHTHALENESULPHONIC ACIDS

C. GHIRVU, M. CONSTANTINESCU *, GH. IONESCU and I. M. POPA

Polytechnic Institute of Jassy, Faculty of Chemical Technology, Department of Physical Chemistry, Splai Bahlui, Jassy 6600, Romania

*** The "Al. I. Cuza" University, Computer Center, Calea 23 August no. 11, Jassy 6600, Romania**

Received April 18, 1983

The effect of sulphonic substitution on the vibrational structure of the α band of naphthalene has been investigated for α- and β-naphthalenesulphonic acids at liquid nitrogen temperature. The experimental data were discussed by using CNDO/2 type calculations for the barriers to internal rotation of the sulphonic group about the C—S bond.

INTRODUCTION

As well known, monosubstituted naphthalenes have different spectral properties. The generalisation of a large number of experimental data has revealed some important characteristics of the ultraviolet electronic spectra of monosubstituted naphthalenes.[1]

The molecules of the $C_{10}H_7X$ type retain the general features of the $\pi \rightarrow \pi^*$ electronic transition due to napthalene.

The perturbation of the energy levels depends on the position of the substituent, the nature of this dependence being accounted for by the following argumentation. In the near ultraviolet spectrum, naphthalene has three absorption bands, [2] namely $^1A \rightarrow {}^1L_b$, located at 312 mμ, $^1A \rightarrow {}^1L_a$ at 286 mμ and $^1A \rightarrow {}^1B_b$ at 221 mμ, using Platt's notation,[3] or α, *p*, β, in Clarr's notation.[4] The first and the third of these bands are polarized along the longitudinal direction, while the second band is polarized perpendicular to the longitudinal direction. Therefore, the substitution in positions 1 and 2 of naphthalene will affect in a different way the $\pi \rightarrow \pi^*$ electronic transition of naphthalene. Therefore the substitution in position 1 of naphthalene extends the conjugation along the transversal direction, thus the p band will be significantly affected, while the substitution in position 2 extends the conjugation along the longitudinal direction and thus the bands polarized along this direction will be affected (α and β bands). These observations are in good agreement with experimental data.[5,6]

The perturbation of the π energy levels of naphthalene upon substitution is due mainly to the conjugation effect of the substituents.

EXPERIMENTAL PART

The study of the influence of the sulphonic substitution on the electronic spectrum of naphthalene has been done by the same experimental method used in the case of benzensulphonic acid.[7] The spectra of the ethanol solutions of spectroscopic purified compounds, naphthalene (N), α-naphthalenesulphonic acid (αNSA) and β-naphthalenesulphonic acid (βNSA), were obtained with a PGS—2 (Zeiss) plane grating spectrograph, in the first order (resolution 7 A°/mm), slit width 25 μ, on Agfa-Gevaert plates of fine granulation (type 23D 56). To obtain rigid glasses a liquid nitrogen cooled cell was used.[8] The density of plates was automatically recorded with the Zeiss Mod II Microphotometer, to which a G_1B_1 recorder was adapted. The spectral data obtained at low temperatures are given in table 1.

Table 1

Spectral data for α-band of naphthalene and naphthalenesulphonic acids (αNSA and βNSA)

Naphthalene (N)		α-Naphthalene sulphonic acid (αNSA)		β-Naphthalene sulphonic acid (βNSA)	
ν, (cm^{-1})	Δν, (cm^{-1})	ν, (cm^{-1})	Δν, (cm^{-1})	ν, (cm^{-1})	Δν, cm^{-1}
31,300.7	0,0	31,259.6	0,0	30,290.2	0,0
31,562.3	261.6	31.562.8	303.2	30,742.7	452.0
32,110.8	810.1	32,006.3	746.7	31,230.5	940.3
32,938.3	1637.6	32,672.0	1412.4	31,689.6	1399.4
—	—	32,991.6	1732.0	31,958.1	1667.9
—	—	—	—	32,696.7	2406.5

* $\Delta\nu = \nu_{0i} - \nu_{00}$

CNDO/2 TYPE CALCULATION OF BARRIERS TO INTERNAL ROTATION

In a previous paper a model of interaction between the sulphonic group and the benzene ring was put forward.[9] This model was considered in the simple LCAO-MO method, as well as in the Pariser-Parr-Pople approximation.[10–12] With this model of interaction we obtained good results in the simple LCAO—MO calculations for α- and β-naphthalenesulphonic acids. However, our model should be valid only when the sulphonic group could rotate freely about the C—S bond. This argumentation has been justified by the CNDO/2 type calculation of the barrier to internal rotation of the sulphonic group about the C—S bond for benzenesulphonic acids.[14]

The above observations prompted us to calculate barriers to internal rotation of the sulphonic group about the C—S band for αNSA and βNSA by the same CNDO/2 method.[15] For practical calculations we considered two extreme geometrical arrangements of the sulphonic group which are given in Fig. 1. In the case of the configuration A the projection of the S—O bonds lies along the x-axis, while this is rotated an angle of 30° about the C—S bond in the case of the configuration B. In our figure the projection of the sulphonic group on the xz plane is shown, while the naphtalene is in the xy plane. As starting geometrical parameters for the sulphonic group Broomhead and Nicol's data were used[16] and for the

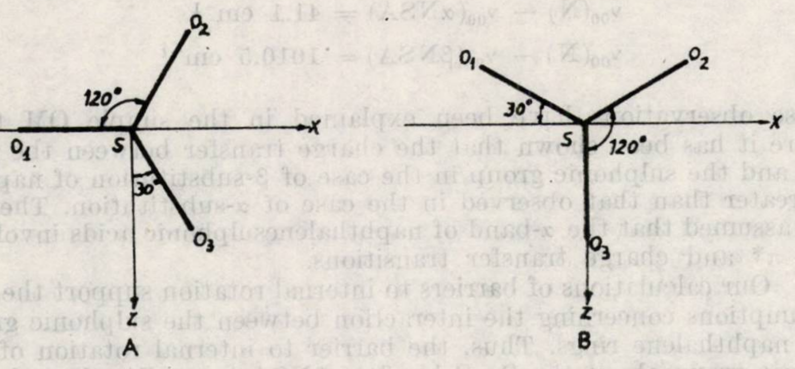

Fig. 1.—Configurations A and B of the sulphonic group.

naphthalene ring the geometry of benzene was considered. The calculation results are given in table 2.

The barrier to internal rotation is defined as being the energy difference between the two extreme configurations of the molecular systems under investigation, namely

$$\Delta E = E_B - E_A$$

Table 2

Calculation results of barriers to internal rotation

Molecule	Total energy (kcal mol^{-1})	Barrier to internal rotation	
		kcal mol^{-1}	kj mol^{-1}
αNSA – A	–89,251.4	1.4	5861.52
αNSA – B	–89,252.8		
βNSA – A	–89,252.6	0.1	418.68
βNSA – B	–89,252.7		

As we know, such barriers for αNSA and βNSA have never been measured experimentally. Nevertheless, the magnitude of these barriers is of considerable theoretical importance for the understanding of the physical nature of both the chemical bonds in the sulphonic group and of the interaction between the sulphonic group and the aromatic nuclei of naphthalene.

DISCUSSION OF THE RESULTS AND CONCLUSIONS

The vibrational structure of the band of naphthalene, denoted as $^1A_{1g} \rightarrow {}^1B_{3u}^-$ in group theory,[17] is not clear both at the room temperature and at low temperatures. However, we can say, from table 1, that in the case of the sulphonic substitution in the α position of naphthalene the modifications of the vibrational structure of the α band of naphthalene are larger than those obtained in the case of α substitution. Also, we can see that:

$$\nu_{00}(\mathrm{N}) - \nu_{00}(\alpha\mathrm{NSA}) = 41.1\ \mathrm{cm}^{-1}$$

$$\nu_{00}(\mathrm{N}) - \nu_{00}(\beta\mathrm{NSA}) = 1010.5\ \mathrm{cm}^{-1}$$

These observations have been explained in the simple OM theory [13] where it has been shown that the charge transfer between the aromatic rest and the sulphonic group in the case of β-substitution of naphthalene is greater than that observed in the case of α-substitution. Therefore, it was assumed that the α-band of naphthalenesulphonic acids involves both $\pi \rightarrow \pi^*$ and charge transfer transitions.

Our calculations of barriers to internal rotation support the previous assumptions concerning the interaction between the sulphonic group and the naphthalene rings. Thus, the barrier to internal rotation of the sulphonic group about the C—S bond of βNSA is smaller than that of the αNSA (see Table 2), therefore the conjugation between the sulphonic group and the naphthalene rings is enhanced in the former case at a larger extent than in the second one. We conclude that the interaction between the sulphonic group and the naphthalene rings, as described above, explains most of the observed experimental data.

REFERENCES

[1] A. E. Lutzkii and L. A. Antropova, *Zhur. Fiz. Himii*, **39**, 2120 (1965).

[2] H. H. Jaffe and M. Orchin, "Theory and Applications of Ultraviolet Spectroscopy", John Wiley and Sons, Inc., New York, 1962, p. 257, 303.

[3] J. R. Platt, *J. Chem. Phys.*, **17**, 484 (1949).

[4] E. Clarr, "Aromatische Kohlerwasserstoffe", Springer-Verlag, Berlin, 1952.

[5] H. Baba and S. Suzuki, *Bull. Chem. Soc. Japan*, **34**, 82 (1961).

[6] T. Iredall and J. White, *Trans. Faraday Soc.*, **56**, 1717 (1960).

[7] C. I. Ghirvu, *Rev. Real. Acad. Ciencias Exaxtas*, Fisicas y Naturales, Madrid Tomo **LXIX**, 683 (1975).

[8] A. Butucelea, *Revista de Chimie*, Bucharest, **19**, 423 (1968).

[9] V. Em. Sahini, C. I. Ghirvu and V. P. Macovei, *Rev. Roumaine Chim.*, **12**, 237 (1967).

[10] V. Em. Sahini and C. I. Ghirvu, *Rev. Roumaine Chim.*, **14**, 275 (1969).

[11] V. Em. Sahini and C. I. Ghirvu, *Rev. Roumaine Chim.*, **15**, 11 (1970).

[12] V. Em. Sahini and C.I. Ghirvu, *Rev. Roumaine Chim.*, **16**, 149 (1971).

[13] C. I. Ghirvu, Doctoral Thesis, Bucharest, 1971.

[14] C. I. Ghirvu, *Theoret. Chim. Acta*, (Berl.), **30**, 115 (1973).

[15] J. A. Pople and G. A. Segal, *J. Chem. Phys.*, **44**, 3289 (1966).

[16] J. M. Broomhead and A. D. I. Nicol, *Acta crystalogr.*, **1**, 88 (1948).

[17] A. Streitwieser, Jr., "Molecular Orbital Theory for Organic Chemists", John Wiley and Sons, Inc., New York, 1961, Chapter 8.

Revue Roumaine de Chimie, **30**, *4*, 333–337 (1985)

ESTUDIO DIPOLAR DE COMPUESTOS OCTAEDRICOS DE TITANIO CON TMDTO Y TEDTO *

M. C. MARTINEZ, M. R. BERMEJO ** y M. GAYOSO

Departamento de Química Inorgánica, Facultad de Química, Centro Coordinado del C.S.I.C.
Universidad de Santiago de Compostela, Galicia, España

Recibido: el 30 de septiembre de 1981

Se han determinado, utilizando el método de Guggenheim, los momentos dipolares, en dioxano a 25°C, de los siguientes complejos : $TiCl_4 \cdot TMDTO$ (8,9 D); $TiBr_4 \cdot TMDTO$ (9,0 D); $TiCl_4 \cdot TEDTO$ (10,0 D) y $TiBr_4 \cdot TEDTO$ (9,1 D). Estos datos sugieren compuestos monómeros con estructura octaédrica y el ligando en posición *cis*, unido a través de los átomos de azufre.

The dipole momentos of $TiCl_4 \cdot TMDTO$ (8.9 D); $TiBr_4 \cdot TMDTO$ (9.0 D); $TiCl_4 \cdot TEDTO$ (10.0 D) and $TiBr_4 \cdot TEDTO$ (9.1 D) have been determined by the Guggenheim method in dioxane at 25°. These results suggest monomer compounds with a *cis* octahedral structure and with the ligands bonded by the sulphur atoms.

INTRODUCCIÓN

En una serie de trabajos anteriores[1] hemos investigado la interacción entre ditiooxamidas totalmente substituidas — tetrametilditiooxamida (TMDTO) y tetraetilditiooxamida (TEDTO) — y tetrahaluros metálicos de transición MX_4 (M = Ti, Zr y X = F, Cl, Br). El estudio realizado permite sugerir que el enlace en los complejos se produce por los dos átomos de azufre y la estructura de los compuestos resulta ser octaédrica en torno al átomo central y con los ligandos ocupando la posición *cis*.

En el presente trabajo se realizó el estudio dipolar de los complejos preparados con el objeto de obtener más evidencia experimental que nos ayudara a conocer como es la estructura de los citados complejos.

PARTE EXPERIMENTAL

Reactivos

La tetrametilditiooxamida y la tetraetilditiooxamida se han preparado por el método de Hurd,[2] partiendo de cloruro de oxalilo, la dialquilamina correspondiente y P_4S_{10}. Se utilizó tetracloruro y tetrabromuro de titanio de la casa Roc/Ric. El dioxano Merck (p.a.) se mantuvo a reflujo 48 horas sobre sodio, se destiló a continuación recogiendo la fracción que pasa a 101°.[3]

---

* Comunicación presentada a „4° Encontro Anual de Sociedade Portuguesa de Quimica" PC 64, Lisboa (1981).

** Autor a quién debe dirigirse la correspondencia.

Se almacenó sobre tamices moleculares Linde 4A. Se utilizó siempre antes de dejar transcurrir dos días. Su constante dieléctrica fue $\varepsilon_1 = 2.2094$.

Preparación de los complejos

Los complejos se preparan como se detalló, [1] añadiendo una disolución del dador sobre otra del aceptor, o viceversa, en la relación molar adecuada. Los compuestos son poco solubles en disolventes de baja constante dieléctrica ; pero lo suficiente como para realizar las determinaciones del momento dipolar en dioxano. Los complejos son muy hidroscópicos lo que determinó que, en todo momento, fuera preciso trabajar en caja seca con atmósfera inerte y guardando las disoluciones en erlenmeyers con cierre esmerilado.

Medidas experimentales

Los momentos dipolares se determinaron, siguiendo el método de Guggenheim. [4,5] En un dipolarimetro WTW DMOI, utilizando una célula DFL I y termostatado a 25°, se midieron las constantes dieléctricas y mediante un refractómetro Bausch/Lomb, termostatable a 25° y con precisión de 0,00003, se midieron los indices de refracción. La técnica utilizada se ha descrito con anterioridad. [6,7]

RESULTADOS Y DISCUSIÓN

Los valores de las constantes dieléctricas y los indices de refración medidos para disoluciones de diferentes fracciones en peso se resumen en la tabla 1.

Tabla 1

Constantes dieléctricas e indices de refracción de disoluciones en dioxano, a 25°C, de los complejos en la concentración que se indica

Compuesto	100 w_{12}	ε_{12}	n_{12}
$TiCl_4 \cdot TMDTO$	0,051	2,2810	1,42005
	0,076	2,2871	1,42012
	0,105	2,3009	1,42021
	0,144	2,3180	1,42028
	0,184	2,3185	1,42043
	0,226	2,3359	1,42053
$TiBr_4 \cdot TMDTO$	0,016	2,2442	1,42008
	0,052	2,2497	1,42014
	0,075	2,2524	1,42021
	0,102	2,2589	1,42030
	0,153	2,2674	1,42033
	0,246	2,2867	1,42052
$TiCl_4 \cdot TEDTO$	0,062	2,2728	1,42002
	0,092	2,2879	1,42015
	0,131	2,2931	1,42024
	0,172	2,3046	1,42039
	0,198	2,3156	1,42052
	0,230	2,3230	1,42064
$TiBr_4 \cdot TEDTO$	0,023	2,2472	1,41996
	0,048	2,2499	1,42002
	0,077	2,2554	1,42008
	0,132	2,2628	1,42014
	0,163	2,2707	1,42017
	0,226	2,2830	1,42032

En la figura 1 y 2 se han representado los valores de $\varepsilon_{12} - \varepsilon_1$ y $n_{12}^2 - n_1^2$ frente a w_{12} para diferentes disoluciones de los compuestos a estudiar. Las rectas obtenidas se ajustaron por minimos cuadrados y sólo se admitieron

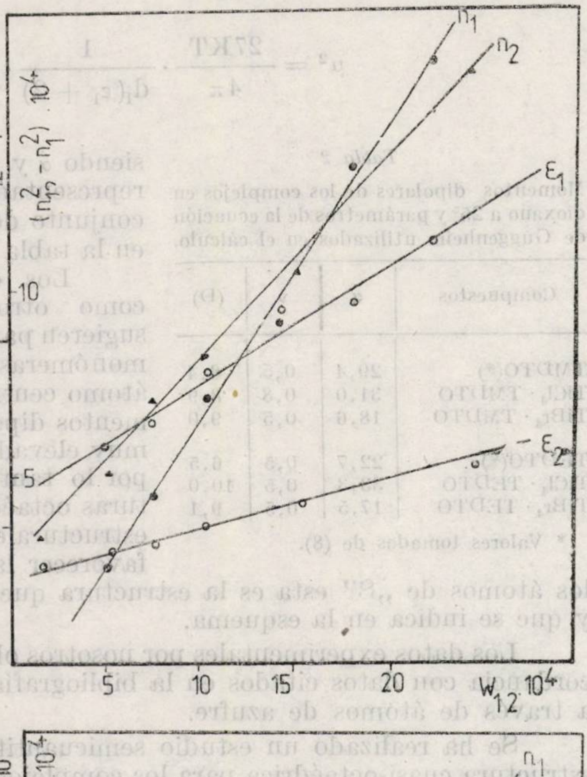

Fig. 1 — Variación de $(\varepsilon_{12} - \varepsilon_1)$ y $(n_{12}^2 - n_1^2)$ frente a la fracciónen peso, para distintas disoluciones de $TiCl_4 \cdot$ TMDTO (1) y $TiBr_4 \cdot$ · TMDTO (2) en dioxano.

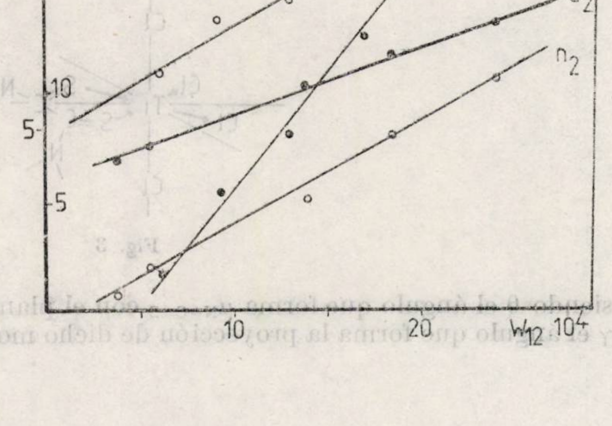

Fig. 2 — Variación de $(\varepsilon_{12} - \varepsilon_1)$-y$(n_{12}^2 - n_1^2)$ frente a la fracción en peso, para distintas disoluciones de $TiCl_4 \cdot$ TEDTO (1) y $TiBr_4 \cdot$ TEDTO (2) en dioxano.

como válidos los experimentos para los que la dispersión lineal fue del orden de R = 0,999.

Los momentos dipolares de los compuestos se han obtenido utilizando la ecuación de Guggenheim. [4]

$$\mu^2 = \frac{27KT}{4\pi} \cdot \frac{1}{d_1(\varepsilon_1 + 2)} \cdot (\alpha - \nu) \cdot M_2$$

siendo α y ν las pendientes de las rectas representadas en las figuras 1 y 2. El conjunto de estos valores se representan en la tabla 2.

Los datos estequiométricos, asi como otros estudios en disolución,[1] sugieren para los compuestos estructuras monómeras y octaédricas en torno al átomo central. Los valores de los momentos dipolares de los complejos son muy elevados para estructuras *trans* y por lo tanto debemos postular estructuras octaédricas *cis*; como los datos estructurales de las ditiooxamidas parece favorecer la coordinación a travérs de los átomos de ,,S'' esta es la estructura que nos parece más probable y que se indica en la esquema.

Tabla 2

Momentos dipolares de los complejos en dioxano a 25° y parámetros de la ecuación de Guggenheim utilizados en el cálculo.

Compuestos	α	ν	(D)
TMDTO(*)	29,4	0,5	6,4
$TiCl_4 \cdot$ TMDTO	31,0	0,8	8,9
$TiBr_4 \cdot$ TMDTO	18,6	0,5	9,0
TEDTO(*)	22,7	0,5	6,5
$TiCl_4 \cdot$ TEDTO	33,3	0,5	10,0
$TiBr_4 \cdot$ TEDTO	17,5	0,5	9,1

* Valores tomados de (8).

Los datos experimentales por nosotros obtenidos están en buena concordancia con datos citados en la bibliografía [9] para ligandos bidentados a través de átomos de azufre.

Se ha realizado un estudio semicuantitativo del μ_{comp} admitiendo estructura cuasi-octaédrica para los complejos y suponiendo que elligando mantiene la estructura más favorable en estado libre (Fig. 3). El momento dipolar se puede obtener como:

$$\mu_{comp} = 2\mu_{X-Ti} \cos 45 + 2\mu_{N-C=S} = \cos \theta \cdot \cos \gamma + \mu_{S-Ti} \cos 45 \qquad (1)$$

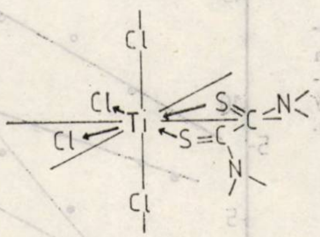

Fig. 3

siendo θ el ángulo que forma $\mu_{N-C=S}$ con el plano ecuatorial del complejo; γ el ángulo que forma la proyección de dicho momento en el plano XY con el eje Y y los otros términos son momentos de enlace y de grupo cuya fuente se indica.

θ y γ son 40,5° y 5° respectivamente[8]

$$\mu_{Cl-Ti} = 2{,}2\ D^{9};\ \mu_{Br-Ti} = 2{,}1\ D^{9}\ y\ \mu_{N-C-S} = 4{,}2\ D^{8}$$

Utilizando la expresión (1) y los datos indicados se puede obtener el valor del momento dador-aceptor μ_{S-Ti} para los diferentes compuestos. Este valor ha resultado ser próximo a cero pero negativo ($\simeq -0{,}4$ D) en todos los casos excepto en $TiCl_4 \cdot$ TEDTO que da $\mu_{Ti-S} = 0{,}4$ D. Estos momentos de enlace dador-aceptor, con valores tan bajos o incongruentes, han sido ya obtenidos para otros sistemas que contienen a estos mismos ligandos[10]. Estos extraños valores sólo pueden deberse a fenómenos disociativos de los complejos, en la disolución de dioxano, del tipo

$$TiX_4 \cdot D \overset{Diox}{\rightleftarrows} TiX_4 \cdot (diox)_x + D(diox)_x \qquad (2)$$

dado que es poco factible postular que el ángulo entre los planos C—C=S se modifiquen lo suficiente como para que el ligando de lugar a una interacción por un átomo de „S" y otro de „N".

La influencia de la disoción sobre los momentos de los complejos puede ser considerable. Asi el compuesto $C_4H_9S(CH_2)_2SC_4H \cdot TiCl_4$ muestra $\mu = 7{,}4$ D[9] en benceno por medida directa; pero cuando se realiza la determinación por medio de valoraciones dielectrométricas, que eliminan toda posible disociación, $\mu = 8{,}8$ D. Debe destacarse que este $\Delta\mu = 1{,}4$ se produce en disolventes benceno, si la media se realizara en dioxano, disolvente más básico, la disociación sería mayor yΔ μ también.

De lo dicho se puede concluir que los datos de momentos dipolares, para los complejos de TMDTO y TEDTO, sugieren que se trata de aductos monómeros con coordinación octaédrica alrededor del átomo central con el ligando en posición *cis* enlazado a través de los átomos de azufre y que en disolvente dioxano se encuentra parcialmente disociado según la expresión (2).

Estas conclusiones están en concordancia con los datos obtenidos espectroscópicamente [1] para estos sistemas.

BIBLIOGRAFIA

[1] M. C. Martínez, M. R. Bermejo y M. Gayoso, *An. Quím* (en prensa).

[2] R. N. Hurd, G. De la Mater, G. C. Mc Elheny, R. J. Turner y H. Wallingford, *J. Org. Chem.*, **26**, 3980 (1961).

[3] H. B. Thompson, *J. Chem. Ed.*, **43**, 66 (1966).

[4] E. A. Guggenheim, *Trans Farad. Soc.*, **45**, 714 (1949).

[5] J. W. Smith, *Trans. Farad. Soc.*, **46**, 394 (1950).

[6] M. R. Bermejo, Tesis Doctoral, Facultad de Ciencias, Santiago de Compostela, España (1972).

[7] J. R. Masaguer y M. R. Bermejo, *An. Quim.*, **69**, 1099 (1973).

[8] J. R. Masaguer, A. Castiñeiras y J. S. Casas, *An. Quim.*, **72**, 734 (1976).

[9] E. N. Gur'yanova, I. P. Gol'dshtein, I. P. Romm, „Donor-acceptor Bond", Keter Pub. House, Jerusalem, 1975 p. 209.

[10] J. R. Masaguer A. Castiñeiras y J. S. Casas *An. Quím.*, **73**, 51 (1977).

Revue Roumaine de Chimie, **30**, *4*, 339–342 (1985)

SYNTHESIS AND CHARACTERISATION OF A PD(II) COMPLEX WITH 2,5-METHOXY-4-CHLORO-BENZENAMINE

GRIGORE TEODORESCU*, CRISTINA MANDRAVEL, MELANIA GUŢUL and GABRIELA TEODORESCU

Polytechnic Institute of Bucharest, National Institute of Chemistry, Str. Polizu, 1, Bucharest Romania

Received September 16, 1982
Revised October 22, 1984

This paper reports elemental analysis, conductimetric measurements, UV absorption and reflectances and IR spectroscopic data in order to characterize the complex formed in the $PdCl_2$ -2,5-methoxy-4-chloro-benzenamine system.

INTRODUCTION

The study of complex compounds with aromatic amines as ligands is of interest in relation to the need to estimate the electron donor properties of the amines. On the other hand increasing attention is paid to the study of transition metal complex compounds in connection with their catalytic properties in oxidation reactions.[1,2]

The system $PdCl_2$–2,5-methoxy.4.chloro-benzenamine (abbreviated "Amine") was studied in this work.

RESULTS AND DISCUSSIONS

To establish the influence of various factors on the complex compounds formation in this system, the synthesis was performed under various conditions by changing the nature of the solvent, the molar ratio of the components and the pH of the solution.

The reproductible results were obtained using slightly acidified aqueous solutions of $PdCl_2$, which were added to alcoholic solution of the "Amine". The complex compound was isolated from the solution as a yellow-gray precipitate.

The synthesis was carried on with various $PdCl_2$: Amine ratios i.e. 1 : 1 ; 1 : 2 ; 1 : 4. The reaction product was always the same, namely $Pd(Amine)_2Cl_2$. The composition was established through elemental analysis as described in the experimental part.

---

* Deceased in 1983.

The molar conductivity of a 10^{-3} m solution of the synthetised compound in DMF, as solvent, is of 23 Ω^{-1} cm^2mol^{-1}. This value indicates a nonelectrolyte character in this solvent. The electronic spectrum of the synthetised complex was obtained by the reflection technique for the solid compound and by absorption technique for the diluted solutions in CCl_4.

The observed bands are given in table 1, which also includes the data for the noncomplexed "Amine".

Table 1

UV spectra

Compound*	λ_{max} (nm)				
$[PdCl_2(Amine)_2]$ solid	275		290		355
$[PdCl_2(Amine)_2]$solution in CCl_4	260		303		400
Amine-solid	215	290	340	355	
Amine-solution in CCl_4	249		310		

* Amine = 2,5-methoxy-4-chlorobenzenamine

The literature[3-6] relative to electronic spectrum of $PdCl_4^{2-}$, given in table 2, proves that d^8 coupled spin configuration exhibits square-plane geometry.

Table 2

The spectral properties of Pd(II) complexes of square planar geometry

Probe	λ max (nm)	ε_{max} (mol^{-1} cm^{-1}l)	Assignments
$[PdCl_4]^{2-}$ (solid K_2PdCl_4)	599	—	$^1A_{1g} \rightarrow {^1A_{2g}}$
	465	—	$^1A_{1g} \rightarrow {^1B_{1g}}$
	429	—	$^1A_{1g} \rightarrow {^1E_{1g}}$
$[PdCl_4]^{2-}$ (aq. solution, chloride ion in excess)	278	12,000	$^1A_{1g} \rightarrow {^1A_{2u}}, {^1E_u}$
	224,5	30,000	$^1A_{1g} \rightarrow {^1E_u}$
$[PdCl_4]^{2-}$ (aq. solution)	434	—	$^1B_{1g} \leftarrow {^1A_{1g}}$
	333,5 (shoulder)	—	$^1E_g \leftarrow {^1A_{1g}}$
	277	—	C.T. (charge transfer)

By comparison, our data also indicate the same geometry.

In order to establish the coordination mode of the ligand we recorded the IR spectra in the 4000—200 cm^{-1} range both for the free "Amine" and for the complex compound.

In agreement with the literature data[7-9] in the "Amine"-IR spectrum were identified absorption bands characteristic for the functional groups of ether (1255, 1050 cm^{-1}), methyl ($\nu_{sym\,CH_3}$ in R—O—CH_3 of R-aryl, at 2850 cm^{-1}), primary amine ($\nu_{sym\,N-H}$ at 3375 cm^{-1} and $\nu_{asym\,N-H}$ at 3460 cm^{-1}), chloride ($\nu_{C_{aryl}-Cl}$ at 720 cm^{-1}).

Examination of the IR spectrum of the complex reveals changes both in the position and intensity of the bands corresponding to the aminogroup. Thus, the $\nu_{\mathrm{sym\,NH}}$ mode is situated in the complex at 3225 cm^{-1} and $\nu_{\mathrm{sym\,N-H}}$ at 3320 cm^{-1}.

The absorption bands of other functional groups were not altered significantly.

The shift to smaller frequencies of the ν_{NH} modes is determined by the formation of the M—N bond,[10] thus suggesting coordination of the ligands to palladium through nitrogen.

The wavenumber of the stretching mode $\nu_{\mathrm{Pd-N}}$ is expected, in agreement with some calculations [11] near 500 cm^{-1}.

The number and position of absorption bands in this region allows to distinguish *cis* and *trans* isomers. The *cis* isomer has a lower symmetry than the *trans* isomer, thus causing the presence of more bands in the IR-spectrum.

Because comparatively few modes of vibration are situated in the 200—500 cm^{-1} region, the interactions between different modes, complicating the spectra are also few. Therefore this region is of great interest for coordination chemistry.

Thus, the compound *cis* $[\mathrm{Pd(NH_3)_2Cl_2}]$ exhibits,[12] in this region two weak bands which belong to $\nu_{\mathrm{Pd-N}}$; in opposition the IR-spectrum of the *trans* isomers [13] shows only a weak band, situated at 496 cm^{-1}. Our new synthetised complex exhibits only a weak band at 465 cm^{-1}, thus indicating a *trans* isomer. In addition, for a *cis*-isomer one would expect two adjoining bands for $\nu_{\mathrm{Pd-Cl}}$, with maxima near 327,336 cm^{-1}, of medium intensity.[14] In the spectrum of our complex a single medium intensity band appears at 330 cm^{-1}. Therefore the vibration spectrum indicates that *trans* $[\mathrm{Pd(Amine)_2Cl_2}]$ was isolated.

EXPERIMENTAL

Preparation of Pd(II) complex

To a slightly acidified aqueous solution of palladium (II) chloride (0.3 g in 50 cm^3) was added dropwise ethanolic solution of "Amine" (0.314 ; 0.634 ; 0.951 and 1.268 g for the different ratios $\mathrm{PdCl_2}$: "Amine") until precipitation of yellow-gray microcrystals ocurred. The mixture was allowed to stand at 0°C for several hours and the precipitate then filtered off, washed with ethanol and ether and dried *in vacuo*.

Elemental analysis for Pd, Cl, and N was performed by methods indicated in [15–17]

Found : Pd, 19.50 ; Cl, 24.07 ; N, 5.25 % ;

$[\mathrm{Pd(Amine)_2Cl_2}]$ requires Pd, 19.27 ; Cl, 25.69 ; N, 5.06 %

The solvents used were of spectral quality.

The conductivity measurements were performed with a RADELKIS TYPE OK 102 conductometer ; the cell constant of conductometer was 0.92 cm. This value was obtained by calibration with standard KCl solutions n/50 and n/100.

Electronic reflectance spectra were recorded on a Beckmann DK-2A spectrophotometer for pressed disks. The 100 % reflectance was established for MgO powder in the 550 nm region. Electronic absorption spectra were recorded on a SPECORD UV—VIS spectrophotometer in diluted $\mathrm{CCl_4}$ solutions.

IR-spectra were recorded on a Perkin-Elmer 571 spectrophotometer in KBr pellets. The spectrophotometer was calibrated in the 3750, 1601 and 900 cm^{-1} region using appropiate polystyrene absorption. Reproductibility was ± 2 cm^{-1}.

REFERENCES

[1] J. Lewis and R. G. Wilkins, "Modern Coordination Chemistry Principles and Methods" Interscience Publishers, New York, 1960, p. 87.

[2] A. Peloso, *Coord. Chem. Rev.*, **10**, 143 (1973).

[3] H. H. Schmidtke, in "Physical Methods in Advanced Inorganic Chemistry", H.A.O. Hill and P. Day, Editors, vol. 3, Interscience, London, 1968, p. 156.

[4] F. R. Hartley, *J. Organomet. Chem.*, **21**, 227 (1970).

[5] P. Day, N. J. Smith and R. J. Williams *J. Chem. Soc. A*, **1968**, 668.

[6] H. P. Gray, in "Transition Metal Chemistry" vol. 1, R. L. Carlin Editor, Wiley, New York, 1965, p. 244, 246.

[7] R. E. Richards *Trans. Faraday Soc.*, **44**, 40 (1948).

[8] H. R. Warner and W. E. Lands, *J. Amer. Chem. Soc.*, **85**, 60 (1963).

[9] M. Avram and G. D. Mateescu "Spectroscopia in infraroşu. Aplicaţii în chimia organică" Ed. Tehnică, Bucharest, 1966, p. 346, 378.

[10] K. Nakamoto, "Infrared Spectra of Inorganic and Coordination Compounds", Wiley, New York, 1962, p. 201.

[11] P. L. Hendra and N. Sadasivan, *Spectrochimica Acta*, **21**, 1271 (1965).

[12] P. B. Powell, *J. Chem. Soc.*, **1956**, 4495.

[13] D. B. Powell, *J. Chem. Ind.*, **1956**, 314.

[14] H. Peny, *Spectrochimica Acta, Part A*, **23**, 1137(1967).

[15] I. M. N. Kukushin and R. I. Bobohodzhaev, "Zakonomernosti transvlyaniya I. I. Chernyaeva" Nauka, Moskow, 1977, p. 43.

[16] C. Wilson and D. Wilson, "Comprehensive Analytical Chemistry. Classical Analysis", vol. I, Interscience, New York, p. 684.

[17] C. Macarovici, "Chimie analitică cantitativă. Gravimetria", Ed. Tehnică, Bucharest, 1959, p. 125.

Revue Roumaine de Chimie, **30**, 4, 343–347 (1985)

STUDIES ON SUBSTITUTED DIARYLIDENECYCLOHEPTANONES

MOHAMED A. ABD-ALLA, MOHAMED T. ISMAIL and AHMED M. EL.-KHAWAGA
Chemistry Department, Faculty of Science, Assiut University, Assiut, Egypt

Received November 5, 1981
Revised November 10, 1984

A number of diarylidencycloheptanones I were prepared and converted to the di- and tetrabromides II and III respectively. The action of silver acetate, methanol, ethanol and silver nitrate on the resulting bromides was studied in an effort to throw some light on the reactivity of both α- and β-bromine atoms. Michael condensation of I with ethyl acetoacetate gave two isomeric compounds VIII and IX. In most cases isomer IX changed rapidly to isomer VIII.

INTRODUCTION

In a previous study Yeh and co-workers[1,2] investigated the action of silver acetate on tetrabromides of dibenzylidenecyclohexanone. They pointed out that the first two bromine atoms to be displaced were those β to the carbonyl group. This finding was supported recently by Islam and Khalaf[3] when they studied the action of silver acetate, silver nitrate and hydrazine hydrate on di- and tetrabromides of substituted dibenzylidenecyclohexanones. Also, they found that the ease with which β-bromine atom was displaced was dependent upon the nature of the substituent present in the phenyl moiety. They reported that, generally, the displacement was accelerated by electron-donating substituents.

Sammour and co-workers[4] investigated the Michael reaction of ethyl acetoacetate with dibenzylidenecyclohexanone. They pointed out that additions of ethyl acetoacetate to ketones were accompanied by a secondary condensation involving the terminal methyl and carbonyl group in the adduct.

In the present work we studied the reactivity of the halogen atoms in di- and tetrabromides of diarylidenecycloheptanones toward displacement reactions to illustrate the behaviour of both α- and β-bromine atoms upon changing the ring size of the ketone. Also, we studied the Michael condensation of diarylidenecycloheptanone with ethyl acetoacetate.

RESULTS AND DISCUSSION

A number of diarylidenecycloheptanones I were prepared by condensing aromatic aldehydes with cycloheptanone. Compounds I were converted to the corresponding di- and tetrabromides II, III by the addition of the required amount of bromine.

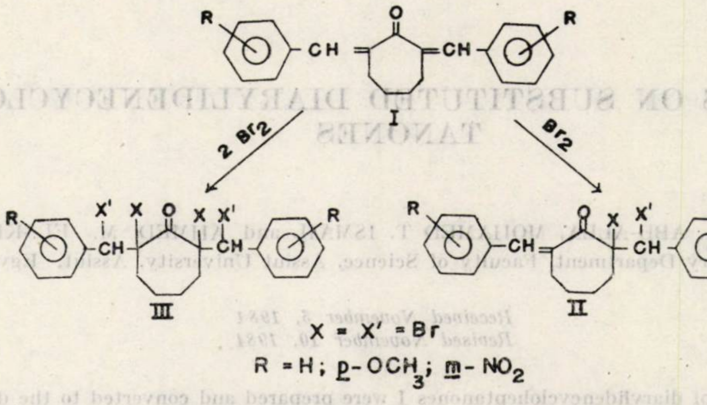

Treatment of the above dibromides and tetrabromides with nucleophilic reagents resulted in displacement of both halogens in the case of dibromides but only of the two β-halogens in the case of tetrabromides. The substitution process was highly enhanced when the substituent R was an electron-donating group and retarded by the presence of an electron attracting group.[2,5,6] Thus, reacting the above bromides IIb, IIIb with silver acetate in glacial acetic acid gave the diacetates IVb and Vb respectively. On the other hand, similar treatment of the bromides IIc, IIIc afforded no displacement products.

The extent to which β-bromines are activated was also shown by the fact that, in tetrabromides, they are readily displaced by methoxyl or ethoxyl groups upon refluxing with methanol or ethanol. Under such mild conditions the tetrabromide IIIb yielded the dibromomethoxy and dibromoethoxy compounds VI, VII respectively.

The activation or deactivation effects of the substituents in the phenyl moiety seem to depend on the extent to which they affect the polarization of β (C—Br) bond. The substituents on the phenyl moiety that increased the electron density at the β-carbon will enhance the polarization and consequently will facilitate the departure of the bromine as a bromide ion. This fact can again be demonstrated by the silver nitrate test. Whereas cold dioxane solution of the bromides IIb and IIIb precipitate AgBr when treated with a dioxane solution of $AgNO_3$, the nitro bromides IIc and IIIc do not give any precipitate even on warming.

From the above discussion one would expect the α-bromine atom to separate as bromonium ion as it is linked to a carbon atom placed between two strong electron attracting groups (the carbonium ion and the carbonyl group) as shown in the following structures:

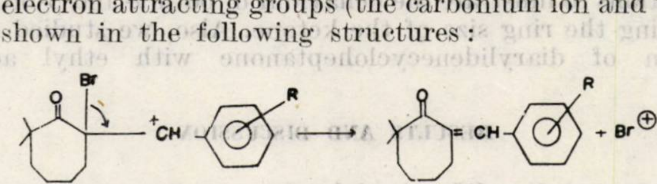

One interesting point about α-bromine atoms in the compounds under discussion is that they are easier to displace in dibromides than in tetrabromides. Whereas both α- and β-bromines in the dibromides IIa and IIb are simultaneously displaced by acetoxyl groups, only β-bromines in the corresponding tetrabromides are displaced under similar conditions. This observed lower reactivity of α-bromine atoms in dibromides is due to the increased steric effects at the other α-position, as well as to the deactivating electronic effects caused by the adjacent non-conjugated carbonyl group.

The preliminary study of the reaction mechanism showed that the reaction of the above bromides with methanol or ethanol is of the first order, not depending upon concentration. With CH_3COOAg, however, it seems even more likely that the reaction proceeds by the S_N1 type mechanism[7].

The Michael condensation products VIII, IX of ethyl acetoacetate with dibenzylidenecycloheptanones I were in agreement with the earlier investigation[5]. The products obtained corresponded to that resulting from secondary condensation of the terminal methyl group with the carbonyl in the primary adducts. Moreover, the products of condensation consisted of the mixture of two isomeric products (a yellow and a white isomer). It was noted that the yellow isomer changed to the white one during separation of the products, except in the case of di (*m*-nitrobenzylidene) cycloheptanone Ic, whereby the isomeric products could be separated by fractional crystallisation from petroleum ether (b.p. 60—80°). The structures of products were confirmed by infrared spectra which exhibited two carbonyl bands, characteristic of nonenolic esters ($COOC_2H_5$) at 1745 cm^{-1} and C=O groups of cyclohexanone derivatives at (1656 cm^{-1}) (cf. Table 1).

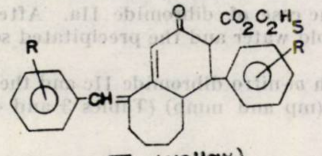

IX (yellow)

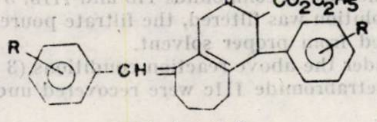

VIII (white)

R = H ; p-OCH_3 ; m-NO_2

Table 1

Condensation products VIII and IX of dibenzylidenecyloheptanones I with ethyl acetoacetate

Compd No.	R	Molecular formula of products*	Yield %	m. p (°C)	Shape and color of crystals	$\nu_{C=O}$ (cm^{-1}) for nonenolic ester	$\nu_{C=O}$ (cm^{-1}) cyclohexanones
VIIIa	H	$C_{27}H_{27}O_3$	86	140	white fluffy	1740	1665
VIIIb	*p*-OMe	$C_{29}H_{31}O_5$	87	156	white fluffy	1742	1670
VIIIc	*m*-NO_2	$C_{27}H_{25}O_7N_2$	65	204	white needles	1743	1660
IX**	m-NO_2	$C_{27}H_{25}O_7N_2$	20	157	yellow rosettes	1743	1656

* Satisfactory elemental analyses were obtained.

** The only isomeric product in which the double bonds are in α-β-position to ketonic function and could be separated by fractional crystallization from petroleum ether (b.p. 60—80°)

As suggested previously by Sammour and co-workers,[5] it is believed that the yellow forms correspond to structures in which the double bonds are in the α, β-position with respect to ketonic functions.

EXPERIMENTAL

Melting points are uncorrected. IR spectra were run on Pye-Unicam SP 200 G spectrophotometer using KBr discs.

The dibenzylidenecycloheptanones (Table 2) were prepared by the method used in literature.[8]

Table 2

Dibenzylidenecycloheptanones I

Compd No.	R	Formula*	Yield %	m. p. (°C)	Solvent of crystalization
I a	H	$C_{21}H_{18}O$	80	106	ethanol
b	*p*-OMe	$C_{23}H_{24}O$	85	116	ethanol
e	*m*-NO_2	$C_{21}H_{19}O_5N_2$	75	180	benzene

General bromination procedure: To a cold solution of the dibenzylidene compound (1 mole) in chloroform was added gradually a chloroform solution of bromine (1 mole in the case of dibromides and 2 moles in the case of tetrabromides) and the reaction mixture was set aside for 1 hr. The solvent was evaporated and the solid collected ewas crystallized from the proper solvent.

Action of silver acetate on the di- and tetrabromides: A mixture of the bromo compound (5 g),, silver acetate (5 g) and glacial acetic acid (50 mL) was heated under reflux on water-bath for 2 hrs in the case of compounds IIb and IIIb, 3 hrs in the case of dibromide IIa. After reflux the hot solution was filtered, the filtrate poured into cold water and the precipitated solid was crystallized from proper solvent.

Under the above reaction conditions (3 hrs) both *m*-nitro dibromide IIc and the corresponding tetrabromide IIIc were recovered unchanged (mp and mmp) (Tables 3 and 4).

Table 3

Dibromodibenzylidenecycloheptanones II and the diacetoxy derivatives

Compd No.	R	Formula *	m.p (°C)	Analysis %			
				Calculated		Found	
				Br	N	Br	N
α, β-Dibromodibenzylidenecycloheptanones (X=X′=Br)							
IIa	H	$C_{21}H_{18}OBr_2$	148	35.87	— —	35.70	— —
b	*p*-OMe	$C_{23}H_{24}OBr_2$	160	33.61	— —	33.82	— —
c	*m*-NO_2	$C_{21}H_{18}O_2NBr_2$	144	29.73	5.20	29.90	5.13
α, β-Diacetoxydibenzylidenecycloheptanones $(X=X'=-\underset{\overset{\|}{O}}{CO}-CH_3)$							
IVa	H	$C_{25}H_{24}O_5$	168	— —	— —	— —	— —
b	*p*-OMe	$C_{27}H_{30}O_5$	179	— —	— —	— —	— —

* Satisfactory analyses for C and H were obtained for all compounds.

Table 4

Tetrabromodibenzylidenecycloheptanones III and the diacetoxy, dimethoxy and diethoxy derivatives

Compd. No.	R	Formula *	m.p (°C)	Analysis %			
				Calculated		Found	
				Br	N	Br	N
α, α′, β, β′-Tetrabromodibenzylidenecycloheptanones (X=X′=Br)							
IIIa	H	$C_{21}H_{18}OBr_4$	187	52.80	— —	52.93	— —
b	*p*-OMe	$C_{23}H_{24}OBr_4$	200	50.31	— —	50.10	— —
e	*m*-NO$_2$	$C_{21}H_{18}O_5N_2Br_4$	205	45.84	4.01	46.09	4.12
α, α′-*Dibromo*-β, β′-*diacetoxydibenzylidenecycloheptanones* (*H*= *Br*, *X*′ = −*O*−*CO*−*CH*$_3$)							
Va	H	$C_{25}H_{24}O_5Br_2$	162	28.36	— —	28.10	— —
b	*p*-OMe	$C_{27}H_{30}O_5Br_2$	172	26.93	— —	27.13	— —
α, α′-*Dibromo*-β, β′-*dimethoxydibenzylidenecycloheptanone* (*X*= *Br*, *X*′ = −*O*−*CH*$_3$)							
VI	*p*-OMe	$C_{25}H_{30}O_3Br_2$	180	27.44	— —	27.55	— —
α, α′-*Dibromo*-β, β′-*diethoxydibenzylidenecycloheptanone* (*X* = *B*, *X*′ = *OC*$_2$*H*$_5$)							
VII	*p*-OMe	$C_{27}H_{34}O_3Br_2$	134	28.26	— —	28.40	— —

* Satisfactory analyses of C and H have been obtained for all compounds.

Action of methanol or ethanol on tetrabromides : A mixture of the tetrabromide (1 g) and methanol or ethanol (50 mL) was heated under reflux for 3 hrs. The resulting solution was reduced to half of its volume, cooled and the separated solid recrystallized from methanol or ethanol.

Reaction of bromo compounds with silver nitrate : To a cold dioxane solution of bromo compounds IIb and IIIb (50 mg each in 5 mL of dioxane) a dilute dioxane solution of silver nitrate (3 mL) was added. In all of the above bromdes a yellowish precipitate was immediately formed whereas the bromides IIc and IIIc did not give yellow precipitate even on warming.

Condensation of dibenzylidenecycloheptanones with ethyl acetoacetate : A mixture of 10 g (0.05 mole) ethyl acetoacetate and alcoholic solution of sodium ethoxide (prepared from 0.3 g ; 0.013 g atom sodium and 140 mL of absolute ethanol) was stirred under anhydrous condition for one hour. After this 0.12 mole of the dibenzylidenecycloheptanone was added and the mixture was refluxed for five hours. On cooling, a pale yellow solid product was obtained which changed to white during the separation. The crude product was crystallized from petroleum ether (b.p. 60−80°) to give white crystalline products in most cases.

REFERENCES

[1] P. Y. Yeh, *Bul. Soc. Chim. Japan*, **27**, 60(1954) ; *J. Chinese Chim. Soc. Taiwan, Ser., II*, **1**, 90(1954).

[2] P. Y. Yeh, Chao. Tung and Su-Len Liu, *Chemistry (Taiwan)*. **1955**, 27.

[3] A. M. Islam and A. A. Khalaf, *Indian. J. Chem.*, **7**, 546(1969).

[4] A. Sammour, A. Marei and M. H. Hassein, *J. Chem. U.A.R.*, **12**, 451 (1969).

[5] S. M. Nadkarni, A. M. Warriar and T. S. Wheeler, *J, Chem. Soc.*, **1937**, 2798.

[6] F. J. Pond and A. S. Schoffstall, *J. Amer. Chem. Soc.*, **22**, 658 (1900).

[7] E. Gould, "Mechanism and Structure in Organic Chemistry" Holt, Rinehart and Winston, New York, 1959, 274.

[8] M. I. Ali, M. F. El-Kaschef, H. G. Abou El-Fotooh and S. A. Khalaf, *J. Chem. Eng.*, **24** 377 (1979).

Revue Roumine de Chimie, **30**, *4*, 349–352 (1985)

CARBON-13 NMR SPECTRA OF SOME 16,17-GLYCOL DITERPENES*

F. GARCÍA, [a] O. COLLERA, [a] J. L. SÁNCHEZ, [a] R. CRUZ, [a] R. SAUCEDO [a] and M. C. PÉREZAMADOR [b]

[a] Instituto de Quimica, Universidad Nacional Autónoma de México, Circuito Exterior Cd. Universitaria, Coyoacán, 04510 México, D.F.

[b] Facultad de Ciencias, Universidad Nacional Autónoma de México, Circuito Exterior Cd. Universitaria, Coyoacán, 04510 México, D.F.

Received September 16, 1981
Revised October 10, 1984

The comparison of the $^{13}C-NMR$ spectra of the glycosides turbicorytin, corymbositin and the recently described ^{13}C spectrum of aureoside with those of cafestol and kahweol, led to the assignment of all the ^{13}C signals of the glycoside turbicorytin as well as for cafestol and kahweol.

The glycosides turbicorytin and corymbositin, [1–3] which are natural products isolated from *Turbina corymbosa* have structures Ia and IIa respectively. These compounds have a kaurane squeleton which is related to kaurene, a precursor in the biosynthesis of gibberelins. In order to compare the carbon-13 NMR spectra and assign the signals, we used the available information from the glycosides found in *Operculina aurea* by Canonica *et al.* [4] and that described by Patra *et al* [5] for tetracyclic diterpenoids. Particularly helpful is the spectra of aureoside, [4] since the aglycone of this glycoside is identical with that from corymbositin. In this context it seemed interesting to compare the $^{13}C-NMR$ spectra of cafestol III and kahweol IV which share a partial structure with turbicorytin and corymbositin, differing only in ring A. The common bicyclic system (rings C and D) have a relatively rigid conformation except for the hydroxymethylene group at C_{17},and this feature is an advantage for the comparison of $^{13}C-NMR$ spectra. On the other hand, ring B in corymbol, aglycone from turbicorytin has considerable flexibility as has been previously established, [6] thus affecting the chemical shifts.

DISCUSSION

Assignments for corymbositin and turbicorytin

Correlation between aureoside and corymbositin allows the assignment of most signals for the last one. For turbicorytin the assignments for C_2, C_3, C_4, C_5, C_8, C_9, C_{10}, C_{11}, C_{12}, C_{13}, C_{14}, C_{15}, C_{16}, C_{17} and C_{20} follow from

---

* Contribution No. 598 of the Instituto de Quimica, U.N.A.M.

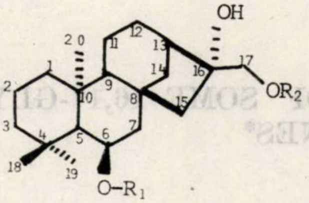
OH
20
1
2
3
4
5
6
7
8
9
10
11
12
13
14
15
16
17
18
19
OR$_2$
O–R$_1$

Ia R_1 = Glu R_2 = H

Ib R_1 = R_2 = Glu

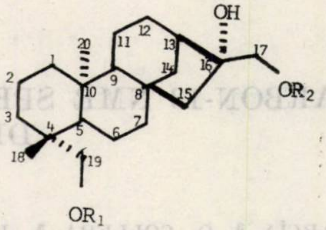
OH
OR$_2$
OR$_1$
1
2
3
4
5
6
7
8
9
10
11
12
13
14
15
16
17
18
19
20

IIa R_1 = Glu R_2= H

IIb R_1 = R_2 = Glu

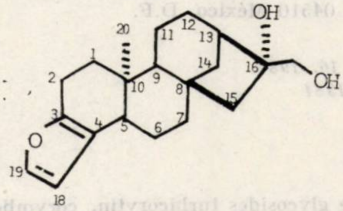
OH
OH
O
1
2
3
4
5
6
7
8
9
10
11
12
13
14
15
16
18
19
20

III

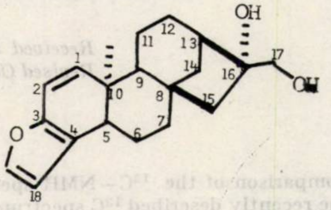
OH
OH
O
1
2
3
4
5
6
7
8
9
10
11
12
13
14
15
16
17
18
19

IV

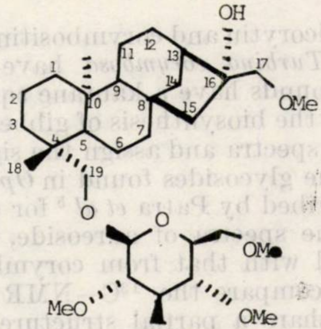
OH
OMe
OMe
OMe
OMe
MeO
O
O
1
3
4
5
6
7
8
10
11
12
13
14
15
16
17
18
19

V

their position in corymbositin. The signal for C_{19} is recognized because there is a quartet at 19.0 ppm which is more exposed to the solvent cell field than C_{20} according to a Dreiding model. Two triple signals appear at 47.2 and 47.1 ppm and are ascribed to C_7 and C_1 (assignments may be exchanged). These signals are downfield shifted by the proximity to the hydroxyl group at C_6. Some signals for the diterpenic portion appear in the same region as the glycosidic carbons whose assignments were made previously.[1] In corymbositin the signal for C_{19} appears as a triplet at 70.9 ppm while that for C_{17} is found at 64.7 ppm also as a triplet and C_{16} as a singlet at 79.8 ppm. In corymbosin the C_{17} triplet appears shifted to 73.7 ppm. In a similar fashion, C_{17} shows up as a singlet at 80.2 ppm for

Table 1

Chemical shifts for compounds I to V

CARBON	I(a and b)		II(a and b)		III$^{(c)}$	IV$^{(c)}$	V$^{(c)}$
C (1)	47.1	48.1	39.5	40.5	35.9	138.4	40.5
C (2)	19.7	20.5	19.9	21.1	23.2	115.2	80.8
C (3)	41.6	42.4	35.5	36.8	148.7	150.2	36.3
C (5)	55.1	56.0	55.2	56.9	52.2	52.2	56.9
C (6)	71.3	72.5	17.5	18.7	19.1	22.6	18.3
C (7)	47.2	48.1	41.9	42.9	40.9	40.4	42.4
C (8)	43.8	44.8	43.8	44.8	44.7	45.1	44.6
C (9)	56.1	57.0	56.1	57.1	53.6	53.4	57.1
C (10)	40.2	41.2	38.3	39.5	38.7	41.9	39.4
C (11)	17.9	18.8	17.4	18.7	20.7	22.2	18.3
C (12)	25.8	26.8	26.1	26.8	26.0	26.0	26.4
C (13)	44.6	46.1	44.2	46.3	45.5	48.4	46.0
C (14)	36.8	37.8	38.3	39.5	37.7	38.2	37.0
C (15)	52.8	54.0	52.4	53.4	53.0	53.0	53.1
C (16)	80.2	81.6	79.9	80.9	82.0	82.0	80.6
C (17)	65.2	66.5	64.7	66.3	66.4	66.4	71.6
C (18)	33.5	33.8	28.1	28.3	108.3	108.7	27.9
C (19)	18.4	19.0	70.9	73.1	140.6	141.2	72.6
C (20)	18.5	19.0	17.4	18.7	13.3	15.6	18.5
GLICOSIDIC PORTION							
C (1)	101.0	102.9	103.0	105.1			103.8
C (2)	73.4	75.4	73.0	75.5			79.8
C (3)	76.7	78.7	76.3	78.7			86.8
C (4)	70.1	71.9	69.6	72.0			74.9
C (5)	76.4	78.4	76.0	78.4			84.1
C (6)	61.0	61.2	60.6	61.2			76 5

Relative to internal TMS

a) in Deuterated DMSO b) in Deuterated Pyridine c) in chloroform

turbicorytin (in DMSO) while C_6 is found at 71.3 ppm as a doublet and C_{17} appears at 65.2 ppm. In turbicoryn the C_{17} triplet signal is shown at 73.7 ppm. The shifts of the C_{17} signals in these spectra are explained by attributing to this carbon atom the second glycosilation position for turbicoryn and corymbosin as represented by structures Ib and IIb respectively. Solvent shifts are large only for those carbon atoms which bear a hydroxyl group directly attached to them. The ^{13}C—NMR spectra of permethylated corymbositin V, was run in chloroform in order to have a correlation point for the spectra of cafestol and kahweol which were also run in chloroform.

Chemical shifts for Cafestol and Kahweol

The signals for C_8, C_9, C_{11}, C_{12}, C_{13}, C_{14}, C_{15} and C_{16} in cafestol and kahweol belong to the bicyclic system (rings C and D) and can be assigned accordingly with due allowance for their multiplicity. The signals for C_2 and C_1 for cafestol are easily located, since they are considerably shifted in the spectra of kahweol. The signal for C_{20} is a quartet which occurs at the highest field. The singlets for C_5 and C_{10} show shifts of 0.1 and 3.15

ppm respectively and can be attributed to the effect of the introduction of a conjugated double bond as well as to the change in geometry induced in ring A. The conformational change consists in a tendency toward planarity including the angle between C_1, C_{10} and C_5. There are also shifts in C_6 and C_7 in ring B (3.5 and 0.5 ppm respectively) which are due to a change in conformation in which C_6 is more exposed to the solvent cell. Accordingly C_6 is assigned to the signal at 19.1 ppm and that at 40.9 to C_7.

The low field resonances in the spectra of cafestol and kahweol belong to the furane ring and in the case of kahweol also to the endocyclic conjugated double bond. The singlets at 148.7 ppm and 120.3 ppm are thus assigned to C_3 and C_4 in cafestol, while 150.2 ppm and 121.8 ppm are the corresponding values for C_3 and C_4 in kahweol. The doublets at 140.6 ppm and 108.7 ppm are ascribable to C_{19} and C_{18} respectively while 141.2 ppm and 108.7 are the corresponding values for kahweol. Kahweol shows two additional signals at 138.4 ppm and 115.4 ppm for carbon atoms C_2 and C_1; these signals are also doublets.

EXPERIMENTAL PART

Turbicorytin and corymbositin were prepared by partial enzymatic hydrolysis from the seeds of ololiuqui (*T. corymbosa)* as previously described. [1-3]

Cafestol and kahweol were isolated from green coffee seeds, bourbon type from Fortin de las Flores, Veracruz, by established procedures. [7,8]

The ^{13}C—NRM were determined using the pulse FT mode, in pyridine, dimethyl sulfoxide and deuterochloroform as solvents, and recorded on Bruker HFX—10, Varian XL—100 and FT—80A instruments operating at 20.1 MHz. The chemical shifts were obtained from the proton decoupled spectra and the multiplicities observed from the CW of resonance spectra. The solvent signals were used as internal standards. The reported chemical shifts are in δ(ppm) downfield from TMS.

ACKNOWLEDGEMENTS : We thank Dr. Pedro Joseph Nathan from Centro de Investigación y Estudios Avanzados (IPN) for the determination of some ^{13}C—NMR spectra used in this work.

REFERENCES

[1] F. Garcia Jiménez, O. Collera, G. Larios, J. Taboada and M. C. Pérezamador, *Rev. Lat. de Quim.*, **10**, 181 (1979).

[2] M. C. Pérezamador, F. Garcia Jiménez, J. Herrán and S. E. Flores, *Tetrahedron*, **20**, 2999 (1964).

[3] F. Garcia Jiménez and M. C. Pérezamador, *Tetrahedron*, **23**, 2557 (1967).

[4] L. Canonica, F. Pelizzoni, G. Ferrari and V. Vecchietti, *Gazz. chim. Ital.*, **107**, 223 (1977) and references therein.

[5] A. Patra, A. K. Mitra, S. R. Mitra, C. L. Kitaniya and N. Adityachandhury, *Org. Magnetic Resonance*, **14**, 58 (1980).

[6] O. Collera, F. Garcia Jiménez and M. C. Pérezamador, *Rev. Lat. de Quim.*, **5**, 54 (1974).

[7] K. H. Slota and K. Neisser, *Ber. dtsch. chem. Ges.*, **71**, 1991 (1938).

[8] H. P. Kaufmann and A. K. Sen Gupta, *Fette, Seifen, Anstrichmittel*, **65**, 529 (1963).

Revue Roumaine de Chimie, **30**, *4*, 353–355 (1985)

A CONVENIENT ONE—STEP CONVERSION OF AROMATIC ALDEHYDES INTO NITRILES

C. I. CHIRIAC

"P. Poni" Institute of Macromolecular Chemistry, Aleea Ghica-Vodă 41 A, Jassy, Romania

Received May 21, 1984

Aromatic nitriles were prepared in high yields from aromatic aldehydes and hydroxylamine hydrochloride in dimethylacetamide as solvent at 140—150° for 4—5 hours. The solvent has an important role in this reaction.

For synthesis of nitriles from aldehydes, many methods use the dehydration of the corresponding oximes with different reagents such as: phenyl chloroformate,[1] benzenesulfonyl chloride,[2] carbodiimides,[3] trichloroacetonitrile,[4] triphenylphosphine — carbon tetrachloride [5] and N,N-carbonyldiimidazole.[6] Saednya obtained nitriles from aldehydes and hydroxylamine in pyridine-toluene.[7]

RESULTS AND DISCUSSION

In a previous communication,[8] we showed that a very simple method for the synthesis of aromatic nitriles consists in heating of an aromatic aldehyde with hydroxylamine hydrochloride in N-methylpyrrolidone as solvent at 135—145° for 3—4 hours, without other reagent.[8]

In this work, we present a method for the synthesis of aromatic nitriles, using dimethylacetamide (DMAC) as solvent. Thus a solution of an aromatic aldehyde and hydroxylamine in DMAC was heated for 4—5 hours at 140—150°, affording the corresponding nitriles.

This reaction involves two stages:

a) in the first stage, the oxime resulted "in situ" by the reaction between the aromatic aldehyde and $NH_2OH \cdot HCl$ at about 100°;

b) by dehydration of the oxime at 140—150° in the second stage, the corresponding nitrile resulted:

$$\underset{(I)}{Ar-CHO} + NH_2OH \cdot HCl \xrightarrow[100^\circ]{DMAC} \underset{(II)}{Ar-CH=NOH} + H_2O + HCl$$

$$II \xrightarrow[140-150^\circ \, -H_2O]{DMAC} \underset{(III)}{Ar-C\equiv N}$$

In this reaction, the dehydration of oxime (II) takes place in high yield by heating at 140 – 150° in DMAC and with very small yield without solvent at the same temperature. Therefore DMAC has an important role in this reaction. Also this reaction occurs with good yields in acetonitrile [9] and in N-methylpyrrolidone [8]. All these aprotic dipolar solvents have high polarity and high dipole moment: acetonitrile $\mu = 3.37$, N-methylpyrrolidone $\mu = 4.09$ and DMAC $\mu = 3.79$.[10] Other aprotic dipolar solvents were also tried. With dimethylsulfoxide, impure products resulted, because this solvent is unstable in the presence of hydrochloric acid, a by-product of this reaction. In nitrobenzene and benzonitrile difficulties occur, because these solvents have poor solubility in water (the final products have been isolated by precipitation with water). In nitromethane having b.p. only 101° the yield of this reaction was smaller and in acetamide with m.p. 60°, it was difficult to obtain an homogeneous solution at the beginning of reaction. We suppose that the formation of the nitriles may proceed *via* the oxime acetate, and the high polarity of DMAC facilitates this reaction. The mechanism of the reaction will be extensively discussed in a separate communication.

The general method for obtaining aromatic nitriles (III) consists thus in dissolving one mole of aromatic aldehyde (I) in DMAC, followed by the addition, under stirring, of 1.1 mole $NH_2OH \cdot HCl$ (a small excess of $NH_2OH \cdot HCl$ improves the yield). After heating for 4 – 5 hours at 140-150°, the final products (III) were obtained by precipitation with water. It can be seen from table 1 that the yields ranged from 61 to 89 %.

Table 1

Aromatic nitriles obtained from the corresponding aldehydes by heating with $NH_2OH \cdot HCl$ in DMAC

Aldehydes	Nitriles [a)]		
	yield [b)] %	M.p. [c)] °C	Reported m.p. [d)] °C
p-$CH_3O-C_6H_4-CHO$	89	58 – 60	59 – 60[11]
p-$Cl-C_6H_4-CHO$	82	92 – 94	93 – 94[11]
p-$O_2N-C_6H_4-CHO$	61	148 – 150	148 – 149[11]
m-$O_2N-C_6H_4-CHO$	69	114 – 116	115 – 117
p-$(CH_3)_2N-C_6H_4-CHO$	77	74 – 76	75 – 76[12]
p-$CH_3-C_6H_4-CHO$	88	58 – 60	58 – 59[11]
o-$Cl-C_6H_4-CHO$	73	41 – 43	42 – 43

[a)] The obtained nitriles were identified by comparison of m.p. and IR spectra with those of authentic samples.

[b)] Yield determined by isolation of the crude products and calculated on aldehyde employed.

[c)] After recrystallisation.

[d)] From "Beilsteins Handbuch der organischen Chemie".

The lower yield in the case of o-$Cl-C_6H_4-CN$ may be determined by a steric hindrance and in the case of p-$O_2N-C_6H_4-CN$, by the nitro group which is a strong electron-attracting substituent.

In conclusion, we present in this work a convenient one-step method for the synthesis of aromatic nitriles directly from the corresponding aldehydes by heating with hydroxylamine hydrochloride in DMAC as solvent.

EXPERIMENTAL

p-Methoxybenzonitrile

To a solution of 4.08 g (0.03 mole) OF *p*-methoxybenzaldehyde in 10 mL DMAC 2.3 g (0.033 mole) hydroxylamine hydrochloride was added under stirring. After stirring for 4–5 hours at 140–150°, the obtained solution was poured into 40–60 mL water with ice under efficient stirring, when the desired product precipitated and was then treated with 5% NaOH solution till pH = 9–10. The product was collected by filtration and washed with 20–30 mL 5% HCl solution and three times with 15–20 mL water. After drying under vacuum at 35–45° and recrystallisation from light petroleum, 3.5 g *p*-methoxybenzonitrile with m.p. 58–60° were obtained (mixed m.p. with pure *p*-methoxybenzonitrile undepressed). Yield 89% (calculated on *p*-methoxybenzaldehyde employed). Anal. calculated for: C_8H_7NO; C, 72.18; H, 5.26; N 10.52 %. Found: C, 72.34; H, 5.22; N, 10.70%.

In similar conditions, the other aromatic nitriles (presented in table 1) were prepared.

REFERENCES

[1] J. M. Prokicak and P. A. Porte, *Canad. J. Chem.*, **49**, 1321 (1971).

[2] M. O. Foxter and H. M. Judd, *J. Chem. Soc.*, **1910**, 254.

[3] E. Vovinekel and J. Bartel, *Chem. Ber.*, **107**, 1221 (1974).

[4] C. M. Wong, *J. Org. Chem.*, **38**, 2241 (1973).

[5] R. Appel and R. Kleinstüch, *Chem. Ber.*, **104**, 2025 (1971).

[6] H. G. Foley and D. R. Dalton, *Chem. Commun.*, **1973**, 628.

[7] A. Saednya, *Synthesis*, **1982**, 190.

[8] C. I. Chiriac, *Revista de Chimie*, **1983**, 67.

[9] J. Nishikido and T. Kato, *Japan Kokai*, **74**, 14, 442 (1974) : *Chem. Abstr.*, **80**, 145.853 s (1974)

[10] A. J. Parker, *Quart. Rev.*, **16**, 163 (1962).

[11] G. A. Olah and A. P. Fung, *Synthesis*, **1980**, 658.

[12] H. M. Blatter and G. Stevens, *J. Amer. Chem. Soc.*, **83**, 2203 (1961).

Revue Roumaine de Chimie, **30**, *4*, 357–364 (1985)

ABOUT THE CALCULATION OF THE I.R AND RAMAN ACTIVE FUNDAMENTALS OF POLYMERS*

ADRIAN O. FULEA
Department of Physical Chemistry, Polytechnic Institute of Bucharest, Blvd. Republicii 13
Bucharest 70031, Romania

Received April 27, 1983
Revised February 13, 1984

There are reported calculations of active fundamentals for an inorganic polymer in order to point out and correct several errors from monographs of infrared spectroscopy of polymers.

In the very useful and widely circulated treatises of infrared spectroscopy of polymers of Zbinden [1] and Elliot [2] we have found several errors with respect to the calculation of the active fundamentals for polymers, ** which either give an oversimplified picture of the vibrational problem for polymers, or can lead to considerable mistakes in this calculation. The difficulties encountered by us in understanding the vibrational analysis for polymers because of those errors[1,2] as well as the relatively long time which was necessary for us to spot them, made us believe that it would be useful for those engaged in the study of molecular vibrations of polymers to have comments on all of them inside a paper, thinking that the books of Zbinden [1] and Elliot [2] are the basic treatises for this study and furthermore that these errors are contained in other publications in the field of the infrared spectroscopy of polymers too. *** The calculation of the active fundamentals of the polymer which is formed in solution of MgI_2 in diethyl ether, whose infrared and Raman spectra were studied by Wieser and Krueger,[6] seemed to the author suitable for the discussion we intend to do here, because there is only one conformation which the chain can have in solution, which also does not require an additional supposition of the extension of the chain, this having a completely stretched structure, owing to the way of linking the atoms in the skeleton of the polymer.

---

* The calculations from this paper were performed by the author in 1972, during his graduate studies at the University of Calgary, Canada, for the Problem 2, Problem Set 5, in the course Chemistry 587 "Infrared and Raman Spectroscopy", taught by Dr. H. Wieser.

** The errors from reference [1] discussed in the present work are also contained in the Russian translation [3] of Zbinden's monograph. The errors of Elliot from reference [2] were copied by Bădilescu in reference.[4] As in the references of the chapter dealing with the theory of the spectra of macromolecular compounds, Bădilescu [4] did not cite reference [2] but reference [5a], these errors [2] appear too in [5a]; it is also possible that at least some of these errors [2] appear in [5b] and in its English original, because reference[5b] is also cited by Bădilescu.[4]

*** See our previous observations regarding references.[3, 4, 5a, 5b]

In the polymer depicted in figure 1 magnesium is sp^3d^2 hybridized. As can be seen from figure 1 the repeat unit * is MgI_2L_2 and not MgI_4O_2 (or MgI_4L_2) as Wieser and Krueger asserted.[6,8]**Thus the number

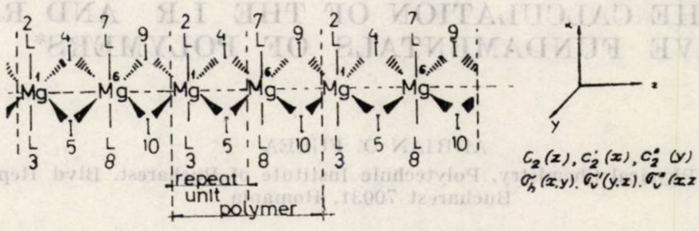

Fig. 1. — The structure of the polymer $(MgI_2L_2)_n$. The side parts are added in order to be met the Born boundary condition; $L = CH_3CH_2OCH_2CH_3$ is considered as one dynamical unit.

of the in-phase vibrations of the chain is $(3\times5 - 4) = 11$ and not $(3\times7-4) = 17$. The factor group of the line group of this inorganic polymer is isomorphous with the point group D_{2h}. Table 1 shows the symmetry operations

Table 1

The symmetry operations for the cosets C_2 and C_2''
$T_2 = T_1^2 = E$, s = skeleton

Coset C_2		Coset C_2''	
T_1C_2	T_2C_2	$T_1C_2''(1)$ $T_2C_2''(4,5)$	$T_2C_2''(1)$ $T_1C_2''(4,5)$
$1 \to 6$	$1 \to 1$	$1 \to 6$	$1 \to 1$
$2 \to 8$	$2 \to 3$	$2 \to 8$	$2 \to 3$
$3 \to 7$	$3 \to 2$	$3 \to 7$	$3 \to 2$
$4 \to 10$	$4 \to 5$	$4 \to 4$	$4 \to 9$
$5 \to 9$	$5 \to 4$	$5 \to 5$	$5 \to 10$
$u(T_1C_2) = 0$	$u(C_2T_2) = 1$	$u(T_1C_2''(1)) = 2$	$u(T_2C_2''(1)) = 1$
$u_s(T_1C_2) = 0$	$u_s(T_2C_2) = 1$	$u_s(T_1C_2''(1)) = 2$	$u_s(T_2C_2''(1)) = 1$
$u(\text{coset } C_2) = 1$		$u(\text{coset } C_2'') = 3$	
$u_s(\text{coset } C_2) = 1$		$u_s(\text{coset } C_2'') = 3$	

The numbering of the atoms is given in figure 1.

of the cosets C_2 and C_2'' and in Table 2 are given the values of u(coset)[9] necessary for the calculation of the active fundamentals. Using formula (1)[1,9] we can calculate the vibrations of the whole polymer and of its skeleton which correspond to the factor group representations.

---

* The (translational) repeat unit is the smallest unit of the chain which can be transformed into an identical unit by a simple translation.[7] It is also called basic (repeating) unit, the repeating unit in the crystallographic sense, or the unit cell. The fact that the degree of the polymerization is equal here with the number of the repeat units is accidental.

** For the four coordinate structure polymer discussed by Wieser and Krueger, the repeat unit is Mg_2X_4 and not MgX_4 as stated previously.[6]

Table 2

The values of u(coset) for all the cosets of line group

Coset	φ	$2\cos\varphi \pm 1$	u(coset)	
			skeleton	whole polymer
E	0	3	3	5
$C_2(z)$	180	−1	1	1
$C'_2(x)$	180	−1	1	3
$C''_2(y)$	180	−1	3	3
$\sigma_h(x, y)$	0	1	3	5
$\sigma'_v(y, z)$	0	1	3	3
$\sigma''_v(x, z)$	0	1	1	3
i	180	−3	1	1

$$n^{\mathrm{f \cdot g \cdot}}_{\alpha} = \frac{1}{H} \sum_{\mathrm{cosets} F_i} \chi_\alpha(F_i) \cdot u(\mathrm{coset}\, F_i)(2\cos\varphi \pm 1) \tag{1}$$

The results of the calculation are:

$$\Gamma^{\mathrm{f \cdot g \cdot}}_{\mathrm{t}} = 2A_g + 2B_{1g} + 3B_{1u} + B_{2g} + 3B_{2u} + B_{3g} + 3B_{3u} \tag{2}$$

$$\Gamma^{\mathrm{f \cdot g}}_{\mathrm{v}} = 2A_g + B_{1g} + 2B_{1u} + B_{2g} + 2\mathrm{B}_{2u} + B_{3g} + 2B_{3u} \tag{3}$$

$$\Gamma^{\mathrm{f \cdot g \cdot}}_{\mathrm{vs}} = A_g + B_{1u} + B_{2u} + B_{3g} + B_{3u} \tag{4}$$

In the above equations we abbreviated : $f \cdot g \cdot$ = factor group, v = vibrations, t = total, s = skeleton.

Therefore there are expected six fundamentals active in infrared spectrum $(2B_{1u} + 2B_{2u} + 2B_{3u})$ and five fundamentals active in Raman spectrum : $(2A_g + B_{1g} + B_{2g} + B_{3g})$. It can be seen that the exclusion rule is functioning because the point group, which is isomorphus with the factor group of the line group, contains the symmetry operation i. For the vibrations of the skeleton there are expected three fundamentals active in infrared spectrum : $(B_{1u} + B_{2u} + B_{3u})$ and two fundamentals active in Raman spectrum : $(\mathrm{A}_g + B_{3g})$.

The polymer depicted in Fig. 1 is also suitable for the analysis of the vibrational modes using the point group of this polymer, the results presenting interest for very small degrees of polymerization and also for our discussion below. The point group is D_{2h} if we admit two approximations : we consider again $\mathrm{L} = \mathrm{O(CH_2CH_3)_2}$ as one dynamical unit and we write the polymer as $(\mathrm{MgI_2L_2})_n\mathrm{I_2}$, adding thus two iodine atoms at one end of the chain in order to increase the molecular symmetry. The real polymer $(\mathrm{MgI_2L_2})_\mathrm{n}$ will have six less vibrational modes and only approximately D_{2h} symmetry. The characters $\chi(R)$ of the reductible representation are given in table 3. The space of this representation has $3N$ dimensions, N being the number of the atoms composing the polymer, $N = 5n + 2$, where n = degree of polymerization.

Table 3

The values of $\chi(R)$

D_{2h}	E	$\sigma(x, y)$	$\sigma(x, z)$	$\sigma(y, z)$	i	$C_2(z)$	$C_2(y)$	$C_2(x)$
n = even	$15n + 6$	2	$3n$	$3n + 2$	0	$-n$	-2	0
n = odd	$15n + 6$	3	$3n$	$3n + 2$	-3	$-n$	-1	-3

n = the degree of polymerization

Using the values of $\chi(R)$ from table 3, we obtain in the usual manner[10] the irreductible representations, the results being given by equations (5), (6), (7) and (8):

n = even

$$\Gamma_t = \left(\frac{5}{2}n + 1\right)A_g + nA_u + (n + 1)B_{1g} + \left(\frac{5}{2}n + 1\right)B_{1u} + 2nB_{2g} + \\ + (2n + 1)B_{2u} + (2n + 1)B_{3g} + (2n + 1)B_{3u} \tag{5}$$

$$\Gamma_v = \left(\frac{5}{2}n + 1\right)A_g + nA_u + nB_{1g} + \frac{5}{2}nB_{1u} + (2n - 1)B_{2g} + 2nB_{2u} + \\ + 2nB_{3g} + 2nB_{3u} \tag{6}$$

n = odd

$$\Gamma_t = \left(\frac{5}{2}n + \frac{1}{2}\right)A_g + nA_u + (n + 1)B_{1g} + \left(\frac{5}{2}n + \frac{3}{2}\right)B_{1u} + 2nB_{2g} + \\ + (2n + 2)B_{2u} + 2nB_{3g} + (2n + 1)B_{3u} \tag{7}$$

$$\Gamma_v = \left(\frac{5}{2}n + \frac{1}{2}\right)A_g + nA_u + nB_{1g} + \left(\frac{5}{2}n + \frac{1}{2}\right)B_{1u} + (2n - 1)B_{2g} + \\ + (2n + 1)B_{2u} + (2n - 1)B_{3g} + 2nB_{3u} \tag{8}$$

The fact that, for n = even and n = odd, the polymer belongs to the same point group, D_{2h}, is accidental. Thus for the tetracoordinate complexed structure,[6] if the degree of polymerization n is odd, $(MgI_2)_n$ belongs to the C_{2v} point group, while, for n even, $(MgI_2)_nI_2$ belongs to D_{2h} point group, $(MgI_2)_n$ having in this case only approximately D_{2h} symmetry. It is also fortuitous that the point group which is isomorphosu with the factor group of the line group of the polymer from figure 1 (in the case of the fulfillment of Born boundary condition), D_{2h}, is the same with the point group of the polymer (without presuming to be met the Born boundary condition).

The balance of this paper is devoted to correct previous errors.[1,2]

1. Elliot asserts in the headings of tables 3.1 and 3.3[2] that a line group (in the case discussed [2], that of polyethylene chain) is isomorphous with a point group (D_{2h}). Bădilescu states also in the text that the line group to which the polyethylene chain belongs is isomorphous (every element of one group corresponds to an element of the other group and reversely) with the point group D_{2h}[4].

Inside the method of Bhagavantam and Venkatarayudu[11] the finite space group is isomorphous with the factor group and the latter is isomorphous with a certain point group, but in that method[11] the authors considered a special case when the number of unit cells is one. When we are considering a chain, composed therefore of at least two repeat units, the above statement is erroneous. Between the point group of interest, the one which is isomorphous with the factor group of the line group and the line group there is only a homomorphism relation : at one element of the point group corresponds a number of elements of the line group equal with the order of the subgroup of translations. This can be very easily seen by looking at table 1 in the present paper or at table VII,[1] *, where to one element of the point group correspond two and three ** elements of the two line groups respectively. It should be noted that, according to table 3.1 [2] and table 3.3 [2], one could think that the line group is isomorphous with the point group, but this is deceptive and it is owing to the fact that under the title of the line group are given only some of the elements of the line group and not all of them. Thus none of the elements RT ($R = E$, $C_2(y)$, $C_2(x)$, $C_2(z)$, i, $\sigma(xz)$, $\sigma_g(yz)$, $\sigma(xy)$; $T \neq E$) is given in table 3.3. [2]

2. The statement that the symmetry elements of the repeat unit together with the unit translation (equivalent to the identity E) form a sub-group of the line group, called a unit cell group or a factor group, [2] is not correct and refers rather to a way of shortening the writing of the elements of the factor group. For example the coset $\{T_1C_2,\ T_2C_2\}$, from table 1, is noted with C_2. The elements of the factor group are the cosets, while the line group has as its elements the symmetry elements themselves. Therefore a symmetry operation is not by itself an element of the factor group and furthermore the factor group cannot be a sub-group of the line group.

Relating to the factor group we have to point out that even for an infinite chain this group is finite *** contrary to the statement of Schachtschneider and Snyder[8] ; only each element of the factor group is formed, in the case of an infinite chain, by an infinite number of symmetry operations.

---

* Some care should be taken regarding Table VII[1] because instead of the elements of symmetry $\sigma_h\ T_i$, as claimed in the headings of this table, are given the elements of symmetry $T_i\sigma_h$.

** There the polymer has three repeat units.

*** An infinite group means a group whose order is infinite.

3. In table 3.1 [2] it is equated the number of the vibrational modes obtained by using formula (1) with the total number of the vibrational modes for an infinite chain. [2] $\Gamma^{f;g}_{t}$, exemplified in this paper by equation (2), represents the vibrations of an infinite polymer chain, or of a finite polymer chain fulfilling the Born boundary condition (including the four zero modes), which can be active in the vibrational spectra if only the translation symmetry requirements would be taken into account. These vibrations are those in which all the repeat units are vibrating in phase and for this reason they are called in-phase vibrations. The addition of the requirements of the other symmetry elements adds more stringent selection rules.

The total number of vibration modes for an infinite chain is infinite and not 18 for polyethylene, as stated previously. [2]*. In the case that we do not suppose that the Born boundary condition is met, we have given above the vibrational modes for our polymer; equations (6) and (8) show also how the number of vibrations of each species is a function of the degree of polymerization n.

The symmetry modes depicted in-figure 3.2 [2] are not all the symmetry modes of the polyethylene chain, but only the in-phase vibrational modes and the symmetry species from table 3.1 [2] are not all the symmetry species of the line group of the polythylene chain, as stated in table 3.1, [2] but only those symmetry species of the line group which are also the symmetry species of the factor group of the respective line group.

4. With respect to the nongenuine vibrations, Zbinden states[1] that they can be evaluated separately by using values given by (64a)[1] and (64b)[1] :

$$\chi(R)^{\text{trans}} = 2\cos\varphi \pm 1 \qquad (64a)^1$$

$$\chi(R)^{\text{rot}} = 2\cos\varphi \pm 1 \qquad (64b)^1$$

Zbinden asserts further that if the symmetry operation R is a translation, φ becomes 0 and eqs. (64)[1] become

$$\chi(R)^{\text{trans}} = \chi(R)^{\text{rot}} = 3 \qquad (67)$$

Equation $\chi(R) = 2\cos\varphi \pm 1$ is valid only for a symmetry operation R whose sole action on the vector is to change its orientation, for example a rotation which does not transform a vector into another one; this equation is widely used for molecules belonging to the point groups. On the other hand any translation $T \neq E$ moves an atom into the place of another atom. The point to be made in our view, in order to demonstrate $\chi(R)^{\text{trans}} = 3$, would not be by applying equation $\chi(R) = 2\cos\varphi \pm 1$ and to put in it $\varphi = 0$, but to point out that in the case of a translation applied on a polymer fulfilling the Born cyclic condition, the vector of the center of the mass of the polymer remains invariant, although none of the atoms is invariant at a translation. This invariance of the vector of the center of the mass leads immediately to $\chi(T)^{\mathrm{trans}} = 3$.

---

* Our previous statement in the title of table 3, [12] that $\Gamma^{f;g}_{t}$ (12 vibrations for poly(methyleneoxide) and 6 vibrations for its skeleton) are the normal vibrations should be completed in the sense indicated above regarding the activity, i.e. as being the in-phase vibrations.

5. In regard to u(coset) from formula (1) Zbinden makes some erroneous assertions[1] which can lead to considerable mistakes in the calculation of the active fundamentals. Thus the author claims that, as implied by nomenclature, u(coset) is the same for any space group element of the same coset.[1] It can be seen, by looking at table 1 that this is not correct. As a matter of fact a nomenclature cannot serve to demonstrate anything. Anyway the nomenclature refers here to the whole coset and therefore cannot suggest anything in regard to a certain space group element belonging to that coset. Furthermore in table XIII,[1] Zbinden equals u(coset) with the number of atoms per unit cell left invariant by a particular operation which is equally wrong. From the definition of u(coset) given by Winston and Halford[9] which introduced it, results that u(coset) is in fact the sum of the atoms from a unit cell which are left invariant by each symmetry operation of the coset, these symmetry operations being applied in turn, after each such an operation adding to the sum obtained previously, the number of the atoms left invariant by this symmetry operation. The definition by which u(coset) is introduced in monograph [1] is : the number of invariant atoms in one unit cell is called u(coset).[1] It is not specified at what the atoms should be invariant. In fact u(coset) is neither the number of the invariant atoms at a symmetry operation nor the number of atoms which remained invariant after the all symmetry operations of a coset were applied *, but the sum of the numbers of invariant atoms from a unit cell when each operation of symmetry of a coset is applied separately, the sum being extended over all the operations of the respective coset.

Taking into account the above discussion we consider that seems justified to write in formula (1) u(coset) as :

$$u(\mathrm{coset}\, F_i) = u_1^i + u_2^i + \ldots + u_N^i \tag{9}$$

u_j^i being the number of the invariant atoms from one unit cell when the symmetry operation $T_j R_i$ is applied, N being the order of the sub-group of translations, equal with the number of the unit cells from the polymer chain. For example in the case of coset C_2'' for our polymer :

$$u(C_2'') = u(T_1 C_2''(1)) + u(T_2 C_2''(1)) = 2 + 1 = 3$$

REFERENCES

[1] R. Zbinden, "Infrared Spectroscopy of High Polymers", Academic Press, New York, 1964 p. 57–59, 84.

[2] A. Elliott, "Infrared Spectra and Structure of Organic Longchain Polymers", Edward Arnold (Publishers) Ltd., London, 1969, p. 38, 39.

[3] R. Zbinden, "Infrakrasnaia spektroscopiya vysokopolimerov", under the editorial care of L. A. Blümenfeld, Izdatelstvo Mir, Moskow, 1966.

---

* We stated previously [12] erroneously that u(coset) represents the number of atoms which remain invariant in unit cell if all operations from a coset are applied to the chain.

[4] S. Bădilescu, M. Toader, M. Giurginca and V. Tălpuş, "Spectroscopia in infraroşu a polimerilor şi auxiliarilor", Ed. Tehnică, Bucharest, 1982, p. 14–16.

[5a] A Elliott, "Infrakrasnyie spectry i struktura polimerov", Mir, Moskow, 1972, cf. ref. 4.

[5b] A. Elliott, "Infrakrasnyie spectry polimerov" in Uspehi Spektroskopii, H. W. Thomson Ed., Izd. Inoster. Liter., Moskow, 1963, cf. ref. 4.

[6] H. Wieser and P. J. Krueger, *Spectrochim. Acta.*, A**26**, 1349 (1970).

[7] J. H. Schachtschneider and R. G. Snyder, *J. Polym. Sci.*, C**7**, 99 (1963).

[8] H. Wieser, Problem Set 5 in the course "Infrared and Raman Spectroscopy", Spring 1972, University of Calgary.

[9] H. Winston and R. S. Halford, *J. Chem. Phys.*, **17**, 607 (1949).

[10] See for example N. B. Colthup, L. H. Daly and S. E. Wiberly, "Introduction to Infrared and Raman Spectroscopy", Academic Press, New York, 1975, p. 146.

[11] S. Bhagavantam and T. Venkatarayudu, *Proc. Indian Acad. Sci.*, **94**, 224 (1939).

[12] A. O. Fulea and M. Leca, *Revista de Fizică şi Chimie*, **AIX**, 71 (1972).

Revue Roumaine de Chimie, **30**, *4*, 365–369 (1985)

IDENTIFICATION D'HYDROCARBURES AROMATIQUES DE QUELQUES FRACTIONS PÉTROLIÈRES. III[1,2]

MÉTHODE n. d. PA

HOCINE KADI[a] et D. P. LAZĂR[b]

[a] Département de Génie chimique, École Polytechnique, Université d'Alger, Algérie

[b] Département de Chimie physique, Faculté de Technologie chimique, Splai Bahlui 71, 6600 Jassy, Roumanie

Reçu le 5 décembre 1983

The n.d. Pa method — frequently used to establish the chemical composition of both crude oil and oil fractions resulting after the primary distillation — belongs to so-called ,,composed criteria'', based on the experimental measurements of several physical parameters (in this particular case : refractive index, relative density and ,,aniline point''). The use of this method enables us to draw a clear distinction between the carbon atoms belonging to the following three main hydrocarbons series : alkanes, naphthenes and aromatics.

La méthode n.d. PA, souvent utilisée pour établir la composition chimique d'un pétrole brut et des fractions pétrolières issues d'une première distillation, fait partie des dits « critères composés » basés sur la mesure de certains paramètres physiques (dans le cas de cette méthode : indice de réfraction, densité relative et « point d'aniline »). L'utilisation de cette méthode permet l'établissement de la composition chimique des fractions pétrolières exprimée en pourcentage d'atomes de carbon appartenant aux trois grandes classes d'hydrocarbures : paraffines, naphtènes et aromatiques.

1. PRÉSENTATION DE LA MÉTHODE n.d. PA

Les hydrocarbures cycliques saturés (cycloparaffines ou naphtènes) possèdent des propriétés physico-chimiques intermédiaires entre celles des hydrocarbures non cycliques saturés (alcanes ou paraffines) et celles des hydrocarbures aromatiques. [3]

L'analyse physico-chimique d'une fraction pétrolière primaire (comme celle discutée dans cet article et distillée entre 90°—209°) peut conduire, quelquefois, à une conclusion erronée, à savoir que la fraction respective ne contient que des hydrocarbures paraffiniques et aromatiques. Pour résoudre cette incertitude, on a cherché à réunir, dans une seule relation, un nombre donné de caractéristiques physiques des fractions pétrolières secondaires et à l'aide de cette relation on peut déterminer la composition quantitative exprimée en pourcentage d'atomes de carbon appartenant aux hydrocarbures paraffiniques ($\%C_P$), naphténiques ($\%C_N$) et aromatiques ($\%C_A$). En admettant que la fraction primaire, ainsi que les fractions secondaires, contiennent des constituants individuels de toutes les trois grandes classes de hydrocarbures, il est nécessaire — du moins théoriquement — d'utiliser trois caractéristiques (grandeurs) physico-chimiques judicieusement choisies, à l'aide desquelles on élimine l'incertitude mentionnée. C'est la raison pour laquelle dans ce travail on fait appel à :

1°. l'indice de réfraction, n_{20}^{D},

2°. densité relative, d_4^{20},

3°. le « point d'aniline », PA (défini comme étant la température la plus basse à laquelle, dans un mélange équivolumétrique de la fraction pétrolière secondaire et d'aniline pure, parfaitement miscibles à des températures plus élevées, apparaît une turbidité observable[4]).

L'utilisation simultanée de ces trois paramètres physiques pour calculer les valeurs $\% \mathrm{C_P}$, $\% \mathrm{C_N}$ et $\% \mathrm{C_A}$ constitue la « méthode n.d.PA », dont le contenu principal est formé par les relations[5] :

$$\% \mathrm{C_A} = 1039{,}4 \; n_{20}^{D} - 470{,}4 \; d_4^{20} - 0{,}315 \; \mathrm{PA} - 1094{,}3 \tag{1}$$

$$\% \mathrm{C_N} = -1573{,}3 \; n_{20}^{D} + 840{,}15 \; d_4^{20} - 0{,}4619 \; \mathrm{PA} + 1662{,}2 \tag{2}$$

$$\% \mathrm{C_P} = 100 - (\% \mathrm{C_A} + \% \mathrm{C_N}) \tag{3}$$

«Le poids moléculaire », M_i, d'une fraction pétrolière secondaire peut être déterminé soit à l'aide de la relation linéaire entre M_i, n_{20}^{D} et PA :

$$M_i = 1705{,}45 \; n_{20}^{D} + 792{,}93 \; d_4^{20} + 4553 \; \mathrm{PA} - 3287 \tag{4}$$

connue sous le nom de « relation de Robert », soit à l'aide de la relation linéaire entre M_i, la « température d'ébullition moyenne » PE_m^0 (définie par : $\mathrm{PE}_m^0 = (t_i^0 + t_f^0)/2$) et n_{20}^{D} :

$$\log M_i = 0{,}001978 \; \mathrm{PE}_m^0 + 1{,}9394 + \log(2{,}1500 - n_{20}^{D}) \tag{5}$$

ou « relation de Hersh ». La grandeur M_i peut être aussi déterminée graphiquement en utilisant un diagramme d_4^{20} en fonction de la température d'ébullition[6] où sont représentées les iso-propriétés des hydrocarbures purs :

1°. la viscosité empirique, mesurée avec un viscosimètre SAYBOLT UNIVERSEL,[7] à la température de 100° F, exprimée en unités secondes — SU (unités $\mathrm{SSU_{100}}$),

2°. le facteur de caractérisation du rapport C/H dans la molécule d'un hydrocarbure pur,[8] défini par :

$$\mathrm{K_{UOP}} = \frac{\sqrt[3]{T(^\circ\mathrm{R})}}{\mathrm{sp.\ gr.\ 60/60}} \tag{6}$$

où T est la température d'ébullition de l'hydrocarbure (en degrés Rankine), sp. gr. 60/60 est la densité relative de l'hydrocarbure à 60° F et UOP est l'abréviation pour Universal Oil Products,

3°. le poids moléculaire, M_i.

2. DÉTERMINATIONS EXPÉRIMENTALES

L'indice de réfraction, n_{20}^{D}, des 23 fractions secondaires a été mesuré sous une lumière monochromatique (lampe de sodium), à la température de 20°, à l'aide d'un réfractomètre HIGLER & WATTS.

La densité relative, d_4^{20}, définie par le rapport :

$$\frac{\text{poids d'un volume donné d'une fraction secondaire}}{\text{poids d'un même volume d'eau, à 4°C}}$$

a été déterminée par picnométrie, à 20° (conformément aux normes internes ASTM — American Society for Testing Materials — la grandeur d_4^{20} s'exprime par le « poids spécifique » de la fraction secondaire, à 60°F, par rapport à un même volume d'eau, toujours à 60°F, et sa notation est « gr. sp. 60/60 »).

Le point d'aniline, PA, a été déterminé en utilisant des volumes égaux de la fraction pétrolière secondaire a examiner et d'aniline pure introduits dans un tube en verre et agités mécaniquement. Le contenu du tube a été chauffé jusqu'à miscibilité totale entre les deux liquides. Le refroidissement du mélange homogène jusqu'à l'apparition d'un trouble a permis d'établir le « point d'aniline », PA.

3. RÉSULTATS

3.1. A l'aide des valeurs expérimentales obtenues pour n_{20}^{D}, d_4^{20} et PA, on a calculé les grandeurs % C_A, % C_N et % C_P, pour toutes les fractions 1—23 (Tableau 1), en utilisant les relations (1)—(3).

Tableau 1

Composition (en pourcentage) des fractions 1—23 déterminée par la méthode n.d.PA

Fraction	Indice de réfraction, n_{20}^{D}	Densité, d_4^{20}	Point d'aniline, PA (°C)	% Aromatiques	% Naphtènes	% Paraffines
1	1,3976	0,7024	58,60	9,5	26,4	64,1
2	1,4018	0,7193	56,80	6,5	34,8	58,7
3	1,4109	0,7330	49,20	11,9	35,5	52,6
4	1,4087	0,7355	54,60	11,4	30,2	58,4
5	1,4090	0,7245	61,80	9,9	25,6	64,5
6	1,4185	0,7409	53,80	14,6	20,1	65,3
7	1,4240	0,7506	52,60	16,2	28,1	55,7
8	1,4189	0,7485	57,80	10,2	32,0	57,8
9	1,4252	0,7553	57,40	13,7	28,0	58,3
10	1,4311	0,7646	53,90	16,6	28,1	55,1
11	1,4343	0,7701	52,70	17,6	28,3	54,1
12	1,4350	0,7706	55,70	17,2	26,2	56,6
13	1,4357	0,7724	54,00	17,6	27,4	55,3
14	1,4368	0,7742	55,60	17,4	26,5	56,1
15	1,4380	0,7784	56,30	16,5	27,7	55,8
16	1,4391	0,7798	56,40	16,9	27,2	55,9
17	1,4399	0,7823	57,20	16,3	27,6	56,1
18	1,4400	0,7824	58,20	16,1	27,1	56,8
19	1,4407	0,7827	59,10	16,4	25,8	57,8
20	1,4415	0,7837	58,60	16,9	25,6	57,5
21	1,4430	0,7880	58,80	16,4	28,8	54,8
22	1,4448	0,7914	57,60	17,0	27,4	55,6
23	1,4464	0,7943	57,10	17,5	27,5	55,0

3.2. A l'aide de la « température d'ébullition moyenne », PE_m^0, et du facteur de caractérisation K_{UOP} (relation 6), on a calculé les grandeurs M_i pour toutes les fractions secondaires 1–23 étudiées (Tableau 2), en utilisant la méthode graphique.

Tableau 2

Détermination des « poids moléculaires » M_i

Fraction	Température ébullioscopique initiale, t_i^0 (°C)	Température ébullioscopique finale, t_f^0 (°C)	Température ébullioscopique moyenne, PE_m^0 (°C)	Facteur de caractérisation[a] K_{UOP}	Poids moléculaire M_i
1	90,0	99,0	94,50	12,4	102
2	99,0	103,5	101,25	12,2	103
3	103,5	115,0	109,25	12,0	106
4	115,0	123,5	119,25	12,3	115
5	123,5	131,0	127,25	12,4	120
6	131,0	137,0	134,00	12,3	122
7	137,0	145,5	141,25	12,1	125
8	145,5	151,0	148,25	12,2	131
9	151,0	157,5	154,25	12,2	133
10	157,5	164,5	160,75	12,0	136
11	164,5	169,0	166,75	12,0	140
12	169,0	172,0	170,50	12,0	142
13	172,0	175,0	173,50	12,0	144
14	175,0	178,0	176,50	12,0	145
15	178,0	182,0	180,00	12,0	146
16	182,0	184,7	183,25	12,0	149
17	184,5	188,0	186,25	12,0	151
18	188,0	191,0	189,50	12,1	153
19	191,0	197,5	195,25	12,1	156
20	197,5	200,5	199,00	12,1	160
21	200,5	202,0	201,25	12,0	161
22	202,0	205,0	203,50	12,0	162
23	205,0	209,0	207,00	12,1	165

[a] Les valeurs spécifiques du facteur K_{UOP} pour certains hydrocarbures :

$K_{UOP} = 10$, hydrocarbures aromatiques purs,

$K_{UOP} = 11$, hydrocarbures naphténiques purs ou aromatiques légèrement substitués,

$K_{UOP} = 12$, hydrocarbures mixtes où le cycle et la chaîne sont équivalents,

$K_{UOP} = 13$, hydrocarbures paraffiniques normaux et iso [8].

CONCLUSIONS

1°. Toutes les fractions secondaires étudiées ont une composition (en pourcentage massique) prépondérante de type paraffinique. Le pourcentage en aromatiques est toujours parmi les plus bas.

2°. A l'exception des fractions n°s 1, 2 et 5, toutes les autres présentent un pourcentage en hydrocarbures aromatiques compris entre 10 % et 17,5 %.

3°. Les fractions 10–23 ont un pourcentage en hydrocarbures aromatiques superiéur à 15 % (moyenne 16,88 % ± 0,51 %) et une distribution particulièrement uniforme.

RÉFÉRENCES

[1] H. Kadi et D. P. Lazăr, *Rev. Roumaine Chim.*, **29**, 497(1984).
[2] H. Kadi et D. P. Lazăr, *Rev. Roumaine Chim.*, **30**, 81(1985).
[3] P. Wuithier, «Le pétrole ; Raffinage et Génie chimique », Tome 1, Editions TECHNIP, Paris, deuxième édition, 1972, p. 55
[4] P. Wuithier, op. cit., p. 30.
[5] P. Wuithier, op. cit , p. 56.
[6] P. Wuithier, op. cit., p. 49.
[7] P. Wuithier, op. cit., p. 10.
[8] P. Wuithier, op cit., p. 49.

Revue Roumaine de Chimie **30**, *4*, 371 (1985)

CORRIGENDUM "ON A CORRECTION TECHNIQUE FOR FRACTIONATION DATA AND ITS APPLICATION TO THE FRACTIONATION OF POLYETHYLENE TEREPHTHALATE"

ADRIAN O. FULEA
Department of Physical Chemistry, Polytechnic Institute of Bucharest, Blvd. Republicii 13
Bucharest, Romania

Received May 29, 1984

The criticism of Haseley's method is withdrawn as unfounded

We are withdrawing our criticism (1) on the Haseley's method (2). It was based on our erroneous understanding that in the formula

$$A'_i = A_i - \sum_{j=1}^{i-1} \omega_j (M > \overline{M}_i) + \sum_{j=i+1}^{n} \omega_j (M < \overline{M}_i)$$

ω_j is the weight in percents of the subfraction j of the fraction i, while in fact, as specified by Haseley, is the weight in percents of the total polymer in the j-th fraction with M greater on less than M_i.

REFERENCES

[1] A. O. Fulea, *Rev. Roum. Chim.*, **25**, 435 (1980).
[2] E. A. Haseley, *J. Polym. Sci.*, **35**, 309 (1959).

NOTE POUR LES AUTEURS

La Revue Roumaine de Chimie publie des articles en englais, français, russe, allemand ou espagnol. Les auteurs sont priés d'envoyer des articles et des comptes rendus inédits.

Les manuscrits seront dactylographiés à double interligne. La bibliographie, les tableaux et la légende des figures seront placés après le texte.

Si l'article partie d'une série numérotée, la partie précédente sera donnée comme première référence.

Chaque article sera précédé d'un résumé comprenant quinze lignes au maximum.

Les références bibliographiques dans le texte seront faites par des exposants sans parenthèses et paraîtront à la fin de l'œuvrage.

Les publications périodiques mentionées dans la bibliographie seront présentées suivant les prescriptions internationales: le nom de l'auteur précédé de l'initiale de prénom, le titre du périodique abrége conformément à « Chemical Abstracts » et souligné par une ligne, le numéro du tome indiqué par des chiffres arabes et souligné par deux lignes, suivi de la première page de l'article: à la fin, l'année de la parution sera placée entre parenthèses. Le numéro de la revue ne sera pas indiqué si les pages du volume sont numérotées consécutivement.

Les textes des livres ou traités inclueront: le nom des auteurs, précédés de l'initiale du prénom, le titre du livre entre guillements et sans être souligné, le numéro du tome précédé par l'abréviation « vol.» (ou « Bd. »), le numéro de l'édition, les éditions (the publisher), la localité de la parution du livre, l'année de la parution et la page de référence précédée(s) par l'abréviation « p » (ou « S »).

Les brevets seront indiqués comme suit : l'auteur ou la firme, le pays et le numéro du brevet, la date de la revue *(Chem. Abstr.* . Par ex.: M. Jones (to Union Carbide Co.) Brit. Pat. 610 238, 2 Sept. 1959: cf. *Chem. Abstr.*, 54, 12808 (1960).

Si la référence n'a pas été lue en original, on indiquera aussi la revue de références consultée.

Les diagrammes seront tracés à l'encre de Chine sur papier calque. Les tableaux et les figures (en nombre strictement nécessaire), ainsi que les courbes dans les figures seront numérotés par des chiffres arabes. Leur explication sera donnée dans la légende des figures. Prière de ne pas inscrire les mêmes dans les tableaux et les figures. Chaque tableau aura un titre. On indiquera dans le texte la place approximative des tableaux et des figures. Les formules chimiques seront incluses dans le texte ; en outre, elles seront transcrites sur papier calque à l'encre de Chine.

Les auteurs sont prés d'indiquer les caractères italiques (en soulignant les lettres au crayon), ainsi que toute autre caractère spécial: les préfixes *ortho, meta, para, cis, trans,* etc. seront soulignés pour indiquer leurs caractères italiques, et ne seront jamais écrits avec des majuscules.

Aucune correction à la main ne sera admise sur le manuscrit. Les corrections seront frappées à la machine. Les lettres greques ou autres symboles spéciaux seront insérés à la main à l'encre clairement.

Le manuscrit sera signé par l'auteur.

Le titre courant aura 50 lettres au maximum.

L'entière responsabilité du contenu des articles appartient aux auteurs.

Sur demande on peut obtenir une note plus complète.

PRINTED IN ROMANIA

ORSZÁGOS MŰSZAKI INFORMÁCIÓS KÖZPONT ÉS KÖNYVTÁR 1983

TRAVAUX PARUS AUX ÉDITIONS DE L'ACADÉMIE DE LA RÉPUBLIQUE SOCIALISTE DE ROUMANIE

GH. MARCU, **Chimia compuşilor coordinativi**, 1984, 415 p.

E. CORDOŞ, C. MANOLIU, **Spectrometria de absorbţie şi fluorescenţă atomică**, 1984, 178 p.

C. BODEA, **Tratat de biochimie vegetală**, p. II, vol. 5, 1984, 438 p.

ELENA CEAUŞESCU, **Cercetări în chimia şi tehnologia polimerilor**, 1983, 519 p.

N. ASANDEI, A. GRIGORIU, **Chimia şi structura fibrelor**, 1983, 395 p.

N. IONESCU, M. CALDARARU, **Oxidarea catalitică a olefinelor inferioare**, 1983, 178 p.

C. CAŞCAVAL, **Studiul polimerilor prin piroliză şi cromatograafie de gaze**, 1983, 220 p.

C. I. SIMIONESCU, F. DENES, **Originea vieţii**, 1983, 110 p.

C. BODEA (editeur), **Tratat de biochimie vegetală**, II, Tome IV, 1982, 408 p.

I. G. MURGULESCU, RODICA VILCU, **Introducere în chimia fizică. Vol. III. Termodinamica chimică**, 1982, 624 p.

ELENA JERCAN, **Analiza cromatografică**, 1982, 286 p.

I. G. MURGULESCU, J. PĂUN, **Introducere în chimia fizică. Vol. I. 3. Nucleul atomic, reacţii nucleare, particule elementare**, 1982, 606 p.

ELENA CEAUŞESCU, **Noi cercetări în domeniul compuşilor macromoleculari**, 1981, 536 p.

I. G. MURGULESCU, TATIANA ONCESCU, E. SEGAL, **Introducere în chimia fizică. Vol. II. 2. Cinetică chimică şi cataliză**, 1981, 1024 p.

V. DRĂGUŢAN, A. T. BALABAN, M. DIMONIE, **Metateza olefinelor şi polimerizarea prin deschidere de inel a cicloolefinelor**, 1981, 254 p.

LYDIA-MARIA VAICUM, **Epurarea apelor uzate cu nămol activ. Bazele biochimice**, 1981, 218 p.

I. GĂLĂŢEANU, **Procese şi metode radiochimice în energetica nucleară**, 1981, 234 p.

O. IORDACHE, **Procese polistocastice aplicate la fenomenele de transfer**, 1981, 186 p.

CR. SIMIONESCU, VALERIA GORDUZA, **Polimeri biocompatibili şi biologic activi**, 1980, 479 p.

ELENA CEAUŞESCU, **Polimerizarea stereospecifică a izoprenului**, 1979, 307 p.

CONST. GH. MACAROVICI, **Analiza chimică cantitativă anorganică**, 1979, 457 p.

M. FLORESCU, **Metode ştiinţifice în dezvoltarea industriei chimice moderne**, 1979, 256 p.

A. T. BALABAN, I. GĂLĂŢEANU, G. GEORGESCU, LIGIA SIMIONESCU, **Compuşi marcaţi şi radiofarmaceutici cu aplicaţii în medicina nucleară**, 1979, 495 p.

I. G. MURGULESCU, E. SEGAL, **Introducere în chimia fizică, Vol. II. 1. Teoria molecular cinetică a materiei**, 1979, 1036 p.

S. STERNBERG, FL. DANEŞ, **Termodinamica chimică aplicată**, 1978, 400 p.

I. G. MURGULESCU, V. EM. SAHINI, **Introducere în chimia fizică. Vol. I. 2. Structura şi proprietăţile moleculelor**, 1978, 604 p.

I. ZUGRĂVESCU, MAGDA PETROVANU, **N-ylid chemistry**, coedition avec McGraw Hill International Book Company, U.S.A., 1977, 396 p.

I. G. MURGULESCU, **Introducere în chimia fizică. Vol. I. 1. Atomi, molecule, legătură chimică**, 1976, 560 p.

ELENA CEAUŞESCU, **Research work on synthesis and characterization of macromolecular compounds. Contributions**, 1974, 251 p.

1985 MAI 2 2

ISSN 0035—4090

I. P. INFORMAŢIA cd. 2773

43426

Lei 40

$ 80 (pour un abonnement annuel)

F 1103

ACADÉMIE DE LA RÉPUBLIQUE SOCIALISTE DE ROUMANIE

REVUE ROUMAINE DE CHIMIE

R 1985 JUN 4

MG

TOME 30

N° 5

Mai 1985

Rev. Roumaine Chim.

RRCHAX, 30, 5, p. 373–438 (1985), Bucarest

EDITURA ACADEMIEI REPUBLICII SOCIALISTE ROMÂNIA

ACADÉMIE DE LA RÉPUBLIQUE SOCIALISTE DE ROUMANIE

COMITÉ DE RÉDACTION

Rédacteur en chef:

I. G. MURGULESCU, membre de l'Académie de la République Socialiste de Roumanie

Rédacteurs en chef adjoints:

A. T. BALABAN et V. EM. SAHINI, membres correspondants de l'Académie de la République Socialiste de Roumanie

Collège de rédaction :

EM. BRATU, ELENA CEAUȘESCU, ECATERINA CIORĂNESCU-NENITZESCU, CR. SIMIONESCU, membres de l'Académie de la République Socialiste de Roumanie ; P. SPACU, membre correspondant de l'Académie de la République Socialiste de Roumanie ; M. BANCIU, M. GHEORGHIU, I. HAIDUC, D. I. MARCHIDAN, I. MOLDOVAN, G. NIAC et D. SĂNDULESCU

La Revue Roumaine de Chimie paraît 10 fois par an. Toute commande de l'étranger sera adressée à ROMPRESFILATELIA — sectorul Export-Import Presă, P.O. Box, 12—201, télex 10376 prsfi r 78104 Bucarest, Calea Griviței nr. 64—66, Roumanie.

Les manuscrits, les livres et les revues proposés en échange, ainsi que toute correspondance seront envoyés à la rédaction

RÉVUE ROUMAINE DE CHIMIE

125, Calea Victoriei, 79717 Bucarest, Roumanie, téléphone 50 76 80

EDITURA ACADEMIEI REPUBLICII SOCIALISTE ROMÂNIA
125, Calea Victoriei, 79717 Bucarest, Roumanie, téléphone 50 76 80

REVUE ROUMAINE
DE
CHIMIE

Tome 30, N° 5 **Mai, 1985**

ELENA CEAUȘESCU, R. BORDEIANU, D. S. VASILESCU, I. MANAFU, IRINA CERCHEZ, P. GHIOCA, RODICA STANCU and E. BUZDUGAN, Characterization of poly(butadiene-b-styrene) by specific refractive index increment measurements 375–380

RODICA VÎLCU and I. GĂINAR, A new method for measuring the small pressure differences at high static pressures 381–384

I. BÂLDEA, V. FĂRCĂȘAN and ILEANA OLTEANU, Kinetics of the Jacobson reaction 385–389

AMALIA CRUSOS, Copolyamides. I. The influence of composition on the physico-chemical properties 391–393

KEEMTI LAL and SITA RANI MALHOTRA, Magnetic and spectral studies on copper(II), nickel(II), cobalt(II), iron(III) and manganese(II) complexes of 3-bromo-2-hydroxy-5-methyl acetophenone hydrazone 395–400

ABDU E. ABDEL RAHMAN and AMAL S. YANNI, Synthesis of some new indophenazinyl-pyrazoline and isoxazoline derivatives 401–404

S. H. DOSS and N. R. ABU ZEID, Bromination of unsaturated sultams and sultones 405–417

M. M. MOHAMED, M. A. EL-HASHASH, M. A. SAYED and A. A. SHEHATA, Reactions of some 2(1H)-pyridones synthesized from 3,4-methylene-dioxybenzylidene- and 4-nitrobenzylidene-p-isopropylacetophenone 419–426

J. M. CAMPELO, A. GARCIA, D. LUNA and J. M. MARINAS, Liquid phase catalytic hydrogenation on $AlPO_4$-supported nickel catalysts. II. Hydrogenation of styrene and α-methyl-styrene 427–434

I. M. POPA, GH. IONESCU and A. TARHON, High-pressure liquid chromatographic analysis of some cephalosporins 435–438

Rev. Roumanie Chim. **30**, *5*, 373–438 (1985), Bucarest

Revue Roumaine de Chimie, **30**, *5*, 375—380 (1985)

CHARACTERIZATION OF POLY(BUTADIENE-b-STYRENE) BY SPECIFIC REFRACTIVE INDEX INCREMENT MEASUREMENTS

ELENA CEAUŞESCU, R. BORDEIANU, D. S. VASILESCU*, I. MANAFU*,
IRINA CERCHEZ, P. GHIOCA, RODICA STANCU and E. BUZDUGAN
Chemical Research Institute ICECHIM, Spl. Independenţei 202, 77208 Bucharest, Romania
* Polytechnic, Lab. of Macromolecular Chemistry, str. Polizu 1, Bucharest, Romania

Received October 19, 1984

Measurements of specific refractive index increments were performed on polybutadiene, polystyrene, mineral oil and oil-extended butadiene-styrene triblock copolymer samples, by dilute solution interferometry in chloroform, benzene, and toluene. It was found that in all the solvents specific refractive indices are additive and offer a reliable and accurate method for compositional characterization of oil-extended butadiene-styrene block copolymers.

INTRODUCTION

An important parameter for characterizing dilute polymer solutions is the specific refractive index increment $\nu = \mathrm{d}n/\mathrm{d}c$. This is the limiting value at $c = 0$ of the ratio $(n - n_0)/c$, where n and n_0 are the refractive indices of the solution and solvent respectively, and c (expressed as g/mL) denotes the concentration of polymer (copolymer) in solution.

It has been proved since long[1] that the appropriate equation is :

$$\frac{n - n_0}{c} = \nu + a_2 c \qquad (1)$$

where a_2 is a coefficient depending on wavelength and temperature. The relationship between refractive index increments in solution and concentration was studied by Lorimer.[2]

However, very often the determination of ν is performed at low concentrations of polymer and the term a_2 may be neglected ; taking into account the experimental errors, a reliable value for ν may be obtained by averaging the results of several experiments carried out at low concentration, especially in the case of routine measurements.

The value of ν, for a given solvent (at constant temperature and wavelength) is needed to calculate average molecular weight, shapes and dimensions of macromolecules in solution, by light scattering.[3] Moreover, once the value of ν for a certain copolymer has been obtained, it becomes easy to calculate its composition, as :

$$\nu = \nu_A w_A + \nu_B w_B \tag{2}$$

where w_i represents the weight fraction of component "i" and ν_i is the corresponding value for the homopolymer "i". The validity of Eq. (2) was demonstrated for a great number of copolymers [4,5]. Sometimes, improved results can be obtained by using mixed solvents.[6]

In a previous paper,[7] results were reported regarding refractive indices and density of non-extended and oil-extended butadiene-styrene block copolymers, over a broad range of compositions.

This work presents the characterization of poly(butadiene-b-styrene) extended with oil and low molecular polybutadiene respectively, by means of specific refractive index increments measurements.

EXPERIMENTAL

The refractive index increments were measured with Zeiss-Jena laboratory interferometer in dilute solution (0.1 – 0.3 g/dL).

Butadiene-styrene block copolymers were obtained by polymerization in the presence of butyllithium in solution; the sample chosen contained 34.4 % (wt) styrene units.[8] The commercial product "Lithene"[9] was used as low molecular polybutadiene ($\overline{M}_w = 2000$; 7 % benzyl end units).

The main parameters characterizing the extender mineral oil were given in a previous work.[10]

In order to obtain a homogeneous blend of Lithene (or extender oil) with the block copolymer, thin films were prepared by spin-casting using a technique already described.[7] These films of preestablished composition were dissolved in chloroform, benzene or toluene, respectively, and the resulted dilute solutions were subjected to interferometric measurements. All solvents were reagent grade.

Prior to these measurements, the method was calibrated by using aqueous NaCl solutions of known concentrations.[3]

RESULTS AND DISCUSSION

The results found for pure polybutadiene (Lithene), polystyrene ($M_w = 80\,000$), poly(butadiene-b-styrene) and extender mineral oil are given in table 1, along with some selected data from the literature.

As can be seen from table 1 the values found for the commercial product Lithene are significantly higher than those reported in literature for polybutadiene; this fact might be explained if taking into account the large amount of terminal benzyl units (7 %)[9] present in this low molecular type of polybutadiene. The values regarding polystyrene are close to those communicated in literature, except for toluene as solvent. In our opinion, it is entirely remarkable that the calculated composition of poly(butadiene-b-styrene), using equation (2) and the values for ν found by us are highly reproducible regardless of the solvent.

Table 1

Specific refractive index values, ν, (mL/g)

Polymer, copolymer or additive	Solvent	Specific refractive index (mL/g)			Calculated Styrene units (% wt)
		Literature		Found	
		Value	Ref.	Value	
Polybutadiene	Chloroform	0.0830	11	0.1262 (a)	
	Benzene	0.0110	12	0.0266 (a)	
	Toluene	—	—	0.0295 (a)	
Polystyrene	Chloroform	0.1690	13	0.1777 (b)	
	Benzene	0.1150	14	0.1187 (b)	
	Toluene	0.1129 0.1080	15 16	0.1634 (b)	
Poly(butadiene-b-styrene)	Chloroform	—	—	0.1440 (c)	34.76
	Benzene	—	—	0.0584 (c)	34.52
	Toluene	—	—	0.0757 (c)	34.50
Mineral oil	Chloroform	—	—	0.0445 (d)	
	Benzene	—	—	0.0096 (d)	
	Toluene	—	—	0.0195 (d)	

(a) Lithene PM, $\overline{M}_n = 1300$

(b) $\overline{M}_w = 80{,}000$ g.mole^{-1}

(c) 34.5 % styrene, $\overline{M}_n = 123{,}200$, $\overline{M}_B = 80{,}000$, $\overline{M}_S = 21{,}200$

(d) paraffinic – naphthenic, $d_4^{25} = 0.8665$ g.cm^{-3}, $n_D^{25} = 1{,}474$

The next step was to verify the additive properties of specific refractive indices for mixtures of poly(butadiene-b-styrene) and Lithene, in three different solvents (see Fig. 1). As the primary mixtures were expressed in parts per hundred parts of rubber (phr), a practice often used in rubber processing industry, it becomes obvious that the obtained curve implies a horizontal asymptote. On the other hand, if Lithene content is expressed as weight percentage, a linear dependence may be noticed. Moreover, even if the composition is expressed in butadiene units (percentage or fraction), a straight line was obtained. Note that both Lithene and poly(butadiene-b-styrene) contain butadiene units. As it can be seen from the data illustrated in Figure 1, the most suitable solvent has proved to be toluene, which offers the highest difference between the values of ν for Lithene and poly(butadiene-b-styrene) respectively.

Since poly(butadiene-b-styrene), as a thermoplastic rubber is often extended with mineral oil, it becomes necessary to have access to rapid and accurate methods to estimate its composition. It has been proved[7] that both the refractive index and the specific volume are additive properties and consequently may be used to calculate the composition of oil extended block-copolymers.

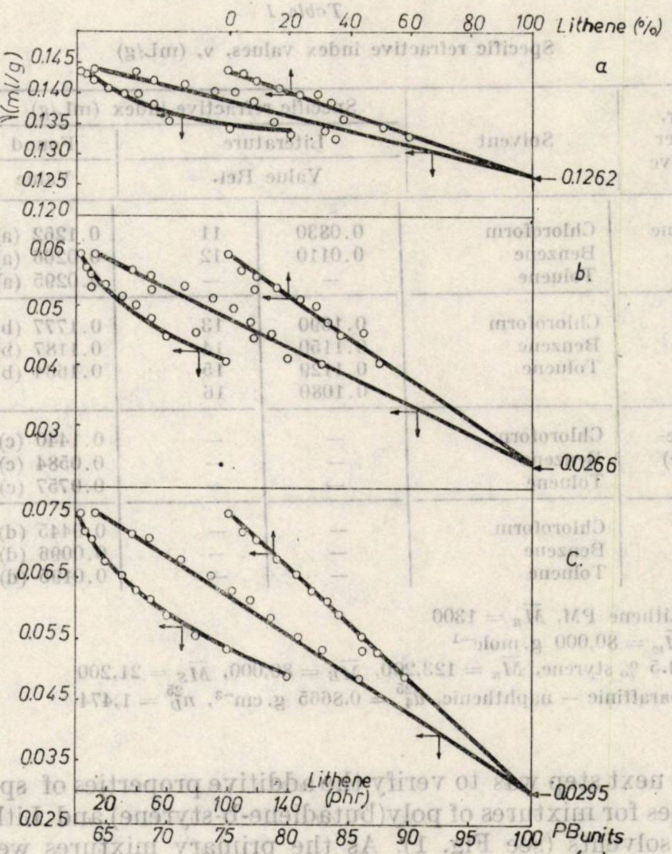

Fig. 1. — Specific refractive index against the composition of the mixture poly(butadiene-b-styrene) — Lithene in various solvents at 25°. a. Chloroform ; b. Benzene ; c. Toluene.

In Figure 2 the specific refractive indices are plotted against extender oil content. The measurements were also carried out in the same three solvents. The linear dependence between specific refractive index and extender oil content can easily be seen. By comparison with the previous graph (Fig. 1), this time the most appropriate solvent is chloroform.

Furthermore, these results could be used to establish the mixture composition with more accuracy than by refractive index measurements, as the relative differences between the corresponding values for TR and extender oil, respectively, are higher in the case of specific refractive indices.

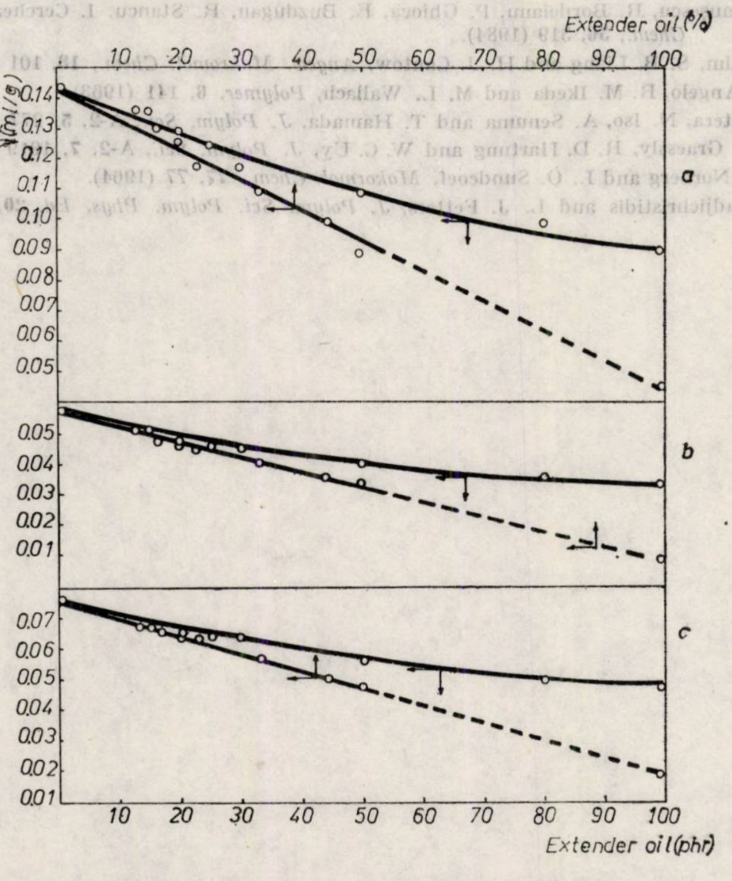

Fig. 2. — Plots of specific refractive index versus extender oil content, in different solvents at 25°. a. Chloroform; b. Benzene; c. Toluene.

REFERENCES

[1] M. B. Huglin, *J. Appl. Polymer Sci.*, **9**, 3963, 4003 (1965).

[2] J. W. Lorimer, *Polymer*, **13**, 46, 52, 274 (1972).

[3] J. Brandrup and E. H. Immergut (Editors), "Polymer Handbook", 2-nd ed., Wiley, N.Y., 1975, IV—267.

[4] W. H. Stockmayer, I. D. Moore, M. Fixman and B. N. Epstein, *J. Polymer Sci.*, **16**, 517 (1955).

[5] W. Mächtle and H. Fischer, *Angew. Makromol. Chem.*, **7**, 147 (1969); W. Mächtle, *Angew. Makromol. Chem.*, **15**, 17 (1971).

[6] P. Kratochvil, B. Sedláček, D. Straková and Z. Tuzar, *Makromol. Chem.*, **148**, 271 (1974).

[7] El. Ceauşescu, R. Bordeianu, P. Ghioca and M. Bălănescu, *Materiale Plastice*, **17**, 201 (1980).

[8] El. Ceauşescu, R. Bordeianu, I. Cerchez, M. Bălănescu and P. Ghioca, *Rev. Roumanine* Chim., **26**, 509 (1981).

[9] Lithene Product Data — Lithene P Series, Revertex Ltd., Harlow, Essex.

[10] El. Ceauşescu, R. Bordeianu, P. Ghioca, E. Buzdugan, R. Stancu, I. Cerchez, *Pure Appl. Chem.*, **56**, 319 (1984).

[11] R. Kuhn, S. B. Liang and H. J. Cantow, *Angew. Makromol. Chem.*, **18**, 101 (1971).

[12] R. I. Angelo, R. M. Ikeda and M. L. Wallach, *Polymer*, **6**, 141 (1963).

[13] A. Kotera, N. Iso, A. Senuma and T. Hamada, *J. Polym. Sci.*, A-2, **5**, 277 (1967).

[14] W. W. Graessly, R. D. Hartung and W. C. Uy, *J. Polym. Sci.*, A-2, **7**, 1919 (1969).

[15] P. N. Norberg and L. O. Sundeoef, *Makormol. Chem.*, **77**, 77 (1964).

[16] N. Hadjichristidis and L. J. Fetters, *J. Polym. Sci. Polym. Phys. Ed.* **20**, 2163 (1982).

Revue Roumaine de Chimie, **30**, *5*, 381–384 (1985)

A NEW METHOD FOR MEASURING THE SMALL PRESSURE DIFFERENCES AT HIGH STATIC PRESSURES

RODICA VÎLCU and I. GĂINAR

Chair of Physical Chemistry and Technological Electrochemistry, Polytechnical Institute of Bucharest, Romania

Received April 25, 1984

The paper presents the construction and use of a baro-resistive differential transducer[1] of high accuracy that should enable the measurement of pressure differences from 10^{-2} to 10^{2} mm Hg, for a wide range of static pressure up to some hundreds kg/cm^2. The accuracy of measurements and the high sensitivity of the device allow its application to different purposes.

The accurate measurement of recorded pressures is important in achieving the control of the running of some accuracy installations as well as the useful operation of many important technological processes. The construction principles of the various types of pressure recording apparatuses and their utilization are given in several works.[2–7]

The analysis of the functional characteristics of such apparatuses, renders evident, in most cases, the existence of rather narrow rangers, determined by the running of the sensitive element of the transducer only from a certain value onward or up to a certain value of the statical pressure. However, transducers with a wide operation range have been also built.

The accuracy of such devices and especially of those run as inductive or capacitive transducers is usually high; they can be used for pressures of the order of mm water column up to hundreds of atm. A general characteristic of such apparatuses is their relatively complex construction, difficult to be reproduced in a laboratory, as well as their high cost.

The present contribution introduces a new type of differential transducer allowing the measurement of some pressure differences from 10^{-2} to 10^{2} mm Hg, for statical pressures up to some hundreds kg/cm^2.

The cost of the apparatus is very low, and it can be constructed, in principles, with the resources available in any laboratory.

CHARACTERISTICS AND CONSTRUCTION

Our differential transducer belongs to the transducers with resistance with mobile mercury contact. Its high sensitivity is ensured by the constructive peculiarities; instead of an electrical resistance, represented by a metallic conductor, semiconductor or coal,[8–9] a thin chromium layer obtained by vacuum evaporation using a glass insulator or ceramic material, was applied.

To obtain such a metallic deposit, with characteristics suitable for a baro-resistive transducer, we proceeded as follows : — a certain number of high spectral blades 4—5 mm in width, are cut. After a thorough cleaning of the surfaces, the blades are mounted on a metallic plate glass where longitudinal furrow grooves, 0.5—1 mm in width, had been previously milled off. The disposition of the blades is such that the furrow grooves should correspond to their middle.

According to the plate length, a wolfram wire of about 0.5 mm is tightly bound up on a stick. The coil is then introduced into the metallizing installation where it is thoroughly padded in high vacuum (10^{-5} — 10^{-6} mm Hg) by passing a sufficiently great current so that the wire should reach incandescence.

The coil is then taken out of the installation and carefully introduced into an electrolysis bath made up of a Cr_2O_3 solution in H_2SO_4.

A Pb rod with 3% Sb is used as anode. The electrolysis bath is kept throughout the process at 45°C.

After obtaining a sufficiently thick chromium deposit, the coil is washed, dried and again mounted in the evaporation installation. The metallic plate should lie 12—15 cm above the coil, best possibly centered longitudinally.

An electric oven is then mounted at about 4—5 cm above the blades. When vacuum is achieved (at least 10^{-2} mm Hg) within the installation the oven is heated until the support reaches 500—600°C.

At that moment the evaporation starts ; the current is then carefully increased in order to obtain a small evaporation rate. If previously two contacts with colloidal Ag had been mounted on a blade, then layer might occur under control, stopping evaporation when a deposit with the suitable ohmic resistance is reached.

The evaporation on a warm support has a double advantage : the first one, the glass adherence and the second one, the high temperature brings about a deposit with a high degree of crystallinity which induces a high stability, in time, of the electrical resistances obtained. The value of the resistance should suitably range from 200 to 400 Ω.

The blades with the deposits obtained on glass, are mounted by a mechanical screwing appliance, on a stainless steel rod. AU-shaped tube is then made of a stainless steel pipe (Fig. 1) which is provided with connecting joints in order to integrate the transducer into the circuit.

The U-tube is filled up with highly purified Hg and then the transducer is mounted ; tightening occurs by teflon packings.

The mercury level in the manometer brings about a certain value of the transducer's electrical resistances. Accordingly, a Wheatstone bridge is constructed, where the transducer *T* represents one of the arms (Fig. 2).

A galvanometer with a $10^{-8}-10^{-9}$ A/mm sensitivity is used as zero instrument. Since the mercury level in the steel tube is also temperature-conditioned and the measurement occurs only by one arm, the transducer should be necessarily well thermostated (± 0.01 °C accuracy).

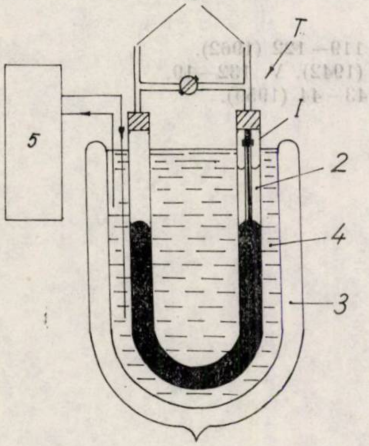

Fig. 1. — General scheme of the baro-resistive differential transducer.

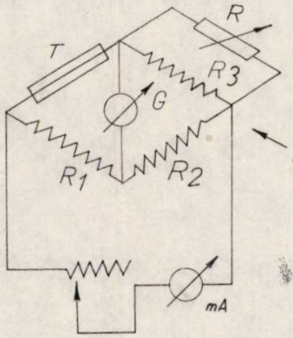

Fig. 2. — Electrical bridge.

If all requirements have been fulfilled, the transducer may be calibrated; to this end it is connected to a manometer with usual mercury that can operate in vacuum or at overpressure.

Using a cathetometer, which enables the measurement of some differences of at least 0.02 mm Hg, the calibration of the transducer may be drawn along the required domain.

The advantages of our transducer are manifold :

- similar apparatuses or even less accurate are more expensive and more complicated in construction;
- the apparatus may be successfully used both in scientifical research and in industry;
- the shortcomings of inductive and capacitive transducers are removed. As such transducers, although accurate, when used for automation purposes, the long connecting conductors bring in parasitic elements.
- on the basis of the differential transducers already described, new automation units may be constructed, such as pressure regulators, pressure valves a.s.o.

The device put forward is easily to be handled, leads to perfectly reproducible data and follows, without any inertia, minute pressure changes.

REFERENCES

[1] Romanian Patent RSR No. 89342, 1977.

[2] F. Grave, "Elektrische Messung nichtelektrischer Grössen" Akademische Verlagsgesellschaft, Leipzig, 1965, p. 268—288.

[3] M. Sorohan "Introducere în fizica și tehnica tensiunilor înalte", Bucharest, Ed. Tehnică 1977

[4] D. M. Considine, "Process Instruments and Controls", Handbook, New York 1957.

[5] P. M. Pfilier, "Elektrisches Messen der mechanischen Grössen", Springer Verlag, Berlin 1948.

[6] E. Schneider, *Elektronik,* **5** (1956).

[7] Capacitive pressure sensors, *Instrum.*, **35**, 5, 119—122 (1962).

[8] O. Müller, Elektrische Druckmessung, ATM (1942), V, 132—19.

[9] H. J. Bommebburg, *Rev. Sci. Instrum.* **30**, 43—44 (1959).

Revue Roumaine de Chimie, 30, 5, 385–389 (1985)

KINETICS OF THE JACOBSON REACTION

I. BÂLDEA[a], V. FĂRCĂŞAN[a] and ILEANA OLTEANU[b]

[a] Faculty of Chemical Technology, Cluj-Napoca, Romania
[b] Medical and Pharmaceutical Institute, Cluj-Napoca, Romania

Received December 14, 1983
Revised June 19, 1984

The kinetics of the oxidation of thiobenzanilide by potassium ferricyanide yielding 2-phenylbenzothiazole has been investigated in alkaline medium. The obtained data suggest a mechanism which assumes the oxidation of thiobenzanilide as a rapid preequilibrium and the ring closure as the rate determining step.

INTRODUCTION

The process of N-arylthioamides oxidation by potassium ferricyanide in alkaline medium yielding benzothiazoles is known as Jacobson reaction.[1] This reaction was largely used in organic syntheses to obtain benzothiazoles, bis-benzothiazoles, naphthothiazoles, benzofurobenzothiazoles, thiazoloacridones, thiazolophenothiazines, a.s.o., having substituted or unsubstituted aromatic rings.[2–7]

As we are aware of, the kinetics of this kind of reactions has not yet been investigated. Such a study could be of interest from a mechanistic point of view, in order to correlate the kinetic data with those obtained in syntheses of benzothiazoles.

We have chosen the system thiobenzanilide-potassium ferricyanide to be studied kinetically.

For this reaction the following mechanistic pathway was supposed[2].

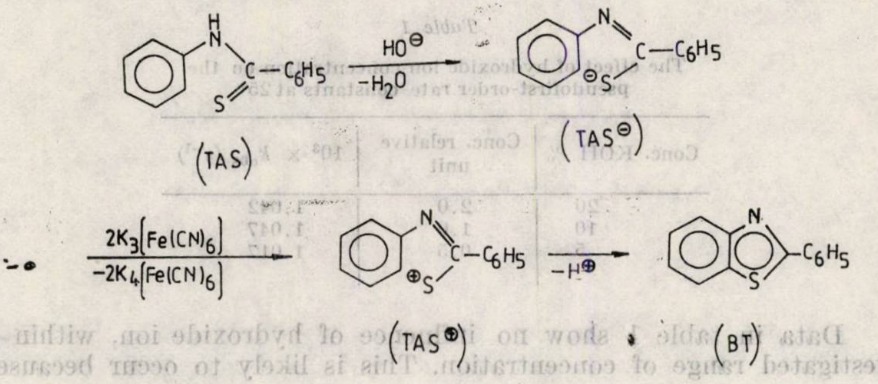

EXPERIMENTAL

Thiobenzanilide was purified by recrystallization. All the other chemicals were of analytical grade purity and used without further purification.

Thiobenzanilide was dissolved in potassium hydroxide solution. Aliquots of 50 mL were mixed with 50 mL potassium ferricyanide solution. All solutions were kept in a thermostate bath before mixing for about 15—20 min. in order to reach desired temperature. The mixtures were stirred at constant temperature for a determined period of time. The progress of the reaction was stopped by adding a required quantity of 1 :1 hydrochloric acid solution to the mixture. The samples were kept at 0°C for an hour, precipitate consisting of the reaction product was quantitatively filtered and thoroughly washed with cold water. After drying the product at 100°C for 1—1.5 hour it was left overnight in a desiccator and was then entirely dissolved in hot chloroform and diluted to a suitable concentration for optical measurements. Ultraviolet spectra were recorded with a UV VIS spectrophotometer and optical densities were read at 300 nm. In such a manner data containing the amount of formed product as a function of time become available. Conditions for pseudofirst-order kinetic were ensured, using both hydroxide and ferricyanide respectively in a large excess for all kinetic experiments.

RESULTS AND DISCUSSION

First-order dependence on thiobenzanilide was deduced from the classical plots of $\ln(E_\infty - E)$ versus time, using an excess of oxidizing agent and potassium hydroxide, the latter being necessary to dissolve the reactant. Slopes of the lines give the first-order rate constants. To be sure that the chosen value of E requested for these plots is an appropriate one a special integrated rate equation, namely Guggenheim method, was used as well.[8] A plot of $\ln(E_{t+\Delta} - E_t)$ versus time was linear, supporting the first-order rate law. The slopes of these plots gave the rate constants in good agreement with those obtained with classical method, attesting that correct values for E have been used. For example, the rate constant for an experiment at 35°C obtained for a first-order plot is $2.60 \times 10^{-3}\,s^{-1}$, while that derived from Guggenheim plot is $2.58 \times 10^{-3}\,s^{-1}$.

In order to deduce the effect of hydroxide ion and ferricyanide ion on the reaction rate some experiments have been carried out using various excess of these chemicals. Tables 1 and 2 contain the pseudofirst-order rate constants as mean from 2—3 individual runs.

Table 1

The effect of hydroxide ion concentration on the pseudofirst-order rate constants at 25°

Conc. KOH %	Conc. relative unit	$10^3 \times k_{obs}$ (s^{-1})
20	2.0	1.042
10	1.0	1.047
5	0.5	1.017

Data in table 1 show no influence of hydroxide ion, within the investigated range of concentration. This is likely to occur because of the fact that in an alkaline solution, the equilibrium

$$\mathrm{TAS} + \mathrm{HO}^{\ominus} \rightleftharpoons \mathrm{TAS}^{\ominus} + \mathrm{H_2O}$$

is completely shifted to the right.

Table 2

The effect of ferricyanide concentration on the first-order rate constants at 25°C. 0.1507 g thiobenzanilide/100 mL KOH 10%

Conc. $K_3Fe(CN)_6$ %	Conc. unit relat.	$10^4 \cdot k_{obs}$ s^{-1}	$\frac{10^4 \cdot k_{obs}}{(\text{rel. conc.})^2}$
10	1	3.84	3.84
20	2	13.89	3.48
30	3	30.50	3.38

Data in table 2 show a second-order dependence of the rate on the oxidizing agent concentration. The following overall rate law may be ascribed to the Jacobson reaction :

$$\frac{-\mathrm{d}(\mathrm{TAS}^{\ominus})}{\mathrm{d}t} = \frac{\mathrm{d}(\mathrm{BT})}{\mathrm{d}t} = k(\mathrm{TAS}^{\ominus})\,(\mathrm{Fe\,(CN)_6}{}^{3\ominus})^2$$

The influence of temperature on the reaction constant was investigated in the range 15—35°C.

Data are presented in table 3.

Table 3

The effect of temperature on first-order rate constants

Temp. °C	$10^4 \cdot k_{obs}\,(s^{-1})$
15	5.74
22	8.13
25	10.42 10.47 10.17
35	25.83

The activation parameters were derived from linear Arrhenius and activated complex theory respectively.

Points lie well on straight lines. The coefficient of determination "r" of the least square plot is quite good, having the value of 0.986.

The activation parameters were calculated from the slope and intercept and are : $E_a = 13.8$ kcal/mole (57.4 kJ/mole), $\Delta H^{\neq} = 13.2$ kcal/mole (55.2 kJ/mole) and $\Delta S^{\neq}$ — derived only from first-order rate constants — is of $-$ 27.8 cal/mole K (-116.3 J/mole K).

This quite small value for activation energy as well as the negative value for the activation entropy suggest a bimolecular rate determining step. Two reaction mechanisms could be taken into account :

(a) The anion $\mathrm{TAS}^{\ominus}$ has a strong nucleophilic and reducing character. Therefore it could associate with metal ion in solution, by displacement of other ligands in the first coordination sphere.

One possible reaction path involves a substitution reaction prior the electron transfer, following the oxidation as rate determining step :

$$\mathrm{TAS}^{\ominus} + \mathrm{Fe(CN)}_6^{3\ominus} \xrightleftharpoons{\text{fast}} \mathrm{TASFe(CN)}_5^{3\ominus} + \mathrm{CN}^{\ominus}$$

$$\mathrm{TASFe(CN)}_5^{3\ominus} + \mathrm{Fe(CN)}_6^{3\ominus} + \mathrm{H_2O} \xrightarrow{k} \mathrm{TAS}^{\oplus} + \mathrm{Fe(CN)}_6^{4\ominus} + \mathrm{Fe(CN)_5\,H_2O}^{3\ominus}$$

The ring closure at the electrophilic attack of the adjacent $S^{\oplus}$ should be quite rapid :

$$\mathrm{TAS}^{\oplus} \xrightarrow{\text{fast}} \mathrm{BT} + \mathrm{H}^{\oplus}$$

This mechanism could explain the second-order dependence on ferricyanide and negative activation entropy.

Such "inner sphere" oxidation steps were presented by Leussing *et al.*[9] in the case of thiol-$Fe^{3\oplus}$ reaction and Agrawal and Mushram[10] in the oxidation of thiourea with ferricyanide.

Wiberg *et al*[11] studied the oxidation of thiols by ferricyanide using labeled cyanide and concluded that the substitution reaction in the coordination sphere of ferric ion has not taken place. This reason rules out the above reaction sequence.

(b) An alternative mechanism which is likely to occur assumes a fast "outer sphere" oxidation in two one-electron consecutive steps. There are some reports on such a mechanism in the oxidation of thiols[11,12]. The rate determining step should be the closure of the thiazole cycle. The reaction sequence is :

$$\mathrm{TAS}^{\ominus} + \mathrm{Fe(CN)}_6^{3\ominus} \rightleftharpoons \mathrm{TAS}^{\bullet} + \mathrm{Fe(CN)}_6^{4\ominus} \quad \text{rapid } K_1$$

$$\mathrm{TAS}^{\bullet} + \mathrm{Fe(CN)}_6^{3\ominus} \rightleftharpoons \mathrm{TAS}^{\oplus} + \mathrm{Fe(CN)}_6^{4\ominus} \quad \text{rapid } K_2$$

$$\mathrm{TAS}^{\oplus} \xrightarrow{k} \mathrm{BT}$$

The oxidative processes should be considered as pre-equilibria. It is supported by our experimental observation that in the presence of $Fe(CN)_6^{4\ominus}$ the rate of reaction decreases. It is worth mentioning that the influence on the yield in benzothiazole of various substituents on the benzene ring[2] supports the ring closure as rate determining step. The relative low activation energy, which is a composite value, could be understood by the exothermic character of the redox pre-equilibria.

REFERENCES

1 P. Jacobson, *Ber. dtsch. chem. Ges.*, **19**, 1067 (1886).
2 J. Metzger and H. Plank, *Chimie et Industrie*, **75**, 930 (1956).
3 C. Finzi and G. Grandolini, *Gazz. chim. Ital.*, **89**, 2558 (1959).

[4] D. Petrova and K. Jakopčić, *Croat. Chem. Acta*, **48**, 319 (1976).
[5] V. Fărcășan and S. Florea, *J. prakt. Chem.*, **312**, 1007 (1970).
[6] V. Fărcășan and I. Balázs, *Stud. Univ. Babeș-Bolyai. Chem.*, **14**, 45 (1969).
[7] S. G. Fridman and D. K. Golub, *Khim. Geterocikliceskich Soedinenie*, **1969**, 247.
[8] E. A. Guggenheim, *Philos. Mag.*, **2**, 538 (1926).
[9] D. L. Leussing, J. P. Mislan and R. J. Goll, *J. Phys. Chem.*, **64**, 1070 (1960).
[10] M. C. Agrawal and S. P. Mushram, *J. Phys. Chem.*, **72**, 1497 (1968).
[11] K. B. Wiberg, H. Maltz and M. Okano, *Inorg. Chem.*, **7**, 830 (1968).
[12] E. J. Meehan, I. M. Kolthoff and H. K. Kiuki, *J. Phys. Chem.*, **66**, 1233 (1962).
[13] R. C. Kapoor, O. P. Kachwaha and P. P. Sinha, *J. Phys. Chem.*, **73**, 1627 (1969).

Revue Romaine de Chimie, **30**, *5*, 391–393 (1985)

COPOLYAMIDES. I

THE INFLUENCE OF COMPOSITION ON THE PHYSICO-CHEMICAL PROPERTIES

AMALIA CRUSOS
Institute of Macromolecular Chemistry "Petru Poni"
Aleea Gr. Ghica Vodă, 41 A, Iaşi, Romania

Received May 7, 1984

The influence of the composition on the physicochemical properties in copolyamides obtained from adipic acid, sebacic acid, hexamethylendiamine and ε-caprolactam is presented. The change of the properties in large limits has important implications on the area of practical applications of copolyamides.

The great number of monomers for polyamides, such as amino-acids, diamines and diacids, allows the obtention of various copolyamides with physico-chemical properties ranging in a large scale of values, that can offer immediate practical solutions of high utilitary in the more and more complex and refined needs of the contemporany technique.

The applicability domains of copolyamides is versatile and include the synthetic fibers, machine parts adhesives, varnishes and impregnation materials.

This paper presents the results of some investigations regarding the correlation between the copolymer composition and its properties carried out in order to obtain certain copolyamides intended to be used as thermoadhesives in textile industry, shoes industry and carpet making, as well as other industrial processees which require the assembling of different items by thermocollage.

The importance of adhesives increased remarkably by their use for making products with new structures such as nonwoven materials, coverings, multilayered (i.e. sandwich type boards etc.).

RESULTS AND DISCUSSION

The investigated copolymerization system has been essentially composed of adipic acid (AA), sebacic acid (SA) hexamethylene diamine (HMD) and ε-caprolactam (CL). Any modification of this composition was made in order to diversify the quality characteristics of synthesized products[1,2].

It is known that polyamides are macromolecular compounds having on the main chain regularly alternating amidic functional groups, i.e. 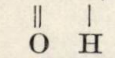 $\underset{\underset{O}{\|}}{-C}-\underset{\underset{H}{|}}{N}$, situated between organic sequences. This arrangement induces the formation at hydrogen bonds which confers significant cohesive properties.

Depending on the magnitude of intermolecular forces, the symmetry of the polymer backbone and the presence of certain bulky substituents which can hinder the formation of hydrogen bonds, the properties of polyamides can be diversified on a large scale affecting the melting temperature, the degree of crystallinity, solubility in different solvents, the humidity resistance and mechanical characteristics.

It has been established that the copolycondensation monomers are randomly disposed on the backbone disturbing the symmetry, so that the establishing of intermolecular links between —CO— and —NH— groups is hindered. Consequently the properties of the resulted products are dependent on copolymer composition.

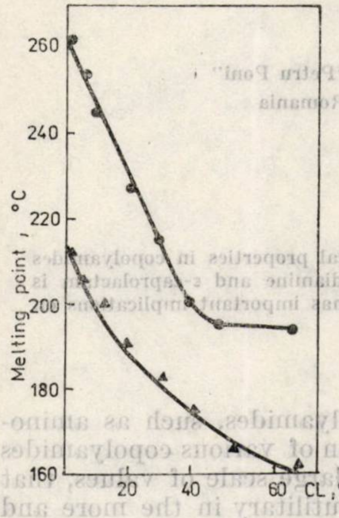

Fig. 1. — The variation of melting point as a function of the CL content, in the system: ● HA-CL; ▲ HS-CL.

One can remark that the system under investigation is composed of monomers used for obtaining polyamide 6, polyamide 66 and polyamide 6.10. These polyamides have a high melting range, i.e. 215 — 260°C.

By quaternary copolymerization it was intended to obtain some thermoadhesive compounds of the "hot melt" type having a lower melting range, i.e. 140 — 170°C, suitable for thermocollage.

In the first stage the influence of ε-caprolactam in the thernary systems AA—HMD—CL and SA—HMD—CL has been investigated. For the sake of simplification, the acids and HMD were plotted as their corresponding salts, i.e. hexamethylene diammonium adipate (HA) and hexamethylene diammonium sebacate (HS). The obtained results are presented in Fig. 1.

One can see that the variation in the investigated systems of the CL content between 5% and 60% does not lead to a satisfactory melting range. Consequently the influence of composition was further investigated in quaternary systems. At this time it can be observed (Fig. 2) that the melting temperatures are dependent on the feed composition and include also the range of interest, i.e. 140 — 170°C.

The lowering of the melting range under these values can be achieved by introducing relatively small amounts of fatty acids in the system.

All the products obtained in the mentioned conditions were physicochemically and physico-mechanically characterized in the thermocollage process. For certain samples the results are listed in tables 1 and 2.

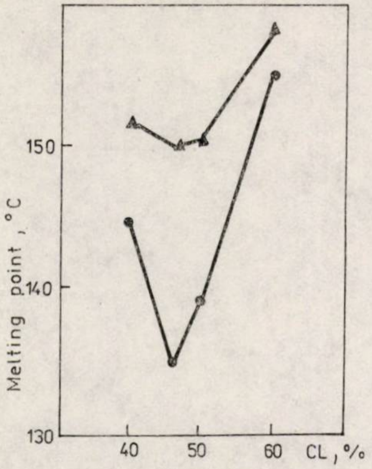

Fig. 2. — The influence of CL in quaternary systems for two ratios between HA and HS.

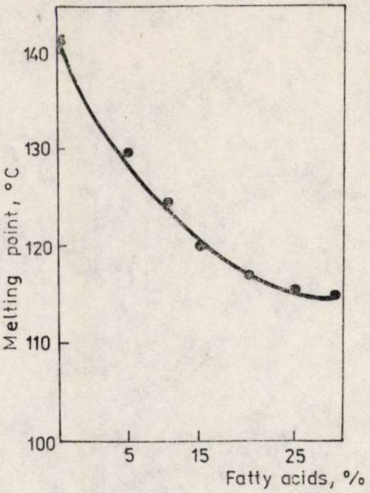

Fig. 3. — The variation of melting point in the quaternary systems as a function of the content of fatty acids.

Table 1

Physico-chemical characteristics

Sample no.	Melting range	[η]	Viscosity (at 170°C) Poise	Soluble products %	Fatty acids %
1	157—163	0.78	1860	3.3	—
2	140—145	0.66	760	2.2	—
3	120—125	0.50	472	5.2	10
4	118—122	0.47	310	5.6	15

Table 2

Physico-mechanical characteristics

Sample no.	Melting range °C	Granulation mm	Recommended fusing conditions	Application. Special features	Tensile strength of thermocollage, gf/cm²
1	135—145	0.1—0.3	10—14 s	Thermosensitive materials	1900—2500
2	135—145	0.1—0.5	10—14 s 20—23 g/m²	Thermosensitive	2900—3000
3	150—165	0.1—0.3 0.3—0.5	10—14 s 20—23 g/m²	Improved fastness to dry cleaning	3000—3700

REFERENCES

[1] A. Crusos and M. Zănoagă, in preparation.

[2] D. Feldman, C. Ungureanu and A. Crusos, Patent R.S.R., 60.215/1.II.1975.

Revue Roumaine de Chimie, **30**, *5*, 395–400 (1985)

MAGNETIC AND SPECTRAL STUDIES ON COPPER(II), NICKEL(II), COBALT(II), IRON(III) AND MANGANESE(II) COMPLEXES OF 3-BROMO-2-HYDROXY-5-METHYL ACETOPHENONE HYDRAZONE

KEEMTI LAL and SITA RANI MALHOTRA
Chemistry Department, D. N. College, Meerut–250002, India

Received October 15, 1981
Revised November 20, 1984

The complexes of Cu(II), Ni(II), Co(II), Fe(III) and Mn(II) with 3-bromo-2-hydroxy-5-methylacetophenone hydrazone were synthesized and characterized on the basis of elemental analysis, magnetic susceptibility and spectral (infrared, electronic and electron spin resonance) studies. The results of the IR spectra reveal that the phenolic proton is lost on complex formation and the nitrogen of the isonitroso group coordinates with metal ions indicating the bidentate nature of the ligand. The magnetic susceptibility of the complexes shows that all the complexes are paramagnetic. The different ligand field parameters were also calculated for these complexes (from electronic spectra). The '*g*' value of the Fe(III) and Cu(II) complexes were calculated and found from E.S.R. spectra to be 1.99 and 2.05 respectively.

INTRODUCTION

2-Hydroxyacetophenone, its oxime and hydrazone, and their substituted derivatives have aroused considerable interest in recent years [1–5] due to their ability to form complexes with a number of transition metal ions. A survey of the literature reveals that no work has been done on 3-bromo-2-hydroxy-5-methyl-acetophenone hydrazone (BHMAH) (Scheme 1). The present work reports the synthesis of Cu(II), Ni(II), Co(II), Fe(II) and Mn(II) complexes :

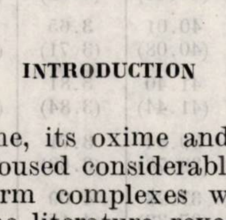

with BHMAH and their characterization on the basis of elemental analysis, magnetic susceptibility, infrared, electronic and electron spin resonance spectral studies.

EXPERIMENTAL

The standard stock solutions of the metal ions were prepared by dissolving (B.D.H., AnalaR grade) samples of metal ions in double distilled water and were standardized gravimetrically.[6]

Magnetic measurements were made in powders at room temperature (27°C) employing Gouy's technique and using $Hg[Co(CNS)_4$ as calibrant ($\chi_g = 16.44 \times 10^{-6}$ cgs Units). The infrared spectra were recorded on a Perkin-Elmer IR spectrophotometer (model 337) in KBr. Electronic spectra of the complexes were recorded on a Beckman DU-2 (manual) spectrophotometer. ESR spectra were recorded on Varian E_4-EPR spectrophotometer, operating at 9.075 GHz with 100 KHz field modulation and phase sensitive detection.

Synthesis of BHMAH

The ligand, BHMAH, was synthesized by refluxing a mixture of 2-hydroxy-3-bromo-5-methylacetophenone[7] (0.1 mole) and hydrazinium sulphate (0.1 mole) in ethanol for about 2 hours and pouring the mixture into cold water. The brown coloured precipitate (BHMAH) was separated and recrystallized from acetone (m.p. 220°C). The results of the elemental analysis are given in table 1.

Table 1

Characteristic and analytical data of BHMAH and its complexes

Compd.	Colour	Dec. Temp.* (°C)	Analysis — Found (Calcd.) % C	H	N	Br	Metal	μ_{eff}
HL	Brown	220**	44.56 (44.44)	4.50 (4.52)	11.47 (11.52)	32.90 (32.92)	— —	— —
MnL_2	Dark- -yellow	235 240	40.01 (40.08)	3.65 (3.71)	10.45 (10.39)	29.76 (29.69)	10.15 (10.19)	—
FeL_3	Reddish- -brown		41.40 (41.44)	3.81 (3.84)	10.81 (10.74)	30.64 (30.70)	7.10 (7.14)	5.72
CoL_2	Yellowish- -brown	270	39.84 (39.78)	3.71 (3.68)	10.23 (10.31)	29.50 (29.47)	10.91 (10.85)	4.50
NiL_2— $2H_2O$	Yellowish- brown	280	37.28 (37.32)	4.09 (4.15)	9.73 (9.68)	27.60 (27.65)	10.10 (10.14)	3.10
CuL·OH— H_2O	Yellowish- brown	230	31.73 (31.76)	3.80 (3.82)	8.20 (8.23)	23.50 (23.53)	18.58 (18.53)	1.85

HL = BHMAH = $C_9H_{11}N_2OBr$
* = Approximate value
** = Melting point

Isolation of the complexes

Aqueous solutions of metal ions were treated with acetonic solution of BHMAH in the ratio 1:2 (metal : ligand). The pH of the Cu(II), Ni(II), Co(II), Fe(III) and Mn(II) ions solutions was adjusted to 5.5—6.0, 9.5—10.5, 3.5—5.0, 3.0—4.0 and 5.0—7.0 respectively by addition of NH_4OH and CH_3COOH and the reaction mixture was refluxed for 4—5 hours until the precipitate appeared. Cu(II), Ni(II), Co(II), Fe(III) and Mn(II) form yellowish brown, yellowish brown, yellowish brown, reddish brown and dark yellow coloured precipitate respectively. These complexes were then filtered, washed with water and dried at 100 — 110°C in an oven.

RESULTS AND DISCUSSION

Elemental analysis

The complexes were analysed for C, H, N, Br and metal. The results of elemental analysis show (M :L) 1 :1 stoichiometry for the Cu(II) complex, 1 : 2 stoichiometry for Ni(II), Co(II) and Mn(II) complexes and 1: 2 stoichiometry for Fe(III) complex.

Infrared spectra

The important frequencies of the ligand and its complexes are shown (Table 2). The IR spectra of the BHMAH shows broad bands in the region 3300 cm^{-1} and 2900 cm^{-1} which may be assigned to assym. and symm. N–H stretching mode of NH_2 and intramolecularly bonded phenolic OH group respectively.[8] In the spectra of the complexes no band is observed at 2900 cm^{-1} (expected for OH group) and the band of 3300 cm^{-1} is shifted to 3400 cm^{-1} suggesting that the hydrogen of OH group, replaced by the metal ions and the NH_2 group is not involved in complexation. A strong band at 1620 cm^{-1} which is assigned to νC = N group in the BHMAH was shifted downfield (by ~ 20 cm^{-1}) indicating M–N bond formation. A strong band at 1320 cm^{-1} which is assigned to phenolic C–O bending vibration was shifted to higher, values ~ 1350 cm^{-1}, which shows M–O bond formation. A band at 980 cm^{-1}, assigned to N–N bond and shifted downfield (~10 cm^{-1}), indicates that nitrogen is taking part in M–N bond formation. The bands at 1540 – 1580 cm^{-1}, 1450 cm^{-1} and 1380 cm^{-1}, and 550 cm^{-1} may be assigned to phenyl ring vibrations, $C-CH_3$ and C–Br groups respectively in the BHMAH and the complexes. In the case of Cu(II) complex a broad band at 1090 – 1070 cm^{-1} is also observed which is assigned to M–OH bond.[9]

Table 2

Some important infrared frequencies (in cm^{-1}) of the BHMAH and its complexes

BHMAH (HL)	MnL_2	FeL_3	CoL_2	$NiL_2 \cdot 2H_2O$	$CuL \cdot HO \cdot H_2O$	Tentative assignment
3300	3390	3410	3420	3420	3440	N–H stretching mode of NH_2 group
2900	--	—	—	—	—	δOH
1620		1605	1610	1600	1600	C=N stretching
980	970	965	975	970	965	νN–N
—	470	490	460	485	470	M–N
—	405	440	400	410	405	M–O

HL = BHMAH = $C_9H_{11}N_2OBr$

Magnetic and electronic absorption spectral studies

Fe(III)-BHMAH complex

The magnetic moment of the Fe(III)—BHMAH complex is found to be 5.72 B.M. which is close to the value for other high spin octahedral Fe(III) complexes. The spectra of Fe(III)—complex show four bands at 13200, 19000, 25000 and 30000 cm^{-1}, which correspond to $^6A_{1g} \rightarrow {}^4T_{1g}$ (G), $\rightarrow {}^4T_{2g}$ (G), $\rightarrow {}^4E_g$(G) and charge transfer respectively.[10] The first transition givs the value of 10 Dq i.e. 13200 cm^{-1}. The value of Racah parameter (B') is found to be 1200 cm^{-1} and β is found to be 0.92.

The E.S.R. spectra of Fe(III)-BHMAH complex were recorded for polycrystalline samples at room temperature. The spectrum consists of a strong, isotropic line at $g = 1.99$. This value is smaller than the free electron value. The low g value ($g < 2.03$) has been suggested[11] for nitrogen, oxygen and halogen coordination. It can be concluded that the deviation of the g tensor value from the electron g values suggests that the unpaired electron is in one of the antibonding e_g orbitals of iron (III).[12]

Co(II)—BHMAH complex

The μ_{eff} value of the Co(II)—BHMAH complex is 4.5. B.M. which is within the range of tetrahedral Co(II) complexes (4.2 – 4.8 B.M.).[13] The electronic spectrum of the complex consists of two bands at 8700 and 19000 cm^{-1}. These transition bands may be due to $^4A_2$ (F) $\rightarrow {}^4T_1$(F)(ν_2) and $\rightarrow {}^4T_1$(P) (ν_3) respectively.[14] Δ, B' and β were calculated and found to be 5063 cm^{-1}, 834 cm^{-1} and 0.86 respectively. The values of ν_2 and ν_3 were also calculated using the equations [15] and found to be 9108 and 20572 cm^{-1} respectively which are in good agreement with the experimental values.

Ni(II)—BHMAH complex

The μ_{eff} value of the present complex is found to be 3.1 B.M. which is higher than the spin only value for two unpaired electrons. The present μ_{eff} value is thus consistent with the assignment of octahedral geometry. The electronic spectra of Ni(II)—BHMAH complex consists of four bands appearing at 9500, 12300, 17400 and 28000 cm^{-1} which correspond to the transitions : (ν_1) $^3A_{2g}$ (F) $\rightarrow {}^3T_{2g}$ (F), (ν_2) $\rightarrow {}^1E_g$, (ν_3) $\rightarrow$ $\rightarrow {}^3T_{1g}$ (F) and (ν_4) $\rightarrow {}^3T_{1g}$ (P) respectively. The ν_3/ν_1 ratio ($\nu_1 = 9500$ cm^{-1}) is found to be (1.83) greater than the range required for the octahedral structure.[16] This suggests considerable distortion from the cubic field and therefore splitting of the ν_1 band.

The value of ν_3 and ν_4 were calculated[17] as follows :

$$\nu_3 = 9/5 \times 10\,\text{Dq}$$

$$\nu_4 = 17000 + 6/5 \times 10\,\text{Dq}$$

and found to be 17100 and 27800 cm^{-1} which are very close to the experimental values. The λ for Ni(II) was also calculated with the relation :

$$-\lambda = 0.27\ \text{B}^2/\text{Dq}$$

and found to be −267.

The first transition is equal to the value of 10 Dq i.e. 9500 cm^{-1}. The other ligand field parameters such as : ligand field stabilization energy, F—P term separation, B' and β are 11400 cm^{-1}, 14535 cm^{-1}, 970 cm^{-1} and 0.93 respectively. The results confirm the octahedral geometry for the complex.

Cu(II)—BHMAH complex

The magnetic moment of this complex is found to be 1.85 B.M.. The tetrahedral Cu(II) complexes are expected to give a single broad band in the near infrared region and no absorption between 10 000 — — 20 000 cm^{-1}. In the Cu(II)—BHMAH complex the band observed at 22 500 cm^{-1} may be due to the transition $^4T_2 \rightarrow {}^2E$ or charge transfer.

The E.S.R. spectrum of Cu(II)—BHMAH complex clearly shows a lower than axial symmetry and contains three peaks. The 'g' values are calculated for all the three peaks which correspond to g_1, g_2 and g_3, and are found to be 2.17, 2.03 and 1.96 respectively. The g_{av} value is found to be 2.05. The 'g' value obtained is very close to the free electron value. These results show that the molecular orbital of the unpaired electron is essentially of the d_z2 type.

On the basis of above results the following stuctures may be assigned to the BHMAH complexes :

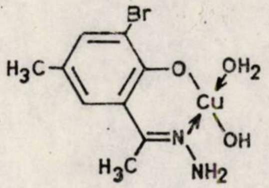

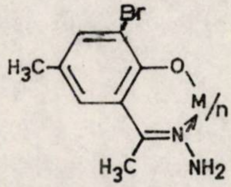

M = Co,Mn & Fe
n = Ox.State

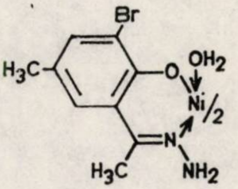

ACKNOWLEDGEMENT. One of us (SRM) is grateful to C.S.I.R., New Delhi, (INDIA) for the award of S.R.F..

REFERENCES

[1] S. N. Poddar, *Z. analyt. Chem.*, **154**, 254 (1957); **155**, 327 (1957); *Analyt. Chem. Acta*, **28**, 586 (1963).

[2] B. D. Gupta, Ph. D. Thesis, Roorkee University, Roorkee (1968).

[3] S. Prakash, Ph. D. Thesis, Delhi University, Delhi (1969).

[4] R. P. Patel, Ph. D. Thesis, Sardar Patel University, Vallabh Vidhyanagar (1971).

[5] K. Lal, Ph. D. Thesis, Meerut University, Meerut (1976).

[6] A. I. Vogel, "A Textbook of Quantitative Inorganic Analysis", Longmans & Green, London, 1971.

[7] K. Lal and S. R. Malhotra, *Nat. Acad. Sci., Letters*, **2**, 381 (1979): *J. Indian Chem. Soc.*, **57**, 233 (1980).

[8] K. Nakanishi and P. H. Solonomon, "Infrared Absorption Spectroscopy", Holden-Day, San Francisco, 1977.

[9] D. Scargil, *J. Chem. Soc.*, **1961**. 4440.

[10] B. N. Figgis, "Introduction to Ligand Field", Interscience, New York, 1967.

[11] B. J. Hathaway and D. E. Billing, *Coordination Chem. Rev.*, **5**, 143 (1970).

[12] J. Kon, *J. Biol. Chem.*, **243**, 4350 (1968).

[13] B. N. Figgis and J. Lewis, "Progress in Inorganic Chemistry" Editor, F. A. Cotton, 1964, Vol. 6, p. 37.

[14] R. S. Drago, "Physical Methods in Inorganic Chemistry", Affiliated East-West Press, New Delhi, 1971.

[15] C. J. Ballhausen, "Introduction to Ligand Field Theory", McGraw Hill, New York, 1962.

[16] D. K. Rastogi, K. C. Sharma, *J. Inorg. Nuclear Chem.*, **36**, 2219 (1974).

[17] C. K. Jorgensen, "Absorption Spectra and Chemical Bonding in Complexes", Pergamon Press, New York, 1964.

Revue Roumaine de Chimie, **30**, 5, 401–404 (1985)

SYNTHESIS OF SOME NEW INDOPHENAZINYL-PYRAZOLINE AND ISOXAZOLINE DERIVATIVES

ABDU E. ABDEL RAHMAN* and AMAL S. YANNI
Chemistry Department, Faculty of Science, Assiut University,
Assiut, Egypt

Received July 13, 1981
Revised December 25, 1983

Some new α,β-unsaturated heterocyclic ketones (IIIa-e) were prepared via the interaction of 6-acetylindophenazine (II), with aromatic aldehydes. The reaction of III with hydrazine hydrate or hydroxylamine in basic catalysis gave the corresponding 3-indophenazinylpyrazoline and isoxazoline derivatives IV, V and VI respectively. The structures of the synthesized compounds were determined by elemental and IR spectroscopic analysis.

The interest in the synthesis of heterocyclic compounds has enormously increased in view of the fact that many of these compounds are successfully applied in various fields, including antibiotics,[1] colour photography as well as various biological uses.[2]

Recently, considerable attention has been directed in our laboratory towards the synthesis of some new heterocyclic compounds containing indophenazine moiety.

RESULTS AND DISCUSSION

6-Acetyl indophenazine (II) was interacted with aromatic aldehydes such as benzaldehyde, *p*-anisaldehyde, *p*-chlorobenzaldehyde, *p*-nitrobenzaldehyde and cinnamaldehyde in the presence of piperidine catalyst, and gave new series of the corresponding α, β-unsaturated heterocyclic ketones (IIIa-e). These compounds had been identified by elemental analysis and spectral data. IR spectra showed absorption bands at 1690 cm^{-1} (ν CO$-$CH $=$ CH$-$) attributed to conjugated carbonyl group.

On the other hand, α,β-unsaturated heterocyclic ketones could be also obtained through another synthesizing route, namely by condensation of substituted cinnamoyl chloride with indophenazine (I) in the presence of dry benzene as a solvent. The identity of compound IIIa obtained by the two mentioned methods was established by their mixed melting points and IR absorption spectra.

N-Cinnamoylindophazines (IIIa-e) were condensed with hydrazine hydrate and/or phenyl hydrazine in the presence of piperidine and ethanol to afford the corresponding 3-(indophanazin-6-yl)-5-aryl pyrazolines IV and V respectively.[3–12]

The IR spectra of these compounds showed absorption bands at 1230 cm^{-1} (ν C$-$N), 1600 cm^{-1} (ν C $=$ N) and 2850 cm^{-1} (ν CH$_2$). The disappearance of the absorption band at 1590 cm^{-1} due to the conjugated carbonyl group indicated the disrupture of this group. These compounds gave also Knorr's[16] colour test characteristic for arylpyrazolines.

On the other hand, the interaction of III with hydroxylamine hydrochloride in the presence of piperidine gave the corresponding 3-(indophenazin-6′-yl)-5-arylisoxazolines (VI). [9–11,13–15] The IR spectra of these compounds showed absorption bands at 2850 cm^{-1} (ν CH$_2$) and the disappearance of the absorption band at 1690 cm^{-1} indicated the formation of the isoxazoline ring.

EXPERIMENTAL

The IR spectra were determined with a Unicam SP 1200 spectrophotometer using the KBr wafer technique. All melting points are uncorrected.

Synthesis of N-cinnamoylindophenazines (IIIa-e)

A mixture of equimolecular amounts (0.05 mol) of II[17,18] and aromatic aldehyde was refluxed in the presence of ethanol (30 mL) and piperidine (0.5 mL) as a basic catalyst for about 8 — 10 hrs. The reaction mixture was cooled and the precipitated products were collected and crystallized from ethanol. Yield 80 %. The cinnamoylindophenazine (III, R = $-$C$_6$H$_5$) was produced also through the interaction of equimolecular amounts of I and cinnamoyl chloride when refluxed in benzene for 3 hrs, m.p. 300°C, mixed m.p. 300°C. The results are listed in table 1.

Table 1

Physical data of compounds III, IV, V and VI

Compound No.	m.p. °C	Molecular formula	Analysis			
			Calcd.		Found	
			N	Cl	N	Cl
IIIa	300	$C_{23}H_{15}N_3O$	12.03	—	11.88	—
b	290	$C_{24}H_{17}N_3O$	11.96	—	11.75	—
c	310	$C_{23}H_{14}N_3OCl$	10.95	9.26	10.81	9.02
d	294	$C_{23}H_{14}N_4O_2$	14.14	—	13.95	—
e	296	$C_{25}H_{17}N_3O$	11.20	—	10.98	—
IVa	310	$C_{25}H_{19}N_5O$	17.28	—	17.08	—
b	305	$C_{26}H_{21}N_5O_2$	16.71	—	16.55	—
c	314	$C_{25}H_{18}N_5OCl$	15.93	8.08	15.80	7.88
d	303	$C_{25}H_{18}N_6O_3$	18.67	—	18.50	—
e	307	$C_{27}H_{21}N_5O$	16.24	—	16.03	—
Va	297	$C_{29}H_{21}N_5$	15.94	—	15.88	—
b	280	$C_{30}H_{23}N_5O$	15.45	—	15.22	—
c	305	$C_{29}H_{20}N_5Cl$	14.78	7.50	14.55	7.32
d	300	$C_{29}H_{20}N_6O_2$	17.35	—	17.12	—
e	310	$C_{31}H_{23}N_5$	15.05	—	14.86	—
VIa	312	$C_{23}H_{16}N_4O$	15.38	—	15.13	—
b	308	$C_{24}H_{18}N_4O_2$	14.81	—	14.65	—
c	302	$C_{23}H_{15}N_4OCl$	14.05	8.91	13.89	8.72
d	300	$C_{23}H_{15}N_5O_3$	17.11	—	16.92	—
d	299	$C_{25}H_{18}N_4O$	14.36	—	14.15	—

Effect of alkali on N-cinnamoylindophenazine

Compound IIIa (0.2 g) was refluxed in ethanolic solution of KOH (0.5 g in 30 mL) for 6 hrs. The reaction mixture was cooled and the yellowish product that separated out crystallized from acetic acid into fine needles of indophenazine II, m.p. 280°C.

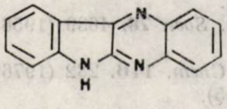
(I)

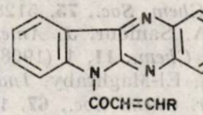
(III)

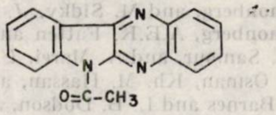
(II)

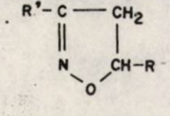
(VI)

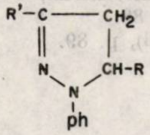
(V)

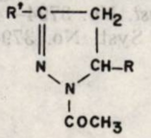
(IV)

IIIa; R = C_6H_5-
b; = p-OCH_3-C_6H_4-
c; = p-Cl-C_6H_4-
d; = p-NO_2-C_6H_4-
e; = C_6H_5-CH=CH-

(IV_V); R'=indophenazin-6'-yl
a; R = C_6H_5-
b = p-OCH_3-C_6H_4-
c = p-Cl-C_6H_4-
d = p-NO_2-C_6H_4-
e = C_6H_5-CH=CH-

(VI); R' = indophenazin-6'-yl
a; R = C_6H_5-
b; = p-OCH_3-C_6H_4-
c; = p-NO_2-C_6H_4-
d; = C_6H_5-CH=CH-

Synthesis of N-acetyl-3-(6-indophenazinyl)-5-arylpyrazolines (IVa-e)

A mixture of N-cinnamoylindophenazines III (0.005 mol), hydrazine hydrate (0.005 mol) ethanol (20 mL), and glacial acetic acid (10 mL) was refluxed for 8—10 hrs. The reaction mixture was concentrated, cooled and poured on ice-water when pale coloured products IV were separated. They were filtered off, washed with water and crystallized from ethanol. Yield 70—75%. The results are reported in table 1.

Synthesis of N-phenyl-3-(6-indophenazinyl)-5-arylpyrazolines (Va-e)

A mixture of equimolecular amounts of III and phenylhydrazine (0.005 mol), ethanol (30 mL) and piperidine (0.5 mL) was refluxed for 8 hrs. The reaction mixture was concentrated, cooled and poured on the acidified ice-water (HCl). The separated products V were filtered off, washed with water and crystallized from methanol. Yield 80 %. The results are given in table 1.

Synthesis of 3-(6-indophenazinyl)-5-arylisoxazolines (VIa-e)

A mixture of III (0.005 mol), hydroxylamine hydrochloride (0.0075 mol), ethanol (30 mL) and piperidine (0.5 mL) was refluxed for 8 hrs. The separated products obtained after cooling and pouring on cold water were filtered off, washed with water and crystallized from ethanol. The results are listed in table 1.

REFERENCES

[1] R. P. Buhs, F. A. Kuehl and Jr. F. J. Wolf, *J. Amer. Chem. Soc.*, **77**, 2344 (1955); P. H. Hidy, R. L. Harned and E.A. Kropp, *ibid*, **77**, 2345 (1955).

[2] V. Knorr, *Chem. Ber.*, **17**, 547, 2032 (1884).

[3] L. Raiford and H. Davis, *J. Amer. Chem. Soc.*, **50**, 156 (1928).

[4] L. Raiford and G. Gundy, *J. Org. Chem.*, **3**, 265 (1938).

[5] S. G. Beech, J. H. Turnbull and W. Wilson, *J. Chem. Soc.*, **1952**, 4686.

[6] A. Samour, M.I.B. Selim and G. H. El-Sayed, *U.A.R.J. Chem.*, **14**, 235 (1971).

[7] A. Samour and M. El Kasaby, *U.A.R.J. Chem.*, **14**, 235 (1971).

[8] A. Samour and M. El Kasaby, *U.A.R.J. Chem.*, **13**, 243 (1970).

[9] A. Schonberg, and M. Sidky, *J. Amer. Chem. Soc.*, **75**, 5128 (1953).

[10] A. Schonberg, A.E.K. Fatten and A.E.A. Samour, *J. Amer. Chem. Soc.*, **78**, 4689 (1956).

[11] A.E.A. Samour, and A. Marei, *U.A.R.J. Chem.*, **11**, 1 (1968).

[12] A. M. Osman, Kh. M. Hassan, and M.A. El-Maghraby, *Indian J. Chem.* **14B**, 282 (1976).

[13] R. P. Barnes and L. B. Dodson, *J. Amer. Chem. Soc.*, **67**, 132 (1945).

[14] V. Auwers and A. Muller, *J. prakt. Chem.*, **137**, 102 (1933).

[15] A. H. Blatt, *J. Amer. Chem. Soc.* **53**, 1133 (1931).

[16] V. Knorrg, *Liebigs Ann. Chem.*, **238**, 200 (1887).

[17] Beilstein Handbuch der organischen Chemie, Berlin, Verlag Von Julius Springer, *XXVI*, *Syst.* No. 3794—4187, 1937, p. 88.

[18] *Ibid*, XXVI, Syst. No. 3794—4187, (1943), p. 89.

Revue Roumaine de Chimie, **30** 5, 405–417 (1985)

BROMINATION OF UNSATURATED SULTAMS AND SULTONES*

S. H. DOSS and N. R. ABU ZEID
National Research Centre, Dokki, Cairo, Egypt A.R.E.

Received December 12, 1980
Revised October 10, 1984

The conflicting views on the bromination of unsaturated sultams and sultones in the light of physico-organic proofs are discussed. Steric and polar effects play a great rôle in the preference for the location of the bromine atom. The canonical structures for the unsaturated sultams reveal the aromatic character of the ring enabling bromination with substitution of the protons at the two methyl groups or those in the two methine groups, rather than the aromatic ring-H of the two double bonds-H of the sultam ring. If the sultam ring is saturated, bromination occurs in the aromatic ring.

INTRODUCTION

Helferich *et al.*[1] reported in 1961 that the two conjugated double bonds of 2,4-dimethyl-butadiene-1,3-sultam (1,4) (I) are not very active particularly because of the presence of the nitrogen atom which is in conjugation with these bonds. N-phenyl-2,4-dimethyl-butadiene-(1,3)-sultam (1,4) can be brominated in the presence of $KHCO_3$ in molar ratios of 1 :1, 1 :2 or 1 :3 moles of bromine to yield the mono, di, or tribromosultam derivatives (with the elimination of 1, 2 or 3 moles of HBr) IIa,b and c. If potassium bicarbonate is not added during bromination to the saturated sultam ring III the formed HBr will destroy the ring giving rise to tribromoaniline and a small amount of the dibromo derivative, where bromine is located in the aromatic nucleus. If bromination is carried out as before and the sultam ring is saturated while the aromatic nucleus is occupied by three methyl groups at positions 2, 4 and 6, two moles of bromine will react giving the dibromo compound IV.

Zeid *et al*[2] reported in 1973 that the bromination occurs in the sultam ring and not in the aromatic ring by substitution of the hydrogen at C_1 giving rise to the monobromo sultam; their proof was the bromination of sultone, then its fusion with aniline. They excluded the possibility

---

* Dedicated to the memory of Prof. Dr. B. Helferich. Preliminary results of this work were presented at Saarlands University before the "Gemeinsames Deutsch-Französisches Seminar mit der Universität Mülhouse" on 12.10. 1976; other results were put forth at the 7th International Congress of Heterocyclic Chemistry, Tampa, Florida 12.8.1979, and the Fourth International Symposium on Novel Aromatic Compounds ISNA 4, Jerusalem, on 30.8.1980 (cf. Conference proceedings p. 11–12).

Scheme 1

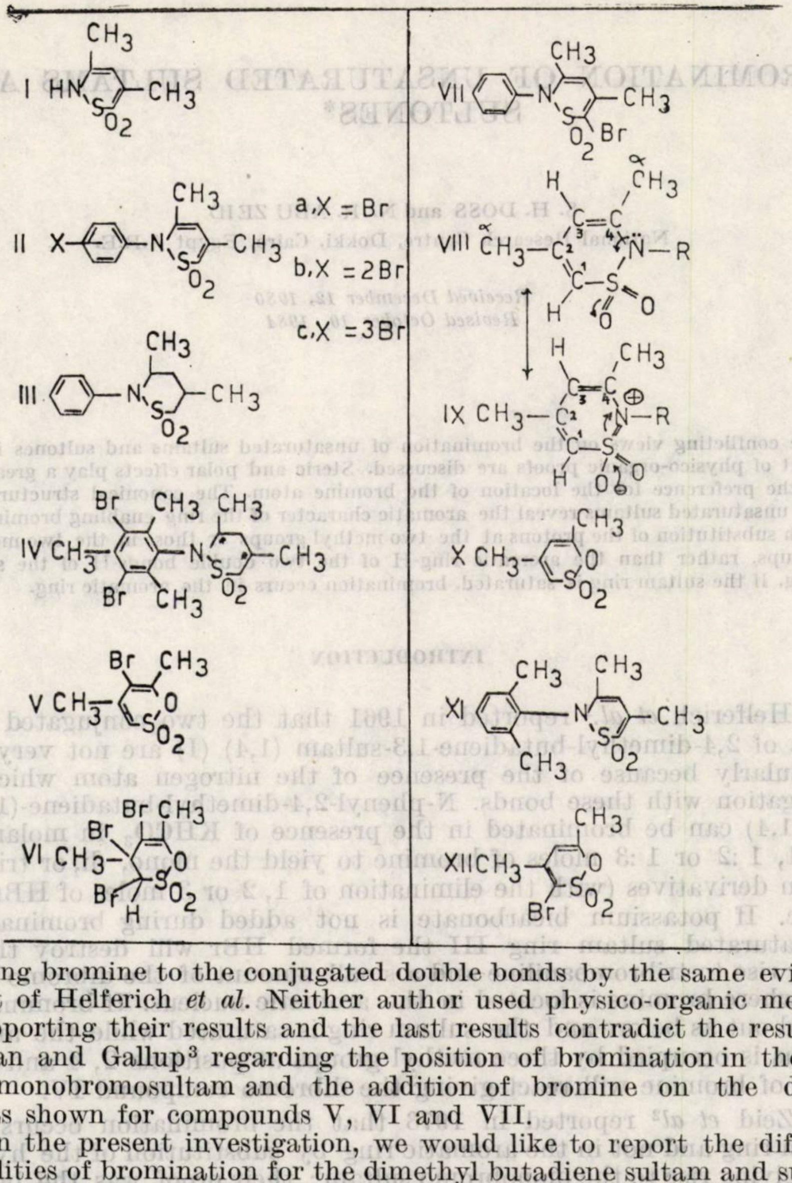

of adding bromine to the conjugated double bonds by the same evidence as that of Helferich *et al.* Neither author used physico-organic methods for supporting their results and the last results contradict the results of Eastman and Gallup[3] regarding the position of bromination in the case of the monobromosultam and the addition of bromine on the double bond as shown for compounds V, VI and VII.

In the present investigation, we would like to report the different possibilities of bromination for the dimethyl butadiene sultam and sultone ring using $^{1}H-NMR$, MS and IR for proving each structure in addition to the classical tool, microanalysis.

RESULTS AND DISCUSSION

It is assumed that the unsaturated sultam ring has a considerable aromatic character, with a large contribution from the canonical structures VII and IX resulting from the alternatively, substantial overlap of

Scheme 1 (continued)

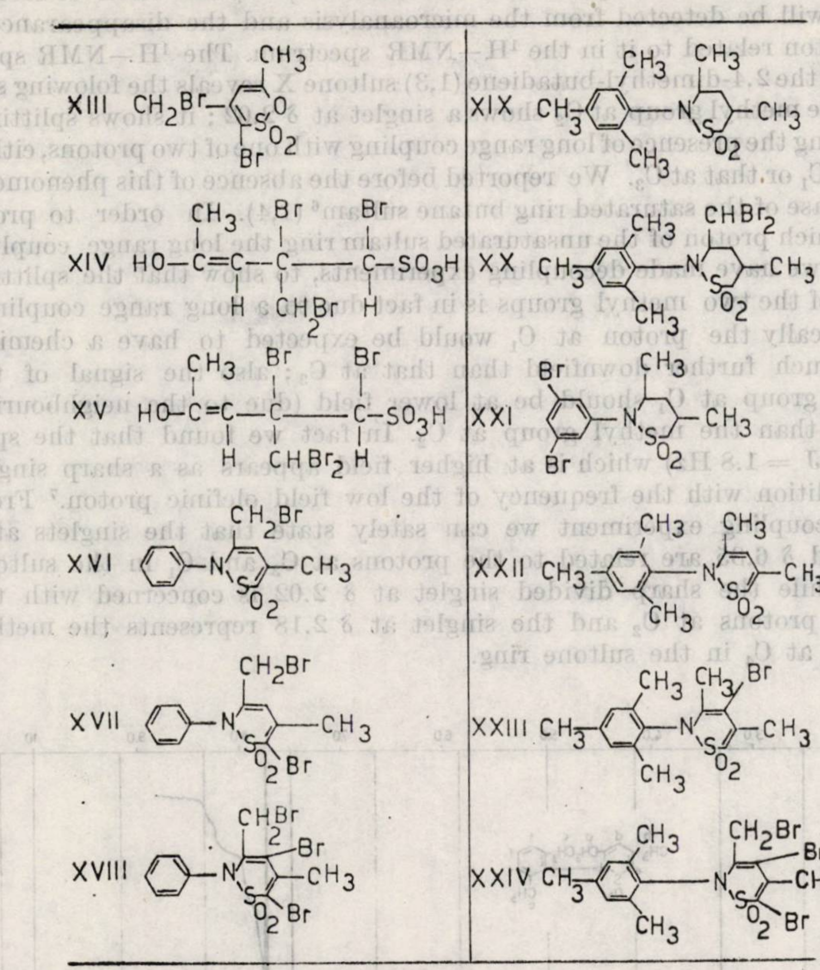

the nitrogen *p* orbitals with a sulphur *d* orbital. At the same time, the methyl groups α and α′ must have an allylic character, like the methyl groups of toluene. Hence, the products of bromination will depend mainly on the reaction conditions; it may be (i) homolytic substitution of the methyl groups, or (ii) electrophilic aromatic substitution. In the case of bromination with N-bromosuccinimide, in the presence of a trace of organic peroxide, substitution should occur in the methyl groups only.[4] The usual considerations (relative numbers of canonical structures contributing to the resonance hybrid of the high energy intermediate) would lead to the expectation that α methyl would be substituted faster than the α′ methyl group which was the case in some examples as will be mentioned later. Electrophilic substitution should be catalysed by $AlBr_3$ [5] or $FeBr_3$. The same sort of approach to relative stabilities of possible intermediates leads to the expectation of preferential bromination at the C_1. The ^1H-NMR spectrum of the free sultone ring will be the criterion for the position of the different protons in the molecule ; any addition of bromin atoms will be detected from the microanalysis and the disappearance o the proton related to it in the ^1H-NMR spectrum. The ^1H-NMR spectrum of the 2,4-dimethyl-butadiene (1,3) sultone X reveals the folowing signals : the methyl group at C_2 shows a singlet at δ 2.02 ; it shows splitting, indicating the presence of long range coupling with one of two protons, either that at C_1 or that at C_3. We reported before the absence of this phenomena in the case of the saturated ring butane sultam[6] (1,4). In order to prove with which proton of the unsaturated sultam ring the long range coupling occurs, we have made decoupling experiments, to show that the splitting of one of the two methyl groups is in fact due to a long range coupling ; theoretically the proton at C_1 would be expected to have a chemical shift much further downfield than that at C_3 ; also the signal of the methyl group at C_4 should be at lower field (due to the neighbouring —O—) than the methyl group at C_2. In fact we found that the split signal (J = 1.8 Hz) which is at higher field appears as a sharp singlet by irradition with the frequency of the low field olefinic proton.[7] From this decoupling experiment we can safely state that the singlets at δ 5.70 and δ 6.35 are related to the protons at C_3 and C_1 in the sultone ring, while the sharp divided singlet at δ 2.02 is concerned with the methyl protons at C_2 and the singlet at δ 2.18 represents the methyl protons at C_4 in the sultone ring.

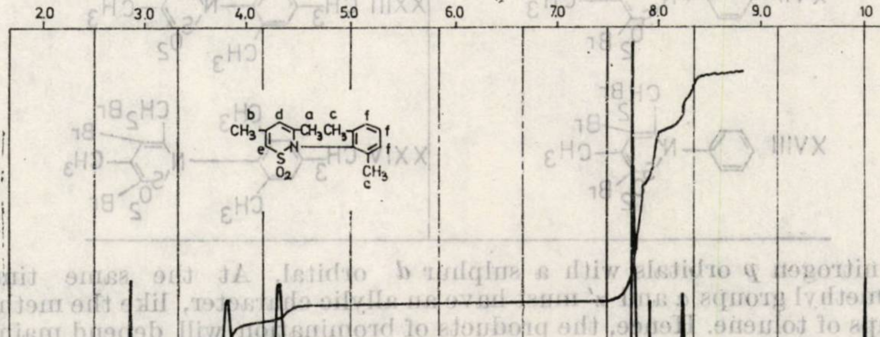

3,5-DIMETHYL-1-(2,6-XYLYL)-2H-1,2-THIAZINE, 1,1-DIOXIDE

Fig. 1

This ^1H-NMR spectrum of sultone was confirmed by another spectrum of N-(2,6-dimethylphenyl)-2,4-dimethyl butadiene (1,3)-sultam (1—4)[1] XI (Fig. 1) where the same phenomenon concerning the long range coupling of the proton at C_1 with the methyl proton at C_2 takes the same general pattern with some downfield shift due to the conversion of the sultone to sultam ring; i.e. due to the presence of nitrogen instead of oxygen in the molecule. Bromination of compound X[7] under the sam conditions,[2] gave a product with the reported m.p. 80—81°C. On carrying out the ^1H—NMR of this compound XII, the downfield singlet at δ 6.35 disappeared (which is related with the protons at C_1); the other singlet at δ 5.7 is deshielded at δ 5.75. The two methyl protons collapse together forming one singlet; its integration shows the presence of six protons at δ 2.18. The deshielding of the methyl singlet at C_2 is due to the presence of the bromine atom in the neighbourhood of C_2; and this proves the assigned structure XII given by Zeid *et al.* Bromination as done by Eastman[3] in carbon tetrachloride gave the monobromo derivative, its m.p. was 75—76°C while that obtained by Zeid *et al.* in chloroform gave m.p. 80—81°C; the mixed m.p. of both samples showed no depression. The bromine atom position was assigned by the first author at C_4 while Zeid *et al.* assigned it to C_1. ^1H—NMR emphasizes the second structure for both products, also the MS showed that both compounds are identical in their fragmentation pathways (Fig. 2) but it was difficult to establish the position of the bromine atom *via* this tool as we got the cyclopropenylium cation fragment at m/e 131 (cf. Chart 1). When bromination was done in the ratio 2 :1 microanalysis and MS showed that two bromine atoms are present in compound XIII. The position of these two bromine atoms in the molecule is clarified from ^1H—NMR, which reveals the methyl singlet situated at C_4 at δ 2.18 (not split), and a singlet δ 4.1; where its integration indicates the presence

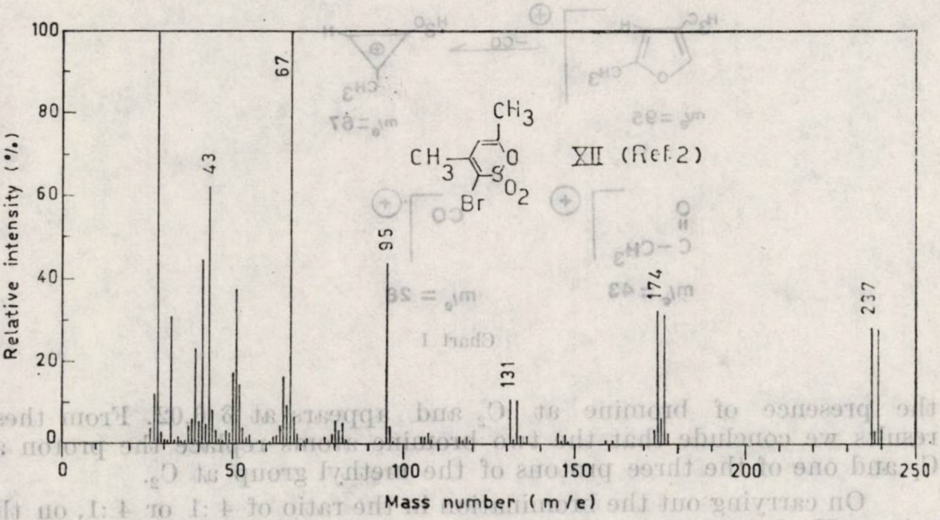

Fig. 2

of 2 protons, its deshielding is due to the presence of the bromine which emphasizes our theoretical base laid before, i.e. the methyl group situated at C_2 is changed to CH_2Br, the proton at C_3 is deshielded due to

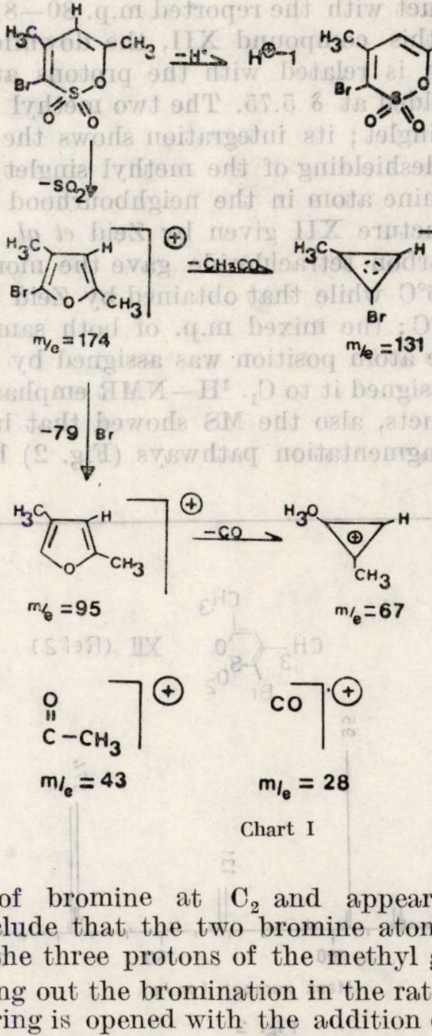

Chart I

the presence of bromine at C_2 and appears at δ 6.02. From these results we conclude that the two bromine atoms replace the proton at C_1 and one of the three protons of the methyl group at C_2.

On carrying out the bromination in the ratio of 4 :1 or 4 :1, on the sultone X, the ring is opened with the addition of two bromine atoms at the Δ^1-double bond in addition to the substitution of the methyl group at C_2 by one bromine atom, (compound XIV) or two bromine atoms (compound XV). ^1H-NMR spectrum of compound XV reveals bands at δ 2.34 (CH_3), a quartet with 1 :3 :3 :1 forming an AB system centered at δ 4.16 ; and a singlet at δ 5.08 (CH). The IR spectrum showed bands at 3000 cm^{-1} (OH stretch), 1610, 1370 cm^{-1} (SO_2-OH), 1190, 1155, 1060 cm^{-1} (SO-stretch). The opening of the sultone ring into the bromosulfonic acid derivatives was also proved by IR and ^1H-NMR, in addition to its accomodation with the results of microanalysis.

When the bromination was done in the ratio 1 :6 we obtained a yellowish brown oil, whose TLC gave 4 spots. The ^1H-NMR of this crude oil showed the presence of methyl protons, methylene protons and methine protons, in addition to the presence of the two protons at C_1 and C_3 in the ratio 2 :1. The separation of this mixture of the different brominated substances is under investigation.

We conclude from the afore-mentioned survey that the bromination of the free sultone occurs firstly at C_1, then at the methyl group at C_2. With more than two moles of bromine, the sultone ring is opened first to yield the sulfonic acid, then addition of two bromine atoms at the Δ^1-double bond while the fourth bromine molecule will substitute the proton at C_1 and that at the methyl group situated at C_2. In order to apply our afore-mentioned theoretical base, bromination of the sultone ring by the use of N-bromosuccinimide in the presence of a trace of an organic peroxide and that with $AlBr_3$ is under current investigation.

The ^1H-NMR spectrum of 2,4-dimethyl-1,3-butadiene sultam (1,4)[3] I reveals the following bands : a doublet at δ 6.23 (J = 2.6 Hz) for the proton at C_1 : singlet at δ 2.1 for the methyl group situated at C_2 : doublet at δ 5.45 (J = 2.6 Hz) for the proton at C_3 : singlet at δ 2.33 tor the methyl group situated at C_4 : and singlet at δ 2.82 (NH). Bromination under the same conditions as Helferich *et al.*[1] for the N-phenyl-2,4-dimethyl butadiene (1,3) sultam (1—4) was carried out in different ratios like that for the free sultone ring. When the ratio was 1 : 1 we obtained substitution of the methyl group at C_4 and not of the proton at C_1 (compound XVI).[8,9] This was emphasized by the ^1H-NMR[10] spectrum since the methyl protons at C_4 which appeared before in the sultone ring at δ 2.18 and in the sultam ring at 2.33 disappeared completely, with the appearance of methylene protons at δ 3.95 ppm. It reveals also a singlet showing long range coupling at 2.14 characteristic for the CH_3 at C_2; another singlet at δ 3.95 its integration representing 2 protons; two other singlets at δ 6.1 and δ 6.4 with some septation, another singlet in the aromatic region at δ 7.47, its integration showing the presence of five aromatic protons. Infrared spectra show characteristic bands for five aromatic neighbouring hydrogen atoms at 870—780 and 690 cm^{-1}. The characteristic sultam band appears at 1290 cm^{-1}, which agrees with our previously published results[11] (Fig. 3). From the afore-mentioned proofs the two supposed structures by Helferich *et al*[1] and Zeid *et al.*[3] do not accomodate formulas IIa, VII with the structure proved by IR and ^1H-NMR for compound XVI. Bromination of compound II in the ratio of 2 :1 gave the product XVII of m.p. 106—108°C. One of the two bromine atoms is situated at the methyl group at C_4 of the sultam ring (as shown from the evidence mentioned before) while the second bromine atoms is situated at C_1. The suggested structure is supported as follows : (1) from integration in the ^1H-NMR spectra, five aromatic protons are present at δ 7.5 ; (2) the methyl group at C_2 lost its long range coupling with the proton at C_1, as replacing by bromine causes deshielding for this methyl at δ 2.47 ; (3) only one proton at C_3 appears as a singlet at δ 5.91, while the second disappeared due to its substitution with bromine ; (4) the methyl singlet at C_4 disappeared and another methylene proton appeared as a singlet at δ 4.10.

In the IR spectrum the five adjacent aromatic protons give the characteristic bands at 890, 760 and 700 cm^{-1} and the characteristic sultam band $^{-1}$ appeared at 1290 cm^{-1}. Bromination of compound II in the ratio 3 :1 gave compound XVIII. ^{1}H—NMR supports the designed structure as it reveals a singlet at δ 2.5 for the methyl proton situated at C_2 : it is deshielded due to the presence of the two surrounding bromine atoms at C_1 and C_3. Another singlet at δ 4.18 for (CH_2Br) is situated at C_4 : the two singlets for the protons at C_1 and C_3 disappeared completely. Another quintet centered at δ 7.45 indicates the presence of five aromatic protons ; such behaviour emphasizes the stability of the aromatic ring towards bromination and agrees with our proposal of the canonical structure including substantial overlap of the nitrogen orbitals with a sulphur *d* orbital. Another proof will be added on applying the method of elimination for the canonical structure *via* the reduction of the two double bonds ; then bromination will occur as homolytic substitution of the methyl groups, if the aromatic nucleus is occupied by three bulky methyl groups. On adding bromine in the ratio 2 :1 to the saturated

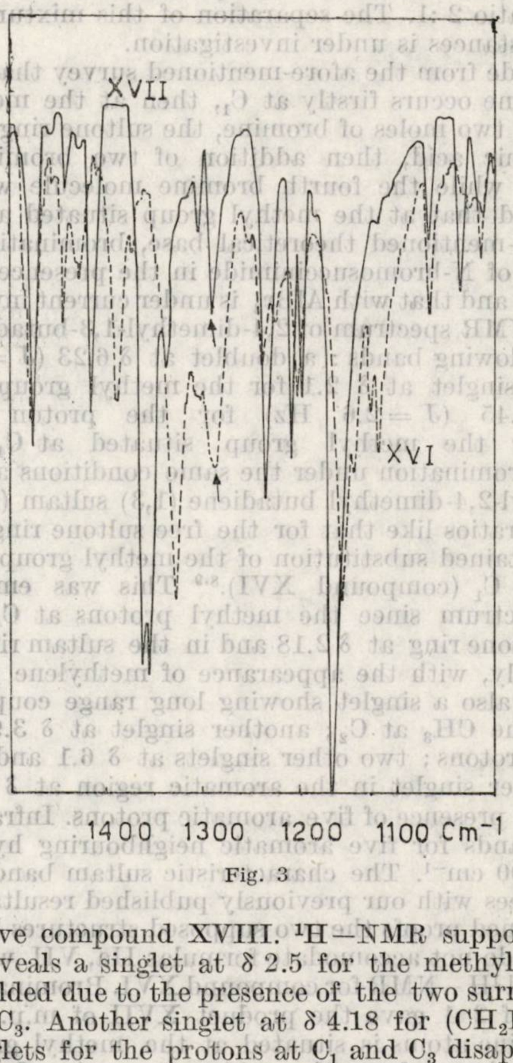

Fig. 3

sultam[1] XIX, ^1H-NMR reveals a quartet centered at δ 1.58 (CH_3 at C_2), a singlet at δ 2.3 (2 methyl groups on the aromatic ring surrounding N) and a singlet at δ 2.5 (3rd methyl group on the aromatic ring). The other three protons on C_2 and C_3 show ill defined multiplets centered at δ 3.45. The two bromine atoms which substitute the methyl group at C_4 indicate the presence of an AB system in the ratio 1 :3 :3 :1 for the group $CHBr_2-CH$; other two aromatic protons constituting on ill defined doublet are centered at δ 7.02. Such results, for compound XX indicate that if the canonical structures are not present and the phenyl nucleus is occupied by bulky methyl groups, then bromination will occur at the methyl group. On the other hand if the canonical structures are not present and the aromatic nucleus is not occupied by bulky groups, then bromination will occur by substitution of the aromatic protons XXI as shown from integration in the ^1H-NMR and the characteristic bands in IR. ^1H-NMR reveals two doublets centered at δ 0.97 and δ 1.18 (two methyls at C_2 and C_4), ill defined multiplets centered at δ 1.65 and δ 1.91 (two methylene groups at C_1 and C_3), ill defined multiplets centered at δ 3.0 and δ 3.2 (two methine groups at C_2 and C_4) and the aromatic protons centered at δ 7.4 and δ 7.88 Infrared spectrum indicates the presence of only three bands at 880, 840 and 760 cm^{-1}.

When the three positions on the aromatic ring are occupied by three methyl groups as in (XXII[1]) bromination of the unsaturated sultam compound will occur at C_3 giving rise to N-2,4,6-trimethyl phenyl-3-bromo-2,4-dimethyl-butadiene 1,3 sultam (1,4) XXIII. ^1H-NMR reveals a doublet centered at δ 1.8 showing that the long range coupling is still operating (which will be connected with the presence of the proton at C_1 forming the singlet at δ 5.84). The other singlet at C_3 disappeared indicating that a bromine atom occupies this position by substitution of the proton at C_3. The three methyls surrounding the nitrogen atom form a doublet centered at δ 2.2, the third methyl group at the aromatic ring appears as a singlet centered at δ 2.35, and the remaining two aromatic protons form a singlet centered at 7.0.

When bromination of compound XXII was done in the ratio 3 :1 three bromine atoms entered, thus obtaining XXIV[8], the two aromatic protons still existed, the two protons at C_1 and C_3 disappeared; the methyl group at C_4 disappeared also giving rise to a singlet centered at δ 4.10 indicating its chage to CH_2Br; the other methyl group appears at δ 2.33 while the three methyl groups on the aromatic ring appear at δ 2.5.

From this comparative study of the bromination of the sultone ring and the sultam compounds whether saturated or unsaturatedwe conclude that the process of bromination is governed by steric and polar factors, if bromination is done under the condition described by Helferich *et al*[1] or Zeid *et al*[2]. In order to accomplish bromination in the sultam ring or in the two methyl groups at C_2 and C_4 or in the aromatic nucleus, bromination on saturated and unsaturated sultam rings with N-bromosuccinimide, $AlBr_3$ and $FeBr_3$ and bromine alone using a 500—1500 W lamp are under investigation.

EXPERIMENTAL

All melting points are uncorrected. IR spectra were obtained on the Perkin-Elmer Spectrophotometer Model 221 with Gitter-Prismen-Austauscheinheit, ^{1}H—NMR spectra were determined in $CDCl_3$ on a Varian A-60 Spectrometer, with TMS as internal reference. MS were obtained with an Atlas CH_4 apparatus. Microanalysis was carried out by the analytical unit, Organisch Chemisches Institut der Universität Saarbrücken W/Germany and the microanalysis department, Faculty of Science, Cairo University, A.R.E.

1-Bromo-2,4-dimethyl-butadiene (*1,3*) *sultone* (*1,4*) *XII*: To a solution of 5 g (0.0312 mole) of sultone X[7] in 30 mL carbon tetrachloride, bromine 5 g (0.0312 mole) was added dropwise within 10 minutes, the solvent was evaporated after adding sodium thiosulphate to eliminate any trace of bromine, the remaining solid (3 g) was crystallized from methanol as white crystals of m.p. 79—80°C. Compound XII is soluble in acetone, chloroform, benzene and ether, partially soluble in water, petroleum ether and acetic acid.

The IR spectrum revealed bands at 1646 cm^{-1} (C=C stretch)[12a], 1355 cm^{-1} and 1185 cm^{-1} (SO_2—O), 755 cm^{-1} (C—Br)[12b], ^{1}H-NMR reveals the absence of the singlet at δ 6.35 indicating that the substitution occurred at C_1. MS : m/e = 239 (M^+). Anal. Calcd. for $C_6H_7BrO_3S$: C, 30.14, H, 2.95. Found : C, 30.0 ; H, 2.9.

On repeating the same experiment using chloroform as solvent we got the same compound with m.p. 77—79°C. On admixture with the first compound, no depression took place, also IR showed the same bands, the singlet at δ 6.13 disappeared in the ^{1}H—NMR spectra, also MS reveals the same fragmentation pathways. Anal. Calcd. for $C_6H_7BrO_3S$: C, 30.14 ; H, 2.95 ; S, 13.41 ; Br, 33.42. Found : C, 30.10 ; H, 3.00 ; S, 13.0 ; Br. 33.1.

1-Bromo-2-bromomethyl-4-methyl-butadiene (*1,3*) *sultone* (*1—4*) *XIII*. To a solution of 5.0 g (0.0312 mole) sultone X, in 25 mL CCl_4, 10.0 g (0.0624 mole) bromine was added dropwise without stirring and the reaction mixture was left to stand overnight and saturated sodium thiosulphate solution was added to get rid of the excess bromine. After extraction with ether, drying with anhydrous sodium sulphate, filtration and evaporation of the ethereal layer, 2.7 g of product remained (27.17 %). Recrystallization from dilute methanol gave colourless crystals, m.p. 98—100°C (2.3 g), which were soluble in acetone, chloroform, benzene and ether, partially soluble in water and petroleum ether.

The IR spectrum reveals bands at 3018, 3034 cm^{-1} (CH_2Br, due to the displacement of the CH frequency under the influence of the halogen atom)[12c], 1640 (thiol ester), 1360, 1180 cm^{-1} (SO_2—O) and 745 cm^{-1} (C—Br), MS. m/e = 318 (M^+). Anal. Calcd. for $C_6H_6Br_2O_3S$ (318) : C, 22.66 ; H, 1.90. Found : C, 22.7 ; H, 1.99.

4-Hydroxy-4-methyl-2-bromomethyl-1,2-dibromo-3-buten-sulfonic acid XIV. To a solution of 1.6 g (0.010 mole) sultone X in 20 mL of carbon tetrachloride, 6.4 g (0.040 mole) bromine was added dropwise while stirring. The reaction mixture was left for 3 days. The precipitated solid (2.4 g) was filtered and recrystallized from dilute methanol as white crystals of m.p 156—157°C (decomp.) (yield 57.55 %). Compound XIV is soluble in acetone, chloroform, ether and benzene, and partially soluble in water and petroleum ether. The IR spectrum reveals bands at 3420 cm^{-1} (broad band OH) 1170, 1050 cm^{-1} (SO_3H).[13a] Anal. Calcd. for $C_6H_9Br_3O_4S$ (417) : C, 17.28 ; H, 2.18 ; S, 7.69. Found : C, 17.7 ; H, 2.06 ; S, 6.9.

4-Hydroxy-4-methyl-2-dibromomethyl-1,2-dibromo-3-butene-1-sulfonic acid XV. To a stirred solution of 1.6 g (0.010 mole) of sultone X in 50 mL carbon tetrachloride, 9.6 g (0.060 mole) of bromine were added dropwise while stirring. The reaction mixture was left for 7 days at room temperature. The solid (1.13 g) which precipitated was recrystallized from dilute methanol to give colorless to pale brown crystals, m.p. 149—150°C. A mixed melting point with XIV was depressed. Compound XV is soluble in acetone, chloroform, benzene, acetic acid and partially soluble in water and petroleum ether. Anal. Calcd. for $C_6H_8Br_4O_4S$ (494) : C, 14.53 ; H, 1.63. Found : C, 14.5 ; H, 1.36.

N-Phenyl-2-methyl-4-bromomethyl-butadiene (*1,3*) *sultam* (*1,4*) *XVI*[9]. To a stirred solution of 2.35 g (0.010mole) N-phenyl-2,4-dimethyl-butadiene (1,3) sultam (1—4) in 50 mL chloroform 4 g (0.040 mole) powdered potassium bicarbonate was added. The reaction mixture was left at room temperature for 15 min then 1.6 g (0.010 mole) of bromine in 15 mL chloroform was added dropwise. Suddenly the colour disappeared. After filtration, the chloroform solution was evaporated under vacuum. The residual oil solidified to give 3.0 g of product (62.8 %) which was recrystallized from methanol yielding 2.6 g colourless crystals, m.p. 134—136°C (shrinking at 127° C). Compound XVI is soluble in chloroform, carbon tetrachloride, partially soluble in benzene and insoluble in alcohol, petroleum ether and water. The IR spectrum reveals bands at 2962 cm^{-1} (CH_3 stretching), 1470 (C—CH_3 deformation), 1385 cm^{-1} (CH_3), 1330 cm^{-1} and 1155 cm^{-1} (SO_2), 1290 cm^{-1} (sultam band)[11], 870, 760 and 690 cm^{-1} (five adjacent aromatic hydrogen atoms)[14b] . Anal. Calcd. for $C_{12}H_{12}BrNO_2S$ (314) : C, 45.87 ; H, 3.85 ; N, 4.46 ; S, 10.20 ; Br, 25.43. Found : C, 45.8 ; H, 3.97 ; N, 4.50 ; S, 9.8, Br, 25.00.

Compound XVI (1.4 g) was dissolved in 80 mL methanol, then reduced with hydrogen in presence of Raney nickel as catalyst for 2 hr ; 200 mL of hydrogen were absorbed, which indicates the presence of two double bonds.

N-Phenyl-1-bromo-2-methyl-4-bromomethyl-butadiene (1,3)-sultam (1—4) XVII. To a stirred solution of 2.35 g (0.010 mole) of compound II in 50 mL chloroform, 6 g (0.060 mole) of powdered potassium bicarbonate were added, then 3.2 g (0.020 mole) of bromine in 20 mL chloroform were added dropwise within 1 hr. After filtration, the chloroform was evaporated under vacuum, and the remaining viscous oil (3 g) was left for 4 days under methanol at 0°C. After solidification and crystallization from methanol colourless crystals (2.7 g, 68.7 %) m.p. 107—108°C dec., were obtained. Compound XVII is sensitive to light, it decomposes in hot weather into a brownish tarry substance. It is insoluble in petroleum ether, benzene and methanol and soluble in chloroform and carbon tetrachloride. The IR spectrum showed bands at 874, 762 and 690 cm^{-1} (characteristic for the presence of 5 adjacent hydrogen atoms)[14b]. Anal. Calc. for $C_{12}H_{11}Br_2O_2S$ (393) ; C, 36.66 ; H, 2.82 ; N, 3.56. Found : C, 36.4 ; H, 2.88 ; N, 3.5.

A solution of 0.17 g in 30 mL methanol was catalytically hydrogenated with Raney nickel for 4 hrs ; 180 mL hydrogen were absorbed indicating that there are two double bonds in the molecule.

N-Phenyl-1,3-dibromo-2-methyl-4-bromomethyl-butadiene (1,3)-sultam (1—4) XVIII[8,9]. To a stirred solution of 2.35 g (0.010 mole) compound III in 30 mL chloroform, 6 g (0.06 mole) of potassium bicarbonate were added, then 4.8 g (0.030 mole) bromine in 40 mL chloroform were added dropwise within $1^{1/2}$ hr. After one hour the colour completely disappeared. After filtration and evaporation of the solvent, 3.5 g of viscous brownish substance was formed which solidified on standing under petroleum ether at 0°C for two days. Recrystallization from benzene-petroleum ether (30—50) gave 3.3 g (69.9 %) colourless crystals, m.p. 163—165°C. The substance is soluble in benzene, chloroform, carbon tetrachloride, methanol, insoluble in petroleum ether and water. Its IR spectrum reveals bands at 1350 and 1165 cm^{-1} (SO_2), 1290 cm^{-1} (sultam band), 912, 752 and 690 cm^{-1} (five adjacent aromatic hydrogen atoms). Anal. Calcd. for $C_{12}H_{10}Br_3NO_2S$ (472) : C, 30.04 ; H, 2.14 ; N, 2.97. Found : C, 31.0 ; H, 2.14 ; N. 2.7.

On hydrogenation of 1.23 g of compound XVIII in methanol using Raney nickel as catalyst, 115 mL of hydrogen were absorbed, indicating the presence of two double bonds in the sultam ring. Trials to resolve the racemic mixture of the saturated sultam products are under investigation.

N-(2,4,6-Trimethyl-phenyl)-2-methyl-4-dibromomethyl-butanesultam (1 — 4) XX. To a stirred solution of 1.4 g (5.0 mmoles) of N-(2, 4, 6-trimethylphenyl)-2,4-dimethyl-butane sultam (1—4) in 30 mL chloroform, 4 g (0.01 mole) of potassium bicarbonate dissolved in a solution of 1.6 g (0.010 mole) of bromine in 20 mL chloroform were added dropwise over 40 min. After filtration, the chloroform evaporated under vacuum ; the remaining yellowish brown oil was crystallized from methanol into colourless prisms (1.6 g) (73.15 %) of m.p. 143—145°C. Compound XX is soluble in ether, chloroform, carbon tetrachloride, insoluble in benzene, petroleum ether, methanol and water. The IR spectrum showed the characteristic bands[14b] for two aromatic protons at 845 and 795 cm^{-1}. Anal. Calcd. for $C_{15}H_{21}Br_2NO_2S$ (439) : C, 41.02 ; H, 4·81 ; N, 3.19 ; S, 7.30 ; Br, 36.39. Found : C, 41.3 ; H, 4.40 ; N, 3.00 ; S, 7.1 ; Br, 36.3.

N-(3,5-Dibromophenyl)-2,4-dimethyl-butanesultam (1—4) XXI. To a solution of N-phenyl-2,4- dimethylbutanesultam (1—4), 2.4 g (0.010 mole) in 30 mL of chloroform a solution of 3.2 g (0.020 mole) of bromine in 20 mL chloroform was dropped while stirring. The bromine color faded slowly. To eliminate the HBr vapors, a stream of nitrogen gas was bubbled through the flask. The reaction mixture was left overnight, whereby a solid substance precipitated. After filtration and recrystallization from methanol, a crystalline solid, m.p. 118—119°C (1.2 g, 52 %), was obtained which agrees with the results of Helferich *et al.*, regarding its identification as tribromoaniline. The filtrate after drying and evaporation under vacuum and recrystallization for several times from dilute methanol gave rise to 0.9 g of solid with m.p. 163—164°C. Compound XXI is soluble in chloroform, carbon tetrachloride, methanol and insoluble in petroleum ether and benzene. Its IR spectrum reveals bands at 878, 815 and 732 cm^{-1} (characteristic for three aromatic hydrogen atoms not adjacent to each other, i.e. substitution of the phenyl ring at 1,3 and 5 positions). Anal. Calcd. for $C_{12}H_{15}Br_2NO_2S$ (397) C. 36.29 ; H, 3.81 ; N, 3.53 ; S, 8.07 ; Br. 40.24. Found : C, 36.7 ; H, 3.82 ; N, 3.8 ; S, 8.5 ; Br, 40.2.

N-(2,4-Trimethylphenyl)-3-bromo-2,4-dimethyl-butadiene-(1,3)-sultam (1—4). XXIII. To a stirred solution of 2.5 g (0.010 mole) of N-(2,4,6-trimethylphenyl)-2,4-dimethyl-butadiene-(1,3)-sultam (1—4)[1] in 30 mL of chloroform, 6 g (0.06 mole) of potassium bicarbonate were added and a solution of 1.6 g (0.01 mole) of bromine in 10 mL chloroform was added dropwise within 20 minutes. After filtration, the chloroform evaporated under reduced pressure, the formed syrup (3.6 g) was left at 0°C for two days in methanol. The solid which formed was recrystallized, after purification with charcoal, affording colourless crystals, m.p. 146—148°C-The crystals are soluble in chloroform, carbon tetrachloride and insoluble in petroleum ether. cyclohexane, benzene and water. The IR spectrum showed bands at 860, 840 and 730 cm^{-1} (characteristic for three aromatic hydrogen atoms not adjacent to each other)[14b]. Anal. Calcd. for $C_{15}H_{18}BrNO_2S$ (356) : C, 50.57 ; H, 5.09 ; N, 3.93 ; S, 9.00 ; Br, 22.43, Found : C, 51.1 ; H, 5.30 ; N, 3.5 ; S, 8.9 ; Br. 22.5.

N-(2,4,6-Trimethylphenyl)-1,3-dibromo-4-bromomethyl-butadiene (1,3)-sultam (1—4) XXIV.[8] To a cooled stirred solution of 2.8 g (0.010 mole) N-(2, 4, 6-trimethylphenyl)-2,4-dimethylbutadiene (1,3)-sultam (1—4) in 30 mL chloroform, 6 g (0.06 mole) potassium bicarbonate were added then a solution of 4.8 g (0.03 mole) bromine in 20 mL chloroform was dropped ; decoloration took place very slowly ; the solution was completely colorless after 2 hrs. After filtration, the chloroform evaporated under vacuum to give a brownish oil (5 g) which solidified on leaving it under methanol for 2 days at 0°C. The formed solid was crystallized from methanol giving crystals, m.p. 168—170°C. Compound XXIV is soluble in chloroform, ether, carbon tetrachloride, insoluble in petroleum, ether, cyclohexane. The IR spectrum reveals bands at 880, 845 and 730 cm^{-1} (characteristic for two aromatic hydrogens not adjacent to each other). Anal. Calcd. for $C_{15}H_{16}Br_3NO_2S$ (514) : C, 35.05 ; H, 3.14 ; N, 2.72. Found : C, 35.3 ; H. 3.25 ; N, 2.6.

Catalytic hydrogenation of 0.4 g of compound XXIV in 30 mL methanol using Raney nickel as a catalyst consumed 34.5 mL hydrogen indicating the presence of two double bonds in the molecule.

CONCLUSION

The positions preferred for bromination of the sultone ring are the proton at C_1, then the methyl group situated at C_2 and then the ring will be opened to yield brominated sulfonic acid with either 3 or 4 bromine atoms. Hence, the two structures assigned for the brominated products by Eastman *et al*[3] are wrong. On the other hand, the positions preferred for the bromination of phenyl sultam II are the methyl group at C_4, then the proton at C_1 then that at C_3. No bromination will occur in the aromtic ring due to the canonical structures of the sultam ring as was explained before. In case of bromination of the saturated sultam ring with the three bulky (2, 4, 6 trimethyl phenyl) groups, the position preferred is the methyl group at C_4 XX. In saturated sultam ring and when no bulky groups are present in the aromatic nucleus, bromination will follow Helferich's view as shown in compound XXI. In unsaturated sultan ring and when the aromatic nucleus is occupied by the three bulky methyl groups XXII, the position preferred for bromina tion will be the proton at C_3 for the monobromo derivative XXIII and the methyl group at C_4 and the proton at C_1 for the tribromo derivative XXIV. Finally, a mixture of the bromo derivative prepared by Helferich's method IIa[1] (m.p. 134—156°C) (the assigned structure XVI) with that prepared by the fusion of monobromosultone with anilines by Zeid's method,[2] m.p. 137°C, shrunk at 124° and melted at 128—132°C, indicating that the compounds differ in the position of the bromine atom on the sultam ring. No bromination in all our examples took place in the aromatic ring due to the aromatic character exhibited by the unsaturated sultam ring arising from overlap of the nitrogen "p" orbitals with the sulphur "d" orbital.

ACKNOWLEDGEMENT. The authors thank Prof. Dr. H. Dürr, Universität des Saarlandes for facilities provided, Prof. Dr. M.R.F. Ashworth for revising the maniscript and Prof. Dr. F. Challenger, Nottingham, England for valuable discussions.

REFERENCES

[1] B. Helferich, R. Dhein, K. Geist, H. Junger and D. Wiehle, *Liebigs Ann. Chem.*, **646**, 32 (1961).

[2] I. Zeid, M. Badawi and I. Ismail, *J. Prakt. Chem.*, **315**, 1166 (1973), cf. also I. Zeid, A. Nada, B. Haggag, I. Ismail, *Egypt. J. Chem.*, **23**, 439 (1980).

[3] R. H. Eastman and D. Gallup, *J. Amer. Chem. Soc.*, **70**, 864 (1948).

[4] C. Djerassi, *Chem. Rev.* **43**, 271 (1948); L. Horner and E. H. Winkelmann, *Newer Methods of Preparative Organic Chemistry*, **3**, 151 (1964); M. Velluz, *Substances naturelles de synthèse*, **7**, 31 (1953).

[5] D. E. Lake and A. A. Asadorian, U.S. Patent 2, 553, 418 (1951); cf. also, S. H. Doss, ISNA 4, 30.8—4.9 (1981) "Conference Proceedings" p. 11—12.

[6] S. H. Doss, *Rev. Roumaine Chim.*, **17**, 905, (1972) and references cited therein.

[7] S. H. Doss and S. R. Michael, *Rev. Roumaine Chim.*, **24**, 605 (1979); cf. also T. Morel and P. E. Verkade, *Rec. Trav. Chim. Pays-Bas*, **68**, 619 (1949).

[8] S. H. Doss, *Appl. Spectrosc.*, **32**, 110 (1978).

[9] E. Fanghanel, H. Mohamed, Y. Keita and R. Radeglia, *J. Prakt. Chem.*, **324**, 353 (1982).

[10] K. H. Albert, H. Dürr, S. H. Doss and J. R. Zahra, *Org. Magn. Reson.*, **14**, 209 (1980); cf. also, R. Radeglia and E. Fanghanel, *Org. Magn. Reson.*, **17**, 10 (1981) and compare M. Kausch, H. Dürr and S. H. Doss, *Org. Magn. Reson.* **10**, 208 (1977).

[11] S. H. Doss, *Chem. Ind.*, 961 (1971); *Acta Chim. Acad. Sci. Hung.*, **72**, 341 (1972), *Rev. Roumaine Chim.*, **17**, 1611 (1972); *Zanco.*, **5**, 208 (1979).

[12] L. J. Bellamy, "*The Infrared Spectra of Complex Molecules*", Methuen & Co., Ltd., London (1966), a) p. 34, b) p. 331, c) p. 44.

[13] For more details on the fragmentation pathways of the sultam ring see H. R. Schulten, H. D. Beckey, G. Eckhardt and S. H. Doss, *Tetrahedron*, **29**, 3861 (1973); S. H. Doss and H.M.A. El-Gamal, *Egypt. J. Chem.*, **19**, 131 (1976); H. R. Schulten and N.M.M. Nibbering, *Biomedical Mass Spec.*, **4**, 55 (1977); S. H. Doss J. L. Derocque, *Rev. Roumaine Chim.*, **24**, 719 (1979).

[14] E. Pretsch, T. Clerc, J. Seibl, W. Simon, "Tabellen zur Strukturaufklärung Organischer Verbindungen mit Spektroskopischen Methoden", Springer-Verlag, Berlin, Heidelberg, New York, 1976. a) p. I 230; b) p. I 55— I 60.

Revue Roumaine de Chimie, **30**, *5*, 419–426 (1985)

REACTIONS OF SOME 2(1H)-PYRIDONES SYNTHESIZED FROM 3,4-METHYLENE-DIOXYBENZYLIDENE- AND 4-NITROBENZYLIDENE-p-ISOPROPYLACETOPHENONE

M. M. MOHAMED, M. A. EL-HASHASH, M. A. SAYED and A. A. SHEHATA
Department of Chemistry, Faculty of Science, Ain Shams University, Abbassia, Cairo, Egypt

Received October 23, 1981
Revised November 14, 1984

In a programme for investigation of the reactivity of α,β-unsaturated carbonyl compounds,[1–5] the authors study the behaviour of the olefinic double bond activated by electron attracting gruop in the base-catalyzed cycloaddition of ethyl acetoacetate and other active methylene compounds as a preparative method for substituted 2 (1H)-pyridones.

A mixture of 3-cyano-4,6-disubstituted-2 (1H)-pyridones **2** (as a major product) and ethyl 2-amino-4,6-disubstituted nicotinates **3** was obtained from the base catalyzed cycloaddition of ethyl cyanoacetate on 3,4-methylenedioxybenzylidene- and 4-nitrobenzylidene-*p*-isopropylacetophenone (**1a** and **1b**) respectively. The reaction was carried out in the presence of ammonium acetate at 120°.

Two routes are possible to explain the formation of compounds **2** and **3** as represented in Chart (1):

The spectral data revealed the existence of lactam-lactimic tautomerism for compounds **2**, and amino-imino tautomerism for compounds **3**.

Chart (1)

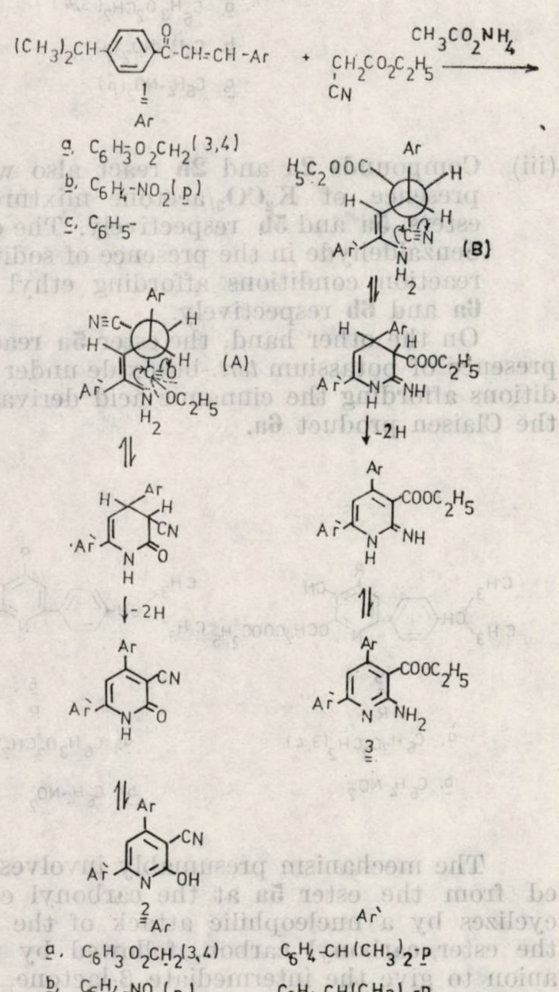
$(CH_3)_2CH-C_6H_4-\overset{O}{C}-CH=CH-Ar$
1
Ar
a. $C_6H_3O_2CH_2(3,4)$
b. $C_6H_4-NO_2(p)$
c. C_6H_5-
+
$CH_2CO_2C_2H_5$
CN
$CH_3CO_2NH_4$
Ar
H_5C_2OOC
H
C≡N
(B)
N
H_2
N≡C
OC_2H_5
(A)
$COOC_2H_5$
NH
-2H
CN
O
OH
NH_2
2
3
Ar
a. $C_6H_3O_2CH_2(3,4)$ $C_6H_4-CH(CH_3)_2-p$
b. $C_6H_4-NO_2(p)$ $C_6H_4-CH(CH_3)_2-p$

The existence of the lactimic form in the cyanopyridones **2a** and **2b** was proved as follows :

(i) Methylation of **2a** by $(CH_3)_2SO_4$ in the presence of K_2CO_3/acetone mixture gave 2-methoxy-3-cyano-4,6-disubstituted pyridine **4a**.

(ii) Similarly, **2b** reacted with $POCl_3$ affording 2-chloro-3-cyano-4,6-disubstituted pyridine **4b**. Compound **4b** reacted with aniline and gave **4c**.

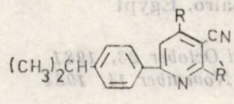

4

	R	R'
a.	$C_6H_3O_2CH_2(3,4)$	$-OCH_3$
b.	$C_6H_4-NO_2(p)$	Cl
c.	$C_6H_4-NO_2(p)$	$-NHC_6H_5$

(iii) Compounds **2a** and **2b** react also with ethyl chloroacetate in the presence of K_2CO_3/acetone mixture and gave the corresponding esters **5a** and **5b** respectively. The esters **5a** and **5b** reacted with benzaldehyde in the presence of sodium ethoxide under the Claisen reaction conditions affording ethyl α-substituted cinnamic esters **6a** and **6b** respectively.

On the other hand, the ester **5a** reacted with benzaldehyde in the presence of potassium *tert.*-butoxide under the Stobbe condensation conditions affording the cinnamic acid derivative **7** and a small amount of the Claisen product **6a**.

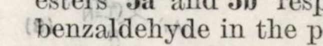

5

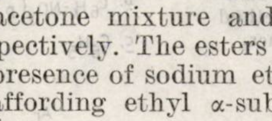

6

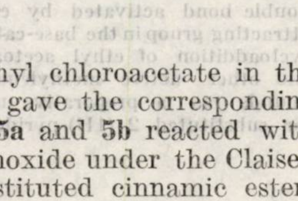

7

R

a. $C_6H_3O_2CH_2(3,4)$

b. $C_6H_4-NO_2$

R

a. $C_6H_3O_2CH_2(3,4)$

b. $C_6H_4-NO_2$

The mechanism presumably involves the attack of the anion derived from the ester **5a** at the carbonyl carbon of benzaldehyde, which cyclizes by a nucleophilic attack of the negatively charged oxygen at the ester carbonyl carbon, followed by the elimination of the ethoxy anion to give the intermediate β-lactone, which undergoes ring opening to give the cinnamic acid derivative **7**. This reaction is analogous with one from our previous work.[7] The mechanism of the reaction is represented in the following Chart (2):

Chart (2)

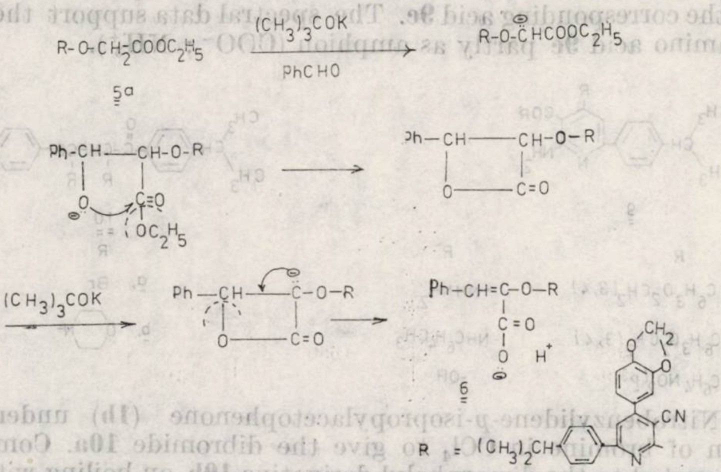

To explain the production of both Stobbe and Claisen products in the presence of potassium *tert*-butoxide (a strong base), it has been reported earlier[8] that the most important factor which leads to the facile occurrence of the Stobbe condensation with succinic esters is the presence of a suitably situated carbalkoxyl group that enables cyclisation to an intermediate paraconic ester (γ-lactonic ring). In ester **5** under investigation β-lactonic ring is formed as intermediate which is less readily formed than the γ-lactonic ring produced in the Stobbe condensation. Consequently, the side reactions such as Claisen condensation compete with the Stobbe condensation.

The cinnamic ester derivative **6a** was also converted to the cinnamic acid derivative **7** on hydrolysis with aq. NaOH.

Further support for the structure of the esters **5** was furnished by the reaction with hydrazine hydrate and *p*-toluidine which gives the corresponding hydrazides **8a**, **8b** and N-*p*-tolylamide derivative **8c** respectively. Alkaline hydrolysis of ester **5a** using 10% aq. NaOH gave the acid **8d** with elimination of cyano group.

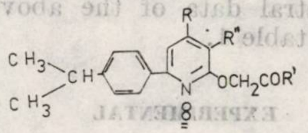

8

	R	R'	R''
a,	$C_6H_3O_2CH_2(3,4)$	$-NHNH_2$	CN
b,	$C_6H_4-NO_2(p)$	$-NHNH_2$	CN
c,	$C_6H_3O_2CH_2(3,4)$	$-NHC_6H_4CH_3(p)$	CN
d,	$C_6H_3O_2CH_2(3,4)$	$-OH$	H

Similarly, the ethyl nicotinate derivative **3a** reacted with hydrazine hydrate and *p*-toluidine affording the hydrazide **9a** and the N-substituted aniline derivative **9b** respectively.

On the other hand, the ester **3b** was hydrolysed with aq. NaOH to give the corresponding acid **9c**. The spectral data support the existence of the amino acid **9c** partly as amphion (COO^- ; NH_3^+).

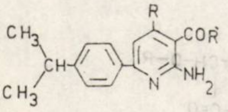

9

	R	R`
a.	$C_6H_3O_2CH_2(3,4)$	$-NHNH_2$
b.	$C_6H_3O_2CH_2(3,4)$	$-NHC_6H_4CH_3$
c.	$C_6H_4NO_2(p)$	$-OH$

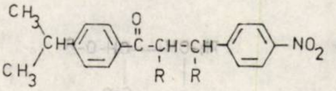

10

	R
a.	Br
b.	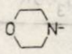

4-Nitrobenzylidene-*p*-isopropylacetophenone (**1b**) undergoes the addition of bromine in CCl_4 to give the dibromide **10a**. Compound **10a** was converted to the dimorpholyl derivative **10b** on boiling with morpholine/ethanol mixture.

Hydrazine hydrate, on the other hand, reacts with the chalcone **1b** in ethanol affording compound **11**, and this gives a blue-violet colour on treatment with $FeCl_3$ in conc. H_2SO_4 which is a characteristic reaction of pyrazolines.[9]

Benzylidene-*p*-isopropylacetophenone (**1c**) reacted with cyclohexanone under the Michael reaction conditions affording the Michael adduct **12**.

On the other hand, ethyl methyl ketone has been added to **1c** under the same reaction conditions and gave the cyclohexenone derivative **13**.

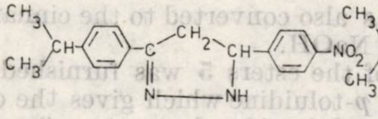

11

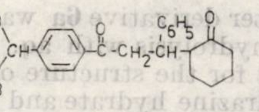

12

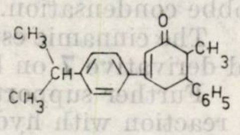

13

The infrared spectral data of the above organic compounds are shown in the following table **1**.

EXPERIMENTAL

The infrared absorption spectra were determined with a Unicam SP 1200 Spectrophotometer using KBr Wafer technique. All melting points are uncorrected.

Reaction of ethyl cyanoacetate with the α,β-unsaturated ketones 1. Formation of the cyanopyridones 2 and ethyl nicotinates 3

A mixture of the chalkones **1** (0.01 mole), ethyl cyanoacetate (4.5 g, 0.04 mole), and ammonium acetate (2.3 g, 0.03 mole) was heated at 140—150° for 8 hrs, washed with water

Table 1

IR spectral data (KBr; cm^{-1})

Compd.	νNH	νCH	$\nu C \equiv N$	νCO of acid or ester	νC=N or νC = C	νCONH
2	3400	2940	2200	pyridones[6] 1500—1400		
3	3440			1737	1610	
4		2900	2200			
5		2940—2910	2200	1735		
6		2930—2900	2200	1730	1610	
7		2950—2820	2205	1700	1610	
8	3300—3280	2900—2820	2200	1700(**8d**)		1645—1640
9a, **9b**	3290	2900—2890				1650—1640
9c	3370	2920		1685		
	νNH_3^+			νCOO^-		
	3220			1565		
10	2890	2960		1680		
11	3300	2980			1610	
12		2960		1720, 1680		
13		2920		1705		

and then dried. The formed oil was fractionally crystallized from the proper solvent to give the cyanopyridones **2** and ethyl nicotinates **3**. The results are listed in table 1.

Methylation of the cyanopyridone 2a. Formation of the methoxy derivative 4a

A mixture of **2a** (0.005 mole), dimethyl sulphate (0.02 mole), anhydrous potassium carbonate (0.02 mole) and dry acetone (50 mL) was refluxed for 20 hrs, the excess solvent was evaporated, and 100 mL of water were then added. The organic material was extracted with ether, the ethereal layer washed with 50 mL of 5% aqueous sodium hydroxide followed by 50 water. Evaporation of dry ether solution left the methoxy derivative **4a**. The results are given in table 1.

Action of phosphorus oxychloride on 2b. Formation of 2-chloro-3-cyano-4,6-disubstituted pyridine 4b

A suspension of **2b** (0.005 mole) and $POCl_3$ (3 mL) was heated on a water-bath for 2 hrs. The reaction mixture was poured gradually into crushed ice (100 g) and the solid that separated was filtered off and crystallized from *n*-butanol to give **4b** as reddish-yellow crystals. See table 1.

Reaction of cyanopyridones 2 with ethyl chloroacetate. Formation of the esters 5

A mixture of **2** (0.01 mole), ethyl chloroacetate (0.04 mole), anhydrous potassium carbonate (0.04 mole) and acetone (20 mL for 1 g of **2**) was refluxed for 20 hrs on a water-bath. The excess of solvent was evaporated and 100 ml of water were then added. The organic substance was extracted with ether and the removal of ether gave the desired products **5**. The results are given in table 1.

Condensation of benzaldehyde with the esters 5. Formation of cinnamic esters 6 or acid 7

A solution of benzaldehyde (0.1 mole) in the ester **5a** (0.15 mole) and (20 mL) *tert*-butanol was added dropwise to a boiling stirred solution of potassium *tert*-butoxide (0.11 mole) in dry *tert*-butanol [potasium metal (0.11 g-atoms); 25 mL of *tert*-butanol for 1g of potassium]. The addition lasted half an hour; heating on a water bath and stirring were then continued for another hour. Most of the alcohol was then removed under reduced pressure and the cooled residue was rendered slightly acidic with dilute hydrochloric acid. The organic material was taken up in ether, the ethereal solution was washed several times with water, then repeatedly with cold sodium carbonate solution (150 mL ; 10 %). The alkaline extract was cooled, acidified with hydrochloric acid/ice (20 mL/200 g) and the precipitated matrial was extracted with ether. Evaporation of the excess ether left the acidic product as an oily product which can be solidified by trituration with light petroleum (b.p. 60—80°). Evaporation of dry ethereal layer left the cinnamic ester derivative **6a** (1.1 g ca. 21 %). The solids obtained were crystallised from the proper solvent to give the cinnamic acid derivatives **6a** and **7**. When the reaction was carried out in the presence of C_2H_5ONa (1.1 mole) in ethanol (50 mL) on steam bath the sole product was the cinnamic ester derivative **6**. The results are given in table 1.

Conversion of 6a to 7

A mixture of the ester **6a** (0.005 mole) and aqueous sodium hydroxide solution (30 mL 10 %) was refluxed for 3 hours. The alkaline mixture was cooled, acidified with hydrochloric acid and ice (15 mL/100 g) and the precipitated material was extracted with ether. Evaporation of ether gave the cinnamic acid derivative **7** which was identified by m.p. and m.m.p. determinations.

Action of hydrazine hydrate on 3a, 5a and 5b, 1b. Formation of the hydrazides 8a, 8b, and 9a and pyrazoline 11

A mixture of **3a**, **5a** and **5b** or **1b** (0.01 mole), hydrazine hydrate (0.01 mole), and ethanol (50 mL) was refluxed for 5 hrs. The solid separated after cooling was crystallized from the proper solvent to give the corresponding hydrazides **8a** and **8b**, **9a** and the pyrazoline **11**. (cf. table 1).

Reaction of the esters 3a and 5a with *p*-toluidine and of chloroderivative 4b with aniline. Formation of 9b, 7c and 4c

A suspension of **3a**, **5a** or **4b** (0.01 mole) and *p*-toluidine or aniline (0.01 mole) was refluxed for 2 hrs then allowed to cool. The reaction mixture was triturated with methanol and the N-substituted amide or amino derivatives **9b**, **8c** or **4c**. See table 1.

Hydrolysis of the ester 3b with aqueous NaOH. Formation of the acid 9c

A mixture of **3b** (0.005 mole) and sodium hydroxide solution (20 mL ; 10 %) was refluxed for 2 hrs. The alkaline mixture was cooled, acidified with 8 mL HCl in 100 g ice, the precipitated solid was extracted with ether. Evaporation of ether gave the acid **9c** (cf. table 1).

Addition of bromine to 4-nitrobenzylidene-*p*-isopropylacetophenone (1b). Formation of the dibromide 10a

A vigorously stirred solution of **1b** (0.01 mole) in carbon tetrachloride (50 mL) was heated on a water-bath to about 60—70° and then treated portionswise with bromine (0.01 mole) during a period of 15 minutes. The mixture was stirred for further 3 hours then poured on ice-water (100 g ice ; 100 g H_2O). The solid that separated was filtered off and crystallized from ethanol to give the dibromide **10a**. The results are listed in table 1.

Reaction of the dibromide 10a with morpholine. Formation of the dimorpholyl 10b

A suspension of the dibromide **10a** (0.001 mole) and morpholine (0.002 mole) was refluxed in ethanol for 2 hours, then allowed to cool. The obtained solid was crystallized from benzene to give the dimorpholyl derivative **10b**.

Base-Catalyzed Michael addition of cyclohexanone and butanone to benzylidene-*p*-isopropylacetophenone (1c). Formation of 12 and 13

A mixture of **1c** (0.01 mole) and cyclohexanone or butanone (0.02 mole) in ethanol (30 mole) was treated with (3 mL ; 50 %) aqueous sodium hydroxide, then set aside at room

Table 2

Characterisations of compounds **2**–**13**

Compound	Yield, % colour	m.p.° solvent	Formula	Analysis, % Calcd.	Found
2a	52	230	$C_{22}H_{18}N_2O_3$	C 73.74	73.50
	yellow	Toluene		H 5.02	5.19
				N 7.82	7.75
2b	51	241	$C_{21}H_{17}N_3O_3$	C 70.19	70.00
	yellowish	Ethanol		H 4.73	4.50
				N 11.69	12.05
3a	29	195	$C_{24}H_{24}N_2O_4$	C 71.28	70.73
	yellow	Benzene		H 5.94	5.61
				N 6.93	7.28
3b	20	177	$C_{23}H_{23}N_3O_4$	C 68.14	68.26
	yellow	P.E. 100–120		H 5.67	5.50
				N 10.37	9.75
4a	73	134	$C_{23}H_{20}N_2O_3$	C 74.19	74.17
	brown	P.E. 100–120		H 5.37	4.98
				N 7.52	7.25
4b	66	284	$C_{21}H_{16}N_3O_2Cl$	C 66.75	66.37
	reddish-yellow	*n*-Butanol		H 4.23	4.13
				N 11.12	11.82
4c	21	235	$C_{27}H_{22}N_4O_2$	C 74.65	74.26
	brown	Benzene		H 5.06	4.62
				N 12.90	13.00
5a	72	179	$C_{26}H_{24}N_2O_5$	C 70.27	70.66
	brown	Benzene		H 5.40	5.62
				N 6.30	5.91
5b	48	162	$C_{25}H_{23}N_3O_5$	C 67.41	67.79
	brown	Benzene		H 5.16	5.18
				N 9.43	9.28
6a	51	159	$C_{33}H_{28}N_2O_5$	C 74.43	74.61
	pale brown	P.E. 100–120		H 5.26	5.67
				N 5.26	5.87
6b	60	212	$C_{32}H_{27}N_3O_5$	C 72.04	72.60
	yellow	Ethanol		H 5.06	5.56
				N 7.87	8.48
7	12	150	$C_{31}H_{24}N_2O_5$	C 73.80	74.23
	yellowish-white	Ethanol		H 4.76	5.12
				N 5.55	6.01
8a	66	194	$C_{24}H_{22}N_4O_4$	C 66.97	67.34
	White	Toluene		H 5.11	5.14
				N 13.02	12.43
8b	71	139	$C_{23}H_{21}N_5O_4$	C 64.03	64.51
	Yellow	Ethanol		H 4.87	5.08
				N 16.24	16.64
8c	82	167	$C_{31}H_{27}N_3O_4$	C 73.66	74.11
	Yellowish	Methanol		H 5.34	5.86
				N 8.31	7.93

Table 2 (continued)

Compound	Yield, % colour	m.p.° solvent	Formula	Analisis,%	
				Calcd.	Found
8d	45	230	$C_{23}H_{21}NO_5$	C 70.58	69.96
	grey	Toluene		H 5.37	4.87
				N 3.58	3.60
9a	69	227	$C_{22}H_{22}N_4O_3$	C 67.69	68.12
	yellowish	Toluene		H 5.64	5.35
				N 14.35	14.28
9b	43	222	$C_{29}H_{27}N_3O_3$	C 74.83	75.06
	pale brown	Ethanol		H 5.80	6.18
				N 9.03	8.88
9c	24	195	$C_{21}H_{19}N_3O_4$	C 66.84	66.37
	yellow	Toluene		H 5.03	5.15
				N 11.14	10.87
10a	77	152	$C_{18}H_{17}NO_3Br_2$	C 47.47	47.25
	yellow	Ethanol		H 3.73	4.13
				N 3.07	3.06
10b	59	147	$C_{26}H_{33}N_3O_5$	C 66.80	65.99
	brown	Benzene		H 7.06	6.64
				N 8.99	9.00
11	82	281	$C_{18}H_{19}N_3O_2$	C 69.90	70.49
	pale yellow	Ethanol		H 6.14	5.85
				N 13.59	14.28
12	24	138	$C_{24}H_{28}O_2$	C 82.75	83.13
	colourless	P.E. 100–120		H 8.04	7.91
13	39	221	$C_{22}H_{24}O$	C 86.84	86.35
	yellowish	Benzene		H 7.89	8.14

temperature for 24 hours. The reaction mixture was poured into crushed ice (50 g) and the solid separated was filtered off, dried and then crystallized from light petrol (b.p. 100–120°) or benzene to give **12** or **13** respectively. (cf. table 1).

REFERENCES

[1] M. El-Hashash and M. M. Mohamed, *Pakistan J. Sci. Ind. Res.*, **20**, 325 (1977).

[2] M. M. Mohamed, M. A. El-Hashash, M. A. El-Nagar, F. Said and W. M. Ali, *Pakistan J. Sci. Ind. Res.*, **23**, 169 (1980).

[3] A. F. Fahmy, M. M. Mohamed, A. A. Afify, M. Y. El-Kady and M. A. El-Hashash, *Rev. Roumaine Chim.*, **25**, 125 (1980).

[4] M. M. Mohamed, M. A. El-Hashash, M. Y. El-Kady and M. A. Hassan, *Rev. Roumaine Chim.*, **25**, 237 (1980).

[5] M. A. El-Hashash, M. M. Mohamed and A. Nagy, *Indian* C. *Chem.*, **16B**, 984 (1978).

[6] A. R. Katritsky and R. A. Jones, *J. Chem. Soc.*, **1960**, 2947.

[7] M. A. El-Hashash, M. M. Mohamed, A. El-Nagar and O. A. El-Sayed, *Rev. Roumaine Chim.*, **34**, 1343 (1979).

[8] W. S. Johnson, A. L. Mc Closkey, and D. A. Dunnigan, *J. Amer. Chem. Soc.*, **72**, 514 (1950).

[9] M. A. El-Hashash and M. El-Kady, *Rev. Roumaine Chim.*, **23**, 1581 (1978).

Revue Roumaine de Chimie, **30**, *5*, 427–434 (1985)

LIQUID PHASE CATALYTIC HYDROGENATION ON $AlPO_4$-SUPPORTED NICKEL CATALYSTS. II

HYDROGENATION OF STYRENE AND α-METHYL-STYRENE

J. M. CAMPELO, A. GARCIA, D. LUNA and J. M. MARINAS
Department of Organic Chemistry, Faculty of Sciences, Cordoba University, Cordoba, Spain

Received December 23, 1981
Revised December 10, 1983

A kinetic study of α-methyl substitution effects in the liquid-phase hydrogenation of the olefinic double bond and in styrene, has been accomplished over a series of new nickel catalysts supported on $AlPO_4$, and $AlPO_4-Al_2O_3$ and $AlPO_4-SiO_2$ systems, containing 5, 10 and 20 wt% nickel and wide ranges of dispersion.
The values of hydrogenation activity per unit of metal surface, r_A, and apparent activation energy, E_a, have been achieved for both substrates. It was found that the r_A varied markedly with the support and it diminished as the nickel content decreased. The order of decreasing activity for the C–C double bond :

$$Ni/AlPO_4-SiO_2 > Ni/AlPO_4 > Ni/AlPO_4\text{-}Al_2O_3$$

is valid for both substrates and it is associated with an effect of metal-support interaction.
The influence of α-methyl substitution operated in two ways; the first, by an inductive effect, increases the reactivity of the olefinic double bond, and manifests itself in a lowering of the E_a values by about two orders of magnitude. The second effect of the methyl substitution is a steric effect that hinders the adsorption of the reactant molecules resulting in similar r_A values of styrene (S) and α-methyl-styrene (MS), although E_a of MS was smaller.

INTRODUCTION

In a recent paper[1] we studied the liquid phase catalytic hydrogenation of acrolein (A) and methyl-vinyl-ketone (MVK) by using new supported nickel catalysts ($Ni/AlPO_4$, $Ni/AlPO_4$-SiO_2 and $Ni/AlPO_4-Al_2O_3$) in methanol as solvent under low hydrogen pressure (0.4 MPa) and temperatures between 298–323 K. We concluded that the methyl group of the MVK, in comparison with A, increases the hydrogenation activity of the olefinic double bond by an electronic effect, and entirely hinders the carbonylic double bond hydrogenation in the MVK by a steric effect. So, we have the possibility of achieving a selective reduction of aldehydes in the presence of ketones.

The purpose of the present paper is to determine if this effect is confined to carbonyl hydrogenation alone or if it may be extended to include the olefinic double bond hydrogenation. Thus, we study here the hydrogenation of S and its α-methyl derivatives, MS, using the same experimental conditions and the same new supported nickel catalysts as in our previous work,[1] in order to see how the double bond C=C hydrogenation is different from or similar to the double bond C=O hydrogenation, since this olefin pair, S and MS, is a structural analogue of the earlier studied α, β-unsaturated carbonyl compound pair.

EXPERIMENTAL

Supported nickel catalysts

As catalysts we have used systems constituted by nickel supported at 5, 10 and 20 wt% on three different supports: a pure aluminium orthophosphate, $AlPO_4$, a $AlPO_4-Al_2O_3$ (75 : 25 wt%) system and a $AlPO_4-SiO_2$ (20 :80 wt%) system; all of them were obtained by gelification with ethylene oxide. These supports, smaller than 200 mesh powder size, were dried at 385 K in air for 24 h, then calcined at 923 K for 3 h and stored in a dessicator. The detailed procedure of synthesis and the textural properties of supports (surface area, pore volume and main pore diameter) determined by nitrogen adsorption have been published elsewhere.[2–5]

Supported nickel catalysts were prepared by impregnating the supports to incipient wetness with solutions with the appropriate concentration of nickel nitrate. The prepared samples were dried and reduced in an ultrapure hyrogen stream (100 mL min^{-1}) at 673 K over a period of 3 h and then were cooled to room temperature in the same hydrogen stream and stored in sealed glass bottles until required.

Before reduction, some samples at 20 wt% were also calcined in air from room temperature to 573 K for 1 h, to produce catalysts of lower dispersions. Thus, at 20 wt%, we have two series of catalysts: Series I, not calcined, and Series II, calcined prior to reduction.

Apparatus and Procedure

According to the procedure previously described,[5] hydrogenation runs were carried out under vigorous shaking in a conventional low pressure hydrogenator (Parr Instruments Co.Md. 3911) equipped with a manometer that allows us to permanently know the hydrogen pressure in the isolated reaction bottle (500 mL). The temperature was maintained constant (± 1 K) by pumping water from a thermostatic bath, through the bottle jacket.

The styrene and α-methylstyrene employed were obtained from Merck p.a. and they were purified by distillation under ultrapure nitrogen and then passed through active acidic aluminium oxide powder for chromatography (Merck) activated at 673 K in flowing ultrapure nitrogen. Then, they were stored under nitrogen in a refrigerator but not for more than a week. Methanol p.a. employed as solvent was used without further purification.

Reactions were developed in a 1M methanolic solution, under initial hydrogen pressure in the range 0.4–0.6 MPa and temperatures between 298 and 323 K. Amounts of catalyst containing $5\,10^{-4}$ mol of Ni, activated in hydrogen stream (100 mL min^{-1}) at 673 K for 1 h, and cooled at room temperature keeping the sample in the hydrogen stream, were added to the reaction bottle containing 25 mL of 1M methanolic solution of substrate (S or MS). In order to avoid the catalyst reoxidation, the air in the bottle was outgassed by a vacuum system until the methanol started to boil, and afterwards, it was alternately filled with hydrogen to 0.3 MPa and vented three times. Then, after the outgassing was finished, the hydrogen was introduced until the total pressure was slightly below the reaction pressure, and the water from the thermostatic bath, at the reaction temperature, was circulated around the reaction bottle for 15 min. A preliminary test was developed in order to determine if there was any reaction while the agitation was not initiated. Next, agitation of the bottle was initiated (5 strokes s^{-1}) and simultaneously hydrogen was introduced until the total pressure reached the desired value. The stirrer and the timer were started simultaneously after the initial hydrogen pressure had been noted. The agitation was started at zero time. The reaction rate was obtained from the initial slope of the plot of hydrogen consumed *vs.* time, and as the plots were always linear until 80% coversion (see Fig. 1, where a typical run appears), the determination of the initial slope was straightforward.

In order to estimate the intrinsic activity of the supported nickel metal for the hydrogenation reaction, the *areal rate*, r_A, is defined as the activity per unit surface area of nickel metal (mol $s^{-1} m_{Ni}^{-2}$) and the metallic surface areas of catalysts were determined by X-ray diffraction (XRD), using a Phillips diffractometer.

The determination of the average crystallite diameter, D_v (XRD), according to the methods of Moss[6], as well as the experimental conditions for the complete reduction of the supported nickel catalysts, determined fom the absence of nickel oxide peaks in their X-ray diffraction diagrams, were reported in a previous paper.[7] The average crystallite diameter, D_v, was calculated from the width of the (111) nickel peak at half the height of the maximum peak.

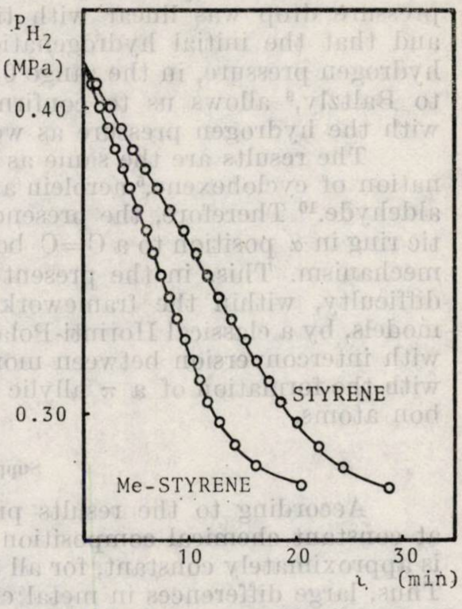

Fig. 1. — Typical plot for hydrogenation of Styrene and α-Methylstyrene on Ni/AlPO$_4$ 20 wt%, Series I, at 298 K and initial hydrogen pressure of 0.41 MPa.

In order to obtain the accuracy of D_v values from the XRD, the catalyst Ni/AlPO$_4$ I 20 wt% has been determined by Transmission electron microscopy (TEM) and, according to the results : $D_{XR} = 77.0$ A ; D_S(TEM) = 76.5 ; D_v(TEM) = 81.4 ; we observe that both procedures, XRD and TEM, are in a very good agreement.

TEM measurements were conducted using a Philips EM-300 electron microscope, capable of greater than 0.3 nm resolution. The samples were prepared by the extractive replica technique.[8] An average of 900—1200 particles from at least five pictures were counted for the sample using enlarged photographs at a magnification of 342000x.

Analysis

The reaction products were analyzed by using a Hewlett-Packard 5830 gas chromatograph fitted with a H.P. 18850 G.C. terminal. The column was packed with 5% Carbowax 20 M on 80/100 Chromosorb G AW-DMCS. Under the experimental conditions the only products detected in the hydrogenation of Styrene and α-Methylstyrene were ethylbenzene and isopropylbenzene, respectively. Neither hydrogenation of the aromatic ring nor hydrogenolysis products were detected in any of the cases.

RESULTS AND DISCUSSION

Kinetics

Previous hydrogenation runs, performed at various agitation regimes and at different amounts of catalyst, have shown that the initial rate measurements were made under conditions where the initial rate was independent of the agitation speed and linearly proportional to the amount of catalyst. Due to this, in the range of operating variables, the reactions were controlled by the chemical step, and the kinetic data are free from transport influences.

Under the experimental conditions of this work, it was found that pressure drop was linear with time until 80–90% conversion, Fig. 1, and that the initial hydrogenation rate was independent of the initial hydrogen pressure, in the range 0.4–0.6 Mpa. This behaviour, according to Baltzly,[9] allows us to confirm that the overall rate was zero order with the hydrogen pressure as well as the olefin concentration.

The results are the same as those previously found in the hydrogenation of cyclohexene,[5] acrolein and methyl-vinyl ketone [1] and E-cinnamaldehyde.[10] Therefore, the presence of a C=O function and/or an aromatic ring in α position to a C=C bond, does not change the hydrogenation mechanism. This, in the present case, may be described, without any difficulty, within the framework of the Langmuir-Hinshelwood kinetic models, by a classical Horiuti-Polanyi type mechanism, non competitive,[11] with interconversion between monoadsorbed and diadsorbed species and with the formation of a π allylic species that is delocalized on three carbon atoms.

Support Effects

According to the results presented in table 1, the areal rate, r_A, at constant chemical composition (the same support and nickel loading) is approximately constant, for all supported nickel catalysts studied here. Thus, large differences in metal crystallite sizes do not imply a different specific chemical reactivity as a function of the particle diameter.

Table 1

Areal rates (r_A) of Styrene and α-Methylstyrene in their hydrogenation at 298 K and 0.14 MPa on different catalysts

CATALYST	D_v[a] (nm)	S[b] ($m^2\ g^{-1}$)	$r_A\ 10^6$ ($mol\ s^{-1}\ m_{Ni}^{-2}$)	
			Styrene	α-Me-Styrene
$Ni/AlPO_4$				
5% I	54	124	2.83	2.83
10% I	76	89	5.00	6.67
20% I	77	88	13.83	10.00
20% II	184	36	13.00	10.33
$Ni/AlPO_4-SiO_2$				
5% I	37	182	9.33	7.83
10% I	44	152	11.83	16.00
20% I	100	68	19.33	16.50
20% II	113	59	21.67	17.50
$Ni/AlPO_4-Al_2O_3$				
5% I	75	90	4.33	3.17
10% I	73	92	4.67	3.33
20% I	61	110	4.00	4.17
20% II	93	63	4.33	4.17

[a] Average crystallite diameter

[b] Metal surface area

So, the olefinic double bond hydrogenation over the catalysts studied here can be considered, according to Boudart's[12] ***structure insensitive.***

On the other hand, the effects of support and metal loading on the areal rate can be analyzed in table 1, where, as it may be seen, the r_A values decrease in the order :

$$Ni/AlPO_4 - SiO_2 > Ni/AlPO_4 > Ni/AlPO_4 - Al_2O_3$$

and, in all cases, the areal rate decreases with the decrease of the nickel concentration.

These results may be ascribed to a metal-support interaction, with an electron transfer between the nickel metal and the support. According to Vannice and Garter,[13] it is possible that oxidizing sites on support surfaces interact with the dispersed metal and reduce the 3d electron density on the nickel metal.

The electron deficient nickel metal results in a stronger and, therefore, more unfavourable adsorption for the hydrogenation of the olefin double bond in styrene or α-methylstyrene. Therefore, it is reasonable that the effects of support on catalytic activity of nickel metal manifest themselves in the apparent activation energy (E_a).

In order to confirm the last assumption, the values of E_a and the preexponential factor, lg A, were obtained from the Arrhenius plots (Fig. 2) in the temperature range of 298—323 K. The results thus obtained are summarized in table 2, and provide the unambiguous evidence that the extent of nickel support interaction clearly decreases in the same order already found in the cyclohexene hydrogenation [5] :

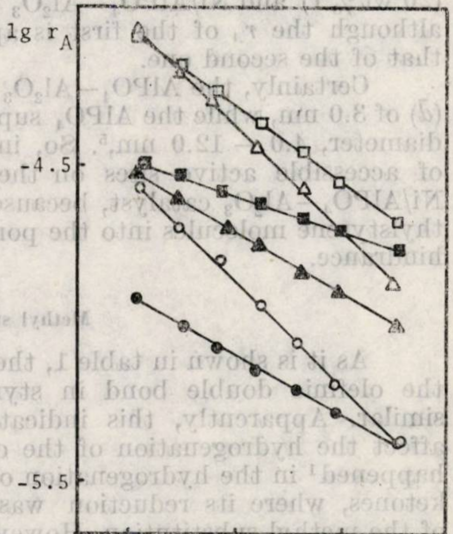

Fig. 2. — Arrhenius plots for hydrogenations on catalysts with Ni at 20 wt% Series I, and with initial hydrogen pressure of 0.41 MPa. *Styrene* : (△) $Ni/AlPO_4$; (□) $Ni/AlPO_4 - SiO_2$; (o) $Ni/AlPO_4 - Al_2O_3$. *α-Methylstyrene* : (▲) $Ni/AlPO_4$; (■) $Ni/AlPO_4 - SiO_2$; (●) $Ni/AlPO_4 - Al_2O_3$.

$$Ni/AlPO_4 - Al_2O_3 \simeq Ni/AlPO_4 > Ni/AlPO_4 - SiO_2$$

for catalysts of the same loading.

However, this order is not obtained with the r_A values. Thus, accepting the fact that the areal rate of a Ni/support catalyst is not only determined by the activity of the nickel surface, which depends on the electron density on nickel, but is also affected by the steric hindrance of the reactant molecules, we can explain that the catalysts Ni/$AlPO_4$ (20 wt% I) and Ni/$AlPO_4$—Al_2O_3 (20wt% I) exhibit the same Ea values, although the r_A of the first is approximately three times greater than that of the second one.

Table 2

Apparent activation energies (E_a) and logarithm of Arrhenius Constants (Log A) of Styrene and α-Methylstyrene on catalysts with Ni at 20 wt% and Series I

CATALYST	Styrene		α-Methylstyrene	
	E_a[a]	Log A[b]	E_a[a]	Log A[b]
Ni/$AlPO_4$	62.1	6.062	35.5	1.245
Ni/$AlPO_4$—SiO_2	44.1	3.095	22.1	−0.887
Ni/$AlPO_4$—Al_2O_3	62.1	5.561	36.8	1.161

[a] kJ. mol^{-2}

[b] $mol^{-1}.m_{Ni}^{-2}$

Certainly, the $AlPO_4$—Al_2O_3 support displays a main pore diameter ($\bar{d}$) of 3.0 nm, while the $AlPO_4$ support displays a much higher main pore diameter, 4.0 — 12.0 nm,[5]. So, in the Ni/$AlPO_4$ catalyst the proportion of accessible active sites on the nickel surface is higher than in the Ni/$AlPO_4$—Al_2O_3 catalyst, because the penetration of styrene and α-methylstyrene molecules into the pores of the last support encounters more hindrance.

Methyl substituent effects

As it is shown in table 1, the values of r_A in the hydrogenation of the olefinic double bond in styrene and α-methylstyrene were nearly similar. Apparently, this indicates that methyl substitution does not affect the hydrogenation of the olefinic double bond, contrary to what happened[1] in the hydrogenation of the carbonylic double bond in methyl ketones, where its reduction was not possible because of the influence of the methyl substitution. However, it should be noted in table 2 that the E_a values in the hydrogenation of styrene were about two times larger than in α-methylstyrene.

Therefore, we see that the methyl group promotes the activation of the olefinic double bond by an inductive effect. But according to such a variation of E_a, the values of r_A for the α-methylstyrene might be rather higher than those of styrene. Only the influence of an important steric effect may explain the similarity between the r_A values on styrene and α-methylstyrene. This steric effect may reside either in a hindered penetration of the reactant molecules by a *sieve effect* or in a hindered adsorption of the olefinic double bond on the active sites, by interaction between the methyl group and the surface of the metal.

One may speculate about the r_A values that might be obtained in the α-methylstyrene hydrogenation if the steric effects of the methyl group were negligible. Thus, from the Arrhenius equation :

$$\lg r_A = \lg A - \frac{\lg e}{RT} E_a$$

and by using the E_a values from MS and the values of lg A, from S both of these values in table 2, we shall obtain the values of the theoretical areal rate, free from steric effects, that we indicate as r^t_A, for each catalyst.

On the other hand, parting from this assumption, we may apply the Arrhenius equation :

$$\lg r_A(\mathrm{S}) = \lg A(\mathrm{S}) - \frac{\lg e}{RT} E_a(\mathrm{S})$$

$$\lg r^t_A(\mathrm{MS}) = \lg A(\mathrm{S}) - \frac{\lg e}{RT} E_a(\mathrm{MS})$$

and combining both expressions :

$$\lg \frac{r^t_A(\mathrm{MS})}{r_A(\mathrm{S})} = \frac{\lg e}{RT} \left[E_a(\mathrm{S}) - E_a(\mathrm{MS})\right]$$

where the factor $\frac{\lg e}{RT}$ has the usual meaning, an its value at 298 K is $0.176 \times 10^{-3} \times \mathrm{mol\ J^{-1}}$, and (S) and (MS) refers to styrene and α-methylstyrene.

The term of the right side was obtained by Tanaka [14,15] as a Catalyst Dependent Constant (K), in the expression of the relative reactivity in a competitive reaction :

$$\lg (R_2/R_1) = \sigma^{**} + K$$

where σ^{**} is related to the substrate size and K to the catalyst property.

Thus, it is also possible to obtain the $r^t_A(\mathrm{MS})$ values from the values of K and r_A of the styrene by the expression

$$r^t_A(\mathrm{MS}) = r_A(\mathrm{S})\, 10^K.$$

The r^t_A values thus obtained are summarized in table 3, where the percentage of difference between the theoretical and real r_A values is also indicated. We think that, as a rough approximation, it is possible to set that percentage as the influence of the steric effect on the lowering of the areal rate. Likewise, these percentages may be representative of the percentage of the active sites where the adsorption of the α-methylstyrene molecules is permitted.

Table 3

Theoretical and real areal rates (mol s^{-1} m^{-2}) in the hydrogenation of α-Methylstyrene on catalysts with Ni at 20wt %, Series I and at 298 K

CATALYST	r_A^t	r_A	% of Difference
$Ni/AlPO_4$	0.656	10.0×10^{-2}	1.52×10^{-3}
$Ni/AlPO_4-SiO_2$	0.158	16.5×10^{-2}	10.40×10^{-3}
$Ni/AlPO_4-Al_2O_3$	0.119	$4{\cdot}2 \times 10^{-2}$	3.49×10^{-3}

According to the negligible differences among these percentages, we may exclude any support effect related to its porosity that affects the penetration of the reactant molecules toward the active sites as the main cause of the methyl substituent effect upon the hydrogenation rate.

We also point out the conclusion that the steric effects of the methyl group must be explained largely, if not exclusively, by a steric hindrance to adsorption on metal surface, so that the catalyst surface may be more densely populated by styrene molecules than by α-methylstyrene molecules.

Certainly, as may be seen from the results in table 3, the steric effects of the methyl group hinder the adsorption of α-methylstyrene molecules in a very high proportion of the active sites, where the adsorption of styrene molecules is possible. However, the entirely hindered hydrogenation of the carbonylic double bond by the substitution effects of a methyl group, [1] under the present conditions, leads us to the conclusion that the adsorption of a α-methyl substituted carbonylic double bond is more sensitive to the steric substituent effects than a α-methyl substituted olefinic double bond.

REFERENCES

[1] J. M. Campelo, A. Garcia, D. Luna and J. M. Marinas, Part I, Accepted for publication to *Bull. Soc. Chim. belges.*

[2] A. Alberola and J. M. Marinas, *An. Quim.*, **65**, 1007 (1969).

[3] J. M. Campelo, J. M. Marinas and R. Perez-Ossorio, in "Proc. 5th Ibero-American Symposium on Catalysis", *Rev. Port. Quim.*, **18**, 84 (1978).

[4] C. Jimenez, J. M. Maronas, R. Perez-Ossorion and J. V. Sinisterna, *An. Quim.*, **73**, 1164 (1977).

[5] J. M. Campelo, D. Luna and J. M. Marinas, *Rev. Roumaine Chim.*, **26**, 867 (1981).

[6] R. L. Moss, "Experimental Methods in Catalytic Research" Vol. 2, Academic Press, New York, 1976, Ch. 2, p. 43.

[7] J. M. Campelo, D. Luna and J. M. Marinas, *Afinidad*, **38**, 299 (1981).

[8] G. Delmai-Imelik, C. Leclerq and I. Mutin, *J. Microscopie*, **20**, 123 (1974).

[9] R. Baltzly, *J. Org. Chem.*, *41*, 920 (1976).

[10] J. M. Campelo, A. Garcia, D. Luna and J. M. Marinas, *React. Kinet. Catal. Lett.*, in press.

[11] M. J. Ledoux and F. G. Gault, *J. Catalysis*, **60**, 15 (1979).

[12] M. Boudart, *Adv. Catal. Relat. Sub.*, **20**, 153 (1969).

[13] M. A. Vannice and R. L. Garten, *J. Catalysis*, **63**, 255 (1980).

[14] T. Chiara and K. Tanaka, *Bull. Chem. Soc. Japan*, **52**, 507 (1979).

[15] Idem., *Ibid.*, **52**, 512 (1979).

Revue Roumaine de Chimie **30**, *5*, 435–438 (1985)

HIGH-PRESSURE LIQUID CHROMATOGRAPHIC ANALYSIS OF SOME CEPHALOSPORINS

I. M. POPA, GH. IONESCU and A. TARHON

Department of Physical Chemistry, Polytechnic Institute Iaşi, 6600,
Splai Bahlui, Romania

Received May 7, 1984

In the present paper the separation of cephalosporin C and 7-amino-cephalosporanic acid in both synthetic mixtures and culture liquids by means of HPLC is reported. The separations were performed with different systems of constant composition mobile phase as well as in solvent gradients.

1. INTRODUCTION

For more than thirty years antibiotics have been used in the therapy of certain bacterial and fungic infections. For their administration it is important to know the concentration within the organism. Besides, during the biosynthesis process it is necessary to dose these antibiotics and byproducts accompanying them.

The high-pressure liquid chromatography proved to be a rapid and precise method also for the identification and dosage of cephalosporins. Several papers published after 1975 reported the separation of some semi-

Table 1

Cephalosporins which can be quantitatively analyzed in biological fluids with liquid chromatography*

Cephalosporins	References
Cephalotin	1–5
Cephalexin	6, 7
Cephalozin	8
Cephalorindine	9
Cephradine	6
Cephoxitin	3
Cefuroxime	10–11
Cefamandole	12
Cefatrizine	13

* Literature references are listed for each.

synthetic cephalosporins by this method showing two advantages in comparison with conventional chromatography. First, mobile phases are "watery" and hence aqueous samples may be injected directly into the chromatograph. Second, dry metabolites which are usually more polar and thus more easily excreted from the body, elute before the parent drug.

2. EQUIPMENT AND EXPERIMENTAL

The chromatographic separations were carried out at room temperature by means of a Model-5020 high-pressure liquid chromatograph, provided with a UV detector of the 254 nm wavelength supplied by Varian (USA). The column of the 250 × 4.7 mm size filled with octadecylsilan was of the Micropak MCH-10 type. The chromatograms were performed at a mobile phase flow rate of 1—1.5 mL/min by using different solvent systems, at both constant compositions of the mobile phase and the solvent gradient. The paper rate was of 0.25 cm/min and the injected sample volume 10 μL.

3. RESULTS AND DISCUSSIONS

Both synthetic mixture and culture liquid containing cephalosporin C, 7-aminocephalosporanic acid and two of the principal degradation products of the structures I, II were submitted to separation under different conditions :

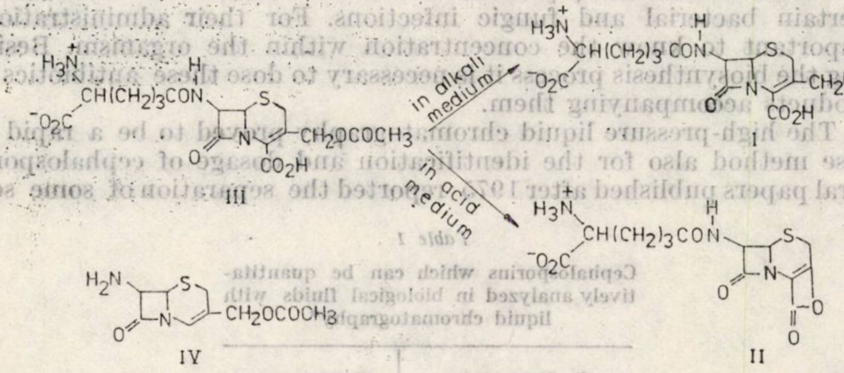

The chromatogram of the compounds I, II, III given in Fig. 1, was recorded with a synthetic mixture containing 2 mg/ml of compound III, by using water 100% as a mobile phase.

The chromatogram in Fig. 2 represents the separation of the compounds III and I by using a 0.25 M aqueous boric acid solution brought to pH = 7 by means of 0.1 M NaOH solution, as a mobile phase.

In Fig. 3 the chromatogram of 7-aminocephalosporanic acid and the compounds I, II with methanol-buffer solution of aqueous 0.05 M KH_2OP_4, as mobile phase is given.

The mobile phase composition was 100% buffer solution at time zero and then modified at 2% /min. methanol for 10 minutes.

In Fig. 4 are given the chromatograms of the compounds I, II, III in the culture liquid.

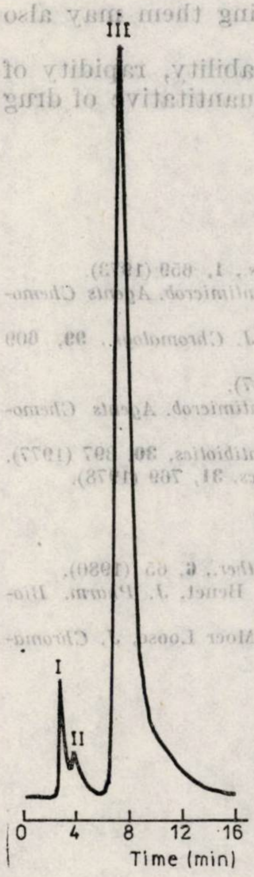

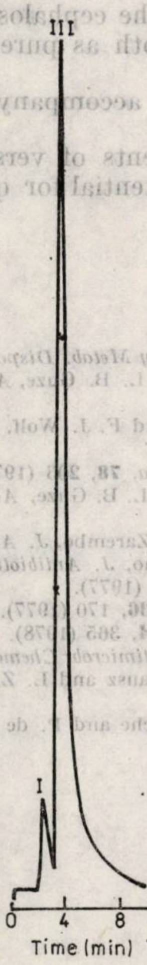

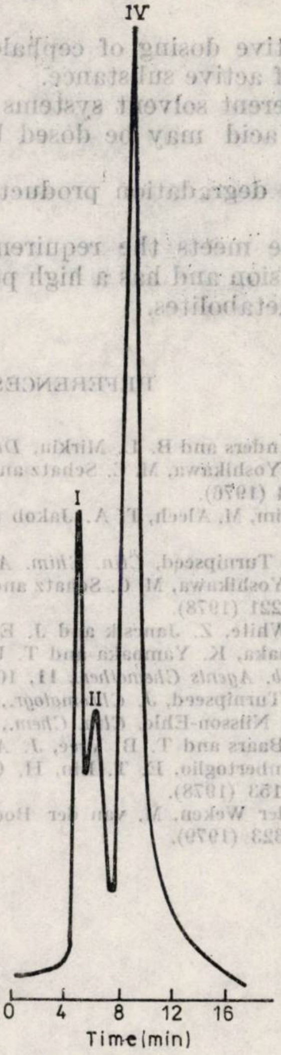

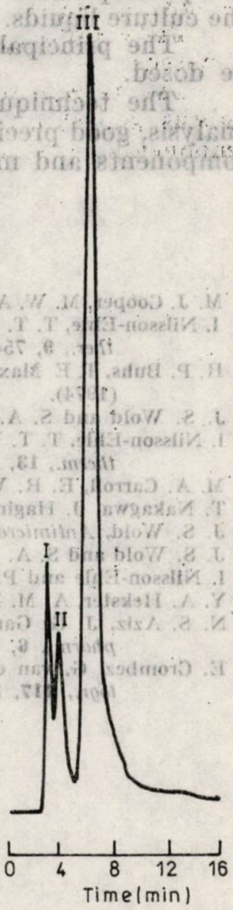

Fig. 1 — The chromatogram of I, II, III compounds in synthetic mixture: (mobile phase 100% H_2O; flow 1 mL/min.; sensibility 0.16 AUFS; retention times: I—2.3 min; II—3.2 min; III—6.8 min)

Fig. 2 — The chromatogram of I, III compounds in synthetic mixture: (mobile phase 0.25 M boric acid in water solution; flow 1 mL/min; sensibility 0.64 AUFS; retention times: I—2.3 min; III—3.8 min)

Fig. 3 — The chromatogram of I, II, IV compounds in synthetic mixture: (mobile phase methanol-buffer solution 0.05 M KH_2PO_4; flow 0.5 mL/min; sensibility 0.32 AUFS; retention times: I—6.0 min, II—7.1 min, IV—9.7 min).

Fig. 4 — The chromatogram of I, II, III compounds in the culture liquid: (mobile phase methanol-buffer solution 0.05 M KH_2PO_4; flow 1 mL/min; sensibility 0.32 AUFS; retention times: I—2.3 min; II—3.8 min, III—6.8 min)

4. CONCLUSIONS

The quantitative dosing of cephalosporins is possible for amounts below 0.1 mg/mL of active substance.

By using different solvent systems the cephalosporin C and 7-aminocephalosporanic acid may be dosed both as pure compounds and in the culture liquids.

The principal degradation products accompanying them may also be dosed.

The technique meets the requirements of versability, rapidity of analysis, good precision and has a high potential for quantitative of drug components and metabolites.

REFERENCES

[1] M. J. Cooper, M. W. Anders and B. L. Mirkin, *Drug Metab. Dispos.*, **1**, 659 (1973).

[2] I. Nilsson-Ehle, T. T. Yoshikawa, M. C. Schatz and L. B. Guze, *Antimicrob. Agents Chemother.*, **9**, 754 (1976).

[3] R. P. Buhs, T. E. Maxim, M. Aleeh, T. A. Jakob and F. J. Wolf, *J. Chromatogr.*, **99**, 609 (1974).

[4] J. S. Wold and S. A. Turnipseed, *Clin. Chim. Acta*, **78**, 203 (1977).

[5] I. Nilsson-Ehle, T. T. Yoshikawa, M. C. Schatz and L. B. Guze, *Antimicrob. Agents Chemotherm.*, **13**, 221 (1978).

[6] M. A. Carroll, E. R. White, Z. Jancsik and J. E. Zarembo, *J. Antibiotics*, **30**, 397 (1977).

[7] T. Nakagwa, J. Haginaka, K. Yamoaka and T. Uno, *J. Antibiotics*, **31**, 769 (1978).

[8] J. S. Wold, *Antimicrob. Agents Chemother.*, **11**, 105 (1977).

[9] J. S. Wold and S. A. Turnipseed, *J. Chromatogr.*, **136**, 170 (1977).

[10] I. Nilsson-Ehle and P. Nilsson-Ehle, *Clin. Chem.*, **24**, 365 (1978).

[11] Y. A. Hekster, A. M. Baars and T. B. Vree, *J. Antimicrob. Chemother.*, **6**, 65 (1980).

[12] N. S. Aziz, J. G. Gambertoglio, E. T. Lin, H. Grausz and L. Z. Benet, *J. Pharm. Biopharm.*, **6**, 153 (1978).

[13] E. Crombez, G. van der Weken, M. van der Boosche and P. de Moer Loose, *J. Chromatogr.*, **117**, 323 (1979).

NOTE POUR LES AUTEURS

La Revue Roumaine de Chimie publie des articles en anglais, français, russe, allemand ou espagnol. Les auteurs sont priés d'envoyer des articles et des comptes rendus inédits.

Les manuscrits seront dactylographiés à double interligne. La bibliographie, les tableaux et la légende des figures seront placés après le texte.

Si l'article fait partie d'une série numérotée, la partie précédente sera donnée comme première référence.

Chaque article sera précédé d'un résumé comprenant quinze lignes au maximum.

Les références bibliographiques dans le texte seront faites par des exposants sans parenthèses et paraitront à la fin de l'ouvrage.

Les publications périodiques mentionées dans la bibliographie seront présentées suivant les prescriptions internationales : le nom de l'auteur précédé de l'initiale du prénom, le titre du périodique abrégé conformément à « Chemical Abstracts » et souligné par une ligne, le numéro du tome indiqué par des chiffres arabes et souligné par deux lignes, suivi de la première page de l'article : à la fin, l'année de la parution sera placée entre parenthèses. Le numéro de la revue ne sera pas indiqué si les pages du volume sont numérotées consécutivement.

Les textes des livres ou traités incluciont : le nom des auteurs, précédés de l'initiale du prénom, le titre du livre entre guillemets et sans être souligné, le numéro du tome précédé par l'abréviation « vol. » (ou « Bd. »), le numéro de l'édition, les éditions (the publisher), la localité de la parution du livre, l'année de la parution et la page de la référence précédée(s) par l'abréviation « p » (ou « S »).

Les brevets seront indiqués comme suit : l'auteur ou la firme, le pays et le numéro du brevet, la date de la revue (*Chem. Abstr.*). Par. ex. : M. Jones (to Union Carbide Co.). Brit. Pat. 610 238, 2 Sept. 1959 : cf. *Chem. Abstr.*, **54**, 12808 (1960).

Si la référence n'a pas été lue en original, on indiquera aussi la revue de références consultée.

Les diagrammes seront tracés à l'encre de Chine sur papier calque. Les tableaux et les figures (en nombre strictement nécessaire), ainsi que les courbes dans les figures seront numérotés par des chiffres arabes. Leur explication sera donnée dans la légende des figures. Prière de ne pas inscrire les mêmes données dans les tableaux et les figures. Chaque tableau aura un titre. On indiquera dans le texte la place approximative des tableaux et des figures. Les formules chimiques seront incluses dans le texte ; en outre, elles seront transcrites sur papier calque, à l'encre de Chine.

Les auteurs sont priés d'indiquer les caractères italiques (en soulignant les lettres au crayon), ainsi que toute autre caractère spécial : les préfixes *ortho*, *meta*, *para*, *cis*, *trans*, etc., seront soulignès pour indiquer leurs caractères italiques, et ne seront jamais écrits avec des majuscules.

Aucune correction à la main ne sera admise sur le manuscrit. Les corrections seront frappées à la machine. Les lettres grecques ou d'autres symboles spéciaux seront insérés à la main à l'encre clairement.

Le manuscrit sera signé par l'auteur.

Le titre courant aura 50 lettres au maximum.

L'entière responsabilité du contenu des articles appartient aux auteurs.

Sur demande on peut obtenir une note plus complète.

PRINTED IN ROMANIA

TRAVAUX PARUS AUX ÉDITIONS DE L'ACADÉMIE DE LA RÉPUBLIQUE SOCIALISTE DE ROUMANIE

1985 MAJ 12

GH. MARCU, **Chimia compuşilor coordinativi**, 1984, 415 p.

E. CORDOŞ, C. MANOLIU, **Spectrometria de absorbţie şi fluorescenţă atomică**, 1984, 178 p.

C. BODEA, **Tratat de biochimie vegetală**, p. II, vol. 5, 1984, 438 p.

ELENA CEAUŞESCU, **Cercetări în chimia şi tehnologia polimerilor**, 1983, 519 p.

N. ASANDEI, A. GRIGORIU, **Chimia şi structura fibrelor**, 1983, 395 p.

N. IONESCU, M. CĂLDĂRARU, **Oxidarea catalitică a olefinelor inferioare**, 1983, 178 p.

C. CAŞCAVAL, **Studiul polimerilor prin piroliză şi cromatografie de gaze**, 1983, 220 p.

C. I. SIMIONESCU, F. DENEŞ, **Originea vieţii**, 1983, 110 p.

C. BODEA (éditeur), **Tratat de biochimie vegetală**, II, Tome IV, 1982, 408 p.

I. G. MURGULESCU, RODICA VÎLCU, **Introducere în chimia fizică. Vol. III. Termodinamica chimică**, 1982, 624 p.

ELENA JERCAN, **Analiza cromatografică**, 1982, 286 p.

I. G. MURGULESCU, J. PĂUN, **Introducere în chimia fizică. Vol. I 3, Nucleul atomic, reacţii nucleare, particule elementare**, 1982, 606 p.

ELENA CEAUŞESCU, **Noi cercetări în domeniul compuşilor macromoleculari**, 1981, 536 p.

I. G. MURGULESCU, TATIANA ONCESCU, E. SEGAL, **Introducere în chimia fizică. Vol. II. 2. Cinetică chimică şi cataliză**, 1981, 1024 p.

V. DRĂGUŢAN, A. T. BALABAN, M. DIMONIE, **Metateza olefinelor şi polimerizarea prin deschidere de inel a cicloolefinelor**, 1981, 254 p.

LYDIA-MARIA VAICUM, **Epurarea apelor uzate cu nămol activ. Bazele biochimice**, 1981, 218 p.

I. GĂLĂŢEANU, **Procese şi metode radiochimice în energetica nucleară**, 1981, 234 p.

O. IORDACHE, **Procese polistocastice aplicate la fenomenele de transfer**, 1981, 186 p.

CR. SIMIONESCU, VALERIA GORDUZA, **Polimeri biocompatibili şi biologic activi**, 1980, 479 p.

ELENA CEAUŞESCU, **Polimerizarea stereospecifică a izoprenului**, 1979, 307 p.

CONST. GH. MACAROVICI, **Analiza chimică cantitativă anorganică**, 1979, 457 p.

M. FLORESCU, **Metode ştiinţifice în dezvoltarea industriei chimice moderne**, 1979, 256 p.

A. T. BALABAN, I. GĂLĂŢEANU, G. GEORGESCU, LIGIA SIMIONESCU, **Compuşi marcaţi şi radiofarmaceutici cu aplicaţii în medicina nucleară**, 1979, 495 p.

I. G. MURGULESCU, E. SEGAL, **Introducere în chimia fizică, Vol. II. 1. Teoria molecular cinetică a materiei**, 1979, 1036 p.

S. STERNBERG, FL. DANEŞ, **Termodinamica chimică aplicată**, 1978, 400 p.

I. G. MURGULESCU, V. EM. SAHINI, **Introducere în chimia fizică. Vol. I. 2. Structura şi proprietăţile moleculelor**, 1978, 604 p.

I. ZUGRĂVESCU, MAGDA PETROVANU, **N-ylid chemistry**, coédition avec McGraw-Hill International Book Company, U.S.A., 1977, 396 p.

I. G. MURGULESCU, **Introducere în chimia fizică. Vol. I. 1. Atomi, molecule, legătură chimică**, 1976, 560 p.

ELENA CEAUŞESCU, **Research work on synthesis and characterization of macromolecular compounds. Contributions**, 1974, 251 p.

CR. SIMIONESCU, VIORICA RUSAN, V. POPA, **Chimia algelor marine**, 1974, 212 p., 1 pl.

ISSN 0035–4090

I.P. INFORMAŢIA, c. 1061

43 426

Lei 40

$ 80 (pour un abonnement annuel)

F 1103

04

ACADÉMIE DE LA RÉPUBLIQUE SOCIALISTE DE ROUMANIE

REVUE ROUMAINE DE CHIMIE

66

1985 JUL 2

MG

TOME 30

N° 6

Juin 1985

Rev. Roumaine Chim.

RRCHAX, **30**, *6*, p. 439–528 (1985), Bucarest

EDITURA ACADEMIEI REPUBLICII SOCIALISTE ROMÂNIA

ACADÉMIE DE LA RÉPUBLIQUE SOCIALISTE DE ROUMANIE

COMITÉ DE RÉDACTION

Rédacteur en chef :

I. G. MURGULESCU, membre de l'Académie de la République Socialiste de Roumanie

Rédacteurs en chef adjoints :

A. T. BALABAN et V. EM. SAHINI, membres correspondants de l'Académie de la République Socialiste de Roumanie

Collège de rédaction :

EM. BRATU, ELENA CEAUŞESCU, ECATERINA CIORĂNESCU-NENITZESCU, CR. SIMIONESCU, membres de l'Académie de la République Socialiste de Roumanie; P. SPACU, membre correspondant de l'Académie de la République Socialiste de Roumanie; M. BANCIU, M. D. GHEORGHIU, I. HAIDUC, D. I. MARCHIDAN, I. MOLDOVAN, G. NIAC et D. SĂNDULESCU

La Revue Roumaine de Chimie paraît 10 fois par an. Toute commande de l'étranger sera adressée à ROMPRESFILATELIA — sectorul Export-Import Presă, P.O. Box 12—201, télex 10376 presfi r Bucarest, Calea Griviţei nr. 64—66, Roumanie.

Les manuscrits, les livres et les revues proposés en échange, ainsi que toute correspondance seront envoyés à la rédaction.

REVUE ROUMAINE DE CHIMIE
125, Calea Victoriei, 79717 Bucarest, Roumanie, téléphone 50 76 80

EDITURA ACADEMIEI REPUBLICII SOCIALISTE ROMÂNIA
125, Calea Victoriei, 79717 Bucarest, Roumanie, téléphone 50 76 80

REVUE ROUMAINE DE CHIMIE

Tome 30, N° 6 Juin, 1985

CRISTOFOR I. SIMIONESCU, BOGDAN C. SIMIONESCU, SILVIA IOAN, MONICA LEANCĂ and CARMEN CHELARU, Plasma-induced polymerization. 12. Low conversion bulk homopolymerization of methyl methacrylate 441–445

GH. DRĂGAN and C. OPREA, Thermomechanical study of amorphous modifications in polyester fibers induced by isothermal annealing 447–452

GEORG GUTT, ŞTEFAN IVAŞCAN, SONIA GUTT and MIHAI GRAMATICU, On the material transport optimization in the electrodeposition of nickel (in German) 453–459

M. A. OMARA, A. A. ELBARBARY, N. ANWAR and S. ELKONI, 1,4-Diarylnaphthalenes. III. Action of Grignard Reagents on some 1,1,4-Triarylbuta-1,3-diene-2,3-dicarboxylic anhydrides and 1,4-diarylnaphthalene-2, 3-dicarboxylic anhydrides 461–466

ALBA A., ARAMENDIA M. A., BORAU V., JIMENEZ C. and MARINAS J. M., Acid-base and redox characteristics of Pd catalysts obtained by ion exchange 467–472

DELIA ISAC, M. MRACEC and Z. SIMON, Thermal and photochemical stability of diazoderivatives 473–481

ELENA VOLANSCHI, A. MISSIR and DIANA MUŞOIU, E.S.R. Spectral study of some polysubstituted thioureide anion radicals 483–489

M. TALABA and C. CALISTRU, Nitric decomposition process of phosphatic raw materials. I. Study on equilibrium of nitric decomposition process of phosphatic raw materials 491–497

I. I. ABD EL-GAWAD, A. M. KHALIL, O.M.O. HABIB and H. A. ETMAN, Synthesis and reactions of some new cyclic β-keto-anilides. Part. 1 . . . 499–505

ALI ALI KHALAF and ROYSTON M. ROBERTS, Modern Friedel-Crafts chemistry. X. Rearrangements accompanying Friedel-Crafts alkylation of benzene with isometric pentanols and pentenes 507–510

M. MITTAL, S. R. MALHOTRA, KEEMTI LAL and S. P. GUPTA, Rare earth chelates of disubstituted 2-hydroxy-acetophenones 511–516

N. H. PAIKE, Reactions of 2,4-pentanedionato complexes-bromination of bis (2,4-pentanedionato) Manganese (II) and tris(2,4-pentanedionato) Manganese (III) 517–524

R. CEA OLIVARES and L. CANTU, Synthesis of the first alkylated spirophosphazenes (in Spanish) 525–528

Rev. Roumaine de Chim. **30**, *6*, 439–528 (1985), Bucarest

Revue Roumaine de Chimie, **30**, *6*, 441–445 (1985)

PLASMA-INDUCED POLYMERIZATION. 12[1]
LOW CONVERSION BULK HOMOPOLYMERIZATION OF METHYL METHACRYLATE*

CRISTOFOR I. SIMIONESCU, BOGDAN C. SIMIONESCU,
SILVIA IOAN[a] MONICA LEANCĂ[a] and CARMEN CHELARU[a]

Department of Organic and Macromolecular Chemistry, Polytechnic Institute
of Jassy, 6600 Jassy, Romania. [a]"P. Poni" Institute of Macromolecular Chemistry.
6600 Jassy, Romania

Received July 25, 1984

Plasma-induced low conversion bulk homopolymerization of methyl metacrylate was studied at room temperature. Experimental data show that ultrahigh molecular weight polymers are obtained and that the reaction can be directed to yield very low polydispersity compounds. Some features of plasma-induced process are underlined, as well as the "living" radical character of the polymerization mechanism.

INTRODUCTION

In some previously published papers, plasma-induced polymerizations and copolymerizations were reported. [1–5] Experimental data showed that a "living" radical mechanism of polymerization has to be considered [6,7] to explain this new approach to polymer synthesis. Some results [8,9] pointed out the possibility to obtain uniform molecular weigth ("monodisperse") polymers and copolymers through this polymerization method.

The present paper is concerned with low conversion plasma-induced bulk homopolymerization of methyl methacrylate (MMA) in an attempt to obtain more data on this process already investigated by Johnson et al.,[10] and to direct the synthesis towards very low polydispersity ultrahigh molecular weight polymers.

EXPERIMENTAL

The experimental procedure used of study the plasma-induced polymerization of MMA was essentially identical to that already reported in this series of papers. The monomer was purified by vacuum distillation under nitrogen, kept on $CaCl_2$ for 24 hours, redistilled, dried on calcium hydride, distilled and used immediately after. The monomer was then introduced in polymerization ampoules, degassed by repeated freeazing and thawing at $10^{-3}-10^{-4}$ Torr, and finally frozen in liquid nitrogen and sealed. Electrical discharges were then operated between two electrodes situated on each ampoule at 1.5 and 3.5 cm from the sample and coupled to a high frequency discharge generator (frequency 2.5 MHz, power 100 W). Two series of experiments were performed, the discharge durations being of 60 seconds and 20 seconds, respectively. Following initiation, the ampoules were kept in dark, at room temperature, for prescribed periods of time, then opened, diluted with benzene and precipitated in methanol.

---

* Part of an invited lecture presented at the IVth Microsymposium on Radical Polymerization, Smolenice, CSSR, April 26–30, 1982.

No mechanical stirring was applied to solutions at any stage, to prevent shear degradation.

Light scattering technique was used to determine weight-average molecular weights ($\overline{M}_w$). Light scattering studies were performed on a P.C.L. Peaker apparatus, at 27°C, in the angular range from 30° to 130°, at 4360 Å; CCl_4 was used as solvent (theta solvent at 27°C according to Fox[11]). Refractive index increments were determined on a Zeiss interferometer, for the same wavelengths and temperatures.

$\overline{M}_w$ values were determined from Zimm plots, as well as according to Berry's method,[12] the extrapolations being made only for angles up to 70°. The experimental errors in the determination of $\overline{M}_w$ were about $\pm 10\%$ for $\overline{M}_w$ values up to $2 \cdot 10^7$ and increased up to $\pm 16\%$ for higher molecular weights.

Light scattering data were also used to determine number-average molecular weights $\overline{M}_n$) according to Miyaki et al.[13], by using the equation

$$yu^2 = (-2/A^2 \cdot \overline{M}_n) + (2/A)u$$

where $y = \overline{M}_w P(\theta) = (R_\theta/Kc)_{c=0}$, $P(\theta)$ is the particle scattering function, R_θ is the Rayleigh intensity, $A = \langle S_0^2 \rangle / M$, ($\langle S_0^2 \rangle$ being the unperturbed mean-square radius of gyration), $u = (4\pi/\lambda)^2 \sin(\theta/2)$, where λ is the wavelength of incident light in the solution.

As concerns the separation of the polymers obtained following the 60 sec. discharge, only those resulting up to 330 hours post-polymerization period are discussed in detail in the present paper. For longer periods of post-polymerization the molecular weight and yield of the polymer still increase, but the monomer — polymer solution becomes extremely viscous and the polymer dissolves very slowly, in time, even at elevated temperature, and only in very large amounts of benzene.

The microstructure of the polymers was determined by ^1H-NMR spectroscopy, the spectra being registered in $CDCl_3$ solutions on a JEOL—C60 HL spectrometer operating at 60 MHz.

RESULTS AND DISCUSSION

Plasma-induced polymerization of MMA has been previously studied by different authors. Thus, Johnson et al.[10] suggest that in the presence of a plasma, monomer vapor is converted into a substance which can later serve as an initiator for polymerization of liquid monomer. Kuzuya et al.[14] present some evidences that operating a low-pressure plasma generated by discharges in a vapor of MMA may produce an allylic radical able to act as an active species to initiate the polymerization of the monomer. All authors accept that the chain propagation during polymerization proceeds via a free radical mechanism.

Figure 1a presents the effect of post-polymerization duration on the $\overline{M}_w$ of the polymers, for both 60 sec. (curve 1) and 20 sec. (curve 2) discharge. The slope of curve 1 increases after a certain period of time, starting from an about 8% conversion (see Figure 1b). One can consider this behaviour as being due to both a self-acceleration process appearing as a consequence of the important increase of the molecular weight, as observed in the low conversion bulk polymerization of styrene[15] and to the intervention of a number of recombinations between the growing macroradicals.

Figure 1b presents the progress of plasma-induced polymerization of MMA. The polymerization rate values were calculated to be about $8.0 \cdot 10^{-7}$ mol$\cdot$L$^{-1}\cdot$s^{-1} (curve 1, 60 sec. discharge) and about $3.3 \cdot 10^{-7}$ mol$\cdot$L$^{-1}\cdot$s^{-1} (curve 2, 20 sec. discharge initiation). The extent of MMA conversion by thermal polymerization, in the absence of plasma initiation, is given by curve 3; the polymerization rate is about $3.9 \cdot 10^{-8}$ mol$\cdot$ $\cdot$L$^{-1}\cdot$s^{-1}. These low values are in agreement with those reported by Johnson et al.,[10] the quoted paper giving, for doubly distilled MMA, a polymerization rate value of about $4.0 \cdot 10^{-6}$ mol$\cdot$L$^{-1}\cdot$s^{-1} and for the polymerization of MMA following the cryogenic purification of the monomer, a rate of about $1.1 \cdot 10^{-6}$ mol$\cdot$L$^{-1}\cdot$s^{-1}. The rate of thermal polymerization of MMA is very low and in agreement with that reported in the literature.[16,17]

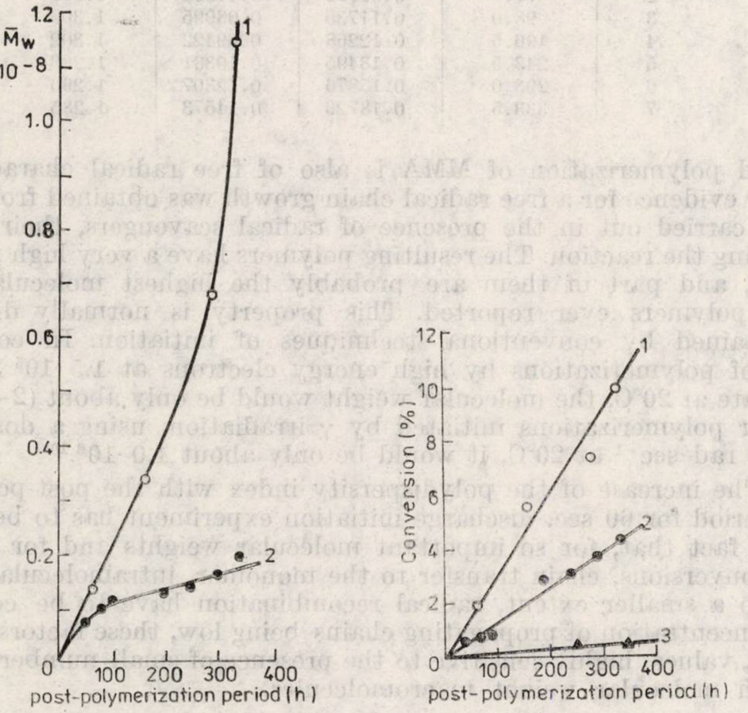

Fig. 1. — Dependence of $\bar{M}_w$ (a) and of monomer conversion (b) on post-polymerization period: 1 — 60 sec. discharge; 2 — 20 sec. discharge; 3 — pure thermal polymerization. The experiments were performed with two portions of MMA, with different purity.

Data concerning the polydispersity of the polymers yielded by the plasma-induced technique are presented in Table 1.

The microstructure of the obtained polymers was found to be in good agreement with the tacticity distribution for radical initiated poly(methyl methacrylate), thus appearing that the propagation of palsma-

Table 1

Molecular weight and polydispersity data

Sample	Post-polym. period (h)	$\overline{M}_n \cdot 10^{-8}$	$\overline{M}_n \cdot 10^{-8}$	$\overline{M}_w/\overline{M}_n$
60 sec. discharge initiation				
1	67.5	0.13495	0.09245	1.455
2	161.5	0.33738	0.20165	1.673
3	281.5	0.67476	0.37185	1.814
4	330.0	1.15674	0.48351	2.392
20 sec. discharge initiation				
1	44.5	0.07497	0.05418	1.384
2	77.5	0.09996	0.07331	1.365
3	98.0	0.11735	0.08995	1.305
4	196.5	0.12268	0.09422	1.302
5	243.5	0.13495	0.10381	1.299
6	293.0	0.15876	0.12307	1.290
7	333.5	0.18726	0.14573	1.285

induced polymerization of MMA is also of free radical character. Yet further evidence for a free radical chain growth was obtained from experiments carried out in the presence of radical scavengers, their presence inhibiting the reaction. The resulting polymers have a very high molecular weight, and part of them are probably the highest molecular weight MMA polymers ever reported. This property is normally difficult to be obtained by conventional techniques of initiation. In comparable cases of polymerizations by high energy electrons at $1.5 \cdot 10^5$ rep. total dose rate at 20°C, the molecular weight would be only about $(2-3) \cdot 10^6$,[18] and for polymerizations initiated by γ irradiation, using a dose rate of $2 \cdot 10^{-2}$ rad$\cdot$sec^{-1} at 20°C, it would be only about $1.0 \cdot 10^6$.[19]

The increase of the polydispersity index with the post-polymerization period for 60 sec. discharge initiation experiment has to be assigned to the fact that, for so important molecular weights and for relatively high conversions, chain transfer to the monomer, intramolecular transfer and, to a smaller extent, radical recombination have to be considered. The concentration of propagating chains being low, these factors influence the $\overline{M}_w$ values, highly sensitive to the presence of small number fractions of high molecular weight macromolecules.

For 20 sec. discharge experiment and low conversion, the polydispersity decreases slowly, but regularly, with the increase of the post-polymerization period. The conversion and molecular weight are less im-portant. Immediately following the discharge — which generates a smaller number of primary radicals as compared to the 60 sec. discharge — part of the radicals recombine, so that only a very limited number of active species become growing macroradicals. As a consequence, with the increase of medium viscosity, diffusion processes become more and more difficult. Both disproportionation — primary mode of termination of MMA polymerization is by disproportionation, as shown by Bevington et al.[20] and by Bamford and Jenkins [21] — and recombination of isolated macroradicals are negligible. The molecular weights of the resulting polymers are almost exclusively controlled by chain transfer reactions, as in the case of thermal polymers,[22] and these reactions have low efficiency at room temperature.

Both peroxides and molecular oxygen influence the rate of MMA radical polymerization.[23] This evidence explains the differences observed on the progress of plasma-induced ploymerization of MMA between the two experiments (polymerization rate values of about $8.0 \cdot 10^{-7}$ mol $\cdot L^{-1} \cdot s^{-1}$ and $3.3 \cdot 10^{-7}$ mol $\cdot L^{-1} \cdot s^{-1}$ for the two discharge times, respectively). Each experiment was performed with highly purified monomer, but the portion used for the 20 sec. discharge one was repeatedly vacuum purified. Thermal polymerization curve was also obtained for ultrapure MMA.

CONCLUSIONS

The present results show that plasma-induced bulk polymerization of MMA yields ultrahigh molecular weight polymers (e.g., in excess of ten millions). Propagation reaction occurs via a free radical mechanism. Both conversion and molecular weight increase with post-polymerization period. For small discharge initiation durations, the polydispersity of the samples decreases in time, this arguing for the "living" radical character of the process.

REFERENCES

[1] Part 11. C. I. Simionescu and B. C. Simionescu, *Chem. Zvesti*, **37**, 685 (1983).
[2] B. C. Simionescu, A. Natansohn, M. Leancă, C. Ananiescu and C. I. Simionescu, *Polym. Bull.*, **3**, 247 (1980).
[3] B. C. Simionescu, A. Natansohn and C. I. Simionescu, *Polym. Bull.*, **3**, 809 (1980).
[4] B. C. Simionescu, M. Leancă, C. Ananiescu and C. I. Simionescu, *Polym. Bull.*, **3**, 437 (1980).
[5] B. C. Simionescu, A. Natansohn, M. Leancă, C. Ananiescu and C. I. Simionescu, *Polym. Bull.*, **4**, 569 (1981).
[6] C. I. Simionescu, B. C. Simionescu, M. Leancă and C. Ananiescu, *Polym. Bull.*, **5**, 61 (1981).
[7] C. I. Simionescu, S. Petrovan and B. C. Simionescu, *Eur. Polym. J.*, **19**, 1005 (1983).
[8] C. I. Simionescu, B. C. Simionescu and S. Ioan, *Makromol. Chem., Rapid Commun.*, **4**, 549 (1983).
[9] C. I. Simionescu and B. C. Simionescu, *Pure Appl. Chem.*, **56**, 427 (1984).
[10] D. R. Johnson, Y. Osada, A. T. Bell and M. Shen, *Macromolecules*, **14**, 118 (1981).
[11] T. G. Fox, *Polymer*, **3**, 111, (1962).
[12] C. G. Berry, *J. Chem. Phys.*, **44**, 4550 (1966).
[13] Y. Miyaki, Y. Einaga and H. Fujita, *Macromolecules*, **11**, 1180 (1978).
[14] M. Kuzuya, K. Kamiya, T. Kawaguchi and T. Okuda, *J. Polym. Sci., Lett. Ed.*, **21**, 509 (1983).
[15] B. C. Simionescu, M. Leancă, S. Ioan and C. I. Simionescu, *Polym. Bull.*, **4**. 415 (1981).
[16] G. M. Burnett and G. L. Ducon, *Makromol. Chem.*, **51**, 154 (1962).
[17] C. Walling and E. R. Briggs, *J. Am. Chem. Soc.*, **68**, 1141 (1946).
[18] T. G. Majury, *J. Polym. Sci.*, **15**, 297, (1955).
[19] A. Chapiro, "Radiation Chemistry of Polymeric Systems", Interscience, New York, 1962.
[20] J. C. Bevington, H. W. Melville and R. P. Taylor, *J. Polym. Sci.*, **12**, 449 (1954).
[21] C. H. Bamord and A. D. Jenkins, *Nature*, **176**, 78 (1955).
[22] M. Stickler and G. Meyerhoff, *Polymer*, **22**, 928 (1981).
[23] C. E. Barnes, *J. Am. Chem. Soc.*, **67**, 217 (1945).

Revue Roumaine de Chimie, **30**, *6*, 447–452 (1985)

THERMOMECHANICAL STUDY OF AMORPHOUS MODIFICATIONS IN POLYESTER FIBERS INDUCED BY ISOTHERMAL ANNEALING

GH. DRĂGAN* and C. OPREA**

* Institute of Chemical Research, ICECHIM–CCF, Spl. Independenţei 202,
Bucharest 77208, Romania
** Textile Research Center, CIMIC, Blvd. Ghencea 79, Bucharest, Romania

Received June 19, 1984

Thermomechanical behaviour of three representative types of polyester raw fibers obtained in similar conditions is established by using a laboratory made apparatus type. The applied method allows to control the initial length of the tested specimens under known load and applying a reproducible heating regime. The observed crystallization process in raw and annealed samples is expressed in normalized units and represented both in Arrhenius and universal representations according to the topoenergetic procedure recently established.

1. INTRODUCTION

Thermomechanical analysis seems to be the most appropriate test for oriented samples taking into account that the other ones strongly modify the initial morphology by preparation of the specimens. DSC measurements, for instance, usually performed on synthetic fibers as a rapid and sensitive test use specimens obtained by chopping the sample in small pieces. The results are not reproducible because of the variable heat transfer between the specimen and the temperature sensor and these are compromised by the chopping operation. On the other hand the oriented samples considered as end products have stored specific internal stresses along orientation direction during their processing and a complete behaviour can be revealed by a p–V–T diagram. A direct correlation between the orientation procedure and thermomechanical behaviour can be established,[1] so that this analysis becomes a rapid, reproducible, sensitive and fair control of a large series of end products. Unfortunately, although such devices are commercially available (Perkin Elmer, Du Pont, Setaram, Linseis, etc.) this kind of analysis is practically unreported in the present literature. In the present work the thermomechanical behaviour of a series of representative polyester fibers obtained on a versatile device built up in the laboratory are presented by using the topoenergetic procedure recently established on significant cases.[2] The values obtained could initiate the creation of a Data Bank in view of identifying and/or optimizing particular behaviours.

2. EXPERIMENTAL DETAILS

Materials. Three types of raw fibers obtained in similar conditions of spinning of monofilaments were considered, namely : polyethylene terephthalate Terom ^{R} grade (PETP) of 76 dtex; copolymer of PETP with dimethyl adipate (PETP/DMA) of 176 dtex, and copolymer of PETP with ethylene glycol (PETP/ETG) of 76 dtex. More structural data on these samples and on their processing conditions will be given in a future work. Samples of approximately 10 g in circular hank were isothermally annealed by oven in the temperature range of $T_{\rm ann}$: 100—200 °C all for 2 hours. The samples were located at room temperature in an aluminium box in which the air had been removed by purging dry nitrogen to minimize thermooxidation.

Thermomechanical apparatus called ATM-1 (Fig. 1a) is to be homologated for routine control in fiber industry. Figure 1 schematically shows it as composed of : a furnace (1) constantly thermostated at 300°C (or in general over T_m^0 of the crystalline phase [2]); a metallic block made of brass (2) in which the test specimens (3) are fixed at room temperature and at controlled initial length (l_0) under constant load (4). The variation of the specimen length is continuously measured by an inductive sensor (5) adapted to a tensometric bridge and to a recorder. The furnace, the metallic block and the sensor are vertically colinear, so that by thermal contact between 1 and 2 the temperature of the specimen reproducibly increases with approximately 20°C/minute. ATM-1 allows to simultaneously analyse four specimens by using the universal bridge of type N 2322/N 2314 (Bucharest-Romania) and the recorder Kutesz 1040/4 (MTA^R-Hungary) both having four channels. The bridge sensitivity was adjusted at 0.8 V per 1 millimetre of real deformation for all channels.

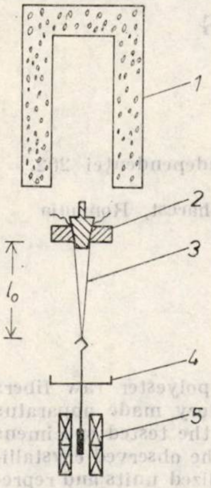

Fig. 1 — Scheme of the thermomechanical apparatus adapted for fiber analysis at initially imposed length of the specimen.

3. RESULTS AND DISCUSSION

Thermomechanical analysis is defined by the following imposed conditions : the initial length of the sample (l_0), the applied load (F) and the thermal regime expressed by the starting temperature and the heating rate. The applied load can be expressed as unitary stress, σ_0 in g/dtex by reporting F to the sample fineness. In Fig. 2 the thermograms of three series of samples containing raw and annealed specimens are reproduced starting at room temperature ($\simeq$ 25°C). The following facts can be noticed : (i) the shrinkage effect prevails and its amplitude decreases with $T_{\rm ann}$; (ii) the real starting temperature of this process corresponds for all three raw samples to T_g(PETP) = 70°C ; [3] and (iii) this starting temperature apparently increases (at constant sensitivity) with $T_{\rm ann}$, but T_g (PETP) has been proved as the real starting temperature by increasing the sensitivity. It is well known that the structural aspect of the isothermal annealing of raw fibers is mainly represented by the crystallization of "oriented" amorphous phases.[4] This process corresponds to an overall transformation process revealing the amorphous-crystalline coupling induced by the particular conditions of specimens synthesis.[5]

The experimental conditions for thermomechanical analysis correspond to standard conditions imposed by the topoenergetic procedure,[2] so that the process amplitude at saturation for a T_{ann} value can be expressed by the relative variation

$$\varepsilon(T_{\text{ann}}) = (|C_{eq}(T_{\text{ann}}) - C_q|/l_0) \times 100 \quad (\text{in } \%) \quad \mathbf{(1)},$$

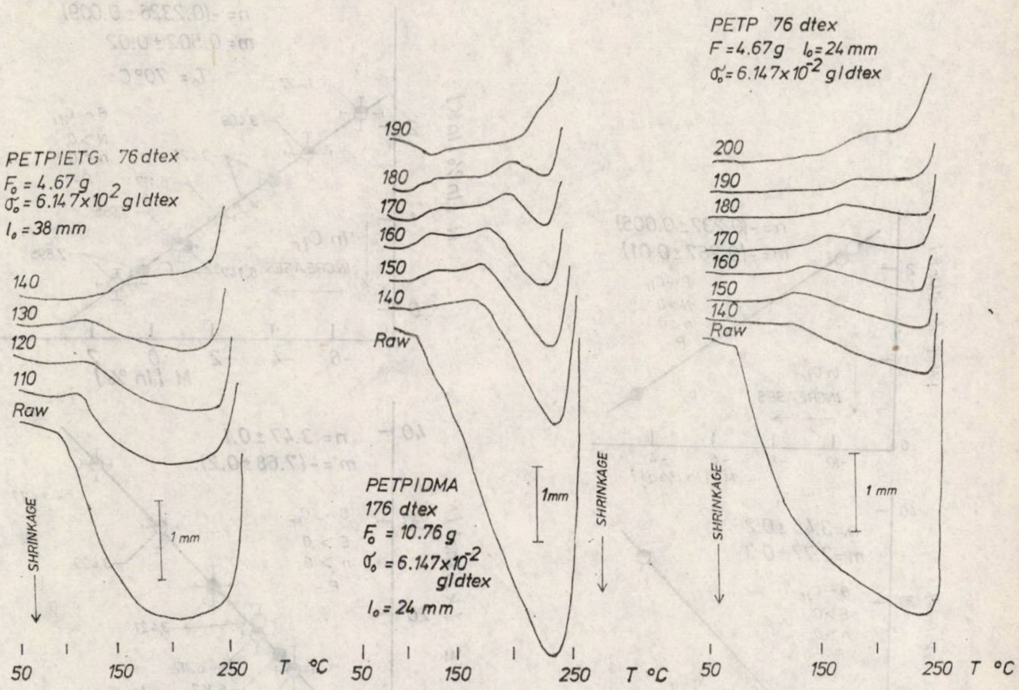

Fig. 2. — Typical thermograms obtained on the same sensitivity for the three series of raw and annealed samples. The figures represent the annealing temperatures.

where $C_{eq}(T_{\text{ann}})$ is the complete shrinkage of the annealed sample (with equilibrated morphology) and C_q — the complete shrinkage for the raw specimen (with quenched morphology). The crystallinity uptake of samples by annealing can be similarly expressed by the relative variation of degree of crystallinity (q), between the two morphologies :

$$\%\, q = (|q_{eq}(T_{\text{ann}}) - q_q|/q_q) \times 100 \qquad (\text{in } \%) \ (2).$$

In Fig. 3 the values of $\%q$ determined by wide angle x-ray scattering on raw and annealed specimens are represented according to Arrhenius and universal procedure ($T_0 = 70$°C). Both eigenvalues (1) and (2) are proportional to the transforming component (C_{tr}), so that the ontogenic values have the meaning given in Fig. 3 and generally established on a large number of particular standard transformation processes and measuring systems (see Table I in[6]). In both representations the process polarity is negative and this fact agrees with the most of ordering processes recently reviewed, especially with the solid-state crystallization revealed by other measuring systems.[2]

In Fig. 4 the values of $\varepsilon(T_{\text{ann}})$ determined according to eqn. (1) for different values of σ_0 are represented according to Arrhenius and universal procedure. The same significance of the ontogenic parameters results like in Fig. 3. It is of the main importance to notice the invariance of the first phylogenic parameter, n, for the two measuring systems, fact predicted by the general topoenergetic theory [2] and which denotes the same nature of the revealed transformation process. Moreover, the n value obtained for solid-state crystallization in dilatometric system for series of other PETP sample and its compounds with inorganic additives was the same (Fig. 6 in[2]).

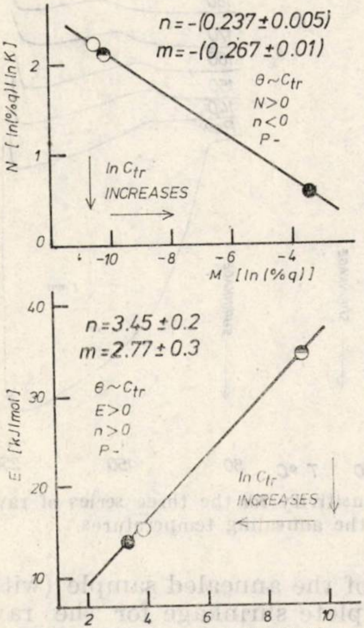

Fig. 3. — Arrhenius and universal representation ($T_0 = 70°C$) of %q values determined by x-ray diffraction according to eqn. (2). (O : PEPT, — : PETP/DMA. ● : PETP/ETG, $\theta = \%q$ in %, $U = T$ in K and $R = 8.32 \times 10^{-3}$ kJ/(mol.K)). The significances of the points are the same.

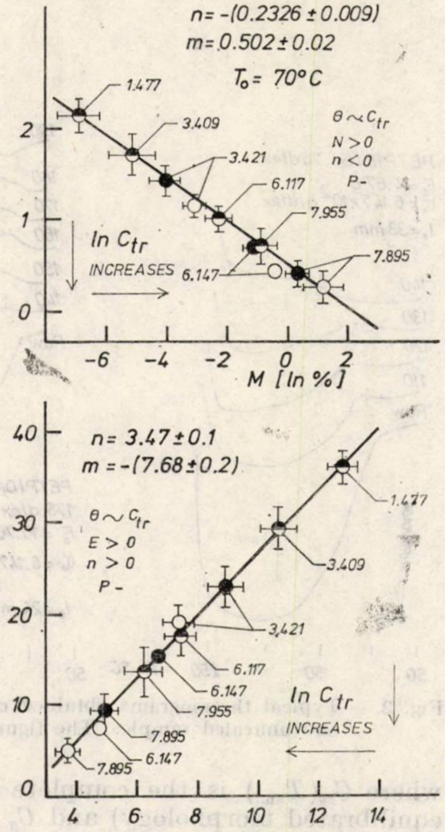

Fig. 4. — Arrhenius and universal representations ($T_0 = 70°C$) of ε (T_{ann}) values determined from thermomechanical diagrams according to eqn. (1) for different values of σ_0 ($\theta = \varepsilon(T_{\text{ann}})$ in %, $U = T$ in K, and $R = 8.32 \times 10^{-3}$kJ/(mol. K)).

One can observe, on the other hand, that the process extent increases with σ_0 and this fact suggests to fit the activation energy as a function of σ_0. In Fig. 5 a linear correlation results for $E(\sigma_0)$ which groups each kind of sample. For these correlations the values of activation energy at $\sigma_0 = 0$ and also the values of σ_0 at $E = 0$ can be determined. A more detailed study of the relationship between the process extent and σ_0 values can be revealed on the parameters M, $-M/N$ and $-N^2/M$ which have been recently defined to reveal the process extent, the value of kinetic entity, c_{tr},[2] and the value of the inert-transforming components coupling or the compatibility-stability (CS) coefficient, respectively (see also Table I, in [6]). The following facts can be noticed from Fig. 6 : (a) ln C_{tr} linearly increases with σ_0, but for each value of σ_0 the process extent increases in the order PETP/DMA, PETP/ETG and PETP as

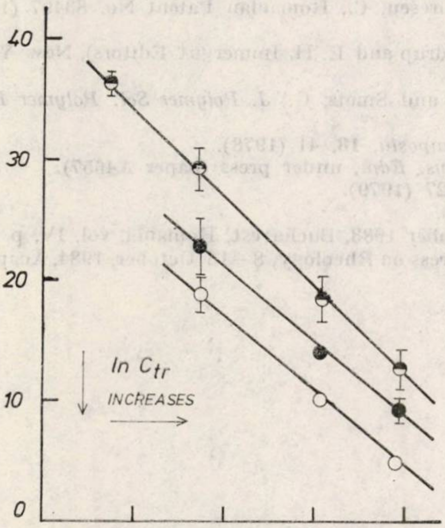

Fig. 5. — Dependence of E determined by Arrhenius representation of ε (T_{ann}) values as a function of σ_0.

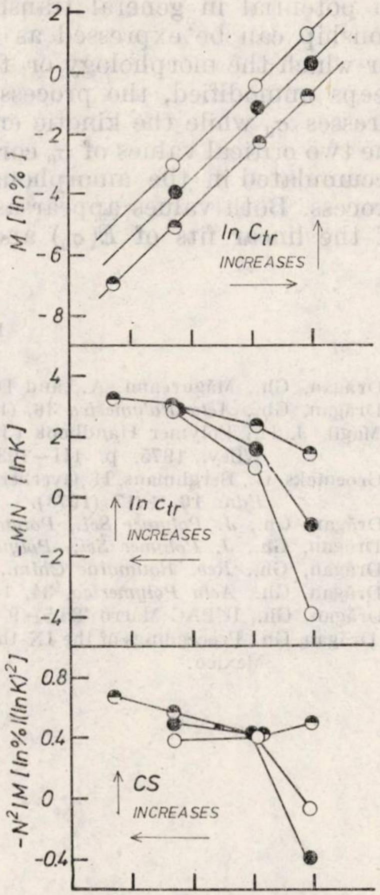

Fig. 6. — Dependences of M, $-M/N$ and $-N^2/M$ on σ_0 and their significances according to the previous standardization. [6]

resulted in Arrhenius representation; (b) the kinetic entity (ln c_{tr}) decreases with σ_0 and the rate of variation or the "stress sensitivity" of samples increases in the same order like in (a); and (c) CS also decreases with σ_0. These three observations are strongly interconnected and agree with the above mentioned remarks on the effects of shear stresses as driven potential in general transformation processes.[7-10] Shortly, this relationship can be expressed as follows: between two critical values of σ_0 for which the morphology or the internal stresses of the tested specimens keeps unmodified, the process extent increases with the external shear stresses σ_0 while the kinetic entity and CS decrease. In the present case the two critical values of σ_0 correspond to zero and to the internal stresses accumulated in the amorphous phase responsible for the crystallization process. Both values appear as the lower and upper limits, respectively, of the linear fits of $E(\sigma_0)$ and $M(\sigma_0)$.

REFERENCES

1 Drăgan, Gh., Măgureanu, A., and Dragomirescu, C., Romanian Patent No. 83497 (1983).
2 Drăgan, Gh., *Acta Polymerica* **36**, (1985).
3 Magil, J. H., Polymer Handbook (J. Brandrup and E. H. Immergut Editors), New York,. Wiley, 1975, p. III—193.
4 Groenicks, G., Berghmans, H.,Overbergh, N. and Smets, G., *J. Polymer Sci. Polymer Phys. Edn.* **16**, 1817 (1978).
5 Drăgan, Gh., *J. Polymer Sci., Polymer Symposia*, **18**, 41 (1978).
6 Drăgan, Gh., *J. Polymer Sci., Polymer Phys. Edn.*, under press (paper A4657).
7 Drăgan, Gh., *Rev. Roumaine Chim.*, **24**, 627 (1979).
8 Drăgan, Gh., *Acta Polymerica*, **34**, 1 (1983).
9 Drăgan, Gh., IUPAC Macro '83,5—9 September 1983, Bucharest, Romania, vol. IV, p./105.
10 Drăgan, Gh., Proceedings of the IX-th Congress on Rheology, 8—13 October, 1984, Acapulco Mexico.

Revue Roumaine de Chimie, **30**, *6*, 453—459 (1985)

ÜBER DIE MÖGLICHKEIT DER STOFFTRANSPORTVERBESSERUNG BEI GALVANISCHEN NICKELNIEDERSCHLÄGEN

GEORG GUTT, ŞTEFAN IVAŞCAN,* SONIA GUTT und MIHAI GRAMATICU
Technische Hochschule, Suceava, Rumänien
*Polytechnisches Institut, Iaşi, Rumänien

Eingegangen am November 27. 1983

Es besteht die Möglichkeit den Stofftransport bei galvanischen Nickelniederschlägen durch künstliche Konvektion zu verbessern. In disem Zweck wurde die Strömung entlang der Katode durch Pendlung, mit verschiedenen Geschwindigkeiten, der Katodenstange erhalten. Da der Stofftransport bei einem gegebenen hydrodynamischen Verhältniss durch den Grenzstrom begrenzt wird, wurde der Zusammenhang zwischen dem Grenzstrom und der Intensität der Strömung festgelegt. Weil durch das Wachsen der Grenzstromdichte die Stromausbeute und der Metallglanz des Niederschlages kleiner wird, erscheint dieses Problem als eine spezifische Optimierung. Die analytischen Ausdrücke, für die experimentell festgelegten grafischen Zusammenhänge, wurden mit Hilfe eines elektronischen Rechners, durch die Methode der kleinsten Quadrate, erhalten.

The paper deals with the possibility of improving the transfer of material during nickel electrodeposition by forced convection. The convection along the cathode is obtained by alternatively moving the cathode bar at different speeds. The transfer of material in the given hydrodynamic conditions is governed by the limit current and the intensity of convection. We consider the problem under discussion a good means of improving efficiency as the more the density of the limit current increases the less is the efficiency and the glitter of metallic electrodeposition. The analytical expressions of the graphical dependences have been established through the regression method by means of an electronic computer.

Der Stofftransport ist geschwindigkeitsbegrenzend in den galvanischen Metallniederschlägen und ist deshalb der wichtigste Faktor in der Produktivitätbestimmung und bei der Dimensionierung der galvanischen Zellen. Es ist bekannt, [1-3,11,13] dass die Metallionen, die sich an der Katode entladen, zur Verarmung der Elektrolytschicht an der Oberfläche der Katode führen. Der Konzentrazionsverlauf an der Katodenoberfläche sieht wie in Abb. 1 aus. Um die Konzentrazion an der Oberfläche aufrecht zu erhalten, muss ein Ionentransport aus dem Bad erzielt werden. Da die Strömung neben der Elektrode wegen der grossen Reibung gleich null ist, wird der Stofftransport durch diese Schicht durch Ionenwanderung und durch Diffusion erzielt.

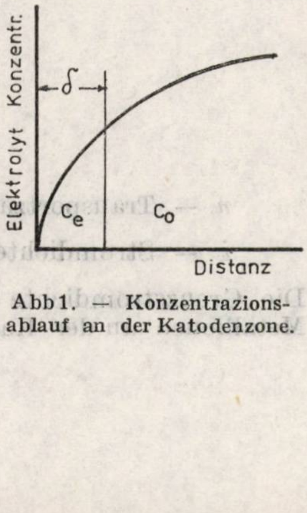

Abb 1. — Konzentrazionsablauf an der Katodenzone.

Wird das erste Fick-sche Gesetz angewandt, so erhält man folgende Gleichung;

$$\frac{\mathrm{d}c}{\mathrm{d}t}=\frac{S\cdot D}{\delta}(C_0-C_e) \tag{1}$$

S — Oberfläche [cm^2]

D — Diffusionskoeffizient [$\mathrm{cm}^2\cdot\mathrm{s}^{-1}$]

C_0 — Badionenkonzentration [mol/L]

C_e — Ionenkonzentration an der Elektrolytoberflache [mol/L].

Die Metallionengeschwindigkeit wird durch;

$$\frac{\mathrm{d}c}{\mathrm{d}t}=\frac{I}{z\cdot F} \tag{2}$$

ausgedrückt. Durch ausgleichen erhält man;

$$\frac{I}{z\cdot F}=\frac{S\cdot D}{\delta}(C_0-C_e) \tag{3}$$

I — Stromstärke [A]

z — Ionenvalenz

F — Faradaysche Zahl [96500 C]

t — Zeit [S]

δ — Diffusionsschichtdicke [cm]

Wird auch der Beitrag der Ionenwanderung in Betracht gezogen, verwandelt sich die Gleichung (3) in;

$$\frac{I}{z\cdot F}=\frac{S\cdot D}{\delta}(C_0-C_e)+\frac{n\cdot I}{z\cdot F} \tag{4}$$

oder

$$i=\frac{z\cdot F\cdot D(C_0-C_e)}{(1-n)\cdot\delta} \tag{5}$$

$$i=\frac{I}{S} \tag{6}$$

n — Transportzahl

i — Stromdichte [$\mathrm{A/cm}^2$].

Die Grenzstromdichte wird dann erreicht wenn die Konzentration der Metallionen an der Katodenoberfläche (C_e) gleich null ist. Vom praktischen Standpunkt gesehen bleiben in dieser Situation zwei Möglichkeiten die Grenzstromdichte zu überschreiten und somit die Produktivität zu steigern;

— Wachsen des Diffusionskoeffizienten (D)

— Verkleinern der Dicke der Diffusionsschicht (δ)

Der Diffusionskoeffizient kann durch Verbesserung der Ionenkonduktivität (λ) oder durch das Wachsen der Temperatur (T) erzielt werden, Gleichung (7);

$$D = \frac{\lambda \cdot R \cdot T}{z \cdot F^2} \tag{7}$$

λ — Ionenkonduktivitat [Ω^{-1}. cm^2]

R — Universelle Gaskonstante [J.Kmol.K]

T — Temperatur [°K]

In der Praxis wird dieses durch Beigabe gutleitender Salze und durch Wachsen der Badtemperatur erzielt. [7-9] Beide Massnahmen haben Grenzen, weil im ersten Fall viele Kationen der beigegebenen Salze sich zusammen mit den Metallkationen an der Katode entladen, und im zweiten Fall, bei der Überschreitung einer gewissen Temperatur die Qualität des Niederschlages leidet [4,5] und die Kosten der Baderwärmung, die Vorteile welche durch das Steigern der Grenzstromdichte erzielt wurden, überschreiten.

Das Verkleinern der Dicke der Diffusionsschicht ist möglich durch die Steigerung der Strömung in der Nähe de Katode. In der Fachliteratur [2-4] gibt es für verschiedene Strömungsytpen Gleichungen, die für eine bestimmte Strömung und Intensität der Strömung, die Grenzströmdichte bestimmen. Diese Gleichungen sind aber in den meisten Fällen für die elektrochemische Massenproduktion, wo es eine relativ einfache Geometrie der beiden Elektroden gibt, festgelegt worden. Da die galvanischen Niederschläge auf Körper mit sehr verschiedener Geometrie und Grösse erzielt werden, ist es nicht immer möglich diese Strömungsarten in der Galvanotechnik anzuwenden. Unser Zeil war eine Strömunsart zu finden die bei der galvanischen Vernickelung anwendbar ist, den Grenzström erhöht unter gleichbleibender oder verbesserter Qualität des Metallniederschlages, kleine Kosten aufweist, und an normalen galvanischen Bädern anwendbar ist ohne die spezifische Investition zu steigern. Diese Strömunsart wurde durch eine Pendlungsbewegung, mit verschiedenen Geschwindigkeiten, der Katodenstange erhalten.

EXPERIMENTELLE ERGEBNISSE

Die experimentelle galvanische Zelle, mit der gearbeitet wurde, ist in Abb. 2 dargestellt. Die Pendelbewegung wurde mit Hilfe einer Kurbelwelle und einer Pleulstange, die von einem Gleichstrommotor angetrieben wurde, erhalten. Der zurückgelegte Weg wurde durch Veränderung der Kurbel modifiziert. Die verschiedenen Pendelfrequenzen erhielten wir durch die

Veränderung der Drehgeschwindigkeit des Gleichstrommotors. Als erste Zielsetzung galt den Zusammenhang zwischen der Grenzstromdichte und der Strömungsintensität unter einer grafischen und analytischen Form zu finden. Weil das Überschreiten der Grenzströmdichte zur Verkleinerung der Strömausbeute führt[6,18], wurde die Grenzströmdichte durch die Bestimmung des Punktes, wo die Strömausbeute stark fällt, festgelegt. Zu diesem Zweck wurden in gleichen hydrodynamischen Verhältnissen die Strömdichte stufenweise gesteigert bis die Ausbeute eine plötzlichen Fall aufwies. Der Punkt wo dieser Fall beginnt bestimmt die Grenzströmdichte. Der Arbeitsgang wurde für 12 verschiedene hydrodynamische Verhältnisse wiederholt (Abb. 3). Die Pendlungsdistanz welche die höchste Stromausbeute und den höchsten Metallglanz des Niederschlages sicherte war 35 mm .[13] Mit den Knickpunkten aus Abb. 3 wurde der grafische Zusammenhang zwischen Grenzstrom und Pendelgeschwindigkeit erzielt (Abb. 4). Durch die Methode der Kleinsten Quadrate und mit Hilfe eines elektronischen Rechners wurde der Ausdruck für diesen Zusammenhang als folgende Gleichung :

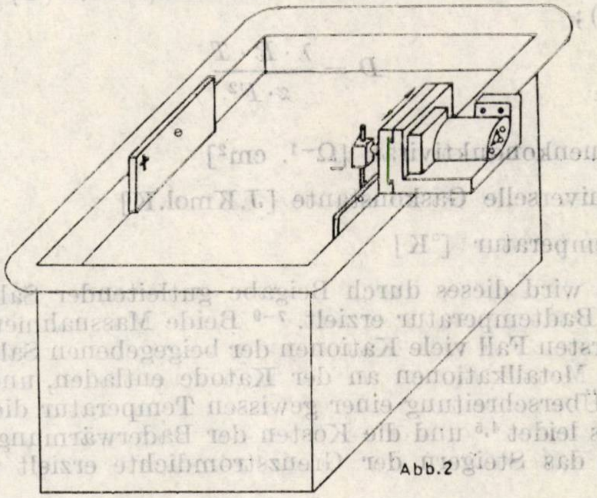

Abb. 2. — Galvanische Zelle mit Pendelbewegungeinrichtung.

$$Y_1 = \frac{(887{,}5 - 167{,}6 \cdot X + 10{,}9X^2)}{X^2} \tag{7}$$

$$Y_1 = \frac{1}{0{,}143 - 0{,}0006 \cdot X + 0{,}002 \cdot X^2} \tag{8}$$

X — Intensität der Strömung [Pendlungen/min.]

Y_1 — Grenzstromdichte [A/cm²]

gefunden. Diese Gleichungen bilden den kynetischen Ausdruck der galvanischen Vernickelung aus dem Watt — Bad bei 35°C und Rürintensitäten von 0—70 Pendl./min Gleichung (7),bzw. Gleichung (8) für 70—120 Pendl./min. Was die praktische Verwendung der ezielten Ergebnisse anbelangt, ist es aus ökonomischen Gründen nicht angebracht den linearen Teil der Kurve aus Abb. 4 zu überschreiten, weil mit dem Wachsen der Rührintensität der Grenzstrom sehr wenig steigt. Wird auch das Sinken der Stromausbeute und das Abnehmen des Metallglanzes des Nickelniederschlages in Grenzstrombedingungen zugleich mit dem Wachsen der Strömung in Betracht gezogen (Abb. 5) und (Abb. 6), so sind folgende analytische Ausdrücke gültig:

$$Y_2 = \frac{1}{0{,}0159 + 0{,}0000227^{X}} \qquad Y_2 - \text{Stromausbeute } \% \tag{9}$$

$$\log Y_3 = 1{,}9109 + 0{,}000689^{X} \qquad Y_3 - \text{Metallglanz } \% \tag{10}$$

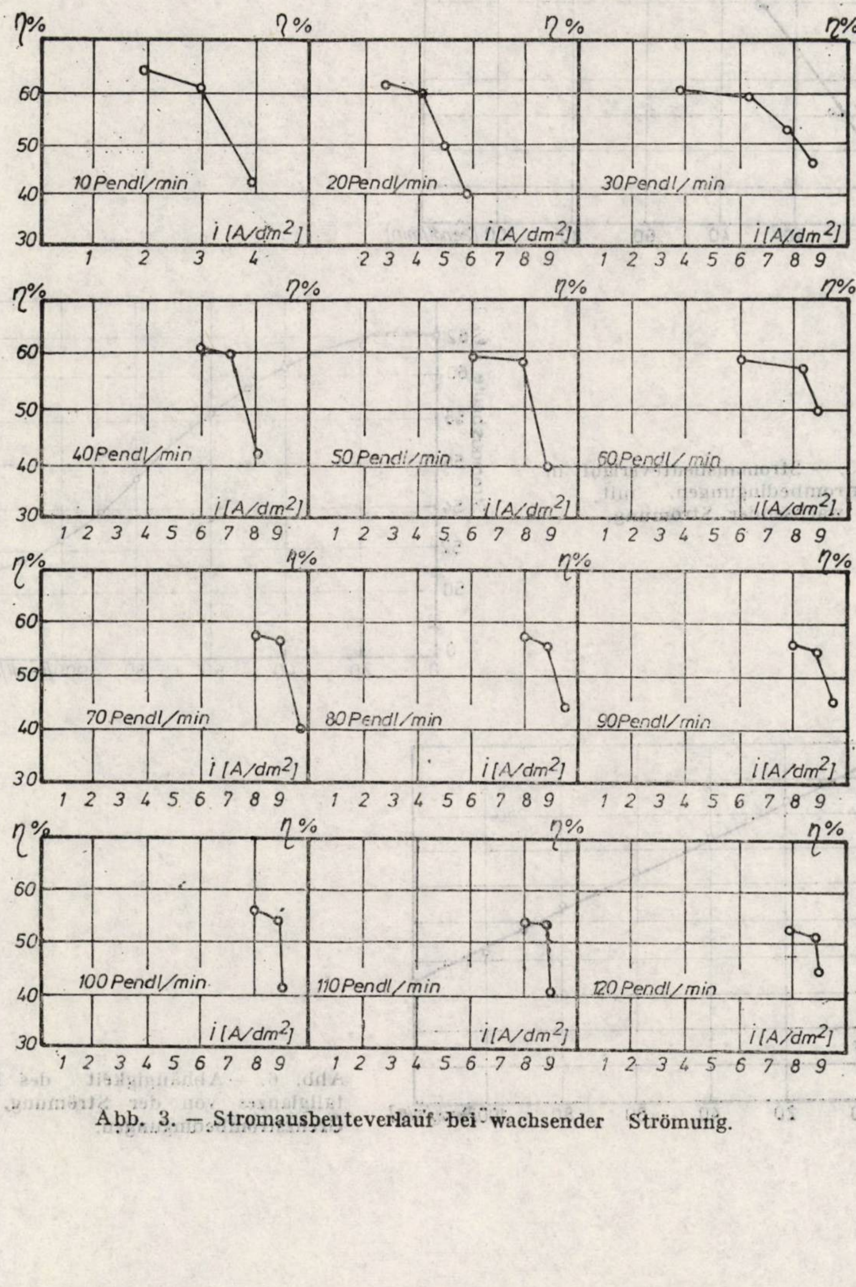

Abb. 3. — Stromausbeuteverlauf bei wachsender Strömung.

Das Problem der Steigerung des Stofftransportes erscheint somit als ein spezifisches Optimierungsproblem. Die optimalen Bedingungen, hinsichtlich des Grenzstromes, der Stromausbeute und des Metallglanzes als qualitativer Faktor, werden durch die gemeinsamen Wurzeln der Gleichungen (7, 8, 9, 10) gegeben.

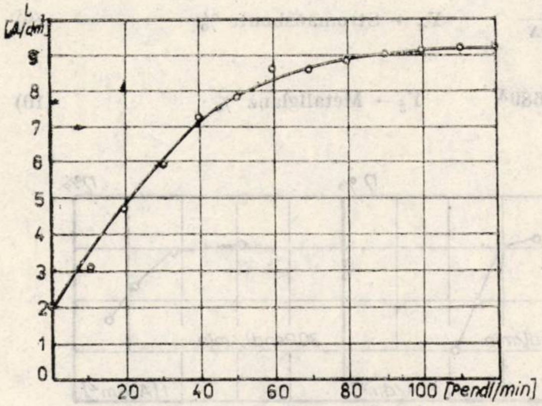

Abb. 4. – Abhängigkeit der Grenzstromdichte von der Strömungsintensität.

Abb. 5. – Stromausbeuteverlauf in Grenzstrombedingungen, mit wachsender Strömung.

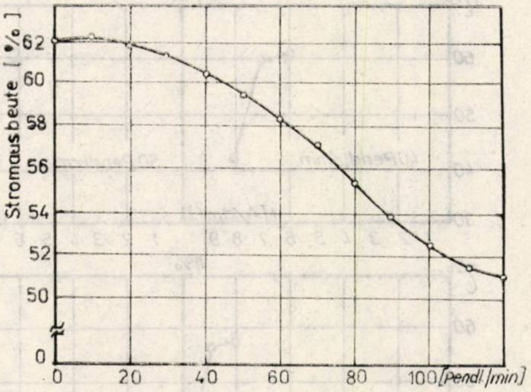

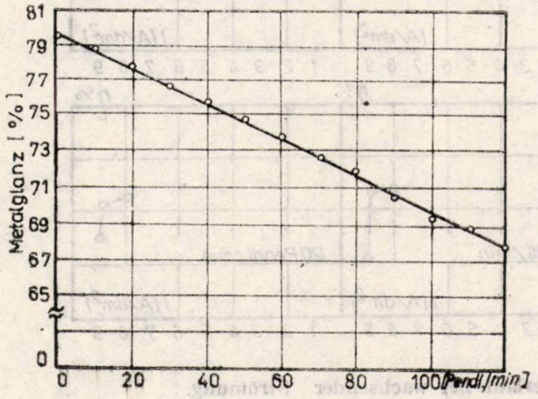

Abb. 6. – Abhängigkeit des Metallglanzes von der Strömung, in Grenzstrombedingungen.

LITERATURHINWEISE

[1] I. Atanasiu, "Electrochimie. Principii teoretice", Ed. Tehnică, Bucureşti, 1958.

[2] N. IBl, "Probleme des Stofftransportes in der angewandten Elektrochemie", *Chemie-Ing.-Technik*, Nr. 5/1963.

[3] N. IBl, "Die Rolle des Stifftransportes bei der Elektrolyse der Metalle", *Chemie-Ign.-Technik-.* Nr. 4/1973.

[4] H. Fischer, Wirkung sorbieter Fremdstoffe aut die elektrolytische Abscheidung und Auflösung von Metallen, *Chemie-Ing.-Technik*, Nr. 6,/1964

[5] C. Wagner, Teorie und Experiment in der elektrochemischen Verfahrenstechnik, *Chemie-Ing,-Technik*, Nr. 1, 1960.

[6] A. Căluşaru, "Electrodeposition of Metal Powders", Elsevier Scientific Publishing Company, Amsterdam, Oxford, New York, 1979.

[7] G. Firoiu, "Tehnologia proceselor electrochimice", Ed. Didactică şi Pedagogică, Bucureşti, 1983.

[8] I. Rădoi, A. Nemeş, "Electrochimie", Ed. Facla, 1974.

[9] A. Maskas, "Tehnica galvanoplastică", Ed. Tehnică, Bucureşti, 1974.

[10] Şt. Ivaşcan und Gh. Gutt, "Einige Ansichten über das Funktionieren der Elketrolytischen Vernickelung, Buletinul Institutului Politehnic Iaşi", Tomul XIX(XXIII), Fasc. 3—4, 1973.

[11] Şt. Ivaşcan und Gh. Gutt, "Betrachtungen über spongiösen Crom und Kegeleffekt bei Hartverchromung", Buletinul Institutului Politehnic Iaşi, Tomul XX (XXIV), Fasc. 1—2, 1974.

[12] Şt. Ivaşcan und Gh. Gutt, Brevet R. S. Romania 72320.

[13] Gh. Gutt und Şt. Ivaşcan, "Cercetări privind posibilitatea de intensificare a transferului la depunerea electrolitică a metalelor", Simpozion Galaţi, 1983, p. 240—248.

Revue Roumaine de Chimie, **30**, *6*, 461–466 (1985)

1,4-DIARYLNAPHTHALENES. III[1].

ACTION OF GRIGNARD REAGENTS ON SOME 1,1,4-TRIARYLBUTA-1,3-DIENE-2,3-DICARBOXYLIC ANHYDRIDES AND 1,4-DIARYLNAPHTHALENE-2,3-DICARBOXYLIC ANHYDRIDES

M. A. OMARA,* A. A. ELBARBARY, M. ANWAR and S. ELKONI

Chemistry Department, Faculty of Science, Tanta University, Tanta, A.R. Egypt

Received January 29, 1982
Revised December 12, 1984

Compounds (I) and (II) were treated with some Grignard reagents to give compound (III) and (IV) respectively. Compounds (I) were also treated with maleic anhydride to give the Diels-Alder adducts (V) which on hydrolysis give the corresponding diacids (VI).

The aim of the present investigation is to study the effect of the different Grignard reagents on the reactivity of compounds I and II.

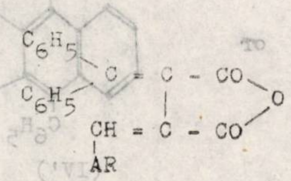

I

a, Ar = C_6H_5
b, Ar = C_6H_4Cl-*o*
c, Ar = C_6H_4Cl-*p*
d, Ar = $C_6H_4OCH_3$-*o*

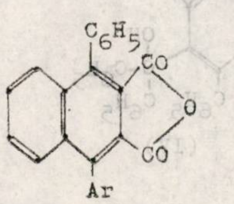

II

a, Ar = C_6H_4Cl-*o*
b, Ar = C_6H_4Cl-*p*
C, Ar = $C_6H_4OCH_3$-*o*

A number of 1,1,4-triarylbuta-1,3-diene-2,3-dicarboxylic anhydrides (Ia-d) and 1,4-diarylnaphthalene-2,3-dicarboxylic anhydrides (IIa-c) were prepared by the previously known methods.[2–5]

---

* Present address: Chemistry Department, Faculty of Science, Sana'a University, P.O. Box 1247 Sana'a, Yemen Arab Republic

Compounds (Ia-d) and (IIa-c) were subjected to the action of some Grignard reagents which attack the anhydride structure giving compounds (IIIa-m) and (IVa-c) respectively.

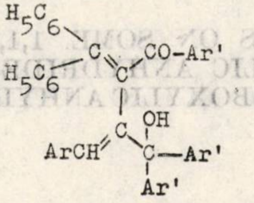
(III)

or

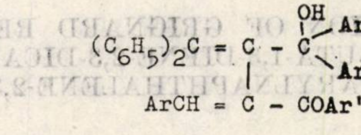
(III')

Ar	Ar′	Ar	Ar′
a, C_6H_5	C_6H_5	g, C_6H_4Cl-*p*	C_6H_5
b, C_6H_5	CH_3	h, C_6H_4Cl-*p*	CH_3
c, C_6H_5	$CH_2-C_6H_5$	i, C_6H_4Cl-*p*	$CH_2-C_6H_5$
d, C_6H_4Cl-*o*	CH_3	j, $C_6H_4OCH_3$-*o*	C_6H_5
e, C_6H_4Cl-*o*	C_6H_5	k, $C_6H_4OCH_3$-*o*	$CH_2-C_6H_5$
f, C_6H_4Cl-*o*	$CH_2-C_6H_5$	l, $C_6H_4OCH_3$-*o*	CH_3
		m, $C_6H_4OCH_3$-*p*	C_6H_5

Structure III′ is excluded due to steric hindrance during attack by the Grignard reagents.

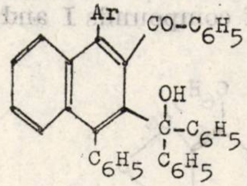
(IV)

or

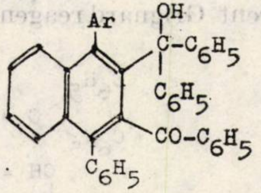
(IV')

a, Ar = C_6H_4Cl-*o*
b, Ar = C_6H_4Cl-*p*
c, Ar = $C_6H_4OCH_3$-*o*

The structures of compounds (III) and (IV) were inferred from :

(i) IR spectral study. All compounds under investigation show absorption bands for the functional groups beside the $\nu C=C$ of the aromatic compounds.
Table 1 shows the characteristic bands for compounds (III) and (IV).

(ii) The ^1H-NMR of compound (IIIa) showed the following signals at $\delta = 6.05$ (1H, singlet of the olefinic proton) ($>CH=C-$), $\delta = 6.6-7.0$ (30 H, multiplet, for the aromatic protons) and at $\delta = 8.15$ (1H, singlet) for the OH group-proton.

Table 1
Characteristic IR bands of compounds III and IV
(KBr, cm^{-1})^{6}

Compound	ν C=C aromatic	ν C=O	ν OH
IIIa	1590^{s}	1775^{vs}	3460^{br}
IIIb	1600^{s}	1775^{s}	3430^{sbr}
IIIc	1605^{m}	1775^{m}	3430^{br}
IIIg	1610^{m}	1770^{vs}	3420^{br}
IIIh	1610^{m}	1770^{vs}	3415^{br}
IIIj	1600^{s}	1770^{sh}	3420^{sbr}
IIIk	1600^{s}	1770^{sh}	3410^{ar}
IIIm	1600^{s}	1775^{m}	3410^{br}
IVa	1600^{s}	1775^{vs}	3400^{sbr}
IVb	1595^{vs}	1775^{m}	3400^{sbr}
IVc	1600^{s}	1760^{m}	3400^{sbr}

* vs = very strong; s = strong; sh = shoulder; br = broad; s.br = strong broad.

The study was extended to a cycloaddition of the Diels-Alder type. Thus, reaction of Ia and Ib with maleic anhydride gives the corresponding adducts (Va, b).[7,8]

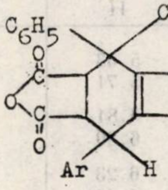

V

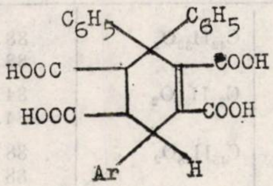

VI

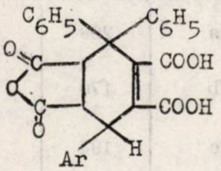

VII

V, VIa, Ar = C_6H_5
b, Ar = C_6H_4Cl-*o*

The structure of compounds V was established by:

(i) IR spectral study. Compounds V show a doublet at 1785 and 1740 cm^{-1} characteristic for νC=O of the anhydrides.

(ii) Hydrolysis of V with 5% hydrochloric acid gives the corresponding dicarboxylic acids (VIa, b). Compounds VI show the characteristic bands at 1700 and 3200 cm^{-1} characteristic for νC=O and νOH respectively.

(iii) Compound VIa was prepared via an independent synthesis starting from 1.1.4-triphenylbuta-1,3-diene-2,3-dicarboxylic acid and maleic anhydride. Compound VII was obtained. Hydrolysis of VII with 5% hydrochloric acid gives VIa.

From the above investigation it is clear that the addition of Grignard reagents or formation of Diels-Alder adduct is much faster than the cyclisation process.

EXPERIMENTAL

The IR spectra were recorded using a Carl Zeis Jena Model UR 10. spectrophotometer The KBr pellet technique was used.

The ^{1}H-NMR spectra were recorded using a Varian A-60 spectrophotometer (in CF_3COOH) All melting points are uncorrected.

Reaction of I and II with Grignard reagents:

A solution of I or II (0.01 mole) in 50 mL dry benzene was added dropwise to a solution of Grignard reagent (0.08 mole) in dry ether. The ether was evaporated and the reaction mixture was heated under reflux for 5 hrs., and then left to stand overnight. The reaction mixture was worked-up as usual. The solid residue was crystallized from the appropriate solvent to give compounds III and IV respectively in 55—60% yield. The results are listed in table 2.

Table 2

Products from the reaction of Grignard reagents with I and II

Compound	M.p. °C	Solvent of cryst.*	Formula	Analysis % Calcd./Found		
				C	H	Cl
IIIa	209	E	$C_{42}H_{32}O_2$	88.75 88.42	5.63 5.71	— —
IIIb	170	P	$C_{27}H_{26}O_2$	84.82 84.59	6.81 6.89	— —
IIIc	194	C	$C_{45}H_{38}O_2$	88.52 88.21	6.23 6.43	— —
IIId	244	E	$C_{27}H_{25}O_2Cl$	77.79 77.64	6.00 6.11	8.52 8.42
IIIe	255	P	$C_{42}H_{31}O_2Cl$	83.65 83.45	5.15 5.49	5.89 5.73
IIIf	178	C	$C_{45}H_{37}O_2Cl$	83.79 83.46	5.74 5.92	5.51 5.33
IIIg	198	M	$C_{42}H_{31}O_2Cl$	83.65 83.43	5.15 5.51	5.89 5.56
IIIh	271	E	$C_{27}H_{25}O_2Cl$	77.79 77.53	6.00 6.11	8.52 8.62
IIIi	160	C	$C_{45}H_{37}O_2Cl$	83.79 83.43	5.74 5.89	5.51 5.31
IIIj	120	P	$C_{43}H_{34}O_3$	86.29 86.10	5.69 5.52	— —
IIIk	103	P	$C_{46}H_{40}O_3$	86.25 86.10	6.25 6.32	— —
IIIl	165	C	$C_{28}H_{28}O_3$	81.16 81.32	6.76 6.72	— —
IIIm	153	P/C	$C_{43}H_{34}O_3$	86.29 86.06	5.69 5.73	— —

Table 2 (continued)

Compound	M.p. °C	Solvent of cryst.	Formula	Analysis % Calcd./Found		
				C	H	Cl
IVa	140	H	$C_{42}H_{29}O_2Cl$	83.93 83.72	4.83 4.99	5.91 5.73
IVb	103	P	$C_{42}H_{29}O_2Cl$	83.93 83.50	4.83 5.01	5.91 5.87
IVc	153	C	$C_{43}H_{32}O_3$	86.58 86.32	5.37 5.51	— —

* E = Ethnaol; P = Petroleum ether b.p. 60–80°C; C = Cyclohexane;
M = Methanol; H = n-Hexane.

Reaction of maleic anhydride with Ia and Ib:

A mixture of Ia or Ib (0.01 mole), maleic anhydride (0.01 mole; 1 g) and dry xylene or tetraline (50 mL) was refluxed for 36 hrs. After hot filtration, concentration and cooling, the solid separated was crystallized from ethanol to give compounds Va, b in 65% yield. The results are given in table 3.

Hydrolysis of Ia, b;

A suspension of Ia or Ib (2 g) in 50 mL 5% ethanolic solution of hydrochloric acid was refluxed for 2 hrs. The solid obtained was crystallized from ethanol to give the corresponding acid Va,b in 60% yield. The results are given in Table 3.

Preparation of an authentic sample of VIa:

A solution of 1,1,4-triphenylbuta-1,3-diene-2,3-dicarboxylic acid (2 g) and maleic anhydride (2 g) in dry xylene (30 mL) was refluxed for 36 hrs. After concentration and cooling the reaction product was crystallized from ethanol to give the compound VII in 65% yield (Table 3).

A suspension of VII (1 g) in 50 mL 5% ethanolic solution of hydrochloric acid, was refluxed for 2 hrs. The solid obtained was crystallized from ethanol to give VIa (mixed melting point with the above sample is underpressed).

Table 3

Characterisation of compounds V–VII

Compound	M.p. °C	Formula	Analysis % Calcd./Found		
			C	H	Cl
Va	213	$C_{28}H_{18}O_6$	74.67 74.38	4.00 4.23	— —
Vb	210	$C_{28}H_{17}O_6Cl$	69.35 69.14	3.51 3.89	7.33 7.42
VIa	201	$C_{28}H_{22}O_8$	69.14 68.96	4.53 4.73	— —
VIb	225	$C_{28}H_{21}O_8Cl$	64.55 64.31	3.03 4.39	6.82 6.72
VII	210	$C_{28}H_{20}O_7$	71.79 71.56	4.27 4.53	— —

REFERENCES

[1] Part II : A. M. El-Abbady, M. A. Omara and A. I. Selim ; *Rev. Roumaine Chem.*, **24**, 11, (1979).

[2] W. I. Awad, G. F. Baddar, M. A. Omara and (in part) S. M. Omaran, *J. Chem. Soc.* (*C*), **1971**, 3721.

[3] F. G. Baddar, El-Assal and Gindy, *J. Chem. Soc.*, **1948**, 1270.

[4] F. G. Baddar, El-Assal and S.H. Doss, *J. Chem. Soc.*, **1955**, 461.

[5] L. S. El-Assal and A. H. Shehab, *U.A.R. J. Chem.*, **13**, 249 (1970).

[6] L. J. Bellamy, "Infrared Spectra of Complex Molecules", Methuen, London, 1964, p. 71.

[7] E. D. Bergmann, *J. Appl. Chem.*, **3**, 145 (1953).

[8] B. Eisler and A. Wasserlann, *J. Chem. Soc.*, **1953**, 1943.

Revue Roumaine de Chimie 30, 6, 467–472 (1985)

ACID-BASE AND REDOX CHARACTERISTICS OF Pd CATALYSTS OBTAINED BY ION EXCHANGE

ALBA A., ARAMENDIA M., A. BORAU V., JIMENEZ C. and MARINAS J. M.
Departamento de Química Orgánica, Facultad de Ciencias,
Universidad de Córdoba, Spain

Received July 20, 1983
Revised October 23, 1984

Acidic, basic, oxidizing and reducing sites of various supports ($AlPO_4$, SiO_2 and SiO_2-AlPO_4 systems), and Pd-supported catalysts, have been evaluated spectrophotometrically, using different titrating agents, in this paper. Hexamethyldisilazane has been used for the specific determination of Bronsted acid sites, the results obtained by UV and IR spectroscopy being practically coincident.

INTRODUCTION

The most outstanding feature of metal-supported catalysts is their metal surface. However, the activity of such catalysts in hydrogenation processes cannot always be accounted for on the basis of their particle size. This kind of processes is termed by Boudart as "structure-sensitive". The catalyst activity is related not only to metal properties, but also to other surface characteristics of the solid which modify the metal-support interaction,[1] facilitate or hinder reagent and product adsorption [2] or favour "spillover".[3]

It is thus necessary to know all the surface properties of the solid which determine its catalytic activity, and the nature and distribution of acidic, basic, oxidizing and reducing surface centres which is, after the metal surface, the most revealing datum as regards the nature of the process occurring on the surface. In earlier papers we showed that Pt catalysts of identical metal surface but differently active in the hydrogenation of xylenes in gas phase, do have different surface acid-base properties.[4]

There are several excellent monographs and reviews on the determination of acidic, basic, oxidizing and reducing centres[5–10] and the role they play in the catalysis of some processes.

The differentiation of Brönsted and Lewis centres has been tackled by a number of researchers. Cook [11] and Saegusa [12] have studied the absorption band of the xanthenecarbonyl group by IR spectroscopy in order to assess Lewis-type acidic centres. Other authors have used ethyl acetate with the same purpose.[13] Hexamethyldisilazane (HMDS) [14,15] has been also widely used to determine Brönsted acidic centres.

The determination of oxidizing and reducing centres has recently received much attention [16-19] due to the widespread assumption that the higher or lower population of this kind of centres determines the catalytic activity of the solid.

In earlier papers [20-22] we assessed the acidity and basicity of $AlPO_4$-supported Pd and Pt catalysts by a spectrophotometric procedure and using amines and carboxylic acids of varying acidic strength and steric hindrance as titrating agents. In this work we have extended the procedure to the determination of surface oxidizing and reducing centres.

EXPERIMENTAL

Supports

The supports utilized were pure aluminium orthophosphate (denominated F) and different SiO_2-AlPO_4 systems (80 : 20%, in weight) gelled in different organic mediums, denominated PM2, EL, F72 and 72P. Pure silica (Merck, 70—230 mesh) denoted by S was also used.

The supports were sifted through 50—200 mesh, then dried in air at 383°C for 24 hours and calcined for 3 hours at 650°C. Their textural properties (specific surface, overall pore volume and average pore size), determined by nitrogen adsorption (BET) were reported elsewhere [23] and are summarized in Table 1.

Table 1

Textural properties of the supports

Supports	Mediums of obtention	$S_{esp} \pm 15$ (m^2/g)	$V_p \pm 0.05$ (mL/g)	$\bar{r}_p$(A)	I.P.
PM2	Propylene oxide	465	0.56	35	4.3
F72	Ammoniacal	310	0.52	35	3.2
EL(*)	Ethylene oxide	420	0.58	32	3.8
72P(*)	Propylene oxide	410	0.56	35	4.0
S	Commercial	395	0.55	28	1.0
F	Ammoniacal	156	0.49	40	3.2

(*) After obtaining the supports they are soaked with isoprophyl alcohol.

S_{esp} = Specific surface as determined by the BET theory.

V_p — Overall pore volume.

r_p = Average pore radius.

I.P. = Isoelectric point or zero point of charge.

Pd-supported systems

All Pd-supported systems used were obtained by ion exchange, from aqueous solutions of $Pd(NH_3)_4Cl$. The synthetic procedure was described in earlier papers [24,25]. The catalysts were finally obtained by calcining the impregnated metallic salt from 25 to 300°C at a heating gradient of 1°/min. Once the upper temperature was reached, the solids were cooled to room temperature and, once again, heated from 25 to 300°C at a gradient of 1°/min, while passing a hydrogen stream through the solid at 60 mL/min.

Catalyst $PdF_{0.97}$ was the only exception as regards the thermal treatment given. The reduction, in a hydrogen flow, was carried out as follows : the catalyst was subjected to a hydrogen flow of 60 mL/min at 180°C for 15 min, and then the temperature was raised at the rate of 1°/min until reaching 320°C, which was kept for a period of 2 hours. Previous studies carried out with catalysts synthesized on pure aluminium orthophosphate supports (i.e. those referred to as F) demand more active reduction conditions in order that all the impregnant salt be reduced to Pd°.

The nomenclaturè of the systems of this series is based on the symbol of the metal, type of support and percentage of metal.

Determination of the amount of titrating agent adsorbed

Sorption experiments were run at the wavelength of maximum absorption (λ_{max}, nm); this wavelength, as well as the concentration range, consistent with the Lambert-Beer law for each of the reagents used, appears in Table 2.

Table 2

Values and concentration range for which the Lambert-Beer law is fulfilled for each of the titrating agents used

Titrating agent	Solvent	λ_{max}(nm)	Concentration range (mol/L)
m-Nitrobenzoic acid	Benzene	279	$0.5\times10^{-4} - 2.0\times10^{-4}$
Phenothiazine	Benzene	317	$1.0\times10^{-4} - 4.0\times10^{-4}$
Tetracyanoethylene	Benzene	384	$1.0\times10^{-4} - 6.0\times10^{-4}$
Cyclohexylamine	Cyclohexane	225	$1.0\times19^{-3} - 3.0\times10^{-3}$
Pyridine	Benzene	282	$1.0\times10^{-3} - 6.0\times10^{-3}$
Acridine	Benzene	338	$0.1\times10^{-4} - 1.6\times10^{-4}$

The procedure used involves the spectrophotometric determination of the amount of titrating agent present in solution, in equilibrium with that adsorbed by the solid in monolayer

A known amount of solid (0.01—0.05 g) is placed in a flask previously dried in a heater, and 10 mL of titrating solution at a C_0 concentration are added, and kept under stirring for 1 hour at 25°C. The solid is then filtered, and the concentration of titrating agent in the supernatant solution, *C*, is determined spectrophotometrically.

The determination has been carried out with each reagent at the λ_{max} shown in Table 2. The evaluation of Brönsted acid centres with HMDS was performed by IR spectroscopy ($\nu_{Si-C} = 1180$ cm^{-1}, $\varepsilon = 289$) using a 0.1 cm thick liquid cell.

The theoretical treatment of the data obtained was carried out by using a form of the Langmuir isotherm :

$$C/X = 1/b\,X_m + C/\,X_m$$

where *C* is the concentration of the reagent in solution, in equilibrium with that adsorbed by the solid; *X*, is the amount of reagent adsorbed per gram of solid; *b* is a constant and X_m, by analogy with the Langmuir isotherm, is the amount of reagent adsorbed in monolayer (constant adsorption) per gram of solid, which corresponds to the theoretical amount of reagent that the solid can adsorb when all the centres were occupied by a particular titrating agent.

RESULTS AND DISCUSSION

Table 1 shows the features of the supports used, all of which have a high specific surface and an acceptable average pore radius which does not favour the diffusion of titrating agents through the solid pores, whose Van der Waals radii are : cyclohexylamine (6.1 A), pyridine (5.1 A) and acridine (10.5 A).

The surface of the metal-support systems has been determined by the BET method. The specific surface and average pore radius found coincide with those of the support in all cases, with an error less than 3 %. This can be explained on account of the low metal loading of the metal-support systems.

In view of the isoelectric point of the supports, their population of surface acidic centres is larger than that of basic ones, as is evident from the data in Table 3. According to Brunelle,[26] for isoelectric point values greater than 7 the catalysts should be synthesized by ion exchange from salts in which the metal is present under cation form. Therefore, we have chosen tetraaminepalladium (II) chloride salts to prepare the catalysts.

Table 3 shows the results obtained in the titration of acidic, basic, oxidizing and reducing sites, using cyclohexylamine, *m*-nitrobenzoic acid, phenothiazine and tetracyanoethylene, respectively.

Table 3

X_m values obtained in the titration with cyclohexylamine, *m*-nitrobenzoic acid, phenothiazine and tetracyanoethylene

System	Acidic centre $(X_m \pm 0.4) \times 10^2$ mol g^{-1}	Basic centres $(X_m \pm 0.1) \times 10^6$ mol g^{-1}	Oxiding centres $(X_m \pm 0.1) \times 10^6$ mol g^{-1}	Reducing centres $(X_m \pm 0.1) \times 10^6$ mol g^{-1}
PM2	31.6	5.9	<0.1	1.3
F72	18.9	0.2	<0.1	<0.1
EL	18.7	8.9	<0.1	0.1
72P	15.8	1.9	<0.1	<0.1
S	15.5	<0.1	<0.1	1.0
F	3.6	<0.1	<0.1	0.2
Pd $PM2_{0 \cdot 74}$	9.5	7.3	<0.1	1.3
Pd $F72_{0 \cdot 77}$	9.2	2.4	<0.1	<0.1
Pd $EL_{0.75}$	9.5	12.5	<0.1	1.0
Pd $72P_{0.74}$	12.0	6.1	1.7	0.9
Pd $S_{0.68}$	8.0	11.2	6.4	0.5
Pd $F_{0 \cdot 97}$	2.0	<0.1	6.8	<0.1

As can be observed, the supports showed an appreciable population of acid centres. The overall acidity (measured against cyclohexylamine, $pK_a = 10.2$) follows the pattern :

$$PM2 > F72 \simeq EL > 72P \simeq S > F$$

On the other hand, when the metal systems are compared with their corresponding supports, a decrease in acidity can be observed when the metal is deposited. This is what might be expected taking into account the fact that these systems have been synthesized by cation exchange. It should be noted that only SiO_2-AlPO_4 supports have an appreciable population of basic centres, although of an order far inferior to the number of acidic ones. In addition, Pd deposition implies a slight increase in the number of basic centres in these systems.

The number of oxidizing centres of the supports titrated with phenothiazine is very low ($<10^{-7}$ mol/g), making it difficult to correctly evaluate them, due to the experimental error introduced by the low population of centres and by the measuring procedure followed. For the systems in which a correct quantification was feasible the deposition of Pd yielded an increase in the number of oxidizing centres.

As regards the number of reducing centres, the order of magnitude found is also small. A slight increase is also observed when Pd is deposited.

Table 4 shows the results obtained in the titration of acidic centres of different strength and accessibility with amines such as: cyclohexylamine, pyridine and acridine.

Table 4

Acidity (mol/g) as a function of different bases used as titrants

Support	Cyclohexylamine[a] $(X_m \pm 0.4) \times 10^4$	Pyridine[b] $(X_m \pm 0.1) \times 10^4$	Acridine[c] $(X_m \pm 0.1) \times 10^5$
PM2	31.6	5.0	2.2
F72	18.9	3.9	4.3
EL	18.7	4.1	2.8
72P	15.8	3.8	2.1
S	15.5	4.0	2.1
F	3.6	1.1	2.3

a $pK_a = 10.20$
b $pK_a = 5.25$
c $pK_a = 5.58$

On comparing the acidity values obtained by using titrants such as cyclohexylamine and pyridine, of similar molecular size (ranging between 5—6 A) but different pK_a (10.2 and 5.25, respectively), it can be concluded that the centres titrated, equally accessible to both reagents, differ in acidic strength in each case. In the titration with pyridine the pattern found is:

$$\mathrm{PM2} > \mathrm{EL} \simeq \mathrm{S} \simeq \mathrm{F72} \simeq \mathrm{72P} > \mathrm{F}$$

From the results obtained by using titrants such as pyridine and acridine, of similar pK_a (5.25 and 5.58, respectively), but different molecular size (5.1 and 10.5 A, respectively), it can be seen that the centres titrated have similar acidic strength but different accessibility to each of the reagents.

Thus we can conclude that when the textural characteristics of a solid are analyzed and one wishes to establish a relationship between its properties and its catalytic activity in a particular process, it is necesary to carry out the study using titrating agents of a molecular size similar to that of the reagents employed.

Finally, the number of Brönsted acid centres determined by IR spectroscopy using hexamethyldisylazane as titrating agent amounts to $(19 \pm 0.4) \times 10^{-4}$ mol/g for the EL support, which implies that the majority of the acid centres of the solid are of Brönsted acid nature. This is what might be expected in view of the low population of oxidizing centres of the solids found when titrating with phenothiazine.

This work has been supported by a grant from the : "Comisión Asesora de Investigacion Cientifica y Técnica", Project nº 0249/81.

REFERENCES

[1] Dalla Betta R. A., Boudart M., Procc. Vth International Congress of Catalysis, p. 1329, Miami Beach, 1972.

[2] Campelo J. M., Garcia A., Luna D., Marinas J. M., *Applied Catalysis*, **10**, 1 (1984).

[3] Neikan W. C., Vannice M. A., Procc. Vth International Congress of Catalysis, p. 609, Miami Beach, 1972.

[4] Aramendia M. A., Borau V., Jimenez C., Marinas J. M., *Bull. Soc. Chim. Belg.*, **91**, 743 (1982).

[5] Tanabe K., "Solid Acid and Bases", Academic Press, New York, 1970.

[6] Forni L.' *Catal. Rev.*, **8**, 65 (1974).

[7] Malinowski S. and Szcepanska S., *J. Catal.*, **2**, 310 (1963).

[8] Take J. I., Kikuchi N. and Yoneda Y., *J. Catal.*, **21**, 164 (1971).

[9] Bakshi K. R. and Gavalas G. R., *J. Catal.*, **38**, 312 (1975).

[10] Yamanaka Y. and Tanabe K., *J. Phys. Chem.*, **79**, 2409 (1975).

[11] Cook D., *Can J. Chem.*, **41**, 522 (1973).

[12] Saegusa Y., Imai H., Ueijima T. and Furukawa J., *Shokubai (Tokyo)*, **7**, 43 (1965).

[13] Lappert M. F., *J. Chem. Soc.*, 542 (1962).

[14] Miyata H., Moffat J. B., *J. Catal.*, **62**, 367 (1980).

[15] Van Roosmalen A. J. and Mol J. C., *J. Phys. Chem.*, **83**, 2748 (1978).

[16] Ghorebl A., Hoang-Van C. and Teichner S. J., *J. Catal.*, **33**, 123 (1974).

[17] Krzywicki A., Marcezwski M., Hombek R. and Malinowski S., *Polish. J. Chem.*, **53**, 487 (1979).

[18] Fedorynska E., Wozniewski T., Malinowski S., Ahmed I. and Madura X., *J. Coll. Int. Sci.*, **69**, 469 (1979).

[19] Grigoryan A. Sh. and Aikazyan A. M., *React. Kinet. Catal. Lett.*, **20**, 129 (1982).

[20] Marinas J. M., Campelo J. M., Jimenez, C., Aramendia M. A., Borau V. and Luna D., 7° Simposio Iberoamericano de Catalisis, p. 69. La Plata, 1980.

[21] Campelo J. M., Luna D. and Marinas J. M., *Afinidad*, **39**, 61 (1982).

[22] Campelo J. M. Garcia A., Gutierrez J. M., Luna D., Luque I. and Marinas J. M., Comunicación 35—28. XIX Reunion Bienal R.S.F.E.Q. Santander, Spain, 1982.

[23] Sinisterra J. V., Jimenez C., Borau V. and Marinas J. M., 5^0 Simposio Iberoamericano de Catalisis, p. 359, Lisboa, 1976.

[24] Aramendia M. A., Climent M. L., Jimenez C. and Marinas J. M., *React. Kinet. Catal. Lett.*, **14**, 489 (1980).

[25] Aramendia M. A., Borau V., Jimenez C., Marinas J. M. and Pajares J. A., *J. Catal.*, **78**, 188 (1982).

[26] Brunelle J. R., *Pure Appl. Chem.*, **50**, 1211 (1978).

Revue Roumaine de Chimie, **30**, *6*, 473–481 (1985)

THERMAL AND PHOTOCHEMICAL STABILITY OF DIAZODERIVATIVES

DELIA ISAC, M. MRACEC and Z. SIMON*

ICECHIM — Center for Plastic Materials, The "SOLVENTUL" Research Laboratory, str. Gării, no. 25, R-1900, Timişoara, Romania,
* Medicine Institute Timişoara, Department of Biophysics,
spl. T. Vladimirescu, no. 14, R—1900, Timişoara, Romania

Received September 7, 1982
Revised December 12, 1984

Molecular diagrams and electronic correlation diagrams for the decomposition reactions were established for diazomethane and for the benzenediazonium cation derivatives, using Hückel molecular orbital calculations (HMO) for diazomethane, diphenyldiazomethane, the 1 and 2 naphthyldiazonium cations and for the cations resulting from their decomposition. Structural parameters were calculated and structure-reactivity correlations for a series of diazonium cations were studied.

The practical importance of diazoderivatives and of the diazonium salts,[1] imposes to elucidate the structure and stability of these compounds. For this reason we shall build Woodward-Hoffmann diagrams for their decomposition reactions to find out the structural peculiarities that might be important for the stability of these compounds. These structural peculiarities will be correlated with the results of the molecular orbital calculations. For this reason HMO calculations were performed for diazomethane, diphenyldiazomethane, 1 and 2 naphthyldiazonium cation and also for the cations resulting from their decomposition. The results are presented in Figs 1 and 2. The parameters used in HMO calculations are those used in the previous papers.[2,3]

For diazomethane, the correlation diagrams for molecular orbitals and electronic states of relatively low energy are given in figures 3 and 4. The position of σ_{CN} and σ_{CN}^* orbitals is given qualitatively, that of π_1, π_2, π_3 and n_N orbitals is given according to the HMO calculations (Fig. 3). For CH_2N_2, the first excited state I(A) could correspond to an n-π^*-transition, the second II(S) to a $\pi-\pi^*$-transition. For the reaction products, $CH_2 + N_2$, the lowest state is a triplet state $^3I(A)$ ($\sigma_C\pi_C$) the lowest singlet state being $^1O(\sigma_C^2)$; the only excited state of relatively low energy in this case could be the $^1I(S)(\sigma_C\pi_C)$ state. The obtained results could be qualitatively correct for the other diazoderivatives too. As for the correlation of the electronic states, the ground state $^1F(S)$ of CH_2N_2 will correlate with the $^1O(S)$ state of $CH_2 + N_2$. The first excited singlet state $^1I(A)$ obtained through light absorption will correlate with a high energy state of the reaction products. The thermal decomposition will take place adiabatically on the potential curve $^1F(S) - {}^1O(S)$, or unadiabatically, by intersection with the $^3I(A)(CH_2N_2) - {}^3I(A)(CH_2 + N_2)$ curve, with production of a triplet methylene radical. The activation energy will be of

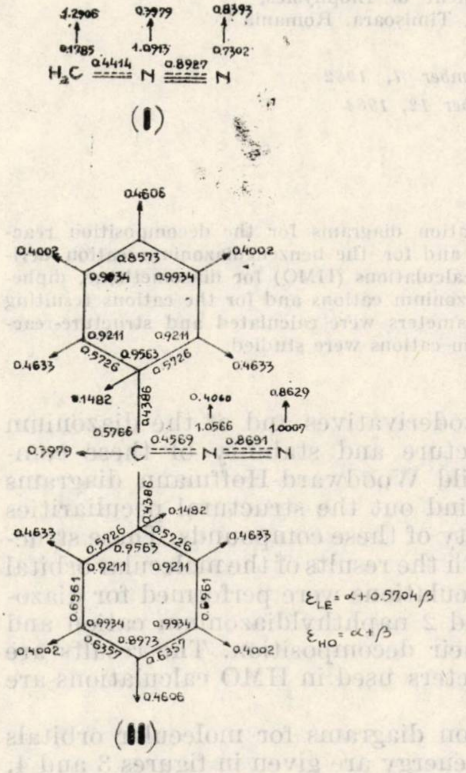
(I)
(II)
H_2C
N
C
$\mathcal{E}_{LE} = \alpha + 0.5704\beta$
$\mathcal{E}_{HO} = \alpha + \beta$

Fig. 1. — Molecular diagrams for diazomethane (I) and diphenyldiazomethane (II).

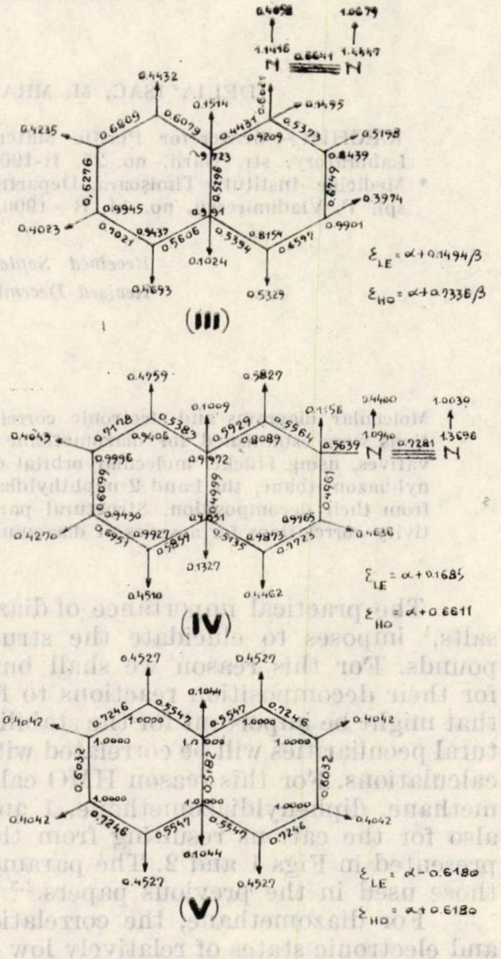
(III)
(IV)
(V)
$\mathcal{E}_{LE} = \alpha + 0.1494\beta$
$\mathcal{E}_{HO} = \alpha + 0.7338\beta$
$\mathcal{E}_{LE} = \alpha + 0.1685$
$\mathcal{E}_{HO} = \alpha + 0.6611$
$\mathcal{E}_{LE} = \alpha - 0.6180$
$\mathcal{E}_{HO} = \alpha + 0.6180$

Fig. 2. — Molecular diagrams for the 1-naphthyldiazonium cation (III), the 2-naphthyldiazonium cation (IV) and the cation resulting from their decomposition (V).

thermodynamic nature. The photochemical decomposition will start from $^1I(A)$; it could take place either by the hot molecule mechanism, or by predissociation, through intersection with the $^1II(S)(CH_2N_2) - {}^1I(S)(CH_2 + N_2)$ potential curve. The results are in agreement with those of Simon and Bădilescu,[2] with exception of the requirement of an intersection with a $\pi\pi^* - \sigma_C\pi_C$ potential curves; the conclusion concerning the increase of predissociation reactivity with increasing of the ε_{LE} orbital energy is preserved.

Using the results of a previous paper,[3] on a similar subject, we shall make the Woodward-Hoffmann correlation diagram for the decomposition of the bezenediazonium cation. Figure 5 gives the scheme of the molecular orbitals involved in the reaction, as they were calculated.[3] The polyelectronic states of interest for the thermal and photochemical decomposition reactions are shown in figure 6. The position of the energy levels is traced qualitatively corresponding to the relative position of ground state and excited states for the reactant and the reaction products. During these reactions the C_{2v} symmetry is preserved[4]; the symmetrical (S) and antisymmetrical (A) notations are made with respect to the molecular plane and the perpendicular plane containing the molecular axis. The activation energy for the thermal decomposition must be of purely thermodynamic nature, without a proper barrier, the diazonium cation is simply more stable than the primary decomposition products. The intersection of a ($^3\pi\sigma^*$) potential triplet curve with that of the ($^1\pi\pi^*$) first excited state could take place in principle as suggested in the paper of Simon and Bădilescu,[2] although because of the higher energy attributed to the decomposition products, such intersection point could be energetically disfavoured.

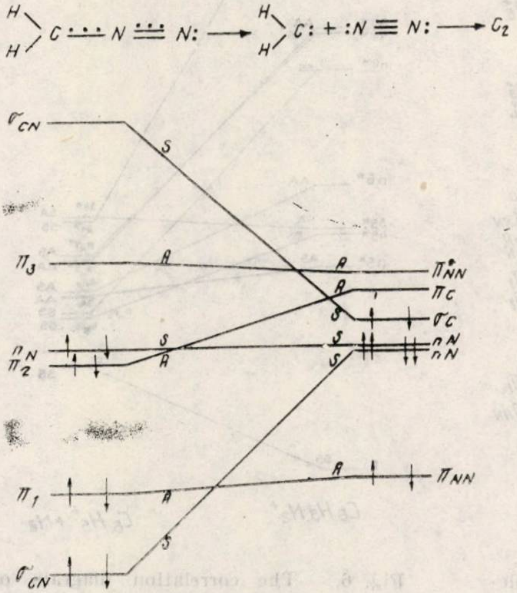
$H_2C \cdots N \cdots N: \longrightarrow H_2C: + :N\equiv N: \longrightarrow C_{2}$
σ_{CN}
π_3
n_N
π_2
π_1
σ'_{CN}
π^*_{NN}
π_C
σ_C
n_N
n_N
π_{NN}
S
A

Fig. 3. — The correlation diagram of molecular orbitals for the decomposition reaction of diazomethane.

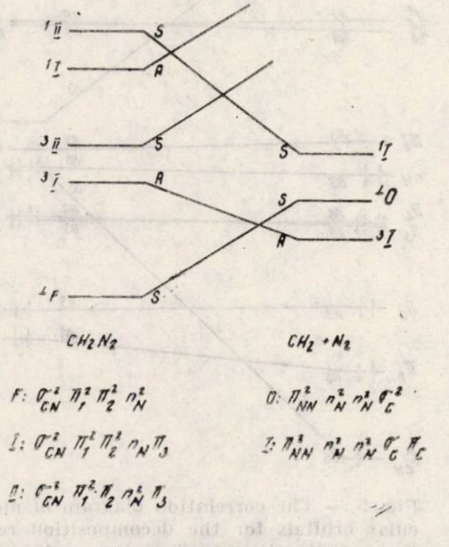
¹II
¹I
³II
³I
¹F
¹I
¹O
³I
S
A
CH_2N_2
$CH_2 + N_2$
F: $\sigma^2_{CN}\,\pi^2_1\,\pi^2_2\,n^2_N$
I: $\sigma^2_{CN}\,\pi^2_1\,\pi^2_2\,n_N\,\pi_3$
II: $\sigma^2_{CN}\,\pi^2_1\,\pi_2\,n^2_N\,\pi_3$
O: $\pi^2_{NN}\,n^2_N\,n^2_N\,\sigma^2_C$
I: $\pi^2_{NN}\,n^2_N\,n^2_N\,\sigma_C\,\pi_C$

Fig. 4. — The correlation diagram of electronic states for the decomposition reaction of diazomethane.

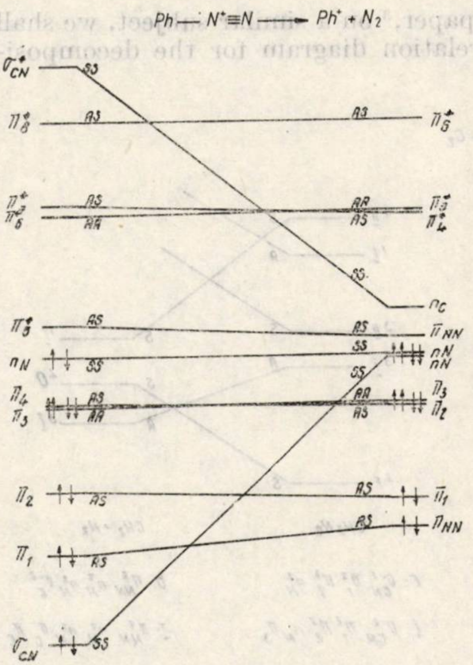
Ph—N⁺≡N → Ph⁺ + N₂
σ*CN
π*8
π*7
π*6
π*5
πN
π4
π3
π2
π1
σCN
SS
AS
AA
π*6
π*3
π*4
nC
πNN
nN
π3
π2
π1
πNN

Fig. 5. — The correlation diagram of molecular orbitals for the decomposition reaction of the benzenediazonium cation.

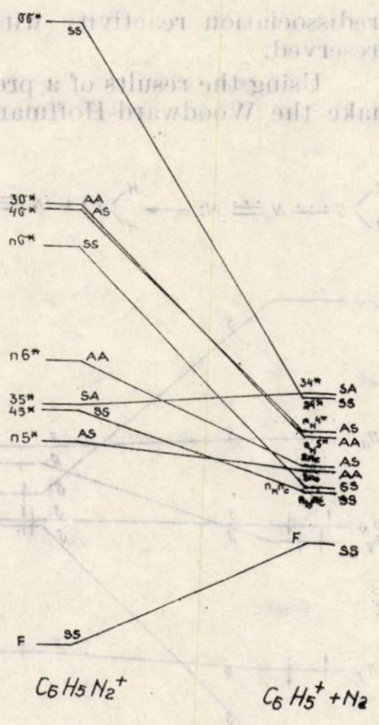
σσ*
3σ*
4σ*
nσ*
n6*
35*
45*
n5*
F
SS
AA
AS
SA
F
C6H5N2+
C6H5+ + N2

Fig. 6. — The correlation diagram of eletronic states for the decomposition reaction of the benzenediazonium cation.

The mechanism taken into account at the thermal and photochemical decomposition of diazonium salts is the ionic one, in water medium, as in the following scheme :[5]

$$\begin{tikzcd}
DV \arrow[r, shift left, "k_1'"] & DV^* \arrow[l, shift left, "k_1=\Delta I"] \arrow[r, "k_2"] & DV' \arrow[r, "k_4"] \arrow[ll, bend left, "k_3"] & Ar^+ + N_2 + X^-
\end{tikzcd}$$

DV = ArN_2X type diazocombination
DV* = excited state
DV′ = intermediate product
Ar =

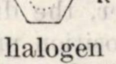

X = halogen
ΔI = absorbed light intensity

The quantitative relation between φ (the quantum yield) and the rate constants is :

$$\varphi = \frac{k_1 k_2 k_4}{(k_3 + k_4)(k_1' + k_2)}$$

The rate constant for the generation of the electronic excited state, DV*, is equal to absorbed light intensity, since the quantum yield for this process is equal to 1. Deviations of the quantum yield from 1 could be due to the deactivation of the electronic excited state by direct transitions to the ground state, or to the generation of a stable excited state, as an intermediate product DV′.DV′ can decompose intro products, in the aqueous solution, or deactivate by transition to the ground state.

In order to establish some relations with the thermal and photochemical reactivity for a series of diazonium cations, alongside with our results,[3,6] the results of the molecular orbital calculations of Simon and Bădilescu [2] and also the experimental data from literature,[7-12] were also considered, and structural parameters pertinent for their thermal and photochemical decomposition were calculated out of the HMO results. New molecular orbital calculations by the Hückel method were performed for the 1 and 2 naphthyldiazonium cations and for the cation resulting from their decomposition. The molecular diagrams for these molecules are given in figure 2.

The thermal stability was characterized by the decomposition rates k for 25°C ($\log k$). In some instances these rate constants were calculated from the values given for the activation energies and preexponential factors.

RESULTS AND DISCUSSIONS

The experimental data and the calculated structural parameters for the thermal and photochemical decomposition of some diazonium cations are shown in table 1.

Using the data in table 1 for the diazonium salts we tried the correlation :

$$\tilde{\nu}_{\text{exp}} = a + b \cdot E$$

the calculations leading to the following results : $r = 0.920$, $s = 1.764$, $a = 3.587$, $b = 36.885$. Here $\tilde{\nu}_{\text{exp}}$ is the wave number for the first absorption maximum of the diazonium salt solution, E the transition energy, $\varepsilon_{\text{LF}} - \varepsilon_{\text{HO}}$, calculated according to the HMO method.

ΔE_{π} (the variation of resonance energy) indicates the stability variation at decomposition; we also tried the correlation :

$$\log k = a + b \cdot \Delta E_{\pi}$$

but the correlation coefficient is only $r = 0.487$ ($s = 1.6$, $a = 46$, $b = -10$).

The ε_{LE} energy was also used for a correlation, as for the diazoderivatives, φ increases with the increasing of this energy, indicating the predissociation mechanism.[13-15] The results of this correlation for diazonium cations

$$\varphi = a + b \cdot \varepsilon_{\text{LE}}^{\text{compound}}$$

are : $r = 0.455$, $s = 0.13$, $a = 0.80$, $b = -2.8$

Table 1

The experimental data and the calculated structural parameters for the thermal and photochemical decomposition of some diazonium cations

Compound	log k (*)	φ (**)	ΔE_{π}	$\varepsilon^{\text{comp.}}_{\text{LE}}$	$\varepsilon^{\text{rad.}}_{\text{HO}} - \varepsilon^{\text{comp.}}_{\text{HO}}$ (***)	$\varepsilon^{\text{comp.}}_{\text{HO}} - \varepsilon^{\text{comp.}}_{\text{LE}}$ (***)	$\varepsilon^{\text{rad.}}_{\text{LE}} - \varepsilon^{\text{comp.}}_{\text{LE}}$ (***)	$\tilde{\nu}^{\text{exp}}$ (cm^{-1})	E^{calc} (β)
1	2	3	4	5	6	7	8	9	10
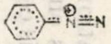	−4.077	0.38	5.114	0.179	0.000	0.821	−1.179	37 879	0.889
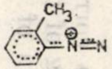	−3.388	0.30	5.172	0.131	−0.037	0.714	−1.131	37 175	0.926
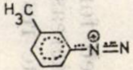	−3.471	0.35	5.108	0.178	−0.015	0.645	−1.178	35 842	0.875
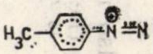	−5.123	0.23	5.176	0.132	−0.110	0.786	−1.132	35 842	0.868
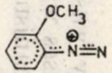		0.18	5.148	0.154	−0.027	0.726	−1.154	28 090 37 879	0.726 0.903
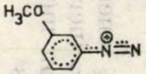	−3.464	0.24		0.178	−0.031	0.706	−1.178	28 571	0.706
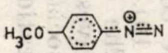	−7.906	0.52	5.146	0.153	−0.093	0.793	−1.153	31 949	0.793
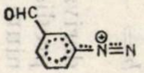	−3.058		5.102	0.179	−0.044	0.865	−0.587		

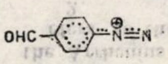	−5.558		5.054	0.255	0.000	0.745	−0.663		
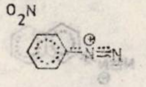	−7.158	0.17	5.104	0.179	−0.042	0.863	−0.465	35 714	0.947
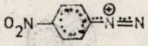	−6.466		5.064	0.248	0.000	0.753	−0.534		
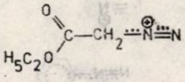	0.046	0.66	4.766	0.128	0.255	1.671	−1.150	37 175	1.617
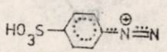	−1.713		5.106	0.179	0.000	0.821	−1.179	33 003 37 175	0.821 0.885
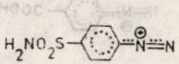	−1.893		5.106	0.179	0.000	0.821	−1.179	31 949 37 175	0.821 0.885
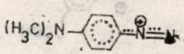		0.58		0.111	0.000	0.635		26 525 40 322	0.635 0.889
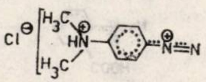		0.58		0.226	0.000	0.774		26 525 40 322	0.774 0.963
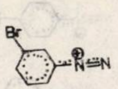	−5.245		5.106	0.182	−0.005	0.799	−1.180		
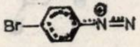		0.35	5.126	0.182	−0.024	0.818	−1.180	34 130	0.818
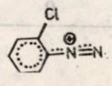	−7.853	0.18	5.104	0.180	−0.004	0.805	−1.165	37 175	0.882

Table 1 (continued)

6	2	3	4	5	6	â	8	9	10
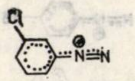	−5.520	0.41	5.106	0.179	−0.004	0.806	−1.164	37 594	0.882
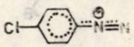	−6.805	0.29	5.108	0.180	−0.019	0.820	−1.165	35 336	0.868
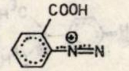	−4.841		5.156	0.229	−0.046	0.817	−0.771		
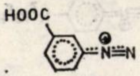	−4.363		5.176	0.179	−0.041	0.862	−0.721		
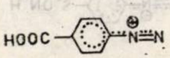	−4.986		5.138	0.232	0.000	0.768	−0.774		
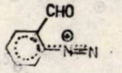	−6.134		5.076	0.251	−0.049	0.798	−0.659		
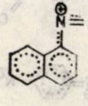	−4.804	0.24	5.208	0.149	−0.116	0.584	−0.767	27 397	0.584
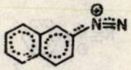	−4.725	0.38	5.137	0.168	−0.043	0.493	−0.786	31 949	0.868

(*) log k refers to the rate constant k at 298.16°; if no determinations at this temperature were available, $k_{298.16}$ was calculated from the Arrhenius equation.

(**) [illegible] efers to the quantum yield for irradiation at the corresponding λ of the first absorption maximum.

(***) [illegible] 2.

As may be seen from Table 1 neither the log k vs.

$$\varepsilon_{\mathrm{HO}}^{\mathrm{radical}} - \varepsilon_{\mathrm{HO}}^{\mathrm{compound}}, \text{ mor the } \varphi \text{ vs. } \varepsilon_{\mathrm{HO}}^{\mathrm{compound}} - \varepsilon_{LE}^{\mathrm{compound}}$$

correlation are satisfactory. All these attempts of correlations with the reactivity are unsatisfactory. This may be due both to the imperfections of the HMO method and to the complex character of this reaction system. So, the hydration of the diazonium cations and of the resulting radicals may present large variations with charge distribution and even with the shapes of the molecules discussed; these factors cannot be taken into consideration simply, by the HMO method.

Concerning the mechanism of the photochemical decomposition of the diazonium salts, the lack of correlation between φ and $\varepsilon_{\mathrm{LE}}$, comparatively with the obvious correlation between them for the diazoderivatives is not in favour of the predissociation mechanism. The photodecomposition of the diazonium salts, probably, takes place through the hot molecule mechanism. Concerning the much increased photoreactivity noticed for the *p*-dimethylaminobenzenediazonium cation,[6] this could be explained in the following way: although existing in a small proportion, the monocation will have, owing to its more extented conjugated system, the absorption maximum much removed towards red, towards the visible domain of the diffuse light in the laboratory. The monocation has also, among the diazonium salts, the highest $\varepsilon_{\mathrm{LE}} = \alpha + 0.111\ \beta$, and therefore the predissociation mechanism could become dominant for this compound.

REFERENCES

[1] K. Winnacker and E. Weingaertner, "Tehnologie chimică organică", vol. 3, Ed. Tehnică. Bucharest, 1959, p. 225.
[2] Z. Simon and I. Bădilescu, *Rev. Roumaine Chim.*, **12**, 243 (1967).
[3] D. Isac, M. Mracec and Z. Simon, *Rev. Roumaine Chim.*, **26**, 341 (1981).
[4] M. A. Vincent and L. Radom, *J. Amer. Chem. Soc.*, **100**, 3306 (1978).
[5] M. Breitenbach, K. H. Heckner and D. Jäkel, *Z. phys. Chem (Leipzig)*, **244**, 377 (1970)
[6] D. Isac, M. Mracec, N. Prosteanu and Z. Simon, *Rev. Roumaine Chim.*, **26**, 29 (1981).
[7] D. Schulte-Frohlinde and H. Blume, *Z. phys. Chem., (Frankfurt)*, **59**, 282 (1968).
[8] D. F. De Tar and A. R. Ballentine, *J. Amer. Chem. Soc.*, **78**, 3916 (1956).
[9] T. Tsunoda and T. Yamaoka, *Nippon Shashin Gakkai Kaishi*, **29**, 27 (1966).
[10] M. L. Crossley, R. H. Kienle and C. H. Benbrook, *J. Amer. Chem. Soc*, **62**, 1400 (1940).
[11] E. M. Evleth and R. J. Cox, *J. Phys Chem.*, **71**, 4082 (1967).
[12] W. Fraenbel, *Z. phys. Chem.*, **60**, 202 (1907).
[13] W. Kirmse and L. Horner, *Liebiegs Ann. Chem.*, **625**, 34 (1959).
[14] I. G. Murgulescu and T. Oncescu, *J. Chim. phys.*, **59**, 78 (1962).
[15] P. E. Millingam and G. G. Pimentel, *J. Chem. Phys.*, **29**, 1405 (1958).

Revue Roumaine de Chimie, **30**, *6*, 483–489 (1985)

E.S.R. SPECTRAL STUDY OF SOME POLYSUBSTITUTED THIOUREIDE ANION RADICALS

ELENA VOLANSCHI, A. MISSIR and DIANA MUȘOIU
Department for Physical Chemistry, Polytechnic Institute, Blvd. Republicii 13,
Bucharest, Romania

Received August 27, 1984

The spectral behaviour of the anion radicals obtained from some polysubstituted thioureides is investigated. The ESR spectra point out a spin distribution characteristic for a nitroaromatic anion radical, in spite of the other structural entities present in the molecule. The second substituent in the aromatic ring determines only minor effects on both ESR and electronic spectra of the anion radicals. MO calculations in the frame of Hückel and McLachlan's procedures account well for the experimental trends.

The thioureea derivatives are known for their physiological activity and are used in the production of different drugs.[1–3] Therefore, the study of the electronic structure and the behaviour of these systems in the oxido-reduction processes presents both a theoretical and practical interest. The influence of the amide and thioamide groups on the molecular structure as outlined by the IR spectra was previously investigated.[4] It was also stated that the nitrosubstitution brings about structural modifications in this type of molecules, allowing the formation of anion radicals. The electronic structure of these anion radicals was studied by means of ESR and absorption spectroscopy.[5]

It is the aim of the present paper to study the spectral behaviour of the anion radicals provided by these systems when several substituents are present, and to establish which one has the determinig role on the electronic structure. Therefore, the ESR and electronic spectra of the anion radicals obtained from derivatives **1**–**3** were investigated and are discussed in connection with those of the corresponding nitrosubstituted anion radicals **4** and **5**, previously reported.[5]

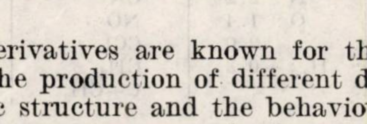

1 : $R = 4\text{–}Cl$, $6 – NO_2$
2 : $R = 4\text{–}CH_3$, $5 – NO_2$
3 : $R = 2\text{–}CH_3$, $5 – NO_2$
4 : $R = H$, $6 – NO_2$
5 : $R = H$, $5 – NO_2$

EXPERIMENTAL PART

The anion radicals were prepared by electrochemical reduction in dimethylsulfoxide (DMSO) and by chemical reduction using alkali metals (Li, Na, K) in dimethylformamide (DMF). For both ESR and optical studies *in situ* techniques were employed. Tetra-*n*-butylammoniumperchlorate was used as supporting electrolyte in concentration 0.1 M.

The ESR spectra were recorded on a JES-3B spectrometer operating in the X-band frequency.

Potassium peroxylaminedisulphonate was used as standard ($a_N = 1.300$ mT).

The electronic spectra were recorded in the visible range on a SPECORD-UV-VIS spectrophotometer. The MO calculations were performed in the frame of Hückel and McLachlan's approximations, on the FELIX C-256 computer of the Polytechnic Institute of Bucharest, using the parameters and equations in Table 1.

Table 1

Parameters and equations used in the MO calculations

Group	h_x	xy	k_{xy}
$>C=S$	1.0	CS	1.2
$-NH-$	1.5	CN	0.8
$-NO_2$	N : 2.2	CN	1.1
	O : 1.4	NO	1.67
$-Cl$	2.0	CCl	0.4
$-CH_3$	$H_3 : -0.3$	CH_3	2.5
		$C-CH_3$	0.9

$$a_H = |25|\rho_C^\pi \quad (1); \quad a_H^{CH_3} = |27|\rho_C^\pi \quad (2); \quad a_H^{CH_3} = |220|\rho_{H_3}^\pi \quad (3)$$

$$a_N^{NO_2} = 99\ \rho_N^\pi - 71.6\ \rho_O^\pi \quad (4); \quad a_H^{NH} = |35|\ \rho_N^\pi \quad (5);$$

$$a_N^{NH^7} = 24.08\ \rho_N^\pi + 3.70 \sum_i \rho x_i \quad (6)$$

$$a_N^{NH^7} = 22.70\ \rho_N^\pi + 3.27 \sum_i \rho x_i \quad (7)$$

RESULTS AND DISCUSSION

a) *ESR Spectra.* The experimental and simulated ESR patterns of the investigated anion radicals are presented in figures 1–3. The hyperfine splittings (hfs) are collected in Table 2.

Examining the data in Table 2 we remark that hfsplittings are apparent only from the nitrosubstituted ring. The greatest hfs., in the range 1.040–1.130 mT, belong to the nitrogen atoms of the nitro groups. The hfcouplings of the protons are in the usual range for the nitroaromatic anion radicals, that is between 0.335–0.390 mT for the positions *ortho* and *para*, and between 0.075–0.105 mT for the position *meta* with respect to the nitro group. This fact attests that, in spite of the thioamide moiety and of the other substituents, the hyperfine spin distribution preserves the features of a nitroaromatic anion radical.

A comparison of the investigated anion radicals with those reported for the nitrothioureide anion radicals outlines the influence of the other substituent. The presence of the chlorine atom enhances the reductibility of the system and the stability of the anion radical. On the contrary, the presence of a methyl group renders the reduction more difficult and leads to more unstable radicals.

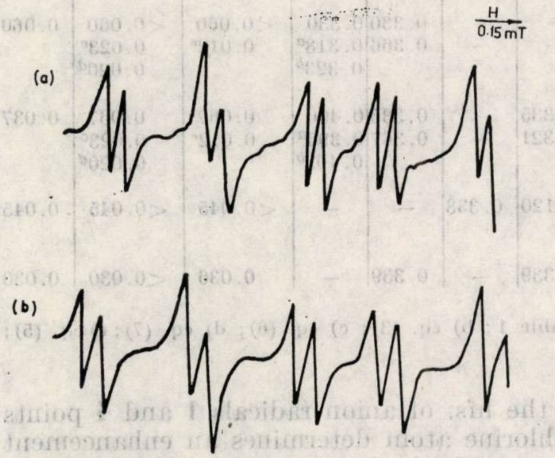

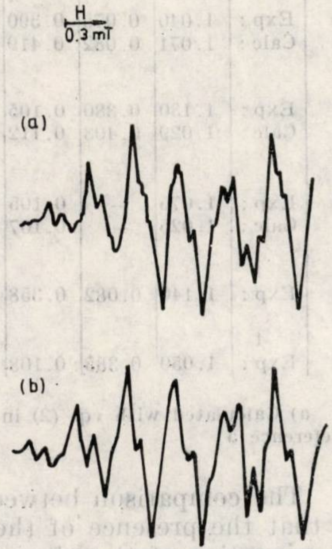

Fig. 1. — ESR spectrum of anion radical 1 (electrochemical reduction in DMSO) a) experimental, b) simulated.

Fig. 2. — ESR spectrum of anion radical 2 : a) experimental ; b) simulated

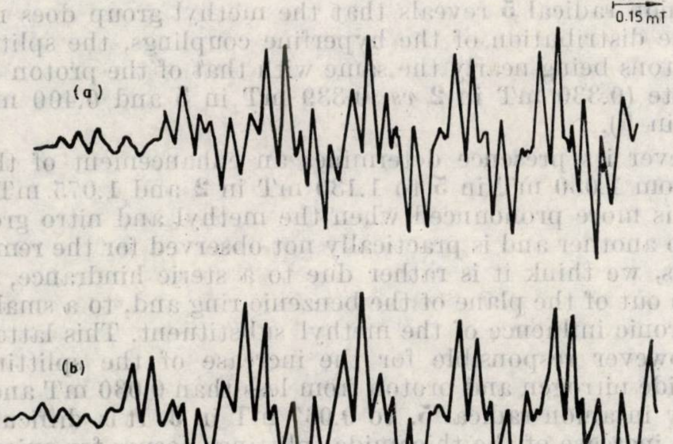

Fig. 3. — ESR spectrum of anion radical 3 : a) experimental ; b) simulated.

Table 2

Experimental and calculated hfs for the investigated anion-radicals (mT)

Anion radical		$a_N^{NO_2}$	a_H^2	a_H^3	a_H^4	a_H^5	a_H^6	$a_H^{CH_3}$	a_H^{NH}	a_N^{NH}	Line-width (mT)
1	Exp :	1.040	0.075	0.390	—	0.360	—	—	<0.037	<0.037	0.037
	Calc :	1.071	0.082	0.419	—	0.390	—	—	0.034^e	0.045^c	
										0.040^d	—
2	Exp :	1.130	0.380	0.105	—	—	0.330	0.330	<0.060	<0.060	0.060
	Calc :	1.029	0.403	0.112	—	—	0.366	0.318^a	0.012^e	0.023^c	
								0.323^b		0.020^d	
3	Exp :	1.075	—	0.105	0.335	—	0.335	0.400	0.067	0.067	0.037
	Calc :	1.025	—	0.107	0.321	—	0.367	0.395^a	0.012^e	0.023^c	
								0.402^b		0.020^d	
4	Exp :[f]	1.140	0.082	0.358	0.120	0.338	—	—	<0.045	<0.045	0.045
5	Exp :[f]	1.050	0.385	0.108	0.339	—	0.339	—	0.036	<0.030	0.030

a) Calculated with eq. (2) in Table 1; b) eq. (3); c) eq. (6); d) eq. (7); e) eq. (5); f) Reference 5

The comparison between the hfs. of anion radicals **1** and **4** points out that the presence of the chlorine atom determines an enhancement of conjugation of the nitro group with the benzenic ring, reflected in a decrease of the nitro group nitrogen splitting and an increase of the *ortho* and *para* proton splittings.

Examination of the hfs. in anion radicals **2** and **3** as compared to those in anion radical **5** reveals that the methyl group does not perturb strongly the distribution of the hyperfine couplings, the splitting of the methyl protons being nearly the same with that of the proton at the substitution site (0.330 mT in **2** *vs.* 0.339 mT in **5** and 0.400 mT in **3** *vs.* 0.385 mT in **5**).

However its presence determines an enhancement of the nitrogen splitting from 1.050 mT in **5** to 1.130 mT in **2** and 1.075 mT in **3**. As this effect is more pronounced when the methyl and nitro groups are in *ortho* one to another and is practically not observed for the remaining ring proton sites, we think it is rather due to a steric hindrance, forcing the nitro group out of the plane of the benzenic ring and, to a smaller extent, to an electronic influence of the methyl substituent. This latter influence may be however responsible for the increase of the splittings due to the thioamide nitrogen and proton from less than 0.030 mT and 0.036 mT respectively in anion radical **5**, to 0.067 mT in **3**. It is difficult to assess if the same increase of the thioamide splittings occurs for anion radical **2**, because the experimental resolution is poorer for this radical (line width 0.060 mT vs. 0.037 mT for **3**).

It is to be noted that the experimental trends are well accounted for by the theoretical spin distributions.

The hfs were calculated using the McLachlan spin densities and the spin — polarization parameters in Table 1, taking into account only the thioamide moiety and the nitrosubstituted ring. The results are collected in Table 2, together with the experimental ones.

A good agreement is obtained for the splittings of the ring protons and nitro group nitrogen atoms. As the thioamide nitrogen is concerned, the Mc Connell type formula, with Q_N^N in the range 3.000—3.500 mT leads to values in disagreement with the experiment. The two parameter formulae which take into account the spin density on the neighbouring carbon atoms [7] give much better results. However the highest calculated value is obtained for anion radical **1** and not for **3**, as it is experimentally observed.

The Hückel calculated π-bond orders for the anion radicals do not differ significantly from those in the parent molecules. Some differences are noted only for anion radical **1** (Table 3), and suggest a higher weight of a formula affecting the thioamide group :

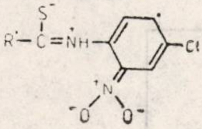

Table 3

Calculated π-bond orders for compound **1** and its anion radical

	p_{C-S}	$p_{C-N(H)}$	$p_{N(H)-C}$	p_{12}	p_{23}	p_{34}	p_{45}	p_{56}	p_{16}	$p_{C-N(O_2)}$
M	0.824	0.425	0.302	0.641	0.672	0.644	0.677	0.612	0.584	0.361
A.r	0.814	0.433	0.280	0.673	0.635	0.632	0.688	0.555	0.533	0.447

This formula also explains the higher value of the splitting due to proton 3, in *para* versus the nitro group, as compared to the similar position in anion radical **4**.

b) *Electronic spectra.* The reduction of the parent compound is accompanied by the appearance of an absorption band in the visible range of the spectrum. As this peak disappears when the electrolysis is interrupted and the solution is exposed to air, it was assigned to the anion radical (Fig. 4).

If the absorption peak of anion radical **1** ($\lambda = 537.6$ nm) is compared to that of the corresponding nitrosubstituted anion radical **4** ($\lambda = = 527.4$ nm), a bathochromic shift is noted. This fact is in agreement with the ESR data which reveal a higher degree of conjugation between the nitro group and the aromatic ring in anion radical **1** as compared to **4**.

Unfortunately, a comparison between the methyl substituted anion radicals **2** and **3** and the corresponding nitrothioureide **5** cannot be done, because their electronic spectra could not be registered in similar conditions*.

The anion radicals **1** and **2** were prepared using different reduction agents and it was noted that the frequency of absorption depends on the cation (Table 4).

Table 4

Dependence of the absorption frequency of the anion radicals on the cation radius (solvent : DMF)

Cation	r(Å)	$1/r$(Å^{-1})	Anion-radical			
			1		**2**	
			λ(nm)	$\bar{\nu}$(cm^{-1})	λ(nm)	$\bar{\nu}$(cm^{-1})
Li^+	0.60	1.66	423.7	23601.6	454.5	22002.2
Na^+	0.96	1.04	543.4	18402.6	598.8	16700.0
K^+	1.33	0.75	510.2	19600.1	709.2	14100.3
$[N(C_4H_9)_4]^+$	3.50	0.28	568.2	17599.4	—	—

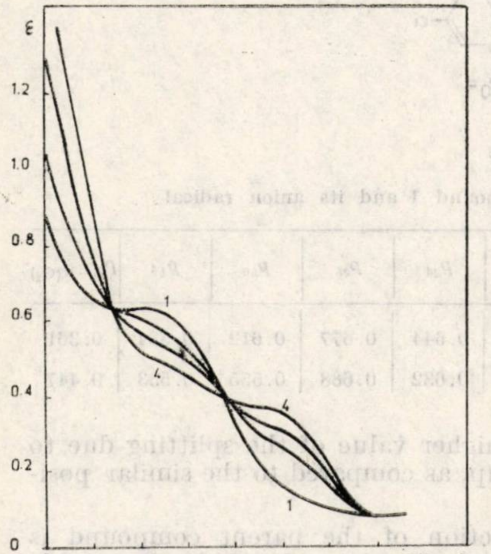

Fig. 4. — Absorption spectrum obtained on the electrochemical reduction of **1** in DMSO 1 — initial; 2—4 — in time;

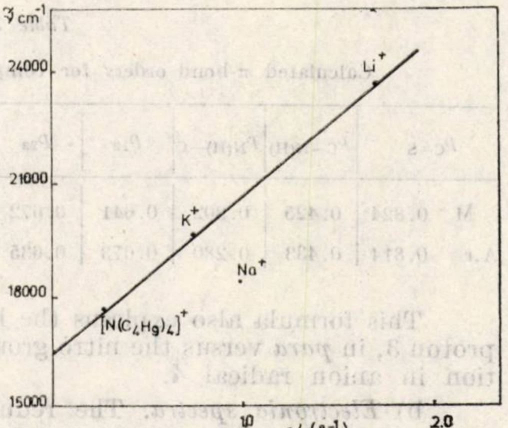

Fig. 5. — Plot of the absorption wave number of anion radical **1** versus the reciprocal of the cation radius (solvent DMF).

If the wavenumber of the absorption peak is plotted against the reciprocal of the cation radius, i.e. for anion radical **1** (Fig. 5), a linear dependence is obtained, excepting Na. This fact points out that the coulombian type ion-pair interaction plays an important role in these systems

---

*) The anion radicals **2** and **3** are unstable, and detectable concentration was reached only employing alkali metals in DMF.

as it was already noted[2] for the unsubstituted nitrothioureide anion radicals.

In conclusion it may be stated that the nitro group exerts a determining role on both spin distribution and energy levels of the thioureide anion radicals, even when other substituents are present. The chlorine atom and methyl groups have only minor influence on both ESR and electronic spectra.

REFERENCES

[1] A. Missir, *Farmacia* **25**, 123 (1977).
[2] A. Missir, *Farmacia* **26**, 183 (1978).
[3] A. Missir, *Farmacia* **27**, 217 (1979).
[4] M. Hillebrand, E. Volanschi and A. Missir, *Bul. inst. Politeh. Bucureşti, Ser. Chim. Mat.*, **42**, (4), 55 (1980).
[5] Elena Volanschi and Melania Voicu, *Rev. Roumaine Chim.*, **28**, 689 (1983).
[6] P. H. Rieger and G. K. Franekel — *J. Chem. Phys.* **39**, 609 (1963).
[7] D. Greatorex, D. B Jenkins and T. J. Kemp — *J. Chem. Soc. Perkin II*, **1973**, 1762.

Revue Roumaine de Chimie, **30**, *6*, 491–497 (1985)

NITRIC DECOMPOSITION PROCESS OF PHOSPHATIC RAW MATERIALS. I.

STUDY ON EQUILIBRIUM OF NITRIC DECOMPOSITION PROCESS OF PHOSPHATIC RAW MATERIALS

M. TALABA and C. CALISTRU
Department of Chemical Technology, Polytechnic Institute,
Splai Bahlui 71, Iaşi, Romania

Received April 24, 1984

The equilibrium of the nitric decomposition process of phosphatic raw materials was studied by means of the double-exchange quaternary diagram at 0°C and the influence of the nitric acid excess, water content and CaO/P_2O_5 ratio on the separation degree of the tetrahydrated calcium nitrate followed.

The investigation of the nitric decomposition process of the phosphatic raw materials involves the equilibrium study. As known, the study of an industrial chemical process makes evident the development possibilities in dependence on the influencing factors.[1]

The study on the nitric decomposition process of the phosphatic raw materials described by the characteristic equation [2]:

$$[Ca_{10}(PO_4)_6F_2 + A_1'']_s + [HNO_3 + H_3PO_4 + Ca(NO_3)_2 + H_2O + A_2'']_l \rightarrow$$

$$\rightarrow [H_3PO_4 + Ca(NO_3)_2\ HNO_3 + HF + H_2O + A_3'']_l + [A_4'']_s$$

is performed by means of the double-exchange quaternary diagram for the system:

$$Ca_3(PO_4)_2 + 6\ HNO_3 \rightleftharpoons 2\ H_3PO_4 + 3\ Ca(NO_3)_2$$

The use of an equilibrium diagram is justified by the quality required for the nitrophosphatic fertilizer obtained in the final stage of the manufacture process, namely a maximum CaO/P_2O_5 ratio of 0.35. Since in the phosphatic raw materials this ratio is situated between 1.3 and 1.8, a certain amount of calcium oxide must be removed from the system. With the technological procedure under study, the Norks-Hydro procedure for obtaining nitrophosphate, the calcium oxide is removed as calcium nitrate crystallized by cooling in one of the following forms:

$$[Ca(NO_3)_2]_s;\quad [Ca(NO_3)_2 \cdot 2H_2O]_s;\quad [Ca(NO_3)_2 \cdot 4H_2O]_s.$$

As can be seen in the equilibrium diagram at 0°C,[4] depicted in Fig. 1, the large area of the crystallization field of the tetrahydrated calcium nitrate assures high separation degrees of the solid phase as well as the concentration of the remaining liquid phase by the inclusion of a significant water amount within the crystalline network of the solid formed. The solution concentration by crystallization determines lower energical consumption in the other technological stages of the obtention of nitrophosphatic fertilizers.

According to the phase law,[1,2] the crystallization process of the calcium nitrate and hence the separation degree of $Ca(NO_3)_2 \cdot 4H_2O$ is influenced by the temperature and chemical composition of the system.

Since the crystallization process of calcium nitrate is exothermal,[3] the cooling temperature decrease determines, according to the Le Chatelier principle,[1] the solubility decrease and hence the increase of the crystallization field of the tetrahydrated calcium nitrate.

The chemical composition of the reaction mixture resulted by the nitric decomposition of the phosphatic raw materials is determined by the nature of the phosphatic raw material expressed by the CaO/P_2O_5 ratio, the nitric acid excess and the water amount in the system expressed by the water number, n_{H_2O} (given by the ratio between the number of H_2O moles and the sum of the molar-ionia fractions of the anhydrous salts).

In the following the influence of the chemical composition variation of the initial system on the separation degree of the tetrahydrated calcium nitrate (ψ^{e}_{cnt}) is studied by means of the equilibrium diagram at °C given in Fig. 1.

The diagram in Fig. 1 shows in detail the crystallization field and the separation conodes of $Ca(NO_3)_2 \cdot 4H_2O$ as a function of the nitric acid excess (toward the stoichiometrical amount necessary for the phosphatic raw material decomposition), between 5–50 % HNO_3, and the water number $n_{H_2O} = 4-15$, considering the reaction between HNO_3 and pure $Ca_3(PO_4)_2$ corresponding to a mole ratio $CaO/P_2O_5 = 3.0$, or mass ratio $CaO/P_2O_5 = 1.183$, the reactant diagonal, R_0. The reactant lines, $R_1 - R_5$, for mass ratio $CaO/PO_5 = 1.3-1.8$ corresponding to their values in the real phosphatic raw materials, table 1, are also drawn.

Table 1

Values of CaO/O_2O_5 molar and mass ratios

CaO/P_2O_5 ratio	R_0	R_1	R_2	R_3	R_4	R_5
$\bar{x}_{CaO}/\bar{x}_{P_2O_5}$ mass ratio	1.183	1.300	1.400	1.500	1.600	1.800
$x_{CaO}/x_{P_2O_5}$ mol ratio	3.000	3.296	3.550	3.800	4.057	4.564

Firstly the influence of the nitric acid excess and water number on the separation degree of the tetrahydrated calcium nitrate for the CaO/P_2O_5 ratio value corresponding to the reactant line R_0 is followed and

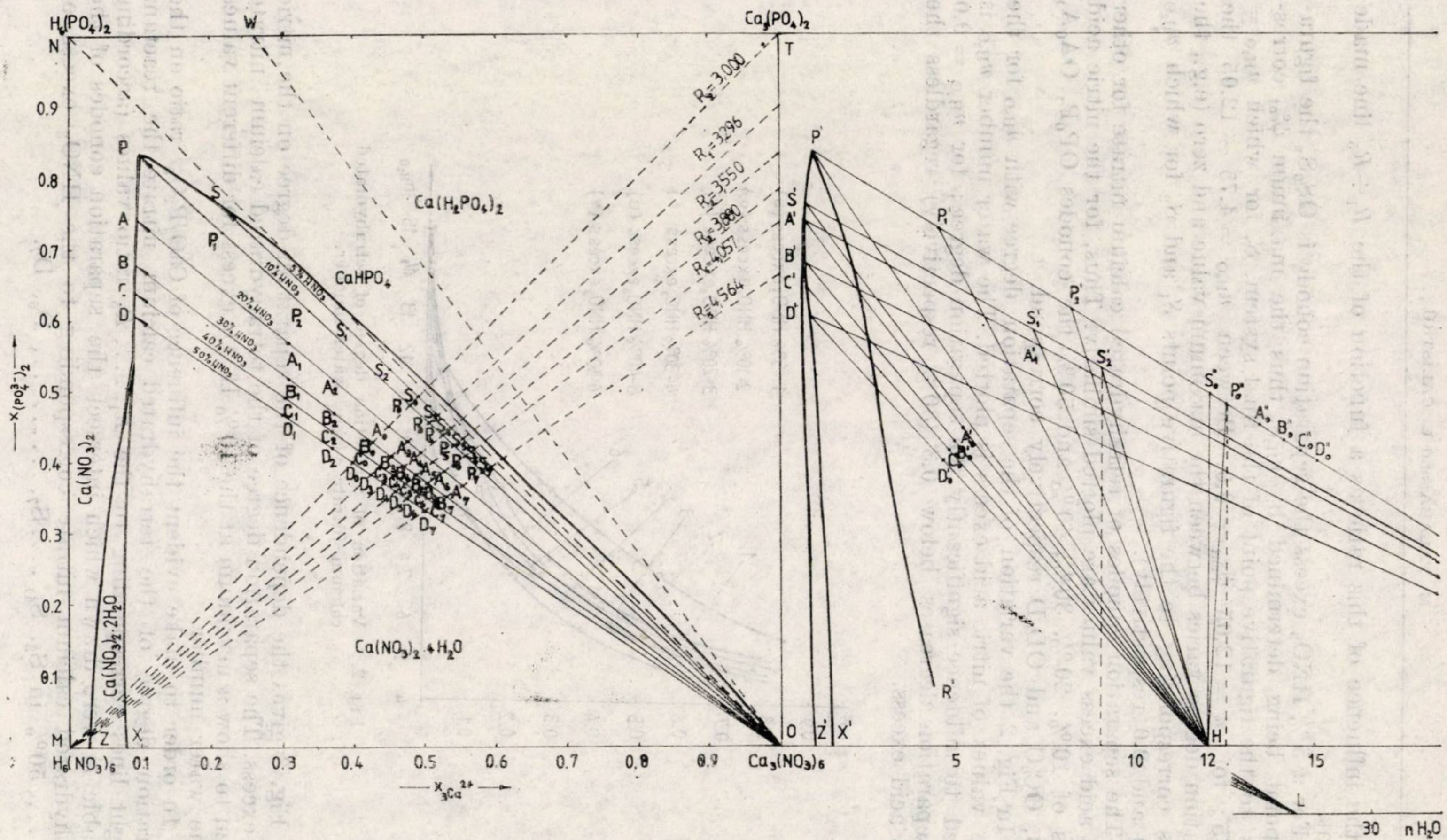

Fig. 1. — Equilibrium diagram for the reciprocal quaternary system :
$Ca_3(PO_4)_2 + 6\ HNO_3 \rightleftharpoons 2\ H_3PO_4 + 3\ Ca(NO_3)_2$, at 0°C.

then the influence of this ratio as a function of the $R_1 \div R_5$ line made evident.

For a 5 % HNO_3 excess the separation conode is OS_0S, the figurative point being determined by n_{H_2O}, thus the maximum ψ^e_{cnt} corresponds to the figurative point of the final system, S, for which $n_{H_2O} = 4.75$; for $n = 12.05$ $\psi_{cnt} = 0.0$. Between $n_{H_2O} = 4.75 - 12.05$ the separation degree varies between the maximum value and zero (e.g., the values corresponding to the figurative points S_1 and S_2 for which n_{H_2O} is 7.0 and 9.0 respectively).

The separation conodes of tetrahydrated calcium nitrate for other nitric acid excess values are plotted similarly. Thus, for the nitric acid excess of 10 %, 20 %, 30 %, 40 % and 50 % the conodes OP_0P, OA_0A, OB_0B, OC_0C and OD_0D respectively correspond.

In Fig. 2 the variation of the separation degree with n_{H_2O} for the above values of nitric acid excess is plotted. The water number n_{H_2O} is noticed to influence significantly the separation degree ; for $n_{H_2O} = 9.0$ the separation decreases below 0.3 (30 % respectively) regardless the nitric acid excess.

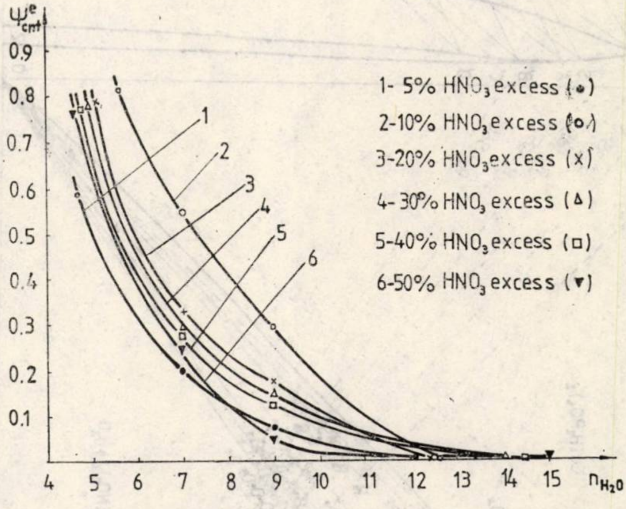

Fig. 2. — Variation of separation degree of tetrahydrated calcium nitrate versus water number.

Fig. 3 gives the dependence of the separation degree on the nitric acid excess. The separation degree of the tetrahydrated calcium nitrate is seen to show a maximum at the 10 % HNO_3 excess for different values of the water number.

In order to make evident the influence of CaO/P_2O_5 ratio on the separation degree of the tetrahydrated calcium nitrate the reactant straight lines corresponding to the $R_1, \ldots, R_5$ ratio values (according to Table 1) were drawn which intersect the separation conodes of the tetrahydrated calcium nitrate corresponding to the HNO_3 excess of 5 %, . . . , 50 % in S_3, S_4, . . . , S_7, ... , D_6, D_7.

By performing these graphical plottings and calculating the separation degrees of the tetrahydrated calcium nitrate corresponding to all figurative points of the initial system, $S_3, \ldots, D_7$ for different values of the water number the data plotted in Figs. 4–6 were obtained.

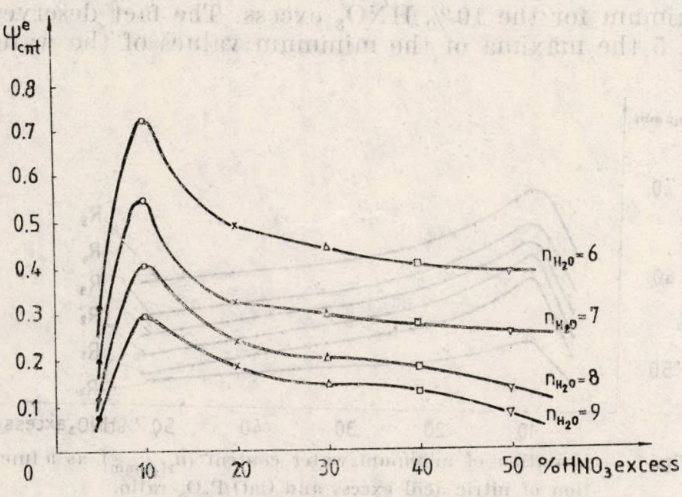

Fig. 3. — Variation of separation degree of tetrahydrated calcium nitrate versus nitric acid excess.

In Fig. 4 the variation curves of the maximum separation degrees as a function of the nitric acid excess are plotted for the R_1-R_5 ratios and for the R_0 ratio for the sake of comparison. Since the maximum values of the separation degrees of the tetrahydrated calcium nitrate correspond to minimum values of the water number when the other factors which

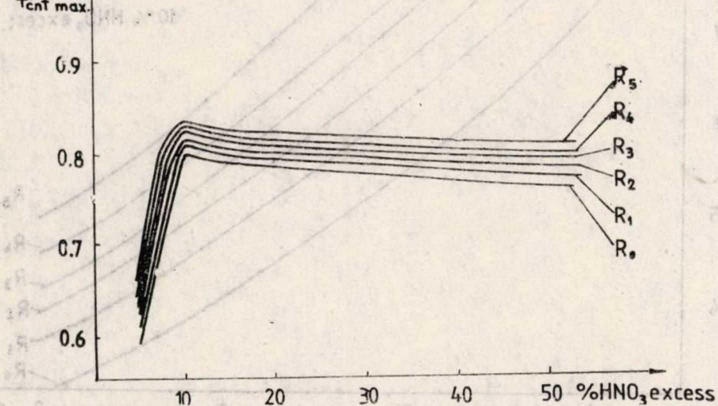

Fig. 4. — Variation of separation degree of tetrahydrated calcium nitrate as a function of nitric acid excess and CaO/P_2O_5 ratio.

would affect the crystallization process are kept constant, the variation curves of the water number as a function of the nitric acid excess for all $R_0 - R_5$ ratios are plotted in Fig. 5.

In Fig. 4 and Fig. 5 the following aspect is evident : regardless the R ratio value all the variation curves of the maximum separation degree show a maximum for the 10 % HNO_3 excess. The fact deserves mention that in Fig. 5 the maxima of the minimum values of the water number

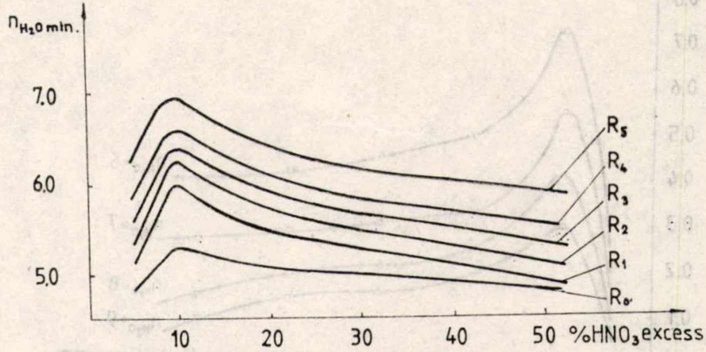

Fig. 5. — Variation of minimum water content ($n_{H_2O\,min}$) as a function of nitric acid excess and CaO/P_2O_5 ratio.

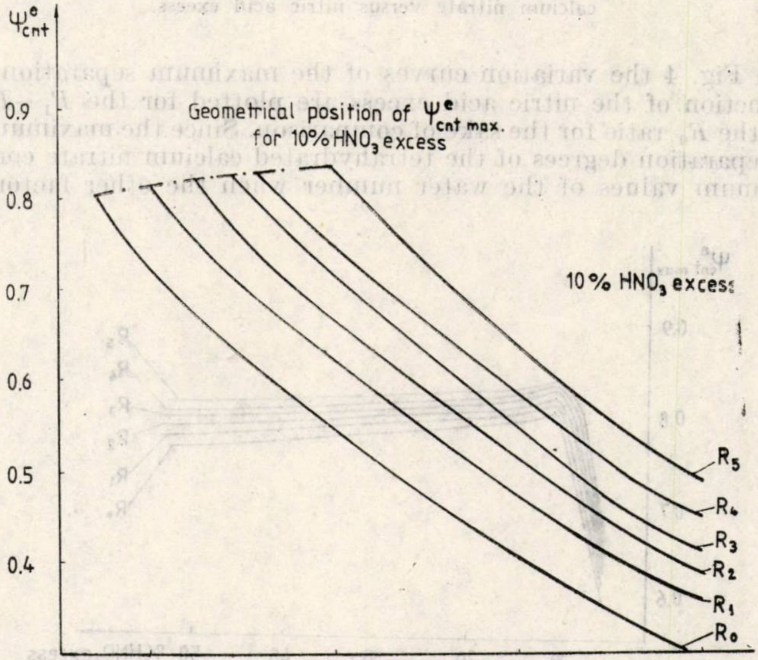

Fig. 6. — The geometrical position of the maximum separation degrees of tetrahydrated calcium nitrate for 10 % HNO_3 excess versus the optimum water number.

correspond to these maxima of the separation degrees, that is the maximum dilutions for obtaining the highest separation degrees of the tetrahydrated calcium nitrate. It may also be noticed that the *R* ratio value increase determines the increase of the maximum separation degree and implicitly of the minimum water number.

By taking these conclusions into account, the variation of the separation degree of the tetrahydrated calcium nitrate was then followed as a function of the water number and the ratio *R*, for 10 % HNO_3 excess, according to the optimum value of the nitric acid excess. By means of the plot in Fig. 6 in which the geometrical position of the maximum separation degrees for 10 % HNO_3 excess was also drawn, the optimum water number values for $R_0 \div R_5$ were obtained.

CONCLUSIONS

1. The equilibrium of the decomposition process of phosphatic raw materials was investigated by means of the double-exchange quaternary diagram at the temperature of 0°C and the influence of nitric acid excess water content (n_{H_2O}) and CaO/P_2O_5 ratio ($R_0 \div R_5$) followed.

2. The optimum value of about 10 % HNO_3 was found for the nitric acid excess determining the maximum separation of the tetrahydrated calcium nitrate.

3. The variation curves of the minimum water number as a function of the nitric acid excess and CaO/P_2O_5 ratio were drawn.

4. The variation curves of the separation degree of tetrahydrated calcium nitrate as a function of the water number and CaO/P_2O_5 ratio for the optimum nitric acid excess (10 % HNO_3) were drawn and the variation curve for maximum separation degrees under these conditions made evident.

REFERENCES

[1] L. Filipescu and E. Pincovschi, "Echilibrul lichid — solid. Aplicații în tehnologia sărurilor minerale", Ed. Tehnică, Bucharest, 1980.

[2] C. Calistru and C. Leonte, "Tehnologia substanțelor anorganice", Ed. Didactică și Pedagogică, Bucharest, 1972.

[3] E. V. Britske, Termiceskie konstanty neorganiceskih vescestv, I.A.N. SSSR, Moskow-Leningrad, 1949.

[4] R. Flatt, G. Brunisholz and A. Denereaz, *Helv. Chem. Acta*, **37**, 274, (1954).

Revue Roumaine de Chimie, **30**, *6*, 499–505 (1985)

SYNTHESIS AND REACTIONS OF SOME NEW CYCLIC β-KETO-ANILIDES*

Part 1

I. I. ABD EL-GAWAD, A. M. KHALIL, O. M. O. HABIB and H. A. ETMAN
Chemistry Department, Faculty of Science, Mansoura University, Egypt

Received March 21, 1984

1,2,3,9,10,10a-Hexahydro-3-oxo-2-phenathrene carboxanilides (IIIa-e) were prepared by Michael condensation of acetoacetanilide with 2-arylidene-1-tetralone. Condensation of III with *o*-phenylene-diamine or *o*-aminophenol afforded diazepinone (Va) and oxazepinone (Vb) *via* anil intermediates (VIa,b) which could be isolated. With polyphosphoric acid or phosphorous oxychloride, III gave naphtho-[2,1-j]-phenanthridione derivatives (VII, VIII). Alkylation of III with acrylonitrile gave IXa,b, while the Mannich reaction yielded the corresponding bases Xc-e.

In our earlier reports [1,2] we described the synthesis of naphthalene annelated α-pyridone from Michael condensation of 2-arylidene-1-tetralone with ethylcyanoacetate. Recently we reported also the synthesis and reactions of some new acetoaceta-iodo-anilides.[3,4] As a sequel to our previous work,[1-4] the synthesis of novel cyclic β-ketoanilides as precursors for the synthesis of new heterocyclic compounds was investigated. Thus, acetoacetanilides Ia,b were readily reacted with 2-arylidene-1-tetralone (IIa-c) in the presence of sodium methoxide and gave the corresponding 1,2,3,9,10,10a-hexahydro-3-oxo-1-phenyl-2-phenanthrene carboxanilides (IIIa-e).

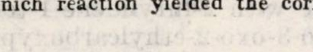

$CH_3-\overset{O}{\overset{\|}{C}}-CH_2-CONHAr'$

I

a, $Ar' = C_6H_5$

b, $Ar' = C_6H_4-Cl-p.$

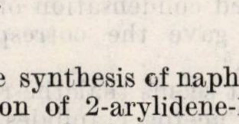

II

a, $Ar = C_6H_5$

b, $Ar = C_6H_4-OCH_3-p$

c, $Ar = C_6H_4-Cl-p$

d, Ar = 2-furoyl

---

* This paper was presented at the Great Lakes Regional Meeting of the American Chemical Society, at Illinois State University, USA, June 7–9 (1982).

The structures of IIIa-e were inferred from correct analytical data and from their IR spectra which showed stretching frequencies at 3030, 1660 and 1630 cm^{-1} characteristic for the $-NH$, $C=O$ and $-CONH-$ groups, respectively.

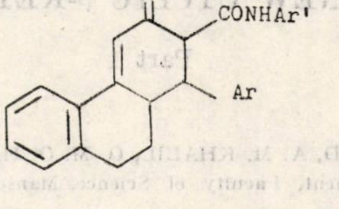

III

a, $Ar = C_6H_5$; $Ar' = C_6H_5$
b, $Ar = C_6H_5$; $Ar' = C_6H_4-Cl-p$
c, $Ar = C_6H_4-OCH_3-p$; $Ar' = C_6H_5$
d, $Ar = C_6H_4-OCH_3-p$; $Ar' = C_6H_4-Cl-p$
e, $Ar = C_6H_4-Cl-p$; $Ar' = C_6H_5$

The formation of β-ketoanilides IIIa-e is analogous to the previously reported condensation of ethyl acetoacetate with 2-furylidene-1-tetralone which gave the corresponding hexahydro-3-oxo-2-ethylcarboxyphenanthrene.[5]

It seems that the reaction involves in its first stage a Michael addition of acetoacetanilides to the exocyclic double bond in the presence of sodium methoxide to give the Michael adduct IV which only appears as an intermediate and cyclizes to the corresponding phenanthrene derivatives IIIa-e under the influence of sodium methoxide.

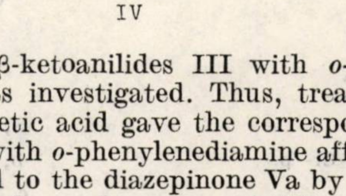

IV

Condensation of β-ketoanilides III with *o*-phenylenediamine and with *o*-aminophenol was investigated. Thus, treatment of IIIa with *o*-phenylenediamine in acetic acid gave the corresponding diazepinone Va, whereas fusion of IIIa with *o*-phenylenediamine afforded the intermediate anils VIa which cyclised to the diazepinone Va by treatment with acetic acid. On the other hand, condensation of IIIa with *o*-aminophenol in acetic acid afforded the anil VIb which cyclised to the corresponding oxazepinone Vb by treatment with polyphosphoric acid.

The structures of Va, Vb, VIa and VIb were deduced from elemental analyses and IR spectra. The compound Va exhibited stretching frequencies at 1645 and 3390 cm^{-1} characteristic for the C=O and $-NH-$ groups, respectively, Vb showed absorption bands at 1600 and 1660 cm^{-1} attributable to the $-C=N-$ and C=O groups, whereas VIb revealed absorption frequencies at 1600, 1630 and 3390 cm^{-1}, characteristic for the $-C=N-$, $-CONH-$ and $-OH$ groups, respectively.

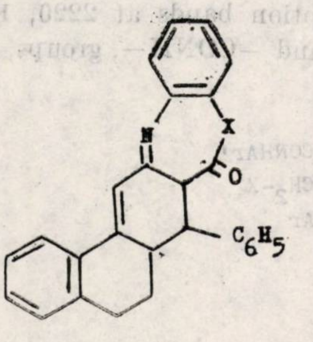

V

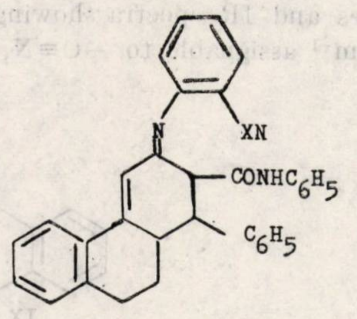

VI

a, X = NH
b, X = O

Since it is well known that acetoacetanilides could be converted into 2-quinolone derivatives by the action of dehydrating agents,[5-8] it became of interest to study the effect of these reagents on the β-ketoanilides III. Thus, treatment of IIIa,b,d with polyphosphoric acid afforded 7, 7a, 8, 9-tetrahydro-7-phenyl-naphtho-[2,1-j]phenanthridine-6(5H)-one derivatives VIIa-c. On the other hand, cyclization of IIIa by treating with phosphorous oxychloride yielded 6-chloro-7,7a,8,9-tetrahydro-7-phenyl-naphtho-[2,1-j] phenanthridine (VIII). Refluxing VIIa with phosphorous oxychloride gave VIII in a good yield.

The IR spectra of VIIa-c showed absorption bands at 3280 and 1660 cm^{-1} characteristic for the $-NH$ and C=O groups, and that of VIII exhibited an absorption band at 1630 cm^{-1} characteristic for the $-C=N-$ group.

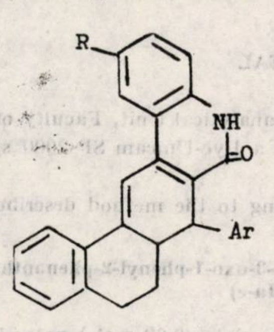

VII

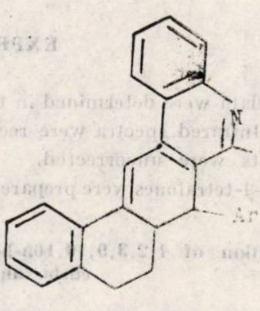

VIII

a, Ar = C_6H_5 ; R = H
b, Ar = C_6H_5 ; R = Cl
c, Ar = $C_6H_4.OCH_3-p$; R = Cl

Alkylation of III with acrylonitrile gave the corresponding cyanoethyl derivatives IXa,b. Similar alkylation was observed when IIIa was treated with formaldehyde and a secondary amine in methanol yielding the corresponding Mannich bases IXc,d.

The structural assignments of IXa,b were based on elemental analyses and IR spectra showing absorption bands at 2220, 1660 and 1630 cm^{-1} assignable to $-C\equiv N$, $C=O$ and $-CONH-$, groups, respectively.

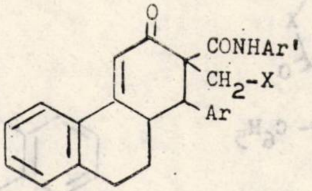

IX

a, $Ar = C_6H_5$: $Ar' = C_6H_5$; $X = CH_2C\equiv N$

b, $Ar = C_6H_4-OCH_3-p$; $Ar' = C_6H_4-Cl-p$; $X = CH_2C\equiv N$

c, $Ar = Ar' = C_6H_5$; $X = C_5H_{10}N$

d, $Ar = Ar' = C_6H_5$; $X = C_4H_8N$

e, $Ar = Ar' = C_6H_5$; $XX = OH$

On the other hand, the structures of IXc,d were deduced by refluxing IIIa with formaldehyde in methanol when the formed hydroxymethyl derivative (IXe) was isolated. Warming IXe with piperidine or morpholine afforded the above Mannich bases IXc,d. These structures were also confirmed from analytical results and IR spectra showing bands at 1720 and 2925 cm^{-1} characteristic for the $C=O$ and $-CH_2$ groups, respectively.

EXPERIMENTAL

Analytical data were determined in the Microanalytical Unit, Faculty of Science, Mansoura University. Infrared spectra were recorded on a Pye-Unicam SP-2000 spectrophotometer. Melting points were uncorrected.

2-Arylidene-1-tetralones were prepared according to the method described previously.[1,2]

Preparation of 1,2,3,9,10,10a-hexahydro-3-oxo-1-phenyl-2-phenanthrene carboxanilides (IIIa-e)

To (0.01 mole) of 2-arylidene-1-tetralones (IIa-c) in (0.02 mole) potassium methoxide, the appropiate acetoacetanilide (0.01 mole) was added. The reaction mixture was refluxed for six hours, poured onto ice-cold dilute hydrochloric acid. The separated solid products were filtered off and crystallized from ethanol to give IIIa-e (Table 1).

Table 1

1,2,3,9,10,10a-Hexahydro-3-oxo-1-phenyl-2-phenanthrene-carboxanilides IIIa-e

Compound No.	M.p. °C	Yield %	Formula	Analyses %			
					C	H	N
IIIa	143	80	$C_{27}H_{23}NO$	Found	82.13	5.72	3.53
				Calcd	82.41	5.89	3.55
IIIb	173	70	$C_{27}H_{22}NO_2Cl$	Found	69.52	4.44	2.90
				Calcd	69.98	4.78	3.02
IIIc	132	75	$C_{28}H_{25}NO_3$	Found	79.13	5.54	3.12
				Calcd	79.40	5.95	3.30
IIId	180	85	$C_{28}H_{24}NO_3Cl$	Found	73.06	4.89	3.01
				Calcd	73.43	5.28	3.05
IIIe	194	80	$C_{27}H_{22}NO_2Cl$	Found	75.36	4.88	3.40
				Calcd	75.78	5.10	3.27

Formation of 6,6a,7,7a-tetrahydro-7-phenylbenzo-[b] phenanthra-[3,2-e] [1,4]-diazepine-8(5H)-one (Va)

A mixture of IIIa (0.01 mole) and *o*-phenylenediamine (0.01 mole) in acetic acid (40 mL) was heated at 70°C for 20 minutes and filtered while hot. The deep-red solid that separated on standing was filtered and crystallized from acetic acid to give Va as deep red crystals, m.p. 128°C, yield 75%.

Analysis : $C_{27}H_{22}N_2O$. Found : C% 82.64; H% 5.14; N% 6.98; Calcd; C% 83.05; H% 5.68; N% 7.18.

Fusion of IIIa with o-phenylenediamine. Formation of carboxanilide (VIa)

A mixture of IIIa (0.01 mole) and *p*-phenylenediamine (0.01 mole) was fused for one hour at 140°C in an oil bath. After cooling, the precipitate was filtered off and crystallized from ethanol to give VIa as a red crystalline solid, m.p. 225°C, yield 65%.

Analysis : $C_{33}H_{29}N_3O$. Found : C% 81.63; H% 6.22; N% 8.47; Calcd : C% 81.96; H% 6.04; N% 8.69.

Compound VIa (0.5 g) was heated in glacial acetic acid (30 mL) at 70—80°C for 30 minutes. The solid product formed on cooling was proved to be Va by m.p. and mixed m.p.

Reaction of IIIa with o-aminophenol

A mixture of IIIa (0.1 mole) and *o*-aminophenol (0.1 mole) was heated in acetic acid (30 mL) at 70—80°C for 30 minutes, filtered while hot to give the 1,2,3,9,10,10a-hexahydro-3-oxo-1-phenyl-2-phenanthrenecarboxanilide-3-(o-hydroxyphenyl) VIb as orange crystals, m.p. 150°C, yield 80%.

Analysis : $C_{33}H_{28}N_2O_3$. Found : C% 82.16; H% 5.41; N% 5.25; Calcd : C% 71.79; H% 5.82; N% 5.78

Compound VIb (0.5 g) was heated in polyphosphoric acid (40 mL) for one hour at 90—110°C. After cooling, the reaction mixture was poured into ice-cold water, and the solid product was filtered off and crystallized from benzene to give 6,6a,7,7a-tetrahydro-7-phenylbenzo-[b]-phenanthro-[3,2-e][1,4]-oxazepin-8(5H)-one (Vb) as reddish-brown crystals, m.p. 243°C, yield 70%.

Analysis : $C_{21}H_{21}NO_2$. Found : C% 82.49; HA 5.58; N% 3.41; Calcd : C% 82.84; H% 5.40; N% 3.57.

Treatment of IIIa,b,d with polyphosphoric acid

Polyphosphoric acid (20 mL) was heated with IIIa,b,d (1.0 g in each case) for one hour at 110—130°C. After cooling, the reaction product was poured into ice-cold water and the formed solid was filtered and crystallized from ethanol to give 7,7a,8,9-tetrahydro-7-phenylnaphtho-[2,1-j]-phenanthridine-6(5H)-one derivatives (VIIa-c) (cf. Table 2).

Table 2

7,7a,8,9 Tetrahydro-7-phenylnaphtho-[2,1-j]phenanthridine-6-(5H)-ones, (VIIIa-c)

Compound No.	M.p. °C	Yield %	Formula		Analysis %		
					C	H	N
VIIa	248	70	$C_{27}H_{21}NO$	Found Calcd	86.04 86.37	5.88 5.64	3.91 3.73
VIIb	193	70	$C_{27}H_{20}NOCl$	Found Calcd.	79.30 79.11	5.32 4.92	3.66 3.42
VIIc	142	65	$C_{28}H_{22}NO_2Cl$	Found Calcd	75.99 76.44	5.15 5.04	3.06 3.18

Effect of phosphorous oxychloride on IIIa

A solution of IIIa (0.5 g) in phosphorous oxychloride (20 mL) was heated on a steam bath for three hours then left to stand for several hours. The separated product was filtered and crystallized from ethanol to give 6-chloro-7-7a,8,9-tetrahydro-7-phenylnaphtho-[2,1-j] phenanthridine (VIII) as red crystals, m.p. 194°C, yield 65%.

Analysis: $C_{27}H_{20}NCl$. Found: C% 82.18; H% 4.49; N% 3.43; C% 8.41; Calcd: C% 82.33; H% 5.12; N% 3.55; C% 9.00.

Reaction of IIIa,c with acrylonitrile

A solution of IIIa,c (0.5 g in each case) in 20 mL acrylonitrile and sodium metal (1,0 g) was heated on a steam-bath for three hours then left to stand several hours. The separated solids were filtered and crystallized from acetone to give 2-2-(2-cyanoethyl)-1,2,3,9,10-10a-hexahydro-3-oxo-1-aryl-2-phenanthrenecarboxanilides (IXa,b) (cf. Table 3).

Table 3

2-(2-Cyanoethyl)-1,2,3,9,10,10a-hexahydro-3-oxo-1-acetyl-2--phenanthrenecarboxanilides (IXa,b)

Compound No.	M.p. °C	Yield %	Formula		Analysis %		
					C	H	N
IXa	282	85	$C_{30}H_{26}N_2O_2$	Found Calcd	80.19 80.69	5.49 5.87	6.02 6.28
IXb	190	80	$C_{31}H_{27}N_2O_3Cl$	Found Calcd	72.52 72.86	5.51 5.33	5.63 5.48

Mannich reaction of IIIa

To a methanolic solution of IIIa (0.01 mole) and the appropriate secondary amine (0.02 mole), (25 mL) 35% aqueous formaldehyde was added. The reaction mixture was refluxed for 24 hrs, and left to stand under cooling. The solid product that separated was crystallized from ethanol to give 1,2,3,9,10,10a-hexahydro-3-oxo-1-aryl-2-(piperidino- or morpholinomethyl)-2-phenanthrene carboxanilides (IXc,d) (cf. Table 4).

Table 4

Mannich bases obtained from the reaction of IIIa with piperidine or morpholine

Compound No.	M.p. °C	Yield %	Formula	Analysis %			
					C	H	N
IXc	172	60	$C_{33}H_{34}N_2O_2$	Found	80.27	6.73	5.63
				Calcd	80.78	6.99	5.71
IXd	125	65	$C_{32}H_{32}N_2O_3$	Found	78.19	6.34	5.32
				Calcd	78.02	6.55	5.69

Formation of 1,2,3,9,10,10a-hexahydro-3-oxo-1-phenyl-2-(hydroxy-methyl-2-phenanthrene carboxanilide (IXe)

To a solution of IIIa (0.01 mole in methanol 50 mL), aqueous formaldehyde (10 mL, 35%) was added. The reaction mixture was refluxed for thirty hours and the solvent was removed under reduced pressure. The product was allowed to solidify by standing, and then crystallized from ethanol to give IXe as a yellow powder, m.p. 300°C, yield 50%.

Analysis : $C_{22}H_{25}NO_3$. Found : C% 79.41; H% 5.43; N% 3.10; Calcd : C% 79.40; H% 5.95; N% 3.30

Conversion of IXe into IXc,d

A mixture of IXe (0.01 mole) and piperidine or morpholine (0.015 mole) was heated on a steam-bath for four hours. The oily residue was triturated with dilute methanol. The formed solid product was proved to be IXc,d (m.p. and mixed m.p.).

REFERENCES

[1] T. Zimaity, A. M. Khalil, I. I. Abd El-Gawad and S. Fouda, *J. Indian Chem. Soc.*, **54** 623 (1977).

[2] I. I. Abd El-Gawad, A. M. Khalil, T. Zimaity and S. Fouda, *J. Indian Chem. Soc.*, **54**, 626 (1977).

[3] I. I. Abd El-Gawad, A. M. Khalil, M. I. Ali and M. M. Girgis, *Indian J. Chem.*, **17B**, 585 (1979).

[4] A. M. Khalil, I. I. Abd El-Gawad, M. I. Ali and M. M. Girgis, *Indian J. Chem.*, **17B**, 627 (1979).

[5] D. A. Peak, P. A. Robinson and I. Walker, *J. Chem. Soc.*, **1936**, 752.

[6] A. Albert, A. J. Brown, and H. Duewell, *J. Chem. Soc.*, **1948**, 1284.

[7] C. E. Kaslow and R. A. Reck, *J. Amer. Chem. Soc.*, **69**, 864 (1947).

[8] R. Huisgen, *Liebigs Ann. Chem.*, **559**, 101 (1948).

Revue Roumaine de Chimie, 30, 6, 507–510 (1985)

MODERN FRIEDEL-CRAFTS CHEMISTRY. X[1].

REARRANGEMENTS ACCOMPANYING FRIEDEL-CRAFTS ALKYLATION OF BENZENE WITH ISOMERIC PENTANOLS AND PENTENES

ALI ALI KHALAF[a] and ROYSTON M. ROBERTS[b]

[a] Department of Chemistry, King Abdulaziz University, Jeddah, Saudi Arabia;

[b] Department of Chemistry, The University of Texas at Austin, Austin, Texas 78712, U.S.A.

Received May 29, 1984

The alkylation of benzene with some isomeric pentanols and pentenes was investigated. The results were interpreted on the basis of our improved knowledge about rearrangements accompanying Friedel-Crafts reactions.

There have been numerous early reports on the Friedel-Crafts alkylation of aromatics with isomeric pentanols and pentenes.[2] However, the poor technique employed for product analysis added to the lack of our present knowledge about the behaviour of carbocations led to questionable and contradictory results especially in regard to isomer distribution in the alkylates. A look at the compiled literature results [2] indicates that confusion existed not only with respect to the extent of rearrangement but also with respect to its occurrence.

In this paper we employed modern techniques to study the alkylation of benzene with some isomeric pentanols and pentenes. The performed experiments are either duplicates of old ones to check their validity or new ones designed to shed some light on the mechanism and the extent of the involved rearrangements.

EXPERIMENTAL

The conditions employed for alkylation together with the results obtained are given in Tables 1 and 2. The experiments of Table 1 duplicated those performed by Streitweiser and co-workers [3] in 1959.

RESULTS AND DISCUSSION

Comparison of our results with those of the earlier workers reveals minor differences in regard to the percentages of the individual components of the mixtures. The confirmation that both 2- and 3-pentanol gave identical product mixtures augmented the proposition that the 2- and 3-

Table 1

Alkylation of benzene with straight-chain pentanols in the presence of BF_3 catalysts[a,b,c]

Entry No.	Alkylating alcohol	Temp. °C	Time hr	Product composition, %			
				2-Phenyl-pentane	3-Phenyl-pentane	*t*-Penthyl-benzene	Other compounds
1	1-Pentanol	60	24	59 (53)	21 (20)	20 (25)	— (3)
2	2-Pentanol	0	1	60 (66)	31 (23)	9.0 (9.0)	— (2)[d]
3	3-Pentanol	0	1	60 (64)	31 (23)	9.0 (10.0)	— (—)

a) These experiments duplicate those of Streitweiser and co-workers.[3]

b) Values between brackets are those reported by Streitweiser and coworkers.[3] c) Yields from 60—70% were obtained. d) This was suggested to be 3-methyl-3-phenylbutane.[3]

Table 2

Alkylation of benzene with branched pentyl alcohols and pentenes

Entry No.	Alkylating agent (mole)	Catalyst (mole)	Temp. °C	Time, hr	Yield %	Production composition, %				
						2-Methyl-3-phenyl-butane	*t*-Pentyl-benzene	Neopentyl-benzene	*t*-Butyl-benzene	Hexyl-benzenes
4[a]	3-Methyl-1-butene)) (0.1)	$AlCl_3$ (0.0007) + traces of H_2O	5—25	1	3	26	50	—	20	4
5[b]	3-Methy-1-butene (0.1)	$AlCl_3$ (0.02) +HClg	21	0.6	70	48	36	1	10	5
6[c]	3-Methyl-2-butene (0.86)	96% H_2SO_4 (30 ml)	25	20	7	—	60	—	30	10
7	3-Methyl-2-butanol (0.05)	$AlCl_3$ (1.8)+ CH_3NO_2 (4 ml)	25	24	65	2	95	—	3	Tr
8[d]	3-Methyl-2-butanol (0.113)	BF_3 (Saturation)	0	1	45	3	52	—	33	12
9	*t*-Pentyl alcohol (0.77)	95.5% H_2SO_4 (100 ml)	25	20	25	—	90	—	7	3

a) Duplicates an experiment by Aldridge and Hunter[16] in which he did not identify the monoalkylates.

b) Duplicates an experiment by Friedmen and Morritz [11] in which they reported 2-methyl-3-phenylbutane as the only product.

c) These results contradicted those of Friedman and Morritz.[11]

d) Duplicates an experiment by Friedman and Morritz in which they reported the product to be probably a mixture of 72% *t*-pentylbenzene and 28% *t*-butylbenzene.[11]

Tabelul 2 (continuare)

Entry No.	Alkytating agent (mole)	Catalyst (mole)	Temp, °C	Time, hr	Yield %	Product composition, %				
						2-Methyl-3-phenyl-butane	*t*-Pentyl-benzene	Neopentyl-benzene	*t*-Butyl-benzene	Hexyl-benzenese
10	*t*-Pentyl alcohol (0.05)	$AlCl_3$ (1.8) CH_3NO_2 (0.05)	35	20	70	2	96	—	2	Tr
11[e]	*t*-pentyl alcohol (0.1)	$AlCl_3$ (0.05)	25—35	1	—	34	66	Tr	Tr	—
				4	—	34	66	Tr	Tr	—
				20	50	39	60	1	Tr	—
12	*t*-Pentyl alcohol (0.1)	$AlCl_3$ (0.15)	23—35	1	—	64	25	8	3	Tr
				4	—	57	29	12	2	Tr
				20	40	66	18	13	3	Tr

e) Under similar conditions Huston and Hsieh [17] reported a yield of 40% *t*-pentylbenzene and 1.8% 2-methylbutane.

phenylpentane ratio was probably determined by the rearrangement of the intermediate carbocations prior to alkylation. It is to be noted that the ratio of 2-phenylpentane to 3-phenylpentane in the products may be compared to the ratios found in the $AlCl_3$ and $AlCl_3/CH_3NO_2$ catalysed alkylation of benzene with 2- and 3-chloropentane where a constant proportion of 2- : 3-phenylpentane of 71 : 2 was attained.[4]

The formation of *t*-pentylbenzene during the alkylation of benzene with 1-, 2- and 3-pentanol is rather interesting. This has been attributed by Streitweiser and co-workers [3,5] to what of recent views, the formation of this isomer can be rationalised in terms of a mechanism involving protonated cyclopropane intermediates.[6-8]

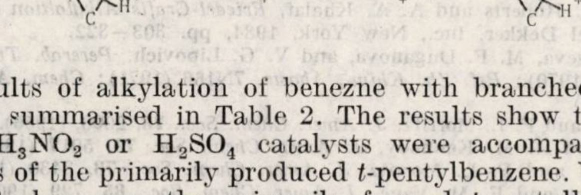

The results of alkylation of benezne with branched pentenes and pentanols are summarised in Table 2. The results show that alkylations with $AlCl_3/CH_3NO_2$ or H_2SO_4 catalysts were accompanied by minor rearragements of the primarily produced *t*-pentylbenzene. With the strong $AlCl_3$ catalyst, however, the primarily formed *t*-pentylbenzene rapidly isomerised to 2-methyl-3-phenylbutane and the latter is more slowly isomerised to neopentylbenzene. These results are in good accord with the findings of other investigators.[9]

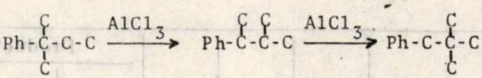

The production of varying amounts of *t*-butylbenzene and *t*-hexylbenzene, especially in alkylations with pentenes is not unexpected since this has been observed by other workers.[3,10,11] Their production can be explained on the basis of bimolecular reactions as formerly proposed for the cleavage of isopentene to isobutane and higher products.[12–15] According to the proposed mechanism a C_{10}-carbocation is the intermediate involved in the formation of C_4 and C_2 fragments :

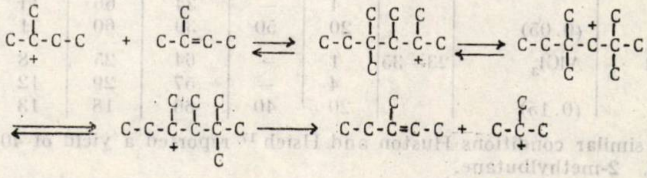

Alkylation of benzene with the latter two fragments yields-t-butylbenzene and hexylbenzene, respectively.

REFERENCES

[1] (a) Part IX : A. A. Khalaf and A. A. El-Khawaga, *Rev. Roum. Chim.*, **26**, 739 (1981); (b) Generous support of this research by the Robert A. Welch Foundation is gratefully acknowledged.

[2] For comprehensive reviews see : (a) G. A. Olah, Ed., *Friedel-Crafts and Related Reactions*, Vols. 1—4, Wiley-Interscience, New York, 1963—1965 ; (b) G. A. Olah, *Friedel-Crafts Chemistry*, John Wiley and Sons, New York, 1973 ; (c) R. M. Roberts and A. A. Khalaf, *Friedel Crafts Alkylation Chemistry*, Marcel Dekker, Inc., New York, 1984.

[3] A. Streitweiser, Jr., D. P. Stevenson and W. D. Schaeffer, *J. Amer. Chem. Soc.*, **81**, 1110 (1959).

[4] R. M. Roberts, S. E. McGuire and I. R. Baker, *J. Org. Chem.*, **41**, 659 (1976).

[5] A. Streitweiser, Jr., W. D. Schaeffer and S. Andreades, *J. Amer. Chem. Soc.*, **81**, 1113 (1959)

[6] G. M. Kramer, *J. Amer. Chem. Soc.*, **91**, 4819 (1969).

[7] D. M. Brouwer and J. M. Oelderik, *Preprints Div. Pet.* Chem, **13**, 184 (1968); *Recl. Trav. Chim. Bays-Bas*, **87**, 721 (1968).

[8] D. M. Brouwer and J. A. Van Doorn, *Recl. Trav. Chim Pays-Bas*, **91**, 895 (1972).

[9] (a) R. M. Roberts and S. E. McGuire, *J. Org. Chem.*, **35**, 102 (1970); (b) For a review see : R. M. Roberts and A. A. Khalaf, *Friedel-Crafts Alkylaltion Chemistry*, 1*st* ed. Marcel Dekker, Inc., New York, 1984, pp. 303—322.

[10] M. F. Polubentseva, M. F. Duganova, and V. G. Lipovich, *Pererab. Tverd. Topl.*, No. 2, 292 (1970); *Ref. Zh. Khim., Abastr.* 7N166 (1971); *Chem. Abstr.*, **76**, 153250a (1972).

[11] B. S. Friedman and F. L. Morritz, *J. Amer. Chem. Soc.*, **78**, 2000, (1956).

[12] A. Schneider and R. M. Kennedy, *J. Amer. Chem. Soc.* **73**, 5017 (1951).

[13] B. S. Friedman and F. L. Morritz, *J. Amer. Chem. Soc.*, **78**, 3430 (1956).

[14] .G J. Karabatsos and F. M. Vane, *J. Amer. Chem. Soc.*, **85**, 729 (1963).

[15] G. J. Karabatsos, F. M. Vane and S. Mayerson, *J. Amer. Chem. Soc.*, **85**, 733 (1963).

[16] G. L. Aldridge and E. A. Hunter, *U. S. Pat.* 3, 0141, 081 (Dec. 19, 1961); *Chem. Abstr.*, **56**, 12800^c^ (1962).

[17] R. C. Huston and T. G. Hsieh, *J. Amer. Chem. Soc.*, **58**, 439 (1936).

Revue Roumaine de Chimie, **30**, *6*, 511–516 (1985)

RARE EARTH CHELATES OF DISUBSTITUTED 2-HYDROXY-ACETOPHENONES

M. MITTAL, S. R. MALHOTRA, KEEMTI LAL and S. P. GUPTA
Chemistry Department, D. N. College, Meerut-250 002, India

Received October 20, 1983

Synthesis and characterisation of chelates of trivalent rare earth metals : La, Pr, Nd, Sm, Gd, Tb, Dy, Ho and Er with 4,5-dimethyl-2-hydroxyacetophenone and 5-chloro-2-hydroxy-4-methylacetophenone are described. These reagents act as bidentate ligands coordinating through phenolic and carbonyl oxygen atoms. The chelates are characterised to be neutral six-coordinated octahedral complexes of the formula ML_3 by elemental analyses, conductance, magnetic, infrared and electronic spectral measurements. The values of nephelauxetic ratio (β), percentage covalency parameter (δ) and bonding parameter ($b^{1/2}$) are also calculated. The stability constant of trivalent lanthanide ions complexes are also determined in 50%(v/v) dioxane-water medium by Calvin-Bjerrum pH titration technique at 27° and various ionic strengths (0.1, 0.05 and 0.01 M $NaClO_4$). The order of stability constant is found $La < Pr < Nd < Sm > Gd < Tb < Dy < Ho$; which is in agreement with the findings of Stagg and Powell.

INTRODUCTION

The literature records a number of reports on the determination of proton-ligand stability constant of 2-hydroxyacetophenone and some of its derivatives and formation constants of their transition metal ions chelates.[1-7] However formation constant and isolation of rare earth chelates of 4,5-dimethyl-2-hydroxyacetophenone (DMHA) and 5-chloro-2-hydroxy-4-methylacetophenone (CHMA) have not been reported so far, and hence there is need for title investigation. We report here the synthesis and charcterisation of trivalent La, Pr, Nd, Sm, Gd, Tb, Dy, Ho and Er chelates with DMHA and CHMA by elemental analyses, conductance, magnetic, infrared and electronic spectral measurements. The stability constant of the chelates are also determined in 50% (v/v) dioxane-water medium at 27° and various ionic strenghts 0.1M, 0.05M and 0.01M ($NaClO_4$) employing Calvin-Bjerrum pH titration technique[8] as applied by Irving and Rossotti.[9]

EXPERIMENTAL

The ligands DMHA and CHMA were prepared as described earlier.[6,10] The rare earths nitrates were procured from M/S Indian Rare Earth Ltd. (Kerla) and used as such. All other chemicals were of AnalaR grade. The solutions of purified dioxane and sodium hydroxide were prepared as earlier.[2] The analyses and physical measurements were carried out as reported earlier.[6,11]

A systronic digital pH-meter type 335 (accuracy 0.01 pH unit) was used for pH measurements. The following titrations were carried out in 50% (v/v) dioxane-water medium at 27° and various ionic strenghts 0.1M, 0.05 M and 0.01M ($NaClO_4$) against carbonte free sodium hydroxide (0.05M) : (i) 2.0 mL perchloric acid (0.05M); (ii), (i) + 10.0 mL ligand (0.01M) and (iii), (ii) + 2.0 mL metal ion (0.01M). Data on B values (pH water readings) versus volume of alkali were corrected in each case.[12,13]

Preparation of Chelates

The metal chelates were synthesised by constant stirring ethanolic solution of the ligand and aqueous solution of metal ion in 5 : 1 mol ratio; pH was adjusted by addition of NH_4OH to just below that for hydrous hydroxide precipitation.[14] Light yellow coloured crystalline solid was filtered off, washed with water, ethanol, acetone and dried.

RESULTS AND DISCUSSION

Calculation

The formation functions, $\bar{n}_A$, $\bar{n}$ and pL were calculated from the pH-titration curves.[9] The pK_1^H values for DHMA and CHMA were obtained by half-integral method. The same value was also evaluated using the graphical method by treating separately the portions on either side of $\bar{n}_A = i$ where $i = 1$ or 2 or 3. Equation (1) was used for this purpose.

$$\log \frac{(i-\bar{n}_A)}{\bar{n}_A-(i-1)} = B - pK_1^H \qquad (1)$$

The average pK_1^H values of the ligands at various ionic strengths so obtained are given (Table 1). The values obtained by different methods are in good agreement with each other and they are accurate to ± 0.02 log units.

Calculation of formation constant of metal chelates was accomplished in two steps :

(i) the formation curves of $\bar{n}$ versus pL and

(ii) the curves were analysed to arrive at the metal-ligand stability constants. The stoichiometric metal-ligand stability constant was determined by half-integral and graphical methods. Equation (2) was used for graphical method.

$$\log \frac{1-\bar{n}}{\bar{n}} = pL - \log K_1 \qquad (2)$$

The average values of $\log K_1$ at various ionic strenghts are reported (Table 1). The value of $\log K_1^{I=0}$ was obtained by extrapolation of $\log K_1$ to ionic strength zero from the graph between $\log K_1$ versus $I^{1/2}$ (I = ionic strength). The change in the free energy ($-\Delta G_1^{I=0}$) in kJ mole^{-1}) was calculated by equation (3) at 27°.

$$-\Delta G_1^{I=0} = 2.303\ RT\ \log K_1^{I=0} \qquad (3)$$

The values of $\log K_1^{I=0}$ and $-\Delta G_1^{I=0}$ are reported (Table 1).

Table 1

Stability constant and free energy change of lanthanide complexes of DMHA and CHMA in 50% (v/v) dioxane-water medium at 27° and various ionic strengths (*I*)

Cations	$\log K_1$ at various I				$-\Delta G_1^{I=0}$
	0.10M	0.05M	0.01M	0.00M	(kJ. mole^{-1})
			DMHA		
H(I)	10.95	11.10	11.28	11.50	66.154
La(III)	4.42	4.50	4.54	4.61	26.519
Pr(III)	4.85	4.91	4.98	5.08	29.223
Nd(III)	5.00	5.08	5.14	5.26	30.258
Sm(III)	5.26	5.34	5.40	5.51	31.696
Gd(III)	5.08	5.18	5.24	5.36	30.834
Tb(III)	5.20	5.31	5.40	5.52	31.754
Dy(III)	5.31	5.42	5.51	5.65	32.502
Ho(III)	5.47	5.59	5.64	5·78	33.250
			CHMA		
H(I)	10.08	10.22	10.42	10.68	61.437
La(III)	3.94	4.06	4.12	4.20	24.161
Pr(III)	4.32	4.40	4.49	4.58	26.347
Nd(III)	4.50	4.60	4.66	4.74	27.267
Sm(III)	4.71	4.82	4.90	5.00	28.762
Gd(III)	4.50	4.64	4.71	4.82	27.727
Tb(III)	4.60	4.70	4.78	4.85	27.900
Dy(III)	4.72	4.84	4.92	5.02	28.878
Ho(III)	4.90	4.98	5.04	5.12	29.453

The order of $\log K_1$ is as follows: La(III) < Pr(III) < Nd(III) < < Sm(III) > Gd(III) < Tb(III) < Dy(III) < Ho(III) which is in agreement with the findings of Stagg and Powell.[15] The explanation for this order of stability constant may be that the lanthanide metal ions differ from each other in the number of electrons in 4f orbital, which are effectively shielded from the interaction with ligand orbitals by electrons in 5s, 5p and 6s orbitals.[16] Hybridisation would involve normally unoccupied higher energy level orbitals and this may be expected to occur with strongly coordinated ligands. Lanthanides, therefore, normally form ionic compounds. This possibility of covalent interaction however cannot be excluded as reported in the case of acetylacetone chelates.[17] If the bonds are ionic, the Born relation: $E = Z^2\left(1 - \dfrac{1}{D}\right)/2r$ should be valid for the complexation equilibrium under study (Z is the charge and r is the radius of the metal ion; D is the dielectric constant of the medium). The stability constants being directly proportional to E, the energy change on complexation of the gaseous metal ion should yield linear plots with Z^2/r. In the present case such plots show some deviation from a strict linear nature suggesting partial covalency.[17] Earlier work on lanthanide complexes support our observation.[18–21]

The plot between $\log K_1$ and atomic number of the lanthanide shows that the $\log K_1$ values of the complexes gradually increase with atomic number from La(III) to Sm(III) and from Gd(III) to Ho(III). The log K_1 values for Gd(III) complexes are lower than Sm(III) complexes resulting in the familiar Gd-break.[17]

Characterisation

The analytical data (Table 2) show that complexes can be represented as ML_3 where M = La(III), Pr(III), Nd(III), Sm(III), Gd(III), Tb(III), Dy(III), Ho(III) and Er(III), and L = deprotonated DMHA or CHMA. The conductivity measurements of 0.001M solutions in DMF show non-electrolytic nature [22] of the complexes ($\Delta_M = 4-8$ ohm^{-1} cm^2 mole^{-1}). The magnetic moments of all the complexes observed at 27° are given (Table 2). The magnetic moments show very little deviation from Van Vleck values [23] indicating, as expected, that 4f electrons are not involved in bond formation in these complexes.

Table 2

Analytical data and magnetic moment of rare earth metal complexes of DMHA and CHMA

Compound	Metal (%)		Cl (%)		Magnetic moment (B.M.)
	Found	Cald.	Found	Cald.	
LaL_3	21.93	22.00	—	—	—
PrL_3	22.27	22.37	—	—	3.62
NdL_3	22.70	22.78	—	—	3.50
SmL_3	23.61	23.51	—	—	1.40
GdL_3	23.39	24.33	—	—	7.80
TbL_3	24.40	24.52	—	—	9.50
DyL_3	24.85	24.94	—	—	10.34
HoL_3	25.30	25.22	—	—	10.52
ErL_3	25.30	25.46	—	—	9.21
LaL'_3	20.47	20.15	15.38	15.45	—
PrL'_3	20.00	20.38	15.22	15.40	3.62
NdL'_3	21.02	20.88	15.40	15.33	3.52
SmL'_3	21.21	21.45	15.06	15.19	1.54
GdL'_3	22.10	22.19	15.22	15.05	7.75
ZbL'_3	22.52	22.41	15.20	15.01	9.41
DyL'_3	22.70	22.74	15.00	14.95	10.28
HoL'_3	23.18	23.06	14.76	14.88	10.52
ErL'_3	23.18	23.27	14.96	14.84	9.20

$L = C_{10}H_{11}O_2$ (Deprotonated DMHA)
$L' = C_9H_8O_2Cl$ (Deprotonated CHMA)

The important bands (in cm^{-1}) of IR spectra of DMHA, CHMA and their lanthanide chelates are described here. The bands at 2940 and 2920 are assigned to ν OH vibration [24] in the spectra of DMHA and CHMA respectively which disappered in all the chelates. This disappearance indicates the loss of phenolic proton on complexation. The bands appearing at 1660 and 1670 are assigned to C=O group [24] which shifts to 1620–30 and 1640–50 in the complexes of DMHA and CHMA respectively. This indicates that keto group is also taking part in complexation. The bands observed at 1220 and 1235 in the spectra of the ligands DMHA and CHMA respectively shift to 1240—50 and 1250—60 in metal complexes which are assigned to phenolic νC—O vibration. This may be due to delocalization of electron density from the oxygen atoms to the lanthanide ions. The weak absorption band around 400 has also been observed in the spectra of all the complexes which may be due to stretching (M—O) vibration.

The absorption bands of trivalent Pr, Nd, Sm, Dy, Ho and Er in visible and near IR region appear due to the transitions from ground levels : $^3H_4$ $^4I_{9/2}$ $^6H_{5/2}$, $^6H_{15/2}$ $^5I_8$ and $^4I_{15/2}$ respectively to the excited J-levels of $4f^n$ configuration.[25] The magnitude of red shift (nephelauxetic effect) is dependent on the change in the interelectronic repulsion parameter. The nephelauxetic ratio (β) and the percentage covalency parameter (δ) were calculated [26] using the equations (4) and (5).

$$\beta = (\nu \text{ complex ion}/\nu \text{ aqueous ion}) \tag{4}$$

$$\delta = (1 - \beta) \times 100/\beta \tag{5}$$

The values of δ were found to be positive in all these complexes indicating electron delocalization from 4f orbital. Henrie and Choppin [27] correlated the bonding parameter ($b^{1/2}$) to the nephelauxetic ratio by equattion (6).

Table 3

The value of nephelauxetic ratio (β), percentage covalency parameter (δ) and bonding parameter ($b^{1/2}$) of some rare earth metal complexes of DMHA and CHMA

Complex	β	δ	$b^{1/2}$
$\mathrm{PrI_2}$	0.9868	1.3376	0.8124
$\mathrm{NdL_3}$	0.9852	1.5022	0.8602
$\mathrm{SmL_3}$	0.9818	1.8537	0.9539
$\mathrm{DyL_3}$	0.9800	2.0408	1.0000
$\mathrm{HoL_3}$	0.9771	2.3437	1.0677
$\mathrm{ErL_3}$	0.9738	2.6905	1.1445
$\mathrm{PrL'_3}$	0.9882	1.1941	0.7681
$\mathrm{NdL'_3}$	0.9854	1.4816	0.8544
$\mathrm{SmL'_3}$	0.9826	1.7708	0.9327
$\mathrm{DyL'_3}$	0.9804	1.9992	0.9899
$\mathrm{HoL'_3}$	0.9774	2.3123	1.0630
$\mathrm{ErL'_3}$	0.9728	2.7960	1.1662

L = Deprotonated DMHA
L′ = Deprotonated CHMA

$$b^{1/2} = [(1 - \beta)/2]^{1/2} \tag{6}$$

The values of $b^{1/2}$ indicate the extent of $4f$ participation in the complexation. The greater the magnitude of $b^{1/2}$, the greater is the contribution of the $4f$ orbital to complex formation. The positive values of δ and $b^{1/2}$ and less than unity values of β in the present complexes point towards the incidence of covalency in the metal-ligand bond. Comparing the values of these parameters (Table 3) in different lanthanides, we find gradual increase in the covalency character with the increase on atomic number of lanthanide. This is in conformity with the lanthanide contraction.

ACKNOWLEDGEMENT. One of us (SRM) is thankful to CSIR, New Delhi for the award of post-doctorate fellowship.

REFERENCES

[1] P. V. Kamat and M. G. Datar, *J. Indian Chem. Soc.*, **47**, 409 (1970); **49**, 261 (1972).

[2] R. P. Patel and R. D. Patel, *J. Inorg. Nuclear Chem.*, **32**, 2591 (1970).

[3] R. P. Patel and M. N Patel, *J. Inorg. Nuclear Chem.*, **34**, 1891 (1972).

[4] K. Lal and S. R. Malhotra, *Rev. Port. Quim*, **21**, 123 (1979).

[5] K Lal, J. Singh and S. P. Gupta, *Chim. Acta Truc.*, **7**, 249 (1979).

[6] M. Mittal, K. Lal and S. P. Gupta, *J. Indian Chem. Soc.*, **57**, 46 (1980); *Rev. Roum. Chim.* **26**, 1335 (1981).

[7] J. K. Verma and R. B. Patel, *J. Indian Chem. Soc.*, **59**, 43 (1982).

[8] J. Bjerrum, "Metal Amine Formation in Aqueous Solution", Haase, Copenhagen, 1941.

[9] H. Irving and H. S. Rossotti, *J. Chem. Soc.*, **1954**, 2904.

[10] R. N. Saksena and K. K. Pandey, *J. Indian Chem. Soc.*, **49**, 779 (1972).

[11] K. Lal, *Rev. Roum. Chim.*, **25**, 355 (1980).

[12] L. G. Van Uitert and C. G. Hass, *J. Amer. Chem. Soc.*, **75**, 451 (1953).

[13] K. Lal, *Talanta*, **26**, 1171 (1979).

[14] T. Moeller and H. E. Kramers, *J. Phys. Chem.*, **48**, 395 (1944).

[15] W. R. Stagg and J. E. Powell, *Inorg. Chem.*, **3**, 242 (1964).

[16] M. M. Jones, "Elementary Coordination Chemistry" Prentice Hall, London, 1964, p. 122.

[17] T. Moeller, *Chem. Rev.*, **65**, 1(1965).

[18] F. H. Speedling, J. E. Powell and E. J. Wheelwright, *J. Amer. Chem. Soc.*, **78**, 34 (1956).

[19] L, K. A. Starely and T. Randall, *Discuss. Faraday Soc.*, **26**, 157 (1958).

[20] G. P. Sengupta and C. R. Bera, *J. Indian Chem. Soc.*, **57**, 558 (1980).

[21] M. S. Mayadeo and S. S. Purohit, *J. Indian Chem. Soc.*, **57**, 1047 (1980).

[22] W. J. Geary, *Coord. Chem. Rev.*, **7**, 81 (1971).

[23] D M. Yost, H. Russel and C.S.S. Garner, "Rare Earth Elements and Their Compounds," Wiley, New York, 1947.

[24] K. Nakamoto, "Infrared Spectra of Inorganic and Coordination Compounds" Wiley, New York, 1963.

[25] G. H. Dicke, "Spectra and Energy Levels of Rare Earth Ions in Crystal" Interscience, New York, 1968, p. 135.

[26] S. P. Sinha and H. H. Schmidtka, *Molec. Phys.*, **38**, 2190 (1965).

[27] D. E. Henrie and G. R. Choppin, *J. Chem. Phys.*, **49**, 477 (1968).

Revue Roumaine de Chimie, **30**, *6*, 517–524 (1985)

REACTIONS OF 2,4-PENTANEDIONATO COMPLEXES

BROMINATION OF BIS(2,4-PENTANEDIONATO) MANGANESE(II) AND TRIS(2,4-PENTANEDIONATO) MANGANESE(III)

N. H. PAIKE

Department of Chemistry, Shri Sharanabasveshwar College of Science,
Gulbarga– 585103, Karnataka

Received October 25, 1983

The synthesis and characterization of a novel compound obtained by the reaction between bis(2,4-pentanedionato) Mn(II) and tris(2,4-pentanedionato) Mn(III) and liquid bromine has been reported in this paper. It is interesting to note that both the parent chelates, bis(2,4-pentanedionato) Mn(III) and tris(2,4-pentanedionato) Mn(III), on the reaction with liquid bromine, produced a reaction product in which manganese is in oxidation state +2. The reaction products were analysed by physical and chemical methods and empirical formula were ascertained. The equilibrium constants were determined for the ionization process

$$\text{Mn (Hacac Br) Br Br}_3 \rightarrow [\text{Mn Hacac Br Br}]^+ + \text{Br}_3]^-$$

and for the solvent extraction process

$$\text{Mn (HacacBr) Br Br}_3 \rightarrow \text{Mn (HacacBr) Br Br} + 2\ \text{Br}$$

by the conductometric and solvent extraction methods respectively.

The composition of the reaction products was ascertained by a number of chemical reactions and spectral observations. It was, however, not successful to obtain a solid adduct, with nitrogen ligands of the semisolid reaction products. The derivatives obtained from the reaction product with many ligands and chelating agents were similar to those obtained with manganese(II) bromide.

INTRODUCTION

A vast amount of physicochemical studies on the chemistry of bis(2,4-pentanedionato)Manganese(II) and tris(2,4-pentanedionato)Manganese(III) have been reported.[1–5] However, the chemistry of bis(2,4-pentanedionato) Mn(II), $Mnacac_2$ is less studied than the tris(2,4-pentanedionato) Mn(III), $Mnacac_3$. Anhydrous $Mnacac_2$, which is polymeric [6] like other acetylacetonates of bivalent first row transition metals, readily forms adducts with one or two molecules of a Lewis base. The dibase adducts presumably contain six coordinate manganese(II). $Mnacac_3$ could be obtained [7] by oxidizing manganese(III) in the presence of acetylacetone with potassium permanganate. The compound is very dark, black to brown material. It is thermally less stable than the complexes of chromium, iron or cobalt. The room temperature X-ray crystal structure of

. $Mnacac_3$ shows regular octahedral arrangements[8] of chelate oxygena bout manganese. Recently the low temperature behaviour in the range 2–100 K for $Mnacac_3$ has been reported [9]. The magnetic data have been found to be compatible with the ligand field calculations based on optical spectrum.

Nakamura et al.[10] have synthesised many complexes of metal halides containing 2,4-pentanedione as a neutral ligand. The work of Nakamura et al. on the bromination of 2,4-pentanedionato complexes of copper and cobalt leads to the fact that the reaction conditions have a deciding effect on the nature of the reaction products. Some interesting findings and observations on the reactions of $Mnacac_2$ and $Mnacac_3$ and with liquid bromine and the bromination product with various ligands have been elucidated in this paper.

EXPERIMENTAL

Bis(2,4-pentenedionato) Manganese, $Mnacac_2$ and tris(2,4 pentanedionato) Manganese (III), $Mnacac_3$ were synthesised and purified by the reported methods.[11–12] A known amount of finely powdered $Mnacac_2$ and $Mnacac_3$ were treated with liquid bromine. The reaction resulted in the formation of a deep yellow viscous mass in both the cases. The excess bromine from the above product was removed by repeated extractions with n-heptane. The removal of unreacted bromine was tested by treating n-heptane washings with aqueous solution of potassium iodide (10% K.I.). The yellow semisolid mass could be solidified in dry ice (–70°C). Both the semisolids lose bromine and produce Manganese(II) bromide and 3-bromo-2,4-pentanedione at elevated temperatures.

The reaction product in dry acetonitrile was treated with different ligands under appropriate conditions to isolate the corresponding derivatives. The following ligands were used;

Nadtc, Hoxin, Phen, bipy, py and tbab.

The products were identified by IR spectra, chemical analysis and melting points.

The elemental analysis of C and H was done at the Micro Analytical Division of the University of Poona. Infrared spectra determined using Nujol mull on Beckman IR-20 spectrophotometer. The electrical conductivity measurements were done on Philips GM-4144 conductivity bridge. The polarographic measurements were made on the recording polarographic instrument at the Central Electro Chemical Research Institute, Karaikudi.

The electronic spectra were recorded in solution in the range 6667 cm^{-1} to 49000 cm^{-1} on DB spectrophotometer.

Magnetic measurements were obtained from the Chemistry Department, Indian Institute of Technology, Bombay. EPR spectra were recorded on standard Varian E-4 instrument, at Indian Institute of Technology, Madras.

RESULTS AND DISCUSSION

The reaction products obtained from Manganese(II) and Manganese(III) were investigated by polarographic technique using acetonitrile as a solvent, and 0.1 M lithium perchlorate as a supporting electrolyte. The results showed a single wave for

Mn(II) → Mn(0), for both the reaction products, with $E = -1.51$ V *vs.* SCE

Mn (II) → Mn(0), E = 1.5 V *vs.* SCE.

This value is in excellent agreement with that reported.[13] This observation, along with the identity of the electronic spectra of both the yellow reaction products which fitted with the octahedral manganese(II) configuration, shows that the reaction products using $Mnacac_2$, and Mna-

Table 1

Elemental analyses

Compound	Chemical formula (F.W.)	% Mn (calc)	%C (calc)	%H (calc)	%Br (calc)	Colour	Solubility in
Mnacac$_2$	$C_{10}H_{14}O_4Mn$ (252.94)	21.6 (21.72)	47.40 (47.44)	5.4 (5.53)	—	Pink	Common organic solvents
Mnacac$_3$	$C_{15}H_{21}O_6Mn$ (351.94)	15.42 (15.61)	51.25 (51.25)	6.0 (5.97)	—	Brown	Common organic solvents
Mn(HacacBr)Br$_4$	$C_5H_7O_2Br_5Mn$	9.90 (9.92)	10.80 (10.83)	— (1.26)	57.85 (57.77)	Orange brown	Acetonitrile, acetone, nitrobenzene

Elemental analysis of the deriavatives

Ligand	Comosition (F.W.)	%C (Calc)	%H (Calc)	%N (Calc)	%Br (Calc)	% Mn (Calc)	Colour
py	Mnpy$_2$Br$_2$ (373.94)	32.12 (32.18)	— (2.68)	7.37 (7.5)	42.85 (42.90)	14 79 (14.73)	Pale Yellow
tbab	(tbab)$_2$MnBr$_4$ (868.9)	44.69 (44.7)	4.83 (4.19)	3.20 (3.26)	37.29 (37.25)	6.38 (6.4)	Yellowish Orange
bipy	Mnbipy Br$_2$ (370.94)	32.15 (32.18)	— (2.68)	7.35 (7.5)	43.10 (43.14)	14.85 (14.73)	Yellow
phen	Mnphen$_2$Br$_2$ (575.0)	49.81 (50.08)	— (2.78)	9.72 (9.73)	26.93 (27.82)	9.53 (9.56)	Yellow
Nadtc	Mndtc$_3$ (499.0)	34.82 (36.07)	5.97 6.01)	8.35 (8.38)	— —	11.35 (11.02)	Black
Hoxin	Mnoxin$_2$ (344.9)	62.57 (62.62)	4.00 (4.06)	8.15 (8.12)	— —	15.87 (15.93)	Yellowgreen

cac_3 starting materials is similar to that reported by Nakamura [14] for the reaction of bromine in dichloromethane with $Coacac_3$. The original compounds, $Mnacac_2$ and $Mnacac_3$, and the reaction product were subjected to elemental analysis. On the basis of elemental analysis, the formula of the reaction product was assigned to be $Mn(HacacBr)\ Br_4$. The analysis of bromine has been useful in assigning the chemical formula of the reaction product. The pressure of two bromine was shown by the iodometric method, while the silver nitrate method showed three bromines per formula weight. The analysis of bromine is again suggestive of the presence of tribromide ionic species in the reaction product. The elemental analysis (Table 1) for the manganese, carbon and hydrogen, agrees well with the formulation $Mn(HacacBr)\ Br^-.\ Br_3^-$.

The reaction product exhibits 1 : 1 electrolytic behaviour in acetonitrile at room temperature from the solution conductivity.[15] On the basis of 1 : 1 electrolytic nature (Table 2), the equilibrium constant for ionization was calculated [16] to be $4.1 \times 10^{-3}\ ML^{-1}$. The conductance measurements for equilibrium constant were based on the assumption that the reaction product ionizes into cation and anion without any chemical decomposition. The calculations of the equilibrium constant using extraction method, (Table 3) assume the decomposition of the tribromide species into bromine and bromide ion.

Table 2

Solution conductivity data

Solvent	Molar concentration			$\Lambda_\infty(ohm^{-1})$
	0.01	0.005	0.0025	
	Λ (in $ohm^{-1}\ l^{-1}\ M^{-1}$)			
Acetonitrile	59.5	63.5	72.4	86.4

Table 3

Data on equilibrium constants

Temp (°C)	pK, by conductometry	pK, by extraction	pK, for (teab) + + Br_2) voltammetry*
25	2.10	6.42	7.3

* I. V. Nelson and R. T. Iwamoto, *J. Electroanal. Chem.*, **7**, 218 (1964).

The data suggest that the processes of decomposition in two methods (extraction and voltammetric) are comparable to each other and both of them are different from conductometric method. It also supportied the fact that the reaction product is a complex containing tribromide on. Thus the yellow reaction product of the bromination reaction appears to be similar to one of the few complexes of transition metals containing tribromide ion.[17]

The two interesting features of the yellow reaction product are:

1) The presence of neutral 3-bromo-2,4-pentanedione in the complex; and

2) The presence of Br_3^- and Br^- as coordinating ions.

The various nitrogen bases and chelating agents were tried to isolate the adducts of Manganese(II) containing tribromide ion. However, it was observed that normal adducts of Manganese(II) bromide with nitrogen bases and other chelating agents were obtained. The derivatives thus obtained were characterized by physical and chemical techniques.

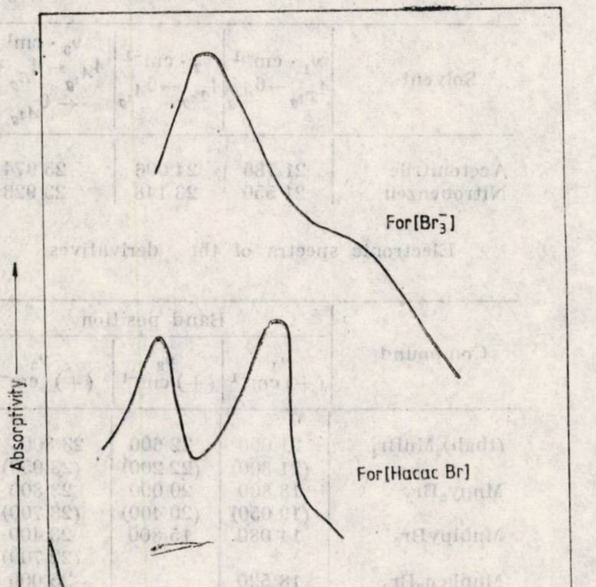

Fig. 1 — Electronic spectra

The electronic spectrum (Fig. 1) of Mn(HacacBr). Br Br_3 was found to exhibit two bands due to the coordinated neutral HacacBr at 31250 cm^{-1} and 46296 cm^{-1}. The tribromide ion, Br_3^- showed as usual two transitions at 27739 cm^{-1} and 34483 cm^{-1}. The transitions due to bromide ion could not be ascertained in the spectrum due to the experimental limitations.

Manganese(II) is a d^5 system with zero crystal field splitting energy, the $d-d$ transitions cannot be obtained. There are many reports on the observation of many spin-forbidden transition,[18-19] particularly $6_{A_{1g}} \rightarrow$ $\rightarrow 4_{T_{1g}}$, $4_{T_{2g}}$, and 4_{E_c}, $4_{A_{1g}}$. Most of these transitions, in solution spectra are mixed with the charge transfer transitions of metal-ligand origin. The electronic spectra (Table 4) of the reaction product have been recorded in acetonitrile and nitrobenzene. The positions and the assignments of these are comparable with the halogen complexes.[19]

Table 4

Electronic spectra of Mn (HacacBr) $Br.Br_3$

Solvent	$\nu_1 \cdot cm^{-1}$ $4_{T_{1g}} \rightarrow 6_{A_{1g}}$	$\nu_2 \cdot cm^{-1}$ $4_{T_{2g}} \rightarrow 6_{A_{1g}}$	$\nu_3 \cdot cm^1$ $4_{A_{1g}} \leftarrow 4_{E_g} \leftarrow$ $\leftarrow 6_{A_{1g}}$
Acetonitrile	21 786	24 096	25 974
Nitrobenzen	21 550	23 148	23 923

Electronic spectra of the derivatives

Compound	Band position		
	ν_1 (+) cm^{-1}	ν_2 (+) cm^{-1}	ν_3 (+) cm^{-1}
$(tbab)_2MnBr_4$	21 000	22 600	23 800
	(21 300)	(22 200)	(23 050)
$Mnpy_2Br_2$	18 800	20 000	23 800
	(19 050)	(20 400)	(23 700)
$MnbipyBr_2$	14 080	15 800	23 400
			(22 700) **
$Mnphen_2Br_2$	18 520		25 000
			(24 300)
$Mndtc_3$	15 500	20 300	28 600
	(16 600)	(19 900)	(28 200)
$Mnoxin_2$	20 800	23 200	27 000
	(21 740)	(24 390)	(28 570)

* Data derived from literature
** Very broad band

The electronic spectra of these derivatives showed the characteristic absorption bands due to spin-forbidden transitions of Mn(II). The only complex, containing Mn(III) is the $Mndtc_3$. The agreement between the observed and reported spectra [19-24] for similar compounds indicated that the nature of the compounds obtained in the present work and that prepared from reported literature is the same. The ground state of Mn(II) is $6_{A_{1g}}$ in octahedral or tetrahedral ligand symmetry. This reflects no spin orbit coupling to affect the magnetic moments to any appreciable extent. Actually the magnetic moments (Table 5) are found to be close to the spin only value and independent of temperature as reported.[25]

The data on the magnetic susceptibilities of the derivatives from the reaction product are found to be quite close to that reported in the literature for similar compounds.[26-31] The result on the electronic spectra and magnetic susceptibilities of the derivatives obtained are normal complexes of Manganese(II) bromide and do not contain any tribromide ion in the coordination sphere.

Table 5

Magnetic susceptibility data of Mn (Hacac Br). Br. Br_3

and derivatives

Temperature K	$\chi_M \times 10^6$ mole observed	$\chi_M \times 10^6$ mole calculated	μ_{eff} B.M. observed
100	42 065	44 936	5.80
150	28 261	29 957	5.70
165	27 050	27 234	5.90
176	24 736	25 532	5.85
188	24 145	23 902	5.95
200	22 241	22 468	5.89
240	18 723	18 723	5.92
260	17 050	17 283	5.88
280	16 430	16 048	5.98
300	14 878	14 979	5.90

Compound	$\chi_M \times 10^6$ mole observed	μ_{eff} B.M. observed
$(tabab)_2\ MnBr_4$	14 068	5.8
$Mnpy_2Br_2$	14 560	5.9
$MnbipyBr_2$	14 068	5.8
$Mnphen_2Br_2$	13 587	5.7
$Mndtc_3$	92 55	4.7
$Mnoxin_2$	14 560	5.9

ACWNOWLEDGEMENTS. The author is very grateful to (late) Prof. A. B. Biswas, I.I. T., Bombay, Dr. S. B. Kulkarni and Dr. G. N. Natu, University of Poona, for their help and guidance. The author is also grateful to Dr. V. R. Phansalkar, Head, Dept. of Chemistry, University of Poona and to the Principal, Shri Sharanabasaveshwar College of Science, for grant of study leave. The financial from U.G.C. New Delhi, is gratefully acknowledged.

REFERENCES

[1] J. P. Fackler, Jr., *Prog. Inorg. Chem,*, **7**, 361 (1966).

[2] D. P. Graddon, *Coord. Chem. Rev.*, **4**, 1 (1969).

[3] D. W. Thompson, *Structure and Bonding*, **9**, 27 (1971).

[4] Q. Fernando, *Adv. Inorg. Chem. Radiochem.*, **7**, 185 (1965).

5 J. Baigh, J. K. Michael and W. David, *J. Chem. Soc., Faraday Trans*, II, **73**, 1561 (1973).

[6] D. P. Graddon and G. M. Mockler, *Austr. J. Chem*, **17**, 1119 (1964).

[7] R. G. Charles, *Inorg. Syn.*, **7**, 193 (1963).

[8] B. Morosin and J. R. Brathvde, *Acta Cryst.*, **17**, 705 (1964).

[9] T. S. Piper and R. L. Carlin, *Inorg. Chem.*, **2**, 260 (1963).

[10] K. Kaeriyama, *Bull, Chem. Soc. Jap.*, **47**, 753 (1974) ; T. Matsushta, I. Masuda and T. Shono, *Technol, Rep-Osaka, Univ.*, **24**, 345 (1974) ; C. A. 81 : 144920 V.

[11] A. K. Gregson, D. M. Doddrell and P. C. Healy, *Inorg. Chem.*, **17**, 1216 (1978).

[12] Y. Nakamura, K. Isobe, H. Morita, S. Yamazaki and S. Kawsguchi, *Inorg. Chem.*, **11**, 1573 (1972).

[13] J. B. Headridge, "Electrochemical Techniques for Inorganic Chemists", Acad. Press, 1969.

[14] Y. Nakamura, M. Gotani and S. Kowaguchi, *Bull. Chem. Soc., Jap.*, **45**, 457, 485 (1972).

[15] W. J. Geary, *Coord. Chem. Rev.* **7**, 81 (1971).

[16] J. M. Wilson, R. J. Newcombe, A. R. Denaro and R.M.W. Rickett, "Experiments in Physical Chemistry", Pergamon Press, 1962, p. 104.

[17] A. I. Popov, "Halogen Chemistry", Vol. 1 (V. Gutmann, ed.) Acad. Press, 1967.

[18] C. J. Ballhausen, "Introduction to Ligand Field Theory", Mc Graw Hill, 1967, p. 198.

[19] C. K. Jorgensen, *Adv. Chem. Phys.*, **1**, *5*, 33 (1963).

[20] D. H. Brown, R. H. Nuttall, D. W. A. Sharp, *J. Inorg. Nucl. Chem.*, **26**, 1151 (1964).

[21] U. St. Nikolov, *Inrog. Chim. Acta*, **4**, 610 (1970).

[22] K. Sone, *J. Am. Chem. Soc.*, **75**, 5207 (1953).

[23] D. P. Madden and S. M. Nelson, *J. Chem. Soc.*, (A). 2342 (1968).

[24] H. A. Goodwin and R. N. Sylva, *Austr. J. Chem.*, **20**, 217 (1967).

[25] B. N. Figgis, "Introduction to Ligand Fields", Wiely-Eastern, 1976, p. 280.

[26] S. Sugden, *J. Chem. Soc.*, 228 (1943).

[27] A. Symal. *J. Ind. Chem. Soc.*, **44**, 989 (1967).

[28] N. S. Gill and R. S. Nyholm, *J. Chem. Soc.*, 3997 (1959).

[29] J. R. Allen, D. H. Brown, R. H. Nuttall and D.W.A. Sharp. *J. Inorg. Nucl. Chem.* **27**, 1865 (1966).

[30] B. A. Kulkarni, Ph. D. Thesis. Poona Univ., 1965.

[31] S. B. Kulkarni, Ph. D. Thesis, Poona Univ., 1965.

Revue Roumaine de Chimie, **30**, *6*, 525–528 (1985)

SÍNTESIS DE LOS PRIMEROS ESPIROFOSFAZENOS ALQUILADOS [*]

R. CEA OLIVARES[**] y L. CANTU

Instituto de Química de la Universidad Nacional Autónoma de México
México 20, D.F.

Recibido el 25 de octubre de 1981

Se informa la síntesis de los espirofosfazenos $((CH_2)_4PN)_3$ y $((CH_2)_4PN)_4$ a partir de $(CH_2)_3PCL_3$ y NH_4Cl, así como su caracterización mediante espectrometría de masas, espectroscopía infrarroja y analisis químico.

The synthesis of spirophosphazenes $((CH_2)_4PN)_3$ and $((CH_2)_4PN)_4$ from $(CH_2)_4PCl_3$ and NH_4Cl is reported as well as their characterization by mass spectrometry, infrared spectroscopy and chemical analysis.

INTRODUCTION

En el campo de la química heterocíclica inorgánica posiblemente los sistemas fosfazénicos han sido los más ampliamente estudiados. Las reacciones de sustitución con reactivos bifuncionales, $H\overset{\frown}{X\ Y}H$ ($X = Y$ ó $X \neq Y$) hacia el hexaclorociclotrifosfazeno, $P_3N_3Cl_6$, y hacia el octaclorociclotetrafosfazeno, $P_3N_3Cl_2$, han dado lugar a una amplia gama de espirofosfazenos.[1] La mayoría de las reacciones que se han llevado a cabo involucran dioles, $X = Y = O$, diaminas ($X = Y = NH$) o hidroxiaminas ($X \neq NH$, $Y = O$). Algunos de estos espirofosfazenos manifiestan interesantes propiedades clatrantes.[2]

Los sistemas ciclofosfazéncios alquilados no pueden ser obtenidos con buenos rendimientos a partir de los fácilmente obtenibles halógenofosfazenos, las reacciones con Grignards o con derivados litiados conducen generalmente al rompimiento del ciclo fosfazénico.[3]

Se conoce un número relativemente pequeño de sistemas fosfazénicos per-alquilados, entre los cuales existen compuestos tales como $(R_2PN)_{3,4}$ ($R = Me$, Et),[4,5] heterociclos con grupos alquílicos diferentes tales como $N_4P_4Me_4(CH_2R)_4$ ($R = Me$, $SiMe_3$, $GeMe_3$, $SnMe_3$)[6] y sistemas perfluorados[7,8] $((CF_3)_2PN)_{3,4}$ y $((C_3F_7)_{3,4}$.

Algunos de ellos, $((CH_3)_2PN)_3$ y $((CH_3)_2PN)_4$ manifiestan interesantes propiedades en su equilibrio térmico[9]. En especial el octametilciclotetrafosfazeno presenta facilidad para actuar como ligante hacia carbonilos metálicos y hacia halogenuros de los metales de transición.[10]

---

[*] Contribución del Instituto de Química de la U.N.A.M.

[**] Autor a quien deberá dirigirse la correspondencia.

En 1960, Burg [11] informó la síntesis del espiroborofosfano alquilado, (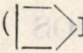$PBH_2)_3$, el cual presenta una estructura poco usual con los tres anillos 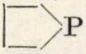P en planos perpendiculares a los planos de un anillo $(PB)_3$ un tanto distorsionado. Sin embargo, hasta donde es del conocimiento de los autores son desconocidos los espirofosfazenos alquilados; dadas sus interesantes propiedades estructurales y el interés que existe sobre los fosfazenos que contienen enlaces fósforocarbono, se procedió a la obtención de los compuestos $((CH_2)_4PN)_3$ (A) y $((CH_2)_4PN)_4$ (B).

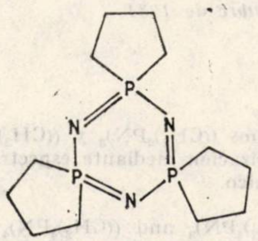

(A)

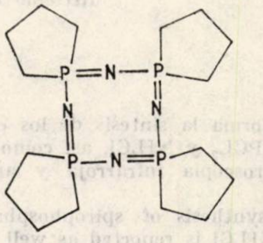

(B)

PARTE EXPERIMENTAL

Los espirofosfazenos alquilados A y B se obtuvieron a través de una reacción de aminólisis directa del ciclotetrametiléntriclorofosforano, $(CH_2)_4PCl_3$, con NH_4Cl en clorobenceno a reflujo. Se siguió un procedimiento semejante al utilizado en la síntesis de los metilciclofosfazenos.[4,9]

Reactivos y determinaciones : El $PSCl_3$ utilizado se obtuvo per el método de Knotz.[12] El $((CH_2)_4P(S))_2$ se sintetizó a partir de $PSCl_3$ y el di Grignard $BrMg(CH_2)_4MgBr$ según la técnica descrita por Schmutzen.[13] El $Br(CH_2)_4Br$ se obtuvo comercialmente. El CCl_4 y el clorobenceno se purificaron y secaron antes de ser utilizados. El Cl_2 se secó haciéndolo pasar sobre H_2So_4 (conc.) y posteriormente sobre CaO. Las placas de alúmina (F_{25},(Tipo T)) que se emplearon en la separacion de los ciclos se obtuvieron comercialmente. El NH_4Cl se precipitó de una solución acuosa con acetona y se secó antes de ser utilizado.

Los espectros de infrarrojo se obtuvieron con un espectrómetro Perkin-Elmer 567. Los espectros de masas de un espectrómetro AEI-MS30. Los análisis elementales fueron realizados por Egmont Pasher en Bonn, Alemania.

Manipulaciones : Les reacciones y manipulaciones hasta la obtención de los ciclos se llevaron a cabo en una atmósfera de argón. En un experimento típico 8 gramos (.0336 moles) de $((CH_2)_4P(S))_2$ se colocaron en 50 ml de CCl_4 y a -10°C y con agitación se hizo pasar una corriente de crolo seco hasta la aparición manifiesta de un sólido blanco. Este sólido blanco formado, el fosforano clorado, se filtró bajo atmósfera de argón y se lavó dos veces con 10 ml de CCl_4. El fosforano en 20 ml de clorobenceno se hizo reaccionar a reflujo con 5.6 gramos de NH_4Cl (.105 moles) durante aproximadamente cuatro horas, produciéndose al inicio de la reacción un violento burbjueo. La mezlca de reacción una vez fría se extrajo con agua y éstos extractos se llevaron casi a saturación con hidróxido de potasio. El sólido que se separa fue extraído con benceno. El disolvente se evaporó a vacío permaneciendo un sólido blanco.

El sólido blanco obtenido por el procedimiento anterior fue triplemente sublimado (140°C, .1mm de Hg) y se recristalizó dos veces de heptano. El espectro de infrarrojo de dicho sólido muestra dos bandas en la región de 1200 cm^{-1}, características de la vibración $P{=}N$ ciclofosfazénica.[14] El análisis elemental es congruente con una relación C_4H_8PN ($C_{calc.} = 47.42\,\%$

$C_{exp} = 46.9\%$; $H_{calc.} = 7.92\%$; $H_{exp.} = 7.74\%$; $P_{calc.} = 30.7\%$, $P_{exp.} = 29.4\%$; $N_{calc.} = 13.9\%$, $N_{exp.} = 13.2\%$).

El sólido blanco es una mezlca de dos compuestos, los cuales fueron separados por cromatografía en capa delgada (cloroformo-acetato de etilo 3 : 2) empleando I_2 como revelador. Las dos fracciones se extrajeron con acetato de etilo y se recristallizaron dos veces de heptano. Se obtuvieron 3.7 gramos de sólido triplemente sublimado y la mezlca consta aproximadamente de un 70% de la primeta fracción y un 30% de la segunda fracción.

CARACTERIZACIÓN Y DISCUSIÓN

Primera fracción: El espectro de infrarrojo de este compuesto muestra bandas supuestamente debidas a las vibraciones de los grupos metilénicos en 2910, 2855, 1438 y 1395 cm^{-1}. En 1158 cm^{-1} aparece una banda muy intensa debida a la vibración P=N del sistema ciclofosfazénico trimérico.[1] En 1300 cm^{-1} no aparece ninguna banda lo cual es evidencia de la ausencia de enlace fósforo-metilo.[4]

El peso molecular de este compuesto, determinado a través de espectrometría de masas, corresponde a 303. Los datos del espectro de masas se muestran en la Tabla 1 (sólo se consideran fragmentos con una abundancia mayor al 9%).

El compuesto presenta un punto de fusión = 195°C

Tabla 1

Espectros de masas des los compuestos $((CH_2)_2PN)_3$ y $((CH_2)_2PN)_4$

$((CH_2)_4PN)_3$			$((CH_2)_4PN)_4$		
m/e	Abundancia	Asignación probable	m/e	Abundancia	Asignación probable
303	22%	$C_{12}H_{24}P_3N_3^+$	404	47%	$C_{11}H_{32}P_4N_4$
302	5%	$C_{12}H_{23}P_3N_3^+$	403	10%	$C_{11}H_{31}P_4N_4$
274	6%	$C_{10}H_{19}P_3N_3^+$	376	15%	$C_{14}H_{22}P_4N_4$
248	100%	$C_8H_{16}P_3N_3H^+$	349	100%	$C_{12}H_{24}P_4N_4H^+$
192	29%	$C_4H_8P_3N_3H^+$	304	13%	$C_{12}H_{24}P_3N_3H^+$
102	11%	$C_4H_8PNH^+$	274	13%	$C_{10}H_{14}P_3N_3$
87	11%	$C_4H_8P^+$	148	52%	$C_2H_{14}P_3N_3H^+$
55	10%	C_4H_7	192	23%	$C_4H_4P_3N_3H^+$
			87	10%	$C_4H_{44}P^+$
			55	22%	C_4H

[a] Sólo se consideran fragmentos con m/e mayor al 9%, salvo cuando sean de interés

Segunda fracción: En el espectro de infrarrojo de este compuesto las bandas supuestamente debidas a los grupos metilénicos aparecen en 2920, 2850, 1438 y 1398 cm^{-1}. En 1200 cm^{-1} aparece una banda muy intensa correspondiente ala vibración P=N tetrámerofosfazénica. Igualmente en 1300 cm^{-1} no aparece ninguna banda.

El peso molecular de este compuesto, determinado por espectrometría de masas, corresponde a 404, en la misma forma que para el compuesto anterior en la Tabla 1 se presentan los datos principales del espectro de masas.

El punto de fusión de este compuesto corresponde a 131—132°C.

Las evidencias espectroscópicas y analiticas son congruentes para la primera fracción con el compuesto trimérico (A) y para la segunda fraccion con el compuesto tetramérico (B).

Los espectros de infrarrojo de ambos compuestos muestran bandas supuestamente debidas a los grupos metilénicos en posiciones muy similares a las de otros compuestos que contienen al sistema heterociclico 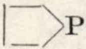P[13]. La frecuencia de vibración P=N ciclofosfazénica aparece a frecuencias ligeramente menores, $\simeq 20$ cm^{-1} que las de los correspondientes derivados metílicos, $((CH_3)_2PN)_3 = 1180$ cm^{-1} y $((CH_3)_2PN)_4 = 1220$ cm^{-1}

Los espectros de masas de ambos compuestos muestran abundantes iones moleculares (véase la Tabla 1). La pérdida de cuatro metilenos, posiblemente provenientes de un sólo fósforo genera el pico base. A diferencia con el $((CH_3)_2PN_4)$ [15] en estos espirofosfazenos alquilados se presentan en sus espectrogramas de masas iones debidos a la pérdida de un hidrógeno a partir del ion molecular. En los espectros de masas aparecen fragmentos en m/e 87 y 55 debidos respectivamente a $C_4H_8P^+$ y a $C_4H_7^+$, comprobatorios de la presencia del heterociclo $(CH_2)_4P$ en los compuestos sintetizados. No se presentan fragmentos debidos a $(M\text{-}15)^+$ que junto con las evidencias en el infrarrojo corroboran la ausencia de grupos metilicos en los compuestos sintetizados.

BIBLIOGRAFIA

[1] R. Shaw, *Pure and Appl. Chem.*, **52**, 1063 (1980).

[2] H. R. Allcock, *Acc. Chem. Res.*, **11**, 81 (1978).

[3] Véase por ejemplo : S. S. Krishnamurthy y A. C. Sau, *Adv. Inrog. Chem. and Radiochem.*, **21**, 41 (1978) y referencias ahi citadas.

[4] H. T. Searle, *Proc. Chem. Soc.*, 7 (1959).

[5] A. J. Bilbo, *Z. Naturforsch.*, **15b**, 330 (1960).

[6] H. P. Calhoun, R. H. Lindstrom, R. T. Oakley, N. L. Paddock, S. M. Todd, *J.C.S. Chem. Comm.*, 343 (1975).

[7] V. N. Prons, M. P. Grinblat, A. L. Klebanskii y N.B. Zaitsev, *Zhur. obshchei. Khim.*, **41**, 2629 (1971 ;)
Chem. Abstr., **77**, 19747 (1972).

[8] V. N. Prons, M. P. Grinblat y A.L. Klebanskii, *Zhur obshchei. Khim.*, **43**, 692 (1973) ; *Chem. Abstr.*, **79**, 42609 (1973).

[9] H. R. Allcock y D. B. Patterson, *Inorg. Chem.*, **16**, 197 (1977).

[10] I. Haiduc, *Chem. in Brit.*, **17**, 330 (1981).

[11] A. B. Burg y P. J. Slota, *J. Amer. Chem., Soc.*, **82**, 2148 (1960).

[12] F. Knotz, *Österr. Chemiker-Z.*, **50**, 128 (1949).

[13] R. Schmutzer, *Inorg. Chem.*, **3**, 421 (1964).

[14] H. R. Allcock, *Chem. Rev.*, **72**, 321 (1972).

[15] A. Soto y R. Cea, *Rev. Roumaine Chim.*, **25**, 529 (1980).

NOTE POUR LES AUTEURS

La Revue Roumaine de Chimie publie des articles en anglais, français, russe, allemand ou espagnol. Les auteurs sont priés d'envoyer des articles et des comptes rendus inédits.

Les manuscrits seront dactylographiés à double interligne. La bibliographie, les tableaux et la légende des figures seront placés après le texte.

Si l'article fait partie d'une série numérotée, la partie précédente sera donnée comme première référence.

Chaque article sera précédé d'un résumé comprenant quinze lignes au maximum.

Les références bibliographiques dans le texte seront faites par des exposants sans parenthèses et paraîtront à la fin de l'ouvrage.

Les publications périodiques mentionnées dans la bibliographie seront présentées suivant les prescriptions internationales : le nom de l'auteur précédé de l'initiale du prénom, le titre du périodique abrégé conformément à « Chemical Abstracts » et souligné par une ligne, le numéro du tome indiqué par des chiffres arabes et souligné par deux lignes, suivi de la première page de l'article ; à la fin, l'année de la parution sera placée entre parenthèses. Le numéro de la revue ne sera pas indiqué si les pages du volume sont numérotées consécutivement.

Les textes des livres ou traités inclueront : le nom des auteurs, l'initiale du prénom, le titre du livre entre guillemets et sans être souligné, le numéro du tome précédé par l'abréviation « vol. » (ou « Bd. »), le numéro de l'édition, les éditions (the publisher), la localité de la parution du livre, l'année de la parution et la page de la référence précédée(s) par l'abréviation « p. » (ou « S. »).

Les brevets seront indiqués comme suit : l'auteur ou la firme, le pays et le numéro du brevet, la date et la revue *(Chem.Abstr.)*. Par. ex. : M. Jones (to Union Carbide Co), Brit. Pat. 601 238, 2 Sept. 1959 ; cf. *Chem Abstr.*, **54**, 12808 (1960).

Si la référence n'a pas été lue en original, on indiquera aussi la revue de référence consultée.

Les diagrammes seront tracés à l'encre de Chine sur papier calque. Les tableaux et les figures (en nombre strictement nécessaire) ainsi que les courbes dans les figures seront numérotés par des chiffres arabes. Leur explication sera donnée dans la légende des figures. Prière de ne pas inscrire les mêmes données dans les tableaux et les figures. Chaque tableau aura un titre. On indiquera dans le texte la place approximative des tableaux et des figures. Les formules chimiques seront incluses dans le texte ; en outre, elles seront transcrites sur papier calque, à l'encre de Chine.

Les auteurs sont priés d'indiquer les caractères italiques (en soulignant les lettres au crayon), ainsi que tout autre caractère spécial ; les préfixes *ortho, meta, para, cis, trans*, etc. seront soulignés pour indiquer leurs caractères italiques et ne seront jamais écrits avec des majuscules.

Aucune correction à la main ne sera admise sur le manuscrit. Les corrections seront tapées à la machine. Les lettres grecques ou d'autres symboles spéciaux seront insérés à la main à l'encre clairement.

Le manuscrit sera signé par l'auteur.

Le titre-courant aura 50 lettres au maximum.

L'entière responsabilité du contenu des articles appartient aux auteurs.

Sur demande on peut obtenir une note plus complète.

PRINTED IN ROMANIA

ORSZÁGOS MŰSZ. INFORMÁCIÓS KÖNYVTÁR 1983

TRAVAUX PARUS AUX ÉDITIONS DE L'ACADÉMIE DE LA RÉPUBLIQUE SOCIALISTE DE ROUMANIE

V. E. SAHINI, M. HILLEBRAND, **Chimie cuantică în exemple și aplicații**, 1985, 378 p.

GH. MARCU, **Chimia compușilor coordinativi**, 1984, 415 p.

E. CORDOŞ, C. MANOLIU, **Spectrometria de absorbție și fluorescență atomică**, 1984, 178 p

C. BODEA, **Tratat de biochimie vegetală**, p. II, vol. 5, 1984, 438 p.

ELENA CEAUŞESCU, **Cercetări în chimia și tehnologia polimerilor**, 1983, 519 p.

N. ASANDEI, A. GRIGORIU, **Chimia și structura fibrelor**, 1983, 395 p.

N. IONESCU, M. CĂLDĂRARU, **Oxidarea catalitică a olefinelor inferioare**, 1983.

C. CAŞCAVAL, **Studiul polimerilor prin piroliză și cromatografie de gaze**, 1983, 220 p.

C. I. SIMIONESCU, F. DANEŞ, **Originea vieții**, 1983, 110 p.

C. BODEA, (sous la direction), **Tratat de biochimie vegetală**, 2^{e} partie, t. IV, 1982, 408 p.

I. G. MURGULESCU, RODICA VÎLCU, **Introducere în chimia fizică. Vol. III, Termodinamica chimică**, 1982, 624 p.

I. G. MURGULESCU, J. PĂUN, **Introducerea în chimia fizică. Vol. I. 3. Nucleul atomic, reacții nucleare, particule elementare**, 1982 606 p.

ELENA CEAUŞESCU, **Noi cercetări în domeniul compușilor macromoleculari**, 1981, 536 p.

I. G. MURGULESCU, TATIANA ONCESCU, E. SEGAL, **Introducere în chimica fizică, Vol. II, 2. Cinematică chimică și cataliză**, 1981, 1024 p.

V. DRĂGUŢAN, A. T. BALABAN, M. DIMONIE, **Metateza olefinelor și polimerizarea prin deschidere de inel a cicloolefinelor**, 1981, 254 p.

LYDIA-MARIA VAICUM, **Epurarea apelor uzate cu nămol activ. Bazele biochimice**, 1981, 218 p.

I. GĂLĂŢEANU, **Procese și metode radiochimice în energetica nucleară**, 1981, 234 p.

O. IORDACHE, **Procese polistocastice aplicate la fenomenele de transfer**, 1981, 186 p.

CR. SIMIONESCU, VALERIA GORDUZA, **Polimeri biocompatibili și biologic activi**, 1980, 479 p.

ELENA CEAUŞESCU, **Polimerizarea stereospecifică a izoprenului**, 1979, 307 p.

CONST. GH. MACAROVICI, **Analiza chimică cantitativă anorganică**, 1979, 457 p.

M. FLORESCU, **Metode științifice în dezvoltarea industriei chimice moderne**, 1979, 256 p.

A. T. BALABAN, I. GĂLĂŢEANU, G. GEORGESCU, LIGIA SIMIONESCU, **Compuși marcați și radiofarmaceutici cu aplicații în medicina nucleară**, 1979, 495 p.

I. G. MURGULESCU, E. SEGAL, **Introducere în chimia fizică. Vol. II. 1. Teoria molecular-cinetică a materiei**, 1979, 1036 p.

S. STERNBERG, FL. DANEŞ, **Termodinamica chimică aplicată**, 1978, 400 p.

I. G. MURGULESCU, V. EM. SAHINI, **Introducere în chimia fizică. Vol. I. 2. Structura și proprietățile moleculelor**, 1978, 604 p.

I. ZUGRĂVESCU, MAGDA PETROVANU, **N-ylid chemistry**, coèdition avec McGraw Hill International Book Company, U.S.A., 1977, 396 p.

I. G. MURGULESCU, **Introducere în chimia fizică. Vol. I. 1. Atomi, molecule, legătură chimică**, 1976, 560 p.

ELENA CEAUŞESCU, **Research work on synthesis and characterization of macromolecular compounds, Contributions**, 1974, 251 p.

CR. SIMIONESCU, VIORICA RUSAN, V. POPA, **Chimia algelor marine** 1974, 212 p., 1 pl.

1985 JUL 1 01

ISSN 0035—3930

I. P. INFORMAŢIA c. 1126

43 426

Lei 40

$ 80 (pour un abonnement annuel)

F 1/03

ACADÉMIE DE LA RÉPUBLIQUE SOCIALISTE DE ROUMANIE

REVUE ROUMAINE DE CHIMIE

R 1985 AUG 27

MG

TOME 30

N° 7

Juillet 1985

Rev. Roumaine Chim.

RRCHAX, 30, 7, p. 529–644 (1985), Bucarest

EDITURA ACADEMIEI REPUBLICII SOCIALISTE ROMÂNIA

ACADÉMIE DE LA RÉPUBLIQUE SOCIALISTE DE ROUMANIE

COMITÉ DE RÉDACTION

Rédacteur en chef :

I. G. MURGULESCU, membre de l'Académie de la République Socialiste de Roumanie

Rédacteurs en chef adjoints :

A. T. BALABAN et V. EM. SAHINI, membres correspondants de l'Académie de la République Socialiste de Roumanie

Collège de rédaction:

EM. BRATU, ELENA CEAUŞESCU, ECATERINA CIORĂNESCU-NENITZESCU, CR. SIMIONESCU, membres de l'Académie de la République Socialiste de Roumanie; P. SPACU, membre correspondant de l'Académie de la République Socialiste de Roumanie; M. BANCIU, M. D. GHEORGHIU, I. HAIDUC, D. I. MARCHIDAN, I. MOLDOVAN, G. NIAC et D. SĂNDULESCU

La Revue Roumaine de Chimie paraît 10 fois par an. Toute commande de l'étranger sera adressée à « ROMPRESFILATELIA » — sectorul Export-Import Presă, P. O. Box 12—201 télex 10376 prsfi r Bucureşti, Calea Griviţei nr. 64—66, Roumanie.

Les manuscrits, les livres et les revues proposés en échange, ainsi que toute correspondance seront envoyés à la rédaction :

REVUE ROUMAINE DE CHIMIE

125, Calea Victoriei, 79717 Bucarest, Roumanie, téléphone 50 76 80

EDITURA ACADEMIEI REPUBLICII SOCIALISTE ROMÂNIA

125, Calea Victoriei, 79717 Bucarest, Roumanie, téléphone 50 76 80

REVUE ROUMAINE DE CHIMIE

ORSZÁGOS MŰSZAKI INFORMÁCIÓS ÉS KÖNYVTÁR 1983

Tome 30, Nº 7 **Juillet, 1985**

M. MRACEC, MARIA MRACEC and Z. SIMON, Optimal parameters in the HMO technique. II. An optimal set of parameters for the hydroxylic phenol function · · · 531–549

C. RADOVAN and MARIA PORAICU, Considérations on the role of the characteristic dimension in the application of the vibrated electrode · · · 551–558

IOANA SARAMET and M. BANCIU, Charge-transfer complexes of some substituted thiazoles · · · 559–564

C. CHELGHOUM, Y. HADDAD, K. ABDEDDAIM and M. H. GUERMOUCHE, Rétention indices and molecular structure of isodécanes (in French) · · 565–569

FAYEZ Y. KHALIL, M. T. HANNA, F. M. ABDEL-HALIM and M. EL-BATOUTI, Kinetic study of the alkaline decomposition of 3-bromopropyltriphenylphosphonium bromide in DMSO-H_2O mixtures · · · 571–574

ION TEOREANU and MARCELA MUNTEAN, Hardening processes in $3(CaO.\,Al_2O_3).\,CaSO_4$ — water system · · · 575–579

R. S. SINDHU and R. P. SINGH, Polarographic studies on the complexes of europium (III) with 2,3-dihydroxypyridine and 2-amino-3-hydroxypyridine 581–583

I. G. DINULESCU, S. STAICU, ANGELA DUMITRIU, AURELIA GHENCIULESCU, F. CHIRALEU and MARGARETA AVRAM, Reaction of acetylenes with transition metals. XI[1] Reaction of 1-chloro-1,2-diphenyl-3-alkyl-π-allylpalladium complexes with alkenes · · · 585–588

NICOLETA ŞTEFAN, PETRU FILIP, ILIE G. DINULESCU and MARGARETA AVRAM, A new dibenzo-$(CH)_{10}$ hydrocarbon : *anti*-dibenzo [*b*, *i*] tricyclo[6.2.0.0 ^{4,7}] deca-2,5,9-triene · · · 589–591

S. ESTEBAN SANTOS, J. M. MARINAS RUBIO and M. P. MARTINEZ-ALCAZAR, Isomerization of *o*-alkylphenols on an aluminium orthophosphate-alumina · · · 593–598

AHMED M. EL-KHAWAGA, ABOEL-MAGD A. ABDEL-WAHAB, MAHER F. ELZOHRY and ALI A. KHALAF, Modern Friedel-Crafts chemistry. XII. On the carbonyl retardation of cyclialkylation of aryl alkenyl ketones under Friedel-Crafts conditions · · · 599–609

E. I. GEORGESCU, FLORENTINA GEORGESCU, M. GHEORGHIU, E. G. GEORGESCU and MAGDA PETROVANU, Dipolar derivatives in the quinoxaline series. IV. (3 + 2) Dipolar cycloaddition reactions of some quinazolium-3-(p-R-benzoyl)-methylides with activated acetylenes (in French) · · · 611–615

Rev. Roumaine Chim. **30**, 7, 529–644 (1985) Bucarest

M. S. ARIAS-PEREZ, C. FERNANDEZ-SANCHEZ and J. M. MARINAS, Esterification of monosubstituted benzoic acids with „kearby" type aluminium orthophosphates as catalysts (in Spanish) · · · · · · · · · · 617–622

CR. I. SIMIONESCU, CLEOPATRA VASILIU-OPREA and JEANA NICOLEANU, Mechano-chemical initiated polymerizations. 9. Influence of mechanical conditions and temperature on polymerization reaction of acrylamide by vibratory milling · 623–629

M. A. KABIL and M. A. MOSTAFA, Elimination of the interfering effects of some organic compounds in the determination of rhodium by atomic absorption spectrophotometry · 631–637

ROBERTO CAO, GILBERTO VICIEDO and HÉCTOR BERTY, Thiosemicarbazone complexes of $3d^{6-10}$ metals. I. Acetophenone and *o*-aminobenzaldehyde thiosemicarbazone · 639–643

Revue Roumaine de Chimie, **30**, 7, 531–549 (1985)

OPTIMAL PARAMETERS IN THE HMO TECHNIQUE. II[1]

AN OPTIMAL SET OF PARAMETERS FOR THE HYDROXYLIC PHENOL FUNCTION

M. MRACEC, * MARIA MRACEC ** and Z. SIMON ***

* The SOLVENTUL Research Laboratory, ICECHIM – Center for Plastic Materials, str. Gării, nr. 25, R-1900, Timişoara, Romania

** Chemical Center Timişoara, blvd Mihai Viteazul, nr. 24, R-1900, Timişoara, Romania

*** Department of Biophysics, Institute of Medicine, Timişoara, spl. Tudor Vladimirescu, no. 14, R-1900, Timişoara, Romania

Received July 21, 1982
Revised November 24, 1984

The effects of the variations of the HMO parameters $\delta_{\ddot{O}-} \in [1.4, 2.6]$ and $k_{\ddot{O}-Ar}$ $[0.4, 1.6]$ for the phenolic hydroxyl group concerning the calculated values of: *i*) π electronic levels; *ii*) π charge densities at the oxygen atom and at the *o*-, *m*- and *p*- positions; *iii*) the ^1L_b transition and *iv*) the first ionization potential (IP) are studied. Using a graphical method for the optimisation of parameters, a new pair, $\delta_{\ddot{O}-} = 2.0$ and $k_{\ddot{O}-Ar} = 0.84$ was proposed for the phenolic hydroxyl group, and tested for the ^1L_b transition of phenol, diphenols and triphenols, for the first vertical ionization potential (VIP) and for the electronic impact ionization potential (EIIP). The π charge densities calculated for phenol are in agreement with PPP and CNDO/2 results and with experimental data for phenol nitration. The calculated electronic spectra, VIP, EIIP and the chemical reactivity are in good concordance with the experimental data.

INTRODUCTION

Despite its empirical character, the HMO method has stayed in use, even in the last years. [2–26] Several papers made use of the HMO results, [27–37] while others proposed new ways for its utilisation. [38,39]

Over the years, several methods for the evaluation of HMO parameters (δ_X and k_{XY}) were used. [40–53] Most of the δ_X – and k_{XY} – values for different heteroatoms in various steric and structural arrangements were collected in a series of reviews and treatises. [51–57] Nevertheless, in several cases the use of these parameters led to poor agreements with experimental data, especially when the parameters were used in attempts to explain unitarily a group of properties for a large series of related molecules.

The aim of this study is to demonstrate the advantages of the application of the graphical method for obtaining a unitary set of HMO parameters. [1] This method is used in the study of the phenolic hydroxyl function. The obtained parameters are used then for the unitary explanation (in the limits of HMO approximations) of the first ^1L_b transition band from UV spectra, of the first ionization potential and of the reactivity of phenol (I) and several related molecules : 1,2- ; 1,3- ; 1,4-dihydroxy benzenes (respectively : pyrocatechol (II) ; resorcinol (III) ; hydroquinone (IV)) and 1,2,3- ; 1,2,3- ; 1,3,5-trihydroxybenzenes (respectively ; pyrogallol (V) ; phlorcglucine (VI) and hydroxydroquinone (VII)).

THE CHOICE OF SIGNIFICANT EXPERIMENTAL DATA FOR PHENOL

In order to obtain a unitary set of HMO parameters using the graphical method, we must choose, from the known set of calculable properties, one or more properties that have been determined by experiments. As a first element of this set for phenol, we selected the energy value of the ^1L_b transition from the electronic spectrum in solution, as a second element — the energy value of the first ionization potential (IP) obtained by photoionization (PIP) and/or the first ionization potential obtained by electronic impact (EIIP).

As we mentioned in the previous note, [1] the numerical experimental values of the properties of the test molecules must be determined with comparable methods and with no doubts as to the assignments. We choose the first $\pi\pi^*$ band of substituted benzenes as such a property (the α band in Clar notation, the $^1B_{2u} - {}^1A_{1g}$ band when one takes into account symmetry of transition, the ^1L_b band in Platt notation or the C band in Forbes notation). [58–63] The reasons for this choice are as follows. First, this band is placed at wavelengths higher than 230 nm, where it is not significantly influenced by solvent impurities, which usually absorb at lower wavelengths. Second, the ^1L_b band was extensively studied from the experimental and theoretical point of view and is assigned without doubts as the first $\pi\pi^*$ benzene band perturbed by an exocyclic function. There are many studies concerning the influence of the solvent polarity, of the temperature and of the intermolecular or solvent hydrogen bonds on this ^1L_b band. Third, the Hückel method can correctly predict especially this ^1L_b band because the etalonation of the resonance integral, $\beta = -2{,}39$ eV was performed for the ^1L_b benzene band.

Let us discuss now the numerical values for these properties (available in literature) regarding phenol and its derivatives.

Phenol exhibits, in the UV range, in solution, two $\pi\pi^*$ bands, ^1L_b and ^1L_a (see Table 1 and the quoted literature). The ^1L_b band presents both in unpolar and polar solvents maxima, patterns that were considered as envelopes of some vibrational bands. In unpolar solvents, this band shows three maxima at 278, 271 and 263 nm. We make the remark that in carbon tetrachloride the reported values are bathochromically shifted

Table 1

Wavelength values (in eV) for ^1L_a and ^1L_b bands of phenol in different solvents.

Solvent		^1L_b (log *A*)		^1L_a (log. A)	Reference
Hexane	276 (3.31)	270 (3.34)	263 (3.15)		61
Hexane	276 (3.32)	269 (3.34)	263 (3.15)	210 (3.78)	63
Hexane	278 (3.40)	271 (3.40)			64
Hexane	277 (3.20)	271 (3.20)	265 (3.10)		65
Hexane	280 (3.40)	270 (3.50)	268 (3.40)		66
Hexane		271 (3.32)			67
Hexane	276 (3.12)	270 (3.20)	265 (3.09)		68
Hexane		270 (3.36)		210 (3.77)	69
Cyclohexane	278 (3.17)	271 (3.35)	265 (3.32)	212 (3.75)	70
Cyclohexane	271 (3.32)	269 (3.34)	263 (3.15)	210 (3.78)	63
Heptane	278 (3.40)	270 (3.40)			71
i-Octane	277 (3.30)	271 (3.30)	264 (3.20)	211 (3.80)	72
n-Pentane/3-Methylpentane 77K	277	270			73
293K	278	271			
i-Octane/ Dioxane	280 (3.20)	273 (3.40)	267 (3.20)	220(3.80)	72
Dioxane		273 (3.32)			74
Carbon-tetrachloride	280 (3.30)	273 (3.30)			64
Ethyl-ether	277 (3.26)	271 (3.34)	266 (3.20)	218 (3.81)	63
Ethyl-ether	276 (3.32)	269 (3.34)	263 (3.15)	210 (3.78)	75
Methanol		271 (3.28)		218 (3.78)	76
Methanol	277	270	264		77*a*
Ethanol		273 (3.26)		218 (3.78)	70
Ethanol	276 (3.16)	271 (3.28)	266 (3.18)	218 (3.78)	63
Ethanol	280 (3.30)	270 (3.50)			78
Ethanol		271 (3.28)			79
Pentane/ Ethanol/ Ethyl-ether		271 (3.28)		218 (3.78)	69
Water	273 (3.10)	268 (3.18)		210 (3.78)	63
Water (pH = 7)		268 (3.18)		210 (3.78)	62
Water (HCl 0.1 N)		268 (3.20)		210 (3.78)	62
Water (NaOH 0.1 N)		285 (3.43)		235 (4.02)	62

and are closer to the dioxan values than those in aliphatic hydrocarbons. Generally, variations in polarity of solvents produce relatively minor shifts. In water, acidic or neutral medium, the shift is hypsochromic. In alkaline medium the $^{1}L_b$ band presents a strong bathochromic shift which is attributed to the phenolate anion. The results of Köhler *et al.*[73] showed that temperature does not significantly influence the $^{1}L_b$ band. The variations in the ratios of the molar extinction coefficients, at different wavelengths of the $^{1}L_b$ band, with the phenol concentration, in cyclohexane and solvents that form hydrogen bonds (methanol, ethanol, water and ethylenglycol), as well as the variations in IR spectra of $-$OH bands at 3640 and 3620 cm^{-1}, lead to the following conclusions :[80, 81] *a*) The small shifts and the variations of absorbance are due to the hydrogen bonds of phenol with proton acceptor solvents, or to the intermolecular hydrogen bonds (that lead to dimers at small concentrations and to polymers at higher concentrations) ; *b*) The phenol can act both as a proton donor when the shift is bathochromic and as a proton acceptor when the shift is hypsochromic ; *c*) The dispersion of the absorption maxima and of the absorbance, obtained by different authors, can be explained by the different ranges of phenol concentrations within which the spectra are recorded. The small shifts in carbon tetrachloride, [64] and dioxane,[74] can be explained by the fact that, in these solvents, phenol acts as a proton donor ; *d*) The hydrogen bonds cannot significantly shift the $^{1}L_b$ maximum because the phenol can act both as a proton acceptor and as a donor.

The phenol spectrum in vapour phase was reported by Robertson and Matsen[82] and they placed the O$-$O transition of $^{1}L_b$ bands at 275.03 nm, while Dearden and Forbes[63] reported five maxima, situated at 261, 264, 266.5, 270 and 273 nm.

From all the available data, we considered a value of 271 nm (4.57 eV) for $^{1}L_b$ maximum of phenol, which is similar to values used by Kiss, [83,84] Baba, [85] Singerman and Jaffé.[86]

The second property considered for obtaining a set of optimal parameters for the OH function was the first IP. This choice was determined especially by the existence of a linear relationship between the HOMO and the IP. [87] In the last years, the calculated values for IP are compared with PIP both for benzene, [88-93] and phenols, [88-94] despite the excellent correlations of the EIIP and HOMO obtained by Streitwieser, [95] because PIP is the true VIP, the one corresponding to Koopmans' theorem. [96]

According to Streitwieser, VIP = EIIP and for the etalonation of α, the coulombic integral, we take for benzene VIP = EIIP = 9.52 eV. [87,95,97-100] With $\beta = -2.39$ eV, the value which yields the correct calculated value for the $^{1}L_b$-maximum of benzene in solution, [1,51,87,101-103] the value resulting for the coulombic integral is $\alpha = -7.13$ eV. The EIIP value of 9.52 eV for benzene, [87,95,104] is comparable, from the experimental point of view, with the 9.16 eV value for phenol. [101,105] In addition, the benzene EIIP leads to an α value (-7.13 eV) close to the values used by different authors, as for example $\alpha = -7.07 \pm 0.09$ eV ($\beta = -2.48 \pm 0.17$ eV), [87,95] or $\alpha = -7.18$ eV. [106]

For benzene, all the authors reported values very close to VIP = 9.24 ÷ 9.25 eV. [88-92,107-115] For $\beta = -2.39$ eV and VIP = 9.25 eV, the

α value is -6.86 eV. The VIP for phenol are also close to this. The old value reported by Watanabe (8.50 eV), [108] was recently confirmed by Palmer *et al.*, (8.56 eV). [93] Many authors adopted the value 8.52 eV for the comparison with their calculated values. [88,114,115] Dewar and David [94] adopt a value of 8.67 eV. From all the available data on VIP we have chosen the recent value reported by Palmer *et al.*, VIP = 8.56 eV. [93]

Theoretical studies made possible to define mathematical relations for the calculation of the values for the most physical properties of the molecules, using quantum-chemical data. For the calculation of the chemical reactivity several indices were proposed, but the reactivity is not yet a well-defined notion. For this reason, the MO calculations allow only a qualitative comparison of the molecular reactivity in a series of related molecules. A set of reactivity indices is defined within the HMO-method and therefore we take into account some kinetic data in order to check our HMO parameters.

The kinetic study of Coombes *et al.* [116] on electrophilic aromatic substitution — the phenol nitration in sulphuric acid medium — evidenced a dependence of the yield (%) of *o*- and *p*- substitution products on the sulphuric acid concentration. For instance the nitration takes place 70% in *o*- and 30% in *p*- for 50% sulphuric acid; 50% in *o*- and 50% in *p*- for 75% sulphuric acid and 40% in *o*- and 60% in *p*- for 86% sulphuric acid.

In a study upon action of phenolase in the electrophilic oxidation of the phenol, Capdeville and Maumy [117] used the catalytic system for phenol oxidation in the presence of Cu_2Cl_2. They concluded that phenol oxidation took place predominantly in *o*-, when phenolase and Cu_2Cl_2 were present, the only reaction product being the pyrochatechol.

For different HF/SbF_5 ratios, phenol oxidation with hydrogen-peroxide yields around 64% hydroquinone, 36% pyrocatechol and 1% resorcinol. [118] Gesson *et al.* [118] supposed that in superacidic media a desactivation of *o*- and *p*- positions was possible and the attack in *m*- position predominates. The presence of resorcinol among the reaction products was observed by Razimovskii *et al.* [119] in the electrophilic oxidation of phenol by ozone (O_3). They explain the resorcinol formation by a five membered cyclic intermediate which involves the *m*- position.

All experimental data indicate only a small difference between the reactivity of *o*- and *p*- positions, and therefore the electronic densities at these positions must be also very close, and significantly higher than the charge density at the *m*-position.

In this optimization study, $\delta_{\ddot{O}-}$ was varied in the range $\mathbb{D} = [1.4, 2.6]$ with a step of $\Delta\delta_{\ddot{O}-} = 0.2$, while $k_{\ddot{O}-Ar}$ was varied in the range $\mathbb{K} = = [0.4, 1.6]$ with a step $\Delta k_{\ddot{O}-Ar} = 0.2$. These domains included all parameters found in literature plus a small, marginal, security range. [9,12,50-56,120-122]

In all following computations, we adopt the inductive model for the C atom bonded to the $-OH$ group. The most frequently used value for its coulombic integral adopted also here is $\alpha + 0.2\ \beta$. [51,52]

The numbering of atoms is consistent with IUPAC recommendation. The oxygen atom participates in the π system with one of the hybrid

sp^3 orbitals. This orbital is occupied by two electrons and has symmetry properties similar to a $2p_z$ orbital. The phenol molecule belongs to the C_{2v} point group. The reducible representation can be reduced by two irreducible representations $\Gamma = 2A_2 + 5B_1$.

RESULTS AND DISCUSSION

The projections of the variation of π energy levels E_π ($\delta_{\ddot{O}-}$, $k_{\ddot{O}-Ar}$) on the $\delta_{\ddot{O}-O}$ E_π and $k_{\ddot{O}-Ar}$ $0E_\pi$ planes are shown in Fig. 1. The energy levels $\alpha \pm \beta$ of A_2 symmetry MO eigenfunctions, as one can see, are independent of the $\delta_{\ddot{O}-}$ and $k_{\ddot{O}-Ar}$ parameters and include only $2p_z$—C—atom orbitals: $\varphi \pm = 2^{-1/2} [(\varkappa_2 - \varkappa_6) \pm (\varkappa_3 - \varkappa_5)]$. Only these MO's preserve both the energy value and the composition corresponding to the benzene system. The other five B_1 eigenfunctions and eigenvalues depend upon the $\delta_{\ddot{O}-}$ and $k_{\ddot{O}-Ar}$ parameters. The level, the strongest influenced by the parameter-variations, is the lowest occupied molecular orbital, with energy values varying between $\alpha + 2.2\beta$ and $\varkappa + 3.6\beta$. It is less influenced by variations in $\Delta_{\ddot{O}-}$ (proportional to the oxygen atom electronegativity) than by variations in $k_{\ddot{O}-Ar}$ (proportional to the π-bond strength between the oxygen and the ring).

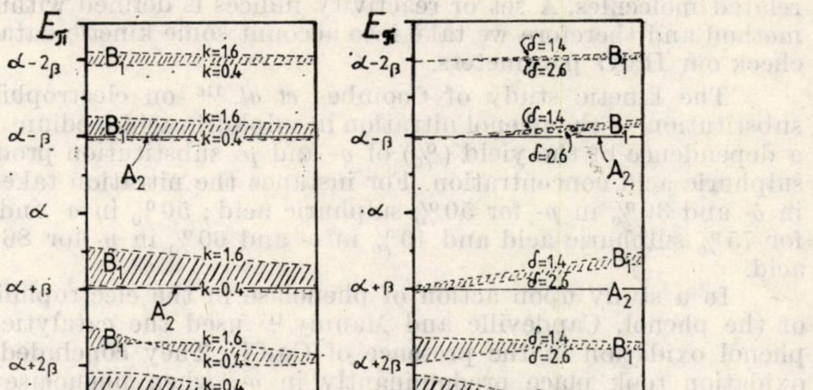

Fig. 1. — The variation of π energy levels $E_\pi(\delta_{\ddot{O}-}, k_{\ddot{O}-Ar})$ — for phenol in the $\delta_{\ddot{O}-}$ $0E_\pi$ and $k_{\ddot{O}-Ar}$ $0E_\pi$ planes, when $\delta_{\ddot{O}-} \in \mathbb{D}$ and $k_{\ddot{O}-Ar} \in \mathbb{K}$.

The variations of the q_{i7} ($\delta_{\ddot{O}-}$, $k_{\ddot{O}-Ar}$), for the sp^3-oxygen atom orbital participation in MO's, with $\delta_{\ddot{O}-}$ and $k_{\ddot{O}-Ar}$, were projected on the $\delta_{\ddot{O}-}$ $0q_{i7}$ and $k_{\ddot{O}-Ar}$ $0q_{i7}$ planes for the lowest occupied MO ($i = 1$) and for the following MO belonging to B_1 symmetry ($i = 2$). These projections are illustrated in Fig. 2, for $\delta_{\ddot{O}-} \in \mathbb{D}$ and $k_{\ddot{O}-Ar} \in \mathbb{K}$. As it results from Fig. 2, the oxygen atom sp^3 hybrid orbital has the highest contribution in the MO corresponding to the lowest occupied ($i = 1$) level for the $\delta_{\ddot{O}-Ar} \leqslant 1.8$ and $k_{\ddot{O}-} \leqslant 0.8$ values. Therefore, we consider that, for $\delta_{\ddot{O}-} \in [1.4, 1.8]$ and $k_{\ddot{O}-Ar} \in [0.4, 0.8]$, the lowest occupied level is a level effectively introduced by the oxygen atom. For $\delta_{\ddot{O}-} > 1.8$ and $k_{\ddot{O}-Ar} > 0.8$, we consider this level ($i = 1$) as a perturbation of the $\alpha + 2\beta$ benzene level. The next occupied level ($i = 2$), corresponding to a MO of B_1 symmetry, has values between $\alpha + 1.5\beta$ and $\alpha + 2\beta$. This level is introduced by the oxygen atom for the range $\delta_{\ddot{O}-} > 1.8$ and $k_{\ddot{O}-Ar} > 0.8$. For lower $\delta_{\ddot{O}-}$ and $k_{\ddot{O}-Ar}$ values it arises from the perturbation of the $\alpha + 2\beta$ benzene level. This inversion (see Fig. 2) is determined by the decrease of the contribution of the oxygen sp^3 hybrid orbital and by the increase in the weights of other AO's.

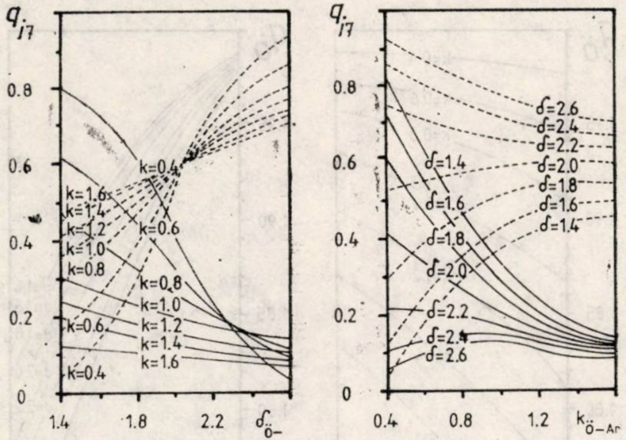

Fig. 2. — The variation of q_{i_7} ($\delta_{\ddot{O}-}$, $k_{\ddot{O}-Ar}$), for the participation of the sp^3 hybrid oxygen orbital in the MO's of B_1 symmetry, for the lowest occupied MO ($i = 1$, ——) and for the next MO ($i = 2$, – – –). Projections in the $\delta_{\ddot{O}-}\ 0q_{i_7}$ and $k_{\ddot{O}-Ar}\ 0q_{i_7}$ planes, when $\delta_{\ddot{O}-} \in \mathbb{D}$ and $k_{\ddot{O}-Ar} \in \mathbb{K}$.

These results are in opposition with the variation diagram given by Matsen.[120] His results can be explained by the fact that he applied a perturbation technique on a very large domain of $\delta_{\ddot{O}-} \in [0.0, 5.0]$, with a single value for $k_{\ddot{O}-Ar}$ ($k = 1.0$). He obtained therefore only one curve projected on a single plane. Applying the perturbation technique for each level, Matsen could produce an independent variation of levels without inversion of the last two occupied levels.

The other B_1 levels derive from the perturbation of $\alpha \pm \beta$ and $\alpha - 2\beta$ benzene levels. Among these levels, the HOMO level is the most strongly perturbed.

The variation of the π charge densities $q\,(\delta_{\ddot{O}-}, k_{\ddot{O}-Ar})$ at the oxygen atom, and also at the *o*-, *m*- and respectively *p*- positions, was projected on the $\delta_{\ddot{O}-}Oq$ and $k_{\ddot{O}-Ar}\,Oq$ planes. These projections can be seen in Fig. 3 and Fig. 4. Because of the level crowding, on certain domains in Fig. 4 only a hatched zone was drawn. This zone was limited by the inferior and superior contour line.

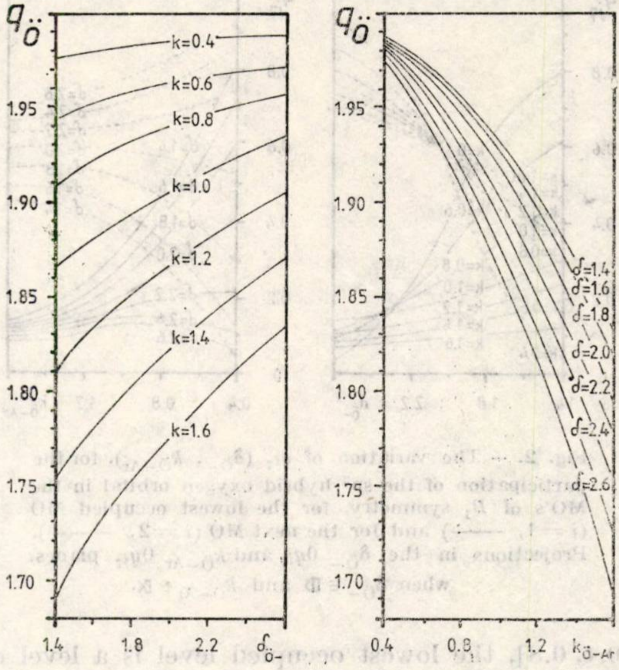

Fig. 3. — Variation of the π charge density, $q\,(\delta_{\ddot{O}-}, k_{\ddot{O}-Ar})$, for the phenolic oxygen. Projections in the $\delta_{\ddot{O}-}\,0q$ and $k_{\ddot{O}-Ar}\,0q$ planes, when $\delta_{\ddot{O}-} \in \mathbb{D}$ and $k_{\ddot{O}-Ar} \in \mathbb{K}$.

The results from Figs 3 and 4 show that the charge density on the oxygen atom and at the *o*- and *p*- positions varies less with electronegativity (i.e. with $\delta_{\ddot{O}-}$), than with bond strength (i.e. with $k_{\ddot{O}-}$). The charge density on the oxygen atom increases with $\delta_{\ddot{O}-}$ and decreases with $k_{\ddot{O}-Ar}$. This order is reversed for *o*- and *p*- charge densities.

The manner of variation of the charge densities at the oxygen atom and respectively at the *o*- and *p*- positions is an argument in favour of a variation of the conjugation between the sp^3 oxygen orbital and the π-ring system. A shift of charge density towards the ring appears when the electronegativity decreases and the conjugation increases.

Another remarkable fact results also from Fig. 4, namely in *o*- and *p*- positions the electrophilic attack is possible only for values $\delta_{\ddot{O}-} > 1.8$ and $k_{\ddot{O}-Ar} > 0.8$. Above these values, the charge density in *o*- position increases more rapidly than that in *p*- position, thus explaining the slight reactivity difference between the two positions for electrophilic attack.[116-119] For lower $\delta_{\ddot{O}-}$ and $k_{\ddot{O}-\mathrm{Ar}}$ values the charge density in *m*- position is greater than that in *o*- and *p*- positions; this fact is in contradiction with the experimental reactivity data.

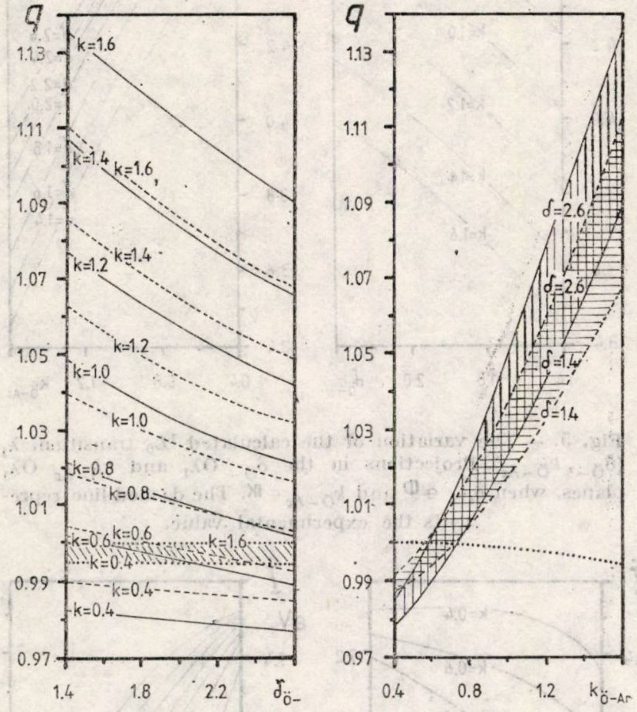

Fig. 4. — Variation of the π charge density, $q\,(\delta_{\ddot{O}-},\ k_{\ddot{O}-\mathrm{Ar}})$ in the *o*- (—), *m*- (. . .), and *p*- (— — —) phenolic positions. Projections in the $\delta_{\ddot{O}-}\ Oq$ and $k_{\ddot{O}-\mathrm{Ar}}\ Oq$ planes, when $\delta_{\ddot{O}-} \in \mathbb{D}$ and $k_{\ddot{O}-\mathrm{Ar}} \in \mathbb{K}$.

Comparatively with the *o*- and *p*- positions, the charge density at the *m*- position varies only to a small extent with the $\delta_{\ddot{O}-}$ and $k_{\ddot{O}-}$ parameters. It is almost independent of the $o_{\ddot{O}-}$ variation, its value being near unity.

In order to explain the oxidation in *m* position in superacidic media,[118] we must admit the addition of a proton at a lone pair of the oxygen-atom. In this case, the ring charges are moved towards the oxygen and the *o*- and *p*- positions are deactivated. The *m*- position is only to a small extent influenced by the substituent electronegativity and will remain with a charge superior to that of the *o*- and *p*- positions. In this case the parameters must be situated in the range $\delta_{\ddot{O}-} < 1.8$ and $k_{\ddot{O}-\mathrm{Ar}} < 0.8$.

The variation of the transition energy $\lambda_1\,(\delta_{\ddot{O}-},\ k_{\ddot{O}-\mathrm{Ar}})$, calculated for the ${}^1L_b$ transition was projected on the $\delta_{\ddot{O}-}\ O\lambda_1$ and $k_{\ddot{O}-\mathrm{Ar}}\,O\lambda_1$ planes; the resulting projections are given in Fig. 5. The projections of the

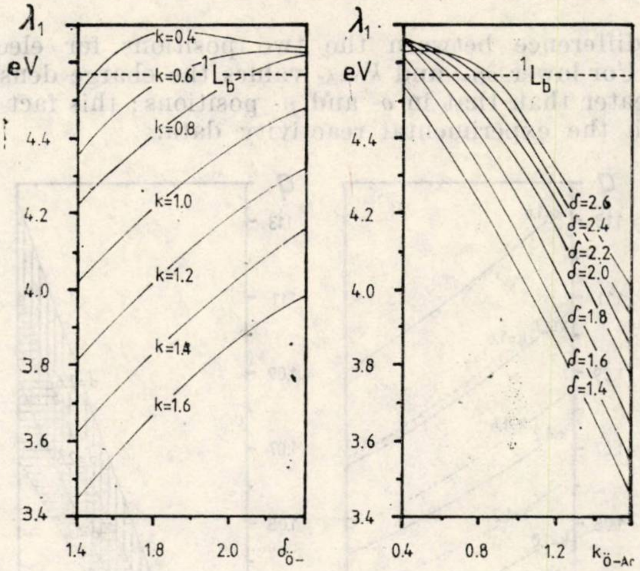

Fig. 5. — The variation of the calculated ^1L_b transition, λ_1 ($\delta_{\ddot{O}-}$, $k_{\ddot{O}-Ar}$). Projections in the $\delta_{\ddot{O}-}$ Oλ_1 and $k_{\ddot{O}-Ar}$ Oλ_1 planes, when $\delta_{\ddot{O}-} \in \mathbb{D}$ and $k_{\ddot{O}-Ar} \in \mathbb{K}$. The dashed line represents the experimental value.

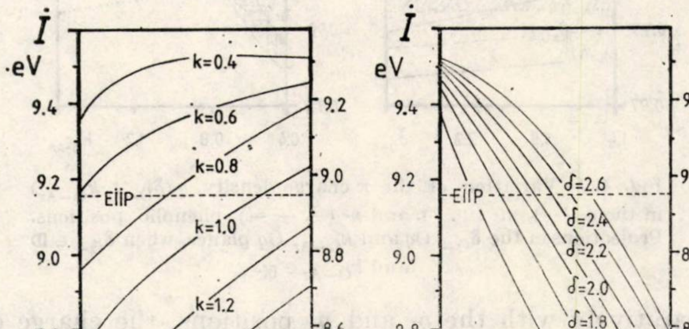

Fig. 6. — The variation of calculated IP, $I\,(\delta_{\ddot{O}-}, k_{\ddot{O}-Ar})$, (EIIP— left scale and PIP — right scale). Projections in the $\delta_{\ddot{O}-}$ OI and $k_{\ddot{O}-Ar}$ OI planes, when $\delta_{\ddot{O}-} \in \mathbb{D}$ and $k_{\ddot{O}-} \in \mathbb{K}$. The dashed lines represent the experimental values.

first ionization potential in eV, $I\ (\delta_{\ddot{O}-}, k_{\ddot{O}-Ar})$, as calculated according to Koopmans' theorem,[96] on the $\delta_{\ddot{O}-}\ Oi$ and $k_{\ddot{O}-Ar}\ OI$ plane are given in Fig. 6. The dashed lines in Figs 5 and 6 represent the experimental values. As we disposed of both IP, EIIP and PIP for phenol, two scales are represented in Fig. 6 : the basis of the first one is the EIIP of benzene (for which $\alpha = -7.13$ eV results) — the left hand side of the diagram, whereas the basis of the second one is the first PIP of benzene (for which $\alpha = -6.86$ eV results) — the right hand side of the diagram.

The concordance domains, obtained from Fig. 5, for the ^1L_b electronic transition are : $\delta_{\ddot{O}-} \in [1.5, 2.6]$ and $k_{\ddot{O}-Ar} \in [0.4, 0.88]$. From Fig. 6, the concordance domains $\delta_{\ddot{O}-} \in [1.4, 2.6]$ and $k_{\ddot{O}-Ar} \in [0.61, 1.14]$ result for EIIP and $\delta_{\ddot{O}-} \in [1.4, 2.6]$ and $k_{\ddot{O}-Ar} \in [0.98, 158]$ for PIP.

The intersection of the $\delta_{\ddot{O}-}$ -domains gives the minimum concordance domain : $\delta_{\ddot{O}-}\ \varepsilon\ [1.5, 2.6]$.

For $k_{\ddot{O}-Ar}$, the intersections over all domains are empty. In this case we intersect the $k_{\ddot{O}-Ar}$ domain for ^1L_b with the $k_{\ddot{O}-Ar}$ domain for EIIP. This last intersection gives a minimum concordance domain $k_{\ddot{O}-Ar} \in$ $\in [0.61, 0.88]$. From these data we conclude that within the limits of the HMO-method one cannot obtain a unitary treatment of the first electronic transition of phenol (^1L_b) with the first VIP because they do not admit a unique set of parameters. Nevertheless, a unitary treatment of ^1L_b with EIIP is possible. Also, from these intersections, we can remark that, in a HMO treatment of exocyclic heteroatom, the parameter related to electronegativity ($\delta_{\ddot{O}-}$) can vary on a large domain, while the parameter related to bond and conjugation strength ($k_{\ddot{O}-Ar}$) can vary only on a very narrow domain.

For ^1L_b and EIIP, the best pair, as resulting from some trials, is $\delta_{\ddot{O}-} = 2.0$, $k_{\ddot{O}-Ar} = 0.84$, a pair similar to the one recommended by Streitwieser [51] and Pullman [52]. This parameter pair was used in HMO calculations for pyrocatechol (II), resorcinol (III), hydroquinone (IV), pyrogallol (V), phloroglucine (VI) and hydroxydroquinone (VII). The calculated first $\pi\pi^*$ transition and the experimental one are given in Table 2.

In order to establish a realistic criterium for comparison of experimental and calculated data, we tried to find some linear relationships of type : $E_{exp.} = a + bE_{calc.}$ (in eV). For the data listed in Table 2, the equation is : $E_{exp.} = -0.597 + 1.167E_{calc.}$ $(r = 0.530)$. For pyrogallol and phloroglucine the differences between the experimental and the calculated data are very important. According to usual elimination criteria these molecules (V and VI) are to be taken away from correlation and a new correlational equation is obtained : $E_{exp.} = -0.335 +$ $+ 1.11OE_{calc.}$ $(r = 0.945)$. [128] Another correlational equation : $E_{exp.} =$ $= -0.665 + 1.181E_{calc.}$ $(r = 0.914)$ is obtained when all the distinct experimental data for each phenol, diphenols, etc. except those for pyrogallol and phloroglucine are considered for the correlation. This last line is shown in Fig. 7.

For the spectra of phenol and diphenols recorded in hydrocarbons (hexane, heptane, cyclohexane) the differences between calculated and experimental transitions are small and almost constant. For the spectra of triphenols recorded in more polar solvents (methanol, ethanol) these differences vary with in relatively large limits, possibly because of the

Table 2

The ^1L_b electronic transition in phenols. Experimental and calculated values with the recommended pair of parameters

Molecule	$\lambda_{calc.}$		$\lambda_{exp.}$		Δ *		References for the experimental data
	nm	eV	nm	eV	nm	eV	
(I)	278	4.460	271	4.570	+ 7	−0.11	Cited literature in Table 1.
(II)	288	4.300	277	4.480	+11	−0.18	77*b*, 122, 123, 124, 125.
(III)	284	4.370	275	4.500	+ 9	−0.13	122, 123, 124.
(IV)	296	4.190	291	4.260	+ 4	−0.06	122, 123, 124, 126.
(V)	289	4.290	267	4.640	+22	−0.35	77*c*.
(VI)	283	4.380	268	4.630	+15	−0.25	77*d*.
(VII)	299	4.150	288	4.310	+11	−0.16	77*e*.

* $\Delta = \lambda_{calc.} - \lambda_{exp.}$

influence of solvent polarity and a certain keto-enol tautomery. However, a comparison of their UV spectra and those of their methyl ethers indicates an enol structure.[129] Taking into account the formation of the hydrogen bonds with the solvent (methanol, ethanol), another possible explanation of the large differences between calculated and experimental ^1L_b transition maxima can be the fact that triphenols act predominantly as proton acceptors with a strong hypsochromic effect. The probability of intermolecular hydrogen bonds is small, because of steric hindrance.

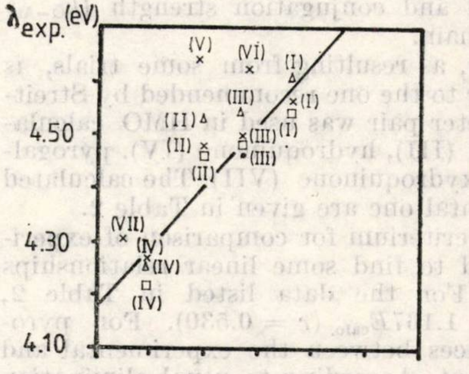

Fig. 7. — The correlation between the experimental and calculated values for the ^1L_b transition in phenol, di- and triphenols (* data from Table 2 ; Δ according to Dearden,[63] according to Senikov,[69] □ according to Kammerer[127]).

The results obtained with the proposed parameters are compared with those obtained from Pariser-Parr-Pople (PPP) or MIM calculations (Table 3).[82,83,123,124,130] We consider them satisfactory.

Table 4 compares the experimental IP data with the calculated ones using this new set of parameters. From the comparison of the EIIP and VIP values, calculated by us, with those obtained by Yoshida and Kobayashi[101] (9.206 eV), and Carbo and Fraga[88] (9.20 eV) respectively, we must not conclude that the HMO technique allows a distinction between the two methods of determination for IP (EIIP and PIP). Our results are due only to the suitable choice of scale. As mentioned, the

Table 3

Comparison between the HMO values for the ^1L_b band for phenol and diphenols, calculated with proposed parameters, and the values obtained by different authors with the PPP method (in eV)

Molecule	E_{calc}	Δ	E_{calc}	Δ	E_{calc}	Δ	E_{calc}	Δ	E_{calc}	Δ	E_{calc}	Δ	E_{calc}	Δ
	a		*b*		*c*		*d*		*d*		*d*		*e*	
(I)	4.460	−0.11	—	—	4.910	+0.34	4.620	+0.05	4.610	+0.04	4.630	+0.06	4.580	+0.01
(II)	4.300	−0.18	4.600	+0.12	—	—	4.400	−0.08	4.390	−0.09	4.420	−0.06	—	—
(III)	4.370	−0.13	4.660	+0.15	—	—	4.490	−0.01	4.480	−0.02	4.500	0.00	—	—
(IV)	4.190	−0.06	4.470	+0.21	—	—	4.290	+0.03	4.270	+0.01	4.310	+0.05	—	—

$\Delta = E_{calc.} - E_{calc.}$

a) calculated with proposed parameters; b) calculated in ref. 124; c) in ref. 130; d) in ref. 122 — three variants of parameters; the results do not differ significantly from the values obtained in refs 82 and 123; e) calculated in ref. 83 with MIM method.

Table 4

The first IP for phenol and diphenols. Comparison between the experimental values and the values calculated with the proposed parameters

Molecule	EIIP (eV)		VIP (eV)	
	calc.	exp. *	calc.	exp. **
(I)	9.19	9.16	8.92	8.56
(II)	9.02	—	8.75	8.56
(III)	9.09	—	8.82	8.63
(IV)	8.95	—	8.68	8.44

* According to refs 104 and 105.
** According to ref. 93.

EIIP value for phenol gives an unempty intersection and that explains the consistence between experimental and calculated EIIP-values. The calculated VIP values for phenol and diphenol differ sensibly from the experimental ones, as expected, because of the empty intersection obtained for the $k_{\ddot{O}-Ar}$-domains. However, the order of VIP for diphenols is correctly predicted by this set of parameters. Although the VIP value obtained by Palmer *et al.*,[93] from an *ab initio* calculation for phenol is almost equal to the experimental VIP value, the *ab initio* calculation for diphenols predicts even more different values than those obtained by us, with the proposed parameters set (Fig. 8).

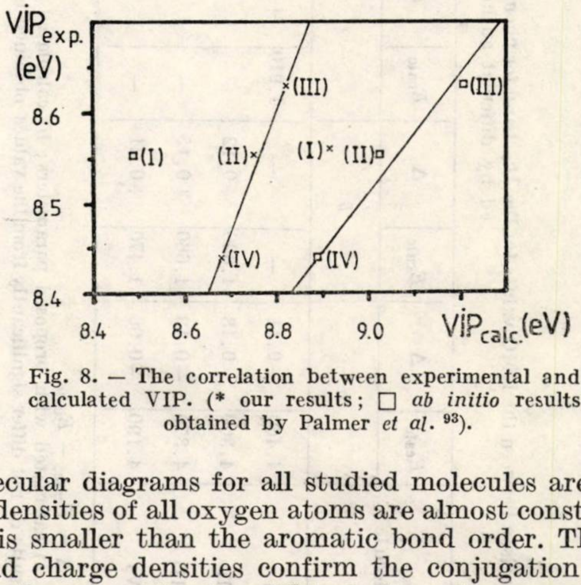

Fig. 8. — The correlation between experimental and calculated VIP. (* our results ; □ *ab initio* results obtained by Palmer *et al.*[93]).

The molecular diagrams for all studied molecules are given in Fig. 9. The charge densities of all oxygen atoms are almost constant. The C—O π bond order is smaller than the aromatic bond order. The values of π bond order and charge densities confirm the conjugation of an oxygen lone pair with the aromatic ring. This fact confers an acidic character to the phenolic hydrogen.

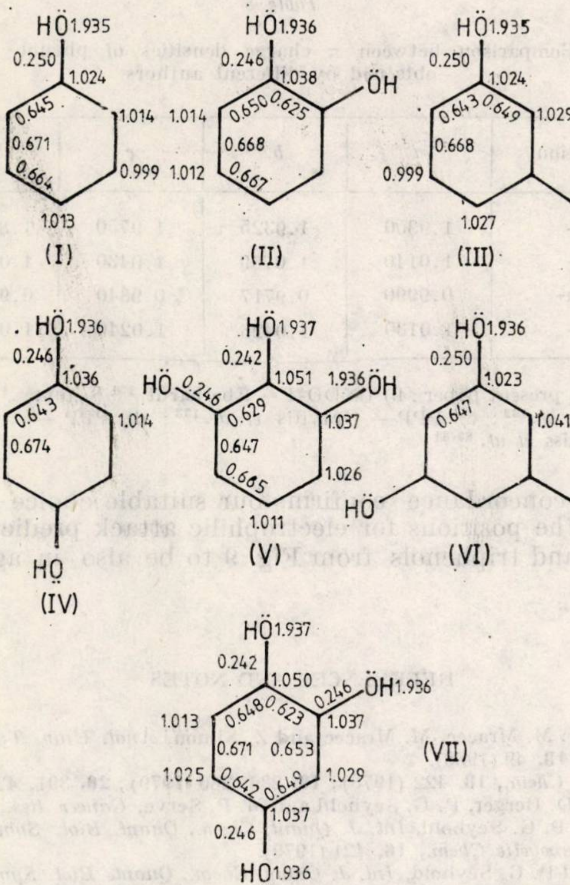
HÖ1.935
0.250
1.024
0.645
1.014
0.671
0.664
0.999
1.013
(I)
HÖ1.936
0.246
1.038
ÖH
1.014
0.650
0.625
0.668
1.012
0.667
(II)
HÖ1.935
0.250
1.024
0.643
0.649
1.029
0.668
0.999
1.027
ÖH
(III)
HÖ1.936
0.246
1.036
0.643
1.014
0.674
HÖ
(IV)
HÖ1.937
0.242
1.051
HÖ
0.246
1.936ÖH
0.629
1.037
0.647
0.665
1.026
1.011
(V)
HÖ1.936
0.250
1.023
0.647
1.041
HÖ
ÖH
(VI)
HÖ1.937
0.242
1.050
0.246
ÖH1.936
1.013
0.648
0.623
1.037
0.671
0.653
(VII)
1.025
0.642
0.649
1.029
1.037
0.246
HÖ1.936

Fig. 9. — The diagrams of π charge densities and bond orders for the studied molecules.

The π charge densities of phenol at oxygen atom and at *o*-, *m*- and *p*- positions obtained by us are consistent with those obtained from PPP or CNDO/2,[83, 84, 131–133] as can be seen from Table 5.

In the phenol molecule the π charge densities are larger than unity in *o*- and *p*- positions, indicating them as sites for an electrophilic attack. A slight difference appears between these two positions, *o*- having a small priority. These differentiations are confirmed by experimental data.[117–119] The priority of the electrophilic attack at one of the two positions depends upon the reaction-conditions,[116, 118] and is not modified in enzymatic catalysis.[117] In order to explain the attack in superacidic media,[118] we must admit that the oxygen-ring conjugation is substantially decreased by the protonation of the oxygen atom. For such situations the oxygen parameter must be $h_{\ddot{O}-Ar} < 0.6$, in order to give for *m*- position a π density charge higher that those for *o*- and *p*- positions (see Fig. 4).

Table 5

Comparison between π charge densities of phenol obtained by different authors

Position	*a*	*b*	*c*	*d*
ö-	1.9350	1.9325	1.9750	1.8717
o-	1.0140	1.0709	1.0430	1.0644
m-	0.9990	0.9717	0.9840	0.9940
p-	1.0130	1.0423	1.0240	1.0358

a) present paper ; b) CNDO/2 — Eberhardt,[131] Seguin *et al.*[132]; c) PPP — Gravitis *et al.*[133]; d) PPP — Kiss *et al.*[83,84]

This good concordance confirms our suitable choice of parameters and we expect the positions for electrophilic attack predicted by charge densities of di- and triphenols from Fig. 9 to be also in agreement with the experiment.

REFERENCES AND NOTES

[1] Preceding paper : M. Mracec, M. Mracec and Z. Simon, *Anal. Univ. Timișoara, ser. Fiz.-Chim.*, **18**, 49 (1980).

[2] W. Gründler, *Z. Chem.*, **18**, 422 (1978) ; **19**, 236, 266 (1979) ; **20**, 391, 425 (1980).

[3] I. A. Smith, G. D. Berger, P. G. Seybold and M. P. Serve, *Cancer Res.*, **39**, 2968 (1978).

[4] I. A. Smith and P. G. Seybold, *Int. J. Quant. Chem., Quant. Biol. Symp.*, 5, 311 (1978) ; *J. Heterocyclic Chem.*, **16**, 421 (1979).

[5] G. D. Berger and P. G. Seybold, *Int. J. Quant. Chem., Quant. Biol. Symp.*, **6**, 305 (1979).

[6] S. Aono and K. Nishikawa, *Bull. Chem. Soc. Japan*, **53**, 4318 (1980).

[7] W. J. Archer, R. Taylor, P. H. Gore and F. S. Kamoun, *J. Chem. Soc. Perkin II*, **1980**, 1828.

[8] L. J. Schaad and B. A. Hess, *Israel J. Chem.*, **20**, 281 (1980).

[9] P. G. Seybold, *Int. J. Quant. Chem., Quant. Biol. Symp.*, **7**, 271 (1980).

[10] P. G. Seybold and A. Graslund, *Int. J. Quant. Chem., Quant. Biol. Symp.*, **7**, 261 (1980).

[11] I. V. Strankevics and O. B. Tomilin, *Zhur. strukt. Khim.*, **21**, 15 (1980).

[12] F. A. van Catledge, *J. Org. Chem.*, **45**, 4801 (1980).

[13] S. Aono, T. Ohmae and K. Nishikawa, *Bull. Chem. Soc. Japan*, **54**, 1645 (1981).

[14] R. B. Bates, B. A. Hess, C. A. Ogle and L. J. Schaad, *J. Amer. Chem. Soc.*, **103**, 5052 (1981).

[15] A. J. Duben, *J. Phys. Chem.*, **85**, 245 (1981).

[16] K. D. Gundermann, C. Lohberger and M. Zander, *Z. Naturforsch.*, **36a**, 276, 297 (1981).

[17] P. Karadakov, O. Castano, F. Fratev and V. Enchev, *Z. phys. Chem. (Wiesbaden)*, **128**, 168 (1981).

[18] L. Musil, B. Koutek, M. Pisová and M. Souček, *Coll. Czech. Chem. Comm.*, **46**, 1148 (1981).

[19] U. Norinder, D. Tanner, B. Thulin and O. Wennerström, *Acta Chem. Scand.*, **B35**, 403 (1981).

[20] P. G. Seybold, R. Vestewing and J. D. Schribner, *Int. J. Quant. Chem., Quant. Biol. Symp.*, **8**, 400 (1981).

[21] H. Vogler, *Theor. Chim. Acta*, **60**, 65 (1981).

[22] R. Brüggemann and J. Voitländer, *Theor. Chim. Acta*, **61**, 387 (1928).

[23] F. Fratev, V. Enchev, O. E. Polansky and D. Bonchev, *J. Mol. Structure*, **88**, 105 (1982).

[24] B. Gimarc and N. Trinajstic, *Inorg. Chem.*, **21**, 21 (1982).
[25] L. J. Schaad and B. A. Hess, *Pure Appl. Chem.*, **54**, 1097 (1982).
[26] H. E. Zimmerman, *Tetrahedron*, **38**, 753 (1982).
[27] C. G. Bollini, J. J. Giambiagi, M. Giambiagi and M. S. Degiambiagi, *Theor. Chim. Acta*, **52**, 27 (1979).
[28] M. S. Degiambiagi and M. Giambiagi, *Letters Nuovo Cimento*, **25**, 458 (1979).
[29] J. A. N. F. Gomes, *Rev. Portugal.*, **21**, 82 (1979); *Croat. Chem. Acta*, **53**, 561 (1980); *Theor. Chim. Acta*, **59** 333 (1981).
[30] L. Vonszentpály, *Chem. Phys. Letters*, **67**, 63 (1979); **77**, 352 (1981).
[31] R. Constanciel, *Theor. Chim. Acta*, **54**, 123 (1980).
[32] M. S. Degiambiagi, M. Giambiagi and H. G. P. Linsdebarros, *Z. Naturforsch.*, **35a**, 1006 (1980).
[33] K. Takeuchi, Y. Yokomichi, Y. Kubota and K. Okamoto, *Tetrahedron*, **36**, 2939 (1980).
[34] K. Takeuchi, Y. Yokomichi and K. Okamoto, *Tetrahedron*, **36**, 2945 (1980).
[35] D. Bonchev, O. V. Mekenyan and O. E. Polansky, *Z. Naturforsch.*, **36a**, 647 (1981).
[36] W. T. Borden and E. R. Davidson, *Acc. Chem. Res.*, **14**, 69 (1981).
[37] R. Gleiter, *Angew. Chem. (Internat. Ed. Engl.)*, **20**, 444 (1981).
[38] A. Julg, in "Growth and Properties of Metal Clusters", J. Bourdon ed., Elsevier, Amsterdam, 1980, p. 255.
[39] S. J. Cyvin, *Tetrahedron Letters*, **22**, 2709 (1981).
[40] J. E. Lennard-Jones, *Proc. Roy. Soc.*, **A158**, 280 (1931).
[41] L. Pauling and J. Scherman, *J. Amer. Chem. Soc.*, **59**, 1450 (1937).
[42] R. S. Mulliken, G. A. Riecke and W. G. Brown, *J. Amer. Chem. Soc.*, **63**, 41 (1941).
[43] G. Wheland, *J. Amer. Chem. Soc.*, **64**, 900 (1942).
[44] R. S. Mulliken, *J. Chim. phys.*, **46**, 497, 535, 675 (1949).
[45] A. Laforgue, *J. Chim. phys.*, **46**, 568 (1949).
[46] C. Sandorfy, *Bull. Soc. chim. France*, **16**, 615 (1949).
[47] R. S. Mulliken, *J. Phys. Chem.*, **56**, 295 (1952).
[48] M. Wolfsberg and L. Helmholz, *J. Chem. phys.*, **20**, 837 (1952).
[49] C. Spanjaard and G. Berthie, *J. Chim. phys.*, **58**, 168 (1961).
[50] C. Vanhooydonk, *Z. Naturforsch.*, **28a**, 933 (1973).
[51] A. Streiwieser, Jr., "Molecular Orbital Theories for Organic Chemists", Wiley, New York, 1961, Chap. 4 and 5.
[52] B. Pullman and A. Pullman, "Quantum Biochemistry", Interscience, New York, 1963, Chap. 1 and 2.
[53] O. E. Polansky, *Monatsh.*, **94**, 43 (1963).
[54] W. P. Purcell and J. H. Singer, *J. Chem. and Eng. Data*, **12**, 285 (1967).
[55] G. Derflinger and H. Lischa, *Monatsh.*, **100**, 1003 (1969).
[56] Z. Simon, "Biochimie cuantică și interacțiuni specifice", Ed. științifică și enciclopedică, București, 1973, p. 41.
[57] S. Moldoveanu and A. Savin, "Aplicații în chimie a metodelor semiempirice de orbitali moleculari", Ed. Academiei, București, 1980, p. 154.
[58] H. H. Jaffe and M. Orchin, "Theory and Application of Ultraviolet Spectroscopy", Wiley, New York, 1964, p. 257.
[59] M. Orchin and H. H. Jaffe, "Symmetry, Orbitals and Spectra", Wiley, New York, 1971, chap. 4 and 8.
[60] H. Suzuki, "Electronic Absorption Spectra and Geometry of Organic Molecules", Academic Press, New York, 1967, Chap. 4, Appendix A1, A2, As and A4.
[60] W. F. Forbes and J. F. Templeton, *Canad. J. Chem.*, **36**, 180 (1958).
[62] W. F. Forbes, A. S. Ralph and R. Gosine, *Canad. J. Chem.*, **36**, 869 (1958).
[63] J. C. Dearden and W. F. Forbes, *Canad. J. Chem.*, **37**, 1294 (1959).
[64] M. Ito, *J. Mol. Spectroscopy*, **4**, 125 (1960).
[65] M. Ito, *J. Mol. Spectroscopy*, **4**. 106 (1960).
[66] W. Zanker and R. Reichel, *Z. Elektrochem.*, **63**, 1133 (1959).
[67] L. Baker and N. W. Holingworth, *J. Appl. Chem.*, **9**, 16 (1959).
[68] J. C. Dearden and W. F. Forbes, *Canad J. Chem.*, **38**, 896 (1960).
[69] P. G. Sennikov, V. A. Kuznetzov, A. E. Egorotcsikin, M. A. Lopatin and YA. I. Korenman *Zhur. obschei Khim.*, **50**, 276 (1980).
[70] L. Lang, "Absorption Spectra in the Ultraviolet and Visible Region", vol 15, 2nd edition, Publishing House of the Hungarian Academy of Sciences, Budapest, 1967, p. 17.
[71] K. Chandra and S. Banerjee, *J. Phys. Chem.*, **66**, 952 (1962).
[72] H. Baba and S. Suzuki, *J. Chem. Phys.*, **35**, 1118 (1961).

[73] G. Köhler, G. Kittel and N. Getoff, *J. Photochem.*, **18,** 19 (1982).

[74] H. KÄmmerer and W. Lewenz, *Spectrochim. Acta*, **24A,** 2059 (1968).

[75] W. F. Forbes, W. A. Mueller, A. S. Ralph and J. F. Templeton, *Canad. J. Chem.*, **35,** 1049 (1957).

[76] F. M. Beringer and I. Lillien, *J. Amer. Chem. Soc.*, **82,** 5135 (1960).

[77] J. G. Grassielli and W. M. Ritchey, "Atlas of Spectral Data and Physical Constants for Organic Compounds", 2nd edition, C.R.C. Press, Cleveland, 1975 ; *a)* Vol. 4, p. 74 (No. p. 720) ; *b)* Vol. 2, p. 286 (No. b 717) ; *c)* Vol. 2, p. 326 (No. b 1097) *d)* Vol. 2. p. 326 (No. b 1099) ; *e)* Vol. 2, p. 326 (No. b 1098).

[78] W. Zanker and R. Reichel, *Z. Elektrochem.*, **64,** 431 (1960).

[79] E. Sawicki, T. R. Hau e and T. W. Stanley, *Analyt. Chem.*, **31,** 2063 (1959).

[80] G. Nemethy and A. Ray, *J. Phys. Chem.*, **77,** 64 (1973).

[81] D. L. Gerrard and W. T. Maddams, *Spectrochim. Acta*, **34A,** 1205 (1978).

[82] W. W. Robertson and F. A. Matsen, *J. Amer. Chem. Soc.*, **91,** 5248 (1950).

[83] A. Martin and A. I. Kiss, *Acta Chim. Acad. Sci. Hung.*, **91,** 105 (1976).

[84] A. I. Kiss and J. Szöke, KFKI 72–58.

[85] H. Baba, *Bull. Chem. Soc. Japan*, **34,** 76 (1961), have used for comparison with ASMO-CI calculations the value 36700 cm^{-1} 272 nm, for the first band of phenol. This value was published by H. B. Klevens and J. R. Platt, "Technical Report Laboratory of Molecular Structure and Spectra. University of Chicago", Part one (1953–1954) p. 145, and American Petroleum Institute Research Project 44, Ultra violet Spectral Data, Serial No. 171.

[86] J. A. Singerman and H. H. Jaffé, *J. Amer. Chem. Soc.*, **103,** 1385 (1981), have used for comparison with VCNDO/S results the value 4.60 eV = 270 nm, for ^1L_b band of phenol. This value was published by K. Kimura and S. Nagakura, *Mol. Phys.*, **9,** 117 (1965).

[87] A. Streit wieser J., "Molecular Orbital Theory for Organic Chemists", Wiley, New York, 1961, Chap. 7 (and cited literature).

[88] R. Carbo and S. Fraga, *An. Fis.*, **65,** 365 (1969).

[89] M. H. Palmer, W. Moyes, M. Spiers and J. N. A. Ridyard, *J. Mol. Structure,* **48,** 105, 1978 ; **55,** 243 (1979).

[90] P. Eilefeld and W. Schmidt, *J. Electron Spectroscopy Relat. Phenom.*, **24,** 101 (1981).

[91] L. von Szent paly, *Chem. Phys. Letters.*, **67,** 63 (1979).

[92] R. J. Jerrard, A. T. Amos and P. A. Brook, *Theor. Chim Acta.*, **61,** 163 (1982).

[93] M. H. Palmer, W. Moyes, M. Spiers and J. N. A. Ridyard, *J. Mol. Structure*, **52,** 293 (1979).

[94] M. J. S. Dewar and D. E. David, *J. Amer. Chem. Soc.*, **102,** 7387 (1980).

[95] A. Streit wieser Jr., *J. Amer. Chim. Soc.*, **82,** 4123 (1960).

[96] T. A. Koopmans, *Physics*, 1, 104 (1933)

[97] J. D. Morrison and A. J. Nicholson, *J. Chem. Phys.*, **20,** 1021 (1952).

[98] F. H. Field and J. L. Franklin, *J. Chem. Phys.*, **22,** 1895 (1954).

[99] I. Omura, K. Higasi and H. Baba, *J. Chem. Phys.*, **24,** 623 (1956) ; *Bull. Chem. Soc. Japan,* **29,** 501 (1956).

[100] H. Baba, I. Omura and K. Higasi, *Bull. Chem. Soc. Japan*, **29**, 521 (1956)

[101] Z. Yoshida and T. Kobayashi, *J. Chem. Phys.*, **54,** 4538 (1971).

[102] I. Bergman, *Trans. Faraday Soc.*, **50,** 829 (1954).

[103] G. J. Hoijitink, *Rec. Trav. chim.*, **74,** 1525 (1955)

[104] M. E. Wacks and V. H. Dibeler, *J. Chem. Phys.*, **31,** 1557 (1959).

[105] G. F. Gabel and G. L. Kearns, *J. Phys. Chem.*, **66,** 436 (1962).

[106] J. A. Howe and J. H. Goldstein, *J. Chem. Phys.*, **26,** 7 (1957).

[107] N. Sato, K. Seki and H. Inokouchi, *J. Chem. Soc. Faraday II*, **77,** 1621 (1981)

[108] K. Watanabe, *J. Chem. Phys.*, **26,** 542 (1957).

[109] R. S. Beker and W. E. Wen worth, *J. Amer. Chem. Soc.*, **85,** 2210 (1963).

[110] D. W. Turner, "Advances in Physical Organic Chemistry", vol.4, V. Gold ed., Academic Press, New York, 1966 p. 31.

[111] A. D. Baker, D. P. May and D. W. Turner, *J. Chem. Soc B*, **1968,** 22.

[112] J. H D Eland, *Int. J. Mass Spectrom. Ion Phys.*, **2,** 471 (1962).

[113] J. W. Robinson, "Handbook of Spectroscopy", vol. 1, C. R. C. Press, Cleveland, 1974, p. 391.

[114] A. Terenin and F. Vilessov, "Advances in Photochemistry", vol. 2, Interscience, New York, 1964, p. 68.

[115] G. Herzberg, "Molecular Spectra and Molecular Structure", Vol. 3, D. Van Nostrand Comp., Princetown, 1966 p 207.

[116] R. G. Coombes, J. G. Golding and P. Hadjigeorgiou, *J. Chem. Soc. Perkin II*, **1979**, 1451,

[117] P. Capdeville and M. Maumy, *Tetrahedron Let ers*, **23**, 1573, 1577 (1982).

[118] J. P. Gesson, J. C. Jacquesy and M. P. Jounnetaud, *Nouveau J. chim.*, **6**, 477 (1982).

[119] D. S. Razimovskii, L. M. Konstantinova and E. G. Zaikov, *Izvest. Akad. Nauk SSSR Ser, Khim.*, **1981**, 1739.

[120] F. A. Matsen, *J. Amer. Chem. Soc.*, **72**, 5243 (1950).

[121] K. Morokuma, H. Kato and K. Fukui, *Bull. Chem. Soc. Japan*, **36**, 541 (1963).

[122] J. Szöke and A. I. Kiss *Acta Chim. Acad. Sci. Hung.*, **92**, 367 (1977)

[123] A I. Kiss and J Szöke, KFKI 72—59.

[124] T. Fuji, S. Suzuki and M. Fujisima, *Bull. Chem. Soc. Japan*, **50**, 847 (1977).

[125] L. V. Smirnov and A. I. Supurenko, *Optika i Spektroskopya*, **8**, 420 (1960).

[126] C. J. Padersen, *J. Amer. Chem. Soc.*, **79**, 5014 (1957).

[127] H. Kämmerer and W. Lewenz, *Spectrochim. Acta*, **24,A** 2059 (1968).

[128] L. Z. Rumsiski, "Prelucrarea matematică a datelor experimentale", Ed. tehnică, București 1974, p. 122, p. 137.

[129] C. D. Nenițescu, "Chimie organică", vol. 2, ed. 6-a, Ed. didactică și pedagogică", București, 1966, p. 484.

[130] Yu. R. Dzelme, Ya. Ya. Slezhis, Ya. A. Gravitis, Yu. K. Yakobson and P. P. Ernish, *Cellulose Chem. Technol.*, **13.** 175 (1979).

[131] M. K. Eberhardt, *J. Org. Chem.*, **37**, 3654 (1972).

[132] J. P. Seguin, P. Bauer, R. Uzan and J. P. Ducet, *Compt. rend.*, **287C**, 293 (1978).

[133] Ya. A. Gravitis, Ya. Ya. Slezhis, Yu. R. Dzele, Yu. K. Yakobson and P. P. Ernish, *Cellulose Chem. Technol.*, **13**, 185 (1979); *Khim. Dreves*, **3**, 65 (1979).

Revue Roumaine de Chimie, **30**, 7, 551–558 (1985)

CONSIDERATIONS ON THE ROLE OF THE CHARACTERISTIC DIMENSION IN THE APPLICATION OF THE VIBRATED ELECTRODE

C. RADOVAN and MARIA PORAICU
I. P. "Traian Vuia" Timişoara, Romania

Received October 22, 1984

From certain literature data neglecting electrode design, a faulty conclusion might be drawn namely that only the vibrational parameters (amplitude and frequency) have an influence upon the efficiency, irrelevant of the characteristic electrode dimension. A similar conclusion might lead to major difficulties when applied to the attempts to transpose small-scale informations on certain technologies when the characteristic dimension in the vibrational direction increases significantly.

The effect of electrode vibrations was first studied some 30 years ago by De Bretevile, Haris and Lindsey [1-3] while obtaining voltamogramms and polarogramms and was attributed to a perturbation of the diffusion layer. Because of the constructive shortcomings of the electrode, the pattern was not applied to polarography. An improved design, permitting to obtain reproducible voltamogramms was reported in 1980 by Moorhean and co-workers[4].

Increase of mass-transfer by electrode vibration in one of the adequate means for intensive process control. A similar aspect was checked in electrogravimetry and hydroelectrometallurgy as well as in other kinds of processes.

In the Romanian speciality literature use of electrode vibration was described in a series of papers [5-11] concerning the fields of electrogravimetry, hydroelectrometallurgy and kinetic studies. On this occasion some quantitative formula were established to characterize the dependence of the mass-transfer coefficient on conditions of vibration. Several authors [12-16] have studied the effect of hydrodynamic conditions and set up relations to express the changes occurring in the velocity of vibrated electrode process.

In previous papers [17-19] while studying simple redox processes Fe^{3+}/Fe^{2+}, Ce^{4+}/Ce^{3+}, $Fe(CN)_6^{3-}/Fe(CN)_6^{4-}$, we have shown some aspects of the dependence of the limit current and the mass-transfer coefficient on the vibration parameters.

A horizontal platinum electrode was used with Ø 0.4 mm, length 5 mm, vibrated perpendicular to the axis with 30–60 Hz and amplitude 0.005–0.2 cm, and 4–12 Hz with 0.05–1.5 cm, respectively.

By a graphical representation of the limit currents under various vibration conditions, determined from the galvanostatic polarization curves in oxidation and reduction (with the exception of the Ce^{4+}/Ce^{3+} system, for which, of known reasons, only reduction was investigated) relations similar to that in fig. 1 shown for the $K_4Fe(CN)_6 - K_3Fe(CN)_6$ system (reduction), were obtained for all systems.

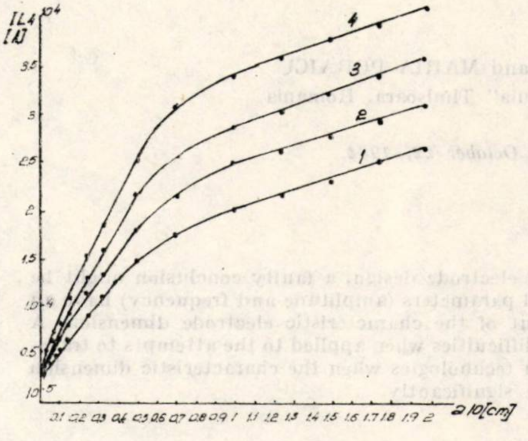

Fig. 1. — Limiting current as a function of amplitude for 5×10^{-3}M $Fe(CN)_6^{3-}$/$Fe(CN)_6^{4-}$ in 1M KCl (reduction at 25°C) 1—30 Hz; 2—40 Hz; 3—50 Hz; 4—60 Hz.

From similar dependences, equations can be written that correlate the limit current with the vibrational amplitude and frequency in linear ranges. Simultaneous dependences of the average limit current (I_L) and the average mass-transfer coefficient (k_L) upon Reynold's vibrational number ($Re = 4afd/\nu$) were established (where d = electrode diameter, a = amplitude, f = frequency, and ν = cinematic viscosity, $\nu = \mu/\rho$ of the solution, μ = dynamic viscosity, ρ = density). By means of these formula complex dependence "spectra" I_L and k_L *v.* Re were traced in the frequency and amplitude interval studied. For constant amplitude or frequency and the associated parameters, and variabile frequency or amplitude, respectively, formulas taking the shape of those established by Radoi [10, 11] were obtained:

$$k_L = m' + n'\mathrm{Re}$$

$$(I_L = m + n\mathrm{Re})$$

Those relations corresponded to a couple of linear variation zones with different slopes for the range of amplitudes and frequencies used, while deviations of the coefficients m' and n', m, n depend on the range of the working variable and the intervals $Re < 20 \simeq 30$ and $Re > 50$. Amplitude variation and frequency variation may give different vibrational effects.

For $Re < 20 \simeq 30$, at frequencies of 30—60 Hz and amplitudes of 0.005—0.05 cm, and/or 4—12 Hz with 0.05—0.15 cm, by correlating the Sherwood number ($Sh = k_L d/D$) and Schmidt number ($Sc = \nu/D$), the expressions were obtained for the Nernst limit layer thickness, at the vibrated electrode, depending on vibrational parameters, where a and f occur with the same exponent, 0.51 and 0.70, respectively.

The expressions for k_L take the shape:

$$k_L = \frac{0.99 D^{0.66} a^{0.51} f^{0.51}}{\nu^{0.18} L^{0.49}} \tag{1}$$

and

$$k_L = \frac{1.11\, D^{0.66} a^{0.70} f^{0.70}}{\nu^{0.36} L^{0.30}} \tag{2}$$

respectively, or

$$k_L = \frac{0.99 D^{2/3} a^{0.51} f^{0.51}}{\nu^{0.18} L^{0.49}} \tag{1'}$$

and

$$k_L = \frac{1.11\, D^{2/3} a^{0.70} f^{0.70}}{\nu^{0.36} L^{0.30}} \tag{2'}$$

respectively, where L is the characteristic dimension (equal to the wire diameter) in the direction of vibration.

For $\mathrm{Re} > 50$, when with an identic Re number, the variation of the vibrational parameter associated, gives different results for the mass-transfer coefficient (greater increase with frequency rise), it was shown that a mechanism could be applied that takes into account the combined effect of the oscillating velocity and concentrations field. [15] According to this mecanism, the mass-transfer coefficient is given by the expression:

$$k_L = \frac{0.808\, D^{2/3} a^{1/3} (2\pi f)^{1/2}}{\nu^{1/6} L^{1/3}} \tag{3}$$

From certain literature data, [5] neglecting electrode design, a faulty conclusion might be drawn to the effect that a 2 mm amplitude, with a vibrational frequency of 50 Hz, would give an increased efficiency irrelevant of the characteristic electrode dimension. Such a conclusion might encounter major difficulties when applied to the attempts to transpose small-scale informations on certain technologies (e.g. production of metal powders, oxidation-reduction processes, formation of oxide electrodes by electrodeposition) to large scale conditions, i.e. when the characteristic dimension in the vibrational direction increases significantly. In cases like that empirical transposal of small-scale data, neglecting adequate electrode design, can yield smaller or even much smaller vibrational efficiencies than those expected as will be shown later (average mass-transfer coefficients and current efficiencies increasing less in oxidation-reduction and powder depositions, smaller current density ranges when obtaining unstrained deposits with oxide electrode deposition).

Those considerations can be rendered evident by a brief analysis of the formula of mass-transfer coefficient, illustrated for Re > 50. For this purpose, the characteristic length of the vertical, large-scale plate electrode, vibrated parallel to the sides, L_M, is taken as the sum of n characteristic lengths of the small-scale electrode, L_m, i.e. $L_M = nL_m$.

Suppose that the vibration takes place in the conditions for which the small-scale electrode satisfies the condition Re $> 50 \sim 60$, e.g., at a frequency of 50 Hz and amplitude 1 and or 2 mm; let L_M take values of 1; 2; 4; 10 and 1000 mm with $a = 1$ mm and/ or 3; 4; 8; 10; 100; and 1000 mm with $a = 2$ mm. Taking the reference condition $L_m = L = 1$ (or 2), i.e. $a/L_M = 1$, and considering the formula of k_L for constant frequency, the vibrational range considered:

$$k_L = \text{const}\ (a/L)^{1/3} \tag{4}$$

and k_L^M, respectively, at large-scale, and k_L^m, at small-scale, show the following relations for an identical amplitude:

$$\frac{k_L^M}{k_L^m} = \frac{L_m^{1/3}}{L_M} \tag{5}$$

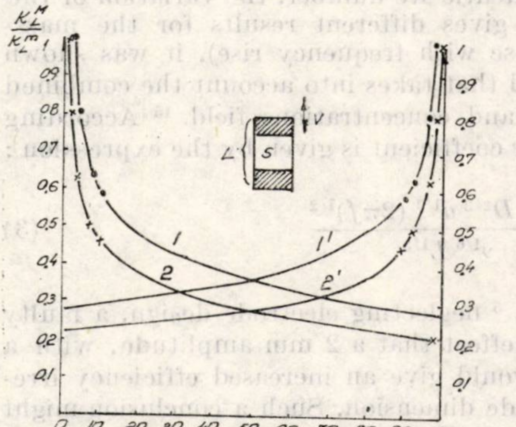

Fig. 2. — Computed dependences k_L^M/k_L^m (reference a/L = 1) vs. L 1 — $a = 1$; 2 — $a = 2$mm

In figs 2 and 3 the computed formulas of the k_L^M/K_L^m ratio vs. L and/ or log. L are given, while the curves 1 apply to amplitude 1 mm, curves 2 and 3 to amplitude 2 mm (reference: $a/L = 1$).

As is evident in both cases the ratio shows a more pronounced decrease in the first part of the interval. Even in the most favourable situation, with $a = 2$ mm, and an increase of the characteristic dimension from 2 to 1000 mm, the k_L^M/k_L^m ratio shows an a about 8-fold decrease, corresponding to a significant diminution of the vibrational effect in the range of this length, as compared to the reference "side" of the electrode. The actual situation is less disadvantageous when both ends of the vertical plate electrode are immersed into electrolyte, in which case

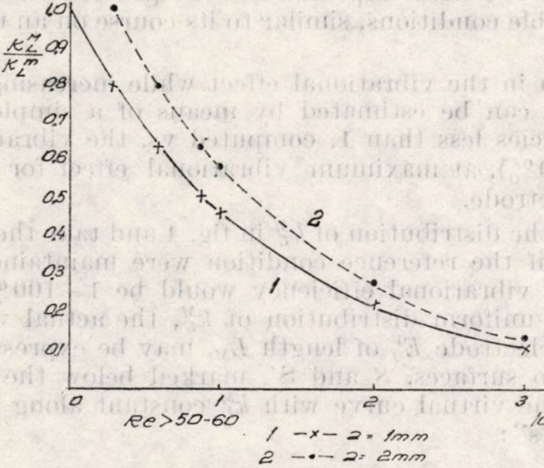

Fig. 3. — Computed dependences k_L^M/k_L^m (reference $a/L = 1$) vs. log L 1 — a = 1mm ; 2 — a =2mm.

a couple of side effects can be manifest, i.e. maximum vibrational effects at the upper and the lower side. For a similar, less unfavourable situation, the ratio k_L^M/k_L^m takes the shape shown in fig. 4.

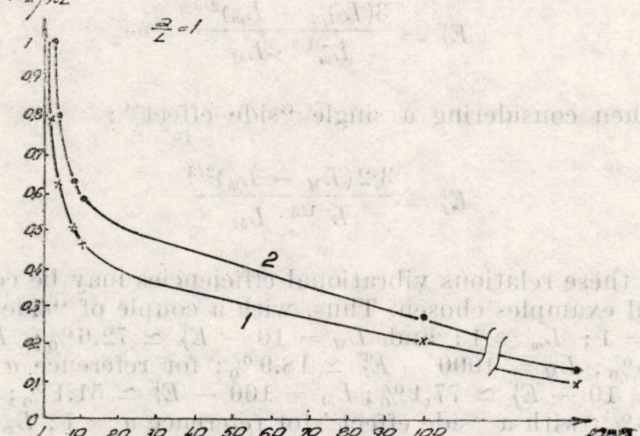

Fig. 4. — Computed dependences k_L^M/k_L^m (reference $a/L = 1$) vs. L when considering a couple of side effects. 1 — a= 1 mm ; 2 — a = 2 mm

As seen from the figure, in this case too there will be a medium range where the vibrational effects is much diminished relative to the expected effect. Hence it follows that for a great current density, taken as an optimal density from small-scale conditions, medium ranges will exist when passing to large-scale conditions, where the vibrational effect will be much less than the effect expected and the process will take place under very unfavourable conditions, similar to its course on an unvibrated electrode.

The change seen in the vibrational effect while increasing the characteristic dimension, can be estimated by means of a simple relation, as vibrational efficiencies less than 1, computed vs. the vibrational efficiency taken as 1 (100%), at maximum vibrational effect for the small-scale use of the electrode.

Let us consider the distribution of k_L^M in fig. 4 and take the reference situation $k_L^M/k_L^m = 1$ (if the reference condition were maintained on the whole length L_m) the vibrational efficiency would be 1–100%). Taking into account the non-uniform distribution of k_L^M, the actual vibrational efficiency on the big electrode E_f^V of length L_M, may be expressed as the ratio between the two surfaces, S and S′, marked below the variation curve of k_L^M and/or the virtual curve with k_L^M constant along L_M. For a couple of "side effects":

$$E_f^V = \frac{S'}{S} = \frac{2\,\text{const.}\,a^{1/3}\displaystyle\int_{L_M}^{L_{M/2}} L^{-1/3}\,dL}{\text{const.}\,a^{1/3}\cdot L^{-1/3}\cdot L_M} \tag{7}$$

Respectively :

$$E_f^V = \frac{3(L_{M/2} - L_m)^{2/3}}{L_m^{-1/3}\cdot L_M} \tag{8}$$

Similarly, when considering a single "side effect" :

$$E_f^V = \frac{3/2(L_M - L_m)^{2/3}}{L^{-1/3}\cdot L_M} \tag{9}$$

By means of these relations vibrational efficiencies may be computed for the numerical examples chosen. Thus, with a couple of "side effects" for reference $a = 1$; $L_m = 1$; and $L_M = 10 - E_f^V \simeq 72.6\%$; $L_M = 100 - - E_f^V \simeq 40.8\%$; $L_M = 1000 - E_f^V \simeq 18.9\%$; for reference $a = 2$; $L_m = 2$; and $L_M = 10 - E_f^V \simeq 77.1\%$; $L_M = 100 - E_f^V \simeq 51.1\%$; $L_M = 1000 - - E_f^V - 23.8\%$; with a "side effect" for reference $a = 1$; $L_m = 1$; $L_M = = 10 - E_f^V - 37.6\%$; $L_M = 100 - E_f^V \simeq 32.1\%$; $L_M = 1000 - E_f^V \simeq 15\%$; for reference $a = 2$; $L_m = 2$ and $L_M = 10 - E_f^V$; $\simeq 75.5\%$; $L_M = 100 - E_f^V \simeq 40.7\%$; $L_M = 1000 - E_f^V \simeq 18.9\%$.

Those deviations from $E_f^V = 1$ (100%), assimilated for widths $l_m = l_M$ increase when the electrode width increases with the ratio l_M/l_m.

From the above considerations it is clear that there is a possible error when recovering the expected effect of vibrational influence on the enhancement of mass-transfer, in passing from small to large-scale conditions, and/ or empirically extrapolating certain laboratory data to vertically vibrated, vertical plate electrodes. A similar diminution of the effect expected was seen by the authors in the attempt to obtain glossy copper foils in the presence of some additives.

The results under small-scale conditions were satisfactory, while with empirical extrapolation of the data to large-scale conditions, side effects developed and the centre zone of the deposits was inadequate. From the same reasons, when producing metal powders (e. g. copper), a diminution of the current efficiencies occurs with increasing characteristic dimension on the vibrational direction. In the case of thin lead dioxide depositions on graphite, on electrodes with small characteristic dimension, thin, glossy deposits were obtained on a large range of current densities, 5—12 A/dm^2. With increasing characteristic dimensions the range significantly narrows, when the danger of straining due to differentiated deposition in the vibrational direction occurs, with a possible late cracking of the deposits. The expected vibrational effects might be also seen in metal refining processes, e. g. copper refining, [6] when nodules or roughnesses on the cathode surface cause local turbulences.

In other situations, e. g. in oxidation or reduction processes, in order to recover the same effect and/ or the same mass-transfer coefficient, a constant a/L ratio should be theoretically observed, thus for instance, when passing from $L = 1$ to $L = 1000$ mm, an absurd situation would result, i.e. an enormous amplitude. The side effect and some irregularities of the electrodes somehow attenuate deviations from the effect expected by an oversimplified prevision.

The actual situation will formally be more beneficial than with simple agitation and might actually be more favourable provided that a smaller value is applied rather than the great optimum current density established with small-scale electrodes. A great characteristic length, with a 1—2 mm amplitude, could shift the control of the large-scale process to disadvantageous conditions or conditions where an unprofitable energy consumption (or associated with an unsignificant effect) for electrode vibration is not warranted.

Design solutions, e.g. with the use of sieve electrodes, grids with wires vibrated normally to the axis, raised surfaces, turbulences promotors associated with the electrode [20] may ensure much improved conditions for the use of large-scale, vibrated electrodes, while maintaining the small-scale effects.

Moreover, taking into account the difficulties connected with the movement of the fluid owing to an increase in amplitude, effects similar to those under small-scale conditions may be obtained when ensuring remedies of the kind reported, consistent with significant process enhancements, preferentially by frequency increase, since with $\mathrm{Re} > 50$, an increase of frequency induced a much greater increase of the mass-transfer coefficient than an amplitude increase.

REFERENCES

[1] A. De Bretevile, E. D. Harris and A. J. Lindsey, *Nature*, **162**, 413 (1948).

[2] E. D. Harris and A. J. Lindsey, *Analyst*, **76**, 647 (1951).

[3] A. J. Lindsey, *J. Phys. Chem.*, **56**, 439 (1952).

[4] E. D. Moorhead, M. M. Stephens and G. A. Bhat, *Anal. Letters*, **13** (A$_3$), 167 (1980).

[5] Gh. Facsko, *Rev. Roumaine Chim.*, **21**, 191 (1966).

[6] Gh. Facsko and I. Radoi, Patent RSR 51266 (1968).

[7] Gh. Facsko, M. Poraicu, *Bul. St. și Tehn. al I.P.T.* Seria Chimie, 18/32/206, 2 (1973).

[8] Gh. Facsko and M. Poraicu, *ibid.*, 2/36/306 (1977).

[9] I. Rădoi, *ibid.* 15/29/86 (1970).

[10] I. Rădoi, *Rev. Roumaine Chim.*, **16**, 3 (1971).

[11] I. Rădoi, *Rev. Roumaine Chim.*, **17**, 1367 (1972).

[12] J. J. Podesta, G. F. Paus and A. J. Arvia, *Electrochim. Acta*, **19**, 583 (1974).

[13] A. M. Al. Taweel, M. I. Ismail and M. Z. El. Abd, *Chem. Ing. Tech.*, **46**, 861 (1974).

[14] H. Gibert and H. Angelino, *Canad. J. Chem. Eng.*, **51**, 319 (1973).

[15] M. I. Ismail, A. M. Al. Taweel and M. Z. El. Abd, *J. Appl. Electrochem.*, **4**, 347 (1974).

[16] A. M. Al. Taweel and M. I. Ismail, *J. Appl. Electrochem.*, **6**, 559 (1977).

[17] M. Poraicu, C. Radovan and Gh. Facsko, *Bul. St. și Tehn. al I. P. Traian Vuia* Timișoara, Seria Chimie, **24** (38), 2 (1979).

[18] C. Radovan, M. Poraicu and Gh. Facsko, The National Congress of the Chemistry, Bucharest 10—14 September (1978).

[19] C. Radovan, M. Poraicu and Gh. Facsko, The National Congress of the Chemistry, Bucharest 10—14 September (1978).

[20] D. Hutin, A. Stock and F. Coeuret, *Inform. Chimie*, **187**, 227 (1979).

Revue Roumaine de Chimie, **30**, 7, 559–564 (1985)

CHARGE-TRANSFER COMPLEXES OF SOME SUBSTITUTED THIAZOLES

IOANA SARAMET[a] and M. BANCIU[b]

[a] Organic Chemistry Department, Faculty of Pharmacy, Traian Vuia Street 6, Bucharest, Romania

[b] Organic Chemistry Department, The Polytechnic, TCH, Spl. Independenţei 313, Bucharest, Romania

Received January 30, 1985

The formation of coloured charge-transfer complexes between substituted thiazoles **1** and tetracyanoethene was proved and investigated by electronic spectrophotometry. The stability constants (K) and ε_{max} values of the complexes were determined from the modified Benesi — Hildebrand equation and discussed.

INTRODUCTION

The charge-transfer complexes between aromatic compounds as electron donors, and various acceptors were extensively investigated becoming even topics of monographs. [1-4] Among the numerous electron acceptors, tetracyanoethene (TCNF) was repeteadly used. [1-11] Two major recent developments of the area should be mentioned. The first one is the new and extremely interesting area of the so-called *organic metals*, compounds in which the intermolecular charge transfer determinates the essential physical properties (e.g. electrical conductivity). [12-18] The second important modern field is the study of *intra*molecular charge transfer interactions which appear between benzenoid rings as donors and various acceptor moieties from the same molecule or ion pair e.g. tetracyano-quinodimethane, [19] tropylium cations, [20] pyrylium cations, [21] pyridinium cations [21] etc.

In spite of these recent developments, the complexation of heteroaromatic compounds as donors with various electron acceptors (e.g. iodine, TCNE, chloranil, dichlorodicyanobenzoquinone etc.) was investigated only sporadically. [22-29] However it has been shown that whereas pyridines are predominantly n-donors, [28, 29] five-membered heteroaromatics e.g. thiophenes [22-27] behave usually as π-donors.

In the present note we describe the formation of 'charge-transfer complexes between substituted thiazoles and tetracynoethene (TCNE).

RESULTS AND DISCUSSION

The thiazoles used in the present work possess the general formula **1**. The synthesis of **1a** from 4-(4′-bromophenylsulphonyl) thiobenzoamide with phenacyl bromide, of **1b** from the same thioamide with monochloroacetone as well as the similar preparation of **1c** — **1e** were reported by one of us previously [30] and will be detailed in a forthcoming paper.

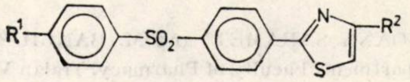

1

a, $R^1 = Br-$; $R^2 = C_6H_5-$

b, $R^1 = Br-$; $R^2 = CH_3-$

c, $R^1 = Br-$; $R^2 = p\text{-}Br\text{-}C_6H_4-$

d, $R^1 = Cl-$; $R^2 = C_6H_5-$

e, $R^1 = Cl-$; $R^2 = p\text{-}Br\text{-}C_6H_4-$

The electronic spectra of thiazoles **1a-e** were also reported previously[30]; neither of them present absorptions over 400 nm.

Treatment of thiazole **1a** with TCNE in dichloromethane solution at room temperature was accompanied by the development of a deep blue colour due to the appearance of a single new absorption band in the electronic spectrum at $\lambda_{max} = 545.5$ nm. Similar treatment of thiazole **1b** conducts to the appearance of a new band in the visible domain having $\lambda_{max} = 500$ nm which confers a yellow-orange colour to the solution. The above mentioned bands, due neither to the electron donor (thiazole) nor acceptor (TCNE) separately, must by attributed to charge-transfer complexes.

The stability constants, K, and ε_{max} values for these charge-transfer complexes were determined using the Benesi-Hildebrand equation [31] as modified by Scott [32] (in order to permit the extrapolation through regions of increasing dilution to the intercept and the determination of initial slope at high dilutions):

$$\frac{C_A \cdot C_B \cdot l}{E} = \frac{1}{K \cdot \varepsilon} + \frac{1}{\varepsilon} \cdot C_A$$

where C_A, C_B are the molarities of reactants, with $C_A > C_B$; E, the absorbance of the complex and l (cm) the cell length.

Good linear correlations were obtained for complexes for both **1a** and **1b**.

From the graphical representation of $\frac{C_A \cdot C_B \cdot l}{E}$ as a function of C_A, the values from table 1 were deduced.

According to the good linearity of the Scott relationship the 1 : 1 stoichiometry of the complexes formed in equilibrium with the reactants is assumed:

$$\mathbf{1a} + \text{TCNE} \xrightleftharpoons{K=5.23} \mathbf{1a}\text{—TCNE}$$

$$\mathbf{1b} + \text{TCNE} \xrightleftharpoons{K=24.86} \mathbf{1b}\text{—TCNE}$$

Table 1

Stability constants (K) and ε_{max} values for charge-transfer complexes between thiazoles **1** and TCNE

Thiazole	Slope	Intercept	K [L.mole^{-1}]	ε_{max} [L.mole^{-1}cm^{-1}]
1a R^1 = Br- $R^2 = C_6H_5$	0.00837	1.6×10^{-3}	5.23	119.4
1b R^1 = Br- $R^2 = CH_3$	0.0920	3.7×10^{-3}	24.88	10.8

The ionisation potential values (I_p) for thiazoles **1a** and **1b** could be estimated from the energies (frequencies) of the charge-transfer bands using the empirical equation :[2]

$$I_p\,[\text{eV}] = a + b \cdot \tilde{\nu}_{CT}\,[\text{cm}^{-1}]$$

explicited for TCNE acceptor (using substituted benzene and polynuclear hydrocarbons as donors) in the form :[25]

$$I_p\,[\text{eV}] = 5.21 + 1.65 \times 10^{-4} \times \tilde{\nu}_{CT}\,[\text{cm}^{-1}]$$

The calculated I_p values are : 8.23 eV for **1a** and 8.51 eV for **1b**, being thus approximately of the same magnitude as those determined[25] e.g. for 2,5-dimethyltiophene (8.21 eV), dibenzothiophene (8.19 eV), or for 2-methylthiophene (8.53 eV). In order to elucidate the nature of the orbitals involved in the charge-transfer interactions, a comparison of calculated I_p values with experimental ones (from mass spectrometry or PE spectra) would be welcome. Such determinations are in progress.

The K value (5.23 L · mole^{-1}) determined for **1a**—TCNE is of the same order of magnitude with those of TCNE complexes of monosubstituted benzenes (e.g. toluene has $K = 3.70$[5]) or diphenyl ($K = 4.09$[5]) being somewhat smaller than the K-value for *p*-xylene ($K = 7.64$[5]). The above data permit the assessment that the complexation of **1a** with TCNE is of $\pi \rightarrow \pi$ type and involves one of the benzenic rings available in the molecule. Most probably the complexation occurs at the monosubstituted benzenoid ring, which is the least hindered one (designated with R^2 in formula **1**).

The lower ε_{max} value found for **1a**—TCNE ($\varepsilon_{max} = 119.4$) in comparison with toluene—TCNE ($\varepsilon_{max} = 3330$[5]) could be ascribed to the greater steric hindrance to complexation exhibited by the arylthiazolyl substituent in **1a** in comparison with CH_3-group in toluene. Indeed, the importance of steric effects in determination of K and ε_{max} — values for charge-transfer interaction was underlined in different cases.[25, 33] Recently, for tri-*o*-tolylborane—TCNE complex, $K = 4.7$ and $\varepsilon_{max} = 135$ values were determined, [33] being thus very near to those obtained for **1a**—TCNE.

On the other hand, we have obtained coloured charge-transfer complexes of thiazoles **1c** — **1e** with TCNE. The λ_{max} values for these complexes : 560 for **1c**, 555 for **1d** and 543 nm for **1e** lie very close to that of **1a** but differ considerably from the **1b**-TCNE absorption. It seems that thiazoles **1a**, **1c**, **1d** and **1e** (but not **1b**) afford the same type of complexes with TCNE.

The bathochromic shift observed on passing from **1a**—TCNE ($\lambda_{max} = 545.5$ nm) to **1c**—TCNE ($\lambda_{max} = 560$ nm) could be ascribed to the bromine + E effect. The bathochromic shift which accompanies the change from **1a**—TCNE ($\lambda_{max} = 545.5$ nm) to **1d**—TCNE complex ($\lambda_{max} = 555$ nm) follows the same trend observed if one compares the absorption spectra of uncomplexed bromobenzene ($\lambda_{max} = 261$ nm) and chlorobenzene ($\lambda_{max} = 265$ nm).

The very different $K = 24.88$ and $\varepsilon_{max} = 10.8$ values obtained for **1b**—TCNE in comparison with **1a**—TCNE suggest another type of complexation. Complexation at one of the two *p*-disubstituted benzenoid rings is ruled out because it is known that *p*-xylene—TCNE complex has $K = 7.64$ and $\varepsilon = 2650$.[5] Formation of the charge-transfer complex may be ascribed in this case only to the thiazole heterocyclic ring. This ring possesses an electron-repelling CH_3 group which increases the donor abilities of the complexing nucleus, conducting to the large observed K value. It cannot be stated at the present stage whether the complex of **1b** with TCNE is of the $\pi \rightarrow \pi$ or $n \rightarrow \pi$ type. Further investigations in this sense (including a larger variety of substituted derivatives) are under way.

EXPERIMENTAL

The electronic spectra were recorded on a SPECORD UV-VIS (C. Zeiss-Jena) spectrophotometer using silica cells with $l = 0.5$ cm.

Reagents. The thiazoles **1a**, m.p. 233°C and **1b**, m.p. 176°C were prepared and purified as previously described. [30] The electronic absorption spectra of **1a** and **1b** indicate no absorption above 400 nm. Tetracyanoethene (TCNE) was recrystallized twice from chlorobenzene ; m. p. 198.5 — 200°C. Dichloromethane was refluxed over P_2O_5 and distilled.

Charge-transfer complexes. Solutions of thiazoles **1** in dichloromethane were prepared according to data from Table 2. The solutions indicate no absorption above 400 nm. The TCNE in CH_2Cl_2 presents a sharp cutoff at 300 nm. Addition of TCNE in determined excess (Table 2) into the dichloromethane solutions of thiazoles **1** at 20°C produces the appearance of a characteristic colour : deep blue for **1a** and yellow-orange for **1b**. The electronic absorption spectra of solutions from Table 2 were registered. Application of Scott's equation [32] conducted to linear correlations $\frac{C_A \cdot C_B \cdot l}{E}$ *vs* $\cdot C_A$ from which K and ε_{max} values were deduced (Table 1).

Treatment of thiazoles **1c**, **1d** and **1e** with excess TCNE in dichloromethane solutions was accompanied by the appearance of single new absorptions in the visible domain having the following λ_{max} values : 560 for **1c** ; 555 for **1d** and 543 nm for **1e**.

Table 2

Charge-transfer complexes of thiazoles **1**
with TCNE ($t = 20°C$; $l = 0.5$ cm ; volume of samples = 2.5 mL)

A. Thiazole **1a** (R^1 = Br- ; R^2 = C_6H_5-) λ_{max} = 545.5 nm

1a		TCNE		$E_{corr.}$	$\frac{C_A \cdot C_B \cdot l}{E}$
mg	mol/L	mg	mol/L		
22.81	0.0199	6.4	0.020	0.11	0.00180
22.80	0.0199	12.8	0.040	0.21	0.001895
22.80	0.0199	19.2	0.060	0.30	0.00199
22.80	0.0199	25.6	0.080	0.34	0.00234

B. Thiazole **1b** (R^1 = Br- ; R^2 = CH_3- λ_{max} = 500 nm

1b		TCNE		$E_{corr.}$	$\frac{C_A \cdot C_B \cdot l}{E}$
mg	mol/L	mg	mol/L		
9.85	0.01	6.4	0.02	0.02	0.005
19.7	0.02	12.8	0.04	0.05	0.008
29.55	0.03	19.2	0.06	0.09	0.010
39.40	0.04	25.6	0.08	0.16	0.010

REFERENCES

[1] G. Briegleb, "Electronen Donator-Acceptor Komplexe" Springer, Berlin, 1961.

[2] R. Foster, "Organic Charge Transfer Complexes", Academic Press, London, 1969.

[3] R. S. Mulliken and W. B. Person, "Molecular Complexes", Wiley, New York, 1969.

[4] L. J. Andrews and R. M. Keefer, "Molecular Complexes in Organic Chemistry", Holden Day, San Francisco, 1964.

[5] R. E. Merrifield and W. D. Philips, *J. Amer. Chem. Soc.*, **80**, 2779 (1958).

[6] E. M. Voigt, *J. Amer. Chem. Soc.*, **86**, 3611 (1964).

[7] A. Zweig, *J. Phys. Chem.*, **67**, 506 (1963).

[8] T. T. Harding and S. C. Wallwork, *Acta Cryst*, **8**, 785 (1955)

[9] M. J. S, Dewar and C. C. Thomson Jr., *Tetrahedron Suppl.*, **7**, 97 (1966)

[10] G. Leroy, *Ann Soc. Sci. Bruxelles* **89**, 115 (1975).

[11] L. A. Singer and D. J. Cram, *J. Amer. Chem. Soc.*, **85**, 1080 (1963).

[12] H. J. Keller (editor), "Chemistry and Physics of One Dimensional Metals", Plenum Press, New York, 1977.

[13] L. Alcácer (editor), "The Physics and Chemistry of Low-Dimensional Solids", Reidel, Dordrecht, Holland 1980.

[14] R. C. Wheland, *J. Amer. Chem. Soc.*, **98**, 3926 (1976).

[15] R. C. Wheland and J. L. Gilson, *J. Amer. Chem. Soc.*, **98**, 3916 (1976)

[16] J. H. Perlstein, *Angew. Chem. Int. Ed. Engl.*, **16**, 519 (1977)

[17] J. B., Torrance, *Acc. Chem. Res.*, **12**, 79 (1979).

[18] V. T. Ciorba, S. Bădilescu, A. Meghea, I. Schiketanz and A. T. Balaban, *Rev. Roumaine Chim.*, **29**, 817 (1984).

[19] K. Iwamura, T. Nakazawa and I. Murata, *Angew. Chem. Int. Ed. Engl.*, **19**, 543 (1980) ; S. Inagaki, K. Yamamura, K. Nakasuji, T. Nakazawa and I. Murata, *J. Amer. Chem. Soc.*, **103**, 2093 (1981) ; I Murata, *Pure Appl. Chem.* **55.** 323 1983) ; K. Nakasuji H. Yamochi, I. Murata, K. Yamamura and S. Inagaki, *J. Org. Chem.*, **48**, 2384 (1983).

[20] T. Nakazawa and I. Murata, *J. Amer. Chem. Soc.*, **99**, 1996 (1977) ; T. Nakazawa N. Abe K. Kubo and I. Murata, *Tetrahedron Letters* **1979**, 4995 ; A. Tajiri, M. Hatano, T. Nakazawa and I. Murata, *Chem. Phys. Lett.*, **76**, 490 (1980).

[21] M. Banciu, A. T. Balaban, C. Drăghici and R. Vlad, *Rev. Roumaine Chim*, **27**, 1037 (1982).

[22] R. P. Lang *J. Amer. Chem. Soc.*, **84**, 4438 (1962).

[23] R. Zahradnić and C. Parkanyi, *Coll. Czechoslov. Chem. Commun* , **30**, 195 (1965).

[24] Z. Yoshida and T. Kobayashi, *Tetrahedron*, **26**, 267 (1970).

[25] G. G. Aloisi and S. Pignataro, *J. Chem. Soc. Faraday I*, **1973**. 534.

[26] A. R. Cooper, C. W. P. Crowne and P. G. Farell, *Trans Faraday Soc.*, **62**, 18 (1966).

[27] T. K. Mukherjee, *J. Phys. Chem.*, **73**, 3442 (1969).

[28] G. G. Aloisi, G. Cauzzo and U. Mazzucato, *Trans. Faraday Soc* , **63**, 1858 (1967).

[29] G. G. Aloisi, G. Beggiato and U. Mazzucato, *Trans. Faraday Soc.*, **66**, 3075 (1970).

[30] I. Şaramet, Thesis, The Polytechnic, Bucharest, 1981 ; N. Bărbulescu, I. Saramet and F. G. Cocu — The II. National Congress of Chemistry, Bucharest 7—10 sept. 1981, Abstract — B. 2.7.

[31] H. A. Benesi and J. H. Hildebrand, *J. Amer. Chem. Soc.*, **71**, 2703(1949) ; L E. Orgel and R. S. Mulliken, *J. Amer. Chem. Soc.*, **79**, 4839 (1957) ; W. B Person, *ibid.*, **87**, 167 (1965).

[32] R. L. Scott, *Req. Trav. Chim.*, **75**, 787 (1956).

[33] J. E. Frey and E. C. Kitchen, *J. Amer. Soc.*, **105**, 2175 (1983).

Revue Roumaine de Chimie, **30**, 7, 565–569 (1985)

INDICES DE RETENTION ET STRUCTURE MOLÉCULAIRE DES ISO-DECANES

C. CHELGHOUM*, Y. HADDAD, K. ABDEDDAIM et M. H. GUERMOUCHE

Institut de Chimie, Université des Sciences et de la Technologie Houari Boumédienne, B.P. nº 9, Dar el Beida, Alger, Algérie

Reçu le 12 janvier 1985

Les indices de rétention de quatre nonanes méthylés, isomères du décane normal, en solution dans le squalane, sont déterminés à différentes températures. Les variations de ces grandeurs, très souvent utilisées dans les problèmes d'identification, sont examinées d'une part en fonction de la température et de l'autre en fonction de la structure moléculaire du soluté.

INTRODUCTION

La connaissance des indices de rétention (I_R) aide non seulement à la résolution des problèmes structuraux en chimie organique, mais aussi à celle des problèmes d'identification dans l'analyse, si dans ce second cas, on ne dispose pas d'un couplage G.C.M.S.

Schroder [1] a récemment publié un remarquable travail de synthèse regroupant sous forme de catalogue l'ensemble des indices de rétention des systèmes hydrocarbures-squalane.

Toutefois, il faut signaler que l'ensemble des données (relatives aux paraffines) se limite aux alcanes légers compris entre les butanes et les nonanes. Par ailleurs, le domaine de température envisagé n'excède pas 50°C.

On se propose dans le présent travail de déterminer les indices de rétention de quelques iso-décanes en fonction de la température. On examinera, en outre, les variations de ces grandeurs en fonction de la structure moléculaire et de quelques propriétés fondamentales du soluté.

CONDITIONS EXÉRIMENTALES

Chromatographe type Perkin Elmer F11 équipé d'un catharomètre, colonne 10 m de long, 4 mm de diamètre intérieur remplie d'une phase stationnaire constituée de 10 % en squalane déposé sur du Chromosorb P.A.W.D.M.C.S. 60 — 80 mesh. Le gaz vecteur utilisé est l'hélium U avec un débit constant égal à 40 ml/min.

Tous les produits utilisés au cours de ce travail proviennent de chez Merck (R.F.A.) et portent la mention „for G.C.".

Tableau 1

Indices expérimentaux et paramètres physico-chimiques des iso-décanes.

Composé	100°C	110°C	120°C	130°C	140°C	150°C	T_{eb} (°C) ref. 3	Code ref. 4	M ref. 5	$\varkappa$ ref. 6	k 100°C	α 25°C	v 25°C
A. Me-5 Nonane	966	965	960	960	964	964	165,1	3610	2	4,807	3,755	9,822	195,2
B. Me-4 Nonane	972	965	960	964	970	970	165,7	3610	2	4,807	3,312	9,813	195,3
C. Me-3 Nonane	979	974	972	972	980	976	167,8	3610	2	4,807	3,305	9,827	195,0
D. Me-2 Nonane	976	966	964	964	972	972	167,03	3610	1	4,770	3,368	9,768	196,9
E. n-Décane	1000	1000	1000	1000	1000	1000	174,154	2800	2	4,914	—	9,814	195,9

RÉSULTATS ET DISCUSSION

Les indices de rétention de Kovats [2] ont été déterminés par la méthode classique entre 100 et 150^{0}C.

Le tableau 1 contient, outre les valeurs expérimentales, les caractéristiques des iso-décanes. Plusieurs remarques peuvent être dégagées :

1^{0} — L'indice de rétention est très peu sensible aux variations de température, en accord avec les auteurs [7,8,9] ;

2^{0} — Pour une température donnée, l'indice de rétention diminue en général à mesure que la ramification se déplace vers le centre de la chaîne carbonée du soluté. Ce même comportement est observé lorsqu'on considère le groupe isocodal 3610 avec $M = 2$ et avec $x = 0{,}807$;

3^{0} — Pour ce même groupe 3610, une diminution de l'indice de rétention est observée lorsque M augmente et lorsque X diminue.

Afin d'apprécier l'importance de l'effet de la structure moléculaire sur le comportement de l'indice de rétention, examinons les variations des facteurs homomorphique (H) et structural ($\delta I_{\mathrm{CH_2}}$).

1° — Relation entre H et I_R

Le facteur H, défini par Schomburg [10] s'exprime par la relation

$$H = I_R\,(\mathrm{HCR}) - I_R\,(\mathrm{HCn})$$

où HCR représente une paraffine ramifiée isomère de la paraffine normale HCn.

Le facteur H diminue (Tableau 2) lorsque la volatilité du soluté s'accroît c'est-à-dire lorsque la ramification se déplace vers le centre de la molécule.

Tableau 2

Valeurs des facteurs $\delta I_{\mathrm{CH_2}}$ et $-$H à différentes températures

Composé	100°C		110°C		120°C		130°C		140°C		150°C	
	$\delta I_{\mathrm{CH_2}}$	$-H$	$\delta I_{\mathrm{CH_2}}$	$-H$	$\delta I_{\mathrm{CH_2}}$	$-H$	$\delta I_{\mathrm{CH_2}}$	$-H$	$\delta I_{\mathrm{CH_2}}$	$-H$	$\delta I_{\mathrm{CH_2}}$	$-H$
1. Me-5 Nonane	66	34	65	35	60	40	60	40	64	36	64	36
B. Me-4 Nonane	72	28	65	35	60	40	64	36	70	30	70	30
C. Me-3 Nonane	79	28	74	26	72	28	72	28	80	20	80	24
D. Me-2 Nonane	76	24	66	34	64	40	64	40	72	28	72	28

2° — Relation entre δI_{CH_2} et I_R

Par définition la contribution d'un CH à l'indice de rétention devrait être égale à 100 s'il n'y avait influence des groupements sur la chaîne paraffinique principale.

En fait cette contribution n'est pas constante (Tableau 2), et dépend de la position de la ramification. On constate que pour toute température, la quantité δI_{CH_2} reste inférieure à 100. On note en outre une similitude dans l'évolution des facteurs δI_{CH_2} et $-H$ en fonction de la structure moléculaire du soluté.

Dans le cas des systèmes hydrocarbures — squalane, molécules apolaires, les interactions sont essentiellement dues aux forces de dispersion de London. L'importance de celles-ci dépend évidemment des propriétés physico-chimiques des molécules à séparer.

Examinons ainsi l'effet des paramètres suivants : température d'ébullition, polarisabilité électronique et volume moléculaire sur le comportement de l'indice de rétention I_R.

1° — Relation entre I_R et température d'ébullition T_{eb}

Différentes relations entre les indices de rétention I_R et les températures d'ébullition T_{eb} des solutés de même nature chimique ont été signalées. [11] La figure 1 montre que la courbe $I_R = f\ (T_{eb})$ est linéaire.

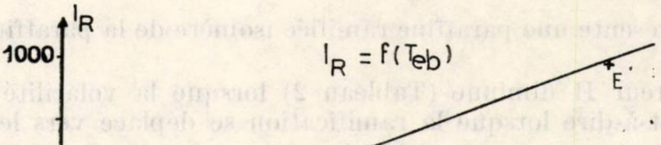

Fig. 1. — Corrélation entre l'indice de rétention I_R à 100°C et la température d'ébullition pour les cinq composés du Tableau 1.

Pour une température égale à 100°C, cette courbe satisfait la corrélation du type $I_R = a\ .\ T_{eb} + b$. Les valeurs des coefficients a, b et R (coefficient de corrélation) sont les suivantes :

$$a = 3{,}537 \quad b = 384{,}498 \quad R = 0{,}994$$

La seconde règle de Kovats

$$\delta I_R \# 5 . \delta T_{eb}$$

n'est pas satisfaite, comme le montrent les résultats expérimentaux (Tableau 1). En effet, le coefficient de proportionnalité k reste inférieur à 5 en accord avec les auteurs [10,12] mais augmente à mesure que la ramification devient interne.

2° — Relation entre polarisabilité électronique, volume moléculaire et I_R

L'examen du tableau 1 montre que le plus élevé indice de rétention I_R est obtenu pour le soluté de petites dimensions v (volume moléculaire) et de haute polarisabilité électronique α.

On constate par ailleurs, que de très faibles variations dans les valeurs de la polarisabilité électronique et du volume moléculaire provoquent d'appréciables différences dans les valeurs de l'indice de rétention I_R.

BIBLIOGRAPHIE

[1] H. Schroder, *High Resol. Chromat. and Column Chromat.*, **3**, 38 (1980).
[2] E. Kovats, *Helv. Chim. Acta*, **41**, 1915(1958).
[3] A. P. I., Data Book édition 1976.
[4] J. M. Takacs et col., *J. Chromatogr.*, **271**, 213 (1983)
[5] A. C. W. Kemenade et H. Groenendijk, *Chromatographia*, **2**, 316 (1969).
[6] R. Kalizan et H. Lamparczyk, *J. Chromatogr. Sci.*, **16**, 246 (1978).
[7] D. A. Tourres, *J. Chromatogr.*, **30**, 357 (1967).
[8] G. Castello, M. Berg and M. Lunardelli, *J. Chromatogr.*, **79**, 23 (1973).
[9] S. Rappoport et T. Gaumann *Helv. Chim. Acta* **56**, 1145 (1973).
[10] G. Schomburg, *J. Chromatogr.*, **23**, 1 1966)
[11] A. Werhli et E. Kovats, *Helv. Chim. Acta*, **42**, 2709 (1959)
[12] V. M. Nabivach et H. V. Kirilenko, *Chromatographia*, **2**, 93 (1980).

Revue Roumaine de Chimie, **30**, 7, 571–574 (1985)

KINETIC STUDY OF THE ALKALINE DECOMPOSITION OF 3-BROMOPROPYLTRIPHENYLPHOSPHONIUM BROMIDE IN DMSO-H_2O MIXTURES

FAYEZ Y. KHALIL,* M. T. HANNA, F. M. ABDEL-HALIM
and M. EL-BATOUTI
Department of Chemistry, Faculty of Science, Alexandria University, Alexandria, Egypt

Received July 20, 1983

This work reports a kinetic study of the alkaline decomposition of 3-bromopropyl-triphenylphosphonium bromide in DMSO-H_2O mixtures. The reaction proceeds according to a third-order rate law, first-order in phosphonium cation and second-order in hydroxyl anion. The presence of an electron withdrawing substituent (3-bromopropyl) attached to the phosphorus in a phosphonium salt accelerates the reaction, and the rate is approximately 80 times faster than for the corresponding tetraphenylphosphonium bromide. The calculated thermodynamic activation parameters of the reaction are discussed.

INTRODUCTION

It is well known[1] that the rate of nucleophilic substitutions on organo phosphorus compounds is strongly dependent on the groups linked to the phosphorus atom. Thus, when alkoxy or dialkylamine groups are substituted for alkyl groups, a great decrease in the rate of nucleophilic substitution is observed.[2–4] Only little work has been done on the substituent effects on the kinetics of the alkaline hydrolysis of quaternary phosphonium salts,[5] which proceeds through a pentacovalent transition state to yield phosphine oxide and hydrocarbon.[6–8] With the aim of elucidating the role of substituent effects on phosphorus upon reaction rates and activation parameters, a comparative study has been made on the kinetics of the alkaline decomposition of tetraphenylphosphonium bromide[9] and 3-bromopropyl-triphenylphosphonium bromide in water and water-DMSO mixtures. The chief differences between the two phosphonium ions are that 3-bromopropyl-containing phosphonium cations easily form phosphoranes in alkaline solution whereas this is not the case with tetraphenylphosphonium ions.

EXPERIMENTAL

Materials and Procedure

3-Bromopropyl-triphenylphosphonium bromide (Fluka, Analytical Grade) was of sufficient purity and used without further purification. Dimethylsulphoxide (BDH) was purified using standard method.[10]

The kinetic procedure used to determine the reaction rate was described earlier.[11]

---

[*] On leave of absence from Alexandria University. Present address: Department of Chemistry, Faculty of Science, University of Maiduguri, P.M.B. 1069 Maiduguri, Nigeria.

RESULTS AND DISCUSSION

Table 1 includes the third-order rate constants measured in the temperature range 30—45°C and in solvent compositions varying from 0 to 50% (v/v) DMSO-H_2O. The observed isocomposition activation energies are listed in the same table. The thermodynamic parameters of activation $\Delta G^{\ddagger}$, $\Delta H^{\ddagger}$ and $\Delta S^{\ddagger}$, calculated according to the standard expressions,[12] are depicted in Table 2.

Table 1

Third-order rate constants k' and activation energies E_c for the alkaline decomposition of 3-bromopropyl-triphenylphosphonium bromide in DMSO-H_2O mixtures at different temperatures

DMSO content			k' (l^2 mol^{-2} min^{-1})				E_c, KJ mol^{-1}
Vol %	wt %	mol %	30°C	35°C	40°C	45°C	
0	0.0	0.0	0.17	0.33	0.63	1.20	106
10	10.8	2.7	0.48	0.91	1.58	3.00	96
20	21.3	5.9	1.91	3.47	6.17	10.90	93
30	31.6	9.6	7.24	12.59	21.87	36.30	88
40	41.5	14.0	36.31	63.09	107.15	177.80	84
50	50.9	19.3	25.19	436.52	707.95	1174.90	77

Figure 1 illustrates a plot of the rate constants of the alkaline decomposition of 3-bromopropyl-triphenylphosphonium bromide against the mol% of DMSO in DMSO-water mixtures. The figure also includes the corresponding plot for tetraphenylphosphonium bromide in DMSO-water mixtures taken from the results of independent measurements.[9] It is evident that in solutions containing the same mol% of DMSO, the rate of the alkaline decomposition of 3-bromopropyl-triphenylphosphonium bromide is always much higher than that of tetraphenylphosphonium bromide. By comparing the activation energies for the alkaline decomposition of the two compounds studied (Fig. 2) it is found that

Table 2

Thermodynamic activation parameters at 40°C

DMSO content		$\Delta G^{\ddagger}$ (kJ mol^{-1})	$\Delta H^{\ddagger}$ (kJ mol^{-1})	$\Delta S^{\ddagger}$ (J mol^{-1} deg^{-1})
vol %	mol %			
0	0.0	88.3	103.4	48.1
10	2.7	85.9	93.8	25.1
20	5.9	82.4	89.9	23.9
30	9.6	79.1	85.5	20.3
40	14.0	74.9	81.1	19.5
50	19.3	70.1	71.9	5.7

there is a drop of approximately 19 kJ mol^{-1} in water from tetraphenyl to 3-bromopropyl triphenylphosphonium compounds, in agreement with the easier formation of the negatively charged 3-bromopropyl ion as compared with the phenyl ion.[13–15] The presence of electron withdrawing substituents attached to the phosphorus in a phosphonium salt would be expected to accelerate the hydrolysis reaction[16] which involves a nucleophilic attack of the hydroxyl ion on the phosphorus atom carrying a small positive charge. The increasing negative inductive effect i.e. electron withdrawing effect, when passing from phenyl to 3-bromopropyl tends to decrease the electronic density of the phosphorus atom and

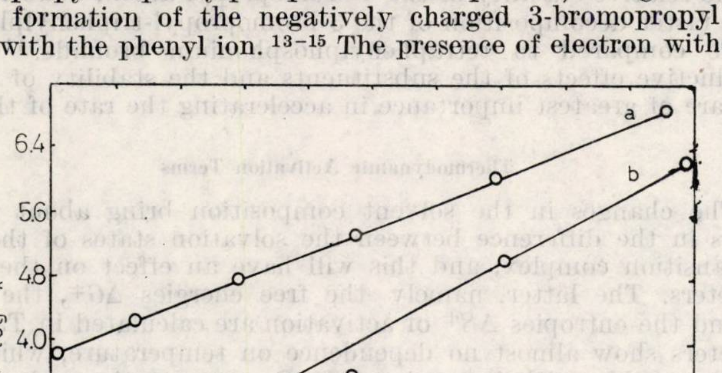

Fig. 1. — Comparative plots of the rate constant, log k', against the mol per cent of DMSO.

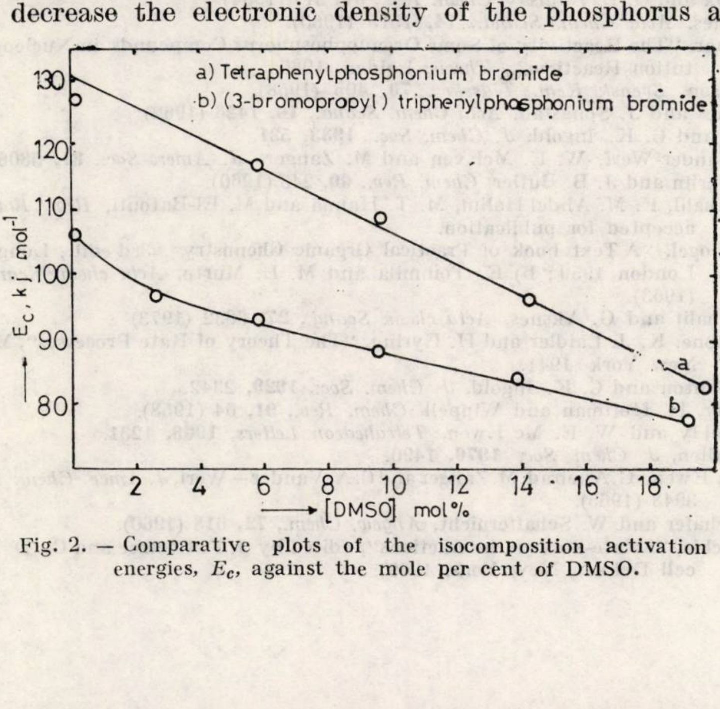

Fig. 2. — Comparative plots of the isocomposition activation energies, E_c, against the mole per cent of DMSO.

hence to increase the attraction of the hydroxyl ion. This factor, together with the relative stability of the 3-bromopropyl anion, doubtless account for the faster decomposition of the 3-bromopropyl-triphenylphosphonium bromide compared to tetraphenylphosphonium bromide.[17] Therefore, the inductive effects of the substituents and the stability of the leaving group are of greatest importance in accelerating the rate of the reaction.

Thermodynamic Activation Terms

The changes in the solvent composition bring about consequent changes in the difference between the solvation states of the reactants and transition complex, and this will have an effect on the activation parameters. The latter, namely the free energies $\Delta G^{\ddagger}$, the enthalpies $\Delta H^{\ddagger}$ and the entropies $\Delta S^{\ddagger}$ of activation are calculated in Table 2. The parameters show almost no dependence on temperature, while $\Delta G^{\ddagger}$ decreases smoothly with increasing DMSO concentration, where the phenomenon of dissolution of the hydroxide anion is encountered.[18,19] The changes in $\Delta G^{\ddagger}$ are reflected in a considerable decrease in the enthalpy $\Delta H^{\ddagger}$. In spite of some compensation by the entropy, appearing in the drop of $\Delta S^{\ddagger}$ with increasing DMSO content, it is the decrease in the enthalpy of activation that constitutes the major factor controlling the reaction.

The activation entropy decreases by 25.8 J × mol^{-1} deg^{-1} in water when a phenyl group ($\Delta S^{\ddagger}$: 73.9)[9] is replaced by a 3-bromopropyl group ($\Delta S^{\ddagger} = 48.1$). This reduction in $\Delta S^{\ddagger}$ is generally believed to be due to a stronger solvation of the transition state.

REFERENCES

[1] J. R. Cox and O. B. Ramsay, *Chem. Rev.*, **64**, 317 (1964)

[2] G. Aksnes, *Acta Chem. Scand.*, **14**, 1515 (1960).

[3] L. Ginjaar, "The Reactivity of Some Organophosphorus Compounds in Nucleophilic Substitution Reactions', *Thesis*, Leiden, 1960.

[4] L. Larsson, *Svensk Kem. Tidsskr*, **70**, 405 (1958).

[5] G. Aksnes and J. Songstad, *Acta Chem. Scand.*, **16**, 1426 (1962)

[6] L. Hey and C. K. Ingold, *J. Chem. Soc.*, **1933**, 531.

[7] C. A. Vander-Werf, W. E. McEven and M. Zanger, *J. Amer. Soc.*, **81**, 3806 (1959).

[8] K D. Berlin and J. B. Butler *Chem. Rev.*, **60**, 243 (1960).

[9] F. Y. Khalil, F. M. Abdel Halim, M. T. Hanna and M. El-Batouti, *Rev. Roumaine Chim.* accepted for publication.

[10] a)A. I. Vogel, "A Text book of Practical Organic Chemistry", 3rd edit., Longmans Green, London 1959 ; b) E. Tommila and M. L. Murto, *Acta chem. Scand.*, **17**, 1947 (1963).

[11] F. Y. Khalil and G. Aksnes, *Acta chem. Scand*, **27**, 3832 (1973)

[12] S. Glasstone, K. J. Laidler and H. Eyring, "The Theory of Rate Processes", Mc Graw-Hill, New York 1941.

[13] G. W. Fenton and C. K. Ingold, *J. Chem. Soc.*, **1929**, 2342.

[14] L. Horner, H. Hoffman and Wippell, *Chem. Rev.*, **91**, 64 (1958).

[15] G. J. Reily and W. E. Mc Ewen, *Tetrahedron Letters*, **1968**, 1231.

[16] D. W. Allen, *J Chem Soc.* **1970**, 1490.

[17] W.E. Mc Ewen, G. Axelrad, M. Zanger and C. A. Vander—Werf, *J. Amer Chem. Soc*, **87**, 3948 (1965).

[18] H. L. Schäfer and W. Schaffernicht, *Angew. Chem.*, **72**, 618 (1960).

[19] C. D. Richie, "Solute-Solvent Interactions", edited by J. F. Coetzee and C. D Richie (Marcell Dekker, New York, 1969).

Revue Roumaine de Chimie, **30**, 7, 575–579 (1985)

HARDENING PROCESSES IN $3(CaO \cdot Al_2O_3) \cdot CaSO_4$ — WATER SYSTEM

ION TEOREANU and MARCELA MUNTEAN

Chair of Silicate Technology and Oxidic Compounds, Polytechnic Institute, Bucharest, Polizu 1–7, Romania

Received December 3, 1984

In the present paper the hardening processes in $3(CaO \cdot Al_2O_3) \cdot CaSO_4$—water system were examined. Information concerning the influence of the binder/ water ratio as well as of the size of the binder particle upon the hydration rate of the $3(CaO \cdot Al_2O_3) \cdot CaSO_4$ is presented. This information is correlated with the nature of the resulted hydrocompounds and the physical-mechanical properties of the normal mortars of calcium aluminate sulphate. To investigate the hydration process and the resulting compounds as well as the mechanical properties of the calcium aluminate sulphate mortars, IR spectral analysis, chemical analysis, electron microscopy and physical-mechanical tests were used.

INTRODUCTION

The study of hydration and framework formation processes in binder of the $C_4A_3\overline{S}$* — water type are relevant for expansive sulphate aluminate masses. [1–3] The information concerning the hydration processes, the factors affecting the hydration rate and consequently, expansion, could explain variations in the mechanical properties of expansive masses which are otherwise similar to their chemical and mineralogical composition.

EXPERIMENTAL

The influence of water/ binder ratio and of $C_4A_3\overline{S}$ particle size after grinding on the hydration process and on the formation of hydrocompounds, and on the hardening structures has been investigated on samples taken after the following durations, measured from the moment of mixing with water : 20 minutes, 1 and 3 hours, 1, 3, 7, and 28 days.

Calcium sulphate-aluminate was prepared by maintaining for 4 hours at 1300°C, an appropriate mixture of chemically pure $CaCO_3$, Al_2O_3 and $CaSO_4 \cdot 2H_2O$. The mixture corresponding to $C_4A_3\overline{S}$ had been finely ground (≤ 63 μm), pelletized at 800 daN/cm^2 in cubes with an edge of 1.41 cm, then fired.

In order to investigate the hydration processes and the resulting compounds, the following techniques have been used ; spectral analysis (X-ray diffraction and IR spectroscopy), electronic microscopy, measurement of the amount of bound water and physical-mechanical measurements.

---

* The following notations are used : $C = CaO$, $A = Al_2O_3$, $\overline{S} = SO_3$.

RESULTS AND DISCUSSION

The amount of the chemically bound water was measured on common pastes with water/ binder ratios 0.5 and 0.62 (the latter corresponds to the potentially total transformation of C_4A_3S in ettringite) and on suspensions water/ binder ratio = 10.

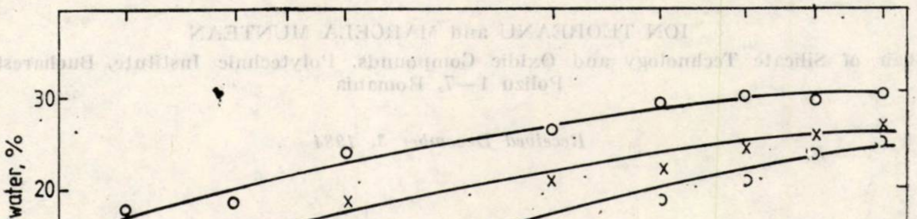

Fig. 1. — Chemically bound water versus time for various water/ binder ratios (Blaine surface area of hydrated $C_4A_3\overline{S}$ 3.770 cm^2/g).

The results are displayed in Fig. 1. Obviously, the greater the amount of water in the system, the higher the rate of the hydration process, mainly in the early stage. After more than 14 days of hydration, the values of bound water are closer to each other, mainly in pastes, where water/ binder ratio is 0.5 and 0.62 respectively.

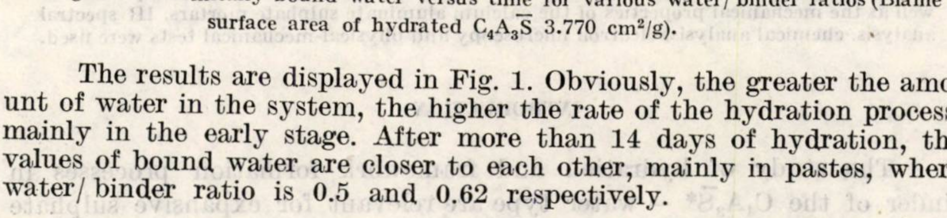

Fig. 2. — Relative intensity for ettringite (9.7 Å) and hydrated calcium monosulphate aluminate (8.9 Å) versus time.

A semiquantitative treatment of X-ray analysis data (Fig. 2) shows that the amount of ettringite, probably formed in solution, is higher in suspension than in the water/ binder = 0.5 paste (see electron micrographs

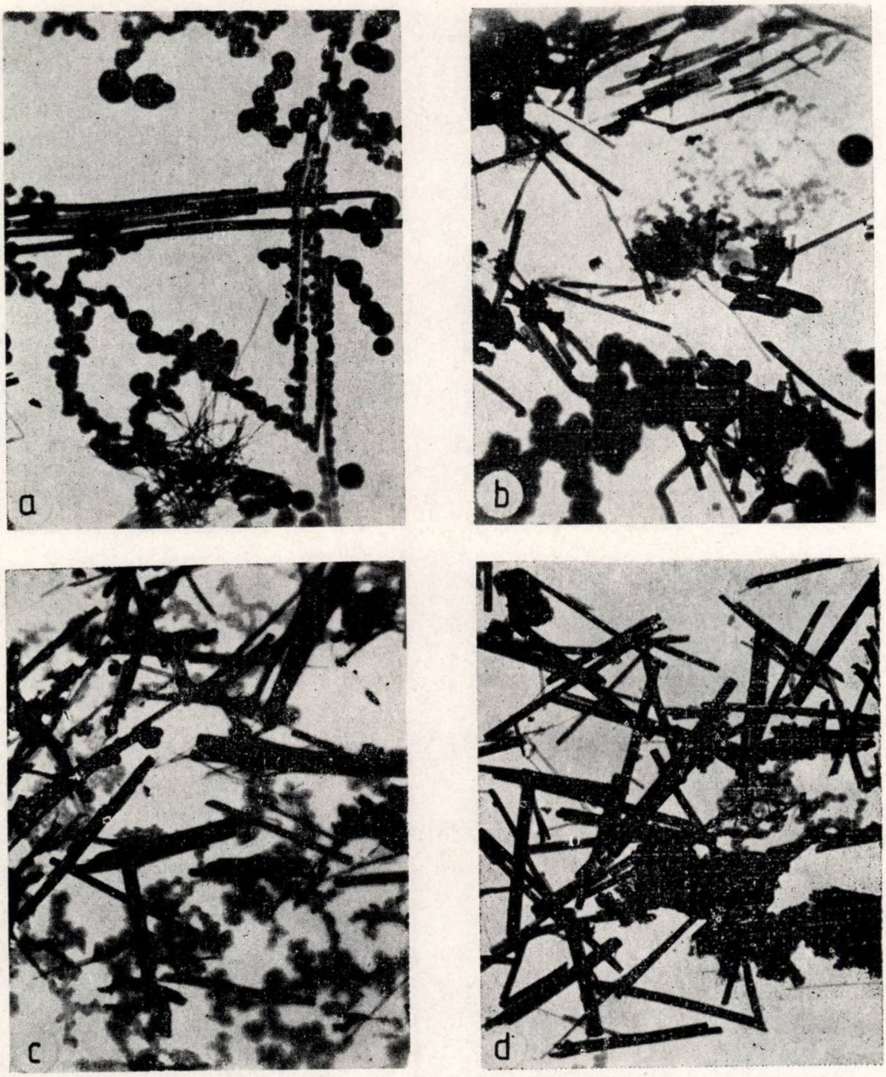

Fig. 3. — Electronmicrographies of hydrated C_4A_3S : in suspension (w/b = 10) for 20 minutes (a) ; one hour (b) ; 24 hours (c) ; 7 days (d) and in pastes (w/b = 0.5) at same times, (a′), (b′), (c′), (d′).

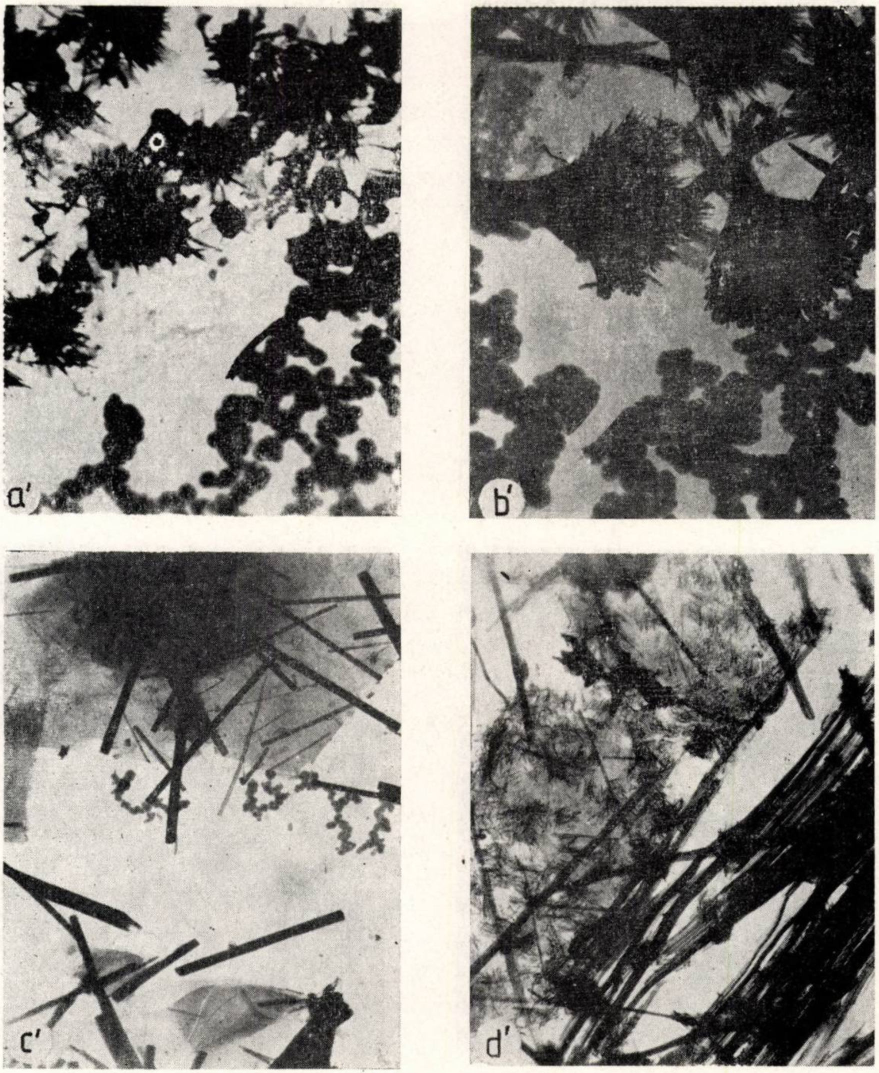

Fig. 3

in Fig. 3, too). In both samples, after longer hydration durations (28 days), an equilibrium of the two hydrated sulphated phases, namely $C_3A.3C\overline{S}.32H_2O$ and $C_3A.C\overline{S}.12H_2O$ is realised.[4,5]

Infrared spectroscopy also proves a higher intensity of the initial hydration in the $C_4A_3\overline{S}$ suspension (water/binder = 10) as compared

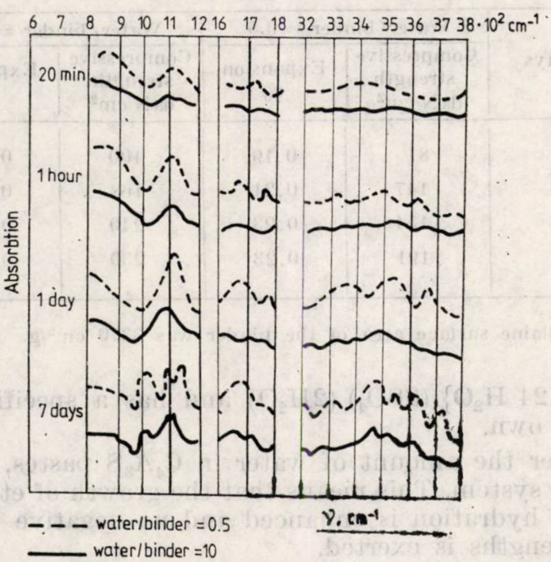

Fig. 4. — Infrared spectra of the hydrated samples of $C_4A_3\overline{S}$ with different water/binder ratios, for the early stages of hydration.

to the paste (water/binder = 0.5) — see Fig. 4. Spectra of the two samples in early stages of hydration (20 minutes, one hour, one day) are quite different, while after 7 days of hydration they tend to become similar to each other. In the IR spectra the evidence of chemically bound water is seen in bounds of different intensities (from HO^- included in H-bonds corresponding to the 3680 cm^{-1} band to a strongly bound HO^-, corresponding to the 3380 cm^{-1} band).

The fact that the amount of water affects the kinetics of the hydration process and its influence on the phase composition of the system might explain the variations noted in some mechanical properties (expansion, mechanical strength). The results obtained working on Kühl microsamples prepared from normal mortars (binder/monogranular sand 0.2—0.4 mm = 1/3) show a better behaviour if water/binder ratio is 0.62 (see Table 1). These results can be explained by taking into consideration the structure of the two hydrated compounds. The hydromonosulphate-aluminate has usually a needle-like structure. This structure is unlikely to be the reason of the expansion, but it could be a potential expansive agent under certain conditions of temperature, provided $CaSO_4$ and $Ca(OH)_2$ are present.

Ettringite has a spatial structure whose framework is composed by adjacent columns whose composition is $\{Ca_3[Al(OH)_6] \cdot 12H_2O\}^{3+}$; between them are channels which contain SO_4^{2-} ions and water molecules. The structural fundamental unit could be described by the formula:

Table 1

Physical-mechanical properties of normal mortars from C_4A_3S*

Days	Water/ binder = 0.5		Water/ binder = 0.62	
	Compressive strength daN/cm²	Expansion %	Compressive strength daN/cm²	Expansion %
1	81	0.19	100	0.29
3	147	0.21	168	0.35
7	154	0.23	240	0.35
28	191	0.23	230	0.34

* Blaine surface area of the binder was 3370 cm²/g.

$\{Ca_6[Al(OH)_6] \cdot 24\ H_2O\}\ (3SO_4)\ (2H_2O)$ and has a specific morphological features of its own.

The higher the amount of water in $C_4A_3\overline{S}$ pastes, the greater the mobility in the system. This means that the growth of ettringite over the early stages of hydration is enhanced and no negative influence on the mechanical strengths is exerted.

The influence of particle size ground $C_4A_3\overline{S}$ on the mechanical strength and expansion of mortars, working on Kühl microsamples has also been investigated. The results are given in Table 2.

Table 2

Physical-mechanical properties of normal mortars from C_4A_3S with different Blaine surface area

Period of hardening days	Blaine surface area, cm²/g					
	2700		3200		3770	
	Compressive strength daN/cm²	Expansion %	Compressive strength daN/cm²	Expansion %	Compressive strength daN/cm²	Expansion %
1	102	0.13	95	—	81	0.19
3	130	0.18	141	0.22	147	0.21
7	133	0.21	146	0.21	154	0.23
28	196	0.215	203	0.22	191	0.23

Obs: water/ binder = 0.5 and the ratio binder/ aggregate = 1/3.

The decrease in particle size after grinding implies an increase in the rate of the reaction with water and consequently, of the expansion of masses. This happens because in an early stage of the interaction with water, important amounts of ettringite are formed. When a small amount of water is present in the system, its consistency is high from the moment of the preparation and therefore the mobility in the system is limited. A too fast ettringite formation rate means a lower initial mechanical strength as compared with the samples in which $C_4A_3\overline{S}$ is ground to a somewhat greater particle size (see the values of compressive strength after one day).

CONCLUSIONS

On the basis of the above described results the following conclusions can be drawn :

— the water/ binder ratio is essential for the determination of the rate of the hydration process of $C_4A_3\overline{S}$, mainly in its early stages; in later stages (over 7 days) the differences in the hydration rates of $C_4A_3\overline{S}$ in the investigated systems become of lesser importance. In the latter case, the amount of chemical bound water is situated between 25—30%, no matter the initial water / binder ratio;

— the nature of hydrocompounds formed in the system in the hydration process is not affected by the water/ binder ratio (in the range 0.5—10), but the initial amount of ettringite is higher in samples with an excess of water. After a longer hardening period (over 28 days) an equilibrium between the two calcium hydrosulphatealuminates ($C_3A \cdot 3CaSO_4 \cdot 32H_2O$ and $C_3A \cdot CaSO_4 \cdot 12H_2O$) is achieved;

— the mechanical properties (expansion and compressive strength) are determined by the initial water/ binder ratio and consequently, by the nature and relative amounts of the hydrocompounds formed in the system and their formation kinetics. The particle size of the binder exerts its own influence which is a function of the mobility in the system and its water/ binder ratio.

REFERENCES

[1] P. K. Mehta and N. Polivka, "Expansive Cements", Paper presented at The VIth International Congress of the Chemistry of Cement, Moscow, 1974.

[2] G. L. Kalousek, "Hydration processes at the early stages of cement hardening", Paper presented at The VIth International Congress of the Chemistry of Cement, Moscow,

[3] M. A. Collepardi, M. Marcialis and R. Turriziani, *Il Cemento*, **69**, 179 1972 .

[4] I. Teoreanu and M. Muntean, *Cement and Concrete Research*, **13**, 711 (1983).

[5] I. Odler and S. Abdul-Maula, *Cement and Concrete Research*, **14**, 133 1984).

Revue Roumaine de Chimie, **30**, 7, 581–583 (1985)

POLAROGRAPHIC STUDIES ON THE COMPLEXES OF EUROPIUM (III) WITH 2,3-DIHYDROXYPYRIDINE AND 2-AMINO-3-HYDROXYPYRIDINE

R. S. SINDHU * and R. P. SINGH **

* Chemistry Department, M. S. College, Saharanpur, 247001

** Chemistry Department, Delhi University, Delhi, 110007

Received April 10, 1984

Interaction of Eu (III) with 2,3-dihydroxypyridine and 2-amino-3-hydroxypyridine has been studied polarographically at $\mu = 0.1$ M ($NaClO_4$) and temperature $20 \pm 0.1°$. With both the ligands 1 : 1 (M : L) composition is found and stability constants with 2,3-dihydroxypyridine and 2-amino-hydroxypyridine are 18.2×10^7 and 9.1×10^7 respectively.

INTRODUCTION

2,3-Dihydroxypyridine (DHP), 2-amino-3-hydroxypyridine (AHP) have been found as potential reagents for the spectrophotometric and complexometric detection and determination of various metal ions. [1] Stability constants of the complexes of some bivalent metal ions with DHP and AHP[2] and rare earths with DHP[2] have been determined potentiometrically. The present paper deals with the polarographic studies of Eu (III) complexes with DHP and AHP at $\mu = 0.1$ M ($NaClO_4$) and temperature $20 \pm 0.1°$.

EXPERIMENTAL

Details of the polarograph and technique have been presented earlier. [3] All the chemicals used were of AR grade. A stock solution of Eu_2O_3 (Sigma Chemicals, U.S.A.) was prepared by dissolving the oxide in the minimum amount of perchloric acid and diluting with double distilled water. Solutions of DHP and AHP (both from Aldrich Chemical Company, U.S.A.), were prepared in double distilled water. The ionic strength was kept constant by using 0.1 M $NaClO_4$ as the supporting electrolyte. The pH was maintained as 5.0 by adjusting with $HClO_4$ and NaOH. All measurements were made at $20 \pm 0.1°$. The test solutions containing 1×10^{-4}M Eu (III) and varying concentrations of DHP or AHP were prepared maintaining the above mentioned conditions and polarographed after bubbling nitrogen gas in the cell for 15 minutes.

RESULTS AND DISCUSSION

In the absence of the ligand, Eu (III) is reduced quasiirreversibly in 0.1 M $NaClO_4$. The reversible $E_{1/2}$ was determined by Gellings method.[4] In presence of each ligand Eu (III) is reduced reversibly which is indicated by the values (61 ± 1mV) of slopes of log plots which are expected for one electron reversible reduction process. The waves in both the cases are diffusion controlled as indicating by the constancy of $i_d\,(h_{eff})^{1/2}$. With increasing ligand concentration $E_{1/2}$ shifts towards more negative potential and i_d decreases which suggests complex formation. The data are analysed for the Fronaeus functions using the expression of De Ford and Hume.[5] F_j [X] functions calculated at a different ligand concentration (Table 1) are then solved for the stability constant by graphical procedure (Fig. 1). The plots of F_1[X] vs. [X] in each case gave straight line parallel to [X] axis which indicates that single 1 : 1 complex is formed in each case. The stability constants are given in Table 1. Higher complex species could exist but we could not identify them because hydrolysis of the metal ion takes place at higher pH (> 5.0).

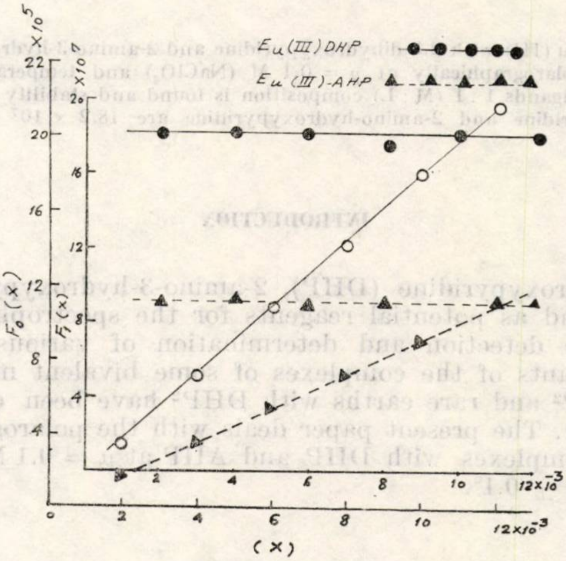

Fig. 1

Eu (III) is a class acceptor. Strength of metal donor bond, therefore, is expected to follow the order 0 > N. The two ligands under study contain respectively phenolic (DHP), amino (AHP) groups on the 2-positions in the vicinity of a phenolic group on 3-position in each pyridine molecule. The stability of the Eu(III) complexes with DHP and AHP is thus expected to follow the order DHP > AHP. The same is found to be true for these ligands (Table 1).

Table 1

Ligand conc. (mM)	$E^r_{1/2}$ (V)	Log $\frac{I_s}{I_c}$	F_0 [X] $\times 10^5$	F_1 [X] $\times 10^7$	β_1
		Eu (III) — DHP			
0.0	0.698 (0.0706)	0.0000	—	—	18.2×10^7
2.0	1.449	0.0317	3.60	18.0	
4.0	1.489	0.0434	7.28	18.2	
6.0	1.510	0.0551	10.88	19.2	
8.0	1.525	0.0671	14.32	17.9	
10.0	1.540	0.0671	18.30	18.3	
12.0	1.553	0.0792	21.72	18.1	
		Eu (III) — AHP			
2.0	1.410	0.0212	1.82	9.1	9.1×10^7
4.0	1.450	0.0317	3.68	9.2	
6.0	1.470	0.0551	5.46	9.1	
8.0	1.489	0.0551	7.28	9.1	
10.0	1.499	0.0551	9.00	9.0	
12.0	1.510	0.0671	11.04	9.2	

The $E_{\frac{1}{2}}$ given in the brackets is quasi reversible $E_{1/2}$ of the Eu (III) in 0.1 M $NaClO_4$

REFERENCES

[1] V. Kushwaha, M. Katyal and R. P. Singh, *Talanta*, **21**, 763 (1974).

[2] D. P. Goel, Ph. D. thesis, Delhi University (1969).

[3] R. S. Sindhu, K. B. Pandeya and R. P. Singu, *Fresenius Z. Anal Chem.*, **316**, 714 (1983).

[4] P. J. Gellings, *Z. Electro Chem.*, **66**, 477, 481, 799 (1962); **67**, 167 (1963).

[5] D. D. DeFord and D. N. Hume, *J. Amer Chem. Soc.*, **73**, 5321 (1951).

Revue Roumaine de Chimie, **30**, 7, 585–588 (1985)

REACTION OF ACETYLENES WITH TRANSITION METALS. XI[1]

REACTION OF 1-CHLORO-1,2-DIPHENYL-3-ALKYL-π-ALLYLPALLADIUM COMPLEXES WITH ALKENES

I. G. DINULESCU[a], S. STAICU[b], ANGELA DUMITRU[a], AURELIA GHENCIULESCU[c], F. CHIRALEU[a] and MARGARETA AVRAM[c,*]

[a] Center of Organic Chemistry — ICECHIM, Spl. Independenţei 202 B, 76300 Bucharest 15, Romania

[b] Research Institute for Pesticides, Spl. Independenţei 202, 77208 Bucharest 15, Romania

[c] Laboratory of Organic Chemistry, Polytechnic Institute — TCH, Spl. Independenţei 313, 72206 Bucharest 16, Romania

Received July 15, 1984

The reaction of 1-chloro-1,2-diphenyl-3-alkyl-π-allylpalladium complexes **1** and **2** with alkenes was studied. On heating under pressure with a large excess of isobutene, **1** gives the diene **3** together with the π-allylpalladium complex **4**; from **2**, the indene **8** was formed, the diene **7** being involved as intermediate.

We have reported [2] on the easy synthesis of 1-chloro-1,2-diphenyl-3-alkyl-π-allylpalladium complexes **1** and **2** from diphenylacetylene, dichloro-bis(benzonitrile) palladium (BNP) and isobutene or ethylene.

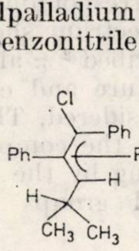

1

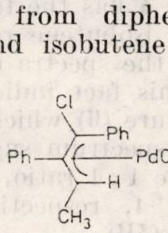

2

The reaction of π-allylpalladium complexes with alkenes has not yet been studied. We mention that Mushak and Battiste [3] obtained *trans*, *trans*-diphenyl-1,3-dienes in the reaction of diphenylacetylene with alkenes in the presence of BNP, and that Maitlis [4] suggested for this reaction a mechanism involving as an intermediate a π-allylic complex, which later reacts with a new molecule of alkene.

It seemed therefore interesting to study the reaction of compounds **1** and **2** with alkenes.

---

[*] Deceased in 1983

REACTION OF COMPLEX 1 WITH ISOBUTENE

By heating complex **1**, in benzene, with excess isobutene, in a sealed vessel, at 100°, the diene **3** and a new π-allylpalladium complex **4** were obtained.

The same compounds, diene **3** and complex **4**, together with hexaphenylbenzene (**5**), were obtained by heating diphenylacetylene with excess isobutene, in the presence of BNP, al 100°, in a sealed vessel.

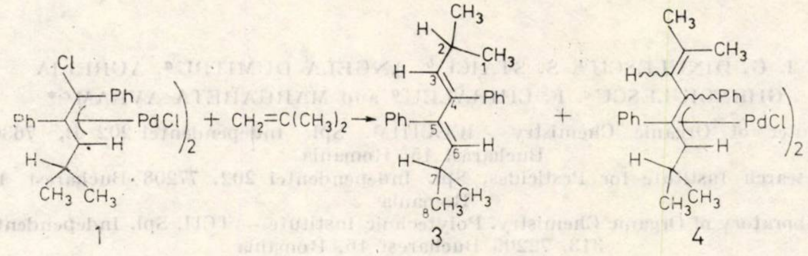

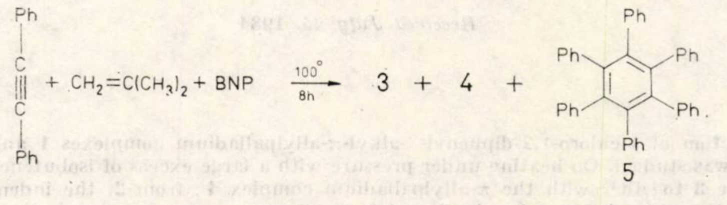

The *trans*, *trans*-2,7-dimethyl-4,5-diphenyl-octa-3,5-dienic structure for the diene **3** was established by means of ^{1}H-NMR and UV spectra.

Complex **4** has the formula $C_{22}H_{25}ClPd$, corresponding to a diphenylacetylene : isobutene ratio 1 : 2. The UV spectrum shows a strong analogy with the spectra of the previously described [2] π-allyl-palladium complexes. This fact indicates a π-allylic structure and excludes a σ-dienilic structure (**6**) which could have been considered. The pattern of the ^{1}H-NMR spectrum suggests the existence in the complex **4** of two isomers (in the 1 : 1 ratio, in chloroform), differing by the configuration at C-3 and C-4, respectively with the phenyl groups situated *anti* (**4A**) and *syn* (**4B**).

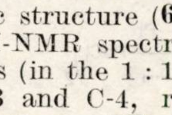

6

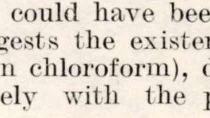

4A

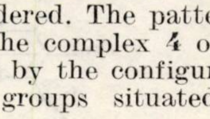

4B

Supporting this assignment, is the splitting into doublets of the signal of the olefinic proton (H-3) and of the allylic proton (H-6), as well as the signals of the aromatic protons in the region δ 7.00—8.00 ppm.

These signals correspond to shielded and deshielded aromatic protons, due to the *syn* configuration (**4B**) and respectively *anti* configuration (**4A**) of the benzene rings.

It should be noted that the ratio **4A** : **4B**, 1 : 1 in chloroform, becomes 2.33 : 1 on addition of 10 % deuterated pyridine. This fact suggests that the isomers are interconvertible.

Complex **4** is formed from the diene **3** and $PdCl_2$ which is present in the reaction mixture. Compounds such as complex **4** are described in the literature, [5,6,7] resulting by the addition of palladium chloride to conjugated dienes.

REACTION OF COMPLEX 2 WITH ETHYLENE

Diphenylacetylene reacts with ethylene, in the presence of BNP, in a more complex way. The reaction has a small degree of reproductibility, because of many possible secondary reactions which occur.

The various experiments carried out in different conditions (temperatures between 20 and 100°, reaction times 8—48 hrs, at normal pressure or 10 at, benzene or chloroform as solvent) showed that the π-allylpalladium complex **2** reacts even at room temperature as soon as it is formed with the excess of ethylene, to give a mixture of unstable compounds, which makes very difficult the isolation and purification of complex **2**.

When complex **2** was treated with ethylene, in benzene, at 80° and atmospheric pressure, only diene **7**, previously described,[3] was isolated.

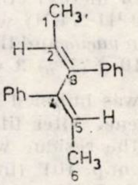

7

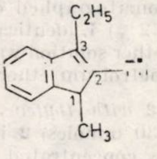

8

By treating complex **2**, in benzene, with ethylene under pressure (5at), at 100°, for 8 hrs, only the indenic compound **8** was isolated as reaction product. This compound is formed, as claimed by Battiste, [3] from the diene **7** under the action of acidity from the reaction medium.

The reaction of π-allylpalladium complexes **1** with isobutene and **2** with ethylene, yielded the diene **3** and the complex **4**, respectively the diene **7** or the indenic compound **8**. The compounds **3**, respectively **7** and **8**, were obtained by Mushak and Battiste[3] by the reaction of diphenylacetylene with isobutene, respectively ethylene, in the presence of BNP, at 70°.

The above presented results demonstrate that a π-allylpalladium complex is formed as an intermediate in this type of reactions.

The reactions of the π-allylpalladium complexes with alkenes different from those involved in their synthesis are under investigation.

EXPERIMENTAL

IR spectra were recorded on a double beam UR-20 Jena spectrophotometer. ^{1}H-NMR spectra were determined with a Varian A-60A spectrometer (TMS as internal standard). UV spectra were recorded on a VSU-Jena spectrophotometer.

Reaction of complex **1** *with isobutene.* A solution of 0.50 g (1.21 mmoles) complex **1** in 30 ml benzene was heated in a sealed vessel with excess of isobutene for 8 hrs at 100°. The cold reaction product was filtered from the separated palladium and evaporated *in vacuo*. The residue was chromatographed on alumina with petroleum ether (fraction A) and then with diethyl ether (fraction B).

From the fraction A, by solvent evaporation, 0.17 g (48 %) **3**, m.p. 178°, were obtained. — Analysis : $C_{22}H_{26}$ (290.5) Calcd. : C, 90.98 ; H, 9.02. Found : C, 90.88 ; H, 9.16. — ^{1}H-NMR ($CDCl_3 + CD_3COCD_3$, δ, ppm) : 0.78 (d, 12H, 4 CH_3 groups, $J_{CH_3.2} = J_{CH_3.7} = 6.0$ Hz), 2.08 (m, 2H, H-2 and H-7, $J_{CH_3.2} = J_{CH_2.7} = 6.0$ Hz, $J_{6.7} = J_{2.3} = 10.0$ Hz), 4.98 (d, 2H, H-3 and H-6, $J = 10.0$ Hz), 7.00 — 7.50 (m, 10 aromatic H). — UV (λ_{max}^{EtOH} (log ε)) : 231.5 nm (4.321), 239.2 (4.313).

The fraction B, after solvent removal, afforded 0.15 g (28.6 %) di-μ-chloro-di-(2,7-dimethyl-4,5-diphenyl-oct-2-en-4-yl)-dipalladium (**4**, mixture of **4A** and **4B**), m.p. 198°. — Analysis : $C_{22}H_{25}ClPd$ (431.3) Calcd. : C, 61.27 ; H, 5.84 ; Cl, 8.22 ; Pd, 24.67. Found : C, 61.74 ; H, 6.13 ; Cl, 8.03 ; Pd, 24.20. — ^{1}H-NMR ($CDCl_3$, δ, ppm) : 0.60 — 2.30 (m, 13H, 4 CH_3 and H-7), 4.01 (d, 1H, H-6 from **4B**), 4.47 (bd, 1H, H-6 from **4A**, long range coupling with H-3 and H-7), 5.24 (bs, 1H, H-3 from **4B**), 5.40 (bs, 1H, H-3 from **4A**), 6.80 — 7.90 (m, 10 aromatic H) ; the characteristic signals of the pure isomers **4A** and **4B** from 4.01 and 4.47 or 5.24 and 5.40 are in ratio 1 : 1). — UV ($\lambda_{max}^{CHCl_3}$ (log ε)) : 270 nm (4.312), 373 (3.645).

Reaction of diphenylacetylene with isobutene and BNP. A solution of 90 g (5.0 mmoles) diphenylacetylene and 1.87 g (5.0 mmoles) BNP in 60 mL benzene was heated in a sealed vessel with an excess of isobutene for 8 hrs at 100°. The cold reaction product was filtered from the separated palladium. The solution was diluted with four volumes of petroleum ether and the separated hexaphenylbenzene was filtered ; 0.15 g (17 %) **5** were obtained. The solution was evaporated *in vacuo* and the residue was triturated with 100 mL petroleum ether. The insoluble material was chromatographed on alumina with diethyl ether-dichloromethane 2 : 1 as eluent, yielding 0.20 g (9.2 %) **4**, identical (m.p., IR and ^{1}H-NMR) with the above described compound. The petroleum-ether solution was evaporated *in vacuo* and the residue was chromatographed on alumina with petroleum ether as eluent ; 0.10 g (7 %) **3** were obtained.

Reaction of complex **2** *with ethylene.* A. Ethylene was bubbled for 8 hrs through a hot (80°) solution of 0.50 g (1.30 mmoles) **2** in 30 mL benzene. After filtration of the separated palladium, the solution was concentrated *in vacuo* and the residue was chromatographed on alumina with petroleum ether, yielding 0.060 g (20 %) **7**, m.p. 101° (lit. [3] m.p. 100 — 101°). — ^{1}H-NMR (CCl_4, δ, ppm) : 1.40 (d, 6H, CH_3-1 and CH_3-6, $J_{CH_3.2} = J_{CH_3.5} = 7.0$ Hz), 5.16 (qu, 2H, H-2 and H-5, $J = 7.0$ Hz), 6.90 — 7.40 (m, 10 aromatic H). — B. A solution of 0.50 g (1.30 mmoles) **2** in 30 mL benzene was heated in sealed vessel with a large excess of ethylene at 5 at for 8 hrs at 100°. After working up as above, 0.20 g (17 %) **8**, colourless oil, were obtained. — Analysis : $C_{18}H_{18}$ (234.3) Calcd. : C, 92.30 ; H, 7.70. Found : C, 91.92 ; H, 7.95. — ^{1}H-NMR (CCl_4, δ, ppm) : 1.16 (d, 3H, CH_3-1, $J = 7.0$ Hz), 1.26 (tr, 3H, CH_3 from ethyl group, $J = 7.0$ Hz), 2.66 (qu, 2H, CH_2, $J = 7.0$ Hz), 3.76 (qu, 1H, H-1, $J = 7.0$ Hz), 7.10 — 7.60 (m, 10 aromatic H).

REFERENCES

[1] Part X : I. G. Dinulescu, S. Staicu, E. Avram, F. Chiraleu and M. Avram, *J. Organometal. Chem.*, **136**, C15 (1977).

[2] S. Staicu, I. G. Dinulescu and M. Avram, *J. Organometal. Chem.*, **113**, C69 (1976).

[3] P. Mushak and M. A. Battiste, *Chem. Commun.*, **1962**, 1146.

[4] P. M. Maitlis, The Organic Chemistry of Palladium, vol. II, Academic Press, New York, 1971.

[5] S. D. Robinson and B. L. Shaw, *J. Chem. Soc.*, **1964**, 5002.

[6] J. Lukas, P. W. van Leewen, H. C. Volger and P. Kramer, *Chem. Commun.*, **1970**, 799.

[7] P. E. Slade and H. B. Jonassen, *J. Amer. Chem. Soc.*, **79**, 1277 (1957).

Revue Roumaine de Chimie, **30**, 7, 589–591 (1985)

A NEW DIBENZO-$(CH)_{10}$ HYDROCARBON : *anti*-DIBENZO[*b*, *i*]TRICYCLO[6.2.0.$0^{4,7}$]DECA-2,5,9-TRIENE[1]

NICOLETA ŞTEFAN, PETRU FILIP, ILIE G. DINULESCU
and MARGARETA AVRAM *
Center of Organic Chemistry, Spl. Independenţei 202 B, 78100 Bucharest 12,
Romania

Received June 18, 1984

The synthesis of dibenzo-$(CH)_{10}$ hydrocarbon **2** starting from the angular dimer of benzocyclobutadiene is described.

The $(CH)_n$ hydrocarbons as well as their benzo and dibenzo derivatives have received considerable attention. [2] In the course of our investigations we have synthetized some $(CH)_n$ hydrocarbons, among which we mention the following: *syn* and *anti*-tricyclo[4.2.0.$0^{2,5}$]deca-3,7-dienes (the dimers of cyclobutadiene), [3,4,5] dibenzo[*c*, *g*]derivative [6,7] and dibenzo[*c*, *g*]cyclooctatetrane, [6] as $(CH)_8$, and tricyclo[4.2.2.0 ^{2,5}] deca-3,7,9-triene *(Nenitzescu's hydrocarbon)*, [8,9,10] and their benzo[*c*], [11] dibenzo[*g*, *j*] [12,13] and dibenzo[*c*, *g*] [14] derivatives, as $(CH)_{10}$. We have also obtained a tetrabenzo-$(CH)_{16}$ hydrocarbon. [13]

As a continuation of these investigations, the synthesis of tricyclo [6.2.0.$0^{4,7}$]deca-2,5,9-triene (**1**), as well as of its benzo derivatives, is of interest. This polycyclic system derives formally from a Kékulé structure of benzene by replacing two double bonds with two cyclobutene rings. In this preliminary note we present a synthesis of the dibenzo[*b*, *i*]derivative **2**.

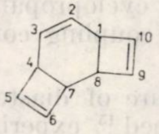

1

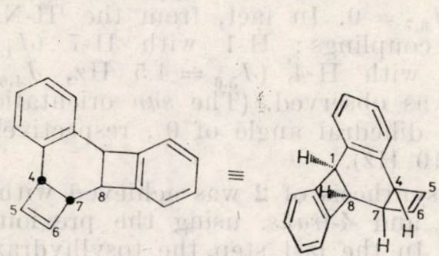

2

---

* Deceased in 1983

The hydrocarbon **2** was obtained starting from the angular dimer of benzocyclobutadiene (**3**), by a sequence of steps which have been successfully used in other case.[15]

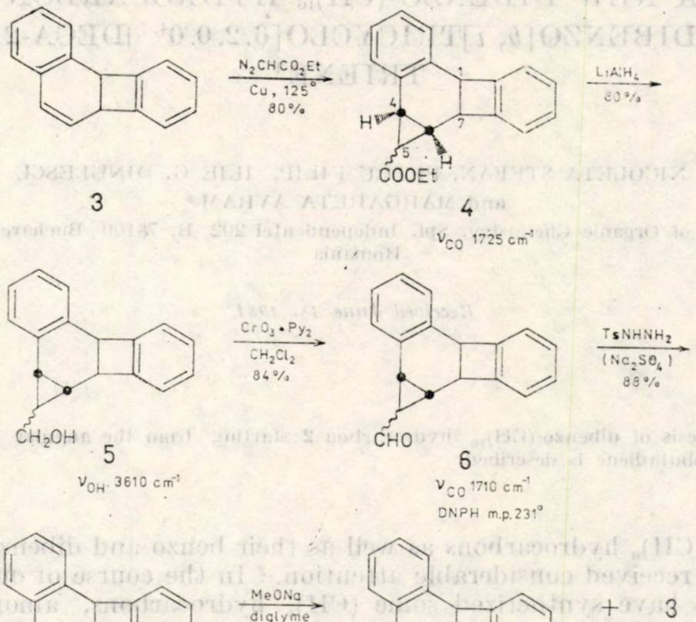
N₂CHCO₂Et
Cu, 125°
80%
1
4
7
5
H
H
COOEt
LiAlH₄
80%
3
4
ν CO 1725 cm⁻¹
CrO₃·Py₂
CH₂Cl₂
84%
TsNHNH₂
(Na₂SO₄)
88%
CH₂OH
5
ν OH 3610 cm⁻¹
CHO
6
ν CO 1710 cm⁻¹
DNPH m.p. 231°
MeONa
diglyme
130°
H
H
+ 3
CH=NNHTs
7
ν NH 3210 cm⁻¹

The reaction of the dimer **3** with ethyl diazoacetate, in the presence of copper bronze, afforded a mixture of esters in which the cyclopropane ring is *anti* in respect to the benzocyclobutene moiety and the carbethoxy groups are *cis* and *trans* oriented.

The *anti* orientation of the cyclopropane ring involves a dihedral angle H-6—C—C—H-7 of approximatively 90°, respectively a coupling constant $J_{6,7} = 0$. In fact, from the ^{1}H-NMR spectra result only the following couplings: H-1 with H-7 ($J_{1,7} = 5.5$ Hz) and H-6 with H-5 and with H-4 ($J_{5,6} = 4.5$ Hz, $J_{4,6} = 9.0$ Hz); no H-6—H-7 coupling was observed. (The *syn* orientation of the cyclopropane ring involves a dihedral angle of 0°, respectively a great coupling constant, $J_{6,7} \sim 8-10$ Hz).

The synthesis of **2** was achieved with the mixture of diastereoisomers **4**-*cis* and **4**-*trans*, using the previously described[15] experimental procedure. In the last step, the tosylhydrazone **7** (*cis-trans* mixture) heated with sodium methoxide (free of methanol), in diglyme, afforded with 20—30% yield, the hydrocarbon **2**; together with **2**, variable amounts of **3** were formed by elimination from carbenoid species.[16,17]

All the compounds which are involved in this synthesis were characterized by elemental analysis, IR and ^{1}H-NMR spectra, which are in good agreement with the proposed structures.

The hydrocarbon **2** presents the following ^{1}H-NMR spectrum (CCl_4, δ, ppm) : 7.40–6.70 (m, 8 aromatic protons), 6.08 (s, 2H, H-5, H-6), 4.58 (d, 1H, H-1, $J_{1,8} = 5.5$ Hz), 3.97 (d, 1H, H-8, $J_{1,8} = 5.5$ Hz), 3.86 and 3.60 (AB system, 2d, 2H, H-4, H-7, $J_{4,7} = 4.5$ Hz). The absence of a coupling between H-7 and H-8 supports the *endo* orientation of H-7 (dihedral angle H-7–C–C–H-8 approximatively 90° and $J_{7,8} = 0$), respectively *anti* orientation for the cyclobutene ring.

Investigations are in progress in order to optimize the synthesis and to establish the thermolytic behaviour of **2**.

REFERENCES

[1] Part LIX in the "Investigations in the Cyclobutane Series". For part LVIII see : N. Ştefan, P. Filip, I. G. Dinulescu, F. Chiraleu and M. Avram, *Rev. Roumaine Chim.*, **29**, 631 (1984).

[2] L. A. Paquette, M. J. Kukla and J. C. Stowell, *J. Amer. Chem. Soc.*, **94**, 4920 (1972) ; M. Elian, M. Banciu, L. Stănescu and E. Ciorănescu, *Rev. Roumaine Chim.*, **21**, 89 (1976) ; E. L. Allred, B. R. Beck and N. A. Mumford, *J. Amer. Chem. Soc.*, **99**, 2694 (1977) ; A. T. Balaban, *Rev. Roumaine Chim.*, **11**, 1097 (1966).

[3] M. Avram, G. D. Mateescu, I. G. Dinulescu, E. Marica and C. D. Nenitzescu, *Tetrahedron Letters*, **1961**, no. 1, 21.

[4] C. D. Nenitzescu, M. Avram, E. Marica, I. G. Dinulescu and G. D. Mateescu, *Angew. Chem.*, **75**, 88 (1963) ; *Angew. Chem. Internat. Edit.*, **1**, 659 (1962).

[5] M. Avram, I. G. Dinulescu, E. Marica, G. D. Mateescu, E. Şliam and C. D. Nenitzescu, *Chem. Ber.*, **97**, 382 (1964).

[6] M. Avram, I. G. Dinulescu, D. Dinu, G. D. Mateescu and C. D. Nenitzescu, *Tetrahedron*, **19**, 309 (1963).

[7] G. D. Mateescu, M. Avram, D. Dinu and C. D. Nenitzescu, *Studii și Cerc. Chimie (Bucureşti)*, **9**, 424 (1961).

[8] C. D. Nenitzescu, M. Avram, J. Pogany, G. D. Mateescu and M. Fărcaşiu, *Studii și Cerc. Chimie (București)*, **11**, 7 (1963).

[9] M. Avram, G. D. Mateescu and C. D. Nenitzescu, *Liebigs Ann. Chem.*, **636**, 174 (1960).

[10] M. Avram, E. Şliam and C. D. Nenitzescu, *Liebigs Ann. Chem.*, **636**, 184 (1960).

[11] L. Enescu, I. G. Dinulescu and M. Avram, *Rev. Roumaine Chim.*, **24**, 995 (1979).

[12] M. Avram, I. G. Dinulescu and C. D. Nenitzescu, *Liebigs Ann. Chem.*, **691**, 9 (1966).

[13] I. G. Dinulescu, J. J. Pogany, A. Dumitriu, E. G. Georgescu and M. Avram, *Rev. Roumaine Chim.*, **25**, 969 (1980).

[14] I. G. Dinulescu, M. S. Pop and M. Avram, *Rev. Roumaine Chim.*, **22**, 1037 (1977).

[15] I. G. Dinulescu, A. Ghenciulescu, L. Enescu, E. Olteanu and M. Avram, *Bull. of the Polytechnic from Bucharest, Ser. Chem. — Metalurg.*, **43**, no. 4, 93 (1981).

[16] L. Friedman and H. Schecter, *J. Amer. Chem. Soc.*, **82**, 1002 (1960).

[17] H. M. Frey and I. D. R. Stevens, *Proc. Chem. Soc.*, **1964**, 144.

Revue Roumaine de Chimie **30**, 7, 595—598 (1985)

ISOMERIZATION OF *o*-ALKYLPHENOLS ON AN ALUMINIUM ORTHOPHOSPHATE-ALUMINA

S. ESTEBAN SANTOS[a], J. M. MARINAS RUBIO[b] and M. P. MARTINEZ-ALCAZAR[c]

[a] Department of General Chemistry and Macromolecules, U.N.E.D., Faculty of Sciences, Ciudad Universitaria, Madrid-3, Spain

[b] Department of Organic Chemistry, Faculty of Sciences, University of Córdoba, Córdoba

[c] Department of Organic Chemistry, Faculty of Chemistry, University Complutense, Madrid-3

Received June 19, 1984

In order to complete the study of alkylation of phenol with alcohols in gas phase with an aluminium orthophosphate-alumina as catalyst, the isomerization of the corresponding *o*-alkylphenols under identical experimental conditions has been investigated. With this catalyst the *meta* and *para* isomerization takes place to a small extent. In contrast, the principal reaction is dealkylation to phenol. This dealkylation increases with the stability of the carbocations formed from the alkyl chains.

INTRODUCTION

The isomerization of alkylphenols in gas phase is normally accompanied by their disproportionation, dealkylation and exchange of hydroxyl group for hydrogen. Nowadays, this process is very often used as a method to synthesize *para* and *meta* alkylphenols.[1] Many catalysts have been employed: aluminosilicates,[2] activated alumina,[3] metallic oxides,[4] natural clays,[5] etc.

On the other hand, numerous papers are dedicated to study the mechanism of these reactions.[6] All of them generally agree that the isomerization of alkylphenols takes place on the acid sites of the catalyst and can be inter- or intramolecular.

In order to complete the study of the alkylation of phenol by alcohols in gas phase with an aluminium orthophosphate-alumina system as catalys carried out by us,[7] we investigate here the isomerization of the *ortho*-alkylphenols that would be produced in those alkylation reactions (*o*-methyl-, *o*-ethyl-, *o*-isopropyl and *o*-*t*-butylphenols) under the same experimental conditions.

RESULTS AND DISCUSSION

With each alkylphenol two sequences of experiences were made, by varying temperature or space time. The results are shown in Tables 1 and 2. From them it can be considered that the isomerization occurs to a small extent (the yields were never higher than 13%). On the contrary, the main reaction is always the dealkylation to phenol, fact that appears too in the rearrangement of phenylethers studied by us with the same catalyst.[8]

Table 1

Total conversions (X_T) and partial conversions (X_i) with the temperature ($W/F = 100$)

o-Alkylphenol	T °C	X_T	X phenol	X $m+p$-alkylphenols	X	X
					alkylbenzenes	xylenols
o-methylphenol	300	6.2	3.7	0.8	—	1.7
	350	9.1	3.7	4.3	1.1	—
	450	25.5	15.3	6.7	1.9	1.6
	550	46.3	23.0	13.8	4.5	5.0
					benzofuran	cresols + xylenols
o-ethylphenol	300	54.7	42.1	12.6	—	—
	350	60.3	47.1	5.9	—	7.3
	450	72.0	36.4	5.4	23.8	6.4
	550	82.5	28.4	2.5	49.8	2.0
					methylbenzofurans	lower alkylphenols
o-isopropylphenol	300	22.5	15.3	7.2	—	—
	350	39.0	31.4	6.3	0.4	0.9
	450	53.0	40.0	2.0	9.0	2.0
	550	68.0	53.0	2.0	8.0	5.0
					methylbenzofurans	lower alkylphenols
o-*t*-butylphenol	300	97.3	81.2	1.1	5.4	9.6
	350	92.0	89.0	1.0	1.0	1.0
	450	80.0	64.0	—	5.0	11.0
	550	91.0	43.0	—	24.0	24.0

Xylenols and alkylbenzenes are also formed in the reactions with *o*-methylphenol. In the other cases, lower alkylphenols are originated through cracking of the reactant or of its *meta* and *para* isomerization products. With *o*-ethylphenol benzofurans appear and with *o*-isopropyl and *o*-*t*-butylphenol methyl and dimethylbenzofurans are formed too, as a result of their dehydrocyclization.[9]

Except for the tests with *o*-methylphenol, isomerization yields decrease with rising temperature (Table 1). In contrast, the temperature favours polyalkylation, cracking to lower alkylphenols and dehydrocyclization, as selectivities also show (Fig. 1).

The effect of space time is more remarkable on the dealkylation to phenol, since its yields increase with that parameter (Table 2).

The formation of phenol at such high rate suggests that there is an important intermolecular reaction. If the chain of *o*-alkylphenol is separated as a cation or "pseudocation" adsorbed on the catalyst surface, then it could attack the aromatic ring, leading to an alkylphenol isomer

Table 2

Total conversions (X_T) and partial conversions (X_i) with the space time ($T = 450°C$)

o-Alkylphenol	W/F	X_T	X phenol	X $m+p$-alkylphenols	X	X
					alkylbenzenes	xylenols
o-methylphenol	60	14.0	10.0	4.0	—	—
	100	25.5	15.3	6.7	1.9	1.6
	140	32.6	24.7	4.5	2.0	1.4
	200	20.0	14.0	3.0	1.0	2.0
					benzofuran	cresols + xylenols
o-ethylphenol	60	59.0	21.0	6.0	27.0	5.0
	100	72.0	36.4	5.4	23.8	6.4
	140	86.5	49.5	7.2	18.5	11.3
	200	86.0	54.0	12.0	12.0	8.0
					methylbenzofuran	lower alkylphenols
o-isopropylphenol	60	49.0	39.0	1.0	8.0	1.0
	100	53.0	40.0	2.0	9.0	2.0
	140	93.0	81.0	2.0	3.0	7.0
	200	86.0	46.0	1.0	25.0	4.0
					methylbenzofurans	lower alkylphenols
o-*t*-butylphenol	60	82.0	63.0	—	8.0	11.0
	100	80.0	64.0	—	5.0	11.0
	140	99.0	89.0	—	3.0	7.0
	200	96.0	90.0	—	3.0	3.0

— pathway a — or suffer an evolution to olefin, and so phenol is originated — pathway b —, as it is represented in Scheme 1.

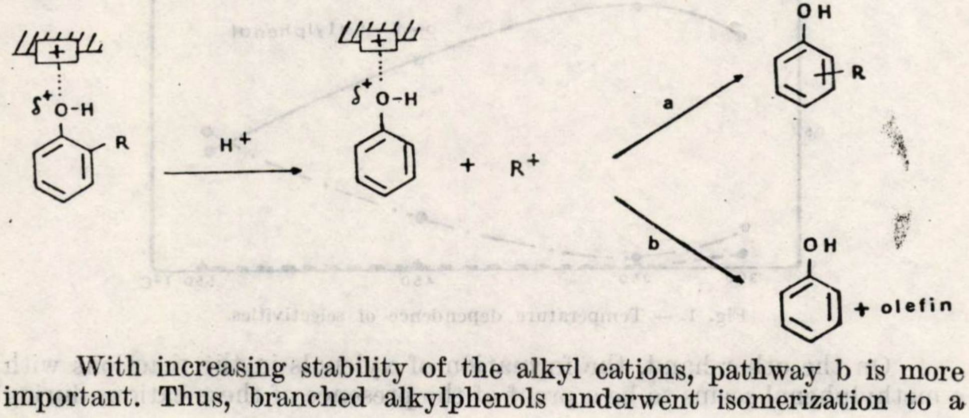

With increasing stability of the alkyl cations, pathway b is more important. Thus, branched alkylphenols underwent isomerization to a lesser extent. For instance, isomerization products from *o*-*t*-butylphenol appear only up to 350°C. This is consistent with the conclusions of Kraus et al. [6]

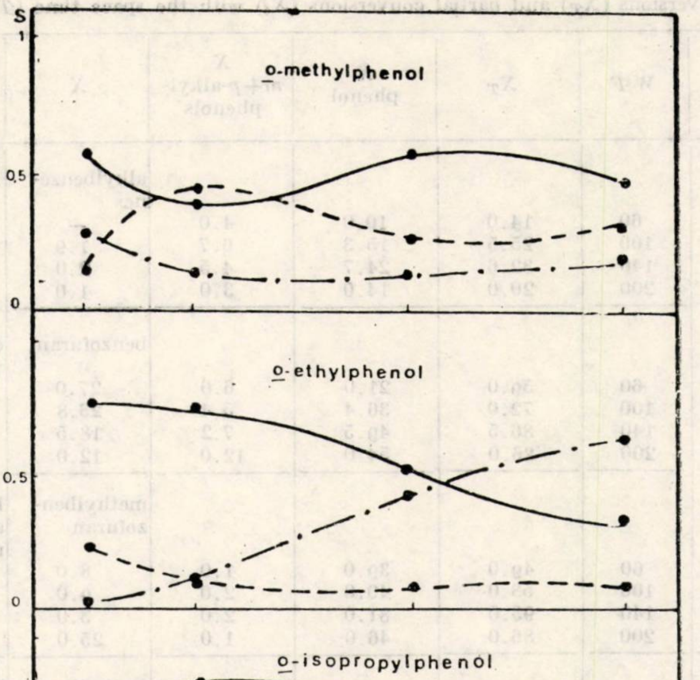

Fig. 1. — Temperature dependence of selectivities.

On the other hand, the formation of xylenols in the reactions with *o*-methylphenol seems to be a proof of the presence of these cations during this process. Xylenols would be originated by attack of the carbocation to the methylphenol.

All above data indicate that this aluminium orthophosphate-alumina promotes dealkylation more than isomerization. This fact might be due to the high acidity of this kind of catalysts, that were successfully employed in cracking reactions of aromatic hydrocarbons.[10]

Thus, with regard to the results obtained when phenol was alkylated by alcohols with this catalyst,[7] the low yields in these isomerization experiences suggest that the *meta* and *para* alkylphenols originated in the alkylation of phenol came from isomerization of the *ortho* isomer. This conclusion agrees with Tanabe,[11] who points out that direct C-alkylation can occur into the three positions, whereas Enomoto and Inoue[6] affirm that it only takes place in *ortho* position.

EXPERIMENTAL

Catalyst. The catalyst consisted of 75% aluminium orthophosphate and 25% alumina gelified in an ammonia medium and compacted in cylindrical pellets of 6/3 mm. The total acidity measured with the indicator 4-dimethylaminoazobenzene by *n*-butylamine titration, was 0.57 meq/g. The basic sites, measured by spectrophotometric titration with phenol (Bausch and Lamb Espectronic 21) were 0.074 mmol/g. The specific surface area (BET method) was 177 m^2/g.[12]

Apparatus and procedure. A modified type CAT-A reactor[12] was used. With each *o*-alkylphenol two sequences of tests were made : a) at a temperature range from 300 to 550°C, with a constant space time (W/F) of 100 ; b) at space time range from 60 to 200 (8 g of catalyst -W- and a feed rate of reactant -F- variable) with a fixed temperature of 450°C.

Analysis of products. The analysis of the products was carried out by gas chromatography (Hewlett-Packard 5750 with a 3 m column of celanesse ester over Chromosorb *W* (80/100) at 180°C). Quantitative analysis was also made with this technique, by the internal normalization method. Spectroscopic techniques, especially MS/GC, in a Variant Mat-711[13] were used too.

NOMENCLATURE

$$W/F = \frac{\text{Catalyst weight (g)}}{\text{Feed rate of reactants (mol/h)}}$$

$$X_T \text{ (total conversion)} = \frac{\text{moles of } o\text{-alkylphenol reacted}}{\text{moles of } o\text{-alkylphenol fed}} \cdot 100$$

$$X_i \text{ (yield of each product or partial conversion)} =$$
$$= \frac{\text{moles of compound } i \text{ produced}}{\text{moles of } o\text{-alkylphenol fed}} \cdot 100$$

$$S_i \text{ (selectivity of each product)} = \frac{\text{Yield of each product } (X_i)}{\text{Total conversion } (X_T)}$$

REFERENCES

[1] N. Kominami, N. Tamura and H. Mikami, Japanese Pat., 76 21, 970 (1976).

[2] I. Pigman, E. del Bel and B. M. Neuworth, *J. Amer. Chem. Soc.*, **76**, 6169 (1954); K. Kochlofl, M. Kraus and V. Bazant, *Coll. Czechoslov. Chem. Commun.*, **24**, 958 (1959).

[3] K. Kochlofl, M. Kraus and V. Bazant, Czechoslovak Pat. 89437 ; RZhKhim, 2L96 (1961) ; J. A. Sharp, R. E. Dean and W. A. Betts, British Pat. I, 232 027 (1971).

[4] P. H. Given, *J. App. l. Chem.*, **7**, 172 (1957) ; P. H. Given, *Chem. and Ind.*, 525 (1956).

[5] Czechoslovak Pat., 93953 ; RZhKhim 17L154 (1961).

[6] M. Inoue and S. Enomoto, *Chem. Pharm. Bull.*, **19 (21)**, 2518 (1971) ; *ibid.*, **20(2)**, 232 (1972) ; P. Schneider, M. Kraus and V. Bazant, *Coll. Czechoslov. Chem. Commun.*, **27**, 9 (1962).

[7] S. Esteban, J. M. Marinas and M. P. Martinez-Alcázar, *React. Kinet. Catal. Lett.*, **24**, 247 (1984).

[8] S. Esteban, J. M. Marinas and M. P. Martinez-Alcázar, *An. Quim.*, **77C**, 251 (1981).

[9] C. Hansch, W. Saltensall and R. Sattle, *J. Amer. Chem. Soc.*, **71**, 943 (1949).

[10] C. Jimenez, J. M. Marinas, R. Perez-Ossorio and J. V. Sinisterra, *An. Quim.*, **72**, 254 (1976).

[11] K. Tanabe and T. Nishizaki, *Proc. Int. Congr. Catal.*, (6th, 1976), **2**, 863 (1977).

[12] M. P. Martinez-Alcázar, Ph. D. Dissertation, Complutense University of Madrid (1981).

[13] S. Esteban, J. M. Marinas and M. P. Martinez-Alcázar, *An. Quim.*, **77C**, 218 (1981).

Revue Roumaine de Chimie, **30**, 7, 599–609 (1985)

MODERN FRIEDEL-CRAFTS CHEMISTRY. XII*

ON THE CARBONYL RETARDATION OF CYCLIALKYLATION OF ARYL ALKENYL KETONES UNDER FRIEDEL-CRAFTS CONDITIONS

AHMED M. EL-KHAWAGA, ABOEL-MAGD A. ABDEL-WAHAB,
MAHER F. ELZOHRY and ALI A. KHALAF
Chemistry Department, Faculty of Science, Assiut University, Assiut, Egypt

Received April 4, 1984

A number of aryl alkenyl ketones (**3**–**6** and **22a-c**) were prepared and subjected to treatment with different Friedel-Crafts catalysts in order to criticize the earlier data claiming facile closures of carbonyl-deactivated systems. Whereas benzylideneacetoenone (**3**), 2-cinnamoylnaphthalene (**5**) and 3-(1-napththyl) acrylophenone (**6**) failed to cyclize under different conditions, 1-cinnamoylnaphthalene (**4**) underwent cyclization to 8,9-dihydro-9-phenylperinapthen-7-one (**8**, 12 %) and 9-phenylperinaphthen-7-one (**7**, 38 %). Also, **5** gave upon treatment with $AlCl_3$ in CS_2 at reflux temperature, in addition to the recovered starting material, a rearrangement product **4** in 16 %. It is worthwhile to mention that synthesis and cyclization of benzoylcyclohexenes (**22a-c**), are described. While treatment of the isomeric mixture **22a-c** with Lewis acid catalysts gave 1,2,3,4-*trans*-10,11-hexahydrofluorenone (**23b**), treatment with Brönsted acid catalysts gave the *cis* derivative (**23a**). Furthermore, reorientation of **11**–**14** and *trans*-acylation of toluene with **11**–**16** were also investigated.

INTRODUCTION

The literature results on the cyclialkylation of carbonyl deactivated compounds such as aryl alkenyl ketones upon treatment with Friedel-Crafts catalysts are rather confusing. [1–28] Whereas some workers claimed facile closure to five [1–5, 7, 8, 10, 14, 16, 19, 21, 26] or six [1, 3, 5, 27, 28] membered ring, others concluded that closure could be effected only under severe conditions. [14, 16, 19, 26] Colonge *et al.* [11] reported, in contrast with the preceding claims, that aryl alkenyl ketones of the general formula **1**

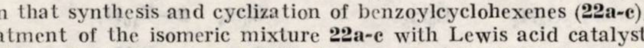

1   2

failed to cyclize to 1-tetralones (**2**) upon treatment with acid catalysts. Recently, some of the confusion was clarified by Pines and Douglas [29, 30] and also by Khalaf and El-Khawaga.[21] Furthermore, confusion was also found in regard to the effect of aromatic substituents. Some authors concluded that α, β-unsaturated aromatic ketones will ring close regardless of the position of the aromatic substituents[22] whereas others indicated that methyl substituents *ortho* and *para* to the closure site promote the closure whereas *meta* to the site inhibits the closure.[1, 3, 5]

---

* Part XI : *Phosphorus and sulfur*, **14**, 000 (1983).

In an endeavour to clarify this interesting problem, we designed some experiments and synthesized a number of aryl alkenyl ketones of special structures to reveal the influence of the different factors affecting ring closure.

RESULTS AND DISCUSSION

The starting aryl alkenyl ketones, benzylideneacetophenone (**3**), 1-cinnamoylnaphthalene (**4**), 2-cinnamoylnaphthalene (**5**) and 3-(1-naphthyl) acrylophenone (**6**) were prepared by condensation of benzaldehyde with acetophenone,[32] with 1-acetylnaphthalene and with 2-acetylnaphthalene or condensation of 1-naphthaldehyde with acetophenone in the presence of basic catalyst, respectively.

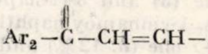

$$\mathrm{Ar_2-\overset{O}{\overset{\|}{C}}-CH=CH-Ar_1}$$

	Ar_1	Ar_2		Ar_1	Ar_2
3	C_6H_5	C_6H_5	**5**	C_6H_5	$2-C_{10}H_7$
4	C_6H_5	$1-C_{10}H_7$	**6**	$1-C_{10}H_7$	C_6H_5

Attempted cyclization of **3** under the reported conditions of Sammour[28c] gave, contrary to his results, the starting material unreacted (Table 1, Entry 1). The starting **3** was also recovered upon treatment with $AlCl_3/H_2SO_4$ catalyst (Table 1, Entry 2) whereas a black tarry material was obtained under more drastic conditions, using $AlCl_3$ at 200°C or $AlCl_3$-NaCl catalysts (Table 1, Entries 3,4). In continuation, treatment of **4** with $AlCl_3$ in CS_2 at 50°C gave a mixture of 9-phenylperinaphth-7-en-9-one (**7**, 38 %) and 8,9-dihydro-9-phenylperinaphthen-7-one (**8**, 12 %). It is worthwhile to mention that none of the perinaphth-7-en-9-one (**9**) could be isolated or detected among the reaction products as claimed by Koelsch.[33]

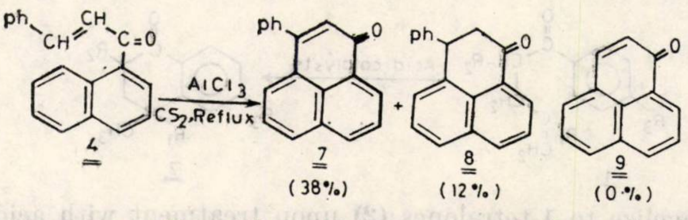

The formation of **7** and **8** could be explained through the electrophilic attack of the carbocation **10** on 8-position followed by loss of proton to form **8** which is in turn dehydrogenated[34] to **7** (Scheme 1). On the

Table 1

Reactions of aryl alkenyl ketones with Friedel-Crafts catalysts

Entry No.	Starting material	Reaction conditions				Reaction products (% yield)
		Catalyst	Solvent	Temp. (°C)	Time (hr)	
1	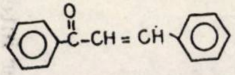	$AlCl_3$	Toluene	110	2	Recovered starting material (85)
2	,,	$AlCl_3/H_2SO_4$	CS_2	25–90	4	,, ,, ,, (84)
3	,,	$AlCl_3$	—	200	1	Black tarry material (90)
4	,,	$AlCl_3/NaCl$	—	200	1	,, ,, ,, (99)
5	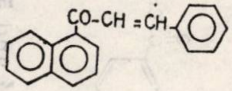	$AlCl_3$	CS_2	RT	2	Recovered starting material (88)
6	,,	,,	,,	Reflux	2	8,9-Dihydro-9-phenylperinaphthen-7-one (12), 9-phenylperinaphthene-7-one (38), unidentified material (8)
7	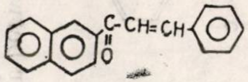	$AlCl_3$	,,	RT	2	Recovered starting material (80)
8	,,	,,	,,	Reflux	2	Starting material (24), 1-cinnamoylnaphthalene (16), 2-(3-phenyl) propinoylnaphthalene (10), unidentified material (20)
9	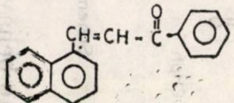	$AlCl_3$	,,	RT	2	Recovered starting material (90)
10		,,	,,	Reflux	2	,, ,, ,, (85)
11	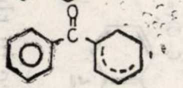	$AlCl_3$	,,	RT	2	Recovered starting material (92)
12	,,	,,	,,	Reflux	2	*trans* 10,11-hexahydrofluorenone (89)
13	,,	$AlCl_3/H_2SO_4$	CS_2	25–90	4	*trans* 10,11-hexahydrofluorenone (73)
14	,,	H_1SO_4	—	RT	24	*Cis* ,, (81)
15	,,	H_3PO_4/ HCOOH	—	90	6	*Cis* ,, (80)
16	,,	H_3PO_4	—	RT	48	*Cis* ,, (68)

other hand, treatment of **5** with $AlCl_3$ in CS_2 under reflux gave a mixture of the starting material (**5**, 24%) 1-cinnamoylnaphthalene (**4**, 16%), 2-(3-phenyl)propionylnaphthalene (**11**, 10%) and an unidentified product

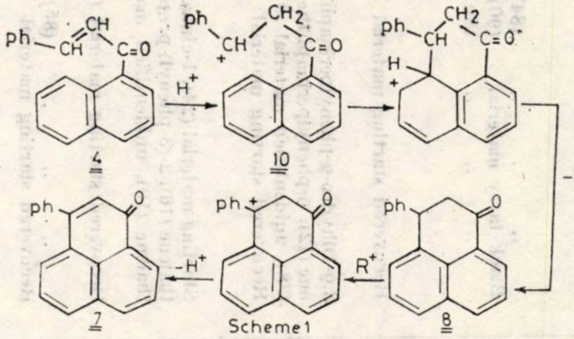

Scheme 1

(20%) (Table 1, Entry 6). The rearrangement [35-37] of cinnamoyl group from 2- to 1-position in the naphthalene ring is very interesting and can be explained in terms of the following mechanism (Scheme 2).

The fact that 1-cinnamoylnaphthalene (**4**), formed *via* rearrangement of **5**, did not undergo any further ring-closure reaction to **7**, can be attributed to the poisoning of the catalyst. However, this was confirmed by the formation of **7** and **8** from **5** upon the addition of fresh amount of $AlCl_3$ to the reaction mixture with further reflux for one hour.

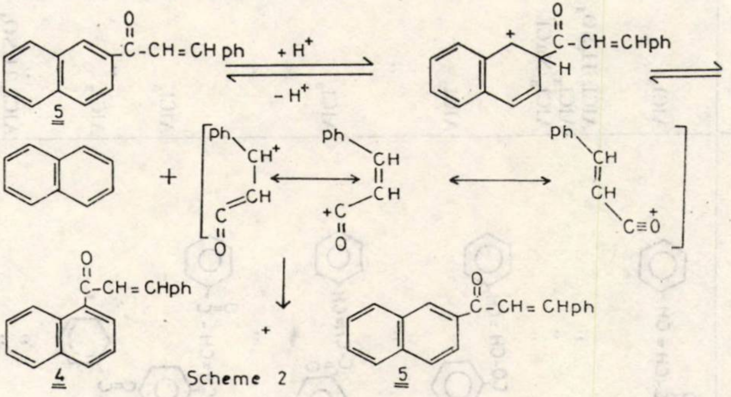

Scheme 2

The difference in the behaviour between **4** and **5** is rather interesting and deserves some comments. In the 1-isomer (**4**), the ring B is not directly attached to the carbonyl group and hence can serve as a site for electrophilic attack resulting finally in ring closure to **7** or **8**. In the 2-isomer, however, ring A, on which closure is expected to occur, is directly deactivated by the carbonyl group and thus ring closure is inhibited. Instead, migration of the cinnamoyl group from the 2- to 1-position constituted the major reaction. To shed more light on the reorientation of cinnamoyl group from 2- to 1-position, the behaviour of other acyl derivatives such

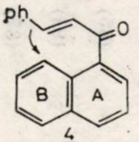

4

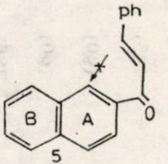

5

as 1-acetylnaphthalene **(11)**, 2-acetylnaphthalene **(12)**, 1-benzoylnaphthalene **(13)** and 2-benzoylnaphthalene **(14)** towards the effect of $AlCl_3$ in CS_2 at reflux temperature was also studied. We found that, under comparable conditions, no migration of either acetyl or benzoyl group took place (Table 2, Entries 1, 3, 5, 7). On the basis of these experiments, it was concluded that the migration of the cinnamoyl group is exceptionally easy due to its resonating ability (Scheme 2). Such resonance, in fact, facilitates the detatchment of this group leading to the migration from 2- to 1-position. We also conducted some experiments on the transacylation reactions between toluene and each of the following acyl derivatives : **11, 12, 13, 14, 15** (acetophenone) and **16** (benzophenone). Whereas no acylated toluene could be found with **11, 12, 13, 14** and **15**, some transacylation was noted with acetophenone (15%) and with benzophenone (18%) (Table 2, Entries 9—14).

To gain more insight into the concerned behaviour of aryl alkenyl ketones, the cyclization of the isomeric **6** under Friedel-Crafts conditions was investigated. Again, no ring closure products could be found (Table 1, Entries 9, 10). Whereas the failure to cyclize on the benzene ring is due to its deactivation by the carbonyl group, that on position 8 is due to the difficulty encountered in forming the carbocation **18** (Scheme 3) in which the position charge is adjacent to carbonyl group.

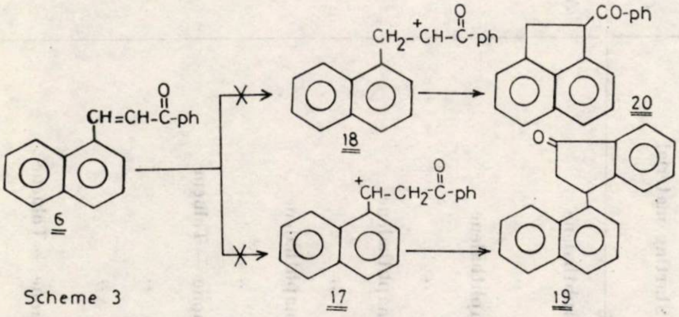

Scheme 3

In the light of the previous results with **3—6**, the reported closure of 1-benzoylcyclopentene **(21)**, [13] 1-benzoylcyclohexene **(22a)** [17, 23, 25] and 1-benzoylcycloheptene, [17] seemed to be either exceptional or in error. Accordingly, the case of **22a** was reinvestigated with the aid of modern methods of analysis. Benzoylcyclohexenes **(22a-c)** were prepared according to Christ and Fuson [38] *via* acylation of cyclohexene with benzoyl chloride in the presence of $AlCl_3$ followed by dehydrohalogenation of the crude

Table 2

Reorientation and transacylation of some aryl ketones

Entry No	Starting material	Reaction conditions				Product composition (%)	
		Catalyst	Solvent	Temp.	Time (hr)		
1	1-Acetylnaphthalene	$AlCl_3$	CS_2	Reflux	2	Recovered starting material	(92)
2	,, ,,	,,	Toluene	,,	2	,, ,, ,,	(85)
3	2-Acetylnaphthalene	,,	CS_2	,,		,, ,, ,,	(90)
4	,, ,,	,,	Toluene	,,	2	,, ,, ,,	(90)
5	1-Benzoylnaphthalene	,,	CS_2	,,	2	,, ,, ,,	(86)
6	,, ,,	,,	Toluene	,,	2	,, ,, ,,	(88)
7	2-Benzoylnaphthalene	,,	CS_2	,,	2	,, , ,	(87)
8	,, ,,	,,	Toluene	,,	2	,, ,, ,,	(85)
9	Acetophenone + Toluene	,,	CS_2	RT	24	,, ,, ,,	(94)
10	,, ,,	,,	CS_2	Reflux	24	,, ,, ,,	(87)
11	,, ,,	,,	Toluene	,,	2	,, ,, ,,	(60) Methyl acetophenones (13)
12	Benzophenone + Toluene	,,	CS_2	RT	24	,, ,, ,,	(94)
13	,, ,,	,,	CS_2	Reflux	24	,, ,, ,,	(89)
14	,, ,,	,,	Toluene	,,	2	,, ,, ,,	(71), Methyl benzophenone (18)

product with alcoholic potassium hydroxide. Contrary to the results of Christ and Fuson, [38] however, glc and mass spectrometric analysis revealed the reaction product to be a mixture of the three possible isomeric cyclohexenes (22a-c) in addition to small amount of benzophenone (16) Scheme 4. The formation of the dehydrogenation product (16) is not unexpected as similar behaviour was noted by other workers. [34]

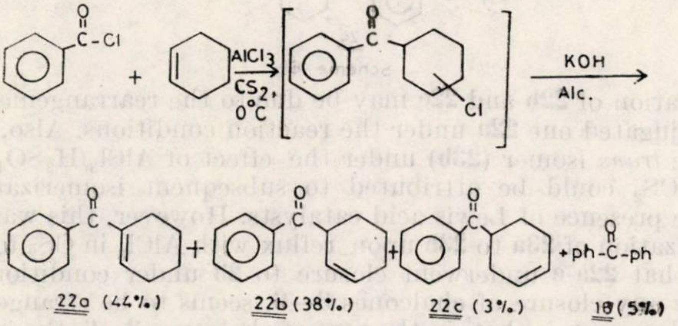
C-Cl
+
AlCl$_3$
CS$_2$,
0°C
Cl
KOH
Alc.
+ph-C-ph
22a (44%)
22b (38%)
22c (3%)
16 (5%)

When the isomeric mixture 22a-c was treated with H_3PO_4/HCOOH catalyst, under the conditions of Braude and Forbes, [17] the product obtained was 1,2,3,4-*cis*-10, 11-hexahydrofluorenone (23a, 80%) (Table 1, Entry 15). However, in contrast to Baker, [13] when the reaction was carried out in the presence of $AlCl_3$ in CS_2 solvent at room temperature no closure took place (Table 1, Entry 11). To gain more insight on the behaviour of **22a** under Friedel-Crafts conditions we also examined its reactions in the presence of H_2SO_4, H_3PO_4, $AlCl_3/H_2SO_4$ and $AlCl_3$ in refluxing CS_2. The closure to **23** successfully occurred and the product had the *trans* configuration with $AlCl_3/H_2SO_4$ and $AlCl_3$ catalysts in refluxing CS_2 but *cis* configuration with H_3PO_4 and H_2SO_4 (Table 1 Entries 14–16). The identification of **23 a** and **b** was confirmed using glc/mass spectrometry whereby the parent ions at m/e 186 and the fragmentation pattern

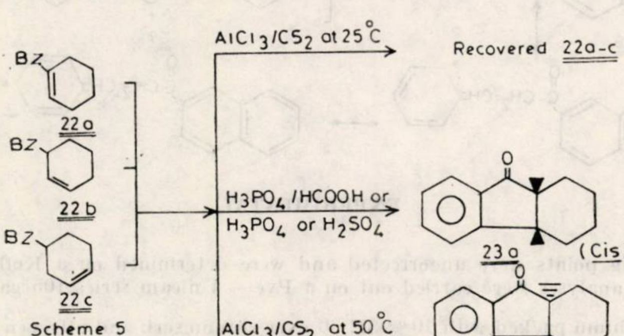
BZ
22a
BZ
22b
BZ
22c
AlCl$_3$/CS$_2$ at 25°C
Recovered 22a-c
H$_3$PO$_4$ /HCOOH or
H$_3$PO$_4$ or H$_2$SO$_4$
23a
(Cis)
AlCl$_3$/CS$_2$ at 50°C
or AlCl$_3$ / H$_2$SO$_4$
23b, (Trans)

Scheme 5

were in accord with the proposed structure. Also, the physical properties of the derivatives of 23 (*cis* or *trans*) were in agreement with the suggested configurations as reported by Braude and Forbes.[17] The closure of 22a

to **23** may proceed according to the mechanism of Pines and Douglas [29, 30] or *via* carbocation **24**, pathway A and B, respectively (Scheme 6).

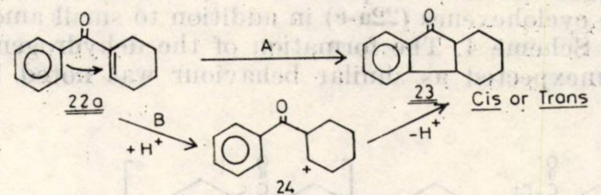

Scheme 6

The cyclization of **22b** and **22c** may be due to the rearrangement to most stable conjugated one **22a** under the reaction conditions. Also, the formation of the *trans* isomer **(23b)** under the effect of $AlCl_3/H_2SO_4$ or $AlCl_3$ in refluxing CS_2 could be attributed to subsequent isomerization of **23a** (*cis*) in the presence of Lewis acid catalysts. However, this was confirmed by isomerization of **23a** to **23b** upon reflux with $AlCl_3$ in CS_2 for one hour. The fact that **22a-c** underwent closure to **23** under conditions that did not induce any closure of chalcones **3**–**6**, seems to be strange. However, one possible reason is that, in the case of chalcones **3**–**6**, the intermediate benzylic carbocations **18, 25, 26,** are less electrophilic in nature than the ordinary carbocations **27** in the case of benzoylcyclohexenes. This is due to delocalization of the positive charge in **18**, **25** and **26** by resonance. Such resonance is of course, not possible in the case of cations **27**.

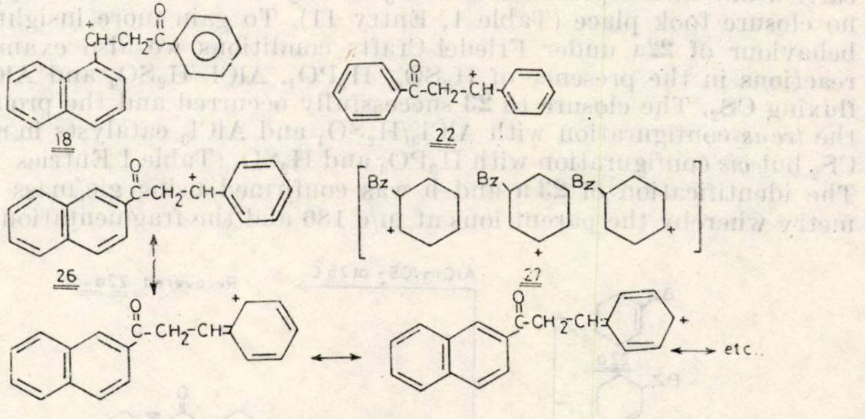

EXPERIMENTAL

All melting points were uncorrected and were determined on a Kofler melting point apparatus. GLC analyses were carried out on a Pye – Unicam series 105 gas chromatograph using $5' \times \frac{1''}{8}$ column packed with 10% SE 30 over chromosorb and nitrogen flow rate 60 mL/min. Separation of products was conducted also using 100 × 2 cm glass column packed with alumina or silica gel as well as 15 × 5 cm glass plates covered with thin film of silica gel. IR spectra were obtained using a Pye-Unicam SP-2000G spectrophotometer. UV spectra were recorded using Pye- Unicam SP-800 spectrophotometer. ^1H-NMR spectra were carried out in $CDCl_3$ and CCl_4 at 60 MHz using EM-360 and at 90 MHz EM-390-spectrometer. GC/MS data were recorded on Hewlett-Packard instrument (model 5992 A) at 70 eV.

Starting materials

The required substrates, benzylideneacetophenone **(3)**, [22] 1-cinnamoylnaphthalene **(4)**, [33] 2-cinnamoylnaphthalene **(5)**, [33] 3-(1-naphthyl) acrylophenone **(6)**, [39] 1-benzoylnaphthalene **(13)** [40] and 2-benzoylnaphthalene **(14)** [40] were prepared as outlined in the cited references.

Benzoylcyclohexenes **(22a-c)** [38] were prepared by dropwise addition of 133 g (0.98 mole) of $AlCl_3$ to a cold mixture of 130 g (1 mole) of benzoyl chloride and 86 g (1.04 mole) of cyclohexene in 600 mL CS_2 while stirring. After stirring for 6 hrs and decomposition with 10% HCl, the product was refluxed in 200 mL alcoholic 30% KOH solution for three hours. The alcohol was distilled and the residue was washed with water, dissolved in ether, dried and the ether was distilled at normal pressure. The residue was fractionated and the product (74 g, 40%) was collected at 147°C/ 8 mm Hg.

Glc/ mass spectrometric analysis showed four peaks, three of the same molecular ion (m/e 186) with fragmentation pattern in accord with the structure of 1-benzoylcyclohexene (**22a**, 44%), 3-benzoylcyclohexene (**22b**, 38%), and 4-benzoylcyclohexene (**22c**, 3%). The fourth product with m/e 186 was identified, using authentic sample, as benzophenone (5%).

1-Acetylnaphthalene **(11)**, 2-acetylnaphthalene **(12)**, acetophenone **(15)** and benzophenone **(16)** were reagent grade and were purchased from Fluka company (Switzerland).

Cyclization procedures

Attempted cyclization of benzylideneacetophenone (**3**) *with $AlCl_3$ in the presence of toluene* [28c]. A mixture of **3** (4.15 g, 0.02 mole) and $AlCl_3$ (4g, 03 mole) was refluxed in 100 mL toluene for two hours. The reaction mixture was decomposed as before and the starting material was recovered (**3**, 84%), Table 1, Entry 1.

Attempted cyclization of **3** *with $AlCl_3/H_2SO_4$ catalyst*. A solution of **3** (4.16 g, 0.02 mole) and $AlCl_3$ (3.24 g, 0.024 mole) in 50 mL carbon disulfide was stirred for 3 hrs at room temperature. The carbon disulfide was removed under reduced pressure and 30 mL of conc. sulfuric acid were added dropwise to the oily residue and the mixture was heated for further one hour at 90°C. The reaction product was cooled, decomposed and extracted with ether. Evaporation of ether afforded the starting material (**3**, 3.5 g., 84%), Table 1, Entry 2,.

Attempted cyclization of **3** *with $AlCl_3$ catalyst at 200°C*. A fused mixture of **3** (4.16 g, 0.02 mole) and $AlCl_3$ (3.24 g, 0.024 mole) was heated for one hour at 200°C. The reaction mixture was cooled to room temperature and decomposed by 10% cold HCl solution. The product was 4 g (80%) of black tarry material (Table 1, Entry 3).

Attempted cyclization of **3** *with $AlCl_3/NaCl$ catalyst*. A mixture of 1 g (0.016 mole) of NaCl and 4.5 g (0.033 mole) of $AlCl_3$ was fused, using direct flame; 3 g (0.01 mole) of **3** were added and then heated at 200°C for one hour. The mixture was decomposed as before and 2.7 g (90%) of black tarry material were isolated by filtration (Table 1, Entry 4).

Reaction of 1-cinnamoylnaphthalene (**4**) *with $AlCl_3$ in CS_2 at RT*. A mixture of 2.5 g (0.01 mole) of **4** and 1.6 g (0.012 mole) of $AlCl_3$ in 50 mL CS_2 was stirred at room temperature (RT) for two hours. After decomposition, **4** was recovered (2.2 g, 88%), Table 1, Entry 5.

Reaction of **4** *with $AlCl_3$ in CS_2 at reflux temperature*. A mixture of 5 g (0.02 mole) of **4** and 10 g (0.074 mole) $AlCl_3$ was refluxed in 200 mL CS_2 for two hours. After decomposition of the reaction mixture, the products were separated using column chromatography on neutral alumina. 8,9-Dihydro-9-phenylperinaphthen-7-one (**8**, 12%) was eluted with petroleum ether (60—80°C)-benzene mixture (1 : 1), mp 115°C (ethanol), IR absorption showed $\nu C = 0$ at 1715 cm^{-1}; UV absorption at λ_{max} 220 nm ($\in$ 1990) and λ_{max} 245 nm (ε 1990) characteristic for benzene and α,β-unsaturated ketones, respectively and ^1H-NMR spectrum : δ3.7—3.8 ppm (d, 2H, CH, α to $C = 0$), 4.7 — 4.0 ppm (t, 1H, CH); δ 7.2 ppm (m, 5H phenyl) and δ7.7——7.9 ppm (m, 6H, naphthyl). 9-Phenylperinaphthen-7-one (**7**, 38%) was eluted with benzene-ether mixture (1 : 1); Yellow crystals from ligroin, mp 143°C, IR absorption at 1690 cm^{-1}, $\nu C = 0$ in conjugation with two double bonds; UV absorption at λ_{max} 220 nm (ε 1300), λ_{max} 245 nm (ε 1800) and λ_{max} 360 nm (ε 1400) and ^1H-NMR spectrum : δ6.5—6.7 ppm (m, 5H, phenyl) and δ7.4 — 8.2 ppm (m, 7H, perinaphthenone moiety). Also, an unknown brown powder (8%) was eluted with ether-methanol mixture (8 : 2), mp 185°C (ethanol), Table 1, Entry 6.

Reaction of **5** *with $AlCl_3$ in CS_2 at RT*. A mixture of **5** (5 g, 0.02 mole) and $AlCl_3$ (3.2 g, 9.24 mole) in 100 mL CS_2 gave after stirring for two hours at room temperature 4 g (80%) of the starting material (Table 1, Entry 7).

Reaction of **5** *with $AlCl_3$ in CS_2 at reflux temperature.* **5** (5 g, 0.02 mole) was treated with $AlCl_3$ (10 g, 0.074 mole) in 200 mL CS_2 at reflux temperature for two hours. TLC showed five compounds in the product mixture. Column chromatography on neutral alumina gave the following fractions: 2-(3-phenylpropionyl) naphthalene (0.5 g, 10 %) eluted with pet. ether (60—80°C)-benzene mixture (4 : 1), mp and mmp 92°C, lit. [41] m.p. 92.5—94°C; 2-cinnamoylnaphthalene (**5**, 1.2 g, 24 %) eluted with pet. ether (60—80°C)-benzene mixture (1 : 1), m.p. as well as mmp 122°C; 1-cinnamoylnaphthalene (**4**, 0.8 g, 16 %) eluted with pet. ether (60—80°C)-benzene mixture (1 : 5), mp, mmp 105°C, lit. [33] mp 105°C; and finally 1 g of unidentified mixture (two spots in glc) was eluted with ether, mp 190—200°C (decomp.), Table 1; Entry 8.

Attempted cyclization of 3-(1-naplthyl) acrylophenone (**6**). Treatment of **6** (5 g, 0.02 mole) with $AlCl_3$ (5 g, 0.057 mole) in CS_2 (50 mL) for two hours at room or reflux temperatures gave only the starting ketone 6 (Table 1, Entries 9 and 10, respectively).

Cyclization of benzoylcyclohexenes (**22a-c**) *with $AlCl_3$*. A mixture of **22a-c** (3.7 g, 0.02 mole) and $AlCl_3$ (3.3 g, 0.024 mole) in 50 mL CS_2 was refluxed for two hours while stirring.

The product was 3.3 g (89 %) of 1,2,3,4-*trans*-10,11-hexahydrofluorenone (**23b**), the mass spectrum showed molecular ion peak at m/e 186 and the 2,4-dinitrophenylhydrazone derivative: mp 189°C, lit. [17] mp 190°C (Table 1, Entry 12).

Treatment of **22a-c** (3.7 g, 0.02 mole) with $AlCl_3$ (3.3 g, 0.024 mole) in 50 mL CS_2 at room temperature gave only the starting material (Table 1, Entry 11).

Cyclization of **22a-c** *with $AlCl_3/H_2SO_4$*. A mixture of **22a-c** (3.7 g, 0.02 mole) and $AlCl_3$ (3.3 g, 0.024 mole) was stirred for three hours at room temperature. The CS_2 was removed under reduced pressure, 10 mL of conc. sulfuric acid were added to the oily residue and then heated for one hour at 90°C on a water bath. The product was 2.1 g (73 %) of **23b**, identified as before (Table 1, Entry 13).

Cyclization of **22a-c** *with H_2SO_4*. Treatment of **22a-c** (3.7 g, 0.02 mole) with 20 mL H_2SO_4 for 24 hrs at room temperature gave 3 g of **23a**, bp 88°C/2 × 10^{-3} mm, lit. [17] bp 86°C/ 2 × $10\_^{3}$ mm, molecular ion peak at m/e 186 and 2,4-dinitrophenylhydrazone derivative mp 160°C, lit. [17] mp 158°C (Table 1, Entry 14).

Cyclization of **22a-c** *with $H_3PO_4/HCOOH$*. **22a-c** (2 g, 0.0107 mole) was added cautiously to an ice-cold mixture of phosphoric acid (4 g, 0.04 mole) and formic acid (14 g, 0.03 mole). The reaction was exothermic and the mixture gradually darkened. After leaving the reaction mixture overnight at room temperature, it was heated at 90°C for 6 hours, cooled, diluted with 100 mL ice-water mixture and extracted with ether. The product was 1.6 g (80 %) of **23a**, identified as before (Table 1, Entry 15).

Cyclization of **22a-c** *with H_3PO_4*. A mixture of **22a-c** (3.7 g, 0.02 mole) and H_3PO_4 (10 g, 0.1 mole, 100 %, solid) was kept at room temperature for 48 hours. The product was **23b** (2.5 g, 68 %) identified as before (Table 1, Entry 16).

Attempted reorientation of 1-acetylnaphthalene (**11**). A mixture of **11** (5 g, 0.02 mole) and $AlCl_3$ (10 g, 0.074 mole) in 100 mL CS_2 was refluxed for two hours, decomposed and treated as described earlier. The starting ketone was recovered (92 %) and no orientation products could be detected (Table 2, Entry 1). Similar treatment of **12, 13** and **14** gave also the starting ketones **12** (90 %), **13** (86 %) and **14** (87 %), respectively (Table 2, Entries 3, 5 and 7).

Attempted trans-*acetylation of toluene with 1-acetylnaphthalene* (**11**). Reflux of a mixture of **11** (4.2 g, 0.024 mole) and $AlCl_3$ (4, 0.029 mole) in 50 mL toluene was carried out for two hours. The product was 3.5 g (83 %) of the starting **11** and no methylacetophenones could be detected (Table 2, Entry 2).

Similarly, when 0.024 mole of each of **12, 13**. and **14** were treated separately with 0.029 mole of $AlCl_3$ in 50 mL toluene as described before with **11**, the starting ketones were recovered in 85 %, 90 % and 88 %, respectively (Table 2, Entries 4, 6 and 8).

Attempted trans-*acetylation of toluene with acetophenone* (**15**) *in CS_2*. Treatment of a mixture of **15** (2.4 g, 0.02 mole) and toluene (1.8 g, 0.02 mole) with $AlCl_3$ (3.3 g, 0.075 mole) in 100 mL CS_2 at room temperature for 24 hours with stirring gave only the starting ketone (**15**, 2.3 g, 94 %), Table 2, Entry 9. Also, repetition of this experiment at reflux temperature gave no *trans*-acetylation product and **15** was recovered (2.1 g, 87 %), Table 2, Entry 10.

trans-*Acetylation of toluene with acetophenone* (**15**). A mixture of **15** (6 g, 0.05 mole) and $AlCl_3$ (7.5 g, 0.055 mole) was refluxed in 100 mL of dry toluene for two hours. Fractional distillation of the crude product gave 3.6 g of **15** and 1.5 g (15 %) of a fraction of bp 215—224°C/atm. pressure. This fraction was identified, using glc and authentic samples, as *p*-methylacetophenones (3 : 1), Table 2, Entry 11.

Attempted trans-*benzoylation of toluene with benzophenone* (**15**) *in CS_2*. Treatment of **15** (3.6 g, 0.02 mole) and toluene (2 g, 0.02 mole) with $AlCl_3$ (3.3 g, 0.024 mole) in CS_2 for 24 hours at room temperature (Table 2, Entry 12) or at reflux temperature (Table 2, Entry 13) gave **15** in 94% yield and 89%, respectively, with no detectable amounts of *p*-methylbenzophones.

trans-*Benzoylation of toluene with benzophenone* (**16**). Treatment of **16** (9.1 g, 0.05 mole), in 100 mL toluene, with $AlCl_3$ (20 g, 0.15 mole) for two at reflux temperature gave using alumina gel column chromatography: 5 g (71%) of **16**, eluted with pet. ether (60–80°C) and 1.5 g (18%) were eluted with pet. ether (60–80°C)-benzene mixture (2 : 1) and identified using gcl and authentic samples as a mixture of *p*- and *m*-methylbenzophenones (4 : 1), Table 2, Entry 14.

REFERENCES

[1] K. Von Auwers and E. Risse, *Liebigs Ann. Chem.*, **502**, 282 (1953).
[2] A. Cohen and J. W. Cook, *J. Chem. Soc.*, **1935** 1570.
[3] L. I. Smith and W. W. Prichard, *J. Amer. Chem. Soc.*, **62**, 772 (1940).
[4] C. F. Koelsch and J. A. Anthes, J. *Org. Chem.*, **6**, 558 (1941).
[5] L. I. Smith and L. J. Spillane, *J. Amer. Chem. Soc.*, **65**, 202 (1943).
[6] C. D. Gutsche and W. S. Johnson, *J. Amer. Chem. Soc.*, **68**, 2239 (1946).
[7] J. Colonge and J. Chambion, *Bull. Soc. Chim. France.*, 999 (1947).
[8] P. A. Plattner, A. Furst and K. Jirasek, *Helv. Chim. Acta.*, **30**, 1320 (1947).
[9] J. Clonge and J. Chambion, *Compt. rend.*, **224**, 128 (1947).
[10] J. H. Burckhalter and R. C. Fuson, *J. Amer Chem. Soc.*, **70**, 4184 (1948).
[11] J. Colonge and E. Grimaud, *Bull. Soc. Chim. France.*, 857 (1951).
[12] L. I. Smith and P. N. Gordon, *J. Amer. Chem. Soc.*, **73**, 3747 (1951).
[13] W. Baker and P. G. Jones, *J. Chem. Soc.*, **1951**, 787.
[14] G. Baddley, G. Holt and S. M. Maker, *J. Chem. Soc.*, **1952**, 3289.
[15] W. S. Johnson, D. K. Banerjee, W. P. Schneider, C. D. Gutsche, W. E. Shelberg and L. J. Chinn, *J. Amer. Chem. Soc.*, **74**, 2832 (1952).
[16] G. Baddeley, G. Holt, S. M. Maker and M. C. Ivinson, *J. Amer. Chem. Soc.*, **74**, 3605 (1952).
[17] E. A. Braude and W. F. Forbes, *J. Chem. Soc.*, **1953**, 2208.
[18] G. Baddely, S. M. Maker and M. G. Ivinson, *J. Chem. Soc.*, **1953**, 3959.
[19] G. Baddely and R. Williamson, *J. Chem. Soc.* **1953**, 2120.
[20] H. Khastgir, S. M. Makherji and B. K. Bhattacharyya, *Indian Chem. Soc.*, **31**, 351 (1954).
[21] W. E. Parham, El. Wheeler and R. M. Dodson, *J. Amer. Chem. Soc.*, **77**, 1166 (1956).
[22] R. W. Layer and L. R. Mac. Greogor, *J. Org. Chem.*, **21**, 1120 (1956).
[23] E. D. Bergmann, *Bull. Res. Council. Israel*, **5A**, 150 (1956); *Chem. Abstr.*, **50**, 15493 (1956).
[24] R. M. Granger, J. Vinas and P. Nau, *Compt. rend.*, **244**, 1048 (1957).
[25] E. D. Bergmann and R. Ikan, *J. Amer. Chem. Soc.*, **83**, 5803 (1958).
[26] S. M. Mahar, H. F. Bassilios and A. Y. Salem, *J. Chem. Soc.*, **1958**, 2437.
[27] a. H. Gilman and J. F. Nelson, *Rec. Trav. Chim.*, **55**, 518 (1936); b-S. A. Fine and R.L. Stern, *J. Org. Chem.*, **32**, 4132 (1967).
[28] a. L. R. C. Barelay, K. L. Adams, H. M. Foote, E. C. Sanford and R. H. Young, *Canad. J. Chem.*, **48**, 2763 (1970); b.H. O. House, V. Pargamian, R. S. Ro and D. J. Wluka, *J. Amer. Chem. Soc.*, **82**, 1457 (1960) and references cited therein, c. A. Sammour and M. Elkasaby, *U.A.R.J. Chem.*, **13**, 409 (1970).
[29] S. H. Pines and A. W. Donglas, *J. Amer. Chem. Soc.*, **98**, 8119 (1976).
[30] S. H. Pines and A. W. Douglas, *J. Org. Chem.*, **43**, 3127 (1978).
[31] A. A. Khalaf and A. M. A. El-Khawaga, *Rev. Roumaine Chim.*, **26**, 739 (1981).
[32] E. P. Kohler and H. M. Chadwell, *Org. Syn. Coll.*, **1**, 77 (1944).
[33] C. F. Koelsch and J. A. Anthes, *J. Org. Chem.*, **6**, 558 (1941).
[34] L. R. C. Barclay and C. C. Stanford, *Canad. J. Chem.*, **46**, 3315 (1968), *ibid.* **46**, 3325 (1968).
[35] J. Kagan, D. A. Agdeppa, S. P. Singh, D. A. Mayers, C. Boyallan, C. Poor Ker and B. E. Firth, *J. Amer. Chem. Soc.*, **99**, 4581 (1976).
[36] J. M. Domagala, R. D. Bach and J. Wemple, *J. Amer. Chem. Soc.*, **98**, 1975 (1976).
[37] J. N. Marx, J. C. Argyle and L. R. Norman, *J. Amer. Chem. Soc.*, **96**, 2121 (1974).
[38] R. E. Christ and R. C. Fuson, *J. Amer. Chem. Soc.*, **59**, 893 (1937).
[39] R. E. Lutz, T. A. Mortin, J. F. Codington, T. M. Amacker, R. I. Allison, N. H. Leake, R. J. Rowlett, J. D. Smith and J. W. Wilson, *J. Org. Chem.*, **14**, 982 (1949).
[40] I. Helbron and H. M. Bunbury, "Dictionary of organic compounds". Vol. III Eyre and Spottis woode (London), 1946.
[41] T. L. Jacobs and S. Singer, *J. Org. Chem.*, **17**, 475 (1952).

gave 15 in 94% yield and 59%, respectively, with no detectable amounts of p-methylbenzophenones.

Transacylation of toluene with benzophenone (15). Treatment of 16 (9.1 g, 0.05 mole), in 100 ml toluene, with AlCl$_3$ (20 g, 0.15 mole) for two at reflux temperature were using alumina gel column chromatography: 3 g (71%) of 16, eluted with pet. ether (60–80°C) and 1.5 g (18%) were eluted with pet. ether (60–80°C)-benzene mixture (2 : 1) and identified using gel and authentic samples as a mixture of p- and m-methylbenzophenones (4 : 1), Table 2, Entry 14.

REFERENCES

[1] K. Von Auwers and E. Risse, Liebigs Ann. Chem. 502, 282 (1933).
[2] A. Cohen and J. W. Cook, J. Chem. Soc., 1935 1570.
[3] L. I. Smith and W. W. Prichard, J. Amer. Chem. Soc., 62, 772 (1940).
[4] C. F. Koelsch and J. A. Anthes, J. Org. Chem., 6, 558 (1941).
[5] L. I. Smith and L. J. Spillane, J. Amer. Chem. Soc. 65, 202 (1943).
[6] C. D. Gutsche and W. S. Johnson, J. Amer. Chem. Soc., 68, 2239 (1946).
[7] J. Colonge and J. Chambion, Bull. Soc. Chim. France, 999 (1947).
[8] P. A. Plattner, A. Fürst and K. Jirasek, Helv. Chim. Acta, 30, 1320 (1947).
[9] J. Colonge and J. Chambion, Compt. rend. 224, 128 (1947).
[10] J. H. Burckhalter and R. C. Fuson, J. Amer. Chem. Soc. 70, 4184 (1948).
[11] J. Colonge and E. Grimaud, Bull. Soc. Chim. France, 857 (1954).
[12] L. I. Smith and P. S. Gordon, J. Amer. Chem. Soc., 73, 3747 (1951).
[13] W. Baker and P. G. Jones, J. Chem. Soc., 1954, 787.
[14] G. Baddeley, G. Holt and S. M. Makar, J. Chem. Soc., 1952, 3289.
[15] W. S. Johnson, D. K. Banerjee, W. P. Schneider, C. D. Gutsche, W. E. Shelberg and L. J. Chinn, J. Amer. Chem. Soc., 74, 2832 (1952).
[16] G. Baddeley, G. Holt, S. M. Makar and M. G. Ivinson, J. Amer. Chem. Soc., 74, 3605 (1952).
[17] E. A. Braude and W. F. Forbes, J. Chem. Soc., 1953, 2208.
[18] G. Baddeley, S. M. Makar and M. G. Ivinson, J. Chem. Soc., 1953, 3969.
[19] G. Baddeley and R. Williamson, J. Chem. Soc. 1953, 2120.
[20] D. Nasipuri, S. M. Mukherji and B. K. Bhattacharyya, Indian Chem. Soc. 31, 581 (1954).
[21] W. E. Parham, H. Wheeler and R. M. Dodson, J. Amer. Chem. Soc., 77, 1166 (1955).
[22] F. W. Lauer and L. R. MacGregor, J. Org. Chem., 21, 1120 (1956).
[23] E. D. Bergmann, Bull. Res. Council Israel, 5A, 130 (1956); Chem. Abstr., 50, 15493 (1956).
[24] R. M. Gerner, J. Vinas and P. Nam, Compt. rend., 245, 1043 (1957).
[25] E. D. Bergmann and H. Ilan, J. Amer. Chem. Soc., 80, 5603 (1958).
[26] S. M. Makar, H. A. Basilios and A. Y. Salem, J. Chem. Soc., 1958, 2187.
[27] a H. Gilman and J. F. Nelson, Rec. Trav. Chim., 55, 518 (1936); b S. A. Fine and H. L. Stern, J. Org. Chem. 32, 4132 (1967).
[28] a L. R. C. Barclay, N. D. Adams, H. M. Foote, E. C. Sanford and D. H. Young, Canad. J. Chem. 48, 2763 (1970); b H. O. House, V. Paragamian, R. S. Ro and D. J. Wluka, J. Amer. Chem. Soc., 82, 1457 (1960) and references cited therein; c A. Salmoun and M. Elkassaby, Indian J. Chem., 13, 409 (1975).
[29] S. H. Pines and A. W. Douglas, J. Amer. Chem. Soc., 98, 8119 (1976).
[30] S. H. Pines and A. W. Douglas, J. Org. Chem., 43, 3127 (1978).
[31] A. A. Khalaf and M. A. El-Khawaga, Rev. Roumaine Chim., 26, 739 (1981).
[32] E. P. Kohler and H. M. Chadwell, Org. Syn. Coll., 1, 77 (1941).
[33] C. F. Koelsch and J. A. Anthes, J. Org. Chem., 6, 558 (1941).
[34] L. R. C. Barclay and E. C. Sanford, Canad. J. Chem., 46, 3315 (1968); ibid 46, 3325 (1968).
[35] J. Kagan, D. A. Agdeppa, S. P. Singh, D. A. Mayers, C. Boyajian, C. Poorker and B. E. Firth, J. Amer. Chem. Soc., 98, 4581 (1976).
[36] J. M. Domagala, R. D. Bach and J. Wemple, J. Amer. Chem. Soc. 98, 1975 (1976).
[37] J. N. Marx, J. C. Argyle and L. R. Norman, J. Amer. Chem. Soc., 96, 2121 (1974).
[38] R. E. Christ and R. C. Fuson, J. Amer. Chem. Soc., 59, 893 (1937).
[39] R. E. Lutz, T. A. Martin, J. F. Codington, T. M. Amacker, R. K. Allison, N. H. Leake, R. J. Rowlett, J. D. Smith and J. W. Wilson, J. Org. Chem., 14, 982 (1949).
[40] I. Heilbron and H. M. Bunbury, "Dictionary of organic compounds" Vol. III Eyre and Spottiswoode (London), 1946.
[41] T. L. Jacobs and S. Singer, J. Org. Chem., 17, 475 (1952).

Revue Roumaine de Chimie, 30, 7, 611–615 (1985)

DÉRIVÉS DIPOLAIRES EN SÉRIE QUINAZOLINIQUES. IV[1]

LES RÉACTIONS DE CYCLOADDITION [3 + 2] DIPOLAIRE DE QUELQUES QUINAZOLINIUM-3-(*p*-R-BENZOYLE)MÉTHYLURES AVEC DES ACÉTYLÈNES ACTIVÉS

E. I. GEORGESCU[a], FLORENTINA GEORGESCU[a], M. GHEORGHIU[b],
E. G. GEORGESCU[c] et MAGDA PETROVANU[d]

[a] Centre de Recherches, Rimnicu Vilcea, Rue Uzinei 1, Roumanie
[b] Institut Polytechnique, Bucarest, Roumanie
[c] Institut Central de Chimie, Bucarest, Roumanie
[d] Institut Polytechnique, Jassy, Roumanie

Reçu le 21 juillet 1984

Le travail présente l'obtention de nouveaux dérivés pyrrolo [1,2-c]quinazoliniques par les réactions de cycloaddition [3 + 2] dipolaire de quelques quinazolinium-ylures avec des acétylènes activés et une nouvelle voie pour la réalisation de ces réactions en partant des méthanolates 1. On présente le mécanisme de la formation des quinazolinium-ylures à partir des méthanolates 1.

The paper presents the synthesis of new pyrrolo [1,2-c] quinazoline derivatives by the [3 + 2] dipolar cycloaddition of certain quinazolinium-ylides with activated acetylenes and a new preparation way of these derivatives starting from methanolates 1. The mechanism of the quinazolinium-ylides formation from methanolates 1 is described.

Dans des travaux antérieurs [2,3] on a présenté les synthèses de
elques dérivés pyrrolo [1,2-c] quinazoliniques par les réactions de
cloaddition [3 + 2] dipolaire de certains quinazolinium-3-(*p*-R-bénzo-
e) méthylures formés „in situ" avec des acétylènes activés. Pour l'ob-
tion des dérivés pyrrolo [1,2-c] quinazoliniques on est parti de la qui-
zoline, des bromures de phénacyle *p*-substitués respectifs et du dérivé
étylénique, utilisant comme agent de déhydrobromuration et comme
vant un époxyde. On a proposé un mécanisme réactionnel qui suppose
formation initiale des sels quaternaires **2**, qui donnent naissance par
hydrobromuration aux dérivés yluriques **3** et ceux-ci avec le dérivé
tylénique conduisent aux produits **10**–**12**. De même, on a montré
les essais d'isoler les quinazolinium-3-(*p*-R-benzoyle) méthylures **3**
échoué à cause de l'instabilité de ces composés.

En étudiant les possibilités d'obtention des sels quaternaires de
nazolinium **2** [1] par la réaction de la quinazoline avec les bromures de
énacyle *p*-substitués on a précisé que nous n'avons pas pu isoler les

sels quaternaires **2** à l'état pur. Pourtant ces sels ont été obtenus à l'état des méthanolates **1**, en effectuant la réaction de quaternisation dans le méthanol.

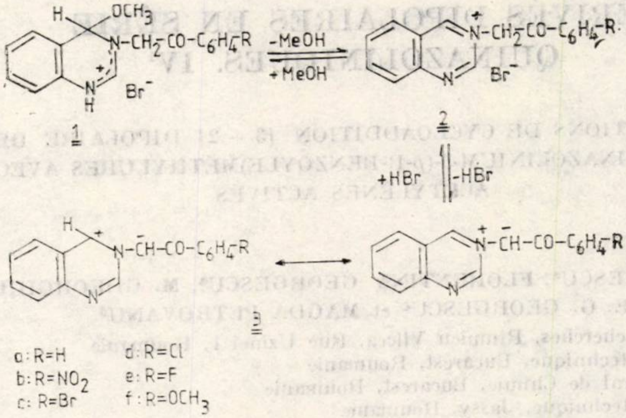

Dans ce travail on présente la synthèse de nouveaux dérivés pyrrolo [1,2-c] quinazoliniques par les réactions de cycloaddition [3 + 2] dipolaire de quelques quinazolinium-3-(*p*-R-benzoyle) méthylures **3** avec des acétylènes activés et une nouvelle voie pour la réalisation de ces réactions en partant des méthanolates **1** et des acétylènes activés. De même, on présente le mécanisme de la formation des quinazolinium-ylures à partir des méthanolates respectifs.

Comme on l'a déjà montré, [1] en solution il y a un équilibre entre les méthanolates **1** et les bromures **2.** Dans les solvants organiques usuels l'équilibre est déplacé en faveur des méthanolates **1.** Mais cet équilibre suggère la possibilité de l'apparition des quinazolinium-3-(*p*-R-benzoyle) méthylures **3** par déhydrobromuration des bromures du 3-(*p*-R-phénacyle) quinazolinium **2.** Ces intermédiaires pourraient être mis en évidence par les produits de la réaction si l'on trouvait des réactants appropriés dans le milieu réactionnel.

Pour capter les quinazolinium-3-(*p*-R-benzoyle)méthylures **3** nous avons utilisé des agents dipolarophiles réactifs comme l'acétylènedicarboxylate de méthyle, le propiolate d'éthyle et la phényle-éthynylecétone. Utilisant des bases usuelles (carbonates et bicarbonates, ou des amines tertiaires) et divers solvants, nous n'avons par réussi à obtenir les cycloadducts. C'est pourquoi nous avons utilisé comme accepteurs d'acide des époxides comme le propylène oxyde et le 1,2-butylène oxyde. Ceux-ci donnent naissance aux ylures des sels quaternaires avec une vitesse beaucoup plus faible, de telle manière que l'ylure sera consommé pendant la réaction avec l'agent dipolarophile à mesure qu'il se forme. De plus, les époxydes se sont révélés de très bons solvants pour les réactions de cycloaddition. [1, 2, 4]

Ainsi, par la réaction des méthanolates **1a-f** avec l'acétylènedicarboxylate de méthyle, la phényle-éthynyle-cétone et respectivement le propiolate d'éthyle, on a obtenu les cycloadducts **10**a-e, **11**a-f resp. **12**a-f. Le produit ayant la structure **10**f n'a pas pu être isolé.

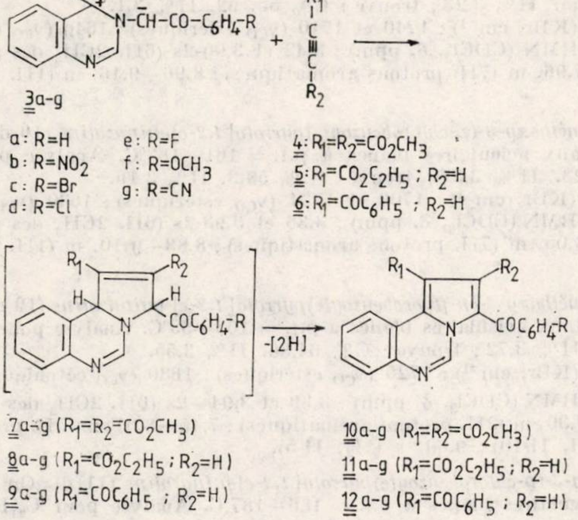

Les cycloadducts **10**g, **11**g et **12**g ont été obtenus par la réaction de la quinazoline avec la ω-brome-*p*-cyanoacétophénone et l'agent dipolarophile acétylénique dans l'époxyde, d'après la méthode décrite antérieurement, [2] parce qu'on n'a pu isoler ni le bromure **2**g, ni le méthanolate **1**g. Ce dernier procédé implique l'obtention ,,in situ'' des sels quaternaires et des ylures et conduit, avec de bons résultats, à des cycloadducts, spécialement dans le cas des bromures de phénacyle très réactifs comme la ω-brome-*p*-nitroacétophénone et la ω-brome-*p*-cyanoacétophénone.

Les analyses élémentaires, les spectres IR et ^{1}H-RMN confirment les structures proposées pour ces cycloadducts.

Donc, les dérivés pyrrolo[1,2-c] quinazolinique peuvent être obtenus d'une manière relativement simple soit par la réaction de la quinazoline avec des dérivés α-halogénocarbonyliques et des acétylènes activés dans l'époxyde, soit par la réaction des méthanolates **1** avec des acétylènes activés dans l'époxyde. Les deux méthodes supposent la formation intermédiaire des sels quaternaires de quinazolinium, respectivement des quinazolinium-ylures.

PARTIE EXPÉRIMENTALE

Les méthanolates **1** ont été obtenus d'après le procédé décrit dans un travail antérieur. Les spectres IR ont été enregistrés sur un spectromètre Perkin Elmer 621-A et les spectres[1] ^{1}H-NMR sur un spectromètre Varian EM 360.

Les points de fusion ne sont pas corrigés.

L'obtention des 3-(p-R-benzoyle)pyrrolo[1,2-c]quinazolines **10—12**. À une suspension de méthanolates **1** (10 mmoles) dans l'époxyde (30 ml) on ajoute 10 mmoles dérivé acétylénique (**4—6**) et on agite 5 jours à la température ambiante. On évapore la moitié du solvant et on ajoute goutte à goutte, sous agitation, 5—10 ml éther éthylique. Le précipité est filtré, lavé sur le filtre avec 5 ml éther éthylique et récristallisé.

1,2-Dicarbométhoxy-3-(p-bromobenzoyle)pyrrolo[1,2-c]quinazoline (**10**c). On obtient 1,12 g (rend. 24 %) de cristaux aciculaires blancs à p. f. = 173—174,5°C. Analyse pour $C_{22}H_{15}N_2O_5Br$: calculé : C% 56,55, H% 3,23 ; trouvé : C% 55, 92, H% 3,1.

Spectre IR (KBr, cm^{-1}) : 1740 et 1710 (ν_{CO} éstériques) ; 1649 (ν_{CO} cétonique).

Spéctre ^1H-RMN ($CDCl_3$, δ, ppm) : 3,42 et 3,99-2s (6H, $2CH_3$ des groupements carbométhoxy) ; 7,60—7,96, m (7H, protons aromatiques) ; 8,96—9,16, m (1H, H-10) ; 9,66, s (1H, H-5).

1,2-Dicarbométhoxy-3-(p-chlorobenzoyle)pyrrolo[1,2-c]quinazoline (**10** d). On obtient 0,84 g (rend. 20 %) cristaux aciculaires blancs à p.f. = 161—163°C. Analyse pour $C_{22}H_{15}N_2O_5Cl$: calculé : C% 58,23, H% 3,37 ; trouvé : C% 58,3, H% 3,15.

Spectre IR (KBr, cm^{-1}) : 1700 et 1734 (ν_{CO} estériques) ; 1630 (ν_{CO} cétonique).

Spectre ^1H-RMN ($CDCl_3$, δ, ppm) : 3,36 et 3,93-2s (6H, $2CH_3$ des groupements carbométhoxy) ; 7,30—8,05, m (7H, protons aromatiques) ; 8,83—9,10, m (1H, H-10) ; 9,61, s (1H, H-5).

1,2-Dicarbométhoxy-3-(p-fluorobenzoyle)pyrrolo[1,2-c]-quinazoline (**10** e). On obtient 1,19 g (rend. 29,4 %) cristaux aciculaires blancs à p.f. = 163—65°C. Analyse pour $C_{22}H_{15}N_2O_5F$: calculé : C% 65,02, H% 3,72 ; trouvé : C% 64,86, H% 3,55.

Spectre IR (KBr, cm^{-1}) : 1725 (ν_{CO} estériques) ; 1630 (ν_{CO} cétonique).

Spectre ^1H-RMN ($CDCl_3$, δ, ppm) : 3,39 et 3,94—2s (6H, $2CH_3$ des groupements carbométhoxy) ; 6,96—7,30, m (2H, protons aromatiques) ; 7,45—8,01, m (5H, protons aromatiques) ; 8,85—9,06, m (1H, H-10) ; 9,60, s (1H, H-5).

1-Carbéthoxy-3-(p-chlorobenzoyle)pyrrolo[1,2-c]quinazoline (**11** d). On obtient 1,1 g (rend. 29 %) cristaux aciculaires blancs à p.f. = 186—187°C. Analyse pour $C_{21}H_{15}N_2O_3Cl$: calculé : C% 66,58, H% 3,99 ; trouvé : C% 66,4, H% 3,75.

Spectre IR (KBr, cm^{-1}) : 1712 (ν_{CO} estérique) ; 1630 (ν_{CO} cétonique).

Spectre ^1H-RMN ($CDCl_3$, δ, ppm) : 1,42, tr (3H, CH_3 du groupement éthyle estérique) ; 4,40, q (2H, CH_2 du groupement éthyle éstérique) ; 7,38—7,97, m (8H, protons aromatiques) ; 9,48—9,71, m (1H, H-10) ; 10,15, s (1H, H-5).

1-Carbéthoxy-3-(p-fluorobenzoyle)pyrrolo[1,2 c]quinazoline (**11** e). On obtient 0,96 g (rend. 26,5 %) de cristaux jaune pâle à p.f. = 174,5—176°C. Analyse pour $C_{21}H_{15}N_2O_3F$: calculé : C% 69,6, H% 4,17 ; trouvé : C% 69,41, H% 3,97.

Spectre IR (KBr, cm^{-1}) : 1705 (ν_{co} estérique) ; 1630 (ν_{co} cétonique).

Spectre ^1H-RMN ($CDCl_3$, δ, ppm) : 1,43, tr., (3H, CH_3 du groupement éthyle estérique) ; 4,43, q (2H, CH_2 du groupement éthyle estérique) ; 7,10—7,46, m (2H, protons aromatiques) ; 7,61—8,13, m (6H, protons aromatiques) ; 9,63—9,86, m (1H, H-10) ; 10,27, s (1H, H-5).

1-Benzoyle-3-(p-chlorobenzoyle)pyrrolo[1,2-c]quinazoline (**12** d). On obtient 1,64 g (rend. 40 %) de cristaux blancs à p.f. = 190,5—192°C. Analyse pour $C_{25}H_{15}N_2O_2Cl$: calculé : C% 73,08, H% 3,68 ; trouvé : C% 73,12, H% 3,7.

Spectre IR (KBr, cm^{-1}) : 1605 et 1622 (ν_{co} cétoniques).

Spectre ^1H-RMN ($CDCl_3$, δ, ppm) : 7,25—8,09, m (13H, protons aromatiques) ; 8,74—8,98, m (1H, H-10) ; 10,30, s (1H, H-5).

1-Benzoyle-3-(p-fluorobenzoyle)pyrrolo[1,2-c]quinazoline (**12** e). On obtient 1,62 g (rend. 41 %) de cristaux blancs à p.f. = 165—167°C. Analyse pour $C_{25}H_{15}N_2O_2F$: calculé : C% 76,13, H% 3,83 ; trouvé : C% 75,95, H% 3,66.

Spectre IR (KBr, cm^{-1}) : 1597 et 1615 (ν_{co} cétoniques).

Spectre ^1H-RMN ($CDCl_3$, δ, ppm) : 7,03—8,06, m ((13H, protons aromatiques) ; 8,68—8,91, m (1H, H-10) ; 10,22, s (1H,H-5).

L'obtention des 3-(p-R-benzoyle)pyrrolo[1,2-c]quinazolines **10**g, **11**g et **12**g

Pour l'obtention de ceux qu'on a produits on est parti directement de la quinazoline, le bromure de phénacyle *p*-substitué et l'agent dipolarophile acétylénique dans l'époxyde, d'après le procédé décrit antérieurement. [2]

1,2-Dicarbométhoxy-3-(p-cyanobenzoyle)pyrrolo[1,2]quinazoline (**10** g). On obtient 0,71 g (rend. 17,1 %) de cristaux jaune pâle à p.f. = 222—223°C. Analyse pour $C_{23}H_{15}N_3O_5$: calculé : C% 66,82, H% 3,65 ; trouvé : C% 66,72, H% 3,70.

Spectre IR (KBr, cm^{-1}) : 1730 et 1716 (ν_{co} estériques) ; 1615 (ν_{co} cétonique) ; 2207 (ν_{CN}).

Spectre ^1H-RMN ($CDCl_3$, δ, ppm) : 4,38 et 4,98–2s (6H, 2 CH_3 des groupements carbométhoxy) ; 8,61–9,16, m (7H, protons aromatiques) ; 9,92–10,24, m (1H, H-10) ; 10,85, s (1H, H-5).

*1-Carbéthoxy-3-(*p*-cyanobenzoyle)pyrrolo[1,2-c]quinazoline* (**11** g). On obtient 0,82 g (rend. 22 %) de cristaux jaunes à p.f. 235–236°C. Analyse pour $C_{22}H_{15}N_3O_2$: calculé : C % 71,53, H % 4,09 ; trouvé : C % 71,41, H % 3,98.

Spectre IR (KBr, cm^{-1}) : 1712 (ν_{co} estérique) ; 1629 (ν_{co} cétonique) ; 2210 (ν_{CN}).

Spectre ^1H-RMN ($CDCl_3$, δ, ppm) : 1,47, tr (3H, CH_3 du groupement éthyle estérique) ; 4,45, q (2H, CH_2 du groupement éthyle estérique) ; 7,61–8,20, m (8H, protons aromatiques) ; 9,69–9,94, m (1H, H-10) ; 10,36, s (1H, H-5).

*1-Benzoyle-3-(*p*-cyanobenzoyle)pyrrolo[1,2-c]quinazoline* (**12** g). On obtient 09,7 g (rend. 24,1 %) de cristaux aciculaires jaunes à p.f. = 258–259°C. Analyse pour $C_{26}H_{15}N_3O_2$; calculé : C % 77,79, H % 3,76 ; trouvé : C % 77,62, H % 3,66.

Spectre IR (KBr, cm^{-1}) : 1600 et 1623 (ν_{co} cétoniques) ; 2207 (ν_{CN}).

Spectre ^1H-RMN ($CDCl_3$, δ, ppm) : 7,41–8,13, m (13H, protons aromatiques) ; 8,77–9,05, m (1H, H-10) ; 10,46, s (1H, H-5).

Les propriétés physiques et spectrales des cycloadducts **10**a-b, **11**a-c, **12**a-c et **12**f ont été décrits dans des travaux antérieurs, [2, 3]

BIBLIOGRAPHIE

[1] Troisième partie : E. I. Georgescu, F. Georgescu, F. Chiraleu et M. Petrovanu, *Rev. Roumaine Chim.*, **28**, 841 (1983).

[2] E. I. Georgescu, I. Druţă et M. Petrovanu, *Rev. Roumaine Chim.*, **26**, 109 (1981).

[3] E. I. Georgescu, I. Druţă et M. Petrovanu, *Bulet. Inst. Politehnic Iaşi*, **tom. XXVII** (XXXI) fasc. 3–4, sect. II, p. 81 (1981).

[4] F. Georgescu, F. Chiraleu, E. I. Georgescu et I. Zugrăvescu, *Rev. Roumaine Chim.*, **26**, 879 (1981).

Revue Roumaine de Chimie, 30, 7, 617–622 (1985)

ESTERIFICACION DE ACIDOS BENZOICOS MONOSUSTITUIDOS, UTILIZANDO ORTOFOSFATOS DE ALUMINIO TIPO "KEARBY", COMO CATALIZADOR

M. S. ARIAS-PEREZ,[a] C. FERNANDEZ-SANCHEZ[a] y J. M., MARINAS[b)]

a) Departamento de Quimica Orgánica de la Facultad de Ciencias Quimicas de la Universidad Complutense de Madrid — España

b) Departamento de Quimica Orgánica de la Facultad de Ciencias de la Universidad de Córdoba — España

Recibido, el 27 de mayo de 1984

Se ha efectuado la esterificación de los ácidos nitro, amino y metoxi benzóicos, con *n*-butanol, utilizando como catalizador un ortofosfato de aluminio de textura y acidez controlada. Los rendimientos obtenidos son buenos, en todos los casos, aunque los mejores resultados se logran con el ácido *p*-nitro benzóico. En el trabajo se comentan, brevemente, los resultados obtenidos.

Esterification of nitro, amino and metoxybenzoic acids with *n*-butanol has been carried out with aluminium orthophosphate of controlled texture and acidity as catalyst. Yields were reasonably high for all of them especially for *p*-nitrobenzoic acid. The results obtained are briefly described in this report.

INTRODUCCION

La reacción de esterificación de ácidos benzóicos *o*-, *m*-y *p*-sustituidos con diferentes alcoholes, ha sido estudiada empleando diferentes catalizadores de naturaleza homogénea [1] o heterogénea. [2]

En trabajos precedentes [3,4] hemos puesto de manifiesto la utilidad de los ortofosfatos de aluminio tipo Kearby [5], como catalizadores de procesos de esterificación, bien con los reaccionantes orgánicos en fase líquida o en fase vapor. En el presente trabajo hemos realizado la esterificación de diferentes ácidos benzóicos sustituidos en *orto*, *meta* y *para*, con alcohol *n*-butilico. Los grupos sustituyentes : nitro, amino u metoxilo nos han permitido el estudio de la influencia de los efectos eléctricos y estéricos de los grupos en el proceso que nos ocupa.

De acuerdo con un mecanismo de esterificación $A_{Ac}2$ y representando a los centros ácidos del catalizador por Cat $\oplus$, el proceso se podría esquematizar en la forma que se indica :

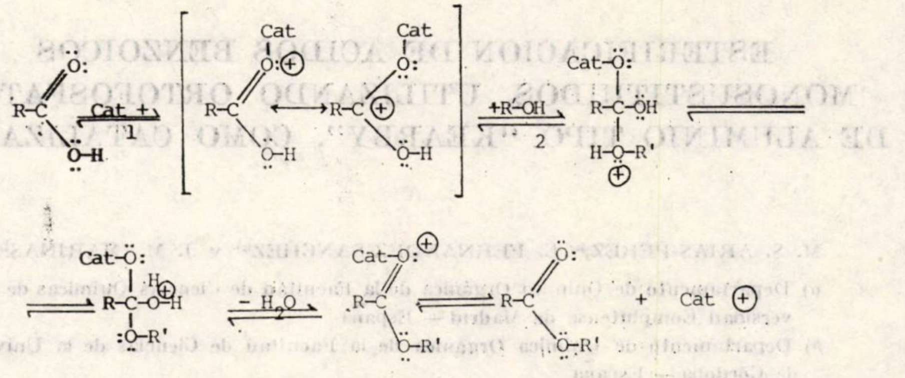

Si el paso determinante del proceso fuera 1, considerado clásicamente como de ,,protonación'' ; en este caso se formará un carbocatión más o menos desarrollado, dependiendo de la acidez del centro catalizador sobre el que se fije el ácido carboxílico, la esterificación transcurrirá mejor cuando se empleen ácidos carboxílicos con grupos dadores de electrones.

Por el contrario, si la fase determinante fuera 2, es decir, el ataque nucleófilo del alcohol, la reacción se producirá tanto más eficientemente cuanto más carga positiva posea la especie atacada por el alcohol. En definitiva, el proceso será acelerado por grupos electroatrayentes situados sobre el ácido a esterificar.

Aparte de estos efectos eléctricos considerados, existen los estéricos que, como veremos, en determinados casos, pueden ejercer una influencia definitiva en el curso del proceso.

METODOLOGIA EXPERIMENTAL

Como catalizador hemos utilizado et ortofosfato de aluminio, catalizador de contacto, elegido por presentar grandes ventajas frente a los catalizadores homogéneos (HCl, H_2SO_4 etc.) tales como : no inducir fenómenos de corrosión y ser más sencilla su separación al finalizar el proceso. El compuesto presenta : una superficie especifica de 316m²/g, un volumen de poros cilindricos de 0,63 cc/g a partir de la isoterma de adsorción-desorción y de acidez superficial total de 1,20 m.e.q./g determinado por el procedimiento de Benesi y de 1,40 m.e.q/g por quimisorción de amoniaco. El sistema de reacción es semejante al utilizado en trabajos precedentes [3], empleando benceno como agente azeotrópico.

En las experiencias se utilizan un mol de alcohol *n*-butilico, 0,2 moles del correspondiente ácido, y cantidades de catalizador correspondientes entre 3,5 y 7 g. (4,2 ; 7,0 y 9,8 m.e.q. de acidez, frente a *p*-dimetilaminoazobenceno). La temperatura es de 110 ± 2°, y la agitación constante, de 390−400 r.p.m.. A intervalos de una hora, se extraen muestras del bruto de reacción, que son sometidas a valoración ácido-base o análisis cromatográfico de gases, con lo que se sigue el progreso de la misma. El análisis fué realizado en un cromatógrafo de gases Hewlett-Packard, modelo 5750, en columna de goma de silicona al 1 % a las temperaturas de 170, 140 y 100°, siendo la velocidad de registro de 0,25 pulgadas/min. El análisis cuantitativo se ha llevado a cabo por el método de normalizacion interna.

En todos los casos se han realizado los correspondientes ensayos en blanco y considerado sus resultados al evaluar el conjunto de la reacción. El tiempo máximo de reacción al que se han realizado las experiencias ha sido, en todos los casos, de nueve horas.

RESULTADOS Y DISCUSION

En las figuras 1, 2 y 3 aparecen las conversiones obtenidas utilizando diferentes proporciones de catalizador (diferentes miliequivalentes de

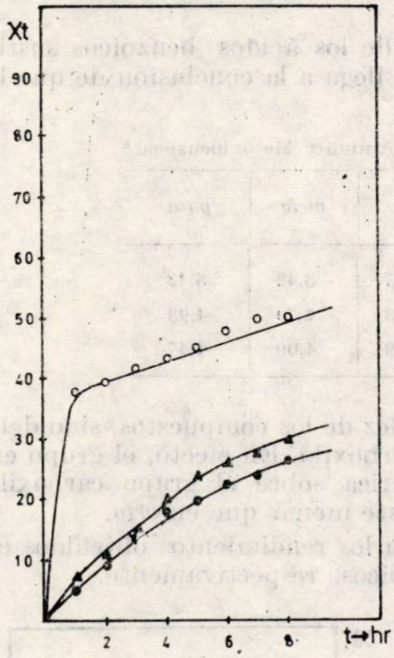

Fig. 1

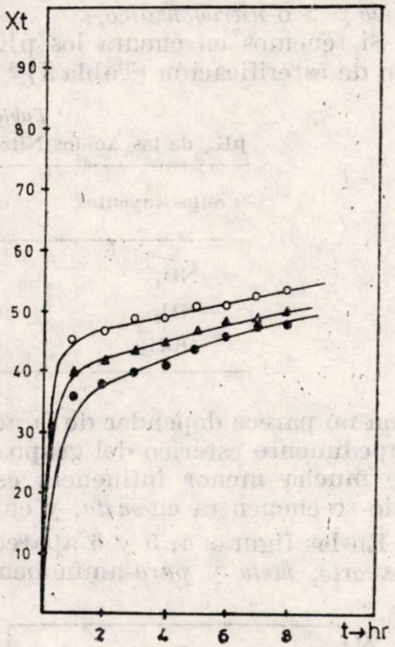

Fig. 2

Fig. 1. — Esterificación de ácido *o*-nitrobenzóico, *n*-butanol.

Fig. 2. — Esterificación de ácido *m*-nitrobenzóico, *n*-butanol.

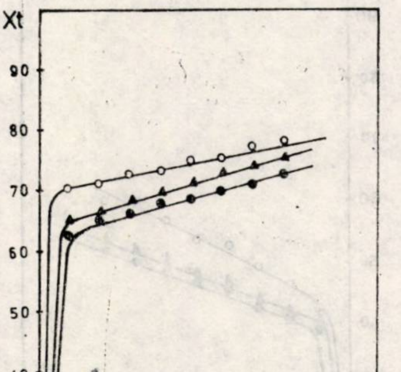

← Fig. 3. — Esterifiación de ácido *p*-nitrobenzóico, *n*-butanol.

acidez), en la esterificación de ácidos *orto*, *meta* y *para*-nitrobenzóicos, respectivamente, en función del tiempo.

Como se puede observar, en igualdad de condiciones de reacción, el rendimiento obtenido sigue el orden : *ácido* p-*nitrobenzóico* > > *m-nitrobenzóico* > > o-*nitrobenzóico.*

Si tenemos en cuenta los pK_a de los ácidos benzóicos sustituidos objeto de esterificación (Tabla I) [6] se llega a la conclusión de que la conversión no parece depender de la acidez de los compuestos, sino del grado de impedimento estérico del grupo carboxilo. En efecto, el grupo en *para* ejerce mucha menor influencia estérica sobre el grupo carboxilo que cuando se encuentra en *meta*, y en éste menor que en *orto*.

Tabla 1

pK_a de los Acidos Nitro, Amino y Metoxibenzóico [6]

Substituyentes	*orto*	*meta*	*para*
$-NO_2$	2,17	3,49	3,43
$-NH_2$	4,98	4,79	4,98
$-OCH_3$	4,09	4,09	4,47

En las figuras 4, 5 y 6 aparecen los rendimientos obtenidos con los ácidos *orto*, *meta* y *para*-aminobenzóicos, respectivamente.

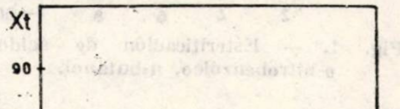

Fig. 4. — Esterificación de ácido *o*-aminobenzóico, *n*-butanol.

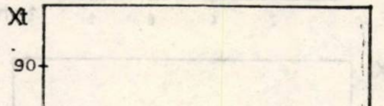

Fig. 5. — Esterificación de ácido *m*-aminobenzóico, *n*-butanol.

De forma semejante a lo que sucede en el caso anterior, el rendimiento sigue el orden : *ácido* p-*aminobenzóico* >> m-*aminobenzóico* > o-*aminobenzóico.*

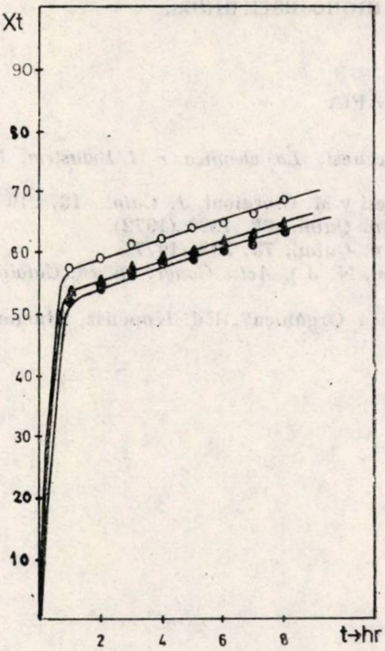

Fig. 6. — Esterificación de ácido *p*-aminobenzóico, *n*-butanol.

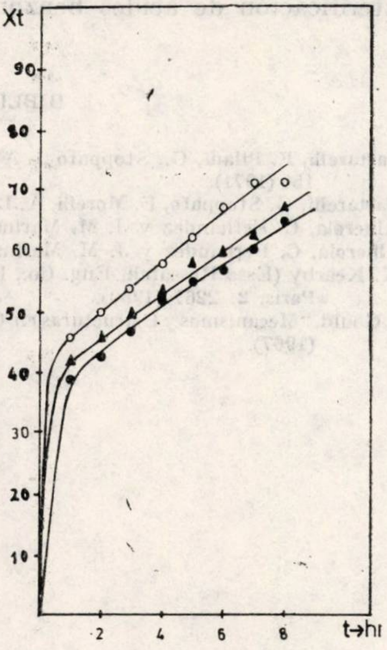

Fig. 7. — Esterificación de ácido *p*-metoxibenzóico, *n*-butanol.

Como se puede comprobar, el efecto espacial sigue predominando : hecho tanto más destacable cuanto que los tres ácidos poseen, prácticamente el mismo pK_a. Por otra parte, en igualdad de condiciones de reacción, los rendimientos obtenidos con los ácidos *orto* ó *meta*-aminobenzóicos, son superiores a los que se logran con los correspondientes ácidos nitrobenzóicos, de acuerdo con el impedimento estérico.

En la figura 7 aparecen los resultados obtenidos en la esterificación del ácido *p*-metoxibenzóico (*p*-anisico). El orden de rendimientos obtenidos con los tres ácidos en *para* es : *ácido* p-*nitrobenzóico* >> p-*metoxibenzóico* > p-*aminobenzóico.*

Suponiendo que, en todos estos compuestos el efecto estérico del sustituyente sobre el grupo carboxilo resulta despreciable, elrendimiento es tanto más elevado cuanto mayor es la acidez del compuesto a esterificar. Esto parece indicar que, en el mecanismo formulado anteriormente para la esterificación, la fase 2 es la determinante del proceso.

Por otra parte, y observando las figuras 1 a 7, se pueden comprobar que, por las condiciones de nuestras experiencias, el óptimo de acidez aparece, en todos los casos, para 7g. de catalizador, hecho que ya había sido observado en trabajos precedentes.

A la vista de los resultados obtenidos, y comparado conotros catalizadores de contacto, los ortofosfatos de aluminio tipo Kearby parecen proporcionar mejores rendimientos y en menor tiempode contacto, por lo que se les puede considerar como buenos catalizadores en procesos de esterificación de ácidos benzóicos monosustituidos.

BIBLIOGRAFIA

[1] R. Tartarelli, F. Piladi, G., Stoppato J. A. Lucchesi, *La chemica e L'Industria*, **53**, (2), 150 (1971).

[2] R. Tartarelli, G. Stoppato, F. Morelli, A. Lucchesi y M. Giorgioni, *J. Catal.*, **18**, 219 (1970).

[3] A. Alberola, C. Fernandez y J. M. Marinas, *An. Quim.*, **68**, 1399 (1972).

[4] A. Alberola, C. Fernandez y J. M. Marinas, *An. Quim.*, **73**, 298 (1977).

[5] K. K. Kearby (Esso Research. Eng. Co., Linden, N. J.), *Actes Congr. Intern. Catalyses*, 2e, Paris, **2**, 2267 (1960).

[6] E. S. Gould, "Mecanismos y Estructuras en Quimica Orgánica", Ed. Kopelisz, Buenos Aires (1967).

Revue Roumaine de Chimie, **30**, 7, 623–629 (1985)

MECHANO-CHEMICAL INITIATED POLYMERIZATIONS. 9

INFLUENCE OF MECHANICAL CONDITIONS AND TEMPERATURE ON POLYMERIZATION REACTION OF ACRYLAMIDE BY VIBRATORY MILLING

CR. I. SIMIONESCU, CLEOPATRA VASILIU-OPREA and JEANA NICOLEANU *
Polytechnic Institute "Gh. Asachi" Iași, Romania

* Institute of Macromolecular Chemistry "P. Poni", Iași, Romania

Received June 5, 1984

Mechanochemical polymerization by vibratory milling of acrylamide is discussed. The influence of temperature and the mechanichal conditions are examined. The reaction products were characterized by chemical and physical methods.

I. INTRODUCTION

The mechanochemical polymerization of the monomers in the solid phase has been little studied; V. A. Karghin polymerized natrium acrylate in the vibratory-dispersion conditions, for the first time.[1] New results concerning the mechanochemical polymerization of methacrylamide were recently published.[2] This paper deals with the influence of temperature and the mechanical conditions on the mechanochemical polymerization of acrylamide.

RESULTS AND DISCUSSION

1. Influence of Mechanical Conditions

1.1. *Influence of Duration and Size of the Grinding Bodies*

Vessels from metal (reaction flask and stainless steel grinding bodies — V_2A —) were used to carry out the grinding experiments. The diameter of the grinding bodies varied from 3 to 15 mm. The experiments were performed at room temperature (18 ± 2°C), in inert atmosphere (purified nitrogen) at a filling ratio of 0.5%. The experimental results were plotted as conversion degree versus time (Fig. 1). The polymerization process develops slowly for a long period of time.

The conversion-time curves show a maximum after 96 hrs (when the grinding bodies with $\Phi = 3$; 6 or 9 mm were used). (Fig. 1; curves 1–3). The maximum shifts towards longer periods of time and it increases getting higher values while the diameter of the grinding bodies increases. (For instance; 120 hrs at $\Phi = 12$ mm curve 4 and 144 hrs at $\Phi = 15$ mm — curve 5).

---

* Preceding part 8 in *Acta Polimerica*, 3/86 (in print)

The shape of the curves is characteristic of the initiated mechanochemical polymerization and it has to be connected with the simultaneous developing of the mechanical degradation of the processes.

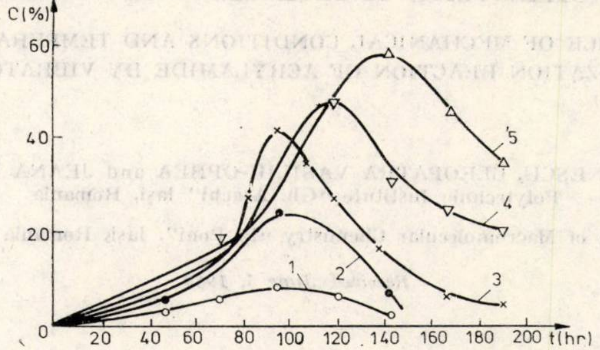

Fig. 1. — The curves of the time-conversion degree for the mechano-chemical polymerization of acrylamide in the presence of the sphere shape-like used as the grinding bodies. The diameters of the spheres (Ø) are : 1—3 mm ; 2—6 mm ; 3—9 mm ; 4—12 mm ; 5—15 mm (Inert medium, $\alpha = 0.5\,\%$; $T = 18 \pm 2$°C).

When the macroradicals reach the critical length, they are able to concentrate on their chains the mechanical energy undergoing a homolytical scission leading to the low molecular compounds which can be removed during the purification processes. The conversion degree decreases in this case. Because, in the case of polyacrylamide (PAA), the soluble fraction is similar to the monomer units, that makes us conclude that the mechanodegradation process performs at the chain ends. The results are in good agreement with the mechano-degradation mechanism of polyacryl- and polymethacrylamide quoted in literature. [3]

The experimental results prove that the shock energy of the system increases at the same time with the diameter of grinding bodies. The fact that there is an optimum diameter of the grinding bodies which ensures the maximum of the conversion degree leads us to the conclusion that the two concurrent processes (polymerization and mechano-degradation) are selectively influenced by the shock-energy magnitude developed in the reaction flask.

On additional evidence concerning the simultaneous development of the mechano-synthesis and mechano-degradation the process is emphasized by the curves which show the variation of the viscosity average molecular weight $\overline{M}_W$* against the length of time.

Figure 2 shows comparatively the time conversion degree (1) and M_W — time curves for the case when the grinding bodies with Ø = 15 mm are used.

---

* $\overline{M}_W$ — was determined according to the method[4], applying the equation: $[\eta] = 3.73\cdot10^{-4}\times\overline{M}_W^{0.66}$

It was noticed besides the fact that the polymerization mechanism was a radicalic one,[2] M_W varied with the duration according to a curve with a shape similar to one which described the conversion-degree-time function (2 by comparison with 1) (Fig. 2). During the first interval of the process (24—144 hrs) prevails the synthesis of the macromolecules. After the maximum of the curve the mechano-degradation becomes the prevailing process, and the molecular weight decreases obtaining a value that might be assumed to be destruction limit (M_d^{**}). This value is specific to the used conditions. In practice, it is admitted that after the critical length of the macromolecules is reached, the molecular weight is continually corrected by the mechano-degradation.

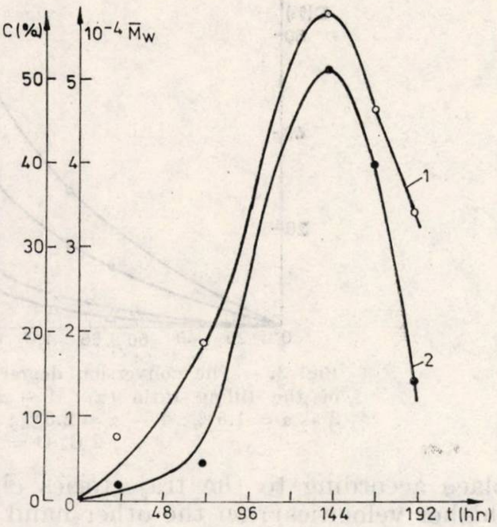

Fig. 2. — The conversion degree-time and M_w-time curves determined for Ø = 15 mm : 1 — conversion degree variation ; 2 — M_w variation.

1.2. *Influence of Duration and Filling Ratio*

The filling ratio ($\alpha = a/p \times 100$), when a is the quantity of the monomer (in g), p is the quantity of the grinding bodies (in g), was varied changing the quantity of the grinding bodies (spheres). So that this parameter gets values from about 0.5 to 2.0% (Fig. 3).

The plotting of the conversion degree-time curves emphasized first of all the importance of the mechanical parameter, that is in the inverse ratio with the monomer transformation degree into polymer. The smallest filling ratio used (0.5%) ensures the maximum conversion degree (about 60%). All plotted curves show the same maximum of the conversion-degree, irrespective of α, which in the system and the studied working conditions is around 144 hrs (Fig. 3).

The influence of the filling ratio must be related with the free volume of the reaction flask which ensures statistical displacements after the rigorously determined trajectory of the grinding-bodies.

** M_d — which is specific to the used experimental conditions.

If the reaction flask volume is kept constant, and small quantities of the grinding bodies (large filling ratios) are used then the free volume available to the shifting will be large. The movement of the spheres takes place according to the trajectories characterized by higher amplitudes (higher velocities); on the other hand the number of the collisions with the vessel wall is smaller. Therefore, the effective overall kinetic energy in the polymerization activity is mainly dependent on the statistical number of the collisions and the shock intensity (when the size of the grinding bodies is taken into account) (Fig. 1). In the case when high quantities of the grinding bodies are used (α is small) the collision frequency increases and in addition the friction intensifies, participating in the polymerization reaction either directly (as a component of the mechanical energy, together with the shock force), or by means of the equivalent caloric contribution resulted in their partial transformation.

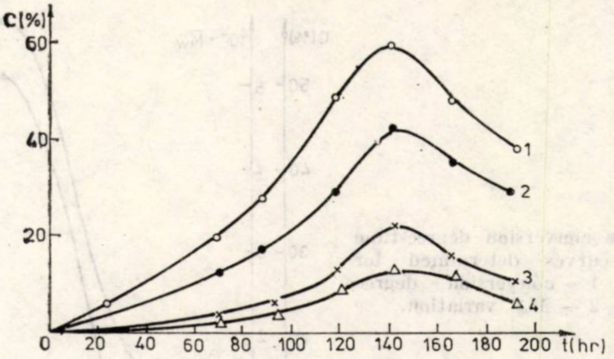

Fig. 3. — The conversion degree-time curves as a function of the filling ratio (α): 1 — $\alpha = 0.5\%$; 2 — $\alpha = 1.0\%$; 3 — $\alpha = 1.5\%$; 4 — $\alpha = 2.0\%$; (Inert medium, $T = 18 \pm 2°C$, $\varnothing = 15$ mm)

2. Influence of Temperature

The recently published data[2] show the fact that the conversion degree amounts in proportion as the caloric supply increases i.e. it is proportional to the network weakening under the thermal stress action. The transformation is on the whole near by the melting point of the monomer ($T = 80°$; $T_t = 84°C$).

With a view to studying deeply the influence of this important parameter on the polymerization reaction, it was obtained the conversion-time curves for six different temperatures ($T = 30°C-80°$).

The millings were carried out for a short duration (1—24 hrs) in inert atmosphere, for the filling ratio of 0.5% and the diameter of the grinding bodies of 9 mm. The conversion degree increases with the length of time for both cases (Fig. 4; curves 1—6) obtaining higher values at $t = 80°C$. The presence of polymer was emphasized after 6 hrs.

The experimental results show a substantial decrease of the polymerization induction period. The conversion-degree obtained under the conditions shown in Fig. 1,3 have non-important values when the duration is below 24 hrs (less 10%), while they increase at 80–90% at 65°C and 80°C respectively.

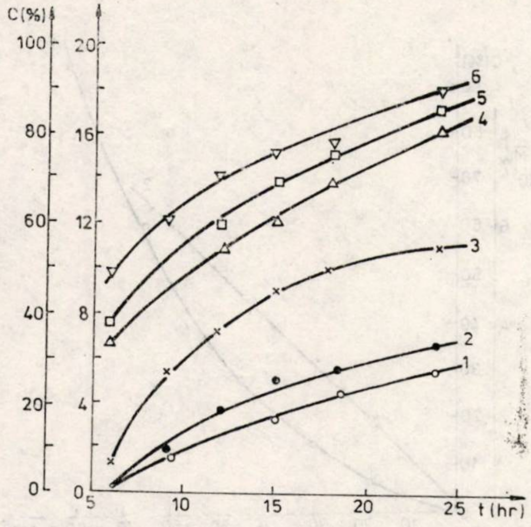

Fig. 4. — The curves of the conversion degree-time for : 1—30°C ; 2—40°C ; 3—50°C ; 4—65°C ; 5—75°C ; 6—80°C (Inert medium, α=0.5%, Ø =9 mm)

The experimental data show an important increase when the mechanical energy participates in the decrease of the thermal activation energy of the monomer polymerization.

The value of the average molecular weight depends both on the length of time and the temperature. The influence of the first factor was already explained.

The relation T *vs.* $\bar{M}_W$ is different from the usual method. Within the limits of the values concerning the period of times and temperatures studied in this paper, one can notice a progressive increase of the average molecular weight depending on the duration of the reaction and implicitly with the increase of the caloric supply, observation proved by the data given in Fig. 5 (curves 1,2) and Fig. 6 (curves 1–4).

The results obtained are due to the increase of the entrance rate of the structural units on the chain thanks to the additional caloric supply towards the system energy on the one hand and polymer obtained for a shorter length of time (6–24 hrs) instead of 24–192 hrs at $T = 18 \pm 2$°C), which does not undergo an important mechano-chemical degradation on the other hand.

Mechanochemically prepared poly(acrylamide) was characterized by elemental analysis and good agreement was obtained (C = 50.7%; H = 7.04%; N = 19.7%). The shape of the IR-spectra concerning the peak adsorption values for the characteristic groups of polymers as well as monomer are identical with the standard one mentioned by the literature. The spectral analysis by X-ray diffraction of PAA showed that the polymer is amorphous. PAA shows a good thermostability (200°C) according to the thermogravimetric measurements carried out on a Paulik Erdely Paulik derivatograph. The weight losses were 5–15% according to the synthesis parameters. PAA is water soluble.

The polymerization initiation must be corroborated with the homolytic splitting up of the chemical bonds of the crystalline lattice in the monomer under the action of mechanical energy, producing the first centers of polymerization. The influence of the electronic flux of the mechano-emission which is inevitably existent at the grinding of the solid compound leading to the anion radical, might be taken into account. The previous data [2] prove on the process developing a concatenation radical mechanism.

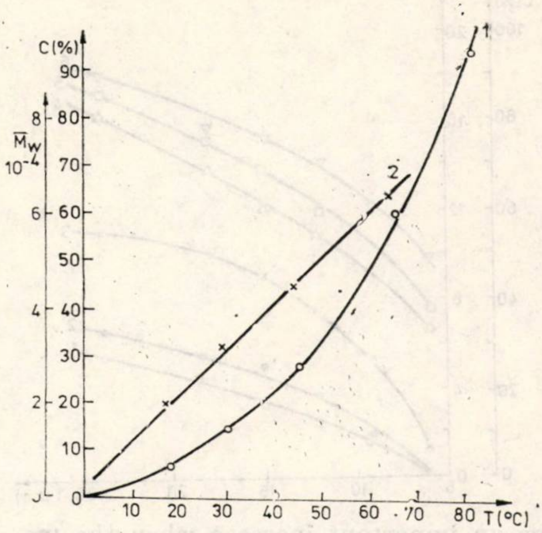

Fig. 5. — The conversion degree-temperature and M_w—temperature determined for 48 hrs ; $\alpha = 0.5\%$, $\varnothing = 9$ mm, inert medium : 1 — conversion degree variation ; 2 — $\overline{M}_w$ variation.

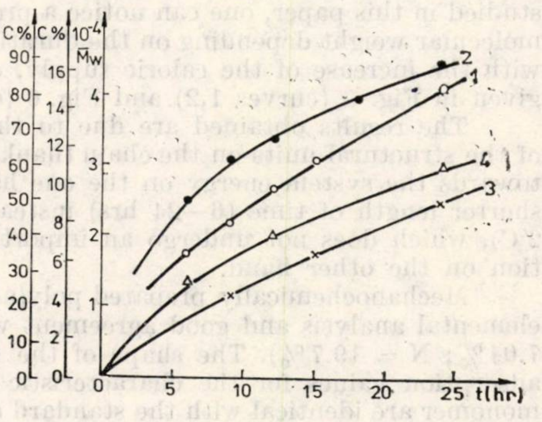

Fig. 6. — The curves of the conversion degree vs. time for : 1—65°C ; 2—80°C and the variation of $\overline{M}_w$ vs. time for : 3—65°C ; 4—80°C.

The amorphous character of the prepared compounds, proved by the X-ray microscopy, shows that the reaction does not develop within the network intimacy ; polymer arises as a new phase within the superficial layers of the crystalline network of monomer mechanically destroyed.

CONCLUSIONS

1. The mechanochemical synthesis of PAA is essentially influenced by the parameters of the mechanical working conditions (length of time, size of the grinding bodies, filling ratio) and temperature.

2. The molecular weight of the synthesized compounds (10.000—50.000 at 18°C) proves the existence of a polymer. Also, the molecular weight depends actually on the temperature.

3. Due to its physical and chemical properties, PAA, mechanically synthesized, shows a good analogy with polymer performed by means of the usual methods.

4. The polymerization process develops after a concentration radical mechanism, in the superficial layers of the crystalline network of monomers, mechanically destroyed.

REFERENCES

[1] V. A. Karghin and N. A. Plate, *Vysokomol. Soedin.*, **1**, 330 (1959).

[2] Cr. I. Simionescu, Cl. Vasiliu-Oprea and J. Nicoleanu, *European Polym. J.*, **19**, 6 (1983).

[3] N. A. Plate, V. A. Karghin, *J. Polym. Sci.*, C_4, 1027 (1963).

[4] W. M. Thomas, "Encyclopedia of Polymer Science", Ed. by H. F. Mark, N. G. Gaylord, N. M. Bikales, Wiley N. Y., 1964.

Revue Roumaine de Chimie, **30**, 7, 631–637 (1985)

ELIMINATION OF THE INTERFERING EFFECTS OF SOME ORGANIC COMPOUNDS IN THE DETERMINATION OF RHODIUM BY ATOMIC ABSORPTION SPECTROPHOTOMETRY

M. A. KABIL and M. A. MOSTAFA
Chemistry Department, Faculty of Science, Mansoura University, Mansoura,
A. R. EGYPT

Received June 25, 1984

The interfering effects of some organic compounds on atomic absorption spectrophotometry (AAS) of rhodium and elimination of these interferences by addition of n-butylamine are investigated. The mechanism of this elimination is discussed. Moreover, the continuous titration method was used to investigate the interference effects of these organic compounds. The purpose of using such technique is to obtain a stoichiometric ratio during the flame processes.

INTRODUCTION

Atomic Absorption Spectrophotometry (AAS) has been successfully used for the determination of most noble metals, but there is very little evidence in the literature concerning the determination of Rh. [1–4] Although no method has been developed to eliminate all potential interferences, Scarborough [3] reported that uranium (10 mg/mL) removes interferences caused by Mo, Pd and Ru in the determination of Rh. Schnepfe and Grimaldi[4] used a mixture of cadmium and copper sulphates to remove interelement interferences on Rh. Also, lanthanum sulphate was used to get rid of serious interferences of Rh. [4–6]

The interferences of organic compounds on the absorption signal of Rh are rarely mentioned in the literature. In the present work, we try to explain the serious depressive effects encountered in some organic compounds. Since Rh forms an amine complex,[7] these interferences are removed by addition of 0.02M n-butylamine to both sample and standard solutions. This amine is a new and better masking agent for determination of Rh.

EXPERIMENTAL

A Unicam SP 90 A (series 2) Atomic Absorption Spectrophotometer with a new HTA photo tube, No. R 270 from EMI, was used throughout. Air was supplied through PU 9003 air compressor. Acetylene was obtained from cylinders after passing through concentrated sulphuric acid and glass wool for purification. Absorbance values were recorded with a PM 8251 single-pen recorder and the results were formulated by CASIO FX-502 P type programmable pocket calculator.

The optimum AAS instrumental parameters are : lamp current, 12 mA ; wavelength, 343.5 nm ; slit width, 0.1 mm ; observation height, 1.0 cm ; air flow rate, 5.0 $dm^3 \cdot min^{-1}$ and fuel flow rate, 1.0 $dm^3 \cdot min^{-1}$.

All solutions were prepared from B.D.H. Chemicals and Analar grades. The stock rhodium solution was prepared from rhodium (III) chloride monohydrate. The nominal concentration of Rh in the stock solution was 1000 ppm. Stock solutions of the organic compounds were prepared ; aliquots were diluted with bidistilled water to give the desired concentration used for the experiments.

RESULTS AND DISCUSSION

Effect of organic compounds

The inhibition release titration method[8] was used to study the interfering effects of the organic compounds under investigation. The changes in the absorption signals of 50 ppm rhodium (4.85×10^{-4}M) as a function of the molar ratio of the [interferent]/ [rhodium] are indicated in Fig. 1. Most of the investigated compounds have depressive effects which are almost consistent after the stoichiometry, whereas the others have diverse effects. Acetylmethylurea decreases the absorption signal of Rh, reaching a minimum with inflection at molar ratio 1 : 1 then, the

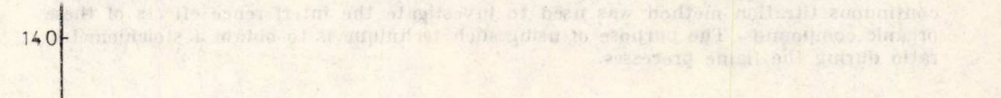

Fig. 1. — Changes in the absorption signal of 50 ppm of rhodium (4.85×10^{-4}M) as a function [interferent ligand]/ [rhodium] ratio : (●) acetylmethylurea, (♦) EDTA, (◉) SSA, (▲) NaDDC (○) pyrogallol, (□) glycine (▲) 4-aminosalicylic acid and (□) gallic acid.

absorption increases, giving a maximum at molar ratio 2 : 1, and gradually falls to the normal recovery percentage (Fig. 1 curve (●)). EDTA shows a minimum absorbance at molar ratio of [EDTA]/[rhodium] 1 : 1, followed by an enhancement to the normal recovery percentage (Fig. 1 curve (■)). Such depressive effect may be due to a complexation phenomenon which takes place in solution or during the flame processes. It has been suggested that[9,10] the disintegration of the solid complex gives atoms and/ or radicals which react with the oxidizing species in the flame, forming a Rh compound(s), especially, RhO (at the inflection point). The rapid enhancement after the inflection may be attributed to the reducing species (NH, CN, ...) which arise from the dissociation of Rh-EDTA complex. Sulphosalicylic acid (SSA) gives a suppressive effect (58 of the recovery percentage) at ratio 1 : 1, followed by a gradual increase in the absorption signal (to 82 of the recovery percentage) and gives a plateau (Fig. 1 curve (•)). The inflection at molar ratio 1 : 1 corresponds to the formation of Rh-SSA complex. On the other hand, Fig. 1 curves (Δ, 0, □, ▼ and X) show distinct break points at molar ratio 2 : 1 for sodium diethyldithiocarbamate (NaDDC) : Rh ; at molar ratio 1 : 1 for pyrogallol, glycine, 4-aminosalicylic acid and gallic acid. The interesting features of these curves are : (a) Definite stoichiometric ratios existed even by changing the analyte and/ or the ligand concentrations, (b) The depressive effect is almost consistent after the stoichiometry is attained.

These compounds enrich the flame plasma by species which may : 1. Quench the flame temperature or 2. Preclude the complete atomization of Rh atoms.

Effect of n-butylamine in eliminating interferences

The changes in the recovery percentage of 50 ppm Rh (4.85×10^{-4}M) as a function of the molar ratio of [n-butylamine]/ [rhodium] is indicated in Fig. 2. The absorbance firstly decreases, reaching a stoichiometric ratio of [n-butylamine]/ [rhodium] 1 : 1, followed by a sharp enhancement (2 folds of the normal recovery percentage) giving a plateau at 4 : 1 ratio. The inflection at molar ratio 1 : 1 corresponds to the formation of Rh-n-butylamine complex. The marked increase in Rh absorbance is attributed to the efficiency of n-butylamine in performing a reducing environment for increasing the Rh atom population in the flame.

A possible explanation of the role of n-butylamine in the flame can be represented in three steps, (i) Vaporization of solid Rh-amine complex, followed by its decomposition giving Rh atoms which react instantaneously with the oxidizing species in the flame forming Rh compound(s), essentially RhO, (ii) After the particular stoichiometric ratio, the excess of the reducing species in the flame (NH, CN, ...) reacts with the Rh compound(s) according to

$$\mathrm{RhO} + \mathrm{CN} \rightarrow \mathrm{Rh} + \mathrm{N} + \mathrm{CO}$$

$$\mathrm{RhO} + \mathrm{NH} \rightarrow \mathrm{Rh} + \mathrm{N} + \mathrm{OH}$$

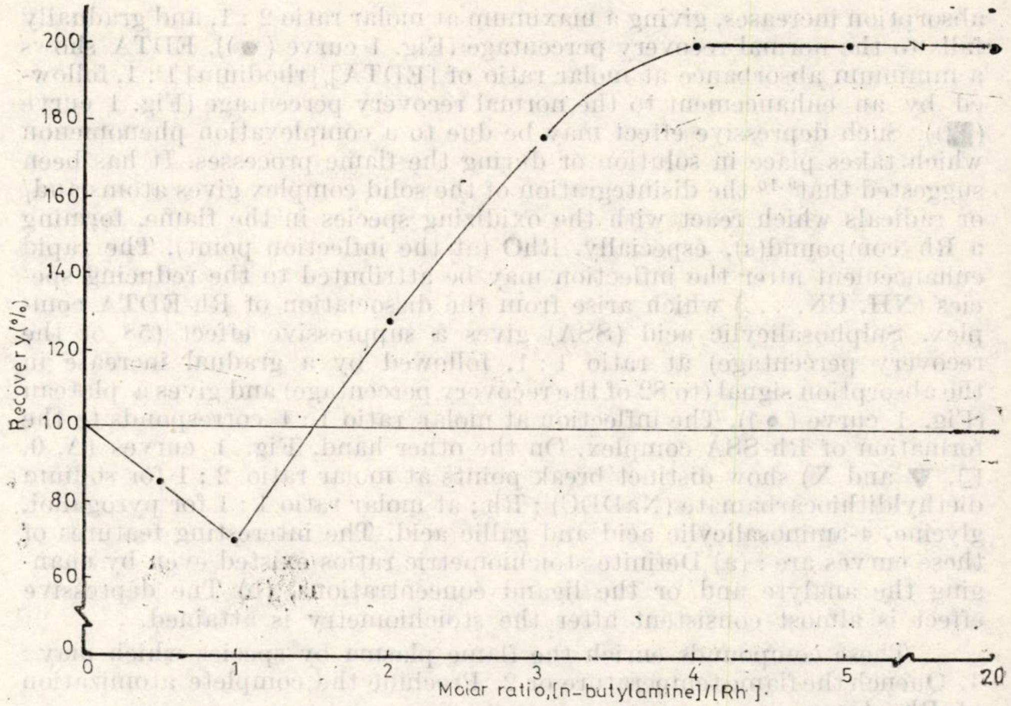

Fig. 2. — Changes of the absorption signal of rhodium as a function of [n-butylamine]/[rhodium] ratio.

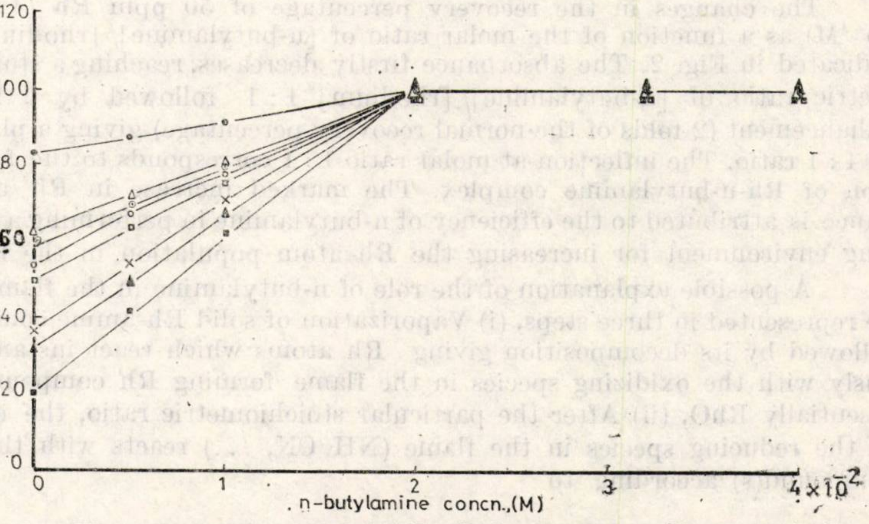

Fig. 3. — Use of *n*-butylamine in eliminating the interferences on 50 ppm of rhodium (4.85×10^{-4}M) encountered from 4.85×10^{-4}M of: (●) acetylmethylurea, (▽) NaDDC*, (◉) SSA, (○) pyrogallol, (□) glycine, (×) gallic acid, (▲) 4-aminosalicylic acid and (■) EDTA.* 9.7×10^{-4} M.

and restores the Rh atom population, and (iii) The continuous increase in the concentration of n-butylamine gives excess reducing species which scavenge the oxidising species in the flame. Accordingly the reducing environment helps in forming neutral atoms of rhodium in the flame.

Data in Fig. 3 and Table 1, support the use of n-butylamine as a flame buffer for rhodium. The addition of 0.02M n-butylamine and 0.05M $HClO_4$ to both samples and standards, restores the rhodium recovery percentage.

Table 1

Interferences of various organic compounds in 4.85×10^{-4}M concentration level on 50 ppm of Rh (4.85×10^{-4}M) absorption without and with addition of n-butylamine in 0.05M $HClO_4$ acid solution

No. 2	Added substance in 4.85×10^{-4}M concentration level	Rh recovery%	
		without addition	with addition of 0.02M n-butylamine
1	Rh*	100	100
2	Rh + CDTA	80	100
3	Rh + Resorcinol	82	100
4	Rh + 8-hydroxyquinoline	92	100
5	Rh + acetamide	95	100
6	Rh + acetylmethylurea	84	100
7	Rh + NaDDC	80	100
8	Rh + SSA	58	100
9	Rh + Pyrogallol	54	100
10	Rh + glycine	50	98
11	Rh + 4-aminosalicylic acid	36	100
12	Rh + Gallic acid	32	100
13	Rh + EDTA	20	98
14	Rh + bromophenol blue	98	100
15	Rh + pyrogallol + resorcinol	45	102
16	Rh+pyrogallol+bromophenol blue	58	100
17	Rh + EDTA + CDTA	85	100
18	Rh + EDTA + acetylmethylurea	80	100
19	Rh + EDTA + Gallic acid	75	100

* The absorbance of 4.85×10^{-4}M of Rb + 0.02M n-butylamine + 0.05M $HClO_4$ was taken as 100 recovery percentage ; all other absorbances were normalized against this value.

Fig. 4 shows the distribution of Rh atoms in the presence of some organic compounds as a function of observation height. The distribution curves indicate that there are some differences in the thermal stabilities of the organic compounds. Likewise, there are different times in the flame required to get the same ratio of the free atoms from the various compounds. This may suggest that the formation of a stable Rh-n-butylamine complex exists in solution and before the aerosol formation is commenced.

On adding 0.02M of n-butylamine all the curves coincide as shown in Fig. 5.

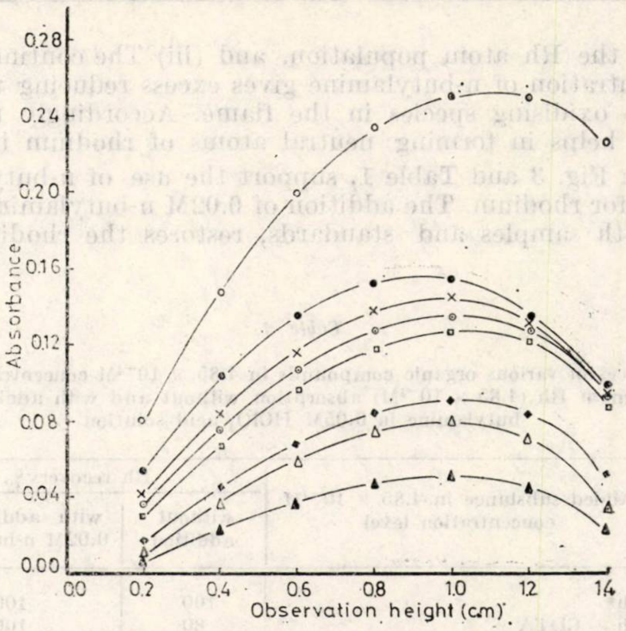

Fig. 4. — Distribution of rhodium atoms, 50 ppm of Rh (4.85 × 10^{-4}M), as a function of observation height for different interferents, each in 485 × 10^{-4}M : (○) Rh only, (●) NaDDC*, (×) SSA, (◉) pyrogallol, (□) glycine, (◆) 4-aminosalicylic acid ( ) gallic acid and (△) EDTA.* 9.7 × 10^{-4}M.

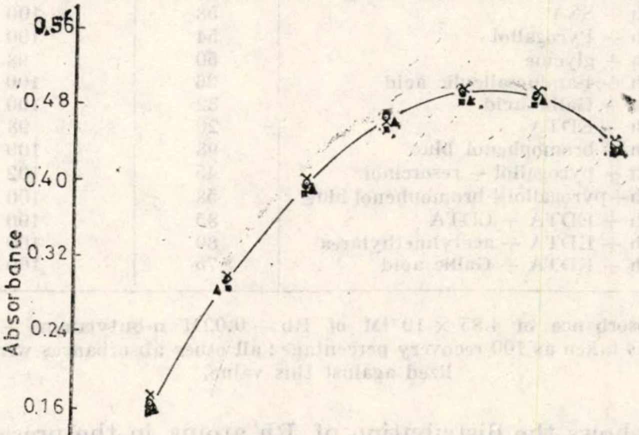

Fig. 5. — Distribution of rhodium atoms (50 ppm of Rh as a function of observation height in the presence of 0.05 M of *n*-butylamine for different interferents (each in 4.85 × 10^{-4}M) : (○) Rh and *n*-butylamine, where the others having Rh, *n*-butylamine and, (●) NaDDC*, (×) SSA, (◉) pyragallol, (□) glycine, (■) 4-aminosalicylic acid, ( ) gallic acid and (△) EDTA. * 9.7 × 10^{-4} M.

REFERENCES

[1] N. K. Belśkii, L. A. Nebolśina, L. K. Shubochkin and G. N. Verkhoturov, *Zh. Anal. Khim.*, **35 (4)**, 799 (1980).
[2] A. Diamantatos, *Anal. Chim. Acta*, **131 (1)**, 53 (1981).
[3] J. M. Scarborough, *Anal. Chem.*, **41**, 250 (1966).
[4] M. M. Schnepfe and P. S. Grimaldi, *Talanta*, **16**, 591 (1969).
[5] M. M. Schnepfe and F. S. Grimaldi, *Talanta*, **16**, 1461 (1969).
[6] J. G. Sen Gupta, *Anal. Chem. Acta*, **63**, 19 (1973).
[7] V. E. Mironov, A. K. Pyartman, Yu. B. Solovév, V. P. Ivankova and M. V. Sofin, *Koord. Khim.*, **6 (8)**, 1233 (1980).
[8] J. Posta and J. Lakatos, *Magy. Kém. Folyoirat*, **86**, 284 (1980).
[9] A. C. Lenzies, *Anal. Chem.*, **32**, 898 (1960).
[10] J. W. Robinson and L. J. Kevan, *Anal. Chim. Acta*, **28**, 170 (1963).

Revue Roumaine de Chimie, **30**, 7, 639–643 (1985)

THIOSEMICARBAZONE COMPLEXES OF $3d^{6-10}$ METALS.

ACETOPHENONE AND *o*-AMINOBENZALDEHYDE THIOSEMICARBAZONE

ROBERTO CAO, GILBERTO VICIEDO and HECTOR BERTY
Faculty of Chemistry, Havana University, Cuba

Received September 10, 1984

Cobalt (II), nickel (II), copper (I) and zinc (II) chloride and bromide complexes with acetophenone thiosemicarbazone of the type ML_2X_2 and ML (L–H)X were obtained. Cobalt (III), nickel (II), copper (II) and zinc (II) chloride and bromide complexes with *o*-aminobenzaldehyde thiosemicarbazone of the type ML (L–H)X, where M : Ni (II), Zn (II), Co $(L-H)_2X$ and $CuLX_2 \cdot H_2O$ are also reported. The complexes were characterized by IR, electronic and ^1H-NMR spectra and molar conductivity and magnetic susceptibility measurements. The influence of the nature of the ligand on the oxidation states of cobalt and copper is discussed.

INTRODUCTION

Since the discovery in 1965 of the antitumoral activity of the pyrydinic derivatives thiosemicarbazones [1] based on the criterion that such activity is due to the chelating action of the thiosemicarbazone on the divalent biometal ions of the first transition series [1–3] these compounds have attracted the attention of coordination chemists.

Complexes with different acetophenone derivatives thiosemicarbazones have been reported by Indian authors.[4,5] In these papers no reduction of copper (II) is reported although such a process is possible in the presence of dialkyl- and alkyl, aryl-monothiosemicarbazones. [6]

In the present work, the synthesis and characterization of the coordination compounds of MX_2 salts, where M ; Co (II), Ni(II), Cu(II), Zn(II) and X : Cl, Br ; with the acetophenone (ATSC) and *o*-aminobenzaldehyde (ABTSC) thiosemicarbazone is reported.

EXPERIMENTAL

The chemicals used in the research work were all AR grade. The thiosemicarbazide was recrystallized in hot water.

IR spectra were recorded on a SP-2000 Pye-Unicam spectrophotometer (3600–200 cm^{-1}) as CsI tablets. Electronic spectra were recorded on a SP-1800 spectrophotometer. Molar conductivities of 10^{-3} mol/L solutions in methanol were measured with a OK-1 Radelkis conductimeter. ^1H-NMR spectra were registered on a H-60 Hitachi spectrometer ; TMS was used as internal reference. The magnetic moments were made by using a Faraday magnetobalance and Hg [Co(SCN)$_4$] as standard (298 K).

The general method of synthesis of the complexes consisted in adding a solution (water-ethanol for ATSC complexes, and methanol for ABTSC) over a solution of the ligand (ethanol for ATSC; methanol for ABTSC). The product was washed with ethanol (or methanol) and ether. In the case of the copper complexes the addition of the copper (II) salt over the ligand was made drop with constant stirring and the resulting mixture was allowed to stand for 24 hours. The analytical data are reported in table 1.

Table 1

Colour, molar conductivity in methanol (10^{-3}mol/L), and analytical data (in weight %)

Complex	Colour	μ_{eff} (BM)	Λ_M ohm^{-1}·cm^2··mol^{-1}	Found			Calculated		
				M	N	X	M	N	X
Co(ATSC)$_2$Cl$_2$	green	4.63	129	11.5	15.6	14.0	11.4	16.3	13.8
Co(ATSC)$_2$Br$_2$	green	4.70	139	10.3	14.0	26.8	9.75	13.9	26.4
Ni(ATSC)$_2$(ATSC-H) Cl	ocre	0	96	12.1	17.8	7.9	12.2	17.5	7.4
Ni(ATSC)$_2$Br$_2$ 2H$_2$O	ocre	0	91	9.7	12.8	25.0	9.2	13.1	25.0
Cu(ATSC)$_2$Cl	yellow	0	4.5	13.0	16.8	7.1	13.1	17.3	7.3
Cu(ATSC)$_2$Br	yellow	0	17.8						
Cu(ATSC)$_2$Br	yellow	0	17.8	11.9	16.1	14.9	12.0	15.9	15.1
Zn(ATSC) (ATSC-K) Cl2H$_2$O	white	0	4.8	12.7	15.8	7.0	12.5	16.1	6.8
Zn(ATSC) (ATSC-H)Br2H$_2$O	white	0	63	11.5	14.1	14.4	11.5	14.9	14.1
Co(ABTSC-H)$_2$Cl	dark brown	0	183	12.4	23.0	7.4	12.2	23.3	7.4
Co(ABTSC-H)$_2$Br	dark brown	0	128	11.0	21.5	15.1	11.5	21.3	15.0
Ni(ABTSC) (ABTSC-H)Cl	reddish brown	3.10	125	12.3	22.8	8.1	12.2	23.3	7.4
Ni(ABTSC) (ABTSC-H)Br	reddish brown	3.11	98	11.4	21.6	15.5	11.5	21.3	15.0
Cu(ABTSC)Cl$_2$ H$_2$O	green	1.50	118	14.8	16.0	16.1	14.6	16.1	16.3
Cu(ABTSC)Br$_2$ H$_2$O	green	1.53	110	14.1	13.0	34.7	14.4	12.8	34.3
Zn(ABTSC) (ABTSC-H)Cl	yellowish white	0	54	13.2	23.2	8.0	13.4	23.0	7.3
Zn(ABTSC) (ABTSCH-)Br	yellowish white	0	48	11.7	21.6	11.8	12.1	21.0	11.9

RESULTS AND DISCUSSION

The assignments of the principal absorption bands in the IR spectra were made according to earlier reports[9, 10] (Table 2). The IR spectra of the corresponding bromides present great similarity with those reported in table 2.

In the IR spectra of all the complexes a shift to lower frequencies is observed for the band assigned as ν CS. This indicates that both thiosemicarbazones coordinate to the metal through the sulphur atom. Greater

Table 2

Frequencies (cm^{-1}) of the principal absorption bands

Compound	ν_{NH}	$\nu_{CN} + \delta_{NH}$	ν_{CS}	ν_{M-X}
ATSC	3400(S), 3240(S) 3140(S)	1515(S)	850(M)	—
Co(ATSC)$_2$Cl$_2$Cl	34030(M), 3300(S)	1530(S)	830(M)	307(S), 300(S) 297(S),
Ni(ATSC)(ATSC-H)Cl	3400(S), 3270(S)	1530(S)	825(M)	—
Cu(ATSC)$_2$Cl	3420(M), 3260(S)	1535(S)	835(M)	308(M) 273(M)
Zn(ATSC)(ATSC-H) Cl2H$_2$O	3420(S), 3300(S)	1535(S)	835(M)	300(S), 302(S) 295(S)
ABTSC	3440(S), 3370(S) 3280(S), 3200(S)	1535(S)	835(M)	—
Co(ABTSC-H)Cl$_2$	3460(M), 3300(S) 3190(S)	1570(S), 1560(S) 1560(S)	800(M)	—
Ui(ABTSC)(ABTSC-H) Cl	3500—3400(S), 3300(S), 3180— 3100(S)	1570(S)	795(M)	—
Cu(ABTSC)Cl$_2$	3420(S), 3260(S) 3160(S)	1570(M), 1555(M)	800(M)	305(S)
Zn(ABTSC)(ABTSC-H)Cl	3440(S), 3310(S) 3220(S)	1570—1550(S)	820(M)	—

S = Strong
M = Medium

shifts are observed for the ABTSC complexes, and according to the metal, they are greater for Ni (II) and smaller for Zn (II) complexes. A shift to higher frequencies is observed for the band assigned as νCN + δNH. This suggests that the iminic nitrogen atom is also involved in the coordination. Therefore, ATSC should be considered in these complexes as a bidentate ligand.

On the other hand, ABTSC should coordinate as a tridentate ligand since a shift to lower frequencies is observed in one of the ν NH bands (3370 cm^{-1}). The additional coordination should take place through the amine group of the benzylic ring.

Once defined the forms of coordination of the ligands, and knowing the values of molar conductivity and magnetic moments, it is possible to consider the most probable structure of each complex. The frequencies of the ν M-X bands are also important elements in the structural assignations. The complexes Co(ATSC)$_2$X$_2$ must have a trigonal bipyramide (TBP) structure. The frequencies of the M-Cl valence bands present a great coincidence with those reported for similar complexes with acetone thiosemicarbazone,[10, 11] which by X-ray studies were reported to have a TBP structure.[12, 13] This criterion disagrees, in the case of Co(ATSC)$_2$X$_2$, from that stated by Tomlinson et al.[14] who considered it to have a tetrahedral structure. These authors reported a splitting in the ν CN + δ NH_2 band which was not observed by us. They considered that coordination only takes place through the sulphur atom.

We must point out that the additional coordination through the iminic nitrogen atom was confirmed by us in the ^1H-NMR spectrum of the complex in dioxane, since the CH_3 signal shifts from 2.25 ppm ppm up to 3.80 ppm.

The fact that $Co(ATSC)_2I_2$ has a tetrahedral structure [13] by a monodentate coordination through the sulphur atom can be explained in terms of the HSAB theory by the softening effect that must exert the iodide ion. Nevertheless, in the bromide and chloride complexes Co(II) must be sufficiently hard to coordinate through the iminic nitrogen atom.

The Ni(II) complexes with ATSC are square-planar diamagnetism. The complexes of Cu(I) and Zn(II) with ATSC ought to present a distorted octahedral structure, with polymeric associations through chloride bridging because of their low solubility in many solvents.

The complexes of Co (III) and Ni (II) with ABTSC should be octahedral. $Cu(ABTSC)Cl_2$ must present chloride bridges with Cu-Cu interactions due to its low μ_{eff} value. The Zn (II) complex, according to the values of its molar conductivities, might correspond to a mixture of bi- and tridentate ligands. This is not surprising since the coordination of ABTSC to Zn(II) is weak and even not well detectable through the NH_2 group.

The electronic spectra of all the complexes present strong absorption bands ($\epsilon = 1000-2500$) at 335—360 nm. The most intensive bands were those of Cu(II). The $Co(ATSC)_2X_2$ complexes change their structures in solution according to the nature of the solvent. Tomlinson reported a tetrahedral structure in — acetone. [14] In aqueous solutions or dioxane-water mixtures, the $Co(ATSC)_2X_2$ complexes present an absorption band at 510 nm ($\epsilon \sim 7$), characteristic of that of octahedral Co(II) complexes, while in pure dioxane the maximum is at 610 nm ($\epsilon \sim 240$). The position of this band and its intensity indicates that in dioxane the complex must be tetrahedral on account of the removal of the halide ion from internal sphere. This is confirmed by the ^1H-NMR spectrum since no additional splitting of the signals of CH_3 (3.80 ppm) nor NH_2(8.00 ppm) group was observed.

The oxidation states of cobalt and copper differ in their complexes with ATSC and ABTSC although synthetized under similar conditions. In ATSC complexes cobalt is 2+ and copper is 1+ while in ABTSC complexes cobalt is 3+ and copper is 2+. Due to the additional amino-group (in *ortho* position) of the ABTSC in respect to ATSC, the former thiosemicarbazone produces a stronger ligand field. This allows the cobalt to oxidize spontaneously.

ATSC is an alkyl, aryl-thiosemicarbazone while ABTSC is a monoaryl-thiosemicarbazone and therefore it is to be expected that copper must have a 1+ oxidation state with the former thiosemicarbazone and 2+ with the latter. [6] This is due to the —I effect of the aryl group that reduces the π-acceptor property of the thiosemicarbazone and, therefore, does not afford to stabilize the 1+ oxidation state of copper.

REFERENCES

[1] F. A. French and E. J. Jr. Blanz, *Cancer Res.*, **25**, 1454 (1965).
[2] A. C. Sartorelli, K. C. Agrawal and E. C. Moore, *Biochem. Pharm.*, **20**, 3119 (1971).
[3] J. A. Crim and H. G. Petering, *Cancer Res.*, **27**, 1278 (1967).
[4] M. S. Patil and J. R. Shah, *J. Indian Chem. Soc.*, **58**, 944 (1981).
[5] L. D. Dave and S. K. Thampy, *J. Indian Chem. Soc.*, **58**, 538 (1981).
[6] M. J. M. Campbell, *Coord. Chem. Rev.*, **15**, 279 (1975).
[7] P. T. Sah and T. C. Daniels, *Rec. Trav. Chim.*, **69**, 1545 (1950).
[8] J. Berstein, H. Yale, K. Losse, M. Holsing, J. Martin and W. Lott, *J. Amer. Chem. Soc.*, **73**, 906 (1951).
[9] M. Mashima, *Bull. Chem. Soc. Jpn.*, **37**, 934 (1964).
[10] B. Beecroft, M. J. M. Campbell and R. Grzeskowiak, *J. Inorg. Nucl. Chem.*, **36**, 55 (1974).
[11] M. J. M. Campbell, R. Grzeskowiak and M. Goldstein, *Spectrochim. Acta A*, **32**, 553 (1976).
[12] M. Mathew and G. J. Palenip, *J. Amer. Chem. Soc.*, **91**, 4923 (1969).
[13] G. Dessy and V. Scaramuzza, *Cryst. Struct.*, **5**, 605 (1976).
[14] C. Bellito, A. A. G. Tomlinson, C. Furlani and G. De Munn, *Inorg. Chim. Acta*, **27**, 269 (1978).

ORSZÁGOS MŰSZAKI INFORMÁCIÓS KÖZPONT ÉS KÖNYVTÁR
1883

NOTE POUR LES AUTEURS

La Revue Roumaine de Chimie publie des articles en anglais, français, russe, allemand ou espagnol. Les auteurs sont priés d'envoyer des articles et des comptes rendus inédits.

Les manuscrits seront dactylographiés à double interligne. La bibliographie, les tableaux et la légende des figures seront placés après le texte.

Si l'article fait partie d'une série numérotée, la partie précédente sera donnée comme première référence.

Chaque article sera précédé d'un résumé comprenant quinze lignes au maximum.

Les références bibliographiques dans le texte seront faites par des exposants sans parenthèses et paraîtront à la fin de l'ouvrage.

Les publications périodiques mentionnées dans la bibliographie seront présentées suivant les prescriptions internationales : le nom de l'auteur précédé de l'initiale du prénom, le titre du périodique abrégé conformément à « Chemical Abstracts » et souligné par une ligne, le numéro du tome indiqué par des chiffres arabes et souligné par deux lignes, suivi de la première page de l'article ; à la fin, l'année de la parution sera placé entre parenthèses. Le numéro de la revue ne sera pas indiqué si les pages du volume sont numérotées consécutivement.

Les textes des livres ou traités inclueront : le nom des auteurs, l'initiale du prénom, le titre du livre entre guillemets et sans être souligné, le numéro du tome précédé par l'abréviation « vol. » (ou « Bd. »), le numéro de l'édition, les éditions (the publisher), la localité de la parution du livre, l'année de la parution et la page de la référence précédée(s) par l'abréviation « p. » (ou « S. »).

Les brevets seront indiqués comme suit : l'auteur ou la firme, le pays et le numéro du brevet, la date et la revue *(Chem. Abstr.)*. Par ex. : M. Jones (to Union Carbide Co.). Brit. Pat. 601 238, 2 Sept. 1959 ; cf. *Chem. Abstr*, **54**, 12808 (1960).

Si la référence n'a pas été lue en original, on indiquera aussi la revue de référence consultée.

Les diagrammes seront tracés à l'encre de Chine sur papier calque. Les tableaux et les figures (en nombre strictement nécessaire) ainsi que les courbes dans les figures seront numérotés par des chiffres arabes. Leur explication sera donnée dans la légende des figures. Prière de ne pas inscrire les mêmes données dans les tableaux et les figures. Chaque tableau aura un titre. On indiquera dans le texte la place approximative des tableaux et des figures. Les formules chimiques seront incluses dans le texte ; en outre, elles seront transcrites sur papier calque, à l'encre de Chine.

Les auteurs sont priés d'indiquer les caractères italiques (en soulignant les lettres au crayon), ainsi que tout autre caractère spécial : les préfixes *ortho*, *meta*, *para*, *cis*, *trans*, etc. seront soulignés pour indiquer leurs caractères italiques et ne seront jamais écrits avec des majuscules.

Aucune correction à la main ne sera admise sur le manuscrit. Les corrections seront tapées à la machine. Les lettres grecques ou d'autres symboles spéciaux seront insérés à la main à l'encre clairement.

Le manuscrit sera signé par l'auteur.

Le titre-courant aura 50 lettres au maximum.

L'entière responsabilité du contenu des articles appartient aux auteurs.

Sur demande on peut obtenir une note plus complète.

PRINTED IN ROMANIA

1985 SEP
51

TRAVAUX PARUS AUX ÉDITIONS DE L'ACADEMIE DE LA RÉPUBLIQUE SOCIALISTE DE ROUMANIE

V. DRĂGUŢAN, A. T. BALABAN, M. DIMONIE, **Olefin metathesis and ring-opening polymerization of cyclo-olefins**, coédition avec John Wiley & Sons, 1985.

GH. MARCU, **Chimia compuşilor coordinativi**, 1984, 415 p.

E. CORDOŞ, C. MANOLIU, **Spectrometria de absorbţie şi fluorescenţă atomică**, 1984, 178 p.

C. BODEA éditeur, **Tratat de biochimie vegetală**, p. I vol. 5, 1984, 438 p.

ELENA CEAUŞESCU, **Cercetări în chimia şi tehnologia polimerilor**, 1983, 519 p.

N. ASANDEI, A. GRIGORIU, **Chimia şi structura fibrelor**, 1983, 395 p.

N. IONESCU, M. CĂLDĂRARU, **Oxidarea catalitică a olefinelor inferioare**, 1983.

C. CAŞCAVAL, **Studiul polimerilor prin piroliză şi cromatografie de gaze**, 1983, 220 p.

C. I. SIMIONESCU, F. DANEŞ, **Originea vieţii**, 1983, 110 p.

C. BODEA (éditeur), **Tratat de biochimie vegetală**, p. II, vol. IV, 1982, 408 p.

I. G. MURGULESCU, RODICA VÎLCU, **Introducere în chimia fizică. Vol. III. Termodinamica chimică**, 1982, 624 p.

I. G. MURGULESCU, J. PĂUN, **Introducere în chimia fizică, Vol. I. 3 Nucleul atomic, reacţii nucleare, particule elementare**, 1982, 606 p.

ELENA JERCAN, **Analiza cromatografică**, 1982, 286 p.

ELENA CEAUŞESCU, **Noi cercetări în domeniul compuşilor macromoleculari**, 1981, 536 p.

I. G. MURGULESCU, TATIANA ONCESCU, E. SEGAL, **Introducere în chimia fizică, Vol. II. 2. Cibernetică chimică şi cataliză**, 1981, 1024 p.

V. DRĂGUŢAN, A. T. BALABAN, M. DIMONIE, **Metateza olefinelor şi polimerizarea prin deschidere de inel a cicloolefinelor**, 1981, 254 p.

LYDIA-MARIA VAICUM, **Epurarea apelor uzate cu nămol activ. Bazele biochimice**, 1981, 218 p.

I. GĂLĂŢEANU, **Procese şi metode radiochimice în energetica nucleară**, 1981, 234 p.

O. IORDACHE, **Procese polistocastice aplicate la fenomenele de transfer**, 1981, 186 p.

CR. SIMIONESCU, VALERIA GORDUZA, **Polimeri biocompatibili şi biologic activi**, 1980, 479 p.

ELENA CEAUŞESCU, **Polimerizarea stereospecifică a izoprenului**, 1979, 307 p.

CONST. GH. MACAROVICI, **Analiza chimică cantitativă anorganică**, 1979, 457 p.

M. FLORESCU, **Metode ştiinţifice în dezvoltarea industriei chimice moderne**, 1979, 256 p.

A. T. BALABAN, I. GĂLĂŢEANU, G. GEORGESCU, LIGIA SIMIONESCU, **Compuşi marcaţi şi radiofarmaceutici cu aplicaţii în medicina nucleară**, 1979, 495 p.

I. G. MURGULESCU, E. SEGAL, **Introducere în chimia fizică. Vol. II. 1. Teoria molecular-cinetică a materiei**, 1979, 1036 p.

S. STERNBERG, FL. DANEŞ, **Termodinamica chimică aplicată**, 1978, 400 p.

I. G. MURGULESCU, V. EM. SAHINI, **Introducere în chimia fizică. Vol. I.2. Structura şi proprietăţile moleculelor**, 1978, 604 p.

I. ZUGRĂVESCU, MAGDA PETROVANU, **N-ylid chemistry**, coédition avec McGraw-Hill International Book Company, U.S.A., 1977, 396 p.

I. G. MURGULESCU, **Introducere în chimia fizică. Vol. I. 1. Atomi, molecule, legătură chimică**, 1976, 560 p.

ELENA CEAUŞESCU, **Research work on synthesis and characterization of macromolecular compounds. Contributions**, 1974, 251 p.

CR. SIMIONESCU, VIORICA RUSAN, V. POPA, **Chimia algelor marine**, 1974, 212 p., 1 pl

ISSN 0035 – 4093

I. P. Informaţia c. 1202

43 426

Lei 40

$ 80 (pour un abonnement annuel)

F 1103 MG

ACADÉMIE DE LA RÉPUBLIQUE SOCIALISTE DE ROUMANIE

R 1985 AUG 27

REVUE ROUMAINE DE CHIMIE

TOME 30
N° 8
Août 1985

Rev. Roumaine Chim.

RRCHAX, 30, 8, 645–764 (1985), Bucarest

EDITURA ACADEMIEI REPUBLICII SOCIALISTE ROMÂNIA

ACADÉMIE DE LA RÉPUBLIQUE SOCIALISTE DE ROUMANIE

COMITÉ DE RÉDACTION

Rédacteur en chef :

I. G. MURGULESCU, membre de l'Académie de la République Socialiste de Roumanie

Rédacteurs en chef adjoints :

A. T. BALABAN et V. EM. SAHINI, membres correspondants de l'Académie de la République Socialiste de Roumanie

Collège de rédaction :

EM. BRATU, ELENA CEAUŞESCU, ECATERINA CIORĂNESCU-NENITZESCU, CR. SIMIONESCU, membres de l'Académie de la République Socialiste de Roumanie; P. SPACU, membre correspondant de l'Académie de la République Socialiste de Roumanie; M. BANCIU, M. D. GHEORGHIU, I. HAIDUC, D. I. MARCHIDAN, I. MOLDOVAN, G. NIAC et D. SĂNDULESCU

La Revue Roumaine de Chimie paraît 10 fois par an. Toute commande de l'étranger sera adressée à «ROMPRESFILATELIA» — sectorul Export-Import Presă, P.O. Box 12—201, télex 10376 prsfir Bucureşti, Calea Griviței nr. 64—66, Roumanie.

Les manuscrits, les livres et les revues proposés en échange, ainsi que toute correspondance seront envoyés à la rédaction :

REVUE ROUMAINE DE CHIMIE

125, Calea Victoriei, 79717 Bucarest, Roumanie, téléphone 50 76 80

EDITURA ACADEMIEI REPUBLICII SOCIALISTE ROMÂNIA
125, Calea Victoriei, 79717 Bucarest, Roumanie, téléphone 50 76 80

REVUE ROUMAINE
DE
CHIMIE

ORSZÁGOS MŰSZAKI INFORMÁCIÓS KÖZPONT ÉS KÖNYVTÁR 1883

Tome 30, N° 8 **Août 1985**

ION TEOREANU, ECATERINA ANDRONESCU and LUCIA CACOVEANU, Thermal phase equilibrium relationships in $2CaO.SiO_2-CaO.Al_2O_3$ system 647–650

ORTANSA LANDAUER, CORNELIA MATEESCU, OLGA IULIAN and G. COSTEANU, Physico-chemical study of tetrahydrofuran-methanol and dioxane-methanol systems (in French) 651–658

P. SPACU, SILVIA PLOŞTINARU, LUMINIŢA PATRON, ADRIANA CONŢESCU and E. SEGAL, Coordination compounds as raw materials for mixed oxides. I. Mixed coordination compounds of lanthanides and Co(III) with salicylic acid 659–665

ION TĂNASE, ION IONECI and CONSTANTIN LUCA, The electrochemical behavior of ethylmercury in aqueous medium 667–678

I. TĂNASE, IULIANA VARTIRES, N.D. TOTIR, I. IONECI and C. LUCA, Determination of microamounts of mercury(II) in high purity reagents by anodic stripping voltammetry 679–687

LUMINIŢA VLĂDESCU and STELA TONEANU, Combined ion exchange-spectrophotometric determination of potassium with sodium tetraphenylborate 689–693

CS. VÁRHELYI, J. ZSAKÓ, GY. LIPTAY and MAGDA SOMAY, On the dioximine complexes of transition metals. LXVII. New sulfito-*bis*-dimethylglyoximino-cobalt(III) complexes and their thermal decomposition 695–702

M. BANCIU, I. POGANY, DANA MOSORA, PATRICIA RUSU, RODICA STĂNCIULESCU and MARIA DEZSÖ, Synthesis of 9,10,19,20-tetrahydro-dibenzo/*a,c*/phenanthro/*g*/cyclodecene and 9,10,19,20-tetrahydro-tetrabenzo/*a,c,g,i*/cyclodecene by sulphone pyrolysis 703–712

M. IOVU, VALERIA RĂDULESCU and M. IQBAL, Decomposition of halomethylethers by secondary amines (in French). 713–717

C.B. SHARMA and P.C. PACHAURI, The reaction of chlorine dioxide with dl-alanine in aqueous solution 719–724

H. HINGORANI, H.C. GOYAL, G. CHANDRA, S.N. SRIVASTAVA, Kinetics of Os(VIII) catalysed chloramine-T oxidation of glycollic acid and lactic acid in alkaline media 725–734

SHRIKANT S. HANMANTGAD, MANOHAR V. KULKARNI and VEMANNA D. PATIL, Synthesis of some biomimetic 4-substituted coumarins. 735–741

A. BODOR, A. GERGELY, R. SCHWARTZ, A. JUHASZ, P. COLTEA and D. BREAZU, The synthesis of 19-hydroxysteroids 743–748

A.M. FAHMY, S.A. MAHGOUB, M.M. ALY and M.Z.A. BADR, The photo formylation of phenols 749–752

C.I. CHIRIAC, Esters from N-acylphthalimides and phenols. 753–755

R.L. MITAL, VINEETA TANEJA, C.L. GUPTA and S.B. GUPTA, Studies in the synthesis of some new polynuclear heterocycles: 6-chloro, 8,13-dihydro-8,13-o-benzenonaphtho[2,3-a]phenothiazin-7(H) ones 757–758

BOGUSŁAW PILARSKI, and KRYSTYNA WISTEROWICZ, Structural studies on imidazolidineacetonitrile derivatives 759–763

Rev. Roumaine Chim. **30**, *8*, 645–764 (1985), Bucarest

Revue Roumaine de Chimie, **30**, *8*, 647–650(1985)

THERMAL PHASE EQUILIBRIUM RELATIONSHIPS IN $2CaO \cdot SiO_2-CaO \cdot Al_2O_3$ SYSTEM

ION TEOREANU, ECATERINA ANDRONESCU and LUCIA CACOVEANU
The Polytechnic Institute Bucharest, Romania

Received February 25, 1985

This paper studies the phasal relations of $2CaO \cdot SiO_2-CaO \cdot Al_2O_3$ binary system that is particularly important for the aluminous cement chemistry. The experimental results allowed to draw the *liquidus* curve for the system zone where the process of melting is completed up to 1500°C. For those compositions whose melting requires higher temperatures, the equilibrium diagram has been assessed on the basis of specific thermodynamic data.

INTRODUCTION

Phase diagrams represent both a fundamental means of investigation and, especially, an instrument to conduct processing into a wide range of ceramic products of phasal composition, having preset textural-structural features and physico-chemical properties. Both in chemistry and cement technologies, particularly aluminous cement, the information supplied by phase diagrams proves scientifically the burning and cooling thermal treatment adequate to obtain certain clinkers with a phasal composition corresponding to higher binding properties. Despite extensive research on thermal equilibrium relations of hydraulic cements, certain systems are still hardly investigated or not investigate at all and therefore are given close attention.

This paper studies the phasal relations of $2CaO . SiO_2 - CaO . Al_2O_3$ binary systems that is particularly important for the aluminous cement chemistry.

EXPERIMENTAL RESULTS

In order to work out the phase diagram of the system, a number of 20 compositions corresponding to various ratios between the dicalcium silicate and monocalcium aluminate have been considered as shown in Table 1.

The compositions shown in Table 1 were mixed from the pre-synthetized components of the system. Melting to define the liquidus curve was the main target. Measurements were made by a high temperature microscope-like device on specimens of about 2 × 2 × 2 mm.

The melting process was studied on the specimens being suspended on a platinum wire next to the Pt—PtRh thermocuple.

The specimen was viewed with an optical instrument-Katetometer KM—6. The rate of temperature rise within the range of melting was under 0.50°C/min, the liquidus temperature being the moment when the specimen becomes entirely transparent. The results are given in Table 1 above. Thus the final melting point cannot be reached for compositions no. 1, 2, 7, 19 and 20 due to the high refraction of dicalcium silicate ($T_f = 2130°C$) and to the working conditions allowing for maximum temperatures of 1500°C. The melting of studies compositions began at 1400°C. The no. 18 sample registers the 1400°C melting considered as invariant of the system. Therefore the nearer the sample (against no. 18 sample) the closer the melting range.

Table 1

Mineralogical composition and *liquidus* temperature

No. sample	Mineralogical composition %Gr		Temperature liquidus °C
	$2CaO.SiO_2$ —	$CaO.Al_2O_3$	
1	75.00	25.00	over 1490
2	50.00	50.00	over 1490
3	40.00	60.00	1440
4	25.00	75.00	1460
5	45.00	55.00	1490
6	42.50	57.50	1460
7	47.50	52.50	over 1490
8	46.25	53.75	1500
9	43.75	56.25	1470
10	44.37	55.63	1485
11	36.70	63.30	1435
12	33.40	66.60	1425
13	35.05	65.95	1430
14	30.00	70.00	1430
15	31.65	68.35	1415
16	34.40	67.60	1420
17	32.12	67.98	1410
18	31.84	68.15	1400
19	55.00	45.00	over 1500
20	60.00	40.00	over 1500

The *liquidus* curve for the zone of the studied compositions is shown in Fig. 1.

The DTA curve made on no. 18 sample shows further to 10°C/min heating of the glass-state sample as per Fig.2.

Quantity ratios among equilibrium phases at 1400°C are shown in the diagram given in Fig. 3.

Since the working conditions allowed for no identification of the melting final temperatures for compositions richer in dicalcium silicate than sample no. 8, having higher monocalcium aluminate concentrations than sample no. 4 respectively, we deemed useful to work out the equilibrium diagram of the system within refractions range based on thermodynamic data to the methodology described in the technical literature [1–7]; the relevant results enabled us to draw-in dashed line the equilibrium diagram corresponding to the specific range (compositions with no experimental informations avaible) — Fig. 1.

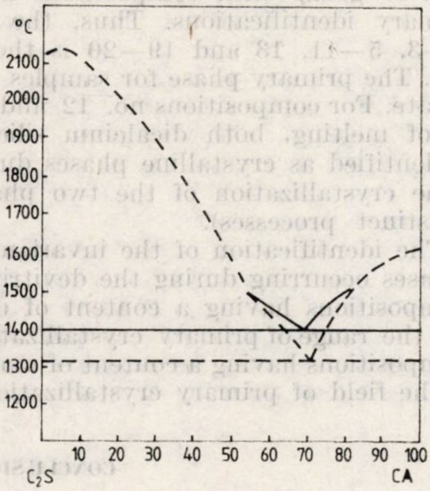

Fig. 1. — Phase diagram of $2CaO.Si_2—CaO.Al_2O_3$ system.

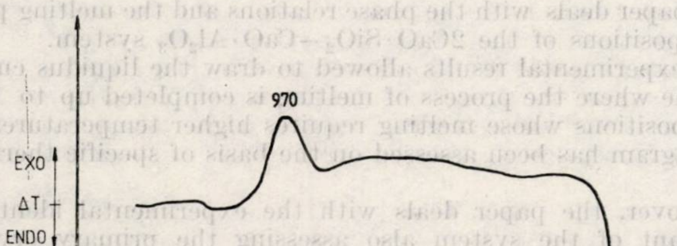

Fig. 2. — The DTA curve for samples no. 18.

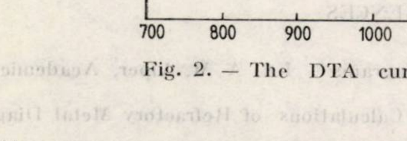

Fig. 3. — Quantity ratios among equilibrium phase at 1400°C.

The same compositions used for experimental investigations have been also studied for the process of crystallizing. With this very end in view the compositions have been arc molten and then subjected to certain treatments of crystallizing within the temperature range 800—1300°C.

The diffractometric analysis (X-ray) and optical microscope analysis allowed to group such compositions according to the crystalline phase of primary identifications. Thus, the primary phase for compositions no. 1—3, 5—11, 13 and 19—20 is the devitrification of the dicalcium silicate. The primary phase for samples no. 4 and 14 is the monocalcium aluminate. For compositions no. 12 and 15—17, probably due to the close range of melting, both dicalcium silicate and monocalcium aluminate were identified as crystalline phases during the process of devitrification (i.e. the crystallization of the two phases could not be separated into two distinct processes).

The identification of the invariant as well as the identifications of the phases occurring during the devitrification allow us to conclude that all compositions having a content of dicalcium silicate over 31.84 % lie within the range of primary crystallization of calcium orthosilicate while the compositions having a content of monocalcium aluminate over 68.16 % lie in the field of primary crystallization of the monocalcium aluminate.

CONCLUSIONS

The paper deals with the phase relations and the melting peculiarities of 20 compositions of the $2CaO \cdot SiO_2 - CaO \cdot Al_2O_3$ system.

The experimental results allowed to draw the liquidus curve for the system zone where the process of melting is completed up to 1500°C. For those compositions whose melting requires higher temperatures, the equilibrium diagram has been assessed on the basis of specific thermodynamic data.

Moreover, the paper deals with the experimental identification of the invariant of the system also assessing the primary crystallization fields for the dicalcium silicate and monocalcium aluminate respectively.

REFERENCES

[1] Y. K. Rao, "Thermodynamics of Phase Diagrams", Ed. A. M. Alper, Academic Press, 1—42 (1970).

[2] L. Kaufman and H. Bernstein, "Computer Calculations of Refractory Metal Diagrams", Academic Press, 46—93 (1970).

[3] P. Holba, *Silikaty*, **23**, 289 (1979).

[4] Z. Panek, *Silikaty*, **23**, 97 (1970).

[5] M. Eliasova, I. Proks and I. Zlatovsky, *Silikaty*, **22**, 97 (1978).

[6] M. Eliasova, I. Proks and K. Adamkomskova, *Silikaty*, **22**, 193 (1978).

[7] L. Barin, "Thermochemical properties of inorganic substances, Academic Press, (1965).

Revue Roumaine de Chimie, **30**, *8*, 651–658 (1985)

ÉTUDE PHYSICO-CHIMIQUE DES SYSTÈMES BINAIRES TÉTRAHYDROFURANNE-ALCOOL MÉTHYLIQUE ET DIOXANNE-ALCOOL MÉTHYLIQUE

ORTANSA LANDAUER, CORNELIA MATEESCU, OLGA IULIAN et G. COSTEANU
Chaire de Chimie-Physique et de Technologie Electrochimique, Institut Polytechnique,
Calea Griviţei 132, Bucarest, Roumanie

Reçu le 14 mai 1984

Les auteurs ont étudié par différentes méthodes physico-chimiques les systemes binaires tétrahydrofuranne-alcool méthylique et dioxanne-alcool méthylique, à diverses concentrations et aux températures de 25, 30 et 40°. D'après les résultats obtenus on a tiré des conclusions sur les associations par liaison hydrogène.

The authors have studied by different physico-chemical methods the binary systems tetrahydrofuran-methyl alcohol and dioxan-methyl alcohol, at different concentrations and at 25, 30, and 40°. On this basis conclusions were drawn concerning the existence of molecular associations by hydrogen bonding.

L'étude des propriétés physico-chimiques d'un grand nombre de composés, hydroxylés en particulier, révèle l'existence d'associations stables entre les molécules par liaison hydrogène.

Pour mettre en évidence de telles associations nous avons étudié la viscosité, la densité, la constante diélectrique et aussi l'indice de réfraction des solutions d'alcool méthylique (AM) dans deux solvants différents : le tétrahydrofuranne (THF) et le dioxanne (Diox). Le premier a un moment dipolaire égal à 1,71 D, alors que le second a un moment nul. On sait que certaines propriétés de ces corps peuvent s'expliquer par la présence des atomes d'oxygène dans leurs molécules. Ces atomes porteurs de paires libres d'électrons sont capables de former, dans certains systèmes, des associations moléculaires par liaison hydrogène, du type O—H. . . .O=, dont le doublet utilisé est un doublet sp_2. Ce sont aussi les forces provenant des atomes d'oxygène qui font de ces deux liquides d'excellents solvants.

Les substances que nous avons utilisées dans ce travail ont été bien purifiées au préalable. Toutes les mesures ont été effectuées dans un ultrathermostat à 25, 30 et 40°.

La viscosité des liquides purs et des solutions de différentes concentrations des systèmes mixtes a été déterminée avec un viscosimètre Ubbelohde. Les résultats obtenus, exprimés en cP, sont rassemblés dans les tableaux 1 et 2. La variation de la viscosité en fonction de la fraction molaire est illustrée par la figure 1.

On voit que la viscosité du système THF—AM varie très peu avec la concentration du mélange, tandis que celle du système Diox—AM croît d'abord régulièrement dans les solutions riches en alcool et ensuite très rapidement à partir de $X > 0,5$.

Tableau 1

Valeurs des viscosités, en cP, du système THF-AM

X_{THF}	$\eta_{25°}$	$\eta_{30°}$	$\eta_{40°}$
0	0,5559	0,5158	0,4576
0,05	0,5529	0,5134	0,4539
0,11	0,5477	0,4978	0,4470
0,18	0,5271	0,4975	0,4359
0,25	0,4969	0,4855	0,4225
0,33	0,4949	0,4609	0,4168
0,43	0,4812	0,4579	0,4144
0,54	0,4796	0,4552	0,4108
0,67	0,4719	0,4528	0,4072
0,82	0,4747	0,4426	0,4055
1,00	0,4900	0,4688	0,4324

Tableau 2

Valeurs des viscosités, en cP, du système Diox-Am

X_{Diox}	$\eta_{25°}$	$\eta_{30°}$	$\eta_{40°}$
0	0,5559	0,5158	0,4576
0,05	0,5666	0,5235	0,4708
0,12	0,5745	0,5337	0,4796
0,14	0,5795	0,5399	0,4827
0,17	0,5826	0,5423	0,4863
0,24	0,6163	0,5708	0,5101
0,32	0,6866	0,6169	0,5391
0,42	0,7315	0,6598	0,5746
0,53	0,8505	0,7234	0,6247
0,66	1,0012	0,7825	0,6913
0,81	1,1444	1,0430	0,7952
1,00	1,1940	1,1375	0,9552

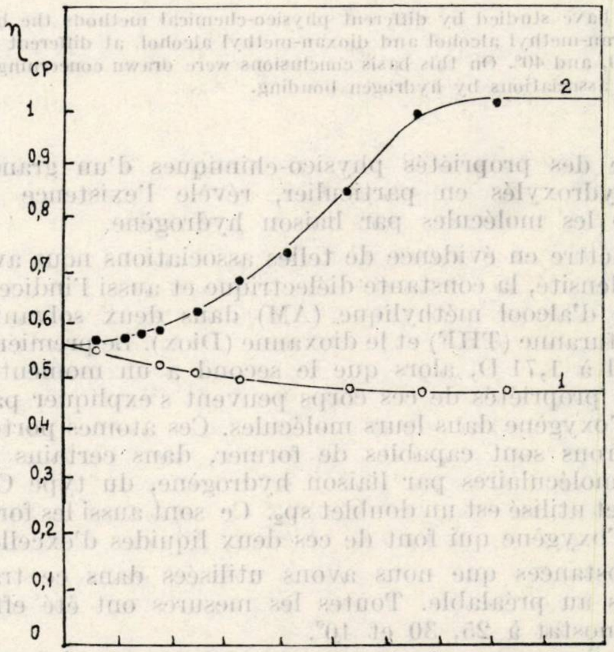

Fig. 1. — Variation de la viscosité avec la fraction molaire.

Les courbes représentatives de l'énergie d'activation de l'écoulement visqueux, E—f(X), sont également très différentes (Fig. 2). On admet que la structure des complexes formés par liaison hydrogène doit jouer un rôle très important dans l'écoulement visqueux.

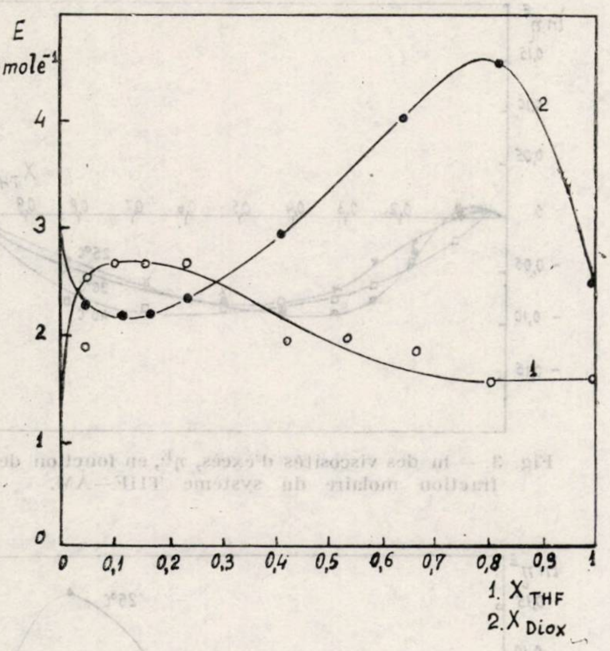

Fig. 2. — Variation de l'énergie d'activation avec la fraction molaire.

Les viscosités d'excès, calculées en utilisant la formule donnée dans un travail antérieur,[1] exprimées en ln η^E sont représentées, en fonction de la fraction molaire, par les courbes des figures 3 et 4.

On remarque la différence entre les deux systèmes et aussi l'influence de la température.

Il est certain que la variation de la viscosité des mélanges liquides est en rapport principalement avec le changement de volume au moment du mélange.

Pour connaître les volumes molaires nous avons mesuré d'abord les densités des solutions mentionnées plus haut, aux mêmes températures, avec un picnomètre à paroi double vidée.

Les résultats sont rassemblés dans les tableaux 3 et 4.

On a calculé, à partir de ces résultats, les volumes molaires moyens et ensuite les volumes molaires d'excès,[1] dont les valeurs en fonction de la fraction molaire sont illustrées par les courbes des figures 5 et 6. On voit que le volume molaire d'excès du système THF—AM a la valeur la plus basse à 40°. Le comportement de ce système est assez différent d'un autre système binaire THF—DMFA, mentionné dans la littérature.[2] Le volume molaire d'excès du système Diox—AM, à 25°, a la valeur la plus petite, à X = 0,8. Nous avons constaté qu'à la même concentration et à la même température les courbes E--f(X) Diox) et ln η^E--f(X_{Diox}) présentent un maximum. (Voir les figures 2 et 4.)

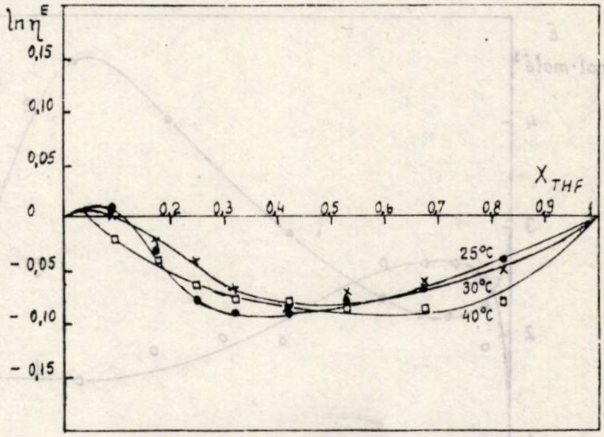

Fig. 3. — ln des viscosités d'excès, η^E, en fonction de la fraction molaire du système THF—AM.

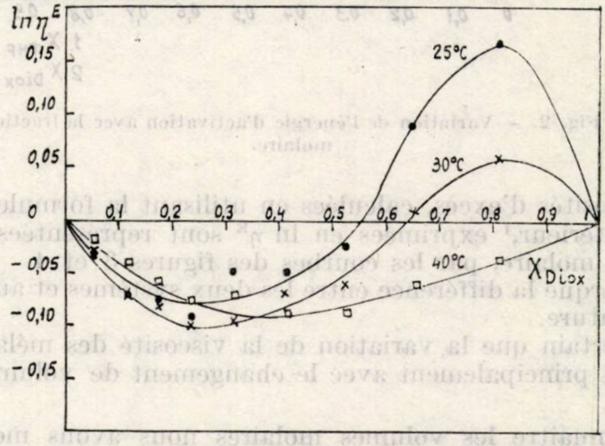

Fig. 4. — ln des viscosités d'excès, η^E, en fonction de la fraction molaire du système Diox—AM.

Il est bien évident qu'à cette concentration de grandes forces intermoléculaires se manifestent entre les deux constituants du système.

Nous admettons, d'après ces résultats, que dans le système Diox—AM il pourrait se former deux types de complexes.

Non moins instructives pour la mise en évidence des liaisons hydrogène est l'étude de la constante diélectrique et, ce qui revient au même, du carré de l'indice de réfraction.

Tableau 3

Valeurs des densités, en gcm^{-3}, du système THF—AM

X_{THF}	$d_{25°}$	$d_{30°}$	$d_{40°}$
0	0,7855	0,7814	0,7734
0,05	0,7965	0,7914	0,7829
0,11	0,8063	0,8040	0,7945
0,18	0,8146	0,8130	0,8036
0,25	0,8260	0,8206	0,8130
0,33	0,8364	0,8300	0,8268
0,43	0,8443	0,8402	0,8332
0,54	0,8542	0,8499	0,8426
0,67	0,8641	0,8568	0,8524
0,82	0,8734	0,8661	0,8601
1,00	0,8810	0,8750	0,8630

Tableau 4

Valeurs des densités, en gcm^{-3}, du système Diox-AM

X_{Diox}	$d_{25°}$	$d_{30°}$	$d_{40°}$
0	0,7855	0,7814	0,7734
0,05	0,8089	0,8013	0,8000
0,12	0,8325	0,8307	0,8235
0,14	0,8455	0,8431	0,8363
0,17	0,8584	0,8565	0,8487
0,24	0,8838	0,8800	0,8729
0,32	0,9077	0,9076	0,9001
0,42	0,9375	0,9323	0,9212
0,53	0,9611	0,9576	0,9450
0,66	0,9889	0,9780	0,9669
0,81	1,0114	1,0011	0,9973
1,00	1,0266	1,0211	1,0124

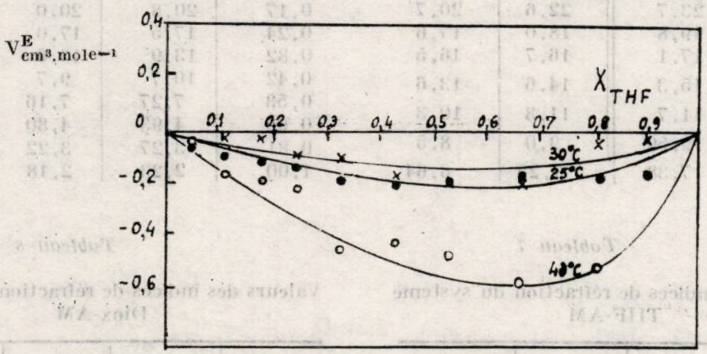

Fig. 5. — Volumes d'excès en fonction de la réaction molaire du système THF-AM.

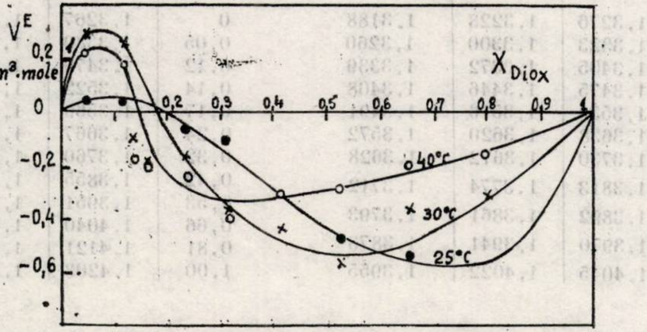

Fig. 6. — Volumes d'excès en fonction de la fraction molaire du système Diox-AM.

Il nous a fallu donc mesurer la constante diélectrique des mélanges considérés, aux mêmes températures, avec un diélcomètre de fréquence 2,5—4 MHz, et les indices de réfraction avec un réfractomètre Abbé. Les résultats sont rassemblés dans les tableaux 5, 6, 7 et 8.

Pour calculer la polarisation électrique du mélange liquide, nous avons utilisé une nouvelle forme de la relation d'Onsager [3,4] : $P = \dfrac{(\varepsilon - n^2)(2\varepsilon + n^2)}{\varepsilon(n^2 + 2)^2}$, P est la „polarisation de mélange", qui se présente comme somme des contributions polaires du mélange, ε est la constante diélectrique et n l'indice de réfraction des mélanges liquides.

Tableau 5

Valeurs des constantes diélectriques du système THF-AM

X_{THF}	ε_{25°	ε_{30°	ε_{40°
0	33,1	32,0	31,3
0,05	31,3	30,5	28,3
0,11	29,1	28,3	26,0
0,18	26,4	25,7	23,2
0,25	23,7	22,6	20,7
0,33	19,8	18,0	17,6
0,43	17,1	16,7	16,5
0,54	15,3	14,6	13,6
0,67	11,7	11,3	10,3
0,82	9,59	9,0	8,5
1,00	7,38	7,25	6,64

Tableau 6

Valeurs des constantes diélectriques du système Diox-AM

X_{Diox}	ε_{25°	ε_{30°	ε_{40°
0	33,1	32,0	31,3
0,05	30,0	28,3	27,7
0,12	25,0	23,6	22,6
0,14	22,6	21,5	20,8
0,17	20,8	20,0	19,3
0,24	17,5	17,0	16,5
0,32	13,9	13,6	12,8
0,42	10,7	9,7	9,2
0,53	7,27	7,16	6,73
0,66	4,93	4,80	4,64
0,81	3,27	3,22	3,19
1,00	2,23	2,18	2,00

Tableau 7

Valeurs des indices de réfraction du système THF-AM

X_{THF}	n_{25°	n_{30°	n_{40°
0	1,3276	1,3228	1,3188
0,05	1,3323	1,3300	1,3260
0,11	1,3405	1,3372	1,3339
0,18	1,3475	1,3446	1,3408
0,25	1,3559	1,3516	1,3491
0,33	1,3638	1,3620	1,3572
0,43	1,3730	1,3672	1,3628
0,54	1,3813	1,3774	1,3712
0,67	1,3892	1,3861	1,3793
0,82	1,3970	1,3941	1,3873
1,00	1,4045	1,4022	1,3955

Tableau 8

Valeurs des indices de réfraction du système Diox-AM

X_{Diox}	n_{25°	n_{30°	n_{40°
0	1,3267	1,3228	1,3188
0,05	1,3380	1,3360	1,3315
0,12	1,3470	1,3450	1,3403
0,14	1,3522	1,3500	1,3454
0,17	1,3569	1,3540	1,3500
0,24	1,3667	1,3645	1,3599
0,32	1,3760	1,3737	1,3689
0,42	1,3855	1,3824	1,3784
0,53	1,3951	1,3914	1,3879
0,66	1,4040	1,4003	1,3967
0,81	1,4121	1,4095	1,4048
1,00	1,4203	1,4172	1,4124

La polarisation expérimentale des deux systèmes diffère de celle déterminée par la règle des mélanges à partir des données relatives aux constituants purs (Fig. 7).

Les courbes présentent une déviation négative par rapport au cas idéal, celle du système Diox-AM étant plus accentuée. Nous avons attribué ces écarts à la linéarité et à la formation des complexes par liaison hydrogène entre les constituants du système. On a calculé aussi les constantes diélectriques d'excès et les indices de réfraction d'excès, dont les résultats sont représentés par les courbes des figures 8 et 9.

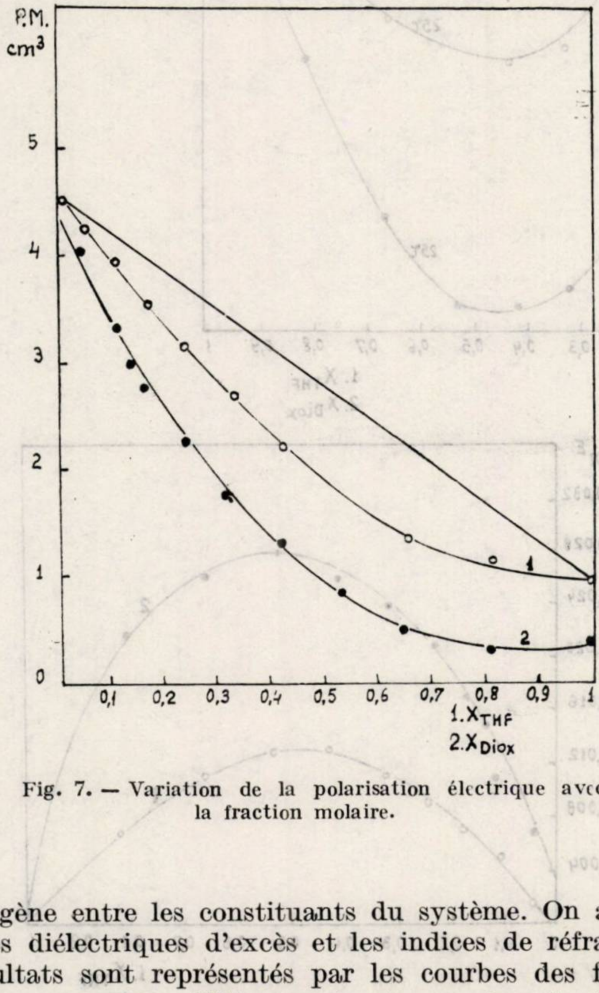

Fig. 7. — Variation de la polarisation électrique avec la fraction molaire.

On remarque un parallélisme entre les courbes de deux systèmes, malgré la différence des valeurs.

D'après les résultats présentés plus haut, on admet la formation des associations moléculaires par liaison hydrogène dans les deux systèmes. Ces associations se font molécule à molécule (association 1——1). Mais il semble que dans l'intervalle des concentrations de 0——1, il pourrait se former aussi des associations 1——2, en particulier dans le système Diox—AM.

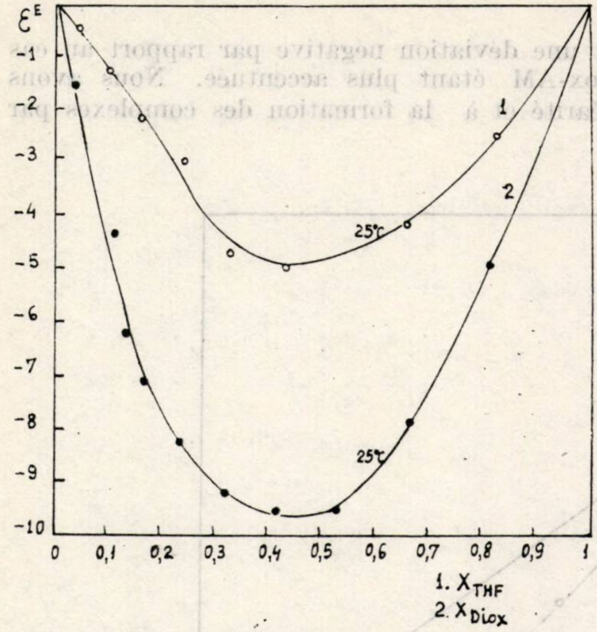

Fig. 8. — Constantes diélectriques d'excès en fonction de la fraction molaire.

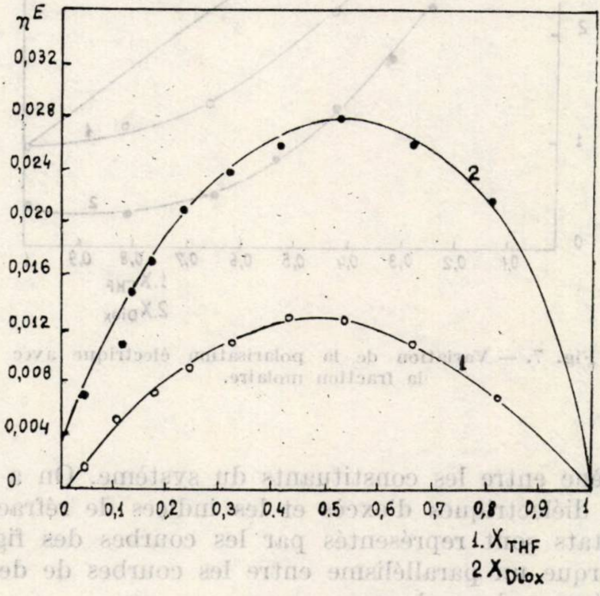

Fig. 9. — Indices de réfraction d'excès en fonction de la fraction molaire.

BIBLIOGRAPHIE

[1] Ortansa Landauer, G. Costeanu et Cornelia Mateescu, *Rev. Roumaine Chim.*, **24**, 1024 (1979).
[2] K. Geier et H. J. Bittrich, *Z. Phys. Chem. (Leipzig)*, **255**, 305 (1974).
[3] J. Barriol et A. Weisbecker, *Compt. rend.*, **259**, 2831 (1964).
[4] J. Barriol et A. Weisbecker, *J. Chim. phys.*, **62**, 623 (1965).

Revue Roumaine de Chimie, **30**, *8*, 659–665 (1985)

COORDINATION COMPOUNDS AS RAW MATERIALS FOR MIXED OXIDES. I

MIXED COORDINATION COMPOUNDS OF LANTHANIDES AND Co(III) WITH SALICYLIC ACID

P. SPACU, SILVIA PLOSTINARU, LUMINIȚA PATRON, ADRIANA CONȚESCU
and E. SEGAL
Center of Physical Chemistry, Bucharest, Romania

Received February 11, 1984

The complex compounds of lanthanides and Co(II) with salicylic acid were characterized by physico-chemical methods (electronic and IR spectra, magnetic and thermogravimetric measurements) in order to establish the nature of the species formed, the coordination of the ligand and the thermal behaviour.

In recent years the mixed oxides of perovskite structure have been focusing increasing attention in relation to their physical properties (piezoelectricity, pyroelectricity, magnetism, electro-optical effects, etc.) as well as to their applications, of which the most interesting is their use in catalytic processes.

These isomorphous oxides have the general formula ABO_3, where A stands for a large ion whose *d* shell is occupied and B for a transition metal ion. Among these oxides the most interesting and extensively studied are the perovskite type mixed oxides of transition metals (Fe^{III}, Co^{III}, Ni^{III}, Mn^{III} etc.). The wide variety of metallic ions accounts for the extensive research perovskites have enjoyed, more so their catalytic applications.[1-3]

Perovskites containing Co^{III}, of $LnCoO_3$ and $Ln_{0.8}Sr_{0.2}CoO_3$[4] type and those containing Mn^{III} [5,6] were tested as catalysts in oxidation-reduction [7] and hydrogenation [8] reactions, respectively. It was also shown that these perovskites may be employed as catalysts in depolution reactions, as their activity is comparable with that of Pt catalysts currently used in this kind of reactions.

Taking into account the importance of those types of oxides, we have undertaken a study aiming at obtaining $LnCoO_3$, where Ln^{III} = La, Pr, Nd, Sm, Eu, Gd, Dy, Ho, Er, Tb.

Several methods of obtaining lanthanide cobaltite are mentioned in the literature : the classical ceramic method [9,10] and the nonconventional methods of coprecipitation followed by pyrolyzing the products obtained [11,12], decomposition of complex compounds [13,14] and explosion [15].

The nonconventional methods offer some advantages : the oxides are obtained at much lower temperatures, the calcination times are shorter.

Because in the literature the studies on mixed complex compounds with lanthanides and Co(II) are scarce, we thought it would be useful to obtain and characterize such complexes with a series of organic ligands, as precursors of $LnCoO_3$. The selection of the ligand was difficult because one had to take into account the very different coordinations of the two elements and of the pH at which the mixed compounds separate.

A characteristic of the coordination chemistry of lanthanides is their pronounced tendency to form stable complex compounds with ligands containing oxygen as donor atom. A comparison with the most transition metals whose donor atoms tend to form complex compounds, in the sequence $N > S > O$ or sometimes $S > N > O$ shows that in lanthanides the sequence is that of alkali earth metals i.e. $O > N > S$.

After testing several organic ligands, the best results were obtained with hydroxycarboxylic acids.

This contribution presents the results obtained with the system $Ln^{III}-Co^{II}$—salicylic acid.

EXPERIMENTAL

Reagents were as follows : Ln_2O_3 99.9% (Mathey and Johnson) ; $Co(NO_3)_2 \cdot 6H_2O$, salicylic acid (Fluka AG). For syntheses the lanthanide oxides were transformed into nitrates. *The synthesis of complexes*. The mixed complex compounds were isolated in aqueous solution by treating the nitrate mixture with a saturated salicylic acid solution (of 1 : 1 : 5 ; 1 : 1 : 8 ; 1 : 1 : 10 ratio). The precipitation of the complex begins only after the addition of aqueous ammonia up to a $pH = 7-8$. After 24 hours, the precipitate is filtered, washed with water and acetone. Crystalline pink complex compounds of the general formula :

$$[LnCo(Sal)_4(OH)] \cdot 4H_2O$$

where Ln^{III} = La, Pr, Nd, Sm, Gd
Sal = salicylic acid

were always obtained, no matter what the amount of ligand employed and the type of lanthanide ion.

The formula was established by elemental chemical analysis : $[LnCo(Sal)_4(OH)]\ 4H_2O$: theoretical : Co, 7.05 ; C. 40.10 ; H, 3.70 ; found : Co, 6.60 ; C. 40.30 ; H. 3.40.

The techniques employed were as follows :

— elemental chemical analysis (C, H) was made by microcombustion ; Co was determined by atomic absorption ;

— the UV and visible spectra were recorded with a VSU-1 Zeiss Jena spectrophotometer in the 240-980 nm range with MgO as standard ;

— the IR spectra were recorded with a UR — 10 Zeiss Jena spectrometer, KBr pellets were employed ;

— the magnetic measurements, on solid samples were effected by Faraday method with Mohr salt as standard ;

— the differential thermal analyses were recorded with a MOM Budapest Paulik-Paulik Erdey derivatograph.

RESULTS AND DISCUSSION

The complex compounds synthetized were characterized from physico-chemical point of view (electronic and IR spectra, magnetic and thermogravimetric measurements) in order to establish the nature of the species formed, the coordination of the ligand and the thermal behaviour.

The elemental chemical analysis shows that the complexes obtained are the same, regardless of the metal/ligand ratio. The carbon and hydrogen content points to the presence of 4 salicylate groups, of 4 moles of H_2O and an OH group. These findings have been supported by the analysis of IR spectra; these spectra were recorded within 400—4000 cm^{-1} range for mixed complexes, for simple Co^{II} and lanthanide complexes and for free salicylic acid. The analysis of spectra points to the fact that the coordination occurs through the carboxylic group evidenced by the existence of two characteristic bands: $\nu_{sym}(1390-1400\ cm^{-1})$ and $\nu_{asym}(1570\ cm^{-1})$.

The formulas we advanced for Co(II) and Ln(III) complex compounds with salicylic acid are supported by the existence of the band at 3600 cm^{-1}, which is characteristic of free OH; this band is very strong in simple Co(II) complex, weak in the mixed complex and absent in the La(III) complex (Fig. 1).

Valuable data on the structure of the complex compounds isolated were obtained from the study of reflectance electronic spectra in UV and visible range. In UV the reflection spectra were recorded within 220—360 nm for the free ligand, the simple complexes of Co^{II} and Ln^{III} and for mixed complexes.

The salicylic acid exhibits two absorption bands at 235 and 315 nm, corresponding to $\pi - \pi^*$ and $n - \pi^*$ transitions in the ligand.

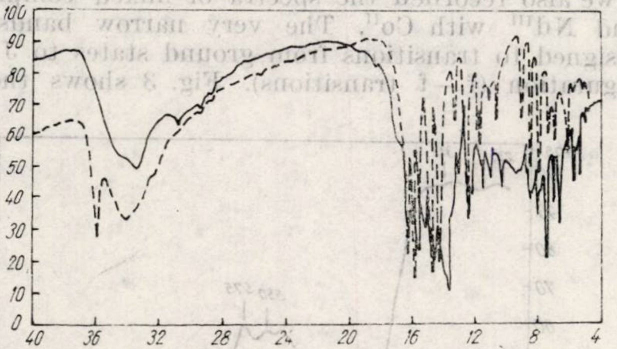

Fig. 1. — IR spectra of ——— $La(Sal)_3 \cdot H_2O$; - - - - $LaCo(Sal)_4(OH) \cdot 4H_2O$.

According to Fig. 2, both the spectrum of simple Co^{II} compound with salicylic acid and of mixed Co^{II} and La^{III} compound with the same acid show absorption bands in this range. These bands were assigned to the transitions in the organic ligand and are therefore proper to the ligand.

The visible, reflection spectra were recorded within 400 — 1000 nm for mixed complex compounds and complex of Co^{II} (Fig. 2). The spectrum of complex compound of Co^{II} with salicylic acid shows a strong band at 540 nm that may be assigned to ν_3 transition, $^4T_{1g} \rightarrow {}^4T_{1g}(P)$, into an octahedral configuration of high spin of Co^{II} ion. The spectrum of

Co^{II} and La^{III} mixed complex compound is identical with that of the simple compound because the La^{III} ion does not exhibit bands in this range.

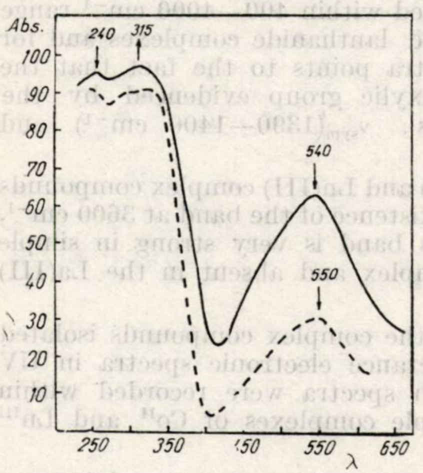

Fig. 2. — Electronic reflectance spectra of
——— $Co(Sal)(OH)(H_2O)_4$;
- - - - $CoLa(Sal)_4(OH).4H_2O$.

Taking into account the fact that a series of lanthanides show bands in visible, we also recorded the spectra of mixed complex compounds of Pr^{III} and Nd^{III} with Co^{II}. The very narrow bands of lanthanide ions are assigned to transitions from ground states to J excited levers of 4f configuration (f – f transitions). Fig. 3 shows the spectrum in visible of the complex compound $[NdCo(Sal)_4(OH)]. 4 H_2O$; apart from the band at 540 nm, there are bands characteristic of Nd^{III} ion. These bands are very narrow but relatively weak and superpose with the charac-

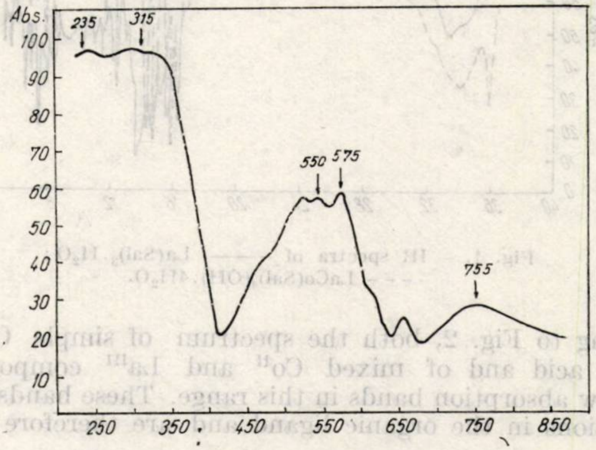

Fig. 3. — Electronic reflectance spectra of $NdCo(Sal)_4(OH) \cdot 4H_2O$.

teristic band of Co^{II} ion of octahedral configuration and high spin located at 540 nm.

In general the formation of chemical bonds in the complex compounds of lanthanides perturbs the "f" orbitals which alter only-slightly the intensity or position of absorption bands; however this allows the obtentions of some indications regarding the nature of chemical bond in these combinations. The case of the mixed complexes synthesized is more complicated because these bands superpose with the much stronger band assigned to Co^{II}. Consequently the spectral data obtained have allowed, in all these compounds, the assigning to an octahedral high spin configuration only for Co^{II} ion.

The determinations of magnetic susceptibility were carried out in the mixed complex compound of La^{III} and Co^{II} and the simple compounds of Co^{II} and La^{III}. The value obtained for the mixed complex i.e. 4.3 BM agrees with the data in the literature supplied for octahedral high spin complex compounds of Co^{II} (4.3–5.2 BM). This value is considerably higher than the single spin value (3.88 BM) corresponding to the odd 3 electron which points to an important contribution assigned to the threefold orbital degeneration of the ground state $^4T_{1g}(F)$ of Co^{II} ion from this configuration.[16] The value of the magnetic moment is the same with that for simple Co^{II} complex, which may be explained taking into account that La^{III} has no magnetic contribution.

Given the aim of this study – the obtention of mixed oxides with perovskite structure by thermal decomposition of the complex compounds synthetized – we have performed a thermogravimetric study to evidence the steps of decomposition and the corresponding effects as a function of temperature.

The curves obtained show that the thermolysis occurs in three steps (Fig. 4): The first step, between 25 and 200°, corresponds to the elimination of constitution water; it is accompanied by the change of complex colour from pink to blue–violet. At room temperature the colour change is reversible. The reaction may be written as:

$$[CoLa(Sal)_4(OH)(H_2O)_4] \rightleftharpoons [CoLa(Sal)_4(OH)]$$

The loss of water at temperatures higher than 100° (see TG curve in Fig. 4) suggests that the four water molecules are coordinated at Co^{II} ion which gives it the octahedral configuration (as Gupta et al.[17] suggested). During the next step between 200–350°, a loss of 13.12% takes place, corresponding to the decomposition of the anhydrous complex. The products of decomposition contain phenol to a large extent. This loss is accompanied by an endothermal effect on the DTA curve.

In a recent study[17] on thermal decomposition of Co^{II} salicylate, the authors have isolated the intermediate products corresponding to the step II and evidenced by chromatography the salicylic acid and phenol among the decomposition products. Step III between 350–700°, corresponds to the formation of oxide mixture and elimination of CO_2 (loss 54.83%). The product obtained was analyzed by X-ray diffraction and evidenced the coexistence of perovskite phase with $Ln_2O_3 + Co_3O_4$ oxide mixture.

The thermogravimetric analysis effected on a series of mixed complexes containing various lanthanides (La^{III}, Pr^{III}, Nd^{III}) leads to the conclusion that the temperature of the three decomposition steps is not influenced by the nature of the lanthanide.

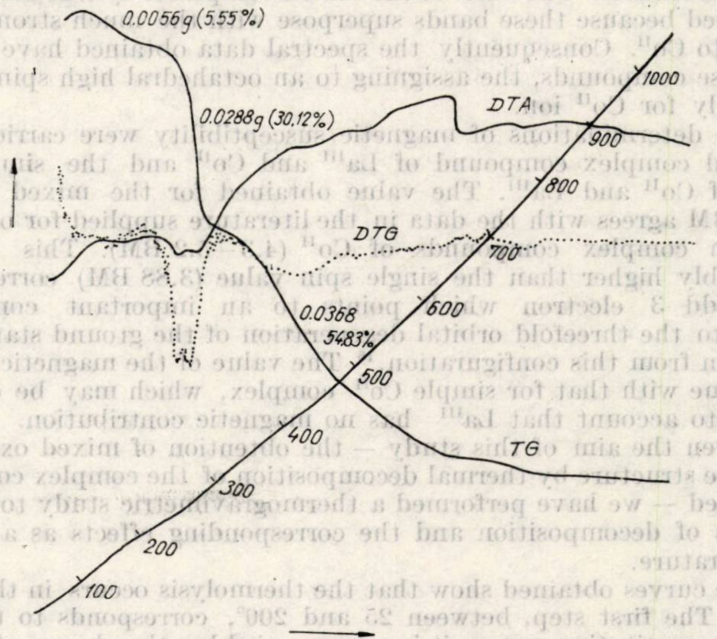

Fig. 4. — Thermal analysis of $CoLa(Sal)_4(OH) \cdot 4H_2O$.

The final products obtained after thermal decomposition are subjected to adequate thermal treatment to yield pure perovskite phase. This was evidenced by X-ray diffraction magnetic determinations, electron and IR spectra.[18]

REFERENCES

[1] Yung-Fang Yu Yao, *J. of Catalysis*, **36**, 266 (1975).

[2] R. H. Voorhoeve, *Science*, **177**, 353 (1972).

[3] T. Nakamura, M. Misowa and Y. Yoneda, *Bull. Chem. Soc. Japan*, **55**, 394 (1982).

[4] J. O. Petunchi, *J. Catalysis*, **70**, 356 (1981).

[5] L. Ray and V. Sunivasan, *J. Catalysis*, **65**, 121 (1980).

[6] T. Arakawa and S. Yosida, *Mat. Res. Bull.*, **15**, 269 (1977).

[7] M. Crespin and H. K. Hall, *J. Catalysis*, **69**, 359 (1981).

[8] P. Lombardo, *J. Chem. Soc., Chem. Commun.*, **1980**, 467.

[9] J. Askham, L. Fankuchen and A. Wold, *J. Amer. Chem. Soc.*, **76**, 1029 (1954).

[10] W. Aaron, E. Banks and B. Post, *J. Amer. Chem. Soc.*, **79**, 6365 (1957).
[11] A. S. Nedil'ko and T. Vasiaghina, *Ukrain. khim. Zhur.*, **46**, 251 (1980).
[12] A. S. Nedil'ko, *Zhur. neorg. Khim.*, **24**, 1395 (1979).
[13] O. Parkash, *Mat. Res. Bull.*, **9**, 1173 (1974).
[14] Y. B. Goodenough and P. M. Racah, *J. Appl. Phys.*, **36**, 1031 (1965).
[15] L. Wachowska, S. Zielinski and A. Burewicz, *Acta Chim. Acad. Sci. Hung.*, **104**, 141 (1980).
[16] F. A. Cotton and G. Wilkinson, "Advanced inorganic chemistry" Intersci. Publish., Wiley, N.Y., 1966, p. 869.
[17] K. Kishore and R. Nagarajan, *J. Therm. Anal.*, **22**, 25 (1981).
[18] P. Spacu, Silvia Ploştinaru, Luminiţa Patron, Adriana Conţescu, N. Stănică and D. Crişan, Proc. Conf. Magnetism, Iaşi, 17—18 Dec., 1983.

Revue Roumaine de Chimie, **30**, *8*, 667–678 (1985)

THE ELECTROCHEMICAL BEHAVIOUR OF ETHYLMERCURY IN AQUEOUS MEDIUM

ION TĂNASE, ION IONECI and CONSTANTIN LUCA
Polytechnical Institute of Bucharest, Faculty of Chemical Technology, Department of Analytical Chemistry, Spl. Independenţei 202, 79611-Bucharest, Romania

Received November 10, 1984

The electrochemical reduction of monoethylmercuric compounds in aqueous solution was investigated by direct current and sinusoidal alternating current polarography and by cyclic voltammetry. The reduction of these compounds takes place in two steps, each of which involving the transfer of a single electron. The first polarographic reduction step proceeds reversibly and results in the formation of the ethylmercuric radical at the electrode surface, whereas the second step proceeds irreversibly, leading to ethane and Hg^0.

The electrochemical behaviour of the organomercuric compounds has been extensively investigated in the latter 25 years, both from an analytical point of view and from that of the mechanism of the electrode reactions.

The electrochemical reduction of the ethylmercuric compounds (EtHgX, where X = halogenide, nitrate, acetate) was noticed for the first time in 1948 by Costa [1] on the occasion of his studies concerning the electrochemical reduction of mercury. Afterwards, various studies have been carried out in connection with the electrochemical behaviour and with the possibility of the electroanalytical determination in other organomercuric compounds.[2–20]

As regards the electrochemical behaviour of the organomercuric compounds, it is generally accepted today that their electrochemical reduction takes place in two steps, each of which involving the transfer of one electron. The first step of the electrochemical reduction leads to the appearance of the organomercuric radical at the surface of the electrode, whereas the second step leads to elemental mercury and, in the case of alkylmercuric compounds, to alkanes.

The opinions of various authors on the two steps of the electrochemical reduction of the organomercuric compounds are divergent; most of them do not take into account the nature of the electrode process. Some of these authors take as irreversible the first step,[1,3,4,12] whereas others take it as reversible.[2,13–16] Vojiř[2] suggests that dimerization of the organomercuric radical may take place after electroreduction, leading to an insoluble layer on the surface of the electrode. Most of the published studies include a series of dimerization or disproportionation reactions, but few authors have given details on the disappearance of the radicals formed in the system or of the formed intermediates. Likewise, some workers note that the direct current polarographic waves have irregularities,[1,3,4,16] or that pre-waves occur,[3,4,9,14-16] but few of them give details concerning such effects. Laviron and Degrand,[13-15] who have given a theoretical classification of the polarographic selfinhibiting phenomena, have also shown that some RHgX-type organomercuric compounds offer a very good opportunity for investigating the type II selfinhibiting phenomena.[13]

Sufficient details on the mechanism of the electrochemical reduction of the organomercuric compounds could be obtained if experimental studies particularized for each compound are carried out; an important role is played by the used technique, solvent and working conditions.

The purpose of this work was to make a complex investigation on the electrochemical reduction of ethylmercury in aqueous solution, using for this the results obtained by direct current and sinusoidal alternating current polarography, and by cyclic voltammetry in order to choose the optimum conditions for the electrochemical determination of the ethylmercury compounds.

EXPERIMENTAL

To carry out the polarographic measurements in direct current and in sinusoidal alternating current, a three-electrode, PRG-3-type Tacussel polarographic complex device was used, together with a RM-06 Tacussel cell provided with thermostating jacket. The capillary used had the following features: $m = 1.510$ mg · s^{-1}, $\tau = 4.15$ s, determined in 0.1N HClO$_4$ at -0.200 V relative to the saturated calomel electrode (SCE), at a height $h = 60$ cm of the mercury column.

The voltammetric curves with cyclic scanning of the potential were obtained by means of a three electrode device consisting of a HP-72 Wenking high-power potentiostat, a GSTP Tacussel triangular signal generator, a NE Orion (Budapest) $X-Y$ recorder and a Tektronix memory oscilloscope. Platinum wire was used first as working electrode, then a mercury electrode with suspended drop.

All measurements were carried out under strictly-controlled temperature conditions, at 25 ± 0.1°C, and the potentials were measured relative to the saturated calomel electrode (a K-401 Radiometer SCE was used).

The substances and reagents used were high-purity or reagent grade, provided by Merck and BDH. To prepare the solutions and to clean the working vessels, tetradistilled water was used (the last distillation being made in a fused silica apparatus).

For the 1.8 – 12 pH range, the measurements were made in a Britton-Robinson buffer, which is considered as adequate for maintaining a constant pH at the dropping mercury electrode.[21] For pH < 1.8, the measurements were carried out in 0.1 N HClO$_4$, whereas for pH > 12, in 0.1 N NaOH. A 0.1 mole · dm^{-3} solution of KCl was used as indifferent electrolyte. Millimolar solutions of the ethylmercuric compound were prepared by weighing the necessary amount, transferring this to a volumetric flask together with the indifferent electrolyte and bringing it to the mark with tetradistilled water. The more diluted solutions were always freshly prepared from the millimolar solutions by dilution in a volumetric flask.

Oxygen was removed from all solutions measured polarographically by bubbling them during 10 minutes with purified argon.

RESULTS AND DISCUSSION

The polarographic reduction of the ethylmercuric cation in aqueous medium (with the Britton-Robinson buffer for pH = 1.8 – 12 ; 0.1N HClO$_4$ and 0.1N NaOH outside this range) gives in direct current two reduction steps of approximately equal heights, whereas in sinusoidal alternating current gives two peaks (Fig. 1), whose half-wave potentials ($E_{1/2}$) or peak potentials (E_p), respectively, depend on the pH of the solution (Fig. 2). The first polarographic step in direct current and the first polarographic peak in sinusoidal alternating current are well-defined; the peak is symmetrical. The second polarographic step in direct current and the corresponding peak in alternating current are strongly distorted due to adsorption processes occurring on the dropping mercury electrode and to polarographic inhibition processes. For both steps of the polarographic reduction, the limiting current varies linearly with the square root of the height of the mercury column (Fig. 3), hence this is a diffusion-controlled current. The diffusion-limited currents, as well as the maximum peak currents, vary linearly with the concentration of the electroactive species in the 1×10^{-3}—1×10^{-4} mole . dm^{-3} concentration range.

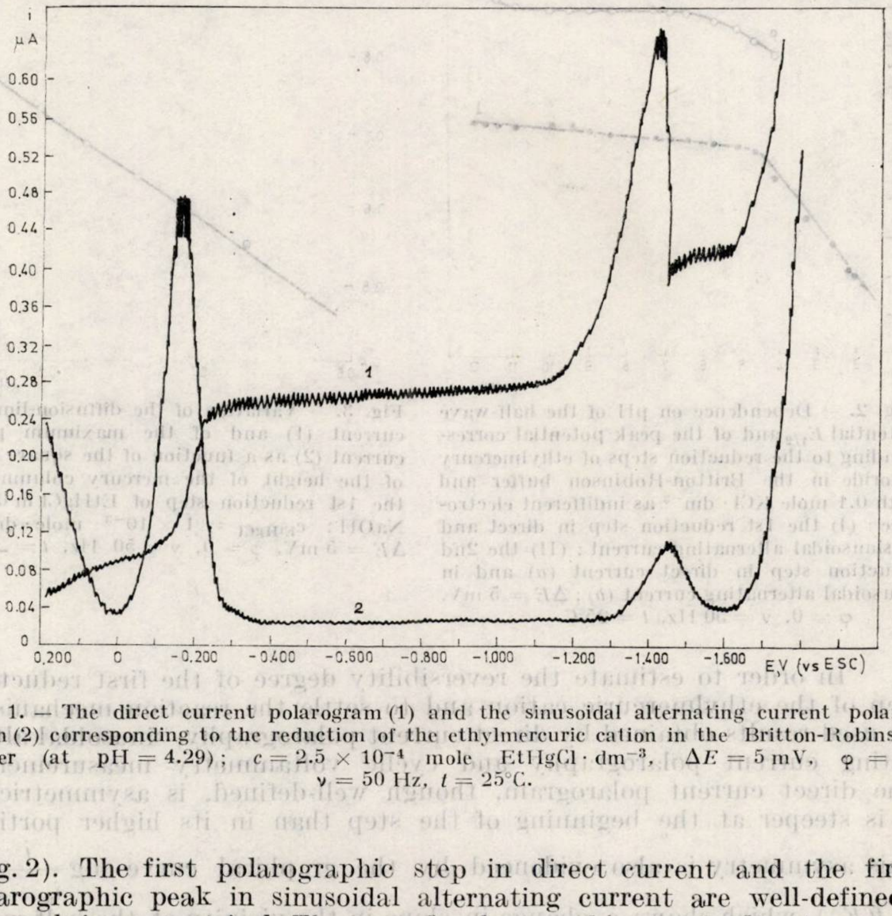

Fig. 1. — The direct current polarogram (1) and the sinusoidal alternating current polarogram (2) corresponding to the reduction of the ethylmercuric cation in the Britton-Robinson buffer (at pH = 4.29); $c = 2.5 \times 10^{-4}$ mole EtHgCl · dm^{-3}, $\Delta E = 5$ mV, $\varphi = 0$, $\nu = 50$ Hz, $t = 25$°C.

The diffusion coefficient of the ethylmercuric cation was estimated from direct-current polarographic data, using the Ilkovič equation; it has the following values: $(1.15 \pm 0.04) \times 10^{-5}$ cm.s^{-1} in 0.1N $HClO_4$ and $(1.17 \pm 0.07) \times 10^{-5}$ cm.s^{-1} in 0.1N NaOH.

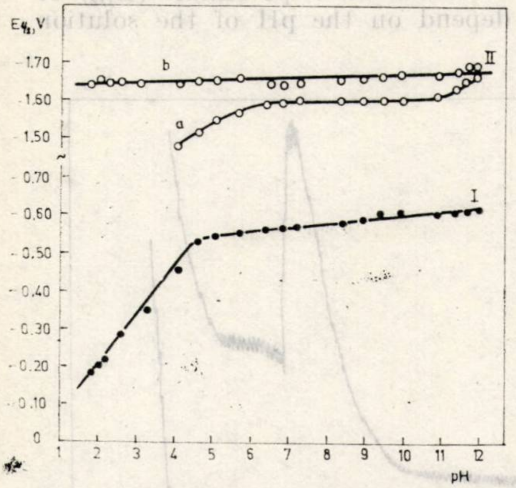

Fig. 2. — Dependence on pH of the half-wave potential $E_{1/2}$ and of the peak potential corresponding to the reduction steps of ethylmercury chloride in the Britton-Robinson buffer and with 0.1 mole KCl · dm^{-3} as indifferent electrolyte : (I) the 1st reduction step in direct and in sinusoidal alternating current ; (II) the 2nd reduction step in direct current (*a*) and in sinusoidal alternating current (*b*) ; $\Delta E = 5$ mV, $\varphi = 0$, $\nu = 50$ Hz, $t = 25$°C.

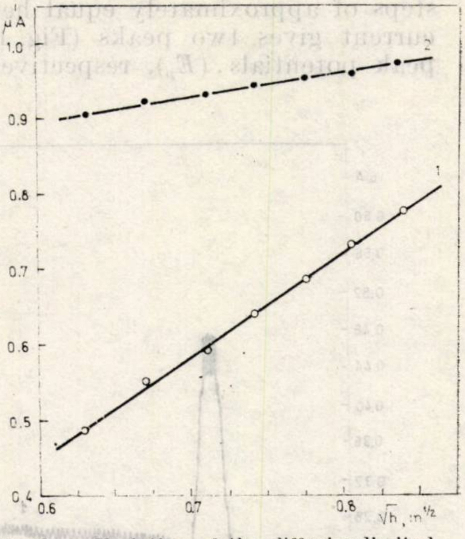

Fig. 3. — Variation of the diffusion-limited current (1) and of the maximum peak current (2) as a function of the square root of the height of the mercury column for the 1st reduction step of EtHgCl in 0.1*N* NaOH ; $c_{EtHgCl} = 1 \times 10^{-3}$ mole · dm^{-3}, $\Delta E = 5$ mV, $\varphi = 0$, $\nu = 50$ Hz, $t = 25$°C.

In order to estimate the reversibility degree of the first reduction step of the ethylmercuric cation and to settle the reaction mechanism, we used results obtained by direct current polarography, sinusoidal alternating current polarography and cyclic voltammetry measurements. The direct current polarogram, though well-defined, is asymmetrical : it is steeper at the beginning of the step than in its higher portion. This asymmetry is also evidenced by the graphical curve $\log \frac{i}{i_d - i} = f(E_{dc})$, which shows a change in slope in the vicinity of the half-wave potential (Fig. 4) for higher concentrations of the ethylmercuric radical. This distortion may be explained by taking into account the evolution of a chemical reaction which follows the electrochemical reduction. To do this, we may write the equations

$$CH_3-CH_2Hg^+ + e^- \rightleftharpoons CH_3-CH_2Hg^\bullet \qquad (1)$$

$$2CH_3-CH_2Hg^\bullet \rightleftharpoons (CH_3-CH_2Hg)_2 \qquad (2)$$

Since the reaction (2) effectively decreases the activity of the ethylmercuric radical, the electrochemical process (1) can be favored, thus increasing the slope of the polarographic step and changing the half-wave potential towards more positive values. Since the reaction (2) is second-order in CH_3CH_2Hg, it could affect little the electrochemical process if the concentration of the ethylmercuric compound is low, as evidenced also by Figure 4.

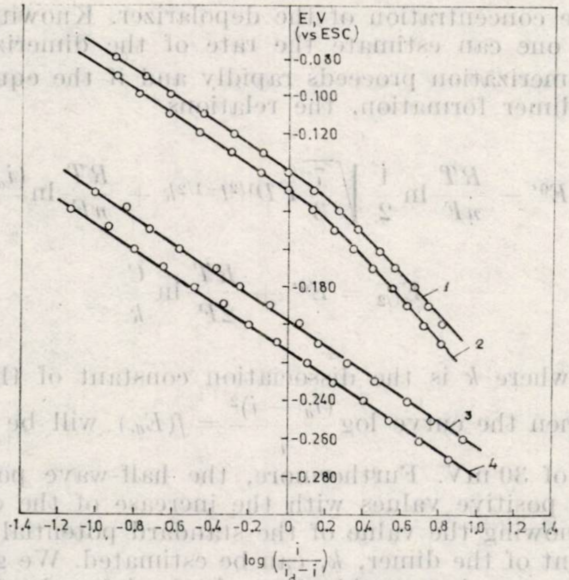

Fig. 4. — Plots of $\log \frac{i}{i_d - i} = f(E_{dc})$ for the direct current polarograms corresponding to the 1st reduction step of EtHgCl in 0.1 N $HClO_4$: (1) 10×10^{-4} mole $EtHgCl \cdot dm^{-3}$, (2) 9×10^{-4} mole $EtHgCl \cdot dm^{-3}$, (3) 4.5×10^{-5} mole $EtHgCl \cdot dm^{-3}$, (4) 1.5×10^{-4} mole $EtHgCl \cdot dm^{-3}$.

Bonatere and Cauquis [22] have given a unified mathematical treatment of the electrochemical reactions which are followed by a chemical dimerization reaction. Two cases have to be mentioned on this line : the first involves the reversible electrochemical reduction followed by an irreversible chemical dimerization, and the second, the reversible reduction followed by a reversible dimerization. In the first case, the inferred equations are similar to those deduced by Hanus,[23] Hanus and Koutecky [24] and Mairanovskii [25,26] :

$$E = E^{0\prime} - \frac{RT}{nF} \ln \frac{i_d}{10^{-3} nFAD^{1/2} K_d^{1/2} C} - \frac{RT}{nF} \ln \frac{i^{2/3}}{i_d - i} \tag{3}$$

$$E = E^{0\prime} + \frac{RT}{3nF} \ln \frac{K_d C t}{4} \tag{4}$$

where A is the average area of the mercury drop, t is the dropping time, K_d is the dimerization rate constant, C is the concentration of the electroactive species and the other constants have their usual meaning. Under these conditions, it is obvious that the graphical representation $\log \frac{i^{2/3}}{i_d - i} = f(E_{dc})$ is a straight line with a slope of 0.059 V for every decadic increase of the concentration of the depolarizer. Knowing the standard potential $E^{0\prime}$, one can estimate the rate of the dimerization reaction.

If the dimerization proceeds rapidly and if the equilibrium favors strongly the dimer formation, the relations

$$E = E^{0\prime} - \frac{RT}{nF} \ln \frac{1}{2} \sqrt{\frac{7}{3}} FD^{1/2}t^{-1/2}k + \frac{RT}{nF} \ln \frac{(i_d - i)^2}{i} \tag{5}$$

$$E_{1/2} = E^{0\prime} + \frac{RT}{2F} \ln \frac{C}{k} \tag{6}$$

can be used, where k is the dissociation constant of the dimer. If we take $n = 1$, then the curve $\log \frac{(i_d - i)^2}{i} = f(E_{dc})$ will be a straight line with a slope of 30 mV. Furthermore, the half-wave potential changes towards more positive values with the increase of the depolarizer concentration. Knowing the value of the standard potential, $E^{0\prime}$, the dissociation constant of the dimer, k, can be estimated. We give in Figure 5 the direct current polarographic data obtained for the first step of the drawn according to equation (5). For high ethylmercuric cation concentrations, the curve $\log \frac{(i_d - i)^2}{i} = f(E_{dc})$ is linear between 10—90% of the height of the polarograms, thus proving that equation (5) describes adequately the present case. A similar situation was pointed out by Heaton and Laitinen,[20] who represented graphically the data obtained by normal pulse polarography in the case of methylmercury reduction; they found that the $\log \frac{(i_d - i)^2}{i} = f(E_{dc})$ dependence remains linear, according to equation (5), for concentrations higher than 2.5×10^{-6} mole·dm^{-3} of $MeHg^+$ in 0.1*N* $HClO_4$, whereas the standard curve $\log \frac{i}{i_d - i} = f(E_{dc})$ is linear only for low concentrations, a fact which may be also noticed in the case of the reduction of the ethylmercuric cation (Fig. 5). The chemical reaction can be therefore neglected for low concentrations of the ethylmercuric cation. The half-wave potential corresponding to the first reduction step shifts towards more negative values when the concentration decreases, and for low concentrations ($\sim 2 \times 10^{-5}$ mole·dm^{-3}) it becomes independent of concentration. Because at very low concentrations the half-wave potential is not influenced by the chemical reaction, it can approach the standard half-wave potential of the electrochemical process. Assuming that the ratio of the diffusion coefficients for the oxidized and the reduced species is equal to 1, the standard potential for the first step of the reduction of the ethylmercuric radical in 0.1N $HClO_4$ is $E^{0\prime} = -0.220$ V relative to SCE. Knowledge of this value enables one

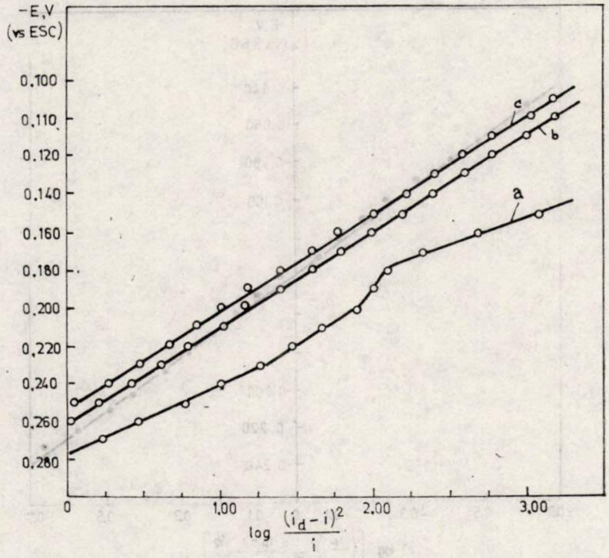

Fig. 5. — Plots of log $\frac{(i_d - i)^2}{i} = f(E_{dc})$ for the direct current polarograms corresponding to the 1st reduction step of EtHgCl in 0.1N $HClO_4$: (a) 10×10^{-4} mole EtHgCl · dm^{-3}, (b) 9×10^{-4} mole EtHgCl · dm^{-3}, (c) 1.5×10^{-5} mole EtHgCl · dm^{-3}.

to estimate the dissociation constant of the dimer by using equation (6). The value thus obtained by us was $k = 3.5 \times 10^{-5}\ \mathrm{cm \cdot s^{-1}}$.

Data related to the reduction of the organomercuric compounds according to equation (3), provided by several authors,[11,12,18,19] lead to the idea that reaction (2) is irreversible; the same authors, however, suggest in their conclusions that the chemical dimerization would be more appropriately described as a fast reversible process rather than an irreversible process. The data obtained in this work support the hypothesis of a reversible reaction (2).

In the case of the sinusoidal alternating current, the peak corresponding to the first reduction step of the ethylmercuric cation is very well defined and symmetrical in all used media, since the reduction is not affected by the chemical dimerization process, unlike the case of the direct current (Fig. 1b). The dependence $\log \left[\left(\frac{i_p}{i} \right)^{1/2} \mp \left(\frac{i_p - i}{i} \right)^{1/2} \right] = f(E_{dc})$ is linear (Fig. 6), the slope of this straight line being 126 mV and the width of the peak at half-height $b = 98$ mV. The temperature coefficient of the maximum peak current is $\beta = 0.61\,\%$, whereas the variation of the maximum peak current as a function of the square root of the height of the mercury column is linear (Fig. 3*b*). All these facts suggest that the electrode process corresponding to the first reduction step of the ethylmercuric cation is reversible in sinusoidal alternating current too.

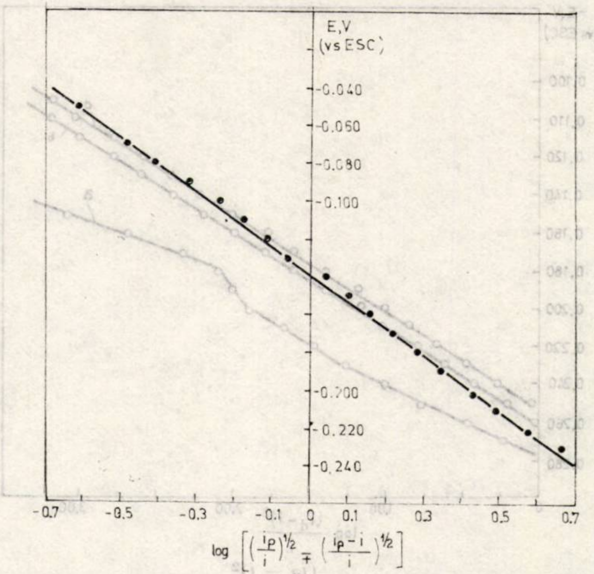

Fig. 6. — Plot of $\log\left[\left(\frac{i_p}{i}\right)^{1/2} \mp \left(\frac{i_p - i}{i}\right)^{1/2}\right] = f(E_{dc})$ for the sinusoidal alternating current polarograms corresponding to the 1st reduction step of EtHgCl in 0.1*N* $HClO_4$; $c = 1 \times 10^{-4}$ mole · dm^{-3}, $E_p = -0.138$ V *vs.* ESC, slope = 128 mV, $b_{1/2} = 96$ mV, $\Delta E = 5$ mV, $\varphi = 0$, $\nu = 50$ Hz.

The cyclic voltammograms recorded for the ethylmercuric cation in 0.1*N* $HClO_4$, 0.1 NaOH and Britton-Robinson buffers have, due to their specific features, a major importance in postulating the reduction. We give in Figure 7 a cyclic voltammogram obtained for the ethylmercuric cation in a Britton-Robinson buffer at pH = 7.00.

Among the features of the curves $i = f(E)$ obtained by cyclic voltammetry, two play a major role in postulating the reduction mechanism. The first of these is the shape of the cathodic and of the anodic peaks. It is obvious that the amplitude of the anodic peak depends on the scanning velocity. The peak virtually does not appear at low scanning velocities, but it appears and increases as the scanning velocity increases. The cathodic peak fits, as concerning its shape, a diffusion-controlled step, whereas the anodic peak does not apparently indicate such a behavior. The shape of the anodic peak is typical of a "stripping" peak, i.e. of a peak which is obtained by destroying a film adsorbed on the electrode or an insoluble film. The fact that the anodic peak is small or nonexistent at low scanning velocities and is large and welldefined at high scanning velocities suggests convincingly that a relatively slow chemical reaction takes place, following the electrochemical reaction. A dilemma now arises, since the polarographic data had suggested that the chemical reaction was fast. To clarify this dilemma, we may rewrite equation (2) as follows :

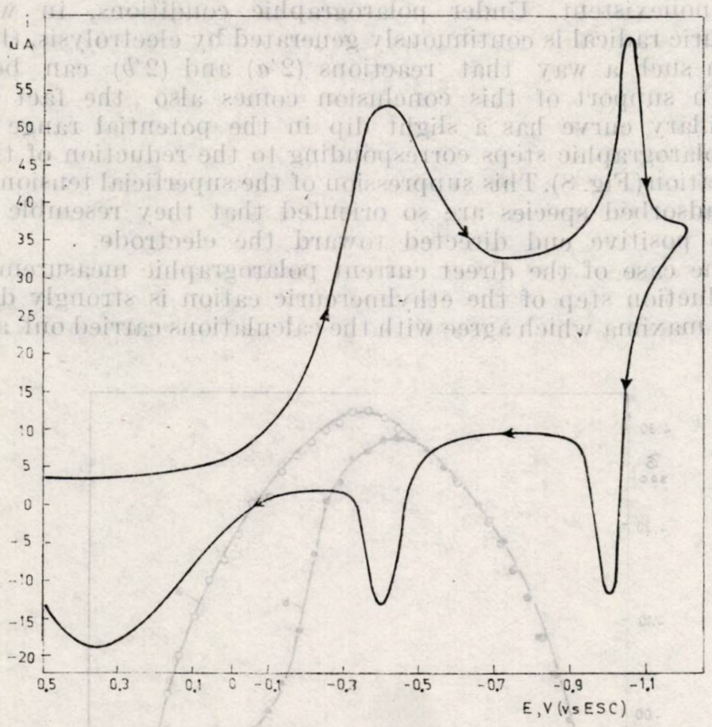

Fig. 7. — The cyclic voltammogram obtained for EtHgCl in the Britton-Robinson buffer (at pH = 7.00), with a platinum electrode.

$$2CH_3-CH_2Hg^{\bullet} \overset{\text{fast}}{\rightleftharpoons} (CH_3-CH_2Hg)_2 \qquad (2\,a)$$

$$(CH_3-CH_2Hg)_2 \overset{\text{slow}}{\rightleftharpoons} CH_3-CH_2-Hg-CH_2-CH_3 + Hg \qquad (2\,b)$$

Reactions (2'*a*) and (2'*b*) account for the cyclic voltammetry data in this way : at high scanning velocities, reaction (2'*b*) may to a large extent not take place during the experiment, so that the voltammogram appears as being due to a process which involves reactions (1) and (2'*a*). At low scanning velocities, reaction (2'*b*) may become involved in the equilibrium. If the equilibrium (2′*b*) favors the product formation, conversion of diethylmercury into diethyldimercury may be slower even than the direct reaction. In this way, reaction (2′*b*) appears as being almost irreversible. The dimer can be effectively converted into an inactive species at low scanning velocities, so that the anodic peak may be very small or nonexistent. Under polarographic conditions, in which the ethylmercuric radical is continuously generated by electrolysis, the system evolves in such a way that reactions (2′*a*) and (2′*b*) can be heterogeneous. In support of this conclusion comes also the fact that the electrocapillary curve has a slight dip in the potential range between the two polarographic steps corresponding to the reduction of the ethylmercuric cation (Fig. 8). This suppression of the superficial tension suggests that the adsorbed species are so oriented that they resemble a dipole having its positive end directed toward the electrode.

In the case of the direct current polarographic measurements, the second reduction step of the ethylmercuric cation is strongly distorted; it contains maxima which agree with the calculations carried out according to Frumkin's theory for the 3rd-order maxima. These maxima can be removed by using common maxima suppressors (gelatine, triton, etc.). A significant modification of the shape of the polarographic curve could be obtained when the indifferent electrolyte was changed from $HClO_4$ to

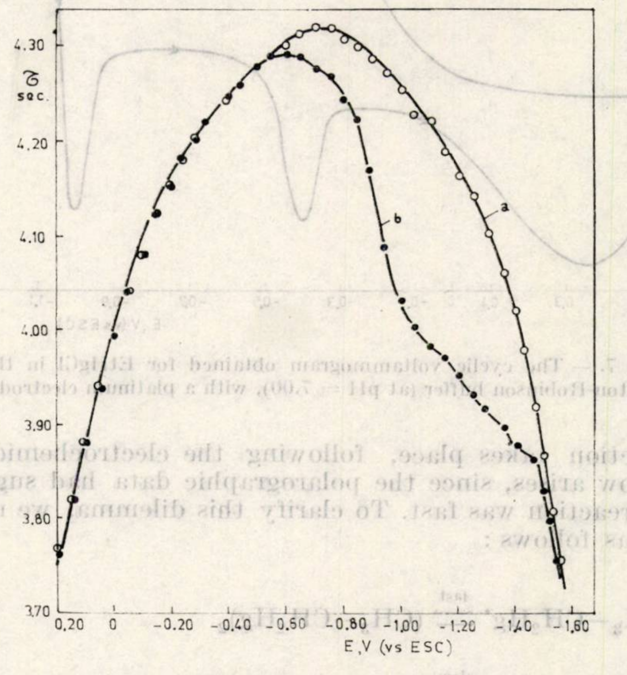

Fig. 8. — The electrocapillary curve of $CH_3CH_2Hg^+$ in 0.1*N* $HClO_4$: (a) 0.1N $HClO_4$, (b) 5×10^{-4} mole $CH_2CH_2Hg \cdot dm^{-3}$ + 0.1*N* $HClO_4$.

NaOH. The shape of the curve makes the reaction to appear as irreversible both in direct current and in sinusoidal alternating current polarographic conditions. The electron transfer is relatively fast, which leads to a well-defined cathodic peak in cyclic voltammetry, even at very high scanning velocities. The irreversible aspect of this reduction step of the ethylmercuric cation can be assigned to two factors : (i) the reaction is chemically irreversible, i.e. the reaction which follows is very fast, but the reversibility rate is negligible because, under the stated conditions, CH_3-CH_3 is inert to the reduction process ; (ii) the electrochemical reduction competes with the chemical dimerization of the radical.

The half-wave potential and the peak potential are independent of the nature of the indifferent electrolyte. For the second reduction step, the dependence of the half-wave potential on the pH is very interesting : for large pH values, $E_{1/2}$ is almost independent of pH, but for values less than 5 the half-wave potential shifts rapidly toward more positive values. This effect may be accounted for as follows : for large pH values, the solution contains very low amounts of H^+ ions and the organomercuric radical can be reduced to elemental mercury and a carbanion. The carbanion can draw a proton from the water molecule to give CH_3-CH_3 and OH^- ions. For low pH values, the reduction of the radical can be also assisted by the attack of a proton, which favors the reduction by shifting the half-wave potential toward more positive values. Since large differences between acidic and basic solutions occur, this explanation suggests a profound modification of the mechanism of the second reduction step of ethylmercuric compounds as a function of pH. The reactions corresponding to the second reduction step can be written as follows :

$$CH_3CH_2Hg^{\bullet} + H^+ + e^- \longrightarrow CH_3-CH_3 + Hg \qquad (7)$$

(in acidic solution)

$$CH_3CH_2Hg^{\bullet} + e^- \rightleftharpoons CH_3CH_2^- + Hg \qquad (8)$$

$$CH_3CH_2^- + H_2O \longrightarrow CH_3-CH_3 + HO^- \qquad (9)$$

(in basic solution)

In sinusoidal alternating current, the peak potential corresponding to the second reduction step of the ethylmercuric cation is practically independent of pH : the peak is poorly defined and broad, and the maximum peak current is small, which suggests the irreversibility of the electrode process in sinusoidal alternating current.

Data obtained by cyclic voltammetry for this reduction step of the ethylmercuric cation show the appearance of a cathodic peak which never disappears completely ; its amplitude is small at low scanning velocities and increases as the scanning velocity increases ; the shape of the peak is typical of a stripping process. The anodic peak is smaller in height and broader, whereas the cathodic peak is high and narrow at lower scanning velocities and similar in magnitude and shape with the former at higher velocities. Since the analyzed process corresponds to the reduction of the ethylmercuric radical and the anodic wave is produced by the oxidation of the same radical, the peaks corresponding to these processes must be very similar. One can notice that his condition is practically fulfilled; the small differences still observed are due to the fact that the peaks appear at different values of the potential.

These remarks support the following reduction mechanism of the ethylmercuric cation in acidic and basic media:

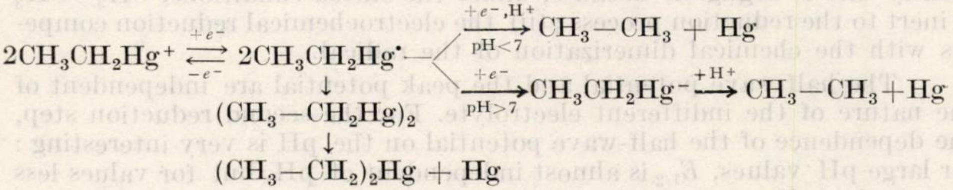

$$2CH_3CH_2Hg^+ \underset{-e^-}{\overset{+e^-}{\rightleftharpoons}} 2CH_3CH_2Hg^{\bullet} \begin{cases} \xrightarrow[pH<7]{+e^-,H^+} CH_3-CH_3 + Hg \\ \xrightarrow[pH>7]{+e^-} CH_3CH_2Hg^- \xrightarrow{+H^+} CH_3-CH_3+Hg \end{cases}$$

$$2CH_3CH_2Hg^{\bullet} \downarrow (CH_3-CH_2Hg)_2 \downarrow (CH_3-CH_2)_2Hg + Hg$$

To conclude, it can be said that the first reduction step of the ethylmercuric cation proceeds reversibly in aqueous media, both in direct and in sinusoidal alternating current, whereas the second step proceeds irreversibly. The polarograms obtained for the first reduction step can be used to determine polarographically the ethylmercuric cation.

REFERENCES

[1] G. Costa, *Ann. Chim. (Rome)*, **38**, 665 (1948).
[2] V. Vojir, *Coll. Czech. Chem. Commun.*, **16**, 489 (1951).
[3] R. Benesch and R. E. Benesch, *J. Amer. Chem. Soc.*, **73**, 3391 (1951).
[4] R. Benesch and R. E. Benesch, *J. Phys. Chem.*, **56**, 648 (1952).
[5] W. L. Wuggatzer and J. M. Cross, *J. Amer. Pharm. Assoc.*, **41**, 80 (1952).
[6] M. L. O'Donnel and C. W. Kreke, *J. Amer. Pharm. Assoc.*, **48**, 268 (1958).
[7] P. J. Casey, J. J. Carrol and N. R. Stalica, *Proc. Pennsylvania Acad. Sci.*, **32**, 63 (1958).
[8] P. J. Casey and W. Waguar, *Proc. Pennsylvania Acad. Sci.*, **36**, 281 (1962).
[9] R. F. Borman and R. W. Murray, *Anal. Chem.*, **17**, 1408 (1965).
[10] N. S. Hush and K. B. Oldham, *J. Electroanal. Chem.*, **6**, 35 (1963).
[11] K. P. Butin, J. P. Beletskaya, A. N. Ryabtsev and O. A. Reutov, *Elektrokhimiia*, **3**, 1318 (1967).
[12] V. G. Toropova, M. K. Saikina and M. G. Khakimov, *Zh. Obshch. Khim.*, **37**, 47 (1967).
[13] E. Laviron and Ch. Degrand, *Bull. Soc. Chim. France*, **7**, 2194 (1966).
[14] Ch. Degrand and E. Laviron, *Bull. Soc. Chim. France*, **5**, 2228 (1968).
[15] Ch. Degrand and E. Laviron, *Bull. Soc. Chim. France*, **5**, 2233 (1968).
[16] B. Fleet and R. D. Jee, *J. Electroanal. Chem.*, **25**, 397 (1970).
[17] B. Fleet and R. D. Jee, *Talanta*, **16**, 1561 (1969).
[18] K. P. Butin, A. N. Kashin, A. B. Ershler, V. V. Strelets, J. P. Beletskaya and O. A. Reutov, *J. Organometal. Chem.*, **39**, 39 (1972).
[19] A. N. Kashin, A. B. Ershler, V. V. Strelets, K. P. Butin, J. P. Beletskaya and O. A. Reutov, *J. Organometal. Chem.*, **39**, 237 (1972).
[20] R. C. Heaton and H. A. Laitinen, *Anal. Chem.*, **46**, 547 (1974).
[21] O. H. Mueller, *Chem. Revs.*, **24**, 95 (1939).
[22] R. Bonaterre and G. Cauquis, *J. Electroanal. Chem.*, **6**, 35 (1963).
[23] V. Hanus, *Chem. Zvesti*, **8**, 702 (1954).
[24] J. Koutecky and V. Hanus, *Coll. Czech. Chem. Commun.*, **20**, 124 (1955).
[25] S. G. Mairanovskii, *Dokl. Akad. Nauk SSSR*, **110**, 593 (1956).
[26] S. G. Mairanovskii, *Izv. Akad. Nauk. SSSR, Otd. Khim. Nauk.*, **12**, 2140 (1961).

Revue Roumaine de Chimie, 30, 8, 679–687 (1985)

DETERMINATION OF MICROAMOUNTS OF MERCURY(II) IN HIGH PURITY REAGENTS BY ANODIC STRIPPING VOLTAMMETRY

I. TĂNASE *, IULIANA VARTIRES **, N. D. TOTIR **, I. IONECI * and C. LUCA *

* Department of Analytical Chemistry, Faculty of Chemical Technology, Polytechnical Institute of Bucharest, Bucharest, Romania

** Center of Physical Chemistry — ICECHIM, 202 Spl. Independenței, 77208-Bucharest, Romania

Received December 15, 1984

Anodic stripping voltammetry with linear sweep of the potential is proposed for the determination of traces of mercury(II) in high purity reagents, using a glassy carbon electrode as working electrode. A NaSCN or KSCN complexing medium was used as indifferent electrolyte; such a procedure allowed to determine mercury(II) in the concentration range $1 \times 10^{-5} - 1 \times 10^{-8}$ mole · dm^{-3}. Mercury(II) was deposited on the glassy carbon electrode under stirring at constant potential ($E_{el} = -0.700$ V *vs.* SCE), whereas the deposit was stripped by anodic voltammetry with linear sweep of the potential. The method was applied to the analysis of some electronic-grade reagents.

The difficulties encountered during analyzing traces of mercury (II) by electrochemical methods are various — as is otherwise the case of the noble metals. To overcome these difficulties, it is necessary in the first place to choose an adequate working electrode, which has to be a solid electrode because stationary mercury electrodes could not be used. The technique most frequently used to determine traces of mercury, particularly in biological samples (after digesting and pretreating them), is atomic absorption spectroscopy (AAS).[1–7] The voltammetric methods, particularly the anodic-stripping voltammetry coupled with a suitable working electrode, offer today an attractive and even better alternative,[8–14] not only for analyzing natural waters [15–17] or drinking water,[18] for which the differential-pulse stripping voltammetry has already become a current method, but also for some biological materials, e.g. for blood fluids, organs, plants, fish or food.[8–14]

Determination of traces of mercury (II) by stripping voltammetry is more accurate and less influenced by interferences than older methods and it can generally be considered as more dependable; it ensures a comparable sensitivity with that offered by AAS for natural waters and biological materials, occasionally even reaching a lower detection limit.[15–18]

The first papers related to the determination of mercury (II) by stripping voltammetry were published during the '60s; the best results were obtained by using carbonaceous electrodes as working electrodes, after carrying out a pre-electrolysis at potentials between 0 and −1.00 V *vs*. SCE and using complexing media (alkali thiocyanates or halogenides, hydrochloric acid, perchloric acid, sulfuric acid, ammonia, hydroxylamine, etc.) as indifferent electrolytes. The first solid electrodes used for determining microamounts of mercury (II) by stripping voltammetry were made of paraffin wax-impregnated graphite,[19−28] of platinum,[29] of carbon paste [30] and then of glassy carbon.[31−36] Another type of solid electrode used of late for the determination of microamounts of mercury(II) by stripping voltammetry is the gold electrode. A series of tests carried out by various authors have made credible the ideas that the use of gold as an electrode material is promising and that a combination of some advanced methodological principles of polarography and voltammetry could bring about optimal performances. The gold electrode, under its various variants (stationary disc, rotatory disc, rotatory ring-disc), has been particularly used for determining mercury in natural waters,[12,37−43] river water,[13] fish,[14] wine [44,45] and biological materials [8,9] by differential-pulse stripping voltammetry; the sensitivity limit reached in such analyses was of the order of 1×10^{-10} mole · dm^{-3}.

This paper proposes the extension of the stripping voltammetry methods to the determination of microamounts of mercury (II) in high purity reagents by using a glassy carbon electrode as working electrode.

EXPERIMENTAL

In order to record the anodic stripping voltammograms with linear sweep of the potential, we used a Tacussel PRG-3 three-electrode polarographic complex. The working cell was made of Teflon and had a capacity of about 50 cm^3; it also had the possibility of mounting the working electrode, the reference electrode and the auxiliary electrode, as well as the glass tubes serving as inlet and outlet ports for the argon used to remove oxygen from the solutions, in the lid of the cell.

The used working electrode was made of Carbon-Loraine V-25 glassy carbon. Carbon gas fitted in a silica tube by means of a thin layer of Araldite and the electrical contact with outer circuitry was achieved with a mercury layer. In order to be usable, the electrode so worked out was polished using the procedure commonly applied to polish metallic surfaces. We used as auxiliary electrode a coiled platinum electrode embedded in a silica tube and as reference electrode a Radiometer K-401 saturated calomel electrode, whose compartment was connected to the cell through a 0.1 mole · dm^{-3} NaSCN salt bridge.

All substances used were high purity or analytical grade compounds provided by Merck or BDH. To prepare the solutions and to clean the vessels before use, tetradistilled water was used, the last distillation being carried out in a silica apparatus.

All measurements were carried out under controlled temperature conditions, at 25 ± 0.5°C, whereas the potentials were measured relative to the saturated calomel electrode. Oxygen was removed from all solutions subjected to voltammetric measurements by bubbling them with purified argon during 10 minutes.

The millimolar solutions of the mercuric compound were prepared by weighing the proper amount of mercury nitrate (Analar, BDH), passing it to a volumetric flask and bringing this to the mark with tetradistilled water. The millimolar solutions of Hg(II) were calibrated by titration with thiocyanate and were kept in polyethylene vessels. The more diluted solutions were always freshly prepared by dilution of the millimolar solution in volumetric flasks.

All laboratory vessels to be used were washed very carefully before use with a sulfonitric mixture (nitric acid : concentrated sulfuric acid in a 1 : 1 volumetric ratio), then were cleaned with bi- and tetradistilled water. The working cell was exposed to the same treatment.

Preparation and processing of the electronic grade reagents subjected to voltammetric measurements were described in earlier papers.[46,47] In order to check up observance of all the precautions devised for preserving the intended purity degree, we always recorded the voltammogram of a blank sample before measurement.

RESULTS AND DISCUSSION

In anodic stripping voltammetry, the pre-electrolysis step can be carried out either under constant current conditions, or under constant potential conditions. In the first case, a 0.3 mA value of the pre-electrolysis current has been shown to be advantageous. Although pre-electrolysis carried out at constant potential is more selective, the optimum value of the potential has to be set up individually for each indifferent electrolyte.

In order to find the optimum conditions for the electrodeposition of mercury at constant potential and its electrodissolution from the glassy carbon electrode, we investigated first the electrochemical behaviour of mercury(II) in various media which have or have not a complexing action on the Hg^{2+} ion. The following indifferent electrolytes were tested: NaSCN, KSCN, NH_4SCN, $HClO_4$, HCl, H_2SO_4, HNO_3 and KNO_3, all of them at 0.1 mole $\cdot$ dm^{-3} concentration. The best defined and the most reproducible intensity-potential curves were obtained in media containing the thiocyanate ion. The results published during the last years have also shown and justified the importance of the complexing action of the thiocyanate ion on the Hg^{2+} ion during the two steps (reduction and oxidation) of its determination by anodic stripping voltammetry.[48-56]

Selection of the optimum pre-electrolysis potential was based on the interpretation of the intensity-potential curves obtained under convection-controlled conditions. To this end, we proceeded first to record the intensity-potential curve for the reduction of the Hg^{2+} ion on the glassy carbon electrode in 0.1 mole NaSCN $\cdot$ dm^{-3}, under conditions identical to those used in the pre-electrolysis step of the analysis by anodic stripping voltammetry. The $i = f(E)$ curve obtained with a cathodic sweep of $+0.500$ to -1.200 V *vs.* SCE (whose potential is $E_{1/2} = -0.375$ V) is given in figure 1. The investigated pre-electrolysis potentials are in the region of the limiting current, at sufficiently negative values, so that no modifications induced by the dilution of the indifferent electrolyte could influence adversely the determinations. We give in figure 2 the variation of the maximum peak current i_p as a function of the pre-electrolysis potential, for a concentration of 5×10^{-6}mole Hg^{2+}. $\cdot dm^{-3}$ and $t_{el} = 5$ min, in 0.1 mole NaSCN $\cdot$ dm^{-3} as indifferent electrolyte. The optimum pre-electrolysis potential established for the determination of Hg^{2+} by anodic stripping voltammetry with linear sweep, with a glassy carbon electrode, was of $-$ 0.700 V *vs.* SCE in the case of using as indifferent electrolyte 0.1 mole NaSCN $\cdot$ dm^{-3} or 0.1 mole KSCN $\cdot dm^{-3}$ + 0.1 mole $HClO_4$ $\cdot$ dm^{-3} solutions.

Taking account of the complexing action of the thiocyanate ion, SCN^-, upon the mercuric ion, Hg^{2+}, we studied the influence of the NaSCN ion concentration, used as indifferent electrolyte,on the peak potential E_p. We give in figure 3 the dependence of thepeak potential E_p on the logarithm of the concentration of the indifferent electrolyte for a 0.01—1.00 mole $\cdot dm^{-3}$ concentration range. This $E_p = f(\log SCN^-)$ dependence is linear, which proves that the Hg^{2+} ion forms in solution a single complexed species with the thiocyanate ion. Although the peak potential is shifted towards more positive values when the concentration of the indifferent electrolyte decreases, which influences the selectivity of mercury determination, the fact that very well defined electrodissolution peaks are also obtained at low concentration of the indifferent electrolyte gives

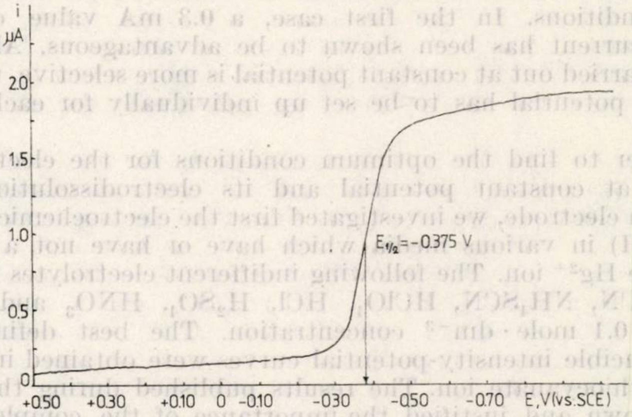

Fig. 1. — The polarographic behavior of the Hg^{2+} ion on a glassy carbon electrode, under convection-controlled conditions. The concentration of Hg^{2+} ions was of 1×10^{-4} mole · · dm^{-3}, in 0.1 mole NaSCN · dm^{-3} as indifferent electrolyte; the sweep rate was of 300 mV/min.

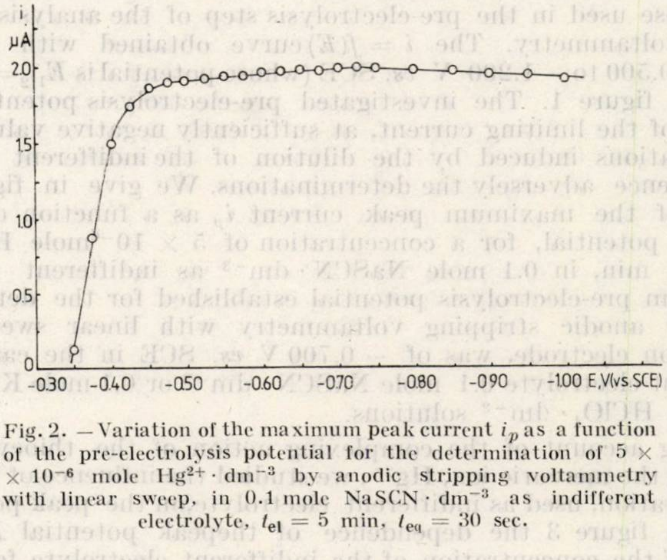

Fig. 2. — Variation of the maximum peak current i_p as a function of the pre-electrolysis potential for the determination of $5 \times \times 10^{-6}$ mole $Hg^{2+} \cdot dm^{-3}$ by anodic stripping voltammetry with linear sweep, in 0.1 mole NaSCN · dm^{-3} as indifferent electrolyte, $t_{el} = 5$ min, $t_{eq} = 30$ sec.

an advantage since in this way the effect of the residual current on the sensitivity of the method could be minimized. For very low mercury concentrations ($< 1 \times 10^{-7}$ mole · dm^{-3}), the residual current strongly affects the voltammetric curves if the indifferent electrolyte concentration is higher than 0.1 mole · dm^{-3}. By examining figure 4 it is obvious that for 5×10^{-8} mole Hg^{2+} · dm^{-3} and a concentration of the indifferent electrolyte of 0.01 mole · dm^{-3}, the residual current decreases appreciably, thus improving the shape of the voltammetric curves and, therefore' the sensitivity of the method.

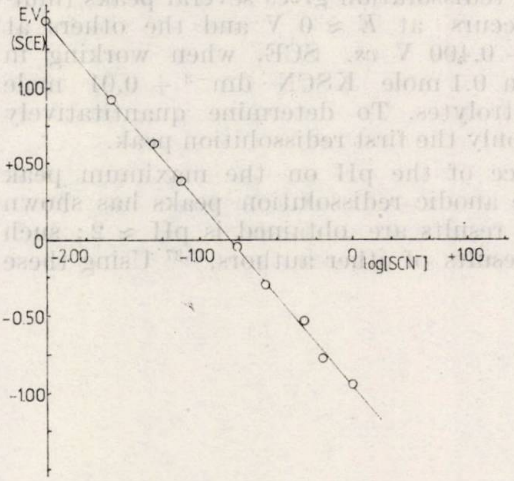

Fig. 3. — Dependence of the peak potential E_p on log [SCN^-] for 5×10^{-6} mole $Hg^{2+} \cdot dm^{-3}$, $t_{el} = 5$ min, $t_{eq} = 30$ sec, $v = 300$ mV/min.

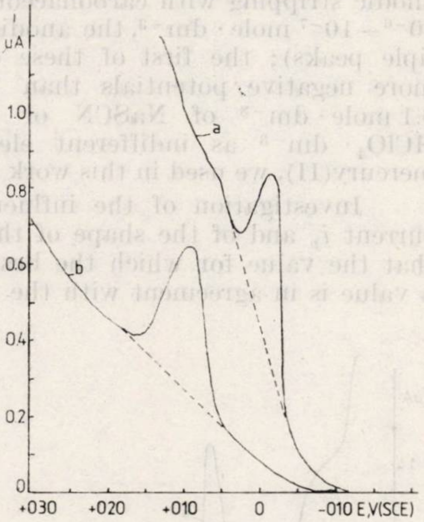

Fig. 4. — The anodic stripping voltammograms with linear sweep obtained for 5×10^{-8} mole $Hg^{2+} \cdot dm^{-3}$ in 0.1 mole $NaSCN \cdot dm^{-3}$ (*a*) and 0.01 mole $NaSCN \cdot dm^{-3}$ (*b*) as indifferent electrolytes. $E_{el} = -0.700$ V, $t_{el} = 30$ min, $t_{eq} = 1$ min, $v = 150$ mV/min.

Another basic parameter which had to be optimized was the pre-electrolysis time. It is known that the height of the anodic redissolution peak increases with the increase of the pre-electrolysis time, but this observation must also be correlated with the concentration of the analyzed species in the solution and with other factors. Thus, for higher mercury(II) concentrations ($10^{-4} \div 10^{-6}$ mole · dm^{-3}) we used pre-electrolysis times of 5 to 10 minutes. It is interesting to note that for a concentration of 5×10^{-6} mole Hg^{2+} · dm^{-3}, the height of the redissolution peak increases with the increase of the pre-electrolysis time up to $t_{el} = 10$ min; for $t_{el} > 10$ min, the height begins to decrease slowly and for $t_{el} = 30$ min the peak becomes poorly defined. This behavior is probably due to the fact that, in these conditions, a simultaneous chemical dissolution of the deposit formed on the glassy carbon electrode takes also place. As a matter of fact, the kinetics of the two steps of the Hg^{2+} determination by stripping voltammetry was dealt with in several papers published lately.[54-56] For concentrations lower than 1×10^{-7} mole Hg^{2+} · dm^{-3} and pre-electrolysis times less than 10 min, the anodic redissolution peak were always very poorly defined; this is why we chose $t_{el} = 20$ min for concentrations of the order of 10^{-7} mole $Hg^{2+} \cdot dm^{-3}$ and $t_{el} = 30$ min for concentrations of the order of 10^{-8} mole $Hg^{2+} \cdot dm^{-3}$.

As the literature data also show,[23,33] to determine mercury by anodic stripping with carbonaceous electrodes, in the concentration range $10^{-6}-10^{-7}$ mole $\cdot$ dm^{-3}, the anodic redissolution gives several peaks (multiple peaks); the first of these occurs at $E \approx 0$ V and the others at more negative potentials than + 0.400 V *vs.* SCE, when working in 0.1 mole $\cdot$ dm^{-3} of NaSCN or in 0.1 mole KSCN $\cdot$ dm^{-3} + 0.01 mole $HClO_4 \cdot dm^{-3}$ as indifferent electrolytes. To determine quantitatively mercury(II), we used in this work only the first redissolution peak.

Investigation of the influence of the pH on the maximum peak current i_p and of the shape of the anodic redissolution peaks has shown that the value for which the best results are obtained is pH $\approx$ 2; such a value is in agreement with the results of other authors.[35,37] Using these

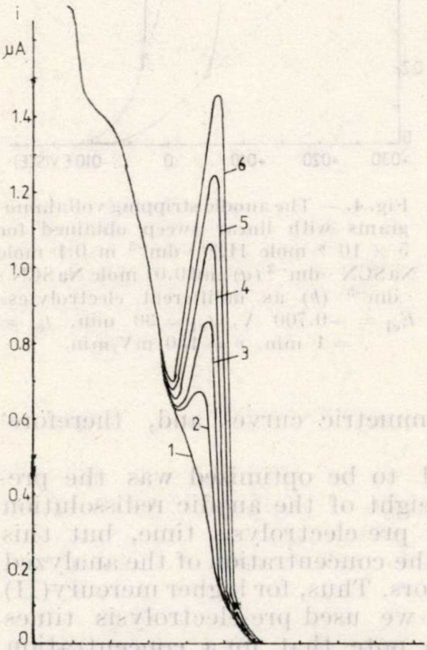

Fig. 5. — The anodic stripping voltammograms with linear sweep obtained for the Hg^{2+} determination in the concentration range $1 \times 10^{-7}-1 \times 10^{-6}$ mole$\cdot dm^{-3}$ using 0.1 mole NaSCN $\cdot$ dm^{-3} as indifferent electrolyte. $E_{el} = -0.700$ V, $t_{el} = 20$ min, $t_{eq} = 1$ min. $v = 150$ mV/min. (1) baseline (0.1 mole NaSCN $\cdot$ dm^{-3}); (2) 1×10^{-7}; (3) 2.5×10^{-7}; (4) 5×10^{-7}; (5) 7.5×10^{-7}; (6) 1×10^{-6} mole $Hg^{2+} \cdot dm^{-3}$.

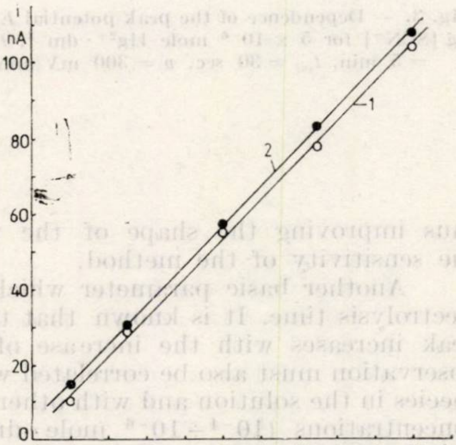

Fig. 6. — The calibration curve drawn for the determination of mercury(II) by anodic stripping voltammetry with linear sweep in the concentration range $1 \times 10^{-7}-1 \times 10^{-6}$ mole $\cdot$ dm^{-3}, using 0.1 mole NaSCN dm^{-3} (1) and 0.1 mole KSCN $\cdot$ dm^{-3} + 0.01 mole $HClO_4 \cdot dm^{-3}$ (2) as indifferent electrolytes. $E_{el} = -0.700$ V (*vs.* SCE), $t_{el} = 20$ min, $t_{eq} = 1$ min.

conditions, we no longer could observe the occurrence of the multiple peaks. This pH value in thiocyanate medium was ensured by adding perchloric acid (0.01 mole $HClO_4 \cdot dm^{-3}$).

Under the conditions discussed above, mercury(II) could be successfully determined in the concentration range $10^{-7}—10^{-8}$ mole · dm^{-3} by anodic stripping voltammetry with linear sweep, using the glassy carbon electrode as working electrode; we obtained a linear dependence of the maximum peak current on the concentration of the mercuric ion in the concentration range $1 \times 10^{-5}—1 \times 10^{-8}$ mole. dm^{-3}. We give in figure 5 the anodic stripping voltammograms with linear sweep obtained for the mercury(II) determination in the concentration range 1×10^{-6}—1×10^{-7} mole · dm^{-3}, using 0.1 mole NaSCN · dm^{-3} as indifferent electrolyte, and in figure 6 the calibration curve drawn for the determination of mercury in this concentration range. Such data suggested that the method could possibly be used to determine traces of mercury(II) in high-purity reagents.

The method herein described was thus applied to check up the mercury(II) content in electronic-grade reagents produced in this country. We give in figure 7 the anodic stripping voltammograms with linear sweep obtained during the determination of mercury in electronic-grade acetone; table 1 presents the results obtained for the mercury(II) determination in some tested electronic-grade reagents by anodic stripping voltammetry.

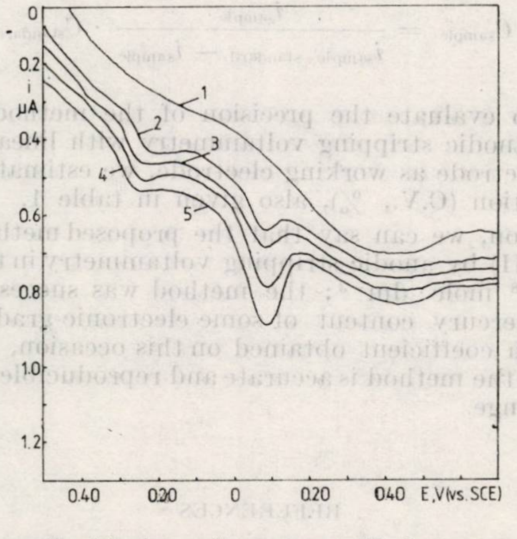

Fig. 7. — The anodic stripping voltamograms with linear sweep obtained for the determination of mercury(II) in electronic-grade acetone produced by ICCF-Bucharest. $E_{el} = -0.700$ V (*vs.* SCE), $t_{el}=20$ min, $t_{eq} = 1$ min, $v = 150$ mV/min. (1) baseline (0.1 mole KSCN · dm^{-3} + 0.01 mole $HClO_4 \cdot dm^{-3}$); (2) indifferent electrolyte + acetone sample; (3) sample (2) + 5×10^{-8} mole $Hg^{2+} \cdot dm^{-3}$; (4) sample (2) + 1×10^{-7} mole $Hg^{2+} \cdot dm^{-3}$; (5) sample (2) + 1.5×10^{-7} mole $Hg^{2+} \cdot dm^{-3}$.

Table 1

Results obtained during the determination of mercury(II) in electronic-grade reagents produced in this country

Sample	No. of determinations	$\bar{C}_{Hg^{2+}}$ $(mole \cdot dm^{-3})$	ppb	C.V.
Ethanol	3	2.5×10^{-8}	5	—
Acetone	5	1.12×10^{-8}	2.25	7.8
Hydrochloric acid	3	2.5×10^{-8}	5	—
Nitric acid	3	2.5×10^{-8}	5	—

Taking into account the linear dependence of the maximum peak current on concentration, up to concentrations of the order of 1×10^{-8} mole $Hg^{2+} \cdot dm^{-3}$, to estimate the mercury concentration in acetone samples, we used the method of the standard addition; the concentration was calculated according to the relation

$$C_{\text{sample}} = \frac{i_{\text{sample}}}{i_{\text{sample+standard}} - i_{\text{sample}}} \cdot C_{\text{standard}}$$

In order to evaluate the precision of the method of determining mercury(II) by anodic stripping voltammetry with linear sweep, using a glassy carbon electrode as working electrode, we estimated the coefficient of percent variation (C.V., %), also given in table 1.

In conclusion, we can say that the proposed method allows determination of Hg(II) by anodic stripping voltammetry in the concentration range $10^{-5}-10^{-8}$ $mole \cdot dm^{-3}$; the method was successfully applied to check up the mercury content of some electronic-grade reagents; the percent variation coefficient obtained on this occasion, always less than 10 %, shows that the method is accurate and reproducible for the examined concentration range.

REFERENCES

[1] U. Harms, *Z. Lebensm. Unters. Forsch.*, **157**, 125 (1975).

[2] M. Bernhard and A. Zattera, in "Marine Pollution and Marine Waste Disposal" (E. Pearson and E. DeFraja Frangipane, Eds.), Pergamon Press, Oxford, 1975, pp. 195–300.

[3] V. Bugdahl and E. V. Jan, *Z. Lebensm. Unters. Forsch.*, **157**, 133 (1975).

[4] M. Bernhard, *Ocean Management*, **3**, 353 (1973).

[5] M. Stoeppler and H. W. Nürnberg, *Ecotox. Env. Safety*, **3**, 335 (1979).

[6] M. Stoeppler, M. Bernhard, F. Backhaus and E. Schulte, *Sci. Tot. Environm.*, **13**, 209(1979).

[7] T. Kempf and M. Sonneborn, *Mikrochim. Acta*, II, 445 (1983).

[8] H. W. Nürnberg, *Proc. Analyt. Chem. Div. Chem. Soc.*, **15**, 276 (1978).

[9] H. W. Nürnberg, *Sci. Tot. Environm.*, **12**, 35 (1979).

[10] M. Kapel and M. E. Komaitis, *Analyst*, **104**, 124 (1979).

[11] H. W. Nürnberg, in "Electroanalysis in Hygiene, Environmental, Clinical and Pharmaceutical Chemistry" (W. F. Smith, Ed.), Elsevier, Amsterdam, 1980, pp. 351–372.

[12] L. Sipos, H. W. Nürnberg, P. Valenta and M. Branica, *Anal. Chim. Acta*, **115**, 25 (1980).
[13] M. Goto, K. Ikenoya and D. Ishii, *Bull. Chem. Soc. Jpn.*, **53**, 3567 (1980).
[14] R. Ahmed, P. Valenta and H. W. Nürnberg, *Mikrochim. Acta*, **I**, 171 (1981).
[15] H. W. Nürnberg, *Chem. Ing. Techn.*, **51**, 717 (1979).
[16] P. Valenta and H. W. Nürnberg, in "Gewässerschutz-Wasser-Abwasser" (B. Böhnke, Ed.), Gess. Förder Siedlungswasserwirtschaft, Aachen, 1980, Bd. 44, pp. 105—204.
[17] L. Mart, H. W. Nürnberg and P. Valenta, *Z. Analyt. Chem.*, **300**, 350 (1980).
[18] P. Klahre, P. Valenta and H. W. Nürnberg, *Vom Wasser*, **51**, 199 (1978).
[19] P. J. Elving and D. I. Smith, *Anal. Chem.*, **30**, 1945 (1958).
[20] P. J. Elving and D. L. Smith, *Anal. Chem.*, **32**, 1849 (1960).
[21] V. G. Barikov and O. A. Sangina, *Zavodsk. Lab.*, **30**, 1184 (1964).
[22] S. P. Perone and W. J. Kretlow, *Anal. Chem.*, **37**, 968 (1965).
[23] P. Emmot, *Talanta*, **12**, 651 (1965).
[24] O. L. Kabanova and E. A. Zalogina, *Zh. Anal. Khim.*, **26**, 826 (1971).
[25] A. I. Kartusinskaia, A. G. Stromberg and N. A. Kalpokova, *Elektrokhimyia*, **7**, 1248 (1971).
[26] E. M. Roizenblat and G. I. Veretina, *Zh. Anal. Khim.*, **28**, 33 (1973).
[27] E. M. Roizenblat and G. I. Veretina, *Zh. Anal. Khim.*, **29**, 2376 (1974).
[28] R. Fukai and L. Huynh-Ngoo, *Anal. Chim. Acta*, **83**, 375 (1976).
[29] V. Vrtilkova and R. Kalvoda, *Chem. Zvesti*, **18**, 410 (1964).
[30] L. Ulrich and P. Rüegsegger, *Fresenius Z. Anal. Chim.*, **277**, 349 (1965).
[31] G. G. Ranev and V. S. Volkova, *J. Anal. Chem. USSR*, **27**, 651 (1972).
[32] D. R. Kendall, *Ana l. Lett.*, **5**, 867 (1972).
[33] V. V. Penev, L. A. Moskovskikh and V. S. Putrova, *Zh. Anal. Khim.*, **28**, 1918 (1973).
[34] R. E. Allen and D. C. Johnson, *Talanta*, **20**, 799 (1973).
[35] L. Luong and F. Vydra, *J. Electroanal. Chem.*, **50**, 379 (1974).
[36] E. M. Roizenblat, T. A. Krapivkina and G. N. Veretina, *Zavodsk. Lab.*, **40**, 370 (1974).
[37] H. W. Nürnberg, P. Valenta, L. Mart, B. Raspor, L. Sipos, *Fresenius Z. Anal. Chem.*, **282**, 357 (1976).
[38] L. Sipos, P. Valenta, H. W. Nürnberg and M. Branica, *J. Electroanal. Chem.*, **77**, 263 (1977).
[39] L. Mart, H. W. Nürnberg, P. Valenta and M. Stoeppler, *Thalessia Jugosl.*, **14**, 171 (1978).
[40] L. Mart, H. W. Nürnberg and P. Valenta, *Z. Anal. Chem.*, **300**, 350 (1978).
[41] L. Sipos, J. Golimowski, P. Valenta and H. W. Nürnberg, *Z. Anal. Chem.*, **298**, 1 (1979).
[42] L. Sipos, H. W. Nürnberg, P. Valenta and M. Branica, *Anal. Chem. Acta*, **115**, 25 (1980).
[43] B. Pihlar, P. Valenta, J. Golimowski and H. W. Nürnberg, *Z. Wasser- und Abwasserforsch.*, **13**, 130 (1980).
[44] J. Golimowski, P. Valenta and H. W. Nürnberg, *Z. Lebensm. Unters. Forsch.*, **168**, 333 (1979).
[45] J. Golimowski, P. Valenta, M. Stoeppler and H. W. Nürnberg, *Z. Lebensm. Unters. Forsch.*, **168**, 439 (1979).
[46] I. Tănase, Ph. D. Dissertation, Polytechnical Institute of Bucharest, 1982.
[47] I. Tănase, I. Vartires, N. D. Totir and C. Luca, *Rev. Chim. (Bucharest)*, to be published.
[48] G. Torsi and G. Mamantov, *J. Electroanal. Chem.*, **34**, 465 (1971).
[49] Kh. Z. Brainina and E. Ya. Neiman, *Zh. Anal. Khim.*, **26**, 875 (1971).
[50] M. Stulikova, *J. Electroanal. Chem.*, **48**, 33 (1973).
[51] S. Combert and S. Dozol, *Electrochim. Acta*, **24**, 1283 (1979).
[52] R. G. Dhaneshwar and A. V. Kulkarni, *J. Electroanal. Chem.*, **99**, 207 (1979).
[53] R. G. Dhaneshwar and A. V. Kulkarni, *J. Electrochem. Soc. India*, **29**, 48 (1980).
[54] H. Verplatse, P. Keikens, E. Temmerman and F. Verbeek, *J. Electroanal. Chem.*, **115**, 235 (1980).
[55] P. Keikens, R. M. H. Verbeeck, H. Donache and E. Temmerman, *J. Electroanal. Chem.*, **147**, 235 (1983).
[56] P. Keikens, M. Bogaert and E. Temmerman, *Mikrochim. Acta*, **III**(1—2), 29 (1983).
[57] R. Neeb, "Inverse Polarographie und Voltammetrie, Neuere Verfahren zur Spurenanalyse", Akademie Verlag, Berlin, 1969, p. 102.

Revue Roumaine de Chimie, **30**, *8*, 689–693 (1985)

COMBINED ION EXCHANGE – SPECTROPHOTOMETRIC DETERMINATION OF POTASSIUM WITH SODIUM TETRAPHENYLBORATE

LUMINIȚA VLĂDESCU and STELA TONEANU

National Institute of Chemistry, Laboratory of Analytical Chemistry,
Splaiul Independenței 202, Bucharest, Romania

Received December 17, 1984

Combined ion exchange – spectrometric determination of potassium with sodium tetraphenylborate offers the conditions necessary for application of spectrometric method in very acid solutions diluted in potassium, hence increasing the domain of applicability and sensitivity of the method and reduces the time required for analysis.

In the chemical analysis of potassium, poor in reagents, sodium tetraphenylborate holds an importante place.

Sodium salt of tetraphenylboric acid is slightly soluble in water, whereas potassium salt is difficultly soluble, a fact that permits its use as a reagent for the quantitative determination of potassium by gravimetric, titrimetric, conductometric, turbidimetric or spectrometric methods.[1-9]

Irrespective of the technique used, precipitation, filtration and washing of potassium tetraphenylborate followed by drying and weighing or by dissolution in an adequate solvent must precede processing of the solution. These numerous operations complicate the working method and increase the time required for analysis.

In addition, indirect spectrometric determination of potassium with sodium tetraphenylborate [10] required strict observance of the pH within the 4–5 range, making this method more difficult to apply in very acid solutions.

The present paper reports on the possibility of using sodium tetraphenylborate in a cation exchange system, thus eliminating precipitation and filtration. By this method, potassium may even be concentrated from solutions in which only traces are to be found. Thus, the solutions obtained by acid desagregation of the samples offer the conditions necessary for application of spectrometric method, hence increasing the domain of applicability and sensitivity of the method.

EXPERIMENTAL

CHEMICAL AND EQUIPMENT

- Strongly acid cation exchange resin Vionit CS-3.
- Aqueous solutions of known titrum of K^+, Na^+, Mg^{2+}, Ca^{2+} and Fe^{3+}.
- Aqueous solution of 0.03 M sodium tetraphenylborate 0.5% aluminium nitrate.
- Aqueous solutions of 0.3 M, 2 M, 4 M HCl.
- Aqueous solution of 10% KSCN.
- Mixed solvent 75% acetonitrile — 25% water.
- SPEKORD UV—VIS and SPECOL spectrofotometers.
- Flame emission spectrofotometer Flapho 4.
- Atomic absorption spectrofotometer Pye Unicam SP 191.

The quantitative determination of cations was performed spectrometrically.[10, 12,13]

The ion exchange took place in glass column 15 cm long, 1 cm in diameter, provided with stopcoks at bottom and funnel with ground joint at top. Known quantities of cation exchanger were transferred in columns, purified, activated in H^+ ionic form and washed with water up to negative Cl^- test.

RESULTS AND DISCUSSION

With a view to establishing the optimal working conditions, we studied the influence of sodium tetraphenylborate on the cation exchange behaviour of potassium.

To this end, after fixing a known quantity of potassium in the cation exchange resin, 50 mL 0.03 M sodium tetraphenylborate solution was passed through the column and it was washed with water up to complete elimination of the excess reagent. Thus, by precipitation, a quantity of tetraphenylborate corresponding to the potassium initially fixed was retained within the resin.

The potassium tetraphenylborate precipitate in the resin was dissolved by passing a 75% acetonitrile — 25% water mixture through the column. The whole quantity of tetraphenylborate was eliminated from the resin into the mixed solvent and was collected in a calibrated flask. The initial quantity of potassium in the sample was calculated by measuring the absorbance of the effluent solution at $\lambda = 260$ nm.

The ion exchange experiments were repeated using potassium solutions with varied HCl content. Table 1 shows that the potassium quantity indirectly determined by the method suggested coincides with that determined by flame emission spectrometry after elution of potassium from the resin with 2 M HCl, and likewise with the quantity of potassium in the sample.

The method was then applied for measuring potassium in synthetic mixtures that contained, besides this ion, Na^+, Mg^{2+}, Ca^{2+} and Fe^{3+}. After fixing several known quantities of these ions in the resin, the same technique was used for indirect determination of potassium with tetraphenylborate. After washing the column with distilled water for removing the mixed solvent, Fe^{3+} was eluted selectively with a 10% KSCN solution, the effluent collected in the calibrated flask being used for the spectrometric determination of iron. Finally, Na^+, K^+, Mg^{2+} and Ca^{2+} were eluted with 2M HCl and determined by emission or absorption flame spectrometry.

Table 1

Results of potassium content determination from solutions with different HCl concentrations

Potassium quantity			
In sample (mg)	Determined by combined ion exchange — spectrometric method (mg)	Determined after elution (mg)	HCl concentration in sample (M)
1.95	1.98	2.01	—
1.95	1.90	1.98	0.5
1.95	1.89	1.86	1
1.95	1.95	1.90	2
1.95	1.87	1.97	4
1.95	1.86	1.88	8

The elution curves in Fig. 1 and the results in table 2 show good agreement of the quantities taken in the sample with those determined after separation. The K^+ content determined by the indirect spectrometric

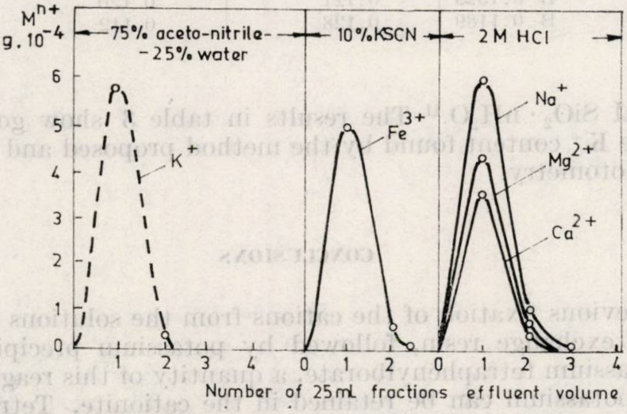

Fig. 1. — Elution curves for combined ion exchange—spectrometric determination of the cations K^+, Na^+, Mg^{2+}, Ca^{2+}, Fe^{+3} in a synthetic mixture.

Table 2

Results of potassium content determination from synthetic samples with different content of Na^+, Ca^{2+}, Mg^{2+}, Fe^{3+}.

Potassium quantity		
In sample (mg)	Determined by combined ion exchange — spectrometric method (mg)	Determined by flame emission or absorption spectrometry (mg)
0.97	0.85	0.90
1.95	1.98	2.04
3.80	4.02	3.79
9.75	10.00	9.86

method with tetraphenylborate was checked by flamephotometry after elution with HCl, obtaining identical results.

Finally, the combined ion exchange — spectrometric method with sodium tetraphenylborate was applied for determining potassium in solutions obtained by the action of concentrated HCl on several samples

Table 3

Results of potassium content determination in acid solutions obtained from industrial $SiO_2 \cdot nH_2O$

Sample	Potassium quantity	
Type (g)	Determined by combined ion exchange — spectrometric method %	Determined by flame emission or absorption spectrometry %
A 0.1243	0.007	0.009
A 0.1250	0.009	0.010
B 0.1329	0.121	0.120
B 0.1189	0.128	0.112

of industrial $SiO_2 \cdot nH_2O$.[11] The results in table 3 show good agreement between the K^+ content found by the method proposed and that obtained by flamephotometry.

CONCLUSIONS

By previous fixation of the cations from the solutions to be analyzed in a cation exchange resin, followed by potassium precipitation in the resin as potassium tetraphenylborate, a quantity of this reagent equivalent to that of potassium can be retained in the cationite. Tetraphenylborate can then be quantitatively recovered by washing the column with a 75 % acetonitrile—25 % water mixture that dissolves the precipitate. Measurement of the absorbance of the effluent collected in the calibrated flask permits calculation of the K^+ content in the analyzed solution.

The combined ion exchange — spectrometric determination of potassium with sodium tetraphenylborate has the following advantages:

— can be applied to solutions of varied acidity, no matter how high without the preparation of some standard solutions of an acidity equal to that of the sample, for each determination;

— eliminates the precipitation, filtration, etc. thus simplifying the working method and shortening the interval necessary for the analysis;

— avoids the introduction of reagents for adjustment of the pH which lowers the sensitivity of the spectrometric method;

— realizes concentration in the resin of the whole quantity of K^+ to be found in traces in the sample analyzed, thus widening the range of applicability of the method to very diluted solutions.

REFERENCES

[1] P. Raff and W. Brotz, *Z. analyt. Chem.*, **133**, 241 (1951).
[2] M. Kohler, *Z. analyt. Chem.*, **138**, 9 (1953).
[3] W. Geilmann and W. Gebauhr, *Z. analyt. Chem.*, **139**, 161 (1953).
[4] H. Flaschka, *Z. analyt. Chem.*, **136**, 99 (1952).
[5] W. Rudorff and H. Zannier, *Angew. Chem.*, **66**, 638 (1954).
[6] R. Neu, *Z. analyt. Chem.*, **143**, 254 (1954).
[7] W. Rudoff and H. Zannier, *Z. analyt. Chem.*, **140**, 1 (1953).
[8] H. Grubitsch, *Z. analyt. Chem.*, **209**, 313 (1965).
[9] Z. Gregorowicz and F. Buhl, *Mikrochim. Acta*, **129** (1961).
[10] R. T. Pflaum and L. C. Howick, *Analyt. Chem.*, **28**, 1542 (1956).
[11] L. Vlădescu, V. Dumitrescu and N. Dumitrescu, *Rev. Chim. (București)*, **00**, 000(1985).
[12] H. Zimmermann, "Photometric Metal and Water Analysis", W.V.C., M.B.H., Stuttgart, 1962, Section B-b 6 1 (61) and 6 2 (61).
[13] M. Pinta, "Spectrometrie d'absorption atomique", Tome II, "Applications a l'analyse chimique", Paris, Masson et Cie, 1971.

Revue Roumaine de Chimie, **30**, *8*, 695–702 (1985)

ON THE DIOXIMINE COMPLEXES OF TRANSITION METALS. LXVII*

NEW SULFITO-*BIS*-DIMETHYLGLYOXIMINO-COBALT(III) COMPLEXES AND THEIR THERMAL DECOMPOSITION

CS. VÁRHELYI *, J. ZSAKÓ *, GY. LIPTAY ** and MAGDA SOMAY *

* Faculty of Chemical Technology, Babeş-Bolyai University, str. Arany János 11, 3400-Cluj-Napoca, Romania

** Department of Inorganic Chemistry, Technical University, 1521-Budapest, Hungary

Received October 1, 1984

Ten new $M[Co(DH)_2(SO_3)X]$ type complexes were synthesized. The bonding of the SO_3 group to the Co atom occurs through the S atom, as shown by IR spectra. Thermal decomposition of eleven sulfito-complexes is studied by derivatography. The decomposition begins with endothermal dehydration reactions. In the case of six complexes kinetic parameters are derived for the first decomposition stage. The dehydration is followed by exothermal reactions, without a clear stoechiometry.

INTRODUCTION

In the present paper the synthesis and characterization of some $M[Co(DH)_2(SO_3)X]$ type complexes is given, where DH_2 stands for dimethylglyoxime and X for aromatic amines or heterocyclic N-bases. A derivatographic study of the thermal decomposition of the complexes obtained is performed. An attempt is made to derive kinetic parameters for the first decomposition stage of several complexes, by using the thermogravimetric curves.

SYNTHESIS OF $M[Co(DH)_2(SO_3)X]$ *TYPE COMPLEXES*

$Na_3[Co(DH)_2(SO_3)_2]$ was used as starting material, which can be easily obtained from $[Co(DH)_2(OH_2)_2]^+$, $[Co(DH)_2(H_2O)Cl]$ by means of a substitution reaction with Na_2SO_3 or by oxidation of cobalt(II) salts in the presence of dimethylglyoxime and Na_2SO_3.[1] In this compound one of the SO_3 — groups is replaced by a water molecule and the resulting sulfito-aquo complex $[Co(DH_2)(SO_3)(H_2O)]^-$ was used for synthesis purposes. The water molecule can be replaced in various anation reactions by other neutral molecules as amines or N-bases. The sulfito-group having the greatest trans effect after the cyanide ion, it is not replaced during these substitution reactions and the products obtained are very pure.

In the present paper new complex salts of the $M[Co(DH)_2(SO_3)$ (amine)]. t H_2O type were obtained by means of anation reactions of

---

* Part LXVI. F. Mánok, Cs. Várhelyi and A. Török, *Stud. Univ. Babeş-Bolyai Chem.*, **29**, 33(1984).

$NH_4[Co(DH)_2(SO_3)(H_2O)]$ with different aromatic amines and heterocyclic N-bases. The aromatic amines with pK_b values comprised between 9 and 13 were observed to co-ordinate easily to the $Co(DH)_2$ nucleus :

$$[Co(DH)_2(SO_3)(H_2O)]^- + \text{amine} = [Co(DH)_2(SO_3)(\text{amine})]^- + H_2O$$

The very weak bases ($pK_b > 14$) (e.g. nitro-anilines nitro-toluidines, sulfanylic — and anthranylic acids) are not suitable for this purpose.

From the ammonium salts resulting from the above anation reactions, the alkaline metal, and heavy metal salts were obtained by means of double decomposition reactions.

The complex salts obtained are characterized in table 1.

Table 1

New sulfito-amino-complexes of the $M[Co(DH)_2(SO_3)(\text{amine})]t\ H_2O$ type

Formula	Yield (%)	Aspect	Analysis calcd.	Analysis found
$Na[Co(DH)_2(SO_3)Py].4\ H_2O$	75	yellow, irregular crystals	Co 10.84	11.05
			S 5.90	6.08
			H_2O 13.17	12.90
$Na[Co(DH)_2(SO_3)(m\text{-}tol)].5\ H_2O$	60	yellow prisms	Co 10.00	10.10
			S 5.44	5.60
			H_2O 15.28	14.96
$Na[Co(DH)_2(SO_3)(p\text{-}tol)].4\ H_2O$	65	short, yellow prisms	Co 10.31	10.25
			S 5.61	5.45
			H_2O 12.52	12.23
$Na[Co(DH)_2(SO_3)(m\text{-}xyl)].4\ H_2O$	75	yellow irregular crystals	Co 10.07	10.11
			S 5.48	5.55
			H_2O 12.22	12.46
$Na[Co(DH)_2(SO_3)(p\text{-}ethylaniline)].4\ H_2O$	80	yellow prisms	Co 10.07	9.88
			S 5.48	5.29
			H_2O 12.22	12.34
$K[(Co(DH)_2(SO_3)(m\text{-}tol)].5\ H_2O$	70	dark yellow microcrystals	Co 9.73	10.03
			S 5.29	5.60
			H_2O 14.87	14.70
$K[Co(DH)_2(SO_3)(p\text{-}tol)].5\ H_2O$	75	dark yellow microcrystals	Co 9.73	9.88
			S 5.29	5.50
			H_2O 14.87	14.66
$K[Co(DH)_2(SO_3)(m\text{-}xyl)].4\ H_2O$	80	orange-yellow long prisms	Co 9.80	10.08
			S 5.33	5.55
			H_2O 11.90	11.70
$K[Co(DH)_2(SO_3)(p\text{-}ethylaniline)].4\ H_2O$	80	dark yellow prisms	Co 9.80	9.70
			S 5.33	5.44
			H_2O 11.90	11.54
$K[Co(DH)_2(SO_3)(m\text{-}Cl\text{-}aniline)].5\ H_2O$	60	long, yellow prisms	Co 9.41	9.33
			S 5.12	5.35
			H_2O 14.35	14.00

Co detn. complexometrically, S as $BaSO_4$

INFRARED SPECTRA

The free SO_3^{2-} ion gives four characteristic bands, which appear both in the IR and Raman spectra. By considering the sulfito-complexes as being $R-SO_3$ type molecules a C_{3v} site symmetry can be assumed, i.e. the same symmetry as with the free SO_3^{2-} ion. Consequently, the same four characteristic bands must appear, in the case of all sulfito-complexes, as with the free ion. The wave number of these bands is modified by the co-ordination, since the formation of the Co—S bond reduces the negative charge of the oxygen atoms and increases the bonding order of the S—O bonds. This is why the symmetric valence vibration band ν_s and especially the band of the double degenerated asymmetric valence vibration is shifted towards higher wave numbers. The wave number ν_s is of 960—1010 cm^{-1} as compared to the value 960—970 cm^{-1}, characteristic for the free SO_3^{2-} ion, and ν_{as} is shifted from 930—950 cm^{-1} up to 1020—1075 cm^{-1}. The bending vibration δ_s appears almost in the same interval of 610—680 cm^{-1} as with the free ion (616—655 cm^{-1}). The bending vibration δ_{as} shows also a slight shift towards higher wave numbers, i.e. it appears at 500—560 cm^{-1} instead of 445—530 cm^{-1}.[2]

In the case of the dimethylglyoximato Co(III) complexes the strong valence vibration of the N—O bond of the oxime appears at about 1050—1150 cm^{-1} and this may partially overlap the strong ν_{as} vibration of the S—O bond. In a similar way, the ν_{Co-N} vibration at 500—530 cm^{-1} is also partially superposed upon the δ_{as} vibration band of the S—O bond. Thus, the exact assignment of ν_s and ν_{as} is rather difficult in the case of these complexes. Anyhow, the presence of all these vibrations is observed in the IR spectra of all the complexes given in table 1, showing that they are sulfito-complexes, with SO_3 ligands linked through the sulfur atom to the Co atom.

In the spectra studied there is an evidence of the formation of strong intramolecular O—H..O hydrogen bridges, giving a weak ν_{O-H} band at 2350—2400 cm^{-1} and a very weak $\nu_{H-O..O}$ band at 1700—1800 cm^{-1}. The same bands are observed also with other bis-dimethylglyoximato-cobalt(III) complexes. These hydrogen bridges are responsible for the trans configurations of the complexes, since they stabilize the coplanar $Co(DH)_2$ ring system.

Other characteristic strong vibration bands of the co-ordinated oxime molecules are situated at 1570—1580 cm^{-1} ($\nu_{C=N}$) and 1240 cm^{-1} (ν_{N-O}). The stretching vibration bands ν_{N-H} of the co-ordinated amines are shifted with 200—250 cm^{-1} towards lower values, as compared to the free amines and they appear at about 3200, 3150 cm^{-1}. This effect indicates the strong covalent character of the Co—N(amine) bond.

ELECTRONIC SPECTRA

The complexes studied show two strong charge-transfer bands at about 33—34 and 41—42 kK similarly to other bis-dimethylglyoximato Co(III) complexes,[3] but no clear crystal field transition can be observed. The wave numbers of the charge transfer bands are given in table 2.

The position of these bands seems to be influenced by the nature of the ligand occupying the trans position to the SO_3 group. Both bands are shifted towards higher wave numbers if the ligand X can give relatively strong π bonds with the Co atom. Thus for X=NCSe, NCO or

Table 2

UV absorption bands of $M[Co(DH)_2(SO_3)X]$ type complexes (Wave numbers in kK)

X	A	B	X	A	B
NCSe	41.6	35.4	Cl	41.2	33.7
NCO	41.4	34.4	Br	41.3	33.8
thioureea	42.1	33.2	pyridine	40.9	33.5
			γ-picoline	41.1	33.5
			aniline	41.3	32.9
			p-toluidine	41.2	33.3
			p-I-aniline	41.0	33.8
			allylthioureea	40.6	33.2
Mean value	41.7	34.3		41.1	33.5

thioureea, the mean values of the wave number of these bands are of 34.5 and 41.7, respectively, but the mean values for other 10 complexes, where X is Cl, Br or pyridine and aniline derivatives, are only 33.6 and 41.3, respectively. This effect allows us to presume that these bands are Co → DH charge transfer bands.

THERMAL DECOMPOSITION

The thermal decomposition of various sulfito-bis-dimethyl-glyoximino Co(III) complexes was studied under dynamic temperature conditions by means of derivatography.

The substances studied generally contain crystallization water. The loss of the water molecules occurs in a wide temperature range comprised between 50 and 190°C. On the thermogravimetric curves appear one, two or even three weight loss stops, corresponding to these dehydration processes. The DTA curves show the same number of endothermal peaks. After the dehydration generally a complex exothermal process begins, leading to the total destruction of the co-ordination sphere without the formation of relatively stable, well defined intermediates. The strong exothermal character of this process pleads for the participation of the atmospheric oxygen in these reactions. Endothermal de-amination processes were observed only in the case of two complexes, but without a clear stoechiometry.

Two typical TG and DTA curvs are given in Fig. 1. The loss of the crystallization water occurs in three stages with $Na_3[Co(DH)_2(SO_3)_2]\cdot 12H_2O$. In the first stage ten molecules of H_2O are evolved and in the following two stages the remaining water molecules are lost one by one. The three stages are marked by three endothermal peaks. The further decomposition begins with a strong exothermal process with no clear stoechiometry. In the case of $K[Co(DH)_2(SO_3)(m\text{-}Cl\text{-}aniline)]\cdot 5\,H_2O$ the water molecules are lost in two stages, followed by another endothermal process consisting presumably in a de-amination reaction. There is no evidence of the formation of a stable intermediate since a very fast strongly exothermal process is partially superposed on the former one. At higher temperature another strongly exothermal reaction occurs.

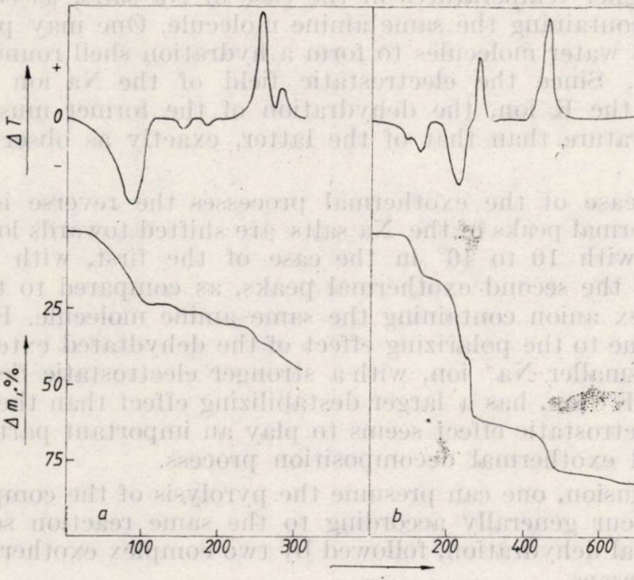

Fig. 1. — DTA and TG curves of : a — $Na_3[Co(DH)_2(SO_3)_2] \cdot 12\,H_2O$; $q = 10°C/min$, $m = 100$ mg ; b — $K[Co(DH)_2(SO_3)(m\text{-}Cl\text{-}aniline)] \cdot 5\,H_2O$ $q = 20°C/min$, $m = 20$ mg

The thermal characteristics of the decomposition reactions are presented in table 3 indicating the DTA peaks observed.

Table 3

Thermal characteristics of the decomposition reactions

Substance	Heating rate K min^{-1}	DTA peak temperatures, °C			temp. range
		endothermal		exothermal	
		dehydration	de-a-mination		
$Na_3[Co(DH)_2(SO_3)_2]$. $12H_2O$	10	85 152 180	—	*255* 285	20—300
$KNH_4[Co(DH)_2(SO_3)NCS]$. $3H_2O$	3	75 100	—	*242*	20—300
$KNH_4[Co(DH)_2(SO_3)NO_2]$. $4H_2O$	3	82	—	*235*	20—300
$Na[Co(DH)_2(SO_3)py]$. $4H_2O$	10	150	—	*260* 340 430	20—1000
$Na[Co(DH)_2(SO_3)(m\text{-}tol)]$. $5H_2O$	20	140	—	*250* 380	20—1000
$Na[Co(DH)_2(SO_3)(p\text{-}tol)]$. $4H_2O$	20	110	—	*240* 330 550	20—1000
$Na[Co(DH)_2(SO_3)(m\text{-}xyl)]$. $4H_2O$	20	102	—	*240* 300	20—1000
$K[Co(DH)_2(SO_3)(m\text{-}tol)]$. $5H_2O$	20	120	—	*260* 440	20—1000
$K[Co(DH)_2(SO_3)(p\text{-}tol)]$. $5H_2O$	20	80	—	*260* 455	20—1000
$K[Co(DH)_2(SO_3)(m\text{-}xyl)]$. $4H_2O$	20	100	190	*280* 465	20—1000
$K[Co(DH)_2(SO_3)(m\text{-}Cl\text{-}aniline)]$. $5H_2O$	20	90 125	220	*280* 460	20—1000

py = pyridine, tol = toludine, xyl = xylidine

From the data presented in table 3 some conclusions can be drawn concerning the thermal decomposition of the $M[Co(DH_2)(SO_3)(amine)]$ type complexes. As seen, the first endothermal peak of the dehydration appears at higher temperatures in the case of Na salts, as compared to the K ones, containing the same amine molecule. One may presume the crystallization water molecules to form a hydration shell round the other sphere cation. Since the electrostatic field of the Na ion is stronger than that of the K ion, the dehydration of the former must occur at higher temperature than that of the latter, exactly as observed experimentally.

In the case of the exothermal processes the reverse is observed, i.e. the exothermal peaks of the Na salts are shifted towards lower temperatures, viz. with 10 to 40° in the case of the first, with 60 to 160° in the case of the second exothermal peaks, as compared to the K salts of the complex anion containing the same amine molecule. Presumably, this shift is due to the polarizing effect of the dehydrated external sphere cations. The smaller Na^+ ion, with a stronger electrostatic field, as compared to the K^+ ion, has a larger destabilizing effect than the latter one. Thus, this electrostatic effect seems to play an important part, especially in the second exothermal decomposition process.

In conclusion, one can presume the pyrolysis of the complex anions studied to occur generally according to the same reaction scheme, viz. an endothermal dehydration, followed by two complex exothermal decomposition processes.

The possibility of endothermal de-amination processes observed, in two cases, is probably related to the weak nucleophylic character of the N atom in the m-Cl-aniline molecule due to the inductive effect of the Cl atom and to steric hindrances both in the case of the m-Cl-aniline and m-xylidine molecules making the Co — ligand bond more unstable.

DERIVING OF KINETIC PARAMETERS

At the thermal decomposition of the complexes studied the only pyrolysis processes corresponding to a clear stoechiometry are the dehydration reactions.

In the case of 6 complexes the **TG** curves allow us to derive apparent kinetic parameters as reaction order n, activation energy E and pre-exponential factor Z. The calculation technique used was a computerized variant of the Coats-Redfern method.[4]

The results are presented in table 4 together with the temperature at which the decomposition degree in the dehydration stage considered is of 0.1, denoted as $T_{0.1} \cdot Z$ values were obtained by giving the heating rate values in $K. s^{-1}$.

As seen from table 4 the dehydration begins at very low temperatures and the apparent activation energy is small. The E and $\lg Z$ values vary in parallel, due to the kinetic compensation effect.[5] The plot

Table 4

Kinetic parameters of some dehydration reactions

Substance	n	E, kJ/mole	lg Z	$T_{0.1}$, K
$Na_3[Co(DH)_2(SO_3)_2] \cdot 12\ H_2O$	0.66	42.7	4.5	313
$K\ NH_4[Co(DH)_2(SO_3)(NCS)] \cdot 3H_2O$	1.39	52.7	5.0	328
$K\ NH_4[Co(DH)_2(SO_3)(NO_2)] \cdot 4H_2O$	0.41	58.6	6.1	323
$Na[Co(DH)_2(SO_3)(py)] \cdot 4H_2O$	0.77	29.3	1.6	341
$Na[Co(DH)_2(SO_3)(m\text{-}tol)] \cdot 5H_2O$	1.64	54.4	5.7	342
$K[Co(DH)_2(SO_3)(m\text{-}tol)] \cdot 5H_2O$	1.17	33.9	2.7	322

of lg Z versus E gives a rather good linearization, showing the validity of a

$$\log Z = aE + b$$

type compensation law. By using the kinetic parameters presented in table 4, the least square method gives for the kinetic compensation parameters a and b the following values:

$$a = 0.145 \text{ mole/kJ}; \quad b = -2.31$$

Jaffé's correlation coefficient [6] is of $\rho = 0.979$ i.e. the linearity is quite good.

The value of the compensation parameter a is very close to those obtained for the dehydration of some dithionates [7] and of $[M(en)_3]X_s \cdot t\,H_2O$ type complexes.[8] According to Garn [9] the compensation parameter a is correlated with the decomposition temperature (T_c), viz.

$$a = 1/2.3\ RT_c$$

By taking for T_c the mean value of $T_{0.1}$ (see table 4), $a = 0.159$ mol/kJ is obtained, which is not in good agreement with the above given experimental value.

EXPERIMENTAL

$Na_3[Co(DH)_2(SO_3)_2] \cdot 12\ H_2O$: 20 m-moles cobalt acetate and 40 m-moles dimethylglyoxime in 80 mL dil. alcohol are oxidized by air bubbling 3—4 hours. Then 40 m-moles $Na_2SO_3 \cdot 7\ H_2O$ in 20—25 mL water are added and the air bubbling continued further for 5—10 minutes. The dark yellow solution is filtered and the disulfito-salt is precipitated with an excess of acetone. Yield : 90 %.

Analysis : Co calcd. 8.02, found 7.96, S calcd. 8.73, found 8.66, H_2O calcd. 29.43, found 29.80

$NH_4[Co(DH)_2(SO_3)(amine)] \cdot t\ H_2O$ salts. 10 m-moles $NH_4[Co(DH)_2(SO_3)(H_2O)]$ are dissolved in 20—25 mL water and treated with 10—12 mmoles of the corresponding amine in 10—15 mL alcohol. The mixture is kept on a water bath for 30—45 minutes. The formed sulfito-amino-salts are separated with an excess of acetone.

$M[Co(DH)_2(SO_3)(amine)]$ salts. 2—3 g $NH_4[Co(DH)_2(SO_3)(amine)]$ are dissolved in 20—30 mL water and treated with an excess of conc. aqueous solution of $NaNO_3$, KCl, 1 % $Pb(NO_3)_2$, 2 % $AgNO_3$, etc. The precipitated corresponding salts were filtered off and washed with ice cooled water.

IR spectra were recorded in KBr pellets by means of an UR 20 Carl Zeiss (Jena) Spectrofotometer. UV and visible spectra were obtained in aqueous solutions (conc. 2.10^{-3} and 1.10^{-4} mole/L) by means of a Specord — Spectrofotometer (Carl Zeiss Jena). The derivatographical measurements were carried out with a MOM Derivatograph.[22] Sample weight : 10—100 mg, atmosphere : static air. Reference material : Al_2O_3. Platinum crucible.

REFERENCES

[1] A. V. Ablov and G. P. Syrzova, *Zhur. neorg. Khim.*, **5**, 122 (1960).

[2] A. Simon, and K. Waldmann, *Z. physik. Chem.*, **204**, 233 (1955); B. Nyberg and B. Larsson, *Acta Chem. Scand.*, **27**, 63 (1973); A. V. Babaeva, Yu. Ya. Kharitonov and E. V. Shendretskaya, *Zhur. neorg. Khim.*, **7**, 1530 (1962).

[3] A. V. Ablov and M. P. Filippov, *Zhur. neorg. Khim.*, **3**, 1565 (1958); **4**, 2204, 2213 (1959); J. Zsakó, J. Sata and Cs. Várhelyi, *Rev. Roumaine Chim.*, **18**, 1759 (1973).

[4] J. Zsakó and J. Zsakó jr., *J. Thermal. Anal.*, **19**, 333 (1980).

[5] J. Zsakó, *J. Thermal Anal.*, **9**, 101 (1976).

[6] H. H. Jaffé, *Chem. Rev.*, **53**, 191 (1953).

[7] J. Zsakó, E. Brandt-Petrik, Gy. Liptay and Cs. Várhelyi, *J. Thermal Anal.*, **12**, 421 (1977).

[8] J. Zsakó, Cs. Várhelyi, Gy. Liptay and K. Szilágyi, *J. Thermal Anal.*, **7**, 41 (1975).

[9] P. D. Garn, *J. Thermal Anal.*, **7**, 465 (1975); **10**, 99 (1976).

[10] F. Paulik and J. Paulik, *Z. analyt. Chem.*, **160**, 291 (1958).

Revue Roumaine de Chimie, 30, 8, 703–712 (1985)

SYNTHESIS OF 9,10,19,20-TETRAHYDRO-DIBENZO/*a,c*/ PHENANTHRO/*g*/CYCLODECENE AND 9,10,19,20-TETRAHYDRO-TETRABENZO/*a, c, g, i*/CYCLODODECENE BY SULPHONE PYROLYSIS

M. BANCIU, I. POGANY, DANA MOSORA, PATRICIA RUSU,
RODICA STĂNCIULESCU and MARIA DEZSÖ
Organic Chemistry Department, The Polytechnic, TCH,
Spl. Independenţei 313, 76206 Bucharest, Romania

Received February 28, 1985

Coupling of 2,2′-bis(mercaptomethyl)biphenyl (**8**) with 9,10-bis(halomethyl)phenanthrenes (**7a, b**) or 2,2′-bis(bromomethyl)biphenyl (**7c**) afforded the corresponding cyclic disulphides **9a, b** which were oxidated to disulphones **10a** and **10b**, respectively. Vacuum gas-phase pyrolysis of **10a** and **10b** afforded the cyclic title compounds **5** and **6**, respectively. Intramolecular cyclization of **8** to the monosulphide **14** was also evidenced. Oxidation of **14** to monosulphone **15** followed by pyrolysis afforded 9,10-dihydrophenanthrene.

INTRODUCTION

Sulphones are well-known valuable intermediates in organic syntheses. An early interesting utilization of sulphones is the Ramberg-Bäcklund reaction[1] affording olefins, a conversion applied some years ago by Bestmann and Schaper[2] for the synthesis of two stereoisomeric tetrabenzo /*a, c, g,i*/cyclododecenes (**1**). On the other hand, the preparative pyrolysis of cyclic sulphones, introduced in practice in 1969 by Vögtle[3] has been developed in the last time to a new simple and general method[4,5] for constructing of a large variety of cyclic compounds e.g. cyclophanes. Using this approach Staab and Haenel[6] synthesized the [2](4,4′-biphenylylene[2](2, 7) phenanthrenophane (**2**) as well as the symmetrical *para*-cyclophanes **3** and **4**.

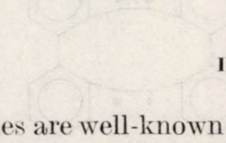
1

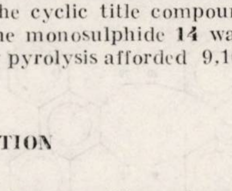
2

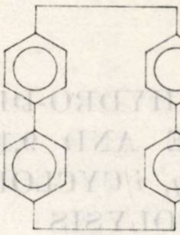

3

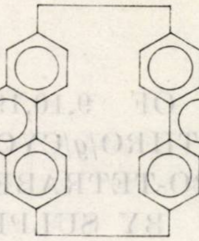

4

In connection with our interest in the domain of benzoannulenes and their valence-isomers[7] we became interested in the synthesis of cyclic disulphones including phenanthrene- and/or biphenyl moieties such as **1**—**4**. These disulphones should be eventually converted either to annulenes or to annulated cycloalkanes using the above mentioned general reactions of sulphones.

In the present paper we describe the application of sulphone pyrolysis in the synthesis of 9, 10, 19, 20-tetrahydro-dibenzo/*a*, *c*/phenanthro/*g*/cyclodecene (**5**) and of 9, 10, 19, 20-tetrahydro-tetrabenzo/*a*, *c*, *g*, *i*/-cyclododecene (**6**); these compounds are isomers of the cyclophanes **2** respectively **3**.

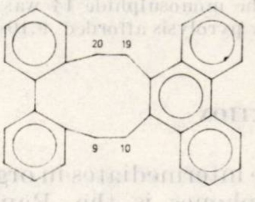

5

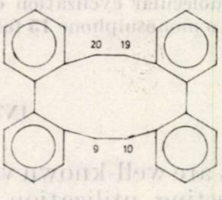

6

A spectrophotometric study of charge-transfer complexes of **5** and **6** as well as of related compounds will be published in a forthcoming paper.

RESULTS AND DISCUSSION

The reaction scheme used in the synthesis of **5** and **6** (Scheme 1) follows the general procedure of Vögtle[3] consisting in coupling of haloderivatives of the type **7** with dithiols of the type **8**, followed by oxidation of the resulted disulphides **9** and pyrolysis of disulphones **10**.

Synthesis of intermediates 7 and 8

9,10-bis(Chloromethylphenanthrene (**7a**) was prepared starting from phenanthrene *via* 9,10-phenanthrene-quinone.[8] Reaction of phenanthrenequinone with methylmagnesium iodide afforded[9] the diol **11**. Treatment

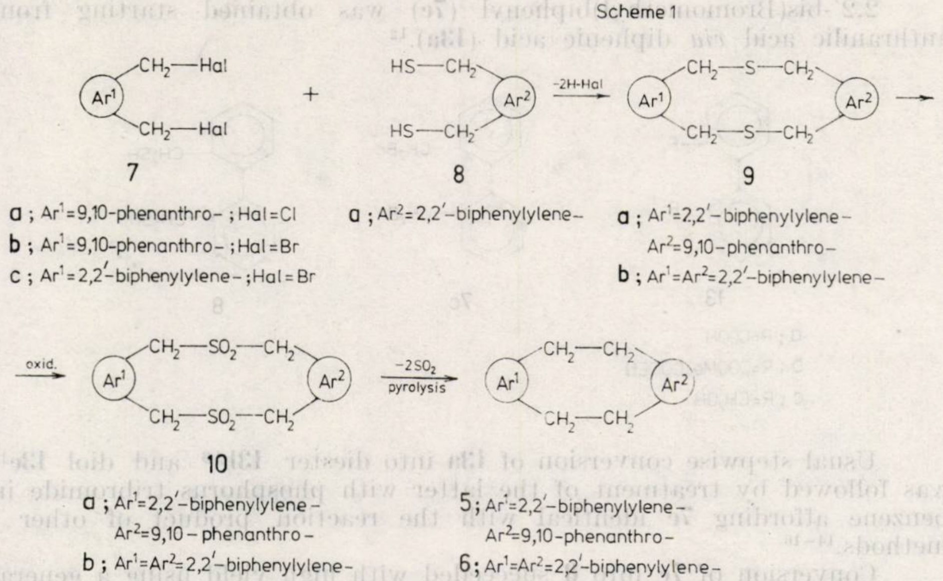
Scheme 1
CH₂—Hal
Ar¹
CH₂—Hal
+
HS—CH₂
Ar²
HS—CH₂
-2H-Hal
CH₂—S—CH₂
Ar¹
Ar²
CH₂—S—CH₂
7
8
9
a ; Ar¹=9,10-phenanthro– ; Hal=Cl
b ; Ar¹=9,10-phenanthro– ; Hal=Br
c ; Ar¹=2,2′-biphenylylene– ; Hal=Br
a ; Ar²=2,2′-biphenylylene–
a ; Ar¹=2,2′-biphenylylene–
Ar²=9,10-phenanthro–
b ; Ar¹=Ar²=2,2′-biphenylylene–
oxid.
CH₂—SO₂—CH₂
Ar¹
Ar²
CH₂—SO₂—CH₂
–2SO₂
pyrolysis
CH₂—CH₂
Ar¹
Ar²
CH₂—CH₂
10
a ; Ar¹=2,2′-biphenylylene–
Ar²=9,10-phenanthro–
b ; Ar¹=Ar²=2,2′-biphenylylene–
5; Ar¹=2,2′-biphenylylene–
Ar²=9,10-phenanthro–
6; Ar¹=Ar²=2,2′-biphenylylene–

of **11** with thionyl chloride in benzene conducted to the methyl-chloromethyl derivative **12a** *via* a dehydration accompanied by allylic rearrangement[10]. Subsequent reaction of **12a** with sulphuryl chloride afforded **7a**.[10]

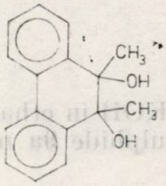
CH₃
OH
CH₃
OH

11

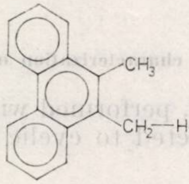

12

a ; Hal = Cl
b ; Hal = Br

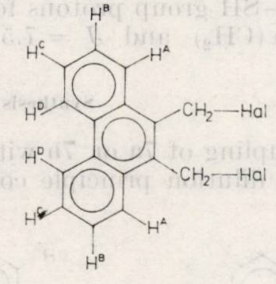
Hᴮ
Hᶜ
Hᴬ
Hᴰ
CH₂—Hal
Hᴰ
CH₂—Hal
Hᶜ
Hᴬ
Hᴮ

7

a ; Hal = Cl
b ; Hal = Br

In the ^{1}H—NMR spectrum of **7a** in d$_6$-DMSO characteristic signals for each proton type could be easily attributed : δ, 5.43 (CH_2 groups); 7.7 (q; H^B, H^C); 8·25 (q; H^A) and 8·8 ppm (q; H^D). Better yields in synthesis of intermediates **7** were obtained for *dibromo*derivative **7b** using the procedure recently described by Staab *et al.*[11] : treatment of **11** with phosphorus tribromide afforded **12b** in an ionic reaction whereas subsequent radicalic bromination of **12b** with N-bromosuccinimide produced **7b** in about 75 % overall yield.

2,2′-bis(Bromomethyl)biphenyl (**7c**) was obtained starting from anthranilic acid *via* diphenic acid (**13a**).[12]

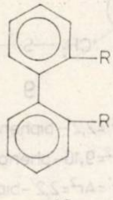

13

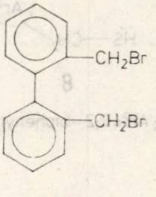

7c

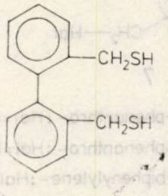

8

a ; R=COOH
b ; R=COOMe (COOEt)
c ; R=CH₂OH

Usual stepwise conversion of **13a** into diester **13b**[13] and diol **13c**[14] was followed by treatment of the latter with phosphorus tribromide in benzene affording **7c** identical with the reaction product of other methods.[14–16]

Conversion of **7c** into **8** succeeded with high yield using a general method applied in other related cases,[6,17] namely the treatment with thiourea followed by alkaline hydrolysis of the intermediate bis(isothiuronium) salt. The 2,2′-bis (mercaptomethyl)biphenyl (**8**) resulted as a yellow oil with penetrating odour, and was identical with the product obtained by Lüttringhaus *et al.*[18] from **7c** with potassium thioacetate and subsequent hydrolysis. In the ^1H-NMR spectrum of **8** (CCl_4 solution) the CH_2-SH group protons form an AB_2 system with $\delta = 1.45$ (SH) and 3.45 ppm (CH_2) and $J = 7.5$ Hz.

Synthesis and characterization of 5

Coupling of **7a** or **7b** with **8**, performed with KOH in ethanol using the high dilution principle conducted to cyclic disulphide **9a** m.p. 257°.

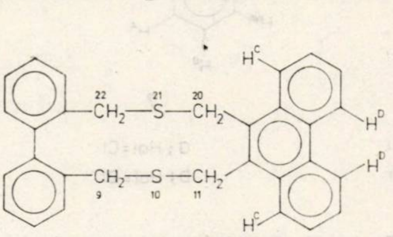

9a

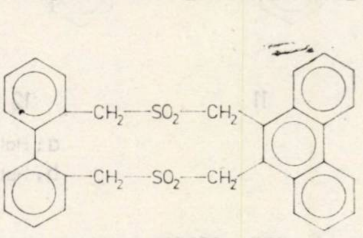

10a

In the ^1H-NMR spectrum of **9a** (in $CDCl_3$) two superimposed AB systems appear for CH_2 protons between 3.6–4.4 ppm ($\delta = 3.85$ and 4.20 ; $J = 14$ Hz ; $\delta = 3.80$ and 4.16 ; $J = 13$ Hz) ; along with these, multiplet for H^C centered at δ, 8.1 ppm, for H^D at δ, 8.6 ppm and between δ 7.0 and 7.8 ppm for the remaining aromatic protons are seen.

Oxidation of **9a** with 30% hydrogen peroxide in acetic acid or with *m*-chloroperbenzoic acid in dichloromethane afforded the disulphone **10a**, m.p. 337 — 8°. In the IR spectrum (KBr) of **10a** the characteristic frequencies of SO_2 groups appear at 1132 and 1320 cm^{-1}. Pyrolysis of disulphone **10a** to 9, 10, 19, 20-tetrahydro-dibenzo/*a*, *c*/phenanthro/*g*/-cyclodecene (**5**) was performed in a laboratory apparatus (see Experimental) in gas phase at 450°C and 1 Torr total pressure in argon atmosphere. Hydrocarbon **5**, m.p. 82 — 84°, was characterized through its IR, UV and ^1H-NMR spectra (see also Experimental). The ^1H-NMR spectrum of **5** (in $CDCl_3$) consists of signals at $\delta = 8.5$ (m, 2H), 7.8 (m, 2H), 6.8 — 7.6 (m, 12H) and 2.8 — 3.2 (broad unsymmetrical singlet, 8H). The last signal, which corresponds to all of the CH_2 groups, reveals a slow conformational motion, probably the inversion of the central ring.

Synthesis and characterization of 6

The steps used in the synthesis of **6** starting from **7c** and **8** were the same as in the synthesis of **5**. Coupling of **7c** with **8**, conducting to a mixture of *meso*- and *racemic*-disulphides **9b**, as well as their *m*-chloroperbenzoic acid oxidation to the corresponding disulphones **10b** were described by Bestman and Schaper.[2] We have found that hydrogen peroxide oxidation of **9b** conducted also with good yields to **10b**. Taking into account the higher temperatures needed in the next step of pyrolysis, no attempt to isolate the diastereoisomers of **10b** was made because it was shown [2] that the *meso*-**10b** rearranges on melting into racemic **10b**.

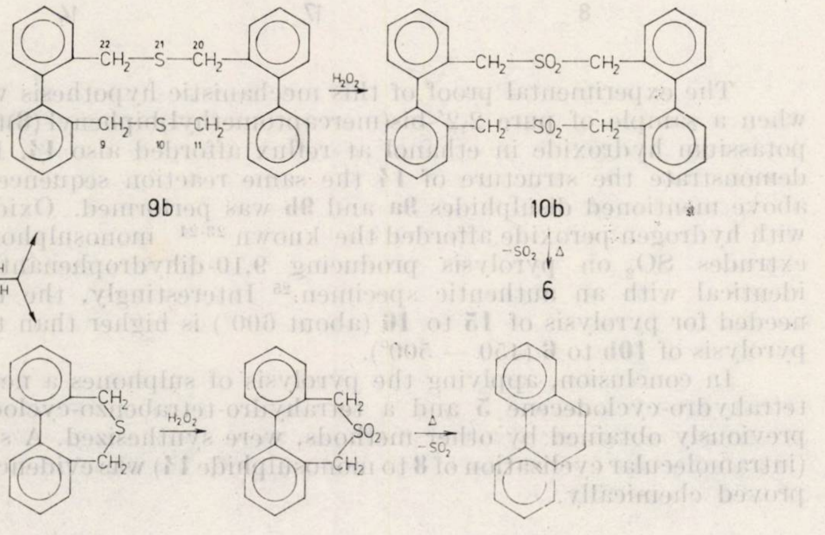

Pyrolysis of **10b** at 450 — 500°C and 0.5 Torr in the same apparatus as above afforded 9, 10, 19, 20-tetrahydro-tetrabenzo/*a*, *c*, *g*, *i*/cyclododecene (**6**) m.p. 263 — 268°. The compound **6** had been obtained by other methods : firstly in 1955 by Wittig and co-workers[19] then by Bestmann and Ruppert[20]; the existence of a *meso-* (m.p. 260 — 261°C) and a *racemic*-form (m.p. 267—268°) was demonstrated[21] and their crystal and molecular structure was also thoroughly investigated.[22] The physical data of our pyrolysis product **6** (see Experimental) are in agreement with those of *racemic* diastereoisomer.

Side-reaction accompanying the coupling of 7c with 8

When the reaction of **7c** with **8** was performed with a smaller KOH : **8** molar ratio and in a somewhat smaller amount of solvent (ethanol), a new product was obtained along with **9b**. This product proved to be the known[23,24] seven-membered ring monosulphide **14**, formed most probably by *intra*molecular cyclization of **8** under the influence of potassium hydroxide available in the reaction medium. The monoanion **17** resulted preferentially from **8** in these conditions suffers an intramolecular nucleophilic substitution affording **14** (whereas from dianion of **8** compound **9b** results after reaction with **7c**).

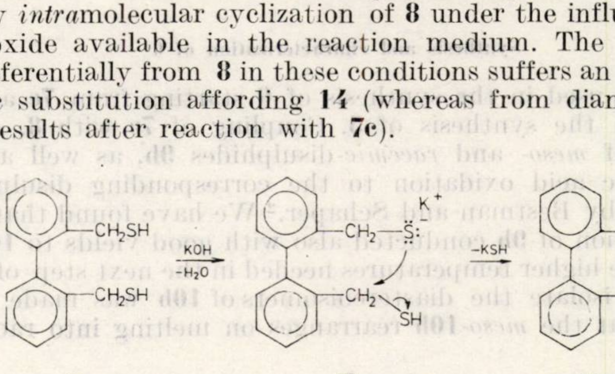

8 17 14

The experimental proof of this mechanistic hypothesis was brought when a sample of pure 2,2′-bis(mercaptomethyl)biphenyl (**8**)treated with potassium hydroxide in ethanol at reflux afforded also **14**. In order to demonstrate the structure of **14** the same reaction sequence as for the above mentioned disulphides **9a** and **9b** was performed. Oxidation of **14** with hydrogen peroxide afforded the known[23,24] monosulphone **15** which extrudes SO_2 on pyrolysis producing 9,10-dihydrophenanthrene (**16**), identical with an authentic specimen.[25] Interestingly, the temperature needed for pyrolysis of **15** to **16** (about 600°) is higher than that for the pyrolysis of **10b** to **6** (450 — 500°).

In conclusion, applying the pyrolysis of sulphones a new annulated tetrahydro-cyclodecene **5** and a tetrahydro-tetrabenzo-cyclododecene **6**, previously obtained by other methods, were synthesized. A side-reaction (intramolecular cyclization of **8** to monosulphide **14**) was evidenced and proved chemically.

EXPERIMENTAL

Melting points are uncorrected. IR spectra were registered with an UR-10 C. Zeiss-Jena double beam spectrophotometer, UV spectra with a SPECORD-UV/VIS spectrophotometer and the ^1H-NMR spectra with a VARIAN A60-A spectrometer using TMS as internal standard.

9,10-bis (Chloromethyl)phenanthrene (**7a**) was prepared following the method of Hauptmann[10] from the diol **11**[9] in two steps (with thionyl-chloride in benzene affording **12a**, m.p. 159°, then with sulphuryl chloride in benzene). **7a**, m.p. 208—210° (from benzene) lit.[10] m.p. 209—210°), yield 53%-calculated on **11**.
IR spectrum (KBr ; cm^{-1}) : 427w, 490m, 555m, 615w, 635m, 680m, 690m, 725s, 765s, 1255m, 1450m, 1495m, 2950w and 3075w.
^{1}*H-NMR spectrum* (see text).

9,10-bis(Bromomethyl)phenanthrene (**7b**) was obtained after Staab *et al*[11]. in two steps starting from the diol **11**[9] (treatment with phosphorus tribromide affording **12b** then with N-bromosuccinimide). **7b**, m.p. 233° (from CHCl$_3$) lit.[11] m.p. 229—231°, yield 70%-calculated on **11**.
IR spectrum (KBr ; cm^{-1}) : 525m, 727s, 766s, 1212m, 1458m, 1495m, 2860 broad and 2930 broad.

The diol **11**, m.p. 164°, used in the preparation of **7a** and **7b** was obtained in 55% yield following a procedure described in the literature[9] from 9,10-phenanthrenequinone[8] and methylmagnesium iodide.

2,2'-bis(Bromomethyl)biphenyl (**7c**). The starting material, anthranilic acid, was converted stepwise into diphenic acid (**13a**),[12] diphenic acid dimethyl- or dietyl esters **13b**,[13] and 2,2'-bis(hydroxymethyl)biphenyl (**13c**)[14] using literature procedures.

A solution of phosphorus tribromide (41 g ; 14.5 mL ; 0.150 moles) in anhydrous benzene (60 mL) was dropped with stirring during 3 hrs into a solution of diol **13c** (40 g ; 0.187 moles) in anhydrous benzene (200 mL). The reaction mixture was then refluxed for 1 hr, cooled and decomposed with 100 mL cold water. The organic layer was washed with water, 5% sodium hydrogen carbonate solution and again with water until pH 7. After drying over anhydrous MgSO$_4$ and solvent evaporation *in vacuo* a crystalline residue of **7c** m.p. 87° was obtained (52 g ; 82% yield). Recrystallization from *n*-heptane afforded a pure product with m.p. 90—91°, identical with the compound described as resulting either on treatment of **13c** with hydrobromic acid[14,15,16d] or on bromination of 2,2'-dimethylbiphenyl.[14b,16] Bromoderivative **7c** presents a strong lacrimatory action.
IR spectrum (KBr ; cm^{-1}) : 541m, 610m, 758m, 772m, 1200m, 1225m, 1440m and 1480m.

2,2'-bis(Mercaptomethyl)biphenyl (**8**). A solution of dibromoderivative **7c** (23 g ; 68 mmoles) and thiourea (12.5 g ; 164 mmoles) in 300 mL 95% ethanol was refluxed for 3 hrs. The solvent was evaporated *in vacuo* and the residue was refluxed with a solution of KOH (14 g ; 250 mmoles) in 300 mL water for 7 hrs. The cooled reaction mixture was acidified with 40% H$_2$SO$_4$ and the separated oil was extracted with benzene. The organic solution was washed with water, dried and evaporated *in vacuo* affording 15 g (90% yield) **8**, yellowish oil, with a penetrating odour.
IR spectrum (CCl$_4$; cm^{-1}) : 1009w, 1036w, 1089w, 1436s, 1476s, 2574w, 2856m, 2936m, 3036m, 3070m, and 3090m.
H-NMR spectrum (see text)

Syntheses of sulphides

10,21-Dithia-9,10,11,20,21,22-hexahydro-dibenzo/a, c/phenanthro/h/cyclododecene (**9a**). Over a stirred boiling solution of potassium hydroxide (4.5 g ; 81 mmoles) in 2.5 L ethanol a solution of **7a** (8 g ; 19.2 mmoles) and **8** (7.15 g ; 29 mmoles) in 300 mL benzene was dropped during 12 hrs. The reaction mixture was refluxed with stirring for other 12 hrs then most of the solvent was evaporated *in vacuo*. The residue was treated with cold water (100 mL), the organic layer was separated and the aqueous one extracted with benzene (3 × 125 mL). The combined organic layers were washed with water until pH 7, dried over anhydrous MgSO$_4$ and evaporated *in vacuo*. The solid residue was recrystallized from chloroform affording **9a** (3.7 g ; 28% yield) as slightly yellow crystals with m.p. 259°—261°.
IR spectrum (KBr ; cm^{-1}) 623w, 728s, 755m, 765s, 1445m, 1460m, 1480m, 1510w, 2935w, 3025w and 3060w.
^{1}*H-NMR spectrum* (*see text*).

Similar results were obtained using dibromoderivative **7b** instead of **7a**.

10,21-Dithia-9,10,11,20,21,22-hexahydro-tetrabenzo/a, c, h, j/-cyclotetradecene (**9b**) was prepared from **7c** and **8** using the procedure and molar ratios presented above for **9a**. The disulphide **9b** resulted as a yellow oily solid in 55% yield and presented ^{1}H-NMR signals in

agreement with the reported ones.[2] No attempt was made to separate the *meso*- and *racemic* isomers.[2] The crude reaction product 9b was used directly in the oxidation step.

5,7-Dihydro-dibenzo/c, e/*thiepine* (**14**)

a) Condensation of **7c** (10 g ; 29.4 mmoles) with **8** (7.3 g ; 29.6 mmoles) using 1100 mL ethanol, 110 mL benzene and 2.8 g (50 mmoles) potassium hydroxide following the procedure described above for **9a** conducted to a crude reaction mixture. This was separated by vacuum filtration in two products : a solid compound **9b** (45 % yield) with m.p. 330 – 350° and an oily yellow compound **14** (50 %) isolated from the filtrate. The last compound, presented an ^{1}H-NMR spectrum identical with an authentic specimen[23,24] (see b.) and was utilized without other purifications in the oxidation step (see below).

b) Heating of **8** (1.2 g ; 4.87 mmoles) with potassium hydroxide (0.3 g ; 5.35 mmoles) in 100 mL ethanol for 12 hrs at reflux followed by the usual work-up (see **9a**) afforded 0.7 g (68 %) of a thick orange-red oil which could be crystallized on grinding with ethanol. The resulted solid, **14**, m.p. 80 – 86°, presented a ^{1}H-NMR spectrum ($\delta = 3.35$; 3.45-two broad peaks for CH$_2$ groups and $\delta = 7.32$ ppm for aromatic H) and afforded a mercuric chloride complex identical with those reported in the literature.[24a,23]

Syntheses of sulphones

10,21-Dithia-9,10,11,20,21,22-hexahydro-dibenzo/a, c/*phenanthro*/h/*cyclododecene-S,S, S′, S′-tetraoxide* (**10a**).

Over a solution of **9a** (1.8 g ; 4 mmoles) in 10 mL anhydrous acetic acid maintained at 100° a solution of 30 % hydrogen peroxide (3.5 mL) was dropped with stirring during 1 hr. The reaction mixture was maintained at 100° for other 6 hrs during which time a solution of hydrogen peroxide (3 mL) in acetic acid (5 mL) was added dropwise with stirring. The cooled reaction mixture was filtered and the obtained solid washed with cold water (10 mL) and methanol (5 mL). The sulphone **10a** resulted (1.5 g ; 73 %) as a white yellowish solid with m.p. 337 – 338°.

IR spectrum (KBr ; cm^{-1}) : 480w, 500m, 538w, 570w, 726m, 766m, 787m, 808w, 880w, 1132s, 1320s, 2930w, 2950w 3020w and 3070w.

^{1}H-NMR spectrum (d_6-DMSO ; δ ppm) : 3.8 – 4.2 (large s ; 8H ; CH$_2$) ; 7.5 – 9.7 (m ; 16Harom).

Similar results (about 80 % yield) were obtained using *m*-chloroperbenzoic acid (in dichloromethane at 30°) instead of hydrogen peroxide.

10,21-Dithia-9,10,11,20,21,22-hexahydro-tetrabenzo/a, c, h, j/*-cyclotetradecene-S, S, S′- S′-tetraoxide* (**10b**) was obtained on 30 % hydrogen peroxide oxidation of **9b**, using the procedure presented above for **10a**. The disulphone **10b**, m.p. 348 – 350° resulted in 80 % yield.

IR spectrum (KBr, cm^{-1}) : 488m, 784m, 1124s, 1164m, 1194m, 1299m, 1321s, 2854m and 2926m.

^{1}H-NMR spectrum was identical with the reported one.[2]

5,7-Dihydro-dibenzo/c, e/*thiepin-S, S-dioxide* (**15**) was obtained on 30 % hydrogen peroxide oxidation of **14** using the procedure described for **10a**. The sulphone **15**, m.p. 208 – 210° (lit.[23] m.p. 209 – 210°) resulted in 75 % yield.

IR spectrum (KBr ; cm^{-1}) : 482m, 520m, 754m, 874m, 1120s, 1159m, 1199m, 1246m, 1260m, 1320s, 1410w, 1445w, 1485w, 2934w, 2976w and 3066m.

^{1}H-NMR spectrum (d_6-DMSO, δ ppm) :3.89 and 4.45 (AB-system ; J = 14 Hz ; CH$_2$) ; 7.3 – 7.7 (m ; Harom).

Pyrolyses of sulphones

Pyrolysis apparatus. The laboratory apparatus used in the pyrolyses of sulphones is presented in fig. 1.

The pyrolysis sample was introduced in a small silica tube having both ends fitted with glass wool. The inert gas flow was regulated by means of stopcocks 2 and 6 in such a way that an excess of inert gas was constantly eliminated through bubbling in the device 5. The working pressure (0.5 – 1 Torr) was regulated with both stopcocks 13 and 6 and measured with the Mc Leod manometer 12. The flow rate of inert gas within the apparatus (15 – 30 mL/min) is measured as volume on the calibrated tube 5 against time when the stopcock 4 was closed (all the inert gas entering from 1 is eliminated through device 3 during such a flow-rate determination). The sample was sublimated on heating the tube 7 with an exterior flame and the resulted vapours mixed with the inert gas pass through the glass wool zone and enter in pyrolysis zone (30 cm length ; 20 mm diameter) heated with the electrical oven. The temperature could be measured with a thermocouple 15. The reaction times at 500°C are about 0.5 s. The reaction product condenses and crystallizes in the vessel 10 cooled with dry-ice

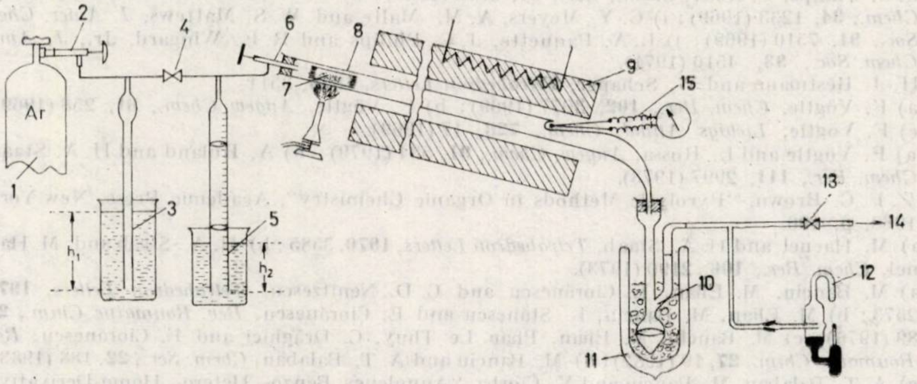

Fig. 1. — Pyrolysis apparatus. 1 — metallic cylinder with inert gas (argon) ; 2 — metallic stopcock ; 3 — bubbler for elimination of excess inert gas ; 4 — glass stopcock ; 5 — device for flow-rate measurements ; 6 — metallic stopcock ; 7 — pyrolysis sample ; 8 — pyrolysis silica tube ; 9 — electrical oven ; 10 — condenser ; 11 — Dewar flask ; 12 — Mc Leod manometer ; 13 — glass stopcock ; 14 — to vacuum pump ; 15 — thermocouple.

*9,10,19,20-Tetrahydro-dibenzo/*a, c*/phenanthro/*g*/cyclodecene* (**5**). Pyrolysis of **10a** (0.5 g ; 0.98 mmoles) at 450°C and 1 Torr total pressure using an argon rate-flow of 15 mL/min afforded **5** (0.29 g ; 77 %), m.p. 82—84°C.

IR spectrum (CS_2 ; CCl_4 ; cm^{-1}) : 725s, 755s, 790s, 1450m, 1480m, 1500m, 2880m, 2920m, 2960m 3025m and 3085m.

UV spectrum (MeOH ; λ_{max}, nm) : 205 ($\varepsilon = 58000$) ; 226 shoulder ($\varepsilon = 31600$) ; 250 shoulder ($\varepsilon = 41600$) ; 256 ($\varepsilon = 49000$) ; 272 ($\varepsilon = 18700$) ; 282 ($\varepsilon = 12500$) ; 293 ($\varepsilon = 10100$) and 305 ($\varepsilon = 10100$).

^{1}H-NMR spectrum (see text).

*9,10,19,20-Tetrahydro-tetrabenzo/*a, c, g, i*/cyclododecene* (**6**) was obtained on pyrolysis of disulphone **10b** at 450—500°C ; 0.5 Torr and argon rate-flow of 20 mL/min. The crude reaction product, obtained in 70—75 % yields has a m.p. 263—268°C. After recrystallization from acetic acid **6** melts at 268°C.

IR spectrum (KBr, cm^{-1}) : 500m, 625m, 726m, 768s, 1015m, 1055m, 1110m, 1180m, 1455s 1500s, 2850w, 2880w, 2950w, 3005w and 3060w.

UV spectrum (MeOH ; λ_{max}, nm) : 211 ($\varepsilon = 37300$) ; 266.5 ($\varepsilon = 1750$) and 273.5 ($\varepsilon = 1450$).
^{1}H-NMR spectrum (d_6-DMSO ; δ ppm) : 2.75s (CH_2) ; 6.75—8 (m ; Harom).

9,10-Dihydrophenanthrene (**16**) resulted on pyrolysis of monosulphone **15** at 600°C, 0.5 Torr and 30 mL/min argon rate-flow. The reaction product obtained in 75 % yield indicated a m.p. of 34.5°C and IR, UV and ^{1}H-NMR spectra identical with those reported in the literature for 9,10-dihydrophenanthrene.[25] Pyrolysis of **15** at 500°C conducted only to unreacted starting material.

AKNOWLEDGEMENTS. The authors address their thanks to Dr. M. Elian for helpful discussions and Dr. C. Drăghici for ^{1}H-NMR spectra.

REFERENCES

[1] a) L. Ramberg and B. Bäcklund, *Arkiv. Kemi Mineral Geol.*, **A13**, No 27, (1940); b) B. Bäcklund, *Thesis*, Uppsala, 1945; c) F. G. Bordwell and G. D. Cooper, *J. Amer. Chem. Soc.*, **73**, 5187 (1951); d) F. G. Bordwell, B. B. Jarvis and P. W. R. Corfield, *J. Amer. Chem. Soc.*, **90**, 5298 (1968); e) N. P. Neureiter, *J. Amer. Chem. Soc.*, **88**, 558 (1966); f) L. A. Paquette and R. W. Houser, *J. Amer. Chem. Soc.*, **91**, 3870 (1969); g) L .A. Paquette and J. C. Philips, *J. Amer. Chem., Soc.*, **91**, 3973 (1969); h) E. J. Corey and E. Block, *J. Org. Chem.*, **34**, 1233 (1969); i) C. Y. Meyers, A. M. Malte and W. S. Mattews, *J. Amer. Chem Soc.*, **91**, 7510 (1969); j) L. A. Paquette, J. C. Philips and R. E. Wingard, Jr., *J. Amer Chem. Soc.*, **93**, 4516 (1971).

[2] H.-J. Bestmann and W. Schaper, *Tetrahedron Letters*, **1975**, 3511.

[3] a) F. Vögtle, *Chem. Ber.*, **102**, 3077 (1969); b) F. Vögtle, *Angew. Chem.*, **81**, 258 (1969); c) F. Vögtle, *Liebigs Annal. Chem.*, **728**, 17 (1969).

[4] a) F. Vögtle and L. Rossa, *Angew. Chem.*, **91**, 534 (1979); b) A. Ruland and H. A. Staab, *Chem. Ber.*, **111**, 2997 (1978).

[5] Y. F. C. Brown, "Pyrolytic Methods in Organic Chemistry", Academic Press, New York, 1980, p. 196.

[6] a) M. Haenel and H. A. Staab, *Tetrahedron Letters*, **1970**, 3585; b) H. A. Staab and M. Haenel, *Chem. Ber.*, **106**, 2190 (1973).

[7] a) M. Banciu, M. Elian, E. Ciorănescu and C. D. Nenitzescu, *Tetrahedron Letters*, **1972**, 2573; b) M. Elian, M. Banciu, L. Stănescu and E. Ciorănescu, *Rev. Roumaine Chim.*, **21**, 89 (1976); c) M. Banciu, M. Elian, Phan Le Thuy, C. Drăghici and E. Ciorănescu, *Rev. Roumaine Chim.*, **27**, 19 (1982); d) M. Banciu and A. T. Balaban, *Chem. Scr.*, **22**, 188 (1983); e) A. T. Balaban, M. Banciu and V. Ciorba, "Annulenes, Benzo-, Hetero-, Homo-Derivatives and Their Valence Isomers", CRC Press, Boca Raton, Florida, 1985.

[8] R. Wendland and J. LaLonde, *Org. Synth.*, col.. voi. 4, Wiley, New York, 1963, p. 757.

[9] T. Zincke and W. Tropp, *Liebigs Annal. Chem.*, **362**, 242 (1908).

[10] S. Hauptmann, *Chem. Ber.*, **93**, 2604 (1960).

[11] H. A. Staab, U. E. Meissner, W. Weinacht and A. Gensler, *Chem. Ber.*, **112**, 3895 (1979).

[12] E. R. Atkinson and H. J. Lawler, *Org. Synth.*, coll. vol. 1, second Ed., Wiley, New York, 1947, p. 222.

[13] H. W. Underwood, Jr., and E. L. Kochmann, *J. Amer. Chem. Soc.*, **46**, 2069 (1924).

[14] a) D. M. Hall and E. E. Turner, *Nature*, **163**, 537 (1949); b) D. M. Hall, M. S. Leslie and E. E. Turner, *J. Chem. Soc.*, **1950**, 711.

[15] C. W. Muth, W.-L. Sung and Z. B. Papanastassiou, *J. Amer. Chem. Soc.*, **77**, 3393 (1955).

[16] a) W. Wenner, *J. Org. Chem.*, **17**, 523 (1952); b) R. Bacon and W. S. Lindsay, *J. Chem. Soc.*, **1958**, 1375; c) T. Sakan and M. Nakazaki, *J. Inst. Polytech. Osaka City Univ.*, **1**, 23(1950), cf. *Chem. Abstr.*, **46**, 5036 (1952); d) B. Eistert and H. Minas, *Chem. Ber.*, **97**, 2479 (1964); e) J. W. Cook, G. T. Dickson and J. D. Loudon, *J. Chem. Soc.*, **1947**, 746.

[17] a) T. Otsubo, M. Kitasawa and S. Misumi, *Bull. Chem. Soc. Japan.*, **52**, 1515 (1979); b) M. Haenel and H. A. Staab, *Chem. Ber.*, **106**. 2203, (1973).

[18] A. Lüttringhaus, U. Hess and H. J. Rosenbaum, *Z. Naturforsch B*, **22**, 1296 (1967).

[19] G. Wittig, G. Hoenig and K. Clauss, *Liebigs Annal. Chem.*, **593**, 127 (1955).

[20] H.-J. Bestmann and D. Ruppert, *Angew. Chem.*, **80**, 668 (1968).

[21] D. Ruppert, Thesis, Erlagen-Nürnberg, 1968.

[22] U. Voll, H. Burzlaff and H.-J. Bestmann, *Chem. Ber.*, **109**, 1324 (1976).

[23] W. E. Truce and D. D. Emrick, *J. Amer. Chem. Soc.*, **78**, 6130 (1956).

[24] a) K. Mislow, M. A. W. Glass, H. B. Hopps, E. Simon and G. H. Wahl, Jr., *J. Amer. Chem. Soc.*, **86**, 1710 (1964); b) R. J. Kurland, M. B. Rubin and W. B. Wise, *J. Chem. Phys.*, **40**, 2426 (1964); c) I. O. Sutherland and M. V. J. Ramsay, *Tetrahedron*, **21**, 3401 (1965).

[25] a) G. Schroeter, H. Müller and J. Y. S. Huang, *Chem. Ber.*, **62**, 645 (1929); b) J. R. Durland and N. Adkins, *J. Amer. Chem. Soc.*, **59**, 135 (1937).

Revue Roumaine de Chimie, **30**, *8*, 713–717 (1985)

LA DESTRUCTION DES HALOMÉTHYLÉTHERS PAR LES AMINES SECONDAIRES

M. IOVU *, VALERIA RĂDULESCU ** et M. IQBAL ***
* Faculté de pharmacie, str. Traian Vuia 6, Bucarest, Roumanie
** Institut de recherches de pédologie et d'agrochimie, str. Mărăşti 61, Bucarest
*** Case Western Reserve University, d. of Chemistry, Ohio, USA

Reçu le 15 octobre 1984

Since chloromethyl methyl ether and bis (chloromethyl)ether used in industry for chloromethylation reactions are cancerigenic, they were tested by destruction methods in the vessels and media where they had been previously employed. The halomethylethers were submitted to the action of secondary amines with which they are very reactive. The best results were obtained by water-miscible solvents, while use for the same amine (dimethylamine, diethylamine, di-*n*-propylamine and piperidine) of solvents which are not water-miscible led to less satisfactory results.

Vu que le chlorométhyl méthyl éther et le bis(chlorométhyl)éther utilisés industriellement dans les réactions de chlorométhylation ont une action cancérigène, ils ont été testés par des méthodes de destruction dans les vases et les milieux où ils avaient été utilisés antérieurement. Les halométhyléthers ont été soumis a l'action des amines secondaires avec lesquelles la réactivité est grande. Les meilleurs résultats ont été obtenus dans des solvants miscibles avec l'eau tandis que les résultats ont été plus faibles lorsqu'on a utilisé pour une même amine (diméthylamine, diéthylamine, di-*n*-propylamine et pipéridine) des solvants non-miscibles avec l'eau.

INTRODUCTION

Le chlorométhyl méthyl éther qui contient aussi une petite quantité de bis(chlorométhyl)éther est utilisé pour la chlorométhylation des composés aromatiques, par exemple le polystyrène réticulé utilisé dans l'industrie d'échangeurs d'anions. Le bis (chlorométhyl)éther peut se former dans une atmosphère contenant de l'acide chlorhydrique et de l'aldéhyde formique [1,2] ou dans l'eau, condition dans laquelle il s'hydrolyse [3].

Le chlorométhyl méthyl éther tout comme le bis (chlorométhyl) éther ont une action cancérigène sur la peau et le tissu sous-cutané des souris.[4]

Le chlorométhyl méthyl éther (2 ppm) et le bis(chlorométhyl)éther (1 ppm) inspirés par les souris accroissent l'incidence des adénomes pulmonaires.[5]

Plus récemment il a été prouvé que ces composés représentent aussi pour l'homme un facteur de risque en fonction de l'intensité de l'exposition et de la durée de l'expérience.[6–8]

Connaissant ce risque on a recherché des méthodes pour la mise en évidence des halométhyléthers dans l'air, dans l'eau et surtout dans les milieux de réaction qui les contiennent.

La détermination quantitative du bis(chlorométhyl)-éther à une concentration de 0,1 ppb a été réalisée par l'absorption sur le Parapak suivie d'une élution thermique à l'aide du spectromètre de masse, mesurant l'intensité des ions à m/e égale à 79,995, $ClCH_2-O-CH_2^+$ avec une résolution de 1/3500.[9−10] La spectrométrie de masse couplée au chromatographe de gaz détectant les ions 79^+ et 81^+ grâce aux isotopes du chlore a été aussi utilisée.[11−14]

LES PROCÉDÉS DE DESTRUCTION DES HALOMÉTHYLÉTHERS

Etant donné l'action cancérigène des halométhyléthers l'Agence Internationale pour la Recherche sur le Cancer, se trouvant à Lyon, a étudié trois méthodes de destruction des halométhyléthers basées sur leurs propriétés chimiques.

Le bis(chlorométhyl)éther subit le phénomène d'hydrolyse dans l'eau à la température d'ébullition,[16] formant un triéther avec les phénoxydes de sodium,[17,18] un polyester avec le sel de sodium du 4,4'-dihydroxydiphényl,[19] des thioéthers avec le thiophénolate de sodium,[20] des bis(N-imidométhyl)éthers avec les sels alcalins des imides [21] et des sels quaternaires d'ammonium avec les trialkylamines.[22] La réaction avec le 2,4,6-trichlorophénoxyde de potassium a été utilisée comme méthode analytique de dosage du bis(chlorométhyl)éther.[23]

Le chlorométhyl méthyl éther réagit à l'aide de l'éthanol et des ions éthoxydes [24] avec les composés contenant un hydrogène actif, comme le diéthylmalonate [25] et le 2,4,6-trichlorophénoxyde de potassium.[26] La réaction du chlorométhyl méthyl éther et du bis (chlorométhyl)éther avec les alkoxydes, les phénoxydes et les thiophénolates des métaux alcalins a été utilisée en chromatographie de gaz analytique. [27]

Pour la destruction des halométhyléthers, l'Agence Internationale de la Recherche sur le Cancer a décis de les traiter avec les composés basiques suivants : l'ammoniaque,[12,28] le phénoxyde de sodium [17−19] et le méthoxyde de sodium [29,30] qui produisent respectivement le hexaméthylène-tétramine, le chlorure d'ammonium et les éthers.

Partant de ces indications, nous avons considéré que la destruction des halométhyléthers peut être favorisée par les amines secondaires, lesquelles sont plus basiques que l'ammoniaque et peuvent être utilisées non seulement en solution aqueuse mais aussi dans les solvants non polaires.

Récemment [31] nous avons démontré que le bis(chlorométhyl)-éther réagit avec les amines secondaires en formant le diaminométhane au lieu du bis(aminométhyl)éther, par exemple :

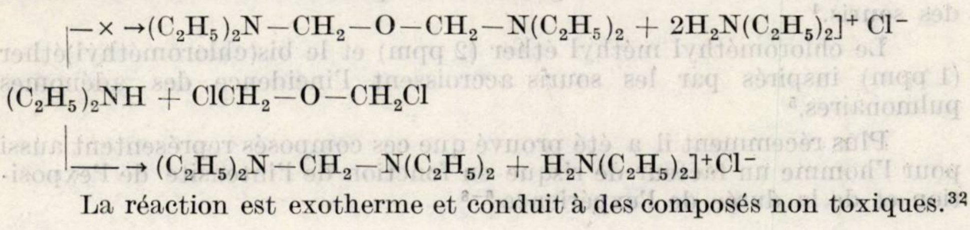

$$\begin{array}{l} \xrightarrow{\times} (C_2H_5)_2N-CH_2-O-CH_2-N(C_2H_5)_2 + 2H_2N(C_2H_5)_2]^+ Cl^- \\ (C_2H_5)_2NH + ClCH_2-O-CH_2Cl \\ \longrightarrow (C_2H_5)_2N-CH_2-N(C_2H_5)_2 + H_2N(C_2H_5)_2]^+Cl^- \end{array}$$

La réaction est exotherme et conduit à des composés non toxiques.[32]

PARTIE EXPÉRIMENTALE

Parmi les amines secondaires on a utilisé celles qui sont plus basiques, comme la diméthylamine, la diéthylamine, la di-*n*-propylamine et la pipéridine.

Les conditions de travail choisies peuvent être rencontrées dans la pratique de destruction des halométhyléthers sans solvant (A), ou avec des solvants miscibles (B et C) ou non-miscibles (D) avec l'eau (tableau 1).

Tableau 1

Méthodes de destruction des halométhyléthers par les amines secondaires

Méthode	Mode de travail
A	A 50 µl d'halométhyléther on ajoute 1 ml d'amine secondaire 20%. Après 15′ on traite avec 1 ml de H_2SO_4 11% et on extrait dans 1 ml de *n*-hexane. On dilue avec 10 ml d'eau et on passe à l'analyse chromatographique.
B	A 50 µl d'halométhyléther on ajoute 1 ml d'amine secondaire 20% et 1 ml d'acétone. Après 15′ on ajoute 1 ml de H_2SO_4 11% et on extrait avec 1 ml de *n*-hexane. Enfin on y ajoute 10 ml d'eau et on effectue l'analyse chromatographique de la solution dans le *n*-hexane.
C	Identique à B, mais au lieu de 1 ml d'acétone on ajoute 1 ml d'éthanol.
D	Identique à B, mais sans acétone, et le *n*-hexane est ajouté dès le début de la réaction.

La détermination quantitative des halométhyléthers a été réalisée grâce au chromatographe de gaz avec capture d'électrons Carlo Erba dans les conditions suivantes :

Colonne en verre de 3,8 m de long et 5,5 mm de diamètre remplie avec du diéthylèneglycole a 10% et du succinate sur le chromosorb W, ,,HP'', de 80—100 mes.

Température dans la colonne : 130°C
Température de l'injecteur : 200°C
Température du détecteur : 275°C
Détecteur : DCE^{63}Ni, type HT-20
Gaz porteur : Azote (30 ml/min)
Temps de rétention pour CMME : 224 sec.
Temps de rétention pour BCME : 250 sec.

RÉSULTATS ET DISCUSSIONS

Le tableau 2 présente les quantités en pourcentage du chlorométhyl méthyl éther et du bis(chlorométhyl)éther non détruites après 15′ de traitement avec les amines secondaires selon les quatre méthodes (A — D).

Avec la même méthode et la même amine secondaire le bis(chlorométhyl)éther a été détruit en plus grande partie que le chlorométhyl méthyl éther.

Quand on a utilisé la di-*n*-propylamine, la méthode A n'a pas été appliquée pour former des solutions à 20%, à cause de la miscibilité nulle de celle-ci avec l'eau. Les autres méthodes ont été applicables grâce à la solubilité de l'amine dans l'acétone, le méthanol ou le *n*-hexane.

Le bis(chlorométhyl)éther utilisé a été pur ; par contre, le chloromèthyl méthyl éther contenait aussi de petites quantités de bis(chlorométhyl)éther, d'ou la présence du bis(chlorométhyl)éther (entre parenthèses dans le tableau 2) après la destruction du chlorométhyl méthyl éther selon les méthodes B, C et D.

Tableau 2

La destruction des CMME * et BCME ** par les amines secondaires

Amine	$(CH_3)_2NH$		$(C_2H_5)_2NH$		$(C_3H_7)_2NH$		$C_5H_{10}NH$	
Méthode	CMME (BCME) %	B BCME %	CMME (BCME) %	BCME %	CMME (BCME) %	BCME %	CMME (BCME) %	BCME %
A	2,91 (–)	1,16	4,24 (–)	2,36	–	–	2,71 (–)	0,55
B	3,08 (–)	0,027	4,24 (2,33)	0,66	2,10 (5,69)	0,13	2,08 (–)	0,04
C	2,63 (–)	0,61	4,22 (–)	0,13	1,66 (1,69)	0,06	2,29 (1,57)	0,035
D	2,05 (–)	0,29	2,08 (15,65)	9,08	1,36 (17,19)	12,74	3,12 (17,93)	14,84

* Chlorométhyl méthyl éther

** Bis(chlorométhyl) éther

Lorsqu'on a employé la diméthylamine, le bis(chlorométhyl)éther (mélangé au chlorométhyl méthyl éther) n'a plus été présent dans les produits de réaction.

La quantité de halométhyléther qui n'a pas réagi avec l'amine a été généralement plus grande lorsqu'on a utilisé un solvant non miscible, comme l'eau et l'hexane.

En étudiant la variation en fonction du temps de la quantité de halométhyléthers non-détruits on a constaté que : après 1 heure la quantité totale de bis(chlorométhyl)éther a été détruite en utilisant par exemple la méthode A, mais en utilisant la diéthylamine il est resté encore 0,38% de la quantité de chlorométhyl méthyl éther. Après deux heures aucun halométhyléther n'a plus été identifié.

CONCLUSIONS

En étudiant la destruction des halométhyléthers par les amines secondaires très basiques, comme la diméthylamine, la diéthylamine, la di-*n*-propylamine et la pipéridine, dans des conditions qui peuvent être rencontrées dans la pratique de destruction des halométhyléthers sans solvant ou avec des solvants miscibles ou non miscibles avec l'eau, on a constaté que les meilleurs résultats s'obtiennent dans des solvents miscibles avec l'eau pour une même amine.

Les meilleurs résultats, après 15′, s'obtiennent en utilisant la diméthylamine.

BIBLIOGRAPHIE

[1] G. J. Kallos et R. A. Solomon, *Amer. Ind. Hyg. Assoc. J.*, **34**, 469 (1973).
[2] L. S. Frankel, K. S. McCallum et L. Collier, *Environ. Sci. Technol.*, **8**, 356 (1974).
[3] J. C. Tou et J. G. Kallos, *Analyt. Chem.*, **48**, 958 (1976).
[4] B. L. Van Duuren, A. Sivak, B. M. Goldschmidt, C. Katz et S. Melchione, *J. Nat. Cancer Inst.*, **43**, 481 (1969).
[5] B. K. J. Leong, H. N. Macfarland et W. H. Reese, *Arch. Environ. Health.*, **22**, 663 (1971).
[6] A. M. Thiess et H. Zeller, *Zentbl. Arbeitsmed.*, **23**, 97 (1973).
[7] N. Nelson, *Ann. N. Y. Acad. Sci.*, **271**, 81 (1976).
[8] W. Weiss et R. L. Moser, *Amer. Rev. Respir. Dis.*, **120**, 1031 (1979).
[9] L. Collier, *Environ. Sci. Technol.*, **6**, 930 (1972).
[10] K. P. Evans, A. Matias, N. Mellor, R. Silvester et A. E. Williams, *Anal. Chem.*, **47**, 21 (1975).
[11] L. A. Shadoff, G. J. Kallos et J. S. Woods, *Analyt. Chem.*, **45**, 2341 (1973).
[12] E. Sawicki, T. Belsky, R. A. Friedel, D. L. Hyde, J. L. Monkman, R. A. Rasmersen, L. A. Riperton et L. D. White, *Health Lab. Sci.*, **13**, 78 (1976).
[13] D. Ellgengausen, *Anal. Lets.*, **8**, 11 (1975).
[14] F. Bruner, G. Bertoni et C. Severini, *Analyt. Chem.*, **50**, 53 (1978).
[15] N. Baggett, Reactions of α-haloethers, dans : J. F. Stoddart, "Comprehensive Organic Chemistry", Pergamon Press, Oxford, 1979, p. 841.
[16] H. Böhme, *Chem. Ber.*, **74B**, 248 (1941).
[17] M. Iovu et G. Cîmpeanu, *Rev. Roumaine Chim.*, **18**, 883 (1973).
[18] M. Iovu et G. Cîmpeanu, *Rev. Chim. (București)*, **27**, 195 (1976); **27**, 373 (1976).
[19] M. Iovu, G. Cîmpeanu et F. Avramescu, *Rev. Chim. (București)*, **28**, 723 (1977); **28**, 925 (1977).
[20] M. Iovu et E. Bădău, *Rev. Chim. (București)*, **34**, 795 (1983).
[21] M. Iovu et M. Iqbal, *Rev. Chim. (București)*, **34**, 591 (1983) .
[22] L. D. Taylor et P. McLanghlin, *J. Appl. Polym. Sci.*, **20**, 225 (1976).
[23] C. C. Yao, H. Zollinger, G. J. Kallos, R. A. Solomon et J. C. Tou, *Analyt. Chem.*, **51**, 299 (1979).
[24] P. Ballinger, P. B. D. de la More, G. Cohnstam et B. M. Prestt, *J. Chem. Soc.*, **1955**, 3641
[25] L. Summers, *Chem. Rev.*, **55**, 301 (1955).
[26] M. L. Lamghorst, R. G. Melcher et G. L. Kallos, *Amer. Ind. Hyg. Assoc. J.*, **42**, 47 (1981).
[27] E. F. Ault et R. A. Solomon, U.S. Patent 3,934,981 (1973), *Of Gazette*, **942**, *4*, 1839 (1976); Brit. Patent 1.479.015 (1977); *Chem. Abstr.*, **87**, 205902p(1977); R. A. Solomon et G. J. Kallos, *Analyt. Chem.*, **47**, 955 (1975).
[28] M. Alvarez et R. T. Rosen, *Int. J. Environ. Analyt. Chem.*, **4**, 241 (1976).
[29] R. A. Solomon, U.S. Patent 3.944.389 (1976), *Of Gazette*, **944**, *3*, 1333 (1976).
[30] E. F. Ault et R. A. Solomon, Brit. Patent 1,478,999 (1977); *Chem. Abstr.*, **87**, 183990m(1977).
[31] M. Iovu et M. Iqbal, *Rev. Roumaine Chim.*, **29**, 333 (1984).
[32] D. Dobrescu, M. Iovu, A. Cristea et M. Iqbal, Brevet RSR 82568 (1981).

Revue Roumaine de Chimie, **30**, *8*, 719–724 (1985)

THE REACTION OF CHLORINE DIOXIDE WITH dl-ALANINE IN AQUEOUS SOLUTION

C. B. SHARMA and P. C. PACHAURI
Chemistry Department, Meerut College, Meerut-25001, U.P.

Received October 18, 1983

Chlorine dioxide oxidises alanine in aqueous solution with the production of acetaldehyde, ammonia, carbon dioxide, hydrogen ion, and chlorite ion. The reaction is first order each with respect to chlorine dioxide and alanine. The second order rate constant, calculated with respect to concentrations of alanine and chlorine dioxide, is approximately $3.1 \times 10^{-2} M^{-1} sec^{-1}$ at $25 \pm 0.1°C$. The order of reaction with respect to hydrogen ion is an inverse one. The influence of chlorides, chlorites, D_2O, and temperature on the reaction rate has been investigated. Various activation parameters have been evaluated. A proton abstraction mechanism is found suitable for the reaction.

INTRODUCTION

In previous papers we have reported oxidation studies of alcohols [1,2] and aldehydes [3] with chlorine dioxide and found different pathways for the reactions. In this paper we report the reaction of dl-alanine with chlorine dioxide in aqueous solution. The desire to understand more fully the reactions of chlorine dioxide with other classes of organic compounds, especially amino acids, prompted the present investigation.

EXPERIMENTAL

Alanine, perchloric acid (about 70%) potassium peroxydilsulphate, and potassium iodide were obtained from Sarabhai M Chemicals. Sodium perchlorate and sodium chlorite were from Thomas and Baker. Deuterium oxide was obtained from BARC, Trombay. Other chemicals used were either of B.D.H. (AnalaR) or Merck (C.P.) grade or of comparable purity. Triple distilled water was used throughout.

The method of Granstrom and Lee [4] modified by Rosenblatt and co-workers [6] was used for the preparation of chlorine dioxide solution.

The reaction was studied at 25°C by adding aqueous chlorine dioxide to alanine solution at constant ionic strength ($\mu = 0.2$). The ionic strength of the solutions was adjusted by adding sodium perchlorate. The reaction was controlled within $\pm$ 0.1°C. The pH of the solutions, where neither hydrogen ions nor other salts were added, was maintained with buffer at 7.5. The concentration of chlorine dioxide was determined iodometrically as described by Ingols and Ridenour[6]. In order to avoid photochemical complications, black bottles were used during the experiments. Due to complex nature of the reaction, the initial rates (k_0) were calculated. All the kinetic runs were carried out in duplicate with the reproducibility of $\pm$ 3%.

Product analysis

Acetaldehyde was isolated as their 2,4-dinitrophenylhydrazone (DNPH) derivative (m.p. 167–168°C, literature,[7] 168°C) and identified by N.M.R. and I.R. spectra. The ammonia was identified by Nesseler's reagent.[8] Carbon dioxide and chlorite ions were identified by their characteristic tests.[9,5]

RESULTS AND DISCUSSION

The order of reaction has been found to be first and first each with respect to alanine (Table 1) and chlorine dioxide (Table 2) concentrations. The rate law (1) is valid for the reaction

$$\frac{-\mathrm{d}[\mathrm{ClO_2}]}{\mathrm{d}t} = k_1[\mathrm{ClO_2}][\mathrm{Alanine}] \qquad \text{(I)}$$

Table 1

Rate constant as a function of alanine concentration at 25°C.
$[\mathrm{ClO_2}] = 0.0050\mathrm{M}$; pH = 7.5 ; $\mu = 0.2$

[Alanine]	(M)	0.010	0.013	0.015	0.022	0.025	0.030
$k_0 \times 10^6$	($\mathrm{Msec^{-1}}$)	1.55	2.10	2.30	3.45	3.70	4.60
$\frac{k_0 \times 10^5}{[\mathrm{Alanine}]}$	($\mathrm{sec^{-1}}$)	15.50	16.1	15.3	15.7	14.8	15.3

Table 2

Rate constant as a function of chlorine dioxide concentration at 25°C.
[Alanine] = 0.020M ; pH = 7.5 ; $\mu = 0.2$

$[\mathrm{ClO_2}]$	(M)	0.0020	0.0030	0.0045	0.0060	0.0075	0.010
$k_0 \times 10^6$	($\mathrm{Msec^{-1}}$)	1.25	1.90	2.80	3.70	4.55	6.10
$\frac{k_0 \times 10^4}{[\mathrm{ClO_2}]}$	($\mathrm{sec^{-1}}$)	6.25	6.33	6.22	6.17	6.07	6.10

EFFECT OF HYDROGEN IONS

The reaction rate decreased linearly with increasing hydrogen ions by increasing perchloric acid concentration (Table 3). A plot of log k_0 versus log $[\mathrm{H^+}]$ gave a straight line with a slope of -1. The inverse one order with respect to $[\mathrm{H^+}]$ gave the rate law (II) for the reaction.

$$\frac{-\mathrm{d}[\mathrm{ClO_2}]}{\mathrm{d}t} = k_2\,\frac{[\mathrm{Alanine}][\mathrm{ClO_2}]}{[\mathrm{H^+}]} \qquad \text{(II)}$$

Table 3

Rate constant as a function of perchloric acid concentration at 25°C.
[Alanine] = 0.020M ; $[ClO_2] = 0.0050M$; $\mu = 0.2$

$[HClO_4]$ (M)	0.015	0.020	0.030	0.035	0.050
$k_0 \times 10^6$ ($Msec^{-1}$)	2.90	2.15	1.40	1.25	0.90

Effect of inorganic salts

The reaction rate of alanine oxidation with chlorine dioxide increased by increasing the concentration of chlorides while decreased by increasing the concentration of chlorites (Table 4).

Table 4

Rate constant as a function of inorganic salts concentration (0.050M) at 25°C.
[Alanine] = 0.020M ; $[ClO_2] = 0.0050M$; $\mu = 0.2$

[Salt]	NaCl	KCl	$BaCl_2$	$NiCl_2$	$NaClO_2$	$KClO_2$
$k_0 \times 10^6$ ($M\ sec^{-1}$)	3.30	3.45	4.40	4.85	1.60	1.75

Solvent isotope effect

The experiments in D_2O medium have shown that the rate decreases in this medium rather than in H_2O medium, giving an inverse isotope effect, $k_{D_2O}/k_{H_2O} = 0.66$. Since D_3O^+ is about three times stronger acid [10,11] than H_3O^+ hence for acid catalysed reactions the inverse isotope effect should be greater than unity but the ratio is less than unity when $[H^+]$ retards the reaction rate as has been observed in the present investigation.

ACTIVATION PARAMETERS

The reaction was carried out at four different temperatures (25–45°C). The kinetic parameters (Table 5) have been calculated. The negative $\Delta S^{\neq}$ value suggested that the water molecule was taking part in the reaction.[12]

Table 5

The kinetic activation parameters for the reaction of alanine with chlorine dioxide.
[Alanine] = 0.020M ; $[ClO_2] = 0.000M$; pH = 7.5 ; $\mu = 0.2$

$\Delta E_a^{\neq}$ (k J $mole^{-1}$)	$\Delta H^{\neq}$ (k J $mole^{-1}$)	$\Delta S^{\neq}$ ($JK^{-1}\ mole^{-1}$)	$\Delta G^{\neq}$ (at 25°C) (k J $mole^{-1}$)
56.6	54.1±1.8	−122.2	90.5

STOICHIOMETRIC FORMULATION

All evidences obtained pointed to the overall reaction (1).

$$\begin{aligned} &CH_3CH(NH_2)COOH + 2ClO_2 + H_2O \rightarrow CH_3CHO + \\ &\quad + CO_2 + NH_3 + 2H^+ + 2ClO_2^- \end{aligned} \tag{1}$$

SIDE REACTIONS

The acetaldehyde and chlorite ions produced in the initial reaction were capable of interacting with each other[5] at low pH according to equation (2).

$$3H^+ + CH_3CHO + 3ClO_2^- \rightarrow CH_3COOH + HCl + 2ClO_2 + H_2O \tag{2}$$

Chlorine dioxide is produced[13] by this side reaction (2), as well as by the decomposition of chlorous acid,[14] and accumulated under appropriate conditions, since it is evolved more rapidly than it can be used up. This is the reason why reaction rate decreased by adding either chlorite ions (Table 4) or hydrogen ions during the oxidation of alanine with chlorine dioxide. When chlorine dioxide is formed in this manner and then consumed by more alanine, the net effect is the following.

$$\begin{aligned} &3CH_3CH(NH_2)COOH + ClO_2 + H_2O \rightarrow CH_3CHO + 2CH_3COOH + \\ &\quad + 3CO_2 + 3NH_3 + HCl \end{aligned} \tag{3}$$

REACTION ORDER

The stoichiometric reaction (1) as shown should require that the kinetics be first order with the alanine and second order with chlorine dioxide. Yet there is no doubt that the reaction is first order in chlorine dioxide concentration. A reasonable way in which this could arise is represented as follows

$$CH_3CH(NH_2)COOH + ClO_2 \rightarrow \text{Intermediate} \tag{4}$$

$$\text{Intermediate} + ClO_2 \rightarrow \text{Products} \tag{5}$$

Since chlorine dioxide does not appear to dimerise[15-18] even at low temperatures,[17] it seems unlikely that the dimer be involved, despite the postulated existence of some type of transition-state chlorine dioxide dimer,[19] it is suggested on the basis of this formulation, that the intermediate in question is a free radical, even though the reaction failed to initiate polymerisation of acrylonitrile.

MECHANISM

On the basis of the evidences obtained, we suggested the following mechanism for the reaction of alanine with chlorine dioxide in aqueous solution.

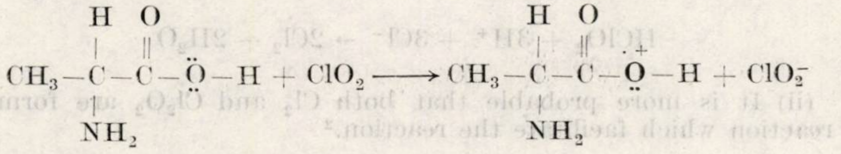

$$CH_3-\underset{NH_2}{\overset{H}{C}}-\overset{O}{\overset{\|}{C}}-\ddot{O}-H+ClO_2\longrightarrow CH_3-\underset{NH_2}{\overset{H}{C}}-\overset{O}{\overset{\|}{C}}-\underset{..}{\overset{\cdot +}{O}}-H+ClO_2^- \tag{6}$$

Alanine

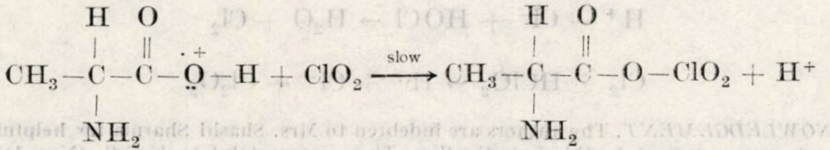

$$CH_3-\underset{NH_2}{\overset{H}{C}}-\overset{O}{\overset{\|}{C}}-\underset{..}{\overset{\cdot +}{O}}-H+ClO_2\xrightarrow{\text{slow}}CH_3-\underset{NH_2}{\overset{H}{C}}-\overset{O}{\overset{\|}{C}}-O-ClO_2+H^+ \tag{7}$$

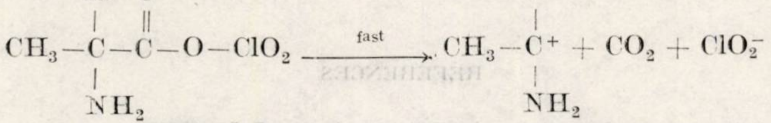

$$CH_3-\underset{NH_2}{\overset{H}{C}}-\overset{O}{\overset{\|}{C}}-O-ClO_2\xrightarrow{\text{fast}}CH_3-\underset{NH_2}{\overset{H}{C^+}}+CO_2+ClO_2^- \tag{8}$$

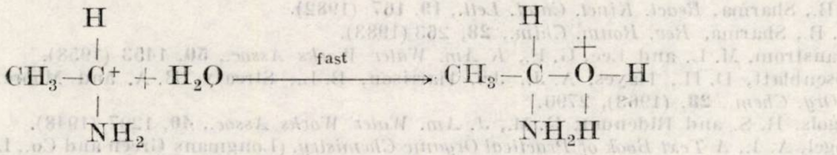

$$CH_3-\underset{NH_2}{\overset{H}{C^+}}+H_2O\xrightarrow{\text{fast}}CH_3-\underset{NH_2H}{\overset{H}{C}}-\overset{+}{O}-H \tag{9}$$

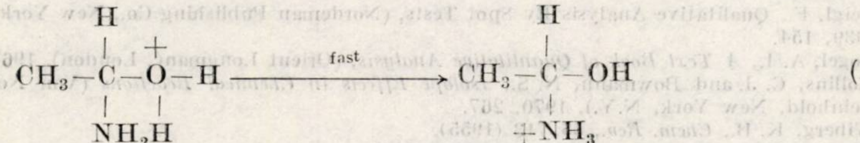

$$CH_3-\underset{NH_2H}{\overset{H}{C}}-\overset{+}{O}\;H\xrightarrow{\text{fast}}CH_3-\underset{+NH_3}{\overset{H}{C}}-OH \tag{10}$$

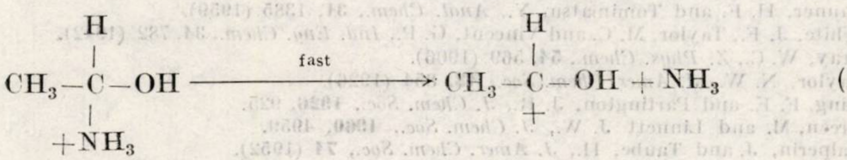

$$CH_3-\underset{+NH_3}{\overset{H}{C}}-OH\xrightarrow{\text{fast}}CH_3-\underset{+}{\overset{H}{C}}-OH+NH_3 \tag{11}$$

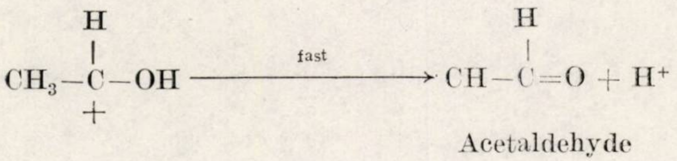

$$CH_3-\underset{+}{\overset{H}{C}}-OH\xrightarrow{\text{fast}}CH-\overset{H}{C}=O+H^+ \tag{12}$$

Acetaldehyde

IN PRESENCE OF CHLORIDE IONS

(i) In presence of chloride ions, the rate enhances due to formation molecular chlorine[1]

$$ClO_2^- + H^+ \rightarrow HClO_2 \qquad (13)$$

$$HClO_2 + 3H^+ + 3Cl^- \rightarrow 2Cl_2 + 2H_2O \qquad (14)$$

(ii) It is more probable that both Cl_2 and Cl_2O_2 are formed in the reaction which facilitate the reaction.[2]

$$H^+ + Cl^- + HClO_2 \rightarrow 2HOCl \qquad (15)$$

$$H^+ + Cl^- + HOCl \rightarrow H_2O + Cl_2 \qquad (16)$$

$$Cl_2 + HClO_2 \rightarrow H^+ + Cl^- + Cl_2O_2 \qquad (17)$$

ACKNOWLEDGEMENT. **The authors are indebted to Mrs. Shashi Sharma for helpful discussion and encouragement to this investigation. They are grateful to U.G.C. (New Delhi) for providing a post-doctoral fellowship (C.B.S.).**

REFERENCES

[1] V. P. Kudesia, and Sharma, C. B., *Acta Ciencia Indica*, **7**, 51 (1981).
[2] C. B., Sharma, *React. Kinet. Catal. Lett.*, **19**, 167 (1982).
[3] C. B., Sharma, *Rev. Roum. Chim.*, **28**, 263 (1983).
[4] Granstrom, M. L. and Lee, G. F., *K Am. Water Works Assoc.*, **50**, 1453 (1958).
[5] Rosenblatt, D. H., Hayes, A. J., Jr., Harrison, B. L., Streaty, R. A. and Moore, K. A., *J. Org. Chem.*, **28**, (1963), 2790.
[6] Ingols, R. S. and Ridenour, G. M., *J. Am. Water Works Assoc.*, **40**, 1207 (1948).
[7] Vogel, A. I., *A Text Book of Practical Organic Chemistry*, (Longmans Green and Co., London), 1956, 334.
[8] Feigl, F., Qualitative Analysis By Spot Tests, (Nordeman Publishing Co., New York, Inc.) 1939, 154.
[9] Vogel, A. I., *A Text Book of Quantitative Analysis*, (Orient Longmané, London), 1967, 326.
[10] Collins, C. J. and Bowmann, N. S., *Isotope Effects in Chemical Reactions* (Von Nostrand Reinhold, New York, N.Y.), 1970, 267.
[11] Wiberg, K. B., *Chem. Rev.*, **55**, 713 (1955).
[12] Sharma, C. B., Rev. Roum. Chim., **28**, 967 (1983).
[11] Launer, H. F. and Tomimatsu, Y., *Anal. Chem.*, **31**, 1385 (1959).
[14] White, J. F., Taylor, M. C. and Vincent, G. P., *Ind. Eng. Chem.*, **34**, 782 (1942).
[15] Bray, W. C., *Z. Phys. Chem.*, **54**, 569 (1906).
[16] Taylor, N. W., *J. Amer. Chem. Soc.*, **48**, 854 (1926).
[17] King, F. E. and Partington, J. R., *J. Chem. Soc.*, **1926**, 925.
[18] Green, M. and Linnett J. W., *J. Chem. Soc.*, **1960**, 4959.
[19] Halperin, J. and Taube, H., *J. Amer. Chem. Soc.*, **74** (1952).

Revue Roumaine de Chimie, **30**, *8*, 725–734 (1985)

KINETICS OF Os(VIII) CATALYSED CHLORAMINE-T OXIDATION OF GLYCOLLIC ACID AND LACTIC ACID IN ALKALINE MEDIA

H. HINGORANI *, H. C. GOYAL **, G. CHANDRA ***, S. N. SRIVASTAVA ****
* Institute of Home Science Khandari, Agra
** Department of Chemistry, Hindu College, Moradabad, India
*** Department of Chemistry, Agra College, Agra
**** Vice-Chancellor, Qumaun University, Nainital

Received October 18, 1983

Os(VIII) catalysed glycollic and lactic acid oxidation by chloramine-T in alkaline medium follow a first order dependence on Chloramine-T and zero order w.r.t. glycollic acid at its all concentration whereas in case of lactic acid the reaction rate is dependent on the reducing substrate concentration. The reaction rate follows a first order kinetics in $[OH^-]$ at lower sodium hydroxide concentrations but at higher concentration of NaOH a zero order dependence on $[OH^-]$ is observed. A direct dependence of reaction rate on Os(VIII) concentration is found and the possibility of uncatalysed reaction is ruled out.

INTRODUCTION

Chloramine-T a two electron accepting oxidant, though a less familiar, is a very potent oxidising agent both in alkaline and acidic medium. Organic compounds like ascorbic acid, glycerol, glycol, manitol, oxalic acid, lactic acid have been appropriately estimated by the help of chloramine-T.[1–6] But very few attempts have been made to investigate the metal ion catalysed oxidation of α-hydroxy acid by chloramine-T. Present investigation deals with Os(VIII) catalysed oxidation of lactic acid and glycollic acid by chloramine-T in alkaline media.

EXPERIMENTAL

B.D.H. AnalaR or E. Merck G.R. grade chemicals were used. Osmium tetraoxide of Johnson & Mathey Company was used. Stock solutions were prepared in double distilled water and stored in pyrex vessel. The reaction was followed by estimating residual chloramine-iodometrically at different intervals. Solymosi and Csik [7] described osmium tetraoxide as general catalyst for chloramine-T oxidation of α-hydroxy acids. The experiments were carried at three different temperatures viz., 45°, 50° and 55°C.

STOICHIOMETRY

The stoichiometry of the solution was studied by taking chloramine-T in excess in the reaction mixture containing (Glycollic acid)/(Lactic acid) = = 0.02 M, (NaOH) = 0.05 M and (Os(VIII)) = 0.00003 M (in case of glycollic acid) and 0.00001 M in case of lactic acid. The mixture was allowed to equilibrate for 12 hours and the remaining chloramine-T was titrated. The results followed the following reactions for glycollic and lactic acid respectively.

$$CH_3C_6H_4.SO_2N.NaCl + CH_2OHCOO^- \xrightarrow[NaOH]{OsO_4} HCO.COO^- + NaCl +$$

$$+ CH_3C_6H_4-SO_2-NH_2$$

$$CH_3C_6H_4-SO_2N-NaCl + CH_3CHOHCOO^- \rightarrow CH_3COCOO^- + NaCl +$$

$$+ CH_3C_6H_4SO_2-NH_2$$

CHLORAMINE-T DEPENDENCE

To find out the effect of change of chloramine-T concentration the reaction was carried at seven concentrations of chloramine-T (0.015 M to 0.0325 M) keeping the concentration of other reactants constant at 50°C. The reaction is first order w.r.t chloramine-T concentration. However the decrease in rate constant by increasing chloramine-T concentration is due to the formation of an intermediate oxidising species whose concentration decreases due to the deactivation with the increase in chloramine-T concentration. The rate of the reaction could be expressed as :

$$R = k\ [\text{chloramine-T}]$$

where R is the reaction rate and k is the observed rate constant (Table 1 A, 2 A).

Table 1 A

Effect of chloramine-T concentration at 50°C
[Glycollic acid] = 0.02M,
[NaOH] = 0.05 M,
[Os(VIII)] = 0.00003 M

Chloramine-T M	$k \times 10^3$ min^{-1}
0.015	6.63
0.020	5.31
0.0223	3.99
0.0250	3.01
0.0275	2.69
0.030	2.39
0.0325	1.866

Table 2A

Effect of Chloramine-T concentration
[Lactic acid]=0.02 M, [NaOH]=
0.05 M, [Os(VIII)] = 0.00001 M,
Temp. = 50°C

[Chloramine-T] M	$k \times 10^3$min^{-1}
0.0175	7.31
0.020	6.51
0.0225	5.56
0.0250	4.07
0.0275	3.56
0.030	2.95

REDUCING SUBSTRATE DEPENDENCE

To ascertain the reducing substrate dependence a set of experiments were carried out in which the concentrations of other reactants were kept constant and the concentrations of glycollic acid (from 0.02 M to 0.03 M) and that of lactic acid from (0.01 – 0.02 M) were varried.

Table 1B

Effect of glycollic acid concentration at 50°C
[Chloramine-T] = 0.02M,
[NaOH] = 0.05 M,
[Os(VIII)] = 0.00003 M

Glycollic acid M	$k \times 10^3$ min^{-1}
0.02	5.22
0.0225	5.45
0.025	5.24
0.0275	5.34
0.03	5.52

Table 2B

Effect of lactic acid concentration
[Chloramine-T] = 0.02 M,
[NaOH] = 0.05 M,
[Os(VIII)] = 0.00001 M, Temp. 50°C

Lactic acid $\times 10^2$ M	$k \times 10^3$ min^{-1}	$10k\left(1 - \dfrac{1}{1 + [\mathrm{Lact}]}\right)$
1.00	3.65	3.65
1.25	4.39	3.51
1.50	4.66	3.11
1.75	5.58	3.18
2.00	6.59	3.29

Table 1 B expresses that the rate constant is independent of glycollic acid concentration and follows the reaction.

$$-\frac{d}{dt}[\text{chloramine-T}] = k\,[\text{chloramine-T}][\text{glycollic acid}]^\circ$$

But in the case of lactic acid the rate of the reaction was found to increase with increasing concentration of lactic acid showing a direct dependence of reaction rate on the reducing substrate concentration $1 - \left(\dfrac{1}{1 + [\text{lactic acid}]}\right)$ Table 2 B.

NaOH DEPENDENCE

The reaction was studied at six different concentrations of NaOH at 50° the concentrations of other reactants were kept constant. The rate of oxidation was highly influenced by altering the concentration of sodium hydroxide. Data in Table 1C, 2 C indicate that the reaction is first order in [NaOH] up to 0.055 M concentration and independent of [NaOH] at higher concentration. Equation

$$-\frac{d}{dt}[\text{chloramine-T}] = k\,[\text{chloramine-T}]\ [\text{Reducing substrate}]\ [\text{NaOH}]$$

$$\text{when } [\text{NaOH}] \leqslant 0.05\ \text{M}$$

$$\text{and } -\frac{d}{dt}[\text{chloramine-T}]=k[\text{chloramine-T}][\text{Reducing substrate}][\text{NaOH}]^{\circ}$$

$$\text{when } [\text{NaOH}] \geqslant 0.5 \text{ M}$$

Table 1C

Effect of NaOH concentration

[NaOH] M	$k \times 10^3$ min^{-1}	$10k$/[NaOH]
0.015	1.55	1.03
0.02	2.28	1.14
0.03	3.54	1.18
0.04	4.29	1.07
0.05	5.24	1.05
0.06	5.34	—

Table 2C

Effect of NaOH concentration
[Chloramine-T] = [Lactic acid] = 0.02 M,
[Os(VIII)] = 0.00001 M, Temp. 50°C

[NaOH] M	$k \times 10^3$ min^{-1}	$\frac{10k}{[\text{NaOH}]}$
0.035	4.35	1.25
0.045	5.61	1.25
0.050	6.59	1.32
0.055	7.317	1.34
0.060	7.34	—
0.065	7.38	—

Os(VIII) DEPENDENCE

In order to investigate the effect of Os(VIII) variation on the reaction rate, sets of kinetic runs with varying concentration of Os(VIII) were carried out at three different temperatures viz. 45°, 50° and 55°C. The concentrations of other reactants were kept constant at [Reducing substrate] = 0.02 M, [NaOH] = 0.05 M and [chloramine-T] = 0.02 Ms.

Table 1D

Effect of Os(VIII) concentration

[Os(VIII)] *M*	$k \times 10^3$ min^{-1} at temperatures		
	45°C	50°C	55°C
0.00002	2.36	2.63	3.86
0.00003	3.59	5.31	5.70
0.00004	5.12	6.19	7.86
0.00005	6.41	7.43	10.55

Table 2D

Effect of Os(VIII) concentration

[Os(VIII)] M	$k = 10^3$ min^{-1} at temperature		
	45°	50°	55C°
0.00001	5.12	6.59	7.10
0.000015	7.46	9.27	10.22
0.00002	9.84	12.90	14.23
0.000025	12.26	16.76	17.87
0.00003	14.54	19.34	21.91

Results depicted in Table 1 D, 2 D indicate that the rate constant increases by increasing the concentration of the catalyst. Thus Rate αOs(VIII) at temperature ranges from 45 to 55°C.

The catalytic activity of Os(VIII) was learnt from a graph plotted between the concentration of Os(VIII) and the rate constant at different concentration. The plots were found to be straight lines passing through the origin, showing a direct dependence of rate constants on the [Os(VIII)] concentration and that the uncatalysed oxidation of glycollic/lactic acid is practically improbable at this temperature range and the fact was actually observed (Fig. 1 and 2).

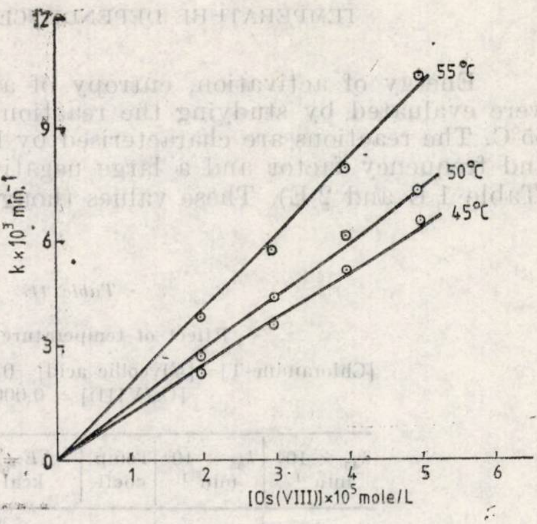

Fig. 1. — Plot of rate constant vs. catalyst concentration at three different temperatures, [Chloramine-T] = = 0.02 M, [CH2OHCOOH] = 0.02 M, [NaOH] = 0.05 M.

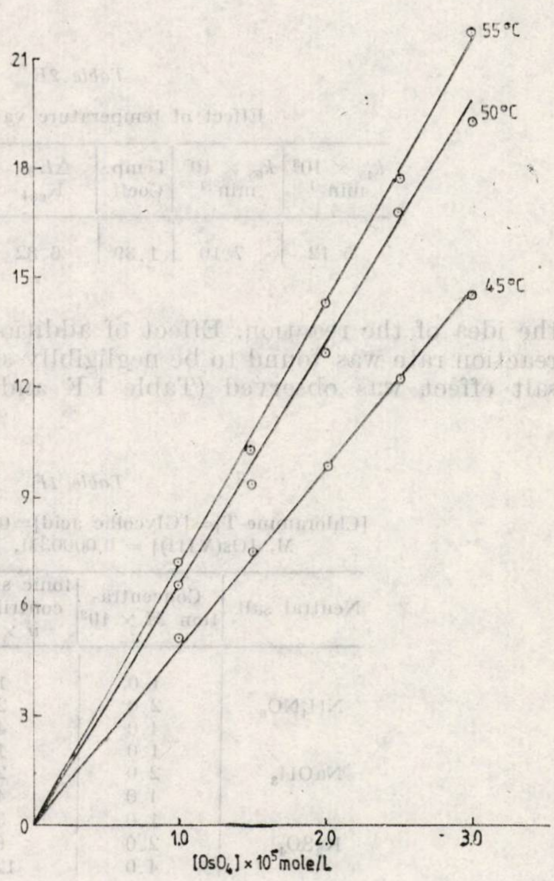

Fig. 2. — Plot of rate constant vs. catalyst concentration at three different temperatures [Chloramine-T] = 0.02M, [CH3CHOHCOOH] = 0.02M, [NaOH] = 0.05 M.

TEMPERATURE DEPENDENCE AND SALT EFFECT

Energy of activation, entropy of activation frequency factor etc, were evaluated by studying the reaction at two temperatures viz. 45°, 55°C. The reactions are characterised by low values of activation energy and frequency factor and a large negative value of activation entropy (Table 1 E and 2 E). These values though of little importance but give the idea of the reaction. Effect of addition of salt concentration on the reaction rate was found to be negligiblly small and only a small negative salt effect was observed (Table 1 F and 2 F).

Table 1E

Effect of temperature variation

[Chloramine-T] = [Glycollic acid] = 0.02 M, [NaOH] = 0.05 M, [Os(VIII)] = 0.00003 M

$k_{45} \times 10^3$ min^{-1}	$k_{55} \times 10^3$ min^{-1}	Temp. coeff.	$\Delta E \neq$ kcal	A sec^{-1}	$\Delta S \neq$ E.U.
3.59	5.70	1.6	9.6	2.3×10^2	−34.80

Table 2E

Effect of temperature variation

$k_{45} \times 10^3$ min^{-1}	$k_{55} \times 10^3$ min^{-1}	Temp. Coeff.	$\Delta E \neq$ K$_{cal}$	A sec^{-2}	$\Delta S \neq$ E.U.
5.12	7.10	1.39	6.82	3.8	−55.2

Table 1F

[Chloramine-T] = [Glycollic acid] = 0.02 M, [NaOH] = 0.05 M, [Os(VIII)] = 0.00003M, Temp. = 50°C

Neutral salt	Concentration $M \times 10^2$	Ionic strength contribution $u \times 10^2$	$k \times 10^3$ min^{-1}
NH_4NO_3	1.0	1.0	5.22
	2.0	2.0	5.18
	4.0	4.0	5.03
$NaOH_3$	1.0	1.0	5.19
	2.0	2.0	5.02
	4.0	4.0	5.01
K_2SO_4	1.0	3.0	5.07
	2.0	6.0	5.05
	4.0	12.0	5.00

Table 2F

Effect of salt concentration

[Chloramine-T] = 0.020 M, [Lactic acid] = 0.02 M,
[NaOH] = 0.05 M, [Os(VIII)] = 0.00001 M, Temp. 50°C

Neutral salt	Concentration $M \times 10^3$	Ionic strength contributed $u \times 10^2$	Rate constant $k \times 10^3$ min^{-1}
NH_4VO_3	1.0	1.0	6.23
	2.0	2.0	6.01
	4.0	4.0	5.83
KNO_3	1.0	1.0	6.12
	2.0	2.0	5.92
	4.0	4.0	5.75
K_2SO_4	1.0	3.0	6.05
	2.0	6.0	5.83
	4.0	4.0	5.59

PRODUCT ANALYSIS AND NON CHAIN REACTION

During the oxidation of glycollic acid by chloramine-T in presence of Os(VIII) the main oxidation product-glyoxalic acid-was confirmed by the spot test. The main oxidation product of lactic acid was identified as pyruvic acid by the usual method. Non chain character was observed in both cases as no significant effect of surface/volume ratio, allylacetate was observed on the reaction rate.

DISCUSSION

The mechanism proposed must explain characteristic features of Os(VIII) catalysed oxidation of glycollic and lactic acid by chloramine-T in alkaline media.

1. Reactions are first order w.r.t. chloramine-T. An increase in oxidant concentration slightly decreases the rate constant.

2. Glycollic acid oxidation is independent of reducing substrate concentration but lactic acid oxidation follows a direct dependence on the factor $\left(1 + \dfrac{1}{1 + [\text{lact.}]}\right)$.

3. At lower concentration of alkali (glycollic acid oxidation up to .05 M, lactic acid oxidation up to 0.55 M NaOH) the reaction follows a first order dependence on alkali. At higher concentration the reaction is independent of it.

4. The reactions occur only in presence of Os(VIII) ion and the order w.r.t. Os(VIII) is the unity. Moreover plots (Fig. 1 and 2) of rate constant vs. Os(VIII) are linear, passing through the origin indicating that the uncatalysed oxidations are not possible.

5. Both oxidations are characterised by low value of temperature coefficient of activation energy.

6. A small negative salt effect was observed in both cases.

7. The reactions are of non chain character.

Chloramine-T hydrolyses in aqueous alkaline solution as follows

$$CH_3.C_6H_4SO_2N.NaCl + H_2O \rightleftharpoons CH_3C_6H_4SO_2N.HCl + NaOH \quad (1)$$

$$CH_3.C_6H_4SO_2N.HCl + NaOH \rightleftharpoons CH_3.C_6H_4SO_2.NH_2 + Na^+ + ClO^- \quad (2)$$

The oxidising species are, therefore, chloramine-T itself and p-toluene sulphochloramide.

In alkaline medium dichloramine-T does not exist and the possibility ClO ion as an oxidising agent is ruled out on kinetic grounds.

At moderate alkali concentration the possibility of p-toluenesulphochloramide formation is rare. Hence chloramine-T itself is main oxidising species.[8]

The essential presence of Os(VIII) as catalyst led to the conclusion that osmium tetroxide complex with chloramine-T in alkaline media is solely responsible for oxidation. Following cyclic structure is proposed for the complex

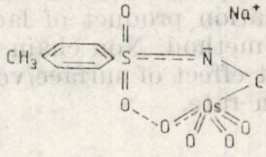

which shows that electron charge density around nitrogen of chloramine-T is reduced and N—Cl bond becomes weaker, subsequently the hybride ion abstracting capacity of chloramine-T is increased after complexation. This results in the interaction with α-hydroxy acid anion.

The following mechanism has been suggested

Chloramine-T forms complex with OsO_4 in presence of alkali

$$CH_3.C_6H_4.SO_2.NaCl + OsO_4 + OH \underset{k_{-1}}{\overset{k_1}{\rightleftharpoons}} Complex \quad (3)$$

The complex reacts with α-hydroxy acid anion

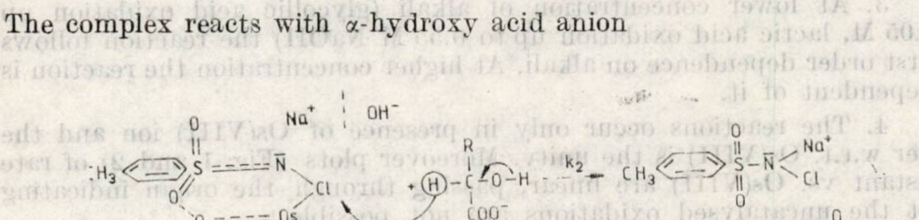 (4)

(here R=H for glycollic and R=CH_3 for lactic acid).

The mechanism is analogous to other hydride ion abstraction mechanisms.$^{9-14}$ This mechanism is further supported by the fact that hydroxy acids which have no hydrogen atom attached to that carbon which is attached to hydroxy group e.g. benzelic, citric acid etc. were not being oxidised under present experimental conditions.

The mechanism proposed leads to the rate expression

$$-\frac{d}{dt}[\text{Chloramine-T}] = k_1[\text{Chloramine-T}][\text{OsO})_4][\text{OH}^-] - k_{-1}[\text{Complex}] \tag{5}$$

The concentration of complex at any time during the reaction is small hence applying steady state assumptions the expression takes the form

$$-\frac{d}{dt}[\text{Chloramine-T}] =$$

$$= k_1[\text{Chloramine-T}][\text{OsO}_4][\text{OH}^-]\left(1 - \frac{1}{1 + \frac{k_2}{k_{-1}}[\text{RCHOHCOO}]}\right) \tag{6}$$

(i) If $k_{-1} \ll k_2$ RCHOHCOO$^-$

$$-\frac{d}{dt}[\text{Chloramine-T}] =$$

$$= k_1[\text{Chloramine-T}][\text{OsO}_4][\text{OH}]\left(\frac{k_2[\text{RCHOHCOO}^-]}{k_{-1} + k_2[\text{RCHOHCOO}^-]}\right) \tag{7}$$

Therefore since

$$\frac{k_2[\text{RCHOHCOO}^-]}{k_{-1} + k_2[\text{RCHOHCOO}^-]} \approx 1$$

Therefore :

$$-\frac{d}{dt}[\text{Chloramine-T}] = k^2[\text{Chloramine-T}][\text{OsO}_4][\text{OH}^-] \tag{8}$$

This rate expression explains the oxidation of glycollic acid at [NaOH] $\leqslant$ $\leqslant$ 0.05 M.

(ii) If $\frac{k_2}{k_{-1}} = 1$

The rate expression (6) reduces to

$$-\frac{d}{dt}[\text{Chloramine-T}] =$$

$$= k_1[\text{Chloramine-T}][\text{OsO}_4][\text{OH}^-]\left(1 - \frac{1}{1 + [\text{RCHOHCOO}^-]}\right) \tag{9}$$

This explains the oxidation of lactic acid where the reaction rate depends on a factor $\left(1 - \frac{1}{1+[\text{Lact.}]}\right)$ w.r.t. reducing substrate. Of course the concentration of alkali must not exceed 0.055 M.

The zero order dependence on alkali at high alkali concentrations ($\geqslant$ 0.05 M for glycollic and 0.055 M for lactic acid) can be explained by considering p-toluene sulphochloramide as oxidising species as its concentration is appreciable at high [NaOH] to carry out oxidation reactions, since the rates are faster under these higher alkali concentrations.

REFERENCES

[1] G. S. Deshmukh and M. L. Eashwar, *J. Sci. Ind. Res.* (India), **19**, 502 (1960); *J. Electroanal Chem.*, **34**, 309 (1962).

[2] L. Brdey and L. Kaplar, *Z. anal. Chem.*, **162**, 180 (1958).

[3] B. Singh, A. Singh and M. Singh, *Res. Bull. of the East, Punjab Univ.*, N**30**, 55 (1953).

[4] A. Borka and J. Zyka. *C. Cskalov, Farm.*, **5**, 335 (1946).

[5] B. Carli and R. Avroldi, *An. Chim. Applicata*, **27**, 56 (1937).

[6] B. N. Afanasev, *Zavodskaya Lab.*, **15**, 1271 (1947).

[7] R. Dietsel and K. Taufil, *Apoth. Ztg.*, 989 (1929), *Apoth Ztg.*, **44**, 1007 (1927).

[8] S. P. Mushran, R. Sahelic and A. K. Bose, *Acta Chim. Acad. Sci.*, **82**(2), 135 (1975).

[9] G. V. Bakore and S. Narain, *J. Chem. Soc.*, 3419 (1963).

[10] F. H. Westheimer, *Chem. Rev.*, **45**, 419 (1949).

[11] H. Kwart and P. S. Francis, *J. Am. Chem. Soc.*, **77**, 4907 (1955).

[12] T. J. Kemp and W. A. Waters, *J. Chem. Soc.*, (1964) 1192.

[13] M. J. S. Dewar, *Research*, **3**, 154 (1950).

[14] S. Sundaram and S. V. Venkatasubramanian, *Curr. Sci.*, **33**, 646 (1964).

Revue Roumaine de Chimie, **30**, 8, 735–741 (1985)

SYNTHESIS OF SOME BIOMIMETIC 4-SUBSTITUTED COUMARINS

SHRIKANT S. HANMANTGAD, MANOHAR V. KULKARNI and VEMANNA D. PATIL *
Department of Chemistry, Karnatak University, Dharwad-580003, India

Received March 10, 1984

4-Bromomethylcoumarins (I) prepared by the reaction of various phenols and 4-bromoethylacetoacetate have been reacted with phenols, anilines and anthranilic acid. Their spectral and antimicrobial properties are reported. Acid hydrolysis and azo coupling of some ethers have also been carried out.

INTRODUCTION

Coumarin nucleus has been the seat of diverse biological properties through its innumerable derivatives, because of its unique delta lactone skeleton.[1] Coumarin derivatives containing aryloxy groups are found to be anti-histaminics,[2] antimycobacterials.[3] Introduction of a secondary amino group in coumarin brings forth neurotropic [4] and anti-bacterial activity.[5,6]

Owing to the importance of nitro group in some antibiotics and the role of amino derivatives in biodegradation, it was thought of immense interest to synthesize biomimetic coumarin derivatives at the allylic position with respect to the 3,4-double bond which is known for its key role in plant and animal metabolisms.[1]

The present paper reports the synthesis of some specifically functionalised 4-aryloxymethyl, 4-arylaminomethyl coumarins, their spectral, anti-bacterial properties, and some of their reactions.

CHEMISTRY

The required 4-bromomethylcoumarins [7] (I) were synthesised by the acid catalysed Pechmann cyclisation from the corresponding phenols and 4-bromoethylacetoacetate,[8] at ice bath temperatures. The allylic bromine in (I) underwent a facile nucleophilic displacement with both phenols and anilines, the latter requiring drastic thermal conditions due to its poor nucleophilicity. In the case of reaction with anthranilic acid, excess of latter was boiled with (I) in xylene. The reactions are shown in scheme 1. Analytical data for these are given in tables 1–3.

Scheme-1

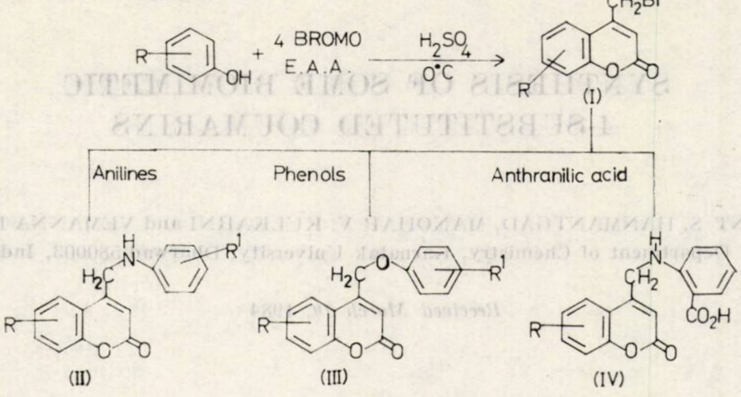

Table 1

Analytical data of 4-(arylaminomethyl) coumarins

R	R¹	m.p. °C	Formula *	Analysis % ** Required N	Found N
6-Methyl	-Methyl	195^a	$C_{18}H_{17}NO_2$	5.01	4.89
6-Methyl	-Chloro	213^a	$C_{17}H_{14}NClO_2$	4.67	4.79
7-Methyl	-Methyl	174^b	$C_{18}H_{17}NO_2$	5.01	5.19
7-Methyl	-Chloro	160^c	$C_{17}H_{14}NClO_2$	4.67	4.49
7-Methyl	-Methoxy	144^a	$C_{18}H_{17}NO_3$	4.74	4.49
7-Methoxy	-Methyl	195^c	$C_{18}H_{17}NO_3$	4.74	4·64
7-Methoxy	-Chloro	202^b	$C_{17}H_{14}NClO_3$	4.43	4.19
7-Methoxy	-Methoxy	165^a	$C_{18}H_{17}NO_4$	4.50	4.34
6-Methoxy	-Chloro	181^d	$C_{17}H_{14}NO_3Cl$	4.43	4.21
6-Methoxy	-Methoxy	166^c	$C_{18}H_{17}NO_4$	4.50	4.40
6-Chloro	-Methoxy	183^a	$C_{17}H_{14}NClO_3$	4.43	4.19

[a] Benzene + Petrol – ether ; [b] Ethanol, [c] Aqueous ethanol ;
[d] Benzene
* Yields are 70–80 %
** All compounds gave satisfactory C, H analyses.

Table 2

Analytical data of 4-(Nitrophenoxymethyl) coumarins

R	R¹	m.p. °C	Formula *	Analysis % ** Required N	Found N
6-Methyl	o-Nitro	270^a	$C_{17}H_{13}NO_5$	4.50	4.29
6-Methyl	p-Nitro	252^a	$C_{17}H_{13}NO_5$	4.50	4.74
7-Methyl	o-Nitro	211^a	$C_{17}H_{13}NO_5$	4.50	4.24
7-Methyl	p-Nitro	229^b	$C_{17}H_{13}NO_5$	4.50	4.74
7-Methoxy	p-Nitro	240^b	$C_{17}H_{13}NO_6$	4.28	4.05
6-Methoxy	o-Nitro	246^c	$C_{17}H_{13}NO_6$	4.28	4.15
6-Methoxy	p-Nitro	250^a	$C_{17}H_{13}NO_6$	4.28	4.10

[a] Acetic acid, [b] Ethanol + dioxan, [c] Xylene
* Yields – 80–90 %
** All compounds gave satisfactory C, H analyses.

Table 3

Analytical data of 4-(alkoxyphenoxymethyl)coumarins

R	R¹	m.p. °C	Formula *	Analysis %			
				Required		Found	
				C	H	C	H
6-Methyl	o-Methoxy	192^b	$C_{13}H_{16}O_4$	72.97	5.40	72.64	5.19
6-Methyl	m-Methoxy	165^c	$C_{18}H_{16}O_4$	72.97	5.40	72.74	5.21
7-Methyl	o-Methoxy	164^c	$C_{18}H_{16}O_4$	72.97	5.40	72.61	5.14
7-Methyl	m-Methoxy	135^d	$C_{18}H_{16}O_4$	72.97	5.40	72.75	5.29
7-Methoxy	m-Methoxy	155^d	$C_{18}H_{16}O_5$	69.23	5.12	69·02	5.29
6-Methoxy	o-Methoxy	150^c	$C_{18}H_{16}O_5$	69.23	5.12	69.04	4.94
6-Methoxy	m-Methoxy	130^c	$C_{18}H_{16}O_5$	69.23	5.12	69.39	4.89

^{b} Ethanol + dioxan ; ^{c} Benzene ; ^{d} Ethanol
* Yields 70–80 %

The condensation product of methyl salicylate (V) when reacted with sulphuric acid even at elevated temperatures, was found to hydrolyse, to the corresponding acid (VI) and does not undergo cyclodehydration at the 3-position of coumarin. Azocoupling in mildly alkaline medium of 7-hydroxy coumarins was reported by Sheshadri et al.[9] During the present investigation the 2-naphthyl ether (VII) containing an equally reactive proton undergoes azocoupling at position-1 of the naphthalene moiety. This is confirmed by the direct condensation of 1-phenylazo-2-naphthol with 4-bromomethylcoumarin resulting in the formation of (VIII) as shown in scheme 2.

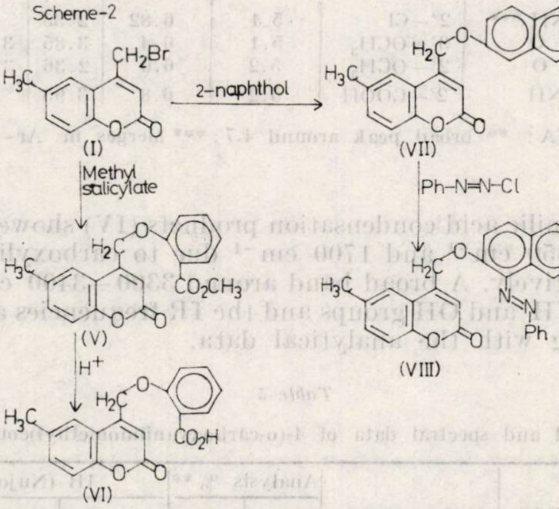

RESULTS AND DISCUSSION

The 4-arylaminomethyl coumarins (II) in the IR spectra showed intense bands around 3400 cm⁻¹ and 1700 cm⁻¹ due to NH and CO stretching vibrations respectively. In the NMR spectral study, the NH proton was found to exchange with D_2O at room temperature. The methylene protons appeared around 4.5 ppm and protonation of the nitrogen lone pair by trifluoroacetic acid causes a downfield shift to 5.4 ppm. Other proton resonances occur at expected fields. The 4-aryloxymethylcoumarins (III) show the long range allylic coupling,[7] between 4-CH_2 protons and coumarin 3—H (J ~ 2 Hz), which is intervened by the quadrupole resonance of nitrogen in the case of compounds (II). PMR spectral data of some of these are mentioned in Table 4.

Table 4

PMR spectral data

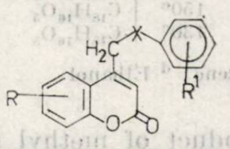

R	x	R^1	4-CH_2	3-H	R	R^1	Ar—H
6-OCH_3	NH **	2′—OCH_3	4.5	6.5	3.9	3.85	6.8—7.4
6—CH_3*	$\overset{+}{\mathrm{N}}$H ***	2′—Cl	5.1	6.82	2.35	—	7.2—7.5
6—OCH_3	O	3′—OCH_3	5.1	6.4	3.85	3.80	6.7—7.4
6—CH_3	O	2′—OCH_3	5.2	6.6	2.36	3.8	6.8—7.3
7—OCH_3‡	NH	2′—COOH	5.2	6.8	3.95	—	7.0—7.3

Spectra : *TFA ; ** broad peak around 4.7 ; *** Merges in Ar—H recorded in : ‡ DMSO-D_2O

The anthranilic acid condensation products (IV) showed two distinct bands around 1650 cm^{-1} and 1700 cm^{-1} due to carboxylic and lactone carbonyls respectively. A broad band around 3300—3400 cm^{-1} indicated the presence of NH and OH groups and the IR frequencies are mentioned in Table 5 along with the analytical data.

Table 5

Analytical and spectral data of 4-(o-carboxyanilinomethyl)coumarins

R	M.P.°C	Formula *	Analysis % **		IR (Nujol) cm^{-1}		
			Required N	Found N	C=O (acid)	C=O (lactone)	N—H, O—H (broad)
6-Methyl	278	$C_{18}H_{13}NO_3$	4.81	4.72	1670	1725	3396
6-Chloro	254	$C_{17}H_{10}NO_3Cl$	4.49	4.21	1670	1720	3400
6-Methoxy	225	$C_{18}H_{13}NO_4$	4.56	4.39	1675	1722	3392
7-Chloro	226	$C_{17}H_{10}NO_3Cl$	4.49	4.28	1675	1720	3395
7-Methoxy	245	$C_{18}H_{13}NO_4$	4.56	4.47	1670	1720	3385
5 : 6-Benz	230	$C_{21}H_{13}NO_3$	4.28	4.45	1680	1725	3394
7 : 8-Benz	259	$C_{21}H_{13}NO_3$	4.28	4.14	1675	1720	3400

* Yields : 60—70 %
** All compounds gave satisfactory C, H analyses.

The carbomethoxy ether (V) displayed only one band around 1700 cm^{-1} due to both lactone and ester carboxyl groups. The high resolution NMR spectrum revealed the presence of methoxyl protons around 3.8 ppm and also exhibited the triplet — doublet pattern for C_3-H and $4-CH_2$ protons ($J = 1.46$ Hz). The hydrolysis product (VI) also showed the presence of C_3-H around 6.5 ppm. In the IR spectrum the acid (IV) exhibited a broad band around 3450 cm^{-1} which further supported its structure.

The azo ether (VIII) also showed the presence of coumarin $3-H$ around 6.5 ppm in the NMR spectrum. This compound was identical in all respects (IR, mp and m.m.p) with the one obtained by the direct synthesis using 1-phenylazo-2-naphthol.

SCREENING RESULTS

Antimicrobial activity

Amongst the compounds tested for antimicrobial activity against *S. aureus* and *E. coli*, in the case of anilinomethyl coumarins (II) 7-methyl and 7-methoxy substitutions in coumarin favoured the growth inhibition of *E. coli*. o-Chloro and o-methoxy groups in the phenoxy moiety favoured the growth retardation of *S. aureus*. The 4-aryloxymethyl coumarins (III) also favoured similar substitution in coumarin moiety. The nitro group in phenoxy moiety enhanced the growth inhibition of *S. aureus* while methoxy groups affected the growth of both the species.

The antibacterial activity was carried out by the agar plate method employing sulphanilamide as standard. All the test compounds were employed as solutions in purified DMF at a dose level of 200 μg/ml.

EXPERIMENTAL

All the melting points are taken in open capillaries and are uncorrected. The IR spectra were recorded on a Perkin-Elmer spectrometer and PMR on a Varion A-60 instrumenet. Chemical shift values are expressed in (δ) ppm downfield from TMS. All PMR spectra were recorded in $CDCl_3$ except otherwise stated.

a) *4-Arylaminomethyl coumarins* (II)

These were prepared by the reaction between 4-bromomethyl coumarins (I) and primary aromatic amines using acetic acid as solvent.[6]

b) *4-Aryloxymethyl coumarins* (III)

These were prepared according to the method of Thyagarajan et al.[10] However in the nitrophenoxymethyl ethers, the condensation products separated out from the acetone solution and were filtered off along with potassium carbonate. The residue when neutralised gave the free ether while acetone solution on dilution did not give any ether.

c) *4-(o-Carboxy anilinomethyl) coumarins* (IV)

In a general method, a substituted 4-bromomethylcoumarin (I) (1.0 g) was reacted with anthranilic acid (2.0 g) in xylene and the mixture was boiled under reflux for two hours. The reaction mixture was thoroughly cooled and the separated solid was washed with saturated sodium bicarbonate solution and water. The residue was recrystallised from a mixture of dioxan, ethanol and water (Table 4).

d) *6-Methyl-4-(o-carbomethoxy phenoxymethyl) coumarin* (V)

This is prepared as mentioned in (b) crystallised from benzene, m.p. 179 (80%).
$C_{19}H_{16}O_5$ required: C, 70.37 ; H, 4.93 ;
found: C, 70.05 ; H, 4.84
IR (Nujol) ; 1710 (C=O)
cm^{-1} 1150, 1080 (C—O—C)
NMR ($CDCl_3$) 2.45 (3H, s, $-CH_3$) ;
250 (MHz) 3.91 (3H, s, $-OCH_3$) ;
5.28 (2H, d, $-CH_2O$),
6.80 (1H, t, C_3—H of coumarin) ;
$J_{allylic} = 1.46$ Hz
7.0—7.99 (7H, m, —Ar—H)

e) *6-Methyl-4-(o-carboxy-phenoxymethyl) coumarin* (VI)

The above ether (V) (1 gm) and conc. sulphuric acid 10 mL were stirred for 30 min and heated for one hour on a water-bath. The thick dark reaction mixture after cooling was decomposed in ice and the separated solid was washed with water and recrystallised from hot water m.p. > 300°C yield (50%), $C_{18}H_{14}O_5$
required : C, 69.67 ; H, 4.51
found : C, 69.41 ; H, 4.29.
IR (Nujol) 3400, (O—H, broad)
cm^{-1} 1725, (C=O lactone),
1695, (C=O acid)
NMR (DMSO-d_6/D_2O) ; 2.4 (3H, s, $-CH_3$) ; 5.4 (2H, d-OCH_2)
6.8 (1H, t, C_3—H) J($\sim$ 2Hz), 7.2—8.2 (7H, m, Ar—H)

f) *Azo ether* (VIII)

This was prepared by the reaction of 6-methyl-4-bromomethyl coumarin (I) and 1-phenylazo 2-naphthol.[11]

The procedure employed was the same as for other 4-aryloxymethylcoumarins.[10]

In this case the azo ether (VIII) was in part separated from acetone solution. The residue when neutralised with (1 : 1) HCl gave the crude azo ether which crystallised as red prisms from alcohol, m.p. 180°C yield (30%).

$C_{27}H_{20}N_2O_3$, required : C, 77.14 ; H, 4.76 ; N, 6.66
found : C, 77.09 ; H, 4.59 ; N, 6.59.
IR (Nujol) 1725 (C=O), 1120, 1180 (C—O—C)
cm^{-1}
NMR ($CDCl_3$) : 2.2, (3H, s, $-CH_3$) ; 5.0, (2H, d, $-CH_2O$)
6.4 (1H, t, $-C_3$—H of coumarin)
6.9—7.6 (14H, m, —Ar—H)

g) *6-Methyl-4-(β-naphthyloxymethyl) coumarin* (VII)

Prepared as given in (b) crystallised from benzene, m.p. 215°C (80%).
$C_{21}H_{16}O_3$, required : C, 79.74 ; H, 5.06 ;
found : C, 79.49 ; H, 4.87.

h) *Coupling of β-napthylether (VII) with benzene diazonium chloride*

To a suspension of (VII) (500 mg) in aqueous sodium hydroxyde (10%, 5 mL) kept at 0°C, was added a solution of benzene diazonium chloride (excess) slowly with stirring and the temperature was maintained below 5°C.

After the addition, the reaction mixture was stirred at room temperature for half an hour, diluted with water and filtered. The residue was found to contain some unreacted (VII) and, another red coloured compound which was found to be the azo ether (VIII) from their mixed mps and IR spectra. Yield (20%).

ACKNOWLEDGEMENTS. Authors thank Prof. V. V. Badiger, Head of the Department of Chemistry, for his encouragement and Mr. V. A. Desai for microanalysis.

REFERENCES

[1] G. Feuer, in "Progress in Medicinal Chemistry", Ed. G. P. Ellis and G. B. West, p. 86, North-Holland, New York (1974).

[2] D. R. Buckle, D. J. Outred, J. W. Ross, H. Smith, R. J. Smith, B. A. Spicer and B. C. Gasson, *J. Med. Chem.*, **22**, 158 (1979).

[3] J. R. Merchant and A. S. Gupta, *Ind. J. Chem.*, **17B**, 410 (1979).

[4] V. L. Savel'ev, N. T. Pryanishnikova, O. S. Artamonova, I. V. Fedina and V. A. Zagorevskii, *Khim. Farm. Zh.* **9**, 10 (1975); *Chem. Abstr.*, **83**, 188296s (1975).

[5] A. M. El-Naggar, F. S. M. Ahmed, A. M. Abd-ElSalam, M. A. Radi and M. S. A. Latif, *J. Heterocyclic. Chem.*, **18**, 1203 (1981).

[6] M. V. Kulkarni and D. V. Patil, *Arch. Pharm. (Weinheim)*, **314**, 708 (1981).

[7] *Ibid*, **316**, 15 (1983) and references therein.

[8] A. Burger and G. E. Ullyot, *J. Org. Chim.*, **12**, 346 (1947).

[9] T. R. Sheshadri and S. Rangaswami, *Proc. Ind. Acad. Sci.*, **9**A, 526 (1939).

[10] B. S. Thyagarajan, K. K. Balasubramaniam and R. Bheemarao, *Tetrahedron*, **23**, 1892 (1967).

[11] B. S. Furniss, A. J. Hannaferd, V. Rogers, P. W. G. Smith and A. R. Tatchell in "Vogels' Text Book of Practical Organic Chemistry" 4th Edition, p. 714, ELBS, London (1978).

Revue Roumaine de Chimie, **30**, *8*, 743–748 (1985)

THE SYNTHESIS OF 19-HYDROXYSTEROIDS

A. BODOR, A. GERGELY, R. SCHWARTZ, A. JUHASZ, P. COLTEA and D. BREAZU
Institute of Chemical and Pharmaceutical Research, str. Fabricii 126,
3400 Cluj-Napoca, Romania

Received July 25, 1984

An improved method for the synthesis of 19-hydroxy androst-4-ene-3,17-dione is described. By the simultaneous reduction and dehydrobromination of the 6, 19-epoxy-5-bromoandrostane-3,17-dione the title compound is obtained in good yield.

Among a great number of syntheses of 19-hydroxyandrost-4-ene-3,17-dione **6**, the sequence by the route of 5-halo, 6-hydroxy derivative proved to be suitable for a large scale production.[1,2]

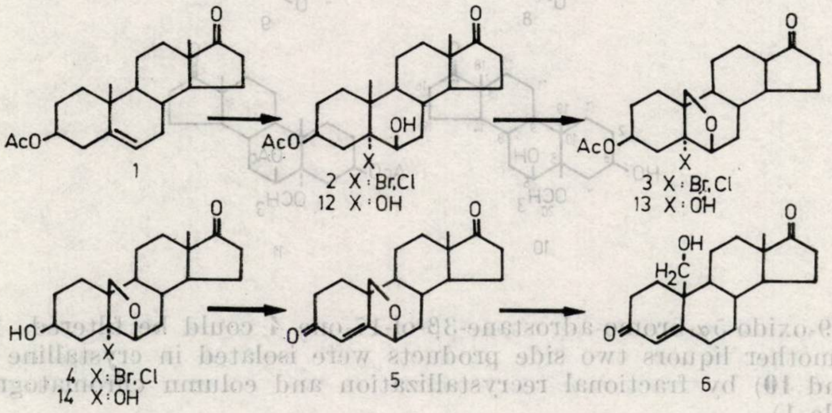

As an alternative to this synthesis it was proposed a route via 3β, 5α, 6β-trihydroxyandrostane-17-one-3-acetate **12**. The epoxidation of dehydroepiandrosterone-3-acetate **1** resulted in the corresponding 5α, 6α-epoxy-3-acetate **8**, which under acidic conditions yielded **12**. The ring closure of the dihydroxy derivative to 6,19 epoxide was effected in an analogous manner as in the halohydrin procedure (**12** → **13** → **14** [3]).

The basic point of the synthesis via halohydrins is the isolation, as pure material of the isomer 5α-bromo, 6β-hydroxy **2** from the reaction mixture which, among several side products contains the another halohydrin isomer, 5α-hydrox, y6β-bromoandrostane-17-one-3β-yl acetate [4].

For this reason we began the synthesis starting from dehydroepiandrosterone-3-acetate **1**, which together with 1,3-dibromo-5,5-dimethyl-hydantoin[5] dissolved in acetone and in the presence of the perchloric acid resulted a rather complex mixture. On adding chloroform to this mixture the expected isomer **2** was isolated in crystalline form, insoluble in this solvent.

However, the other isomer obtained from mother liquors by the usual method of cyclization, by heating of the residue together with sodium acetate, yields 5α, 6-epoxyandrostane-3β-ol-17-one-3-acetate **8**, in good yield. As it was noted before, this compound can also be used as starting material in the alternative procedure presented above.

In the next stages, by irradiating a solution of **2** in methylene chloride, in the presence of iodine, together with lead tetraacetate we obtained a reaction product, which contained mainly the expected 6β, 19-oxido-5α-bromoandrostane-3β-ol-17-one-3-acetate **3**. It was used without purification, in order to obtain **4**. After hydrolysis of the ester **3**, in a medium of aqueous methanol and sodium hydroxide, the crystalline 6β, 19-oxido-5α-bromo-adrostane-3β-ol-17-one **4** could be filtered. From the mother liquors two side products were isolated in crystalline form (**9** and **10**) by fractional recrystallization and column chromatography (Table 1).

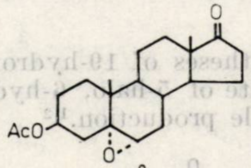

8

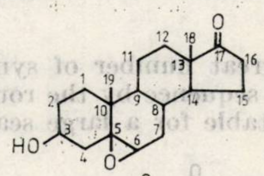

9

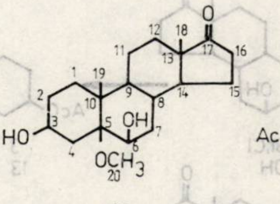

10

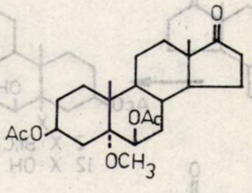

11

Table 1

^{1}H-NMR Spectra of 9 and 10 (δ, ppm)

Comp. no.	Solvent	3 —C—H	6 —C—H	—O—H	—O—CH$_3$	19 —CH$_3$	18 —CH$_3$
9	CDCl$_3$	3.70 t	3.12	2.90		1.03 s	0.86 s
10	CDCl$_3$ DMSO	3.84	3.75 m	3.72 3.66	3.15	1.22 s	0.88 s

The formula for **10** proved to be correct, because the ^1H-NMR spectra show a peak about 3.15 ppm corresponding to the $-O-C\underline{H}_3$ and the peaks 3.72 and 3.66 ppm respectively are assigned to $-O-\underline{H}$ protons

Table 2

^{13}C-Chemical shifts (δ, ppm) of the compounds **9** and **10**

Comp. no.	1	2	3	4	5	6	7	8	9	10	11	12	13	14	15	16	17	18	19	20
9	31.3^{a}	34.9^{b}	68.0	42.0	62.8	62.8	37.0^{b}	29.3	50.8^{c}	47.0	21.5^{d}	30.7^{a}	40.7	51.1^{c}	21.0^{d}	35.4^{b}	219	13.2	17.0	
10	33.1^{a}	34.7^{b}	67.3^{c}	36.9	80.2	69.1^{c}	33.4^{a}	30.9	46.2	40.7	23.0	32.2	49.0	52.3	21.6	35.0^{b}	221	15.1	18.5	48.8

[a, b, c, d] within the group of signals marked with the same letter, assignments are not certain.

Using literature data about related steroids, in the $^{13}C-NMR$-spectra almost all carbons in our compounds could be identified.[6]

One would suppose three several positions for the methoxy group on steroids skeleton. The following facts, however, prove for certain, that the substance **10** is indeed 5α-methoxy derivatives and does possess the constitution proposed.

In the first place, when dissolved in a mixture of acetic anhydride-pyridine at room temperature, the corresponding diacetoxy compound is formed (proof for acetoxy groups 103%). Secondly, in the infrared spectra of acetylated derivative, the characteristic bands of the secondary hydroxyl group are absent while they appear quite clearly in the spectra of 3β, 6β-dihydroxy-5α-methoxy androstane-17-one **10**.

Table 3

The IR spectra of **9**, **10** and **11**

Comp. no.	Frequency (cm^{-1})		
	O−H	C−H	C=O
9	3550, 3430 3400	2950, 2930 2910, 2860	1720
10	3624, 3456	3000, 2930 2900, 2890 2860, 2830	1725
11	—	2954, 2915 2880	1724

The simultaneous presence of the free hydroxyl groups makes somehow difficult to locate the sites of acetylation, but it is not without interest to note that this cautious acetylation does not allow the protection of tertiary hydroxyl group from C—5.[7] It reclaims more drastic conditions, than the use of catalyst. From this it follows that in the monomethoxy compound **10**, the methoxy occupies the C—5 position, and the two hydroxyl groups from C—3 and C—5 respectively were acetylated to form 3β, 6β-diacetoxy-5α-methoxy-androstane-17-one.

Another side product proved to be 5β, 6-epoxyandrostane-17-one-3β-ol **9**. Its structure was confirmed on the basis of ^{1}H—NMR spectra and in accordance with the literature data,[8,9] it showed a signal at 3.12 ppm due to one alpha proton at C—6. Therefore the epoxide ring is oriented in β face.

Based on the structural evidence presented, it is not unreasonable to assume that these compounds are originating from **2**, which remains partly unaffected in the course of epoxidation. While the 5β, 6-epoxide **9** could be easily formed under basic conditions in the course of hydrolysis (**3** → **4**) as a consequence of beta attack of C—6 hydroxyl on C—5, the presence of **11** cannot be explained in terms of a single reaction path by the methoxy anion on C—5 without considering the intermediate rôle of epoxide ring.

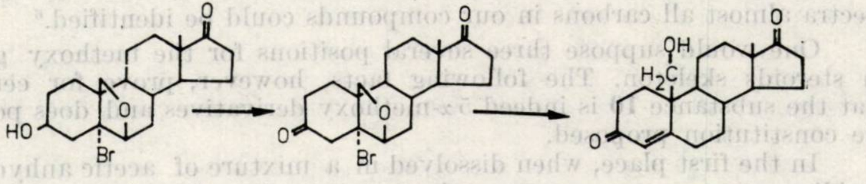

4 7 6

Following the Ueberwasser's original procedure[1,10] we suggested a procedural improvement referring in particular to the facile conversion of **4** into 19-hydroxyandrost-4-ene-3,17-dione **6**. We found to be unnecessary to isolate and purify the intermediate 6β,19-oxidoandrost-4-ene-3,17-dione **5**, because **6** could be obtained by a shorter route. By simultaneous reduction of 6,19-oxido ring and by hydrobromide elimination, we hoped to prepare **6** in good yield.[11]

Oxidation of **4** was carried out according to the standard procedure with Jones reagent in acetone. The resulted bromoketone **7** was isolated by filtration as a yellow crystalline material. This compound however proved to be extremely sensible to air, it was rapidly converted into a dark-brown mass. The reduction takes place in ethanol in the presence of activated zinc under reflux. Evidence obtained from TLC investigations indicates that the dehydrobromination to 3-oxo-4-ene conjugated system, proceeds almost simultaneously with 6,19-epoxide ring opening into 19-hydroxyl. It was impossible to reveal, even temporarily, the presence of **5** in the course of reduction.

In this connection it is interesting to note that neither **7** as starting material, nor 19-hydroxy derivative **6**, as expected product, could be detected in methanolic solution kept under reflux with zinc. The R_f values of the compounds in questions (**6** and **7**) are lower and they differ significantly from the corresponding main fraction, observed on plate. This high *Rf* fraction, owing to its extremely low crystallization tendency from methanolic reaction mixture resisted all attempts of direct identification. We are inclined to suppose the stopping of reduction at an intermediate stage, probably at 19-oxoandrost-4-ene-3,17-dione. It is plausible to presume that the relative low reflux temperature of methanolic medium does not allow completion of reduction to **6**.

Otherwise it was noticed that the supposed 19-oxo compound, appeared to be a by-product in ethanol as well in isopropanol, but it vanished completely at the end of reaction. Since the reduction in isopropanol is a time consuming process (24—36 reflux instead of 10 h as it was proposed for ethanol), its employing as solvent is less recommended.

EXPERIMENTAL

All melting points were taken in a melting point tube and were uncorrected. Infrared spectra were recorded with a Specord IR 75 Carl Zeiss Jena instrument. All NMR spectra were recorded with a Varian S 100 XL spectrometer. Proton chemical shifts are related to internal TMS and are accurate within ± 0.01 ppm. ^{13}C-Chemical shifts are also related to internal TMS. Thin layer chromatography were effected on precoated layer, thickness 0.2 mm (Silica gel Merck G 60). They were eluted with ethyl acetate and benzene in a mixture 4:6, detection with sulfuric acid 40%.

5α-Bromoandrostane-3β,6β-dihydroxy-17-one-3-acetate **2**

We effected this reaction according to the literature though we modified it in a few respects.[5]

In a reaction flask (8.0 L), fitted with stirrer and thermometer were placed 184.5 g (0.559 moles) dehydroepiandrosterone-3-acetate **1**, and 3.35 kg technical acetone. To this solution, chilled to 0—5°C, a solution of perchloric acid (0.06 L 72% diluted with 0.45 L of water) was added, then a solution of 0.2 kg (0.7 moles) 1.3-dibromo-5.5-dimethyl hydantoin in acetone (1.5 kg) was subsequently added dropwise under stirring. The temperature should not rise above 5°C, and it should be maintained continuously for 1—2 hrs, by chilling. Upon pouring the mixture into cold water and sodium thiosulfate (70 g in 800 mL solution) the crude bromohydrin precipitated. After drying the mixture of bromohydrins (220—230 g) was suspended in 750 mL chloroform, chilled to 0—5°C, stirred and filtered off.

Practically pure **2** was obtained (190 g, m.p. = 170—172°C, $/\alpha_D/_{CHCl_3} = +1$).

6β,19 Oxido-5α-bromoandrostane-3β-ol,17-one **4**[12]

1900 g of **2** (4.44 moles) in 18.5 kg methylene chloride and 0.11 kg iodine were irradiated (at sunlight or with lamps of 500 watts). To this mixture a solution of lead tetraacetate (2.74 kg, 6.18 moles) in methylene chloride (18 kg) was added under vigouros stirring. The liquid was irradiated and stirred for 45 minutes. It is easy to control the reaction since it is run at the reflux temperature of methylene chloride.

After working up according to literature, the crystalline residue (which proved to be epoxy-3-acetate **3**) was hydrolised without any previous purification. To this residue 6.36 kg methanol and 0.192 kg sodium hydroxide in water (4 N solution) were added. The temperature was maintained rigorously by cooling at 10—13°C.

First the **3** is gradually dissolved but towards the end of the addition epoxy-3-hydroxide **4** begins to separate. Then to this mixture cold water was added in order to complete the precipitation of **4**. This was sucked off, washed with water and dried. It melts at 199—201°C (1.18—1.19 kg, yield about 55% toward 1).

3β, 6β-Dihydroxy-5α methoxy-androstane-17-one **10**

Water was added to mother liquors of the above hydrolysis, from which after some time 40—50 g of crystals separated. They could be purified by column chromatography, on

a column filled with silica gel (Merck 70—230 mesh), elution with benzene and ethyl acetate finally benzene-acetone. The main fraction proved to be 5β, 6-epoxy-androstane-3β-ol-17-one **9**. Several recrystallizations from acetone yielded pure **9**, m.p. = 167—168°C, $/\alpha_D/_{CHC_3}$ = + 62°
Mass spectra, m/e (relative intensity) 304 (100), 133 (16), 123 (16), 120 (16), 93 (12), 55 (12), 107 (11), 134 (10) ; $M^+ = 304(100\%)$.

After the elimination of **9**, another side product was isolated. Chromatographically it proved to be more polar than **9**. Its repeated crystallization from acetone yielded pure **10**, with m.p. = 250—252°C, $/\alpha_D/_{CHCl_3}$ = + 47° Mass spectra, m/e (relative intensity) 286(100), 304(28), 336(22), 260(15), 123(14), 124(11), 109(12), 55(12) ; $M^+ = 336(22\%)$.

Found : C, 71,77 ; H, 9.60 ; $C_{20}H_{32}O_4$ requires C, 71.39 ; H. 9.51.

3β, 6β-Diacetoxy-5α-methoxy-androstane-17-one **11**

A solution of **10** (1.0 g) in pyridine (20 mL) was treated with acetic anhydride (4.0 g) at room temperature. After completion of acetoxylation (one day), the solution was precipitated on water. After working up, the product was taken up in a mixture methanol-water, refluxed then chilled to 0°C. The precipitated solid was collected. For the analytical specimen this treatment was repeated a number of times ; m.p. = 144—146°C, $/\alpha_D/_{CHCl_3}$ = — 13.5° Found : C, 68.40 ; H, 8.98 ; $C_{24}H_{36}O_6$ requires C, 68.54 ; H, 8.63.

19-Hydroxy-androst-4-ene-3,17-dione **6**

A solution prepared from 472 g chromic anhydride (4.72 moles), 762 g sulfuric acid diluted with water to 3.8 L (Jones reagent), was slowly added to a stirred and cooled solution of 1190 g (3.11 moles) of **4** in acetone (29 kg, 22.9 L). The temperature was maintained at — 2. . .+ 2°C. After 30 minutes of stirring water was added, and the solid crystalline matter was collected by filtration. The obtained 1250—1300 g wet material was used as soon as possible at the next stage.

The bromoketone, ethanol (17.3 kg, 13.68 L) and 2.0 kg zinc, activated in a mixture of acetic acid and water, were refluxed for 10—12 hrs. After cooling to room temperature, the mixture was filtered off. On removal of the zinc by filtration and the alcohol by distillation, the residue was extracted with 1.5—2.0 L of sulfuric acid 10% and 3.3 kg (4.88 L) chloroform. The organic layer after washing with water, sodium bicarbonate and evaporation in vacuum yielded an oily residue. It was treated with acetone in order to induce the crystallization.

After drying at room temperature the white-yellow crystals (610—620 g) melted at 168—170°C (lit. 168—170°C[2, 14]).

ACKNOWLEDGMENT. We express our thanks to Dr. P. Dvortsàk and Dr. Gy. Horvàth (Research Institute for Pharmaceutical Chemistry—Budapest) for ^1H-NMR, ^{13}C-NMR and mass spectra and for helpful discussions.

REFERENCES

[1] H. Ueberwasser, K. Heusler, J. Kalvoda, Ch. Meystre P. Wieland, G. Anner and A. Wettstein, *Helv. Chim. Acta*, **46**, 344 (1963).
[2] A. Bowers, R. Villotti, J.A. Edwards, E. Deust and O. Halpern, *J. Amer. Chem. Soc.*, **84**, 3204 (1962).
[3] G. M. Nascimento, *Rev. Port. Quim.*, **1965**, 133.
[4] N. M. Goncharova and V. I. Maksimov, *Khim. Pharm. Zhur.*, **6**(9) (1972).
[5] D. Rotaru, P. Colțea, A. Gergely, M. Sclifos and D. Tomuș, *Rom. Pat.*, 62121.
[6] Syed Q., A. Rizvi and J. Williams, *J. Org. Chem.*, **46**, 1127 (1981) and literature cited here.
[7] J. Weinman and S. Weinman, *Steroids*, **6**(6), 699 (1965).
[8] Tori and Nakagawa, *J. Org. Chem.*, **29**, 1136 (1963).
[9] A. Cross, *J. Amer. Chem. Soc.*, **84**, 3206 (1962).
[10] S. Schwarz, H. J. Siemann and W. Pohnert, *Experienta*, **21**, 500 (1965).
[11] Bodor A., Gergely A., A. Juhasz, R. Schwartz and D. Breazu, *Rom. Pat.* 96892.
[12] D. Rotaru, P. Colțea, A. Gergely, M. Sclifos and D. Tomuș, *Rom. Pat.*, 60008.
[13] J. Kalvoda, K. Heusler, H. Ueberwasser, G. Anner and A. Wettstein, *Helv. Chim. Acta*, **46**, 1361 (1963).
[14] A. Wettstein, A. Georgand, K. Heusler, *Swiss Pat.* 451925 ; cf. *Chem. Abstr.*, **70**, 4397c (1969).

Revue Roumaine de Chimie, **30**, 8, 749–752 (1985)

THE PHOTO FORMYLATION OF PHENOLS

A. M. FAHMY, S. A. MAHGOUB, M. M. ALY and M. Z. A. BADR *
Chemistry Department, Faculty of Science, Assiut University,
Assiut, Egypt, A.R.E.

Received February 11, 1984

Formylation of phenols, namely: phenol, *o*- and *p*-cresols, p-chlorophenol, p-bromophenol, p-nitrophenol and p-hydroxybiphenyl was achieved through their UV irradiation with chloroform and aqueous potassium hydroxide at 25°C. *ortho*-Formylation products were the only isomers obtained together with chlorine gas. Comparable formylation of p-cresol in darkness reduced the yield from 21% to less than 0.5%. Irradiation pyridine as a solvent gave the pyridine hydrochloride salt together with the usual product. The mechanism of the reaction is discussed.

The reaction of phenols with chloroform under the influence of aqueous alkali to give *o*- and *p*-hydroxybenzaldehydes has long been known as the Reimer-Tiemann reaction. The mechanism is considered to involve the attack of phenoxide ion on dichlorocarbene generated through the action of alkali on chloroform.[1-3]

As far as our observation goes there is no recorded instance for a photo-induced formylation reaction of a phenolic compound with haloform.

The present work deals with the study of a novel formylation reaction of phenols on treatment with chloroform in aqueous potassium hydroxide solution under the influence of UV irradiation.

When a mixture of *p*-cresol in chloroform and aqueous potassium hydroxide was irradiated with vigorous stirring at room temperature (*ca.* 25°C), 2-hydroxy-5-methyl benzaldehyde was formed. The yield was increasing progressively by time reaching its optimum as 21% after 15 h.

Treatment of the same mixture under comparable conditions of reactants concentration and temperature in darkness, leads to a great decrease in the yield to less than 0.5% even after prolonged stirring for more than 15 h; thus the attack on phenoxide ion with dichlorocarbene is not an important route in the reaction.

Similar treatment of several phenols, namely; phenol, *o*- and *m*-cresols, *p*-chlorophenol, *p*-bromophenol, *p*-nitrophenol and *p*-hydroxybiphenol affords formylation forming the corresponding substituted benzaldehyde in relatively moderate yields as shown in Table 1. The most significant feature of these photo- formylation reactions is that the aldehyde group is introduced only in the *ortho*-position with respect to the hydroxy group. No *meta* or *para*-isomers were obtained whenever the structure of the substrate permits as shown from the results of T.L.C. and G.L.C. analyses of the photolysates.

On the other hand, high molecular weight products of resinous nature which are not yet identified are obtained as the sole products on treatment of α- and β-naphthols rather than the expected hydroxynaphthaldehydes.

On irradiation of *p*-cresol and excess chloroform in pyridine as a solvent, pyridine hydrochloride was separated among the reaction products.

Table 1

Photo-formylation of phenols

Phenol	Product	Yield (%)	R_f	Eluent used ether/pet. ether (40 – 60°C)
Phenol	Salicylaldehyde	12.27	0.77	1/16
o-Cresol	2-Hydroxy-3-methylbenzaldehyde	7.64	0.80	1/20
m-Cresol	2-Hydroxy-4-methylbenzaldehyde	9.33	0.70	1/10
p-Cresol	2-Hydroxy-5-methylbenzaldehyde	21.00	0.71	1/20
p-Chlorophenol	5-Chloro-2-hydroxybenzaldehyde	14.72	0.81	1/16
p-Bromophenol	5-Bromo-2-hydroxybenzaldehyde	17.57	0.72	1/16
p-Nitrophenol	5-Nitro-2-hydroxybenzaldehyde	3 %	0.67	1/5
p-Hydroxydiphenyl	3-Formyl-4-hydroxybiphenyl *	18.20	0.73	1/9

* Identified and estimated as 2,4-dinitrophenylhydrazone derivative m.p. and mixed m.p. 270°C.

Furthermore, hydrolysis of the photolysate at the end of the reaction with aqueous potassium hydroxide afforded 2-hydroxy-5-methylbenzaldehyde as the only product as confirmed both by T.L.C. and G.L.C. analyses.

Such results of the photo-formylation reaction point clearly to the difference in the pathway involved as compared to the well known Reimer-Tiemann reaction which implies the dichlorocarbene as the intermediate reacting species.

The process appears to start with the homolysis of the C – Cl rather than the C – H bond as predicted on the basis of homolytic bond dissociation energy values for the C – Cl and C – H bonds being of the order 325 and 410 kJ.mol $^{-1}$ respectively.[4]

There are many instances of homolytic fission of C – Cl bond either on thermolysis [5] or photolysis [6] to form a chlorine atom and the dichloromethyl free radical which subsequently attacks the phenol preferably at the *ortho*-position forming the cyclohexadienyl radical intermediate (a). The normal fate of the chlorine atoms is the oxidation of intermediate (a) through hydrogen abstraction forming hydrogen chloride and the corresponding *o*-hydroxybenzalchloride that subsequently undergoes alkaline hydrolysis to the corresponding aldehyde. Moreover, chlorine gas was evolved albeit in trace amount yet it can be detected by standard spot tests.[7]

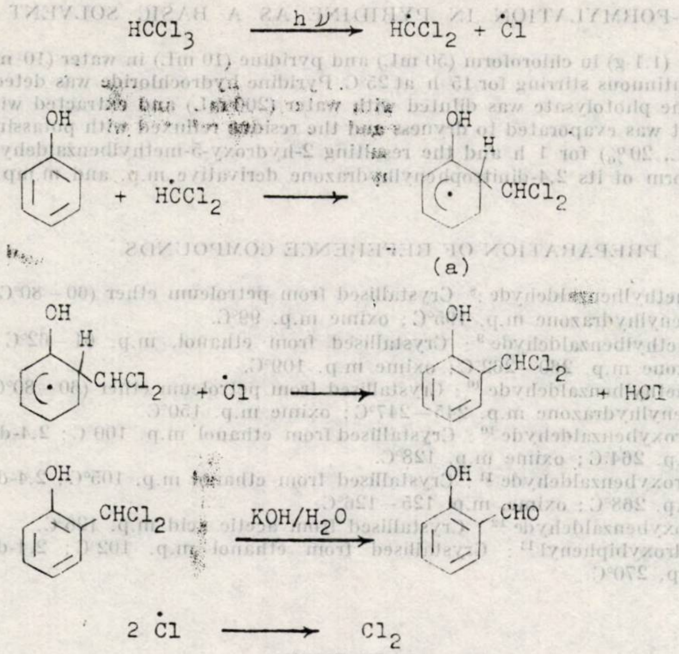
$HCCl_3 \xrightarrow{h\nu} \dot{H}CCl_2 + \dot{C}l$
(a)
$\xrightarrow{KOH/H_2O}$
$2\,\dot{C}l \longrightarrow Cl_2$

EXPERIMENTAL

All m.ps. and b.ps. are uncorrected. The purity of the starting materials as well as of the solvents was checked by gas-liquid chromatographic analysis (GLC) using a Pye-Unicam gas chromatograph, "104" equipped with a dual flame ionization detector, Model 24, using nitrogen as the carrier gas. The products were characterized by comparison of the GLC retention times with those of authentic samples on two columns with different separation characteristics. The columns used were 5 m × 5 mm and packed with 20% SE 30 on Chromosorb W (35–80 mesh) or 10% SE 30 on celite (60–80 mesh). UV irradiation was carried out using a Mallinkrodt 150 W low pressure mercury discharge lamp and the solutions were contained in open-topped pyrex beakers. TLC was carried out on glass plates coated with silica gel (100–150 mesh) and eluted with ether/petroleum ether (40–60°C) in the ratios quoted in Table 1 and the spots were detected by iodine vapour.

GENERAL PROCEDURE

A mixture of the phenolic compound (0.001 mol) in chloroform (50 mL) and potassium hydroxide (2 g) in water (6 mL) was irradiated for 15 h with vigorous stirring at 25°C. The chlorine gas evolved was detected by turning potassium-iodide starch paper blue and fluorescein paper red[7]. The photolysate was acidified and extracted with ether (3 × 100 mL). The combined ethereal extract was dried (anhydrous $MgSO_4$) and evaporated. The phenolic aldehydes were identified either by their R_f values using TLC as compared with authentic samples or through the formation of their 2,4-dinitrophenylhydrazone derivatives and determination of their m.ps. and m.m.ps. with authentic samples. The quantitative estimation of the yield was done using G.L.C. by comparison with mixtures of known concentrations. In the case of *p*-hydroxydiphenyl, the corresponding aldehyde was estimated as its 2,4-dinitrophenylhydrazone derivative.

PHOTO-FORMYLATION IN PYRIDINE AS A BASIC SOLVENT

p-Cresol (1.1 g) in chloroform (50 mL) and pyridine (10 mL) in water (10 mL) was irradiated with continuous stirring for 15 h at 25°C. Pyridine hydrochloride was detected by silver nitrate test. The photolysate was diluted with water (200 mL) and extracted with ether. The ethereal extract was evaporated to dryness and the residue refluxed with potassium hydroxide solution (10 mL, 20%) for 1 h and the resulting 2-hydroxy-5-methylbenzaldehyde was separated in the form of its 2,4-dinitrophenylhydrazone derivative m.p. and m.mp. 245—247°C.

PREPARATION OF REFERENCE COMPOUNDS

2-Hydroxy-3-methylbenzaldehyde :[8] Crystallised from petroleum ether (60—80°C), m.p. 17°C; 2,4-dinitrophenylhydrazone m.p. 195°C; oxime m.p. 99°C.

2-Hydroxy-4-methylbenzaldehyde [9] : Crystallised from ethanol, m.p. 61—62°C; 2,4-dinitrophenylhydrazone m.p. 260—262°C; oxime m.p. 109°C.

2-Hydroxy-5-methylbenzaldehyde [10] : Crystallised from petroleum ether (60—80°C) m.p. 56°C; 2,4-dinitrophenylhydrazone m.p. 245—247°C; oxime m.p. 150°C.

5-Chloro-2-hydroxybenzaldehyde [10] : Crystallised from ethanol m.p. 100°C; 2,4-dinitrophenylhydrazone m.p. 264°C; oxime m.p. 128°C.

5-Bromo-2-hydroxybenzaldehyde [11] : Crystallised from ethanol m.p. 105°C; 2,4-dinitrophenylhydrazone m.p. 268°C; oxime, m.p. 125—126°C.

5-Nitro-2-hydroxybenzaldehyde [12] : Crystallised from acetic acid m.p. 126°C.

3-Formyl-4-hydroxybiphenyl [13] : Crystallised from ethanol m.p. 102°C; 2,4-dinitrophenylhydrazone m.p. 270°C.

REFERENCES

[1] J. Hine, *J. Amer. Chem. Soc.*, **72**, 2438 (1950).

[2] H. Wynberg, *Chem. Rev.*, **60**, 169 (1960).

[3] J. Hine and J. M. Van der Veen; *J. Amer. Chem. Soc.*, **81**, 6446 (1959); *J. Org. Chem.*, **26**, 1406 (1961).

[4] N. S. Isaacs, "Reactive Intermediates in Organic Chemistry", J. Wiley, London, 1974, p. 297.

[5] G. P. Semeluk and R. B. Bernstein, *J. Amer. Chem. Soc.*, **76**, 3793 (1954); *ibid.*, **79**, 46 (1957); J. R. Plimmer and B. E. Hummer, *J. Agr. Food Chem.*, **17**, 831 (1969); J. P. Plimmer, U. I. Klingebiel and B. E. Hummer, *Science*, **167**, 67 (1970).

[6] Dov. Elad, "Organic Photochemistry", Vol. 1 (O. L. Chapman, ed.), Dekker, New York, 1967, p. 180.

[7] F. Feigl, "Spot Test. Inorganic Applications", Elsevier, London (1954) p. 337.

[8] F. Bell and T. A. Henry, *J. Chem. Soc.*, **1928**, 2222.

[9] O. Anselmino, *Ber.*, **50**, 1395 (1917).

[10] H. Weil, M. Traun and S. Morcel, *Ber.*, **55**, 2664 (1922).

[11] H. H. Hodgson and T. A. Jenkinson, *J. Chem. Soc.*, 3041, **1927**.

[12] V. Miller, *Ber.*, **20**, 1929 (1887).

[13] F. Bell and J. Kengon, *J. Chem. Soc.*, 3047, **1926**.

Revue Roumaine de Chimie, **30**, *8*, 753–755 (1985)

ESTERS FROM N-ACYLPHTHALIMIDES AND PHENOLS

C. I. CHIRIAC
"P. Poni" Institute of Macromolecular Chemistry,
Aleea Gr. Ghica-Vodă 41 A, Iași, Romania

Received November 24, 1984

Various esters were prepared by a condensation reaction between N-acylphthalimides and phenoles in pyridine as solvent at reflux 4–5 hours.

C. Palomo [1] presented in 1981 a direct synthesis of the N-acylphthalimides from phthalimide and carboxylic acids in the presence of diphenyl chlorophosphate as reagent. He tried to use the N-acylphthalimides as reagents for acylation of amines, but he obtained a mixture of compounds in which the presence of the corresponding amide was not detected. We verified this reaction with negative results too.

RESULTS AND DISCUSSION

We tried other nucleophile reagents in the reaction with acylphthalimides. Thus, the phenols can react with acylphthalimides resulting the corresponding esters. For example, in the case of reaction between benzoylphthalimide and phenol, we obtained phenyl benzoate in different solvents at reflux as : dioxane, tetrahydrofurane and pyridine. We have chosen the pyridine, because it is a very good solvent for the products of reaction.

The reactivity of acylphthalimides with phenols at low temperature (115–120°) can be explained by the influence of the three acyl groups at the same nitrogen atom. Tribenzoylamine also presents the same reaction, in pyridine at reflux, with phenol, resulting phenyl benzoate and dibenzoylamine as by-product. The dibenzoylamine is inactive at this temperature.

As a result of these investigations, we propose the following mechanism of reaction :

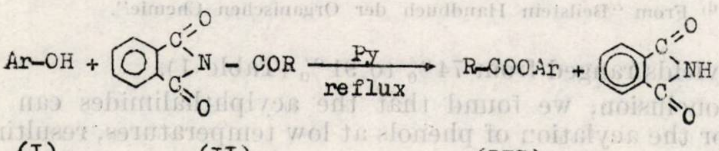

(I) (II) (III)

We supposed, similar as in other cases,[2–5] that this reaction involves a four-centred transition state (IV) :

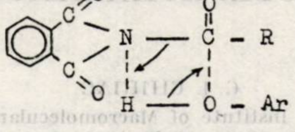

(IV)

In this reaction, phthalimide results as by-product, which was identified by melting point and IR spectra. The phthalimide can be easily recovered and used as starting material for the synthesis of the acylphthalimides(II).

In a typical procedure, to a solution of 1 mole (II) in dried pyridine, 1 mole + 10–15% excess (I) was added under stirring (a small excess improves the yield). Table 1 shows the esters(III) obtained in this way.

Table 1

Esters obtained from acylphthalimides and phenols

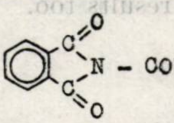	Phenols	Esters[a]		
		Yield[b] %	M.p. [c] °C	Literature m.p. [d] °C
C_6H_5	$C_6H_5-OH_4$	90	68–70	69–71
C_6H_5	p-$Cl-C_6H_4-OH$	81	86–88	86–87
C_6H_5	p-$CH_3-C_6H_4-OH$	74	69–70	70–71
C_6H_5	2-naphthol	85	104–106	105–107
C_6H_5	p-$O_2N-C_6H_4-OH$	83	140–142	141–142
p-$CH_3-C_6H_4$	C_6H_5-OH	78	75–77	76–77[6]
p-$CH_3O-C_6H_4$	C_6H_5-OH	75	74–76	75–76[4]
p-$CH_3O-C_6H_4$	p-$CH_3-C_6H_4-OH$	79	64–66	66–67[6]
CH_3	2-naphthol	91	70–72	70–71
C_2H_5	2-naphthol	88	49–51	50–52

[a] The products were identified by comparison of m.p. and IR spectra with authentic samples.

[b] Yields calculated on acylphthalimide employed.

[c] After recrystallization.

[d] From "Beilstein Handbuch der Organischen Chemie".

The yields ranged from 74% to 91% (Table 1).

In conclusion, we found that the acylphthalimides can be good reagents for the acylation of phenols at low temperatures, resulting esters in high yield.

EXPERIMENTAL

Phenyl benzoate.

A solution of 2.51 g (0.01 mole) benzoylphthalimide and 1.03 g (0.01 mole + 10% excess) phenol in 10 mL dried pyridine was refluxed for 4–5 hours. At the end of reaction, the hot solution (60–80°) was slowly poured into a large volume of water with ice under stirring, when the desired product precipitated. The mixture was treated with 5% NaOH solution till pH = 9–10 and the product was collected by filtration, washed for three times with 15–20 mL water and dried under vacuum at 40–50°. Phenyl benzoate (1.8 g) was obtained with m.p. 68–70° (after recrystallization from ethanol). Yield 90% calculated on benzoylphthalimide employed.

Anal. Found: C, 78.29; H, 5.11%

Calculated for: $C_{13}H_{10}O_2$; C, 78.73; H, 5.05%.

Under similar conditions, the other esters (presented in table 1) were prepared from acylphthalimides and phenols.

REFERENCES

[1] C. Palomo, Synthesis, (1981) 993.
[2] H. O. Becker and K. F. Funk, *J. prakt. Chem.*, **14**, 55 (1961).
[3] C. I. Chiriac, *Rev. Roumaine de Chimie*, **26**, 1001 (1981).
[4] B. Iselin and W. Rittel, *Helv. Chim. Acta*, **40**, 373 (1957).
[5] W. Gerrard and J. A. Cade, *J. Chem. Soc.*, **1954**, 2034.
[6] H. Rheinboldt, *Quimica*, **1951**, (3), 52; *Chem. Abstr.*, **1952**, 7552.

Revue Roumaine de Chimie, **30**, *8*, 757–758 (1985)

STUDIES IN THE SYNTHESIS OF SOME NEW POLYNUCLEAR HETEROCYCLES:

6-Chloro-8,13,dihydro-8,13-o-benzenonaphtho[2,3-a]phenothiazin-7(H) ones

R. L. MITAL *, VINEETA TANEJA, C. L. GUPTA and S. B. GUPTA
Department of Chemistry, University of Rajasthan, Jaipur-302004

Received January 30, 1984

2,3-Dichloro-9,10-dihydro-9,10-o-benzenol-1,4-anthraquinone (I) undergoes condensation with zinc salts of substituted o-amino thiophenols in an equimolar ratio in 95% ethanol to give 6-chloro-8,13-dihydro-8,13-o-benzenonaphtho[2,3-a]phenothiazin-7(H)-ones(IIa-f).

The literature reveals that a few references[1–5] are available for the synthesis of polynuclear heterocycles. This aroused our interest in the synthesis of 6-chloro-8,13-dihydro-8,13-o-benzenonaphtho[2,3-a] phenothiazin-7(H)-ones(II) by a simple procedure and to study the chemistry of these compounds.

2,3-Dichloro-9,10-dihydro-9,10-o-benzeno-1,4-anthraquinone (I; 0.001 mol) underwent condensation with zinc salts of substituted o-aminothiophenols[6,7] (0.0005 mol) to give II in 95% ethanol. The structural assignments of II(a-f) were based on elemental analysis and spectral data. Their IR (KBr) spectra exhibited bands at 3100–3000 (arom. CH),

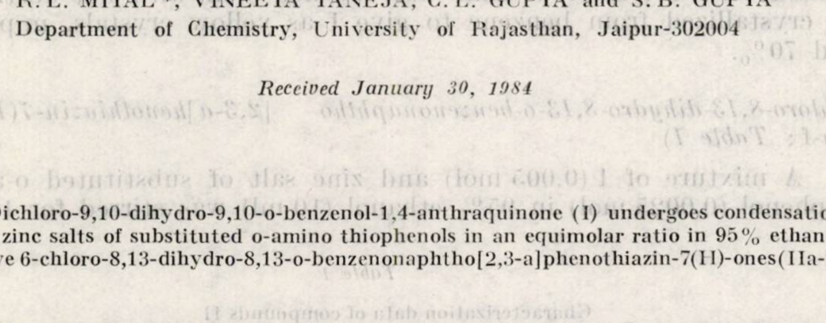

I

II

II, a R_1 = Cl , R_2 = H , R_3 = H
b R_1 = CH_3 , R_2 = H , R_3 = H
c R_1 = H , R_2 = Cl , R_3 = H
d R_1 = H , R_2 = Br , R_3 = H
e R_1 = H , R_2 = CF_3 , R_3 = H
f R_1 = H , R_2 = H , R_3 = CH_3

SCHEME - I

1630—1600, 1600—1590, 1550—1490, 1490—1400, 1390—1340, 1330—1300 (C—C and C—N) and 1380, 1355, 740, 540 cm^{-1} (CF_3, CH_3, Cl and Br). Compounds II(a-f) also exhibited a sharp peak at 1670—1630 cm^{-1} due to C=O group.

2,3-Dichloro-9,10-dihydro-9,10-o-benzeno-1,4-antraquinone (I)

It was prepared by a modification of the reported method.[8] To a boiling solution of anthracene (1.78 g, 0.01 mol) in gl. acetic acid (50 ml) was added chloranil (3.052 g, 0.012 mol) in one lot. The solution became blue green throwing out the yellow product. The reaction mixture was refluxed for 8 hr, filtered while hot, washed well with hot acetic acid and crystallized from benzene to give I as yellow crystals, m.p. 271°, yield 70%.

6-Chloro-8,13-dihydro-8,13-o-benzenonaphtho [2,3-a]henothiazin-7(H) ones (IIa-f; Table 1)

A mixture of I (0.005 mol) and zinc salt of substituted o-aminothiophenol (0.0025 mol) in 95% ethanol (10 ml) was stirred for 1 hr at room temperature and then refluxed for 80 min. The solution was cooled, filtered and washed well with water, 10% aq. HCl, water and finally with dil. ethanol to give II.

Table 1

Characterization data of compounds II

Compound	Yield (%)	Crystallised from	M.P.* °C	Mol. Formula	Found (%)		Calc (%)	
					C	H	C	H
IIa	75	Benzene	154	$C_{26}H_{13}Cl_2NOS$	68.00	2.80	68.12	2.84
IIb	80	Benzene	184	$C_{27}H_{16}ClNOS$	73.92	3.55	73.97	3.65
IIc	70	Benzene	250	$C_{26}H_{13}Cl_2NOS$	68.20	2.80	68.12	2.84
IId	65	Benzene	175	$C_{26}H_{13}BrClNOS$	62.00	2.55	62.03	2.59
IIe	78	Benzene	137	$C_{27}H_{13}F_3NSOCl$	66.30	2.56	66.26	2.66
IIf	60	Benzene	163	$C_{27}H_{16}ClNOS$	73.90	3.70	73.97	3.65

* Melting points are uncorrected.

REFERENCES

[1] J. M. Straley and D. J. Wallace, Brit. Patent, 1.024.654.

[2] M. A. Weaver, J. M. Straley and D. J. Wallace, U.S. Patent, 3, 5 1962.

[3] G. K. Oberoi, Rekha Agrawal and R. L. Mital, *Indian J. Chem.*, **21B** (1982) 584.

[4] N. L. Agarwal and R. L. Mital, *Z. Naturforsch*, **31b** (1976), 106.

[5] R. L. Mital and J. P. Tiwari, *J. Inst. Chem.*, **49** (1977) 286.

[6] S. K. Jain, D. Chandra and R. L. Mital, *Chemy Ind.* (1969) 989.

[7] R. L. Mital and S. K. Jain, *J. Chem. Soc.* (**C**), (1969) 2148.

[8] E. Clar, *Chem. Ber.*, **64B** (1931) 1676; *Chem. Abstr.*, **25** (1931) 5159.

Revue Roumaine de Chimie, **30**, *8*, 759–763 (1985)

STRUCTURAL STUDIES ON IMIDAZOLIDINEACETONITRILE DERIVATIVES

BOGUSŁAW PILARSKI and KRYSTYNA WISTEROWICZ
Department of Organic Chemistry, Medical Academy, 80-416 Gdańsk, ul. K. Marksa 107, Poland

Received February 25, 1984

The structure of seven imidazolidineacetonitrile derivatives were studied by ^{1}H-NMR and IR spectroscopic methods. The 2-ylidene structure has been suggested and for two cyanoesters it has been confirmed by deuteration.

INTRODUCTION

Heterocyclic compounds possessing an active methylene moiety are very interesting from pharmacological and chemical points of view. It is known that heterocyclic compounds with the above mentioned group have an antiinflamatory,[1-2] analgetic [3] and other pharmacological activities.[4]

As a continuation of our interest in the pharmacological activity and chemical properties of heterocycles with active methylene group, the reaction of 2-methylthioimidazoline with active methylene compounds has been studied. The reaction was carried out in two-phase system and the imidazolidineacetonitrile derivatives **1**–**5** obtained were N-alkylated as it has been described in our recent paper.[5]

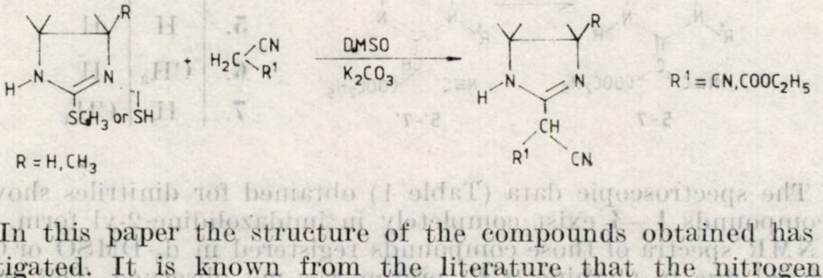

In this paper the structure of the compounds obtained has been investigated. It is known from the literature that the nitrogen six-membered heterocycles with CH/CN/R group can exist in the N–H (ylidene) tautomeric form as reported previously.[6] The ylidene tautomeric form has been described for five membered heterocycles: pyrolidine,[7, 8, 9] oxazole and thiazole,[4] 1,2-benzisothiazole,[9] imidazole.[4]

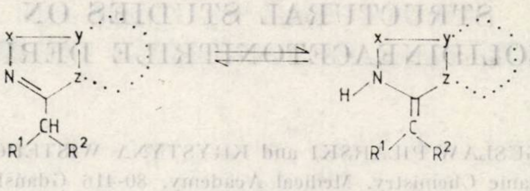

Sandstrom and coworkers [10] studied the ^1H-NMR spectra of several imidazolidine-2-yl -derivatives but in those compounds the tautomerism could not be observed because of the substitution of two nitrogen atoms.

Later on, the *cis-trans* isomerisation of 2-methylpyrrolidine and tetrahydrofurane derivatives has been described [11, 12, 13]; however in that situation it seemed to be of interest to study the structure of the imidazolidine derivatives obtained.

STRUCTURAL INVESTIGATION

Based on the IR and ^1H-NMR spectra, the structure of dinitriles **1 - 4** and cyanoesters **5—7** has been discussed.

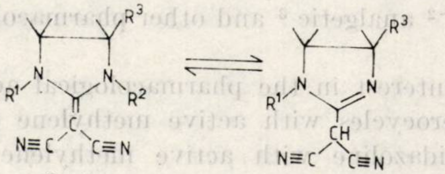

1 - 4 **1'- 3'**

No	R¹	R²	R³
1.	H	H	H
2.	CH_3	H	H
3.	H	H	CH_3
4.	CH_2Ph	CH_2Ph	H

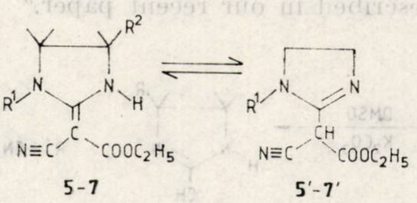

5-7 **5'-7'**

No	R¹	R²
5.	H	H
6.	CH_3	H
7.	H	CH_3

The spectroscopic data (Table 1) obtained for dinitriles show that the compounds **1—4** exist completely in imidazolidine-2-yl form. In the ^1H-NMR spectra of those compounds registered in d_6-DMSO or $CDCL_3$ the signal due to methine (*CH*) proton was not observed. The presence in the ^1H-NMR spectra of compounds **1—3** of a broad signal at about 8 ppm confirms the ylidene /N—H/ structure.

Table 1

Spectroscopic data for compounds **1**—**7**

Compound No	IR ν[cm⁻¹]; KBr				¹H-NMR	
	C≡N	$COOC_2H_5$	C=C	N—H	Solvent	δ p.p.m.; J = [Hz]
1	2180 2200		1600	3260 1600	d_6-DMSO + THF	3.75/4H, s/—NCH_2CH_2N
2	2180br		1560	3260— 3370 1560	d_6-DMSO	3.75/4H, m/—NCH_2CH_2N; 3.2/3H, s/—NCH_3; 8.07/1Hs/br
3	2190br		1600	3250 1600	d_6-DMSO	3.25-4.5/3H, m/; 1.2/3H, d/—HCH_3; J=6; 8.5/2H, d/NH
4	2160 2190		1540		$CDCl_3$	3.3/4H, s/—NCH_2CH_2N; 4.7/4H, s/Z—N—CH_2—Ph; 7.25/10H, s/2Ph
5	2190	1660	1590	3340 3260 1590	$CDCl_3$	3.7/4H, s/—NCH_2CH_2N; 1.2/3H, t/CH_3—CH_2 J=6; 4.1/2H, q/—CH_2—CH_3; J=6 7.0/1H, s/NH br; 6.0/1H, s/NH br
6	2185	1660	1560	3330 3260 1590	$CDCl_3$	3.5/4H, s/—NCH_2CH_2N; 1.15/3H, t/CH_3—CH_2 J=7; 4.05/2H, q/CH_2—CH_3; J=7 8.35/1H, s/NH br.
7	2190	1650	1590	3360 3280 1590	$CDCl_3$	3.0—4.0/4H, m/NCH_2CH—N; 1.1—1.25/6H, m/HCH_3 and CH_3—CH_2— 4.05/2H, q/—CH_2—CH_3; J=7; 6.8/1H, d/NH br; 7.9/1H. d/NH br.

br — broad.

The IR spectra of dinitriles **1**—**4** taken in KBr pellets show a conjugated nitrile split absorption at 2180 and 2190 cm⁻¹. The nitrile split absorption suggests the presence of two different structures in which the nitrile groups are spectrally different. As it is not a result of tautomerism it can be explained by the presence of a dipolar structure typical of nitrile.[10,13,14]

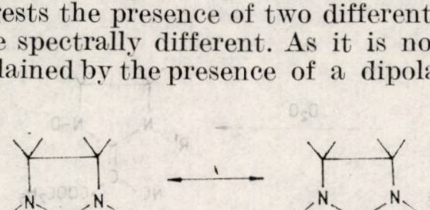

The low barriers to rotation around the carbon-carbon double bond (C=C) are viewed as a consequence of a favourable polar transition state II in which the negative charge is stabilized in the carboanion by nitrile groups.

In the IR spectra of dinitriles **1**—**3** the N—H absorption at 3870—3250 cm^{-1} suggests the intermolecular hydrogen bonding. This absorption was not observed in dibenzyl-**4** derivative.

The symmetrical structure of dinitrile **4** was confirmed by the ^{1}H-NMR spectra. The prochiral substituent ($-CH_2-Ph$) and imidazolidine protons gave a single signal at 3.3 ppm and 4.7 ppm respectively (Table 1).

The spectroscopic analysis of cyanoesters indicates that compounds **5**—**7** possess ylidene structure too. In the ^{1}H—NMR spectra registered in $CDCl_3$ (Table 1) the signal of methine (CH) proton was not detected. The presence of a broad signal at about 8 ppm confirms the N—H structure. These results are in good correlation with the IR spectra taken in KBr pellets. The IR spectra show a conjugated ($=C-C\equiv N$) nitrile band at about 2190 cm^{-1} and the characteristic low frequency of ester carbonyl at 1650 and 1660 cm^{-1}, respectively.

The characteristic low frequency of C=O group can be the result of a conjugation with carbon carbon double bond and on the other hand it suggests the presence of the intramolecular hydrogen bonding between the N—H moiety and ester carbonyl :

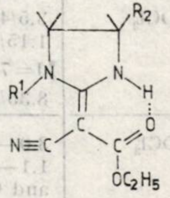

Z-configuration

The intramolecular hydrogen bonding stabilized the ylidene (N—H) form and the Z-configuration of cyanoesters. The stabilization of the ylidene (enamine) form of nitrogen heterocyclic system containing cyanoester group will be the subject of further studies.

The ylidene (enamine) form for compounds **5** and **6** has been confirmed by deuteration.

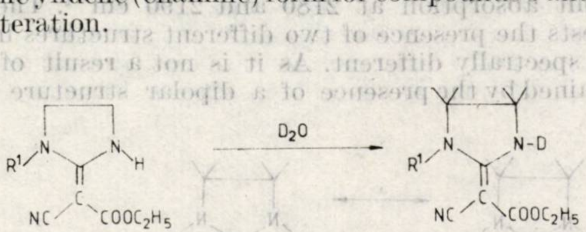

[N-D]-**5**; $R^1 = D$

[N-D]-**6**, $R^1 = CH_3$

Based on the IR spectra of deuterated derivatives [N—D]—**5** and [N—D]—**6** taken in KBr pellets it was found that the N—H absorption bonds were shifted and the $\frac{\nu_{N-H}}{\nu_{N-D}} = 1.35$ what is presented in Fig. 1.

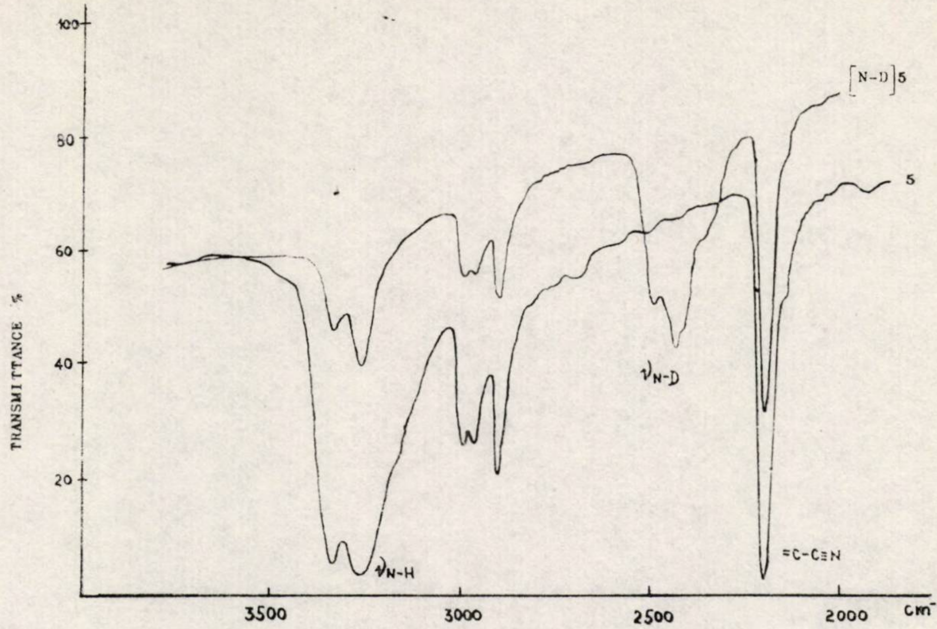

Fig. 1. — IR spectra of compounds **5** and [N—D] **5**.

EXPERIMENTAL

^{1}H-NMR spectra were recorded on Tesla-Brno BS-787 80 MHz spectrometer with H-MDSO as an internal standard. IR spectra were registered on Perkin-Elmer M-357 spectrometer in KBr pellets.

Deuteration exchange

30 mg of compound **5** or **6** were refluxed for 10 hrs with 5 mL D_2O and 5 mL dioxane. Next, the solvents were evaporated to dryness and the products of deuteration were recrystalized from D_2O. The percentage of deuteration was determined by ^{1}H-NMR method (80%).

ACKNOWLEDGMENTS. Authors wish to thank Mrs. E. Kuziak of University of Gdansk for ^{1}H-NMR measurements.

REFERENCES

[1] N. Schwartz and R. J. Mohrbacher, USA Patent 3.901.855 (1975).
[2] W. D. Podmore, *J. Med. Chem.*, **11**, 431 (1968).
[3] G. Nannini, P. N. Giraldi, G. Molgora, G. Biasoli, F. Spinelli, W. Logemann, E. Dradl, G. Zanni, A. Buttioni and R. Tommasini, *Arzneim.-Forsch. (Drug Res.)*, **23**, *8*, 1090 (1973).
[4] G. Satzinger, *Liebigs Ann. Chem.*, **475** (1978).
[5] K. Wisterowicz, H. Foks, *Acta Polon. Pharm.* — in press.
[6] B. Pilarski, H. Foks, K. Ośmialowski, R. Kaliszan, *Monatsh. Chem.* — in press.
[7] B. Thierrichter and H. Junek, *Monatsh. Chem.*, **110**, 729 (1979).
[8] T. Nagasaka, F. Hamaguchi, N. Ozawa and Y. Kosugi, *Heterocycles Jap.*, **14**, 291 (1980).
[9] E. L. C. Carington, K. Clarke, C. G. Huges and R. M. Scrowston, *J. Chem. Soc. Perkin Trans I*, **23**, 3006 (1972).
[10] J. Sandstrom and I. Wennerbeck, *J. Chem. Soc. D*, 1088, **1971**.
[11] N. P. Solovieva, N. B. Martshenko, W. G. Granik and I. N. Sheinker, *Khim. Geterotskl. Soedin.*, **7**, 914 (1982).
[12] J. Shvo and H. Shanan-Atidi, *J. Am. Chem. Soc.*, **91**, 6683 (1969).
[13] C. E. Looney and J. R. Downing, *J. Am. Chem. Soc.*, **80**, 2840 (1958).
[14] G. Scheibe and E. Daltrozzo, *Adv. Heterocycl. Chem.*, **7**, 167 (1966).

NOTE POUR LES AUTEURS

La Revue Roumaine de Chimie publie des articles en anglais, français, russe, allemand ou espagnol. Les auteurs sont priés d'envoyer des articles et des comptes rendus inédits.

Les manuscrits seront dactylographiés à double interligne. La bibliographie, les tableaux et la légende des figures seront placés après le texte.

Si l'article fait partie d'une série numérotée, la partie précédente sera donnée comme première référence.

Chaque article sera précédé d'un résumé comprenant quinze lignes au maximum.

Les références bibliographiques dans le texte seront faites par des exposants sans parenthèses et paraîtront à la fin de l'ouvrage.

Les publications périodiques mentionnées dans la bibliographie seront présentées suivant les prescriptions internationales : le nom de l'auteur précédé de l'initiale du prénom, le titredu périodique abrégé conformément à « Chemical Abstracts » et souligné par une ligne, le numéro du tome indiqué par des chiffres arabes et souligné par deux lignes, suivi de la première page de l'article : à la fin, l'année de la parution sera placée entre parenthèses. Le numéro de la revue ne sera pas indiqué si les pages du volume sont numérotées consécutivement.

Les textes des livres ou traités incluront : le nom des auteurs, l'initiale du prénom, le titre du livre entre guillemets et sans être souligné, le numéro du tome précédé par l'abréviation « vol. » (ou « Bd. »), le numéro de l'édition, les éditions (the publisher), la localité de la parution du livre, l'année de la parution et la page de la référence précédée(s) par l'abréviation « p. » (ou S. »).

Les brevets seront indiqués comme suit : l'auteur ou la firme, le pays et le numéro du brevet, la date et la revue (*Chem. Abstr.*). Par ex. : M. Jones (to Union Carbide Co), Brit. Pat 601 238, 2 Sept. 1959 ; cf. *Chem. Abstr.*, **54**, 12808 (1960).

Si la référence n'a pas été lue en original, on indiquera aussi la revue de référence consultée

Les diagrammes seront tracés à l'encre de Chine sur papier calque. Les tableaux et le figures (en nombre strictement nécessaire) ainsi que les courbes dans les figures seront numérotés par des chiffres arabes. Leur explication sera donnée dans la légende des figures. Prière de ne pas inscrire les mêmes données dans les tableaux et les figures. Chaque tableau aura un titre. On indiquera dans le texte la place approximative des tableaux et des figures. Les formules chimiques seront incluses dans le texte ; en outre, elles seront transcrites sur papier calque, à l'encre de Chine.

Les auteurs sont priés d'indiquer les caractères italiques (en soulignant les lettres au crayon), ainsi que tout autre caractère spécial ; les préfixes *ortho*, *meta*, *para*, *cis*, *trans*, etc. seront soulignés pour indiquer leurs caractères italiques et ne seront jamais écrits avec des majuscules.

Aucune correction à la main ne sera admise sur le manuscrit. Les corrections seront tapées à la machine. Les lettres grecques ou d'autres symboles spéciaux seront insérés à la main à l'encre clairement.

Le manuscrit sera signé par l'auteur.

Le titre-courant aura 50 lettres au maximum.

L'entière responsabilité du contenu des articles appartient aux auteurs.

Sur demande on peut obtenir une note plus complète.

PRINTED IN ROMANIA

1985 SEP 51

TRAVAUX PARUS AUX ÉDITIONS DE L'ACADÉMIE DE LA RÉPUBLIQUE SOCIALISTE DE ROUMANIE

V. DRĂGUŢAN, A. T. BALABAN, M. DIMONIE, **Olefin metathesis and ring-opening polymerization of cyclo-olefins**, coédition avec John Wiley and Sons, 1985, 544 p.

GH. MARCU, **Chimia compuşilor coordinativi**, 1984, 415 p.

E. CORDOŞ, C. MANOLIU, **Spectrometria de absorbţie şi fluorescenţă atomică**, 1984, 178 p.

C. BODEA editeur, **Tratat de biochimie vegetală**, p. I vol. 5, 1984, 438 p.

ELENA CEAUŞESCU, **Cercetări în chimia şi tehnologia polimerilor**, 1983, 519 p.

N. ASANDEI, A. GRIGORIU, **Chimia şi structura fibrelor**, 1983, 395 p.

N. IONESCU, M. CĂLDĂRARU, **Oxidarea catalitică a olefinelor inferioare**, 1983.

C. CAŞCAVAL, **Studiul polimerilor prin piroliză şi cromatografie de gaze**, 1983, 220 p.

C. I. SIMIONESCU, F. DANEŞ, **Originea vieţii**, 1983, 110 p.

C. BODEA (editeur), **Tratat de biochimie vegetală**, p. II, vol. IV, 1982, p. 408.

I. G. MURGULESCU, RODICA VÎLCU, **Introducere în chimia fizică. Vol. III. Termodinamica chimică**, 1982, 624 p.

I. G. MURGULESCU, J. PĂUN, **Introducere în chimia fizică. Vol. I.3 Nucleul atomic, reacţii nucleare, particule elementare**, 1982, 606 p.

ELENA JERCAN, **Analiza cromatografică**, 1982, 286 p.

ELENA CEAUŞESCU, **Noi cercetări în domeniul compuşilor macromoleculari**, 1981, 536 p.

I. G. MURGULESCU, TATIANA ONCESCU, E. SEGAL, **Introducere în chimia fizică, Vol. II.2. Cinematică chimică şi cataliză**, 1981, 1024 p.

LYDIA-MARIA VAICUM, **Epurarea apelor uzate cu nămol activ. Bazele biochimice**, 1981, 218 p.

I. GĂLĂŢEANU, **Procese şi metode radiochimice în energetica nucleară**, 1981, 234 p.

O. IORDACHE, **Procese polistocastice aplicate la fenomenele de transfer**, 1981, 186 p.

CR. SIMIONESCU, VALERIA GORDUZA, **Polimeri biocompatibili şi biologic activi**, 1980, 479 p.

ELENA CEAUŞESCU, **Polimerizarea stereospecifică a izoprenului**, 1979, 307 p.

CONST. GH. MACAROVICI, **Analiza chimică cantitativă anorganică**, 1979, 457 p.

M. FLORESCU, **Metode ştiinţifice în dezvoltarea industriei chimice moderne**, 1979, 256 p.

A. T. BALABAN, I. GĂLĂŢEANU, G. GEORGESCU, LIGIA SIMIONESCU, **Compuşi marcaţi şi radiofarmaceutici cu aplicaţii în medicina nucleară**, 1979, 495 p.

I. G. MURGULESCU, E. SEGAL, **Introducere în chimia fizică. Vol. II. I. Teoria molecular-cinetică a materiei**, 1979, 1036 p.

S. STERNBERG, FL. DANEŞ, **Termodinamica chimică aplicată**, 1978, 400 p.

I. G. MURGULESCU, V. EM. SAHINI, **Introducere în chimia fizică. Vol. I.2. Structura şi proprietăţile moleculare**, 1978, 604 p.

I. ZUGRĂVESCU, MAGDA PETROVANU, **N-ylid chemistry**, coédition avec McGraw-Hill International Book Company, U.S.A., 1977, 396 p.

I. G. MURGULESCU, **Introducere în chimia fizică. Vol. I.1. Atomi, molecule, legătură chimică**, 1976, 560 p.

ELENA CEAUŞESCU, **Research work on synthesis and characterization of macromolecular compounds. Contributions**, 1974, 251 p.

CR. SIMIONESCU, VIORICA RUSAN, V. POPA, **Chimia algelor marine**, 1974, 212 p., 1 pl.

ISSN 0035–4090

I. P. INFORMAŢIA c. 1267

43 426

LEI 40

$ 80 (pour un abonnement annuel)

F 1103 04 T.B.

ACADÉMIE DE LA RÉPUBLIQUE SOCIALISTE DE ROUMANIE

REVUE ROUMAINE DE CHIMIE

R 1985 OKT 1 1

MG

TOME 30

N°s 9—10

Septembre — Octobre 1985

Rev. Roumaine Chim. RRCHAX, **30**, *9—10*, p. 765—890 (1985), Bucarest

EDITURA ACADEMIEI REPUBLICII SOCIALISTE ROMÂNIA

ACADÉMIE DE LA RÉPUBLIQUE SOCIALISTE DE ROUMANIE

COMITÉ DE RÉDACTION

Rédacteur en chef :

I. G. MURGULESCU, membre de l'Académie de la République Socialiste de Roumanie

Rédacteurs en chef adjoints :

A. T. BALABAN et V. EM. SAHINI, membres correspondants de l'Académie de la République Socialiste de Roumanie

Collège de rédaction :

EM. BRATU, ELENA CEAUȘESCU, ECATERINA CIORĂNESCU-NENITZESCU, CR. SIMIONESCU, membres de l'Académie de la République Socialiste de Roumanie ; P. SPACU, membre correspondant de l'Académie de la République Socialiste de Roumanie ; M. BANCIU, M. D. GHEORGHIU, I. HAIDUC, D. I. MARGHIDAN, I. MOLDOVAN, G. NIAC et D. SĂNDULESCU.

La Revue Roumaine de Chimie parait 10 fois par an. Toute commande de l'étranger sera adressée à ROMPRESFILATELIA — sectorul Export-Import Presă, P. O. Box 12—201, télex 10376, prsfi r 78104 Bucarest, Calea Griviței nr. 64—66, Roumanie

Les manuscrits, les livres et les revues proposés en échange, ainsi que toute correspondance seront envoyés à la rédaction

REVUE ROUMAINE DE CHIMIE

125, Calea Victoriei, 79717 Bucarest, Roumanie, téléphone 50 76 80

EDITURA ACADEMIEI REPUBLICII SOCIALISTE ROMÂNIA
125, Calea Victoriei, 79717 Bucarest, Roumanie, téléphone 50 76 80

REVUE ROUMAINE DE CHIMIE

Tome 30, N°s 9—10 Septembre — Octobre 1985

D. OANCEA, V. GOŞA, N. I. IONESCU and D. POPESCU, An experimental method for the measurement of the adiabatic maximum pressure during an explosive gaseous combustion . . . . 767—776

VICTOR DAVID and DAN CIOMARTAN, A method for computing the information entropy of the quantitative analytical data . . . . 777—781

VALENTINA LĂZĂRESCU, M. VASS, J. HERŞCOVICI and ELENA CORLĂTEANU, Potentiodynamic behaviour of raney-copper in potassium hydroxide solutions . . . . 783—790

NICOLETA ŞTEFAN, PETRU FILIP, FILIP CHIRALEU, ILIE G. DINULESCU and MARGARETA AVRAM, Carbocationic rearrangements in dibenzo[*b*, *g*]bicyclo[4.2.0]octa-2,7-diene derivatives . . . . 791—797

C. I. CHIRIAC, Synthesis of amides by a new direct condensation reaction . . . 799—802

R. AGARWAL and P. BAHADUR, Synthesis of diazoketones from β-benzoyl acrylyl chloride and diazoalkanes . . . . 803—806

C. ONISCU, M. MACOVEANU, E. HOROBA, M. COJOCARU and E. POTORAC, The study of the extraction process of vincamine . . . . 807—815

A. K. EL-SHAFEI, A.-B. A. G. GHATTAS and F. A. GAD, Synthesis of some new N-amino-2-pyridone derivatives . . . . 817—822

RODICA VĂŢULESCU, T. BUDIU, GH. MARCU and IRINA PAL, Heteropolytungstates with Ti(IV) and Ni(II). III. The absorption spectra of the heteropolyanions Ni(II)-undecatungstotitanate(IV) and Ni(II)-pentatungstotitanate(IV). . . . . 823—830

RODICA VĂŢULESCU, T. BUDIU, GH. MARCU and IRINA PAL, Heteropolytungstates with Ti(IV) and Ni(II). IV. The thermal behaviour of the potassium salt of the Ni(II)-undecatungstotitanate(IV) anion. . . . . 831—836

P. SPACU, SILVIA PLOŞTINARU, LUMINIŢA PATRON, ADRIANA CONŢESCU and N. STĂNICĂ, Coordination compounds as raw materials for mixed oxides. II. Mixed coordination compounds of lanthanides and Co(II) with derivatives of acetic acid . . . . 837—842

CONSTANTIN LUCA and MOHAMED MAGDI KHALIL, Extraction equilibria of some complex combinations with macrocyclic ligands . . . . 843—850

I. TĂNASE, I. IONECI and C. LUCA, Determination of ethylmercuric compounds by phase-sensitive sinusoidal alternating current polarography . . . . 851—858

G. BOURCEANU, E. GRUNICHIEVICI et M. BOURCEANU, Increase of the free surface energy of terephthalate polyethylene sheets by activation in high frequency plasma (in French) . . . . 859—864

Rev. Roumaine Chim. | **30**, *9—10*, 765 — 890 (1985), Bucarest

C. ANDREI, I. HOGEA and V. DOBRESCU, Photodegradation and photostabilization of the ethylene-vinyl acetate copolymers. I. Aspects of the mechanism of photodegradation reactions 865–873

AURORA SALLO and ANCA TOMESCU, Micellar effects upon the azocoupling reaction 875–881

ORTANSA LANDAUER, CORNELIA MATEESCU and OLGA IULIAN, Influence of solvent on the reaction rate. Alkaline hydrolysis of n-butyl acetate, propionate, butyrate in the water-monoethylenglycol mixed solvent (in French). 883–888

BOOK REVIEWS 889–890

Revue Roumaine de Chimie, **30**, *9–10*, 767–776 (1985)

AN EXPERIMENTAL METHOD FOR THE MEASUREMENT OF THE ADIABATIC MAXIMUM PRESSURE DURING AN EXPLOSIVE GASEOUS COMBUSTION

D. OANCEA*, V. GOȘA**, N. I. IONESCU** and D. POPESCU**

* The Polytechnic Institute, Department of Physical Chemistry and Electrochemical Technology, Blvd. Republicii 13, Bucharest, Romania

** Center of Physical Chemistry, Spl. Independenței 202, Bucharest 77208, Romania

Received July 25, 1984

When a gaseous explosive mixture confined in a cylindrical vessel is centrally ignited, the pressure at the end of combustion, p_e, is linearly correlated with the initial pressure, p_0, at least for a narrow range of initial pressures ($p_0 \div 3p_0$). Theoretical derivation of this correlation, associated with the possibility to calculate the heat losses at the end of combustion, allowed the determination of the adiabatic maximum pressure from the analysis of several pressure-time curves obtained during the explosive combustion, starting from various initial pressures.

INTRODUCTION

The adiabatic maximum pressure (AMP) attained during an explosive combustion of a gaseous mixture confined in a constant volume vessel is a valuable property of both theoretical and practical utility, constituting a basic parameter required to design the equipment containing explosive mixtures, as well as its safety devices. A number of procedures allowing the calculation of the normal burning velocity are also bound up with the knowledge of AMP. [1] As the measured maximum pressure is always lower than the adiabatic value on account of the inherent heat losses, AMP can be obtained, as a rule, on the basis of chemical equilibrium calculations.[2] On the other hand, all these thermodynamic calculations are restricted by the assumption that the chemical equilibrium is completely reached during the combustion process, although this cannot be always true or proved. In addition, the calculated values are strongly dependent on the precision of the thermochemical input data.[2]

A reference experimental value of AMP is consequently worth being obtained. In this paper, a simple method of determining the AMP is proposed, based on the analysis of the laminar combustion process in a closed vessel and the interpretation of the pressure-time curves.

1. THE PHYSICAL MODEL OF THE LAMINAR COMBUSTION IN A CLOSED VESSEL

When an explosive gaseous mixture confined in a spherical closed vessel is centrally ignited, the combustion wave propagates isotropically from the ignition point toward the wall, as a spherical combustion wave.[3] As a result of the burning process, a continuous increase of the pressure results, from the initial value, p_0, to a maximum value, p_{max}, followed by a pressure decrease as a result of the cooling process. Under ideal adiabatic conditions, this maximum pressure would remain constant and would represent an intrinsic property of the explosive mixture (curve *a*, figure 1). Actually, when the combustion wave is close to, or in direct contact with the wall, the heat transfer toward the wall results in the decrease of the flame temperature and consequently of the pressure. A limiting case can be conceived, when the flame front reaches the entire inner surface of the vessel at the same time and the thermal losses begin only after the combustion was already completed (curve *b*, figure 1). In this case, the maximum pressure would stil stand for the AMP. There are, however, several unavoidable phenomena which locate the beginning of the thermal losses before the end of combustion, and the measured maximum pressure is therefore lower than AMP (curve *c*, figure 1). The lowering of the maximum explosion pressure, caused by the thermal losses, is larger when the symmetry of the vessel is lower and when the ignition occurs more eccentrically.

The analysis of the experimental results obtained by different investigators indicates that,[3] even when spherical vessels with central ignition are used, significant thermal losses can be noticed before the end of combustion,[4] either directly or in connection with other observable characteristics of the explosive combustion. The most significant observations revealing the existence of thermal losses are : a) the maximum explosion pressure is dependent upon the size of the spherical vessel,[5] although under the same initial conditions of composition, pressure and temperature, the adiabatic explosion pressure must be the same, irrespective of the volume ; b) the maximum explosion pressure is a function of the degree of turbulence[5] ; c) the pressure-time curve exhibits an inflection point before the maximum pressure is attained[4,6] (curve *c*, figure 1). If the thermal losses would begin after the end of combustion, this curve should exhibit a turning (or break) point instead (curve *b*, figure 1). There are several different mechanisms concerning the heat transfer during the combustion process : 1) radiant energy losses ; 2) heat transfer from the

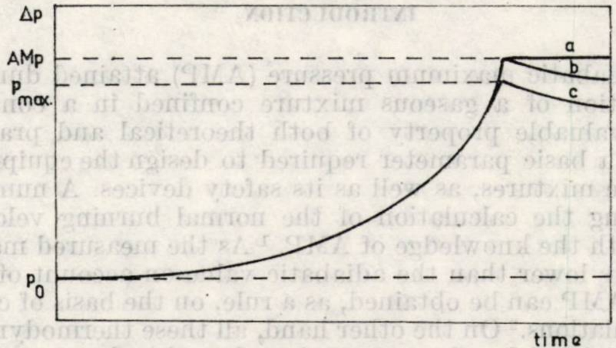

Fig. 1. — Ideal (*a* and *b*) and real (*c*) pressure-time curves during the explosive combustion in a spherical bomb.

unburned gas which is compressed and hence heated; 3) heat transfer from the burned gas in contact with the wall, before the combustion was completed, representing the main contribution to the overall thermal loss. Following this last mechanism, a fraction of heat will be transferred to the electrodes of the initiation source from the beginning of the combustion.

It is obvious that the eccentricity of the ignition point on the one hand, and the natural convection of the flame, accompanied by the loss of the flame sphericity, on the other, will increase the heat losses before the end of combustion. It must be also noticed that owing to the increased pressure, a relatively small volume of the unburned gas contains before the end of combustion an appreciable fraction of the explosive gas, burning while part of the flame front is already in contact with the wall.

When the combustion vessel is no longer spherical, the thermal losses before the end of combustion are larger than in a spherical one of the same volume, and the maximum pressure is smaller. [7] On the other hand, the increased heat losses in a non-spherical vessel can be measured easier under some favourable circumstances. The use of relatively small and symmetrical cylindrical vessels (having the height equal to the diameter) simplifies the calculation of the heat losses, avoiding the natural convection of the flame and preserving a high degree of symmetry.

The measured maximum pressure, $p_{\max}$, attained during an explosive combustion in a closed vessel was found to increase linearly with the initial pressure, p_0, irrespective of the vessel shape. [7] Such a dependence was also found for the thermodynamically calculated maximum pressure. [8] For several cylindrical vessels, we have found the following correlation equation:

$$p_{\max} = ap_0 - b \tag{1}$$

where the parameters a and b are positive and are functions of the mixture composition, initial temperature T_0 and the shape of the vessel. On the other hand, the maximum pressure, $p_{\max}$, does not necessarily coincide with the pressure at the end of combustion, p_e. Although $p_{\max}$ can be measured easier on the pressure-time curve, p_e has a simpler physical meaning and will be consequently used in the following discussion. Using small and symmetrical cylindrical vessels, it was easy to identify p_e on the pressure-time curves. We have also found that p_e is equally well linearly correlated with p_0:

$$p_e = a'p_0 - b' \tag{1'}$$

The model proposed in this paper for the determination of AMP was derived from the interpretation of parameters a' and b' in equation (1') on the basis of the heat balance during the combustion.

2. DERIVATION OF EQUATION (1')

Let us consider an explosive mixture containing a carburant, oxygen and nitrogen, confined in a closed vessel of volume V_0, at an initial pressure p_0 and temperature T_0. The mixture contains n_0 moles and its composition can be given by the volume fraction of each component, r_j. At the end of the combustion, the pressure is p_e and the temperature is $\bar{T}_e$. The mean value for the end temperature is used instead of T_e, because at the end of combustion in a closed vessel a temperature gradient generally exists.[9] Taking into account that the combustion occurs at constant volume V_0, the end temperature will be designed as $\bar{T}_{e,V}$.

As a result of the combustion reaction, the final number of moles n_e is generally different from n_0. Assuming that the law of ideal gases is valid, the following state equations can be written:

$$p_0 V_0 = n_0 R T_0 \tag{2}$$

$$p_e V_0 = n_e R \bar{T}_{e,V} \tag{3}$$

If $\xi = n_e/n_0$ is the molar ratio of combustion, from equations (2) and (3) results:

$$\bar{T}_{e,V} = \frac{T_0}{\xi} \frac{p_e}{p_0} \tag{4}$$

Under adiabatic conditions at constant volume, the heat balance gives:

$$(q_c)_V = (q_{ph})_V \tag{5}$$

where $(q_c)_V$ is the heat evolved during the combustion at constant volume and $(q_{ph})_V$ is the physical heat absorbed by the end products to increase their temperature from T_0 to $\bar{T}_{e,V}$.

If n_1 is the number of moles corresponding to the limiting component of the mixture (the component with a concentration lower than the stoichiometric one) and ν_l its stoichiometric coefficient, then $(q_c)_V$ is:

$$(q_c)_V = n_1 \Delta_c U'/\nu_l = n_0 r_1 \Delta_c U'/\nu_l \tag{6}$$

where $\Delta_c U'$ is the molar heat of combustion (at constant volume and at T_0), corrected for the heat used by the endothermic reactions associated with the combustion at the end temperature. On the other hand:

$$(q_{ph})_V = n_e \bar{C}_{e,V} \cdot \Delta T = n_e \bar{C}_{e,V}(\bar{T}_{e,V} - T_0) \tag{7}$$

where $\bar{C}_{e,V}$ is the molar heat capacity of the end mixture at constant volume, averaged for the end components and for the temperature range T_0 to $\bar{T}_{e,V}$. From the above equations it is easy to obtain:

$$p_e = p_0 \left(\xi + \frac{r_1}{\nu_l} \cdot \frac{\Delta_c U'}{\bar{C}_{e,V} T_0} \right) = k_{a,V} \cdot p_0 \tag{8}$$

If ξ, $\Delta_c U'$ and $\bar{C}_{e,V}$ are independent of p_0 (or their variations compensate each other) within a restricted initial pressure range, equation (8) is a form of the well known thermodynamic correlation equation,[8] $p_e = k_{a,V} \cdot p_0$, where $k_{a,V}$ is the adiabatic coefficient of the pressure increase during the combustion at constant volume.

Under nonadiabatic conditions, when a heat quantity q_{tr} is transferred to the cell before the end of combustion, the heat balance gives :

$$(q_c)_V = (q_{ph})_V + q_{tr} \tag{9}$$

which can be written as :

$$p_e = k_{a,V} \cdot p_0 - q_{tr} \frac{R}{\bar{C}_{e,V} \cdot V_0} \tag{10}$$

where R is the molar constant of ideal gas.

Taking $R = \bar{C}_{e,P} - \bar{C}_{e,V}$, equation (10) becomes :

$$p_e = k_{a,V} \cdot p_0 - q_{tr} \frac{\gamma_e - 1}{V_0} \tag{11}$$

where $\gamma_e = \bar{C}_{e,P}/\bar{C}_{e,V}$ is the adiabatic compression coefficient of the end products.

The resulted equations (10) or (11) have the form given by the experimental correlation (eqn. 1′) in two cases :

1) when q_{tr} is a constant quantity for a given range of initial pressures p_0.

2) when q_{tr} is a linear function of p_0 :

$$q_{tr} = \alpha p_0 + \beta \tag{12}$$

As our measurements indicated, a correlation given by equation (12) seems to describe better the heat losses during the combustion. The measurements of the heat losses were possible on the basis of the interpretation of pressure-time curves, associated with the location of the flame front at different instants, using ionization gauges. A pressure-time curve and its first derivative is given in figure 2.

It can be seen that the end of combustion, indicated by the ionization gauge is not associated with the attainment of the maximum pressure. After the pressure reaches a maximum (point A), the cooling curve exhibits an inflection point (B) which can be easier localized by the minimum of the first derivative (C), which coincides with the end of combustion. As a matter of fact, the maximum pressure reached in A reflects the equality between the pressure increase due to the burning of a small fraction of the remained unburned mixture and the pressure decrease due to the cooling of the burned mixture, in contact with the wall.

The experimental results indicated that the derivatives $(\mathrm{d}p/\mathrm{d}t)_e$ at the end of combustion are also linearly correlated with the initial pressure, p_0:

$$-\left(\frac{\mathrm{d}p}{\mathrm{d}t}\right)_e = -\dot{p}_e = mp_0 + n \tag{13}$$

The heat transferred to the vessel, q_{tr}, from the beginning of the heat loss to the end of combustion can be calculated from the measurable values, $-\dot{p}_e$, as follows. The rate of the gas pressure decrease when the gas is confined in a closed vessel of volume V_0 at a pressure p and a temperature T, as a result of the heat transfer to the vessel having a temperature $T_0 < T$ is given by:

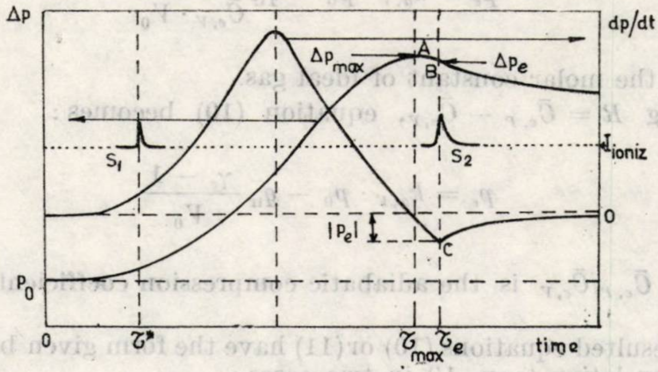

Fig. 2. — Pressure-time curve for an explosion occurring in a cylindrical bomb, its first derivative and signals of the ionisation gauges. S_1 is the signal of the ionization gauge placed on the nearest wall and S_2 — in the top corner. $\Delta\tau_e$ was calculated as $\tau_e - \tau^*$.

$$\frac{\mathrm{d}p}{\mathrm{d}t} = n_e \frac{R}{V_0} \cdot \frac{\mathrm{d}T}{\mathrm{d}t} \tag{14}$$

On the other hand, the heat loss at the end of combustion is given by:

$$q_{\mathrm{tr}} = n_e \overline{C}_{e,V}(\overline{T}_{e,V} - T) \tag{15}$$

Taking the first derivative of eqn. (15) with respect to time, eqns. (14) and (15) lead to

$$\frac{\mathrm{d}q_{\mathrm{tr}}}{\mathrm{d}t} = q_{\mathrm{tr}} \frac{1}{C_{e,V}} \cdot \frac{\mathrm{d}\overline{C}_{e,V}}{\mathrm{d}t} - \frac{V_0}{\gamma_e - 1} \cdot \frac{\mathrm{d}p}{\mathrm{d}t} \tag{16}$$

The first term of the right member in eqn. (16) is generaly less than 2% from the second one and can be neglected. This approximation will be substantiated later on the basis of the experimental results,

At the end of combustion, eqn. (16) becomes:

$$\left(\frac{\mathrm{d}q_{\mathrm{tr}}}{\mathrm{d}t}\right)_e = -\frac{V_0}{\gamma_e - 1}\,\dot{p}_e \tag{17}$$

The heat loss at the end of combustion occurs through the whole surface of the cell (S), while from the beginning of the heat loss, the surface of the cell in direct contact with the flame front increases progressively from zero to S. If we take a mean surface $\bar{S}$ and put $\sigma = \bar{S}/S$, integration of eqn. (17) yields

$$q_{\mathrm{tr}} = -\frac{V_0}{\gamma_e - 1}\cdot \dot{p}_e \sigma \Delta\tau_e \tag{18}$$

where $\Delta\tau_e$ is the time from the beginning of the heat loss to the end of combustion, and $\dot{p}_e$ was considered to be the same within the range $\Delta\tau_e$.

Introducing this result into eqn. (11), we get:

$$p_e = k_{a,V}\cdot p_0 + \dot{p}_e\cdot \sigma\cdot \Delta\tau_e \tag{19}$$

where $\Delta\tau_e$, taken as the time of the heat loss (starting from the moment when the flame front is in contact with the nearest part of the cell to the end of combustion), is a constant within the range of experimental errors, for a relatively narrow range of initial pressures.

Equation (19) can be used to obtain $k_{a,V}$ from a measured set of values of p_0, p_e and $\dot{p}_e$ in two different ways:

1) introducing the correlation parameters a' and b' from eqn(1′) and m and n from eqn. (13) into eqn. (19), $k_{a,V}$ is obtained as:

$$k_{a,V} = a' + b'\frac{m}{n} \tag{20}$$

2) rearranging eqn. (19), we get:

$$\frac{p_e}{|\dot{p}_e|} = k_{a,V}\cdot\frac{p_0}{|\dot{p}_e|} - \sigma\cdot\Delta\tau_e \tag{21}$$

where $|\dot{p}_e|$ is the absolute value of $\dot{p}_e$. It can be seen that $k_{a,V}$ and the product $\sigma\cdot\Delta\tau_e$ can be obtained as the slope and the intercept, respectively, of the linear correlation between the measurable quantities $p_e/|\dot{p}_e|$ and $p_0/|\dot{p}_e|$.

Although the maximum explosion pressure is always higher than the end pressure, the experimental data indicated that $k_{a,V}$ calculated from eqns. (20) or (21) is practically the same as $k_{a,V}$ calculated from the similar correlations :

$$k_{a,V} = a + b\frac{m}{n} \tag{20'}$$

or

$$\frac{p_{\max}}{|\dot{p}_e|} = k_{e,V} \cdot \frac{p_0}{|\dot{p}_e|} - \sigma \cdot \Delta\tau_{\max} \tag{21'}$$

EXPERIMENTAL

The experiments were carried out in a cylinder-shaped stainless steel bomb with $V_0 = 1.7 \cdot 10^{-4} \mathrm{m}^3$ and $\Phi = h = 6 \cdot 10^{-2}$ m, designed to have a minimum dead space. Other details regarding the obtaining of the explosive mixtures and the operating mode were given elsewhere.[10] The derivative of the pressure-time curve was obtained from the main signal of the pressure transducer by means of a shielded RC circuit (with $\mathrm{RC} = 3.4 \times 10^{-4}$s) and monitored on the second channel of the oscilloscope.

The flame front position at different instants was monitored by means of several ionization gauges mounted on the internal surface of the bomb (at the minimum distance from the initiation point and in the top, respectively, the bottom corners). Their signals were monitored alternatively, in different runs, on the second channel of the oscilloscope.

RESULTS AND DISCUSSION

The experimental results are exemplified in tables 1 and 2, for an explosive mixture containing propylene, oxygen and nitrogen.

Table 1

Experimental results for the explosive combustion of a stoichiometric $C_3H_6 - O_2 - N_2$ mixture (5.41% C_3H_6 ; 24.27% O_2 ; 70.32 % N_2)

No.	$p_0 \cdot 10^{-4}$ (Pa)	$p_{\max} \cdot 10^{-5}$ (Pa)	$p_e \cdot 10^{-5}$ (Pa)	$-\dot{p}_e \cdot 10^{-6}$ $(\mathrm{Pa} \cdot \mathrm{s}^{-1})$	$\Delta\tau_e \cdot 10^2$ (s)
1	4.79	4.23	4.18	9.70	1.07
2	6.15	5.61	5.51	10.35	1.07
3	7.57	6.96	6.86	11.83	1.05
4	8.84	8.18	8.08	13.01	1.06
5	10.12	9.41	9.31	14.32	1.08
6	11.39	10.74	10.64	14.79	1.06

From the given data it can be seen that the reliability of the model is well supported by the good agreement between the measured and calculated values of $k_{a,V}$ on the one hand, and by the good correlation coefficients, on the other. If the mean measured value, $k_{a,V} = 10.42$, is compared with the calculated value[8] : $k_{a,V}^{\mathrm{calc}} = 10.29$, a difference of $\simeq 1.5$ % is obtained. At the present time, it is difficult to decide if this difference originates in an overestimation of the experimental value, or in an underesti-

Table 2

Correlation parameters obtained from different equations

Eqn. no.	Slope	Intercept	r_n	$k_{a,V}$
1	9.78	$-4.38 \cdot 10^4$ (Pa)	0.9998	10.42
1′	9.72	$-4.86 \cdot 10^4$ (Pa)	0.9998	10.44
13	81.56 (s^{-1})	$5.57 \cdot 10^6$ (Pa. s^{-1})	0.9850	—
21	10.41	$-8.50 \cdot 10^{-3}$ (s)	0.9998	10.41
21′	10.44	$-7.90 \cdot 10^{-3}$ (s)	0.9999	10.44

mation of the thermodynamically calculated value, due to possible kinetic limitations. From the given results, a reasonable value of the ratio $\sigma = \bar{S}/S$ is also obtained ($\sigma \simeq 0.8$) when the product $\sigma \cdot \Delta\tau_e = 8.50 \cdot 10^{-3}$s is divided by $\Delta\tau_e = 1.06 \cdot 10^{-2}$s.

The usefullness of the proposed method is obvious when it is applied to mixtures having a very complex or even an unknown composition, as well as in the cases when there are kinetic limitations during the combustion process[8].

With the obtained results, the approximation made in eqn. (16) can now be justified using finite differences and observing that it can be written in the following equivalent form:

$$\frac{\Delta\bar{C}_{e,V}}{\bar{C}_{e,V}} \ll 1 \tag{22}$$

where $\Delta\bar{C}_{e,V}$ is the difference between the mean molar heat capacity at the end temperature in adiabatic conditions, i.e. at $T_e = T_0 \cdot k_{a,V}/\xi$, and at the end temperature in nonadiabatic conditions, i.e. at $T'_e = \frac{T_0}{\xi} \cdot \frac{p_e}{p_0}$. For $\xi \simeq 1$, taking the mean heat capacities for the given mixture, one obtains $\Delta\bar{C}_{e,V}/\bar{C}_{e,V} \leqslant 0.02$. In this case, the neglected term is at most 2% from the significant one.

CONCLUSIONS

The adiabatic maximum pressure attained during an explosive combustion in a closed vessel can be measured from a set of several pressure-time curves corresponding to different initial pressures, using the linear correlation between the end and initial pressures and the first derivatives of the pressure-time curves.

REFERENCES

[1] C. J. Rallis and G. E. B. Treemer, *Combust. Flame*, **7**, 51 (1963).

[2] D. D. Agrawal, S. P. Sharma and C. P. Gupta, *J. Inst. Fuel.*, **45**, 43 (1972).

[3] B. Lewis and G. von Elbe, "Combustion, Flames and Explosions of Gases", Academic Press Inc., New York, 1961, p. 367.

[4] S. Crescitelli, G. Russo and V. Tufano, *Arch. Termod. Spalania*, **10**, 465 (1979).

[5] G. Harris, *Combust. Flame*, 11, 17 (1967).

[6] H. E. Perlee, F. N. Fuller and C. H. Saul, U. S. Bureau of Mines Report Investig. no. 7839/1974.

[7] J. C. Leyer, *Rev. Gen. de Thermique*, **98**, 121 (1970).

[8] D. Geană, D. Popescu, M. Mihai and L. Adomnică, *Rev. Chimie* (Bucharest) (to be published).

[9] B. Lewis and G. von Elbe, "Combustion, Flames and Explosions of Gases", Academic Press Inc., New York, 1961, p. 597.

[10] D. Popescu, D. Oancea, V. Goşa, N. I. Ionescu and B. Albu, *Rev. Roumaine Chim.*, **29**, 253 (1984).

Revue Roumaine de Chimie, 30, *9—10*, 777—781 (1985)

A METHOD FOR COMPUTING THE INFORMATION ENTROPY OF THE QUANTITATIVE ANALYTICAL DATA

VICTOR DAVID and DAN CIOMARTAN*

Center of Protection and Hygiene, Str. Pop de Băsești, 59, Sect. 2, Bucharest, Romania
* I.C.P.T.S.C.F., Bd. Chimiștilor, 299—301, Sect. 3, Bucharest, Romania

Received October 20, 1984

A new method for computing the information entropy amount of quantitative analytical results, a priori to an analytical experiment, is proposed, depending on the standard deviation, the concentration domain of analytes and the concentration interval fitted to a given value. By this method, it is found that analytical results of maximum information entropy can a priori to the experiment be known, and a new formula for this entropy is given.

1. INTRODUCTION

An analytical measuring system behaves as a communication system; this system transmits analytical chemical information relating to a sample or a system of samples to be measured. This information has the meaning of lowering in uncertainty with regard to the qualitative and/or quantitative composition of an analytical sample. The problem of measuring the information amount that can be obtained from an analytical measuring system is discussed in a large number of works, e.g.[1-5] The aim of this paper is to suggest a new method for computing the information entropy of the quantitative analytical data, a priori to an analytical experiment.

2. THEORY

For a quantitative analysis, in the conditions of eliminating the systematic errors, there are two kinds of uncertainties about its results, a priori to the experiment :

— uncertainty with regard to the mean value of concentration or to the concentration interval, Δ_c, situated into a concentration domain in which the mean value of concentration of the expected component will be found ;

— uncertainty with regard to the precision of results, i.e. the deviation probability of the experimental results from the mean value. However, there is a possibility as an analytical experiment to be led a pre-established standard deviation σ ; this can be achieved by changing of the parameters which influence the experiment.

A priori to the experiment, the real concentration of an analyte, i, denoted by $\bar{c}_i$, from a given sample, is situated in the concentration domain $[c_{i1}, c_{i2}]$. Let $c_i \pm n\sigma_i$ be denoted by for the interval in which the obtained results can vary with a pre-established standard deviation σ_i. In this manner, the interval $[c_{i1}, c_{i2}]$ can be divided in $s = \frac{(c_{i2} - c_{i1})}{2n\sigma_i}$ number of intervals, $2n\sigma_i$ being thus the measure of an interval. A priori to the experiment, the probability as one of the s intervals to be obtained is given by this simple relation:

$$p'_{ik} = \frac{2n\sigma_i}{(c_{i2} - c_{i1})} \tag{1}$$

The probability as an obtained result denoted by c_i, to deviate from the real value $\bar{c}_i$ is a Gauss function:

$$f(c_i, \bar{c}_i, \sigma_i) = \frac{1}{\sigma_i\sqrt{2\pi}} \exp\left[-\frac{(c_i - \bar{c}_i)^2}{2\sigma_i^2}\right] \tag{2}$$

A priori to an experiment, we can compute the probability as the obtained results $c_i \in [c_{i1}, c_{i2}]$ to be situated in an interval $\bar{c}_i \pm n\sigma_i$:

$$p''_i = \int_{\bar{c}_i - n\sigma_i}^{\bar{c}_i + n\sigma_i} f(c_i, \bar{c}_i, \sigma_i)\,\mathrm{d}c_i = \frac{1}{\sigma_i\sqrt{2\pi}} \int_{\bar{c}_i - n\sigma_i}^{\bar{c}_i + n\sigma_i} \exp\left[-\frac{(c_i - \bar{c}_i)^2}{2\sigma_i^2}\right] \mathrm{d}c_i \tag{3}$$

By changing the variable, $z_i = \frac{c_i - \bar{c}_i}{\sigma_i}$, the integral (3) becomes:

$$p''_i = 2\left\{\frac{1}{\sqrt{2\pi}} \int_0^n \exp\left(-\frac{z^2}{2}\right)\mathrm{d}z\right\} = 2F_L(n) \tag{4}$$

Therefore, the probability p''_i is a Laplace function, $F_L(n)$, which can be known when n is established. This probability does not depend on the standard deviation σ_i, but only on n, which can be established a priori to the experiment.

Thus, the probability as a result of an experiment, c_i, to belong to an interval $\bar{c}_i \pm n\sigma_i$ and at the same time, this interval to represent the real value of the concentration, becomes:

$$p_{ik} = p'_{ik}p''_i = \frac{4n\sigma_i}{(c_{i2} - c_{i1})} F_L(n),\ k = 1, 2, \ldots, s \tag{5}$$

The information entropy of analytical results is computed using Shannon's formula[6]:

$$H_i = -\sum_{k=1}^{s} p_{ik} \log_2 p_{ik} \tag{6}$$

Using p_{ik} given by formula (5), the relation (6) is obtained in the form:

$$H_i = 2F_L(n) \log_2 \frac{(c_{i2} - c_{i1})}{4n\,\sigma_i F_L(n)} \tag{7}$$

In the case of the analysis of N components from a sample, the value of information entropy of analytical results can be computed by the relation:

$$H = \sum_{i=1}^{N} H_i = 2F_L(n) \sum_{i=1}^{N} \log_2 \frac{(c_{i2} - c_{i1})}{4n\,\sigma_i F_L(n)} =$$

$$= 2F_L(n) \log_2 \prod_{i=1}^{N} \frac{(c_{i2} - c_{i1})}{4n\,\sigma_i F_L(n)} \tag{8}$$

When all components have the same concentration domain, i.e. $(c_{i2} - c_{i1}) = (c_2 - c_1)$, $i = 1, \ldots, N$, the formula (8) becomes:

$$H = 2F_L(n) \log_2 \frac{(c_2 - c_1)^N}{4nF_L(n)} \prod_{i=1}^{N} \sigma_i^{-1} \tag{9}$$

From formula (7) it results that H_i increase with the increase of domain $(c_{i2} - c_{i1})$ and with diminution of σ_i. In dependence on n, H_i has a maximum point, as it can be seen from table 1.

Table 1

Some values of information entropy amount H computed for different concentration domains c_1, c_2 and standard deviation

			$c_2 = 10c_1$	H(bits)	$c_2 = 10^2 c_1$	H(bits)	$c_2 = 10^3 c_1$	H (bits)
n	$F_L(n)$	p''	$\sigma = \frac{1}{10} c_1$	$\sigma = \frac{1}{100} c_1$	$\sigma = \frac{1}{10} c_1$	$\sigma = \frac{1}{100} c_1$	$\sigma = \frac{1}{10} c_1$	$\sigma = \frac{1}{100} c_1$
0,25	0.0987	0.1974	1.32	2.60	2.62	3.28	3.28	3.94
0.50	0.1915	0.3830	3.02	4.29	4.34	5.61	5.62	6.51
0.75	0.2734	0.5468	3.71	5.52	5.60	7.41	7.42	9.24
1.00	0.3413	0.6826	4.13	6.39	6.49	8.75	8.76	11.03
1.25	0.3944	0.7888	4.35	6.97	7.08	9.70	9.71	12.33
1.50	0.4332	0,8664	4.43	7.30	7.43	10.31	10.31	13.19
1.75	0.4599	0,9198	4.42	7.47	7.60	10.66	10.66	13.72
2.00	0.4772	0,9544	4.35	7.52	7.65	10.82	10.84	14.00
2.25	0.4878	0,9756	4.25	7.49	7.63	10.87	10.88	14.12
2.50	0.4938	0.9876	4.14	7.42	7.55	10.83	10.85	14.13
2.75	0.4970	0.9940	4.02	7.32	7.45	10.75	10.77	14.07
3.00	0.4987	0.9974	3.90	7.21	7.35	10.66	10.68	13.99

3. APPLICATIONS AND CONCLUSIONS

Let us consider the following example of analytical chemical results relating to the weight fractions of a component from a mixture, found to be in domain [0 ; 0, 100]. This fraction is determined by help of an experiment, with standard deviation a priori to the experiment and found again by experiment $\sigma = 0.0005$ (in the first column of table 2). The concentration domain for the analysed component is divided in portions $\Delta_c = n\sigma$, with σ a priori known. If the results have to be between the limits $\pm\Delta_c = \pm n\sigma$, then from the formula (7) the amount of information entropy is established, which characterizes the obtained results, as a function of variable n, σ and concentration domain. In this manner, for a given standard deviation σ and a known concentration domain $[c_1, c_2]$, we can find n so that the information entropy of the results to be maximum and thus the information amount obtained from experiment to be maximum. Within the framework of this example, the results with the largest information entropy amount are those from the first column, because according to table 1, the maximum of H is obtained for $n = 2.5$.

Table 2

An example of analytical results for a component

ν	I c_1	II c_1	III c_1	IV c_1
1	0.021	0.020	0.02	0.025
2	0.023	0.025	0.02	0.025
3	0.022	0.020	0.02	0.023
4	0.022	0.020	0.02	0.025
5	0.021	0.020	0.02	0.025
6	0.022	0.020	0.02	0.025
7	0.023	0.025	0.02	0.025
8	0.022	0.020	0.02	0.025

$$\bar{c}' = 0.022 \quad \bar{c}'' = 0.021 \quad \bar{c}''' = 0.020 \quad \bar{c}^{IV} = 0.025$$

$$c_i' = c_i \pm 2\sigma \quad c_i'' = c_i' \pm 4\sigma \quad c_i''' = c_i' \pm 18\sigma \quad e_i^{IV} = c_i' \pm 50\sigma$$

$$\bar{c}'' = \bar{c}' - 4\sigma \quad \bar{c}''' = \bar{c}' - 4\sigma \quad \bar{c}^{IV} = \bar{c}' - 6\sigma$$

$$\Delta_c = 0.001 \quad \Delta_c = 0.005 \quad \Delta_c = 0.010 \quad \Delta_c = 0.025$$

It can also be shown that if the results c_i'' are situated in $c_i' \pm n\sigma$ interval, then the following relation can be written :

$$\max |\bar{c}'' - \bar{c}'| = \sigma \tag{10}$$

where :

$$\bar{c}'' = \frac{1}{\nu}\sum_i^{\nu} c_i'' \tag{11}$$

$$\bar{c}' = \frac{1}{\nu}\sum_i^{\nu} c_i' \tag{12}$$

i.e. the condition imposed in seq. 2 is fulfilled.

Finally, an example of choosing is presented, for the results of an experiment that gives the weight fraction of a component, situated in domain $c_1=0.01$ and $c_2= 1.000$, with a standard deviation $\sigma = \frac{1}{10} c_1 = 0.001$. Then, according to table 1, the analytical results of maximum information entropy will be those for which $n = 2$, i.e. the interval of variation for a result will be $\pm$ 0.002. In this manner, the analytical results of maximum information entropy will be those from the following row :

$$\{0.010 ; 0.015 ; 0.020 ; 0.025 ; \ldots ; 1,000\} \tag{13}$$

That means the results 0.011 or 0.012 were fitted to 0.010 ; the results 0.013 ; 0.014 ; 0.016 or 0.017 were fitted to 0.015 ; and so on.

ACKNOWLEDGEMENTS. The authors are indebted to Dr. Costinel Lepădatu for many valuable discussions about this subject.

REFERENCES

[1] K. Eckschlager, "Information Theory as Applied to Chemical Analysis", John Wiley and Sons, New York, Chichester, Brisbane, Toronto (1979).

[2] C. Liteanu and I. Rică, "Teoria şi Metodologia Statistică a Analizei Urmelor", Ed. Scrisul Românesc, Craiova (1979).

[3] K. Eckschlager and I. Vajda, *Collect. Czech. Chem. Commun.*, **39**, 3076 (1974).

[4] K. Eckschlager and V. Stepanek, *Microchim. Acta,* **I,** 107 (1978).

[5] H. Kaiser, *Anal. Chem.*, **42**, 24A (1970).

[6] C. E. Shannon, *Bell Syst. Tech. J.*, **27**, 379, 623 (1948).

Revue Roumaine de Chimie, 30, 9—10, 783—790 (1985)

POTENTIODYNAMIC BEHAVIOUR OF RANEY-COPPER IN POTASSIUM HYDROXIDE SOLUTIONS

VALENTINA LĂZĂRESCU, M. VASS, J. HERŞCOVICI* and ELENA CORLĂTEANU**

ICECHIM — Center of Physical Chemistry, Spl. Independenţei 202, Bucharest, Romania 77208
** ICECHIM — Organic Technology Department, Bucharest, Romania

Received June 25, 1984

Potentiodynamic investigations on Raney-copper and smooth polycrystalline copper were performed at room temperature in KOH solutions. Particular attention was given to the hydrogen region observed only on Raney-copper electrode, where three well-shaped anodic peaks have been noted. The detailed examination of the voltage scan rate influence on the main potentiodynamic parameters led to the conclusion that there are two independent types of adsorption sites without lateral interactions for the hydrogen atoms and a third one, with strong lateral interactions involving hydrogen molecules.

In recent years, it has been pointed out that some of the electrochemical techniques are well-suited to use in the study of catalyst surfaces. [1-3] Giving information concerning the Faradaic processes involved in the surface species adsorption/desorption and metal oxidation/reduction phenomena, the potentiodynamic scan method became an useful instrument for the characterization of the bulk and supported metal catalysts.

In acid or alkaline electrolytes the most metals adsorb/desorb oxygen or/and hydrogen by Faradaic charge transfer processes that are not usually influenced by their division state. McNicol[3] reported that the current-voltage curves of smooth platinum and unsupported finely divided platinum electrodes are very similar, except for the higher currents observed in the second case, as a consequence of the greater metal surface area involved. The Raney catalysts, prepared by leaching from an Al—Me (Me = Ni, Cu) alloy, have not however only a higher division state than the compact metal but also a peculiar structure confering them an important activity in different hydrogenation processes.[4]

In the present investigations the anodic behaviour of the Raney-copper in comparison with that of the smooth copper have been both examined by potentiodynamic scan method in KOH solutions.

EXPERIMENTAL

Cyclic voltammograms for Raney-copper and polycrystalline smooth copper were obtained using a Forschungsinstitut Meinsberg Type PS—20 potentiostat driven by a Tacussel GSTP—2A1 function generator and were registered with a X—Y recorder Hewlett-Packard Type 7001 AM.

---

* Deceased on December 30, 1981

The measurements were performed in stationary 0.1M and 1M KOH (Chemapol pro analyse reagent) solutions in twice distilled water, at room temperature, in a three-electrode electrochemical cell of conventional design. The working electrode potential was measured versus a saturated calomel electrode (SCE). The working electrode was either a polycristalline copper (0.25 mm) sheet (Johnson Matthey spectrographically standardised substance) with a geometric surface area of 1.2 cm^2 or Raney-copper powder placed on a 1.2 cm^2 platinum (or copper) sheet. The Raney-copper was prepared from an original 50% Al—Cu alloy by activation with 3% NaOH (Chemapol pro analyse reagent) at 80°C and contained 0.5% Al, 0.1% Pb, 0.01% Mn, 0.01% Ni (checked by an emission spectrographical method). The influence of the aluminium traces on the potentiodynamic behaviour of the catalyst in alkaline solutions was investigated apart[5] on Al—Cu films containing up to 15% Al. We have found that in the potential region concerned (—1.2 to —0.2 V *vs* SCE) the only new anodic process appearing is the aluminium dissolution observed near —0.3 V *vs* SCE, after the formation of the Cu_2O monolayer.

The copper electrode was washed, prior to each experiment, in a mixture of H_2SO_4, H_2O_2, CH_3COOH, H_2O (3 : 3 : 1 : 10) and rinsed several times with twice distilled water from alkaline permanganate solutions. The Raney-copper electrode was held into the hydrogen evolution potential range for 10 min. prior to the first scan, in order to remove the oxygen traces on its surface. The same treatment was also applied to a copper powder electrode (Johnson Matthey spectrographically standardised substance) with a surface area comparable to that of the catalyst to check up whether a cathodic concentration of the metal ions present in solution, that may possibly take place in this step, has any influence on the next scans. The current-voltage curves recorded before and after the treatment kept the same form and only an increase of peak currents has been observed in both cases.

RESULTS AND DISCUSSION

Typical linear potential scans for Raney-copper and smooth polycrystalline copper in 0.1 M KOH, between −1.2 and −0.2 V *vs* SCE are shown in Fig. 1. The anodic potential scan limit of −0.2V *vs* SCE was imposed by the behaviour of Raney-copper electrode. Going beyond this limit, the catalyst surface is covered with a dark deposit of copper oxide which breaks the electrical contact of the working electrode.

The potentials at which peaks occur on the anodic and cathodic scans were highly reproducible and the peak currents exhibit a discernable time dependence, particularly on the smooth copper, only after 10−12 complete scans.

As seen in Fig. 1, the shapes of the two voltammograms are different. In the same potential range where the smooth copper has a single anodic peak, Raney-copper exhibits three anodic peaks. The anodic peak observed near −0.35 V *vs* SCE and the linear region preceding it are the only common features.

The first anodic process occurring on the smooth polycrystalline copper electrode is, in opinion of Fletcher et al. [6], the Cu(I) dissolution associated with a slow chemical complexation reaction, represented by the linear region A. This is followed by the formation of a Cu_2O monolayer giving rise to peak B.[6,7] Taking into account the common features of the two current-voltage curves we may suppose that the both processes are also taking place on Raney-copper electrode. However, unlike the smooth copper, Raney-copper exhibits a clearly defined hydrogen region with two well-shaped peak. Moreover, it has been observed that after the maintenance of the electrode potential into the hydrogen evolution region for

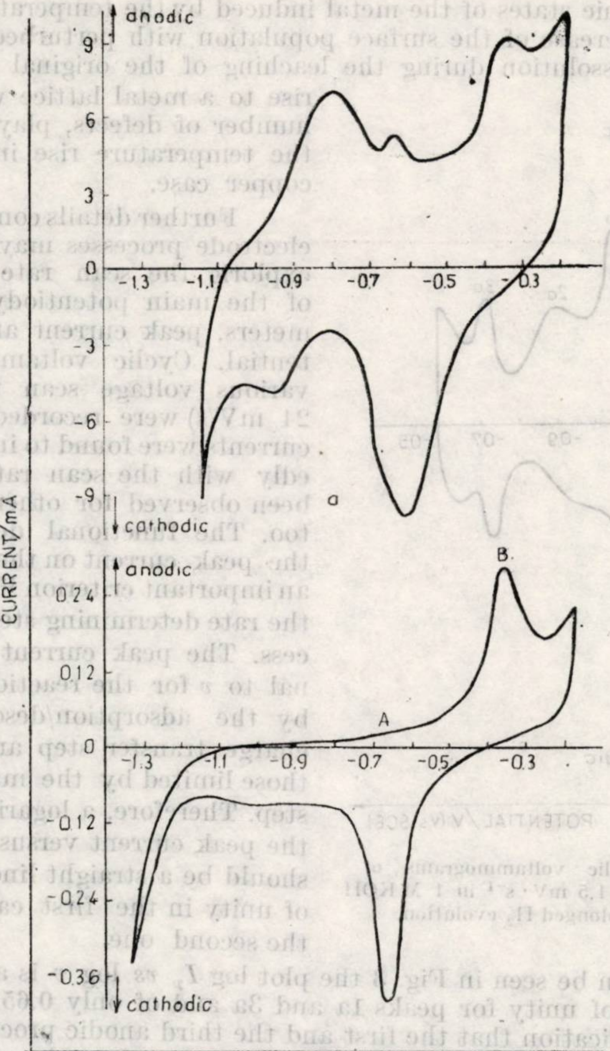

Fig. 1. — Cyclic voltammograms of Raney-copper (a) at $0.9\ \mathrm{mV.s^{-1}}$ and polycrystalline copper (b) at $19\ \mathrm{mV \cdot s^{-1}}$ in 0.1 M KOH.

longer periods of time prior to scan, a new anodic peak together with its cathodic correspondent arise (Fig. 2), increasing slightly in size during the first scans. As the formation of H^+ is the only oxidation state, it is obvious that the peaks represent oxidation processes with different free energies of activation. This is in a good agreement with the results of the volumetric and TPD studies [8] on Raney-copper catalysts, where at least two different adsorption sites have been observed. The hydrogen adsorption on copper, observed only at $T \geqslant 570$ K, was explained[9] by a change of the electronic states of the metal induced by the temperature rise, leading to an increase of the surface population with perturbed atoms. The aluminium dissolution during the leaching of the original alloy, giving rise to a metal lattice with a large number of defects, plays the role of the temperature rise in the Raney-copper case.

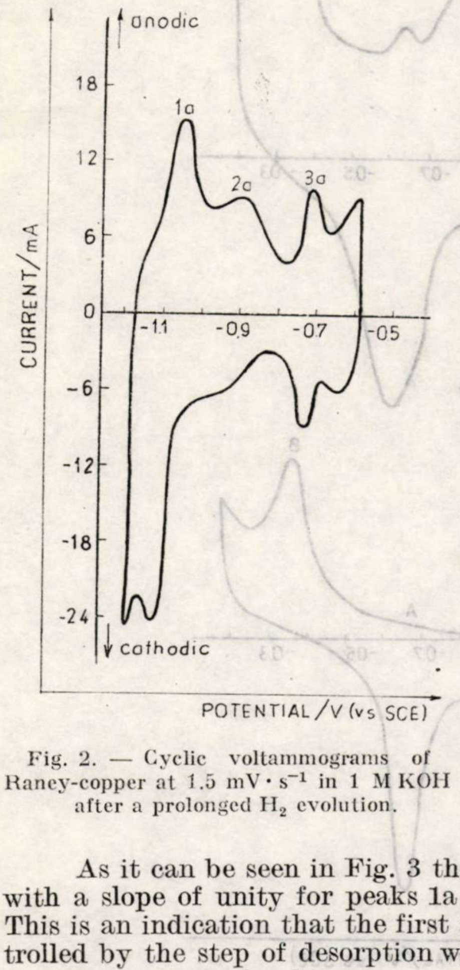

Fig. 2. — Cyclic voltammograms of Raney-copper at 1.5 $mV \cdot s^{-1}$ in 1 M KOH after a prolonged H_2 evolution.

Further details concerning these electrode processes may be obtained explorig the scan rate dependence of the main potentiodynamic parameters, peak current and peak potential. Cyclic voltammograms at various voltage scan rate (0.7 to 24 mV/s) were recorded. The peak currents were found to increase markedly with the scan rate, as it has been observed for other systems [10,11] too. The functional dependence of the peak current on the scan rate v is an important criterion [12,13] to find out the rate determining step of the process. The peak current is proportional to v for the reactions controlled by the adsorption/desorption with charge transfer step and to $v^{1/2}$ for those limited by the mass transport step. Therefore, a logarithmic plot of the peak current versus the scan rate should be a straight line with a slope of unity in the first case and 0.5 in the second one.

As it can be seen in Fig. 3 the plot log I_p *vs* log v is a straight line with a slope of unity for peaks 1a and 3a and of only 0.65 for peak 2a. This is an indication that the first and the third anodic processes are controlled by the step of desorption with charge transfer, whereas the second one obeys a complex kinetics.

The extent to which equillibrium in the adsorption/desorption step is disturbed depends on the specific rate constants of the reaction concerned and on the voltage scan rate v^{14}. The influence of the scan rate on the peak potential E_p may be used to find out what kind of electrode process is involved. It has been demonstrated [13] that for the quasi-equillibrium case the peak potential E_p is independent of v until a specific value is reached, while for a highly irreversible reaction it is proportional to ln v.

Fig. 4 shows plots of E_p *vs* ln v for all the three anodic peaks. It may be seen that the quasi-equillibrium conditions are valid for a rather wide range of scan rate values just for the anodic processes represented

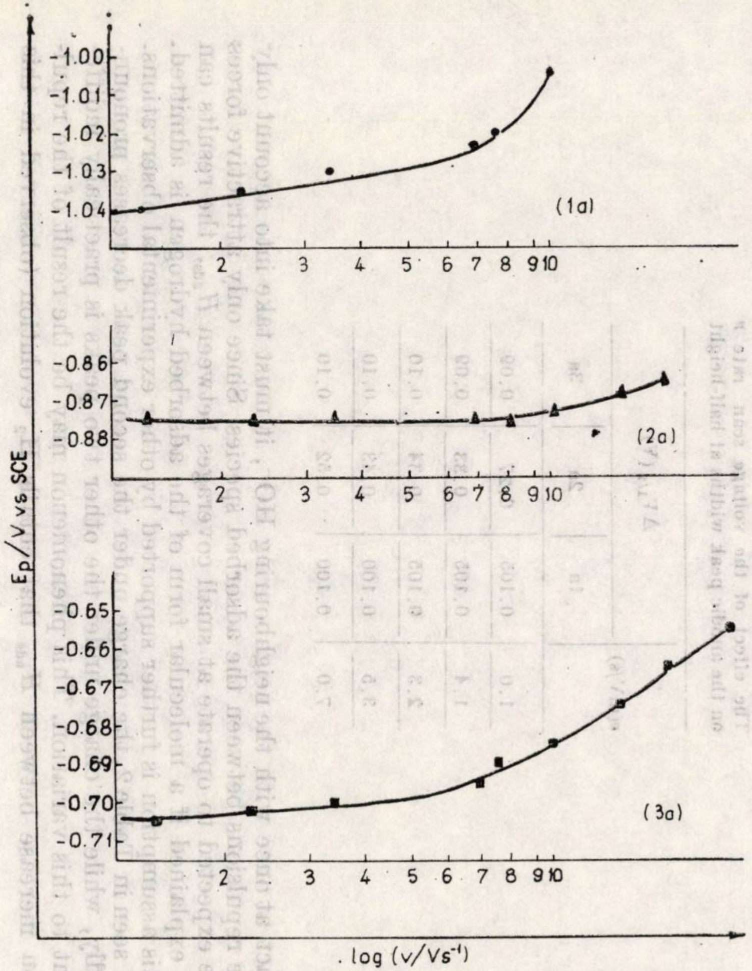

Fig. 4. — Dependence of the peak potential E_p on log v for the anodic peaks in the hydrogen region on Raney-copper (●—1a ; ▲ — 2a ; ■ — 3a).

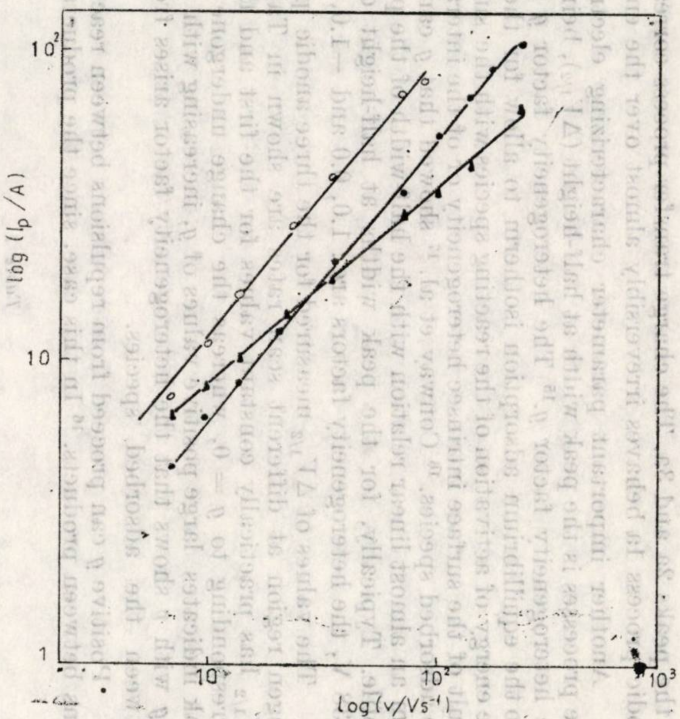

Fig. 3. — Dependence of the peak current I_p on the scan rate v for the anodic peaks in the hydrogen region on Raney-copper (○—1a : ▲ — 2a ; ●— 3a).

by the peaks 2a and 3a. The charge transfer process corresponding to the anodic process 1a behaves irreversibly almost over the entire range of v.

Another important parameter characterizing electrochemical surface processes is the peak width at half-height ($\Delta V_{1/2}$), being a measure of the heterogeneity factor g.[15] The heterogeneity factor g was introduced into the equillibrium adsorption isotherm to allow for the change of the free energy of activation of the reacting species with the surface coverage, result of the surface intrinsec heterogeneity or of the interactions between the adsorbed species.[16] Conway et al.[17] showed that g can be determined from an almost linear relation with the half-width of the potentiodynamic profile. Typically, for the peak widths at half-height of 0.148, 0.090, 0.038 V, the heterogeneity factors are : 1.0, 0.0 and −1.0, respectively.[18]

The values of $\Delta V_{1/2}$ measured for the three anodic peaks in the hydrogen region at different scan rates are shown in Table 1. As seen $\Delta V_{1/2}$ has practically constant values for the first and the third peaks, corresponding to $g = 0$, whereas the change undergone by the second peak indicates large positive values of g, increasing with v. This change of g with v shows that the heterogeneity factor arises from interactions between the adsorbed species.

Positive g can proceed from repulsions between reactants or attractions between products.[16] In this case, since the products are H^+, which react at once with the neighbouring HO^-, it must take into account only the repulsions between the adsorbed species. Since only attractive forces are expected to operate at small coverages between H_{ads}, the results can be explained if a molecular form of the adsorbed hydrogen is admitted. This assumption is further supported by other experimental observations. As seen in Table 2, the charge under the second peak decreases pronouncedly, while the charge under the other two peaks is practically indifferent to this variation. This phenomenon may be the result of the repulsion increase between H_{ads} that entails H_2 evolution (observed in this

Table 1

The effect of the voltage scan rate v on the anodic peak widths at half-height

v(mV/s)	$\Delta V_{1/2}$ (V)		
	1a	2a	3a
1.0	0.105	0.27	0.09
1.4	0.105	0.33	0.09
2.3	0.105	0.34	0.10
3.5	0.100	0.43	0.10
7.0	0.100	0.52	0.10

potential range only at high values of v) and decreases consequently the amount of the molecular hydrogen desorbed by the charge transfer process. Moreover, it was noticed that after the long H_2 evolutions, the second peak area is much greater in the first anodic scan than in the following, ones, reaching a steady value only after the complete ceasing of H_2 evolution. It can be supposed that during the maintenance of the electrode potential into the hydrogen evolution region a number of H_2 does not succeed to leave the surface, remaining partially adsorbed, partially blocked among the catalyst particles. On the anodic potential scan a part of them are evolving but the other are desorbing upon the catalyst surface by a charge transfer process.

Table 2

The effect of the voltage scan rate v on the quantity of charge under the anodic peaks

v(mV/s)	Q(C)		
	1a	2a	3a
0.7	1.3043	1.5942	0.5072
1.0	1.3188	1.4710	0.5072
1.4	1.3768	1.2319	0.5072
2.3	1.4130	0.9999	0.4999
3.5	1.4493	0.8551	0.4783
7.0	1.3587	0.6739	0.4348

CONCLUSIONS

The results of this study may be summarized as follows :

1. The electrochemical behaviour of Raney-copper and smooth polycrystalline copper electrodes has been investigated in KOH solutions using the potentiodynamic scan technique. Between the potential limits -1.2 and -0.2 V *vs* SCE certain features were supposed to be common to the both systems : Cu (I) dissolution and Cu_2O monolayer formation.

2. A major difference between the behaviour of Raney-copper and polycrystalline smooth copper electrodes appears in the hydrogen region. After a long H_2 evolution, three well-defined peaks have been noticed on the anodic potential scan, only for the Raney-copper electrode. The detailed examination of the potential scan rate influence on the main potentiodynamic parameters led to the conclusion that the oxidation of the adsorbed hydrogen on Raney-copper is best treated by considering

two independent types of adsorption sites without lateral interactions ($g = 0$) for hydrogen atoms and a third one, with strong lateral interactions ($g > 0$) involving the molecular hydrogen.

ACKNOWLEDGEMENT. The authors wish to thank Dr. N. Bonciocat for his critical review of the manuscript and Dr. Rodica Grigorovici and Dr. A. Butucelea for performing the spectrochemical investigation of the catalyst.

REFERENCES

[1] D. R. Lowde and J. O. Williams, *Appl. Surface Sci.*, **1**, 215 (1978).
[2] M. Hayes and A. T. Kuhn. Appl. *Surface Sci.*, **6**, 1 (1980).
[3] B. D. McNicol, in : "Characterization of Catalysts", Eds. J. M. Thomas and R. M. Lambert, Wiley-Interscience, New York, 1980, p. 135.
[4] J. A. Stanfield and P. E. Robbins, "Internat. Congr. Catal., 2nd, Paris, 1960", Technip, Paris, 1961, p. 2579.
[5] V. Lăzărescu, M. Vass and O. Radovici, to be published.
[6] S. Fletcher, R. G. Barradas and J. F. Porter, *J. Electrochem. Soc.*, **125**, 1960 (1978).
[7] S. M. Abd El Halem and B. G. Ateya, *J. Electroanal. Chem.*, **117**, 309 (1981).
[8] V. Lăzărescu, P. Budrugeac and M. Vass, to be published.
[9] V. F. Khorykov, G. Lyubarskii and A. I. Gelbstein, *Zhur. Fiz. Khim.*, **45**, 2856 (1971).
[10] B. G. Pound, D. M. Macdonald and J. M. Tomlinson, *Electrochim. Acta*, **25**, 563 (1980).
[11] D. D. Macdonald and D. Owen, *J. Electrochem. Soc.*, **120**, 317 (1973).
[12] P. Delahay, "New Instrumental Methods in Electrochemistry", Interscience, New York, 1954, Ch. 4.
[13] S. Srinivasan and E. Gileadi, *Electrochim. Acta*, **11**, 321 (1966).
[14] P. Stonehart, H. Angerstein-Kozlowska and B. E. Conway, *Proc. Roy. Soc.*, **A 310, 541** (1969).
[5] H. Angerstein-Kozlowska, J. Klinger and B. E. Conway, *J. Electroanal. Chem.*, **75**, 45 (1977)
[6] P. Stonehart, *Electrochim. Acta*, **15**, 1853 (1970).
[7] B. E. Conway, E. Gileadi and M. Dzieciuch, *Electrochim. Acta*, **8**, 143 (1963).
[8] K. Kinoshita and P. Stonehart, *Electrochim. Acta*, **20**, 101 (1975).

Revue Roumaine de Chimie, **30**, *9–10*, 791–797 (1985)

CARBOCATIONIC REARRANGEMENTS IN DIBENZO-[*b*,*g*]BICYCLO[4.2.0]OCTA-2,7-DIENE DERIVATIVES[1]

NICOLETA ŞTEFAN, PETRU FILIP, FILIP CHIRALEU, ILIE G. DINULESCU
and MARGARETA AVRAM *
Center of Organic Chemistry, Spl. Independenţei 202 B,
78100 Bucharest 12, Romania

Received October 1, 1984

The dibenzo[*b*, *g*]bicyclo[4.2.0]octa-2,7-diene derivatives, in reactions which generate a cationic center in the α-position to the cyclobutane ring, could undergo molecular rearrangements. The skeleton of the final products depends upon the molecular fragment which interferes in/or after the ionisation process.

We have shown [2] that the solvolysis of bromoacetoxy derivative **1** under various conditions yields a mixture of bromoacetoxy derivative **2** and diacetate **3** in different ratios, sometimes together with unreacted **1**.

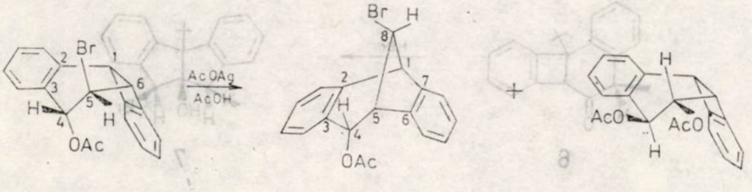

1 2 3

In the diacetoxy derivative **3** the configuration at C-4 and C-5 is reversed with respect to the initial structure. This inversion of configuration has been sustained [3] by an extensive ^{1}H-NMR study of some monoacetoxy and diacetoxy derivatives with a dibenzo[*b*, *g*]bicyclo-[4.2.0]octa-2,7-diene skeleton.

A similar behaviour at solvolysis was reported [2] for the bromomethoxy derivative **4** but the reactions occurring with retention of the skeleton and inversion of configuration were not observed.

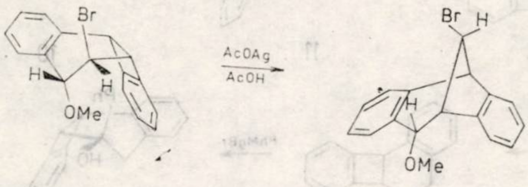

4 5

---

* Deceased in 1983

Table 1 summarizes the experimental data that we have previously reported [2,3] on the solvolysis of **1** and **4**.

Table 1

Reaction products of 1 and 4 in various conditions

Compound	Reagent	Products (% moles)		
		Rearranged compound	Unrearranged compound with reversed configuration	Unreacted compound
1	$AgBr/CCl_4$	95	—	—
	AcOAg/AcOH	25	45	25
	EtCOOAg/AcOH	18.5	81.5	—
	AcOK/AcOH	—	100	—
4	AcOAg/AcOH	100		
	$AgBr/CCl_4$	40	—	60

A different behaviour has been reported [4] for ketone **6**. In acidic media the molecular skeleton is rearranged yielding the bromohydroxy derivative **7** with dibenzo[*b*, *g*]bicyclo[3.3.0]octa-2,7-dienic skeleton.

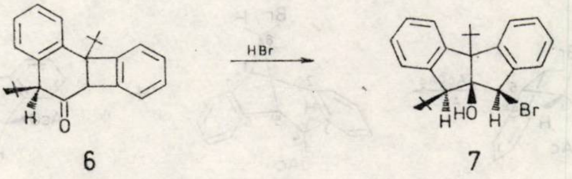

6 7

We wish to report here the behaviour of the ketone **8** and of the phenylhydroxy derivative **9** when a cationic center at C-5 is generated.

These two compounds were obtained from the alcohol **10**, which was prepared [5] from the *endo*-epoxide **11** of the angular dimer of benzocyclobutadiene (**12**), according to the following scheme.

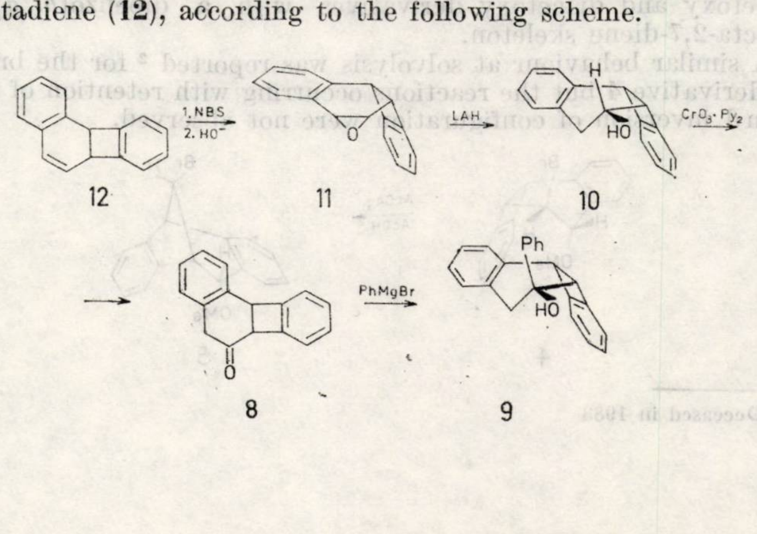

The main arguments for the *exo*-axial orientation of the phenyl group in compound **9** are based on the ^{1}H-NMR and IR spectra. In the IR spectrum the absorption frequency for the OH group appears at 3620 cm^{-1}, in agreement with an *endo*-equatorial orientation of this group. In an *endo*-axial orientation of the OH group, an intramolecular association with the neighbouring π-system is possible, so that the absorption band of the OH group would appear at frequencies less than 3600 cm^{-1}. In the ^{1}H-NMR spectrum the signal of H-1 appears at lower field (δ 4.83 ppm) than in dibenzo[*b*, *g*]bicyclo[4.2.0]octadiene (δ 4.71 ppm)[6] or than in the 5-*endo*-hydroxy-dibenzo[*b*, *g*]bicyclo[4.2.0]octadiene (δ 4.66 ppm).[5] This shift to lower field is due to the deshielding induced by the *exo*-axial phenyl group. In an *endo*-equatorial orientation, the phenyl group would not induce any shielding effect upon H-1.

When ketone **8** was treated with anhydrous hydrobromic acid in dichloromethane, at room temperature, a molecular rearrangement takes place, yielding the bromohydroxy derivative **13** which was reduced to the symmetrical alcohol **14** by treatment with lithium aluminium hydride.

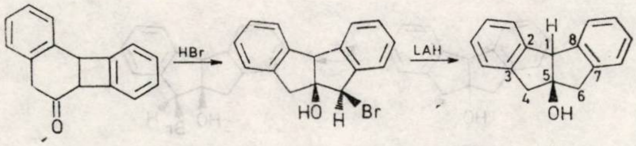

8 13 14

In the IR spectrum of **13** the absorption band of the hydroxy group appears at 3585 cm^{-1} revealing an intramolecular association with the vicinal bromine atom. Such an interaction could exist only if the bromine and hydroxy groups are in *cis* configuration. The symmetrical structure of the skeleton in **14** and respectively in **13** is best revealed in the ^{1}H-NMR spectrum of **14**. This spectrum exhibits, along with aromatic proton signals, only three singlet signals which were attributed to the H-1, the proton from the OH group and to the four equivalent benzylic protons H-4 and H-6. When the spectrum is recorded in the presence of a shift reagent Eu(DPM)$_3$, the signal of benzylic protons is split into an AB system having $J_{AB} = 16$ Hz.

A different behaviour was observed when phenylhydroxy derivative **9** was treated with strong acids. In this case, two products **15** and **16**, were isolated in equal amounts.

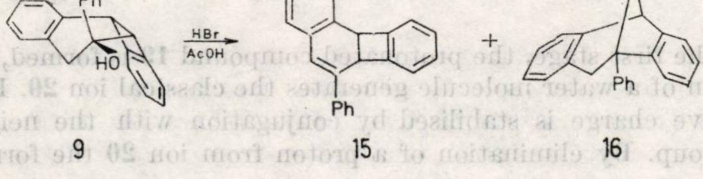

9 15 16

The ^{1}H-NMR spectra for both compounds **15** and **16** are in agreement with the assigned structures.

All experimental data, presented in this paper and in previous works, [2–4] concerning the cationic rearrangements in the dibenzo[*b*, *g*]-bicyclo[4.2.0] octa-2,7-dienic systems can be rationalized accepting that in the case of derivatives **8** and **9** a classical carbonium ion is first formed, while in the case of compounds **1** and **4** the ionisation is assisted by one of the phenyl or acetyl groups.

In acidic media, the ketone **8** is protonated generating the ion **17** which undergoes a rearrangement to the more stable benzylic ion **18**, as shown in the following scheme.

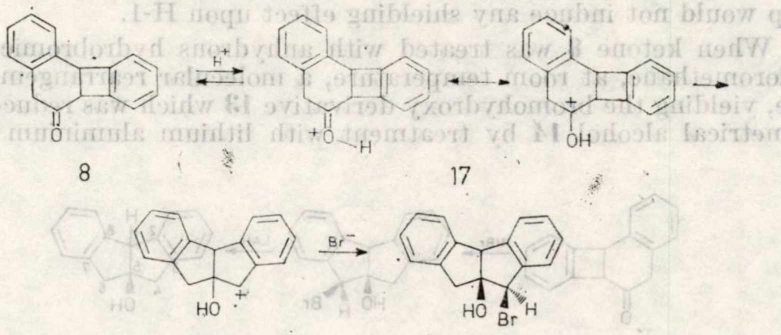

8 17 18 14

The behaviour of the phenyl alcohol **9** in acidic media can be explained by the following mechanism.

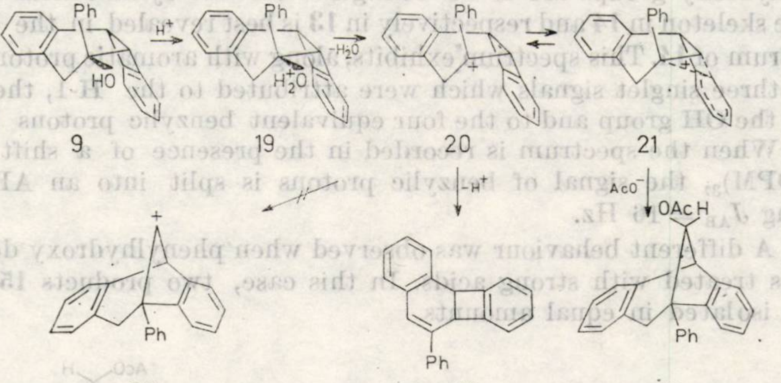

9 19 20 21 22 15 16

In the first stage, the protonated compound **19** is formed, which on elimination of a water molecule generates the classical ion **20**. In this ion the positive charge is stabilised by conjugation with the neighbouring phenyl group. By elimination of a proton from ion **20** the formation of compound **15** is explained. A nonclassical phenonium ion **21** in equilibrium with ion **20** can explain the formation of compound **16** with rearranged skeleton. A classical ion like **22** is probably less stable than the benzylic ion **20** and it can not explain the exclusive *syn* orientation of the acetoxy group in **16**.

The probable mechanism for the rearrangement of **1** (or **4**) is presented in the following scheme.

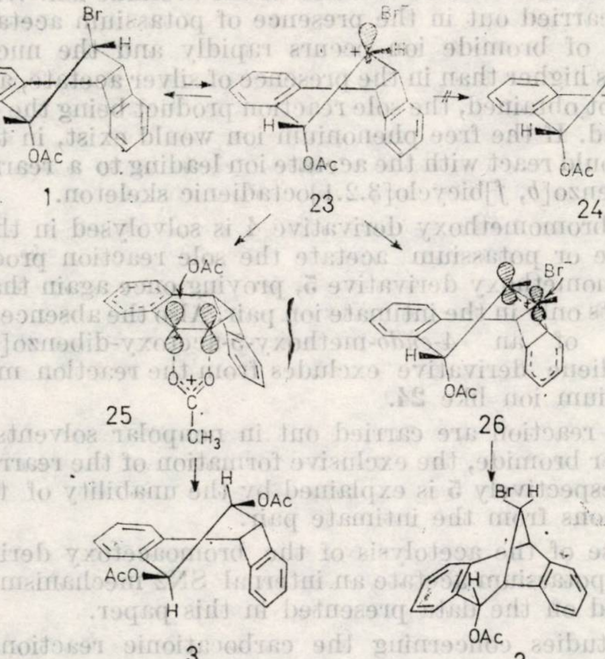

In the first step by ionisation of the bromine an intimate ion pair **23** is formed at equilibrium with **1** (or **4**). In this intimate ion pair the geometry of the skeleton is not yet changed, so that the *p* orbital at C-5 can easily interact with the phenyl group of the benzocyclobutene moiety. In this way in the intimate ion pair the nonclassical phenonium ion **26** appears, explaining the formation of **2**. In the intimate ion pair **23**, van der Waals repulsions exist between the protons at C-5 and C-6 and also between the *endo*-acetoxy group and the aromatic ring of the benzocyclobutene sequence. When the bromine ion is solvated, in the free carbonium ion the molecular geometry is changed, due to the above mentioned repulsions, so that the formation of the acetoxonium ion **25** is favoured.

This ion probably does not exist in equilibrium with the phenonium ion **26**. Also due to the conjugation with the vicinal aromatic ring the positive charge in **25** is localized more at the benzylic position, explaining in this way the formation of diacetate **3** in which the configuration is reversed at C-4 and C-5.

The rearrangement of the bromomethoxy derivative **4** into **5** involves as intermediates only ions like **17** and **20**.

The proposed mechanism is supported by the following data :

i) When **1** was acetolysed in the presence of silver acetate we have not isolated a diacetoxy derivative with rearranged skeleton, proving in this way that the phenonium ion exists only in the intimate ion pair. If a free phenonium ion could exist in this case, the formation of **2** could be also explained if the captation of the bromide ion by the free phenonium ion would be faster than the solvatation of the bromide ion. When the solvolysis of **1** is carried out in the presence of potassium acetate, so that the solvatation of bromide ion occurs rapidly and the nucleophilicity of the medium is higher than in the presence of silver acetate, a rearranged diacetate was not obtained, the sole reaction product being the diacetate **3**, above mentioned. If the free phenonium ion would exist, in the reaction conditions, it would react with the acetate ion leading to a rearranged diacetate with dibenzo[*b*, *f*]bicyclo[3.2.1]octadienic skeleton.

ii) When bromomethoxy derivative **4** is solvolysed in the presence of silver acetate or potassium acetate the sole reaction product is the rearranged bromomethoxy derivative **5**, proving once again that the phenonium ion exists only in the intimate ion pair. Also the absence in the reaction products of an 4-*endo*-methoxy-5-acetoxy-dibenzo[*b*,*g*]bicyclo-[4.2.0]octa-2,7-diene derivative excludes from the reaction mechanism a classical carbonium ion like **24**.

When the reaction are carried out in nonpolar solvents (CCl_4), in presence of silver bromide, the exclusive formation of the rearranged derivatives **2** and respectively **5** is explained by the unability of the medium to remove the ions from the intimate pair.

In the case of the acetolysis of the bromoacetoxy derivative **1** in the presence of potassium acetate an internal SN2 mechanism can not be eliminated based on the data presented in this paper.

Further studies concerning the carbocationic reactions of other derivatives with dibenzo[*b*, *g*]bicyclo[4.2.0]octa-2,7-dienic skeleton in order to elucidate the factors which are governing the rearrangement path are in progress.

EXPERIMENTAL

IR Spectra were recorded with a double beam Jena UR-20 spectrophotometer. ^{1}H-NMR spectra were performed with a Varian A 60-A spectrometer.

5-Hydroxy-dibenzo[b, g]bicyclo[3.3.0]octa-2,7-diene (**14**). A solution of 1.2 g (5.44 mmoles) ketone **8** in 30 mL dichloromethane was saturated with anhydrous hydrobromic acid and left at room temperature for five days. The mixture was poured into water and the organic layer after washing with water and 5% sodium carbonate solution until neutral, was dried. The crude **14** obtained by solvent removal was reduced with lithium aluminium hydride in ethereal solution. After working up, the crude product (0.85 g, 70%) was purified by column chromatography on alumina (activity II) using diethyl ether as eluent, yielding pure **14**, m.p. 121°. — $C_{16}H_{14}O$ (222.3) Calcd. : C, 86.45 ; H, 6.35. Found: C, 86.76 ; H, 6.49. — IR (CCl_4, cm^{-1}) : ν_{OH} 3560. — ^{1}H-NMR ($CDCl_3$, δ, ppm) : 2,55 (broad s, 1H, OH), 3.13 (s, 4H, 2H-4, 2H-6), 4.35 (s, 1H, H-1), 6.95 — 7.40 (m, 8H, aromatic) ; ^{1}H-NMR ($CDCl_3$, δ, ppm ; molar ratio $Eu(DPM)_3$/**14** = 0.07) : 3.65 and 3.91 (4H, 2H-4 and 2H-6, AB system, $J_{AB} = 16.0$ Hz) ; 5.06 (s, 1H, H-1), 6.25 (s, 1H, OH), 7.10 — 7.60 (m, 8H, aromatics).

5-exo-Phenyl-5-endo-hydroxy-dibenzo[b,g]bicyclo[4.2.0]octa-2,7-diene (**9**). A solution of ketone **8** (1.55 g, 7.03 mmoles) in anhydrous diethyl ether (40 mL) was added dropwise, under stirring, to an ethereal solution of Grignard reagent prepared from magnesium (0.6 g, 25 mmoles) and bromobenzene (4.0 g, 25 mmoles), and the mixture was boiled for two hours. After working up, the crude product was purified by column chromatography on alumina (activity II) using diethyl ether as eluent, yielding 1.7 g (81.3%) **9**, m.p. 138°. — $C_{22}H_{18}O$ (298.4) Calcd. : C, 88.55 ; H, 6.08. Found : C, 88.37 ; H, 5.90. — IR (CCl_4, cm^{-1}) : ν_{OH} 3620. — ^1H-NMR ($CDCl_3$, δ, ppm) : 2.10 (broad s, 1H, OH), 2.88 (s, 2H, H-4), 4.33 and 4.83 (2H, H-1, H-6, AB system, J_{AB} = 5.0 Hz), 6.80—7.70 (m, 13H, aromatics).

Reaction of phenylalcohol **9**, *in acidic media*. A solution of 0.7 g (2,35 mmoles) **9** in 20 mL anhydrous acetic acid and 0.2 mL 63% hydrobromic acid was heated for 16 hours at 80°. The mixture was poured into water, extracted with dichloromethane and the organic solution was washed until neutral. After drying and solvent removal, 0.65 g crude mixture containing 50% **15** and 50% **16** were obtained.

By chromatography on alumina column using as eluent petroleum ether with 3% diethyl ether, 0.25 g (38%) *5-phenyl-dibenzo[b, g]bicyclo[4.2.0]octa-2, 4,7-triene* (**15**), m.p. 160°, were isolated. — $C_{22}H_{16}$ (280.3) Calcd. : C, 94.25 ; H, 5.75. Found : C, 94.21 ; H, 5.86. — ^1H-NMR ($CDCl_3$, δ, ppm) : 5.00 (s, 2H, H-1 and H-6), 6.81 (s, 1H, H-4), 6.85—7.90 (m, 13H, aromatics).

Further chromatography using petroleum ether with 10% diethyl ether as eluent yielded 0.25 g (31%) *8-syn-acetoxy-5-phenyl-dibenzo[b, f]bicyclo[3.2.1]octa-2,7-diene* (**16**), colourless oil. — $C_{24}H_{20}O_2$ (340.4) Calcd. : C, 84,71 ; H, 5.85. Found : C, 84.59 ; H, 5.60. — IR (CCl_4, cm^{-1}) : ν_{CO} 1755. — ^1H-NMR ($CDCl_3$, δ, ppm) : 1.70 (s, 3H, OAc), 3.14 and 3.71 (AB system, 2H, H-4, J_{AB} = 17.0 Hz), 4.41 (d, 1H, H-1, $J_{1.8}$ = 4.5 Hz), 5.81 (d, 1H, H-8), 6.70—7.80 (m, 13H, aromatics).

REFERENCES

[1] Part LX of the Investigations in the Cyclobutane Series. For part LIX see : N. Ştefan, P. Filip, I. G. Dinulescu, F. Chiraleu and M. Avram, *Rev. Roumaine Chim.*, **30**, 589 (1985).

[2] N. Ştefan, I. G. Dinulescu and M. Avram, *Rev. Roumaine Chim.*, **21**, 107 (1976).

[3] N. Ştefan, P. Filip and M. Elian, *Rev. Roumaine Chim.*, **29**, 861 (1984).

[4] O. Constantinescu-Simon, I. G. Dinulescu, F. Chiraleu and M. Avram, *Chem. Ber.*, **109**, 1301 (1976).

[5] N. Ştefan, P. Filip, I. G. Dinulescu, F. Chiraleu and M. Avram, *Rev. Roumaine Chim.*, **29**, 631 (1984).

[6] G. I. Fray and D.P.S. Smith, *J. Chem. Soc.* C, **1969**, 2610.

Revue Roumaine de Chimie, **30**, *9—10*, 799—802 (1985)

SYNTHESIS OF AMIDES BY A NEW DIRECT CONDENSATION REACTION

C. I. CHIRIAC
Institute of Macromolecular Chemistry "P. Poni",
Aleea Ghica-Vodă 41 A Jassy, Romania

Received December 3, 1984

Amides were prepared with high to moderate yields by a direct condensation reaction of carboxylic acids with amines in the presence of phosphorous acid and iodine in solution of pyridine at 75—85°, 5—6 hours. The best results were obtained with aliphatic carboxylic acids and aromatic amines.

The classical method for the synthesis of N-mono-substitutes amides consists in the reaction of primary amines with acyl chlorides or anhydrides of carboxylic acids. The last compounds can be obtained from carboxylic acids and reagents with phosphorus or sulfur; for example phosphorus trichloride, thionyl chloride, etc. Different investigators found that the two steps could be combined successfully into one operation. [1,2]

In previous papers, [3] we showed that different reactive phosphorus and sulfur compounds can be used as reagents for the synthesis of amides.

RESULTS AND DISCUSSIONS

Kirby [4] found an ingenious method for the synthesis of monoalkyl phosphate, using the reaction between phosphorus acid, iodine and the corresponding alcohol in the presence of triethylamine as base. The author of this work supposes that this reaction takes place by an anion (IPO_3^{2-}) as reactive intermediary.

In this communication we present a new application of this reagent for synthesis of amides. Therefore, our investigations have shown that the reagent constituted from phosphorous acid and iodine in solution of pyridine (as base and solvent) can be used in this field. By the addition of one mole I_2 to a solution of one mole + 20 % excess $P(OH)_3$ in dried pyridine, an exothermic reaction takes place. At the beginning, the obtained solution has a black-violet colour owing to iodine, but by heating at 75—85°, 30 minutes under stirring, the solution becomes light yellow. This is an indication that the iodine reacted, resulting the reactive intermediary in solution of pyridine. At this solution, one mole of carboxylic acid was added and the heating was continued for about 30 minutes. Then, 1 mole + 10% excess of amine was added and the heating at the same temperature under stirring was continued for 5—6 hours, resulting the corresponding amide (a small excess of amine improves the yield).

We suppose that the reaction between I_2 and $P(OH)_3$ in solution of pyridine can take place by a mechanism which involves an electrophylic attack of iodine atom at the phosphorus atom, resulting a reactive intermediary (I):

$$P(OH)_3 + I_2 \xrightarrow[75-80°,\,30']{Py} (I)$$

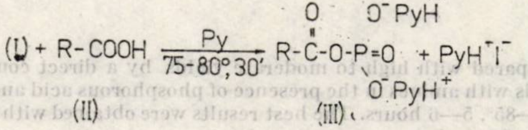

$$(I) + R\text{-}COOH \xrightarrow[75-80°,\,30']{Py} R\text{-}\overset{O}{\overset{\|}{C}}\text{-}O\text{-}P(=O)(O^-PyH^+)_2 + PyH^+I^-$$

(II) (III)

The compound (I) has a reactive bond P—I, which participates in the condensation reaction of carboxylic acids with amines.

The synthesis of amides by this method involves three stages:

— In the first stage, the complex (I) results by the reaction of $P(OH)_3$ with I_2 in solution of dried pyridine.

— In the second stage, the carboxylic acid (II) reacts with the reactive intermediary (I), resulting a reactive complex (III), which can be regarded as a mixed anhydride of phosphoric acid with the corresponding carboxylic acid.

— In the last stage, the reactive complex (III) reacts with the amine (IV) affording the amide (V) and the by-product (VI):

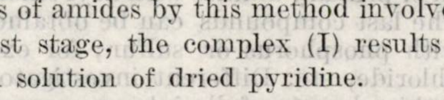

$$(III) + R'\text{-}NH_2 \xrightarrow[75-80°,\,5-6h]{Py} R\text{-}CONH\text{-}R' +$$

(IV) (V)

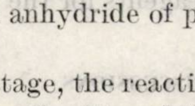

$$HO\text{-}P(=O)(O^-PyH^+)_2$$

(VI)

We supposed, as in other cases, [5-7] that the reaction of the amine (IV) with the reactive complex (III) involves a four-centred transition state

(VII), preceded by a nucleophylic attack of the nitrogen atom at the carbonyl group :

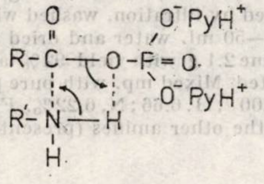

(VII)

The amides (V) obtained by this method are presented in table 1.

Table 1

Amides obtained using $P(OH)_3/I_2/Py$ complex as reagent

Amine	Acid	Amides[a)]		
		Yield[b)] %	M.p.[c)] °C	Reported m.p.[d)] °C
p-Toluidine	Phenylacetic	91	135—137	135—136
Aniline	Phenylacetic	89	115—117	115—116
2-Naphthylamine	Phenylacetic	92	164—166	165—167
Cyclohexylamine	Phenylacetic	53	134—136	134—135[8]
Benzylamine	Phenylacetic	49	109—111	109—110[9]
p-Toluidine	Acetic	85	116—118	117—119
2-Naphthylamine	Acetic	87	132—134	132—133
Cyclohexylamine	1-Naphthylacetic	47	178—180	178—179[10]
p-Toluidine	Benzoic	41	156—158	156—157
Cyclohexylamine	Benzoic	38	146—148	147—149

a) The products were identified by comparison of m.p. and IR spectra with authentic samples ; b) Yields calculated on carboxylic acid employed, before recrystallisation ; c) After recrystallisation ; d) From "Beilstein Handbuch der Organischen Chemie".

From this table we can see that the best results were obtained in the reaction of aliphatic carboxylic acids with aromatic amines, when the yields ranged from 85 to 92 %.

In conclusion, we found a new method for the synthesis of the amides using a reactive intermediate formed from phosphorous acid and iodine in solution of pyridine.

Since our method is very simple, it may be of interest for the synthesis of biologically active compounds.

EXPERIMENTAL

To a solution of 1 g (0.01 mole+20 % excess) $P(OH)_3$ in 7 mL dried pyridine, I_2 2.52 g (0.01 mole), was added under stirring. After 30 minutes at 75—85°, 1.36 g (0.01 mole) phenylacetic acid was added and the heating was continued still 30 minutes in the same conditions. Then

1.5 g (0.01 mole + 10% excess) *p*-toluidine was added and the obtained solution was heated for 5—6 hours at 75—85°. At the end of reaction, the solution still warm was poured into a large volume of water with ice (60—80 mL) under stirring, when the desired product precipitated. The precipitate was collected by filtration, washed with 20—30 mL 7% NaOH solution, 30—40 ml 10% HCl solution, 40—50 mL water and dried under vacuum at 80—100°. Amide of phenylacetic acid with *p*-toluidine 2.1 g with yield 92% and m.p. 135—137° (after recrystallisation from ethyl alcohol) resulted. Mixed mp. with pure product underpressed. Anal. Calculated for : $C_{15}H_{15}ON$ = 225 ; C, 80.00 ; H, 6.66 ; N, 6.22%. Found : C, 79.26 ; H, 6.11 ; N, 6.39%.

Under similar conditions, the other amides (presented in table 1) were prepared.

REFERENCES

[1] T. Wieland and B. Heinke, *Liebigs Ann. Chem.*, **599**, 70 (1956) ; *Chem. Ber.*, **91**, 483 (1958).

[2] G. W. Anderson and R. W. Young, *J. Amer. Chem. Soc.*, **74**, 5304 (1952).

[3] C. I. Chiriac, *Rev. Roum. Chim.*, **24**, 609 (1979) ; **25**, 403 (1980) ; **27**, 747 (1982) ; **28**, 863 (1983).

[4] A. J. Kirby, *Chem. & Ind.*, **1963**, 1877.

[5] W. Gerrard and J. A. Cade, *J. Chem. Soc.*, **1954**, 2034.

[6] B. Iselin and W. Rittel, *Helv. Chim. Acta*, **40**, 710 (1957).

[7] C. I. Chiriac, *Rev. Roum. Chim.*, **26**, 1001 (1981).

[8] L. F. Audrieth, *J. Org. Chem.*, **4**, 54 (1939).

[9] O. C. Dermer and J. King, *J. Org. Chem.*, **8**, 168 (1943).

[10] G. Pala, *Farmaco (Pavia) Ed. Sci.*, **19**, (3) 235 (1964) ; *Chem. Abstr.*, **60**, 14.448 b (1964).

Revue Roumaine de Chimie, **30**, *9—10*, 803—806 (1985)

SYNTHESIS OF DIAZOKETONES FROM β-BENZOYL ACRYLYL CHLORIDE AND DIAZOALKANES

R. AGARWAL and P. BAHADUR
Department of Chemistry, South Gujarat University, Surat—395 007, India

Received May 6, 1983

α-Diazoketones were synthesised from β-benzoyl acrylyl chloride and diazoalkanes and characterized by the action of various reagents on them. Simultaneously the susceptibility of diazoalkanes towards carboxylic acid chloride group, unsaturation and keto group was also studied in a comparative manner when these all are present altogether.

Adopting the method of Ardnt and Eistert,[1] α-diazoketones (I&II) have been synthesized, starting from β-benzoyl acrylyl chloride (1 mol) and, for type I, diazoethane[8]

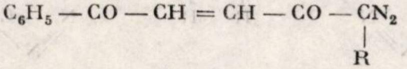

$$C_6H_5-CO-CH=CH-CO-\underset{\displaystyle R}{\underset{|}{C}}N_2$$

(I)

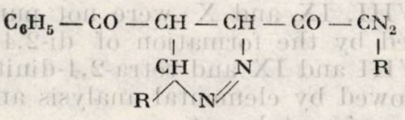

(II)

and diazo-n hexane (each 2 mols), for type II, diazomethane, diazo-n-butane, diazo-n-hexane (each 3 mols) having pyrazoline ring,[4] in dry ether at 0°C, thus affording 1-diazo-1-methyl-4-benzoyl-but-3-ene-2-one III (I, R = $-CH_3$); 1-diazo-1-n-amyl-4-benzoyl-but-3-ene-2-one IV (I, R = n $-$ C_5H_{11}); 4-benzoyl-3-diazoacetyl-pyrazoline V (II, R = H), 4-benzoyl-3-n-propyl-diazoacetyl-5-n-propyl-pyrazoline VI (II, R = n $-$ C_3H_7); 4-benzoyl-3-n-amyl-diazoacetyl-5-n-amyl-pyrazoline VII (II, R = n $-$ C_5H_{11}) as yellow to red mobile liquids.[2] The easily removable diazo group present in them prevented their purification by distillation even under vacuum. The diazoketones were characterized by the formation of cyrstalline 2,4-dinitrophenyl osazones followed by elemental analysis and infrared studies[5,6,7] in the later. However, where the osazones could not be isolated, the diazoketones were characterized by the isolation and subsequent identification of the corresponding benzoates, obtained by treating them with molten benzoic acid. β-Benzoyl acrylyl chloride has three sites of reactivity towards the action of diazoalkanes, thus enabling to find out the maximum susceptibility of all these groups towards diazoalkanes, present altogether.

The diazoketones III, V and VII on warning in molten benzoic acid [3] afforded corresponding benzoyloxy (VIII, R = CH_3 ; Z = $OCOC_6H_5$; IX, R = H, Z = $OCOC_6H_5$; X, R = n — C_5H_{11}, Z = $OCOC_6H_5$) derivatives as liquids.

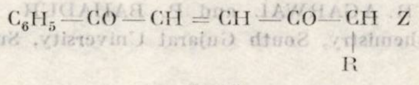

$C_6H_5—CO—CH=CH—CO—\underset{R}{\underset{|}{CH}}\ Z$

(VIII)

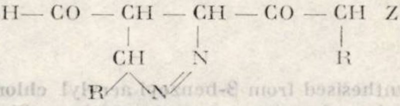

(IX)

On heating the diazoketones in dioxan in the presence of copper powder, [3] after loss of nitrogen, the resulting radicals dimerised to X (R = H, —C_3H_7)

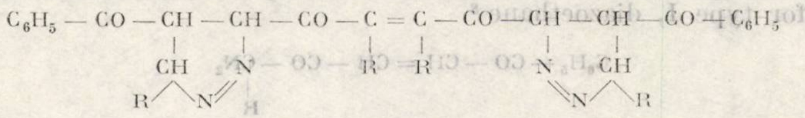

(X)

The products VIII, IX and X were not purified. However, they could be characterized by the formation of di-2,4-dinitrophenyl hydrazone in the case of VIII and IX and tetra-2,4-dinitrophenyl hydrazones in the case of X followed by elemental analysis and infrared studies in them, as given in experimental part.

EXPERIMENTAL

1-Diazo-1-methyl-4-benzoyl-but-3-ene-2-one III (I, R = CH_3)

β-Benzoyl acrylyl chloride (7.78 g; 0.04 mol) was treated with pre-estimated ethereal solution of diazoethane (4.32 g, 0.08 mol) at 0°C. The mobile diazoketone, yield 4.46 g, 52%, failed to give derivative. On treatment with molten benzoic acid, it afforded a benzoate which gave a di-2,4-dinitrophenyl hydrazone, crystallized from ethanol, mp. 161°C (found C = 55.21%, H= 3.49%, N = 16.68% Formula $C_{31}H_{24}O_{10}N_8$ requires C = 55.69%, H = 3.59%, N = 16.76%) absorbed frequencies : (—C=N—) : 1622 cm^{-1}, ($C-NO_2$) : 1332 cm^{-1}, ($O—CO—C_6H_5$) : 1670 cm^{-1}.

1-Diazo-1-n-amyl-4-benzoyl-but-3-ene-2-one IV (I, R = n — C_5H_{11})

β-Benzoyl-acrylyl chloride (2.91 g; 0.015 mol) was treated with pre-estimated ethereal solution of diazo-n-hexane (3.06 g, 0.03 mol) at 0° C. The red oily diazoketone, yield 2.31 g, 56% afforded a di-2,4-dinitrophenyl osazone, crystallized from alcohol, mp. 256°C (found C =

= 50.47%, H = 3.71%, N = 21.19% formula $C_{34}H_{30}O_{12}N_{12}$ requires C = 50.12%, H = 3.77%, N = 21.05%) absorbed frequencies (—C=N—) 1620 cm^{-1}, (C=C) 1680 cm^{-1}, ($C—NO_2$) 1340 cm^{-1}, ($—CH_2—$ in n-amyl group) 760 cm^{-1}

4-Benzoyl-3-diazoacetyl pyrazoline V (II, R = H)

β-Benzoyl acrylyl chloride (5.82 g, 0.03 mol) was treated with pre-estimated diazomethane (3.78 g, 0.09 mol) at 0°C. The yellow mobile diazoketone, yield 2.71 g, 46%, afforded a di-2,4-dinitrophenyl osazone, crystallized from alcohol mp. 116°C (found C = 46.09%, H = 2.82%, N = 25.63% formula $C_{30}H_{20}N_{14}O_{12}$ requires C = 46.76%, H = 2.85%, N = 25.44%); absorbed frequencies: (—C=N—) 1618 cm^{-1}, (—N=N—) 1545 cm^{-1}, ($C—NO_2$) 1340 cm^{-1} (I.R. Graph 'C'). On treatment with molten benzoic acid, it afforded a benzoate which gave a di-2,4-dinitrophenyl hydrazone, crystallized from alcohol, mp. 143°C (found C = 53,96%, H = 3.48%, N = 19.79% formula $C_{31}H_{24}O_{10},N_{10}$ requires C = 53.45%, H = 3.45%, N = 20.01%) absorbed frequencies (—C=N—): 1618 cm^{-1}, ($C—NO_2$): 1320 cm^{-1}, ($O—CO—C_6H_5$): 1704 cm^{-1}. On thermolysis i.e. treating with copper powder in dioxan, it gave X(R=H) which afforded tetra-2,4-dinitrophenyl hydrazone, crystallized from alcohol, mp. 139°C (found C = 50.93%, H = = 3.09%, N = 24.61% formula $C_{48}H_{36}O_{16}N_{20}$ requires C = 50.17%, H = 3.14%, N = 24.39%) absorbed frequencies: (—C=N—) 1628 cm^{-1}, (C=C) 1709 cm^{-1}.

4-Benzoyl-4-n-propyl-diazo-acetyl-5-n-propyl pyrazoline VI (II, R = $n-C_3H_7$)

β-Benzoyl acrylyl chloride (3.89 g, 0.02 mol) was treated with pre-estimated ethereal solution of diazo-n-butane (4.68 g, 0.06 mol) at 0°C. The reddish yellow mobile diazoketone, yield 4.28 g; 68%, afforded a di-2,4-dinitrophenyl osazone, crystallized from alcohol mp. 218°C. It responded to Knorr's test,[4] thus confirming the presence of pyrazoline ring (found C = = 52.91%, H = 4.13%, N = 18.98% formula $C_{36}H_{34}O_{12}N_{14}$ requires C = 53.07%, H = 4.18%, N = 19.18%) absorbed frequencies (—C=N—) 1620 cm^{-1}, ($n—C_3H_7$) 1460 cm^{-1}, ($C—NO_2$) 1340 cm^{-1}, (—N=N—) 1595 cm^{-1} (I.R. Graph 'D'). On thermolysis, it afforded tetra 2,4-dinitrophenyl hydrazone, crystallized from alcohol, mp. 166°C (found C = 53.97%, H = 4.68%, N = 21.15% formula $C_{60}N_{60}O_{16}N_{20}$ requires C = 54.72%, H = 4.57%, N = 21.28%) absorbed frequencies (—C=N—) 1618 cm^{-1}, (—C=C—): 1687 cm^{-1}, ($C—NO_2$): 1334 cm^{-1} ($n—C_3H_7$): 1477 cm^{-1}

4-Benzoyl-3-n-amyl-diazoacetyl-5-n-amyl pyrazoline VII (II, R = $n-C_5H_{11}$)

β-Benzoyl acrylyl chloride (2.14 g, 0.001 mol) was treated with pre-estimated diazo-n-hexane (3.36 g, 0.03 mol) at 0°C. The red mobile diazoketone, yield 2.42 g, 62%, afforded Knorr's test thus confirming the presence of pyrazoline ring. However, the corresponding osazone could not be identified as an oil was obtained. Thus, this diazoketone was characterized by treating with molten benzoic acid, it afforded benzoate which gave di-2,4-dinitrophenyl hydrazoline, crystallized from ethanol, mp. 83°C (found C = 58.17%, H = 5.19%, N = 16.91% formula $C_{41}H_{44}O_{10}N_{10}$ requires C = 58.85%, H = 5.26%, N=16.75%) absorbed frequencies ($O—CO—C_6H_5$) 1695 cm^{-1}, (—C=N—) 1620 cm^{-1}, (—N=N—) 1595 cm^{-1}, ($C—NO_2$): 1330 cm^{-1} ($—CH_2—$ in n-amyl): 722 cm^{-1}

INFERENCE

The above series of experiment has confirmed that the susceptibility towards diazoalkanes goes in descending order i.e. carboxylic acid chloride group, unsaturation and then carbonyl group.

REFERENCES

[1] F. Arndt, B. Eistert, and W. Partale; *Ber. dtsch. chem. Ges.*, **60**, 1364 (1927); R. Robinson, and W. Bradley,; *J. Amer. Chem. Soc.*, **50**, 1310 (1928).

[2] A. K. Bose and P. Yates, *J. Amer Chem. Soc.*, **74**, 4703 (1952).

[3] L. Wolff, *Ann.*, **394**, 23 (1912).

[4] L. Knorr, *Ber. dtsch. chem. Ges.*, **26**, 100 (1893).

[5] L. J. Ballamy, "Introduction to infra-red spectra of complex molecules", Methune & Co.

[6] Colthup, B. Norman, Lawrence H., Daly, Stephen E. Wiberley, "Introduction to infra-red and Raman Spectroscopy", Academic Press, New York.

[7] John R. Dyer, "Applications of absorption spectroscopy of organic compounds", Prentice Hall of India Ltd., New Delhi-1978.

[8] Werner, *J. Chem. Soc.*, **115**, 1093 (1919); Arndt and Amende, *Angew. Chem.*, **43**, 444 (1930).

Revue Roumaine de Chimie, **30**, *9—10*, 807—815 (1985)

THE STUDY OF THE EXTRACTION PROCESS OF VINCAMINE

C. ONISCU, M. MACOVEANU, E. HOROBA, M. COJOCARU and E. POTORAC
Polytechnic Institute of Jassy, Department of Chemistry, Splai Bahlui 71, 6600 Iași, Romania

Received September 10, 1984

The paper studies the extraction process of vincamine from the *Herba Vinca Minor L* plant, in order to establish a direct correlation between the quantity of extracted vincamine and the variables which significantly influence the extraction process. By using the empirical modelling, we can establish an equation which describes quantitatively, and with a high precision, the extraction process.

Likewise, the thermodynamic equilibrium and the kinetics of the extraction process of vincamine from the *Herba Vinca Minor L* plant by using methanol as solvent have been studied. At the same time, the influence of the change in temperature, bath ratio and stirring conditions on the kinetics of the process has been discussed.

1. INTRODUCTION

A special attention has been given lately to natural products, especially to alkaloids used in therapeutics, both their extraction conditions and the possibilities of separation in pure state being studied. One of the natural products, which are extracted from different plants is the vincamine. This is an alkaloid which is extracted from the *Herba Vinca Minor L* plant and has formula[1,2] :

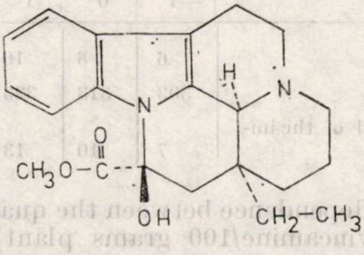

This alkaloid has a powerful hypotensive action ; it regulates the cerebral circulation, determines a better usage of the oxygen by the cerebral matter and is very well tolerated by the human body.

The purpose of this paper is to establish a direct correlation between the quantity of extracted vincamine and the variables which influence the extraction process and, also, to study the thermodynamic equilibrium and the kinetics of the extraction process of vincamine from the *Herba Vinca Minor L* plant by using methanol as a solvent.

2. THE EMPIRICAL MODELLING OF THE PROCESS

2.1. Experimental

To extract vincamine from the *Herba Vinca Minor L plant*, methanol has been used as an extraction solvent. The extraction process has been accomplished in a glass vessel having a 2 L volume. An impeller with the diameter of the active element of 0.5 D (D being the inner diameter of the extractor) has been used. The extractor has been equipped with a return condenser for methanol. The temperature has been kept constant by means of a thermostat. The quantity of plant used for extraction has been constant, namely, 100 g for all our experiments. The extraction process has always lasted 2 h and the used plant has come from the same lot. For analysis we have used 250 mL methanol extract samples which have been concentrated in vacuum up to a 10 mL volume. Then we have added 10 mL H_2SO_4 0.1 N and the distillation of the methanol has been kept on till its complete removal. The concentrate solution has been cooled and filtered in vacuum. Both the vessel and the filtering funnel have been washed with another 10 mL H_2SO_4 0.1 N. The filtrate has been taken to pH = 9 with 25% aqueous ammonia. The alkalized solution has been brought in a separatory funnel and with a quantity of 25 mL chloroform has been dried on anhydrous Na_2SO_4 after which it has been vapourized in dried conditions. The remainder has been dissolved in 1—2 mL chloroform and has been treated by chromatography to separate the vincamine. After chromatography, vincamine is passed in dichloromethane, and the concentration of the solution is spectrophotometrically determined.

2.2. Results and Discussion

The variables whose influence on the extraction process has been studied are: the bath ratio, the temperature and the rotational speed of the impeller.

The extraction process of vincamine has been experimentally accomplished at different values of those three variables. Both the real value of the variables used in the process and their coding are given in Table 1.

Table 1

The variable levels

Variable	Coded and natural Levels			Range	Notation
	—1	0	1		
Bath ratio	6	8	10	4	x_1
Temperature, K	303	313	323	20	x_2
Rotational speed of the impeller, s^{-1}	7	10	13	6	x_3

To determine the dependence between the quantity (y) of the extracted vincamine (grams vincamine/100 grams plant) and the mentioned variables, the following model has been proposed:

$$Y = b_0 + b_1x_1 + b_2x_2 + b_3x_3 + b_{12}x_1x_2 + b_{13}x_1x_3 + b_{23}x_2x_3 + \\ + b_{123}x_1x_2x_3 \tag{1}$$

The experimentation matrix used to statistically model and the obtained data are presented in Table 2.

Table 2

Factorial design 2^3

Experiment	Experimental matrix				Answer $10^3 \cdot y$
	x_0	x_1	x_2	x_3	
1	1	—1	—1	—1	5.790
2	1	1	—1	—1	7.536
3	1	—1	1	—1	9.900
4	1	1	1	—1	10.360
5	1	—1	—1	1	7.857
6	1	1	—1	1	8.100
7	1	—1	1	1	10.056
8	1	1	1	1	10.970
9	1	0	0	0	9.710
10	1	0	0	0	9.710
11	1	0	0	0	9.600
12	1	0	0	0	8.460

As the value y found out during the 12th experiment differs evidently from the values established for the other three experiments (9—11) accomplished under the same conditions, an elimination test of the abnormal results has been applied.[3] We have computed the quantity :

$$Q = \frac{y_s - y_a}{y_{\max} - y_{\min}} = 0.912 \tag{2}$$

where

y_a = the value considered abnormal

y_s = the value immediately superior to y_a

From literature, [3] the Q value found out for an implication level $\alpha = 0.05$ and a number of four determinations is $Q_{(4.5)} = 0.76$.

As the value Q computed by using the experimental data is higher than the listed value, the respective experiment (no. 12) has been eliminated from the subsequent computations.

The computed values [4] of the regression coefficients from the proposed model (1) and the sum of the squares of the regression coefficients, $SP(b_i)$, are given in Table 3.

To estimate the significant influences, the Fischer test has been used. The calculated value (F_c) is given by the relation :

$$F_c = \frac{SP(b_i)}{s_r^2} \tag{3}$$

The computed value of the experimental error [4] is $s_r^2 = 4.05.10^{-9}$.

According to the Fischer test, Table 3, for an implication level $\alpha = 0.05$, we found out that $F_{T(1,2)} = 18.51$.

Table 3

Coefficient	Value	$SP(b_i)$	F_c	Retained coefficients
b_0	0.0090535	0.0008084	198716.0	+
b_1	0.0004240	0.0000014	345.7	+
b_2	0.00150	0.0000180	4444.4	+
b_3	0.0004246	0.0000014	345.7	+
b_{12}	—0.0000769	0.00000005	11.7	—
b_{13}	—0.0001311	0.0000001	24.7	+
b_{23}	—0.0002331	0.0000004	98.7	+
b_{123}	0.0002446	0.0000005	123.0	+

On account of the fact that for all the coefficients, except for b_{12}, the F_c value is higher than the listed one (for $\alpha = 0.05$), we can conclude that y is significantly influenced both by all the studied variables and by their interaction (except to interaction 1—2).

This is the way by which the following equation could have been established :

$$Y = (90.5 + 4.2\,x_1 + 15x_2 + 4.2x_3 - 1.3x_1x_3 - 2.3x_2x_3 - \\ - 2.4x_1x_2x_3) \cdot 10^{-4} \tag{4}$$

The y values computed by means of equation (4) would range about the real value between certain limits, as a function of the experimental errors; these limits could be determined by the relation :

$$Y \pm t_\alpha \sqrt{s^2_{yx_1x_2x_3}} \tag{5}$$

where t_α is found in the Student distribution tables [3]; for $\alpha = 0.05$ and for seven degrees of freedom (the same number of degrees of freedom with which the $s^2_{yx_1x_2x_3}$ dispersion is computed) we have got to $t_{0.05} = 2.365$.

The dispersion of the values noticed around the regression surface has been obtained by the relation :

$$s^2_{yx_1x_2x_3} = \frac{\sum_i (y_i - Y_i)^2}{N - (k+1)} \tag{6}$$

where k is the number of independent variables from equation (4). Thus, the following variation limits of the computed Y values have been determined :

$$Y_i \pm 1.6.10^{-3} \tag{7}$$

To estimate the overall influence of the variation of the examined parameters upon y, the multiple correlation coefficient (R) has been computed by means of the relation :

$$R = \sqrt{1 - \frac{s^2_{yx_1x_2x_3}}{s^2_y}} \tag{8}$$

where s_y^2 is the dispersion of the individual values y_i around the mean value $\bar{y}$:

$$s_y^2 = \frac{1}{N - (k+1)} \cdot \sum_{i=1}^{11} (y_i - \bar{y})^2 \tag{9}$$

We have found that $R = 0.923$, so we can conclude that the variation of the quantity of extracted vincamine is 92.3 % caused by the variation of the studied parameters.

3. THE EQUILIBRIUM OF THE EXTRACTION PROCESS

3.1. Experimental

The study of the equilibrium of the extraction process has been accomplished in the installation described in part 2.1.

The working conditions have been the following:

— the solvent used for extraction has been methanol;

— the bath ratio (mL methanol : g. plant) $M = 10$;

— temperature: 313 K;

— the rotational speed of the impeller: 10 s^{-1};

— the plant quantity: 100 g.

The plant and the methanol ($M = 10$) have been introduced in the extractor. The obtained slurry has been maintained under stirring at a 313 K temperature for 15' hours; after this period the concentration of the extracted vincamine in the solvent has not varied any more.

Then a 250 mL volume of fresh solvent has been used. The procedure has been repeated, thus the dependence between the vincamine concentration from the two phases, namely, solid (plant) and liquid (extraction solvent), being obtained.

The determination of the vincamine concentration from the extract has been done by the method described in part 2.1.

The initial vincamine content of the plant (x_a) has been established by repeated extraction in a Soxhlet apparatus till all vincamine has been drained from the plant. This is the way the value $x_a = 19.81 . 10^{-3}$ g/100 g plant has been obtained.

3.2. Discussion of the Equilibrium Data

By contacting the plant with methanol a stable distribution of the vincamine between the two phases has been achieved after a sufficiently long time.

The variation of the vincamine concentration in the extraction solvent (y), as a function of the vincamine concentration in plant (x), experimentally established for the 313 K temperature, is graphically shown in Figure 1.

As it is more difficult to use a graphical dependence, we have tried to establish a mathematical equation to fit experimental data on the basis of which the curve from Figure 1 has been plotted.

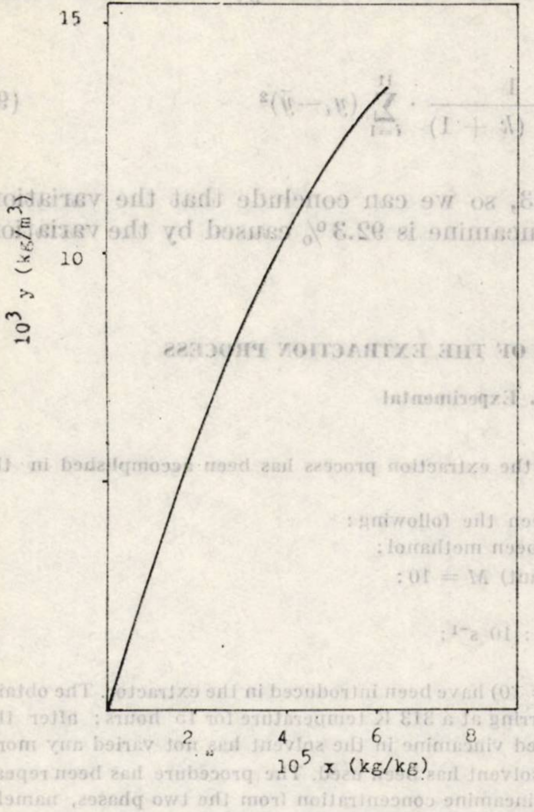

Fig. 1. — The equilibrium curve for the extraction of vincamine with methanol at 313 K.

By using the method of the least squares we have established a polynom-type dependence under the form :

$$y = -0.11278 + 2.38852 . x + 0.27218 . x^2 - 0.08603 . x^3 + 0.00758 . x^4 - 0.00023 . x^5 \qquad (10)$$

where

y is the concentration of the vincamine in the methanol, kg/m^3

x is the concentration of the vincamine in plant, kg/kg

4. THE KINETICS OF THE EXTRACTION PROCESS

4.1. Experimental

The kinetics tests accomplished in the previously-described experimental installation have allowed us to find out the variation of the vincamine concentration with the extraction time both in the extraction solvent and in solid particles, at 313 K and 323 K, at two values of the bath ratio (8 and 10), and at two rotational speed of the impeller (7 and 10 s^{-1}, respectively).

The experimentally obtained results are shown in Figures 2, 3 and 4. The rate of the curves is in agreement with the data presented in literature. [5,6]

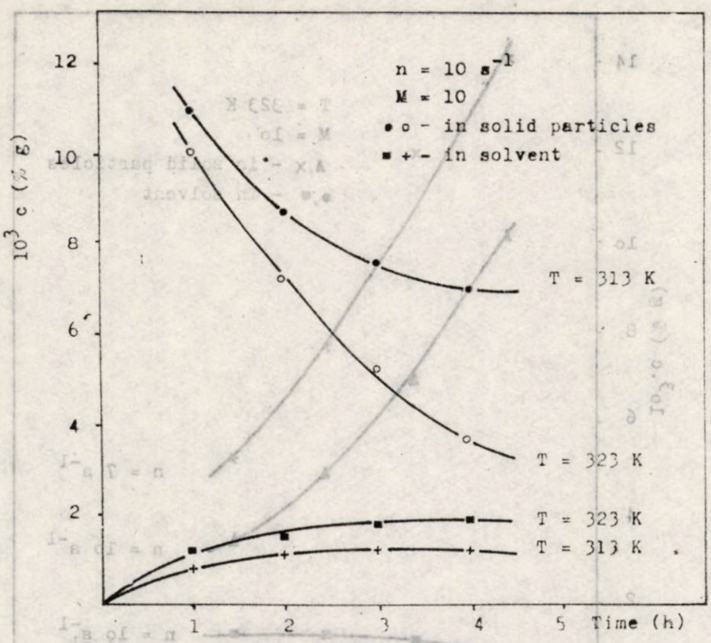

Fig. 2. — The time variation of the vincamine concentration (c) in plant and in the extraction solvent, as a function of temperature.

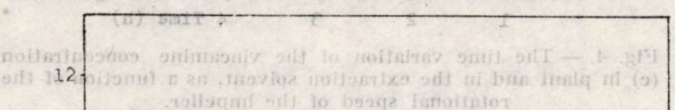

Fig. 3. — The time variation of the vincamine concentration (c) in plant and in the extraction solvent, as a function of the bath ratio.

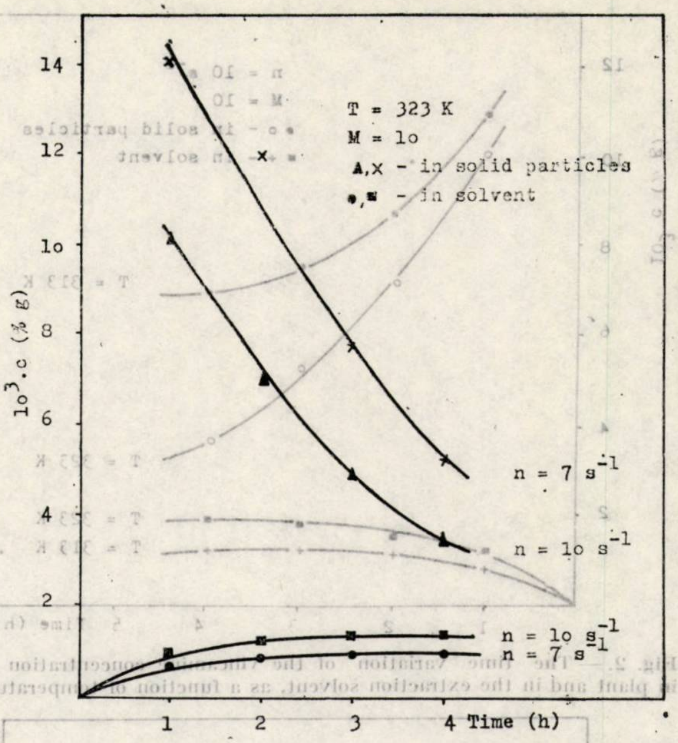

Fig. 4. — The time variation of the vincamine concentration (c) in plant and in the extraction solvent, as a function of the rotational speed of the impeller.

4.2. Discussion of the Kinetics Data

The kinetics of the extraction process contains two elementary processes :

— the internal diffusion which consists in the migration of the soluble substance from the solid particles to their surface;

— the external diffusion, the transfer of the soluble substance through the liquid film from the solid-liquid interface to the mass of the extraction solvent.

In the specialized literature, $^{5-9}$ the internal diffusion is considered as a determinant stage of the process.

If we examine the curves presented in Fig. 2, one can notice that the temperature influences significantly the extraction process when the extraction time has exceeded 1 hour. Consequently, the internal diffusion takes place with a sufficiently high rate in the first hour of extraction; the increase of the temperature in the studied domain being not important in what the acceleration of the extraction process is concerned.

As one can notice from Fig. 3, the concentration gradient of vincamine between the solid and the liquid phase is sufficiently high at the beginning of the extraction process to allow the development of the extraction process with a rate practically independent of the bath ratio. But, in time (after about 2 hours), the influence of the increase of the bath ratio becomes perceptible as it determines the maintaining of a higher concentration gradient.

The influence of the change in the rotational speed of the impeller on the kinetics of the process can be seen in Fig. 4. One can notice that at the same time with the increase of the rotational speed of the impeller the extraction process takes place more rapidly; a fact which indicates the importance of the diffusion through the liquid film from the solid-liquid interface.

On considering as a total the influence of the temperature, bath ratio and the rotational speed of the impeller on the extraction process of vincamine, we can conclude, according to the above-discussed interpretation, that the total rate of the process (for the studied domain) is determined both by the internal diffusion and by the diffusion through the liquid film from the solid-liquid interface.

5. CONCLUSIONS

a) In the studied experimental domain, the quantity of extracted vincamine is a function of the bath ratio, of the temperature, and of the rotational speed of the impeller. The higher the values of these variables are, the greater the quantity of extracted vincamine is.

b) The equation which describes the dependence between the quantity of the extracted vincamine and the variables considered as valid in the studied domain is equation (4).

c) In 95% of the cases the differences between the noted values of y and the $(\bar{Y})$ values computed with the established equation will range between $\pm$ $1.6.10^{-3}$.

d) The variation of the quantity of extracted vincamine is 92.3% caused by the variation of the studied factors, while the remaining percentage is due to other causes.

e) The equilibrium curve of the extraction process of vincamine has been established, a fact which gives the possibility of determining the number of theoretical stages of extraction.

f) The total rate of the extraction process is determined in time both by the internal diffusion and by the diffusion through the liquid film from the solid-liquid interface.

REFERENCES

[1] C. Ruti, "Fondamenti di chimica farmaceutica", Lint, Trieste, 1978, Vol. III, p. 983.

[2] R. H. Monske, "The alkaloids chemisty and physiology", Acad. Press New-York, 1968, Vol. XI, p. 294.

[3] A. Glück, "Metode matematice în industria chimică", Ed. Tehnică, Bucharest, 1971.

[4] R. Mihail, "Introducere în strategia experimentării, cu aplicații în tehnologia chimică", Ed. Științifică și Enciclopedică București, 1976.

[5] H. Yand, C. Y. Brier, A. I. Ch. E. J., 4, 4, 453 (1958).

[6] O. Smigelschi, Gh. Jinescu, C. Balaban, R. Dima, and P. Vasilescu, *Rev. de chimie*, **32**, *2*, 150 (1981).

[7] M. I. Kurochkina, "Extraction and leaching of solid materials", Mir Publishers, Moskva, 1978.

[8] W. Halwachs, *Chem. Eng. Techn.*, **50**, *10*, 767 (1978).

[9] G. J. Gmehling, F. Andersen, and M. J. Prasnitz, I.E.C. Fundamentals, **17**, *4*, 269 (1978).

Revue Roumaine de Chimie, **30**, *9—10*, 817—822 (1985)

SYNTHESIS OF SOME NEW N-AMINO-2-PYRIDONE DERIVATIVES

A. K. EL-SHAFEI, A.-B. A.G. GHATTAS and F. A. GAD*

Chemistry Department, Faculty of Science, Sohag, Egypt, and National Research Centre, Dokki, Cairo

Received October 28, 1984

A convenient one step synthesis of some new 1,6-diamino-3-cyano-4-aryl-5-(2-thioheteroaryl)-2-pyridones 4 and 1,6-diamino-3-cyano-4,5-diaryl-2-pyridones 5 is described. The alkaline hydrolysis of compound 4 afforded the corresponding 1,6-diamino-3-cyano-4-aryl-5-hydroxy-2-pyridones 6. The structure of the obtained products was established both by IR and NMR spectral data.

There are few synthetic procedures which were reported for the preparation of the useful intermediate $^{1-4}$ N-amino-2-pyridones. These compounds are usually obtained $^{5-8}$ in low yield by the reaction of hydrazine with 2-pyrones, which are, in turn, prepared in low yields from open chain compounds; $^{3,9-13}$ however, Soto et al. ^{14} have recently reported a convenient synthesis of N-amino-2-pyridones from benzylidenemalononitriles which are easily accessible through a Knoevenagel condensation of aromatic aldehydes with malononitrile and 2-cyano ethanoic acid hydrazides in methanol in the presence of piperidine. We aim to report here the synthesis of a new series of N-amino-2-pyridones, thus 2-thioheteroarylethanoic acid hydrazides 1 as well as phenylacetohydrazide 2

Table 1

Preparation and spectral data of compounds **1a**—**d**

product No.	Het-Ar	Yield %	mp °C	Molecular formula	Analytical data Calcd./Found % C	H	N	IR KBr ν (Cm^{-1})
1a	pyridyl-	72	80	$C_7H_9N_3SO$ (183)	45.90 45.78	4.91 5.05	22.95 23.07	3290, 3200
1b	pyrimidinyl-	65	133	$C_6H_8N_4SO$ (184)	39.13 39.17	4.34 4.44	30.43 30.32	3320, 3210
1c	benzothiazolyl-	59	162	$C_9H_9N_3S_2O$ (239)	45.18 45.22	3.76 3.62	17.57 17.66	3300, 3210
1d	-phenyl-1,3,4-oxadiazolyl-	55	153	$C_{10}H_{10}N_4SO_2$ (250)	48.00 48.09	4.00 3.89	22.40 22.50	3320, 3200

were allowed to react with arylidene or heteroarylidenemalononitriles **3**. 2-Thioheteroarylethanoic acid hydrazides **1** were obtained by heating 2-mercaptoheteroaryls with ethylchloroacetate in benzene in the presence of triethylamine; the obtained esters were then refluxed with hydrazine hydrate in ethanol. Arylidene and heteroarylidenemalononitriles **3** were prepared as described.[15,16] Phenylacetohydrazide **2** obtained from Aldrich Chemical Co., was used without further purification. The reaction was found to proceed in ethanol at room temperature by stirring a mixture of **1** or **2** with **3** over periods ranging between 1—6 hours in the presence of a catalytic amount of sodium ethoxide. When piperidine was used as the basic catalyst the reaction was found to take more time and in some instances (compounds **5**, cf Scheme 1), the reaction did not afford the desired products. A series of 1,6-diamino-3-cyano-4-aryl-5-(2-thio-heteroaryl)-2-pyridones **4** or 1,6-diamino-3-cyano-4,5-diaryl-2-pyridones **5** is thus obtained in good yields (Table 2). The nature of the substituent present in the benzene ring of the benzylidene-malononitrile **3** and the type of the heteroaryl moiety in **1** has little effect on the reaction, however, phenylacetohydrazide **2** was found to be more reactive than **1**.

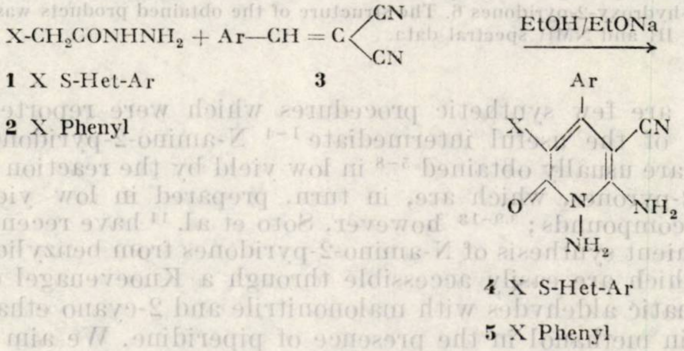

1 X S-Het-Ar

2 X Phenyl

3

4 X S-Het-Ar

5 X Phenyl

Scheme 1

For the mechanism of this reaction cf. ref. 14.

The structure of compounds **4** and **5** was based on analytical and spectral data, in the IR spectra, the band about 1640—1670 cm^{-1} could be assigned to the C=O group of the N-amino-2-pyridones system [6] and the two amino groups are clearly seen in the ^{1}H-NMR spectra (Table 2). A chemical confirmation of the structures **4** was also obtained on hydrolysis in aqueous sodium hydroxide solution; thus **4a** and **4c** are converted into 1,6-diamino-3-cyano-4-aryl-5-hydroxy-2-pyridones **6a, c** which showed an OH group absorption in the IR spectrum. This is suggestive of the easy conversion of a sulphide into hydroxy and mercapto derivatives.[17,18]

EXPERIMENTAL

All melting points were determined on a Kopfler bank and are uncorrected. The IR spectra were recorded using KBr discs on a Pye Unicam SP 1200 spectrophotometer. ^{1}H-NMR spectra were obtained in DMSO-d_6 with a Varian A 60 spectrometer using TMS as internal standard, chemical shifts are expressed in δ ppm.

Table 2

Preparation and spectral data of compounds **4** and **5**

Compound No.	Ar	X	Time of reaction (hours)	mp °C	Molecular formula	Analyses % Calcd./Found			IR ν (Cm^{-1})
						C	H	N	
4a	C_6H_5	2-thiopyridyl-	4	300	$C_{17}H_{13}N_5SO$ (335)	60.89 60.94	3.88 3.79	20.89 20.81	3440, 3330, 2220, 1655
4b	p-$NO_2C_6H_4$	2-thiopyrimidinyl-	4	220	$C_{16}H_{11}N_7SO_3$ (381)	50.39 50.43	2.88 2.98	25.72 25.61	3390, 3320, 2220, 1670
4c	p-$NO_2C_6H_4$	2-thiobenzo-thiazolyl-	6	279	$C_{19}H_{12}N_6S_2O_3$ (436)	52.29 52.36	2.75 2.62	19.26 19.33	3390, 3320, 2220, 1670
4d	C_6H^5	2-thiobenzothiazolyl-	6	228	$C_{19}H_{13}N_5S_2O$ (391)	58.31 58.22	3.32 3.41	17.90 17.98	3480, 3290, 2200, 1665
4e	p$N(CH_3)_2C_6H_4$	5-phenyl-2-thio- 1,3,4-oxadiazolyl-	6	260	$C_{22}H_{19}N_7SO_2$ (445)	59.32 59.21	4.26 4.17	22.02 22.09	3390, 3310, 2210, 1640
5a	C_6H_5	C_6H_5	1	150	$C_{18}H_{14}N_4O$ (302)	71.52 71.44	4.63 4.71	18.54 18.61	3480, 3400, 2220, 1655
5b	p$NO_2C_6H_4$	C_6H_5	1	194	$C_{18}H_{13}N_5O_3$ (347)	62.24 62.19	3.74 3.83	20.17 20.31	3490, 3410, 2215, 1670
5c	p$N(CH_3)_2C_6H_4$	C_6H_5	3	202	$C_{20}H_{19}N_5O$ (345)	69.56 69.48	5.50 5.59	20.28 20.20	3420, 3320, 2220, 1655
5d	4-pyridyl	C_6H_5	2.5	209	$C_{17}H_{13}N_5O$ (303)	67.32 67.39	4.29 4.19	23.10 23.21	3440, 3320, 2220, 1650

Table 2 (continued)

Compound No.	^{1}H-NMR spectral data δ (ppm)
4a	8.44 (br, 2H, C$-$NH$_2$) ; 8.15$-$8.00 (m, 9H, arom. + pyridyl) ; 5.6 (br, 2H, N$-$NH$_2$)
4b	8.60 (br, 2H, C$-$NH$_2$) ; 8.20$-$8.00 (m, 7H, arom. + pyrimidinyl-), 5.53 (br, 2H, N$-$NH$_2$)
4c	8.35 (br, 2H, C$-$NH$_2$) ; 8.20$-$8.00 (m, 8H, arom. + benzothiazolyl-) ; 5.58 (br, 2H, N$-$NH$_2$)
4d	8.45 (br, 2H, C$-$NH$_2$) ; 8.15$-$8.00 (m, 9H, arom. + benzothiazolyl) ; 5.15 (br, 2H, N$-$NH$_2$)
4e	8.73 (br, 2H, C$-$NH$_2$) ; 8.28$-$8.15 (m, 9H, arom.) ; 5.60 (br, 2H, N$-$NH$_2$) ; 3.30 (s, 6H, CH$_3$)
5a	8.75 (br, 2H, C$-$NH$_2$) ; 8.25$-$8.05 (m, 10H, arom.) ; 5.54 (br, 2H, N$-$NH$_2$)
5b	8.60 (br, 2H, C$-$NH$_2$) ; 8.22$-$8.10 (m, 9H, arom.) ; 5.63 (br, 2H, N$-$NH$_2$)
5c	8.55 (br, 2H, C$-$NH$_2$) ; 8.25$-$8.05 (m, 9H, arom.) ; 5.50 (br, 2H, N$-$NH$_2$)
5d	8.50 (br, 2H, C$-$NH$_2$) ; 8.15$-$8.00 (m, 9H, arom.-pyridyl) ; 5.58 (br, 2H, N$-$NH$_2$)

2-Thioheteroarylethanoic acid hydrazides 1a—d; general procedure

A mixture of 0.1 mole of 2-mercaptoheterocyclic compound and ethylchloroacetate (0.1 mole) in 75 mL of dry benzene containing an equivalent amount of triethylamine is heated under reflux with stirring for 1 hour. The solvent is distilled off in vacuo and the residue is washed well with water and crystallized from petroleum ether at 40—60°C. An equivalent amount of the resulting ester (0.05 mole) is then refluxed with 0.05 mole of hydrazine hydrate in ethanol for 2 hours. The reaction mixture is then concentrated and left to cool in the frigo to give the desired products **1** in good yields (Table 1); the corresponding ester of compound **1d** was left to react with hydrazine hydrate at room temperature for 8 hours where the desired product **1d** was obtained by suction filtration and crystallization from ethanol.

1,6-Diamino-3-cyano-4-aryl-5-(2-thioheteroaryl)-2-pyridones 4 and 1,6-diamino-3-cyano-4,5-diaryl-2-pyridones 5; general procedure

A mixture of hydrazide **1** or **2** (0.05 mole) and the appropriate arylidenemalononitrile **3** (0.1 mole) is suspended in dry ethanol (~ 100 ml) under magnetic stirring. When a few drops of an ethanolic solution of sodium ethoxide are added, the reactants begin to dissolve. The reaction mixture is stirred over periods of time ranging between 1—6 hours and left to stand at room temperature overnight. The deposited solid is isolated by suction filtration, washed well with water and ethanol and dried in air. The obtained products are of good purity. Further purification can be achieved by recrystallization from ethanol.

Hydrolysis of 1a, c to 6a, c

To ethanol (10 mL) containing 30% aqueous sodium hydroxide (6 mL) is added **4a** (0.33 g, 0.001 mole) or **4c** (0.43 g, 0.001 mole). The mixture is heated under reflux with stirring for 1 hour and then cooled to room temperature. The resultant solid product is isolated by filtration and washed with ethanol. Warm water is added to the solid, which is stirred until complete dissolution. The solution is acidified with 3 molar hydrochloric acid and stirred at room temperature for 1 hour. The colorless crystals which deposit during the neutralization are isolated by vaccum filtration, washed with water and ethanol. Recrystallization from tetrahydrofuran give **6a** and **6o**, respectively.

6a, yield: 0.15 g (65%) mp (189°C.

$C_{12}H_{10}N_4O_2$	Calcd.	C 59.50	H 4.13	N 23.14
(242)	Found	59.42	4.20	23.22

IR (KBr): cm^{-1} 3560 (OH); 3450, 3340 (NH); 2220 (CN); 1660 (C—O)

^{1}H-NMR (DMSO-d_6): ppm 13.1 (br, 1H, OH); 8.70 (br, 2H, C—NH_2); 7.40 (m, 5H, arom.); 5.58 (br. 2H, N-NH_2).

6c. yield 0.13 g (48%) mp 245°C.

$C_{12}H_9N_5O_4$	Calcd.	C 50.17	H 3.13	N 24.39
(287)	Found	50.13	3.21	24.51

IR (KBr): Cm^{-1} 3350 (OH); 3430, 3310 (NH); 2220 (CN); 1660 (C—O).

^{1}H-NMR (D SO—d_6): ppm 12.4 (br. 1H, OH); 8.80 (br. 1H. C—NH_2); 7.65 (m, 5H, arom.); 5.62 (br, 2H, N-NH_2).

REFERENCES

[1] A. R. Katritzky et al., *Tetrahedron Lett.*, 2691 (1976).

[2] A. R. Katritzky, P. Molina, A. Soler and M. J. Vilaplana, *An. Quim.*, **74**, 1125 (1978).

[3] A. R. Katritzky and P. Molina, *J. Chem. Soc. Perkin Trans.* **1**, 1957 (1979).

[4] P. Molina, M. Alajarin, P. M. Fresneda and A. Soler, *An. Quim.*, **75**, 124 (1979).

[5] R. H. Wiley and S. C. Slaymaker, *J. Amer. Chem. Soc.*, **78**, 2393 (1956).

[6] I. E. El-Kholy, F. K. Rafla and G. Soliman, *J. Chem. Soc.*, 4490 (1961).

[7] I. E. El-Kholy, F. K. Rafla and M. M. Mishrikey, *J. Chem. Soc.* (C), 1578 (1970).

[8] C. W. Rees and M. Yelland, *J. Chem. Soc. Perkin Trans.*, **1**, 77 (1972).

[9] F. Arndt and B. Eistert, *Ber. Dtsch. Chem. Soc.*, **58**, 2318 (1925).
[10] R. Putter and W. Dilthey, *J. Prakt. Chem.*, **149**, 183 (1937).
[11] G. Soliman and I. E. El-Kholy, *J. Chem. Soc.*, 2911 (1955).
[12] I. E. El-Kholy, F. K. Rafla and M. M. Mishrikey, *J. Chem. Soc.*, 2588 (1959).
[13] I. E. El-Kholy, F. K. Rafla and M. M. Mishrikey, *J. Chem. Soc.* (C), 1950 (1969).
[14] J. L. Soto, C. Seoane, P. Zamorano and F. J. Cuadrado, *Synthesis*, **7**, 529 (1981).
[15] B. Corson and R. Stoughton, *J. Amer. Chem. Soc.*, **50**, 2825 (1928).
[16] A. C. Cope and K. E. Hoyle, *J. Amer. Chem. Soc.*, **63**, 733 (1941).
[17] E. D. Hughes and C. K. Ingold, Trans. Faraday Soc., **37**, 657 (1951).
[18] S. Kambe and K. Saito, Synthesis, **7**, 531 (1981).

Revue Roumaine de Chimie, **30**, *9–10*, 823–830 (1985)

HETEROPOLYTUNGSTATES WITH Ti(IV) AND Ni(II). III[1]

THE ABSORPTION SPECTRA OF THE HETEROPOLYANIONS Ni(II)-UNDECATUNGSTOTITANATE(IV) AND Ni(II)-PENTATUNGSTOTITANATE(IV)

RODICA VĂŢULESCU, T. BUDIU, GH. MARCU and IRINA PAL
Chemistry Institute, 30, Fintînele Street, 3400 Cluj-Napoca, Romania

Received September 2, 1983

The paper presents an investigation of the absorption spectra of the heteropolyanions $[H_2ONiTiW_{11}O_{39}]^{6-}$(I) and $[H_2ONiTiW_5O_{20}]^{4-}$ (II) in UV, visible and IR.

1. INTRODUCTION

In our previous papers [1,2] we reported the obtaining of two new heteropolyanions, namely Ni(II)-undecatungstotitanate(IV) and Ni(II)-pentatungstotitanate(IV).

The present paper is devoted to the interpretations of the absorption spectra in UV, visible and IR of the above mentioned anions.

The study of heteropolyanions by means of spectral methods permits, first of all, the obtaining of evidences supporting the structure.[3–13]

Such studies have led to results that confirmed the existence of the heteropolytungstate frame in the case of both anions as well as data that have ascertained the octahedral coordination of the Ni heteroatom.

In the series of the heteropolytungstates of the ratio 1 : 1 : 11, compounds that include two structurally non-equivalent heteroatoms, the interpretation of the absorption spectra in visible has led to spectacular results. These results opened the way to an accurate formulation of the complex anion with the exterior heteroatom hexacoordinated. The series of these spectral studies was initiated by Shimura and Tsuchida.[3]

2. EXPERIMENTAL

The absorption spectra in UV of the potassium salt of the Ni(II)-undecatungstotitanate (IV) and of the sodium salt of the Ni(II)-pentatungstotitanate (IV) have been recorded within the 30000–50000 cm^{-1} range.

The recording was carried out on a Specord UV–VIS spectrophotometer with automatic recording.

The absorption spectra in visible of the potassium salt solution of the I anion and of the sodium salt of the II anion, respectively, have been recorded within the wavelength range of 400—1350 nm and were compared with the spectrum of a $NiSO_4$ solution, that is, of the $[Ni(H_2O)_6]^{2+}$ ion. A Beckman D.K. 2A double-beam spectrophotometer with automatic recording was used in these experiments.

The IR absorption spectra were recorded with a U.R. 10 Carl-Zeiss Jena spectrophotometer and the pelleting technique was used for the preparation of the samples in KBr. These spectra were recorded at room temperature within the 700—1700 cm^{-1} range, for ammonium and potassium salts of the Ni(II)-undecatungstotitanate (IV) anion and for the sodium and amonium salts of the Ni(II)-pentatungstotitanate (IV) anion.

3. RESULTS AND DISCUSSION

The absorption spectra in UV and visible of the potassium salt of the Ni(II)-undecatungstotitanate (IV) anion are identical with those of the ammonium salt of the same anion; similarly the absorption spectra in UV and visible of the potassium or ammonium salts of the Ni(II)-pentatungstotitanate(IV) anion are identical with those of sodium salt of the same anion. Therefore, only one example is given below for each anion, as an illustration.

In figure 1 the UV spectra of the aqueous $K_6[H_2ONiTiW_{11}O_{39}]$ solutions and $Na_4[H_2ONiTiW_5O_{20}]$ are represented, respectively.

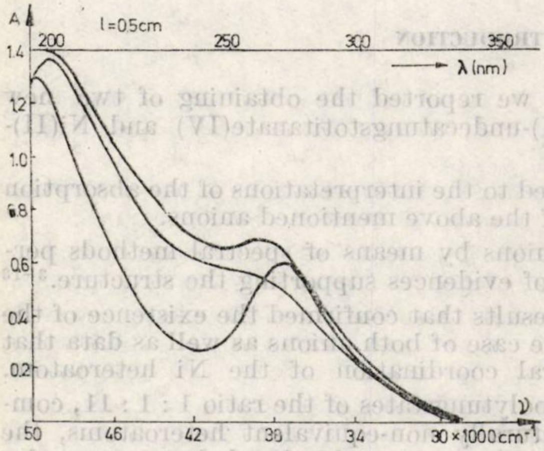

Fig. 1. — The UV absorption spectra of the aqueous solutions:

1) $K_6(H_2ONiTiW_{11}O_{39}]$ $c = 3.6 \cdot 10^{-4}$Mw
2) $Na_4[H_2ONiTiW_5O_{20}]$ $c = 3.1 \cdot 10_{-}{}^{4}$Mw
3) $H_4[TiW_{12}O_{40}]$ $c = 3.4 \cdot 10^{-4}$Mw, obtained by ion exchange.

A rather ill-defined maximum at $\simeq 38500$ cm^{-1} was obtained for the I anion (curve 1) that is, in the same spectral region where this absorption for similar compounds of the series 1 : 1 : 11 is generally encountered.[14-16]

A similar type of absorption is reported with all heteropolytungstate compounds of Keggin structure of ratio 1 : 12, at $\simeq 37800$ cm^{-1}.[17] The shape of the curve differs from the curves of ratio 1 : 1 : 11 in that the absorption maximum is more evident in the series 1 : 12, and the minimum is quite evident at $\simeq 41160$ cm^{-1}.

The absorption band in discussion, characteristic for the polytungstate frame, usually occurs with the compounds of the series 1 : 1 : 11, shifted by ≃ 2000 cm^{-1} towards larger wave numbers, as compared with the Keggin standard structure anions of the ratio 1 : 12.[7]

The same behaviour is obvious in the case of the anion $[H_2ONiTiW_{11}O_{39}]^{6-}$. Comparing the absorption spectrum in UV with the absorption spectrum of the heteropolyacid $H_4[TiW_{12}O_{40}]$ obtained by ion exchange (curve 3), it is evident that the absorption band for the anion I is shifted by 1170 cm^{-1} towards larger wave numbers as compared with the absorption obtained for the acid $H_4[TiW_{12}O_{40}]$.

From the same figure (curve 2) it can be seen that an absorption of approximately the same frequency (≃ 38000 cm^{-1}) is obtained for the anion II, but this time the slope of the curve is less steep; this absorption is also assigned to the pentacondensed polytungstate frame.

The absorption band from 38500 cm^{-1} and 38000 cm^{-1}, respectively, is in the case of both anions situated in the tail of a more intense absorption band with a maximum of ≃ 49000 cm^{-1}. They are charge-transfer bands due to the transitions of the electrons within the W—O—W and W=O bonds of the polytungstate frame.

Pope and his co-workers[18-22] point out that these charge-transfer bands are generally the result of the possibility of charge-transfer from the oxygen atoms to the oxidizing tungsten atoms.

When one or both central atoms of heteropolyanions are transitions metals, other absorption bands appear in the visible field of the spectrum. These bands are due to d—d transitions in the central metal ion and they are ligand-field bands.

In the visible region of the spectrum, as we expected, there will occur, for anions I and II, only the spectrum characteristic for the Ni^{2+} ion of d^8 configuration, because the Ti^{4+} ion has an electronic configuration d°. Therefore, the recording and interpretation of the absorption spectra in visible for anions I and II elucidated the problem of Ni coordination in both heteropolyanions.

In figure 2 the absorption spectra in visible for the anions I and II are presented as compared with the absorption spectrum of the well-known $[Ni(H_2O)_6]^{2+}$ ion.[19]

The absorption spectra in the visible region of the anions $[H_2ONiTiW_{11}O_{39}]^{6-}$ (curve 1), $[H_2ONiTiW_5O_{20}]^{4-}$ (curve 2) and $[Ni(H_2O)_6]^{2+}$ (curve 3 -of the $NiSO_4$ solution) are similar as far as the shape is concerned. They are different only in intensity and those of the anions I and II are a little shifted towards greater wavelengths as compared with that of the hexahydrated Ni^{2+} ion. We reach the conclusion that the Ni^{2+} ion is octahedrally coordinated in both heteropolyanions.

The shape of the spectrum of both anions is similar to that of the other heteropolyanions of the series 1 : 6 or 1 : 1 : 11[5-8,12] that contain Ni^{2+} coordinated in an octahedral space.

Figure 2 shows that the absorption bands recorded for anion I (curve 1) and anion II (curve 2) have their absorption maxima at λ ≃ ≃ 430 nm, in the λ = 700—800 nm and 1100—1250 nm ranges.

The absorption bands of the two anions in discussion are shifted towards higher wavelengths as compared with that of the Ni^{2+} aquoion,

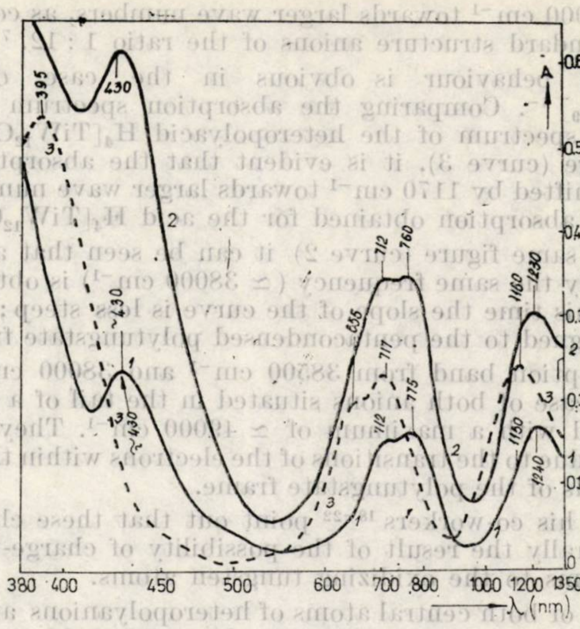

Fig. 2. — The absorption spectra in visible of the aqueous solutions :

1) $K_6[H_2ONiTiW_{11}O_{39}]$ $c = 2.1 \cdot 10^{-2}$ M_{Ni}
2) $Na_4[H_2ONiTiW_5O_{20}]$ $c = 5.7 \cdot 10^{-2}$ M_{Ni}
3) $NiSO_4$ $c = 1.2 \cdot 10^{-1}$ M_{Ni}

which denotes an octahedral coordination of the Ni^{2+} ion in heteropolyanions in a weaker ligand field than in the hydrated ion. The values obtained for the Δ parameter are of 8064 cm^{-1} for the anion $[H_2ONiTiW_{11}O_{39}]^{6-}$ and $\Delta = 8130$ cm^{-1} for anion $[H_2ONiTiW_5O_{20}]^{4-}$, respectively, as compared with $\Delta = 8620$ cm^{-1} for $[Ni(H_2O)_6]^{2+}$ (Table 1). These values are in ageement with those given in literature [4,8] for the octahedral complexes of Ni^{2+} in a ligand field of average strength (7800—8600 cm^{-1}).

Table 1

The experimental data obtained from the interpretation of the anion I and anion II absorption spectra in visible in comparison with the spectrum of the $[Ni(H_2O)_6]^{2+}$ ion

Ion	Conc. (Ni)	λ_1 (nm)	Δ (cm^{-1})	A_1	ε_1	λ_2 (nm)	λ_3 (nm)
$[H_2ONiTiW_{11}O_{39}]^{6-}$	$2.1 \cdot 10^{-2}$ M	1240	8064	0.164	7.8	712 775	430
$[H_2ONiTiW_5O_{20}]^{4-}$	$5.7 \cdot 10^{-2}$ M	1230	8130	0.31	5.5	712 760	$\simeq$430
$[Ni(H_2O)_6]^{2+}$	$1.2 \cdot 10^{-1}$ M	1160	8620	0.245	2	665 717	395

When calculating the ligand field parameter, we took into account the largest wavelength band (noted λ_1, table 1), that occurs as a result of the electron transition from the fundamental state to the first excited state, that is, transition $^3A_{2g} \rightarrow {}^3T_{2g}$ (according to Orgel diagram for a d^8 ion [19]). From figure 2 it is obvious that in the case of both complex anions the band from the 700–800 nm field is wider, almost split, suggesting a "composite" band that must include more transitions in this spectral region. This behaviour was also reported with other heteropolyanions with octahedrally coordinated Ni^{2+}. [4,8] The occurrence of this band is the result of the transition $^3A_{2g} \rightarrow {}^3T_{1g}(F)$. The bell shape of the curve probably covers more transitions in this spectral domain, a fact that may be explained by assuming that the excited state $^3T_{1g}(F)$ is subject to a splitting. This split may be a consequence either of the spin-orbit coupling, or of the reduced symmetry of the NiO_6 octahedron for each anion. The second explanation seems more plausible in the case of Ni^{2+} ion and is supported by the smaller parameter values (as previously shown).

The absorption band that occurs at $\simeq$ 430 nm both in the case of anion I and anion II, is attributed to the transition $^3A_{2g} \rightarrow {}^3T_{1g}(P)$, because it implies the greatest energy.

In the heteropolyanions of Keggin type the oxygen atoms of every WO_6 octahedron are non-equivalent, therefore the WO_6 octahedron is considerably distorted.

When in an octahedron a W atom is replaced by a transition metal (here with Ni^{2+}), we expect the NiO_6 octahedron to be also distorted, but the Ni^{2+} ion polarizes less than tungsten the non-shared oxygen atom of the octahedron. In this way the Ni–O distance in discussion will be longer than the corresponding W–O distance.

The position symmetry of the external heteroatom is reduced and the NiO_6 chromophore group lacks a symmetry centre. This phenomenom provides the explanation for the fact that the intensity of the spectral bands of the anions $[H_2ONiTiW_{11}O_{39}]^{6-}$ and $[H_2ONiTiW_5O_{20}]^{4-}$ (illustrated in table 1 by the extinction molar coeficient values ε), as well as the heteropolyanions of ratio 1 : 1 : 11 in general, is higher as compared with the octahedral aquocomplexes.

The ligand field asymmetry around the Ni^{2+} ion is indicated in both cases directly by the larger values of ε for the bands corresponding to d–d transitions, Laporte-forbidden. The more reduced is the ligand field symmetry (here the NiO_6 octahedron) the higher is the intensity of the respective bands.

The ε coeficient for the anion I (calculated for $\lambda_1 = 1240$ nm) is 3.9 times higher than that of the corresponding band of the symmetrical $[Ni(H_2O)_6]^{2+}$ ion. The ε coeficient for the anion II (calculated for $\lambda_1 =$ $= 1230$ nm) is 2.75 times higher than the one of the same band of the Ni^{2+} aquoion. In both cases the obtained values are within the accepted limits for octahedrally coordinated Ni^{2+}.

In figure 3 are presented the IR spectra recorded at room temperature for the ammonium and potassium salts of the Ni(II)-undecatungstotitanate (IV) anion and for the ammonium and sodium salts of the Ni(II)-pentatungstotitanate (IV) anion, respectively.

It can be noted that all these complex salts present three absorption bands within the 700—1000 cm^{-1} range. The $[H_2ONiTiW_{11}O_{39}]^{6-}$ anion, regardless of the exterior cation, presents these bands at 800 cm^{-1}, 890 cm^{-1} and 960 cm^{-1}, and the $[H_2ONiTiW_5O_{20}]^{4-}$ anion, regardless of the cation, presents bands at 770 cm^{-1}, 880 cm^{-1} and 960 cm^{-1}.

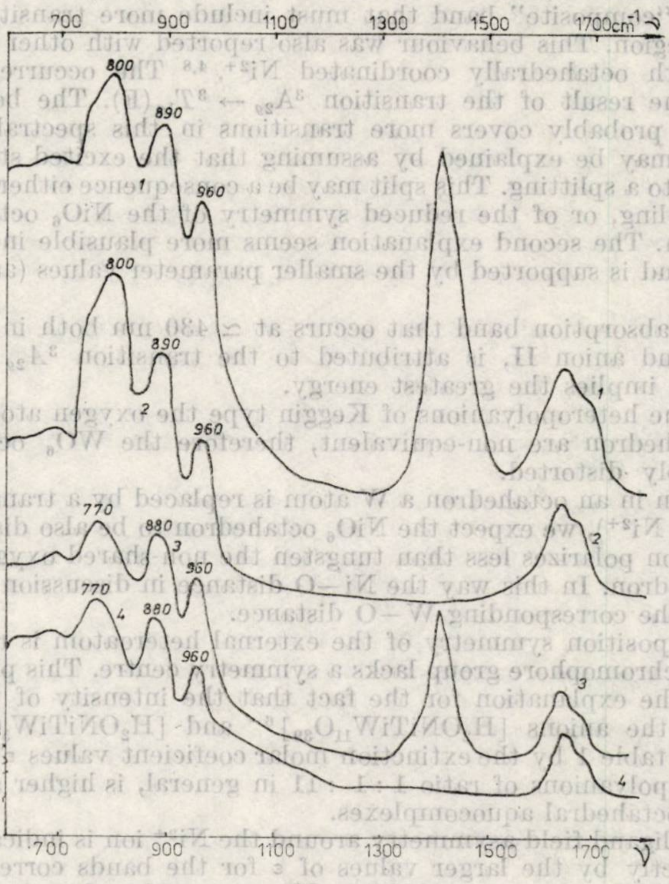

Fig. 3. — IR spectra of the complex salts, recorded at room temperature :

1) $(NH_4)_6[H_2ONiTiW_{11}O_{39}] \cdot 11.5\ H_2O$
2) $K_6[H_2ONiTiW_{11}O_{39}] \cdot 13\ H_2O$
3) $(NH_4)_4[H_2ONiTiW_5O_{20}] \cdot 9\ H_2O$
4) $Na_4[H_2ONiTiW_5O_{20}] \cdot 9\ H_2O$

According to the literature, [20,21] we estimated the position of these bands in spectrum to be characteristic of the heteropolytungstate frame, and to be due to the vibration of the W—O bond. The bands in the 890—1000 cm^{-1} field are assigned to the valency vibrations of the W—O and W—O—W bonds. Just because the W—O-central atom bonds are the most affected by the nature of the central atom, the peaks at ≃ 800 cm^{-1}

(and others lower situated if they occur) are attributed [20] to this bond. This peak ($\simeq$ 800 cm^{-1}) also appears in the structures of the metal tungstates.

By drawing a parallel between the IR spectra of the anion I (curves 1 and 2) and the IR spectra of the anion II (curves 3 and 4) it can be pointed out that in the anion II, as compared with I, only the band attributed to W—O-central atom bond is shifted towards smaller wave numbers (occurs at 770 cm^{-1}). This fact could be interpreted as an evidence for the fact that in the anion II the W—O—central atom bond is more covalent in character than in the case of the anion I.

In the reported IR spectra there also appear the bands characteristic of the deformation vibrations of HOH at 1640 cm^{-1}. For the ammonium salts (curves 1 and 3) a maximum at 1410 cm^{-1} is recorded, characteristic for the NH_3 deformation vibrations.

The deformation vibrations of water from 1640 cm^{-1} appear in spectrum as a shoulder that is constantly present with all salts at $\simeq$ 1670 cm^{-1}.

4. CONCLUSIONS

The UV and IR apsorbtion spectra confirmed the existence of heteropolytungstate frame in both anions noted I and II.

The absorption spectra in visible emphasized each time that the Ni^{2+} ion is octahedrally coordinated.

The spectral studies proved the formulation $[H_2NiO_6TiO_4-W_{11}O_{30}]^{6-}$ or $[H^2ONiTiW_{11}O_{39}]^{6-}$ and the assigning of the anion I to the series 1 : 1 : 11 to be correct.

A new type of structure (to be reported in a following paper) was put forward for the anion II, formulated $[H_2ONiTiW_5O_{20}]^{4-}$, in which the Ni^{2+} ion is also situated in an octahedral surrounding.

REFERENCES

[1] R. Vățulescu, T. Budiu, and Gh. Marcu, *Rev. Roumaine Chim.*, **26**, 971 (1981).

[2] R. Vățulescu, T. Budiu and Gh. Marcu, *Rev. Roumaine Chim.*, **26**, 851 (1981).

[3] Y. Shimura and R. Tsuchida, *Bull. Chem. Soc. Japan*, **30**, 502 (1957).

[4] T. J. R. Weakley and S. A. Malik, *J. Inorg. Nuclear Chem.*, **29**, 2935 (1967).

[5] C. M. Tourné, *Compt. rend.* **266**, 702 (1968).

[6] C. M. Tourné and G. F. Tourné, *Bull. Soc. chim. France*, **(1969)** 1124.

[7] C. M. Tourné, G. F. Tourné, S. A. Malik and T. J. R. Weakley, *J. Inorg. Nuclear Chem.*, **32**, 3875 (1970).

[8] R. Ripan and M. Pușcașiu, *Z. anorg. Chem.* **380**, 102 (1971).

[9] T.J.R. Weakley, *J. Chem. Soc. Dalton Trans.*, **3**, 341 (1973).

[10] Gh. Marcu and M. Rusu, *Rev. Roumaine Chim.*, **22**, 227 (1977).

[11] V. I. Spitsyn, I. D. Kolli, S. V. Kiselev, A. A. Minaev and G. A. Gordeeva, *Zhur. neorg. Khim.*, **24**, 380 (1979).

[12] O. W. Rollins, *J. Inorg. Nuclear Chem.*, **42**, 1368 (1980).

[13] V. I. Spitsyn, I. D. Kolli, S. V. Kiselev, A. A. Minaev and G. A. Godeeva, *Zhur. neorg Khim.*, **26**, 2129 (1981).

[14] Gh. Marcu, M. Rusu and L. Ocheşel, *Rev. Roumaine Chim.*, **22**, 849 (1977).
[15] C. M. Flynn Jr. and M. T. Pope, *Inorg. Chem.*, **10**, 2745 (1971).
[16] C. M. Tourne and G. F. Tourne, *Rev. Chim. Miner.*, **14**, 83 (1977).
[17] D. H. Brown, *Spectrochim. Acta*, **19**, 1683 (1963).
[18] G. M. Varga Jr., E. Papaconstantinou and M. T. Pope, *Inorg. Chem.* **9**, 662 (1970).
[19] M. Dunn, "Modern Coordination Chemistry" (J. Lewis and R. G. Wilkins editors), Interscience Publishers, New-York, 1960, p. 229—300.
[20] D. H. Brown, *Spectrochim. Acta*, **19**, 585 (1963).
[21] O. Glemser, W. Holznagel, W. Höltje and Schwarzmann, *Z. Naturforsch.*, **20b**, 725 (1965).
[22] Hyunsoo So and M. T. Pope, *Inorg. Chem.*, **11**, 1441 (1972).

Revue Roumaine de Chimie, **30**, *9–10*, 831–836 (1985)

HETEROPOLYTUNGSTATES WITH Ti(IV) AND Ni(II). IV[1]

THE THERMAL BEHAVIOUR OF THE POTASSIUM SALT OF THE Ni(II)-UNDECATUNGSTOTITANATE(IV) ANION

RODICA VĂȚULESCU, T. BUDIU, GH. MARCU and IRINA PAL
Institute of Chemistry, 30, Fîntînele Street,
3400 Cluj-Napoca, Romania

Received April 25, 1984

The thermal behaviour of the $K_6[H_2ONiTiW_{11}O_{39}] \cdot 13\ H_2O$ heteropolycompound has been studied by means of the thermogravimetric and thermodifferential analyses combined with the X-ray diffraction analysis in powder and IR spectroscopy.

1. INTRODUCTION

Since 1966 Baker and his co-workers [2] have formulated the heteropolyanions of the series 1 : 1 : 11 with hydrogen atoms in molecule, in this way : $[H_hM^{m+}O_6X^{x+}O_4W_{11}O_{30}]^{(14-m-x-h)-}$. They have pointed out that the hydrogen atoms are indispensable to the partial compensation of the anion electric charge and in some cases the hydrogens are to be found in the form of a water molecule. They assign to the compounds of the series 1 : 1 : 11 a modified Keggin structure supposing that the hydrogen atoms are attached to the unshared oxygen atom of the MO_6 octahedron.

Later, L.C.W. Baker and J. S. Figgis[3] put forward a general formulation for the compounds of the series 1 : 1 : 11, namely :
$[(Y^{y-})M^{m+}O_5X^{x+}O_4W_{11}O_{30}]^{(12-m-x+y)-}$ where Y is a monodendate ligand that takes an isolated coordinative position of M^{m+}.

Y is a molecule of water [2,4–7] for the most of the studied complexes. In 1970, Baker and Figgis [3] and then Weakley [8] indicated that a great variety of ligands may function as Y ($Y = H_2O$, NH_3, pyridine, pyridine derivatives, halogen ion, isoquinoline, pyrazine thiocyanate, thiourea).

The object of the present paper is to report the transformations that take place in the compound $K_6[H_2ONiTiW_{11}O_{39}] : 13\ H_2O$ upon gradual increase of the temperature, as well as isothermally, at several temperatures.

The following technique have been used : the thermogravimetric and thermodifferential analyses, as well as the X-ray diffraction analysis in powder, and IR spectroscopy.

2. EXPERIMENTAL

The thermogravimetric and thermodifferential analyses have been carried out using a Paulik-Erdely Derivatograph OD—102 type without maintaining isothermal conditions, with a heating rate of 4°/minute, the balance sensitivity of 100 mg and the sample weight of 400 mg.

The X-ray diffraction spectra have been recorded by using a Philips installation type PW 1050. A copper anode tube and a nickel β filter have been also used. The diffraction image has been usually recorded on paper with a scanning rate of 1°2θ/minute. During the experiment the sample spinned with a speed of 60 rotation/minute.

The intensity of the diffraction lines has been measured by using a proportional detector with xenon coupled with a height analyser of the impulses.

The compound samples were previously heated for 1/2 hour at different temperatures, up to 800°C. The heating temperatures of the samples have been chosen so that they may correspond to the temperatures situated around the transformation points of the DTA curve.

The IR absorption spectra have been recorded with a U.R. 10 Zeiss Jena apparatus, using the pelleting technique in KBr for the preparation of the samples. There have been used compound samples heated at different temperatures up to 800° C.

3. RESULTS AND DISCUSSION

3.1. THERMAL ANALYSIS

Figure 1 presents the weight loss (TGA — curve 1), its derivative (DTG — curve 3) and its thermodifferential (DTA — curve 2) recorded for the $K_6[H_2ONiTiW_{11}O_{39}] \cdot 13\,H_2O$ complex. A continual weight loss is observed on the TGA curve as the temperature is increasing.

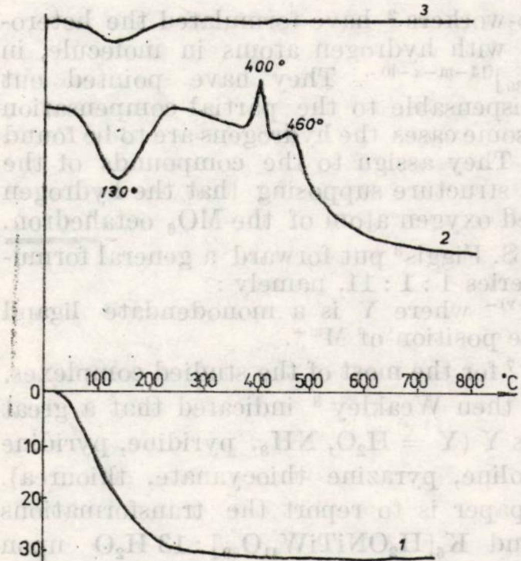

Fig. 1. — Thermal behaviour of the $K_6[H_2ONiTiW_{11}O_{39}] \cdot 13\,H_2O$ complex; 1 — TGA curve; 2 — DTA curve; 3 — DTG curve.

Between 40 — 220°C the weight loss represents 7.23% and it corresponds to 13 crystallization water molecules. The speed of this process is great and it appears on the DTG curve.

Between 220–370°C a small weight loss of 0.55% is observed, corresponding to the loss of a water molecule which is, consequently, strongly connected in the structure. According to our formulation, this molecule represents constitution water, an integrant part of the complex anion.

The speed of the dehydration process within the temperature range 220–370°C is very low; that is why it is not evident on the DTG curve. The total loss of weight obtained from the TGA curve is 7.75%, as compared to 7.78% calculated loss, which means 13 crystallization water molecules and a constitution water molecule.

There is no weight loss above 370°C. A relatively strong endothermal effect is observed on the DTA curve (curve 2, Fig. 1) presenting a minimum at 130°C as a result of the dehydration process. Then, two exothermal effects are recorded, a stronger one at 400°C, and a weaker one at 460°C. Both exothermal effects appear in the region where no weight loss could be noted.

3.2. The X-ray diffraction analyses at different temperatures

The Roentgen spectra have been recorded and the identification of the developed solid phase has been tried in order to make clear the nature of the effects recorded on the DTA curve (curve 2, Fig. 1) obtained by investigating the samples calcined at different temperatures.

In X-ray diffraction spectra on samples heated up to 160° C the same crystalline structure of the complex $K_6[H_2ONiTiW_{11}O_{39}]$ as the one observed at room temperature has been detected (we shall give an account of the crystallographic study of this compound in a future paper). Therefore, in this temperature range the substance loses a part of the crystallization water without decomposing or modifying its crystalline lattice (face – centered cubic lattice).

The spectra of the products obtained at temperatures ranging from 160–300° C indicate the gradual disappearance of the lines of the initial crystalline system and the presence of an amorphous product at $\simeq$ 300° C.

At 400° C begin to appear the first lines of a new crystalline structure on the background of a characteristic amorphous spectrum (two lines: d = 1.404 Å, d = 1.568 Å). Therefore the modification at 400° C has been assigned to the transformation of the amorphous phase in a second crystalline phase. This behaviour has been also reported by other authors.[9]

In the X-ray diffraction spectrum on the sample heated at 440° C the occurrence of some lines could be pointed out; readings and calculation of interreticular distances (d) and relative intensities (I_r) (Table 1) were carried out for these lines. The phase identification (obtained by heating at 440° C) has been made by means of the ASTM Index.

Consulting these cards, we have reached the conclusion that the crystalline phase at 440° C consists of inferior oxides of potassium, titan and tungsten, catalogued $K(WTi)O_3$ in ASTM Index.

The identification has been made on the basis of the lines 3, 1, 2, 4, 5, 6, 7 and 8 out of table 1.

Finally, the recording of the X-ray diffraction spectrum has been made for the complex sample $K_6[H_2ONiTiW_{11}O_{39}]$ heated at 700°C.

Table 1

The values of interreticular distances and relative intensities of the X-ray diffraction spectrum on $K_6[H_2ONiTiW_{11}O_{39}] \cdot 13\ H_2O$ sample, heated at 440° C

Line	1	2	3	4	5	6	7	8	9	10
d(Å)	5.903	3.130	2.977	2.576	2.367	1.984	1.827	1.567	1.491	1.404
I_r	92	64	100	30	14	15	32	24	8	9

Using the same identification technique there has been found that at this temperature the sample consists mainly of WO_3.

The identification of WO_3 has been made on the basis of the lines 1, 2, 4, 6, 7 of table 2.

Table 2

The values of interreticular distances and relative intensities of the X-ray diffraction spectrum on $K_6(H_2ONiTiW_{11}O_{39}] \cdot 13\ H_2O$ sample, heated at 700° C

Line	1	2	3	4	5	6	7	8	9
d(Å)	3.905	3.701	3.162	2.703	2.630	2.181	2.012	1.952	1.860
I_r	40	100	30	85	40	45	30	20	50

As a result of the thermal study to which the complex $K_6[H_2ONiTiW_{11}O_{39}] \cdot 13\ H_2O$ has been subjected, we may appreciate that the field of the thermal stability is relatively wide, as compared to the other heteropolytungstate with transitional metals. [9,10]

The heteropolycompound $K_6[H_2ONiTiW_{11}O_{39}] \cdot 13\ H_2O$ is estimated to be stable up to $\simeq 370°$ C when the decomposition of the complex anion takes place simultaneously with the loss of the last constitution water molecule.

3.3. Temperature dependence of the IR Absorption of $K_6\ [H_2ONiTiW_{11}O_{39}] \cdot 13\ H_2O$

The IR absorption spectra for complex samples $K_6[H_2ONiTiW_{11}O_{39}] \cdot 13\ H_2O$ have been recorded at different temperatures (Fig. 2). The temperature values have been chosen by taking into account the transformational points evidenced in curve DTA (curve 2, Fig. 1).

The IR spectrum of the complex $K_6[H_2ONiTiW_{11}O_{39}] \cdot 13\ H_2O$ at room temperature presents three absorption bands in the 700–1000 cm^{-1} range. These absorption bands are assigned to the valency vibrations of the W–O, W–O–W, W–O–central atom bonds and they are characteristic of the heteropolytungstate frame. The band characteristic of the deformation vibration of water occurs at 1640 cm^{-1}.

At 130° C the IR spectrum (curve 2, Fig. 2) preserves in the 700–1000 cm^{-1} range the same aspect both in the shape of the bands and in intensity. This fact is in agreement with the result of the Roentgen study indicating (as it was previously shown) that the crystalline lattice remains unchanged at temperatures up to ≃ 160°C. In the spectrum of the sample from 240°C (curve 3, Fig. 2) there is a modification of the shape of the maximum from 800 cm^{-1}; at 300° C (curve 4, Fig. 2) the modification of the spectrum shape in the 700—1000 cm^{-1} range is visible in the case of all the three bands (from 800, 880 and 960 cm^{-1}).

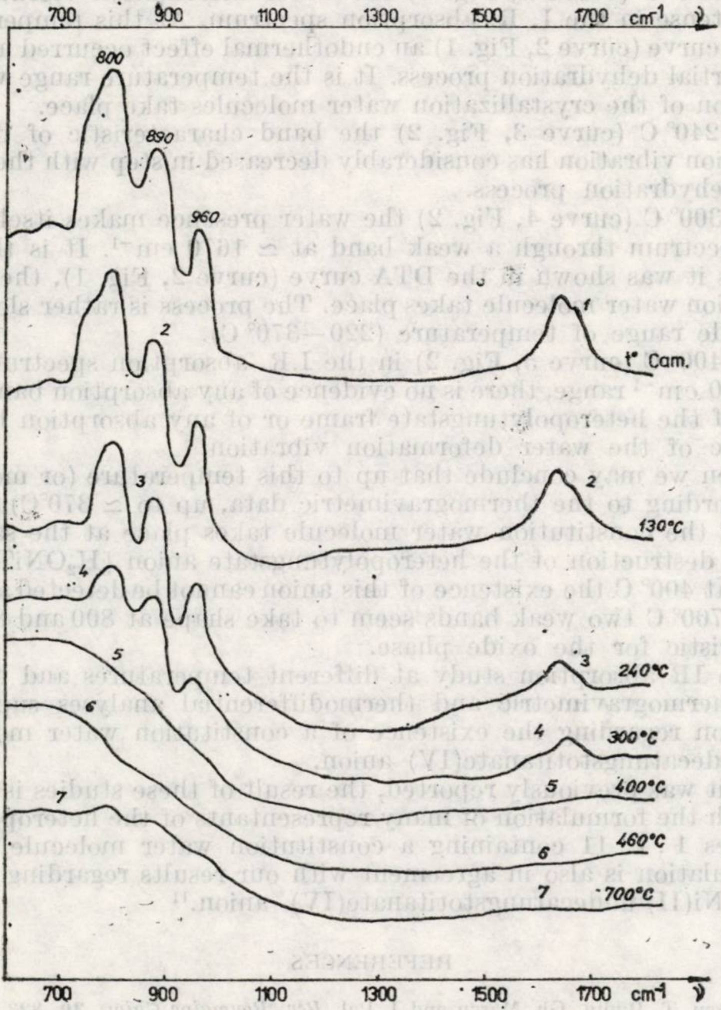

Fig. 2. — The I.R. absorption spectra for complex samples $K_6[H_2ONiTiW_{11}O_{39}] \cdot 13\ H_2O$ at different temperatures: 1 — at room temperature; 2 — at 130° C; 3 — at 240°C; 4 — at 300°C; 5 — at 400 °C; 6 — at 460°C; 7 — at 700° C.

The water deformation vibration from 1640 cm^{-1} (curve 1, Fig. 2) occurs in the spectrum with a shoulder at $\simeq$ 1670 cm^{-1}; this shoulder could be observed also in the spectrum of the same anion, Ni(II) — undecatungstotitanate (IV), at the ammonium salt.[1]

At 130° C (curve 2, Fig. 2) the water deformation vibration band is still intense in the I. R. absorption spectrum. At this temperature on the DTA curve (curve 2, Fig. 1) an endothermal effect occurred as a result of the partial dehydration process. It is the temperature range where the elimination of the crystallization water molecules take place.

At 240° C (curve 3, Fig. 2) the band characteristic of the water deformation vibration has considerably decreased in step with the progress of the dehydration process.

At 300° C (curve 4, Fig. 2) the water presence makes itself obvious in the spectrum through a weak band at $\simeq$ 1670 cm^{-1}. It is the region where, as it was shown in the DTA curve (curve 2, Fig. 1), the loss of a constitution water molecule takes place. The process is rather slow covering a wide range of temperature (220—370° C).

At 400° C (curve 5, Fig. 2) in the I.R. absorption spectrum, in the 700—1000 cm^{-1} range, there is no evidence of any absorption band characteristic of the heteropolytungstate frame or of any absorption band characteristic of the water deformation vibration.

Then we may conclude that up to this temperature (or more precisely, according to the thermogravimetric data, up to $\simeq$ 370°C) the elimination of the constitution water molecule takes place at the same time with the destruction of the heteropolytungstate anion $[H_2ONiTiW_{11}O_{39}]$. That is, at 400° C the existence of this anion cannot be detected any more.

At 700° C two weak bands seem to take shape at 800 and 850 cm^{-1}, characteristic for the oxide phase.

The IR absorption study at different temperatures and the result of the thermogravimetric and thermodifferential analyses support our supposition regarding the existence of a constitution water molecule in Ni(II)-undecatungstotitanate(IV) anion.

As it was previously reported, the result of these studies is in agreement with the formulation of many representants of the heteropolytungstate series 1 : 1 : 11 containing a constitution water molecule,[2,4–7] and the formulation is also in agreement with our results regarding the basicity of Ni(II)-undecatungstotitanate(IV) anion.[11]

REFERENCES

[1] R. Văţulescu, T. Budiu, Gh. Marcu and I. Pal, *Rev. Roumaine Chim.*, **30**, 823 (1985).

[2] L. C. W. Baker, V. Simmons-Baker, K. Eriks, M. T. Pope, M. Shibata, O. W. Rollins, J. H. Fang and L. L. Koh, *J. Amer. Chem. Soc.*, **88**, 2329 (1966).

[3] L. C. W. Baker and J. S. Figgis, *J. Amer. Chem. Soc.*, **92**, 3794 (1970).

[4] T. J. R. Weakley and S. A. Malik, *J. Inorg. Nuclear Chem.*, **29**, 2935(1967).

[5] C. M. Tourne and G. F. Tourne, *Compt. rend.*, **266**, 1263 (1968).

[6] C. M. Tourne and G. F. Tourne, *Bull. Soc. Chim. France*, **4**, 1124 (1969).

[7] O. W. Rollins, *J. Inorg. Nuclear Chem.*, **42**, 1368 (1980).

[8] T. J. R. Weakley, *J. Chem. Soc. Dalton Trans.*, **3**, 341 (1973).

[9] R. Ripan, D. Stănescu and M. Puşcaşiu, *Z. anorg. allg. Chem.*, **391**, 187 (1972).

[10] D. H. Brown, *J. Chem. Soc.*, **1962**, 3189.

[11] R. Văţulescu, T. Budiu and Gh. Marcu, *Rev. Roumaine Chim.*, **26**, 971 (1981).

Revue Roumaine de Chimie, **30**, *9—10*, 837—842 (1985)

COORDINATION COMPOUNDS AS RAW MATERIALS FOR MIXED OXIDES. II

MIXED COORDINATION COMPOUNDS OF LANTHANIDES AND Co(II) WITH DERIVATIVES OF ACETIC ACID

P. SPACU, SILVIA PLOȘTINARU, LUMINIȚA PATRON, ADRIANA CONȚESCU and N. STĂNICĂ

Center of Physical Chemistry, Bucharest, Romania

Received February 11, 1984

The mixed coordination compounds of lanthanides and Co(II) with ligands derived from acetic acid were characterized (by elemental analysis, electronic spectra and IR spectra, magnetic measurements) in order to establish the nature of species formed, the coordination of the ligand and the magnetic behaviour.

In a previous note, we presented the results of a study on mixed complex compounds of lanthanides and Co(II) with salicylic acid; the study aimed at obtaining mixed oxides of perovskite structure.[1]

Other complex compounds with organic ligands have been tested in order to achieve a wider variety of precursors for these mixed oxides.

The best results were obtained with ligands derived from acetic acid, i.e.: mandelic acid, chloromandelic acid and benzylic acid. These polynuclear coordination compounds are easy to obtain with high yield and the thermal treatment applied to obtain the perovskite phase requires much lower temperatures.

RESULTS AND DISCUSSION

The polynuclear coordination compounds of Ln(III) and Co(II) with the above mentioned acids were prepared by treating the nitrate mixture with the ammonium salt of the acid in question. The complex compounds of all Ln(III) and Co(II) with benzylic acid were obtained at room temperature; the precipitation pH is 6—7; the compounds obtained are crystalline and light pink. The complex compounds containing mandelic and chloromandelic acids were obtained at higher pH's (7—8), through heating for 15—20 min; they are pink-violet and light pink, respectively. All complexes were filtered after 24 hours and subsequently washed with water and acetone.

The compounds are little soluble in water and mostly in organic solvents.

To establish the structure of newly synthetized compounds chemical and physico-chemical analyses were performed.

The chemical elemental analysis led to the following formula of mixed complex compounds :

$[\mathrm{Ln\,Co(RCOO)_5}] \cdot n\mathrm{H_2O}$ n = 2.3

for $\mathrm{RCOO^-}$: 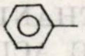 $\mathrm{CHOH{-}COO^-}$ (mandelic acid, Ma) ; Ln(III) = La, Pr, Nd, Ho, Tb

Cl 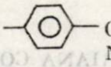 $\mathrm{CHOH{-}COO^-}$ (chloromandelic acid, Cl—Ma) ; Ln(III) = La, Pr, Nd

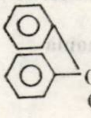 $\mathrm{COH{-}COO^-}$ (benzylic acid, Bz) ; Ln(III) = La, Pr, Nd, Sm, Eu, Gd, Dy, Er, Tb

Information concerning formation of polynuclear coordination compounds and the way the ligands are coordinated was obtained from the analysis of vibration spectra. The IR spectra were recorded for free ligands and mixed complexes within the 700—3600 $\mathrm{cm^{-1}}$ range. The vibration spectra of mixed complex compounds shows a large number of bands which makes impossible their doubtless complete assignment. Because of the complexity of the spectra obtained, we considered and assigned only those bands which evidenced the coordination of ligands.

In general, because of coordination, the vibration spectrum of the complexes differs from that of the free ligand in respect of :

— the absence of some bands proper to the ligand and the presence of new bands;

— the shift or splitting of some bands;

—the intensity.

The coordination of carboxylic acids to metallic ions is determined from the position of the band that corresponds to carbonyl group after the complex formation. The monobasic carboxylic acids exhibit strong bands assigned to C = O group, between 1705 and 1710 $\mathrm{cm^{-1}}$. Introduction of halogen or $\mathrm{CN^-}$ group into the molecule results in a shift of the band corresponding to carboxyl towards higher frequencies. [2] Thus, $\nu_{\mathrm{C=O}}$ shows up in ClMa acid at 1740 $\mathrm{cm^{-1}}$, while in the other acids at about 1700 $\mathrm{cm^{-1}}$. Figures 1 and 2 show the vibration spectra of mixed complexes with benzylic acid and ClMa together with those of free ligands.

As it may be seen, on formation of complexes with these acids, the band corresponding to C = O group in the noncoordinated carboxyl vanishes and is replaced by two bands (ν_{sym} and ν_{asym}) of the $\mathrm{COO^-}$ coordinated groups. It is beyond doubt that the band that appears in the complex, at about 1580—1600 $\mathrm{cm^{-1}}$, is due to the valence vibration ν_{asym} $\mathrm{COO^-}$, while the band at 1370—1400 $\mathrm{cm^{-1}}$ to the symmetric vibration ν_{sym} $\mathrm{COO^-}$.

It is interesting to mention that in Ma and ClMa acids, the band at 1100 $\mathrm{cm^{-1}}$ characteristic for CHOH group, as well as, that at 3400 $\mathrm{cm^{-1}}$ due to OH group, in the free acid, vanish after the formation of the compounds, which points to the possibility that OH group participates in coordination.[3] The data obtained from IR spectra fully agree with the formulas advanced on the basis of elemental chemical analysis performed on the synthetized mixed coordination compounds.

For a more complete study of mixed compounds, UV and visible spectra were recorded. For a better comparison, the spectra of polynuclear coordination compounds, of the free ligands, of simple Co(II) and lanthanide complexes were recorded. In UV, the characteristic of polynuclear coordination compounds studied is the existence of the bands

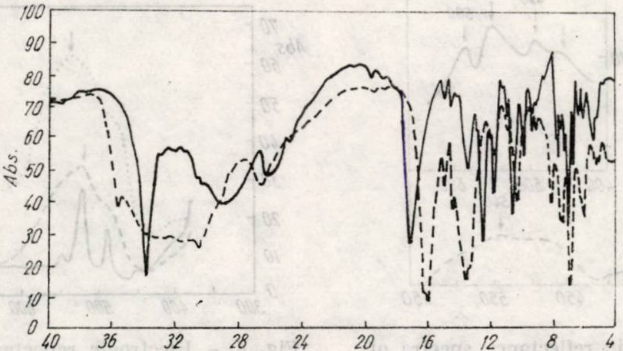

Fig. 1. — IR spectra of — — — — benzylic acid
—— $LaCo(Bz)_5 \cdot 2H_2O$.

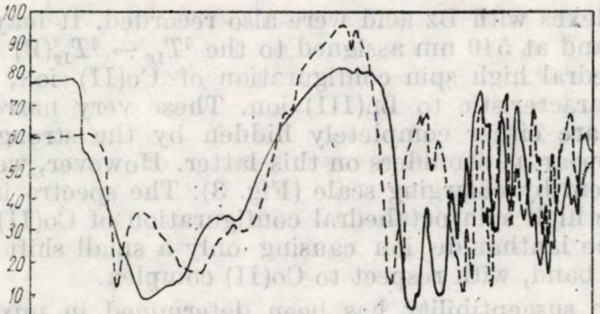

Fig. 2. — IR spectra of — — — chloromandelic acid
—— $LaCo(Cl-Ma)_5 \cdot 3H_2O$.

featured by free ligands. As seen in figure 3, within this range, only the band characteristic to ClMa acid at 265 nm can be evidenced. In visible, the spectra of mixed compounds of Co(II) with Pr, Nd, Ho and Er were studied; these ions exhibit a large number of bands within this range. The very narrow bands that form in the spectra of these complexes are due to transitions from ground states to J excited levels of 4f configuration (f—f transitions).

Generally, the spectra in visible of lanthanide complexes supply information regarding the hypersensitivity and the nefelauxetic effect. They are extracted from the changes occurring in the absorption spectrum of the free ion following coordination.

Figures 3 and 4 present the spectra of polynuclear coordination compounds of Pr(III) and Co(II) with ClMa and Er(III) and Co(II) with Bz acid, respectively. For comparison, the spectra of simple Co(II) and Er(III) complexes with Bz acid were also recorded. It may be seen that besides the band at 540 nm assigned to the ${}^4T_{1g} \rightarrow {}^4T_{1g}(\mathrm{P})$ (ν_3) transition to an octhahedral high spin configuration of Co(II) ion, there appear the bands characteristic to Ln(III) ion. These very narrow, yet fairly weak, bands are either completely hidden by the strong Co(II) band (Fig. 4) or appear as shoulders on this latter. However, we succeeded in evidencing them by enlarging scale (Fig. 3). The spectra in visible have confirmed the high spin octahedral configuration of Co(II) ion, in these compounds the lanthanide ion causing only a small shift of the Co(II) characteristic band, with respect to Co(II) complex.

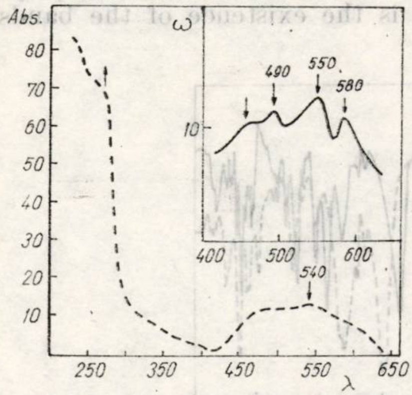

Fig. 3. — Electronic reflectance spectra of $\mathrm{PrCo(Cl{-}Ma)_5\ 3H_2O}$.

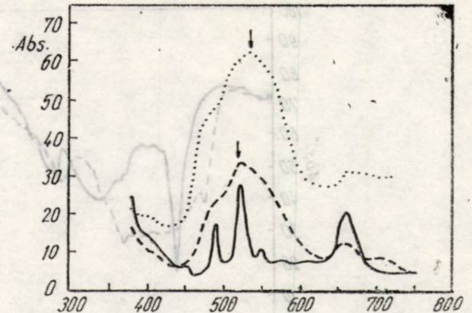

Fig. 4. — Electronic reflectance spectra of
——— $\mathrm{La(Bz)_3}$
— — — — $\mathrm{LaCo(Bz)_5 \cdot 2H_2O}$
.... $\mathrm{Co(Bz)_2 \cdot 2\,H_2O}$

Magnetic susceptibility has been determined in mixed complexes with Ma, Cl—Ma and Bz acids. It is well known that the magnetic behaviour of lanthanides is basically different because the electrons responsible for the magnetic properties are the 4f electrons. The outer layers $5s^2$ and $5p^6$ screen the 4f electrons from the action of the outside field created by the ligands in the complex. This leads the absence of some special interaction between the ligands and the 4f orbitals which causes the complexing group to exert little action upon the permanent magnetic moment of trivalent ions.[4]

In order to determine how the magnetic moment of Ln(III) ion influences the resulting magnetic moment of the polynuclear coordination compounds, the magnetic susceptibilities were determined in a series of complex compounds of Co(II) with various Ln(III) : La, Pr, Nd, Sm, Tb.

The value obtained for the polynuclear coordination compounds of Co(II) with La(III), (5.2 BM) agrees with the data in the literature for high spin octhahedral Co(II) complex compounds (4.3—5.2 BM). This value shows only the contribution of Co(II) ion, because La(III) is diamagnetic.

In polynuclear coordination compounds of Co(III) with Nd(III), with Ma and Bz acids as ligand, values of 5.72 and 5.75 BM respectively, were obtained, pointing to the small contribution of Nd(III), to the resulting magnetic moment and, on the other hand, to the fact that nature of coordinating ligand does not affect the value of magnetic moment.

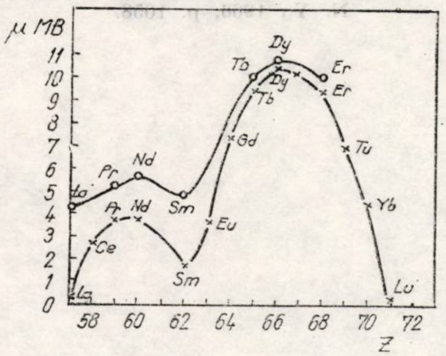

Fig. 5. — Measured and calculated effective magnetic moments (BM) of —x—x—x— lanthanides Ln^{3+} ions —○—○—○— $LnCo(Bz)_5 \cdot 2H_2O$ at 298 K.

The polynuclear compound with Co(II) and Sm(III) gives a value of 4.81 BM for the magnetic moment which agrees with the unusual magnetic behaviour of Sm(III) ion.

For the compound with Tb(III), a high value of magnetic moment was obtained (10.12 BM), which suggests that this ion contributes appreciably to the resulting magnetic moment.

Given the aim of this study, the obtaining of mixed oxides with perovskites structure by thermal decomposition of the polynuclear coordination compounds, we have performed a thermogravimetric analysis to evidence the steps of decomposition.

As shown by the heating curves the thermal decomposition occurs in three steps for the polynuclear coordination compounds with mandelic acid as ligand and in two steps for the polynuclear coordination compounds with benzylic acid as ligand. The decomposition of $LaCo(BZ)_5 \cdot 5\,H_2O$, for instance occurs through:

- the loss of these water molecules in the temperature interval 25—200° C followed by
- the second decomposition step, in the temperature interval 200—450° during which the remaining two molecule of water and ligands are removed as gaseous products.

The X-ray diffraction of the product showed the presence of the mixed oxide with perovskite structure as well as the mixture of unreacted oxides. These products are subjected to adequate thermal treatment to yield pure perovskite phase.

REFERENCES

[1] P. Spacu, Silvia Ploştinaru, Luminiţa Patron, Adriana Conţescu and E. Segal, *Rev. Roumaine Chim.* (under press).

[2] N. Colthup, "Introduction to Infared and Raman spectroscopy", Second Ed. Academic Press. Inc., 1975, p. 426.

[3] N. Colthup, "Introduction to Infrared and Raman spectroscopy", Second Ed., Academic Press. Inc., 1975, p. 299.

[4] F. A. Cotton and G. Wilkinson, "Advanced inorganic chemistry", Intersci. Publ., Wiley, N. Y., 1966, p. 1058.

Revue Roumaine de Chimie, **30**, *9–10*, 843–850 (1985)

EXTRACTION EQUILIBRIA OF SOME COMPLEX COMBINATIONS WITH MACROCYCLIC LIGANDS

CONSTANTIN LUCA* and MOHAMED MAGDI KHALIL**

* Polytechnical Institute of Bucharest, Faculty of Chemical Technology, Department of Analytical Chemistry, Spl. Independenţei 202, 79611 – Bucharest, Romania
** Assiut University, Faculty of Science, Chemistry Department, Assiut, A.R. Egypt

Received June 25, 1984

The extraction equilibria in benzene and dichloromethane were investigated for the complexes formed by Na^+, K^+, Rb^+, Cs^+, Ag^+, and Tl^+ with dibenzo-18-crown-6, coupled with the dipicrylamine anion. The extraction constants of these ion pairs from water into benzene and dichloromethane were determined. The results were interpreted in terms of "caging" the cation into the cavity of the macrocyclic ligand, an effect which depends on the ratio between the diameter of the cation and the diameter of the cavity, on the nature of the coupling anion, and on the nature of the solvent. Feasibility of using the obtained results for analytical purposes is also discussed.

INTRODUCTION

The use of macrocyclic compounds as ligands for forming complexes extractable in organic solvents, initiated by Pedersen[1,2] and Eisenman[3] in 1969, has become lately a major preoccupation in several laboratories all over the world.[4–8] This preoccupation is justified by the various possible applications of the liquid-liquid extraction equilibria in analytical chemistry[9] and in phase-transfer catalysis.[10]

In a process of extraction of an ion pair consisting of the complex cation of a metal cation M^+ with a macrocyclic ligand C and of a suitable anion A^-, the overall equilibrium

$$(M^+)_w + (C)_s + (A^-)_w \rightleftharpoons (MC^+A^-)_s \tag{1}$$

is characterized by the apparent extraction constant

$$K_{ex_0} = \frac{[MC^+A^-]_s}{[M^+]_w[A^-]_w[C]_s} \tag{2}$$

where the indices *w* and *s* stand for the aqueous and organic phases of the extraction system, respectively.

If we consider the equilibrium of formation of the complex cation in aqueous phase, which is characterized by the stability constant

$$\beta_1 = \frac{[MC^+]_w}{[M^+]_w[C]_w} \tag{3}$$

we can define the extraction constant as

$$K_{ex} = \frac{[MC^{+}A^{-}]_s}{[MC^{+}]_w [A^{-}]_w} = R_c \cdot \beta_1^{-1} \cdot K_{ex_0} \tag{4}$$

where R_c is the distribution constant of the macrocyclic ligand C between the two phases of the system,

$$R_c = \frac{[\mathrm{C}]_s}{[\mathrm{C}]_w} \tag{5}$$

By taking into account the equilibrium of association of the complex cation MC^+ with the anion A^- in aqueous phase, characterized by the association constant

$$K_{assoc} = \frac{[\mathrm{MC^{+}A^{-}}]_w}{[\mathrm{MC^{+}}]_w [\mathrm{A^{-}}]_w} \tag{6}$$

the constant K_{ex} can be expressed as

$$K_{ex} = \frac{[\mathrm{MC^{+}A^{-}}]_s}{[\mathrm{MC^{+}A^{-}}]_w} \cdot K_{assoc} \tag{7}$$

or

$$K_{ex} = R_{(\mathrm{MC^{+}A^{-}})} \cdot K_{assoc} \tag{8}$$

where $R_{(\mathrm{MC^{+}A^{-}})}$ is the distribution constant of the ion pair MC^+A^- between the two phases, that is the constant of the equilibrium

$$(\mathrm{MC^{+}A^{-}})_w \rightleftharpoons (\mathrm{MC^{+}A^{-}})_s \tag{9}$$

The constant $R_{(\mathrm{MC^{+}A^{-}})}$ is the fundamental quantity which could possibly attend the rational selection of the C and A^- species in view of optimizing the extraction of the M^+ cation from water into the organic solvent S. The direct determination of this constant is practically not possible because the concentrations of the compound MC^+A^- in aqueous phase are extremely low. Its estimation by means of Eq. (8) is also practically impossible for the same reason, which prevents the prior determination of the association constant K_{assoc}. For these reasons, the extraction processes of this kind are being investigated by means of the extraction constants K_{ex} and K_{ex_0}, which are estimable experimentally and which can play the part of the quantities needed to make a selection of the species C and A^- so that the extraction of species M^+ is optimzed.

In this work, we investigated the equilibria of the extraction from water into benzene and dichloromethane of a series of cations M^+ appearing as compounds of association between the complex cations MC^+, formed with dibenzo-18-crown-6, and the dipicrylamine anion A^-. For this purpose, the values of the constants K_{ex_0} were determined experimentally.

Determination of the extraction constants. In order to estimate the extraction constants K_{ex_0}, the prior experimental determination of the distribution ratio of the dipicrylamine anion (DPA^-) turned out to be necessary; this is expressed as

$$r = \frac{[DPA^-]_s}{[DPA^-]_w} = \frac{[DPA^-]_s}{[DPA^-]_t - [DPA^-]_s} \tag{10}$$

where $[DPA^-]_t$ is the total concentration of dipicrylamine in the system, i.e. the initial concentration of dipicrylamine in the aqueous phase.

Considering the mass balance in the system, we can write

$$[DPA^-]_w = [DPA^-]_t - [DPA^-]_s - \frac{[DPA^-]_s}{R_{(MC+A-)}} = \varphi([DPA^-]_s) \tag{11}$$

$$[M^+]_w = [M^+]_t - [DPA^-]_s - \varphi'([DPA^-]_s) \tag{12}$$

where

$$\varphi'([DPA^-]_s) = \frac{[DPA^-]_s}{R_{(MC+A-)}}\left[\frac{1}{\varphi([DPA^-]_s)\cdot\beta} + 1\right] \tag{13}$$

Taking into account Eqs. (11) – (13), Eq. (10) becomes

$$\frac{1}{r} - \frac{1}{R_{(MC+A-)}} = \frac{[DPA^-]_t - [DPA^-]_s - [DPA^-]_s/R_{(MC+A-)}}{[DPA^-]_s} =$$

$$= \frac{1 + R_C^{-1}}{K_{ex_0}[[C]_t - [DPA^-]_s - \varphi'([DPA^-]_s)][[M^+]_t - [DPA^-]_s - \varphi'[(DPA^-]_s)]} \tag{14}$$

Supposing that only the complex with the stoichiometric ratio 1 : 1, MC^+, is formed in the system, and that the experimental conditions

$$([DPA^-]_t - [DPA^-]_s) \gg [DPA^-]_s\, R^{-1}_{(MC+A-)}$$

$$([M^+]_t - [DPA^-]_s) \gg \varphi'([DPA^-]_s)$$

$$([C]_t - [DPA^-]_s) \gg \varphi'([DPA^-]_s)$$

are fulfilled, Eq. (14) becomes

$$r = K_{ex0}([M^+]_t - [DPA^-]_s)([C]_t - [DPA^-]_s) \tag{15}$$

A straight line graphical representation of $-\log r$ *vs.* $-\log([M^+]_t - [DPA^-]_s)([C]_t - [DPA^-]_s)$ would indicate that a 1 : 1 complex is formed in solution between the metal cation M^+ and the macrocyclic ligand C; the intercept of this line with the abscisa gives the value of the extraction constant K_{ex_0}.

Determination of the distribution ratio of dipicrylamine. To estimate the distribution ratio r of dipicrylamine between the two phases of the system, the concentration of the ion DPA^- in the organic phase, $[DPA^-]_s$, in which this ion is found in the ion pair (MC^+) (DPA^-), was determined. The measurement was carried out spectrometrically, after estimating the molar absorption coefficients. The distribution ratio r was then calculated by means of Eq. (10). The molar absorption coefficients were determined from the spectra recorded with the organic phase after extracting a known amount of DPA^- in the presence of a large excess of the metal cation. In this way, the extraction equilibrium is practically totally shifted towards the organic phase, into which the whole amount of DPA^- is extracted. These molar absorption coefficients were always determined at the wavelength of the maximum of the absorption band, in the range of concentations in which the Beer-Lambert law is obeyed.

EXPERIMENTAL

Operating conditions. Initially, the metal cation M^+ and dipicrylamine are found in the aqueous phase, whereas the macrocyclic ligand in the organic phase. The aim of a first series of experiments was to estimate the molar absorption coefficients of the (MC^+) (DPA^-)-type complexes in organic phase; for this purpose, the absorption spectra of the organic phase, after extraction, were recorded. The spectra obtained for the K^+-dibenzo-18-crown-6-dipicrylamine system in benzene are exemplified in Figure 1. The concentrations of the species involved in the process were chosen in such a way that the whole amount of DPA^- in the aqueous phase would be extracted in the organic phase; this procedure permitted the estimation of the molar absorption coefficients $\varepsilon_{\lambda_{max}}$ at the wavelength corresponding to the maximum of the

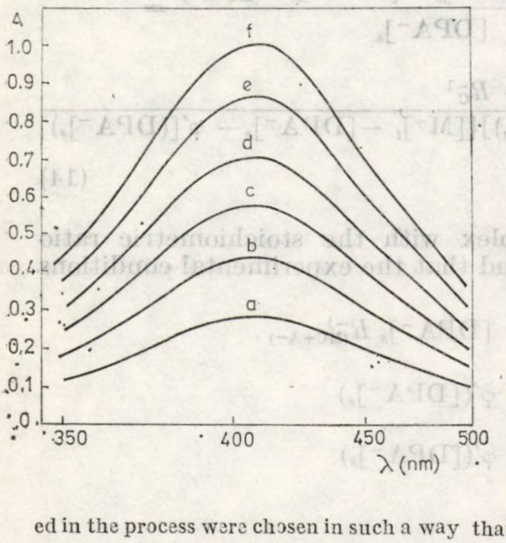

Fig. 1. — The absorption spectra of the ion pair (KC^+) (DPA^-) in benzene, at various concentrations of dipicrylamine: *a.* 2×10^{-5}; *b.* 3×10^{-5}; *c.* 4×10^{-5}; *d.* 5×10^{-5}; *e.* 6×10^{-5}; *f.* 7×10^{-5} mole · dm^{-3}, at $[K^+]_t = 6 \times 10^{-3}$ mole · dm^{-3} and $[C]_t = 2 \times 10^{-4}$ mole · dm^{-3}.

absorption band. The wavelengths $\lambda_{\max}$ and the values $\varepsilon_{\lambda\max}$ determined in this way are given in table 1.

Table 1

Overall extraction constants of the investigated systems

Metal ion M^+ ($\log \beta_1$)	$\lambda_{\max}$(nm)		$\varepsilon_{\lambda\max}$		$\log K_{ex_0}$		Ionic radius (Å)
	C_6H_6	CH_2Cl_2	C_6H_6	CH_2Cl_2	C_6H_6	CH_2Cl_2	
Na^+ (1.16)	410	420	25,000	31,430	6.70	7.96	1.94
K^+ (1.67)	410	420	28,460	32,000	8.88	9.28	2.66
Rb^+ (1.08)	400	420	20,500	32,660	8.28	9.04	2.94
Cs^+ (0.83)	415	420	26,000	32,500	7.26	8.71	3.34
Ag^+ (1.41)	400	420	24,000	31,600	8.63	8.71	2.52
Tl^+ (1.50)	410	420	23,330	32,800	8.94	9.57	2.80

Knowing the coefficients $\varepsilon_{\lambda\max}$ and carrying out a second series of experiments, the distributions ratio of dipicrylamine in all the investigated systems could be estimated. For this purpose, the absorption spectra of the organic phase after extraction of the ion pair (MC^+) (DPA^-) into systems in which the concentrations of the ion M^+ and of dipicrylamine were constant and in excess in comparison with the concentration of the crown ether, were recorded. Figure 2 exemplifies the spectra obtained for the system K^+-dibenzo-18-crown-6-dipicrylamine in ben-

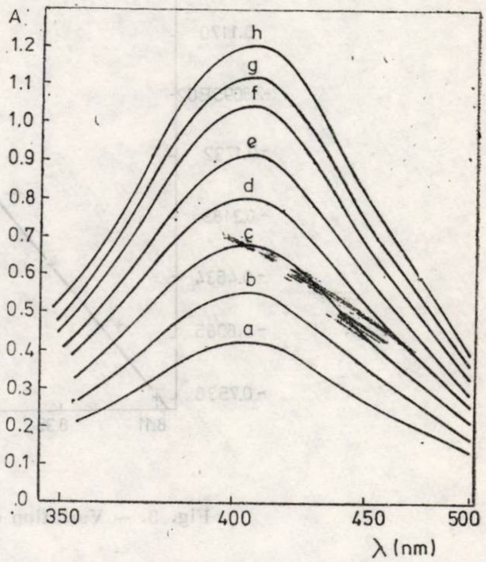

Fig. 2. — The absoption spectra of the ion pair (KC^+)(DPA^-) in benzene, at various concentrations of dibenzo-18-crown-6 : *a*. 3×10^{-5}; *b*. 4×10^{-5}; *c*. 5×10^{-5}; *d*. 6×10^{-5}; *e*. 7×10^{-5}; *f*. 8×10^{-5}; *g*. 9×10^{-5}; *h*. 10^{-4} mole · dm^{-3}, at $[DPA^-]_t = 10^{-4}$ mole · dm^3 and $[K^+]_t = 6 \times 10^{-4}$ mole · dm^{-3}.

zene, with variable concentrations of the crown ether; the experimental data and the data necessary for the estimation of the distribution coefficient r of this system are given in Table 2. The extraction constant K_{ex_0} was then calculated using Eq. (15) and by means of a program written for and run on an Independent—100 computer (Computer Plant of Bucharest). We proceeded similarly for the other investigated systems; the results obtained for the constants K_{ex_0} are given in table 1.

Table 2

Experimental data for the estimation of the extraction constant K_{ex_0} for the K^+-dibenzo-18-crown-6--dipicrylamine system in benzene

$[C]_t \times 10^5$ (mole · dm^{-3})	A (absorbance)	$[DPA^-] = \frac{A}{\varepsilon_1} \times 10^5$	$r = \frac{[DPA^-]_s}{[DPA^-]_t - [DPA^-]_s}$	$-\log r$	$-\log([C]_t - [DPA^-]_s)([M^+]_t - [DPA^-]_s)$
3	0.42	2.951	0.418	0.38	9.55
4	0.55	3.864	0.630	0.20	9.11
5	0.68	4.777	0.915	0.04	8.91
6	0.80	5.620	1.283	−0.11	8.68
7	0.92	6.463	1.828	−0.26	8.54
8	1.04	7.306	2.713	−0.43	8.43
9	1.21	7.869	3.692	−0.57	8.23
10	1.21	8.501	5.671	−0.75	8.11

Variation of r according to Eq. (15) is given in figure 3.

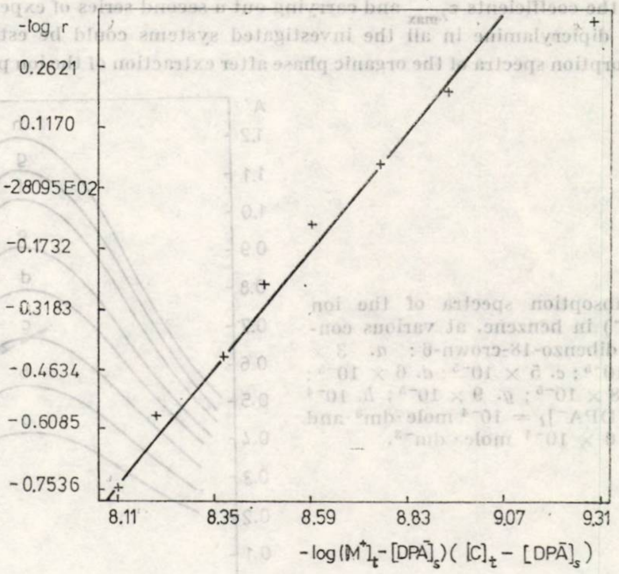

Fig. 3. — Variation of r according to Eq. (15).

Materials and apparatus. All the reagents used in this work were reagent grade, provided by BDH. The extractions were carried out using equal volumes of aqueous phase and of organic phase (benzene and dichloromethane). All measurements were carried out at 25° C. The absorption spectra were recorded with a Carl Zeiss UV/Vis spectrometer (GDR).

RESULTS AND DISCUSSION

In a series of earlier works [5,10] dealing with the extraction of some MC$^+$-type complex cations of crown ethers coupled with the picrate ion, a dependance of the extraction constants K_{ex_0} on the stability of the complexes MC$^+$ in aqueous phase was noticed. Those complexes whose stability constats β_1 has larger values could be more easily extracted in organic phase and has therefore larger extraction constants K_{ex_0}. Since the stability of the complexes with crown ethers depends obviously on the possibility of "caging" the complexes cation into the cavity of the macrocyclic ligand, [11-14] it results that near similarity between the diameter of the complexed cation and the diameter of the cavity of the macrocyclic ligand influences to a large extent the values of the extraction constant K_{ex0} for the ion pair (MC$^+$) (A$^-$). Obviously, near similarity between the cation M$^+$ and the ligand C does not set up the only criterium for foreseeing selectivity for a M$^+$-type series of cations. Structure of the anion A$^-$ with which the complex cation MC$^+$ is coupled, the nature of the organic phase, and the structure of the macrocyclic ligand must also play an important role in these extraction processes.

Thus, the values of the constant K_{ex_0} estimated by Sekine and coworkers [5] for the extraction of the (M-dibenzo-18-crown-6)-(picrate$^-$) ion pair into benzene agree with the stability of the complex cations as expressed by the stability constants β_1, estimated by Shehori and coworkers. [11] A similar observation was made by Jawaid and coworkers [10] for the complexes of Na$^+$ and K$^+$ with dicyclohexyl-18-crown-6, extracted in dichloromethane and coupled with the picrate anion; these invesigators have measured a ratio which agrees with the great stability of the potassium complex. The same authors have however noticed the disappearance of the selectivity for potassium when the picrate anion is replaced with the dipicrylamine anion; in this case, the ratio of the extraction constants may be written as

$$\frac{K_{ex}(\mathrm{K})}{K_{ex}(\mathrm{Na})} = \frac{10^{8.16}}{10^{7.81}} \approx 1$$

One may notice a strong effect of dipicrylamine as compared to the effect of picrate; in the former case, the extraction constants for both alkali ions are increased, while the selectivity of the picrate anion for potassium is significantly decreased.

The data obtained by us in this work on the extraction in benzene and dichloromethane of a series of M$^+$-type cations with dibenzo-18-crown-6 coupled with the dipicrylamine anion indicate:

— a significant increase (by about four units on the logarithmic scale) of the values of the extraction constant as compared to the similar systems with picrate;

— a rather remarkable preservation of the selectivity of the extraction, both in benzene and in dichloromethane, of those cations M$^+$ which have dimensions more appropriate with those of the cavity of the macrocyclic ligand, and consequently a preservation of the agreement between K_{ex_0} and the stability constant β_1.

From the data shown above it results that no correlations of a general nature can yet be established for expressing the contribution of the structure of the reactive species and of the nature of the solvent in the extraction processes of the complex cations with crown ethers coupled with various anions.

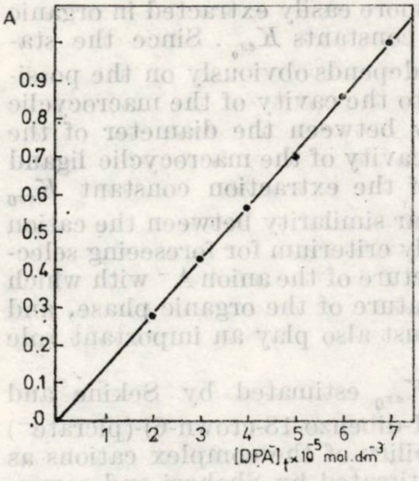

Fig. 4. — Calibration curve for the determination of dipicrylamine.

ANALYTICAL APPLICATIONS

The results obtained on the extraction of the ion pair formed between the complex cation and the dipicrylamine anion can also be used for determining spectrometrically the species involved in this process : dipicrylamine, the M^+ cation, and the crown ether. Thus, *e.g.*, to determine dipicrylamine one can use the extraction of any ion pair investigated in this work. For this purpose, the most advantageous is the system $(KC^+)(DPA^-)$, for which the molar absorption coefficients in benzene and dichloromethane have maximum values, $\varepsilon_{\lambda=410\,\mathrm{nm}} = 28{,}460$ and $\varepsilon_{\lambda=420\,\mathrm{nm}} = 32{,}000$ (see Table 2). Based on the spectra shown in Figure 1, one can draw the calibration curve represented in Figure 4, which allows the spectrometric determination of dipicrylamine in the concentration range $2 \times 10^{-5} - 7 \times 10^{-5}$ mole·dm^{-3}.

REFERENCES

[1] C. J. Pedersen, *J. Amer. Chem. Soc.*, **80**, 7017 (1967).
[2] C. J. Pedersen, *Fed. Pror.*, **27**, 1305 (1968).
[3] G. Eisenman, S. M. Ciani and G. Szabo, *J. Membr.*, **1**, 295 (1969).
[4] A. Sudakane, T. Iwachido and K. Toci, *Bull. Chem. Soc. Japan*, **48** (1), 60 (1975).
[5] T. Sekine, H. Warabayashi and Y. Hasagawa. *Bull. Chem. Soc. Japan*, **51** (2), 645 (1978)
[6] K. Kino, K. Shiroishi and N. Ishiboshi, *Bunseki Kagaku*, **27**, 291 (1978).
[7] A. M. Y. Jaber, G. J. Moody and J. D. R. Thomas, *J. Inorg. Nucl. Chem.*, **39**, 1689 (1967).
[8] I. M. Kolthoff, *Anal. Chem.*, **51** (5), 1R (1979).
[9] E. Weber, *Kontakte*, **1**, 24 (1982).
[10] M. Jawaid and F. Ingman, *Talanta*, **25**, 91 (1978).
[11] E. Shehori, N. Noe and J. Jagur-Frodzinski, *J. Chem. Soc., Dalton Trans.*, 2381 (1975).
[12] H. K. Frensdroff, *J. Amer. Chem. Soc.*, **93**, 4684 (1971).
[13] R. M. Izatt, R. E. Terry, B. L. Haymare, L. D. Hansen, N. K. Falley, A. G. Avondet and J. J. Christensen, *J. Amer. Chem. Soc.*, **98**, 7620 (1975).
[14] M. Joshio and H. Noguchi, *Anal. Letters*, **15** (A15), 1197 (1982).

Revue Roumaine de Chimie, **30**, *9–10*, 851–858 (1985)

DETERMINATION OF ETHYLMERCURIC COMPOUNDS BY PHASE-SENSITIVE SINUSOIDAL ALTERNATING CURRENT POLAROGRAPHY

I. TĂNASE, I. IONECI and C. LUCA
Polytechnical Institute of Bucharest, Faculty of Chemical Technology,
Department of Analytical Chemistry, 79611 – Bucharest, Romania

Received November 17, 1984

The polarographic reduction of ethylmercuric compounds takes place in two steps, each of which involving the transfer of a single electron. The first step of the reduction proceeds reversibly in sinusoidal alternating current and hence the corresponding intensity-potential curve presents analytical importance, enabling determination of these compounds in the concentration range $10^{-7} - 10^{-3}$ mole · dm^{-3}.

The latest 25–30 years have witnessed an important expansion of the industrial production of the organometallic compounds, mainly due to the outstanding role played by such compounds in modern technology, e.g. as stabilizers, catalysts, pesticides, fungicides, medicine drugs, etc. Among organometallic compounds, the organomercuric compounds have reached the most spectacular productions, followed by the organometallic compounds of tin and lead.

Expansion of the uses of these compounds, sometimes uncontrolled, has led to an increase of the concern for the toxicological effects of these compounds and for their degradation and metabolic ways, since it is well known that such organic compounds are generally more toxic than their metallic counterparts. It has been noticed that the alkylmercuric compounds are unique in the sense that their toxic effects can produce irreversible destruction of the central nervous system, unlike the effects produced by inorganic mercury and by arylmercuric compounds, which are to a great extent reversible.[1] For this purpose, analytical methods for determining organometallic compounds as such, as well as their degradation and metabolic products, have been developed.

The electrochemical behavior of the organometallic compounds has been extensively investigated in the latest years, both from an analytical point of view[2–16] and from that of the mechanism of the electrode reactions.[1,17–41] Following our previous study on the electrochemical behaviour of the ethylmercuric compounds, based on measurements carried out by direct current polarography, sinusoidal alternating current polarography and cyclic voltammetry,[42] the work has the purpose to set up the optimum conditions for determining the ethylmercuric compounds by phase-sensitive sinusoidal alternating current polarography.

EXPERIMENTAL

The sinusoidal alternating current polarographic measurements were carried out by means of a PRG-3 Tacussel three-electrode polarographic complex, using a RM-06 Tacussel cell provided with thermostating jacket. The capillary had the following characteristics : $m = 1.152$ mg · s^{-1} and $\tau = 4.15$ s, values determined in 0.1 N $HClO_4$, at -0.200 V relative to the saturated calomel electrode (SCE) and at a height $h = 60$ cm of the mercury column. A Pt—121 Tacussel coiled platinum electrode was used as auxiliary electrode. All measurements were carried out under strictly controlled temperature conditions, at 25 ± 0.1 °C, and the potentials were determined relative to the K—401 Radelkis saturated calomel electrode.

The substances used were high-purity or analytical grade, provided by BDH or Merck. Tetradistilled water was used to prepare the solutions and to clean the vessels (the last distillation of water was carried out in a quartz apparatus). A 0.1 mole · dm^{-3} KCl solution was used as indifferent electrolyte.

The polarographic measurements were carried out both in a buffered medium (Britton-Robinson buffers) for pH = 1.8 — 12 and in unbuffered media (0.1N $HClO_4$ and 0.1N NaOH solutions) outside this range.

The millimolar solutions of ethylmercuric chloride were prepared by weighing the proper amount of ethylmercuric compound, transferring it to a volumetric flask together with the indifferent electrolyte and bringing to the mark with tetradistilled water. The more diluted solutions were always freshly prepared by dilution of the millimolar solutions in volumetric flasks. Oxygen was removed from all solutions subjected to the polarographic measurement by bubbling them with purified argon during 10 minutes.

RESULTS AND DISCUSSION

The polarographic reduction of the ethylmercuric cation in aqueous media leads to two reduction steps of approximately equal height in direct current, whereas in sinusoidal alternating current it leads to two peaks, whose half-wave potential $E_{\frac{1}{2}}$ and peak potential E_p, respectively, depend on the pH of the solution and on the concentration of the electroactive species (Figure 1). It follows that the polarographic reduction of the ethylmercuric cation, and for this matter of other organomercuric cations, proceeds in two steps, according to the mechanism described in a previous paper.[42] The first polarographic step in direct current and the polarographic peak in sinusoidal alternating current, which correspond to the first step of the reduction of the ethylmercuric cation in aqueous media are well defined ; the peak is symmetrical, a fact also evidenced by the linear dependence $\log\left[\left(\frac{i_p}{i}\right)^{\frac{1}{2}} \pm \left(\frac{i_p - i}{i}\right)^{\frac{1}{2}}\right] = f(E_{dc})$ (Figure 2). The polarographic step and the peak corresponding to the second reduction step of the ethylmercuric cation are strongly distorted by the polarographic selfinhibition process.[34,35] The maxima and the distorsions can be removed by using usual maxima suppressors (gelatin, Triton, etc.).

The first reduction step of the ethylmercuric cation at the dropping mercury electrode proceeds reversibly both in direct current and in sinusoidal alternating current, whereas the second step proceeds irreversibly.[42,43] For analytical purposes, i.e. for determining ethylmercuric compounds by direct current polarography, by phase-sensitive sinusoidal alternating current polarography, or by stripping voltammetry, the curves $i = f(E)$ corresponding to the first reduction step of the ethylmercuric cation may be used successfully.

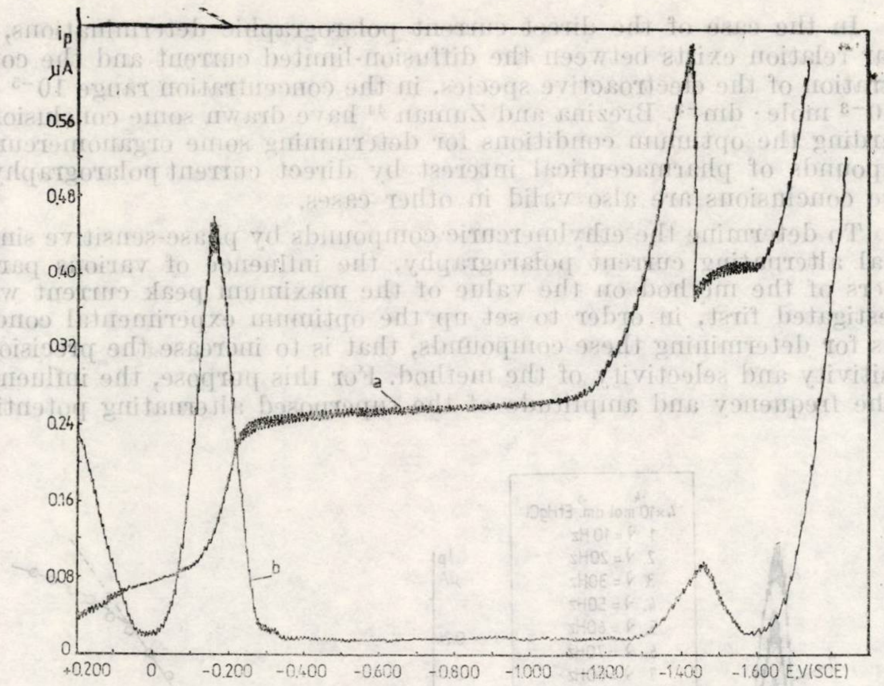

Fig. 1. — The direct current polarogram (*a*) and the sinusoidal alternating current polarogram (*b*) corresponding to the reduction of the ethylmercuric cation ($2.5 \cdot 10^{-4}$ mol · L^{-1}) in a Britton-Robinson buffer; $\Delta E = 5$ mV, $\varphi = 0°$ $\nu = 50$ Hz, pH = 4.19.

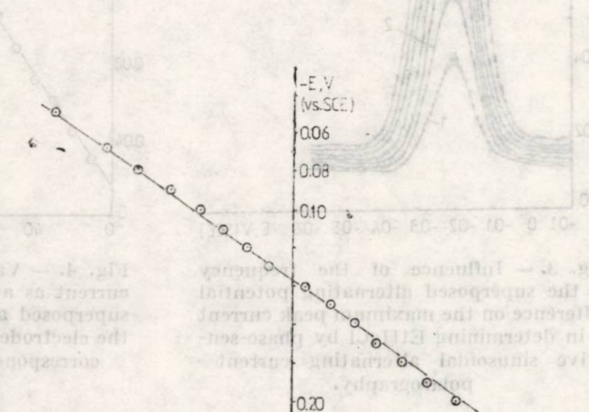

Fig. 2.—The plot of log $\left[\left(\frac{i_p}{i}\right)^{\frac{1}{2}} \mp \left(\frac{i_p - i}{i}\right)^{\frac{1}{2}}\right] = f(E_{dc})$ for the sinusoidal alternating current polarogram corresponding to the first reduction step of the ethylmercuric cation in 0.1 *N* HClO$_4$ as indifferent electrolyte. $c = 1 \times 10^{-4}$ mole EtHgCl · dm^{-3}, $E_p = -0.138$ V (*vs.* ESC), slope 128 mV, $b_{\frac{1}{2}} = 96$ mV, $\Delta E = 5$ mV, $\nu = 50$ Hz, $\varphi = 0°$.

In the case of the direct current polarographic determinations, a linear relation exists between the diffusion-limited current and the concentration of the electroactive species, in the concentration range 10^{-5} — — 10^{-3} mole · dm^{-3}. Brezina and Zuman [44] have drawn some conclusions regarding the optimum conditions for determining some organomercuric compounds of pharmaceutical interest by direct current polarography; these conclusions are also valid in other cases.

To determine the ethylmercuric compounds by phase-sensitive sinusoidal alternating current polarography, the influence of various parameters of the method on the value of the maximum peak current was investigated first, in order to set up the optimum experimental conditions for determining these compounds, that is to increase the precision, sensitivity and selectivity of the method. For this purpose, the influence of the frequency and amplitude of the superposed alternating potential difference and of the detection phase was studied. The polarograms obtained in sinusoidal alternating current which correspond to the first reduction step of the ethylmercuric cation in 0.1N HClO$_4$, at various frequencies of the superposed alternating potential difference, are given in Figure 3. From Figure 4 it results that a linear dependence on frequency of the maxi-

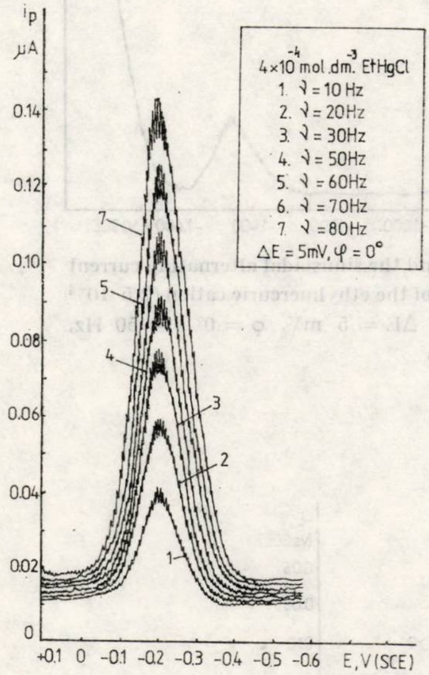

Fig. 3. — Influence of the frequency of the superposed alternating potential difference on the maximum peak current i_p in determining EtHgCl by phase-sensitive sinusoidal alternating current polarography.

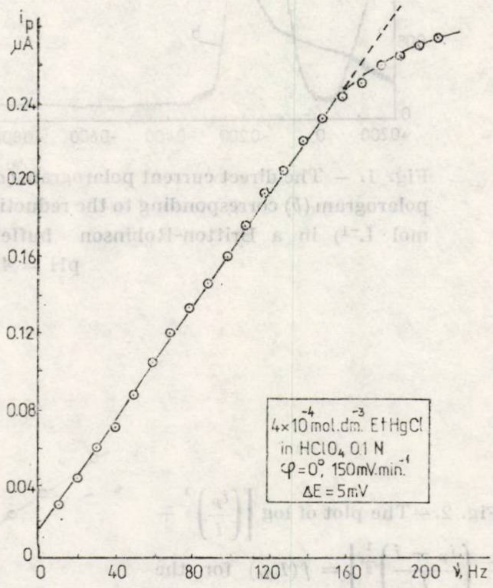

Fig. 4. — Variation of the maximum peak current as a function of the frequency of the superposed alternating potential difference for the electrode process of EtHgCl in 0.1N HClO$_4$, corresponding to the first reduction step.

mum peak current, up to values of the order of 150 Hz, is obtained for a concentration of 4×10^{-4} mole $EtHgCl \cdot dm^{-3}$. It is worth mentioning that the frequency range in which the maximum peak current increases linearly with the frequency becomes less than 100 Hz when the concentration of the electroactive species in the solution decreases. Figure 5 presents the sinusoidal alternating current polarograms corresponding to the first reduction step of the ethylmercuric cation in $0.1N$ $HClO_4$, at various amplitudes of the superposed alternating potential difference. A linear dependence of the maximum peak current on the amplitude ΔE was obtained up to values of 20 mV, for a concentration of 4×10^{-4} mole $EtHgCl \cdot dm^{-3}$. Generally, the linear dependence of the faradaic current on the amplitude of the alternating potential difference is a function of the concentration of the depolarizer; for low concentrations range ($< 1 \times 10^{-5}$ mole. dm^{-3}) this dependence is still linear up to amplitude larger than 30 mV.

Taking into account the high degree of reversibility of the electrode process in sinusoidal alternating current, the most satisfactory results were obtained with a value $\varphi = 0°$ of the detection phase.

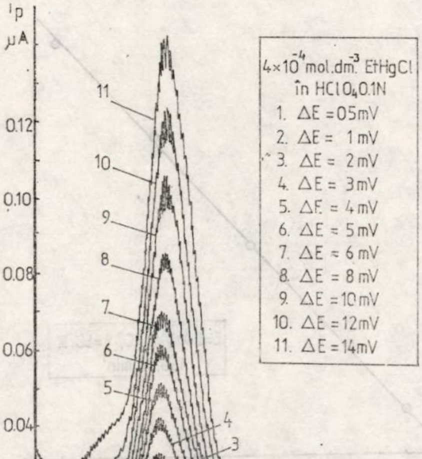

Fig. 5. — Influence of the amplitude of the superposed alternating potential difference on the maximum peak current i_p in determining EtHgCl by phase-sensitive sinusoidal alternating current polarography, when using $0.1N$ $HClO_4$ as indifferent electrolyte.

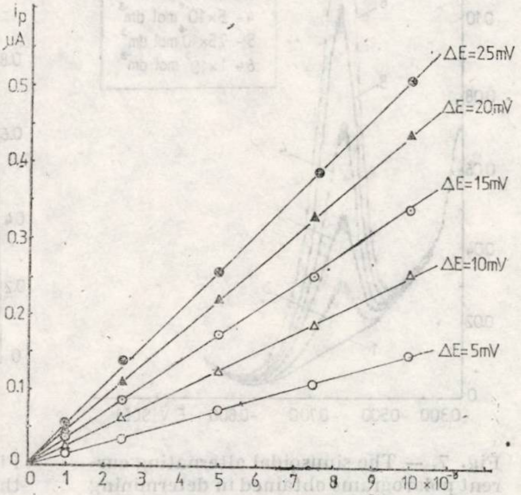

Fig. 6. — Calibration curve obtained for the determination of EtHgCl by phase-sensitive sinusoidal alternating current polarography, for various amplitudes of the superposed alternating potential difference, in the concentration range $1 \times 10^{-5} - 1 \times 10^{-4}$ mole $\cdot$ dm^{-3}, in $0.1N$ NaOH. $\nu = 50$ Hz, $\varphi = 0°$.

In order to evidence more significantly the influence of the superposed alternating potential difference on the increase of the sensitivity of the method, we give in Figure 6 a set of calibration curves, obtained for the determination of the ethylmercuric cation in the concentration range $1 \times 10^{-5} - 1 \times 10^{-4}$ mole · dm^{-3}, and drawn for various values of the amplitude ΔE. It is obvious that by increasing the amplitude ΔE an increase of the slope of the calibration curve, i.e. an improvement of the sensitivity of the method, is obtained.

It results from above that very good results in determining the ethylmercuric compounds in aqueous media (0.1N $HClO_4$, 0.1N NaOH or Britton-Robinson buffers) can be obtained if one works with superposed alternating potential differences whose frequency lies within 25–150 Hz, whose amplitude lies within 5–25 mV and whose detection phase φ is 0°; the selection of the most adequate values within these ranges depends on the concentration of the ethylmercuric cation.

After selecting the optimum parameters, we proceeded to analyze the variation of the maximum peak current as a function of the concentration of the ethylmercuric cation in solution and then to draw the calibration curves for the determination of the ethylmercuric cation, for various concentration ranges. Figure 7 presents the sinusoidal alternating current polarograms obtained for the determination of EtHgCl in 0.1N NaOH, in the concentration range $1 \times 10^{-6} - 1 \times 10^{-5}$ mole · dm^{-3}, whereas Figure 8 presents the calibration curve drawn for this concentration range. The linear dependence of the maximum peak current i_p on the concentration of the electroactive species is obvious for this concentration range.

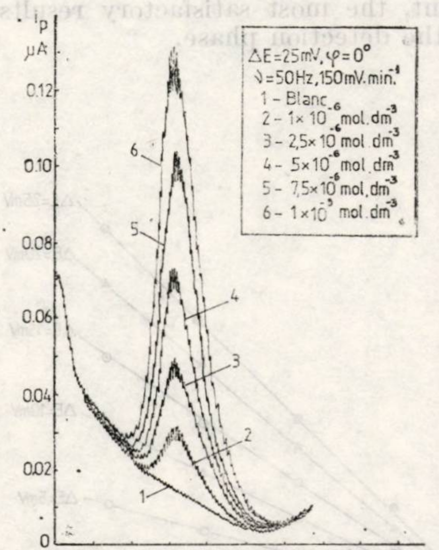

Fig. 7. — The sinusoidal alternating current polarograms obtained in determining EtHgCl, in the concentration range $1 \times 10^{-6} - 1 \times 10^{-5}$ mole · dm^{-3}, when using 0.1N NaOH as indifferent electrolyte.

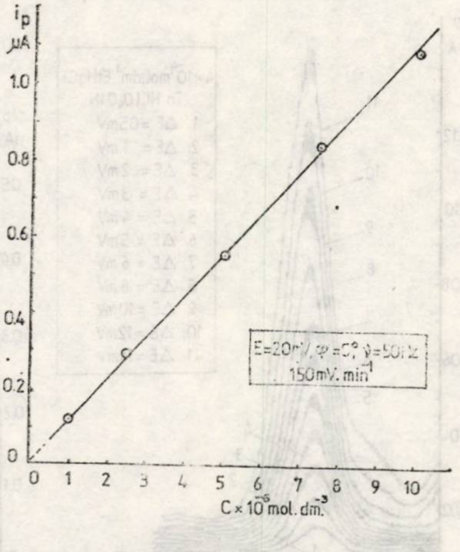

Fig. 8. — The calibration curve drawn for the determination of EtHgCl by phase-sensitive sinusoidal alternating current, in the concentration range $1 \times 10^{-6} - 1 \times 10^{-5}$ mole · dm^{-3}, in 0.1N NaOH.

Well defined peaks and a linear dependence $i_p = f(C)$ were also obtained for the concentration ranges $1\times10^{-5}-1\times10^{-3}$ and $1\times10^{-7}-1\times10^{-6}$ mole · dm^{-3} in all examined media. The sensitivity limit reached in the determination of the ethylmercuric cation by phase-sensitive sinusoidal alternating current polarography was found to be 1×10^{-7} mole · dm^{-3}.

It was also found that in all examined media the peak potential corresponding to the first reduction step of the ethylmercuric cation had different values from those obtained for inorganic or complexed mercury (II) or for phenylmercuric compounds. To exemplify, we give in Figure 9 the sinusoidal alternating current polarogram obtained for the first reduction step of a mixture of phenyl- and ethylmercuric cations, the difference between the corresponding peak potentials being of approximately 340 mV. This difference in the peak potential ensures the possibility to determine sensitively and selectively the ethylmercuric compounds in the presence of phenylmercuric compounds, as well as to determine simultaneously these compounds by using phase-sensitive sinusoidal alternating current polarography.

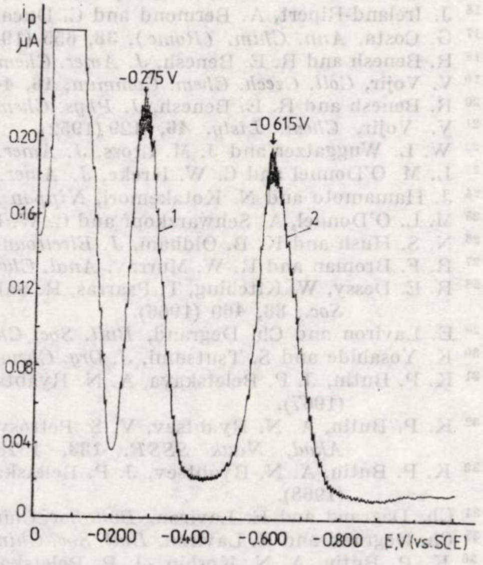

Fig. 9. — The phase-sensitive sinusoidal alternating current polarogram for 5×10^{-5} mole PhHgAc · dm^{-3} + 5×10^{-5} mole EtHgCl · dm^{-3}, using 0.1N NaOH as indifferent electrolyte. $\Delta E = 15$ mV, $\varphi = 0°$, $\nu = 50$ Hz. (1) the peak corresponding to the first reduction step of the cation, (2) for the reduction of the ethylmercuric cation.

In conclusion, we can say that the polarographic method herein described offers a quick and simple way of determining directly, sensitively and selectively the organomercuric compounds, a determination which is not possible by other methods.

REFERENCES

[1] N. B. Fauzder and B. Fleet, in "Polarography of Molecules of Biological Significance" (W. F. Smith, Editor), Academic Press, London — New York — San Francisco, 1979, p. 261.

[2] J. E. Page and J. G. Waller, *Analyst*, **74**, 292 (1949).

[3] T. Kajimura and S. Yamamoto, *Japan Analyst*, **4**, 152 (1955).

[4] S. Usami, *Japan Analyst*, **5**, 499 (1956).

[5] M. Kotakemori and H. Handa, *Ann. Report Takamine Lab.*, **8**, 233 (1957).

[6] N. Shirota, M. Kotakemori and H. Handa, *Ann. Report Takamine Lab.*, **9**, 198 (1957).

[7] P. Casey, J. J. Carroll and N. R. Stalica, *Proc. Penn. Acad. Sci.*, **32**, 63 (1958).

[8] N. Z. Bruja, *Rev. Chim. (București)*, **9**, 685 (1958).

[9] P. Casey and W. Wagner, *Proc. Penn. Acad. Sci.*, **36**, 281 (1962).

[10] V. D. Bezuglyi, Y. P. Ponomarev and V. N. Demitriev, *J. Anal. Chem., USSR, English Transl.*, **19**, 817 (1964).

[11] H. Sato and M. Shimamine, *Esei Shikensho Hohoku*, **83**, 59 (1965).

[12] V. D. Bezuglyi and Y. P. Ponomarev, *J. Anal. Chem. USSR, English Transl.*, **20**, 1274 (1965).

[13] T. M. Hopes, *J. Assoc. Offic. Agr. Chemists*, **49**, 840 (1966).

[14] G. S. Portes, *J. Pharm. Pharmacol.*, **20** (Suppl.), 43 (1968).

[15] B. Fleet and J. D. Jee, *Talanta*, **16**, 1561 (1969).

[16] J. Ireland-Ripert, A. Bermond and C. Ducauze, *Anal. Chim. Acta*, **143**, 249 (1982).

[17] G. Costa, *Ann. Chim. (Rome)*, **38**, 655 (1948).

[18] R. Benesh and R. E. Benesh, *J. Amer. Chem. Soc.*, **73**, 3391 (1951).

[19] V. Vojir, *Coll. Czech. Chem. Commun*, **16**, 448 (1951).

[20] R. Benesh and R. E. Benesh, *J. Phys. Chem.*, **56**, 648 (1952).

[21] V. Vojir, *Chem. Listy*, **46**, 129 (1952).

[22] W. L. Wuggatzer and J. M. Cross, *J. Amer. Pharm. Assoc.*, **41**, 80 (1952).

[23] L. M. O'Donnel and C. W. Kreke, *J. Amer. Pharm. Assoc.*, **48**, 268 (1959).

[24] J. Hamamoto and N. Kotakemori, *Nippon Nogei kagaku Kaishi*, **35**, 48 (1961).

[25] M. L. O'Donnel, A. Schwarzkopf and C. W. Kreke, *J. Pharm. Sci.*, **52**, 659 (1963).

[26] N. S. Hush and K. B. Oldham, *J. Electroanal. Chem.*, **6**, 34 (1963).

[27] R. F. Broman and R. W. Murray, *Anal. Chem.*, **37**, 1408 (1965).

[28] R. E. Dessy, W. Kitching, T. Psarras, R. Salinger, A. Chen and T. Chivers, *J. Amer. Chem. Soc.*, **88**, 460 (1966).

[29] E. Laviron and Ch. Degrand, *Bull. Soc. Chim. France*, **7**, 2194 (1966).

[30] K. Yosahide and S. Tsutsumi, *J. Org. Chem.*, **32**, 463 (1967).

[31] K. P. Butin, J. P. Beletskaya, A. N. Ryabtsev and O. A. Reutov, *Elektrokhimiya*, **5**, 1318 (1967).

[32] K. P. Butin, A. N. Ryabtsev, V. S. Petrosyan, J. P. Beletskaya and O. A. Reutov, *Dokl. Akad. Nauk SSSR*, **183**, 1328 (1968).

[33] K. P. Butin, A. N. Ryabtsev, J. P. Beletskaya and O. A. Reutov, *Zh. Org. Khim.*, **4**, 934 (1968).

[34] Ch. Degrand and E. Laviron, *Bull. Soc. Chim. France*, **5**, 2228 (1968).

[35] Ch. Degrand and E. Laviron, *Bull. Soc. Chim. France*, **5**, 2233 (1968).

[36] K. P. Butin, A. N. Koshin, J. P. Beletskaya and O. A. Reutov, *J. Organometal. Chem.*, **16**, 27 (1969).

[37] B. Fleet and R. D. Jee, *J. Electroanal. Chem.*, **25**, 397 (1970).

[38] K. P. Butin, A. N. Koshin, A. B. Ershler, V. V. Strelets, J. P. Beletskaya and O. A. Reutov, *J. Organometal. Chem.*, **39**, 237 (1972).

[39] J. P. Denisovich and S. P. Gubin, *J. Organometal. Chem.*, **57**, 87 (1973).

[40] J. P. Denisovich and S. P. Gubin, *J. Organometal. Chem.*, **57**, 99 (1973).

[41] R. C. Heaton and H. A. Laitinen, *Anal. Chem.*, **46**, 547 (1974).

[42] I. Tănase, I. Ioneci and C. Luca, *Rev. Roumaine Chim.*, (in press).

[43] I. Tănase, I. Ioneci and C. Luca, communication presented at the 4th meeting "Analytical Chemistry and the Quality Control", Cìmpulung-Muscel, Romania, May 17—18, 1984.

[44] M. Brezina and P. Zuman, "Polarography in Medicine, Biochemistry and Pharmacy", Interscience, New York, 1958, p. 527.

Revue Roumaine de Chimie, **30**, *9–10*, 859–864 (1985)

L'AUGMENTATION DE L'ÉNERGIE LIBRE DE SURFACE DES FEUILLES DE TÉRÉPHTALATE DE POLYÉTHYLÈNE PAR L'ACTIVATION EN PLASMA DE HAUTE FRÉQUENCE. I

G. BOURCEANU, E. GRUNICHIEVICI et M. BOURCEANU
Faculté de Chimie, Splai Bahlui 71, Iași, Romania

Reçu juillet 9, 1984

Les feuilles de téréphtalate de polyéthylène ont été soumises à l'activation dans le plasma de haute fréquence pour augmenter l'énergie libre de surface. L'activation est réalisée pour augmenter l'hydrophilie et pour améliorer leur soudure.

Polyethylene terephthalate films were activated in high frequency plasma in order to increase free surface energy. Activation is aimed at raising hydrophilicity and at improving their welding properties.

1. INTRODUCTION

Il s'est avéré expérimentalement que l'interaction entre les espèces réactives du plasma de haute fréquence (H. F.) et la surface des feuilles de téréphtalate de polyéthylène (TPE) conduit à mettre en évidence les domaines cristallins de ceux amorphes en minimum 300 secondes.[1–5] Cela constitue déjà une méthode de détermination de la structure surmoléculaire des polymères modifiés, qui, à côté d'autres méthodes physiques, contribue à l'obtention des indications importantes concernant le degré de cristallinité, la forme et les dimensions des pseudocristals ainsi que l'orientation de ceux-ci.

Pendant les dernières années on a mis en évidence que l'interaction entre les espèces du plasma et la surface des feuilles TPE conduit à l'activation de la surface des feuilles en permettant un dépôt métallique adhérent,[6] ainsi que la soudure des feuilles activées.[7]

Ce travail se propose de déterminer l'énergie libre de surface des feuilles TPE activées dans le plasma de haute fréquence par le calcul de l'énergie correspondante aux interactions de dispersion de type London, γ_s^d de l'énergie correspondant aux interactions polaires γ_s^p.

2. PARTIE EXPÉRIMENTALE

Le plasma a été réalisé dans une installation décrite dans un travail antérieur.[1] La feuille TPE d'une épaisseur de 175 μ (Fabrication C.F.S. Jassy), initialement lavée en benzène et acétone, a été introduite dans le tuyau de décharge.

On a conduit l'expérience dans le plasma d'oxygène et dans celui d'argon en utilisant des durées différentes d'activation à savoir 15, 30, 60 et 120 s.

Pour le calcul des interactions de dispersion γ_s^d et des interactions polaires γ^p on a effectué des mesurages des angles de raccordement pour deux liquides : l'eau et le formamide.

Dans ce but, on a déposé des gouttes d'eau et de formamide d'un volume de 0,5 μL à l'aide d'une seringue de type Hamilton ayant un volume total de 1 μL.

Des photographies ont été réalisées pour chaque goutte, à 30 $''$ depuis le dépôt.

Ce temps est suffisant pour que la goutte puisse prendre son angle d'équilibre θ, et en même temps suffisamment petit pour négliger les pertes par l'évaporation. [7]

En considérant la goutte comme une section sphérique, l'angle de raccordement θ a été déterminé du diamètre de la base, d et de la hauteur h de la goutte, en utilisant la relation :

$$\mathrm{tg}(\theta/2) = 2\,h/d. \tag{1}$$

L'angle de raccordement θ, utilisé pour le calcul des énergies de surface, représente la moyenne de trois valeurs trouvées expérimentalement.

Pour obtenir des informations sur la durée pendant laquelle la feuille reste activée, on a déterminé l'angle de raccordement et après 24, 48 et 72 heures depuis l'activation pour chaque épreuve.

Dans le but de tester l'autoadhésivité, on a réalisé la soudure à chaud des deux feuilles activées dans le plasma.

A cette fin ont a coupé des échantillons d'une largeur de 14 mm et d'une longueur de 300 mm. Les épreuves ont été soumises à la corrosion pendant 180 s et ensuite passées par deux cylindres à la température de ~ 90°C, la pression entre ceux-ci étant de ~ 15 kgf/mm^2.

Les feuilles, ainsi soudées, ont été soumises à l'allongement en utilisant à cette fin un Dynamomètre Universel Wolpert.

On a trouvé, en moyenne, un allongement de ~ 110% et la force de ~ 40 kgf/mm^2.

Il faut mentionner que les feuilles se sont rompues dans certains points mais elles ne se sont pas décollées.

Il faut aussi souligner que les feuilles TPE nonactivées dans le plasma ne peuvent se souder quelque grande que soit la pression entre les cylindres.

3. LE CALCUL DE L'ÉNERGIE LIBRE DE SURFACE DE LA FEUILLE TPE ACTIVÉE

L'énergie d'adhésion ou la tension d'adhésion d'un liquide à une surface solide est donnée par l'équation combinée Young-Dupré [7] :

$$W_a = \gamma_l (1 + \cos\theta) \tag{2}$$

où γ_l, représente la tension superficielle du liquide et θ est l'angle de raccordement du liquide à la surface du solide.

L'expression (2) n'est valable que pour des petites énergies d'adhésion du liquide à la surface du solide.

Fowkes [8] indique que pour des petites énergies de surface il faut prendre en considération seulement l'énergie de dispersion London, tant pour la surface solide notée γ_s^d que pour le liquide déposé, γ_l^d

Dans ce cas, l'énergie d'adhésion est donnée par la moyenne géométrique des deux énergies γ_s^d et γ_l, c'est-à-dire :

$$W_a = 2\sqrt{\gamma_s^d \cdot \gamma_l^d}\,. \tag{3}$$

Toutefois, il y a des surfaces anorganique ou organiques (ex. la feuille TPE), qui, grâce à leur structure moléculaire ont une certaine polarité.

De même, les liquides qui trempent la surface possèdent des molécules polaires.

Dans ce cas, il faut aussi prendre en considération l'énergie d'interaction dipôle-dipôle.

Ainsi, l'expression (3) de l'énergie d'adhésion devient :

$$W_a = 2(\sqrt{\gamma_s^d \cdot \gamma_l^d} + \sqrt{\gamma_s^p \cdot \gamma_l^p}) . \tag{4}$$

L'énergie libre de surface γ_s est par conséquent la somme des contributions γ_s^d et γ_s^p, c'est-à-dire :

$$\gamma_s = \gamma_s^d + \gamma_s^p \tag{5}$$

La valeur de l'énergie libre de surface, γ_s est facile à déterminer si de l'équation (2) on calcule l'énergie d'adhésion, W_a, de deux liquides pour lesquels on connaît les valeurs de l'énergie de dispersion γ_l^d et de l'énergie des interactions polaires γ_l^p.

En travaillant avec des surfaces de petites énergies, Fowkes[8] a obtenu, pour un grand nombre de liquides, les valeurs γ_l^d et γ_l^p.

Pour la détermination de l'énergie libre de surface de la feuille TPE activée, on a utilisé comme liquides l'eau et le formamide pour lesquels nous avons :

l'eau : $\gamma_l^d = 21{,}8$ mJ.m^{-2} et $\gamma_l^p = 51$ mJ.m^{-2}

le formamide : $\gamma_l^d = 39{,}5$ mJ. m^{-2} et $\gamma_l^p = 18{,}7$ mJ.m^{-2}

En remplaçant ces données dans (4), nous obtenons un système de deux équations avec deux inconnues γ_s^d et γ_s^p :

$$\begin{aligned} W_a^{eau} &= 2\,(\sqrt{\gamma_s^d \cdot \gamma_l^d} + \sqrt{\gamma_s^p \cdot \gamma_l^p}\,) \\ W_a^{form.} &= 2(\sqrt{\gamma_s^d \cdot \gamma_l^d} + \sqrt{\gamma_s^p \cdot \gamma_l^p}) \end{aligned} \tag{6}$$

Après avoir déterminé γ_s^d et γ_s^p à l'aide de l'équation (5), on a déterminé l'énergie libre de surface γ_s de la feuille TPE activée.

Le calcul de l'énergie libre de surface, γ_s, a commencé par calculer l'énergie d'adhésion, W_a conformément à l'équation (2) tant pour l'eau que pour le formamide.

Les valeurs de l'angle θ, ainsi qu'on l'a mentionné, représentent la moyenne pour trois déterminations expérimentales.

En connaissant les valeurs de l'énergie d'adhésion, W_a^{eau} et $W_a^{form.}$ de l'équation (6) on a déterminé les valeurs de l'énergie de surface dues à l'interaction dipôle-dipôle, γ_s^p.

Dans le tableau 1 on présente les valeurs de l'angle de raccordement θ, cos θ, W_a et de l'énergie libre de surface, γ_s, pour la feuille TPE activée dans le plasma à des durées différentes.

Tableau 1

La durée d'activation (s)	La pause après l'activation	Le milieu de plasma	La forme de la goutte	θ	cos θ	1 + cos θ	W_a	γ_s^d mJ · m⁻²	γ_s^p mJ · m⁻²	γ_s mJ · m⁻²
0	—	—	1 (eau) 2 (formamide)	87,1 61,48	0,050 0,477	1,050 1,477	76,44 85,96	32,580	2,627	35,207
15	30 s.	oxygène	1. 2.	22,4 15,3	0,924 0,964	1,924 1,964	140,06 114,30	18,192	49,193	67,385
30	30 s.	—,,—	1. 2.	20,5 12,9	0,936 0,975	1,936 1,975	140,94 114,94	18,517	49,838	68,355
60	30 s.	—,,—	1. 2.	17,2 6,4	0,955 0,994	1,955 1,994	142,32 116,05	18,658	51,000	69,648
60	24 h.	—,,—	1. 2.	38,9 19,2	0,778 0,944	1,778 1,944	129,43 113,14	25,348	33,292	58,640
60	48 h.	—,,—	1. 2.	60,06 38,92	0,499 0,778	1,499 1,778	109,17 113,14	29,1	17,02	46,12
60	72 h.	—,,—	1. 2.	86.9 61,40	0,054 0,478	1,054 1,478	76,73 86,01	32,574	2,625	35,199
15	30 s.	argon	1. 2.	28,3 18,8	0,880 0,946	1,880 1,946	136,86 113,25	19,361	44,966	64,472
30	30 s.	—,,—	1. 2.	28,1 16,6	0,882 0,958	1,882 1,958	137,00 113,95	20,152	44,320	64,472
60	30 s.	—,,—	1. 2.	27,31 9,60	0,888 0,985	1,888 1,985	137,44 115,52	21,882	43,095	64,977
60	24 h.	—,,—	1. 2.	40,01 14,73	0,766 0,967	1,766 1,967	128,56 114,47	28,131	30,624	58,755
60	48 h.	—,,—	1. 2.	58,85 56,28	0,517 0,555	1,517 1,555	110,45 104,83	30,1	17,2	47,3
60	72 h.	—,,—	1. 2.	87,05 61,45	0,050 0,477	1,050 1,477	76,44 85,96	32,580	2,627	35,207

Dans les figures 1 et 2 on a représenté la variation de l'angle de raccordement θ pour l'eau et pour le formamide, en fonction du temps d'activation pour le plasma d'oxygène et respectivement pour le plasma d'argon.

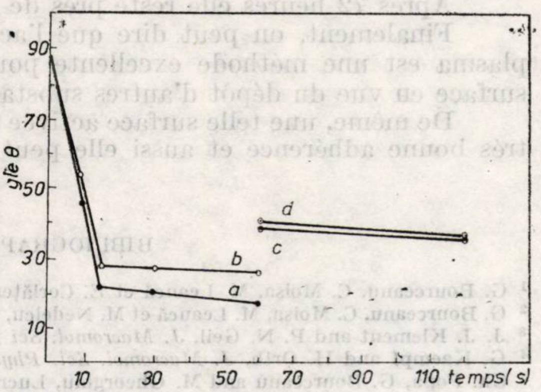

Fig. 1. — La variation de l'angle de raccordement θ, pour la goutte d'eau en fonction du temps d'activation dans le plasma d'oxygène et d'argon : a — dans le plasma d'oxygène à 30″ après l'activation ; b — dans le plasma d'argon à 30″ aprés l'activation ; c — dans le plasma d'oxygène à 24 heures après l'activation ; d — dans le plasma d'argon à 24 heures après l'activation.

Tant de la figure 1 que de la figure 2 on observe que la décroissance rapide de l'angle de raccordement (donc une activation prononcée) est obtenue dans les premières 15 s, après quoi la décroissance de l'angle de raccordement est assez lente tant dans le plasma d'oxygène que dans le plasma d'argon.

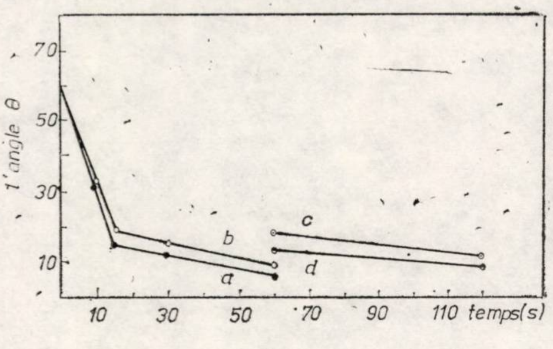

Fig. 2. — La variation de l'angle de raccordement θ, pour la goutte de formamide du temps l'activation dans le plasma d'oxygène et d'argon : a — dans le plasma d'oxygène à 30″ après l'activation ; b — dans le plasma d'argon à 30″ après l'activation ; c) — dans le plasma d'oxygène à 24 heures après l'activation ; d — dans le plasma d'argon à 24 heures après l'activation.

4. DISCUSSION

Ainsi que l'on peut observer du tableau 1, dans le cas de la feuille TPE non-traitée, l'énergie libre de surface γ_s^d due aux forces de dispersion London, est très grande par comparaison à l'énergie de surface γ_s^p donnée par les interactions polaires.

C'est pourquoi l'hydrophilie de la feuille non-traitée est extrêmement diminuée.

Après le traitement, dans le plasma de haute fréquence (H.F) l'énergie γ^p augmente beaucoup tandis que γ_s^d diminue par comparaison à la feuille non-activée.

Des valeurs un peu plus grandes pour γ_s^d sont obtenues si la feuille est activée dans le plasma d'oxygène.

L'activation est réalisée même dans les premières 15 s du traitement dans le plasma de H.F., en restant constante à tout au plus 60 s.

La feuille reste encore activée même après 24 heures, quand elle est encore soudée.

Après 72 heures elle reste près de son état initial.

Finalement, on peut dire que l'activation des feuille TPE dans le plasma est une méthode excellente pour augmenter l'hydrophilie de la surface en vue du dépôt d'autres substances polaires.

De même, une telle surface activée peut être métallisée à l'aide d'une trés bonne adhérence et aussi elle peut être soudée.

BIBLIOGRAPHIE

[1] G. Bourceanu, C. Moisa, M. Leancă et E. Corlăţeanu, *Materiale plastice*, **18**, 51 (1981).

[2] G. Bourceanu, C. Moisa, M. Leancă et M. Nedelcu, *Materiale plastice*, **18**, 226 (1981).

[3] J. J. Klement and P. N. Geil, *J. Macromol. Sci Phys.*, B, **5**, 535 (1971).

[4] G. Kaempf and H. Orth, *J. Macromol. Sci. Phys*, B, **11**, 151 (1975).

[5] Gh. Popa, G. Bourceanu and M. Gheorghiu, Lucrările celei de a patra Conferinţe Naţionale ,,Fizica şi tehnica plasmei'', Bucureşti, 1981.

[6] J. Friedrich and J. Gáhde, *Acta Polymerica*, **31**, 52 (1980).

[7] D. Briggs, D. G. Rance, C. R. Kendall and A. R. Blythe, *Polymer*, **21**, 895 (1980).

[8] F. M. Fowkes, *Adv. Chem. Sci.*, **43**, 99 (1964).

[9] K. D. Owens, *Appl. Polym. Sci.*, **19**, 265 (1975).

Revue Roumaine de Chimie, 30, 9–10, 865–873 (1985)

PHOTODEGRADATION AND PHOTOSTABILIZATION OF THE ETHYLENE-VINYL ACETATE COPOLYMERS. I

ASPECTS OF THE MECHANISM OF PHOTODEGRADATION REACTIONS*)

C. ANDREI [a], I. HOGEA[a] and V. DOBRESCU[b]

[a] Brazi Petrochemical Plant, Research Department, 2000 Ploiești, Romania

[b] ICECHIM — București, Splaiul Independenței 202, Romania

Received May 26, 1984

During UV — irradiation of ethylene-vinyl acetate (EVA) samples, important modifications of copolymer structure occur. Besides new absorption bands, the IR spectrum exhibits a decrease of the intensity of some bands, as well as the increase of intensity of bands in UV spectra (180—210 nm). On the basis of the evolution in time of these spectra, the photooxidation reaction scheme is proposed, with participation in the reaction initiation of the chromophoric group. The scheme emphasizes the decisive role played by chromophoric and hydroperoxidic groups in the process of photodegradation of EVA copolymers.

INTRODUCTION

Manufacturing of ethylene-vinyl acetate (EVA) copolymers took a great development in the last two decades.[1,2]

This evolution is mainly due to the numerous utilizations of these copolymers.

Recently, EVA copolymers are more and more used as films for covering solaria in agriculture and various kinds of constructions as well.

Although there are numerous studies dealing with the photodegradation and photostabilization of polyolefines with backbone carbonyl groups and side chain ketone groups [3–6] have been published, research works concerning the behaviour of differents EVA copolymers are scarce.

In a recent work Buchanan and McGill [7] have studied some aspects of the photodegradation of poly(vinyl esters) by determining the photodegradation products evolved during the process at higher temperature, above glass transition temperature (75°C); some considerations regarding the reaction mechanism were issued.

This contribution is a part of a systematic investigation of degradation of EVA copolymers. Starting from the modification of irradiated polymer we tried to find the mechanism of photodegradation reactions and the efficient system of protection against UV radiation.

---

*) A part of this work was presented at the 28th IUPAC International Symposium on Macromolecules, University of Massachusetts, Amherst, July 12—16, 1982.

This first part of work reports studies by IR and UV absorption spectroscopy on photodegradation of EVA copolymers.

EXPERIMENTAL

EVA copolymers (Bayer and BASF brands) purified by solving in benzene precipitation with methanol, were irradiated, in air, with a high pressure Hg lamp type Romlux (250 W). The distance between the source and the samples was 25 cm and the temperature at sample surface was $27 \pm 0.3°C$.

Determinations were carried out on copolymer layers deposited from solution on KBr windows for IR and on quartz windows for UV.

The IR spectra were recorded by a Specord—IR—75 spectrophotometer and UV spectra with a Hitachi EPS—3 spectrophotometer. UV spectra within 180—220 nm were recorded n nitrogen atmosphere.

RESULTS AND DISCUSSION

During UV — irradiation of EVA samples some important modifications of copolymer structure have occurred.

Fig. 1 shows the IR spectrum of Levapren 450 copolymer between 4000 and 400 cm^{-1}.

It is obvious that new absorption bands appear in the irradiated copolymer: the wide band at 3200—3600 cm^{-1} assigned to stretching vibrations of O—H groups in hydroperoxides, alcohols and acids; the bands at 1710 cm^{-1} and 1690 cm^{-1} assigned to stretching vibrations of C=O groups in aldehydes and ketones, respectively.

The maximum at 3390 cm^{-1} of the absorption band is assigned to hydroperoxide group (OOH) while that at 3465 cm^{-1} to OH group. It is noteworthy that the increase of UV exposure time of EVA copolymer causes the maximum of absorption band characteristic of OH vibrations to shift to higher wavelengths.

This evolution is evidenced by fig. 2 which represents the time variation of absorbance at two wavelengths.

Besides the new absorption bands, the IR spectrum of UV-irradiated EVA copolymer exhibits a decrease of the intensity of bands at 1725 cm^{-1} (assigned to stretching of C = O group), 1225 cm^{-1} (assigned to stretching vibration of C—O—C group) and 1010 cm^{-1} (assigned to stretching vibration of C—C—O group), all belonging to side ester groups, with the increase of irradiation time.

Likewise, the intensity of absorption bands at 2845 and 2920 cm^{-1}, assigned to valence vibrations of methylene groups, decreases.

Fig. 3 shows the behaviour of the intensity of absorption bands C—O—C, C=O and CH_2 groups; the intensity of bands decreases with the increase of the exposure time.

Examination of Fig. 3 shows that the intensity of bands at 2920 cm^{-1} characteristic of methylene groups decreases linearly while the intensity of C—O—C band is larger at the beginning and then decreases slowly.

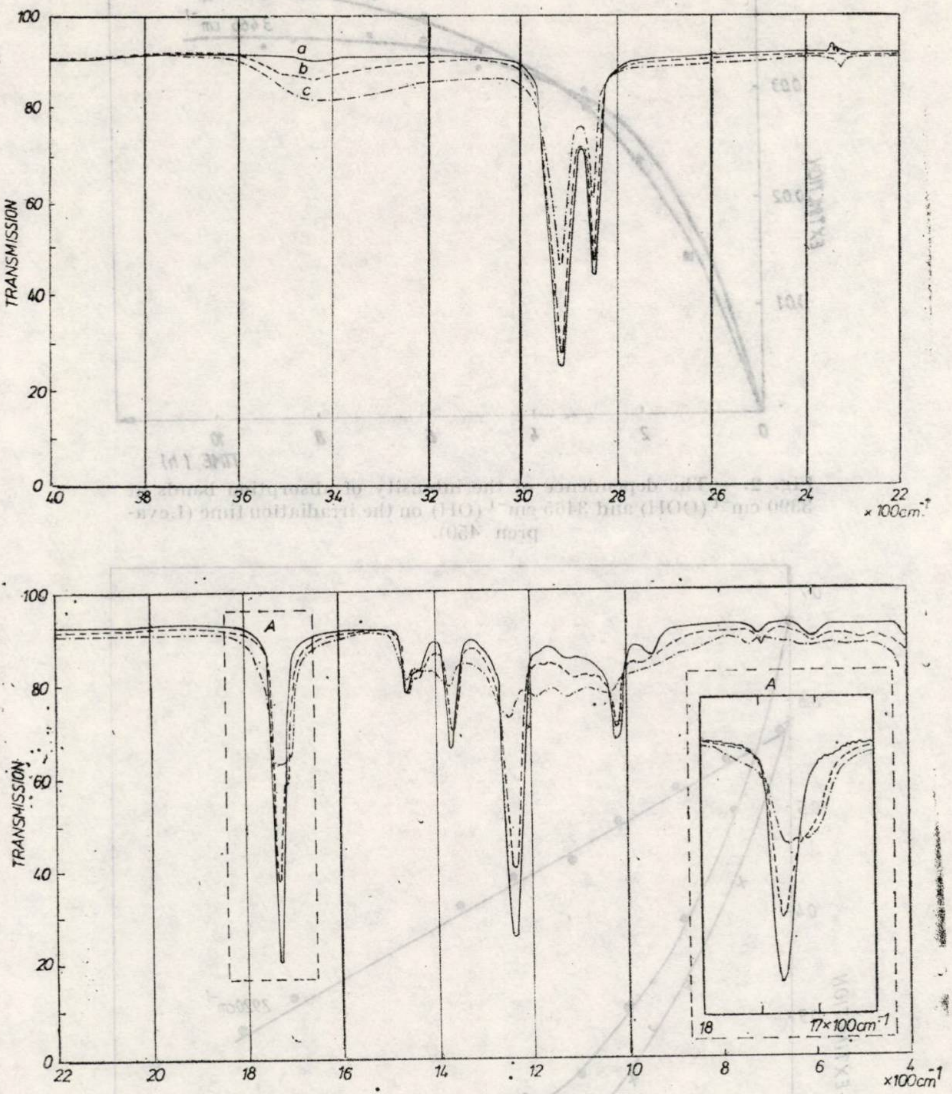

Fig. 1. — IR absorption spectrum of EVA copolymer (Levapren 450) in the range 4000 — 400 cm^{-1} : a. unirradiated ; b. irradiated, 2 h ; c. irradiated, 10 h.

This behaviour supports the idea that the breaking of ester groups occurs by several mechanisms which involves several mechanisms of breaking of side groups.

The decrease of the intensity of band at 2920 cm^{-1} (CH_2) is explained in terms of the formation of double bond in the polymer chain with elimination of acetic acid.

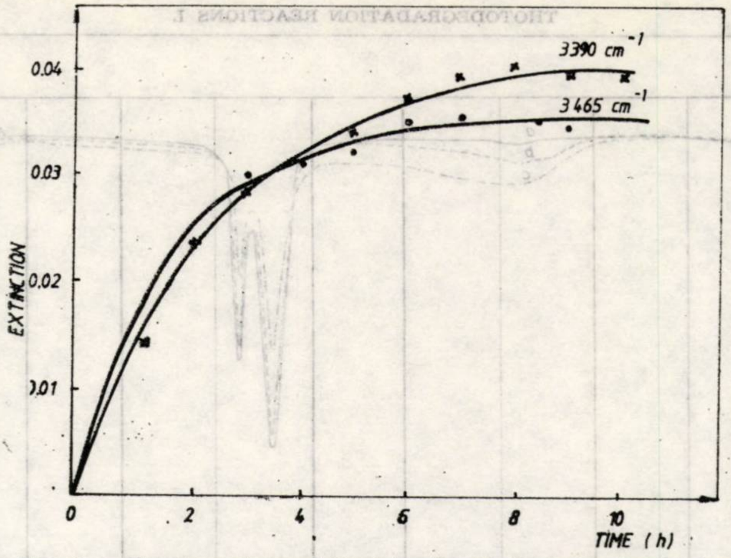

Fig. 2. — The dependence of the intensity of absorption bands at 3390 cm^{-1} (OOH) and 3465 cm^{-1} (OH) on the irradiation time (Levapren 450).

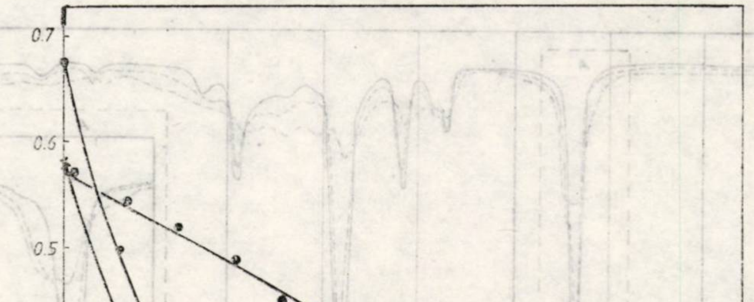

Fig. 3. — The dependence of the intensity of absorption bands at 1225 cm^{-1} (C—O—C), 1725 cm^{-1} (C=O) and 2920 cm^{-1} (CH_2) on irradiation time (Levapren 450).

The formation of double bonds with the increase of irradiation time is also evidenced by UV spectra redorded in nitrogen atmosphere within 180—210 nm range (Fig. 4).

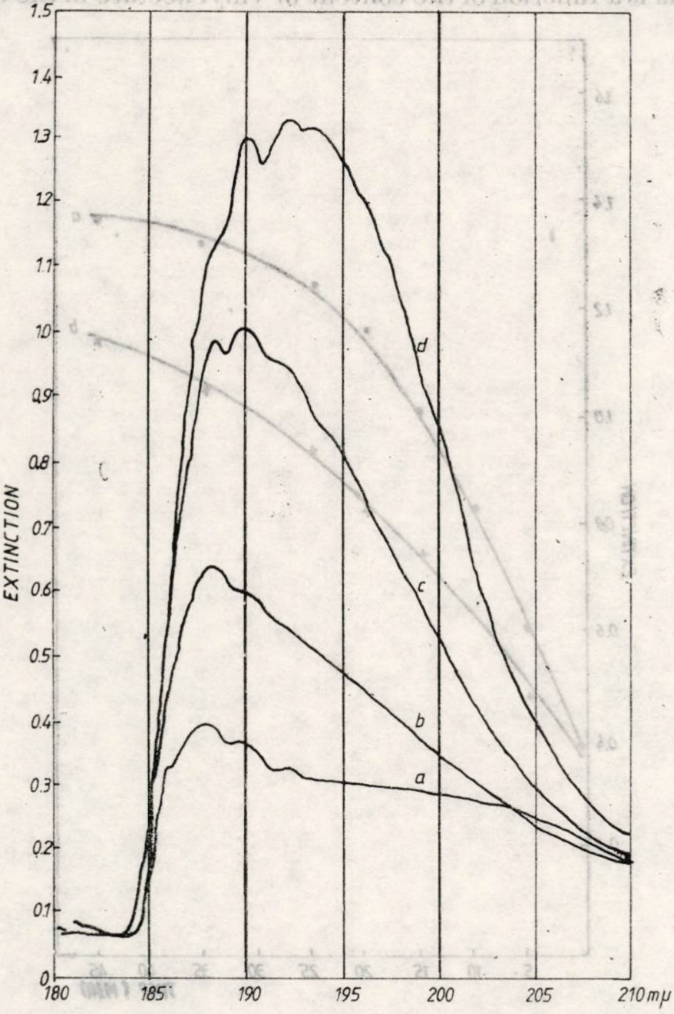

Fig. 4. — The UV absorption spectrum (180 — 210 nm) of EVA copolymer (Levapren 450) : a. unirradiated ; b. irradiated, 5 min ; c. irradiated, 15 min ; d. irradiated, 55 min.

The spectrum evidences a band at 188 nm assigned to double bonds (C= C). The increase of irradiation time causes absorption to shift to higher wavelengths (batochromic effect) because of the interactions in the system.

It is noteworthy that the unirradiated copolymer contains a low number of double bond, which form during synthesis and conditioning of the copolymer.

Fig. 5 shows the variation of the intensity of the band at 190 nm for two EVA copolymers of different vinyl acetate content.

This evolution proves that the rate of increase of the number of double bonds is a function of the content of vinyl acetate in the copolymer.

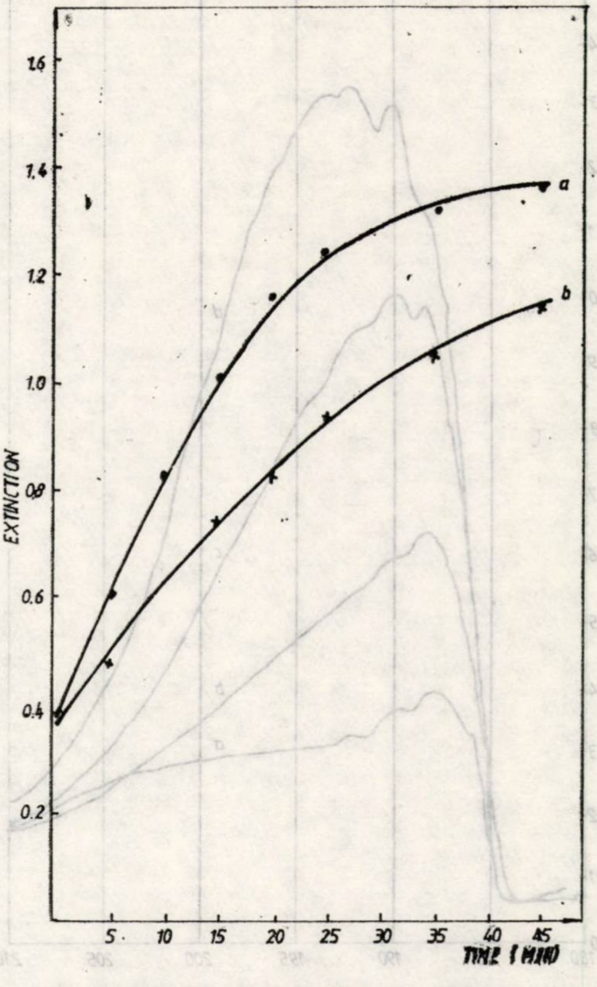

Fig. 5. — The intensity of the band at 190 nm of EVA copolymers on irradiation time: a. Levapren 450 (45% V.A.); b. Lupolen 1201 (30% V.A.).

Thus, the rate of photodegradation of EVA copolymer rises with the increasing content of comonomer in polyolefine chain.

The structural modifications of EVA copolymers subjected to photooxidation by UV (i.e. the decrease of intensity of IR absorption bands at 1725 cm^{-1} (ν C$=$O), 1225 cm^{-1} (ν C$-$O$-$C), 1010 cm^{-1} (ν C$-$C$-$O), 2845 and 2920 cm^{-1} (ν CH_2) as well as the increase of intensity of bands in UV spectra (180$-$210 nm) suggest that the main reaction is the acetic acid elimination through a mechanism which involves a transition state with formation of a six atom ring :

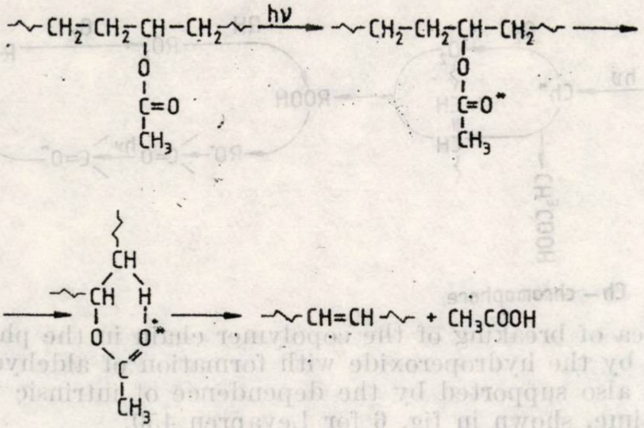

The existence of this reaction agrees with Grant and Grassie's results [8] regarding the pyrolysis of these copolymers and with Geuskens, Borsu and David's works [9] on the photolysis of poly(vinyl acetate) which have also evidenced evolution of acetic acid.

Thermal degradation of these copolymers evolves quantitatively acetic acid ; this reaction has set the foundations of a quantitative method of analysis for the composition of copolymers.[10]

After evolution of acetic acid, the copolymer with double bonds is susceptible to oxidation in the presence of oxygen or singlet oxygen ($^1O_2$) formed on photo-oxidation by energy transfer from excited carbonyl groups in singlet state to molecular oxygen :

$$(>C{=}O)^{*} + {}^{3}O_2 \longrightarrow >C{=}O + {}^{1}O_2$$

The oxidation of the polymer would occur according to the reaction of "ene" process [11,12] with formation of hydroperoxides and exchange of the double bond :

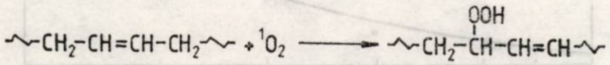

$$\sim CH_2{-}CH{=}CH{-}CH_2\sim + {}^{1}O_2 \longrightarrow \sim CH_2{-}\underset{}{\overset{OOH}{\overset{|}{C}H}}{-}CH{=}CH\sim$$

This reaction is supported by the presence and evolution of the band at 3390 cm^{-1} (OOH).

The presence of hydroperoxides in the polymer initiates new well known reactions which bring about further degradation of the polymer.[13,14]

We consider that the process of photo-degradation of the EVA copolymer occurs according to the following mechanism.[15,16]

The scheme emphasizes the decisive role played by chromophoric and hydroperoxidic groups in the process of photodegradation of EVA copolymers and includes only most important reactions.

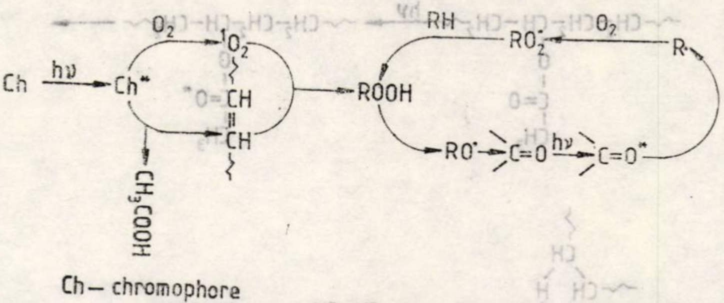

The idea of breaking of the copolymer chain in the photodegradation process by the hydroperoxide with formation of aldehydes, ketones and acids is also supported by the dependence of intrinsic viscosity on irradiation time, shown in fig. 6 for Levapren 450.

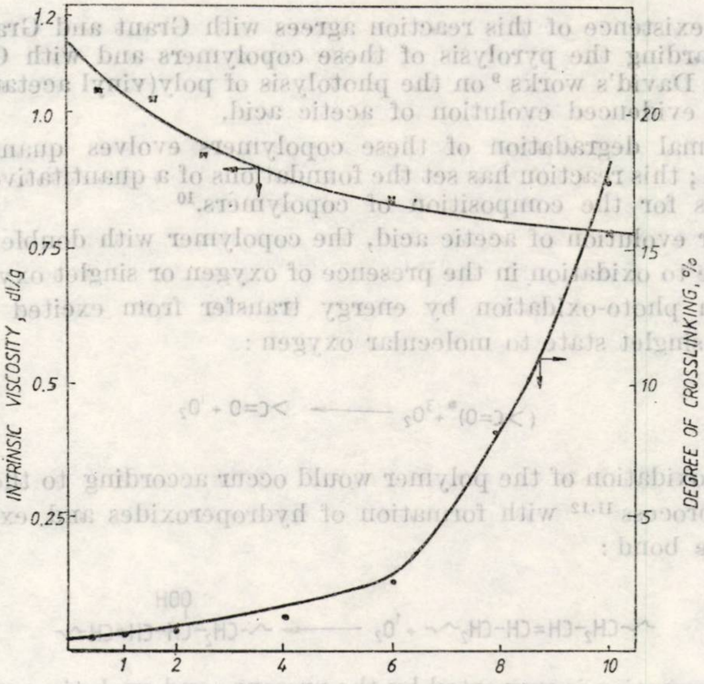

Fig. 6. — The dependence of intrinsic viscosity and crosslinking degree for Levapren 450 copolymer on the time of UV exposure.

On the same figure the variation of the degree of crosslinking with the irradiation time is also shown; this reaction will be considered in a forthcoming work.

REFERENCES

[1] I. Nanu, D. Blum, C. Andrei and G. Musca, *Mat. Plastice*, **16**, 73 (1979).

[2] C. Andrei and V. Dobrescu, 6ème Conférence Européenne des Plastiques, Paris, 7–9 Juin 1982.

[3] K. F. Wissbrun, *J. Amer. Chem. Soc.*, **81**, 58 (1979).

[4] F. Sitek, J. F. Guillet and M. Heskins, *J. Polym. Sci. Symposium*, **57**, 343 (1976).

[5] G. H. Hartley and J. F. Guillet, *Macromolecules*, **1**, 165 (1968).

[6] J. F. Guillet, *Pure Appl. Chem.*, **52**, 285 (1980).

[7] K. J. Buchanan and W. J. McGill, *Europ. Polym. J.*, **16**, 309, 313, 319 (1980).

[8] D. H. Grant and M. Grassie, *Trans. Faraday Soc.*, **48**, 379 (1952) ; **56**, 445 (1960).

[9] G. Geuskens, M. Borsu and C. David, *Europ. Polym. J.*, **8**, 883 (1972).

[10] I. Hogea, G. Andrei, P. Ioana, C. Andrei and V. Dobrescu, The 2nd National Congres of Chemistry, Bucharest — Romania, 7 — 10 sept. 1981.

[11] J. F. Rabek and B. Ranby, *J. Appl. Polym. Sci.*, **23**, 2481 (1979).

[12] J. F. Rabek, J. Lucki and B. Ranby, *Europ. Polym. J.*, **15**, 1089 (1979).

[13] D. M. Wiles and D. J. Carlsson, *Polymer Degradation and stability*, **3**, 61 (1980–81).

[14] C. Andrei and V. Dobrescu, *Rev. de Chimie*, **33**, 317 (1982).

[15] C. Andrei, I. Hogea and V. Dobrescu, IUPAC, 28th Macromolecular Symposium, University of Massachusetts, Amherst, July 12 — 16, 1982.

[16] V. Dobrescu and C. Andrei, The XVth Colloquium of Danubian Countries for Natural and Artificial Ageing of Polymers, 27–30 Sept., 1982, Moscow.

Revue Roumaine de Chimie, **30**, *9–10*, 875–881 (1985)

MICELLAR EFFECTS UPON THE AZOCOUPLING REACTION

AURORA SALLO and ANCA TOMESCU
Chemical Research Centre, B-dul M. Viteazul 24, 1900 Timişoara, Romania

Received June 24, 1983

Studies concerning the kinetics of azocoupling reactions of twelve benzenediazonium tetrafluoroborates ($X-C_6H_5N_2BF_4$, X=H ; p, m–NO_2 ; p, m– ;Cl;p, m–Br ;p, m–CH_3 ; p, m–OCH_3 ; p–OC_2H_5) with l-naphthol-4-sulfonic acid in micellar sodium lauryl sulfate (NaLS) medium, are reported. A retardation of the reaction rate was observed in agreement with Hartley's "sign rule". The degree of this retardation depends upon the nature of the X-substituent. A modest but statistically significant correlation of the log (k_0/k_{obs}) with the hydrophobicity constants, π, is reported for the X-substituents. Preliminary investigations upon the stability of four benzenediazonium tetrafluoroborates indicate that the rate of the dediazoniation reaction in micellar medium does not differ sensibly from the rate in aqueous medium.

INTRODUCTION

During the past decades there has been considerable interest in reactions which can be carried out at interfaces. One aspect of this work has involved the catalysis or inhibition of solution reactions by submicroscopic entities such as polyelectrolytes, cyclodextrins, or micelles. [1–4]These studies opened perspective sconcerning the kinetic directioning of chemical reactions and the modeling of enzymatic reactions (acylation, [5–8] dephosphorilation[11–9]).

The azocoupling of diazonium salts is an electrophylic substitution sensitive to the presence of micelles, but there are only few studies concerning the nature and the effects of this influence. The main results are limited to the statement that micellar effects are affected by the formal charge of reactants, i.e. the diazonium ion and the coupling component [12,13,40] confirming Hartley's "sign rule" [1,14] (Hartely, using simple electrostatic considerations, predicted that cationic micelles enhance the rate of reactions of nucleophilic anions with uncharged substrates, while anionic micelles retard them, but catalyse reactions involving cations). Hartley's ideas are well illustrated by the attended micellar inhibition of the azocoupling between the p-nitrobenzenediazonium and 2-naphthol-6-sulfonate ions. [12] The rate constant for coupling was depressed, relatively to the rate in pure water, in both cationic and anionic micellar solution. By coupling an amphiphilic diazonium salt which yields a micellar pseudophase, Moss at al. [15] succeeded to circumvent Hartley's "sign rule". Based on their kinetic results Moss suggested that, besides the proximity effects, the micromedium created by micelles influences directly the electrophilic substitution, the azocoupling reaction.

The present paper deals with the influence of the micellar sodium lauryl sulfate (NaLS) medium upon the azocoupling reaction rate of substituted benzenediazonium tetrafluoroborates with 1-naphthol-4-sulfonic acid.

Stability of some benzenediazonium tetrafluoroborates was also investigated in micellar medium.

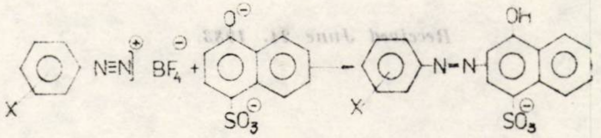

(D) (C) (Az) (1)

$X = H$; p, m $-NO_2$; p, m$-Cl$; p, m$-Br$; p, m$-CH_3$; p, m$-OCH_3$: p$-OC_2H_5$

EXPERIMENTAL SECTION

Materials. The sodium salt of the 1-naphthol-4-sulfonic acid (purum Astranal Austria) was purified by treating the aqueous solution with active coal; the almost colourless solution was passed through an aluminium oxid column. The purity of the solution was checked by TLC, the concentration was determined by nitrozation.[16] The aromatic amines were purified by crystallization and vacuum distillation. The diazotization of amines and the preparation of benzenediazonium tetrafluoroborates were performed according to ref.[17-19] Sodium lauryl sulfate (NaLS) was of 99% purity, with a critical micellar concentration (CMC) equal to the literature value[1] $CMC = 8.1 \cdot 10^{-3}$ mol $\cdot$ L^{-1}.

CMC and PK_a determinations. We studied the thermal decomposition and the azocoupling reactions in water solutions with significant electrolyte concentrations. Therefore we determined the CMC values for our specific conditions. The following results were obtained: for HCl 0.01 N, $CMC = 3.5 \cdot 10^{-3}$ mol $\cdot$ L^{-1}, for phosphate buffer solution (Na_2HPO_4 N/15 and NaH_2PO_4 N/15) $CMC = 1.9 \cdot 10^{-3}$ mol.L^{-1}. CMC was determined by surface tension method.

The acidity constant of 1-naphthol-4-sulfonic acid was determined spectrofotometrically.[21,22] The values determined in aqueous medium and in micellar medium ($[NaLS] = 8.1 \cdot 10^{-3}$ mol.L^{-1}) are equal within the limits of experimental errors. The rate constants were calculated using the $pK_a = 8.2 \pm 0.08$ value.

Kinetic measurements. The stability of diazonium salts was studied in aqueous solution of HCl 0.01 N. Two series of determinations were performed, in aqueous medium and in micellar medium $[(NaLS] = 8,1 \cdot 10^{-3}$ mol L^{-1}). The concentration of the substrate, of the benzenediazonium tetrafluoroborates, was of $1.2 \cdot 10^{-4}$ mol L^{-1}.

The kinetics was followed spectrophotometrically. The undecomposed diazonium ion was coupled with an alkaline solution (Na_2CO_3 0,05 N) of the R salt, 10^{-3} mol $\cdot$ L^{-1}.

The kinetics of azocoupling reactions was followed spectrophotometrically at $\lambda = \lambda_{max}$ of the formed azo dye. The kinetic runs were accomplished in the thermostated cell of a UNICAM SP 800 Spectrophotometer, the exit signal being recorded with a Philips PM 8100 recorder. The concentration of the 1-naphthol-4-sulfonic acid solution was 5.10^{-3} mol $\cdot$ L^{-1}, the concentration of benzenediazonium tetrafluoroborates about 5.10^{-5} mol $\cdot$ L^{-1}. Using the naphthol component in large exces pseudomonomolecular conditions were provided for kinetics here investigated. Phosphate buffer[23] solutions were used. The NaLS concentration was $8.1 \cdot 10^{-3}$ mol $\cdot L^{-1}$. In the presence of NaLS it was not possible to work at a constant ionic strength; these solutions were non homogenous if potasium chloride was present, due to precipitation of the surfactant.[12] The pH measurements were performed on a MV 85 pH-meter (Prăcitronic DDR). The kinetic determinations were accomplished at three different temperatures. Three or four runs were performed at each temperature.

The pseudo first order rate constant, k_ψ was determined by linearization (the least squares method [24]) of log $(E_\infty - E)$ *vs t*, k_ψ being the slope of the regression line. The bimolecular rate constant was calculated by the equation [25,41]:

$$k = \frac{k_\psi(K_a + [H^+])}{c_i \cdot K_a} = [L.\ mol^{-1} \cdot s^{-1}] \tag{2}$$

where : K_a is the acidity constant of naphthol, c_i — initial concentration of naphthol, $[H^+]$ — concentration of hydronium ions, k_ψ — pseudo first order rate constant.

RESULTS AND DISCUSSION

There was investigated the influence of the NaLS micelles on the azocoupling reaction rate of twelve benzenediazonium tetrafluoroborates (equation 1) with 1-naphthol-4-sulfonic acid. Two series of determination were performed : i) in aqueous medium ii) in aqueous medium in the presence of NaLS micelles. The azocoupling reaction with 1-naphthol-4-sulfonic acid was studied by B. Demian [41] and the kinetic equation of the rate constant was established (equation 2). In the condition of kinetic determinations in aqueous medium, the secondary reaction, the thermal decomposition of the diazonium salts, takes place with a negligible rate as compared with that of azocoupling reaction. There was followed the thermal decomposition of four benzenediazonium tetrafluoroborates ($X = H$; m, p$-$cl ; p$-CH_3$) in the presence of NaLS micelles. The results displayed in table 1 show that only in the case of p-chloraniline the rate of thermal decomposition increases (4 times) in micellar medium as compared with that determined in aqueous medium. At a first approximation we may consider that the presence of the micellar pseudophase does not produce sensible modifications on the benzenediazonium ion stability.

Table 1

Spectral data for benzenediazonium tetrafluoroborates

Diazotized amine	λ_{max}, nm		$\Delta\lambda$	$\varepsilon \cdot 10^{-4}$		$\Delta\varepsilon \cdot 10^{-4}$
	aqueous medium	micellar medium[a)]		aqueous medium	micellar medium[a)]	
Aniline	262.0	261.5	0.5	7.50	7.30	0.20
p-Toluidine	277.5	276.5	1.0	8.20	7.80	0.40
m-Cl-Aniline	265.0	264.0	1.0	4.80	4.56	0.24
p-Cl-Aniline	281.0	279.0	2.0	8.95	8.60	0.35

a) [NaLS] = 8.1 10^{-3} mol.L^{-1}

The UV absorption spectra of the investigated diazonium salts is modified in the presence of NaLS micelles. The absorption maximum is shifted towards smaller values and the molar extinction coefficients is diminished (Table 2). These modifications of the absorption spectra indicate a substrate-micelle interaction.

Table 2

Rate constants for thermal decomposition of benzenediazonium tetrafluoroborates

Diazotized amine	[Diazonium salt] mol. L^{-1}	[NaLS] mol. L^{-1}	t° C	$k \cdot 10^5$ (s^{-1})	s
Aniline	$1.2\ 10^{-4}$	—	45	72.30	3.00
	$1.2\ 10^{-4}$	$8.1\ 10^{-3}$	45	71.80	6.40
p-Toluidine	$1.2\ 10^{-4}$	—	45	7.60	0.00
	$1.2\ 10^{-4}$	$8.1\ 10^{-3}$	45	6.90	0.32
m-Cl-Aniline	$1.2\ 10^{-4}$	—	45	3.80	0.29
	$1.2\ 10^{-4}$	$8.1 \cdot 10^{-3}$	45	3.30	0.13
p-Cl-Aniline	$1.2\ 10^{-4}$	—	55	1.19	0.18
	$1.2\ 10^{-4}$	$0.8\ 10^{-3}$	55	1.10	0.35
	$1.2\ 10^{-4}$	$3.5\ 10^{-3}$	55	1.70	0.11
	$1.2\ 10^{-4}$	$8.1\ 10^{-3}$	55	3.80	0.09
	$1.2\ 10^{-1}$	$16.2\ 10^{-3}$	55	3.63	0.18
	$1.2\ 10^{-4}$	$32.4\ 10^{-3}$	55	2.05	0.11
	$1.2\ 10^{-3}$	$8.1\ 10^{-3}$	55	4.00	0.11

The diazonium cation is probably adsorbed on the micelle surface (Stern layer) [26 27 38] with a lower polarity than that of the aqueous medium. The stability of the diazonium ions is not considerably influenced by the nature of the reaction medium, [28,29] so no important modification of the thermal decomposition rate is expected in micellar medium.

The investigated azocoupling reactions (equation 1) are retarded in the presence of NaLS micelles. In table 3 are displayed the rate constants determined in aqueous medium, k_0 and those in the presence of micelles, k_{obs}. Based upon Hartley's "sign rule" we may expect such results. [12,13,15] Application of simple electrostatic arguments suggests that NaLS micelles adsorb cationic diazonium component, but excludes the anionic coupling component (C). According to the pseudophase model [30, 31] we supose that the azocoupling takes place in bulk water. The adsorption of the diazonium component on the micellar pseudophase causes a concentration decrease of one of the reaction parteners, which is reflected in the decrease of the reaction rate. [32] The pK_a value of l-naphthol-4-sulfonic acid, determined in micellar medium, is equal with that in aqueous medium. This fact suggests the absence of the micelle coupling component interaction. The reaction rate is depressed by anionic NaLS micelles only slightly with about one order of magnitude. In the presence of nonfunctional surfactants (NaLS, CTAB), micellar catalysis or inhibition surpasses seldom two orders of magnitude. This is due to the fact that micelle formation and micellar solubilization are dynamic phenomena. [1]

Table 3

Rate constants for azocoupling reactions and π substituent parameters

Substituent	a) k_o L . mol sec^{-1}	b) k_{obs} L.mol sec^{-1}	k_o/k_{obs}	π
H	5.30 10^2	2.00 10^2	2.65	0
p-CH_3	8.18 10	2.36 10	3.46	0.56
m-CH_3	6.77 10^2	2.78 10^2	2.43	0.56
p-NO_2	2.69 10^5	1.11 10^5	2.42	−0.28
m-NO_2	2.04 10^5	1.45 10^5	1.41	−0.28
p-Cl	3.38 10^3	0.48 10^3	7.05	0.71
m-Cl	2.72 10^4	0.23 10^4	11.82	0.71
p-Br	6.26 10^3	1.14 10^3	5.49	0.86
m-Br	2.74 10^4	0.57 10^4	4.80	0.86
p-OCH_3	1.65 10	0.84 10	1.96	−0.02
m-OCH_3	2.82 10^3	0.97 10^3	2.91	−0.02
p-OC_2H_5	1.86 10	0.44 10	4.23	0.38

k_o — is the rate constant in aqueous medium, interpolated at $T = 293$ K

k_{obs} — is the rate constant in the presence of NaLS micelles, interpolated at $T = 293$ K.

The azo-coupling reactions are investigated in buffered solutions at different pH values. The presence of electrolytes may diminish and in some cases even eliminate the effect of ionic micelles upon chemical reactions. [1,33] In the reaction series here studied no correlation was established between sodium ion concentration and the retardation of reaction rates. Thus the variation of k_0/k_{obs} values (Table 3), in the investigated azocoupling reactions, is not due to different concentrations of sodium ion.

Within a rough approximation, that takes into account only the formal charge, the k_0/k_{obs} values are to be similar for the investigated azocoupling reactions. The variation of k_0/k_{obs} ratio with the diazonium component substituent suggests that the nature of the substituent influences the strength of the micelle-substrate interaction.

Log k_0/k_{obs} was correlated with the Hammett (σ) substituent constant. The correlation constant was unsignificant. The diazonium cation is adsorbed by the polar micellar surface, the hydrophobic micelle-substrate interactions being probably very weak. Nevertheless, by correlating log k_0/k_{obs} *vs* hydrophobicity substituent constant π (Table 3) there was obtained a modest but significant correlation coeficient $r = 0.787$ ($n = 12$). The corresponding regressional line was log $k_0/k_{obs} = 0.396 + 0.454\ \pi$. (The hydrophobicity of the substituents can be evaluated by the substituent parameter π. π values are determined from the partition coefficient of a series of compounds, partitioned in an octanol-water system [34]). A difference between the k_0/k_{obs} values was stated at substituents of the same kind but in a different position. The literature indicates the same π values for the *para* and *meta* positions. [34] The behaviour in partition chromatography of some substituted aromatic derivatives suggests that the hydrophobicity is determined not only by the nature of the substituents, but also by their relative positions [35,37]. The different value of the k_0/k_{obs} ratios, for *meta* and *para* substituents, could be caused by the same phenomenon.

CONCLUSIONS

The stability of four benzenediazonium tetrafluoroborate derivatives, studied here, is not influenced significantly by the presence of NaLS micelles, and can be considered to take place with the same rate as in aqueous medium.

The, here studied, azocoupling reactions, are retarded in micellar NaLS solutions. This micellar inhibition can be explained by Hartley's "sign rule". The degree of this inhibition depends upon the substituents of the benzenediazonium cation, there is a modest but statistically significant correlation between $\log k_0/k_{obs}$ and the substituent parameter, π.

REFERENCES

1 J. H. Fendler and E. J. Fendler, "Catalysis in Micellar and Macromolecular Systems", Academic Press, New York, 1975.

2 C. A. Bunton, "Solution chemistry of surfactants", K. L. Mittal Ed., Plenum Press, New York, 1979, vol. 2, p. 520.

3 C. A. Bunton, *Catal. Rev. Sci. Eng.*, **20**, *1*, 1 (1979).

4 T. Kunitake and S. Shinkai, *Advan. Phys. Org. Chem.*, **17**, 435 (1980).

5 Ch. Rav—Acha, M. Chevion, J. Katzhendler and S. Sarel, *J. Org. Chem.*, **43**, 591 (1978).

6 A. Pillersdorf and J. Katzhendler, *J. Org. Chem.*, **44**, 934 (1979) ; *ibid.*, **44**, 549 (1979).

7 R. Ueoka and Y. Matsumoto, *Chem. Lett.*, **1980**, 35.

8 M. Almgren and R. Rydholm, *J. Pyhs. Chem.*, **83**, 360 (1979).

9 C. A. Bunton, G. Cerichelli, Y. Ihara and L. Sepulveda, *J. Amer. Chem. Soc.*, **101**, 2429 (1979).

10 C. A. Bunton and L. Sepulveda, *Israel J. Chem.*, **18**, 298 (1979).

11 J. M. Brown, C. A. Bunton, N. S. Diaz and Y. Ihara, *J. Org. Chem.*, **45**, 4169 (1980).

12 M. Poindexter and B. McKay, *J. Org. Chem.*, **37**, *10*, 1674 (1972).

13 Y. Hashida and K. Matsumura, *Nippon Kagaku Kaishi*, **12**, 1745 (1979).

14 E. Duynstee and E. J. Grunwald, *J. Amer. Chem. Soc.*, **81**, 4540 (1959).

15 R. A. Moss, CH. Rav. — Acha, *J. Amer. Chem. Soc.*, **102**, 5045, (1980).

16 R. P. Lastovski, J. J. Vainstein, "Tehniceski analiz v proizvodstve promejutocinyh produktov i krasitelei, Ed. III, Goshimizdat, Moscow, 1958, p. 218.

17 Houben-Weil, "Methoden der Organischen Chemie", vol. 10/3, Georg Thieme Verlag, Stuttgart, 1965 p. 37 ;

18 E. W. Dürfurt and G. Balz, *Ber. dtsch. Chem. Ges.*, **60**, 116 (1927).

19 H. F. Fierz-David and L. Blangey, "Grundlagende operationen der Farbenchemie" Springer-Verlag, Wien, 1943, p. 240.

20 K. Lindner, "Textilhilfsmittel, Waschrohstoffe"., vol. 2., Wiss. Verlag, Leipzig, 1964 p. 263.

21 A. Albert and E. P. Searjeant, "Ionization Constants of Acid and Bases" Wiley, New York, 1962, p. 69.

22 H. H. Jaffe and M. Orchin", "Theory and Application of Ultraviolet Spectroscopy",Wiley, New-York, 1962, p. 340.

23 I. I. Lurie, "Spravocinik po analiticeskoi Khimii", Izd. Khimie, Moscow, 1967, p. 227.

24 A. G. Worthing and J. Gaffner, "Prelucrarea datelor experimentale", Ed. Tehnică, Bucharest, 1959, p. 225 (Translation from English).

[25] A. Sallo, B. Demian and O. Exner, *Rev. Roumaine Chim.*, **28**, *2*, 169 (1983).
[26] R. B. Dunlap and E. H. Cordes, *J. Amer. Chem. Soc.*, **90**, *16*, 4395 (1968).
[27] A. Finiels and P. Geneste, *Org. Chem.*, **44**, 2036 (1979).
[28] H. Zollinger, "Azo and Diazo Chemistry", Interscience Publishers, New York, 1961, p. 137.
[29] I. Szele and H. Zollinger, *Helv. Chim. Acta.*, **61**, 1721 (1978).
[30] C. A. Bunton, L. S. Romsted and G. Savelli, *J. Amer. Chem. Soc.*, **101**, 5, 1253 (1979).
[31] C. A. Bunton, L. S. Romsted and Ch. Thamavit, *J. Amer. Chem. Soc.*, **102**, 11, 3900 (1980).
[32] F. M. Menger and C. E. Portnoy, *J. Amer. Chem. Soc.*, **89**, 4968 (1967).
[33] J. L. Kurz, *J.Phys. Chem.*, **66**, *11*, 2239 (1969).
[34] C. Hansch, A. Leo, S. H. Unger, K. H. Kim, D. Nikaitani and E. J. Lien, *J. Med. Chem.*, **16**, 1207 (973).
[35] B. Rittich, *J. Chromatogr.*, **197**, 43 (1980).
[36] W. Butte, C. Fooken, R. Klussmann and D. Schuller, *J. Chromatogr.*, **214**, 59 (1981).
[37] J. Sliwiok, A. Macioszyk and T. Kowalaska, *Chromatographia*, **14**, 138 (1981).
[38] S. Riegelman, N. A. Allawala, K. M. Hrenoff and L. A. Strait, *J. Colloid. Sci.*, **13**, 208 (1958).
[39] D. F. Detar and A. A. Ballentine, *J. Amer. Chem.*, **78**, 3916 (1956).
[40] Jvanka Szele and H. Zollinger, in "Topics in Current Chemistry", vol. 112, F. L. Boschke Ed., Springer, Berlin Heidelberg. p. 25.
[41] B. Demian, *Bull. Soc. Chim. France*, **1973**, 769.

Revue Roumaine de Chimie, **30**, *9–10*, 883–888 (1985)

L'INFLUENCE DU SOLVANT SUR LA VITESSE DE RÉACTION. L'HYDROLYSE ALCALINE DE L'ACÉTATE, DU PROPIONATE, DU BUTYRATE DE n-BUTYLE DANS LE SOLVANT MIXTE EAU–MONOÉTHYLÈNEGLYCOL

ORTANSA LANDAUER, CORNELIA MATEESCU et OLGA IULIAN
Institut Polytechnique Bucharest
Chaire de Chimie Physique

Reçu Avril 4, 1984

L'hydrolyse alcaline de l'acétate, du propionate et du butyrate de n-butyle a été étudiée dans le solvant mixte eau-monoéthylène-glycol (MEG) aux températures de 30°, 40° et 50° C et aux concentrations du solvant de $0{,}096 < X_{MEG} < 0{,}65$ (X = fraction molaire). Les données expérimentales ont permis le calcul de l'énergie d'activation, de l'enthalpie d'activation, de l'antropie libre d'activation et de l'enthalpie libre d'activation. Les résultats expérimentaux ont été coordonnés avec la viscosité du solvant mixte. La variation de la vitesse de réaction en fonction de la concentration MEG est atribuée surtout à la variation de la viscosité du solvant.

The alkaline hydrolysis of the n-butyl acetate, propionate and butyrate in the mixed solvent water–MEG was studied at 30°, 40° and 50° C within the concentration range of mixed solvent $0.096 < x_{MEG} < 0.65$ (*X*-mole fraction). The experimental data have enabled us to compute the activation energy, the activation enthalpy, the activation entropy and free activation enthalpy. We have related the results to the viscosity of the mixed solvent. We attribute the variations of the reaction rate depending on the concentration of MEG mainly to the variation of the viscosity of the solvent.

L'hydrolyse alcaline de l'acétate, du propionate et du butyrate de n-butyle a été étudiée dans différents mélanges eau–MEG, à 30°, 40° et 50° C.

Depuis fort longtemps on a tenté d'expliquer les effets cinétiques du milieu sur les réactions chimiques en les reliant à certaines propriétés physiques ou thermodynamiques des solvants : constante diélectrique, viscosité, pression interne, etc.

Toutes ces tentatives ont donné naissance à des théories qui permettent, si une propriété joue un rôle prépondérant, qu'on interprète l'influence du milieu sur la vitesse de réaction par la variation de cette propriété.

Puisque la viscosité du solvant eau–MEG a une variation plus grande que pour les autres solvants[1-4] nous avons cherché de mettre en corrélation les résultats obtenus avec la viscosité du milieu de réaction.

L'influence de la viscosité sur la constante de vitesse s'exprime soit par la relation de E. A. Moelwin—Huges [5]

$$k = \frac{3\pi\eta}{m} \cdot \exp\left(-\frac{E}{RT}\right) = \mathrm{const.}\ \eta$$

où η est la viscosité du solvant, en admettant que la vitesse de réaction est determinée par la diffusion des espèces réactantes à travers le milieu de réaction; soit par la relation de A. Olander [6] :

$$k = \frac{1}{6}\pi\frac{kT}{\eta}\frac{(r_A + r_B)^2}{r_A r_B}\exp\left(-\frac{E}{RT}\right) = \mathrm{const}\ \eta. \qquad \text{(b)}$$

Cette relation admet que la vitesse de réaction dépend surtout de la vitesse d'activation des molécules du réactif.

En tenant compte de ces relations on doit s'attendre que dans certaines conditions le produit $k\eta$ de même que le rapport k/η aient des valeurs constantes.

PARTIE EXPÉRIMENTALE

La purification des substances et la méthode utilisée par nous ont deja été publiées. [7-9]

RÉSULTATS EXPÉRIMENTAUX

Les tableaux 1, 2 et 3 ci-joints réunissent les constantes de vitesse, k, de l'hydrolyse alcaline des trois esters, exprimées en $\mathrm{L \cdot mole^{-1}\,s^{-1}}$ calculées au moyen de l'équation cinétique des réactions du second ordre.

Les résultats expérimentaux nous ont permis de calculer l'énergie d'activation (E), l'enthalpie d'activation (ΔH^*) l'entropie d'activation (ΔS^*) et l'enthalpie libre d'activation (ΔG^*) au moyen des relations déjà connues [3].

Tableau 1

Constante de vitesse de l'hydrolyse alcaline
de l'acétate de n-butyle

X_{MEG}	$k \cdot 10^3$ $\mathrm{L \cdot mol^{-1}\,s^{-1}}$		
	30° C	40° C	50° C
0,096	84,94	115,78	213,70
0,147	46,03	73,80	120,00
0,206	34,67	57,40	92,53
0,278	25,43	44,10	72,44
0,369	18,35	30,20	53,99
0,483	11,83	20,08	37,67
0,638	6,26	11,71	19,20

Tableau 2

Constantes de vitesse de l'hydrolyse alcaline du propionate de n-butyle

X_{MEG}	$k \cdot 10^3$ L . mol^{-1} s^{-1}		
	30° C	40° C	50° C
0,096	57,09	94,95	147,90
0,147	34,85	59,22	95,91
0,206	24,85	40,53	72,44
0,278	17,00	29,96	52,40
0,369	10,76	19,48	34,42
0,483	6,04	12,67	22,12
0,638	3,25	6,99	11,41

Tableau 3

Constantes de vitesse de l'hydrolyse alcaline du butyrate de n-butyle

X_{MEG}	$k \cdot 10^3$ L mol^{-1} s^{-1}		
	30° C	40° C	50° C
0,096	—	—	—
0,147	19,19	34,07	62,00
0,206	11,78	23,44	41,27
0,278	7,83	14,87	27,69
0,369	5,96	10,94	21,67
0,483	3,50	6,98	13,49
0,638	2,24	4,53	8,91

Les valeurs de ces paramètres en fonction de la concentration du solvant mixte, exprimé en fraction molaire du constituant organique (X_{MEG}), sont réunies dans les tableaux 4–6.

Tableau 4

Fonctions thermodynamiques d'activation de l'hydrolyse alcaline de l'acetate de n-butyle

X_{MEG}	E $\frac{\text{kcal}}{\text{mol}}$	ΔH^* $\frac{\text{kcal}}{\text{mol}}$	$-\Delta S^*$ u.e.	ΔG^* $\frac{\text{kcal}}{\text{mol}}$
0,096	9,100	8,498	35,418	19,235
0,147	9,335	8,732	35,865	19,604
0,206	9,724	9,122	35,140	19,774
0,278	10,182	9,580	34,244	19,961
0,369	10,800	10,198	32,850	20,156
0,483	11,303	10,701	32,065	20,421
0,638	11,441	10,839	32,872	20,804

Tableau 5

Fonctions thermodynamiques d'activation de l'hydrolyse alcaline du propionate de n-butyle

X_{MEG}	$E\ \frac{kcal}{mol}$	$\Delta H^*\ \frac{kcal}{mol}$	$-\Delta S^*$ u.e.	$\Delta G^*\ \frac{kcal}{mol}$
0,096	9,257	8,655	35,689	19,474
0,147	9,806	9,204	34,858	19,771
0,206	10,430	9,828	33,471	19,974
0,278	10,472	10,370	32,435	20,202
0,369	11,281	10,679	32,325	20,478
0,483	11,955	11,353	31,248	20,825
0,638	12,236	11,634	31,552	21,198

Tableau 6

Fonctions thermodynamiques d'activation de l'hydrolyse alcaline du butyrate de n-butyle

X_{MEG}	$E\ \frac{kcal}{mol}$	$\Delta H^*\ \frac{kcal}{mol}$	$-\Delta S^*$ u.e.	$\Delta G^*\ \frac{kcal}{mol}$
0,096	—	—	—	—
0,147	11,494	10,892	30,472	20,129
0,206	12,180	11,578	29,178	20,421
0,278	12,303	11,701	29,584	20,669
0,369	12,590	11,988	29,178	20,833
0,483	13,005	12,403	28,867	21,154
0,638	13,447	12,045	28,293	21,422

On observe que les constantes de vitesse diminuent à mesure que la teneur en MEG du solvant augmente et diminuent de l'acétate au butyrate de n-butyle.

Pour les mêmes réactions dans les autres solvants eau—dioxanne (D), [8, 10] eau—acétone (Ac), [11] et eau—tetrahydrofuranne [12] ou constate une variation similaire. E, ΔH^*, ΔS^* et ΔG^*, des trois esters augmentent avec la teneur en MEG.

En représentant graphiquement la variation des fonctions thermodynamiques d'activation en fonction de X_{MEG} (figure 1) on constate que les courbes de l'enthalpie libre d'activation (ΔG^*) ont une allure croissante. On remarque que les enthalpies libres d'activation expriment la résultante des termes enthalpiques et entropiques compensés pour tous les trois esters. (Les courbes de ΔH^* en fonction de X_{MEG} se présentent comme l'image dans le miroir des courbes $-T\Delta S^*$ en fonction de X_{MEG}).

En tenant compte des relations (a) et (b), nous avons calculé la dispersion relative en pourcentages pour k (ε_k) pour le produit $k\ \eta$ ($\varepsilon_{k\eta}$) et pour le rapport $k/\eta(\varepsilon_{k/\eta})$. [13]

Le tableau 7 rassemble les valeurs de ces dispersions relatives en pourcentages.

On voit que les dispersions relatives $\varepsilon_{k/\eta}$ ont des valeurs plus petites que les dispersions relatives ε_k ou $\varepsilon_{k/\eta}$.

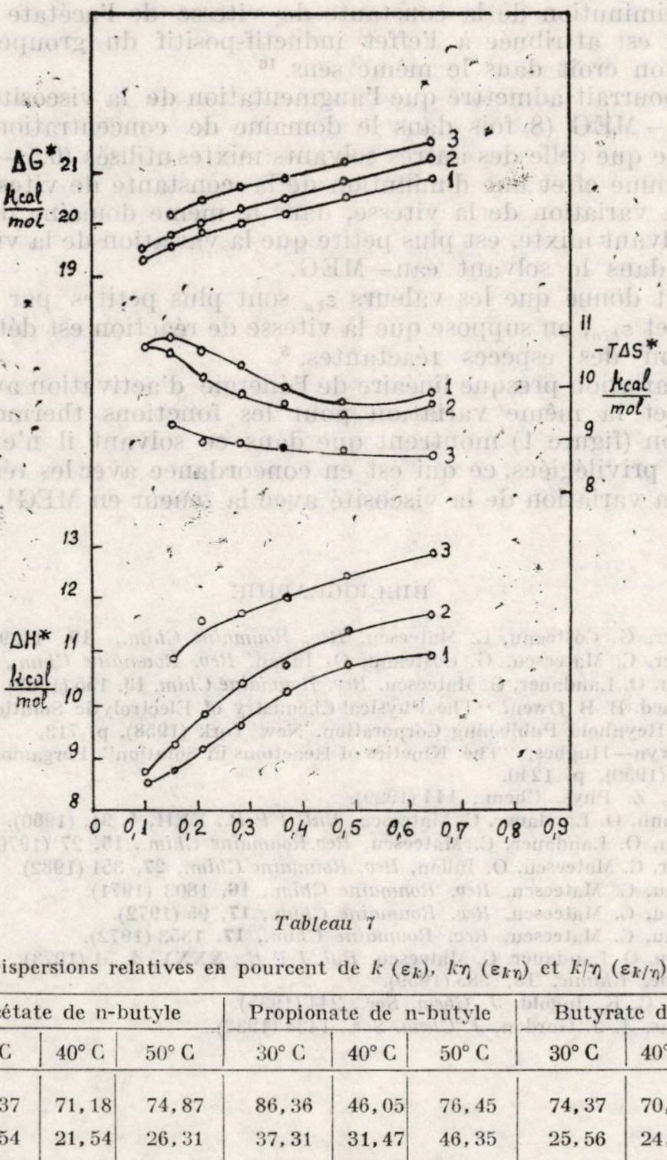

Tableau 7

Dispersions relatives en pourcent de k (ε_k), $k\eta$ ($\varepsilon_{k\eta}$) et k/η ($\varepsilon_{k/\eta}$)

Ester	Acétate de n-butyle			Propionate de n-butyle			Butyrate de n-butyle		
t° C	30° C	40° C	50° C	30° C	40° C	50° C	30° C	40° C	50° C
ε_k	82, 37	71, 18	74, 87	86, 36	46, 05	76, 45	74, 37	70, 56	67, 53
$\varepsilon_{k\eta}$	27, 54	21, 54	26, 31	37, 31	31, 47	46, 35	25, 56	24, 18	27, 60
$\varepsilon_{k/\eta}$	128, 84	415, 41	117, 81	127, 83	163, 91	114, 94	111, 23	286, 60	102, 19

CONCLUSIONS

La diminution des constantes de vitesse avec la teneur en MEG peut être attribuée à l'effet de la liaison des molecules d'eau par les molécules de MEG[14] et aussi à la diminution de la constante diélectrique qui diminue le pouvoir d'ionisation du milieu de réaction[15].

La diminution de la constante de vitesse de l'acétate au butyrate de n-butyl est attribuée à l'effet inductif-positif du groupement alkyle dont l'action croît dans le même sens.[16]

On pourrait admettre que l'augmentation de la viscosité du solvant mixte eau—MEG (8 fois dans le domaine de concentrations utilisées,[7] plus grande que celle des autres solvants mixtes utilisés (0,5 — 0,7 fois [2–4]) a aussi comme effet une diminution de la constante de vitesse. Pour ces solvants la variation de la vitesse, dans le même domaine de concentration du solvant mixte, est plus petite que la variation de la vitesse correspondante dans le solvant eau—MEG.

Étant donné que les valeurs ε_{kn} sont plus petites par rapport aux valeurs ε_k et $\varepsilon_{k/n}$, on suppose que la vitesse de réaction est déterminée par la diffusion des espèces réactantes.[5]

La variation presque linéaire de l'énergie d'activation avec la teneur en MEG et la même variation pour les fonctions thermodynamiques d'activation (figure 1) montrent que dans ce solvant il n'existe pas de structures privilégiées, ce qui est en concordance avec les résultats obtenus pour la variation de la viscosité avec la teneur en MEG[1].

BIBLIOGRAPHIE

[1] O. Landauer, G. Costeanu, C. Mateescu, *Rev. Roumaine Chim.*, **19**, 1429 (1974).
[2] O. Landauer, C. Mateescu, G. Costeanu, O. Iulian, *Rev. Roumaine Chim.*, **27**, 603 (1982).
[3] G. Costeanu, O. Landauer, C. Mateescu, *Rev. Roumaine Chim.* **13**, 155 (1968).
[4] H. S. Harned, B. B. Owen, "The Physical Chemistry of Electrolytic Solutions", IIIe Ed., Reynhold Publishing Corporation, New York (1958), p. 713.
[5] E. A. Moelwyn—Hughes, "The Kinetics of Reactions in Solution", Pergamon Press, Oxford (1950), p. 1240.
[6] A. Olander, Z. Phys. Chem., **144** (1929).
[7] V. Părăușeanu, O. Landauer, C. Mateescu, *Bul. I.P.B.*, **XXII**, **4**, 91, (1960).
[8] G. Costeanu, O. Landauer, C. Mateescu, *Rev.Roumaine Chim.*, **15**, 27 (1970).
[9] O. Landauer, C. Mateescu, O. Iulian, *Rev. Roumaine Chim.*, **27**, 351 (1982).
[10] G. Costeanu, C. Mateescu, *Rev. Roumaine Chim.*, **16**, 1803 (1971).
[11] G. Costeanu, C. Mateescu, *Rev. Roumaine Chim.*, **17**, 95 (1972).
[12] G. Costeanu, C. Mateescu, *Rev. Roumaine Chim.*, **17**, 1353 (1972).
[13] G. Costeanu, O. Landauer, C. Mateescu, *Bul. I.P.B.*, **XXXV**, **4**, 51 (1973).
[14] K. Schwabe, *Chimie*, **13**, 385 (1959).
[15] E. Hughes, C. K. Ingold, *J. Chem. Soc.*, 244 (1935).
[16] D. E. Evans, J. J. Gordon, *J. Chem. Soc.*, 1434 (1938).

Revue Roumaine de Chimie, **30**, *9–10*, 889–890 (1985)

COMPTES RENDUS

"Bio-Organic Heterocycles. Synthetic, Physical Organic and Pharmacological Aspects" (edited by H. C. van der Plas, L. Ötvös and M. Simonyi), Akadémiai Kiadó, Budapest (1984), and Elsevier (Amsterdam) "Studies in Organic Chemistry" vol. 18.

The proceedings of the Third FECHEM Conference on Heterocycles in Bio-Organic Chemistry, held in Balatonfüred (Hungary) on May 20–23, 1984, were published as a clothbound volume totalling 424 pages (the last 14 pages are author and subject indices).

The nine plenary lectures listed below are presented in full and followed by a transcription of the discussions. From the 45 poster presentations 35 are presented as four- to six-page papers, and one as full-length paper, namely "Oxidation of N-alkyl (aryl) pyridinium salts by free and immobilized rabbit liver aldehyde oxidase" by S.A.G.F. Angelino and H.C. van der Plas.

The nine plenary lecturers and the titles of their talks are : G. Snatzke: Circular dichroism and structure of heterocyclic compounds related to natural products ;

H.-P. Husson et al. ; Chiral heterocyclic synthons as intermediates for the synthesis of natural products ;

H. C. J. Ottenheijm : Uncommon amino acids in the synthesis and biosynthesis of natural products ;

P. Krogsgaard-Larsen : *Amanita Muscaria* in medicinal chemistry. Analogues of GABA and glutamic acid derived from muscimol and ibotenic acid ;

M. N. Preobrazhenskaya : Search for antitumor and antiviral compounds among analogues of nucleosides ;

G. Dénes : Chemical structure and biochemical transformation of pyrimidine derivatives ;

D. W. Young : Stereochemical aspecs of the interaction of heterocyclic substrates and drugs with enzymes ;

D. Gröger : Biosynthesis of anthranilic acid derived alkaloids ;

A. Gossauer : Chemistry of plant bile pigments.

All papers are reproduced directly from manuscripts with slight editing for corrections. The editors have supplied uniformly typed titles for all papers, and the discussions for the plenary lectures. This procedure ensured that no errors were introduced and that fast publication was possible.

The high quality of the main lectures consists in providing enough background for the practising organic chemist so as to be able to follow the stereochemical or biochemical details. Several plenary lectures are linked to the problem of new drugs, namely those of Preobrazhenskaya, Denes (formulas C, E and F on p. 131 would need comments to be intelligible), and especially Young) ; they provide a wealth of new information on the stereochemical and chemical interactions between enzymes and pyrimidines or purines, which help in drug design ; much hope is connected with anticancer or antiviral agents which would possess a low toxicity for normal cells. Other highly informative full papers are those by Snalzke and van der Plas.

Among the posters, representing the second half of the book, only a few can be highlighted in this review : new antiarrhythmic agents (14-membered tetraaza-macrocycles) by H. O. Hankovsky, K. Hideg et al.), new hypotensive and antihypertensive agents (Cs. Szantay and coworkers), 1,2,4-triazepines from chalcones (P. Richter and K. Steiner), compressional steric substituent effects in drug-receptor interactions (L. Ötvös).

The FECHEM conferences initiated by Dutch scientists on "Heterocycles in Bio-organic Chemistry" in 1980 represent an area of interest to organic chemists, biochemists, pharmacologists and research workers specializing in drug design. The book is excellently produced and the rich bibliography of each contribution provides further data for the interested reader.

A. T. Balaban

T. TOMINAGA, E. TACHIKAWA, "Modern Hot-Atom Chemistry and Its Applications" (Inorganic Chemistry Concepts, vol. 5), Springer-Verlag, Berlin, 1981, 154 pages (hard cover)

The chemistry of the hot-atoms was initiated fifty years ago by Szilard and Chalmers and its final goal is the elucidation of the mechanism of reactions involving highly excited chemical species (atoms with high kinetic energy or high electric charge). The hot-atom chemistry covers large research field, ranging from theoretical approaches to chemical dynamics or high energy reactions ; it deals with reactions of non-Boltzmann systems, being complementary to conventional chemical studies of systems in thermal equilibrium. This volume illustrates the essential aspects of modern hot-atom chemistry for non-specialists, with considerable emphasis on its applications in the related fields (biochemistry, nuclear medicine, energy-related research).

After a short introduction (Chap. 1), the 2nd chapter describes the main experimental techniques used for the production and analysis of hot chemical species, including some special physical techniques such as charge spectrometry and Mössbauer spectroscopy.

Chapter 3 presents, after a brief theoretical background, the characteristics of hot-atom reactions in gas, liquid and solid phases, with typical exemples (mechanisms and stereochemistry). At the beginning, there are presented the characteristics of monovalent hot-atoms (tritium, fluorine, chlorine, bromine and iodine) as well as those of other multivalent elements (carbon, silicon, sulphur, phosphorus and germanium) in gas phase. The other sections of the 3rd chapter are devoted to condensed phases hot-atom reactions, including solutions of organo-metallic compounds and transition-metal complexes.

The last chapter of the book (Chapter 4) presents various applications of hot-atom chemistry in inorganic, analytical, physical and geochemistry and other fields (nuclear medicine, biochemistry), the principal applications being the production of enriched radioisotopes and the synthesis of labelled compounds.

The special literature cited is not exhaustive but offers to the reader a good background in the field of the hot-atom chemistry. The book contains 57 figures and 34 tables.

Marius Andruh

A. T. SHONO, "Electroorganic Chemistry as a New Tool in Organic Synthesis" (Reactivity and Structure Concepts in Organic Chemistry, vol. 20), Springer-Verlag, Berlin — Heildelberg — New York, 1984, 171 pages, 128 DM (hard cover)

Volume 20 in the Springer Series "Reactivity and Structure Concepts in Organic Chemistry" proves that electroorganic chemistry is indeed useful in organic synthesis.

Since 22 reviews articles and 14 monographs describing electroorganic chemistry from a variety of standpoints have already been published and are cited in the Preface's References, the author attempted to present the material under an aspect which is different from these publications. In this book, electroorganic reactions are divided into two major types, namely oxidation and reduction. Oxidations are classified according to the structure of the substrate (aliphatic carbon—hydrogen and carbon—carbon single bonds, carbon—carbon double bonds, alcohols and derivatives, compounds containing sulphur, phosphorus and boron, organic halides, carbanions, aromatic systems), whereas reductions are classified by the type of reaction (addition, substitution, coupling, elimination, generation of active bases). References are given at the end of each chapter.

This monographs is mainly concerned with organic synthesis, so only few studies carried out from the viewpoint of electrochemical theoretical or analytical chemistry are mentioned.

Since electroorganic chemistry covers a great variety of reactions, the types of reactions described in this book are selected mainly with regards to their application in organic synthesis. Simple transformations of functional groups are only described in particular cases. Well-established processes such as Kolbe electrolysis, pinacolic coupling and hydrodimerisation are only briefly mentioned.

An appendix addresed to those chemists who are not familiar with electroorganic chemistry contains the outlines of operation of three types of reactions (constant current oxidation, controlled potential reduction and indirect oxidation using a mediator).

The book is a valuable source of up-to-date information and emphasized the original contribution of the Japanese school in the field of organic electrochemistry.

Mihaela Ungureanu

NOTE POUR LES AUTEURS

La Revue Roumaine de Chimie publie des articles en anglais, français, russe, allemand ou espagnol. Les auteurs sont priés d'envoyer des articles et des comptes rendus inédits.

Les manuscrits seront dactylographiés à double interligne. La bibliographie, les tableaux et la légende des figures seront placés après le texte.

Si l'article fait partie d'une série numérotée, la partie précédente sera donnée comme première référence.

Chaque article sera précédé d'un résumé comprenant quinze lignes au maximum.

Les références bibliographiques dans le texte seront faites par des exposants sans parenthèses et paraîtront à la fin de l'ouvrage.

Les publications périodiques mentionnées dans la bibliographie seront présentée suivant les prescriptions internationales : le nom de l'auteur précédé de l'initiale du prénom, le titre du périodique abrégé conformément à « Chemical Abstracts » et souligné par une ligne, le numéro du tome indiqué par des chiffres arabes et souligné par deux lignes, suivi de la première page de l'article ; à la fin, l'année de la parution sera placée entre parenthèses. Le numéro de la revue ne sera pas indiqué si les pages du volume sont numérotées consécutivement.

Les textes des livres ou traités inclueront : le nom des auteurs, l'initiale du prénom, le titre du livre entre guillemets et sans être souligué, le numéro du tome précédé par l'abréviation « vol. » (ou «Bd.«, le numéro de l'édition, les éditions (the publisher), la localité de la parution du livre, l'année de la parution et la page de la référence précédée(s) par l'abréviation «p. » (ou « S. »).

Les brevets seront indiqués comme suit : l'auteur ou la firme, le pays et le numéro du brevet, la date et la revue *(Chem. Abstr.)*. Par. ex. : M. Jones (to Union Carbide Co), Brit. Pat. 601 238, 2 Sept. 1959 ; cf. *Chem. Abstr.*, **54**, 12808 (1960).

Si la référence n'a pas été lue en original, on indiquera aussi la revue de référence consultée.

Les diagrammes seront tracés à l'encre de Chine sur papier calque. Les tableaux et les figures (en nombre strictement nécessaire) ainsi que les courbes dans les figures seront numérotés par des chiffres arabes. Leur explication sera donnée dans la légende des figures. Prière de ne pas inscrire les mêmes données dans les tableaux et les figures. Chaque tableau aura un titre. On indiquera dans le texte la place approximative des tableaux et des figures. Les formules chimiques seront incluses dans le texte ; en outre, elles seront transcrites sur papier calque, à l'encre de Chine.

Les auteurs sont priés d'indiquer les caractères italiques (en soulignant les lettres au crayon), ainsi que tout autre caractère spécial ; les préfixes *ortho*, *meta*, *para*, *cir*, *trans*, etc. seront soulignés pour indiquer leurs caractères italiques et ne seront jamais écrits avec des majuscules.

Aucune correction à la main ne sera admise sur le manuscrit. Les corrections seront tapées à la machine. Les lettres grecques ou d'autres symboles spéciaux seront insérés à la main à l'encre clairement.

Le manuscrit sera signé par l'auteur.

Le titre-courant aura 50 lettres au maximum.

L'entière responsabilité du contenu des articles appartient aux auteurs.

Sur demande on peut obtenir une note plus complète.

PRINTED IN ROMANIA

ORSZÁGOS MŰSZAKI INFORM
1983

66

TRAVAUX PARUS AUX ÉDITIONS DE L'ACADÉMIE DE LA RÉPUBLIQUE SOCIALISTE DE ROUMANIE

V. Em. SAHINI, M. HILLEBRAND, **Chimia cuantică în exemple şi aplicaţii**, 1985, 380 p.

N. PETRESCU, **Chimia extracţiei cu solvenţi şi aplicaţii**, 1985, 212 p.

V. DRĂGUŢAN, A. T. BALABAN, M. DIMONIE, **Olefin metathesis and ring-opening polymerization of cyclo-olefins**, coédition avec John Wiley & Sons, 1985, 544 p.

GH. MARCU, **Chimia compuşilor coordinativi**, 1984, 415 p.

E. CORDOŞ, C. MANOLIU, **Spectrometria de absorbţie şi fluorescenţă atomică**, 1984, 178 p.

C. BODEA, **Tratat de biochimie vegetală**, p. II, vol. 5, 1984, 438 p.

ELENA CEAUŞESCU, **Cercetări în chimia şi tehnologia polimerilor**, 1983, 519 p.

N. ASANDEI, A. GRIGORIU, **Chimia şi structura fibrelor**, 1983, 395 p.

N. IONESCU, M. CĂLDĂRARU, **Oxidarea catalitică a olefinelor inferioare**, 1983.

C. CAŞCAVAL, **Studiul polimerilor prin piroliză şi cromatografie de gaze**, 1983, 220 p.

C. I. SIMIONESCU, F. DANEŞ, **Originea vieţii**, 1983, 110 p.

C. BODEA, (editeur), **Tratat de biochimie vegetală**, II, Vol. IV, 1982, 408 p.

I. G. MURGULESCU, RODICA VÎLCU, **Introducere în chimia fizică, Vol. III. Termodinamica chimică**, 1982, 624 p.

I. G. MURGULESCU, J. PĂUN, **Introducere în chimia fizică, Vol. I.3. Nucleul atomic, reacţii nucleare, particule elementare**, 1982, 606 p.

ELENA JERCAN, **Analiza cromatografică**, 1982, 286 p.

ELENA CEAUŞESCU, **Noi cercetări în domeniul compuşilor macromoleculari**, 1981, 536 p.

I. G. MURGULESCU, TATIANA ONCESCU, E. SEGAL, **Introducere în chimia fizică. Vol. II, 2. Cinematică chimică şi cataliză**, 1981, 1024 p.

V. DRĂGUŢAN, A. T. BALABAN, M. DIMONIE, **Metateza olefinelor şi polimerizarea prin deschidere de inel a cicloolefinelor**, 1981, 254 p.

LIDIA-MARIA VAICUM, **Epurarea apelor uzate cu nămol activ. Bazele biochimice**, 1981, 218 p.

I. GĂLĂŢEANU, **Procese şi metode radiochimice în energia nucleară**, 1981, 234 p.

O. IORDACHE, **Procese polistocastice la fenomenele de transfer**, 1981, 186 p.

CR. SIMIONESCU, VALERIA GORDUZA, **Polimeri biocompatibili şi biologic activi**, 1980, 479 p.

ELENA CEAUŞESCU, **Polimerizarea stereospecifică a izoprenului**, 1979, 307 p.

CONST. GH. MACAROVICI, **Analiza chimică cantitativă anorganică**, 1979, 457 p.

M. FLORESCU, **Metode ştiinţifice în dezvoltarea industriei chimice moderne**, 1979, 256 p.

A. T. BALABAN, I. GĂLĂŢEANU, G. GEORGESCU, LIGIA SIMIONESCU, **Compuşi marcaţi şi radiofarmaceutici cu aplicaţii în medicina nucleară**, 1979, 495 p.

I. G. MURGULESCU, E. SEGAL, **Introducere în chimia fizică. Vol. II. 1. Teoria molecular cinetică a materiei**, 1979, 1036 p.

S. STERNBERG, FL. DANEŞ, **Termodinamica chimică aplicată**, 1978, 400 p.

I. G. MURGULESCU, V. EM. SAHINI, **Introducere în chimia fizică, Vol. 1.2. Structura şi proprietăţile moleculelor**, 1978, 604 p.

I. ZUGRĂVESCU, MAGDA PETROVANU, **N-ylid chemistry**, coédition avec McGraw-Hill, International Book Company, U.S.A., 1977, 396 p.

I. G. MURGULESCU, **Introducere în chimia fizică. Vol. I.1. Atomi, molecule, legătură chimică**, 1976, 560 p.

ELENA CEAUŞESCU, **Research work on synthesis and characterization of macromolecular compounds. Contributions**, 1974, 251 p.

CR. SIMIONESCU, VIORICA RUSAN, V. POPA, **Chimia algelor marine**, 1974, 212 p., 1 pl.

ISSN 0035–4090

I. P. Informaţia c. 1345

43 426

Lei 40

$ 80 (pour un abonnement annuel)

~~66~~ F 1103 04

ACADÉMIE DE LA RÉPUBLIQUE SOCIALISTE DE ROUMANIE

REVUE ROUMAINE DE CHIMIE

~~R~~ 1985 DEC 4

MG

TOME 30

N°s 11–12

Novembre–Décembre 1985

EDITURA ACADEMIEI REPUBLICII SOCIALISTE ROMÂNIA

Rev. Roumaine Chim. RRCHAX, 30, *11–12*, p. 891–1078 (1985), Bucarest

ACADÉMIE DE LA RÉPUBLIQUE SOCIALISTE DE ROUMANIE

COMITÉ DE RÉDACTION

Rédacteur en chef:

I. G. MURGULESCU, membre de l'Académie de la République Socialiste de Roumanie

Rédacteurs en chef adjoints:

A. T. BALABAN et V. EM. SAHINI, membres correspondants de l'Académie de la République Socialiste de Roumanie

Collège de rédaction:

EM. BRATU, ELENA CEAUȘESCU, ECATERINA CIORĂNESCU-NENITZESCU, CR. SIMIONESCU, membres de l'Académie de la République Socialiste de Roumanie; P. SPACU, membre correspondant de l'Académie de la République Socialiste de Roumanie: M. BANCIU, M. D. GHEORGHIU, I. HAIDUC, D. I. MARCHIDAN, I. MOLDOVAN ,G. NIAC et D. SĂNDULESCU

La Revue Roumaine de Chimie paraît 10 fois par an. Toute commande de l'étranger sera adressée à ROMPRESFILATELIA — sectorul Export-Import, Presă, P.O. Box 12—201, télex 10376 prsfi r Bucarest, Calea Griviței nr. 64—66, Roumanie.

Les manuscrits, les livres et les revues proposés en échange, ainsi que toute correspondance seront envoyés à la rédaction.

REVUE ROUMAINE DE CHIMIE

125, Calea Victoriei, 79717 Bucarest, Roumanie, téléphone 50 76 80

EDITURA ACADEMIEI REPUBLICII SOCIALISTE ROMÂNIA
125, Calea Victoriei, 79717 Bucarest Roumanie, téléphone 50 76 80

1883

REVUE ROUMAINE DE CHIMIE

Tome 30, N°s 11–12 **Novembre–Décembre, 1985**

RODICA VÎLCU and ŞT. PERIŞANU, The latent heat of vaporization of carboxylic acids 893-902
J. L. CABEZAS, J. C. ARRANZ and J. BERRUETA, Binary vapor–liquid equilibria of benzene-alcohol systems 903-908
M. OLTEANU and STEFANIA ZUCA, Electrical conductivity and density of molten LiI – (Na, K, Rb, Cs)I binary systems 909-916
G. LÓPEZ CUETO and A. ALONSO MATEOS, Coulometric study at controlled potential of the anodic oxidation of the binuclear cyanide complex of Mn(III). I. Oxidation at + 0.2 volts (vs. S.C.E.) : kinetic current and parallel reaction (in Spanish) 917-931
VALENTINA LĂZĂRESCU, M. VASS, O. RADOVICI, CORNELIA DAŞOVEANU, MAGDALENA STANCIU and M. TOLAN, Electrochemical investigation of the oxygen interaction with silver catalysts 933-939
U. G. KRISHNAM RAJU, B. SETHURAM and T. NAVANEETH RAO, Conductometric study of ion-ion and ion-solvent interactions. II. Conductances of trichloroacetic acid in methanol-water mixtures at 25°C 941-947
N. DOCA and E. SEGAL, Dehydrogenation kinetics of lower aliphatic alcohols on copper catalysts. I. Preparation, stabilization and catalytic activity of pure copper powders 649-953
S. STERNBERG, V. BRÂNZOI, A. MATEESCU and L. APĂTEANU, The influence of the Co(II) ions on the $PbSO_4/PbO_2$ electrode in sulphuric acid solutions 955-961
MELANIA BOZEŞANU and N. I. IONESCU, Selfinhibition of the homogeneous pyrolysis of n-heptane 963-967
IOSIF SCHIKETANZ, ANA SCHIKETANZ, MIRCEA D. GHEORGHIU, MIHAI PASCU, AURELIA VASILE and ALEXANDRU T. BALABAN, Aminoketone and oxazole synthesis. VIII. Acylaminoacylations using azlactones of fluoro-substituted hippuric acids and 2,5-diaryloxazoles derived therefrom 969-975
ALEXANDRU T. BALABAN, IOSIF SCHIKETANZ, MIRCEA D. GHEORGHIU and ANA SCHIKETANZ, Aminoketone and oxazole synthesis. IX. 2,2 -(*p*-Phenylene)-bis-(5-aryloxazoles) and 2,2′-(1,4-naphthalenediyl)-bis-(5-aryloxazoles) *via* acylaminoacylation of aromatic hydrocarbons 977-984
Z. SIMON, A. T. BALABAN, D. CIUBOTARIU and T. S. BALABAN, QSAR for carcinogenesis by polycyclic aromatic hydrocarbons and derivatives in terms of delocalization energy, minimal sterical differences and topological indices 985-1000
RODICA VLAD and M. BANCIU, Synthesis of dibenzobullvalene *via* BAMFORD-STEVENS reaction 1001-1004
IULIANA TĂMĂŞAN, OVIDIU MAIOR and TEODOR-SILVIU BALABAN, *O*-substituted aromatic aldoximes of 1-methyl-2-aminooxymethyl-5-nitroimidazole. Synthesis and ^1H–NMR spectra 1005-1013
. S. BOULOS and A. EL KATEB, The reaction of fluorenylidenetriphenyl-phosphoranes and -arsinane with certain dicarbonyl compounds 1015-1017
GH. MIHĂILĂ, C. LUCA, DOINA DRANGA and N. BÎLBĂ, Study of cyclopentene hydration 1019-1024

Rev. Roumaine Chim. | **30,** *11–12,* 891–1078 (1985), **Bucarest**

RODICA VĂŢULESCU, T. BUDIU, GH. MARCU and IRINA PAL, Heteropolytungstates with Ti(IV) and Ni(II). V. The thermal behaviour of sodium and potassium salt of the Ni(II)-pentatungstotitanate(IV) anion. 1025-1030
I. BERDAN, D. ANCUŢA and I. SANDU Complex compounds of Tl(III) with n-donor ligands. Study on the system Tl(III)-2,2-azopyridine (in French) 1031-1037
A. CĂLUŞARU, Structural studies on the aquo-ammino-di-2-mercapto-benzothiazole cobalt complex 1039-1045
LUMINIŢA VLĂDESCU and STELUŢA CHIPER, Combined ion exchange — spectrometric study of the Ce(IV) — Sulphanilic acid system. I. Ion exchange method for eliminating interference in the spectrometric determination of cerium(IV). 1047-1051
ROMANO CIUPE, SZANTO CSABA and STELUŢA BUGNARIU, Simultaneous determination of atmospheric n-hexane, toluene and acetone with activated charcoal tubes using the two-step thermal gas extraction procedure 1053-1058

BOOK REVIEWS 1059-1060
AUTHOR INDEX 1061-1072
SUBJECT INDEX 1073-1078

Revue Roumaine de Chimie, **30**, *11–12*, 893–902 (1985)

THE LATENT HEAT OF VAPORIZATION OF CARBOXYLIC ACIDS

RODICA VÎLCU and ȘT. PERIȘANU

Polytechnic Institute of Bucharest, Department of Physical Chemistry,
13 Blvd Republicii, Bucharest, Romania

Received November 5, 1984

A thermodynamic study of the latent heat of vaporization of compounds associated in the vapour phase, was carried out, by expressing that quantity in two ways :
a) by means of monomeric heat of vaporization, heat of dimerization and equilibrium constant of dimerization ;
b) by means of the slope $\frac{\mathrm{d}\ln p_v}{\mathrm{d}T}$ and the degree of dimerization.

The heats of vaporization calculated by the above mentioned methods for formic and acetic acids were in satisfactory agreement with the experimental ones.
There was some evidence that the latent heat of vaporization of carboxylic acids passes not only through a maximum situated slightly beyond the boiling point (as specified in the literature) but also through a minimum situated about 20 degrees above the triple point.

1. INTRODUCTION

The behaviour of some physico-chemical properties of carboxylic acids is peculiar.[1–3] This is due primarily to the association of their vapour to cyclic and linear oligomers, a process which is both pressure and temperature dependent.

Prediction of the properties of these compounds is complicated, because estimation procedures based on corresponding state theory can hardly be applied, only by consideration of an additional correlation parameter.[4]

The association equilibria of formic, acetic and propionic acids (of NO_2 as well) were investigated in most cases by $P-V-T$ measurements. The data obtained by this method by different authors are quite divergent (see tables 1 and 2) probably because volume is strongly dependent on the nonideal behaviour of the gaseous mixture of monomer and oligomers.

A very accurate study of the association in acetic acid vapour was done by Weltner, [3] by using calorimetric and spectroscopic values of heat capacity. The corresponding values may be different by an order of magnitude. Isobaric vapour heat capacity of carboxylic acids goes through a maximum for a temperature which is pressure dependent.

Table 1

Dimerization equilibrium constants $K_{p\mathrm{dim}}(\mathrm{mm}^{-1})$ of formic acid

Authors / T(K)	B.H.[5]	T.B.[6]	W.[7]	A.G.[2]
298.2	0.3704	0.3942	0.4163	0.44
315.3	0.1038	0.1084	0.1143	0.1190
337.6	0.02344	0.02450	0.02571	0.02622
373.8	$3.227.10^{-3}$	$3.197.10^{-3}$	$3.311.10^{-3}$	$3.396.10^{-3}$

Table 2

Dimerization equilibrium constants $K_{p\mathrm{dim}} \cdot 10^2$ (mm^{-1}) of acetic acid

Authors / T (°C)	R.S.[8]	B.H.[5]	J.N.[9]	T[10]	A.G.[2]	W.[3]
80	3.26	3.59	2.73	3.51	3.95	3.16
90	1.84	2.01	1.59	1.92	2.43	1.79
100	1.10	1.16	0.952	1.09	1.50	0.999
110	0.659	0.692	0.586	0.621	0.87	0.588
120	0.397	0.423	0.369	0.381	0.620	0.356

2. LATENT HEAT OF VAPORIZATION OF CARBOXYLIC ACIDS

Another thermodynamic property which enjoys an abnormal temperature dependence is the latent heat of vaporization. This is considered to go through a maximum at a temperature slightly beyond the normal boiling point, while for most compounds the latent heat of vaporization continually decreases with temperature.[1]

The latent heat of vaporization of a vapour phase associated compound may be written as a sum between a term corresponding to the physical vaporization (with preservation of the molecular state of the liquid phase) and another, corresponding to the dimerization process :

$$L = L_1 + \frac{\beta^g}{2}\Delta H_{\mathrm{dim}} \tag{1}$$

if the liquid phase is considered to consist only of monomers.

The derivative $\frac{\mathrm{d}L}{\mathrm{d}T}$ may be written in the form :

$$\frac{\mathrm{d}L}{\mathrm{d}T} = C^g_{p1} - C^l_p + \frac{\beta^g}{2}\Delta C_{p\,\mathrm{dim}} + \frac{\Delta H_{\mathrm{dim}}}{2}\left(\frac{\mathrm{d}\beta^g}{\mathrm{d}T}\right)_{\mathrm{sat}} \tag{2}$$

Replacing :

$$C^g_{p1} - C^l_p + \frac{\beta^g}{2}\Delta C_{p\,\mathrm{dim}} = \Delta C_{pf} \tag{3}$$

and

$$\left(\frac{\mathrm{d}\beta^g}{\mathrm{d}T}\right)_{\mathrm{sat}} = \beta^g(1-\beta^g)\,\frac{L_1+\Delta H_{\mathrm{dim}}}{RT^2} \tag{4}$$

one obtains:

$$\frac{\mathrm{d}L}{\mathrm{d}T} = \Delta C_{pf} + \beta^g(1-\beta^g)\,\frac{L_1+\Delta H_{\mathrm{dim}}}{RT^2}\cdot\frac{\Delta H_{\mathrm{dim}}}{2} \tag{5}$$

By neglecting the temperature dependence of C_{pf}, the following expression of $\frac{\mathrm{d}^2L}{\mathrm{d}T^2}$ is obtained:

$$\frac{\mathrm{d}^2L}{\mathrm{d}T^2} = \frac{\beta^g(1-\beta^g)(\Delta H_{\mathrm{dim}}+L_1)\,\Delta H_{\mathrm{dim}}}{2RT^4}\left[\frac{\Delta H_{\mathrm{dim}}+L_1}{R}(1-2\beta^g) + \right.$$

$$\left. + \frac{\Delta C_{p\,\mathrm{dim}}+C^g_{p1}-C^l_p}{\Delta H_{\mathrm{dim}}+L_1}T^2 + \frac{\Delta C_{p\,\mathrm{dim}}}{\Delta H_{\mathrm{dim}}}T^2 - 2T\right] \tag{6}$$

The conclusion is drawn, that the dependence $L = f(T)$ passes through an inflexion point, which takes place in the case of acetic acid for $\beta \simeq 0.76$ (but not $\beta \simeq 0.5$ as considered by Armitage and Gray [2]).

Two extremum points should exist, which are situated for the acetic acid as follows: a minimum for $\beta \simeq 0.83$ ($T \simeq 340$ K) and a maximum in the range $\beta = 0.65-0.70$ ($T \simeq 400$ K) (Fig. 1). A similar situation is observed for the formic acid (Fig. 2).

But in the liquid carboxylic acids there is a certain amount of associated forms, so that equation (1) is rewritten in the form:

$$L = L_1 + \frac{(\beta^g - \beta^l)\,\Delta H_{\mathrm{dim}}}{2} \tag{7}$$

The quantities of eq. (7) may be expressed by means of the following relations:

$$L_1(T) = L_1(298)\left(\frac{1-T/T_c}{1-298.2/T_c}\right)^{0.38} \text{(Watson's correlation)} \tag{8}$$

$$\beta^g = 1 - \frac{1}{\sqrt{4K_{x\,\mathrm{dim}}+1}} \tag{9}$$

$$K_{x\,\mathrm{dim}} = \frac{K_{f\,\mathrm{dim}}}{K_{\gamma\,\mathrm{dim}}}\,p \tag{10}$$

$$\Delta H_{\mathrm{dim}} = \Delta H^0_{\mathrm{dim}} + aT + \frac{bT^2}{2} \tag{11}$$

$$K_{f\,\mathrm{dim}} = \exp\left(-\frac{\Delta H^0_{\mathrm{dim}}}{RT} + \frac{a\cdot\ln T}{R} + \frac{bT}{2} + I\right) \tag{12}$$

Equation (7) becomes:

$$L = L_1(298)\left(\frac{1 - T/T_c}{1\,298.2/T_c}\right)^{0.38} + \frac{1}{2}\left(\Delta H^0_{\mathrm{dim}} + aT + \right.$$
$$\left. + \frac{bT^2}{2}\right)\left(1 - \frac{1}{\sqrt{1 + 4K_{f\,\mathrm{dim}} \cdot p/K_{\gamma\,\mathrm{dim}}}} - \beta^1\right) \tag{13}$$

with $K_{f\,\mathrm{dim}}$ given by eq. (12).

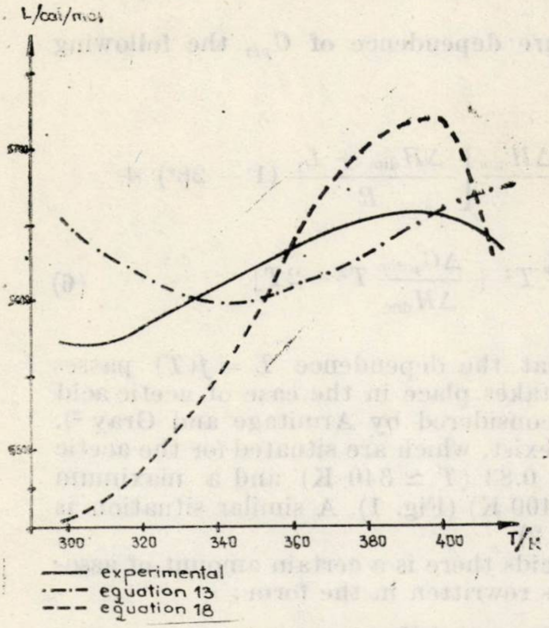

Fig. 1. — Latent heats of vaporization of acetic acid.

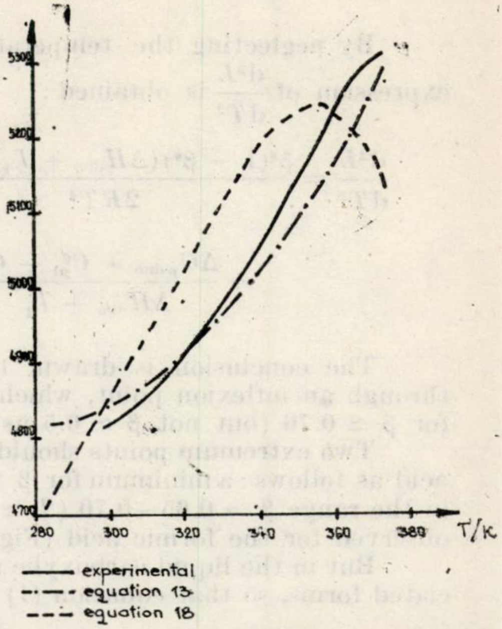

Fig. 2. — Latent heats of vaporization of formic acid.

Knowing some values of the latent heat of vaporization, at different temperatures, $L_1(298)$, $\Delta H^0_{\mathrm{dim}}$, a, b, I and β^l were obtained by an optimization procedure for the formic and acetic acids.

The following approximations were made: K_γ was taken equal with the reciprocal of the activity coefficient of a compound with the same critical temperature as the acid and $Z_c = 0.23$. The values of the above mentioned parameters are given in table 3.

Table 3

Parameters of equation (13)

Acid	formic	acetic
T_c(K)	579.6(est)	594.3
$L_1(298)$ (cal/mol)	11260	12510
$\Delta H^0_{\mathrm{dim}}$(cal/mol)	−15902	−16611
a(cal/mol.K)	−3.2	3.52
b(cal/mol · K^2)	0	$1.510 \cdot {}^{-3}$
I	−16.024	−16.360
β^l	0.02	0.02

3. VAPOUR PRESSURES OF CARBOXYLIC ACIDS

Although continually increasing, the temperature dependence of the vapour pressure of carboxylic acids is different from that of nonassociated compounds. For the latter, the dependence $\log p_v = f(1/T)$ is a curve with the concavity downwards, because of the continual decreasing of the vaporization heat with temperature.

For associated compounds:

$$\frac{\mathrm{d}\ln p_v}{\mathrm{d}T} = \frac{2L}{\Delta Z_v R T^2 (2 - \beta^g)} \tag{14}$$

and

$$\frac{\mathrm{d}\ln p_v}{\mathrm{d}(1/T)} = \frac{2L}{R \Delta Z_v (2 - \beta^g)} \tag{14'}$$

so that:

$$\frac{\mathrm{d}^2 \ln p_v}{\mathrm{d}(1/T)\mathrm{d}T} = -\frac{2}{R\Delta Z_v} \cdot \frac{[\Delta C_{pf} + \beta^g(1-\beta^g)]\dfrac{L_1 + \Delta H_{\mathrm{dim}}}{RT^2} \cdot \dfrac{\Delta H_{\mathrm{dim}}}{2}(2-\beta^g) + \left(L_1 + \dfrac{\beta^g \Delta H_{\mathrm{dim}}}{2}\right)\dfrac{\mathrm{d}\beta^g}{\mathrm{d}T}}{(2-\beta^g)^2} \tag{15}$$

Replacing $\frac{\mathrm{d}\beta^g}{\mathrm{d}T}$ from eq. (4) and rearranging, the following expresion is obtained:

$$\frac{\mathrm{d}^2 \ln p_v}{\mathrm{d}(1/T)\mathrm{d}T} = -\frac{2\Delta C_{pf}}{R\Delta Z_v (2-\beta^g)} - \frac{2\beta^g(1-\beta^g)}{\Delta Z_v}\left[\frac{(L_1 + \Delta H_{\mathrm{dim}})}{RT(2-\beta^g)}\right]^2 \tag{16}$$

In the domain of subatmospheric pressures, the dependence $\ln p_v = f(1/T)$ is nearly linear, especially for the formic acid, where the constant C of the Antoine equation[11]:

$$\ln p_v = A - \frac{B}{T + C} \tag{17}$$

is only 0.5. This fact is due to the reciprocal compensation of the two terms in equation (16).

For expressing the temperature dependence of the vapour pressure of carboxylic acids, the following empirical equation was used:

$$\lg p_v = A + B/T + C \lg T + DT + ET^2 \tag{18}$$

Values of the parameters of eq. (18) for formic and acetic acids are given in table 4. In tables 5 and 6, calculated vapour pressures are compared with experimental ones.

Table 4

Coefficients of equation (18)

Acid	formic	acetic
A	758.761	479.436
B	−16471	−12578
C	−331.320	−201.786
D	0.47245	0.24726
E	-2.58010^{-4}	-1.17810^{-4}

Changes of the curvature of the dependence $\ln p_v = f(1/T)$ are observed for the formic acid at 291.2 and 319.2 K. For the acetic acid, the same graphical representation is concave downwards on the whole temperature range under study.

Equation (14′) was used to calculate the latent heat of vaporization from vapour pressures. No minimum was observed at low temperatures for the vapour pressure calculated heats of vaporization of the two acids.

4. CONCLUSIONS

Tables 7—10 show the calculated latent heats of vaporization obtained, by means of an optimization procedure, with eq. (13) and eq. (14′) respectively. In figure 1 and 2, the temperature dependence of the experimental and calculated heats of vaporization is represented. Some conclusions may be drawn from the examination of the above mentioned tables and figures.

— The agreement between the three kinds of values for the heats of vaporization is generally better than 2%.

— The discrepancies are greater for the formic acid, probably because of the less accurate experimental data.

— The poor agreement for the formic acid in the region of the boiling point is due to its partial decomposition.

— Great discrepancies are observed in the range of low temperatures (less than 20—30 degrees above the triple point). It is supposed that Watson equation (8) is not very accurate in these circumstances. On the other hand, the experimental errors are considerable at low vapour pressures.

For the standard enthalpies of vaporization $\Delta H_v^0(298) = L_1(298)$, the following values are recommended : 11250 cal/mol for formic acid and 12450 cal/mol for acetic acid. Cox and Pilcher[14] recommended 11030 and 12500 cal/mol respectively.

Observation. The degree of dimerization in the liquid phase was considered independent of temperature. It was considered that this approximation does not introduce considerable error, the degree of dimerization in the liquid phase being much smaller than in the vapour phase. For the same reason, its omission in equations 1—6 does not alter qualitatively the conclusions drawn from them.

Table 5

Experimental and calculated (eq. 18) vapour pressures of formic acid*

T(K)	lg $p_{v\,\mathrm{exp}}$	lg $p_{v\,\mathrm{calc}}$	10^3(lg $p_{v\,\mathrm{exp}}$ − lg $p_{v\,\mathrm{calc}}$
283.2	1.27646	1.27989	− 3.43
293.2	1.51983	1.50793	11.90
297.2	1.60206	1.59303	9.03
303.2	1.71767	1.71918	− 1.51
313.2	1.91698	1.91954	− 2.56
317.0	2.0	1.99129	8.71
323.2	2.10003	2.10676	− 6.73
333.2	2.27807	2.28386	− 5.79
343.2	2.44654	2.44614	0.40
353.2	2.60	2.60116	− 1.16
353.5	2.60206	2.60518	− 3.12
363.2	2.74202	2.74240	− 0.38
373.2	2.87703	2.87588	1.15
373.8	2.88081	2.88264	− 1.83

Mean square deviation = $\pm\, 5.44 \cdot 10^{-3}$

* Experimental values from references 12 and 13

Table 6

Experimental and calculated (eq. 18) vapour pressures of acetic acid*

T/(K)	lg $p_{v\,\mathrm{exp}}$	lg $p_{v\,\mathrm{calc}}$	(lg $p_{v\,\mathrm{exp}}$ − lg $p_{v\,\mathrm{calc}}$) · 10^3
290.7	1.00	1.00243	−1.43
293.2	1.06819	1.06711	1.08
303.2	1.31387	1.31297	0.90
313.2	1.54160	1.54029	1.31
316.2	1.60206	1.60525	−2.19
323.2	1.75282	1.75148	1.34
333.2	1.94890	1.94846	0.44
336	2.00	2.00129	−1.29
343.2	2.13354	2.13278	0.76
345.5	2.17609	2.17552	2.57
353.2	2.30600	2.30570	0.30
358.7	2.39794	2.39630	1.64
363.2	2.46790	2.46820	−0.30
368.3	2.54407	2.54731	−3.24
372.2	2.60206	2.60616	−4.10
373.2	2.62024	2.62104	−0.80
378.6	2.69897	2.69978	−0.81
383.2	2.76403	2.76483	−0.80
391.3	2.88081	2.87499	5.82
393.2	2.89982	2.90511	−5.29
403.2	3.02841	3.02696	1.45
413.2	3.15045	3.14585	4.60
416.7	3.18184	3.18559	−3.75

Mean square deviation = $\pm\, 2.61 \cdot 10^{-3}$

* Experimental values from references 12 and 13

Table 7

Data for calculation of the heat of vaporization of the formic acid by means of eq. (13)

Line	T(K)	283.2	298.2	315.3	337.6	353.5	373.8
1	p(mm Hg)	19.5	41.1	91.3	227.5	402.9	763.5
2	$K\gamma_{\mathrm{dim}}$	0.998	0.997	0.993	0.986	0.978	0.965
3	$-\Delta H_{\mathrm{dim}}$ (cal/mol)	14996	14948	14893	14822	14771	14706
4	$K_{f\,\mathrm{dim}}$ (mm^{-1})	1.5644	0.4104	0.1047	$2.188 \cdot 10^{-2}$	$8.113 \cdot 10^{-3}$	$2.569 \cdot 10^{-3}$
5	β^{g}	0.9098	0.8790	0.8398	0.7799	0.7307	0.6602
6	L_{calc} (cal/mol)	4183	4885	4890	5002	5113	5287
7	L_{exp} (cal/mol)*	4810	4840	5035	5035		5310

* Data from references 7,16.

Table 8

Data for calculation of the heat of vaporization of the acetic acid by means of eq. (13)

Line	T/K	298.2	333.2	358.6	379	391.3	413.2
1	p(mm Hg)	15.6	89.1	248.6	508.1	750.7	1401
2	$K\gamma_{\mathrm{dim}}$	0.998	0.988	0.978	0.963	0.949	0.938
3	$-\Delta H_{\mathrm{dim}}$ (cal/mol)	15495	15355	15252	15169	15119	15028
4	$K_{f\,\mathrm{dim}}$(mm^{-1})	1.755	0.114	$2.217 \cdot 10^{-2}$	$7.027 \cdot 10^{-3}$	$3.735 \cdot 10^{-3}$	$1.337 \cdot 10^{-3}$
5	β^{g}	0.9048	0.8441	0.7894	0.7397	0.7069	0.6471
6	L_{calc} (cal/mol)	5655	5601	5607	5628	5650	5672
7	L_{exp}(cal/mol)*	5583		5629	5654	5663	
		(5569)		(5597)	(5648)	(5656)	(5622)

* Data from references 3, 15, 16.

Table 9

Vapour pressure calculated heats of vaporization of formic acid

T(K)	$RT^2 \dfrac{\mathrm{d} \ln p_v}{\mathrm{d}T}$	L_{calc} (cal/mol)	L_{exp} (cal/mol)^{7,16}
383.2	8662	4712	
298.2	8658	4829	4810
315.3	8678	4984	4890
337.6	8631	5171	5036
353.5	8468	5241	
373.8	7999	5133	5310

Table 10

Vapour pressure calculated heats of vaporization of acetic acid

$T(K)$	$RT^2 \dfrac{\mathrm{d} \ln}{\mathrm{d}T} p_v$	L_{calc} (cal/mol)	L_{exp} (cal/mol) ^{3,16}
298.2	10000	5454	5583
333.2	9775	5525	
338.6	9537	5634	5629
379	9405	5701	5654
391.3	9291	5719	5663
413.2	8980	5632	(5622)

SYMBOLS

A—E	**coefficients in equations for vapour pressures**
C	**molar heat capacity**
H	**enthalpy**
I	integration constant in the equation of equilibrium constant (12)
K	equilibrium constant
L	latent heat of vaporization
R	universal constant of ideal gases, $R = 1.987$ cal/mol · K
T	absolute temperature
Z	compresibility factor
a, b	coefficients in the equation for the heat of dimerization (11)
p	pressure
β	degree of dimerization
Δ	finite difference (molar difference for extensive parameters)

Subscripts

c	critical
dim	dimerization
f	fugacity
p	pressure
v	vapour, vaporization
x	mole fraction
1	monomeric
γ	activity (fugacity) coefficient

Superscripts

g	gas (vapour)
l	liquid
0	standard state, $T = 0$ K

REFERENCES

[1] J. D. Chase, *Chem. Eng.*, **1980**, 107.

[2] J. W. Armitage and P. Gray, *Trans. Faraday Soc.*, **58**, 1746 (1962).

[3] W. Weltner Jr., *J. Amer. Chem. Soc.*, **77**, 3941 (1955).

[4] F. A. Gothard, „Echilibre lichid-vapori", vol. I, Ed. Academiei R.S.R., Bucureşti, 1975, p. 41.

[5] J. R. Barton and C. C. Hsu. *J. Chem. Eng. Data*, **14**, 185(1969).

[6] M. D. Taylor and J. Burton, *J. Amer. Chem. Soc.*, **74**, 4151(1952).

[7] W. Waring, *Chem. Revs.*, **51**, 171 (1952).

[8] H. L. Ritter and J. H. Simons, *J. Amer. Chem. Soc.*, **67**, 757(1945).

[9] E. W. Johnson and L. K. Nash, *J. Amer. Chem. Soc.*, **72**, 547 (1950).

[10] M. D. Taylor, *J. Amer. Chem. Soc.*, **73**, 315 (1951).

[11] J. Coolidge, *J. Amer. Chem. Soc.*, **50**, 2166 (1928); **52**, 1874 (1930).

[12] B. P. Nickolski, "Handbuch des Chemikers", Band I, VEB Verlag Technik, Berlin, 1956, p. 625–37.

[13] "Handbook of Chemistry and Physics", Chemical Rubber Publ. Co., Cleveland, 1959, p. 2363.

[14] J. D. Cox and G. Pilcher, "Thermochemistry of Organic and Organometallic Compounds", Acad. Press. London, 1970.

[15] I. Wadsö, *Acta. Chem. Scand.*, **16**, 479 (1982).

[16] J. Konicek and I. Wadsö, *Acta. Chem. Scand.*, **24**, 2612 (1970).

Revue Roumaine de Chimie, **30**, *11–12*, 903 – 908 (1985)

BINARY VAPOR – LIQUID EQUILIBRIA OF BENZENE–ALCOHOL SYSTEMS

J. L. CABEZAS[a], J. C. ARRANZ[a] and J. BERRUETA[b]

[a] Department of Chemical Engineering, University of Valladolid (Burgos), Burgos, Spain

[b] Department of Chemical Engineering, University of Oviedo, Oviedo, Spain

Received January 12, 1985

Experimental data of vapor–liquid equilibrium at 760 mmHg are reported for the following binary systems: methanol – benzene, ethanol – benzene, benzene – n-propanol and benzene – n-butanol. The data were correlated by the Van Laar equation, and they were also predicted by the UNIFAC model. The differences between experimental, correlated and predicted data are analyzed by the integral relative deviation criterion.

1. INTRODUCTION

Measurements of vapor–liquid equilibrium of mixtures benzene-alcohols have received attention by several authors.[1] However, there are deviations in the experimental data reported in the literature, mainly due to the presence of an azeotrope for the mixtures benzene-lower alcohols.

The purpose of this work has been to determine the vapor-liquid equilibrium of the binary mixtures formed by benzene with methanol, ethanol, n-propanol and n-butanol at 760 mmHg. These data have been correlated by the Van Laar equation, and the UNIFAC model has been used for predicting them.

EXPERIMENTAL SECTION

An equilibrium still of the Othmer type[2] with some modifications,[3] was used for the determination of the vapor-liquid equilibria. Depending on the temperature range of the binary mixture, the equilibria were attained in 50—70 minutes.

The vapor and liquid samples were analyzed by density and refractive index. Refractive index measurements were taken at 25°C using a PZO RL2 refractometer which had an accuracy of up to ± 0.0005. The equilibrium temperature was measured by a standard mercury in glass thermometer, the accuracy being of ± 0.1°C. The products were of reagent grade and they were further purified in a laboratory packed distillation column.

RESULTS AND DISCUSSION

Tables 1–4 report the experimental vapor–liquid equilibrium data obtained at 760 mmHg for the systems methanol-benzene, ethanol-benzene, benzene-n-propanol and benzene-n-butanol.

Table 1

Methanol – Benzene system at 760 mmHg

EXPERIMENTAL			VAN LAAR			UNIFAC		
X	Y	t	Y_{VL}	t	$\|Y_{VL}-Y\|$	Y_U	t	$\|Y_U-Y\|$
0,0550	0.4230	63.4	0.4038	65.8	0.0008	0.422	64.6	0.0010
0.0890	0.4800	60.9	0.4709	62.8	0.0091	0.485	61.6	0.0050
0.1285	0.5145	59.7	0.5142	60.8	0.0003	0.521	59.9	0.0065
0.1540	0.5250	59.4	0.5347	60.2	0.0097	0.530	59.3	0.0050
0.2725	0.5500	58.8	0.5701	58.7	0.0201	0.560	58.4	0.0100
0.3400	0.5635	58.6	0.5790	58.5	0.0155	0.568	58.2	0.0045
0.3840	0.5730	58.5	0.5872	58.3	0.0142	0.570	58.2	0.0030
0,4500	0.5815	58.5	0.5900	58.3	0.0085	0.578	58.1	0.0065
0.5255	0.5975	58.4	0.5974	58.2	0.0001	0.588	58.0	0.0095
0.6120	0.6120	58.3	0.6059	58.2	0.0061	0.603	58.0	0.0090
0.6760	0.6250	58.4	0.6205	58.2	0.0045	0.617	58.1	0.0080
0,7450	0.6465	58.5	0,6418	58.4	0.0047	0.641	58.3	0.0055
0.7615	0.6525	58.6	0.6496	58.6	0.0029	0.649	58.4	0.0035
0.7950	0.6705	58.8	0.6703	58.8	0.0002	0.669	58.7	0.0015
0.8300	0.6970	59.2	0.6957	59.2	0.0013	0.695	59.1	0.0020
0.8610	0.7200	59.6	0.7202	59.6	0.0002	0.724	59.6	0.0040
0.8895	0.7595	60.2	0.7575	60,1	0.0020	0.758	60.2	0.0015
0.9320	0.8205	61.3	0,8177	61.2	0.0028	0.823	61.4	0.0025
0.9540	0.8665	62.1	0.8659	62.2	0.0006	0.868	62.2	0.0015
			AAD = 0.0055 IRD = 0.0485			AAD = 0.0047 IRD = 0.0250		

Table 2

Ethanol–Benzene system at 760 mm Hg

EXPERIMENTAL			VAN LAAR			UNIFAC		
X	Y	t	Y_{VL}	t	$\|Y_{VL}-Y\|$	Y_U	t	$\|Y_U-Y\|$
0.0400	0.2590	71.8	0.2356	72.8	0 .0234	0.259	71.7	0.0000
0.0740	0.3000	70.6	0.2909	71.0	0 .0091	0.315	69.0	0.0150
0.1600	0.3655	69.1	0.3608	69.2	0.0047	0.377	66.8	0.0115
0.2255	0.3925	68.7	0.3855	68.7	0.0070	0.405	66.4	0.0125
0.3710	0.4280	68.4	0.4153	68.3	0.0127	0.426	66.3	0.0020
0.4420	0.4420	68.3	0.4277	68.3	0.0143	0.435	66.2	0.0070
0.5235	0.4555	68.4	0.4509	68.3	0.0046	0.443	66.3	0.0125
0.5440	0.4605	68.5	0.4555	68.4	0.0050	0.453	66.3	0.0075
0 .6385	0.4750	68.7	0.4950	69.0	0.0200	0.473	66.7	0.0020
0.6825	0.4980	69.0	0.5151	69.2	0.0171	0.491	67.0	0.0070
0.7140	0.5235	69.4	0.5382	69.6	0.0147	0.516	67.4	0.0075
0.7475	0.5445	69.7	0.5693	70.0	0.0248	0.535	67.8	0.0095
0.8055	0.6000	70.6	0.6200	71.1	0.0200	0.585	68.9	0.0150
0.8570	0.6650	71.7	0.6843	72.4	0.0193	0.650	70.3	0.0150
0.9020	0.7270	73.1	0.7500	73.6	0.0230	0.711	72.1	0.0160
0.9320	0.7935	74.5	0.8104	74.8	0.0169	0.783	73.5	0.0105
0.9640	0.8830	76.4	0.8870	76.4	0.0040	0.874	75.5	0.0090
			AAD = 0.0142 IRD = 0.0756			AAD = 0.0094 IRD = 0.0492		

Table 3

Benzene — n. Propanol system at 760 mmHg

EXPERIMENTAL			VAN LAAR			UNIFAC		
X	Y	t	Y_{VL}	t	$\lvert Y_{VL} - Y \rvert$	Y_U	t	$\lvert Y_U - Y \rvert$
0.0500	0.2025	93.4	0.1987	93.2	0.0078	0.203	92.6	0.0015
0.0925	0.3270	90.4	0.3053	90.3	0.0217	0.323	89.5	0.0040
0.1510	0.4550	86.9	0.4368	86.9	0.0182	0.448	86.1	0.0070
0.1990	0.5185	84.7	0.5031	84.6	0.0154	0.512	84.0	0.0065
0.2420	0.5670	82.9	0.5496	83.1	0.0174	0.559	82.5	0.0080
0.2920	0.6105	81.4	0.5948	81.8	0.0157	0.603	81.1	0.0075
0.3270	0.6200	80.6	0.6205	80.9	0.0095	0.622	80.3	0.0080
0.4300	0.6750	79.1	0.6749	79.2	0.0001	0.676	78.6	0.0010
0.4725	0.6960	78.7	0.6935	78.8	0.0025	0.693	78.1	0.0030
0.5145	0.7090	78.3	0.7070	78.4	0.0020	0.707	77.7	0.0020
0.5400	0.7230	78.1	0.7188	78.2	0.0042	0.715	77.5	0.0080
0.5930	0.7380	77.7	0.7336	77.7	0.0044	0.730	77.2	0.0080
0.6465	0.7520	77.5	0.7497	77.5	0.0023	0.744	76.9	0.0080
0.6830	0.7600	77.4	0.7587	77.4	0.0013	0.753	76.8	0.0070
0.7270	0.7750	77.2	0.7704	77.2	0.0046	0.765	76.7	0.0100
0.7990	0.7990	77.1	0.7950	77.1	0.0040	0.793	76.7	0.0060
0.8540	0.8130	77.2	0.8201	77.2	0.0071	0.813	76.8	0.0000
0.9220	0.8600	77.8	0.8700	77.8	0.0100	0.863	77.4	0.0030
0.9675	0.9140	78.6	0.9250	78.7	0.0110	0.920	78.5	0.0060
			AAD = 0.0084 IRD = 0.0501			AAD = 0.0055 IRD = 0.0295		

Table 4

Benzene — n. Butanol system at 760 mmHg

EXPERIMENTAL			VAN LAAR			UNIFAC		
X	Y	t	Y_{VL}	t	$\lvert Y_{VL} - Y \rvert$	Y_U	t	$\lvert Y_U - Y \rvert$
0.0565	0.2485	111.7	0.2520	111.5	0.0035	0.265	110,0	0.0165
0.0735	0.3210	109.6	0.3168	109.6	0.0042	0.330	108.1	0.0090
0.1045	0.4305	106.1	0.4047	106.7	0.0258	0.442	104.8	0.0115
0.1200	0.4860	104.1	0.4479	105.3	0.0381	0.482	103.3	0.0040
0.1420	0.5280	102.5	0.4973	103.2	0.0307	0.530	101.4	0.0020
0.1800	0.6275	98.6	0.5765	100.4	0.0510	0.607	98.4	0.0195
0.2290	0.6925	95.0	0.6526	96.9	0.0399	0.676	95.2	0.0165
0.2530	0.7180	93.7	0.6784	95.4	0.0396	0.702	93.9	0.0160
0,2955	0.7520	91.6	0.7245	93.2	0.0275	0.737	91.7	0.0150
0.3680	0.7950	88.7	0.7770	90.1	0.0180	0.786	88.9	0.0090
0.4240	0.8225	86.8	0.8055	88.3	0.0170	0.813	87.1	0.0095
0.4600	0.8365	86.0	0.8277	86.6	0.0088	0.826	86.2	0.0105
0.5365	0.8590	84.5	0.8558	84.8	0.0032	0.849	84.6	0·0100
0.6285	0.8780	83.1	0.8790	82.9	0.0010	0.867	83.1	0.0110
0.6540	0.8835	82.8	0.8860	82.5	0.0025	0.873	82.8	0·0105
0.7015	0.8905	82.3	0.8971	81.9	0·0066	0.883	82.3	0.0075
0.8445	0.9265	81.2	0.9249	81.0	0.0016	0.916	80.9	0.0105
0.9080	0.9505	80.7	0.9408	80.7	0.0097	0.941	80.4	0.0095
			AAD = 0.0183 IRD = 0.0556			AAD = 0.0110 IRD = 0.0367		

All the systems, except benzene—n-butanol, showed the presence of an azeotrope, as shown in figure 1, where benzene was taken as reference. Table 5 reports the azeotropic compositions and temperatures, together with values reported in the literature.[4] The azeotropic parameters δ (azeotropic depression) and Δ (boiling points difference) were calculated, and their variations in the homologous series were found satisfactory,[5] as shown in figures 2 and 3.

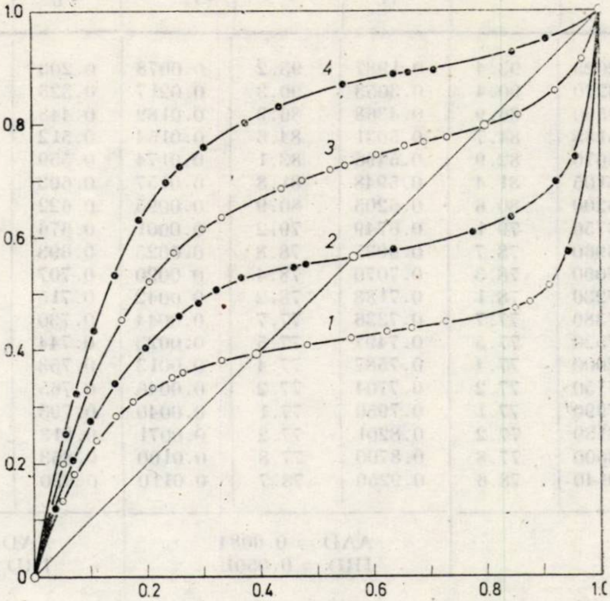

Fig. 1. — Azeotropic vibration for the systems benzene-methanol (1), benzene-ethanol (2), benzene-n-propanol (3) and benzene -n-butanol (4).

Table 5

Azeotropic data

System	$X_{\text{exp.}}$	$X_{\text{bibl.}}$	$t_{\text{exp.}}$	$t_{\text{bibl.}}$	δ	Δ
Benzene — Methanol	0.3880	0.3858	58.3	58.3	21.8	15.2
Benzene — Ethanol	0.5580	0.5516	68.3	67.8	11.8	1.6
Benzene — n. Propanol	0.7990	0.7909	77.1	77.1	3.0	—17.3
Benzene—n. Butanol	—	—	—	—	—	—

The activity coefficients were calculated neglecting the vapor phase fugacity coefficients, according to the equation:

$$\gamma_i = pPy_i/P^0_ix_i$$

Two models e.g. Van Laar[6] and UNIFAC[7-9] were tested to represent the experimental data. The Van Laar constants A and B were obtained using Black's method.[10] Linear regression coefficients higher than 0.999 were obtained for the four systems. Activity coefficients are shown in tables 1—4, together with the deviations between the experimental values of the vapor phase composition (y) and the adjusted ones (y_{VL}) for the same x. The average values of these deviations (AAD) are also included.

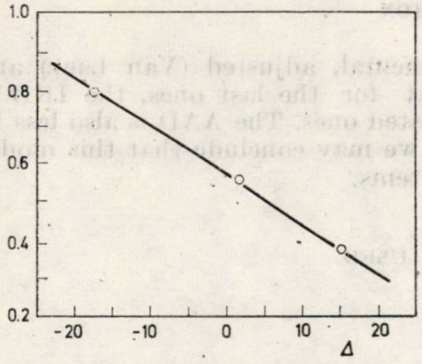

Fig. 2. — δ—x relation in the series.

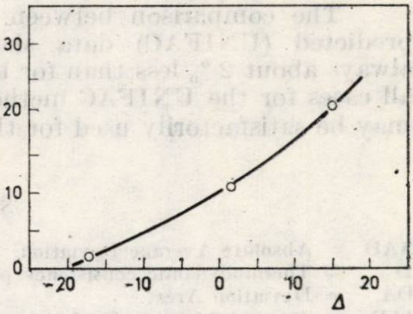

Fig. 3. — δ—Δ relation in the series.

The UNIFAC group and group-interaction parameters were obtained from the bibliography.[8] The calculations carried out in a computer program for the prediction of the activity coefficients consist of straightforward additions and multiplications. Once the activity coefficients are evaluated, iterations are required in order to obtain the $t-y-x$ data, as in the Van Laar method. In Tables 1—4 we have listed again the deviations between the experimental and predicted (y_U) data, as well as the AAD.

The consistency of the experimental data was checked by the criterion of Redlich-Kister[11] and Herington.[12,13] Table 6 shows the results obtained for the parameters D and J. As it is $|D-J| < 10$ in all cases, the experimental data are ***probably consistent***.

Table 6

Thermodynamic consistency parameters

System	D	J	$\|D - J\|$
Methanol — Benzene	0.9068	9.8657	8.9589
Ethanol — Benzene	0.0458	5.1838	5.1380
Benzene — n. Propanol	3.3565	8.6711	5.3146
Benzene — n. Butanol	16.5086	15.9660	0.5426

An integral criterion has been proposed by Mato *et al.*[14] to evaluate the quality of the $y-x$ data. The method consists in calculating the area between the experimental and the "theoretical" lines (*Integral Absolute Deviation*, IAD), and dividing it by the area between the experimental line and the diagonal (*Deviation Area*, DA), the result being called *Integral Relative Deviation* (IRD). Obviously, this is not a thermodynamic consistency test, but it gives a reasonable idea of the quality of the experimental data.

In this work, the IRD were calculated both for the Van Laar and the UNIFAC models in each system, and they appear in Tables 1—4.

CONCLUSION

The comparison between experimental, adjusted (Van Laar) and predicted (UNIFAC) data shows that for the last ones, the IRD is always about 2 % less than for the adjusted ones. The AAD is also less in all cases for the UNIFAC method. So, we may conclude that this model may be satisfactorily used for these systems.

SYMBOLS USED

AAD = Absolute Average Deviation.
D = Thermodynamic consistency parameter.
DA = Deviation Area.
IAD = Integral Absolute Deviation.
IRD = Integral Relative Deviation.
J = Thermodynamic consistency parameter.
P = Total pressure; P° = Vapor pressure.
t = Temperature (°C).
x = Liquid phase composition (mole fraction).
y = Vapor phase composition (mole fraction); y_{VL}, adjusted by Van Laar; y_U, predicted by UNIFAC.
Δ = Difference between the boiling points of the components.
δ = Difference between the boiling points of the reference component and the azeotrope.
γ = Activity coefficients.

REFERENCES

[1] J. Gmehling and, U. Onken, "Vapor-Liquid Equilibrium Data Collection", (D. Behrens, R. Eckermann, Eds.), Dechema Chemistry Data Series, Dechema, Frankfurt (1977).
[2] D. F. Othmer, *Ind. Eng. Chem.*, **20**, 743 (1928).
[3] F. Mato and M. Sanchez, *An. Fis. Quim.*, **67**, 1 (1967).
[4] R. C. Weast, "Handbook of Chemistry and Physics" 63 rd. Ed. CRC Press, Boca Ratón (1982—83).
[5] W. Malesinski, "Azeotropy and other theoretical problems in vapor-liquid equilibrium". Intersc. Pub., New York (1965).
[6] J. J. Van Laar, *Z. Phys. Chem.*, **72**, 723 (1910).
[7] D. S. Abrams and J. M. Prausnitz, *AIChE Journal*, **21(1)**, 116, (1975).
[8] A. Fredslund, R. L. Jones and J. M. Prausnitz, *AIChE Journal*, **21(6)**, 1086 (1975).
[9] J. Gmehling, P. Rasmussen, A. Fredeslund, *Ind. Eng. Chem. Process Des. Dev.*, **21**, 118 (1982).
[10] C. Black, *Ind. Eng. Chem.*, **50**, 403 (1958).
[11] O. Redlich and A. T. Kister, *Ind. Eng. Chem.*, **40**, 345 (1948).
[12] E. F. G. Herington, *Nature*, **160**, 610 (1947).
[13] E. F. G. Herington, *J. Inst. Petrol.*, **37**, 457 (1951).
[14] F. Mato, F. Sobron, F. Fernandez-Polanco and J. Santos, *Anales de Quimica*, **79 (2)**, 275 (1983).

Revue Roumaine de Chimie, 30, *11–12*, 909–916 (1985)

ELECTRICAL CONDUCTIVITY AND DENSITY OF MOLTEN LiI – (Na, K, Rb, Cs)I BINARY SYSTEMS

M. OLTEANU and ŞTEFANIA ZUCA

Center of Physical Chemistry, ICECHIM, Central Institute of Chemistry, Spl. Independenţei 202,
Bucharest, 77208 Romania

Received January 7, 1985

The specific electrical conductivity and density of molten LiI–(Na, K, Rb, Cs)I binary systems have been investigated as a function of composition and temperature. The obtained molar volume and molar (equivalent) conductivity isotherms have been discussed in terms of ionic interactions on mixing and quantitatively related to the ionic parameters (size and polarizability) of the components.

The observation has been made that in mixtures with common anion, the entities participating in the electric transport are the same, no matter if one considers the conductivity of the melt as a whole or the mobilities of individual ionic species, as both processes could be qualitatively explained according to Lumsden's theory of anion polarization.

Our previous results[1] on fused alkali halide systems with common anion have proved the usefulness of a systematic investigation of electrical conductivity as a function of ionic parameters of the two components of the mixture. It has been stated that the electrical conductivity departures from additivity could be expressed in terms of interionic distances and anion polarizability.

In order to complete this systematic study, both electrical conductivity and density were determined for LiI-containing alkali iodide binary systems.

EXPERIMENTAL

All chemicals used were p.a. reagent grade. NaI, KI, RbI and CsI were twice recrystallized from distilled water, dried for 24 h at 423 K and then melted under a current of both throughly dried gaseous HI and argon.

Due to the high hygroscopicity of LiI, a special technique [2] was employed in order to melt it directly into the conductivity cell: commercially available solid LiI was treated and melted in a supplementary vessel attached to the conductivity cell, the melt being then transferred into the latter. Mixtures were prepared by adding the requisite amount of the second alkali iodide; to establish the exact composition of the melt, each mixture was analysed flame-photometrically after the experiment. All melts were tested for neutrality with phenolphthalein before and after each run and the results obtained with consistently neutral melts were only considered.

The specific electrical conductivity (impedance) measurements were carried out by means of an autobalance precision Wayne Kerr B 331 bridge, at a fixed frequency of 1592 Hz (internal operating frequency of the bridge oscillator). U-shaped, previously described[2] silica capillary cells (with constants between 500—700 cm^{-1}) were employed. The precision of specific conductivity measurements was ± 0.1%.

The density measurements were made with a precision of ± 0.2% by means of a hydrostatic method[2], following the same procedure as that for conductivity experiments.

Special care was taken to ensure a carefully controlled atmosphere during specific conductivity as well as density measurements.

RESULTS AND DISCUSSIONS

Both specific conductivity, k (ohm^{-1} cm^{-1}) and density, d (g cm^{-3}), were measured over a temperature range of about 200 K and the whole concentration domain from pure LiI to pure MI (where M = Na, K, Rb, Cs) was covered.

It has been found out[4] that for all compositions of the four studied systems, the density was a linear function of temperature:

$$d = a - bT \tag{1}$$

and the specific conductivity was fitted to a polynomial equation:

$$k = c + dT + eT^2 \tag{2}$$

The values of a, b and c, d, e constants in the two equations are summarized in Tables 1 and 2, respectively, together with validity temperature ranges. In Tables, values are also given for standard deviations (SD) of the experimental results of density and for percent standard errors of estimate (% SEE) in the case of specific conductivity, respectively. These equations have been then employed to compute d and k values at several fixed temperatures. With such obtained d values, the molar volumes, $V_m = M/d$

Table 1

Constants a and b of density equations (1)

System	x_{LiI}	a	$b \times 10^3$	SD	Temperature range (K)
LiI−NaI	0.81	3.4719	0.7081	0.0040	890−1040
	0.67	3.5593	0.8233	0.0021	930−1080
	0.39	3.5936	0.9139	0.0012	910−1090
LiI−KI	0.83	3.5211	0.8710	0.0015	900−1090
	0.50	3.3159	0.8595	0.0019	900−1080
	0.32	3.3270	0.8410	0.0030	910−1120
LiI−RbI	0.87	3.7703	0.9548	0.0019	960−1130
	0.72	3.7499	0.9608	0.0011	950−1090
	0.53	3.6212	0.8651	0.0008	950−1090
LiI−CsI	0.81	3.9283	1.0303	0.0020	890−1100
	0.78	4.0206	1.0867	0.0018	890−1090
	0.47	4.0131	1.0564	0.0031	950−1140

Table 2

Constants *c*, *d* and *e* of equivalent conductivity equations (2)

System	x_{LiI}	$-c$	$d \times 10^3$	$-e \times 10^6$	% SEE	Temperature range (K)
LiI—NaI	0.76	2.1230	9.4937	3.5937	0.07	850—1050
	0.55	−2.2546	− 2.3089	−1.2663	0.16	850—1030
	0.50	−1.0215	− 0.8292	−6.1286	0.12	890—1050
	0.30	3.0449	9.8479	3.9482	0.10	880—1050
LiI—KI	0.72	−0.1564	2.7779	0	0.25	860—1020
	0.65	5.7788	14.8268	9.5157	0.16	880—1030
	0.51	4.0184	10.3178	4.1603	0.14	900—1090
	0.23	5.9621	13.0089	5.4291	0.17	900—1050
LiI—RbI	0.91	2.2490	9.2662	3.3494	0.15	860—1030
	0.55	2.3794	6·3913	2.2363	0.20	860—1030
	0.27	1.6655	4.0677	1.1976	0.23	870—1050
LiI—CsI	0.95	1.4157	7.1013	2.3112	0.40	870—1050
	0.78	3.9933	3.6619	−8.5855	0.28	880—1070
	0.53	6.1092	12.1517	4.6114	0.60	870—1130
	0.28	5.7764	11.6873	4.8111	0.65	860—1000

(where M is molar weight of the mixture) were calculated for all compositions at the corresponding temperatures. In order to compute the equivalent conductivities, $\lambda = kV_m$, the isotherms V_m *vs.* composition were drawn and then V_m values were found by interpolating at compositions so chosen as to correspond to those for specific conductivity measurements. The precision of the reported equivalent conductivity data is ± 0.25 %.

Fig. 1 illustrates the isotherms of molar volume as a function of composition. Contrary to the behaviour of these isotherms which exhibit relatively small departures from additivity (up to 5.5 % in the case of LiI—CsI mixture), the isotherms of equivalent conductivity (Fig. 2) show important negative deviations from linearity.

As graphical analysis of $\log\lambda$ against $1/T$ indicated that all studied mixtures gave straight lines over the whole temperature range, the temperature variation of the equivalent conductivity was expressed by Arrhenius-type equations :

$$\lambda = A \exp(-E_\lambda/RT) \tag{3}$$

The numerical values for pre-exponential factors A and activation energies for equivalent conductivity, E_λ, were obtained by the least square method and are listed in Table 3, together with the standard deviations for E_λ.

The experimental values for λ have been compared with those calculated by additivity relation :

$$\lambda_c = x_1\lambda_1 + x_2\lambda_2 \tag{4}$$

as well as with those calculated by means of Markov's equation[5] :

$$\lambda_M = x_1^2\lambda_1 + x_2^2\lambda_2 + 2x_1x_2\lambda_1 \tag{5}$$

In the above relations, x_1, x_2 are molar fractions and λ_1, λ_2 equivalent conductivities of the two components of the mixture.

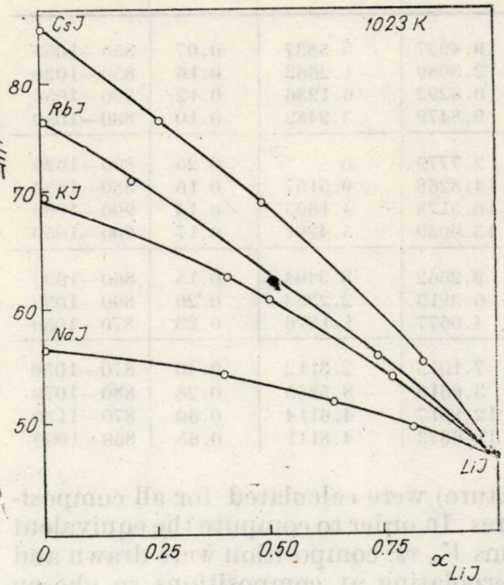

Fig. 1. — Isotherms of molar volumes for alkali iodide mixtures.

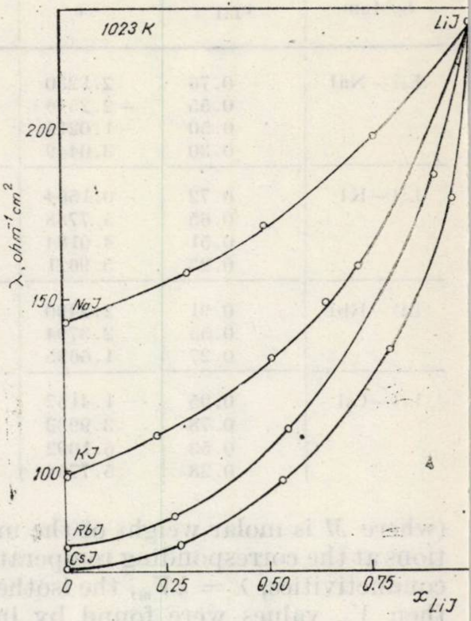

Fig. 2. — Isotherms of equivalent conductivi for alkali iodide mixtures.

Table 3

Pre-exponential factors *A* and activation energies E_λ (kcal/mol) for LiI — MI mixtures

System	x_{LiI}	$A \times 10^{-2}$	E_λ	Standard deviations for E_λ
LiI — NaI	0.76	3.85	1.42	0.025
	0.55	4.11	1.76	0.019
	0.50	3.50	1.46	0.030
	0.30	3.78	1.77	0.025
LiI — KI	0.72	3.51	1.58	0.018
	0.65	3.76	1.87	0.029
	0.51	3.02	1.70	0.031
	0.23	4.17	2.68	0.028
LiI — RbI	0.91	4.69	1.87	0.015
	0.55	6.35	3.53	0.018
	0.27	5.15	3.59	0.018
LiI — CsI	0.95	5.10	2.15	0.026
	0.78	6.17	3.12	0.012
	0.53	8.19	4.26	0.024
	0.28	9.23	4.02	0.005

A comparison between experimental λ's, additive λ_c values and λ_M values calculated according to Markov's equation is given in Table 4, where, in the last two columns, the percent deviations from equations (4) and (5) are listed as well. When comparing the data in Table 4, it is evident that equation (5) predicts the experimental values generally better than equation (4) does. It has been pointed out[5] that there is a correlation between the magnitude of the deviations from equation (5) and the phase diagrams : the more complicated the phase diagrams, the larger the departures. The validity of this statement has been already established in the case of all systems previously studied, no matter if they were with common anion[1] or common cation[6].

Table 4

Comparison between experimental values λ, additive values λ_c and λ_M values calculated according to Markov's equation (all λ's in ohm^{-1} cm^2, T = 1023 K)

System	x_{LiI}	λ	λ_c	λ_M	$100\frac{\lambda-\lambda_c}{\lambda}$	$100\frac{\lambda-\lambda_M}{\lambda}$
LiI−NaI	0.76	197.5	208.5	191.8	− 5.6	+ 2.9
	0.55	175.3	192.1	170.7	− 9.6	+ 2.9
	0.50	172.0	188.5	166.9	− 9.7	+ 2.9
	0.30	158.2	169.4	151.6	− 7.1	+ 4.2
LiI−KI	0.72	158.8	194.2	167.7	−22.1	− 5.5
	0.65	149.0	185.0	155.1	−24.1	− 4.1
	0.51	133.3	166.6	133.7	−24.8	− 0.1
	0.23	110.8	129.7	106.5	−17.1	+ 3.9
LiI−RbI	0.91	186.0	217.2	204.7	−17.0	−10.3
	0.55	112.0	162.2	124.3	−44.0	−11.0
	0.27	86.0	119.3	89.2	−38.4	− 3.5
LiI−CsI	0.95	180.0	218.1	206.3	−21.2	−14.6
	0.78	130.5	195.6	168.0	−49.9	−28.7
	0.53	99.2	155.4	115.4	−60.0	−16.6
	0.28	77.5	116.8	83.7	−50.7	− 8.0

With the exception of LiI−KI mixture,[7] for the other three LiI−MI (M = Na, Rb, Cs) systems there are not available phase diagram data. Yet, the electrical conductivity measurements can be used as a method of physico-chemical analysis : by analogy with the magnitude of the deviations registered in the case of both chlorides and bromides of the same pairs of cations[7,8], some presumptions can be made upon the shape of the phase diagrams of LiI-containing binary mixtures. Thus, as the deviations for LiI−NaI and LiI−KI systems are from 3 to 6 %, one can suppose that these mixtures form well-marked eutectics, while for LiI−RbI and LiI−CsI systems, the large deviations from 8 up to 29 % indicate the formation of LiI · 2MI-type incongruently melting compounds (where M = Rb, Cs). Moreover, the molar volume values (Fig. 1) come to support this supposition that there is a difference between the phase diagrams of LiI−NaI, LiI−KI and, respectively, LiI−RbI, LiI−CsI systems. The first two, which, presumably, form eutectics, exhibit molar volume departures from additivity of only 1.2–1.5 %, while the other two present departures of up to 5.5 % because the formation of the voluminous $\mathrm{LiI \cdot 2\,MI}$ associated compounds.

If negative departures from additivity, $\Delta\lambda = \lambda_{\mathrm{exp}} - (x_1\lambda_1 + x_2\lambda_2)$ (also called excess conductivities) are represented as a function of composition, the thus obtained isotherms exhibit a characteristic evolution (Fig. 3),

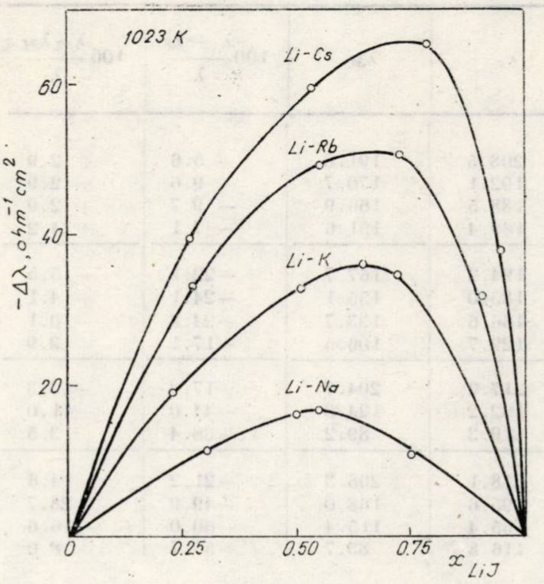

Fig. 3. — Isotherms of excess conductivities of LiI — (Na, K, Rb, Cs)I binary mixtures.

depending on the nature of the ions present in the mixture. One can see that the deviations become greater as the difference between the dimensions of the two uncommon cations rises. With the exception of LiI—NaI mixture, the isotherms are asymmetrical, having a maximum placed within LiI-rich concentration ranges. As the difference between the dimensions of the two cations increases in the sequence: Li — K < Li—Rb < Li—Cs, the maximum is shifted towards higher LiI concentrations.

These specific trends have already been encountered with all previously studied systems [1] and explained in terms of Lumsden's model [9] for common anion polarization in the unsymmetrical field induced by the two cations of different polarization strengths. The present data confirm the finding that the excess conductivity can be fitted to a relation of the form[1]:

$$\Delta\lambda = -a\alpha\left[\frac{1}{(r_{M_1X}-d)^2} - \frac{1}{(r_{M_2X}+d)^2}\right]^2 x_1x_2 \qquad (6)$$

where a is a factor changing with temperature and/or composition, r_{M_1X} and r_{M_2X} are interionic distances [10] in the two salts and d is a package parameter [11] by which interionic separation changes on mixing are accounted for.

According to relation (6), if $\Delta\lambda$ is plotted against parameter $P = -\alpha [1/(r_{M_1X} - d)^2 - 1/(r_{M_2X} + d)^2]^2$, a straight line (isotherm) with the slope equal to a is obtained for mixtures of a given composition. Figure 4 illustrates the results for equimolecular mixtures at 1123 K : making allowance for relative error in $\Delta\lambda_{0.5}$, a straight line can be drawn through the obtained experimental points and the origin of the coordinate system.

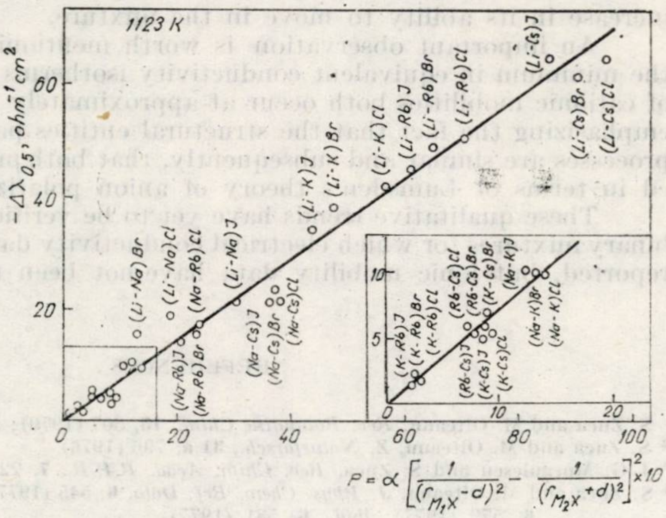

Fig. 4. — Excess conductivities, $\Delta\lambda$, for equimolecular mixtures.

In order to prove the general validity of equation (6), we have completed the present data for LiI-containing mixtures with our own conductivity data for the other 26 alkali halide binary systems with common anion.[11,12] These data illustrate convincingly that the anion polarization plays an important role in the electrical transport in molten salt mixtures with common anion. The decrease in electrical conductivity on mixing is explained by the changes in electrical mobilities of the two cations relative to the common anion.[13] Measurements of relative mobilities in alkali chloride[13] and respectively alkali bromide[14,15] binary mixtures have shown that both cation mobilities decrease monotonously with concentration, but the rate of decrease is greater in the case of smaller cation. At the first sight, the steady decrease in the mobilities of both cations may appear inconsistent with the existence of a minimum in the isotherm of equivalent conductivity for the melt as a whole. That is not so, as smaller cation is such a poor conductor in the nearly pure salt containing the larger cation that the change in composition has a much greater influence on the mobility of smaller one. When the concentration effect is large enough, it leads to the cation mobilities cross-over cited in literature for other alkali halide systems[13–16] as well as for alkali nitrate binary mixtures.[17,18] The crossing over of cation mobilities has also been explained qualitatively[13] in terms of Lumsden's theory. It is apparent that a strengthening of the attractive force between a cation and an anion should lower the mobility of the former relative to the latter. In a mixture $M_1X - M_2X$ (where

$r_{M_1^+} < r_{M_2^+}$), the addition of a single M_2^+ ion to pure M_1X can affect a substantial number of M_1^+ ions by inducing polarization in each of X^- ions in its immediate coordination sphere : the mobility of M_1^+ ions drops rapidly when the first M_2^+ ions are added. Therefore, the asymmetry registered in the case of conductivity *vs.* composition isotherms is placed in the M_1X—rich regions (M_1^+ is smaller cation). As for M_2^+ ion itself, its attraction towards X^- ions is weakened by addition of M_1^+ ions, this effect leading to an increase in its ability to move in the mixture.

An important observation is worth mentioning here, namely that the minimum in equivalent conductivity isotherms and the crossing-over of cationic mobilities both occur at approximately the same composition, emphasizing the fact that the structural entities participating in the two processes are similar and subsequently, that both processes can be explained in terms of Lumsden's theory of anion polarization.

These qualitative trends have yet to be verified with LiI-containing binary mixtures for which electrical conductivity data have been presently reported, but ionic mobility data have not been made available so far.

REFERENCES

[1] S. Zuca and M. Olteanu, *Rev. Roumaine Chim.*, **15**, 307 (1970); *ibid.*, **15**, 1508 (1970).

[2] S. Zuca and M. Olteanu, *Z. Naturforsch.*, **31 a**, 796 (1976).

[3] I. G. Murgulescu and S. Zuca, *Rev. Chim. Acad. R.P.R.*, **7**, 227 (1959).

[4] S. Zuca and M. Olteanu, *J. Phys. Chem. Ref. Data*, **6**, 545 (1977); *ibid.*, **6**, 564 (1977); *ibid.*, **6**, 579 (1977); *ibid.*, **6**, 581 (1977).

[5] I. K. Delimarski and B. F. Markov, "Elektrokhimia Rasplavlenykh Solei", Metallurgizdat, Moscow, cap. I, 1960.

[6] S. Zuca and M. Olteanu, *Rev. Roumaine Chim.*, **13**, 1567 (1968).

[7] G. J. Janz, R. P. T. Tomkins, C. B. Allen, J. R. Downey, G. L. Gardner and S. K. Singer, *J. Phys. Chem. Ref. Data*, **4**, 1005 (1975); *ibid.*, **4**, 1044 (1975); *ibid.*, **4**, 1101 (1975); *ibid.*, **4**, 1105 (1975).

[8] G. J. Janz, R. P. T. Tomkins, C. B. Allen, J. R. Downey and S. K. Singer, *J. Phys. Chem. Ref. Data*, **6**, 485 (1977); *ibid.*, **6**, 495 (1977); *ibid.*, **6**, 514 (1977); *ibid.*, **6**, 516 (1977).

[9] J. Lumsden, 'Thermodynamics of Molten Salt Mixtures", Academic Press, London, 1966, p. 70.

[10] R. W. G. Wyckoff, "Crystal Structure", Interscience, New York, 1948.

[11] S. Sternberg, *St. Cerc. Chim.*, **17**, 1959 (1969).

[12] M. Olteanu, Ph. D. Thesis, Center of Physical Chemistry, Bucharest, 1984.

[13] C. T. Moynihan and R. W. Laity, *J. Phys. Chem.*, **68**, 3312 (1964).

[14] R. W. Laity and A. S. Tenney, *J. Phys. Chem.*, **74**, 3112 (1970).

[15] O. P. Mehta, F. Lantelme and M. Chemla, *Electrochim. Acta*, **14**, 505 (1969).

[16] J. Richter, R. Conradt and R. Becker, *Z. Naturforsch.*, **36 a**, 1100 (1981); J. Richter, E. Kirschbaum and H. Valenta, *ibid*; **38 a**, 880 (1983).

[17] J. A. A. Ketelaar and E. P. Honig, *J. Phys. Chem.*, **68**, 1596 (1964).

[18] F. Lantelme and M. Chemla, *Bull. Soc. Chim. France*, 1963, p. 2200; *Electrochim. Acta*, **11**, 1023 (1966).

Revue Roumaine de Chimie, **30**, *11–12*, 917–931 (1985)

ESTUDIO CULOMBIMÉTRICO A POTENCIAL CONTROLADO DE LA OXIDACIÓN ANÓDICA DEL COMPLEJO CIANURADO BINUCLEAR DE Mn(III). I.

OXIDACIÓN A +0.20 VOLTIOS (vs. S.C.E.): CORRIENTE CINETICA Y REACCIÓN PARALELA

G. LÓPEZ CUETO y A. ALONSO MATEOS *

Departamento de Química Analítica, Facultad de Química, Universidad de Salamanca, España

Recibido el 7 de Enero de 1982
Revisto el 10 de Mayo de 1985

Se realiza un estudio sobre la oxidación electrolítica a potencial controlado de +0.20 volts (vs. S.C.E.) del complejo cianurado binuclear de Mn (III) en medio cianurado. Para concentraciones de $[CN^-] \geqslant 3M$ se observa una corriente cinética. Se calculan los rendimientos en corriente y producto y se propone el siguiente mecanismo : La oxidación electrolítica conduce a la formación de un complejo cianurado binuclear de Mn (III)—Mn IV) que reacciona con el CN^- del medio regenerando la especie inicial. Esta última especie se transforma con el tiempo en otra especie mononuclear de Mn (III) que no se oxida en el electrodo. Esta transformación es mas acusada para $[CN^-] \leqslant 2M$. Se calculan las ecuaciones que relacionan la intensidad de corriente con el tiempo asi como los valores de las constantes de velocidad para la reacción interferente.

A study has been made of the electrolytical oxidation of the Mn(III) brown cyanide complex in cyanide solution to constant-potential of +0.20 volts (as. S.C.E.). For cyanide concentration $CN^- \geqslant 3M$ a kinetic current is observed. From the experimental result a mechanism is proposed : the electrolytical oxidation leads to the formation of a binuclear cyanide complex which reacts with the cyanide of the solution regenerating the initial complex. On the other hand, the Mn(III)—Mn(III) initial species changes to the other mononuclear species nonoxidizable at the electrode. The equations which relate the current with the time and the values of rate constants of the interferent reaction have been calculated.

INTRODUCCION

Cuando el complejo cianurado de Mn(II) se oxida con peróxido de hidrógeno en medio cianurado, se pone de manifiesto la existencia de dos complejos diferentes de Mn(III). La solución parda obtenida inicialmente, se decolora con el tiempo hasta una solución incolora donde el manganeso también se encuentra en estado de oxidación (III).^{1}

La solución parda obtenida inicialmente contiene el complejo hexacianomanganato (III) ya citado por Brauer. ^{2} Esta solución presenta en electrodo de platino y con agitación, dos ondas anódicas reversibles de un electrón a 0.03 y 0.60 volts (vs. S.C.E.). La solución obtenida por decoloración de la anterior solo presenta una onda catódica reversible y de un electrón a −0.55 volts (vs. S.C.E.) (Figura 1). Esta transformación espontánea ocurre según un proceso cinético de primer orden, lo que se ha puesto de manifiesto por estudios espectrofotométricos. [3]

En un trabajo ya comunicado[4] se expusieron los resultados obtenidos al estudiar la influencia de las diferentes variables sobre los dos procesos anódicos y se propuso el siguiente mecanismo para los procesos de difusión que controlan las reacciones en el electrodo : En la primera reacción (0.20 volts) el complejo cianurado binuclear de Mn(III) se oxida hasta el complejo también binuclear mezcla de Mn(III) y Mn(IV), esta especie en la segunda reacción (−0.55 volts) se oxida hasta el complejo binuclear de Mn(IV). Las propiedades diamagnéticas del complejo pardo de Mn(III) confirman su estructura binuclear.

A la vista de los resultados antes mencionados, pareció interesante realizar un estudio culombimétrico a potencial constante de la oxidación del complejo binuclear de Mn(III) en medio cianurado y precisamente a los potenciales de las zonas de difusión de las dos ondas anódicas. El objeto de este estudio es confirmar el mecanismo de las reacciones electroquímicas y la naturaleza de las especies complejas que intervienen en ellas.

EXPERIMENTAL

Reactivos

El hexacianomanganato (III) potásico ha sido obtenido en forma solida por el procedimiento propuesto por Brauer [2]. Su contenido en cuanto al compuesto mononuclear es de 5.7%, hecho puesto de manifiesto por medidas amperométricas.[5] Las soluciones de electrolito soporte se prepararon a partir de CNNa en calidad reactivo análisis. Para ajustar la fuerza iónica se utiliza ClNa de la misma calidad.

Aparatos

El registro de las curvas intensidad-potencial asi como el estudio culombimétrico se ha efectuado mediante el aparato electroanalítico Electroscan−30 Beckman, que lleva incluidos la fuente de energía, el potenciometro y el registrador.

Como electrodos de trabajo(ánodo) se han utilizado dos macroelectrodos de malla de platino cuyas superficies están en la relación 1 : 1,8. El cátodo está constituido por una punta de platino sumergida en una disolución de NaOH 1N separada del resto mediante una placa de vidrio poroso recubierta de agar-agar saturado de ClK. Como electrodo de referencia se utilizó siempre el de calomelanos saturado (S.C.E.). Como celula de electrolisis se utilizó un recipiente Metrohm EA−880 de 50 ml de capacidad, provista de doble fondo para poder termostatar, operación que se efectuó mediante un termostato Tamson de circulación. Agitador magnético con posibilidad de controlar y mantener constante la velocidad de agitación. Se siguió un procedimiento para el pre-tratamiento del electrodo de trabajo que conduce a una buena reproductibilidad de la intensidad de difusión y del potencial de semionda.

Evaluación de las corrientes faradaicas

En un análisis polarográfico, la medida de la intensidad limite de corriente debe ser corregida por el valor de la corriente residual con el fin de determinar correctamente la concentración de la especie deseada. Un problema similar ocurre en el análisis culombimétrico

a potencial controlado, donde la cantidad total de corriente consumida durante la electrolisis debe ser corregida si existen otras corrientes no debidas a la oxidación o reducción de la especie deseada en el electrodo.

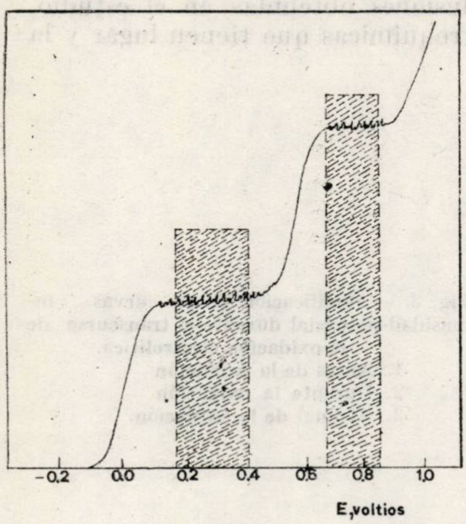

Fig. 1. — Zona de difusión para los dos procesos anódicos.

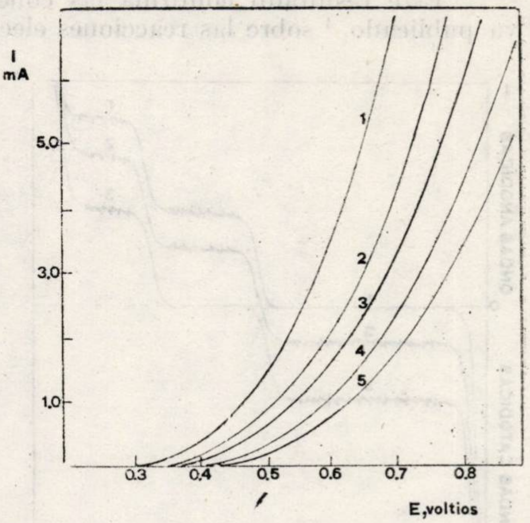

Fig. 2. — Curvas intensidad-potencial de disoluciones cianuradas para diferentes concentraciones.
1. CNNa 5.0 M ; 2. CNNA 4.0 M ; 3. CNNA 3.0 M 4.CNNA 2.0 M ; 5. CNNa 1.0 M.

Según Meites y Moros [6] existen cuatro tipos de corrientes residuales : corriente de *carga*, corriente *faradaica*, corriente *inducida* y corriente *cinética*, las dos primeras se evaluan sólo con el electrolito soporte, en ausencia de la especie que se oxida o reduce en el electrodo.

En la Figura 1 se observa que la zona de difusión de la primera onda anódica está comprendida en el margen de potenciales +0.10 a +0.40 volts (vs. S.C.E.) siendo de +0.70 a +0.90 los límites aproximados de la zona de difusión correspondiente a la segunda onda. Las curvas intensidad-potencial obtenidas para el electrolito soporte (CNNa desde 1 a 5 M) se representan en la Figura 2. Como puede comprobarse para potenciales inferiores a 0.30 volts no se aprecia practicamente ningún tipo de corriente fondo, por lo que si la oxidación culombimétrica se lleva a cabo por debajo de dicho potencial, no será necesario efectuar correcciones para corrientes faradaicas. El potencial de trabajo para esta primera onda, se estableció, como consecuencia de lo anteriormente expuesto, en 0.20 volts. En un trabajo posterior se presentarán los resultados obtenidos en la oxidación culombimétrica a 0.80 volts donde si es necesario previamente evaluar las corrientes faradaicas.

RESULTADOS Y DISCUSION

EVOLUCION DE LAS CURVAS INTENSIDAD-POTENCIAL DURANTE LA OXIDACION

Se efectuó la oxidación electrolítica a 0.20 volts de una disolución reciente de Mn(CN)$_6^{3-}$ 1.12 ×10^{-3} M en CNNa 2.0 M y fuerza iónica 5.0, manteniendo la temperatura a 25°C y registrando las curvas intensidad-potencial en diferentes momentos de la oxidación (Figura 3). Como puede apreciarse, durante el transcurso de la electrolisis la intensidad de la primera onda anódica disminuye, al mismo tiempo que aparece una componente catódica cuya intensidad de difusión crece. La segunda onda anódica no experimenta modificación.

Este resultado confirma las conclusiones obtenidas en el estudio, ya publicado,[4] sobre las reacciones electroquímicas que tienen lugar y la naturaleza de los complejos que intervienen en ellas. Si las dos ondas anódicas que aparecen en las disoluciones cianuradas recientes de $Mn(CN)_6^{3-}$ correspondiesen a la oxidación electroquímica de dos complejos diferentes de Mn(III), la oxidación a potencial controlado debería traducirse en una disminución simultánea de ambas ondas.

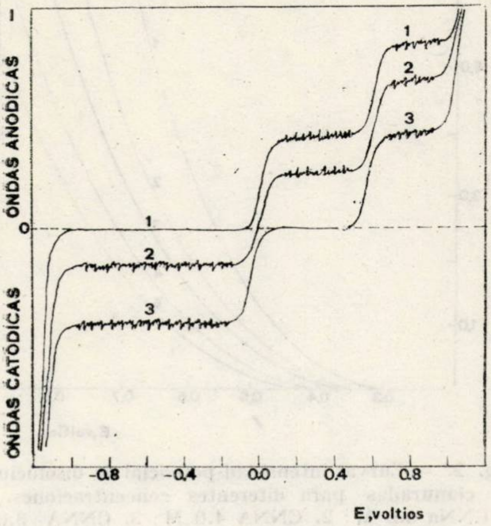

Fig. 3. — Modificación de las curvas intensidad-potencial durante el transcurso de la oxidación electrolítica.

1. Antes de la oxidación
2. Durante la oxidación
3. Al final de la oxidación.

CURVAS INTENSIDAD-TIEMPO DURANTE LA ELECTROLISIS

En un proceso colombimétrico a potencial controlado, la intensidad de corriente decrece exponencialmente según la ecuación de Lingane:

$$i_t = i_0 \cdot e^{-Kt} \qquad (1)$$

donde:

i_0, es la corriente inicial

i_t, es la corriente para un tiempo cualquiera t

K, constante física de electrolisis, $K = \dfrac{DA}{V\delta}$

donde:

D, es el coeficiente de difusión

A, area del electrodo

V, volumen de solución

δ, espesor de la capa límite de difusión.

La ecuación (1) puede expresarse en logaritmos decimales, como :

$$i_t = i_0 \cdot 10^{-Kt} \qquad (2)$$

donde

$$k = 0.4343\ \mathrm{K} \qquad (3)$$

La cantidad de electricidad consumida en el proceso electrolítico será :

$$Q = i_0 \cdot e^{-Kt} = \frac{i_0}{K} = \frac{i_0}{2.303\,\mathrm{k}} \qquad (4)$$

por lo que la cantidad de corriente Q puede ser determinada, representando log i_0 frente a t; la ordenada en el origen es log i_0 y la pendiente de la recta k por lo que el valor de la constante física K es fácil de determinar según (3). Todas estas ecuaciones son correctas para un proceso culombimétrico deal donde no existen corrientes faradaicas, ni inducidas, ni cinéticas.

Fijando la concentración de $\mathrm{Mn(CN)_6^{3-}}$ en 1.12×10^{-3} en M y utilizando el electrodo de malla de platino de superficie menor se han registrado las curvas intensidad tiempo, estudiando la influencia de las variables que puedan afectar de alguna manera al proceso electroquímico. Las condiciones experimentales, exceptuando la variable en estudio han sido : CNNa 1.0 M, fuerza iónica 5.0, temperatura 25°C.

Influencia de la concentración de cianuro

En la Figura 4, se muestran las curvas intensidad-tiempo obtenidas para concentraciones diferentes de CNNa. Como puede apreciarse, para concentraciones iguales o inferiores a 2.0 M en CNNa, la intensidad de corriente decae exponencialmente hasta hacerse practicamente cero. Para concentraciones superiores, la intensidad de corriente llega a alcanzar un valor constante distinto de cero. Este valor final de la corriente de electrolisis aumenta con la concentración de CNNa. Esta morfología de las curvas intensidad-tiempo puede atribuirse a la aparición de una corriente faradaica continua (oxidación del disolvente) o bien a una corriente cinética. Como se dijo anteriormente, al potencial de trabajo de + 0.20 volts no se produce ningún tipo de corriente faradaica, por lo que la intensidad final constante hay que atribuirla a un proceso cinético.

La representación de los valores de log i frente al tiempo conduce a líneas rectas para concentraciones de CNNa 1.0 y 2.0 M pero no así para concentraciones superiores, como puede apreciarse en la **Figura 5,** alcanzándose un valor constante. Esta desviación de la linealidad es característica de un proceso químico en el que se regenera la especie electroactiva inicial a partir del producto de la reacción primaria.

Los valores experimentales obtenidos para K ($K_{\mathrm{exp.}}$) se calculan a partir de la pendiente de las rectas (2). En aquellos casos en que tienen lugar una corriente cinética (CNNa $\geqslant$ 3.0 M), el valor de $K_{\mathrm{exp.}}$ se obtiene a partir de la pendiente trazada en el origen pues la corriente cinética es practicamente nula en los primeros instantes. El valor teórico que debería de tener K (K_{calc}) para las condiciones experimentales de trabajo se obtiene a partir de la expresión (4), donde i_0 se obtiene por extrapolación a tiempo cero de las rectas $\log(i - t)$y el valor de Q_{calc}, expresado en milifaradays, a partir de la cantidad inicial de $\text{Mn(CN)}_6\text{K}_3$.

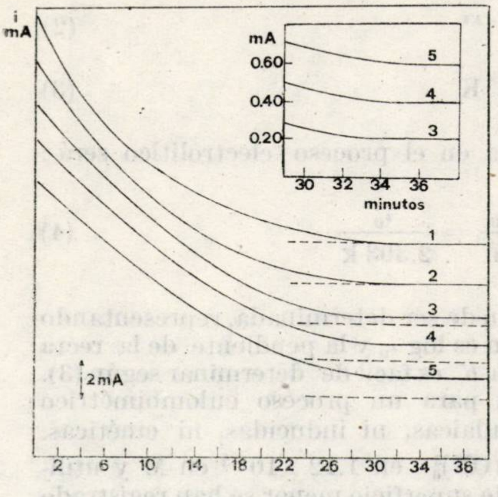

Fig. 4. — Curvas intensidad-tiempo. Influencia de la concentración de CNNa
1. CNNa 0.1 M; 2. CNNa 2.0 M; 3. CNNa 3.0 M
4. CNNa 4.0 M; 5. CNNa 5.0 M.

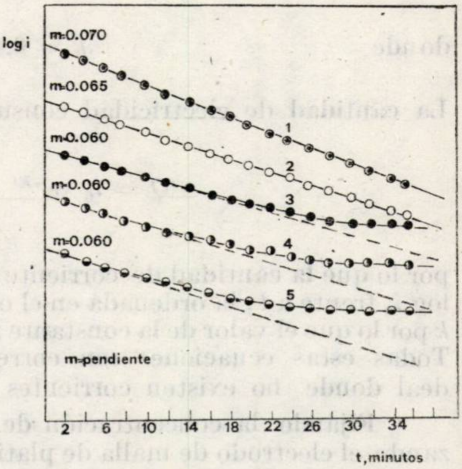

Fig. 5. — Curvas log i frente al tiempo. Influencia de la concentración de CNNa.
1. CNNa 1.0 M; 2. CNNa 2.0 M; 3. CNNa 3.0 M
4. CNNa 4.0 M; 5. CNNa 5.0 M.

En la Tabla 1 se representan los valores de K_{calc} y K_{exp} para las distintas concentraciones de CNNa estudiadas. El valor de K_{calc} permanece constante como era de esperar. Para concentraciones de CNNa 3.0 M ó superiores los valores coinciden, para concentraciones inferiores puede apreciarse que los valores de K_{exp} resultan superiores a los de K_{calc}. Este hecho indica que la concentración de la especie inicial disminuye con mayor velocidad que la debida exclusivamente a la electrolisis, es decir, que tiene

Tabla 1

Influencia de la concentración de CNNa
Valores de $K_{\text{calc.}}$ y $K_{\text{exp.}}$

CNNa M	I_0 mA	m min^{-1}	$K_{\text{cal.}}$ min^{-1}	$K_{\text{exp.}}$ min^{-1}
1.0	12.4	0.070	0.138	0.161
2.0	12.3	0.065	0.137	0.150
3.0	12.4	0.060	0.138	0.138
4.0	12.4	0.060	0.138	0.138
5.0	12.4	0.060	0.138	0.138

lugar una reacción, paralela a la oxidación electrolítica, en la que interviene dicha especie, reacción cuya velocidad es mayor a bajas concentraciones de cianuro tal como se deduce de los datos de la Tabla 1. A la vista de estos hechos parece evidente que dicha reacción paralela no es otra que la evolución del complejo inicial hacia una forma no oxidable, fenómeno durante el que se produce una decoloración que ya ha sido descrita.

Influencia de la fuerza iónica

Para todos los valores de fuerza iónica estudiados, desde 1.0 hasta 5.0, la intensidad de corriente decae hacia cero lo que indica que en ningún caso tiene lugar de modo apreciable el proceso cinético(NaCN 2.0 M). La representación de los valores de log i frente al tiempo conduce en todos los casos a líneas rectas.

En la Tabla 2, se representan los valores de K_{exp} y K_{cal} obtenidos los primeros a partir de las pendientes de las rectas semilogarítmicas. Como puede apreciarse, K_{calc}, disminuye ligeramente a medida que aumenta la fuerza iónica, debido a la modificación del coeficiente de difusión $\left(K = \frac{DA}{VS}\right)$. Para todos los valores de fuerza iónica estudiados, K_{cal} es inferior a K_{exp}, lo que indica que en estas condiciones experimentales la evolución de la especie oxidante (decoloración) tiene lugar en magnitud apreciable. Cuanto menor es la fuerza iónica, el valor de K_{exp} se desvia en mayor grado de K_{cal}, lo que está de acuerdo con el hecho de que el proceso de decoloración se produce a mayor velocidad en estas condiciones. [3]

Tabla 2

Influencia de la fuerza iónica. Valores de $K_{cal.}$ y K_{exp}:

f. iónica	I_0 mA	m min^{-1}	$K_{cal.}$ min^{-1}	$K_{exp.}$ min^{-1}
1.0	13.9	0.170	0.155	0.391
2.0	13.5	0.110	0.150	0*254
3.0	13.3	0.095	0.148	0.219
4.0	12.9	0.080	0.143	0.184
5.0	12.4	0.070	0.138	0.161

Influencia de la temperatura

En todos los casos estudiados para diferentes temperaturas (entre 5° y 40°C), la intensidad de corriente decrece hasta hacerse cero, lo que indica que en las condiciones experimentales en que se trabaja (CNNa 2.0 M y fuerza iónica 5.0) no ocurre de modo apreciable el proceso cinético. La representación de los valores de log i frente al tiempo conduce en todos los casos a líneas rectas.

El valor de K_{calc} (Tabla 3) aumenta con la temperatura por hacerlo también el coeficiente de difusión D. Los valores de K_{exp} obtenidos a partir de las pendientes, se desvian de K_{calc}, en mayor grado a medida que aumenta la temperatura. Este hecho refleja el incremento de la velocidad del proceso de decoloración a temperaturas elevadas. Para temperaturas de 5 y 15°C los valores de K_{exp} y K_{calc} son muy próximos, lo que indica que apenas tiene importancia el proceso antes mencionado.

Tabla 3

Influencia de la temperatura. Valores de $K_{\mathrm{cal.}}$ y K_{exp}.

T °C	I_0 mA	m min^{-1}	$K_{\mathrm{cal.}}$ min^{-1}	K_{exp} min^{-1}
5	8.2	0.040	0.091	0.092
15	10.0	0.050	0.111	0.115
25	12.4	0.070	0.138	0.161
30	14.1	0.085	0.157	0.196
40	17.3	0.150	0.194	0.346

Influencia de la superficie del electrodo

Como queda reflejado en la Tabla 4, los valores de K_{cal}, son proporcionales a la superficie del electrodo, como se deduce de la constancia de $K_{\mathrm{cal}}/\mathrm{A}$. Los valores de K_{exp} son mayores que los valores calculados, debido sin duda a la evolución de la especie electroactiva (decoloración).

Tabla 4

Influencia de la superficie del electrodo. Valores de $K_{\mathrm{cal.}}$ y K_{exp}.

S_r	I_0 mA	m min^{-1}	$K_{\mathrm{cal.}}$ min^{-1}	$K_{\mathrm{exp.}}$ min^{-1}	$K_{\mathrm{cal.}}/S_r$
1	12.4	0.070	0.138	0.161	0.138
1.8	21.8	0.115	0.242	0.265	0.135
2.8	34.9	0.160	0.388	0.414	0.137

RENDIMIENTO EN CORRIENTE Y PRODUCTO

La reacción electroquímica que tiene lugar en las disoluciones cianuradas recientes del complejo $\mathrm{Mn(CN)_6K_3}$ a un potencial anódico de +0.20 volts (vs. E.C.S.) puede representarse mediante la ecuación :

$$\mathrm{Mn(III) - Mn(III) - 1e^- \rightarrow Mn(III) - Mn(IV)} \qquad (5)$$

Por tanto, el rendimiento en corriente R_c, en tanto por ciento vendrá definido por la expresión :

$$R_c = \frac{\text{mmoles formados Mn(III)}-\text{Mn(IV)}}{\text{mF de corriente consumidos}} \times 100 \qquad (6)$$

y el rendimiento en producto

$$R_p = \frac{\text{mmoles Mn(III)} - \text{Mn(IV) formados}}{\text{mmoles Mn(III)} - \text{Mn(III) inicial}} \times 100 \qquad (7)$$

Según la ecuación (5) el rendimiento en corriente será del 100 % siempre que la corriente se invierta exclusivamente en la reacción primaria que tiene lugar en el electrodo, es decir, siempre que no se produzca ninguna otra reacción.

Como ya se mencionó anteriormente, a +0.20 volts no se producen corrientes faradaicas, ni tampoco a lo largo de la oxidación electrolítica existen procesos de inducción pues se traduciría en un aumento de los valores iniciales de intensidad de corriente, pudiendose comprobar en todas las experiencias realizadas que dichos valores se mantienen practicamente constantes siempre que lo sean las condiciones de transferencia de masa y la superficie del electrodo. Para concentraciones de CNNa 3M si existe una corriente cinética, en estas condiciones la reacción electroquímica no es estequiométrica y el rendimiento en corriente que es inferior al 100 % se calcula mediante la expresión (6).

El numerador de dicha expresión viene dado experimentalmente por la diferencia entre la cantidad de Mn(III)–Mn(III) inicial y la que queda sin oxidar, puesto que la evolución paralela (decoloración) es despreciable en estas condiciones:

$$\begin{aligned} \text{mmoles formados Mn(III)} - \text{Mn(IV)} &= \\ \text{mmoles iniciales Mn(III)} - \text{Mn(III)} &- \\ - \text{mmoles finales Mn(III)} - \text{Mn(III)} & \qquad (8) \end{aligned}$$

Teniendo en cuenta la proporcionalidad existente entre intensidades y concentraciones

$$\text{mmoles formados Mn(III)} - \text{Mn(IV)} =$$

$$= \text{mmoles iniciales Mn(III)} - \text{Mn(III)} \text{-mmoles iniciales Mn(III)} - \text{Mn(III)} \cdot$$

$$\cdot \frac{i_K}{i_0} = \text{mmoles iniciales Mn(III)} - \text{Mn(III)} \, \frac{i_0 - i_K}{i_0} \qquad (9)$$

El denominador de la ecuación (6) (Q_{exp}) es necesario obtenerlo por integración, ya que la representación de log i frente a t no es lineal. Sustituyendo (9) en (6) resulta:

$$R_c = \frac{\text{mmoles iniciales Mn(III)} - \text{Mn(III)} \; \dfrac{i_0 - i_K}{i_0}}{Q_{\text{exp}}} \times 100 \qquad (10)$$

expresión mediante la que se calcula el rendimiento en corriente cuando este es inferior al 100 % (en presencia de corriente cinética).

En rendimiento en producto se calcula a partir de la expresión (7). Cuando la reacción electroquímica es estequiométrica, $k_c = 100\ \%$, la cantidad formada de Mn(III) – Mn(IV) equivale a la corriente consumida, por lo que el numerador de la expresión (7) viene dado por :

$$\text{mmoles formados Mn(III)} - \text{Mn(IV)} = Q_{\text{exp}} \tag{11}$$

y la expresión (7), se transforma en :

$$R_p = \frac{Q_{\text{exp}}}{\text{mmoles iniciales Mn(III)} - \text{Mn(III)}} \times 100 \tag{12}$$

Si el rendimiento en corriente es inferior al 100 % la cantidad formada de Mn(III) – Mn(IV) se calcula a partir de la expresión (9), con lo que la ecuación (7) se transforma en :

$$R_p = \frac{i_0 - i_K}{i_0} \times 100 \tag{13}$$

Resultados obtenidos

El rendimiento en producto aumenta inicialmente al aumentar la concentración de CNNa (Figura 6), debido a que la evolución de Mn(III) – Mn(III), paralela a la oxidación electrolítica, es tanto más lenta cuanto mayor es la concentración de cianuro del medio. No obstante para cianuro 3M ó mas concentrado, se pone de manifiesto la corriente cinética de regeneración de Mn(III)–Mn(III), con lo que el rendimiento en producto vuelve a disminuir. El rendimiento en corriente es inferior al 100 % para concentraciones de cianuro elevadas (Figura 7), condiciones en las que corriente cinética tiene lugar con magnitud apreciable.

Para todos los valores de fuerza iónica estudiados, el rendimiento en producto aumenta al hacerlo la fuerza iónica, como puede verse en la Figura 8. La falta de cuantitatividad en la electrolisis se debe exclusivamente al proceso de decoloración, cuya velocidad disminuye al aumentar la fuerza iónica. El rendimiento en corriente, al no existir corriente cinética es para todos los casos del 100 %.

Al aumentar la temperatura, disminuye el rendimiento en producto, ya que la velocidad del proceso de decoloración se intensifica (Figura 9). Como para los valores de temperatura estudiados no se aprecia practicamente proceso cinético de regeneración, el rendimiento en corriente es del 100 % para todos los casos.

Un aumento de la superficie del electrodo, se traduce en un rendimiento en producto más elevado, ya que, al ser menor el tiempo de electrolisis, menor es también la cantidad de Mn(III)–Mn(III) decolorada. El rendimiento en corriente es siempre del 100 %.

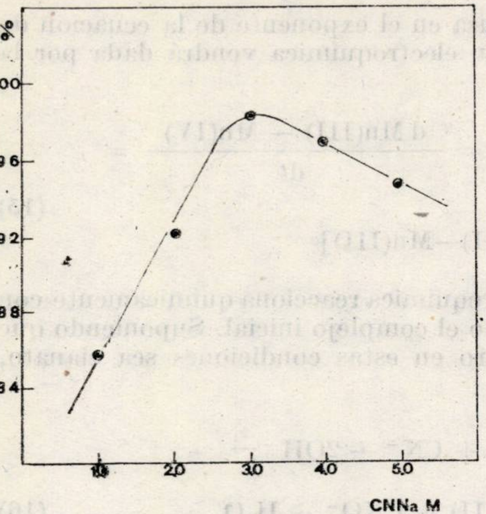

Fig. 6. — Rendimiento en producto. Influencia de la concentración de CNNa.

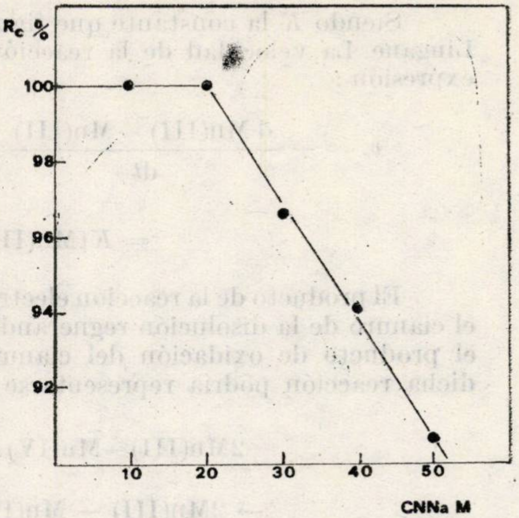

Fig. 7. — Rendimiento en corriente. Influencia de la concentración de CNNa

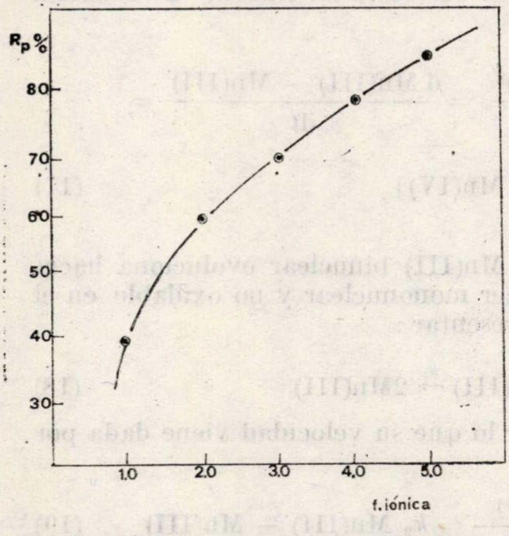

Fig. 8. — Rendimiento en producto. Influencia de la fuerza iónica.

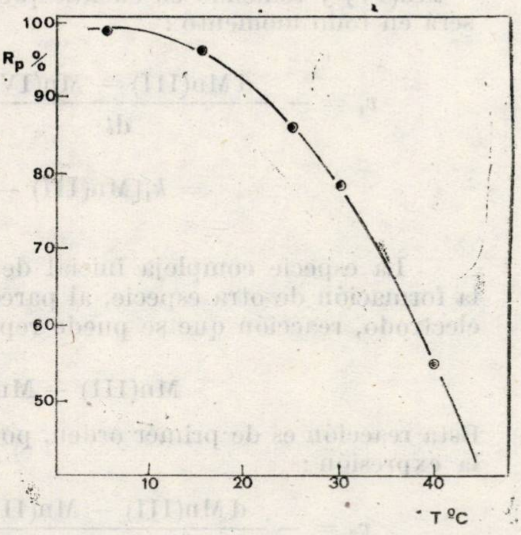

Fig. 9. — Rendimiento en producto. Influencia de la temperatura.

MECANISMOS

Como ya se mencionó anteriormente, la oxidación electrolítica del complejo cianurado binuclear de manganeso (III) a un potencial anódico de + 0.20 conduce a la formación de un complejo binuclear de valencia mixta Mn(III)—Mn(IV) :

$$\mathrm{Mn(III)}-\mathrm{Mn(III)}-1e^- \xrightarrow{K} \mathrm{Mn(III)}-\mathrm{Mn(IV)} \qquad (14)$$

Siendo K la constante que figura en el exponente de la ecuación de Lingane. La velocidad de la reacción electroquímica vendrá dada por la expresión :

$$v_e = -\frac{\mathrm{d\,Mn(III)-Mn(III)}}{\mathrm{d}t} = \frac{\mathrm{d\,Mn(III)-Mn(IV)}}{\mathrm{d}t} = K[\mathrm{Mn(III)-Mn(III)}] \qquad (15)$$

El producto de la reacción electroquímica reacciona químicamente con el cianuro de la disolución regnerando el complejo inicial. Suponiendo que el producto de oxidación del cianuro en estas condiciones sea cianato, dicha reacción podría representarse :

$$\mathrm{2Mn(III)-Mn(IV) + CN^- + 2OH^-} \xrightarrow{k_1} \mathrm{2Mn(III) - Mn(III) + CNO^- + H_2O} \qquad (16)$$

Si la reacción es de primer orden con respecto al complejo Mn(III) — Mn(IV) y teniendo en cuenta que el $\mathrm{CN^-}$ está en exceso, su velocidad será en todo momento :

$$v_1 = -\frac{\mathrm{d\,Mn(III)-Mn(IV)}}{\mathrm{d}t} = \frac{\mathrm{d\,Mn(III)-Mn(III)}}{\mathrm{d}t} = k_1[\mathrm{Mn(III)-Mn(IV)}] \qquad (17)$$

La especie compleja inicial de Mn(III) binuclear evoluciona hacia la formación de otra especie, al parecer mononuclear y no oxidable en el electrodo, reacción que se puede representar :

$$\mathrm{Mn(III) - Mn(III)} \xrightarrow{k_2} \mathrm{2Mn(III)} \qquad (18)$$

Esta reacción es de primer orden, por lo que su velocidad viene dada por la expresión :

$$v_2 = -\frac{\mathrm{d\,Mn(III)-Mn(III)}}{\mathrm{d}t} = k_2\ \mathrm{Mn(III) - Mn(III)} \qquad (19)$$

El conjunto de estas tres reacciones que tienen lugar simultáneamente puede representarse por el siguiente esquema :

$$\begin{tikzcd}
\mathrm{Mn(III)-Mn(III)} \arrow[r, "k_2"] \arrow[d, shift left, "k_1"] & \mathrm{2Mn(III)} \\
\mathrm{Mn(III)-Mn(IV)} \arrow[u, shift left, "K"]
\end{tikzcd}$$

Deducción de las ecuaciones corriente-tiempo

La intensidad de corriente que pasa por el circuito será proporcional a la velocidad de la reacción electroquímica y por tanto a la concentración de la especie electroactiva Mn(III) — Mn(III) :

$$i = K_d[\mathrm{Mn(III)} - \mathrm{Mn(III)}] \tag{20}$$

donde K_d, constante de proporcionalidad entre intensidad y concentración ha sido evaluada voltamétricamente.[4]

La velocidad global, expresada mediante la variación de la concentración del complejo inicial Mn(III) — Mn(III) con respecto al tiempo, vendrá dada por :

$$v = v_e - v_1 + v_2 \tag{21}$$

es decir :

$$v = -\frac{\mathrm{d\,Mn(III) - Mn(III)}}{\mathrm{d}t} = (K + k_2)[\mathrm{Mn(III)} - \mathrm{Mn(III)}] - $$

$$- k_1[\mathrm{Mn(III)} - \mathrm{Mn(IV)}] \tag{22}$$

La integración de esta ecuación es complicada, pero puede llevarse a cabo de manera aproximada teniendo en cuenta que, para concentraciones de cianuro sódico 2.0 M o inferior la reacción redox del complejo Mn(III) — Mn(IV) con el cianuro (16) tiene lugar a velocidad despreciable en comparación con otras reacciones, mientras que para cianuro $\geqslant$ 3.0 M es la evolución de la especie compleja inicial (18) la reacción cuya velocidad es prácticamente despreciable. En consecuencia se pueden plantear dos casos particulares :

1. *Para* $CN^- \leqslant 2M$, se cumple $v_1 \ll v_e$ y $v_1 \ll v_2$
por lo que la ecuación (22) se transforma en :

$$v = (K + k_2)[\mathrm{Mn(III)} - \mathrm{Mn(III)}] \tag{23}$$

separando variables e integrando, se obtiene después de sustituir en (20) :

$$i = K_d[\mathrm{Mn(III)} - \mathrm{Mn(III)}]_0 \cdot \mathrm{e}^{-(K+k_2)t} \tag{24}$$

donde $[\mathrm{Mn(III)} - \mathrm{Mn(III)}]_0$ es la concentración inicial de la especie electroactiva.

2. *Para* $CN^- \geqslant 3M$, se cumple $v_2 \ll v_c$ y $v_2 \ll v_1$
por lo que la ecuación (22) se transforma en :

$$v = K[\mathrm{Mn(III)} - \mathrm{Mn(III)}] - k_1{=}\mathrm{Mn(III)} - \mathrm{Mn(IV)}] \tag{25}$$

por otra parte en las condiciones experimentales de $\mathrm{CN}^- \geqslant$ 3.0 M, prácticamente el proceso de decoloración no ocurre, por lo que

$$[\mathrm{Mn(III)} - \mathrm{Mn(IV)}] = [\mathrm{Mn(III)} - \mathrm{Mn(III)}]_0 - [\mathrm{Mn(III)} - \mathrm{Mn(III)}] \tag{26}$$

stituyendo la expresión (26) en (25) e integrando y posteriormente sutituyendo en (20):

$$i = K_d[\mathrm{Mn(III)} - \mathrm{Mn(III)}]_0 \frac{1}{K + k_1} [k_1 + K \cdot e^{-(K+k_1)t}] \tag{27}$$

Comprobación

Para comprobar la validez de las ecuaciones propuestas para la intensidad en función del tiempo en $CN^- \leqslant 2M$(24) y en $CN^- \geqslant 3M$ (27), se han calculado los valores de i a diferentes tiempos para concentraciones de CNNa, 1, 2, 3, 4 y 5M y se han representado junto con los datos experimentales (Figura 10). Los resultados obtenidos permiten apreciar una buena concordancia entre los valores teóricos y experimentales, de donde puede afirmarse que los mecanismos propuestos así como las ecuaciones deducidas

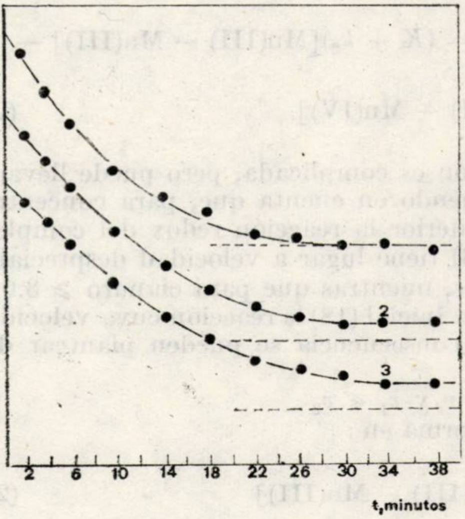

Fig. 10. — Valores de i experimentales y calculados para distintas concentraciones de CNNa.

1. CNNa 1.0 M; 2. CNNa 3.0 M; 3. CNNa 5,0 M

— Valores experimentales

● Valores calculados

Cálculo de las constantes de las reacciones interferentes

1. Cálculo de k_2

La constante de velocidad de la reacción de transformación del complejo binuclear de manganeso (III) hacia la especie no oxidable, puede calcularse a partir de la ecuación (24), pues de la representación lineal se deduce el valor de la pendiente:

$$K_{\mathrm{exp}} = K + k_2 \tag{28}$$

de donde se deduce el valor de k_2. Los valores de K son los obtenidos teoricamente, K_{calc}. Los valores obtenidos para k_2 en las distintas condiciones experimentales se representan en la Tabla 5 junto con los obtenidos por Lopez Cueto [1] por un método amperométrico y como puede comprobarse son concordantes.

2. Cálculo de k_1

Para calcular la constante de velocidad de la reacción entre el complejo Mn(III) — Mn(IV) y el CN^- de la solución, se ha hecho uso de la ecuación (27), pues para $[CN^-] \geqslant 3M$ y para tiempos infinitos (valor constante para la intensidad, i_K) se obtiene

$$i_K = i_0 \frac{k_1}{K + k_1} \tag{29}$$

donde : i_K es el valor final constante de la intensidad de corriente
K, el valor hasta ahora denominado K_{cal}.

En la tabla 6 se muestran los valores de k_1 obtenidos mediante la expresión (29).

Tabla 5

Cálculo de la constante k_2 para diferentes condiciones experimentales

		$k_{exp.}$ min^{-1}	K min^{-1}	$k_2 \cdot 10^3$ min^{-1}	$k_2 \cdot 10^3$ min^{-1} (*)
CNNa M	1.0	0.161	0.138	23	15.0
	2.0	0.150	0.137	13	8.4
f. iónica	1.0	0.391	0.155	236	140.6
	2.0	0.254	0.150	104	112.4
	3.0	0.219	0.148	71	69.6
	4.0	0.184	0.143	41	44.2
	5.0	0.161	0.138	23	19.0

*) Valores obtenidos por Lopez Cueto por un procedimiento espectrofotométrico.

Tabla 6

Cálculo de la constante k_1 para concentraciones de CNNa igual o superiores a 3.0 M.

CNNa M	I_0 m A	I_k m A	K min^{-1}	$K_1 \cdot 10^3$ min^{-1}
3.0	12,4	0.2	0.138	2.3
4.0	12.4	0.4	0.138	4.6
5.0	12.4	0.6	0.138	7.0

BIBLIOGRAFIA

[1] G. Lopez Cueto, Doctoral Tesis. Salamanca (1972).

[2] G. Brauer, "Química Inorgánica Preparativa", Ed. Reverté, Barcelona, 1958.

[3] G. Lopez Cueto y J. Hernandez Mendez, *Quim. Anal.*, **28**, 106 (1974).

[4] G. Lopez Cueto y A. Alonso Mateos, *Anl. Lett.*, **11**, 43 (1978).

[5] G. Lopez, Cueto y A. Alonso Mateos, *Stvdia Chemica*, **VI**, 55 (1975).

[6] L. Meites. y S. A. Moros, *Analyt. Chem.*, **31**, 23 (1959).

Revue Roumaine de Chimie, **30**, *11–12*, 933–939 (1985)

ELECTROCHEMICAL INVESTIGATION OF THE OXYGEN INTERACTION WITH SILVER CATALYSTS

VALENTINA LĂZĂRESCU *, M. VASS *, O. RADOVICI **, CORNELIA DAȘOVEANU***, MAGDALENA STANCIU *** and M. TOLAN ***

* ICECHIM – Center of Physical Chemistry, Spl. Independenței 202, Bucharest 15, Romania 77208

** IPB – National Institute of Chemistry, Faculty of Chemical Technology, Chemistry Department, Bucharest, Romania

*** Central Institute of Chemistry, I.C.I.T.P.R. Ploiești, Romania

Received June 30, 1984

Cyclic voltammetry has been used to investigate the oxygen interaction with silver catalysts in KOH solutions. This study revealed the existence of two layers of Ag_2O, a surface one and a subsurface one. It was found that the amount of subsurface Ag_2O is greater in the presence of Cl^-, suggesting a close relation to the catalyst selectivity in the ethylene epoxidation.

The utility of the electrochemical techniques for the study of the catalysts surface has been often pointed out in recent years. Giving information concerning the processes involved in the surface species adsorption/desorption and metal oxidation/reduction phenomena, the cyclic voltammogram may be considered a genuine finger-print [1] for a definite surface. Therefore, the cyclic voltammetry could become a useful instrument for the characterization of the bulk and supported metal catalysts.

In the present paper, we report the results obtained in the study of the oxygen interaction with silver catalysts by cyclic voltammetry.

EXPERIMENTAL

Cyclic voltammograms for silver catalysts were obtained using a Tacussel Bipotentiostat Type Bipad coupled with a Tacussel GSTP—2A1 waveform generator and were registered with an X—Y Hewlett-Packard recorder Type 7001 AM.

The measurements were performed in stationary 1M KOH and 1M KOH + KCl (Chemapol pro analyse reagents) solutions in twice distilled water, at room temperature, in a three-electrode cell of conventional design. The working electrode potential was measured versus a saturated calomel electrode (SCE). Samples of 10 mg catalyst powder with definite particle size ($\leqslant$ 0.06 mm) placed on a 1.2 cm^2 platinum sheet represented the test electrode. The catalyst used in these studies was 15.5% $Ag/\alpha Al_2O_3$ obtained by a usual impregnation technique. When no other mention is made, the catalyst was held into the hydrogen evolution region for 15 minutes prior to the first run, in order to remove the oxygen sorbed in the sample.

In some experiments, a polycrystalline silver 0.1 mm sheet (Goodfellow Metals 99.95%) with a geometric surface area of 1.1 cm^2 was used as working electrode. The silver electrode was washed before each experiment in a mixture of H_2O_2 : NH_4OH : H_2O (1 : 1 : 4) and rinsed several times with twice distilled water.

The potential sweeps were constantly carried out with a sweep rate of 10 mV/s in a potential range limited to the first step of the anodic oxidation of silver (— 0.35 to + 0.45 V vs SCE).

RESULTS

A typical cyclic voltammogram for a catalyst containing 15.5% Ag/αAl_2O_3 is shown in Fig. 1, in comparison with that of a polycrystalline smooth silver electrode, in 1M KOH. The two curves resemble closely : the same three peaks are seen in the anodic branch of each of them, only peak 2*a* is better shaped in the catalyst case.

The potentials at which peaks appear on the direct and reverse sweeps are highly reproducible but the peak currents exhibit a discernable time dependence, particularly for the catalyst electrode. In this case, the anodic peak areas and therefore, the coulombic charges *Q* involved in the corresponding electrode processes, decreased markedly during the first runs. This diminution is more pronounced in the second cycle, as it can be seen in Table 1, but only for peaks 2a and 3a. The charge under the first peak Q_{1a} has not been significantly changed during these repeated sweeps.

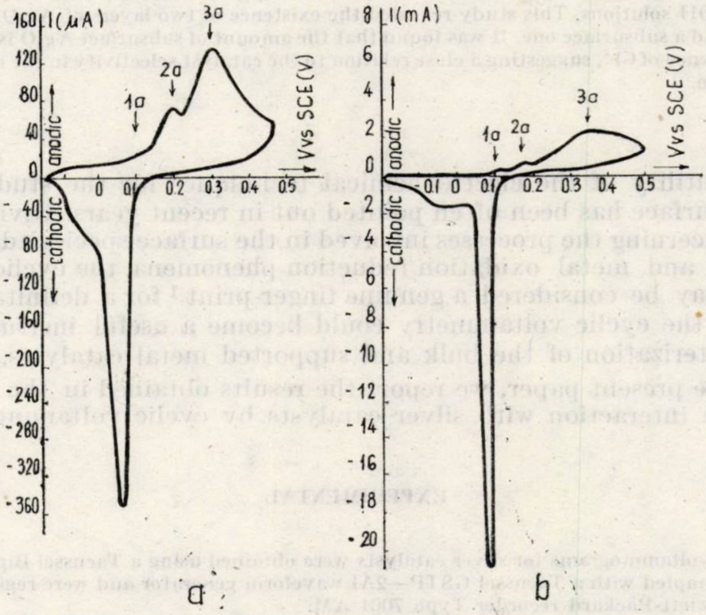

Fig. 1. — Typical cyclic voltammograms for : a) 15.5% Ag/αAl_2O_3 and b) polycrystalline silver electrode, in 1M KOH at a sweep rate of 10 mV s^{-1}.

The curves were found to be superimposable after 7—8 cycles. In the stationer voltammogram, the coulombic charge involved in the second anodic process Q_{2a} decreased at about one third and that corresponding to the third anodic peak Q_{3a} at about half in respect of the values noted in the first cycle. This phenomenon is closely related with the fact that the total anodic charge Q_a is greater than the cathodic one Q_c in all the cycles performed. This difference is greatest in the first run, as it can also be observed in Table 1.

Table 1

The influence of the repeated potential sweeps on the coulombic charge Q involved in the anodic oxidation of the catalyst 15.5 % Ag/α Al_2O_3 in 1M KOH

Cycle	Coulombic charge (mC)		
	Q_{2a}	Q_{3a}	Q_a/Q_c
1	1.24	4.24	1.82
2	0.72	3.08	1.51
8 (stationer)	0.40	2.20	1.19

The shape of the current-potential curve is strongly dependent in the catalyst case on the surface pre-treatment too. In order to remove the oxygen sorbed in the sample, this was held into the hydrogen region for various periods of time prior to the first run. It has been observed that Q_{2a} and Q_{3a} have increased but not in same way. As seen in Fig. 2 Q_{2a} measured in the first cycle is increasing steadily as long as the period of treatment increases, as Q_{3a}, measured in the same conditions, reaches a constant value after a treatment of 15 minutes. This phenomenon suggests a slower rate of releasing the reaction sites for process 2*a*.

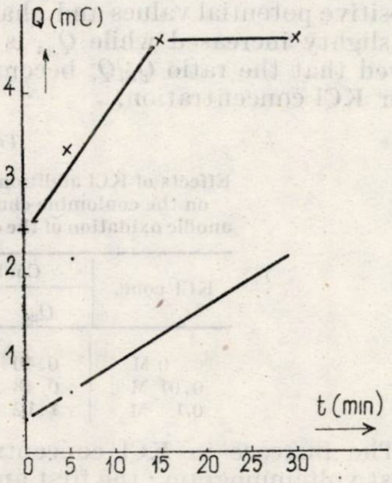

Fig. 2. — Variations of the coulombic charge Q involved in the anodic processes 2*a* (●) and 3*a*(×) in the first cycle performed after different periods of H_2 evolution.

Performing the potential sweeps in KOH solutions containing different amounts of KCl, new changes appear in the catalyst voltammogram. The effect of Cl^- ions upon the electrode processes taking place in the anodic oxidation of silver catalyst is illustrated in Fig. 3 for two KCl concentrations : 0.01 M and 0.1M. It can be observed that the presence of the smaller KCl concentration brings about a shift of the third anodic peak towards less positive potential values and changes of Q_{2a} and Q_{3a}. As seen in Table 2, Q_{2a} is slighty increased while Q_{3a} is markedly reduced. It has been also observed that the ratio Q_a/Q_c becomes unitary in solution containing the smaller KCl concentration.

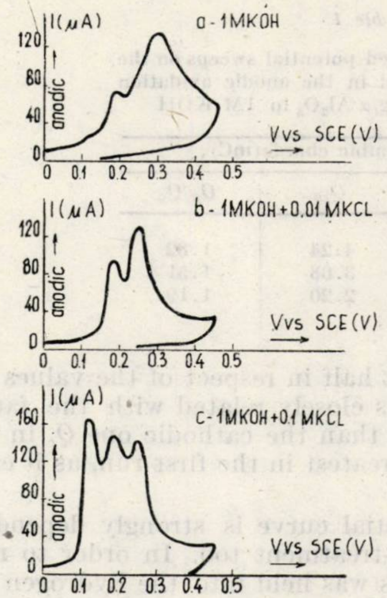

Fig. 3. — Typical voltammograms for 15.5% $Ag/\alpha Al_2O_3$ in a) 1M KOH b) 1M KOH + 0.01 M KCl c) 1M KOH + 0.1 M KCl at a sweep rate of 10 mVs^{-1}.

Table 2

Effects of KCl additions to the base electrolyte on the coulombic charge Q involved in the anodic oxidation of the catalyst 15.5 % $Ag/\alpha Al_2O_3$

KCl conc.	Coulombic Charge (mC)		
	Q_{2a}	Q_{3a}	Q_a/Q_c
0 M	0.40	2.20	1.19
0.01 M	0.48	1.40	1.00
0.1 M	1.12	1.36	1.10

The increase in KCl concentration yields further changes of the catalyst voltammogram : the first anodic peak is, somewhat unexpectedly, greatly enhanced and Q_{2a} continues to raise up. The only process unaffected in these conditions is 3*a*, keeping constant both the position and the involved charge. The total anodic charge Q_a is again greater than the cathodic one Q_c.

DISCUSSION

It is well established [2–12] that the first stage of the anodic oxidation of Ag in alkaline solutions is Ag_2O formation. Usually, this phenomenon is characterized by two peaks, when investigated by a potential sweep method [2,5,7,8,11]. There are however, several reports [2,5,7,13,14] concerning a third minor peak prior to these two main ones. This was considered to be either the result of the carbonate impurities, [7] an artifact due to the metal fabrication, [5,13] or it was simply ignored.[2,14]

Recent investigations[15] of the influence of the carbonate traces in 1M KOH on the smooth polycrystalline silver electrode voltammogram, in solutions containing up to 10% K_2CO_3, have shown however, that the interaction between CO_3^{2-} ions and Ag surface yields only a slight decrease of the usual oxidation peaks. Moreover, as the results reported here show, the peak 1*a* is present on the smooth silver electrode as well as on the catalyst electrode, revealing the weakness of the previous suppositions.

Careful studies performed in our laboratory[15] have pointed out the conditions favourable to process 1*a* (high KOH or KCl concentration) showing that the Faradaic dissolution of silver as $Ag(OH)_2^-$ is fitted the best to the characteristics revealed :

$$Ag \rightleftharpoons Ag^+ + e^- ;\ Ag^+ + 2HO^- \rightarrow Ag(OH)_2^- \tag{1}$$

Our results are in a good agreement with both the predicted behaviour[16] which indicated that in alkaline solutions, dissolution should precede the lowest oxide formation and the conclusions of the Faradaic impedance measurements,[10] namely that dissolution takes place before the phase formation on the silver electrode.

The hydroxy complex ions $Ag(OH)_2^-$ may diffuse away into solution or discharge themselves on the electrode in the next step, together with HO^- ions :

$$Ag + Ag(OH)_2^- \rightleftharpoons Ag_2O + H_2O + e^- \tag{2}$$

$$2Ag + 2HO^- \rightleftharpoons Ag_2O + H_2O + 2e^- \tag{3}$$

The oxidation of Ag to Ag_2O takes place in two steps, as a lot of galvanostatic,[21] potentiodynamic [7,9,11] and Faradaic impedance[7,9,10,17–20] studies have shown. These are represented by peaks 2*a* and 3*a* in the silver voltammogram. The more anodic peak (3*a*) is generally recognized to correspond to the formation of a thick Ag_2O layer[5,7,8,11,12] but the more cathodic one (2*a*) has been variously assigned as AgOH, [2,5] H_{ads} [12] or $Ag(OH)_2^-$. [7,8,10,11]

The electron and X-ray diffraction and electron microscopy investigations [3] on the texture, growth and orientation of the anodically formed Ag_2O showed, however, a quite clear evidence for two types of Ag_2O, making a distinction between the initial dense thin layer (estimated variously as 3–100 layers[21,22]) and the thick porous layer, subsequently formed.

The experimental results presented here have pointed out certain features of the process corresponding to peak 2*a*. It has been observed that this is favoured both by the more porous structure of the catalyst, being better shaped in its voltammogram and the increased surface roughness resulted after the enhanced dissolution of silver in higher Cl^- concentration. We have also to add the slower rate of releasing the reaction sites for this process, mentioned before. All these experimental facts suggest, in our opinion, the formation of a subsurface oxide layer, as a result of the oxygen atoms penetration in the silver lattice. Development of such a layer is certainly favoured by a greater number of lattice defects and its reduction needs a longer period of time to allow O^{2-} diffusion-migration towards the surface.

The occurrence of process 2*a* is limited by O^{2-} diffusion in the silver lattice. Therefore, when the electrode potential becomes more positive, the kinetics of silver oxidation is changed : oxygen remains on the surface and Ag^+ cations diffuse this time through the initial dense layer up to the surface[4,7-19]. It is also important to mention here the observation that the $Ag(OH)_2^-$ discharge (2) could be regarded as a process of silver lattice reconstruction coupled with a simultaneous oxygen atoms incorporation.

The existence of the subsurface oxygen is generally accepted in all recent studies of the oxygen interaction with silver.[23-26] Modern methods of the surface physics (LEED,[23] HREELS,[24] IS,[25] TPD[26]) revealed three distinct species in oxygen adsorption on silver : a diatomic oxygen, stable only at $T \leqslant 173K$, a monoatomic chemi-adsorbed oxygen in fourfold coordination and a subsurface oxygen. Recent investigations on the reactivity of the oxygen adsorbed on silver in the epoxidation of ethylene [27,28] have pointed out the important result that the ethyleneoxide is formed only if both surface (chemi-adsorbed) and subsurface oxygen are present.

It is also well known the fact that small amounts of some elements added to silver increase the catalyst selectivity in the reaction mentioned above. In this context, the effects of Cl^- addition (one of the most frequent catalyst activator used) to the base electrolyte, on the two anodic oxidation processes leading to Ag_2O, become interesting. The results presented in Tab. 2 show that small amounts of Cl^-(0.01M) yield a slight increase of the subsurface oxide in contrast with the surface oxide which is markedly reduced. The inhibition of the surface oxide formation has the same origin as the pronounced decrease of the amount of the monoatomic chemiadsorbed oxygen observed in the system $Ag/O_2 + Cl_2$. [29] The chlorine preadsorption on the silver surface reduces the number of the four bare neighbouring silver atom assemblies required by O^{2-} ions, fourfold coordinated both on a silver surface [29] and in the Ag_2O lattice. The slight increase of the amount of oxygen penetrating the silver lattice may be, on the other hand, the consequence of the electrostatic repulsions enhanced by the Cl^- ions preadsorption on the surface. It should also be mentioned that only in the presence of this small amount of Cl^- (0.01M) the total cathodic charge becomes equal to the anodic one, suggesting changes in Ag—O bond strength. Tëmkin's supposition, [30] according to which, the increase in the surface coverage with such an electronegative element results in a lowering of the reactive oxygen bond strength, facilitating its participation in reaction is thus in a good agreement with our results. This phenomenon may be the result of the change undergone by the Fermi level position, the most important factor in determining the catalyst properties in some authors' opinion.[28] The fact that process *3a* is taking place at potentials less positive in presence of Cl^- ions is probably due to the same modification of the electronic structure.

CONCLUSIONS

The anodic oxidation of a catalyst containing $15.5\,\%$ $Ag/\alpha Al_2O_3$ in 1M KOH, between the limits $-\ 0.35 + 0.45$ V (SCE) leads to the formation of two layers of Ag_2O, a subsurface one and a surface one, preceded by a minor process of silver dissolution. The addition of small amounts of Cl^- to the base electrolyte, changes the ratio of the two Ag_2O layers, weakening, at the same time, the Ag—O bond strength. By these results, the cyclic voltammetry proved to be a sensible method for studies of the silver catalyst surface properties, useful in investigations concerning the factors contributing to its performances.

REFERENCES

[1] R. Parsons, *Surface Sci.*, **101**, 316 (1980).

[2] T. P. Dirkse and D. B. De Vries, *J. Phys. Chem.*, **63**, 107 (1959).

[3] G. W. D. Briggs, M. Fleischmann, L. J. Lax and H. R. Thirsk, *Trans. Faraday Soc.*, **64**, 3120 (1968).

[4] M. Fleischmann. D. J. Lax and H. R. Thirsk. *Trans. Faraday Soc.*, **64**, 3128 (1968).

[5] P. Stonehart, *Electrochim. Acta*, **13**, 1789 (1968).

[6] T. P. Dirkse, D. De Wit and R. Shoemaker, *J. Electrochem. Soc.*, **114**, 1196 (1967).

[7] B. V. Tilak, R. S. Perkins, H. A. Kozlowska and B. E. Conway, *Electrochim. Acta*, **17**, 1447 (1972).

[8] B. G. Pound, D. D. Macdonald and J. W. Tomlinson, *Electrochim. Acta.*, **25**, 563 (1980).

[9] Z. Takehara, Y. Namba and S. Yoshizawa, *Electrochim. Acta*, **13**, 1395 (1968).

[10] R. D. Giles, J. A. Harrison and H. R. Thirsk, *J. Electroanal. Chem.*, **22**, 375 (1969).

[11] R. D. Giles and J. A. Harrison, *J. Electroanal. Chem.*, **27**, 161 (1970).

[12] T. G. Clarke, N. A. Hampson, J. B. Lee, J. R. Morley and B. Scanlon, *Canad. J. Chem.*, **46**, 3437 (1968).

[13] P. Stonehart and F. P. Portante, *Electrochim. Acta*, **13**, 1805 (1968).

[14] B. Miller, *J. Electrochem. Soc.*, **117**, 491 (1970).

[15] V. Lăzărescu, O. Radovici and M. Vass, to be published.

[16] B. C. Pound, D. D. Macdonald and J. W. Tomlinson, *Electrochim. Acta*, **24**, 929 (1979).

[17] B. N. Kabanov and D. I. Leiks, *Z. Electrokem.*, **62**, 660 (1958).

[18] D. I. Leiks G. L. Vidovitch, L. L. Kuoz and B. N. Kabanov, *Z. Physik. Chem. (Leipzig)*, **214**, 334 (1960).

[19] G. L. Vidovitch, D. L. Leiks and B. N. Kabanov, *Doklady Akad. Nauk SSSR*, **124**, 855 (1959).

[20] G. L. Vidovitch, D. I. Leiks and B. N. Kabanov, *Doklady Akad. Nauk SSSR*, **142**, 109 (1962).

[21] A. Hickling and C. Taylor, *Discuss. Faraday Soc.*, **1**, 277 (1947).

[22] B. D. Cahan, J. B. Ockerman, F. F. Amlie and P. Ruetschi, *J. Electrochem. Soc.*, **107**, 725 (1960).

[23] W. M. H. Sachtler, C. Backx and R. A. Van Santen, *Catal. Rev.*, **23**, 127 (1981).

[24] R. W. Joyner and M. W. Roberts, *Chem. Phys. Lett.*, **60**, 459 (1979).

[25] M. H. Barteau and R. J. Madix, *Surface Sci.*, **97**, 101 (1980).

[26] G. Rovida, F. Pratesi and E. Ferroni, *Appl. Surface Sci.*, **5**, 121 (1980).

[27] C. Backs, J. Moolhuysen, A. Geenfen and R. A. Van Santen, *J. Catal.*, **72**, 364 (1981).

[28] R. Haul, D. Hoge, G. Neubauer and U. Zeeck, *Surface Sci.*, **122**, LL 622 (1982).

[29] P. A. Kilty, N. C. Rol and W. M. H. Sachtler, in : "Proc. 5th Internat. Congress Catal., Palm Beach 1972" Palm Beach 1973, Paper 64.

[30] M. I. Tëmkin, *Adv. Catal.*, **28**, 173 (1979).

important factor in determining the catalyst properties in some authors opinion.[27] The fact that process 3a is taking place at potentials less positive in presence of Cl⁻ ions is probably due to the same modification of the electronic structure.

CONCLUSIONS

The anodic oxidation of a catalyst containing 13.0% Ag α-Al$_2$O$_3$ in 1M KOH, between the limits — 0.35 + 0.45 V (SCE) leads to the formation of two layers of Ag$_2$O, a subsurface one and a surface one, preceded by a minor process of silver dissolution. The addition of small amounts of Cl⁻ to the base electrolyte changes the ratio of the two Ag$_2$O layers, weakening at the same time, the Ag—O bond strength. By these results, the cyclic voltammetry proved to be a sensible method for studies of the silver catalyst surface properties, useful in investigations concerning the factors contributing to its performances.

REFERENCES

[1] R. Fausch, Surface Sci. 101, 418 (1980).
[2] T. P. Gilkes and D. D. De Vries, J. Phys. Chem., 63, 107 (1959).
[3] G. W. D. Briggs, J. Fleischmann, D. J. Lax and H. R. Thirsk, Trans. Faraday Soc., 64, 3120 (1968).
[4] M. Fleischmann, D. J. Lax and H. R. Thirsk, Trans. Faraday Soc., 64, 3128 (1968).
[5] P. Stonehart, Electrochim. Acta, 13, 1789 (1968).
[6] R. P. Larkin, D. De Witt and R. Shoemaker, J. Electrochem. Soc., 111, 1180 (1964).
[7] B. V. Tilak, R. S. Perkins, H. A. Kozlowska and B. E. Conway, Electrochim. Acta, 17, 1447 (1972).
[8] B. G. Pound, D. D. Macdonald and J. W. Tomlinson, Electrochim. Acta, 25, 563 (1980).
[9] Z. Takehara, Y. Nambu and S. Yoshizawa, Electrochim. Acta, 13, 1295 (1968).
[10] B. D. Giles, J. A. Harrison and H. R. Thirsk, J. Electroanal. Chem., 20, 475 (1969).
[11] B. D. Giles and J. A. Harrison, J. Electroanal. Chem., 27, 161 (1970).
[12] P. G. Clarke, N. A. Hampson, J. B. Lee, J. R. Morley and B. Scanlon, Canad. J. Chem. 46, 3437 (1968).
[13] P. Stonehart and F. P. Portante, Electrochim. Acta, 13, 1805 (1968).
[14] B. Miller, J. Electrochem. Soc., 117, 491 (1970).
[15] V. Cărăușescu, G. Hadovici and M. Vass, to be published.
[16] B. G. Pound, D. D. Macdonald and J. W. Tomlinson, Electrochim. Acta, 24, 929 (1979).
[17] B. N. Kabanov and D. I. Leikis, Z. Elektrochem., 62, 660 (1958).
[18] D. I. Leikis, G. L. Vidovitch, L. L. Knots and B. N. Kabanov, Z. Physik. Chem. (Leipzig) 214, 334 (1960).
[19] G. L. Vidovitch, D. I. Leikis and B. N. Kabanov, Doklady Akad. Nauk SSSR, 124, 855 (1959).
[20] G. L. Vidovitch, D. I. Leikis and B. N. Kabanov, Doklady Akad. Nauk SSSR, 142, 109 (1962).
[21] A. Hickling and D. Taylor, Discuss. Faraday Soc., 1, 277 (1947).
[22] B. D. Cahan, J. B. Ockerman, R. F. Amlie and P. Ruetschi, J. Electrochem. Soc., 107, 725 (1960).
[23] W. M. H. Sachtler, C. Backx and R. A. Van Santen, Catal. Rev., 23, 127 (1981).
[24] R. W. Joyner and M. W. Roberts, Chem. Phys. Lett., 60, 459 (1979).
[25] M. H. Barteau and R. J. Madix, Surface Sci., 97, 101 (1980).
[26] G. Rovida, F. Pratesi and E. Ferroni, Appl. Surface Sci. 5, 121 (1980).
[27] C. Backx, J. Moolhuysen, A. Geenen and R. A. Van Santen, J. Catal., 72, 364 (1981).
[28] R. Haul, D. Hoge, G. Neubauer and U. Zeeck, Surface Sci. 122, L622 (1982).
[29] P. A. Kilty, N. C. Rol and W. M. H. Sachtler, in: "Proc. 5th Internat. Congress Catal., Palm Beach 1972" Palm Beach 1973, Paper 64.
[30] M. Kilty, Adv. Catal., 28, 173 (1979).

Revue Roumaine de Chimie, **30**, *11–12*, 941–947 (1985)

CONDUCTOMETRIC STUDY OF ION-ION AND ION-SOLVENT INTERACTIONS. II.*

CONDUCTANCES OF TRICHLOROACETIC ACID IN METHANOL-WATER MIXTURES AT 25°C

U.G. KRISHNAM RAJU, B. SETHURAM and T. NAVANEETH RAO
Department of Chemistry, Osmania University, Hyderabad-500 007, India

Received July 15, 1980
Revised February 2, 1984

Conductances of trichloroacetic acid in methanol-water mixtures were measured at 25°C. The association constants and molar conductances at infinite dilution were calculated using the Fuoss-Hsia equation with Fernandez-Prini coefficients. The association constants of the acid were found to be 7.18 in 20% MeOH, 12.80 in 40% MeOH, 32.94 in 60% MeOH and 96.53 $dm^3\ mol^{-1}$ in 80% MeOH at 25°C. These association constant values were compared with those predicted by Bjerrum, Fuoss, Denison-Ramsey and Ebeling-Kraeft-Yokoyama-Yamatera theories. The experimental results are in better agreement with the predictions of Denison-Ramsey theory. The Walden products were calculated and the results are interpreted to find the nature of the ion-ion and ion-solvent interactions and the structure of the ion-pairs.

Trichloroacetic acid (TCA) is used in biology and medicine as precipitant of proteins and fixative in microscopy. It is suitable as titrant for bases like amines and amino acids in non-aqueous solvents. [1] Conductances of TCA were studied in acetone, butanol and formamide. [2,3] Aqueous solutions of the acid were studied by pH, Raman and NMR methods. [4,5] The dissociation constants were reported in methanol [6] and higher alcohols using indicator methods. [7] Thus it is evident that these studies were confined to the solutions of TCA in pure solvents only. It is well known that the solvent mixtures offer a wide and continuous range of dielectric and viscous properties that are not accessible for pure solvents. Therefore in the present study the conductances of TCA in mixtures of water with a protic solvent i.e. methanol were determined with a view to study the possible ion-ion and ion-solvent interactions solutions and also to estimate the association constants. Conductometry was used because it is a very sensitive physical method for studying electrolyte solutions and a precision of ± 0.05 % could be obtained without much difficulty. Conductance data obtained were analysed using the Fuoss-Hsia equation[8] with Fernandez-Prini coefficients. Apart from, discussing the applicability of various theories of ion-pair formation such as those of Bjerrum,[10] Fuoss,[11] Denison-Ramsey [12] (DR) and Ebeling-Kraeft-Yokoyama-Yamatera (EKYY), [13,14] the Walden products were also evaluated to get an insight into the possible ion-solvent interactions and structure of the ion-pairs.

---

* Part I, *Bull. Chem. Soc.* (Japan), **52** (1979) 3076.

EXPERIMENTAL

Trichloroacetic acid (E. Merck) was purified as reported earlier[15]. Methanol (BDH electrolyte grade) was used without further purification. The specific conductance of this was found to be 5.0×10^{-8} Scm^{-1}. Water with a specific conductance less than 5×10^{-7} Scm^{-1} was used. Due correction was made for the solvent conductance values of all salt solutions, All solutions were prepared freshly just before use. Experimental arrangement was the same as reported earlier[16]. The overall accuracy of the measured molar conductances was better than $\pm 0.05\%$ and had a reproducibility of $\pm 0.1\%$.

RESULTS AND DISCUSSIONS

The molar conductances of the solutions of TCA in 20, 40, 60 and 80 % (w/w) methanol-water mixtures at 25°C are given in Table 1. The dielectric constants and viscosities of the methanol-water mixtures were taken from the literature.[17] The conductance data were analysed using the Fuoss-Hsia equation[8] with Fernandez-Prini coefficients[9] as in the following :

$$\Lambda = \Lambda_0 - s(\alpha c)^{1/2} + E\alpha c \ln(\alpha c) + J_1 \alpha c - J_2(\alpha c)^{3/2} - K_A \Lambda y_{\pm}^2 \alpha c) \qquad (1)$$

where the various symbols have their usual significance. The activity coefficients ($y_{\pm}$) were calculated by the equation

$$-\log y_{\pm} = A(\alpha c)^{\frac{1}{2}} / \{1 + Ba(\alpha c)^{\frac{1}{2}}\} \qquad (2)$$

Eq (1) was solved as originally described by Justice.[18] The procedure envisages the replacement of the distance of closest approach of ions (a) by the Bjerrum critical distance (q). The standard deviation (σ) values were calculated from the relation

$$\sigma = \{\Sigma(\Lambda_{\mathrm{exp}} - \Lambda_{\mathrm{cal}})^2/(N - 3)\}^{\frac{1}{2}} \qquad (3)$$

All the calculations were done on TDC−12 Computer and the results are recorded in Table 2. The association parameters of TCA in water are also presented in this table for the sake of comparison. These results are taken from our earlier work. [15]

The functional dependence of log K_A on $1/D$ was used to test the applicability of various theories of ion-pair formation. A linear plot passing through origin is expected according to the DR theory whereas Fuoss theory predicts a straight line with a finite intercept. Bjerrum and EKYY theories predict curves which are concave downwards. The least square regression

Table 1

Conductances of trichloroacetic acid in methanol — water mixtures at 25°C

20 % MeOH – H_2O $D = 69.75$ $\eta = 0.01400$ poise		40 % MeOH–H_2O $D = 60.93$ $\eta = 0.01593$ poise		60 % MeOH – H_2O $D = 51.67$ $\eta = 0.01410$ poise		80 % MeOH – H_2O $D = 42.60$ $\eta = 0.01050$ poise	
10^5 c	Λ	10^5 c	Λ	10^5 c	Λ	10^5 c	Λ
mol dm^{-3}	S cm^2 mol^{-1}	mol dm^{-3}	S cm^2 mol^{-1}	mol dm^{-3}	S cm^2 mol^{-1}	mol dm^{-3}	S cm^2 mol^{-1}
116.09	234.57	211.07	150.56	217.13	114.29	277.16	79.523
99.506	234.92	180.91	151.17	186.11	115.20	245.49	80.016
87.068	235.29	158.30	151.76	162.85	115.86	214.80	81.464
77.393	235.68	140.71	152.20	144.76	116.55	190.93	82.488
69.654	235.84	126.64	152.59	130.28	117.28	171.84	83.554
58.045	236.24	105.53	153.14	108.57	118.02	143.20	84.977
49.753	236.61	90.457	153.28	93.057	118.64	122.74	86.177
43.534	236.87	79.150	153.70	81.425	119.29	107.40	87.402
38.697	237.10	70.356	154.00	72.378	119.65	95.467	88.359
34.827	237.26	52.767	154.80	65.140	120.10	85.920	88.983
29.023	237.68	45.229	155.24	54.283	120.67	71.600	90.002
21.767	237.97	39.575	155.67	46.529	121.17	61.371	91.098
		33.681	155.87	40.713	121.58	53.700	91.881

Table 2

Association parameters and Walden products of TCA for $a = q$

Solvent	a/A	Λ_0 S cm^2 mol^{-1}	K_A dm^3 mol^{-1}	σ	$\Lambda_0\,\eta$
Water	3.578	385.05	3.532	0.193	3.428
20% MeOH	4.003	239.86	7.180	0.085	3.358
40% MeOH	4.598	157.95	12.80	0.210	2.516
60% MeOH	5.423	124.91	32.94	0.129	1.761
80% MeOH	6.578	98.307	96.53	0.377	1.032

line required by the experimental points had a correlation coefficient of 0.997 and had a definite intercept. In the dielectric constant range 40—80 all the expressions except DR predict almost the same magnitude for K_A for a given value of a in the range of 1.0 to 20A. It appears from fig. 1 that experimental K_A values coincide with K_B and K_{EKYY} suggesting the applicability of Bjerrum and EKYY theories also. But the plot of log K_A vs $1/D$ is a straight line with a near unity correlation coefficient indicating either DR or Fuoss theory to be more appropriate. Both these theories predict a slope of $|Z_+Z_-|e^2/2.303\ a\ k\ T$ but intercepts predicted by these two theories are different. The Fuoss theory predicts an intercept of $\log 4\pi Na^3/3000$ whereas DR theory predicts the intercept to be zero. The experimental line had a slope of 131.7 and an intercept of —1.0714. Therefore, the Fuoss theory predicts different a values of 1.85A and 3.83A from the slope and intercept values of the same plot for the same ion-pair studied. On the other hand the finite intercept of the experimental line could be accommodated in the modified DR expression as

$$\log K_A = -\ 1.0714 + 131.7/D \tag{4}$$

$$\text{or } K_A = 0.1418 \exp(303.4/D) \tag{5}$$

$$\text{and } a = 1.85\text{Å}$$

Eq (5) is similar to the modified DR expression[19] as

$$K_A = K_A^0 \exp(|Z_+\,Z_-|e^2/a\ D\ k\ T) \tag{6}$$

The expression (6) could be obtained by adding a pre-exponential factor i.e., K_A^0 to DR expression for K_A. The physical significance of introducing this pre-exponential factor is that the forces involved in ion-pair formation are not purely electrostatic as assumed in the derivation of the simple DR expression. Further, the pre-exponential in the Fuoss expression is an explicit function of the ion-size parameter (a) and may lead to different and contradictory a values from the slope and intercept values of the same equation for the same ion-pair. This inconsistant feature can be tacitly circumvented by eq. (6) in which the pre-exponential factor which is an arbitary adjustable parameter depending on the solute-solvent system under consideration, was added. Hence DR theory may be considered as more flexible and convenient to apply for various solute-solvent systems.

Alternatively, the ion-size parameter (a_K) required to give experimental K_A values were calculated *via* the various theories. The Fuoss, Bjerrum and EKYY theories required the a values in the range of 0.90 to 1.38 Å whereas DR theory required 2.88 to 5.67 Å. The effective ion-size parameter for trichloroacetate ion was taken as equal to that of acetate ion i.e., 1.27 Å. As the radius of proton is of the order of 0.0001 Å, it was neglected as compared to the radius of trichloroacetate ion and the a value of trichloroacetic acid was taken as 1.27 Å. As the a of TCA is 1.27 Å, an a value of <1.27Å for H^+ TCA^- is incompatible. Therefore, it is clear that DR theory is in better agreement with the experimental results than all the other theories compared, because getting >1.27Å for a can be explained by considering the solvent separated ion-pairs. Theoretical $\log K_A$ *vs* $1/D$ plots according to Bjerrum, Fuoss, DR and EKYY theories using 1.27 Å for a are also shown in Fig. 1.

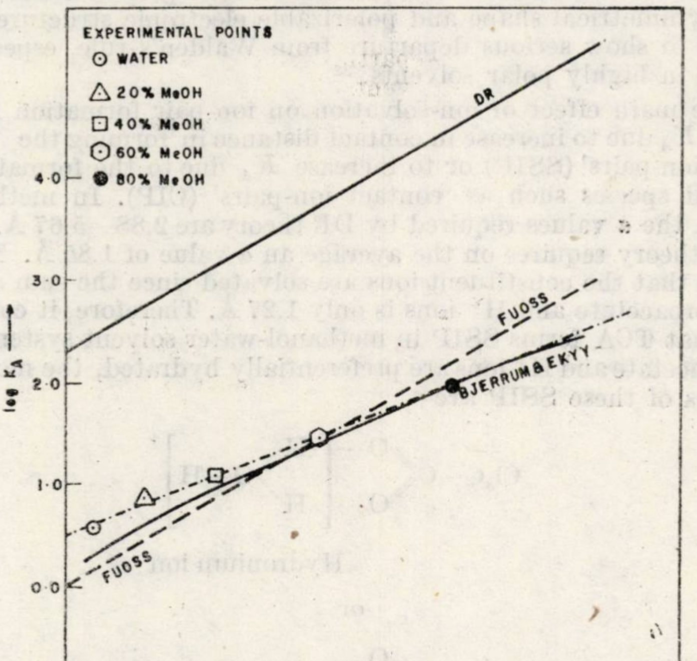

Fig. 1

The Walden products [20] for TCA in methanol-water mixtures are presented in Table 2. These values reveal that as we go from water to higher percentages of methanol, the Walden products decrease abnormally i.e.,

$\Lambda_0\eta$ decreases more than the decrease expected by the changes in viscosities of the solvent mixtures. This could be explained on the basis of proton jump mechanism. It is quite probable that the acid conductance mechanism in alcohol solvents is similar to that in water. Even then, the rate determining step consists of the orientation of ROH molecules in the field of ROH_2^+ ions followed by the classical proton transfer. In this aqueous alcoholic solutions the equilibrium

$$ROH_2^+ + H_2O \rightleftharpoons ROH + H_3O^+$$

is set up and lies far to the right since H_2O is relatively a stronger base than MeOH. Thus, when small amounts of water are added to alcoholic acid solutions the water molecules steal protons from ROH_2^+ ions thereby diminishing the extent of $ROH_2^+ - ROH$ proton jumping. The proton jumping from H_3O^+ ions to alcoholic molecules is energetically unfavourable. Addition of more and more water progressively increases the chances of $H_3O^+ - H_2O$ proton transfers and the molar conductance increases steadily as the solvent becomes more and more aqueous. Ions having small size, unsymmetrical shape and polarizable electronic structures would be expected to show serious departure from Walden's rule, especially when dissolved in highly polar solvents. [22]

The main effect of ion-solvation on ion-pair formation is either to decrease K_A due to increase in contact distance in forming the 'solvent separated ion-pairs' (SSIP) or to increase K_A due to the formation of the associated species such as 'contact ion-pairs' (CIP). In methanol-water mixtures, the a values required by DR theory are 2.88 – 5.67 Å. The modified DR theory requires on the average an a value of 1.85 Å. This clearly indicates that the constituent ions are solvated since the sum of the radii of trichloroacetate and H^+ ions is only 1.27 Å. Therefore, it could be concluded that TCA forms SSIP in methanol-water solvent systems. As both trichloroacetate and H^+ ions are preferentially hydrated, the most probable structures of these SSIP are

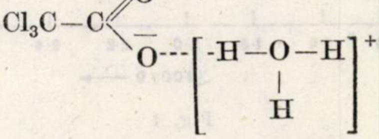

Hydronium ion

or

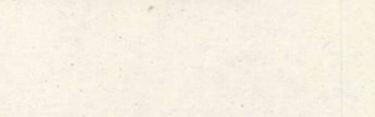

Hydronium ion

ACKNOWLEDGEMENT. One of the authors (U.G.K.R.) is thankful to C.S.I.R, New Delhi for the award of a research fellowship.

REFERENCES

[1] C. A. Streuli, "Treatise on Analytical Chemistry" Part I, Vol. II ed. by I. M. Kolthoff, and P. J., Elving, (John Wileby & Sons, N.Y.) 1975 p. 7059.
[2] H. Hunt and H. T. Briscoe, *J. Phys. Chem.*, **33**, 1945(1929).
[3] H. H. Loyd and J. B. Wiesel, *Carnegie Inst. Pub.* No. 260, 119(1918).
[4] J. Kurtz and J. M. Farrar, *J. Amer. Chem. Soc.*, **91**, 6057(1969).
[5] O. D. Bonner, H. B. Flora and H. W. Aliken, *J. Phys. Chem.*, **75**, 2402 (1971).
[6] H. Goldschmidt and H. Aarflot, *Z. Phys. Chem.*, **117**, 312 (1925).
[7] V. I. Dulova, N. V. Lichkova, N. V. Arkhipova and Sh. R. Tillyashaikhova, *Izv. Vyssh. Ucheb. Laved., Khim. Khim. Tekhn (USSR)*, **11**, 867(1968).
[8] R. M. Fuoss and K. L. Hsia, *Proc. Natl. Acad. Sci. (USA)* **57**, 1550(1966); **58**, 1818 (1967).
[9] R. Fernandez-Prini, *Trans. Faraday, Soc.*, **65**, 3311(1969).
[10] N. Bjerrum, *Kgl. Danske. Vidensk, Selsk*, **7**, No. 9, 1(1926).
[11] R. M. Fuoss, *J. Amer. Chem. Soc.*, **80**, 5059(1958).
[12] J. T. Denison and J. B. Ramsey, *J. Amer. Chem. Soc.*, **77**, 2615(1955).
[13] H. Falkenhagen, W. Ebeling and W. D. Kraeft, "Ionic Interactions", Vol. I ed. by S. Petrucci, (Academic Press, N.Y.), 1971 p. 104.
[14] H. Yokoyama and H. Yamatera, *Bull. Chem. Soc. (Japan)*, **48**, 1970(1975).
[15] U. G. Krishnam Raju, J. Ananthaswamy, B. Sethuram and T. Navaneeth Rao, *Z. Physik. Chem. (Leipzig)*, in press.
[16] J. Ananthaswamy, B. Sethuram and T. Navaneeth Rao, *Indian J. Chem.*, **15A**,9(1977).
[17] a) R. A. Robinson and R. H. Stokes, "Electrolyte Solutions" (Butterworths, London) 1965 p. 457 & 458; b) A. K. Covington and T. Dickinson, "Physical Chemistry of Organic Solvent Systems" (Plenum Press, London & N.Y.) 1973 p. 18. c) R. Parsons, "Handbook of Electrochemical Constants" (Butterwotths, London), 1959 p. 11,
[18] J. C. Justice, *J. Chim. Phys.*, **65**, 353(1968).
[19] J. Ananthaswamy, B. Sethuram and T. Navaneeth Rao, *J. Inorg. Nucl. Chem.*, in press.
[20] P. Walden and E. Birr, *Z. Phys. Chem.*, **153A**, 1(1931).

Revue Roumaine de Chimie, **30**, *11–12*, 949–953 (1985)

DEHYDROGENATION KINETICS OF LOWER ALIPHATIC ALCOHOLS ON COPPER CATALYSTS. I

PREPARATION, STABILISATION AND CATALYTIC ACTIVITY OF PURE COPPER POWDERS

N. DOCA * and E. SEGAL **

* Chemical Research Center, Blvd. Mihai Viteazul 24, Timişoara, R. S. Romania

** Chair of Physical Chemistry and Electrochemical Technology, Faculty of Chemical Engineering, Polytechnical Institute of Bucharest, Blvd Republicii 13, Bucharest, R.S. Romania.

Received October 1, 1984

Metallic powdered copper catalyst was prepared by reduction of CuO with hydrogen, followed by stabilisation against reoxidation (by means of N_2 or CO_2 adsorption). The kinetic parameters for the dehydrogenation of ethyl, *n*-propyl, *i*-propyl, *n*-butyl and 2-butyl alcohols were determined by the chromatographic pulse technique. The fresh copper catalyst is very active, but its activity decreases with the amount of the reactant. The kinetic of the low aliphatic alcohols dehydrogenation is described by a first order equation.

The dehydrogenation of low aliphatic alcohols on metallic catalysts was used as model reaction for testing the general theories of heterogeneous catalysis, mainly the geometric and energetic factors.[1–4]

Kinetic studies were performed with the purpose to find the mechanisms and limiting steps.[5, 6] Thus, on copper catalysts the desorption of the reaction product is the limiting step, and the kinetics is described by Balandin's equation.[7, 8]

These series of works aim:

— to prepare a series of stabilised copper catalysts, containing small amounts of Cr, Mn, Fe and Ni;

— to investigate the kinetics of ethyl, n-propyl, i-propyl, n-butyl and 2-butyl alcohols dehydrogenation on these catalysts, by the chromatographic pulse technique;

— to establish the influence of added transition metal on the copper activity in the dehydrogenation reaction.

CATALYST PREPARATION

The copper oxide was obtained by precipitation of 2n Cu $(NO_3)_2$ solution with a 5n Na_2CO_3 solution at 80° and 8.5–9 final pH value, drying at 60° in vacuum and calcining 5 h at 300°. The prepared copper (II) oxide was reduced to metal and stabilised against later oxidation by nitrogen or carbon dioxide adsorption. The laboratory equipment and operational procedure were described earlier.[9] The experimental conditions were : hydrogen flow : 0.5 mL/s for 10 g copper-oxide ; heating rate up to 400° ≃ 3°/min ; reduction time : 6 h at 400°.

The temperature *vs.* time variation during the stabilisation is presented in figure 1.

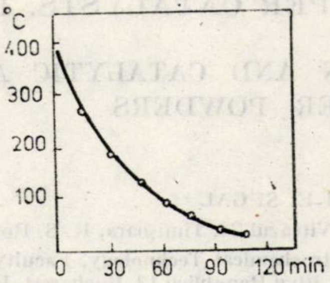

Fig. 1.— Stabilization diagram for the copper catalyst

The laboratory equipment allowed at the same time to check the catalyst stability by measuring the ignition temperature of the stabilisated sample.[9] The catalyst samples exhibited stability up to 200° for carbon dioxide as stabilising gas, and 270° for nitrogen respectively.

KINETICS OF ALCOHOLS DEHYDROGENATION

For the evaluation of the kinetic parameters, the chromatographic pulse technique was used. The alcohol/aldehyde (or ketone) mixture resulted as reactor effluent was separated on a 4 mm diameter, 2 m length steel column packed with 20% Carbowax 101 on Celite 545, at 60° with nitrogen as eluent.

All measurements were performed in the following conditions:

— catalyst weight : 0.150 g ;

— reactor temperatures : 200, 240 and 280°C ;

— eluent flow rates : 60, 90 and 120 mL/min ;

— volume of injected alcohol : 2 μL.

The stability of copper catalyst activity was studied by carrying out successively alcohol injections and determining the corresponding conversions. In figure 2 the conversion decrease *vs.* the injection number is given for isopropylic alcohol dehydrogenation at 200° and 60 mL/min nitrogen. To determine the kinetic parameters of alcohols dehydrogenation on copper catalyst, the initial values of conversion were used.

For a first order kinetic controlled by the surface reaction, the rate constant k is given by[10,11] :

$$k = \frac{q \cdot \ln 1/(1-Z)}{K \cdot V_e} \tag{1}$$

where Z is the reactant conversion, q is the flow rate of carrier gas in reactor (mL/min), $V_c = 0.065$ mL is the catalyst bed volume, and K is the adsorption equilibrium constant (mL of gas/mL of catalyst) determined by means of the reactant retention time in the presence and the absence of catalyst respectively, $K = (t_c - t)/t_c$. The small values of the determined difference $(t_c - t)$ and its random variation increase the uncertainess of the calculated adsorption constant K, thus one has determined the product $kK = (q \cdot \ln 1/(1 - Z))/V_c$.

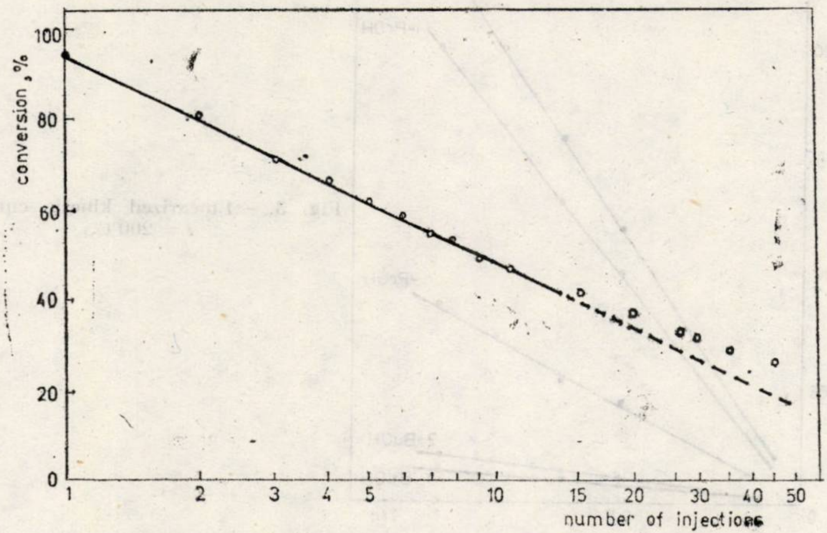

Fig. 2. — Copper catalyst deactivation during the reaction.

The apparent activation energy $E_{ap} = E_a - Q$ (where E_a is the activation energy of the surface reaction and Q is the adsorption heat) was evaluated from the slope of the $\ln kK$ vs $1/T$.

The linearity of the plot $\ln \dfrac{1}{1 - Z}$ v.s. $1/q$ (Fig. 3) shows a first order kinetics. The values of the kinetic parameters are given in table 1.

The value of the apparent activation energy for ethanol dehydrogenation shows a satisfactory agreement with the value obtained in a steady state flow reactor (70.6 kJ/mole). As far as the values of the activation energy for the dehydrogenation of the other alcohols are concerned one can notice a trend to increase from the inferior alcohols to the superior ones. The value of the activation energy for i-Propanol smaller than the corresponding value for n-Propanol should be also noticed.

CONCLUSIONS

1. The possibility to stabilise a freshly prepared copper catalyst against reoxidation by chemisorption of inert gases (nitrogen or carbon dioxyde) was proved.

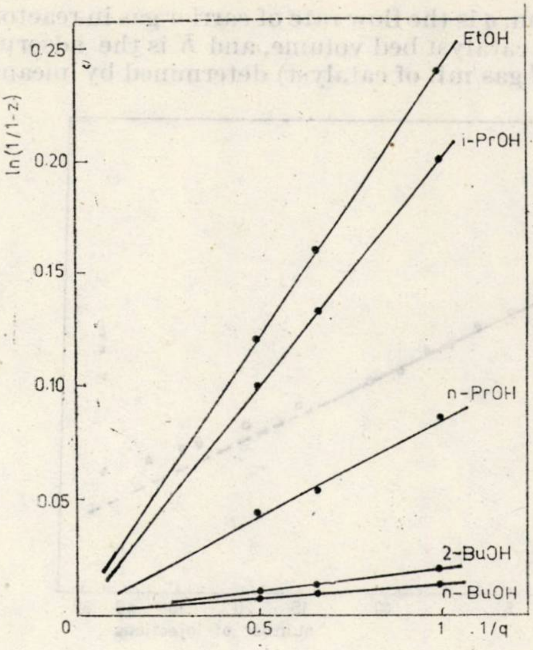

Fig. 3. — Linearized kinetic curve for $t = 200°C$.

Table 1

Kinetic parameters of alcohols dehydrogenation on copper catalyst

Reactant	Temperature °C	$Z = f(q)$, % q, cm³/min 60	 90	 120	$kK \cdot s^{-1}$	E_{ap} kJ/mole
Ethanol	200	21.22	14.74	11.21	3.70	75.5
	240	66.14	51.42	41.81	16.61	
	280	97.96	93.55	85.74	59.74	
n-Propanol	200	8.20	5.53	4.18	2.01	85.0
	240	37.10	26.55	20.66	7.10	
	280	86.10	73.17	62.72	30.26	
i-Propanol	200	18.11	12.41	9.51	3.06	82.4
	240	64.61	50.03	40.56	15.96	
	280	98.60	94.16	86.90	65.36	
n-Buthanol	200	1.24	0.83	0.62	0.19	96.4
	240	8.20	5.54	4.18	1.31	
	280	35.63	25.45	19.77	6.76	
2-Buthanol	200	1.94	1.30	0.98	0.30	92.8
	240	11.74	8.00	6.05	1.92	
	280	45.47	33.25	26.15	9.30	

2. The fresh copper catalyst is very active in the alcohols dehydrogenation but its activity decreases rapidly with the amount of needed reactant.

3. The kinetics of low aliphatic alcohols dehydrogenation is described by a first order equation.

4. The chromatographic pulse technique allowed us a quick and easy determination of the kinetic parameters for all the five investigated dehydrogenation reactions.

REFERENCES

[1] A. A. Balandin, *Uspekhi Khim.*, **31**, 1265 (1962).

[2] A. A. Balandin, "Multipletnaia teoria kataliza", tom. I i II, Izd. MGU, Moskva, 1963.

[3] A. A. Tolstopiatova and A. A. Balandin, "Fizika i fiziko-himia kataliza", ed. S. Z. Roginski and O. V. Krilov, *Izd. Akad. Nauk SSSR*, Moskva, 1960, p. 351.

[4] A. A. Balandin, *Zhur. fiz. Khim.*, **31**, 746 (1957).

[5] Yu. S. Mardoseev, O. G. Grebenscikova, B. V. Erofoev and A. V. Muklasevskii, *Vestnik, Akad. Nauk Belorus. SSSR, Ser. Khim. Nauk*, **2**, 56 (1973).

[6] O. G. Grebnscikova, Yu. S. Mardoseev, G. K. Tvetkova and B. V. Erofoev, *ibid.*, **4**, 14 (1973).

[7] I. Horescu, doct. thesis, Univ. Moscow, 1965.

[8] A. A. Balandin, A. P. Rudenko and. I. Horescu, *Rev. Roumaine. Chim.*, **14**, 619 (1969).

[9] V. Medeleanu, N. Doca, M. Ştefănescu and A. Bibolaru, *Revista de Chimie* (Bucureşti) **30**, 751 (1979).

[10] D. W. Bassett and H. W. Habgood, *J. Phys. Chem.*, **64**, 769 (1960).

[11] A. G. Gaziev, B. I. Filinovskii and M. I. Ianovskii, *Kinetica i kataliz.*, **4**, 688 (1963).

Revue Roumaine de Chimie, **30**, *11–12*, 955–961 (1985)

THE INFLUENCE OF THE Co(II) IONS ON THE $PbSO_4/PbO_2$ ELECTRODE IN SULPHURIC ACID SOLUTIONS

*) S. STERNBERG, *) V. BRÂNZOI, **) A. MATEESCU and ***) L. APĂTEANU

*) Dept. of Physical Chemistry, The Polytechnic Institute of Bucharest, Romania

**) Acumulatorul'' Enterprise, Bucharest, Romania

***) The Institute of Chemical and Biochemical Energetics, Bucharest, Romania

Received April 24, 1984

The influence of cobalt sulphate, in small amounts, on the polarization behaviour of the lead electrode in sulphuric acid solutions was studied using the potentiodynamic method. The lead microelectrode was cycled within the potential range of + 800 mV to + 1650 mV and back to + 800 mV.

The analysis of potentiograms shows the increase of the microelectrode capacity with the number of cycles, as well as the decrease of the overvoltage of the oxygen evolution and the reduction of the microelectrode capacity at the cobalt sulphate addition.

INTRODUCTION

The peculiar importance of lead acid batteries as power sources lead to the considerable development of studies concerning the influence of different additives in paste or in electrolyte on the performances of the batteries. Literature data [1–10] also refers to the corrosion resistance of the lead grids of the batteries, as a function of different alloying elements as well as of the presence of some additives in paste or in electrolyte.

In the present paper the influence of cobalt sulphate addition on the polarization behaviour of the lead electrode in a solution of sulphuric acid (of a density of $\rho = 1.24$ g/cm^3) within a potential range varying from + 800 mV to + 1650 mV and back to + 800 mV, was studied.

This potential range has been chosen because the potential scan studied (way and back) within this range very well simulates the processes occurring at the positive plate of the acid battery during the charging-discharging cycles.

EXPERIMENTAL PART

In order to test the polarization curves in the above mentioned potential range the potentiodynamic technique was used. For this purpose an "Orion" type pulse generator was coupled with 179 Model-Princeton Applied Research Potentiostat and this one with the working cell with three electrodes and with an x-y recorder. The totalisation of the triangular pulses of the generator with the constant and continuous pulse of the potentiostat resulted in a potential scan from + 800 mV to + 1650 mV and back to + 800 mV (this represented a cycle). The

scheme of the electronic device and of the polarization cell was described in detail in an earlier paper.[11] It must be mentioned that in order to study the influence of the cobalt sulphate the microelectrode tehnique was used, that is : the working electrode was made of a lead wire with the length of 1.5 cm and the diameter of 1 mm. This microelectrode was placed in the center of the cell and was surrounded by a platinum net which acted as counterelectrode. The $Hg/Hg_2SO_4/H_2SO_4$ 4.15 M electrode was used as reference electrode. A Haber — Luggin capillary was used in order to connect the cell compartment with the reference electrode. The experiments were carried out in a $\rho = 1.24$ g/cm^3 solution of sulphuric acid without cobalt sulphate and with different amounts of cobalt sulphate. A number of 10 cycles was done for each determination, in order to obtain a porous, active and reproducible surface of the microelectrode. The potential scan of the lead microelectrode was done with a constant rate of 400 mV/min. Potentiograms were automatically registered by means of an x-y recorder and the potential of the working electrode was measured, all the time, by means of an electronic voltmeter, versus the above mentioned reference electrode. For each solution, for each concentration of cobalt sulphate solution respectively, several determinations were done till a good reproducibility of the results was obtained. The electricity amount used during the anodic and cathodic processes, as well as the whole cycle, were automatically registered by means of the coulometric module of the potentiostat. The temperature in the working cell was maintained at a constant value of 20°C, by means of a UM-210, thermostat, with a precision of ± 0,01°C.

RESULTS AND DISCUSSIONS

In a previous paper, [17] we had shown that in sulphuric acid solutions, free of additives as a result of the successive recyclings, the $PbO_2/PbSO_4$ electrode capacity (measured by Q_c) increases progressively and a porous microelectrode with a sufficiently high capacity and with reproducible properties obtains, after about ten cycles. A similar behaviour can be seen in sulphuric acid solutions with $CoSO_4$ addition, as indicated in Fig. 1.

Figure 1 shows comparatively the polarization curves of the lead microelectrode in a solution of H_2SO_4 (1.24 g/cm^3 $= 4.15$ M) $+ 4 \cdot 10^{-4}$ M $CoSO_4$ (*a*, *b* and *c*) and in "pure" sulphuric acid solution (Fig. 1 *d*). Analysis of the potentiograms from the figure shows that at the first cycle (Fig. 1 *a*) during the anodic increasing potential scan (the dashed curve) no maximum of current obtains.

Within the ($+800 \div +1350$) mV potential range, the current has a very small value. This is the passive range. The microelectrode surface is covered by a dense and compact layer of lead sulphate which hinders the ions penetrability to the lead microelectrode, resulting in a very small current intensity.

At potential values higher than + 1350 mV (Fig. 1 *a*) a sudden increase of the current occurs, as a result of the oxygen evolution, simultaneously with the oxidation of the lead sulphate layer to α- and β-PbO_2.[11-15] At the reverse potential scan, from + 1650 mV to + 800 mV there appear for the first cycle, three maxima of current denoted by P, M and N. The (P) peak, which appears at a potential of + 1200 mV, during the reverse potential scan, is an oxidation peak corresponding to the remanent oxidation of the lead sulphate layer (unoxidated during the increasing anodic scan) to lead bioxide. This oxidation peak is immediatly followed ($\Delta E_p \cong$ $\cong 30$ mV) by a reduction (M) peak, representing the formed PbO_2 reduction, respectively the Pb^{4+} to Pb^{2+} reduction. The (M) peak area was coulometrically measured (Q_c) and represents the microelectrode capacity. $Q_c \ll Q_a$ because at the anodic polarization a high fraction of the current

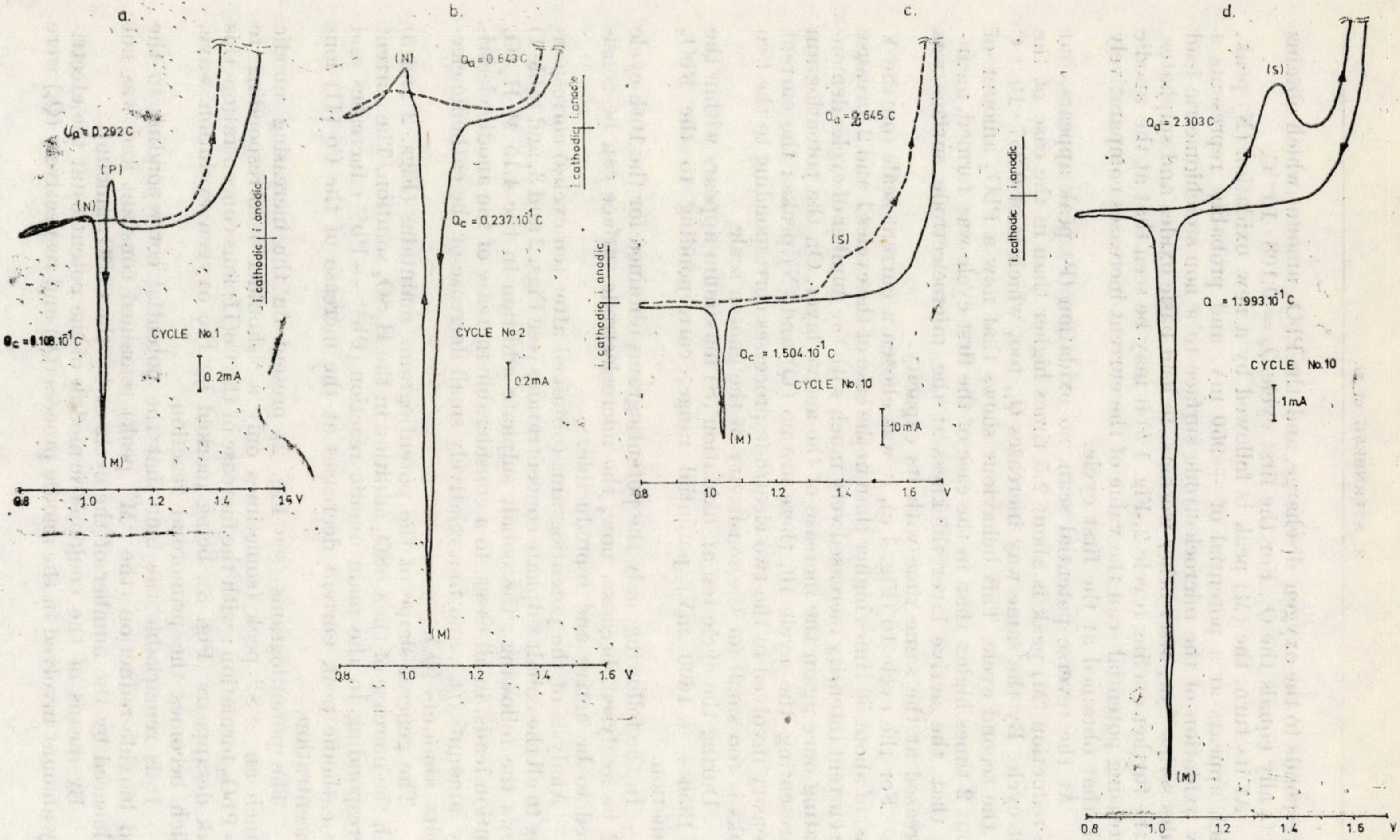

Fig. 1. — The potentiograms of the pure lead in: *a*, *b*, and *c*—1.24 g/cm³ H_2SO_4 solution containing 4.10^{-4} M $CoSO_4$; *d* — 1.24 g/cm³ H_2SO_4 solution. The potential scan rate = 400 mV/min.

corresponds to the oxygen discharge, and the PbO_2 amount which obtains practically equals the Q_c. For the first cycle $Q_c = 0.108 \cdot 10^{-1}C$.

At its turn, the (M) peak is followed by a new oxidation (N) peak, which appears at a potential of + 950 mV and probably represents a new oxidation of the microelectrode surface to a non stoichiometric lead oxides series[16] or, after other workers, to lead basic oxides and sulphates. At the further cycling (cycle 2, Fig. 1 *b*) it may be seen that at the anodic increasing potential scan the value of the current increases comparatively with that obtained at the first cycle.

At the reverse potential scan, no oxidation (P) peak appears, but the reduction (M) peak is about 2.5 times higher than in the case of the first cycle. By the same way increases Q_c, too, which is of $0.237 \cdot 10^{-1}$ C for the second cycle. This behaviour shows that now a PbO_2 amount of about 2 times higher than in the case of the first cycle was formed, meaning that the active layer thickness at the microelectrode surface was increased at the same time with its capacity.

For the cycle 10 (Fig. 1 c), it was chosen a current scale (on the Y axis) of about 50 times higher than in the case of the cycles 1 and 2, because the current intensity increased very much with the number of cycles demonstrating once again the increase of the active layer. On the potentiogram representing the cycle 10, there are no (Q) and (N) peaks : the current intensity involved in the two electrode processes corresponding to the two peaks is too small for the sensitivity of the chosen scale.

During the cycle ten an oxidation (S) maximum appears within the $(+1350 \div +1600$ mV) potential range, corresponding to the PbO_2 formation.

In the following, only the potentiograms obtained for the 10th cycle will be analysed, because, now, the microelectrode surface can be considered to be active and reproducible.

Analysis of the potentiograms (obtained after ten cycles) corresponding to all the cobalt sulphate concentrations (see Figs. 2 and 3, and table 1) shows the following : the cobalt sulphate addition in the 4.15 M H_2SO_4 solution leads, in all cases, to a considerable increase of the anodic electricity amounts (Q_a), and to a relatively small decrease of the cathodic electricity amounts (Q_c).

The general shape of the potentiograms maintains (Figs. 2 and 3) with the increase of the $CoSO_4$ addition in the H_2SO_4 solution. The current corresponding to the main anodic reaction ($Pb^{2+} \rightarrow Pb^{4+}$) increases and the cathodic peak current decreases at the increase of the Co (II) ions concentration.

The potentiograms (see Fig. 2) present on the increasing anodic branch an "S" peak (sometimes only a "shoulder") corresponding to the PbO_2 formation ; with the increase of the Co(II) ions concentration this peak desappears (Fig. 3), being marked by the oxygen evolution wave, which becomes the primordial reaction.

It is remarkable the fact that the potential corresponding to the lead bioxide reduction (the "M" peak) remained constant and was not influenced by the number of the cycle or by the $CoSO_4$ amount.

By means of the coulometric module of the potentiostat the electricity amount involved in the anodic process (Q_a) and respectively (Q_c) were

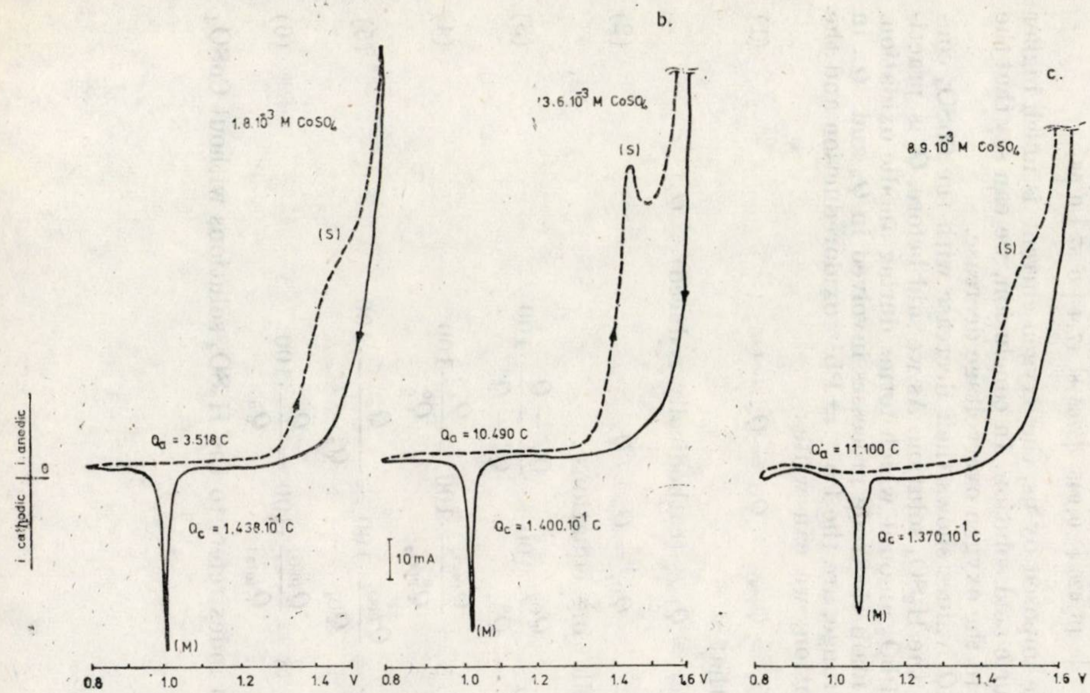

Fig. 2 — The potentiograms of the pure lead (for the cycle 10) in 1.24 g /cm³ H_2SO_4 solution + $xCoSO_4$: *a* — *x* = 1.8. 10^{-3} M ; *b* — *x* = 3.6. 10^{-3}M ; *c* — *x* = 8.9. 10^{-3}M. The potential scan rate = 400 mV/min.

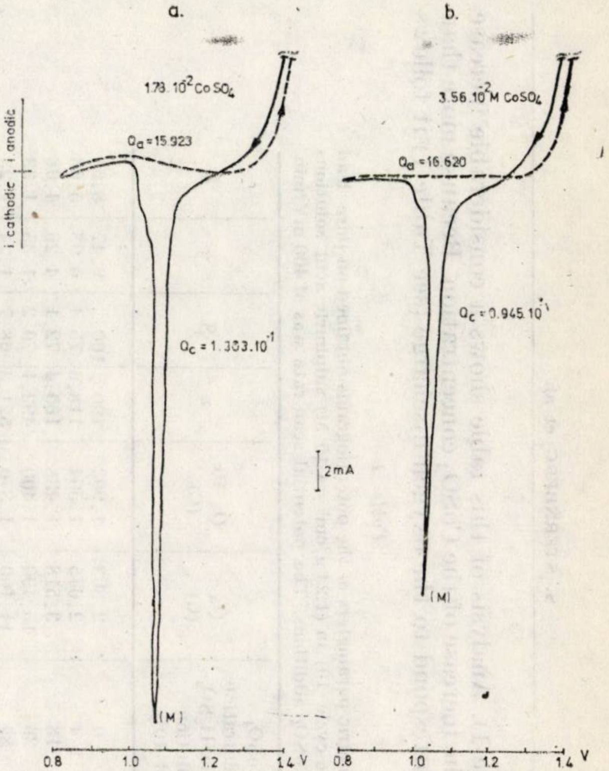

Fig. 3 — The potentiograms of the pure lead (for the cycle 10) in 1.24 g/cm³ H_2SO_4 solution + x $CoSO_4$: *a* — *x* = =1.78. 10^{-2}M ; *b* — *x* = 3.56. 10^{-2} M. The potential scan rate = 400 mV/min.

measured (Table 1). Analysis of this table shows a considerable increase of the Q_a with the increase of the $CoSO_4$ concentration. Because more than 90% from Q_a correspond to the oxygen discharge (see Table 1) it follows that at an overvoltage imposed by us, the oxygen current is much higher than in "pure" sulphuric acid solution. In conclusion, we can say that the $CoSO_4$ addition leads to the oxygen overvoltage decrease.

Table 1

Coulometric parameters of the potentiograms obtained on pure lead (for the cycle 10) in ($1.24\ g/cm^3 = 4.15\ M$) sulphuric acid solutions with $CoSO_4$ additions. The potential scan rate was of 400 mV/min.

$CoSO_4$ concentration in the H_2SO_4 solution ($M \cdot 10^4$)	Q_a (C)	$Q_c \cdot 10$ (C)	α	β	γ	δ
0	2.303	1.993	100	100	9.47	8.65
4	2.645	1.504	118.6	75.4	6.03	5.68
18	3.518	1.438	160.4	72.1	4.26	4.08
36	10.490	1.400	492.1	70.2	1.35	1.33
89	11.100	1.370	521.3	68.7	1.24	1.23
178	15.923	1.320	750.9	65.3	0.82	0.81
356	16.620	0.945	785.8	47.4	0.57	0.56

Analysis of the Q_c values shows their decrease with the $CoSO_4$ concentration increase in the H_2SO_4 solution. As we said before, Q_c is practically equal with the PbO_2 amount which forms during anodic oxidation. Considering that the main electrode processes involved in Q_a and Q_c, in the studied potential range, are the $Pb^{2+} \rightleftarrows Pb^{4+}$ oxidoreduction and the gaseous oxygen evolution, we can write:

$$Q_a = Q_{PbO_2} + Q_{O_2} = Q_c + Q_{O_2} \tag{1}$$

where we considered that:

$$Q_{PbO_2}(\text{anodic}) = Q_{PbO_2}\ (\text{cathodically reduced}) = Q_c$$

Hence:

$$Q_{O_2} = Q_a - Q_c \tag{2}$$

We can write the following equations:

$$\alpha = \frac{Q_{O_2}}{Q^0_{O_2}} \cdot 100 = \frac{Q_a - Q_c}{Q^0_a - Q^0_c} \cdot 100 \tag{3}$$

$$\beta = \frac{Q_{PbO_2}}{Q^0_{PbO_2}} \cdot 100 = \frac{Q_c}{Q^0_c} \cdot 100 \tag{4}$$

$$\gamma = \frac{Q_{PbO_2}}{Q_{O_2}} \cdot 100 = \frac{Q_c}{Q_a - Q_c} \cdot 100 \tag{5}$$

$$\delta = \frac{Q_{PbO_2}}{Q_{\text{total}}} \cdot 100 = \frac{Q_c}{Q_a} \cdot 100 \tag{6}$$

where the "o" superior index refers to the H_2SO_4 solutions without $CoSO_4$ addition.

The coulometric "ratios", α, β, γ, δ, defined by (3) ÷ (6) equations can give interesting information regarding the influence of different factors on the electrode processes. Table 1 gives the coulometric ratios, α, β, γ, δ calculated with the equations presented before. The α ratio increases at the $CoSO_4$ addition and at the maximum concentration of the addition, becomes of about 800 % higher comparatively with the "pure" H_2SO_4 solution. Hence, there is a remarkable decrease of the oxygen overvoltage in the presence of the $CoSO_4$, the Co ion being an electrocatalyser for the oxygen evolution reaction.

The β ratio decreases at the $CoSO_4$ addition, but only with maximum 50 % in the studied concentration range.

The decrease of Q_{PbO_2} amount can be explained by the fact that in solutions containing $CoSO_4$ the oxidation process, $Pb^{2+} \rightarrow Pb^{4+}$, is disfavoured comparatively with the oxygen discharge process. The ratio between Q_{PbO_2} and Q_{O_2} (γ) is of about 10 % in pure H_2SO_4 solution, but becomes only 0.57 % in the solution with the maximum concentration of the additive.

The δ coulometric ratio has a similar evolution with the $CoSO_4$ concentration.

In conclusion, the $CoSO_4$ addition considerably decreases the oxygen overvoltage, favouring the oxygen evolution within the working range of the positive electrode of the lead-acid battery. This behaviour could have positive effects on the grid functioning, hindering its corrosion. As other additions[18] it is possible that the $CoSO_4$ addition influences the grid behaviour but not that of the active mass, too, which is in a very high amount. Because of that the effect of the increase of the $PbO_2/PbSO_4$ electrode capacity, observed by us, probably has no negative influence on the active mass capacity of the battery. It is confirmed the practical observation[19] that an addition of only 0.02 M $CoSO_4$ is sufficient to determine a considerable decrease of the oxygen overvoltage.

REFERENCES

[1] J. Visscher, *Power Sources*, **1**, 257 (1977).
[2] K. R. Bullock, *J. Electrochem. Soc.*, **11**, 360 (1979).
[3] D. Pavlov and G. Papazov, *J. Electrochem. Soc.*, **127**, 10 (1980).
[4] M. A. Dasoian, "Surse de curent chimice", Editura Tehnică, Bucharest, 1964.
[5] P. Delahay and W. C. Tobias, "Advances in Electrochemistry and Electrochemical Engineering", vol. 8., New York, 1971.
[6] A. Pierson, *Electrochem. Technol.*, **5**, 323 (1967).
[7] D. Pavlov, G. Papazov and V. Iliev, *J. Electrochem. Soc.*, **119**, 1(1972).
[8] P. Ruetschi and R. Angestadt, *J. Electrochem. Soc.*, **111**, 1323 (1964).
[9] C. F. Yarnell and M. C. Weeks, *J. Electrochem. Soc.*, **126**, 1 (1979).
[10] K. R. Bullock and D. H. McClelland, *J. Electrochem. Soc.*, **124**, 1478 (1977).
[11] S. Sternberg, V. Brânzoi, L. Apăteanu and A. Mateescu, *Rev. Roumaine* Chim. **28**, 6 (1983).
[12] J. Gersche, N. Anastasjevic and K. Wiesener, *Electrochim. Acta*, **26**, 10 (1981).
[13] B. K. Mahato, *J. Electrochem. Soc.*, **11**, 124 (1977).
[14] B. K. Mahato, *J. Electrochem. Soc.*, **7**, 128 (1981).
[15] B. K. Mahato, *J. Electrochem. Soc.*, **127**, 8 (1980).
[16] J. Perkins and M. T. Coyle, *J. Electrochem. Soc.*, **124**, 4 (1977).
[17] S. Sternberg, A. Mateescu, V. Brânzoi and L. Apăteanu, *Rev. Roumaine Chim.*, **29**, 9(1984).
[18] S. Sternberg and A. Matteescu, *Revista de Chimie*, **35**, 6 (1984).
[19] M. A. Dasoyan and I. A. Aguf, "Sovremennaia teoria svintsovogo acumuliatora", Ed. Energhia, Leningrad (1975).
[20] P. Ruetschi and R. T. Angstadt, *J. Electrochem. Soc.*, **111**, 1964, p. 1323.

Revue Roumaine de Chimie, **30**, *11–12*, 963–967 (1985)

SELFINHIBITION OF THE HOMOGENEOUS PYROLYSIS OF n-HEPTANE

MELANIA BOZEŞANU and N. I. IONESCU
ICECHIM-Center of Physical Chemistry, Splaiul Independenţei 202, 77208 Bucharest, Romania

Received March 30, 1985

The use of kinetic equations for different reaction orders in homogeneous pyrolysis of n-heptane was discussed. In this reaction, two processes, namely selfinhibition and variation of reaction order with temperature appear together, without determining one another.

The pyrolysis of hydrocarbons from natural gases, refinery gases or petroleum in tubular reactors between 500 and 900°C is the most important reaction in petrochemical processes. Depending on charge and reaction conditions a complex mixture of products is obtained, ethene and propene being the most important.

In the group of liquid alkanes, n-heptane presents the highest conversion and yield of ethene, being particularly suitable for studies of kinetics and mechanism of pyrolysis.[1]

As kinetic data on homogeneous pyrolysis of n-heptane are not in a good agreement,[1-6] in this paper we aim to study some aspects concerning the determination of the kinetic constants of this reaction.

EXPERIMENTAL PART

The experiments were carried in a flow tubular reactor made of silica [2] within the temperature range 509–660°C at contact times between 5 and 90 s. Under these conditions, the conversion of n-heptane ranged from 1.5 to 95 percents.

The analysis of reaction products was performed by a gas chromatographic method.[2]

RESULTS AND DISCUSSIONS

In a previous paper, [3] assuming that the reaction order is one, by means of the variation of n-heptane conversion as a function of contact time, the kinetic constants for different temperatures were calculated.

These data show that the rate constants decrease with the conversion increase and the higher the temperature the steeper the decrease.

This behaviour named selfinhibition has also pointed out in the pyrolysis of other hydrocarbons [4] not only n-heptane [5] and it could be assigned to: 1) an inhibition due to some pyrolysis products, 2) the fact that the n-heptane conversion could not always be described in terms of a first order kinetic equation 3) both of them.

In order to make a distinction between these hypotheses, the experimental data were calculated by means of the equation[5]:

$$\frac{dx}{dt} = \frac{k}{C_1^0}\left[\frac{C_1^0(1-x)}{1+(E_v-1)\,x}\right]^n [1+(E_v-1)\,x] \tag{1}$$

where

k — rate constant
x — n-heptane conversion
t — contact time
C_1^0 — initial concentration of n-heptane
E_v — expansion of reaction at $x - 1$
n — reaction order

This relationship describes the variation of n-heptane conversion as a function of contact time for any value of the reaction order.

By integrating equation 1 for $n = 0.5$; 1 ; 1.5 and 2, the following expresions of the rate constants were obtained:

for $n = 0.5$

$$k = \frac{(C_1^0)^{1/2}}{t}\cdot\frac{1}{\sqrt{\alpha}}\cdot \text{arc sin}\ \frac{\alpha - 1 - 2\alpha x}{1+\alpha} \tag{2}$$

where $\alpha = E_v - 1$

for $n = 1$

$$k = \frac{2.303}{t}\cdot \log\frac{1}{1-x} \tag{3}$$

for $n = 1.5$

$$k = \frac{1}{(C_1^0)^{1/2}\,t}\left[2\sqrt{\frac{1+\alpha x}{1-x}} + 2\sqrt{\alpha}\ \text{arc tg}\sqrt{\frac{1+\alpha x}{\alpha(1-x)}}\right] \tag{4}$$

for $n = 2$

$$k = \frac{1}{C_1^0 t}\left[\alpha \ln(1-x) + \frac{1+\alpha}{1-x}\right] \tag{5}$$

By means of equations (2)—(5) the rate constants for every reaction order, at different temperatures were calculated and the values thus obtained were plotted as a function of conversion (figures 1—4).

From the examination of these figures one may notice that irrespective of the reaction order for which the rate constant is calculated, this constant decreases with conversion increase.

These data show that the selfinhibition by reaction products which is assumed to be a possible explanation for the decrease or rate constant is really present in pyrolysis of n-heptane and is as evident as temperature is higher.

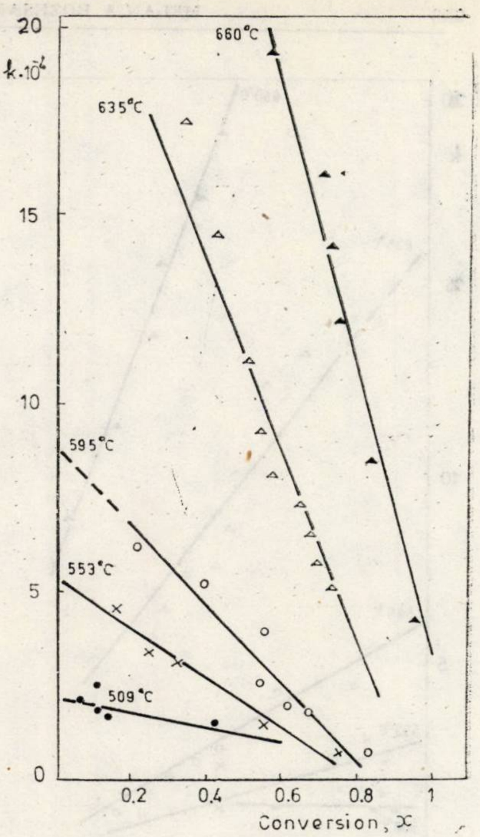

Fig. 1. — Rate constant variation with n-heptane conversion for reaction order $n = 0.5$, at different temperatures.

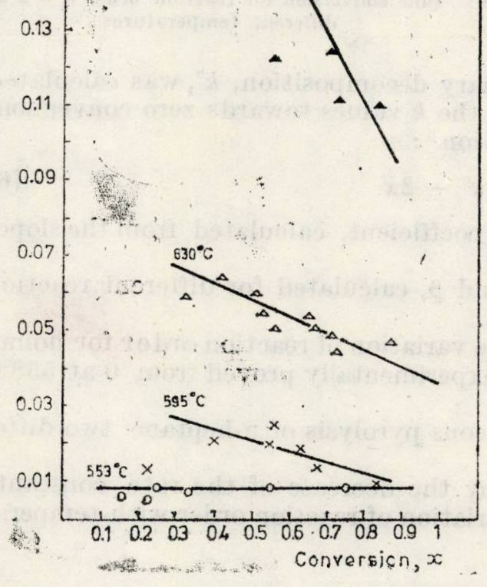

Fig. 2. — Rate constant variation with n-heptane conversion for reaction order $n = 1$, at different temperatures.

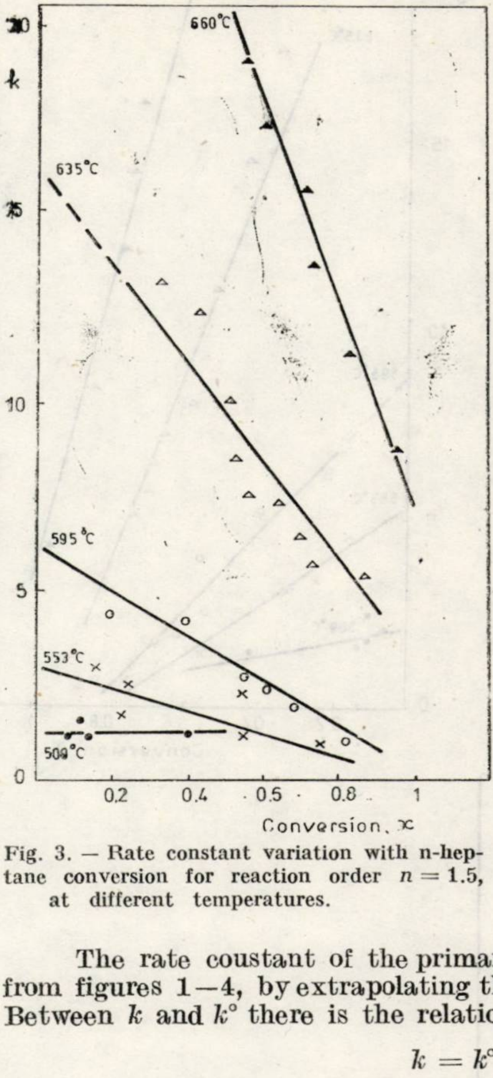

Fig. 3. — Rate constant variation with n-heptane conversion for reaction order $n = 1.5$, at different temperatures.

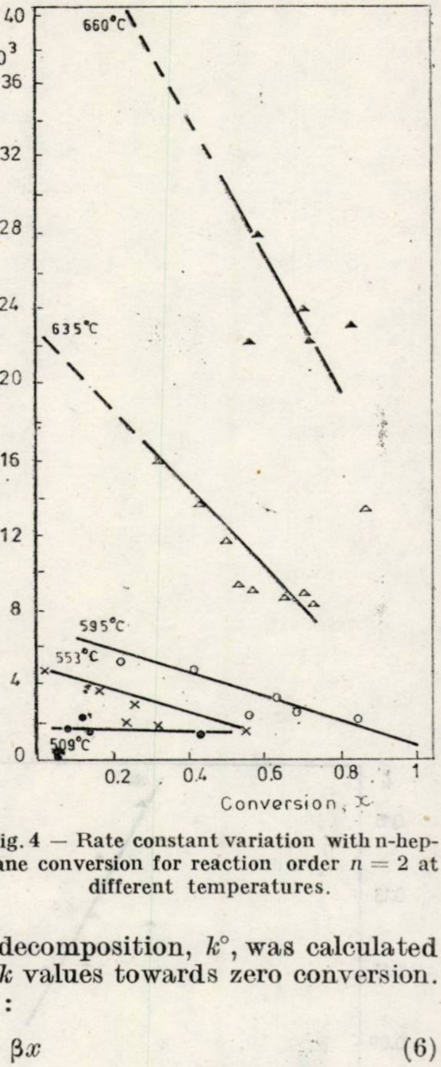

Fig. 4 — Rate constant variation with n-heptane conversion for reaction order $n = 2$ at different temperatures.

The rate coustant of the primary decomposition, k°, was calculated from figures 1—4, by extrapolating the k values towards zero conversion. Between k and k° there is the relation[5]:

$$k = k^\circ - \beta x \tag{6}$$

where β represents the inhibition coefficient, calculated from the slopes of the straight lines (figures 1—4).

In table 1, the values of k° and β, calculated for different reaction orders and temperatures are listed.

In another previous paper, [7] the variation of reaction order for homogeneous pyrolysis of n-heptane was experimentally proved from 0 at 558°C to one at 695°C.

In conclusion, in the homogeneous pyrolysis of n-heptane two different processes occur :

1) selfinhibition, manifested by the decrease of the rate constants with the increase of conversion 2) variation of reaction order with temperature.

Table 1

Rate constants k° and inhibition coefficients, β, for different reaction orders and temperatures

T °C	$n = 0.5$		$n = 1$		$n = 1.5$		$n = 2$	
	$k^\circ \times 10^{-4}$	$\beta \times 10^{-4}$	$k^\circ \times 10^{-3}$	$\beta \times 10^{-2}$	k°	β	$k^\circ \times 10^{3}$	$\beta \times 10^{3}$
509	2.1	1.6	2.4	0	1.2	0	1.8	0
553	4.7	5.9	8.0	0	3.0	3.3	4.4	6.0
595	8.5	9.7	36.0	3	6.2	5.9	6.7	6.4
635	24.7	26.6	80.0	5	18.1	16.6	21.2	21.1
660	47.5	46.3	256.0	18	38.8	32.4	48.8	36.6

These two processes appear together, whithout determining one another.

REFERENCES

[1] M. Bajus and V. Vesely, *Ind. Eng. Chem., Res. Dev.*, **16**, 30(1979).

[2] I. Iosif, M. Bozeşanu, N. I. Ionescu and Gr. Pop, *Rev. Chimie*, **31**, 231(1980).

[3] I. Iosif, N. I. Ionescu, M. Bozeşanu and Gr. Pop, Symposium über Aktuelle Wissenschaftliche Probleme der Pyrolyse von Kohlenwassaerstoffen, Leipzig, 1979, p. 130.

[4] A. Y. Dintses and A. V. Frost, *Dokl. Akad. Nauk SSSR*, **3**, 510(1934).

[5] V. Illes, K. Welther and I. Pleszkats, *Acta Chim. Acad. Sci. Hung.*, **78**, 357(1973).

[6] G. Ivănuş, Ph. D. Thesis, Oil and Gas Institute, Ploieşti, 1978.

[7] N. I. Ionescu, I. Iosif, M. Bozeşanu and Gr. Pop, *Z. Phys. Chemie*, (Leipzig), **264**, 1209(1983).

Revue Roumaine de Chimie, **30**, *11–12*, 969–975 (1985)

AMINOKETONE AND OXAZOLE SYNTHESIS. VIII.[1] ACYLAMINOACYLATIONS USING AZLACTONES OF FLUORO-SUBSTITUTED HIPPURIC ACIDS AND 2,5-DIARYLOXAZOLES DERIVED THEREFROM

IOSIF SCHIKETANZ, ANA SCHIKETANZ, MIRCEA D. GHEORGHIU,
MIHAI PASCU, AURELIA VASILE and ALEXANDRU T. BALABAN*

Polytechnic Institute, Organic Chemistry Department, Splaiul Independenţei 313,
76206 Bucharest, Romania

Received May 20, 1985

Electrophilic acylaminoacylation of aromatic hydrocarbons (benzene, toluene, *m*- and *p*-xylene) with the azlactone of *o*- or *p*-fluorohippuric acid in the presence of anhydrous $AlCl_3$ yields aroylaminoketones **4**, whose dehydration affords 2,5-diaryloxazoles **5**. The IR, UV, ^1H-NMR and ^{19}F-NMR spectra of these compounds are discussed, and the laser emission of fluoro-substituted 2,5-diaryloxazoles is described.

With the exception of hydrogen isotopes, fluorine substituents in aromatic rings introduce the smallest steric perturbation owing to the fact that the van der Waals radius of fluorine is the next smallest after that of hydrogen. However, the difference in electronegativity is very large because the electronegativity of fluorine surpasses that of any other element; nevertheless, Hammett's sigma-value σ_p for a *p*-fluoro substituent is small and negative because the $+E$ effect prevails over the $-I$ effect; only in *meta*, where the $-I$ effect operates exclusively, is σ_m for fluorine moderately positive (smaller than for other halogens and for groups such as RCO, CN, COOR, CF_3 or NO_2).[2]

We decided to investigate *o*- and *p*-fluorosubstituted azlactones[3] of hippuric acid in the acylaminoacylation of aromatic hydrocarbons ArH with various Ar groups: **a**) phenyl; **b**) *p*-tolyl; **c**) 2,4-xylyl; **d**) 2,5-xylyl. The resulted α-acylamino-ketones **4** were then converted into 2,5-diaryloxazoles **5**, where the 2-aryl group is either *o*-(**A**) or *p*-fluorophenyl (**B**).** Such oxazoles are interesting for dye lasers owing to their strong fluorescence and strong C–F bonds; among the numerous substituted 2,5-diaryloxazoles investigated by Hayes, Ott and their coworkers [3,4] as liquid scintillators, it was found that fluorine substituents did not quench the fluorescence like bromo and especially iodo substituents. The presence of strong chemical bonds is a prerequisite for steady functioning of dye lasers; for filling in the gaps between various wavelengths, as many substituents as possible are necessary, therefore fluoro substituents are attractive.

---

* Correspondence author.

** The notation used in the present paper employs capital letters **A** and **B** to denote *o*- and *p*-fluorophenyl, respectively, and small letters **a**–**d** for Ar groups derived from benzene, toluene, *m*- and *p*-xylene, respectively.

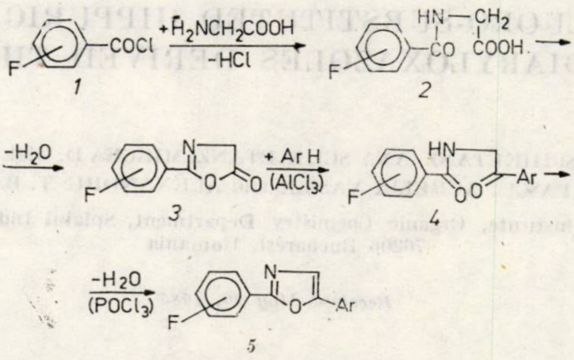

Aroyl chlorides **1A** and **1B** were converted into fluoro-substituted hippuric acids **2A, B** which had been described by Coppola. [5] The melting point for **2A** is significantly higher (150°) than indicated earlier (121°).[5] These acids were converted into the corresponding azlactones **3** using a method described by Kumar, Mishra and Mukerjee [6] which employs ethyl chloroformate and triethylamine as dehydrating agent. The IR and ^1H—NMR spectra of the azalctones agree with their structures. The *p*-substituted azlactone **3B** had been reported earlier by one of us.[7]

The acylaminoacylation of benzene, toluene, *m*- or *p*-xylene was carried out in excess of these hydrocarbons as solvents in the presence of anhydrous aluminium chloride. The crude products **4** were recrystallized from 80% ethanol when the melting points increased only with 2—10° indicating that the reaction proceeded with remarkable regioselectivity. The α-acylaminoketones **4** were characterized by elemental analysis, IR and ^1H—NMR spectrometry (Tables 1 and 2).

Table 1

Data for α-acylaminoketones **4**

Comp.	Ar	M.p. (°C)	Yield (%)	Formula	N %	
					Calc.	Found
4Aa	C_6H_5	115[a]	62	$C_{15}H_{12}FNO_2$	5.44	—
4Ab	4-MeC_6H_4	158	64	$C_{16}H_{14}FNO_2$	5.16	5.00
4Ac	2,4-$Me_2C_6H_3$	140	44	$C_{17}H_{16}FNO_2$	4.91	4.64
4Ad	2,5-$Me_2C_6H_3$	95	33	$C_{17}H_{16}FNO_2$	4.91	4.85
4Ba	C_6H_5	134[b]	58	$C_{15}H_{12}FNO_2$	5.44	5.15
4Bb	4-MeC_6H_4	151	59	$C_{16}H_{14}FNO_2$	5.16	4.90
4Bc	2,4-$Me_2C_6H_3$	135	47	$C_{17}H_{16}FNO_2$	4.91	4.73
4Bd	2,5-$Me_2C_6H_3$	118	44	$C_{17}H_{16}FNO_2$	4.91	4.91

[a] Lit. m.p. 116—117° (ref. [3])

[b] Lit. m.p. 135—6° (ref.[7]) and 134—5° (ref. [3])

Table 2

^{1}H-NMR Spectra of acylaminoketones **4** (δ values, ppm)

No.	Ar	H_{arom}(m)	CH_2(d)	NH	CH_3(s)	Solvent
4Aa	Ph	7.10–8.23	5.00	8.00	—	$CDCl_3$
4Ab	4-MeC_6H_4	7.00–8.20	4.90	8.00	4-Me : 2.40	$CDCl_3$
4Ac	2,4-$Me_2C_6H_3$	7.00–8.26	4.83	8.00	2-Me : 2.60 4-Me : 2.33	$CDCl_3$
4Ad	2,5-$Me_2C_6H_3$	7.00–8.33	4.87	8.10	2-Me : 2.60 5-Me : 2.37	$CDCl_3$
4Ba	Ph	6.96–8.16	4.80	3.33	—	$(D_3C)_2CO$
		6.90–8.10	4.93	7.50	—	$CDCl_3$
		7.10–8.16	4.73	8.83	—	DMSO
4Bb	4-MeC_6H_4	7.07–8.20	4.83	3.23	4-Me : 2.40	$(D_3C)_2CO$
		7.03–8.00	4.86	7.60	4-Me : 2.40	$CDCl_3$
		7.10–8.07	4.70	8.77	4-Me : 2.33	DMSO
4Bc	2,4-$Me_2C_6H_3$	7.00–8.00	4.73	7.33	2-Me : 2.50 4-Me : 2.33	$CDCl_3$
4Bd	2,5-$Me_2C_6H_3$	7.00–8.00	4.70	7.30	2-Me : 2.50 5-Me : 2.33	$CDCl_3$

Dehydration of compounds **4** by refluxing with phosphorus oxychloride proceeded smoothly affording 2,5-diaryloxazoles **5** in 80–90% yield. The oxazoles **5** were characterized by elemental analysis, UV–VIS, IR and ^{1}H–NMR spectrometry (Tables 3 and 4).

Table 3

Data for 2,5-diaryloxazoles **5**

Comp.	Ar	M.p. (°C)	Formula	N%	
				Calc.	Found
5Aa	C_6H_5	83[a]	$C_{15}H_{10}FNO$	5.86	5.77
5Ab	4-MeC_6H_5	78	$C_{16}H_{12}FNO$	5.53	5.23
5Ac	2,4-$Me_2C_6H_3$	98	$C_{17}H_{14}FNO$	5.24	5.02
5Ad	2,5-$Me_2C_6H_3$	97	$C_{17}H_{14}FNO$	5.24	4.98
5Ba	C_6H_5	83[b]	$C_{15}H_{10}FNO$	5.86	5.62
5Bb	4-MeC_6H_3	130	$C_{16}H_{12}FNO$	5.53	5.74
5Bc	2,4-$Me_2C_6H_3$	80	$C_{17}H_{14}FNO$	5.24	5.35
5Bd	2,5-$Me_2C_6H_5$	91	$C_{17}H_{14}FNO$	5.24	5.08

[a] Lit. m.p. 84–85° (ref.[3])

[b] Lit. m.p. 81° (ref.[7]) and 81–82° (ref.[3]).

^{1}H–NMR SPECTRA

An interesting feature appears in the ^{1}H–NMR spectra of *o*-fluoroderivatives **2A**–**4A**, namely a long-range heteronuclear coupling between the fluorine nucleus and the methylene protons. The latter protons usually appear in related compounds as a doublet because of homonuclear coupling with the vicinal NH proton, as shown by decoupling experiments or

Table 4

^{1}H-NMR Spectra of oxazoles **5**(δ values, ppm)

No.	H_{arom} (m)	CH_3 (s)	Solvent
5Aa	7.10–8.13	—	CCl_4
5Ab	7.03–8.17	4-Me : 2.30	$CDCl_3$
5Ac	6.90–8.26	2-Me : 2.46 4-Me : 2.33	CCl_4
5Ad	7.00–8.20	2-Me : 2.47 5-Me : 2.26	$CDCl_3$
5Ba	7.03–8.13	—	$CDCl_3$
5Bb	7.10–8.17	4-Me : 2.30	$CDCl_3$
5Bc	7.03–8.20	2-Me : 2.43 4-Me : 2.30	$CDCl_3$
5Bd	7.00–8.13	2-Me : 2.40 5-Me : 2.30	$CDCl_3$

by deuteration to ND ; in both cases the doublet becomes a singlet. However, *o*-fluoroderivatives exhibit for the CH_2 protons a supplementary long-range splitting $^6J_{^{19}F-^1H}=0.3$ Hz (in the methyl ester of **2**, methyl *o*-fluorohippurate). A similar value was noticed for the acylaminoketone **4Aa** in $CDCl_3$. Such long-range coupling between an *o*-fluorine atom and a phenacyl-ω-proton was noticed earlier in the literature[8] with a similar *J* value : compound **6** has $J_{^{19}F-^BH}= 3.1$ Hz and $J_{^{19}F-^AH}= 1.7$ Hz ; there is an analogous coupling also in the $^{13}C-NMR$ spectra of **6** between the fluorine atom

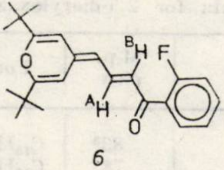

6

and the carbon atom bonded to H^A ; likewise *o*-fluoroacetophenone has a coupling between fluorine and the methyl carbon in the $^{13}C-NMR$ spectra. Another noteworthy feature is the lowest field 1 : 2 : 1 triplet (J = 7 Hz for *o*-^{1}H and ^{19}F) of closely-spaced doublets (J = 2 Hz) for another aromatic proton centered at 7.92 ppm, assigned to the aromatic proton *ortho* to the carbonyl group in compounds **2A**–**4A**.

The *p*-fluoro-derivatives **2B**–**4B** have the normally expected ^1H-NMR spectra, with supplemental splittings of the AA′BB′-type aromatic protons owing to the *para*-fluoro atom.

The *m*-protons relative to the carbonyl group, which are strongly coupled to the vicinal *p*-fluorine atom, give signals at higher field than the *o*-protons. Thus, *p*-fluorohippuric acid (**2B**) has the *o*-protons as a quartet at δ = 7.97 ppm (H^B), the *m*-protons as a triplet at δ = 7.24 ppm (H^A), and the coupling constants are J_{AB} = 9 Hz, J_{H^AF} = 9 Hz, J_{H^BF} = 6 Hz.

The assignment of the methyl peaks in Tables 2 and 4 is based on the comparison between the *p*-tolyl-substituted systems (**4b**, **5b**) which have an unambiguous assignment, and the systems with two methyl groups. It can be observed that one of the two methyl groups coincides within 0.07 ppm with the position of the *p*-tolyl methyl protons, therefore this methyl group is assigned to the 4- (in **4c**, **5c**) or 5-standing methyl group (in **4d**, **5d**). The remaining methyl is therefore the *ortho*-standing one with respect to the carbonyl group or oxazole ring, respectively, and appears slightly deshielded relatively to the other methyl.

^{19}F—NMR SPECTRA

The ^{19}F—NMR spectral data of model compounds (*p*-fluoroacetophenone and methyl *p*-fluorohippurate) and of several products described in the present paper are indicated in Table 5. The data are consistent and indicate that the ^{19}F chemical shifts of acylaminoketones (e.g. **4Ba**) are closely similar to those of methyl *p*-fluorohippurate because the structure is very similar. On cyclization of hippuric derivatives to azlactones (e.g. **3B**) the *p*-fluorine nucleus is slightly deshielded, whereas on cyclization of acylaminoketones to oxazoles (e.g. **5Bb**) the through-bond and through-space effects shield slightly the *p*- ^{19}F nucleus. *p*-Fluoroacetophenone is seen from Table 5 to resonate at much lower field than all other compounds from the same Table, because its carbonyl group has only C—C bonds, while all other compounds have a C—N bond.

Table 5

^{19}F-NMR Spectral data : chemical shifts relative to $CFCl_3$ (Φ^*, ppm) and coupling constants (Hz) in $CDCl_3$ ($Ar = p\text{-}FC_6H_4$)

Compound	$\Phi^{*\,a}$ (ppm)	$J_{^{19}F-H(o)}$ (Hz)	$J_{^{19}F-H(m)}$ (Hz)
$ArCOCH_3$	105.2	8.5	5
$ArCONHCH_2CO_2Me$	125.8	8.5	5
3B (azlactone)	118.8	9.5	5.5
4Ba ($ArCONHCH_2Bz$)	125.5	9.0	5.5
5Bb (oxazole)	127.3	8.5	5.5

[a] ^{19}F-chemical shifts determined relatively to $CFCl_3$ without extrapolation to infinite dilution.

ELECTRONIC ABSORPTION SPECTRA

The ultraviolet absorption spectra of 2,5-diaryloxazoles in cyclohexane were investigated in detail by Ott, Hayes and coworkers. [3,4] We recorded UV absorption spectra of the longest-wavelength absorption band in methanol. Data are presented in Table 6, in comparison with literature data for compounds which had been described earlier.

Table 6

UV absorption spectra of oxazoles in methanol

Compound	λ_{max} (nm)	ε_{max}	Literature[4] data λ_{max} (ε_{max})
5Aa	304	33 900	303 (26 800)
5Ab	308	23 600	—
5Ac	309	25 800	—
5Ad	307	24 000	—
5Ba	303	33 000	303 (29 000)
5Bb	308	34 000	—
5Bc	305	31 000	—
5Bd	306	26 000	—

Despite the different solvents, the agreement between our data and those of Ott et al.[4] is good for λ_{max} values and satisfactory for ε_{max} values. It may be noted that methyl substitution causes bathochromic shifts which may be useful for dye lasers.

FLUORESCENCE AND LASER EFFECT

The fluorescence of some compounds described in this paper was investigated under conditions of the laser effect in ethanol (10^{-2} mol/L, 5 mL cells). The most intense effect was obtained with 2-(*o*-fluorophenyl)-5-phenyl-oxazole **5Aa** (emission at 375–386 nm); a less intense effect was observed with 2-(*p*-fluorophenyl)-5-phenyl-oxazole **5Ba** (emission at 378–383 nm); still less intense emissions were observed with 2-(*o*-fluorophenyl)-5-(*p*-tolyl)-oxazole **5Ab** (370–379 nm) and 2-(*o*-fluorophenyl) 5-(2′, 4′-xylyl)-oxazole **5Ac** (375–405 nm). Determinations were carried out in conditions similar to those reported in an earlier paper.[9]

EXPERIMENTAL

Commercial fluorobenzene acids were converted into acid chloride **1A**, **B** with thionyl chloride. A Specord-Jena spectrophotometer was used for UV spectra, and a Varian EM-360L instrument was used for the 60 MHz ^{1}H-NMR and ^{19}F-NMR spectra.

Fluoro-substituted hippuric acids **2** were prepared by adding acid chlorides **1** into a solution of glycine dissolved in aqueous sodium hydroxide with stirring and external cooling at 0° during one hour. On acidification with concentrated hydrochloric acid, the precipitated fluorohippuric acids were filtered off, washed on the Buchner funnel with water, and recrystallized from water in the presence of animal carbon. The yield was 95 % for **2A**, m.p. 150° (m.p. lit.[3] 121°), and 92 % for **2B**, m.p. 169° (m.p. lit.[3] 161°). For elucidation of ^{1}H-NMR features the methyl esters were also prepared; that of **2A** was an oil, but that of **2B** had m.p. 114° (from water).

o-Fluorohippuric acid (**2A**) presents in DMSO-d_6 the methylene doublet at 3.99 ppm ($J = 6$ Hz).

Methyl *o*-fluorohippurate presents in CCl_4 the ν(NH) band at 3450 cm^{-1}, and two strong IR absorption bands at 1770 and 1695 cm^{-1}; its ^{1}H-NMR methyl peak appears as a singlet in $CDCl_3$ at 3.73 ppm and the CH_2 protons as a doublet at 4.23 ppm ($J = 6$ Hz).

Acid **2B** has in KBr pellet the ν(CO) band at 1730 cm^{-1}, and in the ^{1}H-NMR spectrum dry DMSO-d_6 as solvent) the CH_2 protons resonate at 3.90 ppm (d, $J = 7$ Hz) coupled (deuteration, decoupling) to the NH proton at 8.83 ppm (t, $J = 7$ Hz); the two aromatic protons H^A *ortho* to carbonyl appear as a multiplet centered at 7.98 ppm, and the other two aromatic protons H^B as a multiplet approximating a 1 : 2 : 1 triplet centered at 7.24 ppm. Coupling constants are $J_{AB}=9$ Hz, $J_{^{19}F-H^A}=6$ Hz, $J_{^{19}F-H^B}=9$ Hz. The methyl ester of **2B** in $CDCl_3$ presents the methyl protons at 3.73 ppm, the methylene doublet at 4.15 ppm, the aromatic multiplets close to the values mentioned above, and the NH proton superimposed on the aromatic protons around 7.20 ppm.

Azlactones **3** were preapared by stirring at room temperature 3 g (15 mmol) acid **2** in 75 mL benzene with 1.6 g (15 mmol) triethylamine, followed by addition of 1.7 g (15 mmol) ethyl chloroformate. The stirring is continued till the exothermal reaction subsides and the triethylamine hydrochloride is removed by filtration. The red filtrate was concentrated and the residue was left for several days to crystallize. On recrytstallization from cyclohexane, azlactone **3A** (m.p. 123°, containing according to ^{1}H-NMR data traces of **2A**) was obtained; the corresponding azlactone **3B**, m.p. 125° was described earlier,[5] with m.p. 118°. Yields were practically quantitative.

In the IR spectra (in KBr pellet) of azlactone **3A** strong bands at 1680 and 1820 cm^{-1} may be noted; the ^{1}H-NMR spectrum presents the CH_2 group as a singlet at 4.33 ppm.

Azlactone **3B** has strong IR bands at 1680 and 1830 cm^{-1}, and the ^{1}H-NMR CH_2 peak (in $CDCl_3$) at 4.39 ppm as a singlet.

Acylamninoketones **4** were prepared by stirring 3.6 g azlactone **3** (20 mmol) in 50 mL aromatic hydrocarbon ArH (**a**—**d**) with 8 g (60 mmol) freshly sublimed and ground aluminium chloride, during 5 hours at room temperature, then it was left overnight. After hydrolysis with dilute hydrochloric acid, the solid crude product was filtered off; another smaller crop was obtained by evaporating the upper organic layer of the filtrate under reduced pressure. The products were recrystallized from 80% ethanol with animal carbon. Yields and melting points are indicated in Table 1.

2,5-Diaryloxazoles **5**. Acylaminoketones **4** (1.5 g) were refluxed for 4 hrs in 30 mL phosphorus oxychloride, then the excess of $POCl_3$ was evaporated and the residue was poured in ice-water. The precipitated oxazoles were filtered off, washed on the Buchner funnel with 5% aqueous sodium hydrogen carbonate solution, and recrystallized from 80% ethanol in the presence of animal carbon. Yields are about 80%. Melting points are presented in Table 3.

ACKNOWLEDGEMENT. We express our thanks to the E.I. Du Pont de Nemours Company for a gift of Cl_3CF used as standard for ^{19}F-NMR spectra.

REFERENCES

[1] Part VII, I. Schiketanz, A. T. Balaban and E. Ciorănescu, *Rev. Roumaine Chim.*, **27**, 1125 (1982).

[2] C. D. Johnson, "The Hammett Equation", Cambridge University Press, 1973; P. R. Wells, *Chem. Rev.*, **63**, 171 (1963); "Linear Free Energy Relationships", Academic Press, London, 1968.

[3] F. N. Hayes, B. S. Rogers and D. G. Ott, *J. Amer. Chem. Soc.*, **77**, 1850 (1955).

[4] D. G. Ott, F. N. Hayes, E. Hansbury and V. N. Kerr, *J. Amer. Chem. Soc.*, **79**, 5448 (1957).

[5] F. Coppola, *Gazz. Chim. ital.*, **13**, 522 (1883).

[6] P. Kumar, H. D. Mishra and A. K. Mukerjee, *Synthesis*, 836 (1980).

[7] A. T. Balaban, L. Bîrlădeanu, I. Bally, P. T. Frangopol, M. Mocanu and Z. Simon, *Tetrahedron*, **19**, 2199 (1963).

[8] A. T. Balaban, M. Fahmy, M. D. Gheorghiu and V. Wray, *Liebigs Ann. Chem.*, 1807 (1983) and further references therein.

[9] C. Rullière, J. Joussot-Dubien, J. Bellocq and A. T. Balaban, *J. chim. phys.*, **75**, 961 (1978).

Revue Roumaine de Chimie, **30**, *11–12*, 977–984 (1985)

AMINOKETONE AND OXAZOLE SYNTHESIS. IX.*

2, 2′-(*p*-PHENYLENE)-bis-(5-ARYLOXAZOLES) AND 2,2′-(1,4-NAPHTHALENEDIYL)-bis-(5-ARYLOXAZOLES) *via* ACYLAMINOACYLATION OF AROMATIC HYDROCARBONS

ALEXANDRU T. BALABAN, IOSIF SCHIKETANZ, MIRCEA D. GHEORGHIU
and ANA SCHIKETANZ

Organic Chemistry Department, Polytechnic Institute TCH, Splaiul Independenței 313,
76206 Bucharest, Romania

Rceived May 20, 1985

Reaction of bis-azloactones 3A or 3B prepared starting from glycine and terephthaloyl or 1,4-naphthalenedicarbonyl dichlorides respectively, with excess of various aromatic hydrocarbons (benzene, toluene, *o*-, *m*- or *p*-xylene, mesitylene, pseudocumene) leads by double acylaminoacylation to bis-(α-acylamino)-ketones 4 whose dehydration affords the title bis-oxazoles 5. Products were characterized by IR, UV-VIS, ^{1}H-NMR and mass spectra, except for the naphthalene-bis-oxazoles whose insolubility precluded NMR studies. The mesityl-substituted bis-oxazole 5Af has its longest-wavelength shifted hypsochromically by about 20 nm owing to steric factors. The fluorescent bis-oxazoles may be used as solutes for scintillators, as textile brightening agents, or dye lasers.

INTRODUCTION

A preceding paper in the present series reported [1] the formation of bis-oxazoles **5A** starting from the bis-azlactone (**3A**, R=H) of N, N′-terephthaloyl-bis(glycine) (**2A**, R=H), and two moles of aromatic hydrocarbons ArH (benzene, toluene and *p*-xylene) which were the reaction sol-

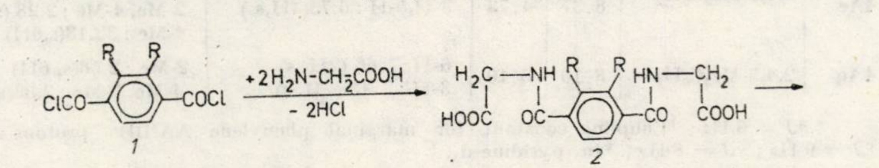

---

* Part VIII, preceding paper.

vents, in the presence of anhydrous aluminium chloride, *via* the bis (α-acylamino) ketones **4A** (R=H). *

The present paper extends this reaction to oxazoles derived similarly either from (i) terephthaloyl dichloride (**1A**, R=H) or from (ii) 1,4-naphthalenedicarbonyl dichloride (**1B** where R, R indicate a —(-CH=CH-)$_2$— chain), and various aromatic hydrocarbons : **a**, benzene ; **b**, toluene, **c**, *p*-xylene ; **d**, *m*-xylene ; **e**, *o*-xylene ; **f**, mesitylene ; **g**, pseudocumene.

Reaction of 2,2′-*p*-phenylene-bis[5(4*H*)-oxazolone] 2A with di- and trimethylbenzenes ArH (d—g)

The bis-azlactone **2A** prepared as described previously, [1] was reacted with *m*-xylene, *o*-xylene, mesitylene or pseudocumene **d—g**, respectively, in excess (as reaction solvents), in the presence of anhydrous aluminium chloride. The bis (α-acylamino) ketones **4Ad—g** which resulted in 45—70 % yield were recrystallized from acetic acid and were characterized by ^{1}H—NMR and IR spectrometry. (Table 1). Melting points and elemental analyses are presented in Table 2.

Table 1

^{1}H-NMR Spectra (δ, ppm) of bis-aminoketones 4 (in trifluoroacetic acid unless otherwise stated)

Comp.	Ar	H_{arom} (s, 4H)	CH$_2$[a] (d, 4H)	H_{arom} (side-rings)	CH$_3$
4Ab[b]	4-MeC$_6$H$_4$	8.07	5.13	2-H,6-H : 8.00 (4H. d)[c] 3-H,5 H : 7.40(4H, d)[c]	4-Me : 2.50 (s, 6H)
4Ac	2,5-Me$_2$C$_6$H$_3$	8.07	5.10	6-H : 7.67 (2H, m) 3-H,4-H : 7.23 (4H, m)	2-Me : 2.53 (s, 6H)
4Ad	2,4-Me$_2$C$_3$H$_3$	8.07	5.10	6-H :7.92 (2H, d) 3-H,5-H : 7.20 (4H, m)	2-Me : 2.73 (s, 6H) 4-Me : 2.43 (s, 6H)
4Ae	3,4-Me$_2$C$_6$H$_3$	8.13	5.20	2H : 8.00 (2H, s) 5-H : 7.36 (2H, d) 6-H : 7.83 (2H, d)	3-Me, 4-Me : 2.46 (s, 12H)
4Af	2,4,6-Me$_3$C$_6$H$_2$	8.07	4.87	3-H,5-H : 6.93 (4H, s)	2,4,6-Me$_3$: 2,33(s, 18H)
4Ae		8.37	4.73	3-H,5-H : 6.73(4H,s)	2-Me, 4-Me : 2.28 (s,12H) 4-Me : 32.13(s,6H)
4Ag	2,4,5-Me$_3$C$_6$H$_2$	8.10	5.10	6-H ;7.66 (2H, s) 3-H : 7.13 (2H, s)	2-Me : 2.56(s, 6H) 4-Me, 5-Me : 2.33(s,12H)

[a] $J = 6$ Hz ; [b] Coupling constant for marginal phenylene AA′BB′ protons : 9 Hz ; [c] $J = 9$ Hz ; [d] $J = 8$ Hz ; [e] In pyridine-d$_5$.

The cyclization to bis-oxazoles **5Ad—g** was effected by refluxing with phosphorus oxychloride. Yields were about 80%. Owing to the low

---

* In the notation employed in the present paper, **A** and **B** indicate terephthalic and 1,4-naphthalenedicarboxylic acids, respectively, while the Ar residues are : **a**, phenyl ; **b**, *p*-tolyl ; **c**, 2,5-dimethylphenyl ; **d**, 2,4-xylyl ; **e**, 3,4-xylyl ; **f**, 2,4,6-trimethylphenyl ; **g**, 2,4,5-trimethylphenyl. The bis-oxazoles **5Aa-e** were reported in the previous paper[1], and their physical constants or preparation will not be repeated here ; however, their ^{1}H-NMR spectra will be discussed comparatively because earlier no detailed assignments had been given.

Table 2

Data for *p*-phenylenebis(α-acylamino) ketones **4** (N,N′-bis-phenylterephthaldiamides)

Comp.	Ar	M.p. (°C)	Yield (%)	M	Formula	N %	
						Found	Calc.
4Ad	2,4-$Me_2C_6H_3$	250	69	456.5	$C_{28}H_{28}N_2O_4$	6.35	6.14
4Ae	3,4-$Me_2C_6H_3$	256-8[a]	71	456.5	$C_{28}H_{28}N_2O_4$	6.05	6.14
4Af	2,4,6-$Me_3C_6H_2$	245	44	484.5	$C_{30}H_{32}N_2O_4$	6.19	5.78
4Ag	2,4,5-$Me_3C_6H_2$	230	62	484.5	$C_{30}H_{32}H_2O_4$	6.01	5.78

[a] May be better recrystallized from dimethylformamide.

solubility of the bis-oxazoles, ^1H-NMR spectra were determined in trifluoroacetic acid (TFA) and only exceptionally in pyridine$-d_5$ or deuterochloroform. Analytical data are presented in Table 3 and ^1H-NMR data in Table 4.

Table 3

Data for 2,2′-(p-phenylene)bis(5-aryloxazoles)

Comp.	Ar	M.p. (°C)	Recryst. from	M	Formula	N %	
						Found	Calc.
5Ad	2,4-$Me_2C_6H_3$	257	toluene	420.5	$C_{28}H_{24}N_2O_2$	7.16	6.66
5Ae	3,4-$Me_2C_6H_3$	262	toluene	420.5	$C_{28}H_{24}N_2O_2$	6.55	6.66
5Af	2,4,6-$Me_3C_6H_2$	186	cyclohexane	448.5	$C_{30}H_{28}N_2O_2$	6.43	6.25
5Ag	2,4,5-$Me_3C_6H_2$	250	toluene	448.5	$C_{30}H_{28}N_2O_2$	6.39	6.25

Table 4

^1H-NMR Spectra (δ, ppm) of bis-oxazoles **5A** (in trifluoroacetic acid unless otherwise stated)

Comp.	Ar	H_{arom} (s, 4H)	$H_{oxazole}$ (s, 2H)	H_{arom} (side-rings)	CH_3
5Aa[a]	C_6H_5	8.66	8.06	7.5−8.0(10H, m)	—
5Ab[a,b]	4-MeC_6H_4	8.60	8.06	2-H,6-H : 7.80 (4H, d) 3-H,5-H : 7.30 (4H,d)	4-Me : 2.50 (s, 6H)
5Ac[a]	2,5-$Me_2C_6H_3$	8.66	8.00	6-H : 7.74 (2H, s) 3-H,4-H : 7.73 (4H,s)	2-Me : 2.63 (s, 6H) 5-Me : 2.50 (s,6H)
5Ad	2,4-$Me_2C_6H_3$	8.60	7.87	6-H : 7.67 (2H, s) 3-H, 5-H : 7.30(4H, s)	2-Me : 2.57 (s, 6H) 4-Me : 2.37 (s, 6H)
5Ae	3,4-$Me_2C_6H_3$	8.60	7.93	2-H,5-H,6-H ; 7.2−7.7 (6H, m)	3-Me, 4-Me : 2.40 (s, 12H)
5Af	2,4,6-$Me_3C_6H_2$	8.13	7.13	3-H,5-H : 6.90 (4H, s)	2-Me, 6-Me : 2.27 (s, 12H) 4-Me : 2.33 (s, 6H)
5Af[c]		8.27	7.33	3-H,5-H : 6.87 (4H, s)	2-Me, 4-Me, 6-Me : 2.27 (s, 18H)
5Ag	2,4,5-$Me_3C_6H_2$	8.70	7.93	6-H : 7.70 (s, 2H) 3-H : 7.27 (s, 2H)	2-Me : 2.60 (2, 6H) 4-Me, 5-Me : 2.44 (s, 12H)

[a] Reported earlier[1] without detailed assignments; [b] Coupling constant for marginal phenylene AA′BB′ protons : 8 Hz; [c] In pyridine-d_5.

Assignments in Tables 1 and 4 are based on the chemical shifts of methyl peaks in the *p*-tolyl derivatives **4Ab** and **5Ab** ; *para*-standing methyl protons appear at higher field than of *o*-standing methyl groups in **4Ad** or **4Ag**. A marked shielding of all methyl protons is observed in the mesityl derivative **4Af** : in TFA all methyl protons are accidentally degenerate at 2.33 ppm, at appreciably higher field than in all other ketones **5Aa**–**e**, **g** ; this effect is due to steric factors which will also be discussed in connection with electronic absorption spectra. The degeneracy is removed by ASIS (aromatic solvent induced shift) in pyridine-d_5, where unlike all other cases, the *ortho*-methyl groups appear at higher field than the *para*-methyl. This effect indicates that in **4Af** the aryl and carbonyl groups are not coplanar, as known from UV spectra of mesityl ketones. [2]

Electronic absorption spectra of bis-oxazoles **5Aa**–**f** in methanol (Table 5) revealed a pronounced hypsochromic shift amounting to about 20 nm of the longest-wavelength absorption band of the mesityl derivative **5Af** ($\lambda_{max} = 334$ nm) relatively to all other analogous compounds (with $\lambda_{max} = 352-360$ nm). This effect is certainly due to sterically-caused non-coplanarity of the oxazolyl and mesityl (Ar) groups in **5Af**. For the same reason, the less intense band around 240 nm in bis-oxazoles **5Aa**–**e**, **g** is displaced hypsochromically by about 10 nm in **5Af**. Whereas bis-oxazoles **5Aa-e**, **g** have, in addition, a weak band around 270 nm, this band is not visible in the spectra of **5Af** ; it may exist, submerged under the more closely situated stronger bands discussed previously.

Preparation of bis-oxazoles derived from 1,4-naphthalenedicarboxylic acid 9

The reaction of glycine with 1,4-naphthalenedicarbonyl dichloride **1B** was not yet described in the literature. Compound **1B** was obtained either (i) starting from naphthalene **6** *via* the 1,4-dibromide 7, [3] dinitrile 8, [4] and the dicarboxylic acid **9**, [5] or more simply (ii) *via* oxidation of 1,4-dimethylnaphtalene with aqueous sodium dichromate in an autoclave at 250°, in conditions similar to those described in the literature.[6]

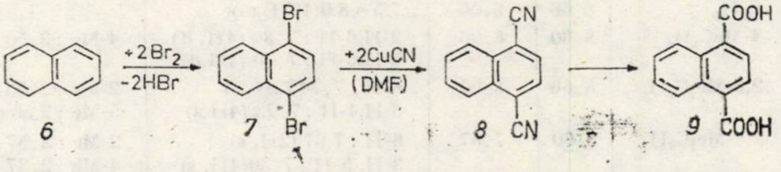

The dichloride **1B** was prepared according to literature data [7,8] from the acid **9**, and afforded with glycine in conditions similar to published procedures[1,9] the N, N′-(1,4-naphtalenediyl)-bis(glycine) **2B**. Attempts to convert this product into the bis-azlactone **3B** by dehydration with hot acetic anhydride gave unsatisfactory results, unlike the analogous conversion **2A** → **3A** ; however, the conversion **2B** → **3B** was effected by means of dicyclohexyl-carbodiimide[10,11] (which had proved to be unsuitable for the preparation of **3A**). The reason for this difference is the much higher solubility of the bis-azlactone **3B** than of **3A**.

The bis-azlactone **3B** was reacted with excess benzene (**a**) or toluene (**b**) affording the bis (α-acylamino) ketones **4Ba** and **4Bb**, respectively.

These compounds were characterized by elemental analysis, IR and ^{1}H–NMR spectrometry, as well as by mass spectrometry (Table 6). Cyclizations to the bis-oxazoles **5Ba** and **5Bb** were effected by the usual reagent ($POCl_3$) and the resulting bis-oxazoles were characterized by the same methods except ^{1}H-NMR; the mass spectra are presented in Table 6. Isotopic peaks in mass spectra, as well as the fragmentation pattern are consistent with the structure.

Electronic absorption spectra of the bis-oxazoles **5Ba** and **5Bb** were recorded in methanol, and are very similar (Table 5).

Table 5

Electronic absorption spectra of bis-oxazoles **5** λ_{max}, nm ($\varepsilon_{max} \times 10^{-4}$) in methanol

Comp.	Ar	Lower λ band	Main band	Other bands
5Aa[12]	C_6H_5	230 sh (2.06)	358 (5.52)	
5Aa	C_6H_5	232 sh (0.62)	360 (2.28)	
5Ab	4-MeC_6H_4	236 (1.36)	362 (3.44)	
5Ac	2,5-$Me_2C_6H_3$	240 (0.57)	358 (2.05)	
5Ad	2,4-$Me_2C_6H_3$	245 (0.13)	362 (0.32)	
5Ae	3,4-$Me_2C_6H_3$	235 (0.13)	365 (0.29)	242 sh (0.11) ; 349 sh (0.25 ; 387sh (0.18)
5Af	2,4,6-$Me_3C_6H_2$	208 (4.32)	334 (4.15)	
5Ag	2,4,5-$Me_3C_6H_2$	246 (0.37)	361 (0.90)	
5Ba	C_6H_5	246 (1.79)	374 (2.57)	207 (3.12) ; 282 (1.61)
5Bb	4-Me-C_6H_4	246 (0.52)	378 (1.62)	206 (2.56) ; 282 (1.03)

All bis-oxazoles described in the present paper present strong fluorescence and can therefore be used both as scintillators for detecting ionizing radiations, and as solutes for dye lasers. However, the naphthyl derivatives have a very low solubility. Since this low solubility of the naphthalene-bis-oxazoles **5B** precluded the study of their NMR spectra, the mass spectra of some of these compounds were recorded (Table 6). Oxazoles **5B** have the molecular peak as base and an intense doubly ionized M^{2+} peak, but the bis-acylaminoketones **4B** have low-intensity molecular peaks. Their base peaks are either $ArCO^+$ ions or $ArCOCH_2NHCOC_{10}H_6CO^+$ ions; in both cases **4Ba** and **4Bb** these are the two most intense fragment peaks. Fragmentations are consistent with the structures.

EXPERIMENTAL PART

^{1}H–NMR Spectra were recorded with a 60 MHz Varian EM–360 L instrument, IR spectra, with a Jena UR–20 spectrophotometer in potassium bromide pellet, and electron-impact mass spectra with a Du Pont–102 instrument. UV–VIS Spectra were recorded with a Jena Specord UV–VIS spectrophotometer

Reaction of N, N'-terephthalolyl-bis(azlactone) **3A** *with aromatic hydrocarbons ArH* (**d**–**g**). The bis-glycine **2A** was prepared as described in the

Table 6

Electron impact mass spectra of bis (acylaminoketones) **4B** and of bis (oxazoles) **5A**

Aminoketones			Oxazoles		
4Ba Ar = Ph	**4Bb** Ar=*p*-tolyl	Assignment	**5Ba** Ar=Ph	**5Bb** Ar=*p*−MeC_6H_4	Assignment*
451 (0.3)	479 (2.2)	M + 1	417 (0.2)	445 (1.0)	M + 3
450 (1.7)	478 (6.3)	M	416 (4.5)	444 (6.7)	M + 2
	460 (1.6)	$M-H_2O$	415 (30.9)	443 (38.9)	M + 1
422 (1.2)			414 (100.0)	442 (100.0)	M
421 (7.1)	449 (20.8)	$M-CH_2NH$	385 (3.0)	413 (2.3)	M−CHO
	421 (0.9)		358 (2.3)	386 (2.2)	M−CHO−HCN
	358 (0.6)		344 (0.3)	372 (2.0)	
331 (1.3)	345 (2.0)	$M-ArCOCH_2$	330 (0.6)	358 (1.0)	M-2CO-H-HCN
318 (2.1)			309 (2.5)	323 (1.2)	M−ArCO
317 (23.2)			296 (7.3)	310 (2.5)	M−CH−ArCO
316 (100.0)	330 (82.4)	$M-ArCOCH_2NH$	282 (4.4)	296 (2.7)	M-ArCO-HCN
314 (1.9)			269 (1.6)	283 (1.6)	$M-ArC_3NO-H$
299 (5.9)	313 (8.2)		254(1.3)	268 (1.5)	
298 (6.8)	312 (5.4)	$M-ArCOCH_2NH$ $-H_2O$			
			240(2.4)	254 (1.8)	
	302 (1.2)		226 (0.7)	240 (1.4)	
	285 (1.2)		214 (0.7)	228(1.3)	
	273 (1.1)				
	211 (1.3)	M−2ArCO $-CH_2NH$			
	210 (1.7)				
	201 (2.2)		207 (15.1)	221 (15.6)	M/2
	198 (2.3)				
182 (3.5)	182 (9.4)	$M-2ArCOCH_2NH$			
155 (2.3)					
154 (9.1)	154 (12.1)	M−CO $-2ArCOCH_2NH$			
153 (3.9)					
126 (5.3)	126 (7.1)	$M-2ArCOCH_2$ $\vert$ CONH			
			164 (0.9)	164 (0.6)	$M-ArCO-ArC_3NO$
125 (1.5)			150 (0.6)	150 (0.5)	
106 (2.0)			138 (2.5)	138(1.8)	
105 (24.0)	119 (100.0)	ArCO	105 (7.1)	119 (4.6)	ArCO
78 (2.1)			89 (2.4)	103 (2.0)	ArC
77 (6.9)	91 (18.4)	Ar	77 (7.6)	91 (5.6)	Ar

* The oxazole skeleton has the molecular formula C_3NO

preceding part; to 10 mmoles (2.44 g) of **2A** in 40 mL aromatic hydrocarbon [m-xylene (**d**), *o*-xylene (**e**), mesitylene (**f**) and pseudocumene (**g**)], freshly sublimed and powdered anhydrous aluminium chloride (8.0 g, 60 mmoles) was added. The mixture was stirred at 60–65° for 10 hours, then hydrolyzed with dilute hydrochloric acid; the product was filtered off, washed with water and ethyl ether, and purified by recrystallization from glacial acetic acid (Table 1). The melting point of the crude product increased by 5–8° indicating that practically one isomer resulted in the acylaminoacylation of aromatic hydrocarbons **d**, **e** and **g**, where several regio-isomers were possible.

2, 2′-(p-Phenylene)-bis(5-aryloxazoles) **5Ad**–**g** were prepared from the above bis (α-acylamino) ketones as described in the preceding part,[1] and purified by recrystallization from toluene or cyclohexane (Table 2).

1, 4-Naphthalenedicarboxylic acid (**9**). *Method* (*i*) *via the dinitrile.* The dibromination of naphtalene **6** was effected with the bromine-dioxane adduct.[3] 1,4-Dibromonaphtalene **7** (1 mole) was converted[4] into the dinitrile **8** with 2.3 moles of cuprous cyanide in dimethylformamide at 160°–170°, for 10 hours, and the dinitrile (84% yield) was recrystallized from acetic acid yielding a product with m.p. 206°.[5] The hydrolysis of **8** to the acid **9** in sulfuric acid, according to literature data,[5] yielded a product with m.p. 303° (uncorr.).

Method (ii), by oxidation of 1,4-dimethylnaphthalene. By analogy with oxidations described in the literature, 1,4-dimethylnaphthalene was oxidized with aqueous sodium dichromate at 250° for 18 hrs. in an autoclave (yield 88%).

1, 4-Naphthalenedicarbonyl dichloride (**1B**) was prepared (i) by refluxing **9** (1 mole) with 2 moles of thionyl chloride and pyridine (2 moles) for 15 hrs, but the product resulted only in 76% yield and had m.p. 78°. A better method (ii) consisted in heating **9** (1 mole) with 2.2 moles of phosphorus pentachloride, affording a product with m.p. 80° (in agreement with literature data[5]) in 80% yield.

The best method (iii) was[8] from the diacid **9** (11 g, 50 mmol) refluxed for 4 hrs with 36 g (22 mL, 300 mmol) thionyl chloride and 1.5 g (20 mmol) dimethylformamide. After evaporating the excess thionyl chloride, the residue was recrystallized from petroleum ether yielding 10 g **1B** (80% yield) yellow crystals with m.p. 88°. This m.p. is higher than the literature data.

Reaction of 1B with glycine. Method (i). According to the method described previously,[1,5] the N, N′-(1,4-naphthalenediyl)-bis(glycine), **2B** was prepared in 80% yield from **9** with glycine in cold dioxane in the presence of magnesium oxide. The product had m.p. (crude) 235°, and after recrystallization from water in the presence of active carbon, 245–247°. Anal. found: N, 9.05%; $C_{16}H_{14}N_6O_6$ requires N, 8.48%.

Method (ii). The diacid dichloride **1B** (10 g, 40 mmol) was suspended in 50 mL methylene dichloride and added during one hour to a solution of glycine (6 g, 80 mmol) in aqueous 10% sodium hydroxide at 0°–5° with efficient stirring. The mixture was then stirred for 30 min. at room temperature. The organic layer was discarded and the aqueous layer was acidified with hydrochloric acid yielding **2B** (10 g, 76% yield).

2, 2′-(1, 4-Naphthalenediyl)-bis[5(4H)-oxazolone], **3B**. The dehydration of **2B** (1 mole) to the bis-azlactone **3B** was performed by stirring with two moles of dicyclohexylcarbodiimide in methylene chloride at room temperature for five hours. After separating the resulting dicyclohexylurea by filtration, the solvent was removed under reduced pressure. The crude product (89 % yield) had m.p. 217° (dec.) and after recrystallization from benzene had m.p. 225°. Anal. found : N, 8.90 %; $C_{16}H_{10}N_2O_4$ requires : N, 9.52 %.

Reaction of the bis-azlactone **3B** *with aromatic hydrocarbons ArH* (**a**,**b**). The bis-azlactone **3B** (3 g, 10 mmoles) in 50 mL aromatic hydrocarbon [benzene (**a**) or toluene (**b**)] was treated at 0° with freshly sublimed and powdered anhydrous aluminium chloride (8 g, 60 mmoles) and stirred for 48 hrs at room temperature, or for 2 hrs at 50°. The mixture was decomposed with dilute hydrochloric acid, affording in 60−67 % yield the bis-(α-acylamino)-ketones by filtration.

Compound **4Ba** (Ar=Ph) had m.p. 222° (from ethanol). Anal. found : N, 6,26 %; $C_{28}H_{22}N_2O_4$ requires : N, 6.22 %. ^{1}H−NMR (DMSO−d_6) : 4.84 (d, 4H, CH_2, J = 7 Hz), 9.00 (t, 2H, NH, J = 7 Hz), 7.5−8.6 ppm (m, 16 H, arom.)

Compound **4Bb** (Ar = p-C_6H_4Me) had m.p. 225° (from ethanol or toluene) Anal. found : N, 5.50 %; $C_{30}H_{26}N_2O_4$ requires : N, 5.85 %.

Preparation of 2, 2′-(1,4-naphthalenediyl)-bis(5-aryloxazoles) **5Ba**,**b**. On refluxing in excess $POCl_3$ for ten hours the above bis(acylamino)ketones **4B**, followed by evaporation of the unreacted phosphorus oxychloride, by decomposition of the mixture with ice-water, and by filtration, the oxazoles **5B** were obtained in 80 % yield. They were purified by column chromatography on alumina from benzene.

Compound **5Ba** (Ar=Ph), yellow crystals with m.p. 218° (from aqueous dioxane). Anal. found : N, 6.82 %; $C_{26}H_{18}N_2O_2$ requires : N, 6.76 %.

Compound **5Bb** (Ar=p-C_6H_4Me), m.p. 192°. Anal. found : N, 6.52 %; $C_{30}H_{22}N_2O_2$ requires : N, 6.33 %.

REFERENCES

[1] I. Schiketanz, A. T. Balaban and E. Ciorănescu, *Rev. Roumaine Chim.*, **27**, 1125 (1982).

[2] M. T. O'Shaughnessy and W. H. Rodebush, *J. Amer. Chem. Soc.*, **62**, 2506 (1940); G. D. Hedden and W. G. Brown, *ibid.*, **75**, 3744 (1953); L. H. Schwartzman and B. B. Corson, *ibid.*, **76**, 781 (1954); W. F. Forbes and W. A. Mueller, *ibid.*, **79**, 6495 (1957); *Canad. J. Chem.*, **33**, 1145 (1955); **34**, 1340, 1347 (1956); E. A. Braude and F. Sondheimer, *J. Chem. Soc.*, 3745 (1955); E. A. Braude and E. S. Waight, in "Progress in Stereochemistry" (ed. W. Klyne), Butterworths, London 1954, p. 126.

[3] R. W. Bayer and E. Y. O'Reilly, *J. Org. Chem.*, **23**, 311 (1958).

[4] L. Friedman and H. Schechter, *J. Org. Chem.*, **26**, 2522 (1961).

[5] R. Scholl and H. Neumann, *Ber. dtsch. chem. Ges.*, **55**, 121 (1922).

[6] L. Friedman, D. L. Fishel and H. Schechter, *J. Org. Chem.*, **30**, 1453 (1965).

[7] J. M. Griffing and L. F. Salisbury, *J. Amer. Chem. Soc.*, **70**, 3416 (1948).

[8] L. F. Fieser and M. Fieser, "Reagents for Organic Synthesis", vol. 1, Wiley, New York, 1967, p. 1158.

[9] C. S. Cleaver and B. C. Pratt, *J. Amer. Chem. Soc.*, **77**, 1544 (1955).

[10] N. Engel and W. Steglich, *Liebigs Ann. Chem.*, **1978**, 1916.

[11] F. M. F. Chen, K. Kuroda and N. L. Benoiton, *Synthesis*, **1979**, 230.

[12] D. G. Ott, F. N. Hayes, E. Hansbury and V. N. Kerr, *J. Amer. Chem. Soc.*, **79**, 5448 (1957).

Revue Roumaine de Chimie, 30, *11–12*, 985–1000 (1985)

QSAR FOR CARCINOGENESIS BY POLYCYCLIC AROMATIC HYDROCARBONS AND DERIVATIVES IN TERMS OF DELOCALIZATION ENERGY, MINIMAL STERICAL DIFFERENCES AND TOPOLOGICAL INDICES

Z. SIMON [a], A. T. BALABAN* [b], D. CIUBOTARIU [c], and T. S. BALABAN [b]

[a] Medicinal Institute of Timişoara, Department of Biophysics, Pţa. 23 August, 2, Timişoara 1900, Romania

[b] Polytechnical Institute of Bucharest, Department of Organic Chemistry, Spl. Independenţei 313, Bucharest 76206, Romania

[c] Polytechnical Institute of Timişoara, Department of Organic Chemistry, Str. Bocşa 6, Timişoara 1900, Romania

Received April 2, 1985

Experimental carcinogenesis data from the literature concerning polycyclic aromatic hydrocarbons (PAH's : benz[a]anthracene, benzo[a]pyrene and their derivatives) are interpreted in terms of QSAR using as parameters Hückel molecular orbital delocalization energies (DE), minimal steric differences (MTD), and/or topological indices (J, w, or χ). It was found that DE plus MTD account satisfactorily for partitioning PASH's into very active, moderately active and inactive structures, and allow mapping of the hypermolecule modelling the receptor site. When topological indices were used in addition to DE, it was found that the average distance sum connectivity (J) gives more significant correlations than Wiener's index w or Randić's index χ, and that a triparametric correlation, DE plus MTD plus J improves the overall correlation.

Abbreviations

BA = Benz[a]anthracene
BaP = Benzo[a]pyrene
DE = Delocalization Energy
EV = Explained Variance
HMO = Hückel Molecular Orbital
MC = Methylcholanthrene
MTD = Minimal Topological Difference
PAH = Polycyclic Aromatic Hydrocarbon
QSAR = Quantitative Structure-Activity Relationship
SCF = Self-Consistent Field
SIBIS = Steric Interactions in Biological Systems

1. INTRODUCTION

The bay region theory for carcinogenesis by benzenoid polycyclic aromatic hydrocarbons showed that the diol-epoxide derivatives are directly implied in the carcinogenic process. As demonstrated by Jerina et al.,[1] there is a good parallelism between the reactivity of the corresponding diol-epoxide I (i.e. the stabilisation of the triol-carbenium ion II resulted by ring opening of the diol-epoxide) and the carcinogenicity of the parent hydrocarbon, but metabolic and stereochemical factors are also critically important.

---

* To whom requests for reprints should be sent

Here we establish QSAR's for the carcinogenicity of a series of benz[a]anthracene derivatives, as listed by Huggins, Pataki and Harvey [2] and for benzo[a]pyrene derivatives [3]. The carbenium ion stabilisation energy, calculated by the simple HMO-method, will be used as reactivity index, while the MTD-method [4a] and topological indices [5] will be used to take into account steric effects, for partitioning the above hydrocarbons into very active, moderately active or inactive ones, and to make predictions.

Regulation of growth homeostasis in mammalian tissues is an intricate process and one may expect any mutation which affects genes involved in this process to contribute to carcinogenesis. A diol-epoxide molecule (I), acting as carcinogen by alkylation of a DNA-base, can interact (by intermolecular forces or chemical reactions) with at most 2–3 pairs of DNA bases. Therefore, one can hardly expect any specificity concerning the alkylation of certain "carcinogenic" genes or an attack at oncogenic sites of chromosomal DNA. Rather, there should be a good parallelism between somatic mutagenicity and carcinogenicity for a given animal and tissue. There may be, nevertheless, a specific targeting for a certain tissue, by enzymes transforming the aromatic hydrocarbon molecule into the alkylating diol-epoxide or by membrane transport mechanisms. Steric effects are expected to play a part in such enzyme–hydrocarbon interactions and also in the diol-epoxide–DNA interaction.

2. METHOD

a) EXPERIMENTAL CARCINOGENIC ACTIVITIES

It is difficult to establish structure-activity relationships, especially quantitative ones (QSAR's) for carcinogenic activities, since these activities are usually expressed only in a qualitative or at most semiquantitative way. For the data of Huggins, Pataki and Harvey [2] of Table 1, we use as experimental activity, A, the quotient (approximated to one significant figure):

$$A = \frac{\text{rats with sarcoma}}{\text{total number of rats in the experiment}} \qquad (1)$$

These data refer to production of muscle sarcoma in rats by a series of $N = 29$ benz[a]anthracene derivatives (including also benzo[a]pyrene and 3-methylcholantrene). The same quotient is used for the production of skin tumours (papilloma) in rats by methylbenzo[a]pyrene derivatives (3) of Table 2, but all compounds less active than the control (6% animals with tumours) were considered as inactive, i.e. with $A = 0.0$.

A QSAR is a relationship between structural parameters and the affinity towards a certain receptor. The very active compounds, i.e. those producing tumors in all animals, with $A = 1$ according to eq. (1), may have any affinity higher than an upper threshold; the inactive compounds, with $A = 0$, any affinity below a second threshold. For the moderately active compounds, producing tumors in some (but not all) animals, the 0 to 1 range, given by eq. (1) for A, may reflect well these affinities, but if very active and inactive compounds are also considered, this range should be extended. The linear correlation coefficient, r, is not so meaningful as the possibility to classify the compounds according to the calculated activities $\hat{A}$ (by the QSAR): very active for $\hat{A} \geq 1$, moderately active for $1 > \hat{A} > 0$ and inactive for $\hat{A} \leq 0$. As discussed below in the section "Results", this classification is improved if the 0 to 1 scale for "experimental" activities is enlarged, considering threshold values $A = -0.5$ for the inactive compounds and $A = 1.5$ for the very active ones.

b) CARBOCATION STABILISATION ENERGIES

The reactivity of the diol-epoxide derivative (I) in DNA alkylation should be parallel to the reactivity toward hydrolysis. Jerina et al.[6] found indeed a good correlation between solvolysis rate constants and carbocation stabilisation energies. They concluded that there is no significant difference between the correlational results obtained with carbocaton stabilisation energies calculated via a perturbational approach within the framework of the simple HMO method and those obtained with much more sophisticated SCF-MO-methods.

Here we shall use the ω-HMO-method to calculate carbocation stabilisation energies as differences between delocalisation energies of structures III and IV. Structures III and IV are simplified models for biologically relevant compounds II and I, respectively.

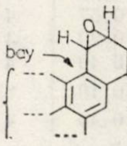

I

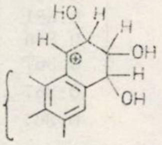

II

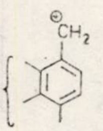

III

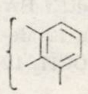

IV

$$DE = DE\,(III) - DE\,(IV) \quad \text{in } \beta\text{-units} \tag{2}$$

The results, in β units, are listed under the corresponding headings in Tables 1 and 2.

Alkyl and alkoxy-substituents to the aromatic moiety were considered as heteroatoms with two π-electrons and with the following parameters (CH_3 stands for any alkyl group):

$$\alpha_{CH_3} = \alpha + 2\beta \qquad \beta_{C-CH_3} = 0.6\,\beta$$
$$\alpha_{OCH_3} = \alpha + 2\beta \qquad \beta_{O-CH_3} = 0.8\,\beta \tag{3}$$

The calculations were performed on the FELIX M–18 computer of the Biophysics-Department in Timişoara.

Table 1

Carcinogenic benz[a]anthracene derivatives

i	Derivative	*A*	DE(β)	MTD	$\hat{A}(5)$	MTD$^+$	$\hat{A}(7)$
	a) Very active derivatives						
1	3-MC	⩾1.0	0.871	3	1.05	2	1.57
2	BaP		0.867	3	1.01	3	0.87
3	7-Me-BA		0.867	4	0.71	3	0.87
4	6-Me-BA		0.891	4	0.94	3	1.41
5	7-MeO-12-Me-BA		0.884	4	0.87	3	1.25
6	7-Et-12-Me-BA		0.867	4	0.71	3	0.87
7	7,12-diMe-BA		0.867	3	1.01	2	1.48
8	7-EtO-12 Me-BA		0.884	5	0.57	4	0.64
	b) Moderately active derivatives						
9	7-nPr-12-Me-BA	0.7	0.867	5	0.40	4	0.26
10	12-Me-BA	0.7	0.846	4	0.51	3	0.40
11	8-ME-BA	0.6	0.853	4	0.57	3	0.56
12	7-Me-12-Et-BA	0.6	0.867	4	0.71	3	0.87
13	7,12-diMeO-BA	0.5	0.885	5	0.58	4	0.66
	c) Inactive derivatives						
14	1-Me-BA	⩽0.0	0.848	6	−0.08	5	−0.78
15	2-Me-BA		0.848	6	−0.08	5	−0.78
16	3-Me-BA		0.848	6	−0.08	5	−0.78
17	4-Me-BA		0.848	6	−0.08	5	−0.78
18	5-Me-BA		0.847	6	−0.09	5	−0.80
19	9-Me-BA		0.848	5	0.22	4	−0.16
20	10-Me-BA		0.853	6	−0.03	4	−0.05
21	11-Me-BA		0.848	6	−0.08	4	−0.16
22	BA		0.848	5	0.22	4	−0.16
23	7-Et-BA		0.867	5	0.40	4	0.26
24	7-nBu-BA		0.867	7	−0.20	6	−0.96
25	7-MeO-BA		0.881	5	0.57	4	0.57
26	12-Et-BA		0.846	5	0.20	4	−0.21
27	7,12-diEt-BA		0.867	5	0.40	4	0.26
28	7-nBu-12-Me-BA		0.867	6	0.10	5	−0.35
29	7-MeOCH$_2$-12-Me-BA		0.867	5	0.40	4	0.26

A — biological activities (rats with sarcoma per total rats); DE(β) — cation stabilisation energy, in β units; MTD — miniml steric difference according to the receptor map $\boldsymbol{S}(5)$; $\hat{A}(5)$ — calculated biological activity according to eq. (5); MTD$^+$ and $\hat{A}(7)$ — the same, according to the receptor map $\boldsymbol{S}^+$ (Fig. 2) and eq. (7); 3-MC : 3-methylcholanthrene ;BaP-benzo[a]pyrene ; BA : benz[a]anthracene.

c) THE MTD METHOD

The MTD method (4) describes the spatial structures by a topological network of points (vertices) symbolizing atoms other than hydrogen (the hypermolecule) obtained by superposition of the considered molecules, M_i. The vertices, $j = 1, 2, \ldots, M$, of the hypermolecule correspond to the approximate position of atoms of the M_i, s in their complex with the receptor. If vertex j is occupied by M_i, we have $x_{ij} = 1$, whereas $x_{ij} = 0$ if j is not occupied. These vertices are assigned to the receptor cavity ($\varepsilon_j = -1$), the receptor walls ($\varepsilon_j = +1$) or to the external space ($\varepsilon_j = 0$) by an optimisation procedure. The minimal steric (topological) difference (MTD_i) o

Table 2

Carcinogenic methyl-benzo[a]pyrene derivatives

i	Derivative	A	DE(β)	MTD	$\hat{A}(6)$	MTD$^+$	$\hat{A}(8)$
	a) Active derivatives						
1	11-Me-BaP	0.9	0.866	2	0.89	2	0.84
2	1-Me-BaP	0.8	0.886	3	1.01	3	1.01
3	3-Ma-BaP	0.8	0.885	—	—	4	0.45
4	12-Me-BaP	0.7	0.886	4	0.59	3	1.01
5	BaP	0.7	0.867	3	0.50	3	0.35
6	4-Ne-BaP	0.7	0.886	4	0.59	4	0.49
7	2-Me-BaP	0.4	0.867	—	—	3	0.35
8	5-Me-BaP	0.3	0.867	—	—	4	−0.16
9	6-Me-BaP	0.2	0.866	4	0.06	4	−0.20
	b) Inactive derivatives						
10	7-Me-BaP	$\leqslant 0.0$	0.867	4	0.09	4	−0.16
11	8-Me-BaP		0.867	4	0.09	4	−0.16
12	9-Me-BaP		0.867	4	0.09	4	−0.16
13	10-Me-BaP		0.867	4	0.09	4	−0.16

Legend : see Table 1 : A — experimental activities (rats with papilloma per total number of rats). MTD — values are not given for molecules with i : 3, 7, 8 as they occupy also vertices which are not contained in the receptor map $S(5)$.

molecule M_i is a measure for its misfit into the receptor and is calculated according to the formula :

$$\mathrm{MTD}_i = s + \sum_{j=1}^{M} \varepsilon_j x_{ij} \tag{4}$$

with s being the total number of cavity ($\varepsilon_j = -1$) vertices.

The hypermolecule corresponding to the $N = 29$ compounds of Table 1 is depicted on Figure 1. The bay-region benzene ring which is transformed into the diol-epoxide moiety occupies always the same position (the six-membered ring indicated by an asterisk in Fig. 1) The vertices occupied by all the 29 compounds are not numbered. Vertices $j = 1 - 12$ correspond to the same substituent-positions in benz[a]anthracene. The 12-ethyl group occupies vertices $j = 12, 13$; the 7-ethyl group occupies vertices $j = 7, 14$ or $j = 7, 17$ and the 7-n-butyl group occupies vertices $= 7, 14, 15, 16$ or $j = 7, 17, 21, 22$. The attributions ε_j for vertices

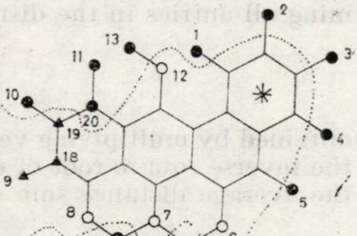

Fig. 1. — Hypermolecule and receptor map $S(5)$. Numberings correspond to the j-vertices ; ε_j-assignments : full black circles, ●, $\varepsilon_j = +1$; full open circles, ○ , $\varepsilon_j = -1$; triangles, ▲, $\varepsilon_j = 0$. The marked (*) six-membered ring in benzopyrene and benzanhracene derivatives is attacked to give the carcinogenic bay-region diol-epoxide. The dotted line, . . , is the predicted limit for the receptor cavity walls.

$j = 17, 21, 22$ are not allowed to be more "favourable" than for $j = 14$, 15, 16 ; if not, the ethyl or butyl group would adopt the alternative, more "favourable" conformation. The benz[a] anthracene (BA) system occupies the common (non-numbered) vertices and $j = 18, 19, 20$; 3-methylcholanthrene (MC) occupies the common vertices and $j = 7, 8, 9, 18, 19, 20$; benzo[a]pyrene (BaP) occupies the common vertices and $j = 6, 7, 8, 14, 17$.

For the $N = 13$ compounds of Table 2, the methyl groups in positions 1, 4, 6, 7, 8, 9, 10, 11 and 12 of the benzo[a]pyrene system occupy, correspondingly, the vertices $j = 18, 15, 5, 4, 3, 2, 1, 12$ and 20 of the hypermolecule.

Our hypermolecule contains $M = 22$ vertices and this is also the number of ε_j-parameters which must be assigned to the -1, 0 or $+1$-values by the MTD-optimisation procedure. For only $N = 29$ experimental A-values, such an assignment, per se, can be but of a very low reliability In order to avoid unnatural, fortuitous, ε_j-assignements we shall introduce some restrictions in the sense of the vertex connectivity conditions of the SIBIS-method [7]. Namely, all cavity ($\varepsilon_j = -1$) vertices should form a single connected network, corresponding to the molecule which fits perfectly into the receptor cavity ; also, we shall avoid isolated wall ($\varepsilon_j = +1$ or external ($\varepsilon_j = 0$) vertices which do not fit into the representation of a receptor cavity with a single, or only a few, opening(s) to the exterior

d) TOPOLOGICAL INDICES

Three topological indices from the various available ones (reviews refs.[4b,5-8]) were selected : Wiener's index :[9]

$$w = \frac{1}{2} \sum_{k=1}^{n} s_k$$

half of the sum of all distance sums or distance degrees obtained by summing all entries in the distance matrix ; Randić's index : [10]

$$\chi = \sum_{q \text{ edges } kl} (v_k v_l)^{-1/2}$$

obtained by multiplying vertex degrees of endpoints for each edge, takin the inverse square root of the product, and summing for all q edges ; an the average distance sum connectivity : [11,12]

$$J = \frac{q}{\mu + 1} \sum_{q \text{ edges } kl} (s_k s_l)^{-1/2}$$

obtained analogously to χ but multiplying distance sums instead of verte degrees and averaging by the factor $q(\mu + 1)^{-1}$, where q is the numbe of edges and $\mu = q - n + 1$ is the cyclomatic number of the graph wit q edges and n vertices. Distance sums s_k for each vertex k are sums of topological distances from vertex k to all other vertices in the graph ; summing the adjacency matrix over rows or columns leads to distance sums s

just as summing analogously the adjacency matrix leads to vertex degrees, v_k: Topological index J was calculated by a specially devised computer program on a Hewlett-Packard HP–9830 desk-top computer from adjacency data [13].

3. RESULTS

a) CARCINOGENICITY *VERSUS* DE AND MTD

A first set of correlational equations was obtained considering the limits $A = 1.0$ for the activity of very active derivatives and $A = 0.0$ for the inactive derivatives.

The correlations with carbocation stabilisation energies, DE, are modest, but significant at a 95 % level : $r = 0.559$ for the $N = 29$ derivatives of Table 1 and $r = 0.621$ for the $N = 13$ compounds of Table 2.

The MTD-optimisation procedure was applied to the set (5) of $N=29$ derivatives of Table 1, considering DE as a second structural parameter, along with MTD. The optimisation was performed considering the restrictions discussed in section 2c. The following receptor map $S(5)$ and correlational results were obtained (see also Fig. 1) * :

$$S(5) \begin{cases} j(\varepsilon = -1) : 6-8,\ 12 \text{ and common vertices} \\ j(\varepsilon = 0) : 9,\ 18,\ 19 \\ j(\varepsilon = +1) : 1-5,\ 10,\ 11,\ 13-17,\ 20-22 \end{cases}$$

$$\begin{gathered} \hat{A}(5) = -6.397 + 9.597 \text{ DE } -0.303 \text{ MTD} \\ r = 0.860,\ N = 29,\ s = 0.222,\ \text{F} = 26.0,\ \text{EV} = 0.738 \end{gathered} \tag{5}$$

The partial correlation and intercorrelation coefficients are :

$$r(\text{MTD}) = -0.816,\ r(\text{DE}) = 0.559,\ r(\text{MTD, DE}) = -0.369$$

The ε_j-attributions of $S(5)$ are optimal according to the $\Delta Y(\varepsilon_j)$ criterion [4]. A 95 % level of reliability for the ε_j-assignments would require $\Delta Y \geqslant 0.8\ Y = 1.06$; as seen from Table 3, no attribution meets this condition. Especially for any of the vertices $j : 1-5$, the $\varepsilon_j = 0$ attribution is almost as good as $\varepsilon_j = +1$, while for any of the vertices $j :\ 9-11$ and 20, $\varepsilon_j = 0$ is almost equivalent to $\varepsilon_j = +1$.

The set (6) of $N = 10$ molecules from Table 2, whose atoms occupy only the vertices assigned to atoms in molecules of Table 1, can be considered as a test series. With MTD's calculated with $S(5)$ and eq. (4), and DE's the following correlational results are obtained :

$$\begin{gathered} \hat{A}(6) = -21.250 + 26.532 \text{ DE} - 0.146 \text{ MTD} \\ N = 10,\ r = 0.941,\ s = 0.131,\ \text{F} = 15.5,\ \text{EV} = 0.853 \\ r(\text{DE}) = 0.573,\ r(\text{MTD}) = -0.695 \end{gathered} \tag{6}$$

---

* Here and in all subsequent QSAR's, F is the Fisher test, EV the explained variance, and s the standard deviation.

Table 3

Reliability of vertex attributions in $S(5)$

j	$i(x_{ij} = 1)$	$\Delta Y(-1)$	$\Delta Y(0)$	$\Delta Y(+1)$
1	14	+0.25	+0.04	0
2	15	+0.25	+0.04	0
3	16	+0.25	+0.04	0
4	17	+0.25	+0.04	0
5	18	+0.25	+0.04	0
6	2,4	0	+0.20	+0.75
7	1,3,5−9,12,13,23−25,27−29	0	+0.60	+2.50
8	1,2,11	0	+0.25	+1.10
9	1,19	+0.34	0	+0.01
10	20	+0.32	+0.07	0
11	21	+0.25	+0.04	0
12	5−10,12,13,26−29	0	+0.67	+2.60
13	12,13,26	+1.60	+0.51	0
14 and 17	2,5,6,8,9,13,23−25,25−29	+2.65	+0.68	0
15 and 21	8,9,24,28,29	+1.00	+0.12	0
16 and 22	28	+0.47	+0.15	0
18, 19	1,3−29	+0.08	0	+0.10
20	1,3−29	+0.35	+0.08	0

j-Vertices of the hypermolecule of Fig. 1; $i(x_{ij} = 1)$ — molecules i in which vertex j is occupied, $\Delta Y(-1)$, $\Delta Y(0)$, $\Delta Y(+1)$ represent the increase in the sum (4):

$$Y = \sum_{i=1}^{N} (A - \hat{A})^2$$

when the ε_j — atribution of the receptor map $S(5)$ is changed into -1 and 0 or $+1$, respectively. A 95% — reliability of the ε_j attribution in $S(5)$ requires $\Delta Y \geqslant 1.06$ or both alternative attributions (see main text, in the Results-section 3a).

This excellent result can be considered as a test for the ε_j-attributions for vertices j : 1−8, 12, 14, 15, 18, 20, occupied also by the BaP-derivatives of Table 2. The receptor cavity, as depicted by the receptor map of Figure 1, should accomodate almost perfectly the 6, 7, 8, 12-tetramethyl-benz[a]anthracene molecule, but one cannot be sure if the receptor walls include also vertices j : 10, 11, 20, or if some of these vertices are in the external region.

The correlational results (5) and (6) can be considered as satisfactory; the predicted receptor map is reasonable from the chemist's point of view, but if $\hat{A} \geqslant 1.0$ and $\hat{A} \leqslant 0.0$-limits are considered for very active and inactive molecules, respectively, several false very active—to—moderately active and moderately active—to—inactive predictions result by the $\hat{A}(5)$ and $\hat{A}(6)$— calculated activities listed in Tables 1 and 2.

In order to improve the prediction of very active, moderately active and inactive compounds we performed a rather unorthodox attempt: $A = 1.5$ (instead of 1.0) will be considered for the very active compounds, and $A = -0.5$ (instead of 0.0) for the inactive ones. Also, we extended the hypermolecule and receptor map of Fig. 1 in order to achieve as good as possible an agreement with the qualitative carcinogenicities of the polynuclear hydrocarbons of Table 4. For this purpose, the vertices corresponding to the common molecular core will be attributed to the cavity ($\varepsilon_j = -1$). Vertices $j = 10, 11, 20$ will be attributed to the exterior ($\varepsilon_j = 0$), in order to obtain reduced MTD-values for hydrocarbons $i = 4$ and 6, with weak carcinogenic activity but very low reactivity indices. Supplementary vertices will be considered in the exterior ($\varepsilon_j = 0$), except those which obviously fall beyond the receptor wall limits of the receptor map $S(5)$ of Fig. 1. The receptor map S^+ depicted in Fig. 2 results therefrom; the corresponding receptor cavity is a sort of flat plateau bordered of three sides by the receptor walls and by a precipice on the fourth (the left-hand side of Fig. 2).

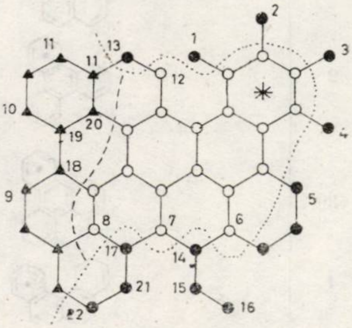

Fig. 2 — Hypermolecule and generalised receptor map S^+. Legend – see Figure 1. The dotted line, ..., denotes the cavity/receptor wall border; the interrupted line, — — — —, marks the cavity/external space border.

For the $N = 29$ compounds of Tab. 1, the corresponding correlational equation is:

$$\hat{A}(7) = -16.703 + 22.387\ \mathrm{DE} - 0.611\ \mathrm{MTD}^+$$

$$r = 0.840,\ s = 0.482,\ \mathrm{F} = 20.0,\ \mathrm{EV} = 0.684 \qquad (7)$$

$$r(\mathrm{MTD}^+) = 0.775,\ r(\mathrm{DE}) = 0.573$$

For the $N = 13$ compounds of Tab. 2:

$$\hat{A}(8) = -27.796 + 34.260\ \mathrm{DE} - 0.517\ \mathrm{MTD}$$

$$r = 0.480,\ s = 0.323,\ \mathrm{F} = 6.4,\ \mathrm{EV} = 0.615 \qquad (8)$$

The classification into very active ($\hat{A} \geqslant 1.0$), moderately active ($1.0 > \hat{A} > 0.0$) and inactive ($\hat{A} \leqslant 0.0$) compounds is improved, but there remain a few false predictions (overlaps between neighbouring, not between the extreme classes). As to the qualitative data of Tab. 4, the agreement between activity vs. DE and MTD$^+$ is good, except compound $i = 4$ which is calculated as inactive although it is slightly active.

b) CARCINOGENICITY *VERSUS* DE, MTD, AND TOPOLOGICAL INDICES

Table 5 presents three topological indices (the Wiener index w, the Randić index χ, and the average distance sum connectivity J) for each carcinogenic hydrocarbon of Table 1 which have no substituent or only one methyl substituent. It may be observed that, according to expectations,

Table 4

Various carcinogenic polycyclic aromatic hydrocarbons

i	Hydrocarbon	A	DE(β)	MTD⁺
1	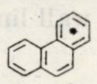	—	0.658	5
2	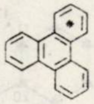	—	0.664	7
3	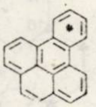	—	0.714	7
4	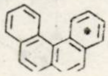	+	0.600	5
5	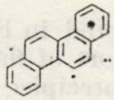	+	0.640	3
6	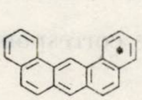	+	0.722	4
7	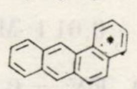	+	0.766	4
8	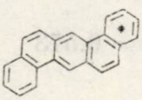	+++	0.738	3
9	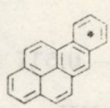	++++	0.794	3
10	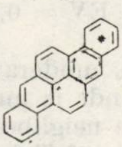	++++	0.845	3
11	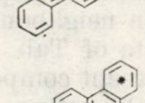	++++	0.870	3

A — approximate carcinogenicity according to Jerina et al. (1); — : inactive; +, +++, ++++ : various increasing activities.

The hydrocarbons are arranged such as to bring the epoxidated six-membered ring (marked by *) in the same position (right-upwards) for all molecules. DE(β) are carbocation stabilisation energies calculated by Jerina et al. (1) by a perturbational HMO-method (instead of the ω — HMO method used for the derivatives in Tabs. 1 and 2). For other notation — see legend of Table 1.

there is no degeneracy of J values i.e. no two different structures have the same J index. Interestingly, the degeneracy of the Randić index χ is quite high, and that of the Wiener index w is low; this fact is due to J and w being based on topological distances which vary appreciably with varying structures whereas χ is based on vertex degrees which vary little among position isomers. The last four columns of Table 5 represent activities $\hat{A}$ calculated according to the correlational equations (9)—(12) for the molecules in this Table.

$$\hat{A}_{\mathrm{MTD}} = -23.949 + 30.805\ \mathrm{DE} - 0.568\ \mathrm{MTD}$$

$$r = 0.920\,;\ \mathrm{F} = 18.29\,;\ \mathrm{EV} = 0.818\,;\ s = 0.340 \tag{9}$$

$$\hat{A}_J = -53.572 + 50.051\ \mathrm{DE} + 6.898\ J$$

$$r = 0.819\,;\ \mathrm{F} = 6.79\,;\ \mathrm{EV} = 0.611\,;\ s = 0.496 \tag{10}$$

$$\hat{A}_W = -46.349 + 53.041\ \mathrm{DE} + 0.001786\ w$$

$$r = 0.794\,;\ \mathrm{F} = 5.69\,;\ \mathrm{EV} = 0.564\,;\ s = 0.256 \tag{11}$$

$$\hat{A}_\chi = -48.481 + 46.139\ \mathrm{DE} + 0.984\ \chi$$

$$r = 0.823\,;\ \mathrm{F} = 6.98\,;\ \mathrm{EV} = 0.618\,;\ s = 0.492 \tag{12}$$

It should be stressed that eq. (9) refers only to the 14 molecules of Table 5, while the analogous equation (7) containing the same parameters (DE and MTD) was based on all 29 molecules of Table 1.

Table 5

Sarcoma induction *versus* MTD and topological indices

i	Hydrocarbon	A	DE	MTD$^+$	J	w	χ	$\hat{A}_{\mathrm{MTD}}$	$\hat{A}_J$	$\hat{A}_w$	$\hat{A}_\chi$
1(2)	BaP	$\geqslant 1.0$	0.8675	3	1.4872	680	9.916	1.07	0.50	0.88	1.30
2(3)	7-Me-BA		0.8667	3	1.5622	624	9.343	1.04	0.98	0.74	0.70
3(4)	6-Me-BA		0.8914	3	1.5524	628	9.326	1.81	0.22	2.05	1.82
4(10)	12-Me-BA	0.7	0.4856	3	1.5735	620	9.343	0.39	−0.01	−0.34	−0.27
5(11)	8-Ma-BA	0.6	0.8527	3	1.5207	640	9.326	0.61	−0.01	−0.02	−0.03
6(14)	1-Me-BA	$\leqslant 0.0$	0.8480	5	1.5410	632	9.326	−0.67	−0.11	−0.24	−0.18
7(15)	2-Me-BA		0.8480	5	1.5215	641	9.310	−0.67	−0.30	−0.22	−0.20
8(16)	3-Me-BA		0.8480	5	1.4954	652	9.310	−0.67	−0.42	−0.20	−0.20
9(17)	4-Me-BA		0.8480	5	1.5213	640	9.326	−0.67	−0.24	−0.23	−0.18
10(18)	5-Me-BA		0.8469	5	1.5412	632	9.326	−0.70	−0.16	−0.30	−0.23
11(19)	9-Me-BA		0.8478	4	1.4941	652	9.310	−0.10	−0.44	−0.21	−0.20
12(20)	10-Me-BA		0.8528	4	1.5021	648	9.310	0.05	−0.13	0.04	0.02
13(21)	11-Me-BA		0.8476	4	1.5296	636	9.326	−0.11	−0.21	−0.25	−0.19
14(22)	BA		0.8480	4	1.5122	553	8.916	−0.10	−0.31	−0.38	−0.42

The numbers in parentheses (after i), refer to i of Table 1.

A, DE and MTD$^+$ — values, as in Table 1. For the definition of the topological indices J, w, χ — see section 2d (main text).

$\hat{A}_{\mathrm{MTD}}$, $\hat{A}_J$, $\hat{A}_w$, $\hat{A}_\chi$ are calculated activities according to eqs. (9), (10), (11) and (12), respectively.

Table 6

Intercorrelation and partial correlation coefficients for *Sarcoma* induction

	A	DE	MTD	J	w	χ
DE	0.792	1	−0.583	0.207	0.118	0.404
MTD	−0.841		1	−0.252	0.016	−0.289
J	0.367			1	−0.364	−0.209
w	0.150				1	0.822
χ	0.511					1

The A, DE, MTD, J, w and χ – values are those of Table 5.

Table 6 indicates the partial correlation and intercorrelation coefficients between parameters DE, J, w and χ for the 14 compounds listed in Table 5. The negative $r(J, w)$ and $r(J, \chi)$ intercorrelation coefficients are due to the fact that whereas J increases with increased branching, χ and w decrease with increased branching.

Table 7

Papilloma induction versus MTD and topological parameters

i	Hydrocarbon	A	DE	MTD$^+$	J	w	χ	$\hat{A}_J$	$\hat{A}_w$	$\hat{A}_\chi$	$\hat{A}_{MTD,J}$
1	11-Me-BaP	0.9	0.8659	2	1.5201	762	10.326	0.36	0.05	−0.05	0.95
2	1-Me-BaP	0.8	0.8856	3	1.4896	778	10.326	0.62	0.67	0.71	0.79
3	3-Me-BaP	0.8	0.8855	4	1.4892	778	10.326	0.62	0.67	0.71	0.42
4	12-Me-BaP	0.7	0.8860	3	1.5112	766	10.326	0.91	0.80	0.73	1.09
5	BaP	0.7	0.8675	3	1.4872	680	9.916	0.01	0.87	0.66	0.29
6	4-Me-BaP	0.7	0.8858	4	1.5036	770	10.326	0.80	0.75	0.72	0.55
7	2-Me-BaP	0.4	0.8675	3	1.4720	788	10.310	−0.18	−0.13	0.03	0.16
8	5-Me-BaP	0.3	0.8668	4	1.5121	766	10.326	0.29	0.05	−0.02	0.01
9	6-Me-BaP	0.2	0.8657	4	1.5195	762	10.343	0.35	0.04	−0.09	0.04
10	7-Me-BaP	$\leqslant 0.0$	0.8675	4	1.4874	778	10.326	0.01	−0.03	0.01	−0.18
11	8-Me-BaP		0.8675	4	1.4635	792	10.310	−0.29	−0.16	0.03	−0.38
12	9-Me-BaP		0.8675	4	1.4736	786	10.310	−0.16	−0.11	0.03	−0.29
13	10-Me-BaP		0.8675	4	1.4989	772	10.326	0.15	0.02	−0.01	−0.08

The A, DE and MTD$^+$ values, as in Table 2. For the definition of the topological indices J, w, χ-see section 2d (main text), $\hat{A}_J$, $\hat{A}_w$, $\hat{A}_\chi$ and $\hat{A}_{MTD,J}$ are calculated activities according to eqs. (14), (15), (16) and (13), respectively.

Table 7 presents the analogous data as in Table 5, but referring to Papilloma induction; the polycyclic aromatic hydrocarbons are the same as in Table 2. The last four columns in Table 7 indicate calculated carcinogenic activities for 13 hydrocarbons having at most one methyl substituent, according to the equations:

$$\hat{A}_{\mathrm{MTD},\,J} = -39.138 + 32.480\ \mathrm{DE} + 8.506\ J - 0.468\ \mathrm{MTD} \qquad (13)$$

$$r = 0.861;\ \mathrm{F} = 5.74;\ \mathrm{EV} = 0.655;\ s = 0.290$$

$$\hat{A}_J = -46.621 + 32.474 \text{ DE} + 12.411 \ J \tag{14}$$

$$r = 0.682 \,;\ \text{F} = 2.60 \,;\ \text{EV} = 0.358 \,;\ s = 0.417$$

$$\hat{A}_w = -26.620 + 38.933 \text{ DE} - 0.00924 \ w \tag{15}$$

$$r = 0.714 \,;\ \text{F} = 3.12 \,;\ \text{EV} = 0.411 \,;\ s = 0.400$$

$$\hat{A}_\chi = -17.262 + 38.849 \text{ DE} - 1.591 \ \chi \tag{16}$$

$$r = 0.634 \,;\ \text{F} = 2.02 \,;\ \text{EV} = 0.283 \,;\ s = 0.441$$

Table 8

Intercorrelation and partial correlation coefficients for *Papilloma* induction

	A	DE	MTD	*J*	*w*	χ
DE	0.554	1	−0.023	0.099	0.137	0.188
MTD	−0.616		1	−0.230	0.311	0.248
J	0.451			1	−0.227	0.267
w	−0.371				1	0.877
χ	−0.200					1

The A, DE, MTD, *J*, *w* and χ-values are those of Table 7.

Table 8 indicates, analogously to Table 6, the intercorrelation and partial correlation coefficients for Papilloma induction among MTD, DE, *J*, *w* and χ.

4. DISCUSSION OF THE RESULTS AND CONCLUSIONS

Correlations (5)—(8) between HMO delocalisation energies (DE) and MTD give satisfactory agreement ($r = 0.82$ to 0.86, with a test series (6) having $r = 0.94$) and allow a classification of the compounds into three categories : (i) very active, (ii) moderately active, and (iii) inactive, which is correct for most compounds (41 out of 53) ; there are no false assignments between classes (i) and (iii) but only between neighbouring ones, (i) and(ii) or (ii) and (iii).

The receptor map S^+ (Fig. 2) could map the active receptor site of the enzyme responsible for converting a polycyclic hydrocarbon into the diol-epoxide which is considered to be the ultimate carcinogen. The receptor map S^+ is in agreement with the qualitative conclusions of Huggins, Pataki and Harvey [2], that the carcinogenicity of benz[a]anthracene is increased by substituents in positions 6, 7, 8 and 12 that at least one surface "top" or "bottom" of the PAH should not be higher than cca. 4 Å.

Correlations involving only DE and one of the three topological indices *J*, *w* and χ are at best comparable to those involving DE and MTD. On adding *J*, *w* or χ, as a second parameter to DE for Papilloma induction the *r* value increases significantly from 0.554 to 0.682, 0.714 and 0.634, respectively (see Table 8 and eqs. (14)—(16)) ; for Sarcoma induction the corresponding increases are from 0.792 to 0.819, 0.794 and 0.823, respectively (see Table 6 and eqs. (10)—(12)).

If one considers the regression coefficients and the partial correlation coefficients for J, they are comparable for both series of activities (Papilloma and Sarcoma), while for w and χ they are negative for Papilloma induction and positive for Sarcoma induction. A summary of all these correlational data is presented synoptically in Table 9.

Table 9

Summary of correlational results of DE and topological indices

Coefficient \ Parameters	DE	DE+ J	DE+ w	DE+ χ
A. Sarcoma induction (see Tab. 5)				
Correlation coefficient, r	0.792	0.819	0.794	0.823
Partial correlation coeff.	—	0.367	0.150	0.511
Regressional coefficient	—	6.898	0.00179	0.984
Equation no.	—	(10)	(11)	(12)
B. Papilloma induction (see Tab. 7)				
Correlation coefficient, r	0.554	0.682	0.714	0.634
Partial correlation coeff.	—	0.451	−0.371	−0.200
Regressional coefficient	—	12.411	−0.00924	−1.591
Equation no.	—	(14)	(15)	(16)

Partial correlation coefficients and regressional coefficients in column DE+ J, DE+ w and DE+ χ refer to the parameters J, w and χ, respectively.

One may conclude from Table 9 that among the three topological indices investigated in the present paper, the increase of correlation coefficient by adding either w or χ to DE might be due to chance correlations since the partial correlation coefficients and the regressional coefficients for w and χ are of opposite sign in the two series of similar biological activities. Therefore it appears that J is better suited for this type of correlation because it gives comparable increase of r values in biparametric correlations together with DE, conserving the sign and magnitude of partial correlation coefficients and regressional coefficients.

It is also apparent from Tables 6 and 8 that there is a strong intercorrelation between w and χ (0.822 and 0.877, respectively) but not between J and these two parameters (intercorrelation coefficients from 0.20 to 0.33). This supports the above conclusion.

In comparison with correlations based on DE and MTD, the correlations involving DE and a topological index are inferior; moreover, the MTD optimized map of the receptor is easier to interpret in terms of molecular structure. However, topological indices have the advantage of being unique numbers for a given molecular structure, unlike MTD which implies a large number of adjustable ε_j parameters.

The triparametric correlation (13) in terms of DE, MTD and J improves markedly the overall results, both as far as correlation coefficients are concerned, and with regard to partitioning the hydrocarbons into the three categories (i)—(iii). The correlation coefficient r increases from 0.824 (eq.) 18) for DE and MTD) to 0.861 (eq. (13). The biparametric correlation DE + MTD (Table 2 and eq. (7)) has four misfits with regard to partitioning, the biparametric correlation DE + J (Table 7 and eq. (14)) three misfits, the triparametric correlation DE + J + MTD (Table 7 and eq. (13)) has only one misfit.

5. SOME CONCLUSIONS CONCERNING THE CARCINOGENESIS MECHANISM AND PREDICTIONS

The successful classification of a wide variety of PAH's and derivatives by carbocation stabilisation energies and MTD (a parameter for the steric misfit of the effector into the receptor site) suports Jerina's mechanism (the diol epoxide as ultimate carcinogen) and the common nature of pacemaker steps in carcinogenesis.

The variation range of the calculated DE-values, 0.045 β, (about 3—4 kj/mol) may explain a rate increase factor of about 5 for carbocation formation (at cca 300 K). The regressional coefficient for DE in eq. (7), -22.4, yields a range of about 1.0 logarithmic units for the calculated activity $\hat{A}$.

The usual DNA-alkylation site is the N_7-guanine atom. In the receptor map S^+ of Fig. 2, the alkylating moiety of the carcinogen should occupy the inner corner of the receptor cavity (marked by the asterisk, *) ; thus a carcinogen—base pair—intercalation, favouring the alkylation, is difficult to reconcile with this receptor map. Rather, S^+ should correspond to the receptor site of an enzyme converting the PAH's into diol-epoxides. The carcinogenic potency of a PAH should be given by both the diol-epoxide formation rate and its carbocation forming ability.

A cautionary note is needed concerning the too literal interpretation of the notion "receptor map" : the mechanism by which methyl groups on positions 1—4 of benz[a]anthracene inhibit carcinogenic activity is probably different (interference with the formation and/or stereochemistry the bay-region diol epoxide) from the mode in which methyl groups on other sites increase or decrease the activity ; therefore "cavity walls" are mathematical models rather than a physical reality.

The receptor map S^+ is in agreement with the conclusions of Huggins, Pataki and Harvey (2), see also Lowe and Silverman (14), that the carcinogenicity of benz[a]anthracene is enhanced by substituents in positions 6, 7, 8 and 12. Therefore 6,7,8,12-tetra- or 6,7,8-trimethyl-benz[a]anthracene (V) and also the phenanthrene derivatives VI and VII all with $MTD^+ = 0$, are predicted to be strong carcinogens.

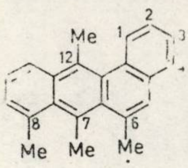

V

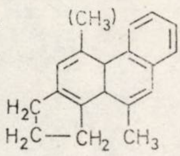

VI

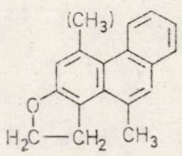

VII

ACKNOWLEGEMENTS. Thanks are expressed to dr. G. I. Mihalaş from the Biophysics Department, Timişoara Medical Institute, for computations.

REFERENCES

[1] D. M. Jerina, J. M. Sayer, D. R. T., Thakker, H. Yagi, W. Levin, A. W. Wood and A. H. Connery, (1980), "Carcinogenicity of polycyclic aromatic hydrocarbons : the bay-region theory", in B. Pullman, P.O.P. Ts'o, and H. Gelboin, (Eds.), "Carcinogenesis. Fundamental Mechanisms and Environmental Effects", p. 1–12. D. Reidel Publ. Corp., New York.

[2] C. B. Huggins, J. Pataki and R. G. Harvey, *Proc. Nat. Acad. Sci. USA*, 58, 2253 (1967).

[3] T. J. Slaga, G. L. Gleason, G. Mills, L. Ewald, P. P. Fu, H. M. Lee and R. G. Harvey, *Cancer Res.*, **40**, 1981 (1980).

[4] A. T. Balaban, A. Chiriac, I. Moţoc, and Z. Simon, (1980). *Steric Fit in QSAR*, Lecture Notes in Chemistry No. 15, Springer Verlag Berlin : (a) chapter 5, p. 77–108; (b) chapter, 2, p. 22–51.

[5] A. T. Balaban, I. Moţoc, S. Bonchev, and O. Mekenyan, (1983), Topological indices for structure-activity correlations, in M. Charton and I. Moţoc, (Eds.), *Topics Curr. Chem.* 114, 23–53.

[6] J. M. Sayer, R. E. Lehr, D. L. Whalen, H. Yagi, and D. M. Jerina, *Tetrahedron Letters*, **23**, 4431 (1982).

[7] I. Moţoc and D. Filimonescu, *Math. Chem.*, **12**, 117 (1981).

[8] L.B. Kier, and L.H. Hall, *"Molecular Connectivity in Chemistry and Drug Research"*, Academic Press, New York, 1976.

[9] H. Wiener, *J. Amer. Chem. Soc.* **69**, 17 (1947).

[10] M. Randić, *J. Amer. Chem. Soc.*, **97**, 6609 (1975).

[11] A. T. Balaban, *Chem. Phys. Letters*, **83**, 399 (1982).

[12] A. T. Balaban, *Pure Appl. Chem.*, **55**, 199 (1983).

[13] A. T. Balaban, and P. Filip *Math. Chem.*, **16**, 163 (1984).

[14] J. P. Lowe and B. D. Silverman, *Acc. Chem. Res.*, **17**, 332 (1984).

Revue Roumaine de Chimie, **30**, *11–12*, 1001–1004 (1985)

SYNTHESIS OF DIBENZOBULLVALENE *VIA* BAMFORD-STEVENS REACTION

RODICA VLAD and M. BANCIU

Organic Chemistry Laboratory, TCH, Polytechnic Institute
Bucharest, Spl. Independenţei 313, 76206 Bucharest 16, Romania

Received May 23, 1985

The synthesis of dibenzobullvalene **3** through anionic Bamford-Stevens reaction of the corresponding tosylhydrazone **18** is described. From all presently known methods for the synthesis of dibenzobullvalene (**3**) this reaction affords the best yields and involves the simplest work-up.

INTRODUCTION

The interest and fascination exerted by $(CH)_{10}$ valence isomers[1] were extended in the last years to the benzo$(CH)_{10}$ hydrocarbons — investigated by Vedejs, [2] Paquette [3] and Murata [4] — as well as to dibenzo $(CH)_{10}$ valence isomers — studied mainly by Nenitzescu and co-workers. [5] Although among $(CH)_{10}$ hydrocarbons, bullvalene (**1**) focused numerous investigations, its monobenzo-(**2**) and dibenzo-derivatives (**3**) were less investigated until now.

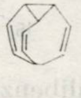
1

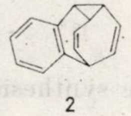
2

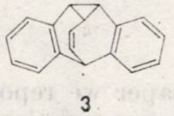
3

Bullvalene (1) was first obtained by Schröder [6] on UV irradiation of the cyclooctatetraene dimer 4, then by Doering[7] in a "rationale synthesis" from diazoketone 5, *via* 6 and 7.

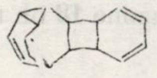
4

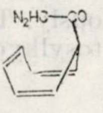

5

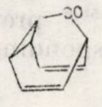

6

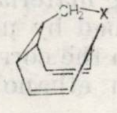

7, a ; X=CO
b ; X=$CHOCOCH_3$

Bullvalene results also on photolysis of : bicyclo[6.2.0] deca-2,4,6,9-tetraene, [8] *cis*- and *trans*-9,10-dihydronaphthalene,[8–10] bicyclo[4.2.2]

deca-2,4,7,9-tetraene (prebullvalene) **8**[11] and tricyclo $[5.2.1.0]^{4,10}$ deca-2,5,8-triene (triquinacene) [12] as well as (*inter alia*) on thermolysis or photolysis of various polycyclic azoderivatives. [13]

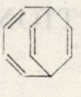

8

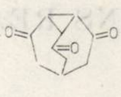

9

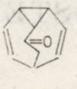

10

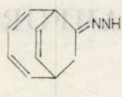

11

Beside these reactions hydrocarbon **1** resulted in about 20 % yield[14] from a Bamford-Stevens reaction of the tris-tosylhydrazone of triketone **9**. Interestingly, treatment of bullvalone **10** with tosylhydrazine produces a rearranged tosylhydrazone **11** which affords prebullvalene **8** on decomposition. [15]

Benzobullvalene (**2**) was first obtained on UV-irradiation of benzo-[g]bicyclo[4.2.2]deca-2,4,7,9-tetraene (**12**) (the benzoderivative of **8**) [2i] then, *via* a Bamford-Stevens reaction of the tosylhydrazone of **13** [16] in 30 % yield.

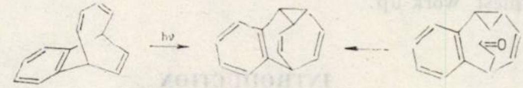

12 2 13

Dibenzobullvalene (**3**) was synthesized [5b,e] from "dibenzobullvalene bromide" **14** by dehydrobromination, from alcohol **15** by dehydration as well as from the butadienic-bridged hydrocarbon **16**, by UV irradiation.

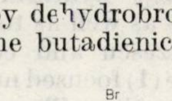

14

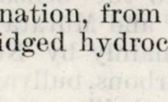

15

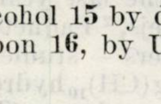

16

In this paper we report the synthesis of dibenzobullvalene (**3**) *via* a Bamford-Stevens reaction.

RESULTS AND DISCUSSION

The starting material for the synthesis of **3** was the dibenzotricyclic ketone **17** described by us [5b,e] previously. The ketone **17** was converted in 85 % yield into the corresponding tosylhydrazone **18** on treatment with tosylhydrazine in ethanol.

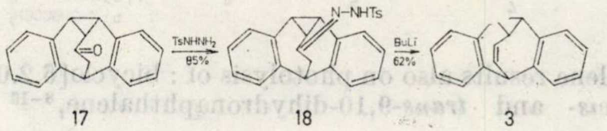

17 18 3

The tosylhydrazone **18**, m.p. 191–3°, was characterized through its IR and ^1H–NMR spectra (see Experimental), and was subjected to Bamford-Stevens decomposition. This reaction[17] was performed in the anionic procedure which proceeds usually without rearrangements [4b, 5g, 16, 18]. Thus, treatment of **18** with excess butyllithium in benzene/hexane solution at 0°–5°C followed by the usual work-up afforded in about 62% yield dibenzobullvalene **3**, identical with an authentic sample.[5b,e] The formation of **3** in the reaction of **18** with butyllithium may be explained through the admitted anionic mechanism,[17] including the tosylhydrazone anion **19**, the diimidic anion **20** and the vinylic anion **21** as sequentially formed (unisolated) intermediates:

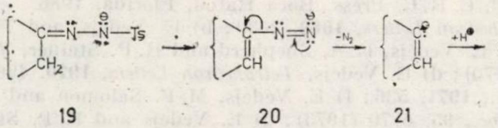

Thus, the anionic Bamford-Stevens reaction in the dibenzobullvalene series proceeds without rearrangement as in the monobenzobullvalene series, and differently from the non-annulated bullvalene series. The presence of two benzo groups in **18** effectively blocks the possibility of rearrangement.

EXPERIMENTAL

Melting points are uncorrected. IR spectra were recorded on a UR-10 Carl Zeiss Jena double-beam spectrophotometer and the ^1H-NMR spectra on a Varian A-60A spectrometer using TMS as internal standard.

Dibenzo[b,g]*tricyclo*[3.3.2.0^{4,6}] *deca-2,7-dien-10-one tosylhydrazone* (**18**). To a solution of ketone **17**,[5b,e] m.p. 227–228°C (1 g; 4.06 mmoles) in 125 mL ethanol, 1 g (5.3 mmoles) tosylhydrazine and 0.5 mL concentrated HCl were added at room temperature. The reaction mixture was kept for 24 hrs in a refrigerator then decomposed by pouring into 100 mL water. The tosylhydrazone **18** was filtered, washed with water and dried in a vacuum desiccator. Tosylhydrazone **18**, m.p. 192–5°C, was obtained in about 85% yield (1.45 g).
IR spectrum (KBr, cm^{-1}): 548m, 564m, 673m, 691m, 716s, 753s, 813m, 1160vs, 1332s, 1395m, 1494m, 1600m, 2918w, 3026w, 3064w, and 3181m.
^{1}*H-NMR spectrum* (d_6–DMSO, δ ppm): 2.4 (s, 3H, CH_3); 2.7–3.1 (m, 5H, CH_2 and cyclopropanic H); 3.6(s, 1H, NH); 4.18(t, J = 5.5 Hz; 1H; Aryl-C*H*-Aryl); 7.1–8.1(m, 12H; Harom).

Dibenzobullvalene (**3**). Over a cooled (0°C) stirred suspension of tosylhydrazone **18** (1.4 g; 3.3mmoles) in 70mL anhydrous benzene maintained under a dry argon atmosphere, a 15% solution of *n*-butyllithium in hexane (10 mL, 16.4mmoles) was dropped in 1 hr. During the dropping the reaction mixture becomes clear and brown coloured. After an additional stirring for 1 hr at 0° and 2 hrs at room temperature the reaction mixture was poured into 150 mL cold water. The organic layer was separated and the aqueous one extracted with six 50 mL portions of benzene. The combined organic layers were washed with saturated natrium chloride solution until pH=7, dried over anhydrous $MgSO_4$ then evaporated *in vacuo* affording a thick yellow oil. The liquid chromatography of this product on a neutral alumina column (diameter 2 cm; height 33 cm) afforded successively: a) 0.35 g (44.5%; *vide infra*) dibenzobullvalene (**3**), m.p. 103–106° (lit.[5b] m.p. 108°) from the first two fractions of 75 mL each eluted with petroleum ether (b.p. 30–40°); b) 0.04 g of a yellow oil (probably hydrocarbon — after IR spectrum) on elution with 150 mL petroleum ether; c) 0.035 g of an orange oil (probably hydrocarbon — after IR spectrum) on elution with petroleum ether: diethyl ether in ratios of 95 : 5 to 85 : 15; d) 0.246 g of a yellowish solid on elution with petroleum ether: diethylether mixtures of 3 : 1 to 1 : 1 v/v ratios. This solid proved to be (IR, ^1H-NMR spectra and m.p.) the starting ketone **17** which could be used in a new preparation of **18** without other purification. Taking into account the amount of recovered ketone **17** the yield of **3** increases to 62.2%. The dibenzobullvalene **3** obtained in the above mentioned procedure presented identical IR and ^{1}H-NMR spectra with an authentic material prepared by other methods.[5b-e]

ACKNOWLEDGEMENTS: The authors express their thanks to Professor Ecaterina Ciorănescu-Nenitzescu for helpful discussions and Dr. C. Drăghici for ^{1}H-NMR spectra.

REFERENCES

[1] For recent reviews see : a) A. T. Balaban and M. Banciu, *J. Chem. Educ.*, **61**, 766 (1984); b) A. T. Balaban, M. Banciu and V. Ciorba, "Annulenes, Derivatives and Valence Isomers", C. R. C. Press, Boca Raton, Florida, 1986.

[2] a) E. Vedejs, *Tetrahedron Letters*, **1968**, 2633; b) E. Vedejs, and T. Shepherd, *ibid.*, **1970**, 1863; c) E. Vedejs, R. A. Shepherd and R. P. Steiner, *J. Amer. Chem. Soc.*, **92**, 2158 (1970); d) E. Vedejs, *Tetrahedron Letters*, **1970**, 4963; e) E. Vedejs, *Chem. Commun.*, **1971**, 536; f) E. Vedejs, M. F. Salomon and P. D. Weeks, *J. Amer. Chem. Soc.*, **95**, 6770 (1973); g) E. Vedejs and R. P. Steiner, *Chem. Commun.*, **1973**, 599; h) E.Vedejs and E.S.C. Wu, *Tetrahedron Letters*, **1973**, 3793; i) E. Vedejs M. F. Salomon and P. D. Weeks, *J. Amer. Chem. Soc.*, **95**, 6770 (1973); j) E. Vedejs, R. P. Steiner and E.S.C. Wu, *ibid.*, **96**, 4040 (1974).

[3] a) L.A. Paquette and J. C. Stowell, *Tetrahedron Letters*, **1970**, 2259; b) L. A. Paquette and J. C. Stowell, *J. Amer. Chem. Soc.*, **92**, 2584 (1970); c) L. A. Paquette, M. J. Kukla and J. C. Stowell, *ibid.*, **94**, 4920 (1972).

[4] a) I. Murata and Y. Sugihara, *Tetrahedron Letters*, **1972**, 3785; b) I. Murata, Y. Sugihara and N. Ueda, *ibid.*, **1973**, 1183.

[5] a) M. Avram, I. G. Dinulescu and C. D. Nenitzescu, *Liebigs Annal. Chem.*, **691**, 9 (1966); b) M. Banciu, M. Elian, E. Ciorănescu and C. D. Nenitzescu, *Tetrahedron Letters*, **1972**, 2573; c) M. Banciu, M. Elian, C. Drăghici and E. Ciorănescu, *Rev. Roumaine Chim.*, **19**, 1179 (1974); d) I. G. Dinulescu, M. Pop, F. Chiralcu, M. Avram and C. D. Nenitzescu, *ibid.*, **19**, 1197 (1974); e) M. Elian, M. Banciu, L. Stănescu and E. Ciorănescu, *ibid.*, **21**, 89 (1976); f) M. Banciu, *ibid.*, **21**, 1083 (1976); g) M. Banciu, M. Elian, Phan Le Thuy, C. Drăghici and E. Ciorănescu, *ibid.*, **27**, 19 (1982); h) M. Banciu and A. T. Balaban, *Chem. Scr.*, **22**, 188 (1983).

[6] a) G. Schröder, *Angew. Chem.*, **75**, 722 (1963); b) G. Schröder, *Chem. Ber.*, **97**, 3131, 3140 (1964).

[7] W. v.E. Doering, B. M. Ferrier, E. T. Fossel, J. H. Hartenstein, M. Jones, Jr., G. Klumpp, R. M. Rubin and M. Sanders, *Tetrahedron*, **23**, 3943 (1967).

[8] a) S. Masamune, R. T. Seidner, H. Zenda, M. Wiesel, N. Nakatsuka and G. Bigam, *J. Amer. Chem. Soc.*, **90**, 5286 (1968); b) S. Masamune and R. T. Seidner, *Chem. Commun.*, **1969**, 542; c) S. Masamune and N. Darby. *Acc. Chem. Res.*, **5**, 272 (1972).

[9] E. E. van Tamelen and T. L. Burkoth, *J. Amer. Chem. Soc.*, **89**, 151 (1967).

[10] W. v. E. Doering and J. W. Rosenthal, *J. Amer. Chem. Soc.*, **88**, 2078 (1966).

[11] a) M. Jones, Jr. and L. T. Scott, *J. Amer. Chem. Soc.*, **89**, 150 (1967); b) K. Hojo, R. T. Seidner and S. Masamune, *J. Amer. Chem. Soc.*, **92**, 6641 (1970); c) W. v. E. Doering and J. W. Rosenthal, *Tetrahedron Letters*, **1967**, 349; d) M. Jones, Jr., S. Reich and L. T. Scott, *J. Amer. Chem. Soc.*, **92**, 3118 (1970).

[12] D. Bosse and A. de Meijere, *Angew. Chem.*, **86**, 706 (1974).

[13] a) R. Jösel and G. Schröder, *Liebigs Annal. Chem.*, **1980**, 1428; b) S. Masamune, H. Zenda, M. Wiesel, N. Nakatsuka and G. Bigam, *J. Amer. Chem. Soc.*, **90**, 2727 (1968).

[14] J. Font, F. Lopez and F. Serratosa, *Tetrahedron Letters*, **1972**, 2589.

[15] J. Cassas and F. Serratosa, *Ann. Quim.*, **73**, 300 (1977).

[16] A. Eisenstadt, *Tetrahedron*, **30**, 2353 (1974).

[17] a) W. R. Bamford and T. S. Stevens, *J. Chem. Soc.*, **1952**, 4735; b) R. H. Shapiro, in "Organic Reactions", vol. 23, Wiley, New York, 1976, p. 405.

[18] L. Enescu, I. Dinulescu and M. Avram, *Rev. Roumaine Chim.*, **24**, 995 (1979).

Revue Roumaine de Chimie, **30**, *11–12*, 1005–1013 (1985)

O-SUBSTITUTED AROMATIC ALDOXIMES OF 1-METHYL-2-AMINOOXYMETHYL-5-NITROIMIDAZOLE. SYNTHESIS AND ^{1}H–NMR SPECTRA

IULIANA TĂMĂŞAN,[a] OVIDIU MAIOR[b] and TEODOR-SILVIU BALABAN[c]

[a] Institute for Chemical Pharmaceutics, Bucharest, Romania
[b] The Polytechnic, Organic Chemistry Department, Splaiul Independenţei 202B, Bucharest, Romania
[c] Centre for Organic Chemistry, Splaiul Independenţei 202B, Bucharest, Romania.

Received May 27, 1985

1-Methyl-2-aminooxymethyl-5-nitroimidazole was condensed with various aromatic aldehydes yielding new hydroxylamine derivatives which were isolated only as *E* (*syn*) configurational isomers. ^{1}H-NMR Spectra are presented and discussed. For two compounds, molar induced shifts by $Eu(fod)_3$ in $CDCl_3$ solution are given.

INTRODUCTION

The *O*-benzylated derivatives of hydroxylamine as well as their condensation products with aldehydes, the *O*-substituted aldoximes **1**, are described as having important pharmacological activities such as: analgetic, antiinflammatory, antipyretic, hypocholesterolemiantic, hypotensive and tranquilizing. A few of the known derivatives **1** have instead of the Ar group a heterocyclic ring.[1] The R group is usually an alkyl group:

$$\mathbf{1}: \ Ar-CH_2-O-N=CH-R.$$

The broad spectrum of biological activities for compounds **1** prompted us to synthesize and to investigate the pharmacological properties of such hydroxylamine derivatives in which the Ar group is an imidazolyl moiety and R is an aromatic ring: a phenyl, a substituted phenyl, or a heterocyclic ring.

The availability of 1-methyl-2-hydroxymethyl-5-nitroimidazole, **2**, an intermediate product in the synthesis of the veterinarian-use drug Ronidazol, led us to prepare the corresponding benzyloxyamine which on condensation with aromatic aldehydes yielded the title compounds. We report here the synthesis and the ^{1}H–NMR spectra of 14 such condensation products (**6a–6n**) which were not previously described.

SYNTHESIS

The existing methods for obtaining *O*-benzylated derivatives of hydroxylamine have as starting material a benzyl halide which is condensed in alkaline medium with a mono-, or di-N-substituted derivative of hydroxylamine such as : (i) acetone oxime,[1-3] (ii) hydroxamic acid,[1,3] (iii) N-hydroxyurethanes,[4-7] or (iv) cyclicN-hydroxyimides.[1,3,4,8-12] Among the latter derivatives, most used is the readily available N-hydroxyphtalimide. The resulting intermediates are descomposed by acids or bases affording the corresponding benzyloxyamine.

Methods (i)—(iii) yield low melting intermediates which are difficult to isolate and purify thus leading to an impure final product. Also the decomposition requires energic conditions which may affect the desired benzyloxyamine, thus lowering the yield. Procedure (iv) avoids these drawbacks, the intermediate condensation products (e.g. **3**) are easily isolated and decomposed in mild conditions by hydrazine hydrate leading to improved yields of purer benzyloxyamines. These are isolated as salts, usually hydrochlorides, which in order to obtain the *O*-benzyl-substituted aldoximes, are condensed with aldehydes in alcoholic solutions, in the presence of bases, such as sodium carbonate,[2,7] sodium acetate,[13] or pyridine.[14]

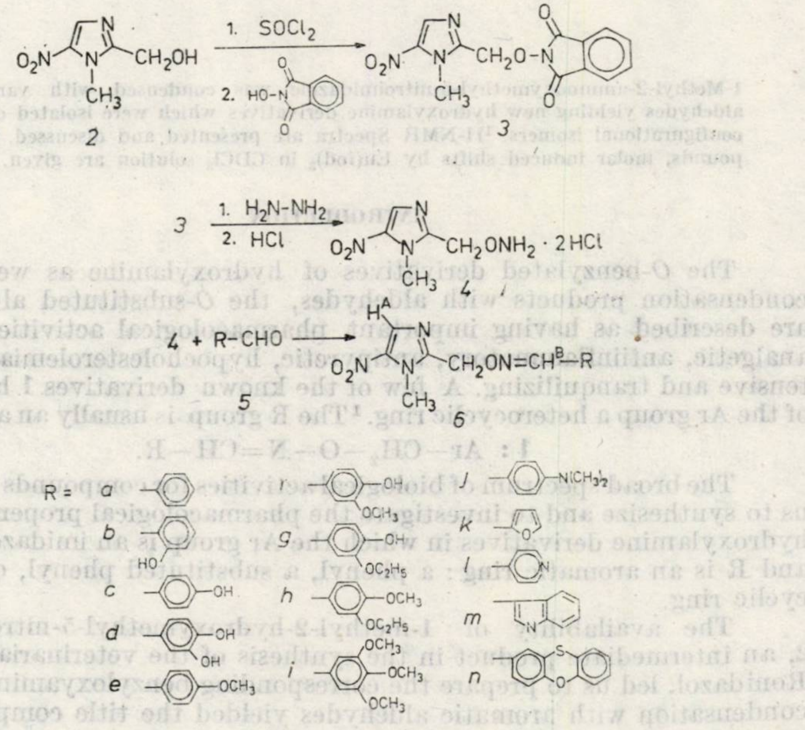

Scheme 1

The synthesis of the novel 2-aminooxymethyl-1-methyl-5-nitroimidazole **4** follows method (iv) and is presented in Scheme 1. Treatment of **2** with thionyl chloride formed the 2-chloromethyl derivative which was condensed with N-hydroxyphthalimide. The resulting intermediate **3** (m.p. 229—30°) on hydrazinolysis afforded **4**, which was isolated as dihydrochloride salt in an overall yield (based on **2**) of 65%. Condensation of the benzyloxyamine **4** with different substituted N-benzaldehydes **5a**—**5n**, in ethanol, in the presence of sodium carbonate, yielded the desired *O*-substituted benzaldoximes **6a**–**6n.** Pure samples were obtained by recrystallisation from ethanol.

Table 1 presents the newly synthesized aldoximes **6**, thier melting points, elemental analysis and yields based on the benzyloxyamine **4**.

^{1}H–NMR SPECTRA

Table 2 presents the ^{1}H–NMR spectra of compounds **6**. According to their solubility, the aldoximes were dissolved either in $CDCl_3$ or in anhydrous DMSO–d_6*. Compound **5n** is practically insoluble in these solvents but is readily dissolved by trifluoroacetic acid (TFA); its ^{1}H–NMR spectrum is given in Table 3.

Table 3 also presents the ^{1}H–NMR spectra in TFA of the benzyloxyamine **4** (dihydrochloride), the N-phthalimide **3**, and for comparison, he 4-methoxybenzaldoxime **6e.** It is evident from Table 3 that of the two ignals (1H each) which appear at $\delta > 8$ ppm in **6e** and **6n,** the one which is at higher field (8.30 and 8.13 ppm respectively) must be assigned to he aldehydic proton H^B, as this signal is missing in the spectra of **3** and **4**. Although the NH^+_3 group in **4** or the phthalimido group in **3** are more elecron-withdrawing than the –N=CH–Ar group in **6e** or **6n** (this is reflected n the O–CH_2 chemical shifts), the absorption for the 4-imidazolyl proton H^A, must be the lower field signal (8.45 ppm in **6e** and 8.40 ppm in **6n**), n order to be consistent with the chemical shifts in **3** and **4** (8.52 and 8.43

Table 1

Melting points, elemental nitrogen analysis and yields of title compounds **6**

6	M.p. (°C)	Formula	Nitrogen (%)		Yield [a] (%)
			Required	Found	
a	130	$C_{12}H_{12}N_4O_3$	21.53	21.08	84
b	164	$C_{12}H_{12}N_4O_4$	20.29	19.85	70
c	212	$C_{12}H_{12}N_4O_4$	20.29	20.20	75
d	199	$C_{12}H_{12}N_4O_5$	19.17	18.78	70
e	189	$C_{13}H_{14}N_4O_4$	19.31	18.80	84
f	162	$C_{13}H_{14}N_4O_5$	18.30	17.93	80
g	144	$C_{14}H_{16}N_4O_5$	17.50	17.48	76
h	115	$C_{15}H_{18}N_4O_5$	16.76	16.39	82
i	141	$C_{15}H_{18}N_4O_6$	16.00	15.53	80
j	170	$C_{14}H_{17}N_5O_3$	23.10	22.74	70
k	71–2	$C_{10}H_{16}N_4O_4$	22.40	22.00	60
l	125–6	$C_{11}H_{11}N_5O_3$	26.82	26.30	58
m	195–7	$C_{14}H_{13}N_5O_3$	23.41	23.15	70
n[b]	187–90	$C_{18}H_{14}N_4O_4S$	15.30	15.10	72

[a] based on the bezyloxyamine **4**.
[b] sulphur analysis : required 8.56, found 8.74.

---

* Dimethylsulphoxide-d_6

Table 2

^{1}H-NMR spectra[a] of aldoximes **6**

6	Solvent	N-CH_3 (3H,s)	CH_2 (2H,s) δ (ppm)	aldehyde- - CH^B(1H,s) δ (ppm)	imidazole- -CH^A(1H,s)	R: Group	R: Aromatic protons δ (ppm)	R: J(Hz)[b]	R: Other protons δ(ppm) J(Hz)
a	$CDCl_3$	4.08	5.30	8.02	8.15	C_6H_5	7.45 (m)	—	—
b	DMSO	4.07	5.37	8.08	8.52	2-HOC_6H_4	6.85–8.12 (m)	—	c
c	DMSO	4.03	5.30	8.03	8.15	4-HOC_6H_4	6.83 (2H, d) 7.43 (2H, d)	J = 8.5	c
d	DMSO	4.03	5.28	8.10	8.15	3,4-$(HO)_2C_6H_3$	6.79 (1H, d)-5 6.98 (1H, d)-6 7.13 (1H, s)-2	$J_{5,6}$ = 8.5	c
e	$CDCl_3$	4.12	5.30	8.03	8.10	4-$MeOC_6H_4$	6.93 (2H, d) 7.55 (2H, d)	J = 9	3.86 (3H, s)
f	$CDCl_3$	4.13	5.32	7.98	8.07	3-MeO-4-HOC_6H_3	6.86 (1H, d)-5 7.05 (1H, d)-6 7.20 (1H, d)-2	$J_{5,6}$ = 8.5	3.92 (3H, s)
g	$CDCl_3$	4.03	5.30	8.05	8.17	3-EtO-4-HOC_6H_3	6.83 (1H, d)-5 7.07 (1H, dd)-6 7.15 (1H, s)-2	$J_{5,6}$ = 8.5 $J_{2,6}$ = 1.5	1.37 (3H, t) 4.05 (2H, q) J = 7
h	$CDCl_3$	4.08	5.28	7.95	8.03	3-EtO-4-$MeOC_6H_3$	6.83 (1H, d)-5 7.07 (1H, dd)-6 7.18 (1H, d)-2	$J_{5,6}$ = 8.5 $J_{2,6}$ = 1.5	4.13 (2H, q) 3.92 (3H, s) 1.48 (3H, t) J = 7
i	$CDCl_3$	4.08	5.30	7.93	8.02	3,4,5-$(MeO)_3C_6H_2$	6.80 (2H, s)	—	3.91 (9H, s)
j	DMSO	4.02	5.25	8.07	8.15	4-$NMe_2C_6H_4$	6.75 (2H, d) 7.50 (2H, d)	J = 8.5	2.97 (6H, s)
k	DMSO	4.00	5.30	8.02	8.22	2-furfuryl	6.63 (1H, dd)-4 6.87 (1H, d)-5 7.78 (1H, d)-3	$J_{3,4}$ = 3.5 $J_{4,5}$ = 1.5	—
l	DMSO	4.07	5.43	8.07	8.36	4-pyridyl	7.57 (2H, dd) 8.68 (2H, dd)	$J_{2,3}$ = 6 $J_{2,5}$ = 1	—
m	DMSO	4.03	5.28	8.08	8.45	3-indolyl	7.73 (1H, s)-2 6.80–7.90 (4H, m)	—	—

---

[a] Signal multiplicities are abbreviated as follows: s = singlet ; d = doublet (may be unequal) ; dd = double doublet ; t=triplet ;

Table 3

^{1}H-NMR spectra in TFA (δ in ppm)

Compound	$N-CH_3$	CH_2	CH^B	CH^A	R		
					Group		
3	4.53	5.88	—	8.52	$\overset{+}{N}H_3$	—	
4[a]	4.43	6.09	—	8.43	$N(CO)_2C_6H_4$	8.00	(4H, s)
6e	4.40	5.58	8.30	8.45	$4\text{-}MeOC_6H_4$	4.00 7.03 7.95	(3H, s) (2H, d)[b] (2H, d)[b]
6n	4.33	5.56	8.13	8.40	2-phenoxathiin	7.03 − 7.50	(7H, m)

[a] Dihydrochloride salt

[b] J=8.5Hz

ppm respectively). The solvent influence on the chemical shifts is seen by comparing the data from Tables 2 and 3. Only a slight increase in chemical shifts is observed when changing the solvent from $CDCl_3$ to DMSO. This increase becomes significant (about 0.25 ppm) when TFA is used as solvent and can be explained by salt formation.

The most significant feature of the ^1H-NMR spectra of compounds **6** is the complete absence of the signals which could be assigned to a less stable configurational *E*/*Z* isomer. This isomer could not be detected even after heating, treatment with acids, or by keeping the samples in solution for several days. The sharp melting points of compounds **6** (Table 1) indicate also that only one configurational isomer is present.

Early observations by ^1H-NMR spectroscopy on syn-anti isomerism in ketoximes[15] were later expanded by Karabatsos and coworkers who have extensively studied by ^1H-NMR the configurational and conformational isomerism due to the C=N double or partially double bond.[16] Mixtures of *E*/*Z* isomers are present in the case of ketone and most aldehyde derivatives (semicarbazones, hydrazones, etc.). The assignment of signals to one or the other isomer was made [17] by comparison of chemical shifts (δ) and by comparison of aromatic solvent induced shifts (ASIS). Marked differences were observed in δ and ASIS values for corresponding protons in the *E* and *Z* isomers (significant $\Delta\delta_{E-Z}$ and $\Delta ASIS_{E-Z}$ values). Analysis of coupling constants gave detailed information on the predominant conformation.[17]

Mixtures of *E* and *Z* isomers were also detected in a study by Tronchet et al.[18] on a series of sugar aldoximes and *O*-methylaldoximes. The assignment of signals, facilitated as in the above cases by the presence of both isomers in unequal quantities, was based on Karabatsos's studies which have become classic.

In the present case, as only one isomer is evidenced by the ^1H-NMR spectra, its configuration cannot be readily established as no $\Delta\delta_{E-Z}$ or Δ $ASIS_{E-Z}$ values are available.

A similar absence of configurational isomerism was detected in the case of all aldehyde N,N-dimethylhydrazones[16] and N-methyl-N-phenylhydrazones;[19] for these compounds the *syn* (*E*) configuration **7** was assigned based on the overall correspondence to the analogous *syn*- but not *anti*-isomers of ketoxime *O*-methyl ethers. The latter compounds were shown [20] to exist also as *syn-anti* mixtures (**8**), and the influence of steric interactions on the *Z*/*E* populations was studied.[20] Thus, the ratio of *Z*—**8** is increased from 2 % when R=Me, to 16 % when R=Et and to 61 % when R=iPr. This effect is explained by the tendency of the phenyl ring to be in conjugation with the C=N bond. In *Z*—**8** the methoxy group forces the phenyl out of conjugation, while in *E*—**8** the conjugation is lost only when phenyl—R interactions become important. U.V. Spectra for compounds **7** and **8** support the importance of steric interaction in loss of conjugation and confirm the assignment of **7** as *syn*.

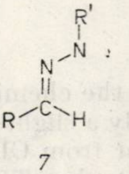

7

R' = Me, Ph

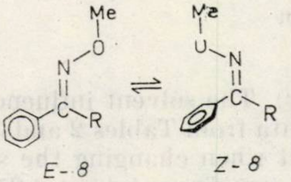

E-8 Z-8

R = Me, Et, iPr

A reasonable assumption is that on lowering the steric requirements of the R group in **8** (e.g. R=H*), less than 2 % of the *Z* isomer are to be expected. The same effect should be obtained by increasing the steric requirements of the *O*-substituent. Both these modifications are met in the present case. This leads to assigning for all *O*-substituted aldoximes derivatives **6** the more stable *syn* configuration **9** in which steric interactions are avoided. The conjugation between the aromatic ring R and the C=N bond is not affected by the interaction between the imidazolyl moiety and H^B in the *syn* configuration. This would not be the case for the *anti* configuration where imidazolyl moiety-aromatic ring interactions force the aromatic ring out of conjugation.

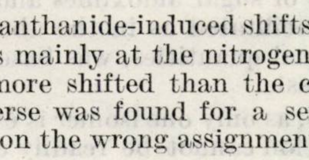

^1H—NMR SPECTRA IN THE PRESENCE OF $Eu(fod)_3$ **

Previous studies of lanthanide-induced shifts on oximes [21] have shown that complexation occurs mainly at the nitrogen lone pair, as the protons of the *anti* isomer are more shifted than the corresponding protons in the *syn* isomer. The reverse was found for a series of ketoximes,[22] but probably, this was based on the wrong assignment*** of signals to *syn* and *anti* isomers.

---

* *O*-methyl benzaldoxime was not studied in ref. 20.

** Europium(III)-tris(1,1,1,2,2,3,3-heptafluoro-7,7-dimethyl-4,6-heptanedione).

*** Cf. footnote in ref. 16.

Tronchet and coworkers[16] have studied the $Eu(dpm)_3$ induced shifts on the above-mentioned sugar aldoximes and aldoxime-*O*-methyl ethers, and they have found in all cases smaller induced shifts for the *O*—methyl derivatives compared to those of corresponding oximes.

The authors conclude that although the lanthanide probe method is useful in configurational and conformational analysis, in their case the data are not readily interpretable; more than one factor (i.e. the Eu-complexation site distance) had to be taken account.

We investigated the ^1H-NMR spectra of compounds **6h** and **6i** in the presence of $Eu(fod)_3$. Molar induced shifts (MIS) values in ppm, derived from the slopes of chemical shifts versus the molar ratio ρ, Eu chelate/substrate, (with $\rho < 0.25$) are shown as boldface figures in Scheme 2. The figures in brackets represent relative induced shifts, taking as standard the $N-CH_3$ induced shift.

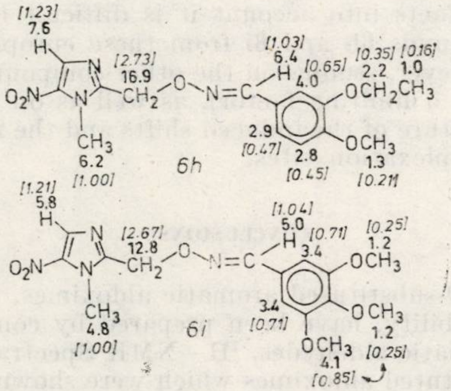

Scheme 2

The following items deserve mention:

(i) Although the MIS values are slightly larger for **6h**, the relative values of corresponding protons are practically identical in **6h** and **6i**.

(ii) The largest MIS value is at the OCH_2 group, suggesting a significant contribution of the oximic nitrogen lone electron pair as a complexation site. However, if only this complexation site is considered, the observed induced shifts cannot be accounted for. A second complexation site might be at the 3-imidazolic nitrogen which should also afford a large MIS value for the OCH_2 group. It is known[23] that N-methyl pyrrole and nitroderivatives do not afford complexes with europium chelates. On the other hand, ethers are weak donors towards lanthanides so that complexation at the ethereal oxygen is less probable, though not excluded.

(iii) The three methoxy groups in **6i** appear isochronous in the absence of $Eu(fod)_3$, (see Table 2) while in the presence of $Eu(fod)_3$, one methoxy group is approx. 3.4 times more strongly shifted than the other two which remain isochronous, and have comparable MIS values to those of the corresponding groups in **6h**. Two explanations seem possible:
a) The more strongly shifted methoxy group is the 4-OMe group and a new complexation site is offered by this group in **6i** in contrast to **6h**;

this new site can account for the smaller absolute MIS values in **6i** relative to **6h**, and also for the fact that the two aromatic protons remain isochronous even at $\rho > 0.2$.
b) The more strongly shifted methoxy group in **6i** is the 5–OMe which is absent in **6h**. Owing to the restricted rotation around the C-aryl bond, only one *meta*-standing methoxy group (i.e. 5–OMe) is in close proximity of the europium atom, coordinated probably at the oximic nitrogen lone-pair. However, the induced shifts of the aromatic protons in **6h** (or their assignment) are not in accord with this.

(iv) No attempts have been made to verify the validity of the pseudocontact model, or to elucidate the stoichiometry of the complexes. The many possible conformations in which the imidazolyl moiety can exist in respect to the aryl group, are due to the unrestricted rotation around the single bonds indicated by the curved arrows in **9**. These make computational approaches to induced shifts difficult and time consuming.

Taking these facts into account it is difficult to ascribe a certain geometry to compounds **6h** and **6i** from these europium induced shifts measurements. However, studies on the other compounds (their low solubility in $CDCl_3$ was a limiting factor), as well as on model compounds, can elucidate the nature of the induced shifts and the relative importance of the various complexation sites.

CONCLUSIONS

Several new *O*-substituted aromatic aldoximes, with possible pharmacological applicability, have been prepared by condensing compound **4** with various aromatic aldehydes. ^1H–NMR Spectra have been presented for the *O*-substituted aldoximes which were shown to exist only as *E* (*syn*) isomers. Shifts induced by $Eu(fod)_3$ in $CDCl_3$, as in previous studies on sugar aldoxime *O*-methyl ethers,[18] are not readily interpretable, owing probably to pluri-site complexation of the europium atom.

EXPERIMENTAL

Melting points were determined on a hot-stage melting point apparatus, and are uncorrected. ^1H-NMR spectra were recorded on a Varian A-60-A Spectrometer with TMS as internal standard. Carefully dried $CDCl_3$ and TMS were used for the $Eu(fod)_3$ (Aldrich) spectra. Measurements of induced shifts were made for **6h** and **6i** in identical conditions with an estimated error of less than 5%. Six points were run by adding anhydrous $Eu(fod)_3$ to the sample solution; a regression analysis yielded straight lines with a correlation coefficient of at least 0.996. No scavenging effects were noted.

2-Aminooxymethyl-1-methyl-5-nitroimidazole **4**. 16.3 g (0.1 mol) of 1-methyl-2-hydroxymethyl-5-nitroimidazole (**2**) and 11 ml (0.15 mol) thionyl chloride were refluxed for 3 hrs in 1600 ml benzene. After concentration in vacuo, the residue solidified on cooling. The crude chloromethyl derivative was added to a solution of 15 g (0.09 mol) N-hydroxyphthalimide and 10 g (0.10 mol) triethylamine in 80 ml dimethylformamide. After heating for 2 hrs at 100° the reaction mixture was allowed to cool and 200 ml water were added. The precipitate **3** was then filtered, washed first with water, subsequently with acetone and, afterwards air dried. It weighed 23 g (yield 76% and after recrystallization from isopropanol it had m.p. 229–230°. Intermediate **3**, 30.2 g (0.10 mol) was suspended in 800 ml methanol. To this boiling mixture, 7 g (0.11 mol) of 80% hydrazine hydrate were added and after the solution cleared it was refluxed for an additional 30 min. The mixture was concentrated to 1/3 and cooled at −5°. The precipitated phthalylhydrazine was filtered off and to the cold, clear filtrate, 18 ml of concentrated hydrochloric acid were added. Ethyl ether (300 ml) precipitated 4 which after filtering and drying weighed 21 g (yield 85%) and had m.p. 169−171°.

Condensation of **4** *with aromatic aldehydes.* To 5 g (0.02 mol) **4**, 60 ml ethanol and 2.12 g (0.02 mol) sodium carbonate were added. The mixture was stirred for a few minutes at room temperature after which the aromatic aldehyde was added. The mixture was refluxed for 30 min. and after cooling at room temperature, 100 ml of water were added. In most cases the O--substituted aldoxime precipitated and was filtered off. Otherwise, (mostly for the heterocyclic aldoximes) the reaction mass was concentrated, filtered from NaCl, and left to crystallize. All aldoximes were recrystallized from ethanol.

ACKNOWLEDGEMENT. The recording of most ^{1}H-NMR spectra by Dr. Filip Chiraleu and the stimulating discussions with Dr. Antonie Dinculescu are gratefully acknowledged.

REFERENCES

[1] Gyogyszerkutate Intezet, Ger. Offen., 2206890 (Cl C07cd, A61k), (1972).
[2] Yu. V. Markova, N. G. Ostroumova and N. N. Shchukina, *Zhur. Org. Khim.*, **3**, 1207 (1967).
[3] E. L. Schumann, R. V. Heinzelmann, M. E. Greig and W. Veldkamp. *J. Med. Chem.*, **7**, 329 (1964).
[4] B. J. R. Nicolaus, G. Pagani and E. Testa, *Helv. Chim. Acta*, **45**, 1381 (1962).
[5] S. A. Lepetit, UK Patent, 964721 (Cl C07c), (1964); cf. *Chim. Abstr.* **61** P9467 (1964).
[6] J. H. Biel and J. E. Robertson, US Patent, 3192110 (Cl 167−65), (1965); cf. *Chem. Abstr.* **63** P8258 (1965).
[7] Yu. V. Markova, N. G. Ostroumova, L. N. Zenkova and M. N. Shchukina, *Zhur. Org. Khim.*, **2**, 239 (1966).
[8] A. A. Aroyan and T. A. Khachaturyan, USSR Patent, 396318 (Cl C07c), (1973).
[9] A. Chimiak and T. Kolosa, *Bull. Acad. Pol. Sci. Ser. Sci. Chim.*, **22**, 195 (1974).
[10] A. Pougny and M. Daudon, *Bull. Soc. Chim. France*, **5**, 833 (1976).
[11] E. Fischer and G. Zinner, *Chem. Ztg.*, **103**, 371 (1979).
[12] V. L. Plakidin and P. P. Gnatyuk, *Zhur. Org. Khim.*, **9**, 167 (1973).
[13] E. L. Schumann, US Patent, 3167563 (Cl 260−296); cf. *Chim. Abstr.* **62**, 10418 (1965).
[14] L. J. Fliender, Ger. Offen., 2326462 (Cl C07cd, Ablk), (1973).
[15] E. Lustig, *J. Phys. Chem.*, **65**, 491 (1961).
[16] G. J. Karabatsos and R. A. Taller, *Tetrahedron*, **24**, 3923 (1968) and previous papers in this series.
[17] G. J. Karabatsos and R. A. Taller, *J. Amer. Chm. Soc.*, **85**, 3624 (1963) and previous papers in this series.
[18] J. M. J. Tronchet, F. Barbalat-Rey and M. Le-Hong, *Helv Chim. Acta*, **54**, 2615 (1971).
[19] G. J. Karabatsos and K. L. Krumel, *Tetrahedron*, **23**, 1097 (1967).
[20] G. J. Karabatsos and M. Hsi, *Tetrahedron*, **23**, 1079 (1967).
[21] K. D. Berlin and S. Rengaraju, *J. Org. Chim.*, **35**, 2912 (1971).
[22] Z. W. Wolkowski, *Tetrahedron Lett.*, 825 (1971).
[23] For reviews on LSR-substrate interactions see e.g.: J. Reuben, *Progr. NMR Spectroscopy* **9**, 1 (1973); A. F. Cockerill, G. L. O. Davies, R. C. Harden and D. M. Rackham, *Chem. Rev.*, **73**, 553 (1973). For conformational analysis by LSR see: F. Inagaki and T. Myiazawa, *Progr. NMR Spectroscopy*, **14**, 67 (1981).

Revue Roumaine de Chimie, **30**, *11–12*, 1015–1017(1985)

THE REACTION OF FLUORENYLIDENETRIPHENYLPHOSPHORANES AND -ARSINANE WITH CERTAIN DICARBONYL COMPOUNDS

L. S. BOULOS and A. EL KATEB
National Research Centre, Dokki-Cairo, Egypt

Received December 3, 1984

The present work has been carried out in order to study the behaviour of fluorenylidenetriphenylphosphorane(Ia), 2,7-dibromofluorenylidenetriphenylphosphorane (Ib) and fluorenylidenetriphenylarsinane (Ic) towards 1,2-benzophen-azine-3,4-quinone(II) and 2N-phenyl-α,β-naphtho-1,2,3-triazolequinone(III). Structural assignments of the obtained products are based on analytical, chemical, and spectroscopic results.

INTRODUCTION

Although fluorenylidenetriphenylphosphorane (FTP, Ia), a stable phosphinemethylene, has been found unreactive with the carbonyl group of ketones,[1] it showed a remarkable activity towards some *o*-quinones.[2] In continuation to our work on the reaction of FTP with carbonyl functions,[3–5] we have now investigated its behaviour towards certain heterocyclic nitrogen *o*-quinones, namely 1,2-benzophenazine-3,4-quinone (II) and 2N-phenyl-α,β-naphtho-1,2,3-triazolequinone (III).

EXPERIMENTAL

Benzene (thiophene-free) was dried (over Na). The analyses were carried out in the Microanalytical Lab., National Res. Centre (Cairo). Infrared spectra were measured on a Perkin-Elmer Infracord Model 137 Spectrophotometer using KBr Wafer technique. The mass spectra were recorded at 70 eV on Varian MAT 711 Spectrophotometer.

Reaction of Fluorenylidenetriphenylphosphorane (Ia) with 1,2- Benzophenazine-3,4-quinone (II):

Fluorenylidenetriphenylphosphorane (Ia)[6] (0.86 g, 0.002 mol) was added to a suspension of quinone (II)[7] (0.001 mol) in benzene (25 mL) and the reaction mixture was refluxed for 5h. After filtration, the solid material thus obtained (90%) was crystallized from chloroform to give (IVa) as deep violet crystals, m.p. 250°C. Anal. Calcd. for $C_{29}H_{16}N_2O$: C, 85.27 ; H, 3.94 ; N,6.86. Found : C, 85.13 ; H,3.95 ; N,6.83%.

Reaction of 2,7-Dibromofluorenylidenetriphenylphosphorane (Ib) with 1,2-Benzophenazine-3,4-quinone (II):

A mixture of (Ib)[8] (0.9 g, 0.0015 mol) and quinone (II) (0.001 mol) in benzene (25 mL) was boiled under reflux for 4h. After cooling, the precipitated material was collected (95%), crystallized from acetone to give (IVb) as deep brown crystals, m.p. 330°C. Anal. Calcd. for

$C_{29}H_{14}N_2Br_2O$, C, 61.49 ; H,2.49 ; N, 4.94 ; Br, 28.35%. Found : C, 61,38 ; H,2.52 ; N,4.93 ; Br, 28.35%.

Reaction of Fluorenylidenetriphenylarsinane (Ic) with 1,2-Benzophenazine-3,4-quinone (II) :

Similarly the reaction of phosphorane (Ic)[9] (0.002 mol) with quinone (II) (0.001 mol) in dry benzene (50 mL) for 4h reflux afforded (IVa) as deep violet crystals (m.p., mixed m.p., comparative IR and mass spectra).

Reaction of Fluorenylidenetriphenylphosphorane (Ia) with Quinone (III) :

A mixture of phosphorane (Ia) (0.002 mol) and compound (III) (0.001 mol) in toluene (25 mL) was refluxed for 20 h. After cooling the substance that separated was collected (90%) and recrystallized from tetrahydrofuran to give (Va) as green crystals, m.p. 270°C. Anal. Calcd. for $C_{29}H_{17}N_3O$: C, 82.24 ; H,4.04 ; N, 9.92. Found : C, 82.28 ; H,4.1 ; N,9.94%.

Reaction of 2,7-Dibromofluorenylidenetriphenylphosphorane (Ib) with Quinone (III) :

A mixture of phosphorane (Ib) (0.002 mol) and compound (III) (0.001 mol) in toluene (52 ml) was boiled under reflux for 10 h. After cooling, the substance that separated was collected (95%) and crystallized from acetone to give (Vb) as brown crystals, mp. 220°C. Anal. Calcd. for $C_{29}H_{15}N_3Br_2O$: C, 59.90 ; H,2.60 ; N,7.23 ; Br, 27.51. Found : C, 59.87 ; H,2.63 ; N, 7.28 ; Br, 27.56%.

Similarly, the reaction of phosphorane (Ic) with quinone (III) afforded (Va) in 90% yield (mixed m.p. and comparative IR spectra).

In all the above reactions triphenylphosphine oxide and/or triphenylarsine oxide were isolated from the filtrate in quantitative yield and identified (m.p., mixed m.p. and comparative IR spectra with authentic sample).[10,11].

RESULTS AND DISCUSSION

We have found that phosphoranes (I) react with 1,2-benzophenazine-3,4-quinone (II), in dry benzene, to give colored crystalline substances with assigned structures (IV) (Scheme 1) The structure of adduct (IVa),

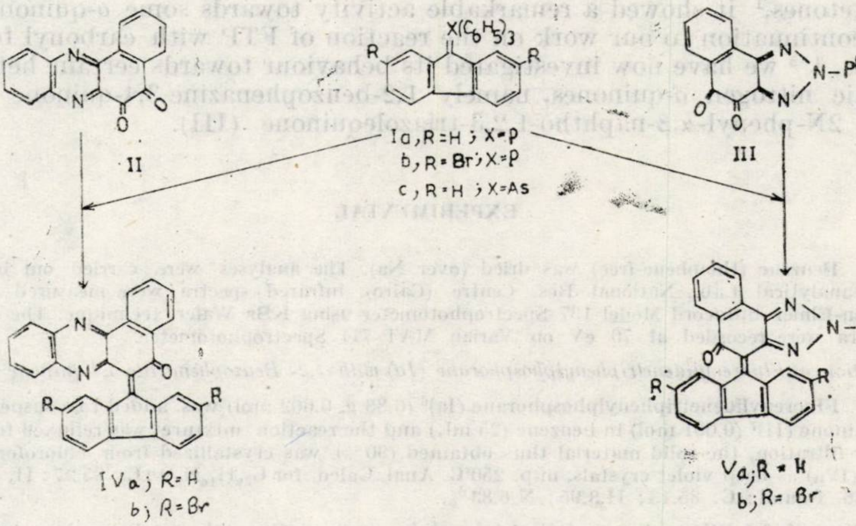

taken as example, was established from the following : (i) Correct elemental and mass spectroscopic analyses, (ii) t.l.c. (one spot), (iii) IR spectrum (in KBr) lacks the absorption band at 1720 cm^{-1}, characteristic for the carbonyl group at position 3 which absorbed sharply in the parent molecule (II), but it showed a strong absorption band at 1665 cm^{-1} (C=O,aryl)[12] allocated for the carbonyl number 4. Similar treatment of 1,2-benzophenazine-3,4-quinone(II) with phosphorane (Ib) afforded (IVb) in 95% yield. Structure (IVb) was inferred from correct analytical values, t.l.c. (one spot), mass spectroscopic data and IR spectrum which showed only one carbonyl absorption band at position 4. Quinone (II) has also been found to react with fluorenylidenetriphenylarsinane (Ic), yielding the same compound (IVa) and triphenylarsine oxide.

Similar treatment of quinone (III) with fluorenylidenetriphenylphosphorane (Ia) and its 2,7-dibromo-derivative (Ib) in toluene for 20 h and 10 h respectively, afforded the corresponding ethylenes (Va) and (Vb) in 90 and 95% yield respectively. The identity of compounds (Va) and (Vb) was established from concordant analytical values, mass spectroscopic data, and IR spectra which showed a single carbonyl absorption (C=O, aryl) band at 1685 cm^{-1} for (Va) and at 1690 cm^{-1} for (Vb), respectively. These assignments are obviously in favour of structure (V). Similarly fluorenylidenetriphenylarsinane (Ic) reacts with quinone (III) to give the corresponding ethylene (Va) (mixed m.p. and comparative IR spectra).

From the present investigation we concluded that the reaction of fluorenylidenetriphenylphosphoranes and fluorenylidenetriphenylarsinane with heterocyclic nitrogen-*o*-quinone undergoes the normal Wittig pattern to yield the corresponding ethylenes. The significance of this finding is not only the demonstration of the possible reaction route undertaken by heterocyclic nitrogen-*o*-quinones with stable ylides (I) but also the synthesis of new olefinic compounds by simple methods.

REFERENCES

[1] Johnson, A. W., "Ylid Chemistry" Academic Press, New York and London, 1966; Johnson, A. W., *J. Org. Chem.*, **24**, 282 (1959).

[2] Sullivan, W. W., Ullman, D. and Shechter, H., *Tetrahedron Letters*, (**1969**) 457.

[3] Sidky, M. M., and Boulos, L. S. *Phosphorus and Sulfur*, **4**, 299 (1978).

[4] Sidky, M. M., Mahran, M. R., and Boulos, L. S., *Phosphorus and Sulfur*, **8**, 365 (1980).

[5] Sidky, M. M., and Boulos, L. S., *Phosphorus and Sulfur*, **14**, 71(1983).

[6] Pinck, L. A., and Hilbert, G. E., *J. Amer. Chem. Soc.*, **69**, 723 (1947).

[7] Fischer, O., *Ber. dtsch. Chem. Ges.*, **36**, 3622 (1903).

[8] Schönberg, A., Brosowski, K. H., and Singer, E., *Chem. Ber.*, **95**, 2144 (1962).

[9] Pascal, M. P., *Bull. Soc. Chim.*, **33**, 171 (1923).

[10] Michaelis, A., and Gleichman, L., *Chem. Ber.*, **15**, 801 (1882).

[11] Coste, L. and Michaelis, A. *Ann.*, **201**, 243 (1880).

[12] Bellamy, "The Infrared Spectra of Complex Molecules" John Wiley and Sons Inc. N.Y. (1962).

Revue Roumaine de Chimie, **30**, *11—12*, 1019—1024 (1985)

STUDY OF CYCLOPENTENE HYDRATION

GH. MIHĂILĂ, C. LUCA, DOINA DRANGA and N. BÎLBĂ
Department of Chemical Technology, Polytechnic Institute, Splai Bahlui 71, Iași, Romani

Received May 29, 1984

Thermodynamic study of cyclopentene hydration in the temperature range of 298—342.24 K has shown that conversion of cyclopentene to cyclopentanol is unfavourably influenced by temperature and its value is between 0.7376 and 0.9516, for the molar ratio, water to cyclopentene, of 1, 2 and 3. The experiments on cyclopentene hydration in liquid phase, using 60—70% sulphuric acid as catalyst, have pointed out that the reaction does not take place at temperatures lower than 333 K and the maximum yield, 46.5%, was obtained at 338 K, for a reaction time of 60 minutes and the sulphuric acid concentration of 70%.

INTRODUCTION

Cylopenetene is a petrochemical by-product obtained by processing of refinery C_5 fractions as starting material. Cyclopentene itself, is a minor recoverable component, but much larger amounts of it can be obtained by recovery of hydrogenation of the more abundant component cyclopentadiene.[1] Recent processes of ethylene production based on the high temperature steam cracking of heavy hydrocarbon feed streams give larger amounts of C_5 fraction, fact that determines a significant increase of the amount of recoverable cyclopentene. [2] This product, by polymerization [3] leads to polypentene, a readily vulcanizable elastomer and, by oxidation under different conditions leads to 3- and 5-isopropoxycyclopentene, cyclopentanone, cyclopentene oxide, cyclopentanol, acrylaldehyde, glutaraldehyde etc.[4-7]

In the present work we have investigated the cyclopentene hydration in order to find out the experimental conditions under which the cyclopentene transformation takes place with high yields in cyclopentanol, starting material for production of the δ-aminopentanoic acid lactam, necessary in nylon 5 manufacture.

THERMODYNAMIC STUDY

The thermodynamic study of cyclopentene hydration, in liquid phase, at atmospheric pressure, was performed in the temperature range from 298 up to 342.24 K, boiling point of cyclopentene for the molar ratios water to cyclopentene of 1, 2 and 3. For the narrow temperature range mentioned above, the dependence of the reaction enthalpy on temperature was neglected.

The reaction enthalpy, under standard conditions, calculated on the basis of thermochemical reaction

$$C_5H_8(l) + H_2O(l) \rightarrow C_5H_9{-}OH(l)\,;\ \ \Delta H_{298} = -\ 60.61\ \ \mathrm{kJ \cdot mol^{-1}}$$

using the standard formation enthalpies of reactants[8,9] and reaction product, listed in table 1 is $-60.61\ \mathrm{kJ \cdot mol^{-1}}$.

Table 1

Standard formation enthalpy and entropy of the reactants and reaction products[8,9]

Compound	State	ΔH_{298}, kJ.mol^{-1}	S_{298}, J.mol^{-1}K^{-1}
C_5H_8	l	4.2636	201.267
H_2O	l	$-$285.5776	188.518
C_5H_9OH	l	$-$300.124	205.99

In order to find out if the reaction is possible from the thermodynamic point of view, the free enthalpy of reaction, ΔG(298.15 K) was calculated using the relation

$$\Delta G_{298} = \Delta H_{298} - T\Delta S_{298} \tag{1}$$

where ΔS_{298} is the reaction entropy, $\mathrm{J \cdot mol^{-1} \cdot K^{-1}}$ and T is the temperature in K. Its value is $-5.839\ \mathrm{kJ \cdot mol^{-1}}$.

Based on the relation

$$\Delta G_{298} = -RT \ln K_c \tag{2}$$

the value of equilibrium constant at different temperatures was calculated. Its values are presented in table 2.

Table 2

Dependence of equilibrium conversion on temperature and molar ratio water to cyclopentene

T (K)	K_c	X		
		$r = 1$	$r = 2$	$r = 3$
298	10.67	0.7376	0.9203	0.9564
303	10.26	0.7329	0.9176	0.9546
308	9.88	0.7287	0.9141	0.9529
313	9.52	0.7271	0.9119	0.9516

Dependence of conversion X, at equilibrium, on K_c and the molar ratio, water to cyclopentene, r, is given by the relation

$$\frac{X}{(1 - X)(r - X)} = K_c \tag{3}$$

developed based on the mass-action law.

The values of the equilibrium conversion, calculated with the relation (3) are summarized in table 2 too. The data of table 2 show that the temperature influences unfavourably the conversion, it increases as the molar ratio, water to cyclopentene, increases.

EXPERIMENTAL

The cyclopentene hydration was carried out in homogeneous catalysis, in the presence of 60 – 75 % sulphuric acid (molar ratio, sulphuric acid to cyclopentene, of 2 :1), at temperatures ranging from 303 to 323 K, reaction time of 30 – 120 minutes, at the molar ratio, water to cyclopentene, for hydrolysis step, from 5 :1 up to 25 :1, in nitrogen stream. The purity of cyclopentene was verified by means of double-bond determination, using Kaufman and Baltes[10] method and refractometrically, using an Abbé refractometer. The employed sulphuric acid, indigeneous production, was analytical grade. The purity of cyclopentanol obtained was verified refractometrically and by the determination of its boiling point.

Cyclopentene hydration was carried out in a laboratory plant with mechanical stirring, represented in figure 1, according to the example given below.

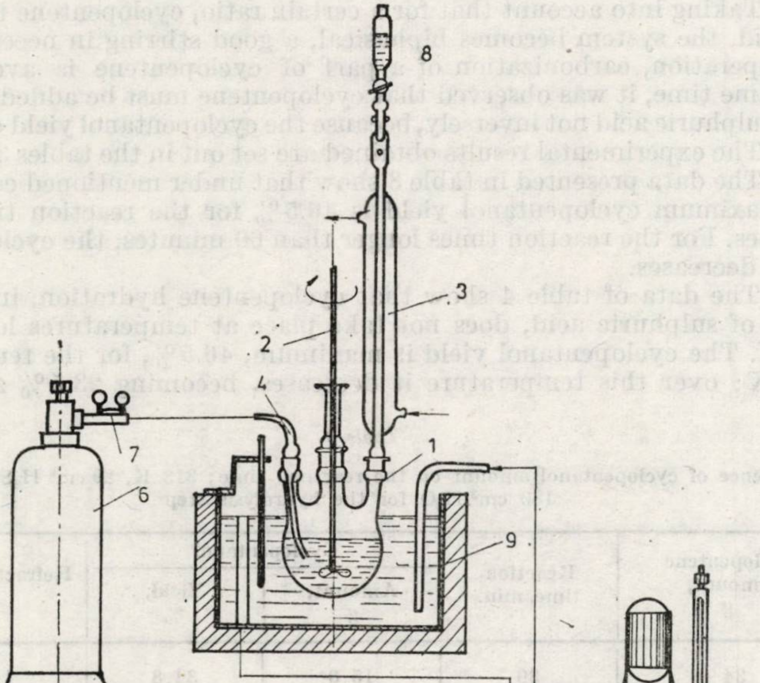

Fig. 1. — Laboratory plant with mechanical stirring employed for the investigation of cyclopentene hydration:
1 — tree-necked flask; 2 — impeller; *3* — water cooler; *4* — capillary tube for nitrogen bubbling, *5* — thermostat; *6* — nitrogen cylinder; *7* — pressure reducer; *8* — dropping funnel; 9 — thermostated vessel.

In a 750 cm^3 three-necked flask with stirrer, provided with upward water cooler for refluxation and a capillary tube for nitrogen bubbling, 89 cm^3 (144 g) 70% H_2SO_4 solution was poured. Then, 34 g (44 cm^3) cyclopentene were added dropwise and the reaction mixture was maintained at 313 K, under stirring in nitrogen stream for 60 minutes. After this, 140 cm^3 distilled water were added for hydrolysis, then, by heating, was distilled in nitrogen stream too. At the beginning, at 317 K, unreacted cyclopentene was collected, after which, in the temperature range of 348—371 K, steam distillation of cyclopentanol took place. Separation of cyclopentanol was carried out using a tap funnel and its further purifications were made by distillation, obtaining pure cyclopentanol, cyclopentene and an organic residue.

RESULTS AND DISCUSSION

The thermodynamic study of cyclopentene hydration, in liquid phase, has shown that the reaction is possible in the temperature range of 298 ÷ 342.24 K with conversions ranged between 0.7576 and 0.9876, for the molar ratios, water to cyclopentene, of 1, 2 and 3.

Taking into account that for a certain ratio, cyclopentene to sulphuric acid, the system becomes biphasical, a good stirring in necessary; by this operation, carbonization of a part of cyclopentene is avoided. At the same time, it was observed that cyclopentene must be added dropwise over sulphuric acid not inversely, because the cyclopentanol yield decreases.

The experimental results obtained are set out in the tables 3, 4 and 5.

The data presented in table 3 show that under mentioned conditions, the maximum cyclopentanol yield is 46.5% for the reaction time of 60 minutes. For the reaction times longer than 60 minutes, the cyclopentanol yield decreases.

The data of table 4 show that cyclopentene hydration, in the presence of sulphuric acid, does not take place at temperatures lower than 308 K. The cyclopentanol yield is maximum, 46.5%, for the temperature 313 K; over this temperature it decreases, becoming 23.5% at 323 K.

Table 3

Dependence of cyclopentanol amount on the reaction time; 313 K, 89 cm^3 H_2SO_4 70% and 180 cm^3 H_2O for the hydrolysis step

Cyclopentene amount, g	Reaction time, min.	Cyclopentanol		Refractive index, n_D^{20}
		Amount, g	Yield, %	
34	30	15.0	34.8	1.4548
34	60	20.0	46.5	1.4547
34	90	18.9	43.9	1.4549
34	120	18.1	42.1	1.4548

The cyclopentanol yield depends substantially on concentration of sulphuric acid employed. At concentrations of sulphuric acid less than 60% the reaction does not take place and, at the concentration of 75%, only traces of cyclopentanol are obtained and an intense process of cyclopentene carbonization occurs. The optimum concentration of sulphuric acid is 70%. Of course, for a certain concentration of sulphuric acid, the cyclopentanol yield depends on the amount of sulphuric acid employed, table 5.

Table 4

Dependence of cyclopentanol amount on temperature; 60 min., 89 cm^3 H_2SO_4 70 % and 180 cm^3 H_2O for the hydrolysis step

Cyclopentene amount, g	Temperature, K	Cyclopentanol		Refractive index, n_D^{20}
		Amount, g	Yield, %	
34	303	—	—	—
34	308	10.0	23.2	1.4548
34	313	20.0	46.5	1.4547
34	323	10.1	23.5	1.4548

The data summarized in table 5 show that the cyclopentanol yield is maximum, 46.5 %, if 100 % excess is employed; a larger excess of sulphuric acid leads to cyclopentanol yield decreasing.

Of great importance over the cyclopentanol yield is also the water amount employed in the hydrolysis step. Using for hydration, the same amount of cyclopentene (34 g) and sulphuric acid of 70 % (89 cm^3), at operating temperature of 313 K and reaction time of 60 minutes and, for hydrolysis step, the molar ratio, water to cyclopentene, from 5 : 1 up to 25 : 1, it was seen that the maximum cyclopentanol yield, i.e. 46.5 %, was obtained for the ratio 20 : 1 after which it remains approximately the same.

Table 5

Dependence of cyclopentanol amount on quantity of H_2SO_4 70 %; 313 K, 60 min. and 180 cm^3 H_2O for the hydrolysis step

Cyclopentene amount, g	Quantity of 70% H_2SO_4	Cyclopentanol		Refractive index, n_D^{20}
		Amount, g	Yield, %	
34	71	14.5	33.7	1.4548
34	89	20.0	46.5	1.4549
34	107	14.6	33.9	1.4548
34	143	14.8	34.4	1.4549

CONCLUSIONS

From the study of cyclopentene hydration in liquid phase, presented above, the following conclusions may be drawn:

1. Cyclopentene hydration, in liquid phase, is an exothermal reaction, possible from thermodynamic stand point, with an equilibrium conversion of 0.7376 − 0.7516 in the temperature range of 298 ÷ 342.24 K at the molar ratio, water to cyclopentene, between 1 and 3.

2. The maximum cyclopentanol yield, i.e. 46.5 %, was obtained at 313 K, for the reaction time of 60 minutes and the sulphuric acid concentration of 70 %;

3. The cyclopentanol yield depends on the molar ratio, water to cyclopentene, employed for hydrolysis of cyclopentyle acid sulphate, its optimum value being 20 : 1.

REFERENCES

[1] Fr. Gothard, Gr. Pop, D. Breabăn, D. Radu, Gh. Ionescu, A. Cobzaru and T. Rogojin, Rom. Pat. 67011/1979.

[2] L. Lassau, D. V. Quang and M. Hellin, *Hydroc. Proces.*, **52**, 109, 1973.

[3] * * * "Encyclopedia of Polymer Science and Technology", vol. 8, Wiley and Sons, New York, London, Sydney, Toronto, 1968, p. 592.

[4] J. Brandrup and E. H. Immergut, "Polymer Handbook", 2nd Edition, Wiley and Sons Inc., New York, 1975.

[5] B. C. Anderson, C. I. Hoover and O. Vogl, *Macromolecules*, **2**, 286, 1969.

[6] K. Wedemeyer and A. Klein, Ger. P. 2261657/1974.

[7] H. Waldmann, W. Schwerdtel and W. Swodenk, Ger. P. 2252674/1972.

[8] L. Abbas and F. D. Rossini, *J. Phys. Chem.*, **65**, 476, 1961.

[9] * * * "Spravocinik khimika", vol. I, Goskhimizdat, Leningrad, 1962.

[10] Houben-Weyl, "Metody organiceskoi khimii", 2, Izd. "Himia", Moskow, 1967, p. 291.

Revue Roumaine de Chimie, 30, 11—12, 1025—1030 (1985)

HETEROPOLYTUNGSTATES WITH Ti(IV) AND Ni(II).V[1] THE THERMAL BEHAVIOUR OF SODIUM AND POTASSIUM SALT OF THE Ni(II)-PENTATUNGSTOTITANATE(IV) ANION

RODICA VĂŢULESCU, T. BUDIU, GH. MARCU and IRINA PAL
Institute of Chemistry, 30, Fintinele Street, 3400 Cluj-Napoca, Romania

Received October 20, 1984

The thermal behaviour of the sodium and potassium salt of the heteropolyanion $[H_2ONiTiW_5O_{20}]^{4-}$ ($Na_4[H_2ONiTiW_5O_{20}]\cdot 9\,H_2O$ and $K_4[H_2ONiTiW_5O_{20}]\cdot 10\,H_2O$ respectively) has been investigated by means of thermogravimetric and thermodifferential analyses and IR absorption spectroscopy.

1. INTRODUCTION

As far as the 2 : 5 series is concerned, there are relatively few data mentioned in literature regarding both the studies in solution and in the solid state. Firstly, this is due to the fact that only a few representatives with molybdenum[2–8] and tungsten[9–12] of the 2 : 5 series are known. On the other hand, the representatives of the 2 : 5 series were mentioned or obtained sometimes as degradation products of the larger series.[7,13]

The present paper summarizes our studies concerning the thermal behaviour of heteropolysalts $Na_4[H_2ONiTiW_5O_{20}]\cdot 9\,H_2O$ and $K_4[H_2ONiTiW_5O_{20}]\cdot 10\,H_2O$. By interpreting the thermogravimetric and thermodifferential analyses as well as the IR absorption spectra obtained at different temperatures, the transformations that take place depending on the temperature were pointed out and it was supposed that the heteropolytungstic anion in discussion contains a constitution water molecule.

2. EXPERIMENTAL

The thermogravimetric and thermodifferential analyses have been recorded using a Paulik-Erdely type OD-102 derivatograph, without maintaining isothermal conditions, with a heating rate of 4°/minute and a balance sensitivity of 100 mg. We worked on a sample of 600 mg compound for both sodium and potassium salt of the Ni(II)-pentatungstotitanate(IV) anion. The IR absorption spectra were recorded using an UR 10 Zeiss-Jena apparatus and the pelleting technique in the preparation of samples. Samples heated for half an hour at different temperatures, up to 800°C, were also investigated.

3. RESULTS AND DISCUSSION

3.1. THE THERMAL ANALYSIS

3.1.1. $Na_4[H_2ONiTiW_5O_{20}]\cdot 9\,H_2O$

In figure 1 are given the weight loss (TGA-curve 1), its derivative (DTG-curve 3) and the thermodifferential (DTA-curve 2) recorded for the complex $Na_4[H_2ONiTiW_5O_{20}] \cdot 9\,H_2O$. From the TGA curve (curve 1) it can be seen that within the temperature range 40–420°C a continual process of weight loss is recorded.

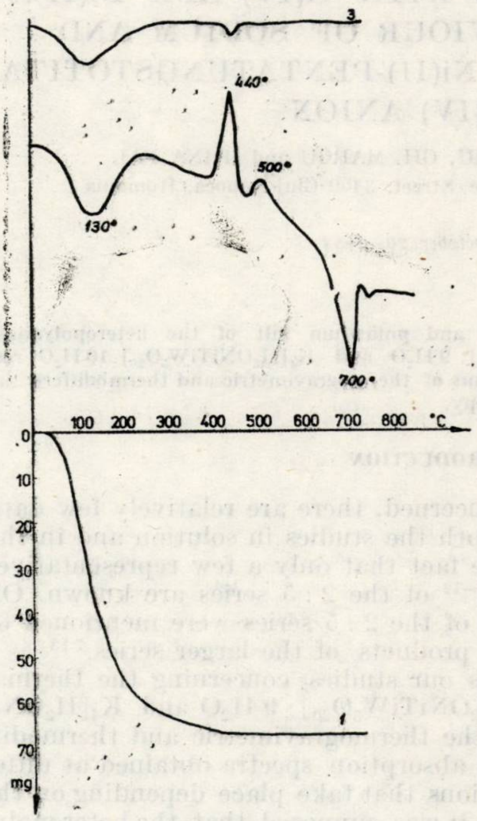

Fig. 1. — The thermal behaviour of the $Na_4[H_2ONiTiW_5O_{20}] . 9\,H_2O$ complex ; 1 — the TGA curve ; 2—the DTA curve ; 3—the DTG curve.

Within this temperature range, the recorded weight loss is 11.1 % as compared to 11.12 % calculated for 10 water molecules.

It is obvious that up to 240–250°C the rate of the dehydration process is higher ; the weight loss is 10.01 % and corresponds to 9 crystallization molecules ; this high rate of the dehydration process explains why it is visibly marked on the DTG curve (curve 3).

A water molecule, representing a loss of weight of 1.11 %, is difficultly removed from the molecule, within a wide temperature range and at a higher temperature. We consider this to be a constitution water molecule because it is stronger bound than the 9 crystallization water molecules.

As it will be further seen in the analysis of the IR absorption spectra, a destruction of the heteropolytungstate frame takes place simultaneously with the removing of this water molecule. This fact enabled us to consider it as an integrant part of the complex anion and to formulate the latter as $[H_2ONiTiW_5O_{20}]^{4-}$. Furthermore, we can observe when examining the

TGA curve (curve 1) that the slope of the curve is steeper in the portion corresponding to the elimination of the crystallyzation water as compared with the smoother slope of the curve in the last portion, corresponding to the elimination of the constitution water.

Above the temperature of 430°C no weight loss is recorded.

There are several thermal effects which occur on the DTA curve (curve 2), namely :

— an endothermal effect at 130°C, that is due to the dehydration process ;

— a strong exothermal effect at 440°C, assigned to a transformational process, from an amorphous phase (formed during the heating process) to a crystalline phase, another than the initial, complex one ; [1]

— a weak exothermal effect at 500°C that would mark the formation of lower oxides ; this process is achieved at a higher temperature ;

— the endothermal effect at 700°C marks the existence of a molten phase at this temperature in the system.

3.1.2. $K_4[H_2ONiTiW_5O_{20}]$. 10 H_2O

In figure 2 are given the weight loss (TGA-curve 1), its derivative (DTG-curve 3) and the thermodifferential (DTA — curve 2) recorded for complex $K_4[H_2ONiTiW_5O_{20}] \cdot 10\,H_2O$.

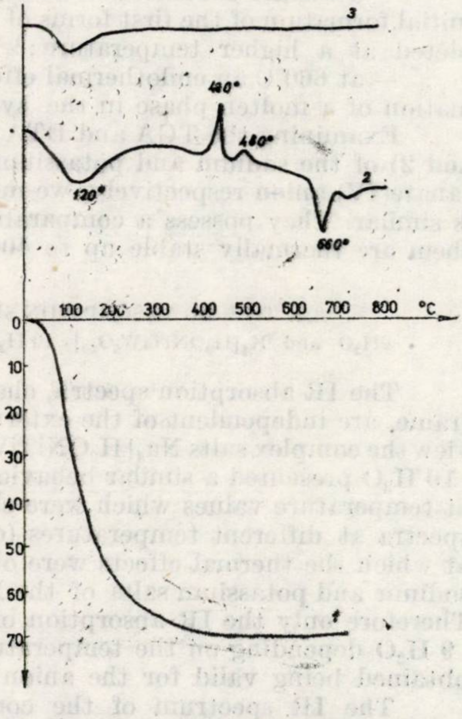

Fig. 2. — The thermal behaviour of the $K_4[H_2ONiTiW_5O_{20}]$. 10 H_2O complex ; 1 — the TGA curve ; 2 — the DTA curve ; 3 — the DTG curve.

Examining the TGA curve (curve 1) one can point out that a continual process of weight loss takes place when increasing the sample temperature from 40 to 420°C. This weight loss totalizes 11.66 % compared with 11.64 %, calculated for a dehydration process equivalent to the removal of 11 water moles for a complex mole.

In the first part of the TGA curve (curve 1), where the slope is more decided (up to $\simeq$ 240°C) a loss of 10 crystallization water molecules takes place (loss of 10.58 %) while within the temperature range 240–420°C there is only the elimination of one constitution water molecule (loss of 1.061 %). In this temperature range the slope of the TGA curve (curve 1) is much smaller.

As it is obvious, the first part of the process is developing with higher speed and is detectable on the DTG curve (curve 3) while the loss of the constitution water develops with lower speed, within a wide range of temperature. The speed of this last process is no longer visible in the DTG curve.

Above the temperature of 420°C there is no weight loss on the TGA curve (curve 1).

Following the DTA curve (curve 2) we can observe the occurrence of several thermal effects, namely :

— an endothermal effect at 120°C corresponding to the dehydration process on the TGA curve ;

— a stronger exothermal effect at 430°C, due to the formation of a new crystalline phase, other than the one stable at room temperature ;

— a weaker exothermal effect at 480°C that might correspond to the initial formation of the first forms of the metal oxides. This process is completed at a higher temperature ;[1]

— at 660°C an endothermal effect is recorded which denotes the formation of a molten phase in the system.

Examining the TGA and DTA curves (curves 1 and 2 from figures 1 and 2) of the sodium and potassium salts of the Ni(II)–pentatungstotitanate(IV) anion respectively, we may state that their thermal behaviour is similar. They possess a comparable thermal stability, namely, both of them are thermally stable up to 400–420°C.

3.2. THE IR ABSORPTION SPECTRA OF $Na_4[H_2ONiTiW_5O_{20}]\cdot 9H_2O$ and $K_4[H_2ONiTiW_5O_{20}]\cdot 10\,H_2O$ AT DIFFERENT TEMPERATURES

The IR absorption spectra, characteristic of the heteropolytungstate frame, are independent of the external cation. From the thermal point of view the complex salts $Na_4[H_2ONiTiW_5O_{20}]\cdot 9H_2O$ and $K_4[H_2ONiTiW_5O_{20}]\cdot 10\,H_2O$ presented a similar behaviour ; the thermal effects were recorded at temperature values which were close to each other. The IR absorption spectra at different temperatures (chosen depending on the temperatures at which the thermal effects were obtained) are actually identical for the sodium and potassium salts of the Ni(II)-pentatungstotitanate(IV) anion. Therefore only the IR absorption of the compound $Na_4[H_2ONiTiW_5O_{20}]\cdot 9\,H_2O$ depending on the temperature will be presented here, the results obtained being valid for the anion $[H_2ONiTiW_5O_{20}]^{4-}$.

The IR spectrum of the complex $Na_4[H_2ONiTiW_5O_{20}]\cdot 9\,H_2O$ at room temperature, presents three absorption bands within the 700–1000 cm^{-1} range due to the valency vibrations of the W–O, W–O–W and

W–O– central atom bonds and characteristic of the heteropolytungstate frame.[14] They occur, irrespective of the exthernal cation, at 770, 880 and 960 cm^{-1} (curve 1, figure 3). At 1640 cm^{-1} there occurs the bond characteristic of the water deformation vibration.

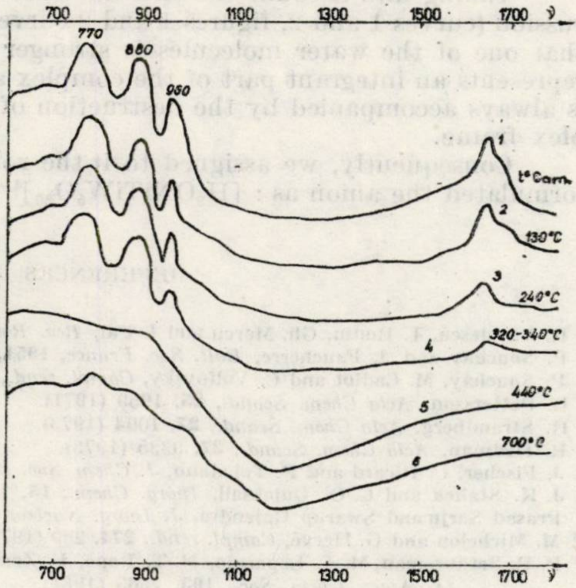

Fig. 3. — The IR absorption spectra of the $Na_4[H_2ONiTiW_5O_{20}] . 9 H_2O$ complex at different temperatures: 1 — at room temperature; 2 — at 130°C; 3 — at 240°C; 4 — at 320—340°C; 5 — at 440°C; 6 — at 700°C.

With the samples heated at 130°C (curve 2, figure 3) and within the 700–1000 cm^{-1} domain the IR spectrum preserves the same aspect as the one recorded at room temperature. As the temperature increases, the absorption bands within the 700–1000 cm^{-1} range start modifying their shapes.

Around 1640 cm^{-1} (curve 2, figure 3) there occurs in the spectrum the water deformation vibration with a shoulder at $\simeq$ 1670 cm^{-1}, observed also with the salts of the Ni(II)-undecatungstotitanate(IV) anion.[14]

At 130°C the water deformation vibration band is still intense. Within this temperature range we recorded on the TGA and DTA curves (figure 1) the dehydration process, that is, there took place the elimination of crystallization water.

At 240°C (curve 3, figure 3) the band characteristic of the water deformation vibration is much lowered in intensity. According to the thermal study we estimated that the removing of the crystallization water took place at a temperature around 240°C and the elimination of one water molecule, stronger bound in structure, took place within the temperature range of 240–420°C. In agreement with this, in the IR spectrum, at 240°C (curve 3, figure 3) and at temperature of 320–340°C (curve 4, figure 3), the band around 1640 cm^{-1} occurs as a band of weaker intensity and becomes even weaker as the temperature increases.

The IR absorption spectrum, recorded on samples heated at 440°C (curve 5, figure 3) (the exact temperature where, according to the DTA curve, the exothermal transformation into a new crystalline phase occurs), presents no absorption band within the 700—1000 cm^{-1} range and no water deformation band. As a consequence, we may conclude that the heteropolytungstic anion $[H_2ONiTiW_5O_{20}]^{4-}$ is actually decomposed at 440°C.

Taking into account the thermal behaviour of the anion under discussion (curves 1 and 2, figures 1 and 2 curves 2—5, figure 3) we conclude that one of the water molecules is stronger bound in the structure and represents an integrant part of the complex anion, because its elimination is always accompanied by the destruction of the heteropolytungstic complex frame.

Consequently, we assigned to it the role of constitution water and formulated the anion as : $[H_2ONiTiW_5O_{20}]^{4-}$.

REFERENCES

[1] R. Văţulescu, T. Budiu, Gh. Marcu and I. Pal, *Rev. Roumaine Chim.*, **30**, 831 (1985)

[2] P. Souchay and J. Faucherre, *Bull. Soc. France*, **1951**, 355.

[3] P. Souchay, M. Cadiot and C. Volfovsky, *Compt. rend.*, **269**, 826 (1969).

[4] L. Pettersson, *Acta Chem. Scand.*, **25**, 1959 (1971).

[5] R. Strandberg, *Acta Chem. Scand.*, **27**, 1004 (1973).

[6] B. Hedman, *Acta Chem. Scand.*, **27**, 3335 (1973).

[7] J. Fischer, L. Ricard and P. Toledano, *J. Chem. Soc. Dalton*, **9**, 941 (1974).

[8] J. K. Stalick and C. O. Quicksall, *Inorg. Chem.*, **15**, 1577 (1976).

[9] Prasad Sarju and Swarup Rajendra, *J. Inorg. Nuclear Chem.*, **30**, 1337 (1968).

[10] M. Michelon and G. Hervé, *Compt. rend.*, **274**, 209 (1972).

[11] P. R. Sethuraman, M. A. Leparulo, M. T. Pope, F. Zonnevijlle, C. Brevard and J. Lemerle, *J. Amer. Chem. Soc.*, **103**, 7665 (1981).

[12] W. H. Knoth and R. L. Harlow, *J. Amer. Chem. Soc.*, **103**, 1865 (1981).

[13] P. Souchay, "Ions Minéraux Condensés", Masson et Cie, Paris, 1969, p. 105—109.

[14] R. Văţulescu, T. Budiu, Gh. Marcu and I. Pal (in press).

Revue Roumaine de Chimie, **30**, *11—12*, 1031—1037 (1985)

COMBINAISONS COMPLEXES DU Tl(III) AVEC DES LIGANDS N-DONNEURS. ÉTUDE DU SYSTÈME Tl (III) — 2, 2′-AZOPYRIDINE

I. BERDAN, D. ANCUŢA et I. SANDU
Institut Polytechnique « Gh. Asachi », Faculté de Technologie Chimique
71, Splai Bahlui, Iaşi

Reçu le 8 décembre, 1984

Dans ce travail on présente les résultats obtenus concernant l'étude du système de réaction TlX_3 — AP, où : X = Cl, Br et AP = 2,2′-azopyridine.
Le comportement de l'ion Tl(III) comme acide Lewis de classe « b » (M) vis-à-vis du ligand N-donneur, 2,2′-azopyridine (L), a été mis en évidence par la formation de combinaisons complexes, mononucléaires, polaires, de type Tl(III). L. La détermination des constantes globales de stabilité des espèces complexes de Tl(III), par voie spectrophotométriques, donne les valeurs : $\beta_1 = 5{,}7 . 10^2$ l. mol^{-1} (X = Cl) et $\beta_1' = 4{,}6 . 10^2$ l. mol^{-1} (X = Br).
L'étude des complexes à l'état solide, en utilisant la spectroscopie électronique et d'absorption en I. R., nous a permis de conclure sur le mode de coordination du ligand à l'ion Tl (III). En effet, les caractéristiques spectrales des molécules complexes prouvent que la coordination du AP se réalise tant par l'atome d'azote donneur du groupement azo que par celui du noyau pyridinique.

The paper reports the characterization of some Tl(III) complexes with 2,2′-azopyridine (AP). The complexes correspond to the general type TlX_3 . AP (X = Cl, Br). The structural characterization of the complexes is based upon elemental analysis data, molecular weight, dipolmoment and electric conductivity determinations, electronic and infrared spectra.

1. INTRODUCTION

La plupart des combinaisons du Tl(III) se comportent comme acides Lewis et réagissent avec certaines bases Lewis avec formation de complexes.

L'ion Tl(III) manifeste un caractère d'acide Lewis de classe « b » [1] puisque la coordination des ligands autour de lui se réalise à base de liaisons covalentes. Ce caractère est illustré par sa haute capacité de former des combinaisons complexes avec un grand nombre de ligands inorganiques et organiques. [2]

D'autre part, les combinaisons contenant Tl(III) sont peu stables et réagissent comme agents oxydants. C'est la raison pour laquelle les équilibres de complexation peuvent être compliqués par l'apparition de certains processus rédox, surtout vis-à-vis des ligands à caractère réducteur. De tels processus rédox ont été saisis dans les systèmes de réaction entre Tl(III) et ligands du type des amines organiques.[3–5]

Evidemment, la stabilité des complexes formés dépend aussi de l'état d'hybridation de l'atome d'azote donneur qui assure une certaine basicité au ligand. D'une manière générale, la basicité des ligands N-donneurs varie de la sorte :

$$N(sp^3) > N(sp^2) > N(sp)$$

Dans une série de travaux antérieurs,[6–8] les auteurs ont étudié les systèmes de réaction du Tl(III) avec des ligands N-donneurs de type des hétérocycles organiques. En poursuivant ces études, dans cette note on présente les résultats obtenus sur le système Tl(III) — 2,2'-azopyridine.

2. PARTIE EXPÉRIMENTALE

Comme source de Tl(III) nous avons employé les halogénures, TlX_3 (X = Cl, Br) préparés d'après une recette citée dans la littérature[9]. Le ligand, 2,2'-azopyridine (L), a été préparé par oxydation de 2-aminopyridine à l'aide de NaClO.

La synthèse des combinaisons complexes a été réalisée en faisant réagir, à température ordinaire, la solution de ligand, AP, en éther éthylique, sur une solution fraîchement préparée de TlX_3 en acétonitryle. En refroidissant le mélange à zéro degrés, les complexes séparent sous forme de produits cristallins colorés (jaune pour X = Cl et brun-rougeâtre pour X = Br) qui sont purifiés par recristallisations. Les complexes sont stables vis-à-vis de lumière et d'humidité. La formule moléculaire générale de ceux-ci est $TlX_3 . L$, où X = Cl, Br.

Les complexes obtenus ont été caractérisés à l'aide des méthodes chimiques et physiques, à savoir : analyse élémentaire, déterminations de masses molaires, de conductibilités électriques molaires et de dipolmoments, spectres électroniques et spectres d'absorption en infra-rouge.

Les déterminations de masses molaires ont été effectués par la méthode cryoscopique en utilisant le benzène et le sulpholane comme solvants.[10] La conductibilité molaire des complexes, en solution d'acétonitryle, a été déterminée avec un conductomètre type OK-102. Les spectres électroniques ont été obtenus en utilisant le spectrophotomètre type Spekord UV-VIS (Carl Zeiss Jena) alors que les spectres d'absorption en I.R. ont été enregistrés avec les appareils de types : SP-200 (5000—650 cm^{-1}) et Perkin Elmer (400—200 cm^{-1}).

3. RÉSULTATS ET DISCUSSIONS

3.1. La formation des complexes en solution

La formation des complexes talliques, dans le système TlX_3—L, en solution eau-alcool éthylique (1 : 1) a été suivie par voie spectrophotométrique. Ainsi, on a enregistré les spectres électroniques des sels, TlX_3, du ligand, AP, et des solutions TlX_3—AP pour différents rapports molaires ; fig. 1. Les halogénures de Tl(III) présentent une bande d'absorption intense, dans l'ultra-violet, situé à $\lambda = 230$ nm (X=Cl) respectivement $\lambda' = 240$ nm (X=Br).

Le spectre électronique du ligand, préparé sous la forme trans, présente trois bandes d'absorption : une première bande, I, ($\pi \rightarrow \pi^*$) localisée aux noyaux pyridiniques qui apparaît à $\lambda_{max.} = 225$ nm relativement intense, une deuxième, II ($\pi \rightarrow \pi^*$), caractéristique à la molécule entière du ligand avec $\lambda_{max.} = 313$ nm et la troisième bande, III, ($n \rightarrow \pi^*$) avec $\lambda_{max.} = 455$ nm qui caractérise le groupement azo. L'isomère cis du même ligand ne présente que les deux premières bandes.

Dans les spectres électroniques des solutions TlX_3—AP, de différents rapports molaires, on retrouve les trois bandes du ligand libre avec certaines modifications qui apparaissent surtout pour les bandes I et III Ceci prouve tout d'abord que le ligand conserve sa forme trans dans la molécule du complexe formé et que la capacité donneuse du ligand se manifeste tant par l'atome d'azote du noyau pyridinique que par celui du groupement azo. Evidemment, la bande correspondante à la transition qui caractérise la molécule entière du ligand, III, est peu affectée à la suite de la coordination du AP à l'atome central.

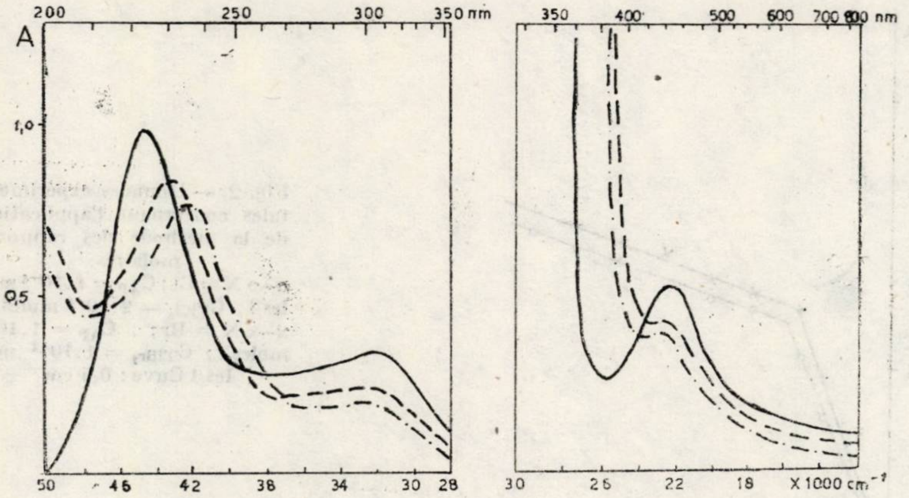

Fig. 1.—Spectres d'absorption électronique ; a. en ultra-violet : —AP ; $C=1.10^{-4}$ moles/l ; - - - $TlCl_3$.AP ; $C = 1.10^{-4}$ moles/l ; -·-·-$TlBr_3$.AP ; $C=1.10^{-2}$ moles/l ; b. en visible : concentration des espèces chimiques = 1.10^{-2} M ; solvant : eau — alcool éthylique = 1 : 1 ; cuve : 0,5 cm.

3.2. La détermination de la composition et de la stabilité des complexes talliques

Le rapport molaire de combinaison Tl(III)/L a été déterminé par voie spectrophotométriques, en utilisant les méthodes des rapports molaires,[11] des variations continue[12] et d'Edmonds-Birnbaum.[13] Les déterminations d'absorbance ont été effectuées à $\lambda_{max.} = 450$ nm (X=Cl) respectivement $\lambda_{max} = 451$ nm (X= Br), longueurs d'onde pour lesquelles se vérifie la loi de Lambert-Beer.

Dans la fig. 2 on présente les résultats expérimentaux concernant l'application de la méthode des rapports molaires. La représentation graphique de la fonction A = f[L/Tl(III)], où : A = absorbance et le rapport L/Tl(III) s'exprime en volumes de solutions équimolaires, conduit à deux droites dont l'intersection correspond au rapport molaire TlX_3 : L= 1 : 1. Le même résultat a été obtenu par l'utilisation de la méthode des variations continues — fig. 3, où la représentation de la fonction A = f(composition du système) met en évidence un maximum correspondant au rapport molaire 1 : 1. La méthode d'Edmonds-Birnbaum permet, à la fois, la détermination du rapport molaire de combinaison Tl(III)/L et de la constante globale de stabilité du complexe tallique. Cette méthode se base sur la détermination de l'absorbance d'une série de solutions Tl(III)—L, préparées en maintenant constante la concentration du Tl(III) et en faisant varier la concentration du ligand, ajouté en grand excès par rapport à l'ion Tl(III). Ainsi, la constante globale de stabilité, β_n, d'une espèce complexe, est calculée à l'aide de la relation :

$$\beta_n = \frac{A_2 \cdot C^n_{L_1} - A_1 \cdot C^n_{L_2}}{C^n_{L_1} \cdot C^n_{L_2}(A_1 - A_2)}$$

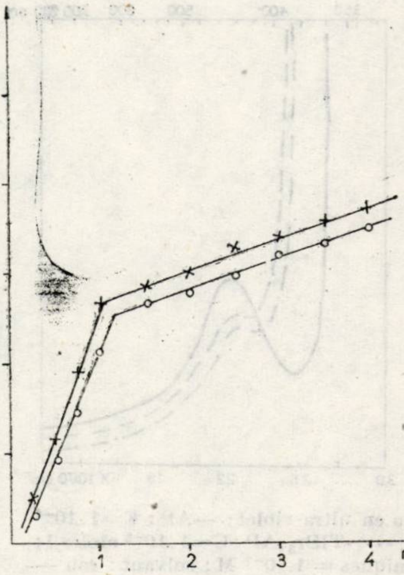

Fig. 2. — Données expérimentales concernant l'application de la méthode des rapports molaires. o–o X = Cl ; $C_{AP} = 1.10^{-4}$ moles/l ; $C_{TlCl_3} = 2.10^{-4}$ moles/l ; x–x X = Br ; $C_{AP} = 1.10^{-4}$ moles/l ; $C_{TlBr_3} = 1.10^{-4}$ moles/l Cuve : 0,5 cm

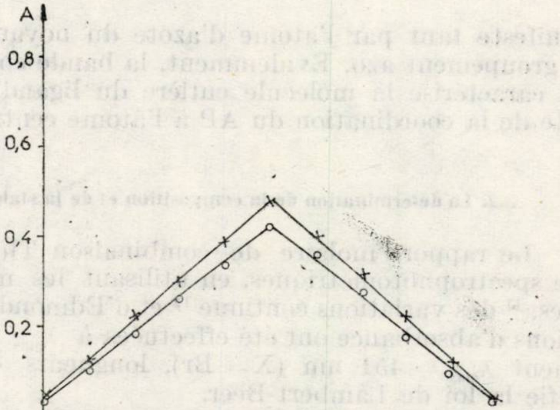

Fig. 3. — Données expérimentales concernant l'application de la méthode des variations continues o–o X = Cl ; x–x X = Br ; $C_{AP} = 5.10^{-4}$ moles/l ; $C_{TlX_3} = 5.10^{-4}$ moles/l

où : C_L = concentration molaire du ligand ;
A = absorbance des solutions ;
n = nombre de coordinence ;
les indices (1) et (2) se réfèrent à deux séries de solutions.

Le calcul de β_n se fait pour différentes valeurs de « n », mais on retient la valeur « n » pour laquelle on obtient une constance raisonable de la constante de stabilité. Les données expérimentales obtenues sont présentées dans le tableau 1.

Tableau 1

Données expérimentales concernant l'application de la méthode d'Edmonds-Birnbaum

C_{TlX_3} (moles/l) X=Cl, Br	C_L (moles/l)	A		β_n					
		X=Cl	X=Br	n = 1		n = 2		n = 3	
				X = Cl	X=Br	X = Cl	X = Br	X = Cl	X=Br
1	2	3	4	5	6	7	8	9	10
	1.10^{-3}	0,22	0,24						
2.10^{-4}	2.10^{-3}	0,32	0,34	6.10^2	$5,2.10^2$	$1,4.10^6$	$1,35.10^6$	$1,8.10^9$	$1,7.10^9$
	2.10^{-3}	0,32	0,34						
2.10^{-4}	5.10^{-3}	0,44	0,46	$6,1.10^2$	$4,6.10^2$	$0,2.10^5$	1.10^7	$0,5.10^8$	7.10^7
	5.10^{-3}	0,44	0,46						
2.10^{-4}	10.10^{-3}	0,505	0,54	$5,1.10^2$	4.10^2	$0,1.10^6$	$0,15.10^6$	$0,2.10^7$	4.10^6

En effet, on retrouve le même rapport molaire de combinaison Tl(III)/L = 1 : 1, car β_n prend des valeurs rapprochées uniquement pour n = 1 : $\beta_1 = 5,6 \cdot 10^2$ (X=Cl) ; $\beta_1' = 4,6 \cdot 10^2$ l·mol.$^{-1}$ (X= Br). Ces valeurs montrent que les espèces complexes ont une stabilité moyenne, comparable avec celle du cation complexe $[Cu(NH_3)_4]^{2+}$.

3.3. Quelques propriétés des complexes TlX_3 .AP

Les complexes séparés à l'état solide ont été caractérisés par analyse élémentaire, déterminations de masses molaires, conductibilité électrique molaire et de dipolmoment et par spectroscopie d'absorption en infra-rouge.

Dans le tableau 2 on présente quelques propriétés physiques des complexes $TlX_3 \cdot AP$.

Les valeurs des masses molaires, des conductibilités molaires et des dipolmoments correspondent à la formation des espèces complexes mononu-

Tableau 2

Quelques propriétés physiques des complexes TlX_3.AP

Formule moléculaire du complexe	$M_{calc.}$	$M_{déter.}$	Λ_M ($\Omega^{-1}.cm^2.mol^{-1}$)	μ (Debye)	Couleur	Point de fusion (°C)
$TlCl_3 . C_{10}H_8N_2$	494	514	105,4	6,24	jaune	194
$TlBr_3 . C_{10}H_8N_2$	628	636	95,4	6,15	brun-rougeâtre	182—184

cléaires, polaires, de rapports molaires Tl(III) : L = 1 : 1. En solution d'acétonitryle, ces complexes se dissocient selon le schèma d'ionisation des électrolytes univalents :

$$TlX_3 \cdot L + (S) \rightleftharpoons [TlX_2 \cdot L(S)]^+X^-,$$

où (S) = molécule de solvant.

Les complexes présentent une polarité assez élevée, ce qui signifie la formation des complexes à transfert de charge.

L'étude des spectres d'absorption en infra-rouge des complexes talliques, à l'état solide, fournissent des informations utiles concernant leur structure.

Dans les figures 4 et 5 on présente les spectres I.R. des complexes TlX_3. AP dans les domaines 5000—650 cm^{-1} et 400—200 cm^{-1}.

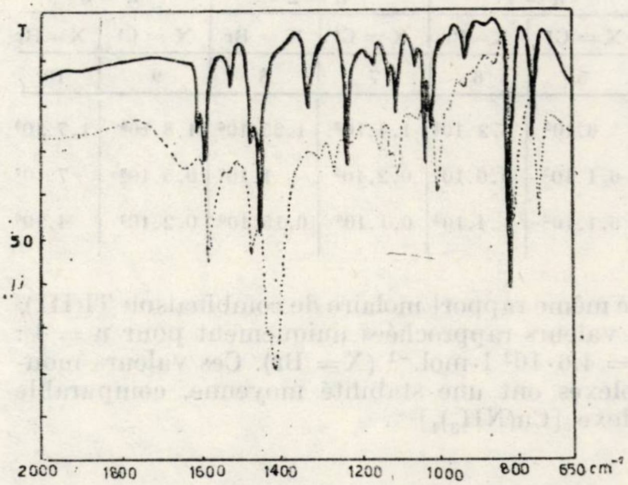

Fig. 4. — Spectres d'absorption en infra-rouge (5000—650 cm^{-1}).
------ AP (suspension en Nujol) ;
—— $TlCl_3$. AP (suspension en Nujol)

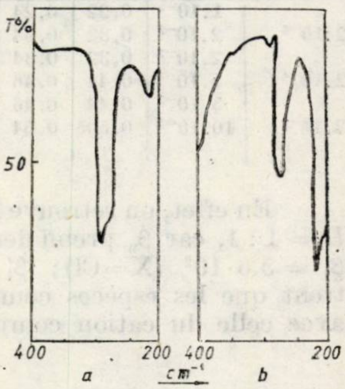

Fig. 5. — Spectres d'absorption en infra-rouge (400—200 cm^{-1}).
a. $TlCl_3$ .AP ; b. $TlBr_3$. AP

Le spectre du ligand libre, 2,2'-azopyridine, présente trois bandes caractéristiques :

- $\nu_{C=N} = 1585$ cm^{-1}; vibration de valence;
- $\nu_{N=N} = 1410$ cm^{-1}; vibration de valence;
- bande située à 991 cm^{-1}; vibration du noyau pyridinique ou vibration de squelette.

Dans les spectres I.R. des complexes, des modifications plus profondes s'observent aux bandes $\nu_{N=N}$ et $\nu_{squ.}$; la première se retrouve à 1440 cm^{-1} (X=Cl) respectivement 1442 cm^{-1} (X=Br) alors que la deuxième se scinde en deux composantes situées à 1010 cm^{-1} et 1070 cm^{-1} (X=Cl) respectivement à 1012 cm^{-1} et 1078 cm^{-1} (X=Br). La scission de la deuxième bande relève la présence dans les molécules des complexes tant du noyau pyridinique coordonné que de celui libre (non-coordonné). En effet, l'existence des noyaux pyridinique non-équivalents est en accord avec la conservation, dans les molécules des complexes, de la forme trans du ligand, de sorte que sa coordination se fasse, à la fois, par l'intermédiaire de l'atome d'azote pyridinique et par celui du groupement azo. Dans ces circonstances, à l'état solide, les complexes ont une structure bipyramidale-triangulaire, correspondant au nombre de coordination 5. Dans la chimie du Tl(III), une configuration semblable à été postulée pour le complexe du $TlCl_3$ avec le diméthyle-sulfoxyde (DMSO), à savoir $TlCl_3 \cdot 2DMSO$.[14]

L'étude des spectres I.R. dans le domaine 400—200 cm^{-1} a permis d'attribuer certaines bandes aux modes de vibration correspondant à la liaison Tl—N formée. Ainsi, dans les spectres des complexes (fig. 5), les vibrations de valence ν_{Tl-N} sont représentées par les bandes caractéristiques situées à 290 cm^{-1} ($X=Cl$) respectivement 268 cm^{-1} ($X=Br$). Evidemment, les bandes correspondant aux vibrations ν_{Tl-X}, qui se conservent dans les molécules des complexes, devront apparaître à des fréquences plus basses

4. CONCLUSIONS

Dans le système de réaction TlX_3 — 2,2'-azopyridine, se forment, en solution aqueuse, des complexes mononucléaires, polaires, de rapport molaire 1 : 1, qui ont une stabilité moyenne ($\beta_1 = 5.10^2\ l \cdot mol^{-1}$, pour $X=Cl$ et $\beta_1' = 4.10^2\ l \cdot mol^{-1}$). En solution d'acétonitryle, les complexes présentent une dissociation correspondante aux électrolytes univalents, 1 : 1. Dans ces conditions, leurs molécules contiennent l'ion Tl(III) hexacoordonné, le sixième point coordinatif étant assuré par la molécule de solvant (acétonitryle).

A l'état solide, la structure des complexes peut être interprétée en admettant l'ion Tl(III) pentacoordonné, ayant une structure bipyramidale-triangulaire.

BIBLIOGRAPHIE

[1] S. Ahrland, J. Chatt et N. R. Davies, *Quart. Rev. (London)*, **12**, 265(1958).

[2] A. J. Carty, *Coord. Chem. Rev.*, **4**, 29(1969).

[3] N. Calu et I. Berdan, *An. şt. Univ. Iaşi, Secţ. I*, t. **XVII**, f. 2, 149(1971).

[4] N. Calu et I. Berdan, *An. şt. Univ. Iaşi, Secţ. I*, t. **XVII**, f. 2, 159(1971).

[5] N. Calu et I. Berdan, *An. şt. Univ. Iaşi, Secţ. I*, t. **XIX**, f. 2, 125(1973).

[6] I. Berdan, *Bul. Inst. Politehnic Iaşi, Secţ. II*, t. **XXVI(XXX)**, f. 3—4, 21(1980).

[7] N. Calu, I. Berdan et Al. Caşcaval, *Bul. Inst. Politehnic Iaşi, Secţ. II*, t. **XXVI(XXX)**, f. 3—4, 41(1980).

[8] I. Berdan et N. Calu, *Bul. Inst. Politehnic Iaşi, Secţ. II*, t. **XXVII(XXXI)**, f. 1—2, 9(1981).

[9] I. Berdan, Thèse de doctorat, I.P. Iaşi, 1974.

[10] C. H. Lanford, *J. Amer. Chem. Soc.*, **81**, 3799(1959).

[11] J. H. Joe et A. L. Jones, *Ind. Engl. Chem. Anal.*, **16**, 111(1944).

[12] P. Job, *Ann. Chem.*, **9**, 10, 113(1928).

[13] S. Edmonds et H. Birnbaum, *J. Amer. Chem. Soc.*, **63**, 1471(1941).

[14] F. A. Cotton, B. F. G. Johnson and R. M. Wing, *Inorg. Chem.*, **4**, 502(1958).

Revue Roumaine de Chimie, 30, *11–12*, 1039–1045 (1985)

STRUCTURAL STUDIES ON THE AQUO-AMMINO-DI-2-MERCAPTO-BENZOTHIAZOLE COBALT COMPLEX

A. CĂLUŞARU

Institute of Chemical Research, Spl. Independenţei 202, Bucharest, Romania

Recived May 11, 1985

Chemical analysis, thermal behaviour, NMR and IR spectra were used in order to determine the structure of the complex formed by cobalt (II) ion with 2-mercaptobenzothiazole in amoniacal medium. It has been found that the structure corresponds to an aquo-ammino-di-2-mercaptobenzothiazole cobalt complex, in which water and ammonia form hydrogen bonds with the sulphur atoms. This interligand conformer structure confers special properties to both water and ammonia molecules embedded in a relatively symmetrical steric skeleton.

The 2-mercaptobenzothiazole can be expressed in two tautomeric forms: thiolic and thionic. The pure substance in solid state is predominantly in thione form, as it has been shown by infrared spectroscopy.[1−3]

A defined assignment of the IR absorption bands for 2-mercaptoqenzothiazole can be found in[4]; the bands near 1036 cm^{-1} and 1287 cm^{-1} are mainly produced by the 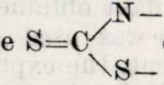 $S{=}C\begin{smallmatrix}\diagup N-\\ \diagdown S-\end{smallmatrix}$ couple; the band at 750 cm^{-1} was assigned as a streching vibration of the four adjoint hydrogen atoms of the aromatic ring and the band at about 726 cm^{-1} was assigned as a streching frequency of the NH couple.

We can expect that in ligand form the structure of the 2-mercaptobenzothiazole will be modified owing to the bonds between metal ion and sulphur atoms; therefore the thione form will be displaced in the thiol one.

Several complexes of the mercaptobenzothiazole with metal ions, especially Pb^{2+} and Cu^{2+}, were studied by Spacu and Kuraş[5] for analytic purposes, but no IR spectra nor detailed structural data of these complexes are yet available.

In the present work we study a cobalt complex with 2-mercaptobenzothiazole in order to clarify a multiligand structure and to determine some properties of this complex.

EXPERIMENTAL

The 2-mercaptobenzothiazole and the other substances were of reagent grade, commercially available.

For the preparation of the complex a solution of 1 % 2-mercaptobenzothiazole in 2.5 % ammonia was mixed with amonium chloride-ammonia — cobalt chloride solution. It is important to maintain the pH of the resulting solution near 8. At lower pH values the precipitation of the 2-mercaptobenzothiazole occurs, while at higher pH values the cobalt ammonia complexes are too stable, hindering the precipitation of the mercapto-complex. The cobalt 2-mercaptobenzothiazole complex is formed as a green precipitate which can be separated by filtration. After washing with distilled water, the precipitate was left to dry in air at room temperature. The product is soluble in a series of solvents such as : acetone, chloroform, dimethylformamide, carbon tetrachloride, dimethylsulfoxide and is insoluble in methyl- and ethyl alcohols.

The precipitate of cobalt complex, prepared as mentioned, contains also a more insoluble compound, whose amount varies in time and depends on the drying conditions. This amount of the insoluble compound is minimal when the precipitate is dried at a lower temperature.

The combustion elemental analysis was carried out with a Carlo Erba "Elemental Analyser" 1106 type ; the IR spectra were recorded with a Karl Zeiss (Jena) "Specord 75 IR" instrument ; the polarographic analysis was carried out with a Radelkis "OH 105" polarograph ; for the thermal analysis a thermogravimetrical balance "Stanton" and a thermogravimetrical analyser Du Pont 1090 type were used. The NMR spectra were recorded with a "Varian" A 60 A type instrument.

EXPERIMENTAL RESULTS

The experimental determinations were focused to establish the composition by means of chemical and instrumental analysis and to study some properties of this complex.

1. Chemical analysis

The experimental results obtained by combustion elemental analysis, thermogravimetry and polarography are presented in Table 1 ; the corresponding theoretical values for three possible complexes are given. In order to evaluate the precision of the data obtained by combustion elemental analysis, 2-mercaptobenzothiazole was used as reference compound. It appears that for the carbon percent, the experimental data can be lower with about 6%, as compared with the theoretical value. For the assumed complexes, the calculated values which are not in agreement with the corresponding experimental ones are marked with asterisk.

The best agreement between both the experimental and theoretical values was obtained for the aquo-ammino-di-2-mercaptobenzothiazole complex, i.e. $[Co(C_7H_4NS_2)_2(NH_3)(H_2O)]^{\pm 0}$. For the complexes containing two ammonia or two water molecules as ligands, larger deviations were obtained for the values of both hydrogen and nitrogen contents. On the other hand if the complexes with one or three molecules of 2-mercaptobenzothiazole as ligand are considered, strong deviations of all the values presented in table 1 are obtained.

2. Thermal behaviour

In order to interpret the thermal behaviour of the $[Co(C_7H_4NS_2)_2(NH_3)(H_2O)]^{\pm 0}$ complex, it is necessary to know this behaviour of the ligand alone. For the 2-mercaptobenzothiazole the variation of the weight as a function of temperature is given in Fig. 1, together with the corresponding derivative curve. Only one sharp decrease of the weight is produced between

Table 1

Comparison of the analytical experimental data with the calculated values for several possible structures of cobalt 2-mercaptobenzothiazole complexes

Compound	Combustion			Residue at 900°	Cobalt %
	Carbon %	Hydrogen %	Nitrogen %		
2-Mercaptobenzothiazole					
Experimental	47.0	2.9	8.5	1.4	—
Calculated	50.2	3.0	8.4	0	—
Cobalt(II)-complex					
Experimental	37.5	3.1	9.2	17.0	12.9
Calculated					
$[Co(C_7H_4NS_2)_2(NH_3)(H_2O)]$	39.4	3.05	9.4	17.6	13.8
$[Co(C_7H_4NS_2)_2(NH_3)_2]$	39.6	3.3*	13.2*	17.6	13.9
$[Co(C_7H_4NS_2)_2(H_2O)_2]$	39.4	2.84*	6.56*	17.5	13.6

* Disagreement with the experimental values

245.6° and 316.8°, with a halfplateau value at 287.2°, followed by a slower continuous decrease. At 900° the residue value is 1.4, as it is shown in Table 1.

In the case of the cobalt complex the thermogravimetric curves are shown in Fig. 2. After the elimination of a small quantity (0.416%) of of non-bounded water below 100°, two sharp steps of weight losses are produced. The first step is located in the range of 151.9° and 174.4°, with a halfplateau value at 161.2°. This step can be assigned to the elimination of both water and ammonia molecules bound as ligand in complex structure. We can see however that the experimental value of 6.32% is lower, although of the same order, as compared with the theoretical value of 8.22%. This difference can be explained if we take into account that some reactions occur with the formation of hydroxy-compound or cobalt oxide. The second step is located in the range of 247.5° and 312.7° with a halfplateau value at 271.2°, which is the same as in the case of pure 2-mercaptobenzothiazole (Fig. 1). Also in this case the percentage of the weight loss is somewhat lower, owing to the formation of cobalt sulphide which is oxidised slower than the decomposition of the non bound ligand.

The thermal behaviour is therefore in agreement with the structure shown in Table 1.

3. Nuclear magnetic resonance and magnetic susceptibility

The problem which arises when the complex is dissolved in solvents is the slow oxidation of the Co(II) to Co(III), visible by the change of the green colour in the brown one. The fastest oxidation occurs in acetone. We used the hexadeutero-dimethylsulfoxide as solvent for recording

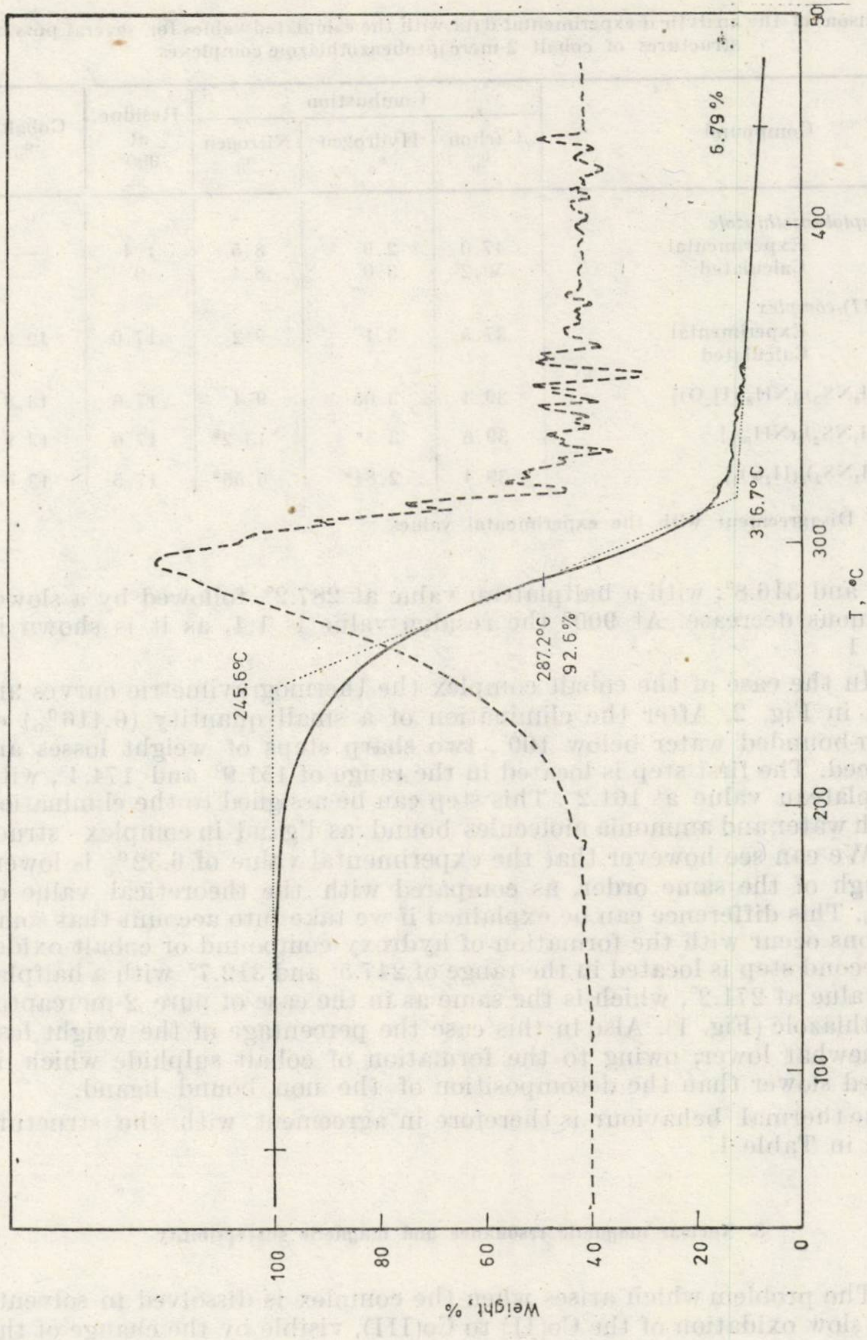

Fig. 1. — Thermal behaviour of the 2-mercaptobenzothiazole : weight loss full line, derivative dotted line.

NMR spectra. Two kinds of protons were found : (1) bonded to the aromatic ring, located at 8.25 ppm and (2) OH and NH proton type located at 4.33 ppm. The bands are broadened, without fine structure, owing to the paramagnetic properties of the Co(III) fraction, resulted by air oxidation. The determination of the magnetic susceptibility of some solid samples indicated a value $\chi = 3 \cdot 5 \times 10^{-6}$ cm^3/g, produced by the paramagnetic properties of the traces of a Co(III) fraction.

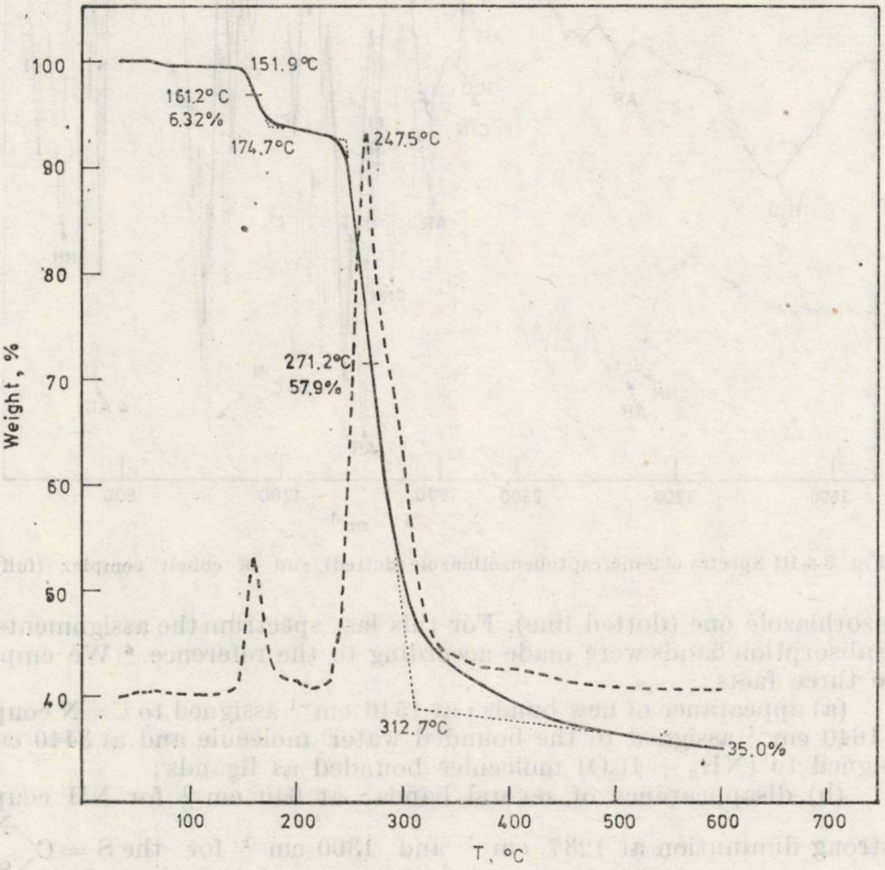

Fig. 2. — The same as in Fig. 1 for the cobalt complex.

The two species of protons indicated by NMR spectra are also in good agreement with the structure in Table 1.

4. Infrared spectra

The infrared spectrum of the aquo-ammino-di-2-mercaptobenzothiazole complex is given in Fig. 3 (solid line), compared with the 2-mercapto-

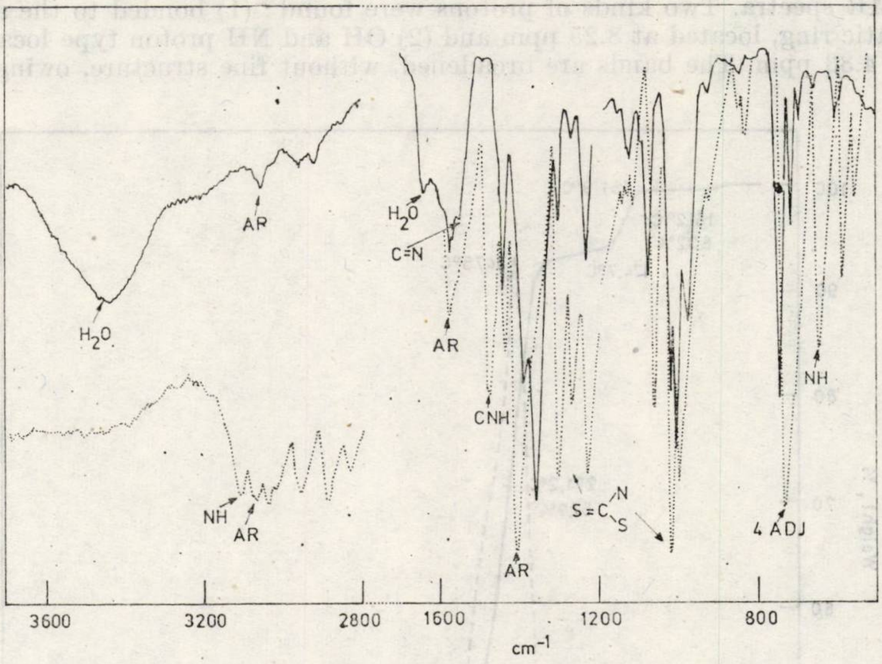

Fig. 3 — IR Spectra of 2-mercaptobenzothiazole (dotted) and of cobalt complex (full).

benzothiazole one (dotted line). For this last spectrum the assignments of the absorption bands were made according to the reference.[4] We emphasize three facts :

(a) appearance of new bands : at 1546 cm^{-1} assigned to C=N couple, at 1640 cm^{-1} assigned to the bounded water molecule and at 3440 cm^{-1} assigned to $(NH_3 + H_2O)$ molecules bounded as ligands ;

(b) disappearance of several bands : at 640 cm^{-1} for NH couple, a strong diminution at 1237 cm^{-1} and 1300 cm^{-1} for the $\mathrm{S} = \mathrm{C}\genfrac{}{}{0pt}{}{\diagup \mathrm{N}-}{\diagdown \mathrm{S}-}$ couple, at 1480 cm^{-1} for CNH couple, in the range of 2800–3040 cm^{-1} (non assigned) and at 3110 cm^{-1} for NH couple ;

(c) displacement of several bands : at 740 cm^{-1} for the four H adjoints to the aromatic ring, in the range of 973–1072 cm^{-1} for $\mathrm{S}{=}\mathrm{C}\genfrac{}{}{0pt}{}{\diagup \mathrm{N}-}{\diagdown \mathrm{S}-}$ couple and at 1360 cm^{-1} for the aromatic ring.

DISCUSSION

All the data presented above can be correlated for finding the cobalt complex structure. As it has been shown, the chemical analysis, NMR spectra and thermal analysis allow to conclude that an aquo-ammino-di-2-mercaptobenzothiazole cobalt complex is formed when a 2-mercaptobenzothiazole in ammonia solution is mixed with Co^{2+} ions at pH about 8.

The IR spectra show undoubtedly that the ligand suffers a major structural transformation when it is bound in ligand form. The most obvious is the disappearence of all bands corresponding to the NH couple : at 640 $\mathrm{cm^{-1}}$, 1840 $\mathrm{cm^{-1}}$ and 3110 $\mathrm{cm^{-1}}$. This fact, correlated with the strong modifications of the bands in the range of 973—1072 $\mathrm{cm^{-1}}$ and at 1273 and 1300 $\mathrm{cm^{-1}}$, is a certain proof that the thione form of the free 2-mercaptobenzothiazole is changed into a thiol one. We can also take into account the IR spectrum of the di(benzothiazol-2-yl) disulphide, which is a "dimer" of the 2-mercaptobenzothiazole, where the thione form is converted into the thiol one.[4] Also in this case the bands in the above mentioned regions, corresponding to the $\mathrm{S{=}C}\begin{smallmatrix}\diagup\mathrm{N}-\\ \diagdown\mathrm{S}-\end{smallmatrix}$ couple, are modified in a similar manner as for the cobalt complex bands. The stronger band at about 1010 $\mathrm{cm^{-1}}$ (Fig. 3) is produced in the cobalt complex spectrum by the couple $-\mathrm{S}-\overset{\|}{\mathrm{C}}-\mathrm{S}-$ which is in agreement with the thiol form of the ligand.

On the basis of the above mentioned experimental findings we can conclude that the structure of the aquo-ammino-di-2-mercaptobenzothiazole cobalt complex is of the type represented in Fig. 4. The four sulphur atoms of the two 2-mercaptobenzothiazole ligand molecules are coplanar with the cobalt ion in the center. Above and below the axis perpendicular to this plane are located the water and ammonia molecules. We emphasize that in this complex both water and ammonia ligands form in addition interligand hydrogen bonds, similarly with a series of organic molecules.[6] The conformer type structure shown in Fig. 4 explains the higher stability of the complex when water or ammonia ligand are bounded in the molecule. These molecules are "embedded" in the complex structure and therefore their properties must be modified. Some properties of the embedded water and ammonia molecules in cobalt complexes of the aquo-ammino-di-2-mercaptobenzothiazole type are studied polarographically and will be published elsewhere.

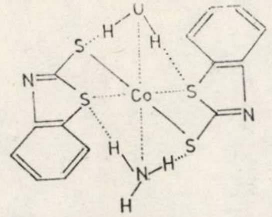

Fig. 4. — Structure of the aquo-ammino-2-mercaptobenzothiazole cobalt (II) complex.

REFERENCES

[1] K. S. Suresh, J. Ramachandran and C.N.R. Rao, *J. Sci. Ind. Res.* (India), **20 B**, 203 (1961).
[2] C. N. R. Rao and R. Venkataraghavan, *Spectrochim. Acta*, **18**, 541 (1962).
[3] I. Suzuki, *Bull. Chem. Soc. Japan*, **35**, 1286, 1449 and 1456 (1962).
[4] N. B. Colthup, L. H. Dely and S. E. Wiberley, "Introduction to Infrared and Raman Spectroscopy", Academic Press, New York, San Francisco, London, 1975, p. 442.
[5] Gh. Spacu and M. Kuraş, *Z. anal. Chem.*, **104**, 88 (1936).
[6] S. Mager and M. Horn, "Stereochemistry of Organic Compounds" (in Romanian), Dacia, Cluj-Napoca (Romania), 1984, pp. 263—264.

Revue Roumaine de Chimie, 30, *11—12*, 1047—1051 (1985)

COMBINED ION EXCHANGE–SPECTROMETRIC STUDY OF THE Ce(IV) – SULPHANILIC ACID SYSTEM. I

ION EXCHANGE METHOD FOR ELIMINATING INTERFERENCE IN THE SPECTROMETRIC DETERMINATION OF CERIUM(IV)

LUMINIŢA VLĂDESCU and STELUŢA CHIPER
National Institute of Chemistry, Laboratory of Analytical Chemistry, Splaiul Independenţei 202, Bucharest, Romania

Received December 17, 1984

In this paper the optimal working conditions of ion exchange utilisation for eliminating the interferences in the spectrometric determination of cerium (IV) with Sulphanilic acid were studied and established.

Sulphanilic acid was first used in the analytical chemistry of cerium by Montignie.[1] The reaction is sensitive and as other rare earths proved not to interfere; it was used as the basis of a method for the spectrometric determination of cerium(IV).[2]

In connection with the method described in the literature, mention is made of the interference of manganese, chromium, copper, cobalt, nickel, iron. Likewise, strong oxidants such as bismuthate, bromate, dichromate, periodate, permanganate, persulphate and lead dioxide oxidize sulphanilic acid and thus interfere with the determination of cerium.[2]

These interferences can be eliminated by double extraction of cerium with 4,4,4-trifluoro-1-(2-thyenyl)-1,3-butanedione in xylene,[3] controlled potential electrolysis with platinium electrodes,[4] or oxalate precipitation of cerium.[5]

Each of these methods is laborious, involves numerous operations and solves only partially the problem of interferences.

The present paper reports on the use of ion exchange resins for eliminating interferences in the spectrometric determination of cerium(IV) with sulphanilic acid.

EXPERIMENTAL

CHEMICALS AND EQUIPMENT

- — Strongly acid cation exchange resin Vionit CS-3
- — Strongly basic anion exchange resin Vionit AT—1.
- — Aqueous solutions of known titrum of Ce (IV), Ce (III), Mn (II), Co (II), Ni (II), Cu (II), Fe (II), Mg (II), Ca(II), Cr(III), Al(III), Fe(III).

— Aqueous solutions of sulphanilic acid 10^{-2} M and 10^{-1} M.

— Aqueous solution of sulphosalicylic acid 20%.

— Aqueous solutions of HCl 4 M, 6 M ; H_2SO_4 2M, 4M ; HNO_3 2M, 4 M ; NH_3 25%.

— Aqueous solutions of sodium or potassium bismuthate, bromate, dichromate, periodate, permanganate, persulphate.

— SPECOL Carl Zeiss Jena spectrophotometer.

— MV — 84 pH — meter.

The quantitative determination of Ce (IV) was performed by spectrophotometry in the presence of sulphanilic acid, [2] or of sulphosalicylic acid.[6]

The ion exchange took place in glass column 15 cm long, 1 cm in diameter, provided with stopcoks at bottom and funnel with ground joint at top.

Known quantities of cation or anion exchange resins were transferred into each column, purified, activated in H^+ or Cl^- form respectively, and washed with distilled water up to negative Cl^- test.

RESULTS AND DISCUSSION

In order to establish optimum working conditions the study was carried out on the influence of the type and ionic form of the resin, of pH and the working method on the ion exchange behaviour of cerium(IV) in the presence of sulphanilic acid.

To this end, two methods were used : (A) accurately measured volumes of Ce(IV) and sulphanilic acid solutions of known titrum were introduced into the funnel at the end of the resin column. The solution was passed through the resin at a rate of 0.1 ml/min. The resulting effluent after passing the sample through the resin and after washing, was collected in 25 ml calibrated flasks and was used for spectrometric determination of cerium, measuring absorbance at $\lambda = 495$ nm ; (B) a known amount of Ce(IV) was fixed in the resin and then eluted with sulphanilic acid solution.

The Ce(IV) amount retained in the cationite following the passage of sulphanilic acid through the column was measured after cerium elution with HCl 4M.

The pH used was 1.5 and 2, optimal values for the spectrometric determination, but also restrictive because at pH < 1 the absorbance decreases and at pH 2.3 a precipitate appears.

The results obtained are given in table 1.

Table 1

Influence of type and ionic form of the resin, of pH and of working method on the ion exchange behaviour of Ce(IV) in the presence of sulphanilic acid

Resin		pH	Working method	Cerium (IV) quantity		
				In sample (mg)	Determined	
Type	Ionic form				In resin (mg)	In effluent (mg)
CS-3	H^+	1.5	A	2.80	—	2.94
		2.0	A	2.80	—	2.75
		1.5	B	2.80	2.88	—
	NH_4^+	1.5	A	2.80	—	2.90
		2.0	A	2.80	—	2.85
		2.0	B	2.80	2.70	—
AT-1	Cl^-	2.0	A	2.80	—	2.76

The reaction bright-red product was strongly fixed in the anion exchange resin from which it could not be eluted with high concentrations of HCl, H_2SO_4 or HNO_3 solutions nor did it disappear under the action of certain oxidant or reducing solutions.

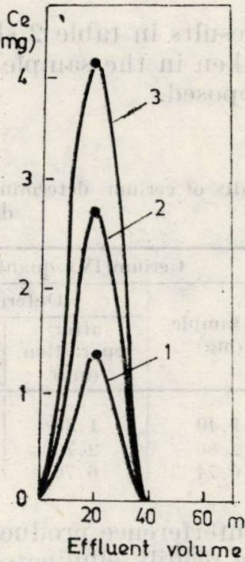

Fig. 1. — Determination of cerium (IV) by the combined ion exchange-spectrometric method in the presence of sulphanilic acid, in solutions with different contents of Ce(IV).
Cerium (IV) quantity in sample: 1) 1.40 mg ; 2) 2.80 mg ; 3) 4.20 mg

On using (B) method no colour appeared in the effluent, proof that the reagent could not act on the cerium in the resin. The cerium amount was again found by elution with HCl 4 M.

With (A) method, irrespective of the ionic form of the resin, the absorbance of the effluent solution corresponded to and was the measure of the amount of cerium introduced in the sample. After passing a HCl 4 M solution through the cationite, the complete cerium amount taken in the sample was again found.

The cation exchange experiments repeated with samples having varied amounts of Ce(IV), in the presence of the reagent in excess, showed absorbance of the effluent solution to be proportional to the amount of cerium taken in the sample (Fig. 1).

Therefore, contact of the solution with the resin did not have a negative influence on cerium determination. In contrast, by this simple operation, all the other cations, which do not react with sulphanilic acid, but produce interferences owing to thier specific colour, are taken out of solution.

The results of the ion exchange experiments on the binary mixtures Ce(IV)—M (M = Mn(II), Co(II), Ni(II), Cu(II), Fe(II), Mg(II), Ca(II), Cr(III), Al(III)) showed good agreement between the amount of cerium taken in the sample and those determined after passage through a cationite column. In the absence of this operation, the spectrometric method led to marked positive errors. Contact of the sample to be analyzed with the cationite is followed by retention in the resin of all the interfering cations, while the product of the reaction between Ce(IV) and sulphanilic acid can be completely recovered in the effluent which is used for correct determination of the cerium amount.

The ion exchange method was checked on samples containg known amounts of Ce(IV) and variable amounts of the cations previously mentioned.

The results in table 2 show a good agreement between the cerium amounts taken in the sample and those found again after applying the method proposed.

Table 2

Results of cerium determination from synthetical mixtures containing different cations

Cerium(IV) quantity			Elements present in sample
In sample (mg)	Determined after separaition (mg)	Determined without separation (mg)	
1.40	1.38	2.66	Mn(II), Co(II), Ni(II), Cr(III), Fe (II), Cu (II), Al(III), Ca(II), Mg(II)
2.80	2.76	5.02	
6.74	6.70	7.15	

The interference produced by strong oxidants which attack the reagent can be readily eliminated as all these compounds are found in the solution as anions. By passing the sample — in which cerium is to be determined — through a column with anion exchange resin (in ionic form SO_4^{2-}) bismuthate, bromate, dichromate, periodate, permanganate, persulphate anions are retained in the anionite, releasing into the solution an equivalent amount of SO_4^{2-} ions which does not act in any way on the reaction of Ce(IV) with sulphanilic acid.

Table 3

Results of cerium(IV) determination from synthetical mixtures containing different oxidants

Cerium(IV) quantity			Oxidants present in sample
In sample (mg)	Determined after separation (mg)	Determined without separation (mg)	
1.40	1.36	0.30	$KBrO_3$, $K_2Cr_2O_7$, KIO_4, $KMnO_4$, $Na_2S_2O_8$
2.80	3.00	0.27	
6.70	6.82	0.38	

The results of the ion exchange experiments in table 3 show that cerium can be determined with good precision in the synthetical mixtures containing known quantities of cerium (IV) in the presence of the oxidants mentioned.

Therefore, the quantitative determination of cerium can be achieved under good conditions by using sulphanilic acid as reagent in the presence of any chemical species considered to interfere, if the spectrometric method is combined with a simple ion exchange procedure.

In this way, by passing the solution to be analyzed through a column with anion exchange resin, in SO_4^{2-} ionic form, followed by washing with distilled water, a solution containing only the cations in the initial sample and the SO_4^{2-} anions is obtained. This solution to which sulphanilic acid is added is then passed through a column with cation exchange resin. The effluent quantitatively collected in a calibrated flask is used for spectrometric determination of cerium by measuring absorbance at $\lambda = 495$ nm.

Table 4

Retults of cerium (IV) determination from synthetical mixtures containing different cations and oxidants

Cerium(IV) quantity (mg)	In sample	1.40	2.80	5.60	6.74
	Determined after separation	1.35	2.97	5.49	6.83

Table 4 shows the results of some of the applications of this working method using synthetical mixtures of variable compounds. In all the cases the quantity of cerium taken in sample was found by this procedure, with an error corresponding to the precision of the determination method.

CONCLUSIONS

By coupling the method of spectrometric determination of cerium(IV) with sulphanilic acid, with an ion exchange method, all the interferences noticed are eliminated by a simple, rapid method, without consumption of reagents.

Contact of the sample to be analyzed with an anion exchange resin leads to the release of all the interfering anions.

Contact with the cation exchange resin is obtained after adding the reagent to the solution with cerium only in the presence of the cations of the initial sample and the SO_4^{2-} anions from the anionite.

The effluent solution collected quantitatively contains only the reaction product between Ce(IV) and sulphanilic acid, which is used for accurate determination of the cerium content in the sample to be analyzed.

REFERENCES

[1] E. Montignie, *Bull. Soc. chim. France*, **6**, 889 (1939).
[2] P. L. Sarma and L. H. Dieter, *Talanta*, **13**, 347 (1966).
[3] G. W. Smith and F. L. Moore, *Analyt. Chem.* **29**, 448 (1957).
[4] G. F. Smith, G. Frank and A. E. Kott, *Ind. Eng. Chem., Anal. Ed.*, **12**, 268 (1940).
[5] R. C. Vickery, "Analytical Chemistry of Rare Earths", Pergamon Press, Oxford, 1961, p. 19—22, 60.
[6] K. A. Das, *J. Indian Chem. Soc.*, **10**, 306 (1972).

Revue Roumaine de Chimie, 30, *11—12*, 1053—1058 (1985)

SIMULTANEOUS DETERMINATION OF ATMOSPHERIC n-HEXANE, TOLUENE AND ACETONE WITH ACTIVATED CHARCOAL TUBES USING THE TWO-STEP THERMAL GAS EXTRACTION PROCEDURE

ROMANO CIUPE, SZANTO CSABA and STELUȚA BUGNARIU
Institute of Hygiene and Public Health, Pasteur Str. 6, Cluj-Napoca

Received August 10, 1984

The present paper presents a two-step procedure for the determination of some volatile polluants from air using charcoal sample tubes and a direct thermal desorption device.

INTRODUCTION

Hygiene and work safety legislation have been settling the workers' exposure to toxic vapours, applying the Maximum Allowable Concentration (M.A.C.). The assessment of the workers' real exposure during a whole shift has become an increasingly important and up-to-date general problem. Several techniques have been used for sampling and analysing organic vapours in air. A direct sampling of air is useful when the time weighted average as M.A.C. is well above the analyser's limit of detection. Greater sensitivity is achieved by absorption in a bubbler or by adsorption in large adsorption tubes on a solid adsorbent, followed by thermal desorption and direct periodical introduction into the gas chromatograph. [1] A much more convenient sampling technique was developed using activated charcoals miniature sampling tubes [2,3] and low flow pumps. For analysis, the adsorbant beds are removed and desorbed by extraction with a polar solvent, or directly thermally desorbed, incorporating the tube into the carrier gas line of the chromatograph by a Thermal Desorption Attachment. [1,4–6] The advantages of the thermal desorption were applied to the Badges-type passive sampling systems too, by insertion of the diffusive monitors suitable for thermal desorption. [7] In order to maintain the advantages offered by thermal desorption almost as ideal technique by its simplicity and minimal sample handling with few opportunities for artifact introduction, different approaches were done to enlarge its applicability. Thus a stepwise gas extraction was used by Suzuki et al.[4] for evaluating the occluded solvents in adhesive tape and by Kolb and Pospisil [8] for determining the monomers in polymers, residual solvents in printed films and ethylene oxide in sterilized material. In a similar manner, called Multiple Headspace Extraction, Kolb et al. [9] using the standard headspace sampling device quantitatively analyzed the volatile compounds in solid samples, such as vinyl chloride monomer and water in a P.V.C. resin and also the residual solvents in food packaging printed films.[10] It has been found that only two extraction steps are usually enough to obtain the final result by extrapolation.[4,8,11] This method seems also attractive at the direct determination of adsorbed organic vapours from larger single charcoal bed tubes. These tubes allow a much greater air volume to be sampled without breakthrough and gives greater sensitivity. To avoid the excessive broadening of chromatographic peaks through the large desorption carrier gas volume required (usually under 30 mL) [12] by strongly retained vapours, the stepwise thermal gas extraction procedure, first used by Ciupe, [1] together with the two-step total peak area evaluation may be the most opportune method for the determination of organic vapours in an industrial work environment. The present method was applied for the toluene, hexane and acetone determination using an original device for heat desorption appropriate for reusable tubes.

EXPERIMENTAL

A volatile compound concentration is estimated by summing the partial areas of all the peaks corresponding to an "i" extraction; applying the two-step total area evaluation, the following formula obtained by Kolb et al. is reproduced:

$$SA_i = A_1^2/A_1 - A_2 \qquad (1)$$

SA_i = total area of compound

A_1 = peak area of the first extraction step

A_2 = second extraction peak area.

The procedure of the two-step gas extraction can be performed since the semilogarithmic plot of the peak areas of compounds versus the number of extraction from charcoal sample tubes represents a straight line, as the experimental data show in Fig. 1.

The Heat Disorber shown in Fig. 2 was constructed at the Institute of Hygiene, Cluj-Napoca according to the original design conceived by one of the authors (R.C.)[5]. It consists of sampling tube connection clamps (1) which are set in a ceramic heating block (2) and a six-way stopcock (4). The temperature of the block can be regulated from the room temperature up to 250°. This device is directly attached to the inlet part of a gas chromatograph Carlo-Erba, Fractovap 2450, with FID.

The sample tube included in this device is 70 mm length and 5 mm I. D. filled with 250 mg MERCK 9624, 0.50—0.75 mm charcoal.

Gas chromatographic analysis was carried out under the following operational conditions:

Column: stainless tube, 5 mm I.D.X 5 m., with 10% SP-1000 on Chromosorb WAW sil., 100—120 mesh stationary phase; temperature of column 130° isothermal and sample desorption temperature 110°.

The analytical and calibration sample preparation data are the following:

— volume of calibration compound into a stoppered 10 L glass bottle: 0.05 mL for n-hexane (H), acetone (A) and toluene (T);

— volume of vapours generated into a calibration bottle: 0.0089 L (H), 0.0162 (A), 0.0114 (T).

— compound concentration (mg/m^3) in the calibration bottle: 3.200 (H), 3900 (A), 4300 (T).

— compound concentration (ppm) of the same calibrated atmosphere: 890 (H), 1620 (A), 1140 (T).

— weight (mg) of sampled compound in 1 L of air: 3.2 (H), 3.9 (A), 4.3(T).

Procedure: The sample tube is set in the heating block maintained at 110° and is allowed to stand for 5 min. Then the stopcock is turned to the injection position illustrated in Fig. 2

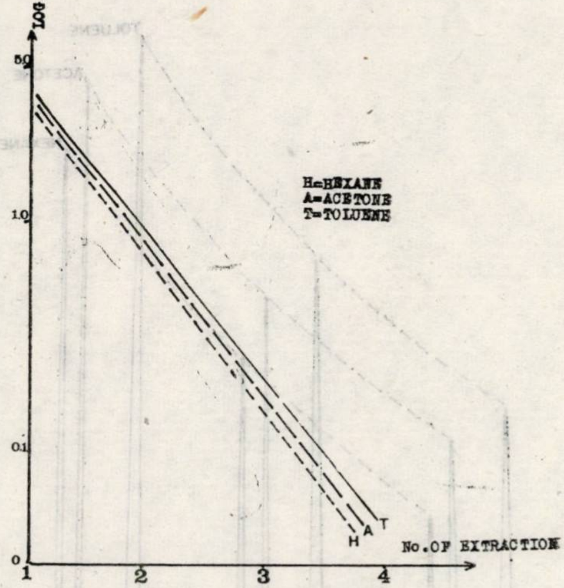

Fig. 1. — Semi-logarithmic plot of the peak areas of hexane, acetone and toluene, versus the number of extractions from the sample tube.

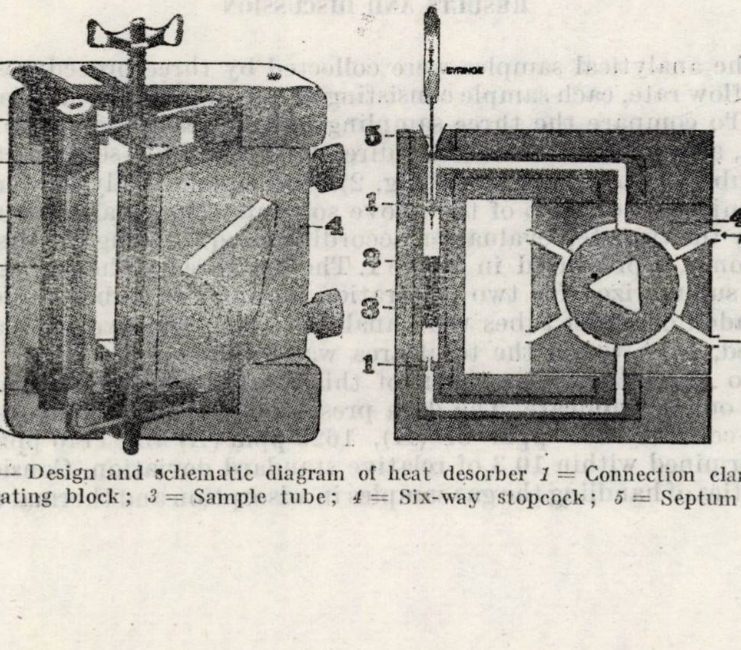

Fig. 2. — Design and schematic diagram of heat desorber *1* = Connection clamps ; *2* = Heating block ; *3* = Sample tube ; *4* = Six-way stopcock ; *5* = Septum cap.

(right) for a fixed period of 3 sec. and again returned to the initial position. The second and the subsequent gas chromatograms of the same sample are obtained by repeating the same procedure mentioned above with a periodic cycle of 10 min. The three chromatograms in Fig. 3 show the exponential decrease of the peak heights from the three successive extractions.

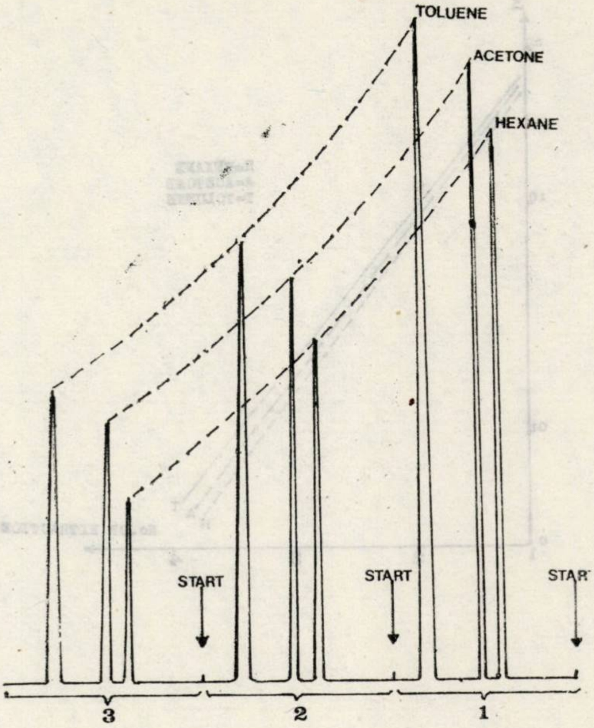

Fig. 3. — Gas chromatographic analysis of a mixed system of hexane, acetone and toluene from sample tube by the stepwise heat gas extraction procedure.

RESULTS AND DISCUSSION

The analytical samples were collected by three procedures with 0.1 L/min. flow rate, each sample consisting of 1 L air from the standard atmosphere. To compare the three sampling procedures an adequate sample of hexane, acetone and toluene was directly injected via septum cap in sampling tube (5 μL of each, 5 in Fig. 2). Subsequent analyses were done by direct injection of 1 μL of the above solvents. The total peak area calculated by the two-step evaluation according to eq. 1, using the first two area values only, is presented in Table 1. The total area of the two-step evaluation is summarized for two calibration methods in Table 2 and Table 3. The loaded charcoal tubes were analysed twice and two peak areas were obtained, from which the total area was calculated by eq. 1.

To evaluate the precision of this method the measurements were carried out in triplicate. The data presented in Table 1 indicate that the sample content 860 ppm of (H), 1620 ppm (A) and 1140 ppm (T), can be determined within 10.3 of relative standard deviation. Considering the difficulties of handling the gas samples in adsorption and thermal desorption

Table 1

Precision data

Total peak area calculation by the two-step evaluation in a hexane, acetone and toluene analysis from the calibrated atmosphere

No of extractions	Sample no.			$\overline{X}$	*SD* (RSD%)
	1	2	3		
Hexane					
1	27562	32970	29553	44291	4562 (10.3)
2	8353	10625	9925		
Total area	39545	48647	44681		
Acetone					
1	41974	43631	42881	63705	568.6 (0.89)
2	14227	14048	13820		
Total area	63495	64350	63273		
Toluene					
1	48831	51570	50075	74760	2844(3.80)
2	15629	17251	16630		
Total area	71816	77492	74974		

Table 2

Calibration data

Total peak area calculation by the two-step evaluation of direct in-tube injected hexane, acetone and toluene

No. of extraction	Sample no.			$\overline{X}$	*SD* (RSD%)
	1	2	3		
Hexane					
1	33528	34927	34029	48275	1186 (2.3)
2	9727	10315	9920		
Total area	47230	49565	48030		
Acetone					
1	45583	45118	45825	67859	141.2 (0.20)
2	14929	15082	14954		
Total area	67782	67773	68022		
Toluene					
1	50974	54498	53547	78121	2088(2.67)
2	16737	17388	16992		
Total area	75893	80033	78437		

Table 3

Accuracy data

Peak area obtained by direct in-gas chromatograph injected equivalent volume of hexane, acetone and toluene

	Sample no.			$\overline{X}$	SD (RSD%)
	1	2	3		
Hexane	44502	44390	44630	44507	120 (0.3)
Acetone	65803	63288	62878	63989	1583(2.5)
Toluene	73759	75925	74730	74804	1085(1.45)

procedure at constant pressure and temperature, the relatively large deviations are rather satisfactory for the determination in this field. The 2.67 highest relative standard deviation obtained by direct in-tube injected solvents as shown in Table 2 indicates opportunities of acceptable handling errors which occur in the adsorption-desorption step. The data presented in Table 3 show the similitudes between the average values obtained by the first two methods utilizing the two-step evaluation and the third direct injection calibration method. Good agreement between the results of these methods indicates the RSD.

The amount of the compounds in the mixture to be analysed with the present method using the active carbon sampling tube, thermal desorption and finally the two-step evaluation of the chromatographic peak area, can be calculated finally from the following equation :

$$C = 1000\ C_e\ A\ n_e\ A_e^{-1} n^{-1}\ (\mathrm{mg/m^3}) \qquad (2)$$

$$C' = C\ 24.45\ G^{-1} \qquad (\mathrm{ppm}) \qquad (3)$$

C = compound concentration in air expressed as mg/m^3 ; C_e = compound of interest concentration in the gas standard ; C' = compound concentration in air expressed as ppm ; A = total area of the sample compound ; A_e = total area of the calibration gas compound ; n_e = volume (liters) of gas standard used for calibration ; n = volume (liters) of sample ; G = molecular weight of compound to be determined.

The advantages offered by the presented method (time saving, handling facilities, the re-use of the sample tubes, a greater sensitivity compared to the NIOSH tube) justify its frequent application to the sampling of some occluded volatiles in the solid matrix as cited above.

REFERENCES

[1] R. Ciupe, *Igiena (București)*, **21**, 425, (1972).

[2] P. W. West, B. Sen and N. A. Gibson, *Anal. Chem.*, **30**, 1390 (1958).

[3] R. Ciupe, E. Fagarasan and L. Pop, *Rev. de Chimie*, București, **28**, 575 (1977).

[4] M. Suzuki, T. Shin and T. Tsugio, *Anal. Chem.*, **42**, 1705 (1970).

[5] R. Ciupe and T. Bud, Romanian Patent No. 71965, 1979.

[6] * * * *Chrompack News*, **10**, 3 (1983).

[7] W. J. Lautenberg, E. V. Kring and J. A. Morello, *Amer. Ind. Hyg. Assoc. J.*, **41**, 737 (1980).

[8] B. Kolb and P. Pospisil, *Chromatographia*, **10**, 705 (1977).

[9] B. Kolb, M. Auer and P. Pospisil, *Applied Chromatography*, **35 E** (1981), Perkin-Elmer.

[10] B. Kolb, P. Pospisil and M. Auer, *J. Chromatogr.*, **204**, 371 (1981).

[11] C. D. Mc. Auliffe, *Chem. Techn.*, 46 (1971).

[12] D. T. Coker and A. M. Mc. Dougall, Paper presented at the Intl. Environment Safety Conference, London 1982.

Revue Roumaine de Chimie, **30**, *11* *12*, 1059—1060 (1985)

COMPTES RENDUS

"Complex Chemistry" (Structure and Bonding, vol. 57), Springer Verlag, Berlin, 1984, 199 pages, 110 DM (hard-cover)

Volume 57 in the well known series "Structure and Bonding" contains four reviews of major interest in the chemistry of coordination compounds.

The first of them (53 pages), written by R. D. Ernst, is devoted to "Structure and Bonding in Metal-Pentadienyl and Related Compounds". Despite the fact that the first transition-metal pentadienyl compound, $Fe(C_5H_7)(CO)_3{}^+ClO_4{}^-$, was reported in 1962, it is only now clear that pentadienyl ligands offer substantial promise for the future of organo-metallic chemistry. The pentadienyl ligand (C_5H_7) as well as its various methylated derivatives have similarities to both the allyl and cyclopentadienyl ligands and it was demonstrated that the corresponding complexes possess not only thermal stability but also catalytic activity. Pariticular emphasis is given to the bis-(pentadienyl)-metal compounds ("open metallocenes"). The author presents a perspective view of the main physical, structural and chemical aspects of pentadienyl and metal-pentadienyl chemistry, including electronic and energetic considerations, as well as experimental and theoretical studies of pentadienyl anions or radicals and of transition-metal pentadienyl compounds. The literature is surveyed up-to-date (271 references).

The second review, entitled "A New Look at the Stereochemistry and Electronic Properties of Complexes of the Copper (II) Ion", is written by B. J .Hathaway, a well known name for the research workers in this field. It is typical for the copper (II) coordination compounds to illustrate a variety of stereochemical features, many of them being characterized by distorsions from regular octahedral, tetrahedral or square-planar geometries. The main reason for this behaviour arises from the d^9 electron configuration and the operation of the Jahn-Teller effect and its secondary consequences (the plasticity effect, fluxional copper (II) stereochemistry, cooperative Jahn-Teller effect, second order Jahn-Teller effects). This article is an attempt to establish a relationship between structural data and the electronic properties, *i.e.* electronic and *e.s.r.* spectra. The author presents also some electronic criteria of copper (II) stereochemistry, useful for the study of new copper (II) coordination compounds. The article is a valuable source of up-to-date information in this field and the literature cited includes many original papers of the author.

"Calculation of the Jahn-Teller Coupling Constants for d* Systems in Octahedral Symmetry via the Angular Overlap Model" (26 pages), written by K. D. Warren, is the third review. C. K. Jørgensen and C.E. Schäffer developed in 1965 the so-called Angular Overlap Model (AOM), describing the chemical bonding in complexes. Since this date, the AOM was applied to the explanation of many properties of coordination compounds, *e.g.* electronic spectra, magnetic properties, stereochemistry and stability. In this paper, the AOM is applied to the calculation of the Jahn-Teller coupling constants for all possible ground states of ML_6 (d*) systems in O_h symmetry, using both weak and strong field approaches, including the effect of spin-orbit coupling. The quenching of the Jan-Teller activity due to spin-orbit coupling is also evaluated. This article is useful for chemists interested in the electronic structure of coordination compounds.

The last article (44 pages), entitled "The Composition, Structure and Hydrogen Bonding of the β-Diketones" (author: J. Emsley) is of considerable interest to organic, inorganic and physical chemists. The β-dicarbonyl compounds exhibit slow proton transfer but strong intramolecular hydrogen bonding, providing the best known examples of keto-enol tautomerism. By means of theoretical calculations and using the results of experimental techniques (^{1}H-NMR spectra, talking into account the substitution effects and the proton — deuterium NMR isotopic shifts, X — ray and neutron diffraction data, microwave spectroscopy, vibrational spectra) the author shows that the hydrogen bonding of the *cis* enol tautomers of β-diketones is strong ($>$ 50 kJ/mol), short (245—255 pm), centered and non linear. The proton of the O—H...O bond is situated in a double minimum potential energy, well separated by an energy barrier that is not higher than its ground state vibrational energy level; through this barrier the proton tunnels easily if symmetry requirements are met. The review quotes 156 references.

All four reviews are valuable sources for up-to-date information on the subjects which are discussed. They are highly readable; the figures and all the formulas are drawn with care.

Volume 57, like others in the series "Structure and Bonding", is characterized by an excellent printing.

The volume contains an author and a subject index.

Marius Andruh

"Food Industries and the Environment" International Symposium — Budapest — Hungary — 9—11 September 1982, — Edited by J. Holló — Akadémiai Kiadó — Budapest — 1984.

Published in the series "Developments in Food Science", the volume "Food Industries and the Environment" benefits from worthy contribution of the well-known Hungarian scientist, prof. dr. doc. J. Holló, member of the Hungarian Academy of Sciences, manager of the Central Institute for Chemical Research from Budapest.

Organised by the Hungarian Scientific Society for Food Industry under the auspices of the Committee of Technical Chemistry of the Hungarian Academy of Sciences, the Symposiom whose works are the subject-matter of this volume, comprises papers of 64 contributors from 20 countries. Though structured into apparently different chapters, the volume represents a perfect unity, offering to the readers an insight into one of the most urgent problems which faces mankind; the relationship between man and his environmental surroundings. The main purpose of the volume is to achieve, in the conditions of a tremendous development of agriculture and food industry, a healthier view, contributing to the implementation of the most efficient methods for the maintaining of ecological equilibrium. Underlining the fact that "the use of agressive techniques aimed to the conquest and subduing of Nature has reversed against mankind", Prof. J. Holló insists upon the necessity of using "advanced scientific methods aimed to the compensation of this destructive effort".

As a reponse to this major imperative, the volume "Food Industries and the Environment" represents a top contribution to the technical literature of the field. The 3 plenary conferences; "Opening Address" by J. Holló, "Food Industry and Environmental Protection in Hungary" by I. Kovács, and "Resources and Environmental Considerations in the Agro and Food Industrry" by Nay-Thun, are followed by highly specialized contribtuions (60 papers) organised into; a. General Topics; b. Canning Industry; c. Dairy Industry; d. Meat Industry; e. Other Indutrial Branches and f. Noise-Stench. The first chapter deals with modern processes involved in effluent reduction, membrane technology, electroflotation, anaerobic, aerobic and enzyme treatments of by-products. These processes are likely to show premises for the achievement of highly integrated technologies without harmful consequences upon natural environment, when used together with classical systems for environment conservancy. For the canning industry, 7 papers analyse aspects concerning a higher use of raw materials, energy production from solid wastes and the highgrading of by-products, mainly for animal feeding uses. As in the dairy industry, whey is the most important by-product, its use for specialty products, single-cell protein, ethyl alcohol, protein concentrates, processing beverages, desserts and lactic acid manufacture are contributing to the lowering of dairy effluents pollution and to the simultaneous obtainment of useful products. These aspects are analysed in 8 papers. Owing to the complexity of the chemical composition of wastes in the meat industry, the recovery and utilisation of valuable components from animal wastes and industrial wastewaters are to be considered together with complex treatment methods for effluents containing animal proteins and fats. 18 papers are devoted to such aspects. For other branches of food industry, the treatment of potato fruit juice and effluents from starch industry and sugar works, the use of brewer's dried grains as animal feed, and the development of a waste-poor alcohol production technology are thoroughly analysed in 7 papers. Other aspects, such as the reduction of air pollution and of noise — which accompanies the advance of mecanization — and the microbiological environment control, are also dealt with.

Continuing the 80 years tradition of the Commission Internationale des Industries Agricoles et Alimentaires, this symposium covers one of the most urgent problems facing man today — the relationship between industry and environment — underlining the tasks of researchers and scientists. Its works shall become a vade mecum for industrial activity, underlining the usefulness of the biotechnological approach to the problem of creating a new "metabolism" between mankind and nature.

Radu Giurcă

Revue Roumaine de Chimie, **30**, *11–12*, 1061–1078 (1985)

INDEX DES AUTEURS

A

ABD-ALLA A. MOHAMED and MOHAMED T. ISMAIL, AHMED M. EL-KHAWAGA, Studies on substituted diarylidenecycloheptanones . . . 343
ABDEDDAIM K., voir CHELGHOUM C. . . . 565
ABD EL-MOATY, voir HASSAN M.A. . . . 245
ABD EL-GAWAD I. I., A. M. KHALIL, O. M. O. HABIB and H. A. ETMAN, Synthesis and reaction of some new cyclic β-keto-anilides. Part 1. . . . 499
ABDEL-HALIM F. M., voir FAYEZ Y. KHALIL . . . 571
ABDEL RAHMAN A. E. and AMAL S. YANNI, Synthesis of some new indophenazinylpyrazoline and isoxazoline derivatives . . . 401
ABDEL-RASSOUL A. A. voir EL-NAGGAR H. A. . . . 179
ABDEL-WAHAB M. voir ABOEL MAGED A. . . . 41
ABDEL-WAHAB A. voir AHMED M. EL-KHAWAGA . . . 599
ABOEL-MAGD A. voir AHMED M. EL-KHAWAGA . . . 599
ABOEL MAGED A. and ABDEL-WAHAB MOHAMED, S. K. YOUSSEF, GUNTER HELMCHEN, Mass spectra of diastereomeric substituted secondary valer- and butyramides . . . 41
ABU ZEID N. R. voir DOSS S. H. . . . 405
AGARWAL R. and P. BAHADUR, Synthesis of diazoketones from β-benzoyl acrylylchloride and diazoalkanes . . . 803
AHMED M. EL-KHAWAGA and ABOEL-MAGD A., ABDEL-WAHAB, MAHER F. ELZOHRY, ALI A. KHALAF, Modern Friedel-Crafts chemistry. XII. On the carbonyl retardation of cyclialkylation of aryl alkenyl ketones under Friedel-Crafts conditions . . . 599
ALBA A. and ARAMENDIA M. A., BORAU V., JIMENEZ C., MARINAS J. M., Acid-base and redox characteristics of Pd catalysts obtained by ion exchange . . . 467
ALY M. M., voir FAHMY A. M. . . . 749
ANCUTA D. voir BERDAN I. . . . 1039
ANDREI C. and I. HOGEA, V. DOBRESCU, Photodegradation and photostabilization of the ethylene-vinyl acetate copolymers. I. Aspects of the mechanism of photodegradation reactions . . . 865
ANDRONESCU E. voir TEOREANU I. . . . 647
ANDRUH M., voir LEPĂDATU C. . . . 217
ANDRUH M., voir BREZEANU M. . . . 229
ANWAR N., voir OMARA M. A. . . . 461
APĂTEANU LILIANA, voir BRÂNZOI V. . . . 199
APĂTEANU LILIANA, voir STERNBERG S. . . . 105
APĂTEANU L., voir STERNBERG S. . . . 955
ARIAS-PEREZ M. S. and C. FERNANDEZ-SANCHEZ, J. M. MARINAS, Esterification of monosubstituted benzoic acid with "kearby" type aluminium orthophosphates as catalysts (in Spanish) . . . 617
ARRANZ J. C. voir CABEZAS J. L. . . . 903
ARAMENDIA M. A. voir ALBA A. . . . 467
ARORA R. K. voir GUPTA D. R. . . . 37
ASHOK KUMAR and B. K. PURI, A. L. J. RAO, Thermodynamics of complex formation : Zinc-ε-caprolactam system . . . 49
ATTIA I. A. and E. A. SOLIMAN, Synthesis and some reactions of acetyl-cyclohexenone derivatives . . . 267
AVRAM MARGARETA, voir MĂNOIU D. . . . 223
AVRAM MARGARETA, voir DINULESCU ILIE G. . . . 585
AVRAM MARGARETA voir ŞTEFAN NICOLETA . . . 589
AVRAM MARGARETA voir ŞTEFAN NICOLETA . . . 791

B

BACALOGLU R., voir GLATT H.-H. 125

BADEA F. and F. IORDACHE, AURELIA MEGHEA, A. T. BALABAN, ROXANA MARINESCU, ANA-MARIA GHIVIRIGĂ, Carbanions and free radicals derived from 1,2-diphenylpyrazolidine-3,5-diones. I. Trapping of the free radical formed in phenylbutazone oxidation 189

BADR M. Z. A., voir FAHMY A. M. 749

BALABAN A. T., voir BADEA F. 189

BALABAN ALEXANDRU T. and IOSIF SCHIKETANZ, MIRCEA D. GHEORGHIU and ANA SCHIKETANZ, Aminoketone and oxazole synthesis. IX. 2,2-(*p*-Phenylene)-bis-(5-aryloxazoles) and 2,2'-(1,4-naphthalenediyl)-bis-(5-aryloxozoles) *via* acylaminoacylation of aromatic hydrocarbons 977

BALABAN ALEXANDRU, T. voir SCHIKETANZ IOSIF 975

BALABAN A. T., voir SIMON Z. 985

BALABAN T. S., voir SIMON Z. 985

BALABAN T. S., voir TOMESCU I. 1005

BAHADUR P. voir AGARWAL R. 803

BÂLDEA I. and V. FĂRCĂŞAN, ILEANA OLTEANU, Kinetics of the Jacobson reaction 385

BANCIU M. and I. POGANY, DANA MOSORA, PATRICIA RUSU, RODICA STĂNCIULESCU, M. DEZSÖ, Synthesis of 9,10,19,20-tetrahydro-dibenzo/*a*, *c*/-phenanthro/*g*/cyclodecene and 9,10,19,20-tetrahydro-tetrabenzo/*a*,*c*,*g*,*i*/cyclodecene by sulphone pyrolysis 703

BANCIU M., voir SARAMET IOANA 559

BANCIU M. voir VLAD RODICA 1001

BANCIU ILEANA and E. TĂRNĂUCEANU, V. DOBRE, I. NICULESCU-DUVĂZ, Potential anticancer agents. XXV. Aliphatic and cycloaliphatic N-nitrosoureas and N-nitrosourethanes 317

BARRY MAMADOU FOULA, voir H.—H. GLATT 125

BERDAN I., D. ANCUŢA and I. SANDU, Complex compounds of T1(III) with *n*-donor ligands. Study on the system T1(III)-2,2 azopyridine (in French) 1031

BERMEJO M. R., voir MÁRTINEZ M. C. 333

BERRUETA J. voir CABEZAS J. L. 903

BERTY HÉCTOR, voir CAO ROBERTO 639

BÎLBĂ N. voir MIHĂILĂ GH. 1019

BODOR A. and A. GERGELY, R. SCHWARTZ, A. JUHASZ, P. COLTEA, D. BREAZU, The synthesis of 19-hydroxysteroids 743

BORAU V., voir ALBA A. 467

BORDEIANU R., voir CEAUŞESCU ELENA 375

BOULOS L. S. and A. EL-KATEB, The reaction of fluorenylidene-triphenyl-phosphoranes and -arsinone with certain dicarbonyl compounds 1005

BOURCEANU G. and E. GRUNICHIEVICI, M. BOURCEANU, Increase of the free surface energy of terephthalate polyethylene sheets by activation in high frequency plasma (in French) 859

BOURCEANU M. voir BOURCEANU G. 859

BOZEŞANU MELANIA and N. I. IONESCU, Self inhibition of the homogeneous pyrolysis of n-heptane 963

BREAZU D. voir BODOR A. 743

BRÎNZAN GH., voir I. GĂNESCU 309

BRÂNZOI V., voir STERNBERG S. 105

BRÂNZOI V. and S. STERNBERG, LILIANA APĂTEANU, Electrode processes in $Pb/H_2SO_4 + Na_2SO_4$ system 199

BRÂNZOI V., voir STERNBERG S. 955

BREZEANU MARIA and M. ANDRUH, LUMINIŢA PATRON, V. T. POPA, Coordination compounds formation within the $MCl_2-SnCl_2-\alpha,\alpha'$-bipyridine ($M = Co$, Ni) system 229

BRUMĂ MARIA and ION SAVA, Ordered polyesterimides 239

BUDIU T., voir VĂŢULESCU RODICA 823

BUDIU T., voir VĂŢULESCU RODICA 831

BUDIU T., voir VĂŢULESCU RODICA 1025

BUGNARIU STELUŢA voir CIUPE ROMANO 1052

BUZDUGAN E., voir CEAUŞESCU ELENA 375

C

CABEZAS J. L. and C. ARRANZ, J. BERRUETA, Binary vapor-liquid equilibria of benzene-alcohol systems . . . 903
CACOVEANU LUCIA., voir TEOREANU I. . . . 647
CALISTRU C., voir TALABA M. . . . 491
CALU N., voir I. GĂNESCU . . . 309
CĂLUȘARU A., Structural studies on the aquo-ammino-di-2-mercapto-benzothiazole cobalt complex . . . 1039
CAMPELO J. M. and A. GARCIA, D. LUNA, J. M. MARINAS, Liquid phase catalytic hydrogenation on $AlPO_4$-supported nickel catalysts. II. Hydrogenation of styrene and α-methyl-styrene . . . 427
CANTU L., voir CEA OLIVARES R. . . . 525
CAO ROBERTO and GILBERTO VICIEDO, HÉCTOR BERTY, Thiosemicarbazone complexes of $3d^{6-10}$ metals. I. Acetophenone and o-aminobenzaldehyde thioșemicarbazone . . . 639
CEA OLIVARES R. and I. CANTU, Synthesis of the first alkylated spirophosphazenes (in Spanish) . . . 525
CEAUȘESCU ELENA and R. BORDEIANU, D. S. VASILESCU, I. MANAFU, IRINA CERCHEZ, P. GHIOCA, R. STANCU, E. BUZDUGAN, Characterization of poly (butadiene-b-styrene) by specific refractive index increment measurements . . . 375
CERCHEZ IRINA., voir CEAUȘESCU ELENA . . . 375
CHANDRA G., voir HINGORANI H. . . . 725
CHELARU., C. voir SIMIONESCU CRISTOFOR . . . 441
CHELGHOUM C. and Y. HADDAD, K. ABDEDDAIM, M. H. GHERMOUCHE, Retention indices and molecular structure of isodecanes (in French) . . . 565
CHIPER STELUȚA, voir VLĂDESCU L. . . . 1047
CHIRALEU F., voir DINULESCU I. G. . . . 585
CHIRALEU FILIP, voir ȘTEFAN NICOLETA . . . 791
CHIRIAC C. I., A convenient one-step conversion of aromatic aldehydes into nitriles . . . 353
CHIRIAC C. I., Esters from N-acylphthalimides and phenols . . . 753
CHIRIAC C. I., Synthesis of amides by a new direct condensation reaction . . . 799
CIOMARTAN DAN, voir VICTOR DAVID . . . 777
CIUBOTARIU D., voir SIMON Z. . . . 985
CIUPE ROMANO and SZANTO CSABA, STELUȚA BUGNARIU, Simultaneous determination of atmospheric n-hexane, toluene and acetone with activated charcoal tubes using the two-step thermal gas extraction procedure . . . 1053
CIUREANU M. and M. HILLEBRAND, V. EM. SAHINI, E. VOLANSCHI, U.H.E. spin density calculations on substituted nitroaromatic anion radicals . . . 97
COJOCARU M., voir ONISCU C. . . . 807
COLLERA O., voir GARCIA F. . . . 349
COLTEA P., voir BODOR A. . . . 743
CONSTANTINESCU M., voir GHIRVU C. . . . 329
CONȚESCU ADRIANA, voir SPACU P. . . . 659
CONȚESCU ADRIANA, voir SPACU P. . . . 837
CORLĂTEANU E., voir LĂZĂRESCU V. . . . 783
COSTEANU G., voir LANDAUER ORTANSA . . . 651
C. CRISTESCU, *as*-triazine derivatives with potential therapeutic action. XIX. Synthesis of 5-(substituted-benzyl) thio-6-azauridines . . . 117
CRISTESCU C. and SILVIA SITARU, *as*-Triazine derivatives with potential therapeutic action. XX. Cyanoethylation of 5-substituted-6-azauracil and 4-thioxo-5-substituted-azauracil . . . 233
CRUSOS AMALIA, Copolyamides. I. The influence of composition on the physico-chemical properties . . . 391
CRUZ R., voir GARCIA F. . . . 349
CSABO SZANTO, voir CIUPE ROMANO . . . 1053
CSUNDERLIK CAROL, voir GLATT H.-H. . . . 125
CUETO G. LOPÉZ and A. ALONSO MATEOS, [Coulometric study at controlled potential of the anionic oxidation of the binuclear cyanide complex of Mn(III). Part I. Oxidation at +0.2 volts (*vs*. SCE); kinetic current and parallel reaction (in Spanish) . . . 917

D

DAŞOVEANU CORNELIA, voir LĂZĂRESCU VALENTINA 933
DAVID VICTOR and DAN CIOMARTAN, A method for computing the information entropy of the quantitative analytical data 777
DEZSÖ M. voir BANCIU M. 703
DINULESCU ILIE G., voir MĂNOIU DUMITRU 223
DINULESCU I. G. and S. STAICU, ANGELA DUMITRIU, AURELIA GHENCIULESCU, F. CHIRALEU, MARGARETA AVRAM, Reaction of acetylenes with transition metals. XI. Reaction of 1-chloro-1,2-diphenyl-3-alkyl-τ-allylpalladium complexes with alkenes 585
DINULESCU ILIE G., voir ŞTEFAN NICOLETA 589
DINULESCU ILIE G., voir ŞTEFAN NICOLETA 791
DOBRE V., voir BARACU ILEANA 317
DOBRESCU V., voir ANDREI C. 865
D. DOCA and E. SEGAL, Dehydrogenation kinetics of lower aliphatic alcohols in copper catalysts. I. Preparation, stabilization and catalytic activity of fine copper powders 949
DOSS S. H. and N. R. ABU ZEID, Bromination of unsaturated sultams and sultones 405
DRĂGAN GH. and C. OPREA, Thermomechanical study of amorphous modifications in polyester fibers induced by isothermal annealing 447
DRĂGĂNOIU MIHAELA, voir STERNBERG S. 209
DRĂGUŢ M., voir VÎLCU R. 289
DRANGA D., voir MIHĂILĂ GH. 1019
DUMITRIU ANGELA, voir DINULESCU I. G. 585

E

EL-BARBARY A. A., Some chemical aspects of 5-aryl-1,3,4-oxadiazoles 257
EL-BARBARY A. A., voir OMARA M. A. 461
EL-BATOUTI M., voir FAYEZ Y. KHALIL 571
EL-BORAI M., voir HASSAN M. A. 245
EL—HASHASH M. A., voir MOHAMED M. N. 419
EL-KADY M., voir HASSAN M. A. 245
EL-KATEB A., voir BOULOS L. S. 1015
EL-KHAWAGA M. AHMED, voir ABD-ALLA M. A. 343
ELKONI S., voir OMAR M. A. 461
EL-NAGGAR H. A., A. RAMADAN and A. A. ABDEL-RASSOUL, Synergistic and antagonistic extraction of protactinum (V) by bis(2-ethyl hexyl) phosphoric acid and tributyl phosphate mixture 179
ELZOHRY F. MAHER, voir AHMED M. EL-KHAWAGA 599
EL-SHAFEI A. K., A.—B. A. G. GHATTAS and F. A. GAD, Synthesis of some new N-amino-2-pyridone derivatives 817
ETMAN H. A., voir ABD EL-GAWAD I. L. 499

F

FĂRCĂŞAN V., voir BÂLDEA I. 385
FAHMY A. M. and S. A. MAHGOUB., M. M. ALY, M. Z. A. BADR, The photo formylation of phenols 749
FAYEZ Y. KHALIL, and M. T. HANNA, F. M. ABDEL-HALIM, M. EL-BATOUTI, Kinetic study of the alkaline decomposition of 3-bromopropyl-triphenylphosphonium bromide in DMSO—H_2O mixtures 571
FERNANDEZ-SANCHEZ C., voir ARIAS-PEREZ M. S. 617
FILIP PETRU, voir ŞTEFAN NICOLETA 589
FILIP PETRU, voir ŞTEFAN NICOLETA 791
FULEA ADRIAN O., About the calculation of the I. R. and Raman active fundamentals of polymers 357
FULEA ADRIAN O., Corrigenda "On a correction technique for fractionation data and its application to the fractionation of polyethylene terephthalate" 371

G

GAD F. A., voir EL-SHAFEI A. K. 817
GĂINAR I., voir VÎLCU R. 381
GĂNESCU I. and N. CALU, GH. BRÎNZAN, C. VÁRHELYI, New substitution products of $K_3[Cr(NCS)]$ with chinaldine (in German) 309

GARCIA A. voir CAMPELO J. M. 427

GARCIA F. and O. COLLERA, J. L. SÁNCHEZ, R. CRUZ, R. SAUCEDO, M. C. PEREZAMADOR, Carbon-13 NMR spectra of some 16—17-glycol diterpenes 349

GAYOSO M., voir MARTINEZ M. C. 333

GEORGESCU E. I. and FLORENTINA GEORGESCU, M. GHEORGHIU, E. G. GEORGESCU, MAGDA PETROVANU, Dipolar derivatives in the quinoxaline series. IV. (3+2) Dipolar cycloaddition reactions of some quinazolium-3-(p-R-benzoyl)-methylides with activated acetylenes (in French) 611

GEORGESCU FLORENTINA, voir GEORGESCU E. I. 611

GEORGESCU E. G., voir GEORGESCU E. I. 611

GERGELYI A., voir BODOR A. 743

GHATTAS A.-B. A. G., voir EL-SHAFEI A. K. 817

GHENCIULESCU AURELIA, voir DINULESCU I. G. 585

GHEORGHIU M. D., voir GEORGESCU E. I. 611

GHEORGHIU MIRECA D., voir SCHIKETANZ IOSIF 975

GHEORGHIU MIRECA D., voir A. T. BALABAN 977

GHIRVU C. and M. CONSTANTINESCU, GH. IONESCU, I. M. POPA, Considerations on the electronic spectra and barrier to internal rotation of α- and β-naphthalenesulphonic acids 329

GHIOCA P., voir CEAUŞESCU ELENA 375

GLATT HANS-HORST and MAMADOU FOULA BARRY, CAROL CSUNDERLIK, RADU BACALOGLU, M. MEDELEANU, MARIA LANTOS, Imines of aminoazoles. I. Synthesis and characterization of some imines of 2-aminobenzoimidazole (in German) 125

GHIVIRIGA ANA-MARIA, voir BADEA F. 189

GOŞA V., voir OANCEA D. 767

GOYAL H. C., voir HINGORANI H. 725

GRAMATICU MIHAI ,voir GUTT GEORG 453

GRUNICHIEVICI E., voir BOURCEANU G. 859

GUERMOUCHE M. H., voir CHELGHOUM C. 565

GUPTA D. R. and R. R. ARORA, Synthesis of some biologically active N'-picolinoyl-4-(substituted azo)-alkyl/aryl pyrazoles 37

GUPTA S. P., voir MITTAL M. 511

GUPTA C. L., voir MITAL R. L. 757

GUPTA S. B., voir MITAL R. L. 757

GUTT GEORG and ŞTEFAN IVAŞCAN, SONIA GUTT, M. GRAMATICU, On the material transport optimization in the electrodeposition of nickel (in German) 453

GUTT SONIA, voir GUTT GEORG 453

GUŢUL MELANIA, voir TEODORESCU GRIGORE 339

H

HABIB O. M. O. voir ABD EL-GAWAD I. I. 499

HADDAD Y., voir CHELGHOUM C. 565

HANMANTGAD S. S. and M. V. KULKARNI, V. D. PATIL, Synthesis of some biomimetic 4-substituted coumarins 735

HANNA M. T., voir FAYEZ Y. KHALIL 571

HASSAN M. A. and M. EL-KADY, M. EL-BORAI, A. A. ABD EL-MOATY, Base catalyzed additions of dehydroacetic acid and its 3-cinnamoyl derivatives 245

HAVLIK IULIA, T. SIMONESCU and I. HAVLIK, New pyrazolone compounds of bis-methylaminoantipyryl-propane and bis-methylaminoantipyryl-butane 55

HAVLIK I., voir HAVLIK IULIA 55

HELMCHEN GUNTER, voir ABOEL MAGED A. 41

HILLEBRAND MIHAELA, voir CIUREANU M. 97

HERŞCOVICI J., voir LĂZĂRESCU VALENTINA 783

HINGORANI H. and H. C. GOYAL, G. CHANDRA, S. N. SRIVASTAVA, Kinetics of Os(VIII) catalysed chloramine-T oxidation of glycollic acid and lactic acid in alkaline media 725

HOGEA I., voir ANDREI C. 865

HOROBA E., voir ONISCU C. 807

I

IOAN SILVIA, voir SIMIONESCU CR. I. 441

IONECI ION, voir TĂNASE I. 667

IONECI I., voir TĂNASE I. 679

IONECI I., voir TĂNASE I. 851

IONESCU D., voir MEGHEA AURELIA 297

IONESCU GH., voir GHIRVU C. 329

IONESCU GH. voir POPA I.M. 435

IONESCU N. I., voir OANCEA D. 767

IONESCU N. I., voir BOZEŞANU MELANIA 963

IORDACHE F., voir BADEA F. 189

IOVU M., VALERIA RĂDULESCU and M. IQBAL, Decomposition of halomethylethers by secondary amines (in French) 713

IQBAL M., voir IOVU M. 713

ISAC DELIA, M. MRACEC and Z. SIMON, Thermal and photochemical stability of diazoderivatives 473

ISMAIL T. MOHAMED, voir ABD ALLA A.M. 343

ISTUDOR ANCA, voir MOKHALLALATI A.O. 31

IULIAN OLGA, voir LANDAUER ORTANSA 651

IULIAN OLGA, voir LANDAUER ORTANSA 883

IVAŞCAN STEFAN, voir GUTT GEORG 453

J

JUHASZ A., voir BODOR A. 743

JIMENEZ C., voir ALBA A. 467

K

KABIL M.A. and M.A. MOSTAFA, Elimination of the interfering effects of some organic compounds in the determination of rhodium by atomic absorption spectrophotometry 631

KADI HOCINE and D.P. LAZĂR, Identification of aromatic hydrocarbons in different petroleum fractions. II. Component identification by HPLC (in French) 81

KADI HOCINE and D.P. LAZĂR, Identification d'hydrocarbures aromatiques de quelques fractions pétrolières. III. Méthode n.d.PA 365

KEEMTI LAL and SITA RANI MALHOTRA, Magnetic and spectral studies on copper (II), nickel (II), cobalt (II), iron (III) and manganese (II) complexes of 3-bromo-2-hydroxy-5-methyl acetophenone hydrazone 395

KEEMTI LAL, voir MITTAL M. 511

KEREK FR., voir VLĂDEA R. 157

KHALAF ALI ALI and ROYSTON M. ROBERTS, Modern Friedel-Crafts chemistry. K. Rearrangements accompanying Friedel-Crafts alkylation of benzene with isometric pentanols and pentenes 507

KHALAF A. ALI, voir EL-KHAWAGA A.M. 599

KHALIL A.M., voir EL-GAWAD ABD I.I. 499

KHALIL MOHAMED MAGDI, voir LUCA CONSTANTIN 843

KUDESIA V.P., voir KUMARI RAMESH 141

KULKARNI M.V., voir HANMANTGAD S. S. 735

KUMARI RAMESH and A.D. TANEJA, V.P. KUDESIA, Studies of enolization of some substituted acetoacetarylamides at different temperatures and concentrations 14

L

LANDAUER ORTANSA and CORNELIA MATEESCU, OLGA IULIAN, G. COSTEANU, Physico-chemical study of tetrahydrofuran-methanol and dioxane-methanol systems (in French) 651

LANDAUER ORTANSA and CORNELIA MATEESCU, OLGA IULIAN, Influence of solvent on the reaction rate. Alkaline hydrolysis of n-butyl acetate, propionate, butyrate in the water-monoethylenglycol mixed solvent (in French) 883

LANTOS M., voir GLATT H.-H., 125

LAZĂR D. P., voir KADI HOCINE 81

LAZĂR D.P., voir KADI HOCINE 365

LĂZĂRESCU VALENTINA, and M. VASS, J. HERȘCOVICI, E. CORLĂTEANU, Potentiodynamic behaviour of raney-copper in potassium hydroxide solutions 783

LĂZĂRESCU VALENTINA and M. VASS, O. RADOVICI, CORNELIA DAȘOVEANU, MAGDALENA STANCIU, M. TOLAN, Electrochemical investigation of the oxygen interaction with silver catalysts 933

LEANCĂ MONICA, voir SIMIONESCU CR. I. 441

LEPĂDATU C. I., Global similarity and shape recognition in experimental chemistry 3

LEPĂDATU C. I., The concept of electronegativity in *Slater*'s theory of the atom . . . 111

LEPĂDATU C. I. and MARIUS ANDRUH, Factorisation of orbital energies in transition — metal complexes. I. Factorisation of the overlap integrals 217

LINGVAY I., voir STERNBERG S. 7

LIPTAY GY., voir VÁRHELYI CS. 695

LUCA C., voir MOKHALLALATI A.O. 31

LUCA CONSTANTIN, voir TĂNASE I. 667

LUCA CONSTANTIN, voir TĂNASE I. 679

LUCA CONSTANTIN and MOHAMED MAGDI KHALIL, Extraction equilibria of some complex combinations with macrocyclic ligands 843

LUCA C., voir TĂNASE I. 851

LUCA CORNELIA, voir MIHĂILA GH 1019

LUCINESCU E., voir VÎLCU R. 289

LUNA D., voir CAMPELO J.M. 427

M

MACOVEANU M., voir ONISCU C.. 807

MAHGOUB S.A., voir FAHMY A.M. 749

MAHMOUD F. ABD EL-ALLE, voir SALAH M. ABD EL-KADER 61

MAIER OVIDIU, voir TĂMĂȘAN IULIANA 1005

MALHOTRA S.R., voir MITTAL M. 511

MALHOTRA S.R., voir KEEMTI LAL 395

MANAFU I., voir CEAUȘESCU ELENA 375

MANDRAVEL CRISTINA voir TEODORESCU GRIGORE 339

MĂNOIU DUMITRU and MARIA MĂNOIU, ILIE G. DINULESCU, MARGARET AVRAM, Friedel-Crafts acylation of alkynes V. Reaction of alkynes with aroyl chlorides in the presence of silver perchlorate 223

MĂNOIU MARIA, voir MĂNOIU D. 223

MANOVICIU I., voir MUNTEANU D. 23

MANOVICIU VIRGINIA, voir MUNTEANU D. 23

MARCU GH. voir VĂȚULESCU RODICA 823

MARCU GH., voir VĂȚULESCU RODICA 831

MARCU GH., voir VĂȚULESCU R. 1025

MARINAS J.M., voir CAMPELO J.M. 427

MARINAS J.M., voir ALBA A. 467

MARINAS J.M., voir ARIAS PEREZ M.S. 617

MARINESCU ROXANA, voir BADEA F. 189

MARTINEZ-ALCAZAR M.P., voir SANTOS S. ESTEBAN 593

MARTINEZ M.C. and M.R. BERMEJO, M. GAYOSO, Dipolar study of titanium octahedral compounds with TMDTO and TEDTO (in Spanish) 333

MATEESCU CORNELIA, voir LANDAUER ORTANSA 651

MATEOS A. ALONSO, voir CUETO G. LÓPEZ 917

MATEESCU CORNELIA, voir LANDAUER ORTANSA 883

MATEESCU A., voir STERNBERG S. 955

MEDELEANU MIHAI, voir GLATT H.-H. 125

MEGHEA AURELIA, voir BADEA F. 189

MEGHEA AURELIA and FLORICA ZĂLARU, D. IONESCU, Some new copper (II) complex compounds with nitroimidazole derivatives 297

MIHĂILA GH. and C. LUCA, DOINA DRANGA, N. BÎLBĂ, Study of cyclopentene hydration 1019

MISSIR A., voir VOLANSCHI ELENA 483

MITTAL M. and S. R. MALHOTRA, KEEMTI LAL, S. P. GUPTA, Rare earth chelates of disubstituted 2-hydroxy-acetophenones 511

MITAL R.L., VINEETA TANEJA, C.L. GUPTA and S.B. GUPTA, Studies in the synthesis of some new polynuclear heterocycles: 6-chloro, 8,13-dihydro-8,13-o-benzononaphtho[2,3-a]phenothiazin-7(H) ones 757

MOHAMED M. M. and M. A. EL-HASHASH, M. A. SAYED, A. A. SHEHATA, Reaction of some 2(1H)-pyridones synthesized from 3,4-methylene-dioxybenzylidene- and 4-nitrobenzylidene-p-isopropylacetophenone 419

MOHAMADY A. FAKHR EL-DEIN, voir SALAH M. ABD EL-KADER 61

MOISESCU LIANA, voir STERNBERG S. 7

MOKHALLALATI A. O. and ANCA ISTUDOR, D. VÎRTOSU, C. LUCA, Potentiometric gas sensor for carbon dioxide 31

MOSORA DANA, voir BANCIU M. 703

MOSTAFA M.A., voir KABIL M.A. 631

MRACEC M., voir ISAC DELIA 473

MRACEC M. and MARIA MRACEC, Z. SIMON, Optimal parameters in the HMO technique. II. An optimal set of parameters for the hydroxylic phenol function 531

MRACEC MARIA, voir MRACEC M. 531

MUNTEAN MARCELA, voir TEOREANU ION 575

MUNTEANU D. and VIRGINIA MANOVICIU, I. MANOVICIU, Separation of oligo(1,2-propylene terephthalate)s by gradient elution high performance liquid chromatography 23

MUŞOIU DIANA, voir VOLANSCHI E. 483

N

NICOLEANU JEANA, voir SIMIONESCU CR. I. 623

NICULESCU-DUVĂZ I., voir BARACU ILEANA 317

NICU M., Synthesis and uses of α-methylstyrene-*p*-sulphonate (II). Sulphonation of isopropylbenzene (IPB) with H_2SO_4 (d = 1.831 g/ml.) 17

O

OANCEA D. and V. GOSA, N. I. IONESCU, D. POPESCU, An experimental method for the measurements of the adiabatic maximum pressure during an explosive gaseous combustion 767

OLTEANU ILEANA, voir BÂLDEA I. 385

OLTEANU M. and ŞTEFANIA ZUCA, Electrical conductivity and density of molten $LiI-(Na, K, Rb)I$ binary systems 909

OPREA C., voir DRĂGAN GH. 447

OMARA M.A. and A.A. ELBARBARY, N. ANWAR, S. ELKONI, 1,4-Diarylnaphthalenes. III. Action of Grignard Reagents on some 1,1,4-Triaryl-buta-1,3-diene-2,3-dicarboxylic anhydrides and 1,4-diarylnaphthalene-2,3-dicarboxylic anhydrides 461

ONISCU C. and M. MACOVEANU, E. HOROBA, M. COJOCARU, E. POTORAC, The study of the extraction process of vincamine 807

P

PACHAURI P. C. voir SHARMA C.B. 719

PAIKE N.H., Reactions of 2,4-pentanedionato complexes-bromination of bis (2,4-pentanedionato) Manganese (II) and tris(2,4-pentanedionato Manganese (III) . . 517

PAL IRINA, voir VĂŢULESCU R. 823

PAL IRINA, voir VĂŢULESCU R. 831

PAL IRINA, voir VĂŢULESCU R. 1025

PATIL V.D., voir S.S. HANMANTGAD 735

PATRON LUMINIŢA, voir BREZEANU MARIA 229

PATRON LUMINIŢA, voir SPACU P. 659

PATRON LUMINIŢA, voir SPACU P. 837

PERIŞANU ŞT., voir VÎLCU RODICA 893

PÉRÉZAMADOR M.C., voir GARCIA F. 349

PETROVANU MAGDA, voir GEORGESCU E. I. 611

PILARSKI B. and K. WISTEROWICZ, Structural studies on imidazolidine-acetonitrile derivatives 759

PLOŞTINARU SILVIA, voir SPACU P. 659

PLOŞTINARU SILVIA, voir SPACU P. 837

POGANY I., voir BANCIU M. 703

POPA I.M., voir GHIRVU C. 329

POPA I.M. and GH. IONESCU and A. TARHON, High-pressure liquid chromatographic analysis of some cephalosporins 435
POPA M., voir VASILIU OPREA CL. 69
POPA V.T., voir BREZEANU MARIA 229
POPESCU D., voir OANCEA D. 767
PORAICU MARIA, voir C. RADOVAN 551
POTORAC E., voir ONISCU C. 807
PURI B.K., voir ASHOK KUMAR 49

R

RADOVAN C. and MARIA PORAICU, Considerations on the role of the characteristic dimension in the application of the vibrated electrode 551
RADOVICI O., voir LĂZĂRESCU VALENTINA 933
RĂDULESCU VALERIA, voir IOVU M. 713
RAJU U.C. KRISHNAM and B. SETHURAM, T. NEVANEETH RAO, Conductometric study of ion-ion and ion-solvent interactions. II. Conductances of trichloroacetic acid in methanol-water mixtures at 25°C 941
RAMADAN A., voir EL-NAGGAR H.A. 179
RAO A.L.J., voir ASHOK KUMAR 49
RAO NAVANEETH T., voir RAJU K.U.G. 941
ROBERTS R.M. voir KHELAF ALI ALI 507
RUBIO J.M. MARINAS, voir SANTOS S. ESTEBAN 593
RUSU PATRICIA, voir BANCIU M. 703

S

SALAH M. ABD EL-KADER and MAHMOUD F. ABD EL-ALLE, MOHAMADY A. FAKHR EL-DEIN, SALAH A. TURK, Isolation and characterization of arabinogalactan from Lima Bean *(Phaseolus Limensis)* Seed 61
SALAH A. TURK, voir SALAH M. ABD EL-KADER 61
SAHINI VICTOR EM., voir CIUREANU M. 97
SANTOS S. ESTEBAN and J. M. MARINAS RUBIO, M. P. MARTINEZ-ALCAZAR, Isomerization of *o*-alkylphenols on an aluminium orthophosphate-alumina . . . 593
SALLO AURORA and ANCA TOMESCU, Micellar effects upon the azocoupling reaction 875
SÀNCHEZ J.L., voir GARCIA F. 349
SANDU I., voir BERDAN . . . v 1031
SARAMET IOANA and M. BANCIU, Charge-transfer complexes of some substituted thiazoles 559
SAVA ION, voir BRUMĂ MARIA 239
SAUCEDO R., voir GARCIA F. 349
SAYED M.A., voir MOHAMED M.M. 419
SCHIKETANZ IOSIF and ANA SCHIKETANZ, MIRCEA D. GHEORGHIU, MIHAI PASCU, AURELIA VASILE, ALEXANDRU T. BALABAN, Aminoketone and oxazole synthesis. VIII. Acyl aminoacylations using azlactones of fluoro-substituted hippuric acids and 2,5-diaryloxazoles derived therefrom 975
SCHIKETANZ ANA, voir SCHIKETANZ IOSIF 975
SCHIKETANZ ANA, voir BALABAN A.T. 977
SCHIKETANZ IOSIF, voir BALABAN A.T. 977
SCHWARTZ R., voir BODOR A. 743
SEGAL E., voir SPACU P. 659
SEGAL E., voir DOCA N. 949
SETHURAM B., voir RAJU K.U.G. 941
SHARMA C. B. and P. C. PACHAURI, The reaction of chlorine dioxide with dl-alanine in aqueous solution 719
SHEHATA A.A., voir MOHAMED M.M. 419
SIMIONESCU BOGDAN C., voir SIMIONESCU CRISTOFOR I. 441
SIMIONESCU CRISTOFOR I. and BOGDAN C. SIMIONESCU, SILVIA IOAN, MONICA LEANCĂ and CARMEN CHELARU, Plasma induced polymerization. 12. Low conversion bulk homopolymerization of methyl methacrylate 441
SIMIONESCU CR. I., CLEOPATRA VASILIU-OPREA and JEANA NICOLEANU, Mechano-chemical initiated polymerizations. 9. Influence of mechanical conditions and temperature on polymerization reaction of acrylamide by vibratory milling 623
SIMONESCU T., voir HAVLIK IULIA 55

SIMON Z., voir ISAC DELIA 473

SIMON Z., voir MRACEC M. 531

SIMON Z. and A.T. BALABAN, D. CIUBOTARIU, T.S. BALABAN, QSAR for carcinogenesis by polycyclic aromatic hydrocarbons and derivatives in term of delocalization energy, minimal sterical differences and topological indices . . . 985

SINDHU R.S., and R.P. SINGH, Polarographic studies on the complexes of europium (III) with 2,3-dihydroxypyridine and 2-amino-3-hydroxypyridine 581

SINGH R.P., voir SINDHU R.S. 581

SITARU S., voir CRISTESCU C. 233

SMARANDACHE VICTORIA A., voir TERDIC MARIUS H. 133

SOLIMAN E.A., voir ATTIA I.A. 267

SOMAY MAGDA, voir VARHELYI GS. 695

SPACU P. and SILVIA PLOŞTINARU, LUMINIŢA PATRON, ADRIANA CONŢESCU, E. SEGAL, Coordination compounds as raw materials for mixed oxides. I. Mixed coordination compounds of lanthanides and Co(III) with salicylic acid 659

SPACU P. and SILVIA PLOŞTINARU, LUMINIŢA PATRON, ADRIANA CONŢESCU, N. STĂNICĂ, Coordination compounds as raw materials for mixed oxides. II. Mixed coordination compounds of lanthanides and Co(II) with derivatives of acetic acid 837

SRIVASTAVA S.N., voir HINGORANI H. 725

STAICU S., voir DINULESCU I.G. 585

STANCIU M., voir LĂZĂRESCU V. . . . .

STĂNCIULESCU RODICA, voir BANCIU M. 703

STANCIU MAGDALENA, voir LĂZĂRESCU VALENTINA 933

STANCU RODICA, voir CEAUŞESCU ELENA 375

STĂNICĂ N., voir SPACU P. 837

ŞTEFAN NICOLETA and PETRU FILIP, ILIE G. DINULESCU, MARGARETA AVRAM, A new dibenzo.(CH)$_{10}$ hydrocarbon : *anti*-dibenzo [*b,i*] tricyclo[6.2.0.0^{4,7}] deca-2,5,9-triene 589

ŞTEFAN NICOLETA and PETRU FILIP, FILIP CHIRALEU, ILIE G. DINULESCU, MARGARETA AVRAM, Carbocationic rearrangements in dibenzo[*b,g*]bicyclo [4.2.0]octa-2,7-diene derivatives 791

STERNBERG S. and I. LINGVAY, T. VIŞAN, LIANA MOISESCU, Electrochemical behaviour of silicon electrodes in molten chlorides 7

STERNBERG S. and MIHAELA UNGUREANU, V. BRÂNZOI, LILIANA APĂTEANU, Polarization behaviour of the *n*-type and *p*-type silicon in sulphuric acid-hydroquinone solutions 105

STERNBERG S., voir BRÂNZOI V. 199

STERNBERG S. and MIHAELA DRĂGĂNOIU, The mean thermodynamic activity of $CuSO_4$ in the ternary systems : $CuSO_4+MgSO_4+H_2O$ and $CuSO_4+MnSO_4+H_2O$ 209

STERNBERG S. and V. BRÂNZOI, A. MATEESCU, L. APĂTEANU, The influence of the Co(II) ions on the $PbSO_4/PSO_2$ electrode in sulphuric acid solutions 955

T

TALABA M. and C. CALISTRU, Nitric decomposition process of phosphatic raw materials. I. Study on equilibrium of nitric decomposition process of phosphatic raw materials 491

TĂMĂŞAN IULIANA and OVIDIU MAIER, TEODOR-S. BALABAN, *O*-substituted aromatic aldoximes of 1-methyl-2-aminooxymethyl-5-nitroimidazole. Synthesis and ^1H-NMR spectra 1005

TĂNASE I., ION IONECI and CONSTANTIN LUCA, The electrochemical behaviour of ethylmercury in aqueous medium 667

TĂNASE I., I. VARTIRES, N. D. TOTIR, I. IONECI and C. LUCA, Determination of microamounts of mercury(II) in high purity reagents by anodic stripping voltammetry 679

TĂNASE I. and I. IONECI, C. LUCA, Determination of ethylmercuric compounds by phase sensitive sinusoidal alternating current polarography 851

TOMESCU A., voir A. SALLO 875

TANEJA A.D., voir KUMARI RAMESH 141

TANEJA VINETA, voir MITTAL R.L. 757

TARHON A., voir POPA I.M. 435

TĂRNĂUCEANU EUTANȚA, voir BARACU ILEANA 317

TEODORESCU GRIGORE and CRISTINA MANDRAVEL, MELANIA GUȚUL, GABRIELA TEODORESCU, Synthesis and characterisation of a Pd(II) complex with 2,5-methroxy-4-chlorobenzanamine 339

TEODORESCU GABRIELA, voir TEODORESCU G. 339

TEOREANU ION and MARCELA MUNTEAN, Hardening processes in $3(CaO.Al_2O_3).CaSO_4$ — water system 575

TEOREANU ION and ECATERINA ANDRONESCU, LUCIA CACOVEANU, Thermal phase equilibrium relationship in $2CaO.SiO_2 - CaO.Al_2O_3$ system 647

TERDIC H. MARIUS and VICTORIA A. SMARANDACHE, Disubstituted phenothiazones. III. Synthesis of dimethyl-3H-phenothiazin-3-ones 133

TOLAN M., voir LĂZĂRESCU VALENTINA 933

TOMESCU ANCA, voir SALLO AURORA 875

TONEANU STELA, voir LUMINIȚA VLĂDESCU 689

TOTIR N.D., voir TĂNASE I. 679

U

UNGUREANU MIHAELA, voir STERNBERG S. 105

V

VÁRHELYI C., voir GĂNESCU I. 309

VÁRHELYI CS. and J. ZSAKÓ, GY. LIPTAY MAGDA SOMAY, On the dioximine complexes of transition metals. LXVII. New sulfito-*bis*-dimethyl-glyoximino-cobalt (III) complexes and their thermal decomposition 695

VARTIRES IULIANA, voir TĂNASE I. 679

VASILESCU D.S., voir CEAUȘESCU ELENA 375

VASILIU-OPREA CLEOPATRA and POPA M., Mechanochemically initiated copolymerization. 6. Synthesis and characterization of acrylonitric-vinyl-acetate-α-methyl styrene copolymers obtained by vibratory milling (in Russian) 69

VASILIU OPREA CLEOPATRA and FELICIA WEINER, Mechanochemically initiated polymerization. 6. Influence of mechanical parameters on the polymerization of styrene by vibratory grinding 273

VASILIU-OPREA CLEOPATRA, voir SIMIONESCU CR. I. 623

VASS M., voir LĂZĂRESCU V. 783

VASS M., voir LĂZĂRESCU VALENTINA 933

VĂȚULESCU R. and T. BUDIU, GH. MARCU, IRINA PAL, Heteropolytungstates with Ti(IV) and Ni(II). III. The absorption spectra of the heteropolyanions Ni(II)-undecatungstotitanate(IV) and Ni(II)-pentatungstotitanate(IV) 823

VĂȚULESCU R. and T. BUDIU, GH. MARCU, IRINA PAL, Heteropolytungstates with Ti(IV) and Ni(II). IV. The thermal behaviour of the potassium salt of the Ni(II)-undecatungstotitanate(IV) anion 831

VĂȚULESCU RODICA and T. BUDIU, GH. MARCU, IRINA PAL, Heteropolytungstates with Ti(IV) and Ni(II). V. The thermal behaviour of sodium and potassium salt of the Ni(II)-pentatungstotitanate (IV) anion 1025

VICIEDO GILBERTO, voir CAO ROBERTO 639

VÎLCU R. and E. LUCINESCU, M. DRĂGUȚ, Excess values in binary systems of carboxylic acids with n-heptane and benzene 289

VÎLCU RODICA and I. GĂINAR, A new method for measuring the small pressure differences at high static pressures 381

VÎLCU RODICA and ȘT. PERIȘANU, The latent heat of vaporization of carboxylic acids 893

VÎRTOSU D., voir MOKHALLALATI A. O. 31

VIȘAN T., voir STERNBERG S. 7

VLAD RODICA and M. BANCIU, Synthesis of dibenzobullvalene *via* Bamford — Stevenson reaction 1001

VLĂDEA RADU, Catalytic influence in the electrooxidation of olefines in non-aqueous solution I. Experimental aspects 151

VLĂDEA RADU and FRANCISC KEREK, Catalytic influence in electrooxidation of olefins in non-aqueous solutions. II. Diisobutylene and styrene oxidation products 157

VLĂDEA RADU, Catalytic influence in electrooxidation of olefins in non-aqueous solutions III. Kinetic study of diisobutylene and styrene oxidation 249

VLĂDESCU LUMINIȚA and STELA TONEANU, Combined ion exchange-spectrophotometric determination of potassium with sodium tetraphenylborate 689

VLĂDESCU LUMINIȚA and CHIPER STELUȚA, Combined ion-exchange-spectrometric study of the Ce(IV)-Sulphanilic acid system. I. Ion exchange method for eliminating interference in the spectrometric determination of cerium (IV) . . . 1047

VOLANSCHI ELENA, voir CIUREANU MARIANA 97

VOLANSCHI ELENA and A. MISSIR, DIANA MUȘOIU, E. S. R. Spectral study of some polysubstituted thioureide anion radicals 483

W

WEINER FELICIA, voir VASILIU-OPREA CLEOPATRA 273

WISTEROWICZ K., voir B. PILARSKI 759

Z

ZĂLARU FLORICA, voir MEGHEA AURELIA 297

ZSAKÓ J., voir VÁRHELYI CS. 695

ZUCA ȘTEFANIA, voir OLTEANU M 909

Y

YANNI AMAL S., voir ABDELY RAHMAN A. E. 401

YOUSSEF S. K. M., voir ABOL MAGED A. 41

INDEX DES SUJETS

A

Acetyl-cyclohexenone derivatives. Synthesis and some reactions of. . .,I. A. ATTIA and E. A. SOLIMAN 267

Acetylenes with transition metals XI. Reaction of 1-chloro-1,2-diphenyl-3-alkyl-π-allylpalladium complexes with alkenes. Reaction of —, I. G. DINULESCU, S. STAICU, A. DUMITRIU, A. GHENCIULESCU, F. CHIRALEU and M. AVRAM 585

N-Acylphthalimides and phenols. Esters from —, C. I. CHIRIAC 753

Additions of dehydroacetic acid and its 3-cinnamoyl derivatives. Base catalyzed —, M. A. HASSAN, M. EL-KADY, M. EL-BORAI and A. A. ABD EL-MOATY 245

Acid-base and redox characteristics of Pd catalysts obtained by ion exchange, ALBA A., ARAMENDIA M. A., BORAU V., JIMENEZ C. and MARINAS J. M. 467

Alkaline decomposition of 3-bromopropyl-triphenylphosphonium bromide in DMSO—H_2O mixtures. Kinetic study of the —, FAYEZ Y. KHALIL, M. T. HANNA. F. M. ABDEL-HALIM and M. EL-BATOUTI 571

Alkylation of benzene with isometric pentanols and pentenes. Modern Friedel-Crafts chemistry. X. Rearrangements accompanying Friedel-Crafts —, ALI ALI KHALAF and ROYSTOM M. ROBERTS 507

Alkynes V. Reaction of alkynes with aroyl chlorides in the presence of silver perchlorate. Friedel-Crafts acylation of —, D. MĂNOIU, M. MĂNOIU, I. G. DINULESCU and M. AVRAM 223

Amides by a new direct condensation reaction. Synthesis of —, CHIRIAC I. 799

2-Aminobenzoimidazole. Imines of aminoazoles. I. Synthesis and characterization of some imines of —, H. H. GLATT, M. FOULA BARRY, C. CSUNDERLIK, R. BACALOGLU, M. MEDELEANU and M. LANTOS 125

Aminoketone and oxazole synthesis VIII. Acylaminoacylations using azolactones of fluoro-substituted hypuric acids and 2,5-diaryloxazoles derived therefrom, I. SCHIKETANZ, A. SCHIKETANZ, M. D. GHEORGHIU, M. PASCU, A. VASILE and 975
A. T. BALABAN— —. IX. 2,2'-(*p*-Phenylene)-bis-(5-aryloxazoles) and 2,2'-(1,4-naphthalenediyl)-bis(5-aryloxazoles) *via* acrylaminoacrylation of aromatic hydrocarbons, A. T. BALABAN, I. SCHIKETANZ, M. D. GHEORGHIU and A. 977
SCHIKETANZ

N-Amino-2-pyridone derivatives. Synthesis of some new —, A. K. EL-SHAFEI, A.-B. A. G. GHATTAS and F. A. GAD 81

Anodic oxidation of the binuclear cyanide complex of Mn(III). I. Oxidation at +0.2 volts (*vs.* SCE): kinetic current and parallel reaction. Coulometric study at controlled potential of the —, (in Spanish), G. LÓPEZ CUETO and A. ALONSO MATEOS 917

Aquo-ammino-di-2-mercapto-benzo-thiazole cobalt complex. Structural studies on the —, A. CĂLUȘARU 1039

Arabinogalactan from Lima Bean *(Phaseolus Limensis)* seed. Isolation and characterization of —, SALAH M. ABD EL-KADER, M. F. ABD EL-ALLE, M. A. FAKHR EL-DEIN and S. A. TURK 61

Aromatic aldoximes of 1-methyl-2-aminooxymethyl-5-nitroimidazole. Synthesis and ^1H-NMR spectra *O*-substituted —, I. TĂMAȘAN, O. MAIER and T. S. BALABAN 1005

Aromatic hydrocarbons in different petroleum fractions. II. Component identification by HPLC — (in French), HOCINE KADI and D. P. LAZĂR 81
— — III. Méthode n.d. PA, HOCINE KADI and D. P. LAZAR 365

5-Aryl-1,3,4-oxadiazoles. Some chemical aspects of —, A. A. EL-BARBARY 257

Atmospheric n-hexane, toluene and acetone with activated charcoal tubes using the two-step thermal gas extraction procedure. Simultaneous determination of —, R. CIUPE, S. CSABA and S. BUTNARIU 1053

Benzene-alcohol systems. Binary vapor-liquid equilibria of —, J. L. CABEZAS, J. C. ARRANZ and J. BERRUETA 903

Binary systems of carboxylic acid with n-heptane and benzene. Excess values in —, R. VÎLCU, E. LUCINESCU and M. DRĂGUȚ 289

Biomimetic 4-substituted coumarins. Synthesis of some—, S. S. HANMANTGAD, M. V. KULKARNI and V. D. PATIL 735

Book reviews — 89, 90, 91, 92, 281, 282, 283, 284, 285, 286, 289

Calculation of the I. R. and Raman active fundamentals of polymers. About the—, ADRIAN O. FULEA 357

Carbanions and free radicals derived from 1,2-diphenylpyrazolidine-3,5-diones. I. Trapping of the free radical formed in phenylbutazone oxidation, F. BADEA, F. IORDACHE, A. MEGHEA, A. T. BALABAN, R. MARINESCU and A.-M. GHIVIRIGĂ . . . 189

Carbocationic rearrangements in dibenzo (*b, g*) bicyclo [4.2.0] octa-2,7- diene derivatives, N. ȘTEFAN, P. FILIP, F. CHIRALEU, I. G. DINULESCU and M. AVRAM 791

Carbon-13 NMR spectra of some 16,17-glycol diterpenes, F. GARCIA, O. COLLERA, J. L.SÁNCHEZ, R. CRUZ, R. SAUCEDO and M. C. PEREZAMADOR . . . 349

Carboxylic acids. The latent heat of vaporization of —, R. VÎLCU and ST. PERIȘANU 893

Catalytic hydrogenation on AlPO$_4$ -supported nickel catalysts. II. Hydrogenation of styrene and α-methyl-styrene, J. M. CAMPELO, A. GARCIA, D. LUNA and J. M. MARINAS . . . 427

Cyclialkylation of aryl alkenyl ketones under Friedel-Crafts conditions. Modern Friedel-Crafts chemistry XII. A. M. EL-KHAWAGA, ABOEL MAGD A. ABDEL WAHAB, M. F. ELZOHRY and ALI A. KHALAF . . . 599

Cyclic β-keto-anilides. Synthesis and reactions of some new — I. I. I. ABD EL-GAWAD, A. M. KHALIL, O. M. O. HABIB and H. A. ETMAN . . . 499

Cyclopentene hydration. Study of —, GH. MIHĂILĂ, C. LUCA, DOINA DRANGA and N. BÎLBĂ . . . 1019

Charge-transfer complexes of some substituted thiazoles, I. SARAMET and M. BANCIU 559

Chlorine dioxide with dl-alanine in aqueous solution. The reaction of—, C. B. SHARMA and P. C. PACHAURI . . . 719

Complex with 2,5-methoxy-4-chloro-benzenamine. Synthesis and characterisation, GR. TEODORESCU, C. MANDRAVEL, M. GUȚUL and G. TEODORESCU 339

Complexes of 3-bromo-2-hydroxy-5-methyl acetophenone hydrazone. Magnetic and spectral studies on copper(II), nickel(II), cobalt (II), iron(III) and manganese (II), KEEMTI LAL and SITA RANI MALHOTRA . . . 395

Complex compounds of Tl(III) with n-donor ligands. Study on the system Tl(III)-2,2-azopyridine, I. BERDAN, D. ANCUȚA and I. SANDU (in French) . . . 1031

Conductometric study of ion-ion and ion-solvent interactions II. Conductances of trichloroacetic acid in methanol-water mixtures at 25°C, U.G. KRISHNAM RAJU, B. SETHURAM and T. NAVANEETH RAO . . . 941

Conversion of aromatic aldehydes into nitriles. A convenient one-step —.C. I. CHIRIAC 353

Coordination compounds as raw materials for mixed oxides. I. Mixed coordination compounds of lanthanides and Co(III) with salicylic acid, P. SPACU, S. PLOȘTINARU, L. PATRON, A. CONȚESCU and E. SEGAL . . . 659

Coordination compounds formation within the MCl$_2$-SnCl$_2$-α,α′-bipyridine (M = Co, Ni) system, M. BREZEANU, M. ANDRUH, L. PATRON and V. T. POPA . . . 229

Coordination compounds as raw materials for mixed oxides. II. Mixed coordination compounds of lanthanides and Co(II) with derivatives of acetic acid, P. SPACU, S. PLOȘTINARU, L. PATRON, A. CONȚESCU and N. STĂNICĂ . . . 837

Copolyamides. I. The influence of composition on the physico-chemical properties, AMALIA CRUSOS . . . 391

Copper(II) complex compounds with nitroimidazole derivatives, A. MEGHEA, F. ZĂLARU and D. IONESCU . . . 297

Corrigendum "On a correction technique for fractionation data and its application to the fractionation of polyethylene terephthalate", A. O. FULEA . . . 371

Dehydrogenation kinetics of lower aliphatic alcohols on copper catalysts I. Preparation, stabilization and catalytic activity of pure copper powders. N. DOCA and E. SEGAL 949

1,4-Diarylnaphthalenes. III. Action of Grignard reagents of some 1,1,4-triaryl-buta-1,3-diene-2,3-dicarboxylic anhydrides and 1,4-diarylnaphthalene-2,3-dicarboxylic anhydrides, M. A. OMARA, A. A. ELBARBARY, N. ANWAR and S. ELKONI 461

Diazoderivatives. Thermal and photochemical stability of —, D. ISAC, M. MRACEC and Z. SIMON . . . 473

Diazoketones from β-benzoyl acrylyl chloride and diazoalkanes. Synthesis of —, B. AGARWAL and P. BAHADUR . . . 803

Dibenzo-(CH)$_{10}$ hydrocarbon : *anti*-dibenzo [*b, i*] tricyclo [6.2.0.0.^{4,7}] deca-2,5,9-triene. A new —, N. ȘTEFAN, P. FILIP, I. G. DINULESCU and M. AVRAM . . . 589

Dibenzobullvalene *via* Bamford-Stevens reaction. Synthesis of —, R. VLAD and M. BANCIU . . . 1001

Dioximine complexes of transition metals. LXVII. New sulfito-*bis*-dimethylglyoximinocobalt(III) complexes and their thermal decomposition. CS. VÁRHELYI, J. ZSAKÓ, GY. LIPTAY and M. SOMAY 695

Dipolar study of titanium octahedral compounds with TMDTO and TEDTO, M. C. MARTINEZ, M. R. BERMEJO and M. GAYOSO (in Spanish) 333

Electrochemical behaviour of ethylmercury in aqueous medium, I. TĂNASE, I. IONECI and C. LUCA 667

Electrochemical behaviour of silicon electrodes in molten chlorides. S. STERNBERG, I. LINGVAY, T. VIŞAN and L. APĂTEANU 7

Electrodeposition of nickel. On the material transport optimization in the—, G. GUTT, ST. IVAŞCAN, S. GUTT and M. GRAMATICU (in German) 453

Electrode processes in Pb/$H_2SO_4+Na_2SO_4$ system, V. BRÂNZOI, S. STERNBERG, and L. APĂTEANU 199

Electronegativity in *Slater*'s theory of the atom. The concept of —, C. I. LEPĂDATU 111

Electronic spectra and barrier to internal rotation of α- and β-naphthalenesulphonic acids. Considerations on the —, C. GHIRVU, M. CONSTANTINESCU, GH. IONESCU and I. M. POPA 329

Electrooxidation of olefins in non-aqueous solutions. I. Experimental aspects — R. VLĂDEA 151

Electrooxidation of olefins in non-aqueous solutions II. Diisobutylene and styrene oxidation products, R. VLĂDEA 157

Electrooxidation of olefins in non-aqueous solution. III. Kinetic study of diisobutylene and styrene oxidation. Catalytic influences in—, R. VLĂDEA 249

Enolization of some substituted acetoacetarylamides at different temperatures and concentrations, R. KUMARI, A. D. TANEJA and V. P. KUDESIA 141

Esterification of monosubstituted benzoic acids with "kearby" type aluminium orthophosphates as catalysts (in Spanish), M. S. ARIAS-PEREZ, C. FERNANDEZ-SANCHEZ and J. M. MARINAS 617

Ethylmercuric compounds. Determination by phase-sensitive sinusoidal alternating current polarography, I. TĂNASE, I. IONECI and C. LUCA 851

Extraction equilibria of some complex combinations with macrocyclic ligands, C. LUCA and M. MAGDI KHALIL 843

Factorisation of orbital energies in transition-metal complexes. I. Factorisation of the overlap integrals, C. I. LEPĂDATU and M. ANDRUH 217

Fluorenylidenetriphenyl-phosphoranes and -arsinane with certain dicarbonyl compounds. The reaction of — , L. S. BOULOS and A. EL KATEB 1015

Halomethylethers by secondary amines. Decomposition of (in French), M. IOVU, V. RĂDULESCU and M. IQBAL 713

Hardening processes in 3(CaO . Al_2O_3). $CaSO_4$—water system, I. TEOREANU and M. MUNTEAN 575

Heteropolytungstates with Ti(IV) and Ni(II). III. The absorption spectra of the heteropolyanions Ni(II)-undecatungstotitanate (IV) and Ni(II)-pentatungstotitanate (IV) R. VĂŢULESCU, T. BUDIU, GH. MARCU and I. PALL 823

— — — IV. The thermal behaviour of the potassium salt of the Ni(II)-undecatungstotitanate(IV) anion. R. VĂŢULESCU, T. BUDIU, GH. MARCU and I. PAL . . 831

— — — V. The thermal behaviour of sodium and potassium salt of the Ni(II) pentatungstotitanate(IV) anion, R. VĂŢULESCU, T. BUDIU, GH. MARCU and I. PAL 1025

19-Hydroxysteroids. The synthesis of —, A. BODOR, A. GERGELY, R. SCHWARTZ, A. JUHASZ, P. COLŢEA and D. BREAZU 743

Imidazolidineacetonitrile derivatives. Structural studies on —, B. PILARSKI and K. WISTEROWICZ 759

Indophenazinyl-pyrazoline and isoxazoline derivatives. Synthesis of some new—, ABDU E. ABDEL RAHMAN and AMAL S. YANNI 401

Ion exchange-spectrophotometric determination of potassium with sodium tetraphenylborate. Combined —, L. VLĂDESCU and S. TONEANU 689

Ion exchange-spectrophotometric study of the Ce(IV) — sulphanilic acid system I. Ion exchange method for eliminating interference in the spectrometric determination of cesium (IV). L. VLĂDESCU and S. CHIPER 1047

Ion Co(II) on the $PbSO_4/PbO_2$ electrode in sulphuric acid solutions. The influence of the —, S. STERNBERG, V. BRÂNZOI, A. MATEESCU and L. APĂTEANU . 955

Isomerization of *o*-alkylphenols on an aluminium orthophosphate-alumina. S. ESTEBAN

SANTOS, J. M. MARIÑAS RUBIO and M. P. MARTINEZ-ALCAZAR 593

Jacobson reaction. Kinetic of the —, I. BÂLDEA, V. FĂRCĂȘAN and I. OLTEANU 385

Liquid chromatographic analysis of some cephalosporins. I. M. POPA, GH. IONESCU and A. TARHON 435

Mass spectra of diastereometric substituted secondary valer- and butyramides, ABOEL MAGED A. ABDEL-WAHAB, M. S. K. YOUSSEF and G. HELMCHEN . . . 41

Mechanochemically initiated copolymerizations. 6. Synthesis and characterization of acrylonitrile-vinyl acetate-α-methyl styrene copolymers obtained by vibratory milling (in Russian). CL. VASILIU OPREA and M. POPA 69

Mechanochemically initiated polymerizations. 6. Influence of mechanical parameters on the polymerization of styrene by vibratory grinding. CL. VASILIU OPREA and F. WEINER 273

— — — 9. Influence of mechanical conditions and temperature on polymerization reaction of acrylamide by vibratory milling, CR. I. SIMIONESCU, CL. VASILIU OPREA and J. NICOLEANU 623

Method for computing the information entropy of the quantitative analytical data, V. DAVID and D. CIOMARTAN 777

Method for measuring the small pressure differences at high static pressures. A new-, R. VÎLCU and I. GĂINAR 381

Method for the measurement of the adiabatic maximum pressure during an explosive gaseous combustion. D. OANCEA, V. GOȘA, N. I. IONESCU and D. POPESCU 767

α-Methyl-styrene-*p*-sulphonate (II). Sulphonation of isopropylbenzene (IPB) with H_2SO_4 (d_4^{20}= 1.831 g/mL). Synthesis and uses of—, M. NICU 17

Micellar effects upon the azocoupling reaction, A. SALLO and A. TOMESCU 875

Microamounts of mercury(II) in high purity reagents by anodic stripping voltammetry. Determination of—, I. TĂNASE, I. VARTIRES, N. D. TOTIR, I. IONECI and C. LUCA 679

Molten LiI-(Na, K, Rb, Cs)I binary systems. Electrical conductivity and density of —, M. OLTEANU and Ș. ZUCA 909

Nitric decomposition process of phosphatic raw materials. I. Study on equilibrium of —, M. TALABA and C. CALISTRU . . . .

Oligo(1, 2-propylene terephthalate)s by gradient elution high performance liquid chromatography. Separation of —, D. MUNTEANU, V. MANOVICIU and I. MANOVICIU 23

Optimal parameters in the HMO technique. II. An optimal set of parameters for the hydroxylic phenol function, M. MRACEC, MARIA MRACEC and Z. SIMON 531

Ordered polyesterimides, M. BRUMĂ and I. SAVA 239

Os(VIII) catalysed chloramine — T oxidation of glycollic acid and lactic acid in alkaline media. Kinetics of —, H. HINGORANI, H. C. GOYAL, G. CHANDRA and S. N. SRIVASTAVA 725

Oxygen interaction with silver catalysts. Electrochemical investigation of the —, V. LĂZĂRESCU, M. VASS, O. RADOVICI, C. DAȘOVEANU, M. STANCIU and M. TOLAN 933

72,4-Pentanedionato complexes. Reactions of —. Bromination of bis-(2,4-pentanedionate) manganese(II) and tris(2,4-pentanedionate) manganese (III), N. H. PAIKE . . 517

Phenols. The photo formylation of —, A. M. FAHMY, S. A. MAHGOUB, M. M. ALY and M. Z. A. BADR 749

Phenothiazones disubstituted. III. Synthesis of dimethyl-3H-phenothiazin-3-ones. M. H. TERDIC and V. A. SMARANDACHE 133

Photodegradation and photostabilization of the ethylene-vinyl acetate copolymers. I. Aspects of the mechanism of photodegradation reactions, C. ANDREI, I. HOGEA and V. DOBRESCU 865

N′-picolinoyl-4-(substituted azo)-alkyl/aryl pyrazoles. Synthesis of some biologically active —, D. R. GUPTA and R. K. ARORA 37

Plasma-induced polymerization. 12. Low conversion bulk homopolymerization of methyl methacrylate. CR. I. SIMIONESCU, B. C. SIMIONESCU, S. IVAN, M. LEANCĂ and C. CHELARU 441

Polarization behaviour of the *n*-type and *p*-type siliconin sulphuric acid-hydroquinone solutions, S. STERNBERG, M. UNGUREANU, V. BRÂNZOI and L. APĂTEANU 105

Polarographic studies on the complexes of europium (III) with 2,3-dihydroxypyridine and 2-amino-3-hydroxypyridine, R. S. SINDHU and R. P. SINGH 581

Poly(butadiene-b-styrene) by specific refractive index increment measurements. Characterization of —. E. CEAUŞESCU, R. BORDEIANU, D. S. VASILESCU, I. MANAFU, I. CERCHEZ, P. GHIOCA, R. STANCU and E. BUZDUGAN . . 375

Polynuclear heterocycles : 6-chloro, 8,13-dihydro-8,13-o-benzenonaphtho[2,3-a]phenothiazin-7(H) ones. Studies in the synthesis of some new —, R. I. MITAL, V. TANEJA, C. L. GUPTA and S. B. GUPTA 757

Potential anticancer agents. XXV. Aliphatic and cycloaliphatic N-nitrosoureas and N-nitrosourethanes, I. BARACU, E. TĂRNĂUCEANU, V. DOBRE and I. NICULESCU-DUVĂZ 317

Potentiodynamic behaviour of raney-copper in potassium hydroxide solution. V. LĂZĂRESCU, M. VASS, J. HERŞCOVICI and E. CORLĂTEANU 783

Potentiometric gas sensor for carbon dioxide. A. O. MOKHALLALATI, A. ISTUDOR, D. VÎRTOSU and C. LUCA 31

Products of K_2[Cr(NCS)] with chinaldine. New substitution- (in German), I. GĂNESCU, N. CALU, GH. BRÎNZAN und C. VÁRHELYI 309

Pyrazolone compounds of bis-methylaminoantipyryl-propane and bis-methylaminoantipyryl-butane, I. HAVLIK, T. SIMIONESCU and I. HAVLIK 55

2(1H)-pyridones synthesized from 3,4-methylene-dioxybenzylidene- and 4-nitrobenzylidene-p-isopropylacetophenone. Reactions of some—, M. M. MOHAMED, M. A. EL-HASHASH, M. A. SAYED and A. A. SHEHATA 419

Pyrolysis of n-heptane. Selfinhibition of the homogeneous —, M. BOZEŞANU and N. I. IONESCU 963

Quinoxaline series. IV. (3+2) Dipolar cycloaddition reactions of some quinazolium-3-(p-R-benzoyl)-methylides with activated acetylenes. Dipolar derivatives in the — (in French), E. I. GEORGESCU, F. GEORGESCU, M. GHEORGHIU, E. G. GEORGESCU and M. PETROVANU 611

QSAR for carcinogenesis by polycyclic aromatic hydrocarbons and derivatives in terms of delocalization energy, minimal sterical differences and topological indices. Z. SIMON, A. T. BALABAN, D. CIUBOTARIU and T. S. BALABAN 1001

Reaction rate. Alkaline hydrolysis of n-butyl acetate, propionate, butyrate in the water-monoethylenglycol mixed solvent. Influence of solvent on the — (in French), O. LANDAUER, C. MATEESCU and O. IULIAN 883

Rare earth chelates of disubstituted 2-hydroxy-acetophenones, M. MITTAL, S. R. MALHOTRA, KEEMTI LAL and S. P. GUPTA 511

Retention indices and molecular structure of isodecanes (in French). C. CHELGHOUM, Y. HADDAD, K. ABDEDDAIM and M. H. GUERMOUCHE 565

Rhodium determination by atomic absorption spectrophotometry. Elimination of the interfering effects of some organic compounds in the — M. A. KABIL and M. A. MOSTAFA 631

Similarity and shape recognition in experimental chemistry, C. I. LEPĂDATU 3

Spirophosphazenes. Synthesis of the first alkylated — (in Spanish), R. CEA OLIVARES and L. CANTU 525

Substituted diarylidenecycloheptanones. Studies on —, MOHAMED A. ABD-ALLA. M. T. ISMAIL and AHMED M. EL-KHAWAGA 343

Sultams and sultones. Bromination of unsaturated —, S. H. DOSS and N. R. ABU ZEID 405

Synergistic and antagonistic extraction of protactinum (V) by bis (2-ethyl hexyl) phosphoric acid and tributyl phosphate mixture, H. A. EL-NAGGAR, A. RAMADAN and A. A. ABDEL-HASSOUL 179

9,10,19,20-Tetrahydro-dibenzo/*a,c*/phenanthro/*g*/cyclodecene and 9,10,19,20-tetrahydrotetrabenzo/*a,c,g,i*/cyclodecene by sulphone pyrolysis. Synthesis —, M. BANCIU, I. POGANY, D. MOSORA, P. RUSU, R. STĂNCIULESCU and M. DEZSÖ 703

Tetrahydrofuran-methanol and dioxane-methanol systems. Physico-chemical study of — (in French), O. LANDAUER, C. MATEESCU, O. IULIAN and G. COSTEANU 651

Terephthalate polyethylene sheets by activation in high frequency plasma. Increase of the free surface energy of — (In French), G. BOURCEANU, E. GRUNICHIEVICI and M. BOURCEANU 859

Thermal phase equilibrium relationships in 2CaO.SiO$_2$-CaO.Al$_2$O$_3$ system. I. TEOREANU, E. ANDRONESCU and L. CACOVEANU 647

Thermodynamic activity of $CuSO_4$ in the ternary systems :$CuSO_4$ $MgSO_4+H_2O$ and $CuSO_4$ $+MnSO_4+H_2O$. The mean S. STERNBERG and M. DRĂGANOIU 209

Thermomechanical study of amorphous modifications in polyester fibers induced by isothermal annealing, GH. DRĂGAN and C. OPREA 447

Thiosemicarbazone complexes of $3d^{6-10}$ metals. I. Acetophenone and *o*-aminobenzaldehyde thiosemicarbazone. R. CAO, G. VICIEDO and H. BERTY 639

Thioureide anion radicals. E. S. R. Spectral study of some polysubstituted —, E. VOLANSCHI, A. MISSIR and D. MUȘOIU 483

as-Triazine derivatives with potential therapeutic action. XIX. Synthesis of 5-(substituted-benzyl)thio-6-azauridines, C. CRISTESCU 117

as-Triazine derivatives with potential therapeutic action. XX. Cyanoethylation of 5-substituted-6-azauracil and 4-thioxo-5-substituted-6-azauracil. C. CRISTESCU and S. SITARU 233

U.H.F spin density calculations on substituted nitroaromatic anion radicals, M. CIUREANU, M. HILLEBRAND, V. EM. SAHINI and E. VOLANSCHI 97

Vibrated electrode. Considerations on the role the characteristic dimension in the application of the —, C. RADOVAN and M. PORAICU 551

Vincamine. The study of the extraction process —, C. ONISCU, M. MACOVEANU, E. HOROBA, M. COJOCARU and E. POTORAC 807

Zinc-ε-caprolactam system. Thermodynamics of complex formation —, ASHOK KUMAR, B. K. PURI and A. L. J. RAO 49

NOTE POUR LES AUTEURS

La Revue Roumaine de Chimie publie des articles en anglais, français, russe, allemand ou espagnol. Les auteurs sont priés d'envoyer des articles et des comptes rendus inédits.

Les manuscrits seront dactylographiés à double interligne. La bibliographie, les tableaux et la légende des figures seront placés après le texte.

Si l'article fait partie d'une série numérotée, la partie précédente sera donnée comme première référence.

Chaque article sera précédé d'un résumé comprenant quinze lignes au maximum.

Les références bibliographiques dans le texte seront faites par des exposants sans parenthèses et paraîtront à la fin de l'ouvrage.

Les publications périodiques mentionnées dans la bibliographie seront présentées suivant les prescriptions internationales : le nom de l'auteur précédé de l'initiale du prénom, le titre du périodique abrégé conformément à « Chemical Abstracts » et souligné par une ligne, le numéro du tome indiqué par des chiffres arabes et souligné par deux lignes, suivi de la première page de l'article ; à la fin, l'année de la parution sera placée entre parenthèses. Le numéro de la revue ne sera pas indiqué si les pages du volume sont numérotées consécutivement.

Les textes des livres ou traités inclueront : le nom des auteurs, l'initiale du prénom, le titre du livre entre guillemets et sans être souligné, le numéro du tome précédé par l'abréviation « vol. » (ou « Bd. »), le numéro de l'édition, les éditions (the publisher), la localité de la parution du livre, l'année de la parution et la page de la référence précédée(s) par l'abréviation « p. » (ou « S. »).

Les brevets seront indiqués comme suit : l'auteur ou la firme, le pays et le numéro du brevet, la date et la revue *(Chem. Abstr.)* Par. ex. : M. Jones (to Union Carbide Co), Brit. Pat. 601 238, 2 Sept. 1959 ; cf. *Chem. Abstr.*, *54*, 12808 (1960).

Si la référence n'a pas été lue en original, on indiquera aussi la revue de référence consultée.

Les diagrammes seront tracés à l'encre de Chine sur papier calque. Les tableaux et les figures (en nombre strictement nécessaire) ainsi que les courbes dans les figures seront numérotés par des chiffres arabes. Leur explication sera donnée dans la légende des figures. Prière de ne pas inscrire les mêmes données dans les tableaux et les figures. Chaque tableau aura un titre. On indiquera dans le texte la place approximative des tableaux et des figures. Les formules chimiques seront incluses dans le texte ; en outre, elles seront transcrites sur papier calque, à l'encre de Chine.

Les auteurs sont priés d'indiquer les caractères italiques (en soulignant les lettres au crayon), ainsi que tout autre caractère spécial ; les préfixes *ortho*, *meta*, *para*, *cis*, *trans*, etc. seront soulignés pour indiquer leurs caractères italiques et ne seront jamais écrits avec des majuscules.

Aucune correction à la main ne sera admise sur le manuscrit. Les corrections seront tapées à la machine. Les lettres grecques ou d'autres symboles spéciaux seront insérés à la main à l'encre clairement.

Le manuscrit sera signé par l'auteur.
Le titre-courant aura 50 lettres au maximum.
L'entière responsabilité du contenu des articles appartient aux auteurs.
Sur demande on peut obtenir une note plus complète.

PRINTED IN ROMANIA

DEC 1 9

TRAVAUX PARUS AUX ÉDITIONS DE L'ACADÉMIE DE LA RÉPUBLIQUE SOCIALISTE DE ROUMANIE

V. DRAGUTAN, A. T. BALABAN, M. DIMONIE, **Olefin Metathesis and Ring-Opening Polymerization of Cyclo-olefins**, coèdition avec John Wiley and Sons, 1985, 514 p.
C. LITEANU, I. RÎCA, **Optimizarea proceselor analitice**, 1985, 360 p.
N. PERESCU, **Chimia extracției cu solvenți și aplicații**, 1985, 212 p.
V. E. SAHINI, M. HILLEBRAND, **Chimie cuantică în exemple și aplicații**, 1985, 378 p.
GH. MARCU, **Chimia compușilor coordinativi**, 1984, 415 p.
E. CORDOȘ, C. MANOLIU, **Spectrometria de absorbție și fluorescență atomică**, 1984, 178 p.
C. BODEA, **Tratat de biochimie vegetală**, p. II, vol. 5, 1984, 438 p.
ELENA CEAUȘESCU, **Cercetări în chimia și tehnologia polimerilor**, 1983, 519 p.
N. ASANDEI, A. GRIGORIU, **Chimia și structura fibrelor**, 1983, 395 p.
N. IONESCU, M. CĂLDĂRARU, **Oxidarea catalitică a olefinelor inferioare**, 1983, 178 p.
C. CAȘCAVAL, **Studiul polimerilor prin piroliză și cromatografie de gaze**, 1983, 220 p.
C. I. SIMIONESCU, F. DANEȘ, **Originea vieții**, 1983, 110 p.
C. BODEA (sous la direction), **Tratat de biochimie vegetală**, 2^{e} partie, t. IV, 1982, 408 p.
I. G. MURGULESCU, RODICA VÎLCU, **Introducere în chimia fizică. Vol. III, Termodinamica chimică**, 1982, 624 p.
I. G. MURGULESCU, J. PĂUN. **Introducerea în chimia fizică. Vol. I. 3. Nucleul atomic, reacții nucleare, particule elementare**, 1982, 606 p.
ELENA CEAUȘESCU, **Noi cercetări în domeniul compușilor macromoleculari**, 1981, 536 p.
I. G. MURGULESCU, TATIANA ONCESCU, E. SEGAL, **Introducere în chimia fizică, Vol. II. 2. Cinematică chimică și cataliză**, 1981, 1024 p.
LYDIA-MARIA VAICUM, **Epurarea apelor uzate cu nămol activ. Bazele biochimice**, 1981, 218 p.
I. GĂLĂȚEANU, **Procese și metode radiochimice în energetica nucleară**, 1981, 234 p.
O. IORDACHE, **Procese polistocastice aplicate la fenomenele de transfer**, 1981, 186 p.
CR. SIMIONESCU, VALERIA GORDUZA, **Polimeri biocompatibili și biologic activi**, 1980, 479 p.
ELENA CEAUȘESCU, **Polimerizarea stereospecifică a izoprenului**, 1979, 307 p.
C. GH. MACAROVICI, **Analiza chimică cantitativă anorganică**, 1979, 457 p.
M. FLORESCU, **Metode științifice în dezvoltarea industriei chimice moderne**, 1979, 256 p.
A. T. BALABAN, I. GĂLĂȚEANU, G. GEORGESCU, LIGIA SIMIONESCU, **Compuși marcați și radiofarmaceutici cu aplicații în medicina nucleară**, 1979, 495 p.
I. G. MURGULESCU, E. SEGAL, **Introducere în chimia fizică. Vol. II. 1. Teoria molecular-cinetică a materiei**, 1979, 1036 p.
S. STERNBERG, FL. DANEȘ, **Termodinamica chimică aplicată**, 1978, 400 p.
I. G. MURGULESCU, V. EM. SAHINI, **Introducere în chimia fizică. Vol. I. 2. Structura și proprietățile moleculelor**, 1978, 604 p.
I. ZUGRĂVESCU, MAGDA PETROVANU, **N-ylid chemistry**, coédition avec McGraw Hill International Book Company, U.S.A., 1977, 396 p.
I. G. MURGULESCU, **Introducere în chimia fizică. Vol. I. 1. Atomi, molecule, legătură chimică**, 1976, 560 p.
ELENA CEAUȘESCU, **Research work on synthesis and characterization of macromolecular compounds, Contributions**, 1974, 251 p.
CR. SIMIONESCU, VIORICA RUSAN, V. POPA, **Chimia algelor marine**, 1974, 212 p., 1 pl.

ISSN 0035—3930

I. P. INFORMAȚIA

43 426

Lei 40
$ 80 (pour un abonnement annuel)